



Abstract Volume
17th Swiss Geoscience Meeting

Fribourg, 22nd + 23rd November 2019

Geoscience goes underground: understanding resources & processes

sc | nat

Swiss Academy of Sciences
Akademie der Naturwissenschaften
Accademia di scienze naturali
Académie des sciences naturelles

UNI FR

UNIVERSITÉ DE FRIBOURG
UNIVERSITÄT FREIBURG

Geoscience goes underground

Knowledge of the shallow and deep underground has ever-growing importance in modern society. This is especially true for Switzerland, which has a longstanding tradition of exploring the deep that was acquired over the course of decades of building tunnels throughout its territories. Hydrocarbon exploration of the Alpine Molasse Basin and the Jura fold-and-thrust belt yielded modest successes, but the public controversy regarding shale gas exploration and induced seismicity in the wake of deep geothermal exploration has highlighted the importance and the role of communication of our geoscientific knowledge to the public.

The extraction of geothermal energy, building management, and land use planning will increasingly rely on knowledge of the near and deep subsurface geology. Natural resources of the underground, such as geothermal energy (from shallow to deep), CO_2 sequestration, shale gas, reservoir technology, water exploitation, subsurface energy storage, or "classic" mineral resources will thereby play a central role in the future. Geodata, GeoBIM, GeoCIM projects, and 3D geology models will reshape future management and use of underground resources and geoscientists must not miss the opportunity to get involved. Indeed, geoscientists should reach out to politicians and the public and take a position in a debate that will become increasingly more complex.

Cover Phoro credits: Pierre Dèzes

17th Swiss Geoscience Meeting, Fribourg 2019

Table of contents

Abstracts

1	Structural Geology, Tectonics and Geodynamics	2
2	Mineralogy, Petrology, Geochemistry	44
3	Stable isotope geochemistry: development and applications	90
4	Palaeontology	106
5	Stratigraphy	152
6	Seismic Hazard and Risk in Switzerland: From Science to Mitigation	166
7	Deep geothermal energy and CO_2 storage	196
8	Quaternary environments: landscapes, climate, ecosystems and human activity during the past 2.6 million years	238
9	Geomorphology	284
10	Soil: Formation, Processes, and Conservation	312
11	Cryospheric Sciences	223
12	Hydrology, Limnology and Hydrogeology	382
13	Public Engagement with Climate Change: Interdisciplinary Challenges	416
14	Environmental Biogeochemistry of Trace Elements	426
15	Atmospheric Processes and Interactions with the Biosphere	456
16	Phenology and seasonality	456
17	Aerosols and clouds in a changing world	456
18	Remote Sensing of the Spheres	482
19	Geoscience and Geoinformation – From data acquisition to modelling and visualisation	502
20	Taking stock of transformative research and education on mountains. What future avenues?	520
21	Human Geographies: Bodies, Cultures, Societies	534
22	Human Geographies: Cities, Regions, Economies	550
23	Human Geographies: Materials, Natures, Politics	566
24	The limits to Earth: thinking social-ecological transitions in a post-extractive economy	578
25	Towards the sustainable management and governance of land resources and land systems	578

Organisation

Host Institution

Department of Geosciences of the University of Fribourg

Patronnage

Platform Geosciences of the Swiss Academy of Sciences SCNAT

Local Organizing Committee

Christine Bichsel
Reynald Delaloye
Anneleen Foubert
Olivier Graefe (President SGM 2019)
Bernard Grobéty
Christian Hauck
Martin Hölzle
Matthias Huss
Walter Joyce
Afifé El Korh
Jon Mosar
Nadine Salzmann
Silvia Spezzaferri

Coordination

Pierre Dèzes

Sponsors

Swiss Geological Survey, swisstopo
CHGEOL
Swiss Academy of Sciences (SCNAT)

Participating Societies and Organisations

Commission for the Swiss Journal of Palaeontology
Forum Landscape, Alps, Parks (FOLAP)
Georesources Switzerland Group
Interdisciplinary Centre for Mountain Research
International Union of Geodesy and Geophysics, Swiss Committee (IUGG)
International Union of Geological Sciences, Swiss Committee (IUGS)
Mountain Research Initiative
Schweizerischen Gesellschaft für Erdbebeningenieurwesen und Baudynamik (SGEB)
Swiss Association of Geographers (ASG)
Swiss Association for Geographic Education (VGDch)
Swiss Commission for Phenology and Seasonality (CPS)
Swiss Commission for Remote Sensing (SCRS)
Swiss Commission on Atmospheric Chemistry and Physics (ACP)
Swiss Committee for Stratigraphy (Platform Geosciences/SCNAT)
SWISS DRILLING
Swiss Geodetic Commission (SGC)
Swiss Geological Society (SGG/SGS)
Swiss Geological Survey (swisstopo)
Swiss Geomorphological Society (SGGm/SSGm)
Swiss Geophysical Commission (SGPK)
Swiss Geothermal Society
Swiss Hydrogeological Society (SGH)
Swiss Hydrological Commission (CHy)
Swiss Paleontological Society (SPG/SPS, Swiss Geological Society)
Swiss Snow, Ice and Permafrost Society (SIP)
Swiss Society for Hydrology and Limnology (SGHL/SSHL)
Swiss Society for Quaternary Research (CH-QUAT)
Swiss Society of Mineralogy and Petrology (SMPG/SSMP, Swiss Geological Society)
Swiss Tectonics Studies Group (Swiss Geological Society)

1. Structural Geology, Tectonics and Geodynamics.

Guido Schreurs, Neil Mancktelow, Paul Tackley

Swiss Tectonics Studies Group of the Swiss Geological Society

TALKS:

1.1 Akker I.V., Schrank C.E., Jones M.W.M., Kewish C.M., Berger A., Herwegh M.: From slow-slip to fast earthquakes – a look into the paleo-earthquake record in eastern Switzerland

1.2 Borderie S., Souloumiac P., Maillot B., Mosar J.: Propagation of compressive deformation beyond a décollement topography: application to the Mandach Thrust (Jura Mountains, Switzerland)

1.3 Candioti L.G., Schmalholz S.M., Duretz T.: Impact of convection in the mantle transition zone on long-term lithospheric deformation during the Alpine cycle

1.4 Dielforder, A., Brune S., Frasca G., Ford M.: Formation of the Iberian-European convergent plate boundary fault and its effect on intraplate deformation in central Europe

1.5 Leith, K., Li, Y., Perras, M. A., Loew, S.: A first look at a new thermodynamic model to track time-dependant creep in crystalline rock

1.6 Li Y., Leith K., Wu R., Moradian O., Perras M.A., Loew S.: Initial insights into progressive failure during relaxation of Herrnholz granite subjected to three-point bending

1.7 Moscariello A., Clerc N., Eruteya O.E., Omodeo-Salé S., Guglielmetti L.: Complex shortening tectonic style of the Western Swiss Alpine foreland and implications for subsurface geo-fluid circulation.

1.8 Omodeo-Salé S., Cassola T., Moscariello A.: Structural evolution of the triangle zone in the fold-and-thrust Swiss Alpine belt (St. Gallen): Implications for geo-energy

1.9 Ricchi E., Gnos E., Bergemann C., Berger A., Rubatto D., Whitehouse M., Walter F.: Miocene deformation in the Tauern Window (Eastern Alps, Austria) constrained by in-situ Th-Pb dating of fissure monazite

1.10 Ruh J., Vergés J., Burg J.-P.: Paul Niggli Medal Recipient lecture: Importance of fluid overpressure for the structural evolution of the Makran accretionary wedge

1.11 Schmid T., Adam, J., Hollis, D., Schreurs, G., Zwaan, F.: 4D analysis of analogue extensional models

1.12 Winkler W., Wiederkehr M.: Cenozoic basin inversion in the North Penninic Valais domain of Eastern Switzerland (Prättigau)

1.13 Wu R., Moradian O., Li Y., Leith K., Loew S.: Acoustic emission observation during staged loading and relaxation of Herrnholz granite subjected to three-point bending

1.14 Zwaan F., Corti G., Keir D., Sani F., Muluneh A., Illsley-Kemp F., Papini M.: Multiphase rotational extension along the Western Afar Margin in East Africa

POSTERS:

P 1.1 Diehl T., Madritsch H., Spillmann T., Kraft T., Schnellmann M.: Imaging of Seismotectonic Processes in the Upper Crust of the Northern Alpine Foreland of Switzerland

P 1.2 Gilgannon J., Waldvogel M., Poulet T., Fusseis F., Berger A., Barnhoorn A., Herwegh M.: High shear strain ductile deformation produces stable porous domains

P 1.3 Gouffon Y., Kempf O., Möri A., Wiederkehr M.: Tectonic Map of Switzerland 1:500000: A new concept

P 1.4 Gventsadze A., Alania V., Enukidze O., Kvavadze N.: Structural architecture of active back-thrust zone of the eastern Achara-Trialeti fold-and-thrust belt (Kumisi-Teletei area), Georgia

P 1.5 Hauvette L., Sommaruga A., Mosar J., Fiebig B., Meyer M.: New insight into the Geneva Basin structural framework based on recently acquired 2D seismic data

P 1.6 Hetényi, G., Greenwood A., Baron L., Hetényi G., Pistone M., Holliger K., Ziberna L., Zanetti A., Müntener O., DIVE Site Survey Field Teams: Active seismic surveys at project DIVE's three drilling target sites (Ivrea zone, N-Italy)

P 1.7 Kakurina M.: In-situ stress estimation from fault slip triggered during fluid injection

P 1.8 Lanza F., Diehl T., Kraft T.,Deichmann N., Wiemer S., Nussbaum C.,Schefer S.: Seismotectonic analysis of seismicity in the vicinity of the Mont Terri rock lab

P 1.9 Laziz O., Bouaja F., Benabbas C.: Travertine occurrences along major neotectonic normal fault zones in the Hammam Debar- Roknia Guelma Region, Nort-East Algeria

P 1.10 Mannini S., Ruch J., Hollingsworth J., Swanson D.A., Johanson I., Cousseau F.: Multi-temporal analysis of ground deformation at the Koa'e fault system (Kīlauea volcano, Hawaii) using structural field observation and high resolution imagery.

P 1.11 Musso Piantelli, F., Herwegh M., Berger A., Wiederkehr M., Kurmann E., Möri A., Baumberger R.: Structural evolution of the western Aar Massif (external Central Alps, Switzerland): insights from 3D geological modelling

P 1.12 Nibourel L., Heuberger S., Galfetti T.: Automated extraction of layer orientation and thickness information from geological maps to support the characterisation of siliceous limestone deposits

P 1.13 Panza E., Ruch J., Martin F.: Influence of faulting on magma propagation during volcano-tectonic events and structural mapping using UAVs in NW Iceland.

P 1.14 Schenker F.L., Tagliaferri A., Ambrosi C., Scapozza C., Czerski D., Maino M., Gouffon Y.: The tectonics of the Simano, Cima-Lunga, Adula and Maggia nappes in the southern Lepontine dome

P 1.15 Simon V., Kraft T., Diehl T., Wiemer S.: High-resolution Imaging and Analysis of Seismicity Patterns in Swiss Microearthquake Sequences

P 1.16 Tackley P., Jain C., Rozel A., Lourenco D., Gerya T.: Geodynamic models of non-subduction generation of Archean continental TTG crust

P 1.17 Tagliaferri A., Corti L., Spalla M.I., Zucali M.: Multiscale structural analysis of the Variscan Basement and Permo-Mesozoic covers, at Frisson Lakes (Argentera Massif, Maritime Alps)

P 1.18 Vaughan-Hammon, J.D., Luisier, C., Schmalholz, S.M., Baumgartner, L.: Outcrop-scale pressure variations in the Monte Rosa nappe?

P 1.19 Zwaan F., Schreurs G., Rosenau M.: Rift development and propagation in orthogonal and rotational extension as seen in 4D analogue models

1.1

From slow-slip to fast earthquakes – a look into the paleo-earthquake record in eastern Switzerland

Ismay Vénice Akker[1], Christoph E. Schrank[2], Michael W. M. Jones[3], Cameron M. Kewish[4,5,6], Alfons Berger[1] and Marco Herwegh[1]

[1]Institute of Geological Sciences, University of Bern, Bern, Switzerland
[2]School of Earth, Environmental, and Biological Sciences, Queensland University of Technology, QLD 4000, Australia
[3]Central Analytical Research Facility, Institute of Future Environments, Queensland University of Technology, QLD 4000, Australia
[4]Department of Chemistry and Physics, La Trobe Institute for Molecular Science, La Trobe University, Victoria 3086, Australia
[5]Australian Nuclear Science and Technology Organisation, Australian Synchrotron, Victoria 3168, Australia
[6]ARC Centre of Excellence in Advanced Molecular Imaging, La Trobe Institute for Molecular Sciences, La Trobe University, Victoria 3086, Australia

Recent advances in geophysical techniques enable quantification of episodic tremor and slow-slip (ETS) in plate-convergent settings. Compared to megathrust earthquakes with reoccurrence times in the order of 100 years, ETS is more frequent, showing reoccurrence times of only 0.5 to 2 years. Fluids play an important role, and in the geological record, ETS is recognized in exhumed fault-and shear zones by en-echelon crack-seal, shear and extension veins. We study how fluids release and migrate over a multitude of scales and what their effect on the deformation is. To this end, we combine field observations from the European Alpine exhumed accretionary wedge with high-resolution trace-element maps from synchrotron X-ray fluorescence microscopy (SXFM). Fluids are moved along an up-scale cascade: 1) On the µm-cm scale in the slate matrix dynamic dissolution-precipitation processes make phyllosilicate seals, which eventually leads to hydrofracturing under increasing pore fluid pressure, as seen by ultrathin veinlets (widths of 10 µm) with very high spatial frequencies. The mutual overprint of these ductile processes in the matrix and the brittle fracturing of veinlets with such high frequency is indicative for cyclic slow slip and related tremor. On these small scales fluids are pervasively collected, and the energy release by fracturing is low. 2) The collected fluids feed into foliation sub-parallel veins making up m-scale vein arrays. The foliation sub-parallel veins are larger (widths of 1 cm) and have smaller spatial frequencies compared to the veinlets, indicating less frequent fracturing with an increased energy release. 3) Eventually these fluids channel into mega-arrays (widths of 100 m), which themselves feed into deca-km scale thrusts. The enormous localized fluid collection on thrust planes builds up high pore fluid pressures and could eventually lead to rupture of megathrust earthquakes.

1.2

Propagation of compressive deformation beyond a décollement topography: application to the Mandach Thrust (Jura Mountains, Switzerland)

Sandra Borderie[1], Pauline Souloumiac[2], Bertrand Maillot[2] & Jon Mosar[1]

[1]Unit of Earth Sciences, Geosciences Department, University of Fribourg, Chemin du Musée 6, CH-1700 Fribourg (sandra.borderie@unifr.ch)
[2]Laboratoire GEC, Maison Internationale de la Recherche, Université de Cergy-Pontoise, 1 rue Descartes, F-95000 Neuville-sur-Oise

In fold-and-thrust belts, the *décollement* can be offset, notably by normal basement faults inherited from former extensive tectonic episodes. This can create a basement topography, characterized by steps in the *décollement* surface. Such discontinuities in the *décollement* are believed to localize and concentrate the deformation.

In this study, we used the Limit Analysis Theory and the software OptumG2 to investigate the mechanical parameters that control the propagation of compressive deformation beyond an upward step of the *décollement*.

Firstly, we conducted a parametric study using a simple prototype. This was done in an attempt to quantify the general conditions in which an upward step of the *décollement* can significantly influence the propagation of deformation. We tested (i) the impact of the position of an upward step below a hinterland wedge and (ii) its height, (iii) the *décollement* friction and (iv) the slope of the wedge. Results confirm that an upward step in the *décollement* helps to localize deformation.

Furthermore, we found that the propagation of deformation beyond the step is more dependent on the friction of the *décollement* and on the position of the step with respect to a pre-existing topography, as opposed to the height of the step. Four major structural styles are defined, corresponding to different ranges of geometric and rheological parameters. Results indicate that even a small perturbation in the *décollement* relief can have a relevant impact on the deformation.

In the subsequent step, we compared the modelled data to the mechanical conditions for activation of the Mandach Thrust in the eastern part of the Jura Mountains. In this area, the *décollement* is partially offset and shows upward steps. We utilised eight structural cross sections positioned across the Mandach Thrust. This allows defining rheological parameters for this part of the Jura, and testing their compatibility with proposed geometries. Results indicate that for the given geometries, several *décollements* can be activated, even for high strengths of the *d*écollement*s*. The final component of this study, which is still ongoing, aims to resolve the associated stress fields in this area.

1.3

Impact of convection in the mantle transition zone on long-term lithospheric deformation during the Alpine cycle

Lorenzo G. Candioti[1], Stefan M. Schmalholz[2], Thibault Duretz[3]

[1]Institut des sciences de la Terre, Université de Lausanne (Lorenzo.Candioti@unil.ch)
[2]Institut des sciences de la Terre, Université de Lausanne
[3]Univ. Rennes 1, UMR CNRS 6118, France

The geodynamic history of the Western Alpine orogeny comprises periods of distinct phases of lithospheric deformation. Ultra-slow to slow spreading during ca. 40 Myrs formed the ca. 300-400 km wide Piemonte-Liguria basin. This basin was bounded by magma-poor, hyper-extended continental margins of the European and Adriatic plate and consisted mainly of exhumed and partially serpentinized sub-continental mantle. Subsequently, post-extension cooling took place for ca. 70 Myrs with insignificant tectonic activity. Then, convergence of the basin-margin system started at ca. 90 Ma causing the closure of the basin during subduction and the formation of an orogenic wedge during continent-continent collision.

Modelling the long-term geodynamic history (>100 Myrs) of orogens such as the Alps, including the pre-orogenic extension and cooling stages, remains challenging. For example, thermal convection in the upper mantle and transition zone becomes significant over long time scales. The resulting viscosity, temperature and density distribution in the lithosphere and transition zone is crucial for subduction initiation and evolution of the subduction zone. Effects of convection can be modelled by either (1) directly modelling small-scale mantle convection, or by (2) artificially scaling the thermal parameters of the sub-lithospheric mantle without modelling convection.

We perform 2D high resolution thermo-mechanical numerical simulations of more than 120 Myrs of lithospheric deformation. The models include the mantle transition zone down to a depth of 660 km to model the Western Alpine cycle including three subsequent deformation phases: (1) formation of a ca. 400 km wide basin of exhumed mantle bounded by two hyper-extended passive margins during a 30 Myrs rifting period. (2) Thermal relaxation of the margin system for 70 Myrs with no far-field tectonic activity. (3) Convergence of the passive margin system leading to subduction initiation, basin closure and orogenic wedge formation.

We perform three types of simulations: (1) We resolve and model sub-lithospheric convection during lithospheric extension, cooling and convergence. (2) We scale the thermal conductivity of the sub-lithospheric mantle without modelling and resolving the convection. (3) We replace the top 7.5 km of exhumed mantle material in the basin with material that is describe by an antigorite flow law 1 Myrs before the onset convergence. We discuss and quantify the general differences of the model results for the extension, cooling and subduction phase as well as the impact of a serpentinite layer on top of the subducting lithosphere. We further quantify differences in effective viscosities in the models and their impact on the extension and subduction dynamics.

1.4

Formation of the Iberian-European convergent plate boundary fault and its effect on intraplate deformation in central Europe

Armin Dielforder[1], Sascha Brune[1], Gianluca Frasca[2] & Mary Ford[3]

[1]GFZ German Research Centre for Geosicences, Telegrafenberg, D-14473 Potsdam (armin.dielforder@gfz-potsdam.de)
[2]IPGS, EOST-CNRS, Université de Strasbourg, 1, Rue Blessig, F-67084 Strasbourg
[3]Centre de Recherches Pétrographiques et Géochimiques, 15 rue Notre Dames des Pauvres, F-54500 Vandœuvre-lès-Nancy

In the Late Cretaceous plate convergence between Africa, Iberia, and Europe commenced. Simultaneously central Europe experienced a pulse of intraplate deformation lasting some 15–20 Myr. This deformation event documents area-wide deviatoric compression of Europe and has been interpreted as a far-field response to plate convergence. However, the factors that governed the compression of Europe and conditioned the transient character of the deformation event have remained unclear. Based on geological reconstructions, mechanical considerations, and numerical simulations, we examine how the dynamics of intraplate deformation related to the formation of a convergent plate boundary fault between Iberia and Europe. During the Late Cretaceous, plate convergence was accommodated by the inversion of a young hyperextended rift system that separated Iberia from Europe. Our analysis shows that the strength of the lithosphere beneath this rift was initially sufficient to transmit large compressive stresses far into Europe at the onset of plate convergence, though the lithosphere beneath the rift was thinned and thermally weakened. Continued plate convergence forced the formation of a plate boundary fault between Iberia and Europe. The fault evolved progressively and constituted a lithospheric-scale structure at the southern margin of Europe that weakened rheologically. This development caused a decrease in mechanical coupling between Iberia and Europe and a reduction of upper plate compression, which eventually terminated intraplate deformation in Central Europe. Taken together, we propose that the Late Cretaceous intraplate deformation event records a high force transient that relates to the earliest strength evolution of a lithospheric-scale plate boundary fault.

1.5

A first look at a new thermodynamic model to track time-dependant creep in crystalline rock

Kerry Leith[1], Ying Li[1], Matthew A. Perras[2], Simon Loew[1]

[1]Geological Institute, ETH, Sonneggstrasse 5, CH-8092 Zürich (kerry.leith@erdw.ethz.ch)
[2]Department of Civil Engineering, York University, 4700 Keele St, Toronto

The manner in which crystalline rock responds to permanent natural or anthropogenic changes in load, pore water chemistry, and / or temperature conditions over periods of hours to years is controlled by a phenomena known as static fatigue. Static fatigue is an overarching term to describe a range of processes that facilitate crystal glide and stable crack propagation in rock subjected to subcritical loading conditions. This can be attributed to chemo-physical properties of crystal boundaries, and pre-existing crack tips, and can be described by considering a combination of thermodynamic effects, and balance of energies present during deformation.

While a number of numerical techniques have been applied to capture the effects of static fatigue, particularly under controlled laboratory conditions, these very commonly have limited wider applicability as they rely on calibrated ‘damage’ parameters with little physical meaning. In this study we present a new method to reproduce creep behaviour in a fine grained granite core (Herrnholz granite) subjected to unconfined compressive loading in the new Rock Physics and Mechanics Lab at ETH Zurich. Employing a finite element model in COMSOL Multiphysics, we track time-dependant micro crack formation and plastic shear on connected fractures using parameters primarily derived from physical properties of the test specimen. We account for the release of thermal, seismic, and fracture surface energy in order to ensure the density of fractures contributing to material damage is consistent with energy converted from mechanical loading, and thermodynamic properties.

By developing a model around readily measurable physical properties, we expect to demonstrate an efficient, scalable method of assessing time-dependant creep at scales well beyond that of isolated laboratory specimens. Likely applications include the assessment of distributed strains around caverns, boreholes, and natural rock slopes under both static, and variable environmental conditions.

1.6

Initial insights into progressive failure during relaxation of Herrnholz granite subjected to three-point bending

Ying Li[1], Kerry Leith[1], Rui Wu[1], Omid Moradian[1], Matthew A Perras[2], Simon Loew[1]

[1]Geological Institute, ETH, Sonneggstrasse 5, CH-8092 Zürich (ying.li@erdw.ethz.ch)
[2]Department of Civil Engineering, York University, 4700 Keele St, Toronto

The propagation of fractures through intact rock under constant or reducing load conditions is known as static fatigue. This phenomena controls the progression of failure events in both natural rock environments (i.e. alpine rock slopes), and engineered settings (e.g. dam abutments, tunnels, and underground nuclear waste storage facilities). The physics of such progressive crack growth is, however, not captured in traditional rock mechanical analyses, making the prediction of long-term behaviour of bedrock in such settings complicated. Here, we presents results from single edge notch bending (SENB) tests undertaken on 400 × 90 × 90 mm prisms of Herrnholz granite subjected to alternating phases of loading at constant displacement rate, followed by load relaxation under constant displacement. These tests were undertaken in the new Rock Physics and Mechanics Lab at ETH Zurich, and provide new insight into the time-dependant behaviour of a fine-grained granite subjected to constant or reducing load conditions.

Four samples were tested in the SENB configuration, for which the first two were loaded to failure under load-point displacement (piston) control at a rate of 1 μm/s. This provided an indication of the peak strength and fracture toughness of the Herrnholz granite. The next two samples were subjected to staged loading increases (ranging from 50% to 98% of the average peak load) with load-point displacement maintained for up to 30 minutes between each load stage. Results demonstrate an exceptionally consistent failure load of 14.54 kN, ± 0.18 kN, suggesting a (theoretical) average fracture toughness of 1.82 MPa $m^{1/2}$.

Progressive failure characteristics during the load relaxation phase of the two staged tests were observed through an attached crack mouth opening displacement sensor, and digital image correlation. When loaded to between 50% and 90% of the peak load, crack mouth opening rates reduced to around 1% of the rate at the initiation of the hold period (10^{-4} mm/s) within 10 to 20 minutes. However, when the displacement was held at 98% of the peak, the creep rate demonstrated an acceleration toward failure as the load dropped by 5% over a four-minute interval.

Ongoing tests planned for more than 100 similar specimens are expected to provide data to constrain the physical properties controlling sub-critical cracking in Herrnholz granite, and the response of critically stressed cracks to changes in imposed environmental conditions. This unique dataset will provide much-needed insight into the long-term behaviour of natural and engineered rock sites.

1.7

Complex shortening tectonic style of the Western Swiss Alpine foreland and implications for subsurface geo-fluid circulation.

Andrea Moscariello[1], Nicolas Clerc[2], Ovie Emmanuel Eruteya[1], Silvia Omodeo-Salé[1], Luca Guglielmetti[1]

[1]*Department of Earth Sciences, University of Geneva Rues des Maraîchers, 13; 1205 Geneva, Switzerland (andrea.moscariello@unige.ch).*
[2]*Service de géologie, sols et déchets (GESDEC), Etat de Genève, Geneva, Switzerland*

The Swiss Alpine foreland located between the Alpine front and the folded Jura chain is described as generally undisturbed plateau where the shortening related to the Alpine compression is accommodated mostly by deeply rooted sliding of the thick Mesozoic series over the Triassic evaporites (Sommaruga, 1999). In addition to the basal sliding, proving the thin-skin tectonic character of the regional deformation, a series of several-km long N-S and NW-SE regional strike slip faults formed resulting in the lateral compartmentalization of the undeformed thick succession of Mesozoic and Cainozoic sediments. The role of high-angle faults deeply rooted in the underlying Hercynian basement in the deformation of the swiss Plateau is still under debate. However, evidence of a relationship between the occurrence of buttress of Hercynian basement and the development of anticlinal structures in the overlying Mesozoic, targeted in the past by hydrocarbon exploration, seems to indicate the importance of these Palaeozoic structures in explaining the present day deformation style of the Swiss Plateau subsurface.

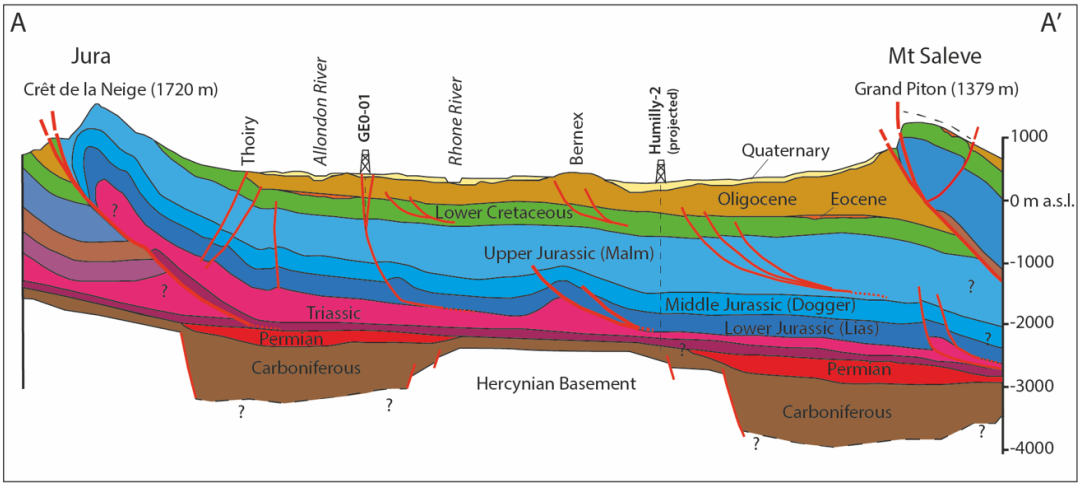


Fig. 1. Geological section crossing the Geneva Basin from NW (A) to SE (A') summarizing the key stratigraphic and structural elements present in the basin. This synthetic section has been drawn from the assemblage of several 2D seismic lines and borehole data.

In this area, the detailed examination of vintage reprocessed and newly acquired 2D reflection seismic lines highlights the discontinuity of the regional NW-SE strike-slip lineaments originally thought to cross the Geneva Basin. Instead, the occurrence of a higher degree of deformation at smaller scale distributed within several stratigraphic intervals within the Mesozoic succession has been highlighted.
These deformation consist of low-angle inverse faults/thrusts which root generally in shale and marly intervals. Thrust anticlines formed in the low-angle hanging wall have also been observed. These compressional features have an axis generally oriented parallel to the main deformation of the Jura domain, which display a progressive rotation from NE-SW to NW-SE direction.
These observations indicate a higher structurally complexity than previously thought. It reflects a complex history of deformation indicating that shortening is accommodated by small low-angle inverse faults and thrusts displaying tens to few hundreds of meters of lateral displacement with little vertical offset.

Deformation is controlled by contrasting lithologies occurring within the Jurassic and lower Cretaceous (carbonates vs marls and shales). Different phases of deformation include compression, rotation and development of both transpressive and transtensional strike slips.
In places fault and dense fracture network associated with these deformations are connected crossing throughout the entire thickness of the Mesozoic sequence above the Triassic anhydrites showing a listric character rooted in the Lower Jurassic shale intervals (e.g. Toarcian; Fig. 1).

In the framework of the ongoing study of the Geneva Basin subsurface aiming at developing a strategy for Geothermal energy exploration (Moscariello 2016), the understanding of geometry, direction and continuity at depth of these structural features is therefore crucial as they can play a key role in controlling the subsurface circulations of both hydrocarbons and geothermal fluids.

REFERENCES

Moscariello, A. 2016: Geothermal exploration in SW Switzerland. *Proceedings* European Geothermal Congress 2016 Strasbourg, France, 19-24 Sept 2016, 10 pp.

Sommaruga A. 1999: Decollement tectonics in the Jura foreland fold-and-thrust belt. Marine and Petroleum Geology 16, 111-134

1.8

Structural evolution of the triangle zone in the eastern fold-and-thrust Swiss Alpine belt (St. Gallen): Implications for geo-energy

Omodeo-Salé, S.[1], Cassola, T.[2] and Moscariello, A.[1]

[1]*Department of Earth Science, University of Geneva (Switzerland)*
[2]*Schlumberger GmbH, Aachen (Germany)*

The term triangle zone is used to describe frontal structures in fold and thrust belts, triangular and bounded by thrusts of opposite vergence (Von Hagke and Malz, 2018). These structures have been intensively studied as they provide relevant keys to understand the process forming an orogenic belt. Furthermore, in these areas, hydrocarbon traps can form (McKay et al., 1996; Zamora-Valcarce and Zapata, 2015).
There are several uncertainties on the mechanic and kinematic mechanisms forming a triangle zone in a fold-thrust belt. It can be the result of the play of single and/or multiple detatchement surfaces, their frictional and geometrical characteristics, the fluids overpressure and of the differential strength of the stratigraphic cover(McKay et al., 1996; Von Hagke and Malz, 2018). A useful tool to elucidate these mechanisms is by balancing and restoring a 2D geological cross-section (e.g., Bally et al., 1966). By this method, a kinematic model, consistent with the present-day geometry and structures, can be defined. Furthermore, the original thickness and geometry of the stratigraphic units can be reconstructed.
The structuration of triangle zones in the fold-thrust belts forelands can have an effect on the occurrence of hydrocarbons, in terms of maturation, expulsion and migration processes. Tectonic stacking can provoke an acceleration in the source rock maturation and hydrocarbons expulsion. Furthermore, the stacking of soft sediment can create overpressure zone that can strongly control fluids circulation. Finally, traps can be formed in opposite verging thrusts (McKay et al., 1996).
In this work, by combining structural restoration with basin modelling, the structural evolution of the triangle zone formed in the eastern sector of the Swiss Alpine fold-and-thrust belt (St. Gallen area), is reconstructed. The sequence of restored sections obtained were used to model the thermal evolution of the area, thus the hydrocarbons generation, migration and accumulation processes (Figure 1). The results provided by this work permit to individuate the areas, in the frontal part of a fold-and-thrust belt, with the highest probabilities to find hydrocarbons occurrence, thus that could represent a relevant risk for the geothermal drilling exploration activity.

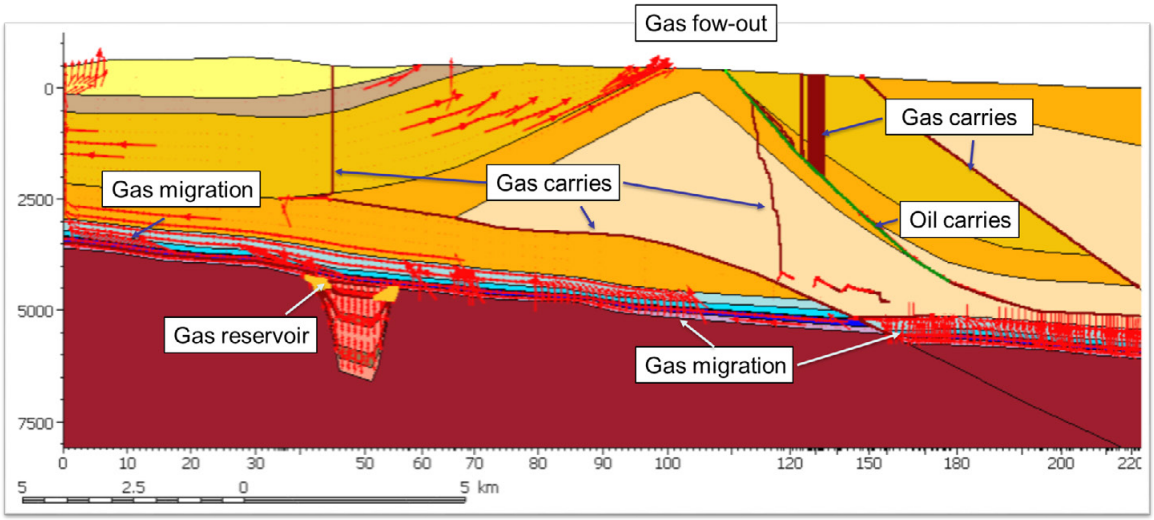


Figure 1. Potential hydrocarbons occurrence in a triangle zone (St. Gallen area, eastern Switzerland) (From Omodeo-Salé et al., 2019).

REFERENCES

Bally, Albert W., P. L. Gordy, & George Alan Stewart. “Structure, seismic data, and orogenic evolution of southern Canadian Rocky Mountains.” Bulletin of Canadian Petroleum Geology 14.3 (1966): 337-381.

MacKay, P. A., Varsek, J. L., Kubli, T. E., Dechesne, R. G., Newson, A. C., & Reid, J. P. (1996). Triangle zones and tectonic wedges: An introduction. Bulletin of Canadian Petroleum Geology, 44(2), I-1.

Omodeo-Salé, S., Cassola, T., Eruteya, O.E., & Moscariello, A. (2019). Petroleum system evolution in a fold-and-thrust belt triangle zone: a case study from the Swiss Alps. ICE AAPG 2019, Buenos Aires, Argentina.

von Hagke, C., & Malz, A. (2018). Triangle zones–Geometry, kinematics, mechanics, and the need for appreciation of uncertainties. Earth-science reviews, 177, 24-42.

Zamora-Valcarce, G., & Zapata, T. (2015). Building a valid structural model in a triangle zone: An example from the Neuquén fold and thrust belt, Argentina. Interpretation, 3(4), SAA117-SAA131.Beograd.

1.9

Miocene deformation in the Tauern Window (Eastern Alps, Austria) constrained by in-situ Th-Pb dating of fissure monazite

Emmanuelle Ricchi[1], Edwin Gnos[2], Christian Bergemann[1], Alfons Berger[3], Daniela Rubatto[3], Martin Whitehouse[4], Franz Walter[5]

[1]Department of Earth Sciences, University of Geneva, Rue des Maraîchers 13, 1205 Geneva, Switzerland
[2]Natural History Museum of Geneva, Route de Malagnou 1, 1208 Geneva, Switzerland
[3]Institute of Geological Sciences, University of Bern, Baltzerstrasse 1+3, 3012 Bern, Switzerland
[4]Institute of Earth Sciences, University of Lausanne, Geopolis, Lausanne, 1015 Switzerland
[5]Swedish Museum of Natural History, Box 50007, SE104-05 Stockholm, Sweden
[6]Institut für Erdwissenschaften, Karl-Franzens-Universität, Universitätsplatz 2, 8010 Graz, Austria

Hydrothermal monazite-(Ce), a LREE phosphate concentrating Th and little U, is found in Alpine fissures and clefts that formed under peak to retrograde metamorphic conditions. In the eastern part of the Tauern Window (TW) fissure monazite was estimated to crystallise at temperatures of ~200-300°C (Gnos *et al.*, 2015), thus postdating early fissure formation.

Fissures are generally oriented roughly perpendicular to the foliation and lineation of their host rocks and may experience prolonged phases of deformation. In the TW two generations of parallel fissures are oriented sub-vertically. Early fissures formed during E-W extension in association with N-S compression and folding and are oriented perpendicular to the main fold axis (and lineation; e.g. Gnos *et al.*, 2015; Rosenberg *et al.*, 2018). Younger fissures are oriented pependicular to sinistral strike-slip (e.g. Rosenberg *et al.*, 2018) or sinistral oblique-slip faulting. These faults develop parallel to the axial plane of upright folds and are restricted to the central and western TW. Interaction of fluid-filled fissures with the surrounding rock leads to dissolution of minerals in the rock wall and mineral precipitation in the fissure.

As long as deformation continues fluid-filled clefts will react to deformation via dissolution-precipitation cycles due to disequilibrium between fluid, rock wall and mineral assemblage within the cleft. This chemical disequilibrium can lead to crystallization or reprecipitation of fissure monazite and to resetting of its isotopic system (e.g. Seydoux-Guillaume *et al.*, 2002, 2012; Grand'Homme *et al.*, 2016). Therefore, hydrothermal monazite is able to record several deformation events through multiple growth and dissolution episodes (e.g. Berger *et al.*, 2013; Bergemann *et al.*, 2017; Ricchi *et al.*, 2019).

Thorium-Pb crystallization ages of hydrothermal monazites from the western, central and eastern TW provide new insights into Miocene tectonic evolution of the Tauern metamorphic dome. Growth domain crystallization ages range from 21.69 ± 0.30 Ma to 7.69 ± 0.88 Ma. Three major periods of monazite growth are recorded between ~22 – 17, 17 – 15 and 13 – 8 Ma, respectively interpreted to be related to E-W extension, contemporaneous N-S shortening, beginning strike-slip movements, and reactivation of strike-slip/normal faulting. Fissure monazite crystallization ages largely overlap with zircon and apatite fission tracks cooling data. Monazite dates reflect crystallization due to tectonic movements that took place during the formation of the dome. Thus, monazite growth appears to be episodic and related to tectonic movements along the shear zones in the TW. Geochronological and structural data from the Pfitschtal area in the western Tauern Window, show the existence of two cleft generations separated in time by 4Ma and related to strike-slip to oblique-slip faulting.

Extreme Th/U ratios observed in fissure monazites reflect monazite growth under higly oxidizing conditions in association with hematite, in line with previous observations.

REFERENCES

Bergemann, C. A., Gnos, E., Berger, A., Whitehouse, M., Mullis, J., Wehrens, P., Pettke, T. & Janots, E. (2017). Th-Pb ion probe dating of zoned hydrothermal monazite and its implications for repeated shear zone activity: An example from the central Alps, Switzerland. Tectonics 36, 671–689.

Berger, A., Gnos, E., Janots, E., Whitehouse, M., Soom, M., Frei, R. & Waight, T. E. (2013). Dating brittle tectonic movements with cleft monazite: Fluid-rock interaction and formation of REE minerals. Tectonics 32, 1176–1189.

Gnos, E., Janots, E., Berger, A., Whitehouse, M., Walter, F., Pettke, T. & Bergemann, C. (2015). Age of cleft monazites in the eastern Tauern Window: constraints on crystallization conditions of hydrothermal monazite. Swiss Journal of Geosciences 108, 55–74.

Grand'Homme, A., Janots, E., Seydoux-Guillaume, A. M., Guillaume, D., Bosse, V. & Magnin, V. (2016). Partial resetting of the U-Th-Pb systems in experimentally altered monazite: Nanoscale evidence of incomplete replacement. Geology 44, 431–434.

Ricchi, E., Bergemann, C. A., Gnos, E., Berger, A., Rubatto, D. & Whitehouse, M. J. (2019). Constraining deformation phases in the Aar Massif and the Gotthard Nappe (Switzerland) using Th-Pb crystallization ages of fissure monazite-

(Ce). Lithos 342-343, 223-238.
Rosenberg, C. L., Schneider, S., Scharf, A., Bertrand, A., Hammerschmidt, K., Rabaute, A. & Brun, J. P. (2018). Relating collisional kinematics to exhumation processes in the Eastern Alps. Earth-Science Reviews 176, 311–344.
Seydoux-Guillaume, A. M., Montel, J. M., Bingen, B., Bosse, V., de Parseval, P., Paquette, J. L., Janots, E. & Wirth, R. (2012). Low-temperature alteration of monazite: Fluid mediated coupled dissolution-precipitation, irradiation damage, and disturbance of the U-Pb and Th-Pb chronometers. Chemical Geology 330–331, 140–158.
Seydoux-Guillaume, A. M., Paquette, J. L., Wiedenbeck, M., Montel, J. M. & Heinrich, W. (2002). Experimental resetting of the U-Th-Pb systems in monazite. Chemical Geology 191, 165–181.

1.10

Importance of fluid overpressure for the structural evolution of the Makran accretionary wedge

Jonas B. Ruh[1], Jaume Vergés[2] & Jean-Pierre Burg[1]

[1]Structural Geology and Tectonics Group, Geological Institute, Department of Earth Sciences, ETH Zürich, Sonneggstrasse 5, 8092 Zürich, Switzerland (jonas.ruh@erdw.ethz.ch)
[2]Institute of Earth Sciences "Jaume Almera" - CSIC, Carrer Solé I Sábaris s/n, 08028 Barcelona, Spain

In accretionary wedge systems, fluid overpressure plays a dominant role when it comes to the localization of major décollement horizons. Furthermore, it effects the overall internal strength of the shortened and imbricated sedimentary sequence. Numerical experiments on evolving accretionary wedges usually implement predefined weak basal decollements and constant strength parameters for overlying compressed sequences, although fluid pressure ratio, and therefore brittle strength, can vary strongly in sedimentary basins. A two-dimensional finite difference model with a visco-elasto-plastic rheology is used to investigate the influence of different simplified fluid pressure ratio distributions on the structural evolution of accretionary wedge systems. Results show that a linear increase in fluid pressure ratio towards the base leads to toeward-verging thrust imbrication and underplating of strata, while simulations with a predefined décollement form conjugate shear zones supporting box-fold-type frontal accretion. Surface tapers are in agreement with the critical wedge theory, which here is modified for cases of varying fluid pressure ratio. Numerical experiments with high fluid pressure result in both thrust imbrication and local normal faulting during large-scale shortening due to converging minimal and maximal critical taper angles. Similar findings have observed in the Makran accretionary wedge, SE Iran, where large listric normal faults occur along the coast line dipping towards the wedge toe.

Furthermore, landwards from the coast, the onshore Iranian Makran accretionary wedge exhibits closed minibasins developed onto a regional-scale olistostrome with a shaly matrix. Minibasins are sagging synformal depocenters surrounded by upsurging ductile material reproducing typical salt tectonic halokinetic patterns. It is expected, that the fluid-saturated and non-lithified olistostrome deposits rheologically behave in a ductile manner, often also referred to as "mobile shale". Two-dimensional numerical experiments were carried out to investigate whether the growth of such minibasins above a shale-dominated unit is feasible and how the presence of a regional, shale-dominated olistostrome may affect the structural evolution of active accretionary wedges. Model results indicate that rapid mass-flow emplacement triggers thickening of the rear of the wedge while minibasins grow in a more frontal, tectonically quiet region. Further wedge growth leads to a jump forward of frontal accretion. Compared to the case history, this jump would explain the structural characteristics of the Coastal Makran in Iran.

1.11

Deformation in crust and mantle as observed in 4D analogue extensional models

Timothy Schmid[1], Frank Zwaan[1], Guido Schreurs[1]

[1]*Institute of Geological Sciences, University of Bern, Baltzerstrasse 1, CH-3012 Bern (timothy.schmid@geo.unibe.ch)*

In stable continental lithosphere at least two strength peaks occur (Fig. 1). One peak is located below the Moho, defined by the presence of a high strength mantle, and a second one in the upper crust. Hence, old continental lithosphere is at first order considered to be composed of four layers: An upper brittle crust, a lower ductile crust and lithospheric mantle consisting of a brittle upper and a ductile lower part. Ductile layer strength is governed by extension velocity (i.e. strain rate); an increase in strain rate increases ductile crust strength, thus enhancing the coupling between crust and mantle lithosphere.

Our study aims at investigating how extension velocity (and thus strain rate and eventually the ductile layer strength) influences deformation in the mantle and crustal lithosphere by means of extensional analogue models. The experimental machine consists of two rigid sidewalls with a base of alternating plexiglass and foam bars in between (Fig. 1). By moving the sidewalls apart, the foam expands evenly allowing a homogeneous extension at the base of the model. Simultaneously, one of the base plates can move laterally to simulate oblique extension. Quartz sand and viscous mixtures of PDMS/ corundum sand with known rheological properties are used to simulate brittle deformation in the upper crust and uppermost mantle, as well as ductile behaviour in the lower crust and lower mantle lithosphere, respectively. A rod of ductile material ("seed"), placed on top of the lower viscous layer acts as a structural weakness at the base of the lower brittle layer, and ensures that deformation initializes in the mantle lithosphere (Fig.1).

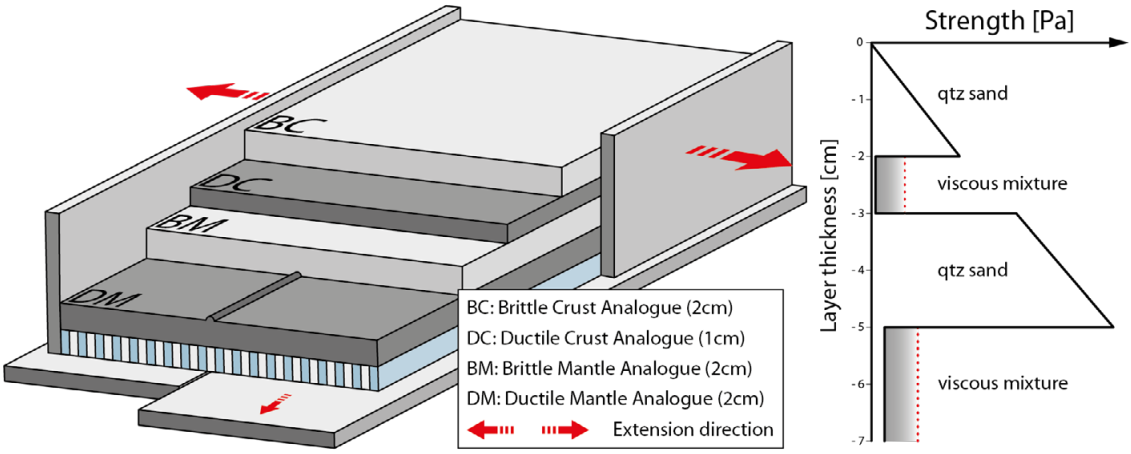


Figure 1. Four-layer model set up with a rod of ductile material placed at the base of the lower brittle layer (left). Extension directions, applied by the side walls and one basal plate, are indicated by red arrows. Associated strength profile with strength peaks in the modelled brittle crust and mantle lithosphere (right).

Next to standard top view time lapse photography and 3D photogrammetry, we plan to monitor our experiments with 4D X-ray computed tomography (CT) methods, allowing additional 3D digital volume correlation (DVC) analysis and quantification of internal deformation. In combination with 3D digital image correlation (DIC) techniques applied to monitor model surface evolution we produce fully quantified analogue models that help understanding the relations between internal model deformation and surface evolution.

Preliminary results of orthogonal extension experiments for a relatively low mean strain rate (values of ca. 9 10^{-16} s^{-1} in nature) are shown in figure 2; single mantle necking occurs in the centre of the model (above the weak seed) and deformation is transfered to the brittle crust via the viscous lower crust that takes up deformation in a diffuse fashion. The first deformation visible at the surface is expressed by two parallel narrow rifts in the brittle crust, confining a horst structure above the weak seed. With continued stretching, additional parallel rifts develop further away from the central horst in the upper crust while the brittle mantle is thinned out allowing the ductile mantle to come into contact with the ductile crust. The lack of isostatic rebound, due to the absence of a low viscosity layer beneath the model leads to collapse of the central horst in the upper crust. For a higher strain rate, we expect multiple necking, i.e. boudinage of the brittle mantle. Future models in this series will address the coupling of deformation in oblique extensional systems in continental settings.

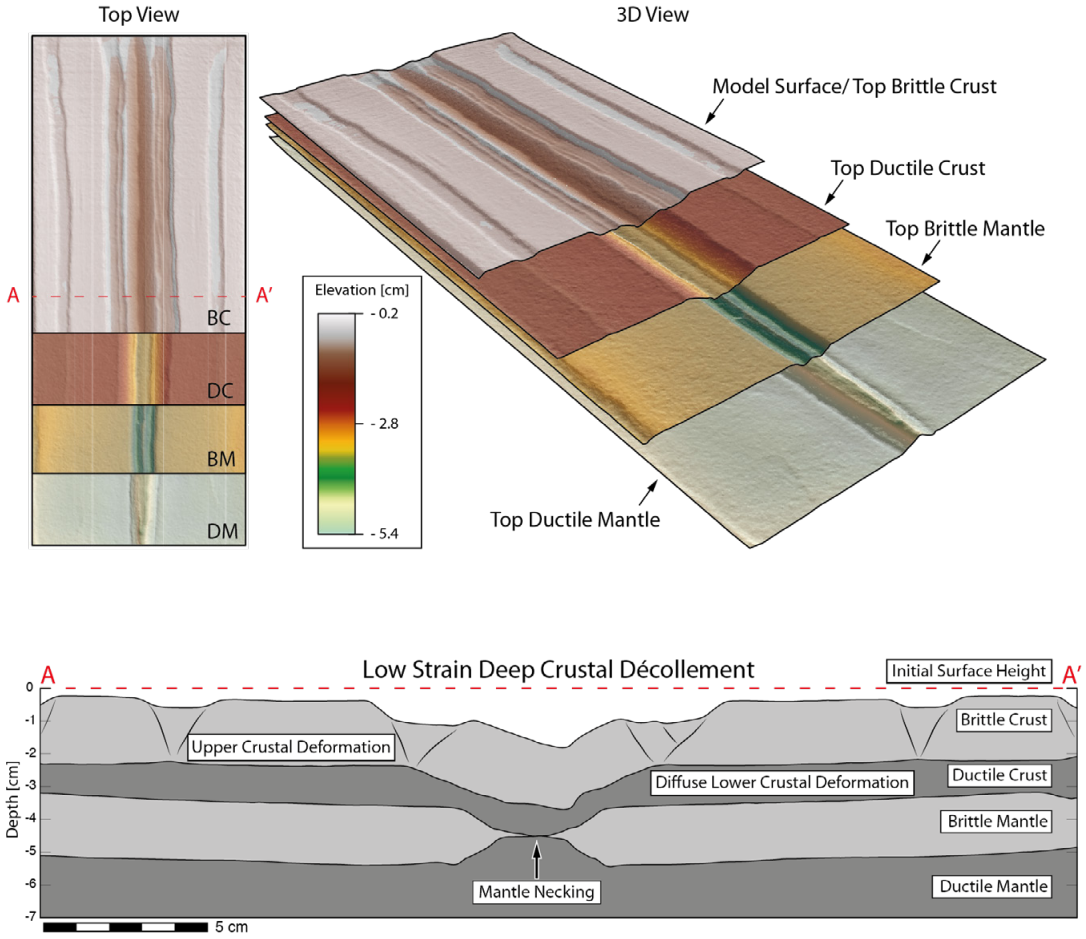


Figure 2. Top view of superposed layer surfaces of the final model stage (top left) and 3D view (top right). Digital elevation models are made with Agisoft Photoscan photogrammetry software. Red dashed line indicates the position of the cross section A-A' (bottom).

1.12

Cenozoic basin inversion in the North Penninic Valais domain of Eastern Switzerland (Prättigau)

Wilfried Winkler[1], Michael Wiederkehr[2]

[1]Geological Institute, Department of Earth Sciences, ETH Zurich, Sonneggstrasse 5, 8092 Zurich, Switzerland (wilfried.winkler@erdw.ethz.ch)
[2]Bundesamt für Landestopografie swisstopo, Landesgeologie, Seftigenstrasse 264, 3084 Wabern, Switzerland

As part of a joint mapping project under direction of the Swiss Geological Survey at swisstopo, several researchers work on the revision of geological maps in the Grison area. Here we refer directly to the Bündnerschiefer- and flysch deposits in the Prättigau district. They consist throughout of sandy-shaley turbiditic deposit of confusingly low lithological variability with the exception of the topping Palaeocene Oberälpli and Lower Eocene Ruchberg fms. (Nänny 1948). In a larger frame, these series are attributed to the Grava Nappe, which is overthrusted by the Tomül Nappe of more southern origin. Both contain in their lower stratigraphic section similar lithologies, in particular the Aptian–Albian Nolla Tonschiefer and Valzeina Fm., respectively (Steinmann 1994).

After a long time of research important points remained enigmatic with regard to what do the sediments tell us about the triggering tectonic processes und how do they fit with current basin models and inversions. There is common consensus that during the Alpine orogeny the inversion of basins initiates the formation of flysch and mélange deposits, i.e. by the transition from extension to subduction. It is also obvious that inversion of basins migrated in time from south (Cretaceous) to north (Eocene–Oligocene).

At Nänny's (1948) time the dominant geosynclinal model demanded the Tethys-wide simultaneity of the tectono-sedimentary processes. Consequently, on various geological maps of the Prättigau half-window the transition from Prättigauschiefer to flysch is still drawn at the base of the Turonian Pfävigrat Fm.

The mapping results on the map sheets Schiers, Serneus, Sulzfluh and Schesaplana we summarize as follows: The Cretaceous sedimentary sequence (i.e. Klus, Valzeina, Sassauna, Pfävigrat, Fadura, Gyrenspitz and Eggberg fms.) were formed during basin extension and mantle exhumation in southern parts of the basin as inferred by Steinmann (1994). These turbiditic formations show a simple composition by varying contents in quartz and carbonate matrix as typical for passive margin deposits. From grain-size trends, Nänny (1948) inferred detrital sources to the north which we can confirm. The dark shales and minor sandstones of the Palaeocene Oberälpli Fm. show only local and thin occurrences. The depostits of the Lower Eocene Ruchberg Fm. prograded from south to north over the entire basin area culminating in up to metric coarse-grained arkosic sandstones and conglomerates. Both Cenozoic fms. we mapped mainly on top of the Eggberg but also on the Gyrenspitz and Sassauna/Pfävigrat fms. The observed switch of detrital supply of the basin from south is also evident from detrital zircon U-Pb age spectra. Few analysed Cretaceous extension related sandstone beds show a limited detrital zircon age variation whereas those of the Oberälpli and Ruchberg fms. imply a more heterogeneous sourcing typical for Central Alpine flysch deposits (Bütler et al. 2011, Beltrán-Triviño et al. 2013). Distinctly, there are also Triassic zircons identified pointing to a supply from early Alpine nappe stacks including Eastern/South Alpine Triassic units (Beltrán-Triviño et al. 2016). Considering the Oberälpli Fm. as remnant from local basins forming during the inversion to a subduction basin we see ambiguities with the structural analysis of Weh and Froitzheim (2001) suggesting a multiple-phase deformation post-dating the deposition of the Ruchberg Fm. and ending in the Early Oligocene. Although the Ruchberg sandstones prove to be much more competent in deformation, in fine facies we observe only simple folding.

In conclusion, our mapping of sedimentary and compositional trends revealed the inversion from extension to southward subduction in the North Penninic basin should have occurred somtimes around the Cretaceous/ Cenozoic transition. Hence, it preceded the HP/LT metamorphic peak event measured in the Valais domain at 42–40 Ma (Wiederkehr et al. 2009) for about 20 mys.

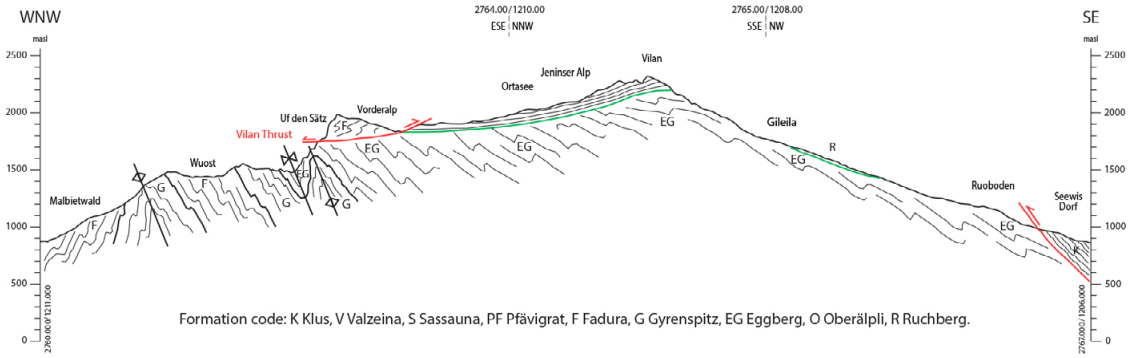


Fig. 1: Interpreted geological section across the larger Vilan area after Nänny (1948) and own observations.

REFERENCES

Beltràn-Triviño, A., Winkler, W., von Quadt, A. 2013. Tracing Alpine sediment sources through laser-ablation U-Pb dating and Hf-isotopes of detrital zircons. Sedimentology 60, 197-224.

Beltràn-Triviño, A., Winkler, W., von Quadt, A., Gallhofer, D. 2016. Triassic magmatism on the transition from Variscan to Alpine cycles: evidence from U–Pb, Hf, and geochemistry of detrital minerals. Swiss Journal of Geosciences 109, 309-328, DOI 10.1007/s00015-016-0234-3

Bütler, E., Winkler, W., Guillong, M. 2011. Laser ablation U/Pb age patterns of detrital zircons in the Late Maastrichtian - Early Eocene Schlieren Flysch (Central Switzerland): new proves on the detrital sources. Swiss Journal of Geosciences 104, 225-236.

Nänny, P. 1948. Geologie der Prättigauschiefer zwischen Rhätikon und Plessur. Mitt. Geol. Institut ETH u. Univ. Zürich, Serie C, Nr. 30, 127 p.

Weh, M. & Froitzheim, N. 2001. Penninic cover nappes in the Prättigau half-window (Eastern Switzerland): Structure and tectonic evolution. Eclogae geol. Helv. 94, 237-252.

Steinmann, M. 1994. Ein Beckenmodell für das Nordpenninikum der Ostschweiz. Jb. Geol. B.-A. 137, 675-721.

Wiederkehr, M., Sudo, M., Bousquet, R., Berger, A., & Schmid, S.M. 2009: Alpine orogenic evolution from subduction to collisional thermal overprint: The 40Ar/39Ar age constraints from the Valaisan Ocean, central Alps. Tectonics 28, doi:10.1029/2009TC002496.

1.13

Acoustic emission observation during staged loading and relaxation of Herrnholz granite subjected to three-point bending

Rui Wu[1], Omid Moradian[1], Ying Li[1], Kerry Leith[1], Simon Loew[1]

[1]Geological Institute, ETH, Sonneggstrasse 5, CH-8092 Zürich (rui.wu@erdw.ethz.ch)

Time-dependent fracture propagation at sub-critical crack tip stress intensities known as subcritical crack growth (SCG), is gaining increasing attention, as it is seen to be the next step required to understand of the precursory phase and triggered failure of catastrophic geohazards. In particular, tensile fractures, in which rupture propagates along a plane perpendicular to the applied tensile stress can be observed in various engineering projects (e.g. hydraulic fracturing and underground excavations), and natural disasters (e.g. landslides). One of the major challenges is to figure out what controls the SCG mechanism.

Acoustic emissions (AE) are elastic waves that are emitted from brittle rock caused by microcracks and can provide valuable physical insights behind SCG. However, a number of researches indicate that no or very low AE activity is detected during SCG as cracks propagate with low energy release rate. To have a deeper understanding of AE activity during SCG, we studied AE signals of Herrnholz granite under single edge notch bending (SENB) tests using a combined AE setup under room environment conditions. Two sets of AE sensors from Physical Acoustic Corporation (PAC), and KRNBB-PC sensors with different sensitivities (PAC: ~1 V/nm, KRNBB-PC: ~0.015 V/nm), contact area (PAC: face contact, KRNBB-PC: point contact) and frequency ranges (PAC: resonant, KRNBB-PC: flat, wideband) were attached to a 400 × 90 × 90 mm SENB specimen.

For the 1st and 2nd stages, the rock specimen was loaded under constant load-point displacement rate of 1 μm/s until 50% and 60% of the estimated peak load (from preliminary testing results) and then went through stress relaxation under constant displacement for 10 minutes, respectively. Then the specimen was loaded again until 91% of the peak load and 20 minutes under stress relaxation (3rd stage). The staged loading under constant displacement rate and then stress relaxation cycles was repeated progressively up to the 98% of the peak load where the specimen failed within 4 minutes.

PAC sensors, with higher sensitivity, could detect more signals (620 events occurred within 222 s) and show that crack numbers increase logarithmically after the 4th staged loading (98% of the estimated peak load), while most signals from KRNBB-PC sensor are recorded in the last 10 seconds or completely after the failure. Though they detect fewer AEs, KRNBB-PC sensors are still useful as they have a wideband frequency range and therefore can provide information on energy partitioning. The 3D AE locations from KRNBB-PC sensors show that most microcracks distributed within an apparent zone of nearly 4 cm width during the last relaxation stage, which are centered around the notch but relatively scattered probably caused by anisotropic velocity model, signal to noise ratio, sensor locations, etc. However, they have similar trends with the results of other techniques such as digital image correlation (DIC). In the next step, improvements will be made in the source locations and other pieces of information related to source mechanisms, crack direction, etc. will be studied.

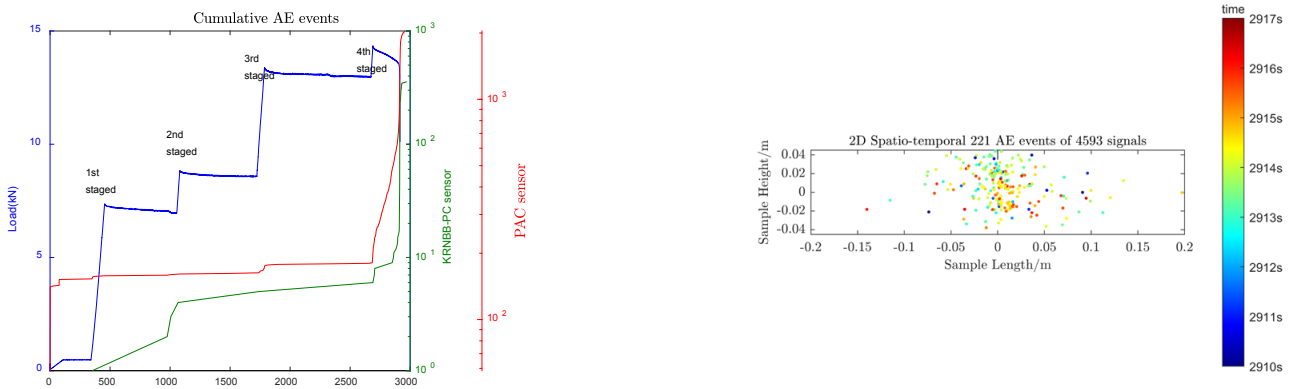


Figure 1. AE results from a SENB test. *Left*: loading data and cumulative AE events from 2 different AE sensors. *Right*: 2D AE locations from KRNBB-PC sensors during the last relaxation stage.

The initial results of this study demonstrated that resonant sensors can detect much more crack events than their broadband counterparts during progressive failure of rocks, and therefore observe earlier precursors before the catastrophic failure. This study will continue by conducting creep tests on more than 100 similar specimens under different mechanical and environmental conditions (temperature, humidity, surface water, etc.) to better understand the long-term behavior of natural and engineering settings.

1.14

Multiphase rotational extension along the Western Afar Margin in East Africa

Frank Zwaan[1], Giacomo Corti[2], Derek Keir[1,3], Federico Sani[1], Ameha Muluneh[4], Finnigan Illsley-Kemp[5] & Mauro Papini[1]

[1]Dept. of Earth Sciences, University of Florence, Italy (frank.zwaan@unibe.ch)
[2]National Research Council of Italy, Florence, Italy
[3]Dept. of Ocean and Earth Science, University of Southampton, United Kingdom
[4]School of Earth Sciences, University of Addis Ababa, Ethiopia
[5]School of Geography, Environm. and Earth Sc., V. University Wellington, NZ

The Afar Rift in Ethiopia forms the northernmost segment of the East African Rift System (EARS) and represents one of the rare locations where active continental break-up and the formation of a young passive margin can be examined. A key element in the system is the poorly studied Western Afar Margin (WAM) along the western edge of the Afar, which marks a sharp decrease in topography from the Ethiopian Plateau into Afar (Fig. 1a). In this multidisciplinary study we aim to create the first integral structural interpretation of the margin and its tectonic history.

We apply various methods to chart the structures in the study area. First, using satellite imagery and digital elevation models we draft a detailed fault map of the whole WAM, showing how the N-S striking margin is dominated by NNW-SSE oriented faults and remarkable right-stepping marginal grabens (Fig. 1a). Additionally, earthquake data show that the margin is tectonically active and T-axis analysis of focal mechanisms provides associated extension directions. These are ca. E-W along the WAM, but rotate to ca. SW-NE in the Afar rift floor. Extension directions from fault measurements taken along the margin are in line with the extension orientation obtained by T-axis analysis. Combined with current GPS data of the Danakil Block, these findings nicely fit the rotational opening of Afar due to the counterclockwise pivoting Danakil Block (Fig. 1a).

We also examine the structural history of the Afar margin in light of the current tectonics and known geological record. Previous work suggests that the current rotational motion of the Danakil block was only established some 11 Ma. However rifting in Afar started ca. 25 Ma as a result of the clockwise rotation of the Arabian plate about a rotational pole in Egypt (Fig. 1b). Simple geometrical relations and the large-scale en-echelon fault patterns are best explained by a ca. SW-NE extension direction along the WAM during 25-11 Ma (Fig. 1b), which is quite different from the current situation (Fig. 1a). We therefore propose a multiphase evolution with an initial phase of SW-NE extension due to the rotation of Arabia, creating the large-scale structures of the WAM, followed by E-W extension and fault reactivation associated with the more local rotation of the Danakil Block (Fig. 1c-f).

Next to these large-scale interpretations, we also created the first-ever well-calibrated structural sections of the WAM, which in combination with detailed earthquake analysis suggest that deformation along the WAM is accommodated by the antithetic faulting. Also these results are of great interest for a better understanding of the WAM and its implications for passive margin formation.

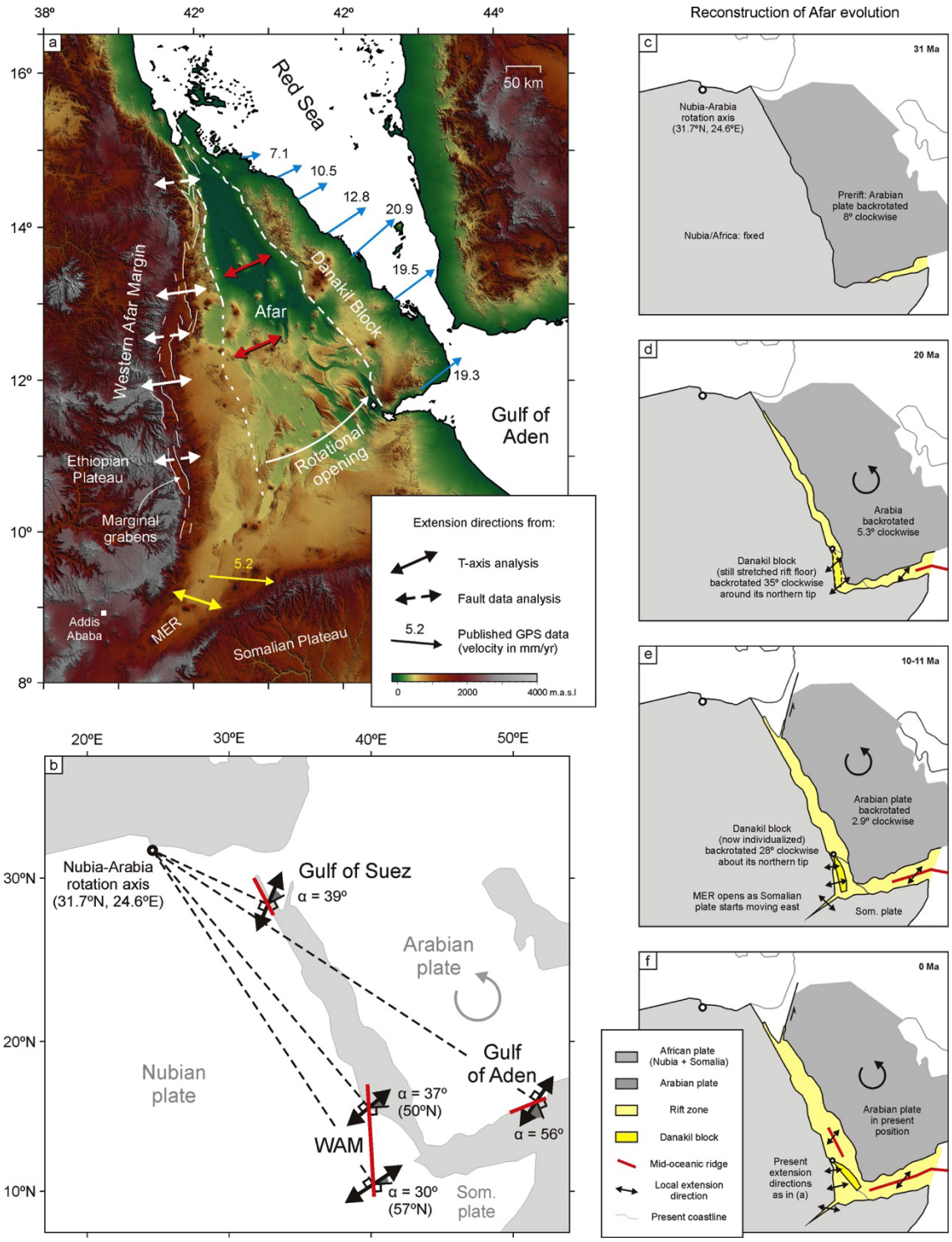


Figure 1. (a) Combined overview of current tectonic setting in Afar as derived from (1) T-axes analysis, (2) field measurements and (3) GPS data. White: Western Afar Margin (WAM), Red: Afar, Yellow: MER (Main Ethiopian Rift), Blue: Danakil Block. (b) Theoretical oblique extension directions (described by angle α between the normal to the rift trend and the general extension direction) in the Red Sea, Afar and the Gulf of Aden a result of the rotation of the Arabian plate around a pole at 31.7˚N, 24.6˚E. The orientation of the WAM should result in a ca. NE-SW extension direction (50˚-57˚N). (c-f) Multiphase evolution of Afar within the regional tectonic development.

P 1.1

Imaging of Seismotectonic Processes in the Upper Crust of the Northern Alpine Foreland of Switzerland

Tobias Diehl[1], Herfried Madritsch[2], Thomas Spillmann[2], Toni Kraft[1], Michael Schnellmann[2]

[1]Swiss Seismological Service, ETH Zurich, 8092, Switzerland (tobias.diehl@sed.ethz.ch)
[2]Nagra (National Cooperative for the Disposal of Radioactive Waste), Wettingen, Switzerland

Since 2011, the Swiss Seismological Service (SED) significantly densified the seismic monitoring network across north-eastern Switzerland. On behalf of the National Cooperative for the Disposal of Radioactive Waste (Nagra), the existing network was extended by 18 permanent and semi-permanent weak-motion stations, including three borehole sensors at depths between 120 and 150 m. The collaborative project aims to lower detection thresholds and location uncertainties of seismicity, in order to image and characterize seismically active structures in northern Switzerland at high resolution. Combined with information from focal-mechanisms, tomographic models and reflection seismic surveys, the imaged seismicity contributes to an improved understanding of seismotectonic processes in the low-strain environment of the northern Alpine Foreland.

The magnitude of completeness (Mc) within the densified network reaches 1.0 and hypocentre location uncertainties were significantly reduced. In addition, high-resolution velocity models derived by a recent three-dimensional Pg and Sg tomography improved the accuracy of hypocentres. In this study, we will present a consistently relocated earthquake catalogue of the region, including high-resolution relative relocations. The interpretation of the catalogue is focused on seismicity in the upper crust and is complemented with updated compilations of focal-mechanisms, structural information from exploration seismic surveys as well as geological data.

Recent earthquake sequences near Schlattingen (TG), Hilzingen (D), and northwest of Konstanz (D) suggest ongoing NE-SW directed extension along the NW-SE striking Hegau-Bodensee Graben system. Further to the west, a series of earthquakes defines another similar striking regional basement structure stretching approximately from Pratteln to Läufelfingen undergoing active NE-SW extension. In addition to these findings, we present an analysis of very shallow seismicity in the region of Eglisau and provide a summary map of tectonic and seismogenic structures of the region, which will be the base of an improved seismotectonic model explaining deformation patterns in the northern Alpine foreland.

P 1.2

High shear strain ductile deformation produces stable porous domains

James Gilgannon[1], Marius Waldvogel[1], Thomas Poulet[2], Florian Fusseis[3],Alfons Berger[1], Auke Barnhoorn[4], Marco Herwegh[1]

[1]Institute of Geological Sciences, University of Bern, Baltzerstrasse 1+3, CH-3012 Bern, CH (james.gilgannon@geo.unibe.ch)
[2]CSIRO Mineral Resources, 26 Dick Perry Avenue, Kensington, WA 6151, AUS
[3]School of Geosciences, The University of Edinburgh, Grant Institute, EH9 3JW, UK
[4] Faculty of Civil Engineering and Geosciences, TU Delft, Stevinweg 1, Delft, NL

Dynamic recrystallisation is a major grain size reduction mechanism in shear zones and it is observed or interpreted for almost all of Earth's major constitutive minerals (e.g. calcite: Bestmann and Prior (2003); quartz: Stipp et al. (2002); feldspar: Kruse et al. (2001); olivine: Michibayashi et al. (2006)). We revisit the torsion experiments of Barnhoorn et al. (2004) on Carrara Marble and show that grain size reduction by dynamic recrystallisation produces domains of syn-kinematic pores, called creep cavities. Furthermore, these domains show evidence for mass transfer which was likely mediated by fluids. Continuous wavelet analysis finds sheets of porosity that have distinct orientations and spacing. Our results demonstrate that dynamic recrystallisation occurs in a highly ordered fashion and that once recrystallisation is complete an anisotropic porosity is sustained. For the first time, this shows experimentally that the ductile deformation of a natural starting material necessarily produces a dynamic permeable porosity and that this porosity is highly anisotropic. Our findings have ramifications for a multitude of solid Earth settings where ductile deformation is observed, like ice sheets, major thrust contacts, strike slip and low-angle normal faults in the earth's crust as well as mantle shear zones.

REFERENCES

Barnhoorn, A., Bystricky, M., Burlini, L. & Kunze, K. 2004: The role of recrystallisation on the deformation behaviour of calcite rocks: large strain torsion experiments on Carrara marble, Journal of Structural Geology, 26, 885-903.

Bestmann, M., Prior, D. 2003: Intragranular dynamic recrystallization in naturally deformed calcite marble: diffusion accommodated grain boundary sliding as a result of subgrain rotation recrystallization, Journal of Structural Geology, 25, 10 1597-1613.

Kruse, R., Stünitz, H., Kunze, K. 2001: Dynamic recrystallization processes in plagioclase porphyroclasts, Journal of Structural Geology, 23,11, 1781-1802.

Michibayashi, K., Ina, T., Kanagawa, K. 2006: The effect of dynamic recrystallization on olivine fabric and seismic anisotropy: Insight from a ductile shear zone, Oman ophiolite, EPSL, 244, 3-4, 695-708.

Stipp, M., Stünitz, H., Heilbronner, R., Schmid, S.M. 2002: Dynamic recrystallization of quartz: correlation between natural and experimental conditions, GSL Special Publications, 200, 171-190.

P 1.3

Tectonic Map of Switzerland 1:500000: A new concept

Yves Gouffon, Oliver Kempf, Andreas Möri, Michael Wiederkehr

Bundesamt für Landestopografie swisstopo, Wabern

The nomenclature of tectonic units in Switzerland today is strongly influenced by different schools and concepts. Authors of scientific publications or of geological maps frequently use different terms for similar units or use the same terms in different ways. This is particularly a problem if regional data sets have to be compiled or if a nationwide data set is to be established. Moreover, geographic information systems (GIS) require data models with consistent and unambiguous attributes.

To establish a widely accepted concept, a tectonic working group was convened at swisstopo including experts from Swiss universities and geology-related companies, as well as from the Swiss Geological Commission, with the aim of developing a tectonic concept as a basis for the Tectonic Data Model of the Swiss Geological Survey. The aim of the working group was to achieve a consistent terminology, while maintaining, as far as possible, compatibility of the new concept with existing literature. This new concept will finally be integrated into a new Tectonic Map of Switzerland 1:500 000 for future teaching and as base for scientific as well as applied projects.

The new tectonic concept for Switzerland classifies the tectonic units according to a 4-level (orders) hierarchy. The 1st order includes tectonic domains, i.e. Autochthonous North Alpine Foreland, Sheared North Alpine Foreland, Helvetic, Penninic, Salassic*, Austroalpine, South Alpine and Cenozoic magmatic provinces, often subdivided into 2nd order subdomains. The 3rd order includes the classical nappes, but also nappe complexes, slice complexes, etc. If applicable, their subdivisions are listed in the 4th order.

The coming new Tectonic Map of Switzerland 1:500 000 follows this concept and shows units up to the 3rd order. A first draft is proposed here in order to animate the discussion and to collect remarks and proposals of everyone.

** Salassic is a new tectonic domain (1st order) that groups the Dent-Blanche and Mont Mary nappes and the Sesia Zone in western Switzerland/Italy, and the Margna and Sella nappes in eastern Switzerland/Italy. These tectonic units have an Adriatic palaeogeographic affinity but their tectono-metamorphic history is quite different from that of the other Adriatic-derived units (Austroalpine and South Alpine domains). The Simmen nappe of the Préalpes, which is considered to be the sedimentary cover of the Dent-Blanche nappe, is also assigned to the Salassic domain. These particular continentally-derived mainly basement units are interpreted to have been rifted-off the most distal part of the Adriatic margin during the Middle Jurassic opening of the Piemont-Ligurian Ocean, forming extensional allochthons referred to as the Margna-Sesia fragment (Schmid et al. 2004) or Cervinia (Pleuger et al. 2007, Froitzheim et al. 2008). The term «Salassic» stems from a Celtic tribe, the Salasses, which occupied the Aosta valley and Sesia region.*

REFERENCES

Froitzheim, N., Plašienka, D. & Schuster, R. (2008): Alpine tectonics of the Alps and Western Carpathians. In: McCann, T. (Ed.): The Geology of Central Europe. Vol. 2: Mesozoic and Cenozoic (p. 1141–1232). – London.

Pleuger, J., Roller, S., Walter, J.M., Jansen, E. & Froitzheim, N. (2007): Structural evolution of the contact between two Penninic nappes (Zermatt-Saas zone and Combin zone, Western Alps) and implications for the exhumation mechanism and palaeogeography. – International Journal of Earth Sciences 96/2, 229–252.

Schmid, S.M., Fügenschuh, B., Kissling, E. & Schuster, R. (2004): Tectonic map and overall architecture of the Alpine orogen. – Eclogae geologicae Helvetiae 97, 93–117.

P 1.4

Structural architecture of active back-thrust zone of the eastern Achara-Trialeti fold-and-thrust belt (Kumisi-Teletei area), Georgia

Alexander Gventsadze, Victor Alania, Onise Enukidze, Nino Kvavadze

*Iv. Javakhishvili Tbilisi State University, Institute of Geophysics, Tbilisi, Georgia (***aleko.gventsadze@tsu.ge***)*

The Achara-Trialeti fold-and-thrust (ATFTB) belt is located within the northernmost part of the Lesser Caucasus orogen and is associated with Arabia-Eurasia convergency. The collision between the Arabian and Eurasian plates caused inversion of the relief and at the place of intra-arc and back-arc basins were formed two fold-and-thrust belts of the Achara-Trialeti and Greater Caucasus with the intermontane basin in between (e.g. Adamia et al., 2010; Banks et al., 1997; Mosar et al., 2010; Sosson et al., 2016). Present day's geometry of the Achara-Trialeti fold and thrust belt is related to the northward thrusting of the basement wedge and had been developed during late Alpine times. Within eastern ATFTB several principal structural units have been found from south to north: south-vergent backthrust zone, north-vergent forethrust zone and triangle zone (Alania et al., 2017). The study object is Teleti-Kumisi area including back-thrust zone of the eastern ATFTB. The surface area of the study territory is mainly built of Cretaceous, Paleogene, Neogene and Quaternary volcanic rocks. Our interpretation has integrated 2-D seismic reflection profiles, several oil-wells, and the surface geology data to reveal structural characteristics of the study area. Seismic reflection data reveal the presence of structural wedge and south-vergent back-thrust. The main style of deformation within the back-thrust belt is a series of fault-propagation folds whose front limb is broken by thrust faults. Interpreted 2-D seismic refection profiles, structural cross-sections, and earthquakes reveal the presence of an active blind wedge under back-thrust zone. The kinematic evolution of south-vergent back-thrust zone is related to northward propagating structural wedge. 2-3D structural models show that Kumisi and Teleti earthquakes related to a north-vergent blind wedge thrust system.

REFERENCES

Adamia, Sh., et al. 2010: Evolution of the Late Cenozoic basins of Georgia (SW Caucasus): a review. Geological Society of London, Special Publication no. 340, 239-59.

Alania, V., et al. 2017: Structural model of the eastern Achara-Trialeti fold and thrust belt using seismic reflection profiles. Geophysical Research Abstracts, Vol. 19, EGU2017-5064.

Banks, C. et al. 1997: Structure and regional tectonics of the Achara-Trialeti fold belt and the adjacent Rioni and Kartli foreland basins. Republic of Georgia. American Association of Petroleum Geologists Memoir no. 68, 331-36.

Mosar, J., at al. 2010: Cenozoic–Recent tectonics and uplift in the Greater Caucasus: a perspective from Azerbaijan. Geological Society of London, Special Publication no. 340, **261-79.**

Sosson, M., et al. 2016: The Eastern Black Sea-Caucasus region during Cretaceous: new evidence to constrain its tectonic evolution. Compte-Rendus Geosciences, v. 348, Issue 1, 23-32.

P 1.5

New insight into the Geneva Basin structural framework based on recently acquired 2D seismic data.

Louis Hauvette[1/2], Anna Sommaruga[1], Jon Mosar[1], Bernd Fiebig[2] & Michel Meyer[3]

[1]Unit of Earth Sciences, Geosciences Department, University of Fribourg, Chemin du Musée 6, CH-1700 Fribourg (louis.hauvette@unifr.ch)
[2]Geneva Geo Energy, Rue des vieux grenadiers 8, CH-1205 Genève (GGE)
[3]Services industriels de Genève, chemin Château-Bloch 2, CH-1219 Le Lignon

In the North Alpine Foreland, fault zones in the Mesozoic cover represent the main targets for drilling campaigns, as part of the 2020 Geothermal project of the Canton Geneva. Hence, a structural mapping and modelling of this Canton subsurface appears, to be a crucial step of the project. In this context, a 2D seismic reflection campaign was run during winter 2018 leading to acquisition of 86km of high resolution 2D seismic lines, complementing the >750km of pre-existing 2D seismic lines (Geneva Canton and neighbouring France).

The Molasse Basin in the Geneva area is located between the Jura fold-and-thrust belt and the Subalpine Molasse. This whole domain is part of the detached foreland and is characterized by compressive and transpressive multiphase tectonic structures. The aim of this research project is to present the geometry and the kinematic concept of these structures by computing a 3D geological model and balanced NW-SE cross-sections across the whole basin.

After a proper seismic to well calibration using the reference drilling from the area (e.g.Humilly-2), the interpretation of the seismic lines reveals new tectonic features, and reduces uncertainties of previously interpreted structures. Surface data and well data are also integrated as key information to support the interpretation. This poster will present the settings of the project and examples of our in progress interpretation.

Several scientific hypotheses concerning the geodynamics of this ongoing project are investigated. We propose that several detachment levels in the Mesozoic cover series have played a role during the different phases of deformation. In addition to the main Triassic (Keuper Group) decollement level of the Western Swiss Molasse Basin, marls in the lower part of the Malm and/ in the Cretaceous interval are linked to the development of “shallow” SW-NE thrusting structures.

Moreover, the major NW-SE strike-slip faults in the Mesozoic cover linking the Jura Mountains and the frontal Penninic thrust are going to be explored in more details, particularly considering their complexity along strike geometries.
The kinematics of the basin and differential subsidence potentially linked with faults will also be investigated; mainly using thickness maps of Mesozoic sediments (Triassic and Jurassic) in relation to Paleozoic grabens or basements highs. Balanced cross-sections will subsequently help obtain a better understanding of the tectonic development.

P 1.6

Active seismic surveys at project DIVE's three drilling target sites (Ivrea zone, N-Italy)

Andrew Greenwood[1,2], Ludovic Baron[1], György Hetényi[1], Mattia Pistone[1,3],Klaus Holliger[1], Luca Ziberna[4], Alberto Zanetti[5], Othmar Müntener[1] & DIVE Site Survey Field Teams

[1]Institut des Sciences de la Terre, Faculté des Géosciences et de l'Environnement, Université de Lausanne, Géopolis, CH-1015 Lausanne (gyorgy.hetenyi@unil.ch)
[2]now at: Montanuniversität Leoben, Austria
[3]now at: University of Georgia, USA
[4]Università degli studi di Trieste, Italy
[5]IGG-CNR & Università degli studi di Pavia, Italy

The Drilling the Ivrea-Verbano zonE (DIVE) project aims at sampling rocks of the lower crust and the Moho transition zone for petrological, geophysical, hydrological, thermal, microbiological and educational goals, among others. To bridge across a range of spatial scales and to support the drilling proposal, we have carried out active seismic surveys at the three target drilling locations in 2017 and 2019.

The first campaign in 2017 near Boccioleto and Balmuccia (Val Sesia) crosses the Insubric Line, and aims at determining its dip at depth so that the drilling strategy can be refined. The seismic source was a 400 kg weight drop. Migrated images of crystalline rocks along the acquired profiles reach ca. 1 km depth: the pervasive structural fabric suggests that the continuity of geological units from the surface to this depth is fairly unsurprising, and no major faults offset the near vertical structures. A deeper-reaching campaign providing images down to 5 km depth has already been planned.

The second campaign near Ornavasso (Val d'Ossola) aims at resolving the geometry of a dipping-axis anticline buried beneath Quaternary sediments. The third campaign near Megolo (Val d'Ossola) is the simplest structural geometry based on geological data at hand, without major folds or faults. At both sites, 2D with partial 3D infill acquisition geometries were deployed, and a vibrator truck source used to reliably image at relatively far offsets. Additionally, at the longitude of Premosello, we acquired a 2D refraction/reflection line to map the bottom of the valley infill.

Preliminary results, as of the SGM2019 conference, will be presented and we invite geological and geophysical experts to come discuss and comment on our poster.

P 1.7

In-situ stress estimation from fault slip triggered during fluid injection

Maria Kakurina[1], Yves Guglielmi[2], Christophe Nussbaum[3], Benoît Valley[1]

[1]University of Neuchâtel, Rue Emile-Argand 11, 2000 Neuchâtel, Switzerland (maria.kakurina@unine.ch)
[2]Lawrence Berkeley National Laboratory, 1 Cyclotron Rd, Berkeley, CA 94720, USA
[3]Swisstopo, Seftigenstrasse 264, 3084 Wabern, Switzerland

Standard in situ stress measurement methods using fluid injection in deep boreholes are based on the analyses of pressure, flowrate and pre- and post-injection fracture mapping. Here we apply a new methodology to improve the estimation of the in situ stress by adding the record of three-dimensional (3D) displacement in the pressured interval measured continuously during the injection. We use the displacement-flowrate-pressure data from a fault reactivation experiments conducted in shale rocks at the Mont Terri rock laboratory, Switzerland. The experiment consisted in fluid injections into the fault damage zone in order to reactivate the fault planes and to measure the slip during the injection. The experiment protocol followed the step-rate injection method for fracture in situ properties (SIMFIP) developed by Guglielmi et al. (2013).

Stress orientations and magnitudes are estimated using the geology of the injected interval, measured slip orientation, normal and vertical stress on the reactivated fracture. Firstly, we created a grid search over all possible reduced stress tensor in order to identify the ones compatible with measured slip orientation. Seconldy, we sorted the possible reduced stress tensor keeping only those with a FIT > 90% , i.e. allowing for a max misfit angle between measured and calculated slip of 5.7° or less. Thirdly, we calculated absolute principal stress magnitude values by considering the accepted reduced stress tensor and estimations of the vertical and fracture normal stress. Finally, we reduced the number of possible solutions by ensuring that only solutions showing high slip tendency on the considered fracture are kept.

The presented methodology allows estimation of the full stress tensor from a single set of fracture activation measurements. Some uncertainties remains concerning what exact fracture is activated but this does not affect the robustness of the stress estimation on the analyzed site.

REFERENCES

Guglielmi, Y., Cappa, F., Lançon, H., Janowczyk, J. B., Rutqvist, J., Tsang, C. F., & Wang, J. S. Y. (2013). ISRM suggested method for step-rate injection method for fracture in-situ properties (SIMFIP): Using a 3-components borehole deformation sensor. In The ISRM Suggested Methods for Rock Characterization, Testing and Monitoring: 2007-2014 (pp. 179-186). Springer International Publishing.

P 1.8

Seismotectonic analysis of seismicity in the vicinity of the Mont Terri rock lab

Federica Lanza[1], Tobias Diehl[1], Toni Kraft[1], Nicolas Deichmann[1], Stefan Wiemer[1], Christophe Nussbaum[2] & Senecio Schefer[2]

[1]Swiss Seismological Service, Swiss Federal Institute of Technology, ETH Zurich, Sonneggstrasse 5 CH-8092 Zurich (federica.lanza@sed.ethz.ch)
[2]Swiss Geological Survey, Federal Office of Topography, swisstopo, Seftigenstrasse 264, 3084, Wabern

The analysis of shallow seismicity has fundamental implications for the interpretation of upper-crustal seismotectonic processes. It is also critical for the assessment of potential induced seismicity for geothermal projects or nuclear waste underground repositories and consequent hazard mitigation strategies.
In March and April 2000, five earthquakes with magnitude reaching M_L 3.2 occurred near St-Ursanne, in the vicinity of the Mont Terri rock laboratory and close to Haute-Sorne, which is currently being considered as a suitable site for the development of a new geothermal power project. The sequence is dominated by strong and long-lasting surface waves, indicating a shallow source and may represent a rare evidence for an active décollement beneath the Jura Mountains. The focal mechanism available for the biggest event of the sequence suggests a low-angle thrust mechanism; however, the solution is characterized by high uncertainties. In this study, in order to produce a robust microearthquake catalogue, and taking advantage of mini-arrays operating since 2014, we perform a template matching analysis of the sequence for the period 1998-to-date. Preliminary results from a single-station approach identified 46 additional events with a cross-correlation value > 0.55 with one template being persistent during the entire investigation period. Comparison with other available earthquake catalogues (SED, University of Stuttgart) will allow for a detailed assessment of the active seismicity in the area and its link with potentially related faults exposed in the Mont Terri rock lab. Forward modelling of synthetic waveforms will be also used to further assess the focal depths and fault plane solutions of the new events and discern the lithology (sediments versus basement) for the 2000 events. This is the first step forward into the seismotectonic characterization of the Swiss north-western Jura belt.

P 1.9

Travertine occurrences along major neotectonic normal fault zones in the Hammam Debar- Roknia Guelma region, North- East Algeria

Ouided laziz[1], Foued Bouaja[1], Chaouki Benabbas[1]

Université Des frères Mentouri Constantine. ouidedlaziz@gmail.com
Université frères Mentouri Constantine. bouedjaf@yahoo.fr
Université Constantine 3. benabbas.chaouki@gmail.com
*Geology and Envirmnment laboratory, Constantine University Ain Elbey Constantine Algeria

The tectonic analysis of Pliocene-Quaternary structures has been documented in Guelma region from Quaternary travertines and faults relationships. Quaternary travertines deposited from hot springs can reveal much about the neotectonic attributes and histories of structures. The largely developed travertines in the Roknia- Hammam Debar are subdivided into several sequences including the most recent Are observed at the level of the Hammam Debar recent sources. For facies are observed; th hummocky and reed facies in proximal bed, massive and laminated facies in distal bed. In Roknia- Hammam Debar structural studies, field mapping and tectono-stratigraphical considerations on Pliocene and Quaternary units indicate two fault populations: N10 ° E are associated with Block detachments, collapses and the development of several fibrous calcite generations. These observations prompted us to Classify as probably seismic tectonic structures. N140 ° E structures already mapped as Seismic structures (Maouche et al 2013) are also affected Roknia travertine .

P 1.10

Multi-temporal analysis of ground deformation at the Koa'e fault system (Kīlauea volcano, Hawaii) using structural field observation and high resolution imagery.

Stefano Mannini[1], Joël Ruch[1], James Hollingsworth[2], Donald A. Swanson[3], Ingrid Johanson[3], Florian Cousseau[4]

[1]Department of Earth Science, University of Geneva, Switzerland (stefano.mannini@unige.ch)
[2]ISTerre Université Grenoble Alpes, UMR 5275 CNRS, 1381 Rue de la Piscine, 38610 Gières, France
[3]U.S. Geological Survey – Hawaiian Volcano Observatory, 1266 Kamehameha Ave., Hilo, HI 96720, United States of America
[4]Institute F.A. Forel, University of Geneva, Switzerland

Kīlauea volcano is one of the most active volcanoes on Earth and is considered as a model for flank instability studies on large volcanic islands. The Koa'e is an active fault system (11 km long, ~3 km wide) located 5 km south of the Kīlauea caldera and is structurally connected to the east and southwest rift zones, playing a key role in accommodating part of the unstable volcano flank. The origin and evolution of the Koa'e fault system are still poorly understood, including its role in controlling magma pathway in the area. This zone presents several structural features as monoclines, nested grabens and en-echelon cracks. Our aim is to map and quantify the structural features that characterise this zone using structural field observations (mid-term, centuries) and air photo correlation (short-term, from the 1950's). We expect to provide a structural model that can explain what are the tectonic and magmatic conditions that precede an eruption by studying recurrent volcano-tectonic events. The Koa'e and Kīlauea's East Rift Zone have been subject to several volcano-tectonic events with large earthquakes (e.g. Kalapana 1975 MW7.7) and eruptions in the past decades and are ideal candidates to analyze recurrent ground deformation related to the volcano flank motion.

We collected ~750 structural measurements in two areas of Koa'e fault system during June 2019. We measured the fracture direction and the fracture opening orientations by fitting asperities on both sides of the fracture walls. Preliminary results show obliquity with both right and left lateral opening components, with areas of dominant left lateral opening in correspondence with other structures, e.g. with a dike intrusion north of the Ohale fault. These data are useful to define the kinematics and undestanding magma propagation to the surface. We then used a ground photogrammetry setup (i.e. using a camera on top of a pole) to collect vertical and oblique photos to build up a 3D model of a monocline structure, reprensatitive of a magma intrusion related structure. We acquired 122 images along an outcrop (10 m long, 8 m wide and 4 m high) and processed the data using Agisoft, producing a DEM and an orthophoto.

We then use an optical imagery correlation technique that allows to quantify the ground deformation covering the period from the 1950s. We analyzed the 1975 earthquake because it is one of the largest event in the area, producing massive faulting. We used 12 and 10 photos for the pre-event (October 1974 and July 1975, respectively) and 6 and 7 photos for the post-event time period (December 1976 and March 1977, respectively). Preliminary results show ground displacements of several meters on Kīlauea's south flank (Hilina fault system), in agreement with EDM measurements of 8 meters horizontal displacement measured at the coastline.

These structural data and air photo correlations will be later integrated with geophysical data to provide a better quantification on ground deformation and comprehension of the mechanisms that precede an eruption.

P 1.11

Structural evolution of the western Aar Massif (external Central Alps, Switzerland): insights from 3D geological modelling

Ferdinando Musso Piantelli[1], Marco Herwegh[1], Alfons Berger[1], Michael Wiederkehr[2], Eva Kurmann[2], Andreas Möri[2] and Roland Baumberger[2]

[1]Institute of Geological Sciences University of Bern, Baltzerstrasse 1+3, 3012 Bern, Switzerland
[2]Federal Office of Topography swisstopo, Seftigenstrasse 264, 3084 Bern, Switzerland

3D modelling of complex and irregular geological bodies is an expanding discipline that combines two-dimensional cartographic and structural data managed with GIS technology. In this study, geological information has been processed to build a 3D model of major stratigraphic and tectonic boundaries. The investigated area is located in the western part of the Aar Massif (external Central Alps, Switzerland) characterized by pronounced topographic (600–<4000 m) and structural relief. A complex deformation sequence, characterized by multiple deformation stages, shaped the investigated area throughout the Alpine deformation. Due to the geometric and overprinting relationships of different structural elements, four different large-scale deformation phases can be discriminated in the model:

(i) Kiental phase (30 – 20 Myr): emplacement and deformation of the Doldenhorn Nappe (Burkhard 1988);
(ii) Handegg phase (20 – 12 Myr, mainly observed in the basement units): steep-reverse faults, which are caused by buoyancy-driven sub-vertical extrusion of the Aar Massif (Wehrens et al. 2016);
(iii) Pfaffenchopf phase (~12 Myr): NW-vergent thrusting along moderately SE dipping shear planes cutting through basement-cover contacts (Wehrens et al. 2017);
(iv) Oberaar phase (~12 Myr): steeply oriented dextral strike-slip shear planes cutting through the previous structures (Wehrens et al. 2016).

The integration of all accessible geological information and background knowledge with the generation of a 3D model offers the chance to visualize in detail the current structural disposition of the western Aar Massif and the relative geometric and overprinting relationships of the above-mentioned deformation phases.

REFERENCES:

Burkhard, M.: L'Helvétique de la bordure occidentale du massif de l'Aar (évolution tectonique et métamorphique), Eclogae Geol. Helv., 81, 63–114, https://doi.org/10.5169/seals-166171, 1988.

Wehrens, P., Berger, A., Peters, M., Spillmann, T., and Herwegh, M.: Deformation at the frictional-viscous transition: Evidence for cycles of fluid-assisted embrittlement and ductile deformation in the granitoid crust, Tectonophysics, 693, 66–84, https://doi.org/10.1016/j.tecto.2016.10.022, 2016.

Wehrens, P., Baumberger, R., Berger, A., and Herwegh, M.: How is strain localized in a meta-granitoid, mid-crustal basement section? Spatial distribution of deformation in the central Aar massif (Switzerland), J. Struct. Geol., 94, 47–67, https://doi.org/10.1016/j.jsg.2016.11.004, 2017.

P 1.12

Automated extraction of layer orientation and thickness information from geological maps to support the characterisation of siliceous limestone deposits

Lukas Nibourel[1], Stefan Heuberger[1], Thomas Galfetti[2]

[1]Fachgruppe Georessourcen Schweiz, Departement Erdwissenschaften, ETH Zürich, Sonneggstrasse 5, 8092 Zürich (lukas.nibourel@erdw.ethz.ch)
[2]Landesgeologie, Bundesamt für Landestopografie swisstopo, Seftigenstrasse 264, 3084 Wabern

The potential of mineral deposits is defined by their geometry (volume and shape) and quality of the raw material of interest. Robust 3D geological models of a deposit require amongst others data on orientation and thickness of strata, which are typically collected during exploration campaigns and/or through desktop studies. Traces of stratigraphic units on geological maps yield important information on the spatial distribution and orientation of deposits. We test and develop approaches to assess the consistency of mapped traces and to automatically extract orientation and thickness estimates from the 1:25'000 geological map sheets of Switzerland, e.g. trace information extraction toolbox (Rauch et al., 2019) and moment of inertia best fit plane algorithm (Fernández, 2005). Preliminary results will be shown for the Helvetic Kieselkalk-Formation of the Upper Helvetic in Central Switzerland – a stratigraphic unit commonly used as raw material for railway and road infrastrucuture.

REFERENCES

Rauch, A., Sartori, M., Rossi, E., Baland, P. & Castelltort, S. 2019: Trace Information Extraction (TIE): A new approach to extract structural information from traces in geological maps, Journal of Structural Geology, 126, 286-300.

Fernández, O. 2005: Obtaining a best fitting plane through 3D georeferenced data. Journal of Structural Geology, 27, 855-858.

P 1.13

Influence of faulting on magma propagation during volcano-tectonic events and structural mapping using UAVs in NW Iceland.

Elisabetta Panza[1], Joël Ruch[1], François Martin[2]

[1]Department of Earth Sciences, University of Geneva, Rue des Maraîchers 13, CH-1205 Genève (Elisabetta.Panza@unige.ch)
[2]Services Industriels de Genève (SIG), Chemin Château-Bloch 2, Ch-1219 Vernier

Volcano-tectonic events result from the interaction of magmatic and tectonic processes and are found in various geological settings, included extensional environments. In these events, earthquakes and volcanic eruptions release over days or weeks tectonic strain accumulated over several decades or hundreds of years.

Laying both on an extensional plate boundary and on a mantle plume, Iceland counts several rifting episodes in its volcanic systems in the last centuries. Such volcano-tectonic events, traditionally called “Fires”, have been reported since the first settlements around 870 AD. The Icelandic Fires involve transport of magma in the crust, associated to eruption and often relate to the formation of graben structures, with reactivation of pre-existing structures. Therefore, the volcanically active and spreading zone of Iceland, crossing the country from North to South, is a natural laboratory to investigate the interactions of magma and crustal structures during magma propagation.

However, classical models of magma propagation assume Earth’s upper crust as homogeneous and fully elastic and they do not account for pre-fractured medium. This study aims at analyse the role of pre-existing crustal structure on the propagation of magma in extensional environments.

We gathered literature information on the Icelandic Fires and their return periods. 18 events have been historically reported in Iceland, located mostly in the North, East, and West Volcanic Zones. The return period in between two volcano-tectonic events (i.e. Fires) within the same volcanic system is on average in the order of 200 years, suggesting a cyclic nature of strain deficit loading and subsequent release. At divergent plate boundaries stress is released not continuously but stepwise through volcano-tectonic events: magma emplacement (through dike intrusion) is associated with a crustal opening of the same order of magnitude than the strain deficit accumulated since the previous event in the same area. On this basis, we identified structurally relevant fieldwork areas. We focused on the North Volcanic Zone, specifically Fjallagjá, a graben ~15-20 m deep and ~1 km wide that extends parallel to Sveinagjá graben for ~18 km. Sveinagjá graben subsided 3 to 6 m during a volcano-tectonic event in 1875, contemporaneous to Askja central volcano eruption and caldera collapse. Both Fjallagjá and Sveinagjá grabens are part of the Askja volcanic system, whose main volcano is located ~60 km to the South. Here we mapped a representative portion of the Fjallagjá graben with a fixed-wing UAV with a ground resolution down to 1 $cm \cdot px^{-1}$ in August 2019. To obtain centimetre accuracy of the georeferencing of the drone images, we installed a GPS base to allow using PPK correction, avoiding the deployment of aerial targets as GCPs. With this setup we managed to perform 21 flights, covering an area of ~15 km^2.

The processing of the drone images resulted in a 3D model and an orthorectified representation of the fieldwork area. We then performed a detailed morphological and structural analysis, looking at the shape of the overall graben and the effect of the topography on the faulting processes. We further look at fractures and potential kinematic indicators to reconstruct the paleostress history of this area of the plate boundary.

Parallel to field observations, we are building up an analog experiment setup to investigate the processes that cause the observed structures. The experiments will include injection tests to analyse the role of the structure’s presence and reactivation during magma propagation. The expectation is to show how magma follows pre-existing fractures, even if they are not ideally oriented with the current stress field, like what happened in the 2014-2015 Bárðarbunga event.
The expected results will shed light on the processes governing magma propagation at divergent plate boundaries, which exert a fundamental influence on eruptions locations.

P 1.14

The tectonics of the Simano, Cima-Lunga, Adula and Maggia nappes in the southern Lepontine dome

Filippo Luca Schenker[1], Alessia Tagliaferri[1], Christian Ambrosi[1], Cristian Scapozza[1], Dorota Czerski[1], Matteo Maino[2] & Yves Gouffon[3]

[1]Institute of Earth Sciences, University of Applied Sciences and Arts of Southern Switzerland (SUPSI), Campus Trevano, CH-6952 Canobbio (filippo.schenker@supsi.ch)
[2]Dipartimento di Scienze della Terra e dell'Ambiente, University of Pavia, via Ferrata 1, 27100 Pavia, Italy
[3]Swiss Geological Survey, Federal Office of Topography swisstopo, Seftigenstrasse 264, CH-3084 Wabern

New structural data, geological maps and cross sections (1:10'000) collected and elaborated in the framework of the Bellinzona, Osogna and Grono sheets of the Geological Atlas of Switzerland 1:25'000 (sheets no. 1313,1293 and 1294) are used to discuss the still controversial tectono-stratigraphy of the southern margin of the Lepontine Dome that includes the Simano, Cima-Lunga, Adula and Maggia nappes.

Particular interest is given to the position of the disrupted calcsilicate-paragneiss-amphibolite-peridotite sequence of the Cima-Lunga. To the north, it is folded and pinched between Simano gneisses, in the central part, it is overthrusted by the Maggia nappe and in the southeastern part, it lays at the base of the Adula nappe. This geometry and the structural data do not fit with the classical nappe stack architecture and question the lateral continuation of the Cima-Lunga into the Adula nappe. Different tectonic scenarios will be discussed: 1) a post-nappe emplacement folding of the Cima-Lunga nappe, 2) an Alpine intra-Simano channel flow of the Cima Lunga series and 3) a pre-Alpine Cima-Lunga mélange, metamorphosed at high pressure and reworked during the Eocene.

More to the south, the Oligocene-Miocene migmatites and the synchronous normal and oblique ductile faults obliterated the cylindrical continuation of the units into the Southern Steep Belt. There, part of the exhumation and disruption of the HP mafic and ultramafic rocks occurred during doming of the migmatites.

P 1.15

High-resolution Imaging and Analysis of Seismicity Patterns in Swiss Microearthquake Sequences

Verena Simon[1], Toni Kraft[1], Tobias Diehl[1] & Stefan Wiemer[1]

[1]Swiss Seismological Service, Earth Sciences, ETH Zürich, Switzerland (verena.simon@sed.ethz.ch)

Earthquakes tend to cluster in space and time forming earthquake sequences. Each sequence shows a different spatiotemporal occurrence behavior, which often can roughly be classified as mainshock-aftershock, foreshock-mainshock-aftershock or swarm-like. While many ruptures are followed by a significant number of aftershocks, foreshocks seem to be rare, and their underlying mechanisms are still debated. The controversy on foreshock mechanisms is fostered by inconsistency and incompleteness of many earthquake catalogs and by the lack of a consistent definition and identification of foreshocks. In the past decades, immediate foreshocks have been studied intensively on the centimeter scale in laboratory experiments. However, for real earthquakes, only a few high-resolution observations are available today and are mainly limited to magnitudes above M4. Due to the big observational gap between laboratory and field scale, it is not fully understood if and how results can be transferred between the two different scales.

We want to overcome these obstacles by studying the seismicity patterns of microearthquake sequences in Switzerland, which has one of the densest and most sensitive seismic networks in the world. To further assure the highest data quality, our study concentrates on the operation period of the digital broadband network (2002 to present). We start with a systematic analysis of the earthquake catalog of the Swiss Seismological Service to consistently identify and classify all earthquake sequences. In a next step, we enhance the earthquake catalog by a matched filter analysis that ensures a uniform detection sensitivity and consistent magnitude estimation for each sequence. To better resolve the spatiotemporal behavior of the seismicity, we perform a high-precision relative relocation and a high-resolution statistical analysis of the enhanced catalogs for significant sequences. Based on these improved data sets, we plan to systematically investigate the occurrence and behavior of foreshocks.

In this presentation, we show the results of the systematic analysis of the Swiss catalog and the identification and classification of the seismic sequences. We will discuss the differences in their occurrence patterns considering geological and seismotectonic conditions. For selected sequences, we will present the first results of the high-resolution analysis of the enhanced catalogs.

P 1.16

Geodynamic models of non-subduction generation of Archean continental TTG crust

Paul J. Tackley[1], Charitra Jain[2], Antoine B. Rozel[1], Diogo Lourenco[3] & Taras V. Gerya[1]

[1]Institut für Geophysik, Departement Erdwissenschaften, ETH Zürich, CH-8092 (ptackley@ethz.ch)
[2]Department of Earth Sciences, Durham University, UK
[3]Department of Earth and Planetary Sciences, University of California, Davis, USA

The tectonic mode in the Archean, and when and how continents formed, are two key unresolved questions. Here we investigate these issues using global simulations of Earth evolution from post magma ocean to the present day, including self-consistently calculated production of basaltic oceanic crust and TTG continental crust. The mantle starts with a uniform pyrolytic composition and has an initially hot core. Basaltic crust is formed by partial melting of pyrolytic material, while TTG is formed by partial melting of basalt in certain (P,T) windows in the presence of water. Produced magma is erupted at the surface and intruded into the crust with a ratio that is specified a priori. After an early overturn of post-magma-ocean-formed crust, we find that the tectonic mode was likely neither modern-day plate tectonics nor a rigid lid, but rather, one characterized by abundant mostly intrusive magmatism resulting in a hot, weak, deformable lithosphere – a "Plutonic Squishy lid" (PSL) [Lourenco, 2017]. In this mode, a thick basaltic crust is recycled at its base by eclogite drips plus episodic delamination of depleted lithosphere [Sizova, 2015]. Abundant TTG crust is produced, with a production rate far exceeding typical continental crustal growth curves [Rozel 2017; Jain 2018]. At the same time it can also be destroyed by entrainment in downwellings. These models thus indicate that (i) subduction was not necessary for the production of early continental crust, (ii) intrusive magmatism was dominant during the Archean (as opposed to "heat pipe" extrusive magmatism), and (iii) Archean tectonics was characterised by a weak, hot deformable lithosphere undergoing extensive delamination as well as significant horizontal motion.

REFERENCES

Lourenço, D. J. 2017: The influence of melting on the thermo-chemical evolution of rocky planets' interiors, Doctoral thesis, ETH Zurich, DOI:10.3929/ethz-b-000228308

Sizova, E., T. Gerya, K. Stüwe & M. Brown 2015: Generation of felsic crust in the Archean: A geodynamic modeling perspective, Precamb. Res, *271*, 198-224.

Rozel, A. B., G. J. Golabek, C. Jain, P. J. Tackley & T. Gerya 2017: Continental crust formation on early Earth controlled by intrusive magmatism, Nature 545, 332-335.

Jain, C., A. B. Rozel, P. J. Tackley, P. Sanan & T. V. Gerya 2019: Growing primordial continental crust self-consistently in global mantle convection models, Gondwana Res. 73, 96-122.

P 1.17

Multiscale structural analysis of the Variscan Basement and Permo-Mesozoic covers, at Frisson Lakes (Argentera Massif, Maritime Alps)

Alessia Tagliaferri[1,2], Luca Corti[2], Maria Iole Spalla[2], Michele Zucali[2]

[1]Scuola Universitaria Professionale della Svizzera Italiana (SUPSI), Dipartimento Ambiente Costruzione e Design, Istituto Scienze della Terra, Campus Trevano, CH-6952 Canobbio (alessia.tagliaferri@supsi.ch)
[2]Università degli Studi di Milano Statale, Dipartimento di Scienze della Terra "Ardito Desio", Via Luigi Mangiagalli 34, IT-20133 Milano

This contribution consists in a new structural map of the Frisson Lakes area, which synthesizes structural and metamorphic data useful to the detection of the tectono-metamorphic history of an area registering two superposed orogenic cycles. The analysed area is located in the south-east portion of the Argentera crystalline Massif, where both rocks of the Variscan metamorphic basement and Permo-Mesozoic sedimentary covers are deformed together during Alpine convergence. The crystalline basement belongs to the Gesso-Stura-Vésubie metamorphic complex, mainly consisting of migmatitic gneiss and paragneiss, locally containing mafic layers and lenses. The most common Permo-Mesozoic rock in the area is a metamorphic conglomerate, deformed and re-equilibrated under greenschist facies conditions. The structural map at 1:2'000 scale integrate lithostratigraphic boundaries, compositional heterogeneities in the main rock types, superposed foliation trajectories, fold axes, axial planes and ductile and fragile shear zones. Microtextural analysis on thin sections allowed the recognition of mineral assemblages marking superposed fabrics.

The mesoscale structural analysis detected 4 ductile deformation phases followed by faults and fractures. The first three groups of structures (D1-D3) are recorded only in the Variscan crystalline basement; D4 deformed coherently both basement and Permo-Mesozoic cover rocks. S1 is the mylonitic foliation affecting granulites, marked by alternating layers amphibole- and plagioclase-rich containing garnets and pyroxenes. S2 is the relict foliation in micaceous migmatites marked by mica films separating quartz-feldspathic domains. S2 is folded and transposed till the parallelisation to S3. S3 is the dominant foliation in micaceous and amphibolic migmatites. S4 is the dominant fabric in meta-conglomerates and carbonatic schists.

The multiscale structural analysis, synthesised in the structural map, permits to separate the Alpine from the Variscan structural and metamorphic history, and to identify the latest deformation phase affecting coherently both the Variscan crystalline basement and the metamorphosed sedimentary cover.

P 1.18

Outcrop-scale pressure variations in the Monte Rosa nappe?

Joshua D. Vaughan-Hammon[1], Cindy Luisier[1], Stefan M. Schmalholz[1], Lukas Baumgartner[1]

[1]Institute of Earth Sciences, University of Lausanne, Lausanne 1015, Switzerland (joshua.vaughan-hammon@unil.ch)

The Monte Rose nappe consists of pre-Variscan paragneisses, which were intruded by Permian-age granitic bodies. The current position of the basement complex resides within the collisional Austroalpine-Penninic wedge, and derives originally from the upper crust of the pre-Alpine distal European passive margin. During the Alpine orogeny, the Monte Rosa incurred a high-P imprint interpreted as subduction of continental crust below the overriding Austroalpine units. The peak pressure conditions for subduction have been inferred from “whiteschist” bodies (chloritoid, talc, phengite, quartz ± kyanite/garnet) that occur as local hydrothermal alterations within the metagranite throughout the nappe. Recent studies revealed peak conditions for these whiteschist bodies are between 2.2 and 2.5 GPa and ~570 °C. However, locally the host metagranite exhibits ca. 1.4 GPa and ~550 °C. The reasons for this disparity in peak P are currently disputed and need to be further investigated. This is essential for the reconstruction of the tectonic history of the Monte Rosa nappe, in order to confirm whether pressure of ca. 1.4 GPa (~48 km lithostatic depth) or ca. 2.4 GPa (~82 km lithostatic depth) is representative for the maximum burial depth of the nappe. We will present: (i) detailed structural analysis of the Monte Rosa nappe, (ii) newly discovered peak Alpine assemblages within metapelites in close proximity to the high-P whiteschist bodies, and (iii) the tectonic implications of outcrop-scale pressure variations.

(i) Detailed structural analysis in the study area shows strong strain partitioning within the metagranite. The highest strain intensities are present: (1) near the intrusion-country rock contact, and (2) surrounding the high-pressure whiteschist lenses. Several phases of deformation are observed from early top-N weak augen gneiss shear zones to later top-S mylonite shear zones associated with intense folding. Large areas of the metagranites are undeformed and show pristine magmatic textures, even preserving original intrusive contacts with country rock metapelites, indicating the structural coherence of the Monte Rosa nappe in this study area. Here, we have collected samples of basement metapelites for detailed petrological analysis in order to verify peak Alpine metamorphic conditions.

(ii) Newly discovered metapelitic samples (preserving equilibration at peak Alpine conditions) consist of a unique mineral assemblage: muscovite, paragonite, chloritoid and staurolite. The absence of kyanite and garnet in this assemblage allows us to constrain metamorphic conditions between 1.4-1.7 GPa and ~590 °C. Analysis has also been undertaken for peak Alpine metapelitic assemblages: garnet, muscovite, paragonite, chlorite and quartz. Metramorphic conditions have been constrained ca. 1.3-1.4 GPa and 550 °C. These results consistently highlight a pressure disparity of 0.5-0.8 GPa when compared to estimates for whiteschist assemblages (negligible temperature differences). Our hypothesis is that the whiteschist represents an area of local overpressure deviating from lithostatic.

(iii) The consequences these pressure variations have on the kinematics reconstruction of the Monte Rosa nappe within the Alpine orogeny are significant. The difference between maximum burial depths of ~48 km or ~82 km require vastly different exhumation mechanisms. Exhumation from 48 km can be explained via models of wedge-type dynamics during continental collision (e.g. Escher and Beaumont, 1997). Whereas, exhumation from >80 km requires models such as channel flow (e.g. Chemenda et al., 2000) or “transmantle” diapirism (e.g. Hacker and Gerya, 2013).

REFERENCES

Chemenda, A.I., Burg, J.-P., Mattauer, M., 2000. Evolutionary model of the Himalaya–Tibet system: geopoem: based on new modelling, geological and geophysical data. Earth and Planetary Science Letters, 174(3-4): 397-409.

Escher, A., Beaumont, C., 1997. Formation, burial and exhumation of basement nappes at crustal scale: a geometric model based on the Western Swiss-Italian Alps. Journal of Structural geology, 19(7): 955-974.

Hacker, B.R., Gerya, T.V., 2013. Paradigms, new and old, for ultrahigh-pressure tectonism. Tectonophysics, 603: 79-88.

P 1.19

Rift development and propagation in orthogonal and rotational extension as seen in 4D analogue models

Frank Zwaan[1], Guido Schreurs[1] & Matthias Rosenau[2]

[1]*Institute of Geological Sciences, University of Bern, Baltzerstrasse 1+3, CH-3012 Bern, Switzerland (frank.zwaan@geo.unibe.ch)*
[2]*Helmholtz Centre Potsdam – GFZ German Research Centre for Geosciences, Telegrafenberg, Potsdam 14473, Germany*

A common simplification is that rifts develop under constant along-strike extension conditions. However, extension rates often change laterally along strike in natural settings, due to the rotation about a vertical axis for small-scale settings or about an Euler pole for global scale systems (Fig 1a). Such gradients are thus found in various rift structures or whole ocean basins and even compressional deformation on the other side of the rotation pole is observed in nature (e.g. in the Arctic, Fig. 1c).

Yet analogue and numerical modelers traditionally use a constant along-strike extension rate and few have applied rotational motion in their tectonic experiments. To date, a systematical analysis of the structures developing under these two fundamentally different conditions is lacking. We therefore apply simple brittle-viscous analogue models to compare rift development and rift propagation in either a orthogonal extension setting (involving constant extension rates along strike) or a rotational extension setting (involving extension rate gradients along strike) (Fig. 1a, d). The models are analyzed with state-of-the-art CT-scanning and digital image correlation techniques.

Our models provide a good first-order insight in large-scale rift processes and the structural differences between rifts developing in orthogonal versus rotational extension settings: in the former case, a rift basin with constant along-strike features develops, whereas rotational extension leads to an along-strike structural gradient (Fig. 1d). Rotational extension is furthermore a key factor for rift propagation (Fig. 1d). By contrast, rift structures tend to develop instantaneously along the whole length of the model in orthogonal extension (Fig. 1d). In cases where rifts do propagate in our orthogonal extension models, this involves slight rotational motion, related to strain partitioning along the model sides that do not occur in natural settings (Fig. 1e). The recognition of such boundary effects are of importance for modelers, as they may lead to incorrect interpretations when for instance studying fault evolution.

The rifts in some models are similar to features observed at locations where an oceanic rift enters continental crust. We interpret that the presence of two such domains with different rift styles (i.e. distributed vs. localized) may lead to delayed propagation or even halted propagation and the development of a transform fault separating both domains (e.g. in the Arctic, Fig. 1c).

The clear differences between orthogonal and rotational extension boundary conditions are valid from a purely kinematical point of view. However, various geological processes such as magmatism can significantly affect a developing rift system (e.g. in Afar, Fig. 1b).

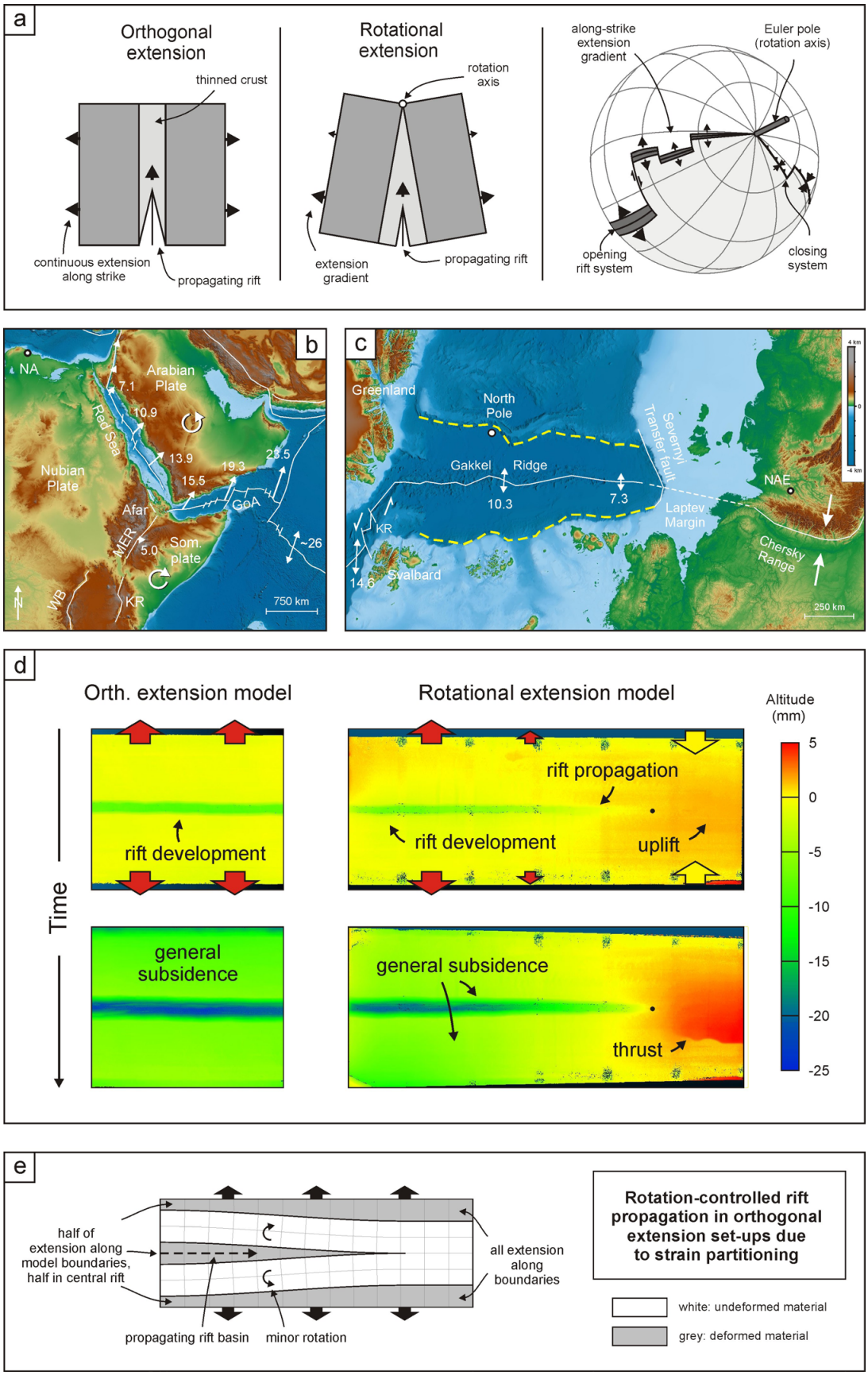


Figure 1. (a) Geometries of orthogonal vs. rotational tectonics. (b-c) extension gradients in the Red Sea and the Arctic (velocities in mm/y). (d) Top view evolution of models (CT-derived topography). (e) Rift propagation in orthogonal extension, due to local rotation.

02. Mineralogy, Petrology, Geochemistry

Sébastien Pilet, Bernard Grobéty, Eric Reusser

Swiss Society of Mineralogy and Petrology (SSMP)

TALKS:

2.1 Bégué F., Baumgartner L., Escrig S., Bouvier A.-S., Robyr M., Meibom A.: Dissolution-reprecipitation reaction of dolomite: investigation of self- and tracer-diffusion using SIMS mini-spot and NanoSIMS profiles

2.2 Chevallaz J., Robyr M.: Pre-Himalayan metamorphism in the High Himalayan Crystalline of Zanskar?

2.3 Curry A., Caricchi L., Davies J., Ovtcharova M.: Zircon petrochronology of four large, rapid-succession, caldera-forming eruptions in the central San Juan caldera cluster, Colorado

2.4 Degen S., Franz L., Krzemnicki M.S. , Wang H.A.O. , Berger A.: Petrology and mineralogy of gem-quality “Paraíba- type” tourmaline bearing granitic pegmatite from Parelhas, Brazil

2.5 Demers-Roberge A., Jollands M., Müntener O.: Testing whether orthopyroxene can reliably record mantle water signatures: an experimental study

2.6 Vieira Duarte J., Piccoli F., Hermann J., Pettke T.: Redox conditions across the antigorite dehydration reaction constrained by sulfide-oxide-silicate mineral geochemistry

2.7 Georgatou A., Chiaradia M.: What can magmatic sulphides tell us about magma fertility in porphyry systems?

2.8 Grosjean M., Moritz R., Rezeau H., Melkonyan R., Hovakimyan S., Ulianov A.: Temporal, spatial and geochemical evolution of the magmatism and associated Cenozoic porphyry and epithermal deposits of the South Armenian Block, Lesser Caucasus

2.9 Hakim K.: Geochemistry of the Inorganic Carbon Cycle on Rocky Exoplanets

2.10 Hantsche A.L., Kouzmanov K., Milenkov G., Vassileva R.D., Dini A., Laurent O.: Relative timing of calc-silicate formation during distal skarn metasomatism

2.11 Higgins O., Sheldrake T., Melekhova L., Blundy J., Ulyanov A., Kouzmanov K., Caricchi L.: Geochemical and temporal evolution of the St Kitts magmatic system, Lesser Antilles

2.12 Jollands M., Baumgartner L.P.B., Tollan P., Muntener O.: H diffusion in quartz: unravelling timescales of explosive volcanism

2.13 Marxer F., Ulmer P.: Polybaric fractional crystallisation of arc magmas – an experimental study

2.14 McCarthy A., Chelle-Michou C., Blundy J.D., Vonlanthen P., Meibom A., Escrig S.: Plagioclase glomerocrysts: taking the pulse of volcanic eruptions

2.15 Morel M., Serneels V.: Iron metallurgy on northeastern coast of Madagascar: How could slag mineralogy help us understand the temperature and reduction conditions in a low furnace?

2.16 Nformidah S., Tollan P., Hermann J.: A Mantle Source For Anomalous CO_2 Along The Cameroon Volcanic Line

2.17 Saintilan N.J., Selby D., Hughes J., Schlatter D., Kolb J., Boyce A.: Exploratory concepts into a refined view of the “Mesoarchaean gold event” and its aftermath – Insights from paragenetic studies and sulphide Re-Os geochronology in the Nuuluk Greenstone Belt, Tartoq, Greenland

2.18 Tollan P., Gurenko A., Hermann J.: Deciphering the evolution of the most primitive Icelandic melts using olivine trace element systematics

2.19 Weber G., Simpson G., Caricchi L.: Thermochemical controls on the diversity of magma chemistry sampled by volcanoes

POSTERS:

P 2.1 Anand A., Pape J., Wille M., Hofmann B., Mezger K.: Mn-Cr chronological constraints on the thermal evolution of ordinary chondrite parent bodies

P 2.2 Ravindran A., Mezger K., Balakrishnan S., Kooijman E., Schmitt M., Upadhyay D., Berndt J.: Genesis of Early Archaean Continents: Constraints from Initial Sr- and Hf-Isotopes from Apatite and Zircon in the Western Dharwar Craton

P 2.3 Blattmann F.R., Eglinton T.I., Haghipour N., van der Voort T.S., Bontognali T.R.R.: Microbial mat growth rates inverted from $\delta^{14}C$ profiles

P 2.4 Chairi R., Triki,A., Mahmoud.,N: Organic matter flux Characterization by pyroloyse Rock Eval in the Majerda river

P 2.5 Maggetti M., Grobéty B., Neururer C.: Maghemite (γ-Fe_2O_3) as a black pigment on a late 18th century tiled stove from Fribourg

P 2.6 Maurer A., Meyer C.A., Franz L.: Geochemistry and diagenesis of fossil tetrapod bones from the Late Triassic of Northern Switzerland

P 2.7 Reynes J., Hermann J., Lanari P.: $Ca_3Ti_2H_2Si_2O_{12}$ – A new hydrogarnet ?

P 2.8 Bovay T., Bisch A., Piccoli F., Lanari P., Rubatto D..: Highlighting complex textures by major and trace element mapping in high-pressure garnet

P 2.9 Foley M., Guillhermin Z., Seitz S., Putlitz B., Baumgartner L.: Oxygen isotope characterization of the silicic Jurassic volcanics from Chon Aike Province (Patagonia): Investigating the origin of rhyolites linked to crustal melting

P 2.10 Peverelli V., Ewing T., Wille M., Rubatto D., Lanari P., Villa I.M., Herwegh M., Berger A.: Epidote as a geochronometer in veins

P 2.11 Giacomazzi L., Baumgartner L.P.: Internal structure of a felsic intrusion: the Catedral granite, Torres del Paine, Patagonia

P 2.12 Serneels K.I., Serneels V.: Understanding minor elements i9n iron bloomery slag from archaeological excavations

P 2.13 Surdez M., Serneels V.: Reconstruction of the supply of lithic materials in the Roman city of Aventicum (VD, Switzerland)

P 2.14 Naumenko-Dèzes M., Rolland Y., Gallet S.: Geochronology of the Terre Adélie Craton (East Antarctica)

P 2.15 Weber S., Diamond L.W.: Pumpellyosites as markers of chemically evolved hydrothermal discharge in the oceanic crust, and their relation to massive sulfide (VMS) deposits

P 2.16 Liu P., Chung S., Li X., Li Q., Zhou M., Lai Y., Ghani A.A., Sihotang T., Sheldrake T.E., Simpson G., Caricchi L.: Rate of eruptible magma assembly preceding Toba's super-eruptions

P 2.17 Jorgenson C., Caricchi L., Weber G., Giordano G., Marxer F., Ulmer P., Tollan P.: Consequences of magma-CO_2 interaction for explosive volcanism at Colli Albani (Italy)

P 2.18 Sheldrake T., Caricchi L.: Probabilistic graphical models to assess tectonic controls on arc volcanism

P 2.19 Musu A., Morgavi D., Spina L., Corsaro R.A., Perugini D.: Experimental model for lava fountaining: the case study of 26 January – 24 June 2000 at south east crater (Mt. Etna, Italy)

P 2.20 Abd El-Rahman Y., Gutzmer J., Li X., Seifert T., Li C.: Geochemistry Of The Sturtian-Aged Hamama Iron Formations: Implication On The Origin Of Neoproterozoic Banded Iron Formations Of The Arabian-Nubian Shield

2.1

Dissolution-reprecipitation reaction of dolomite: investigation of self- and tracer-diffusion using SIMS mini-spot and NanoSIMS profiles

Florence Bégué[1], Lukas Baumgartner[1], Stéphane Escrig[2], Anne-Sophie Bouvier[1], Martin Robyr[1] & Anders Meibom[2]

[1]Institute of Earth Sciences, University of Lausanne, CH-1015 Lausanne (florence.begue@unil.ch)
[2]Laboratory for Biological Geochemistry, Federal School of Technology Lausanne (EPFL), CH-1015 Lausanne

Recrystallization of minerals due to fluid infiltration modifies their original chemical and isotopic signature. Such processes are sought after as they give access to timescales of geologic processes, which are commonly quantified using diffusion chronometry. Here, we focus on hydrothermal veins forming in dolomitic marbles in contact metamorphic environments. The large chemical and isotopic contrast in composition between the magmatic fluids and sedimentary protolith greatly facilitates tracing fluid pathways and reaction mechanism. In addition, they represent a good natural laboratory to study diffusion along recrystallization fronts in minerals.

Dolomite crystals at the vein boundary are characterized by up to 100µm thick, crystallographically continuous recrystallization zones. This new generation of dolomite is characterized by lower $\delta^{18}O$ (about 16 ‰) and $\delta^{13}C$ values (about 6 ‰), and slightly higher Fe (~1000 ppm) and Mn (~100 ppm) concentrations.
$\delta^{18}O$ diffusion profiles across the recrystallization fronts were measured with SIMS, using “mini-spots” of 3µm. The newly installed RF Hyperion source on the NanoSIMS was used to measure Fe and Mn profiles with a beam size of ~200nm.

Diffusion distances of 10-20 μm were obtained for oxygen isotope profiles. Fitting the results to the diffusion equation, results in geologically plausible timescales (1-5 Myrs for temperatures of 500-600°C). Surprisingly, however, the Mn and Fe profiles are extremely sharp, with measured diffusion distances ranging from 150 to 300nm. With the available diffusion coefficients for Fe and Mn in dolomites, such distances result in geologically unrealistic times of less than 1 year. In addition, the profiles are likely even sharper, since the beam size is very similar to the overall diffusion distances. Hence this raises the question whether Fe and Mn diffusion profiles in these dolomites can actually be spatially resolved here or if we are only measuring analytical mixing due to the beam size.

Further investigations are required to understand this large discrepancy between results from these two types of diffusers. Could they be the result of distinct diffusion mechanisms between oxygen self-diffusion versus Fe and Mn tracer diffusion?

2.2

Pre-Himalayan metamorphism in the High Himalayan Crystalline of Zanskar?

Jade Chevallaz[1] & Martin Robyr[1]

[1]*Institute of Earth Sciences, University of Lausanne (martin.robyr@unil.ch), Geopolis, 1015 Lausanne*

The High Himalayan Crystalline (HHC) corresponds to the metamorphic core zone of the Himalayan range. This HHC thrusts over the low-grade sedimentary series of the Lesser Himalaya along the MCT, an intracontinental thrust developed within the Indian margin during Early Miocene. In most section across the range, this metamorphic core zone is separated from the overlying low-grade sedimentary series of the Tethyan Himalaya by the NE-dipping extensional structures of the STDS that initiated during Early Miocene. According to the classical kinematic model for the HHC, the metamorphic imprint in this unit results from the NE underthrusting of the HHC high grade rocks below the Tethyan Himalaya. Most of the tectonic, metamorphic and geochronological data suggest that the Himalaya is essentially the consequence of a single orogenic cycle associated with the India-Asia collision during the Cenozoic era. As a consequence, the metamorphic assemblages and the tectonic structures observed in the Himalayan belt are, de facto, interpreted as belonging to the Cenozoic post-collisional Himalayan history. However, recent investigations in the Zanskar region strongly suggest that the sediments deposited on the northern Indian margin were not necessarily preserved from metamorphism prior to the Cenozoic Himalayan orogenic cycle. Textural and chemical investigations on garnets collected in the footwall of the Zanskar Shear Zone, a local equivalent of the STDS, reveal that these rocks likely experienced a contact metamorphism during the intrusion of an Ordovician granite exposed now in the footwall of the Zanskar Shear Zone. More interestingly, these particular garnets contain inclusion trails marked by staurolite suggesting than an even older metamorphic event may have occurred in the Precambrian to Cambrian sediments deposited on the northern Indian margin. In the same area, foliated xenoliths of metapelites are cross-cut by the undeformed Ordovician Kade granite supporting the hypothesis of a pre-Himalayan metamorphism. Were a metamorphic event indeed had occured in the Palaeozoic time, then it would be necessary to deeply reinterpret the thermal history of the Himalayan range since all the models proposed to explain the tectono-metamorphic evolution of the HHC are all based on the assumption that the thermal events and deformation phases are associated with the Himalayan history.

2.3

Zircon petrochronology of four large, rapid-succession, caldera-forming eruptions in the central San Juan caldera cluster, Colorado

Adam Curry[1], Luca Caricchi[1], Joshua Davies[2], and Maria Ovtcharova[1]

[1]Department of Earth Sciences, University of Geneva, Rue des Maraîchers 13, CH-1205 Geneva (adam.curry@unige.ch)
[2]Département des sciences de la Terre et de l'atmosphère, Université du Québec à Montréal, 201 Avenue du Président-Kennedy, Montréal, Québec, H2X 3Y7

The Rat Creek Tuff (RCT; ~150 km3), Cebolla Creek Tuff (CCT; ~250 km3), Nelson Mountain Tuff (NMT; >500 km3), and Snowshoe Mountain Tuff (SMT; >500 km3) erupted between 26.91 ± 0.02 Ma (RCT) and 26.87 ± 0.02 Ma (SMT) according to single-crystal sanidine 40Ar/39Ar ages. No other ignimbrite flare-up in the world produced a similarly large volume of ignimbrite in such rapid succession. The eruption deposits alternate between zoned (crystal-poor to crystal-rich) and unzoned (crystal-rich) and provide an excellent opportunity to study the evolution of large, silicic crustal magmatic systems. Using U-Pb geochronology (CA-ID-TIMS and LA-ICP-MS), trace elements (LA-ICP-MS and EPMA), and δ18O (SIMS) of zircons, we document the chemical and temporal evolution of this unique sequence. Initial ID-TIMS U-Pb zircon dates show pre-eruptive magma accumulation over less than 600 k.y. before each eruption (<~27.5 Ma). Some zircon dates extend back to 1.4 to 4.3 m.y. before eruption. Zircon oxygen isotope δ18O values are homogeneous among eruptions, rims, and interiors, ranging between 5.1 to 6.3 ‰ and precluding assimilation of low-δ18O crustal rocks as a major process. The average Ti-in-Zr temperatures shift towards cooler values from the oldest RCT to the younger CCT and NMT. The youngest SMT shifted geographically to the Creede Caldera and has the highest average Ti-in-zircon temperature of the four eruptions. Trace elements show an increase in variance with decreasing Ti-in-zircon temperatures. Our results indicate the presence of a large region of magma accumulation and evolution active for at least 600 k.y prior to eruption. The comparison between our data and thermal modelling results suggests that the San Luis systems experienced progressive thermal maturation with temperature becoming generally lower, which is typical of systems constructed by prolonged magma injection into the crust. We are currently performing tailored thermal models that will allow us to quantify the rate of magma injection into the magmatic system to account for zircon ages and trace element distributions.

2.4

Petrology and mineralogy of gem-quality “Paraíba-type” tourmaline bearing granitic pegmatite from Parelhas, Brazil

Sarah Degen[1], Leander Franz[1], Michael S. Krzemnicki[2], Hao A. O. Wang[2] and Alfons Berger[3]

[1]*Institute of Mineralogy and Petrography, University of Basel, Bernoullistrasse 32, CH-4056 Basel*
[2]*Swiss Gemmological Institute SSEF, Aeschengraben 26, 4051 Basel, Switzerland*
[3]*Institute of Geological Sciences, University of Bern, Switzerland*

Granitic pegmatites from the Borborema province in the state of Rio Grande do Norte in northeastern Brazil are amongst the most essential sources of tantalum, beryllium and gemstones, such as “Paraíba-type” tourmaline.

According to LA-ICP-TOF-MS analysis and subsequent geochronological investigation performed on zircon, the genesis of the LCT-type Boqueirão granitic pegmatite has been confirmed to have occurred in a late stage of the Brasiliano-Pan-African orogeny in the Late Cambrian, 491±26 Ma ago (see fig. 1), which is in agreement with a recently published paper by Strmic Palinkas et al. (2019).

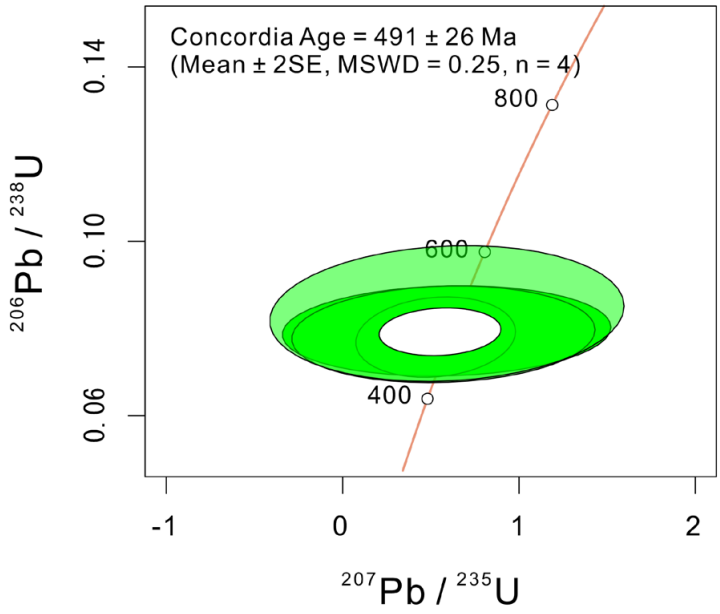


Figure 1. Concordia plot of age dating performed on zircon

The core of zoned garnet crystals indicate initiating crystallisation from the melt in the wet-solidus range of granite, as garnet-phengite geothermobarometry yielded temperatures of 711-763°C (± 60°C). Measurements of the rim revealed temperatures of 619-664°C (± 60°C) and thus suggest a retrograde cooling. This observation is supported by the presence of secondary clinozoisite-epidote, zoisite and prehnite, which are indicative of overprints in the greenschist and the prehnite-pumpellyite facies, respectively.

Moreover, the proceeding crystallisation of mostly water-free minerals led to accumulation of hydrothermal fluids, resulting in alterations in mineralogy such as complete replacement of kalifeldspar by clay or evolution of hydrothermal zircon. Late selective replacement of zoned elbaite by Li-bearing mica has been observed. As previously described by Beurlen et al. (2011), the purple core experienced the highest amount of replacement, whereas the blue rim was left mostly intact.

The analysed tourmalines have been classified as elbaites with elevated amounts of Cu, Mn and Zn, hence falling in the category of the “Paraíba-type”.

The highest amounts of Cu (up to 2.3 wt.-%), have been detected in blue tourmaline samples. Turquoise crystals contain, in addition to their elevated Cu-content, high amounts of Mn (up to 2.5 wt.-%). Moreover, up to 2.4 wt.-% Zn was registered.

Pink colours are due to a dominance in Mn and a depletion in Cu and Zn compared to the other samples as previously described by Beurlen et al. (2011).

The green tourmaline species receive their colour by enhanced Fe-contents (up to 0.8 wt.-%) in combination with high amounts of Mn (up to >2 wt.-%) and medium Cu-concentrations (up to 0.4 wt.-%).

The typical blueish-green, greenish-blue and “neon-blue” hues are seen as a consequence Cu- and Mn-abundance, which has been discussed extensively in previous publications (e.g. Okrusch et al., 2016; Perretti et al., 2009 and references therein). The analysed tourmalines display a blueish shade of green and contain both Mn as well as high amounts of Cu like the blue samples and elevated amounts of Fe, analogous to the green samples.

The investigated samples are not clearly distinguishable from material origi–nating from other areas from Brazil (such as Paraíba-state), however, there is a clear difference in trace elements towards Paraíba-type tourmalines from Nigeria (which have higher Ga-, Ge- and Pb-concentrations) and Mozambique (elevated Be, Sc, Ga, Pb and Bi contents).

REFERENCES

Beurlen, H., de Moura, O., Soares, D., Da Silva, M. 2011: Geochemical and geological controls in the genesis of gem-quality “Paraíba Tourmaline” in granitic pegmatites from northeastern Brazil. Canadian Mineralogist, Vol. 49, pages 277-300

Okrusch, M., Ertl, A. Schüssler, U., Tillmanns, E. 2016: Major- and Trace-element Composition of Paraíba type Tourmaline from Brazil, Mozambique and Nigeria. Journal of Gemmology, Vol. 35, pages 120-139

Perretti, A., Bieri, W., Reusser, E., Hametner, K, Günther, D. 2009: Chemical Variations in multicolored “Paraíba”-type tourmalines from Brazil and Mozambique: Implications for Origin and Authenticity Determination. Contributions to Gemology, Volume 9

Strmic Palinkas, S., Palinkas, L., Neubauer, F., Scholz, R., Borojevic Sostaric, S., Bermanec, V. 2019: Formation Conditions and $^{40}Ar/^{39}Ar$ Age of the Gem-Bearing Boqueirao Granitic Pegmatite, Parelhas, Rio Grande do Norte, Brazil. Minerals, Volume 9, pages 232-248

2.5

Testing whether orthopyroxene can reliably record mantle water signatures: an experimental study

Alexandra Demers-Roberge[1], Michael Jollands[1], Othmar Müntener[1]

[1]*ISTE, Université de Lausanne, 1015, Lausanne*

Experiments have been conducted to assess the effects of temperature, oxygen fugacity, crystallographic orientation, silica activity and chemical composition on the diffusivity and substitution mechanisms of H in orthopyroxene. Axially oriented ~cuboids of natural tanzanian opx were dehydrated at 1 bar in a gas mixing furnace (H_2-CO_2 mix) at three different oxygen fugacities (~QFM-1,~QFM+1, ~QFM-7), and two different silica activity buffers (olivine+pyroxene or pyroxene+quartz) between 700°C and 1000°C. Profiles of hydrogen content versus distance were extracted from experimental samples using Fourier-Transform Infrared (FTIR) Spectroscopy with diffusion coefficients extracted using relevant analytical solutions and numerical approximations of Fick's second law. Diffusion is the fastest along [001] ($D_{[001]}>D_{[010]}>D_{[100]}$). Fitting the diffusion coefficients to the isobaric Arrhenius relationship ($logD=logD_0+(-Q/(2.303RT))$ gives activation energies (Q) and pre-exponential factors ($logD_0$) from 127 to 162 kJmol^{-1} and –4.29 to -5.42 m^{2}s^{-1} for ~QFM-1 and 145 kJmol^{-1} and -4.64 m^{2}s^{-1} for ~QFM+1.

Diffusion appears to be faster at QFM+1 than at ~QFM-1 and -7. The hydrogen diffusion coefficients extracted are faster than previously measured by 0.5 to up to 5 orders of magnitude (Carpenter Wood (2000), Stalder and Skogby (2003), Stalder and Behrens (2006)) and are strikingly similar to those of the fastest known diffusivity of H in olivine (Kohlstedt and Mackwell, 1998), suggesting a mechanism akin to proton-polaron exchange. Tian et al. (2017) proposed that hydrogen diffusion in mantle orthopyroxenes of the Tianchang xenoliths is controlled by metal vacancies, which is ~3 to 4 orders of magnitude slower than hydrogen self-diffusion or proton-polaron exchange. Experiments on the San Carlos enstatite (Carpenter Wood, 2000), which also comes from mantle xenoliths, yield hydrogen diffusion coefficients 0.5 to 1.5 orders of magnitude slower than the results from this study. Thus, the observation that mantle orthopyroxenes appear to be more reliable recorders (than olivine) (e.g. Tian et al., 2017) of original water contents should lay on the type of substitution mechanisms or is not a simple function of relative diffusivities. It seems that there is a disconnection between experimental and natural observations.

The study of infrared peaks of the diffusion profiles, determined using a deconvolution algorithm, at ~QFM-1 and QFM+1, shows 2 peaks (3330 cm^{-1}, 3460 cm^{-1}) out of 9 (3085 cm^{-1}, 3360 cm^{-1}, 3385 cm^{-1}, 3420 cm^{-1}, 3515 cm^{-1}, 3545 cm^{-1}, 3600 cm^{-1}) that do not follow a core to rim dehydration but rather show a higher concentration at the rim than in the core. However, at ~QFM-7, peaks at 3085 cm^{-1} and 3600cm^{-1} behave differently. Different substitution mechanisms must thus occur in response to changing oxygen fugacity, influencing the peaks behavior.

REFERENCES

Carpenter Wood J., (2000), The Pennsylvania State University, Dissertation Abstracts International, Volume: 64-07, Section: B, page: 3145.; 249 p.

Kohlstedt, D.L., Mackwell S.J., (1998). Zeitschrift fur Physikalische Chemie, 207, 1-2, 147-162

Stalder, R., Behrens, H., (2006), Phys Chem Minerals (2006) 33:601–611

Stalder, R., Skogby, H., (2003), Phys Chem Minerals (2003) 30: 12 – 19

Tian et al. (2016). Geology (2017) 45 (1): 87-90.

2.6

Redox conditions across the antigorite dehydration reaction constrained by sulfide-oxide-silicate mineral geochemistry

Joana Vieira Duarte, Francesca Piccoli, Jörg Hermann & Thomas Pettke

University of Bern, Institute of Geological Sciences, Baltzerstrasse 1+3, 3012 Bern

Antigorite breakdown is arguably the most important dehydration reaction occuring during subduction, thought to release oxidizing fluids to the mantle wedge. However, stabilities of oxide and sulfide minerals across this dehydration reaction have remained poorly constrained, despite their importance for the redox state of the fluids released and the residual rock-forming slab.

We performed a detailed petrographic and geochemical study of oxide and sulfide minerals in ultramafic rocks from Cerro del Almirez (Spain). Our results indicate that prograde to peak magnetite ± ilmenite + pentlandite ± pyrrhotite coexist in both the antigorite-serpentinites and chlorite-harzburgites. Retrogression is variably prominent and includes the formation of talc after orthopyroxene, hematite exsolutions from ilmenite, crack-filling low-T serpentine along with magnetite, and rare phosphates and sulfates. Hence, an in-situ approach is required to reliably constrain the redox evolution across the antigorite dehydration reaction.

Textural relationships identify multiple oxide and sulfide mineral growth stages that can be linked precisely to the prograde silicate mineral evolution (Bretscher et al., 2018). Successive growth stages are chemically distinct. In antigorite-serpentinite, anhedral magnetite is zoned, showing a decrease in Cr, Ni, along with most other trace elements from core to rim and to the isolated matrix grains intergrown with pentlandite. In chlorite-harzburgite, magnetite inclusions in olivine, orthopyroxene, and chlorite show the highest Cr contents (up to 28 wt% Cr_2O_3), suggesting formation rather than consumption of magnetite during antigorite breakdown. Polygonal magnetite aggregates stable with euhedral pentlandite additionally document recrystallization of primary magnetite.
Enrichments in chalcophile and/or redox-sensitive elements are observed in all opaque phases of chlorite-harzburgite relative to those in antigorite-serpentinite, notably, Zn, Ga, Sn, V, Mo, and W in magnetite and Cu, As, Se, Mo, Tl, Pb, and Bi in pentlandite.

Neoformation of magnetite coexisting with pentlandite in the antigorite dehydration product mineral assemblage documents rock-buffered conditions. Moreover, pentlandite stability demonstrates limited S mobility in dehydration fluids along with modest redox budget escape via aqueous fluid release. Our findings are in stark contrast to claims made in the literature (e.g., Debret et al., 2015) that highly oxidizing fluids escape from dehydrating Atg-serpentinites in subduction zones. Moreover, observed differences in oxide and sulfide modes between antigorite-serpentinite and chlorite-harzburgite likely relate to variations imposed upon variable extents of ocean floor hydration (Bretscher et al., 2018). We conclude that antigorite-dehydration fluids only carry a moderate redox budget and thus may not account for the relatively oxidized nature of arc magmas.

REFERENCES

Bretscher, A., Hermann, J., Pettke, T., 2018: The influence of oceanic oxidation on serpentinite dehydration during subduction, Earth and Planetary Science Letters, 499, 173-184.

Debret, B., Bolfan-Casanova, N., Padrón-Navarta, J.A., Martin-Hernandez, F., Andreani, M., Garrido, C.J., López Sánchez-Vizcaíno, V., Gómez-Pugnaire, M.T., Muñoz, M., Trcera, N. 2015: Redox state of iron during high-pressure serpentinite dehydration. Cont. Min. Petrol. 169:36.

2.7

What can magmatic sulphides tell us about magma fertility in porphyry systems?

Ariadni Georgatou[1], Massimo Chiaradia[1]

[1]Department of Earth Sciences, University of Geneva, Rue des Maraichers 13, CH-1205 Geneva, Switzerland

Early sulphide saturation plays a crucial role on magma fertility in porphyry systems by retaining Cu and other chalchophile elements in depth before these metals get enriched in the exsolving mineralising fluid. Nonetheless, porphyry deposits are present in areas that have undergone different degrees of sulphide saturation and that are characterised by subduction and post-subduction settings. This study compares for both mineralised and barren systems, magmatic sulphide and chalcophile metal behaviour during the evolution of compositionally different magmas in diverse geodynamic settings. The study areas are: (a) the Quaternary Ecuadorian volcanic arc (host to the Miocene Llurimagua Cu-Mo and Cascabel Cu-Au porphyry deposits) (Subduction), (b) the Miocene Konya magmatic province (hosting the Doganbey Cu-Mo-W porphyry) (PostSubduction) and (c) the Miocene Usak basin (Elmadag, Itecektepe and Beydagi volcanoes, the latter associated with the Kisladag Au porphyry) in Western Turkey (PostSubduction). For comparison we also investigate (d) the barren Plio-Quaternary Kula volcanic field, west of Usak (Intraplate).

All study areas present multiphase sulphides composed of a Cu-poor/Ni-rich (mss) and one/two Cu-rich (iss) phases independently of; (i) magma composition (basalts to andesites/dacites and from high K-calc-alkine to shoshonitic series), (ii) geodynamic setting (subduction, post-subduction and intraplate-OIB), (iii) fertile or barren system (Cu and/or Au porphyry or no mineralisation). However not all study areas present all sulphide types and although all areas show similar initial metal contents of the magmas (inferred from similar mss-84 and iss-16 (area%) for all areas) only areas associated to porphyry deposits show the highest Cu values in later stage magmatic sulphides. In addition, sulphide composition is determined by the nature of the sulphide host mineral phase, in particular the Cu-richests sulphides are hosted exclusively by magnetite.

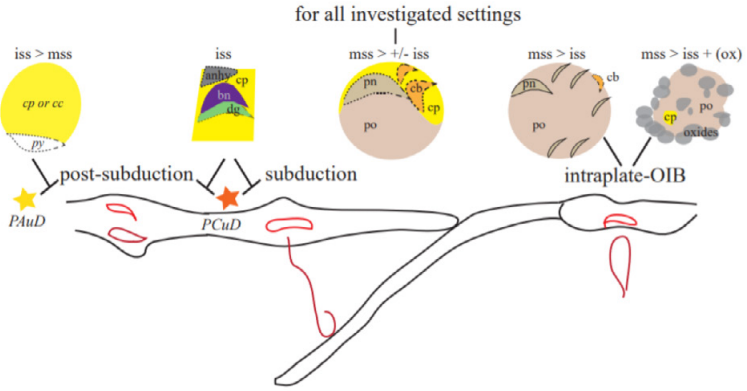


Figure 1. Graphical abstract summarising the sulphide occurence and composition for the different study areas characterised by different geodynamic settings.

2.8

Temporal, spatial and geochemical evolution of the magmatism and associated Cenozoic porphyry and epithermal deposits of the South Armenian Block, Lesser Caucasus

Marion Grosjean[1], Robert Moritz[1], Hervé Rezeau[1,°], Rafael Melkonyan[2], Samvel Hovakimyan[1,2] & Alexey Ulianov[3]

[1]Department of Earth Sciences, University of Geneva, Switzerland
[2]Institute of Geological Sciences, National Academy of Sciences, Yerevan, Armenia
[3]Institute of Earth Sciences, University of Lausanne, Lausanne, Switzerland
°Present address: Department of Earth, Atmospheric, and Planetary Sciences, MIT, Cambridge, USA

The South Armenian block (SAB), in the Lesser Caucasus underwent dextral strike-slip tectonics (Hovakimyan et al., 2019) during Cenozoic collision of the Arabian and Eurasian plates. This setting controlled Cenozoic magmatism and spatially associated porphyry and epithermal deposits in the SAB.

Whole-rock geochemical and geochronological data of magmatic rocks from the SAB and dating of the ore deposits allow us to offer an integrated geodynamic, magmatic and metallogenic model (Figure 1). This study focuses on three areas, including from north to south: (1) the Tejsar pluton (TP) and the Meghradzor epithermal Au deposit, (2) the Amulsar intrusions and the Amulsar epithermal Au deposit, and (3) the Meghri-Ordubad pluton (MOP), which hosts the giant Kadjaran porphyry Cu-Mo deposit.

Calc-alkaline magmatism in the MOP between 49 and 43 Ma is attributed to subduction of the southern Tethys underneath the SAB, and Iran and Anatolia (Moritz et al., 2016; Rezeau et al., 2016, 2017). A magmatic lull. in the southern SAB at the MOP from 41 to 38 Ma is attributed to collision with Arabia (Rezeau et al., 2016, 2017). By contrast, concomitant magmatic activity in the northern TP resulted in the emplacement of shoshonitic intrusions accompanied by emplacement of the Meghradzor deposit, and a younger ultra-alkaline ring intrusion. This stage is attributed to the beginning of slab roll-back triggering back-arc extension in the northern SAB. Progressive southward slab roll-back generated further shoshonitic magmatism at ca. 35-34 Ma in the SAB, culminating with the emplacement of the Amulsar epithermal gold deposit at 30 Ma, and of the Kadjaran porphyry Cu-Mo deposit in the MOP, southern SAB, at ca. 26-27 Ma (Moritz et al., 2016; Rezeau et al., 2016). Finally, Miocene adakitic-like magmatism in the MOP (Rezeau et al., 2016, 2017) and the TP is attributed to slab break-off underneath the SAB propagating westwards into Anatolia (Rabayrol et al., 2019).

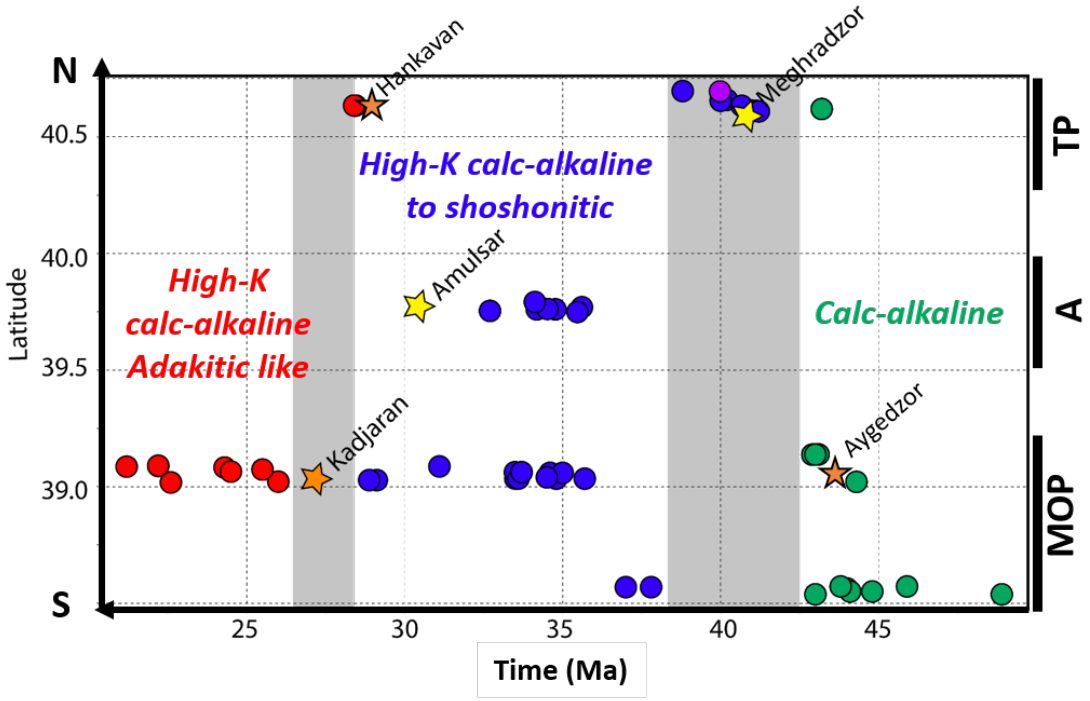


Figure 1. Temporal spatial and geochemical evolution of the magmatism and associated Cenozoic porphyry and epithermal deposit of the SAB. A=Amulsar, MOP=Meghri-Ordubad pluton, TP= Tejsar Pluton.

REFERENCES

Hovakimyan S, Moritz R, Tayan R, et al 2019. Cenozoic strike-slip tectonics and structural controls of porphyry Cu-Mo and epithermal deposits during geodynamic evolution of the southernmost Lesser Caucasus, Tethyan metallogenic belt. Econ Geol

Moritz, R., Melkonyan, R., Selby, D., Popkhadze, N., Gugushvili, V., Tayan, R., and Ramazanov, V. 2016: Metallogeny of the Lesser Caucasus: From arc construction to postcollision evolution. Society of Economic Geologists Special Publication 19, 157–92.

Rabayrol F, Hart CJR, Thorkelson DJ, 2019 Temporal, spatial and geochemical evolution of late Cenozoic post-subduction magmatism in central and eastern Anatolia, Turkey. Lithos 336–337:67–96.

Rezeau, H., Moritz, R., Leuthold, J., Hovakimyan, S., Tayan, R., and Chiaradia, M. 2017: 30 Myr of Cenozoic magmatism along the Tethyan margin during Arabia–Eurasia accretionary orogenesis (Meghri–Ordubad pluton, southernmost Lesser Caucasus). Lithos 288–289, 108–24.

Rezeau, H., Moritz, R., Wotzlaw, J.-F., Tayan, R., Melkonyan, R., Ulianov, A., Selby, D., d›Abzac, F.-X., Stern, R.A., 2016. Temporal and genetic link between incremental pluton assembly and pulsed porphyry Cu-Mo formation in accretionary orogens. Geology 44, 627–630.

2.9

Geochemistry of the Inorganic Carbon Cycle on Rocky Exoplanets

Kaustubh Hakim

University of Bern, Center for Space and Habitability, 3012 Bern

The long-term carbon cycle (also known as the silicate-carbonate cycle) acting on a timescale of the order of hundreds of thousands of years provides the essential negative feedback to maintain temperate climates on Earth. With the discovery of almost a thousand rocky exoplanets and ongoing hunts for an Earth-twin, it is imperative to understand the working of the carbon cycle on such planets. The aim is to investigate the factors of the Earth's carbon cycle that are critical to stabilize and destabilize carbon cycles on rocky exoplanets. These factors could be dependent on the orbital, planetary and stellar parameters as well as planet-specific properties such as rock composition, land and ocean fractions, among other factors. In this study, we focus on modeling the chemical kinetics of rock-water interaction for different rock types (depending on the planet's surface composition), as well as pH. We incorporate a set of silicate weathering reactions leading to the formation of carbonates. In addition to continental silicate weathering, we explore the effects of seafloor weathering especially in the context of varying land-mass fractions, and shallow and deep ocean fractions. Other components of the carbon cycle such as subduction, ridge and arc volcanism are parameterized based on previous studies. The effects of planet size, oxidation states, and tidal locking are also investigated.

2.10

Relative timing of calc-silicate formation during distal skarn metasomatism

Aaron Hantsche[1], Kalin Kouzmanov[1], Georgi Milenkov[1], Rossitsa Vassileva[2], Andrea Dini[3], Oscar Laurent[4]

[1]Department of Earth and Enviromental Sciences, University of Geneva, Rue des Maraîchers 13, CH-1205 Geneva (arron.hantsche@unge.ch)
[2]Bulgarian Academy of Sciences, Acad. G. Bonchev St. 24, 1113 Sofia, Bulgaria
[3]Instituto di Geoscienze e Georisorse, CNR - Pisa, Via Moruzzi 1, 56124 Pisa, Italy
[4]Institute of Geochemistry and Petrology, ETH Zürich, Clausiusstrasse 25, 8092 Zürich, Switzerland

The distribution of distal Pb-Zn skarn bodies in the Madan district (Central Rhodopes) is structurally and lithologically controlled (Bonev, 1984; Vassileva et al., 2009). Skarn formation occurs as a result of fluid transport in two modes: 1. Fluid flow along fracture-controlled vein systems; 2. Fluid propagation along litholigal contacts, resulting in the selective replacement of reactive minerals (Marchev et al., 2005). In marble host rocks, this results in the complete replacement of the original carbonate by Mn-rich clinopyroxene, followed by hydrous silicate overprint. In aluminous host rocks, selective replacement of Al-bearing and Fe-Mg minerals by epidote group minerals occurs in successive stages, leading to the eventual pervasive replacement of the host. These calc-silicate assemblages are precursory to Pb-Zn sulfide mineralization and significantly influence the ore distribution in the Madan deposits (Marchev et al., 2005).

Linking the relative timing with the chemical composition of these metasomatic calc-silicates is important to understanding district scale distribution of the Pb-Zn mineralization. Despite the lack of high-precision geochronometers in the skarn bodies, a relative timing can be inferred from the chemical composition of the dominant calc-silicate minerals, pyroxene and epidote. These analyses have been performed using back-scatter electron imaging (BSE), electron probe microanalysis (EPMA), and laser ablation – inductively coupled plasma mass spectrometry (LA-ICP-MS).

Pyroxene major element geochemistry suggests two distinct generations of metasomatic pyroxene in the Madan district. An early diopside-hedenbergite formed by selective replacement of amphibolite host rocks at the Marzian deposit, located in the southern extent of the district. This early pyroxene was later overprinted by garnet-epidote skarn mineralization and Cu-Fe sulfides, and the relationship to the main Pb-Zn hydrothermal mineralization in the district remains unclear. Another style of Mn-rich pyroxene skarn forms in marble hosts, ranging from $Jo_{54}Hd_{35}Di_{11}$ to $Jo_{97}Hd_{2}Di_{1,}$ with a general increase in MnO (wt. %) to the north. Trace element composition of this pyroxene shows an increase in Zn, Y, and REE with increasing johannsenitic component.

Major element geochemistry of epidote group minerals is governed by the relative timing and crystallization style of the epidote: early (foliation controlled), late (pervasive replacement), or open space crystallization in veins. The foliation-controlled epidote is more ferric than the later, more aluminous epidote in the massive replacement bodies and veins. The trace element composition of this epidote shows progressive increase in Mn, Zn, K, Rb, Ce, and REE over the relative timing sequence of epidote crystallization.

Based on the increasing Mn, Zn, and REE concentrations in these two calc-silicate minerals, we propose that these phases are both formed during prograde skarn formation, with both early and late epidote corresponding to the crystallization of Jo-Hd series pyroxene. Overprinting by hydrous skarn minerals and later sulfide precipitation is potentially linked to the increase in volatile elements in the vein-style epidote. The relative timing shows that these calc-silicate minerals record the early stages of evolution of the system in different host-rocks.

REFERENCES

Bonev, I. K. (1984) Mechanisms of the hydrothermal ore deposition in the Madan lead-zinc deposits, Central Rhodopes, Bulgaria. IAGOD, 69-73

Marchev, P., Kaiser-Rohrmeier, M., Heinrich, C., Ovtcharova, M., von Quadt, A., Raicheva, R. (2005) Hydrothermal ore deposits related to post-orogenic extensional magmatism and core complex formation: The Rhodope Massif of Bulgaria and Greece. Ore Geology Reviews, 27, 53-89.

Vassileva R.D., Atanassova R., Bonev I.K. (2009) A review of the morphological varieties of the ore bodies in the Madan Pb-Zn deposits, Central Rhodopes, Bulgaria. Geochemistry, Mineralogy and Petrology 47, 31-49.

2.11

Geochemical and temporal evolution of the St Kitts magmatic system, Lesser Antilles

Oliver Higgins[1], Thomas Sheldrake[1], Lena Melekhova[2], Jon Blundy[2], Alexey Ulyanov[3], Kalin Kouzmanov[1], Luca Caricchi[1]

[1]Department of Earth Sciences, University of Geneva, Rue de Maraîchairs 13, CH-1205 Genève (Oliver.Higgins@unige.ch)
[2]Department of Earth Sciences, University of Bristol, Wills Memorial Building, Queens Road, Bristol BS8 1RL, UK
[3]University of Lausanne, Géopolis, Quartier Mouline, CH-1015 Lausanne

Detailed petrological and geochemical study of plutonic and cumulate rocks can provide insights into the inner workings of transcrustal magmatic systems (e.g. Melekhova et al., 2017; Otamendi et al., 2016). This crustal architecture in turn influences the eruptive style, chemical diversity, thermal evolution and erupted volume at the associated volcanic system. Here we focus on the volcanic island of St. Kitts in the Lesser Antilles, an island that is largely uninterrupted by sediment contamination and pre-existing crustal structure.

Whole rock major and trace element analysis of volcanic and pyroclastic rocks show two distinct magmatic lineages that can be ascribed to differentiation at various crustal depths. We use major element modelling to show the cumulate assemblages needed to generate these trends. In-situ mineral trace element data for the cumulate and plutonic xenoliths are used to constrain the differentiation process as well as mineral reactions, particularly between clinopyroxene and amphibole. Thermodynamic modelling provides estimates of the equilibrium P-T (Pressure-Temperature) conditions for the cumulate xenoliths; this technique acts as a complement to multiple reaction thermobarometers or as an alternative when suitable phase assemblages are unaivalable.

Collectively, these techniques allow us to develop a clearer picture of the magmatic system below St. Kitts.

REFERENCES

Melekhova, E., Blundy, J., Martin, R., Arculus, R., & Pichavant, M. 2017: Petrological and experimental evidence for differentiation of water-rich magmas beneath St. Kitts, Lesser Antilles. Contributions to Mineralogy and Petrology, 172 (11-12), 98.

Otamendi, J.E., Tiepolo, M., Walker Jr, B.A., Cristofolini, E.A. and Tibaldi, A.M., 2016: Trace elements in minerals from mafic and ultramafic cumulates of the central Sierra de Valle Fértil, Famatinian arc, Argentina. Lithos, 240, 355-370.

2.12

H diffusion in quartz: unravelling timescales of explosive volcanism

Michael C. Jollands[1], Lukas P. Baumgartner[1], Peter M.E. Tollan[2], Othmar Müntener[1]

[1]*Institute of Earth Sciences, University of Lausanne, 1015 Lausanne, Switzerland*
[2]*Institute of Geology, University of Bern, Balzerstrasse 1+3, 3012 Bern, Switzerland*

Hydrogen diffusion in quartz is presented as a potential tool for understanding very short (minutes to hours at 700-800 °C) timescales of eruption processes that involve changing water fugacity prior to quenching. The system also allows new insights into diffusive processes in general – H is a trace element but does not behave as a tracer diffusant, and has multiple sites even in the simple quartz structure.

Oriented cubes were cut from various optically perfect quartz crystals (Brazil, Tibet, Madagascar), all of which contained some structurally bound OH groups, but with different defect populations and water contents (2 to 90 wt. ppm H_2O). The crystals were then dehydroxylated (1 bar), or hydroxylated/deuteroxylated (1 kbar) at 400-900 °C.

Dehydroxylation was done in air, placing the crystals in Au containers, either alone or packed into a lithium disilicate-quartz powder (to induce Li^+-H^+ inter-diffusion). Experiments were conducted for minutes to weeks, then doubly polished and analysed using FTIR spectroscopy. Total OH versus distance from the crystal edge shows simple error function shapes, but resolved profiles show diffusion-induced OH band fractionation.

Following hydroxylation or deuteroxylation, profiles do not conform to the error function, rather they show two-step profiles (including plateaus) or linear concentration decreases, often with kinks. These shapes can be explained using a diffusion plus reaction model, were H diffuses along a pathway associated with one defect (e.g. associated with non-bridging O^{2-}) then hops into association with another defect (associated with Al^{3+}).

Despite clear differences between the different experimental series, the in-diffusion and out-diffusion (of H^+) can be approximately described by the same diffusion-reaction model. In the out-diffusion experiments the H^+ is already on its most stable site (Al^{3+} associated) so inter-site reaction is limited/negligible, and in the in-diffusion experiments the H^+ moves partially on a less favourable site, then hops into the more favourable Al-associated site.

Then, timescales of the last moments of silica-saturated volcanic eruptions can be unravelled, in the case where crystals do not experience considerable post-eruption heating. Diffusion is fast enough that easily measurable profiles (hundreds of µm) are formed in just minutes to hours at 700-800 °C.

2.13

Polybaric fractional crystallisation of arc magmas - an experimental study

Felix Marxer[1], Peter Ulmer[1]

[1]*Institute of Geochemistry and Petrology, ETH Zürich, Clausiusstrasse 25, CH-8092 Zürich (felix.marxer@erdw.ethz.ch)*

To date, the principal crustal depth of arc magma differentiation is still highly debated. Implications from field observations, natural rock data and experimental studies are partly contradictory and cannot be combined into one single differentiation model. Therefore, we propose an alternative scenario, namely polybaric fractional crystallisation, inferring that arc magmas progressively differentiate by crystal fractionation and interaction with crystal mushes/cumulates upon ascent through the continental crust.

This hypothesis is tested through a series of experiments along three different pressure - temperature ascent trajectories, simulating the buoyant rise of evolving arc magmas in the continental crust. Running concomitant equilibrium (closed-system) crystallisation experiments allows us to directly elaborate the impact of crystal fractionation on magma differentiation. Phase equilibria data, chemical compositions of stable mineral phases, liquid lines of descent as well as the evolution of crystal/melt ratios were established and provide crucial information to improve our understanding of the evolution of the calc-alkaline magmatic series.

Experimental results support theoretical considerations on the effect of decreasing crystallisation pressure on mineral phase equilibria: the olivine-clinopyroxene cotectic curve is shifted towards more cpx-rich compositions (equivalent to a stabilisation of olivine at the expense of clinopyroxene) rendering residual melts more metaluminous and, therefore, circumventing a rapid evolution of liquid lines of descent towards and into the peraluminous compositional field. Enhanced plagioclase precipitation with decreasing pressures further affects the liquid line of descent. The polybaric evolution of the experimental liquids more closely approaches the prevalent compositions of intermediate to SiO_2-rich plutonic and volcanic rocks observed at convergent plate margins.

2.14

Plagioclase glomerocrysts: taking the pulse of volcanic eruptions

Anders McCarthy[1], Cyril Chelle-Michou[2], Jonathan D. Blundy[1], Pierre Vonlanthen[3] , Anders Meibom[4], Stéphane Escrig[4]

[1]School of Earth Sciences, University of Bristol, Wills Memorial Building, BS8 1RJ, Bristol, UK (anders.mccarthy@bristol.ac.uk)
[2]Institute of Geochemistry and Petrology, Department of Earth Sciences, Eidgenössische Technische Hochschule Zürich, Clausiusstrasse 25, CH-8092 Zürich, Switzerland
[3]Institute of Earth Sciences, University of Lausanne, CH-1015 Lausanne, Switzerland
[4]Laboratory for Biological Geochemistry, School of Architecture, Civil and Environmental Engineering, Ecole Polytechnique Fédérale de Lausanne (EPFL) and Center for Advanced Surface Analysis, Institute of Earth Sciences, University of Lausanne, CH-1015 Lausanne, Switzerland.

Volcanic eruptions result from complex interplay of magmatic processes including the ascent and storage of magma in the crust, volatile exsolution and crystallization. The dynamics of crystallization in shallow subvolcanic systems and the consequences of interaction between ascending magmas and gases remain largely unconstrained. Mineral clusters, or glomerocrysts, provide a novel tool to infer magmatic processes occurring in vertically integrated subvolcanic systems. Here, we target cm-wide glomerocrysts formed of radially oriented plagioclase from Tolbachik volcano, Kamchatka, Russia. We use glass inclusion data, mineral textures and diffusion chronometry on olivine and plagioclase and show that cm-size glomerocrysts can grow in days to weeks in a dynamic and melt-rich system prior to or during volcanic eruption. Rhythmic CO_2-fluxing by degassing of deep-seated magmatic reservoirs controls the crystallization and resorption of plagioclase and might well lead to significant overpressure in shallow subvolcanic systems, thereby controlling the rhythmicity of volcanic eruptions. Radially oriented plagioclase glomerocrysts represent the volcanic counterpart of radial magmatic layering found in shallow magmatic plutons, namely plagioclase-dominated comb layers and orbicular rocks (McCarthy and Müntener, 2016). Long timescales and slow cooling are mechanisms generally required to form well-developed magmatic layering according to fundamental and long-standing tenets of igneous layered intrusions (Wager and Brown, 1963, McBirney and Noyes, 1979). We argue however that vertical, radial magmatic layering dominated by plagioclase crescumulates found in shallow subvolcanic systems and sampled as mineral clusters in erupted products should be reassessed as monitors of fluctuating P-T-H_2O-CO_2 conditions on eruptive timescales.

REFERENCES

McCarthy, A., & Müntener, O. 2016: Comb layering monitors decompressing and fractionating hydrous mafic magmas in subvolcanic plumbing systems (Fisher Lake, Sierra Nevada, USA), Journal of Geophysical Research, 121, 8595-8621.

Wager, L.R., & Brown, G.M.,1967: Layered Igneous Rocks, WH Freeman

McBirney A.R., and Noyse, R.M., 1979: Crystallization and layering of the Skaergaard Intrusion, Journal of Petrology, 20(3), 487-554,

2.15

Iron metallurgy on northeastern coast of Madagascar: How could slag mineralogy help us understand the temperature and reduction conditions in a low furnace?

Mélissa Morel[1], Vincent Serneels[1]

[1]*Institut de Géologie de l'Université de Fribourg, Chemin du Musée 6, CH-1700 Fribourg (melissa.morel@unifr.ch)*

On the northeastern coast of Madagascar lived between the 7th and th 17th century a Islamized population so-called Rasikajy. This still poorly known population produced iron, probably only for local uses, in workshops located along the coast between the modern cities of Vohémar and Antalaha (Serneels *et al*., 2018; Serneels *et al*., 2019).

Between 2017 and 2019, three excavation and survey campaigns have been undertaken. More than 80 slag heaps were located and some of them were excavated. The study of archaeological remains and the analysis of metallurgical wastes such as slags or tuyeres allow us to reconstruct the structure of the furnaces. Hence the furnaces were bowl furnace, directly dug into the sand, with small walls also made with sand. It seems that they were single-tuyere fireplaces with bellows. Iron-rich lateritic ores, which are easy to find in the surrounding hills, were crushed and then smelted inside the furnace in order to produced metallic iron.

From one workshop to another, little variations of the archaeological remains and artefacts can be observed. However, these variations are small and could correspond to local variability. This tends to demonstrate the use of a same technology throughout the period of metallurgical production (11^{th}-15^{th} century).

However, it is still difficult to reconstruct what were the temperature and reduction conditions inside such furnaces. The study of minerals inside iron slags (Fayalite, Hercynite, Ulvöspinel, Wüstite,…) could help us to understand the variability of the production or the heterogeneity inside these bowl furnaces. The study of these metallurgical wastes allow us to reconstitute how much iron were produced.

REFERENCES

Serneels, V., Morel, M., Nitsche, C., Radimilahy, C., Rakotoarisoa, J.-A., Rasoraifetra, B., Schreurs, G. 2018: Pierre et Fer à Madagascar (1) – Vestiges sidérurgiques de Benavony et de la rivière Matavy, SLSA Jahresberich 2017, p.109-156.

Serneels, V., Morel, M., Nitsche, C., Radimilahy, C., Rakotoarisoa, J.-A., Rasoraifetra, B., Schreurs, G., Velomora, S. accepted : Pierre et Fer à Madagascar (2) – Les scories d'Amboronala et les carrières de Milanoa, SLSA Jahresberich.

2.16

A mantle source of anomalous CO_2 along the Cameroon Volcanic Line

Siggy Nformidah[1], Peter Tollan[1], Jörg Hermann[1]

[1]*Institut für Geologie, Universität Bern, Baltzerstrase 1+3, 3012 Bern (ndah.nformidah@geo.unibe.ch)*

Periodic, violent outgassing of CO_2 along the Cameroon Volcanic Line (CVL) indicates a deep CO_2 reservoir. However, the origin of this CO_2 remains enigmatic. One possibility is that the CO_2 is mantle derieved, either via ancient subduction-related metasomatism during the Pan-African orogeny or by recent plume-related carbonatite metasomatism. In order to test these hypotheses, we measured major and trace element concentrations (including H) in silicate minerals from clinopyroxene-bearing spinel hazburgites recovered from Cenozoic alkaline basalts from the northernmost part of the CVL.

The three investigated xenoliths show protogranular to porpyroclastic textures. High ol (0.91-0.92) and opx (0.92-0.93) Mg# coupled with relatively high modal proportions of cpx (5-8%) and a remarkably wide range in cpx Mg# (0.91-0.94) are interpreted to reflect high degrees of partial melting followed by chemical and modal metasomatic refertilisation. This is confirmed by strong LREE (and to a lesser extent, HREE) enrichments in cpx compared to those anticipated for the percentage of partial melting indicated by ol Mg#. The diversity in cpx Mg# is also mirrored by variations in concentrations of highly incompatible trace elements, notably LREE and both Th and U.

Primitive mantle normalised trace element patterns of cpx show negative Ti and Nb anomalies and a positive Sr anomaly but contrastingly a negative Pb anomaly, which indicates the absence of subduction-related metasomatism. On the other hand, negative Ba and Nb anomalies are inconsistent with metasomatism by alkaline melt. Instead, such features combined with strong enrichments in U and Th indicate the involvement of a carbonatite fluid component.

Despite this, Ti/Eu ratios, a commonly used discriminant between silicate and carbonatite metasomatism, do not indicate the ubiquitous involvement of carbonatite fluid. We suggest that the cpx initially precipitated from a dominantly silicate melt, but were subsequently overprinted by carbonatite metasomatism. Such a process could explain the difference in metasomatic signatures between strongly and moderately incompatible trace elements.

To test further the involvement of carbonatite fluids, H_2O was measured in all silicate minerals. In sample Ka1, opx and cpx have H_2O contents of ~20 ppm and ~100 ppm at their cores respectively. Low water contents compared to typical sub-continental peridotites reflect lower water activities of carbonatitic melts relative to alkaline melts.

Although the precise tectonic associations of the distinct metasomatic fluids is yet to be constrained, our new data indicates that the mantle has undergone 3 main events: partial melting, addition of cpx during silicate metasomatism and a subsequent partial overprinting during carbonatite metasomatism. The identification of pervasive carbonatite metasomatism in cpx could be a potential source of the CO_2 release during periodic degassing along the CVL.

2.17

Exploratory concepts into a refined view of the "Mesoarchaean gold event" and its aftermath – Insights from paragenetic studies and sulphide Re-Os geochronology in the Nuuluk Greenstone Belt, Tartoq, Greenland

Nicolas J. Saintilan[1],‡, David Selby[1], Joshua Hughes[1], Denis Schlatter[2], Jochen Kolb[3], & Adrian Boyce[4]

[1]Department of Earth Sciences, University of Durham, Durham DH1 3LE, UK (nicolas.saintilan@erdw.ethz.ch)
[2]Helvetica Exploration Services GmbH, Carl-Spitteler-Strasse 100, 8053 Zürich, Switzerland
[3]Institute of Applied Geosciences, Geochemistry and Economic Geology Group, Karlsruhe Institute of Technology, Adenauerring 20b, 76131 Karlsruhe, Germany
[4]Isotope Geoscience Unit, SUERC, Rankine Avenue, East Kilbride, Glasgow G75 0QF, UK
‡Present address: Institute of Geochemistry and Petrology, Department of Earth Sciences, ETH Zürich, Clausiusstrasse 25, 8092 Zürich, Switzerland

A "Mesoarchaean gold event" of magmatic origin might have added the bulk of gold to the nuclei of the future cratons around the time of the global onset and establishment of crust generation by plate tectonic processes at ca. 3.2–3.0 billion years (Ga; Shirey and Richardson, 2011; Næraa et al., 2012; Tang et al., 2016). The timing of this major magmatic event may coincide with the aftermath of the ca. 3.2 Ga major bombardment of the Earth-Moon system (Glikson, 2001). Although a logical link between these events is tempting, it has not really been investigated in detail, and the origin of the "Mesoarchaean gold event" remains rather enigmatic if not truly controversial with regard to its trigger and whether magmatic processes actually led to this pronounced gold endowment in those nuclei (cf. Frimmel, 2008). Here, our study focuses on the Nuuluk greenstone belt in the Tartoq district in southwestern Greenland where volcanic and magmatic rocks and accompanying lower crustal harzburgite cumulates were emplaced at ca. <3.19–3.01 Ga (Kisters et al., 2012; Szilas et al., 2013, 2014; van Hinsberg et al., 2018). We use detailed sulphide and sulpharsenide petrography in gold-mineralized shear zones in this greenstone belt and complement our observations with rhenium-osmium-sulphur (Re-Os-S) isotope geochemistry of individual mineral separates of arsenopyrite and pyrite. In light of our findings, we propose to relate the "Mesoarchaean gold event" to the precipitation of ca. 2.98 Ga (Re-Os model ages) massive arsenopyrite on the seafloor. Indeed, arsenopyrite with primary invisible gold may result from the hydrothermal alteration and serpentinization of a <3.19–3.01 Ga oceanic crust comprising basaltic rocks and lower crustal harzburgite cumulates. This alteration mobilized arsenic, Re, and Au that were fixed in arsenopyrite. In major shear zones, retrograde greenschist-facies metamorphism overprinted the ca. 3.01–2.82 Ga pervasive amphibolite-facies metamorphic assemblages and caused local dissolution of arsenopyrite. During this retrograde tectono-metamorphic stage, in gold-rich shear zones, the Re-Os geochronometer in arsenopyrite was reset to a Neoarchaean age while invisible gold was liberated and deposited as native gold with 2.66 Ga pyrite (Re-Os isochron ages). The initial Os isotope ratios of Neoarchaean arsenopyrite ($^{187}Os/^{188}Os_i$ = 0.13 ± 0.02) and gold-bearing pyrite (0.12 ± 0.02) overlap with the estimated $^{187}Os/^{188}Os$ ratio of the Mesoarchaean mantle (0.11 ± 0.01) and preclude contribution of radiogenic crustal Os from evolved lithologies in the accretionary complex, but instead, favour a local contribution in Os from basaltic rocks and serpentinized harzburgite protoliths by metamorphic fluids. Thus, the ca. 2.66 Ga lode gold mineralization identified in the North Atlantic Craton may illustrate a gold endowment in shear zones in Earth's stabilizing continental crust at the time of the 2.75–2.55 Ga Global Gold Event (Goldfarb et al., 2001, 2005; Bierlein et al., 2006), through metamorphic upgrading of bulk gold originally extracted from the Mesoarchaean mantle and concentrated in massive arsenopyrite deposits on the seafloor of the reduced Mesoarchaean ocean.

REFERENCES

Bierlein, F.P., Groves, D.I., Goldfarb, R.J., and Dubé, B. 2006: Lithospheric controls on the formation of provinces hosting giant orogenic gold deposits, Mineralium Deposita, 40, 874-886.

Frimmel H.E. 2008: Earth's continental crust gold endowment, Earth and Planetary Science Letters, 267, 45-55.

Glikson, A. Y. 2001: The astronomical connection of terrestrial evolution: crustal effects of post-3.8 Ga mega-impact clusters and evidence for major 3.2±01 Ga bombardment of the Earth-Moon system, Journal of Geodynamics, 32, 205-229.

Goldfarb, R.J., Groves, D.J., and Gardoll, S. 2001: Orogenic gold and geologic time: a global synthesis, Ore Geology Reviews, 18, 1-75.

Goldfarb, R.J., Baker, T., Dubé, B., Groves, D.I., Hart, C.J.R., and Gosselin, P. 2005: Distribution, character, and genesis of gold deposits in metamorphic terranes. In: Hedenquist, J.W., Thompson, J.F.H., Goldfarb, R.J., Richards, J.P. (Eds.), Economic Geology One Hundredth Anniversary Volume. Society of Economic Geologists, Littleton, pp. 407-450.

Kisters, A.F., van Hinsberg, V.J., and Szilas, K. 2012: Geology of an Archean accretionary complex – the structural record of burial and return flow in the Tartoq Group of South West Greenland, Precambrian Research, 220-221, 107-122.

Næraa, T., Scherstén, A., Rosing, M.T., Kemp, A.I.S., Hoffmann, J.E., Kokfelt, T.F., and Whitehouse, M.J. 2012: Hafnium

isotope evidence for a transition in the dynamics of continental growth 3.2 Gyr ago, Nature, 485, 627-631.
Shirey, S.B., and Richardson, S.H. 2011: Start of Wilson cycle at 3 Ga shown by diamonds from subcontinental mantle, Science, 333, 434-436.
Szilas, K., van Hinsberg, V.J., Kisters, J.E., Hoffmann, T.F., Kokfelt, A., Scherstén, A., Windley, B.F., and Münker, C. 2013: Remnants of arc-related Mesoarchean oceanic crust in the Tartoq Group, SW Greenland, Gondwana Research, 23, 436-451.
Szilas, K., van Hinsberg, V.J., Creaser, R.A., and Kisters, A.F. 2014: The geochemical composition of serpentinites in the Mesoarchean Tartoq Group, SW Greenland: Harzburgitic cumulates or melt-modified mantle? Lithos, 198-199, 103-116.
Tang, M., Chen, K., and Rudnick, R.L. 2016: Archean upper crust transition from mafic to felsic marks the onset of plate tectonics, Science, 351, 65-75.
Van Hinsberg, V.J., Crotty, C., Roozen, S., Szilas, K., and Kisters, A.F. 2018: Pressure-temperature history of the >3Ga Tartoq greenstone belt in Southwest Greenland and its implication for Archaean tectonics, Geosciences, 8, 367.

2.18

Deciphering the evolution of the most primitive Icelandic melts using olivine trace element systematics

Peter Tollan[1], Andrey Gurenko[2], Jörg Hermann[1]

[1]*Intitut für Geologie, Universität Bern*
[2]*Centre de Recherches Pétrographiques et Géochimiques, Université de Lorraine*

Melt inclusions hosted by high forsterite (*Fo*) olivine phenocrysts are generally regarded as the best tool for understanding the chemical and physical characteristics of the underlying mantle source. However, post-entrapment processes such as crystallisation and diffusive exchange can significantly modify the original melt inclusion composition and can be hard to identify and correct for. An alternative is to use the host olivine chemistry instead. Modern laser ablation ICP-MS techniques combined with the interpretative framework provided by experimental studies have resulted in an expanded range of trace elements that can be routinely utilised. The signifcant variance in chemical affinities of these elements are sufficient to open up new possibilities for tracing the evolution of Earth's most primitive melts.

We demonstrate such an approach using olivine macrocrysts hosted by the Borgarhraun lava flow, northern Iceland. This historical lava flow is the most primitive on Iceland, highlighted by the highly forsteritic olivine macrocryst compositions, which form an approximately bimodal population distribution ($Fo_{92.2\text{-}90.9}$ and $Fo_{90.0\text{-}87.7}$). Trends between *Fo* and minor elements obtained by microprobe (Ni and Mn) are unable to distinguish any clear genetic differences between these olivine populations. Trace elements, on the other hand, show striking differences. Clear trends between Cr and other elements (Li, Na, Ca, Al, Ti, Y) within the high *Fo* group are consistent with concurrent mixing and crystallisation of two subtely different high-Mg primary melt compositions. The low *Fo* group, conversely, show much poorer trends between major, minor and trace elements, discounting any distinct genetic relationship between the crystals comprising this population.

High resolution LA-ICP-MS scanning across the crystal-matrix interface shows convergence of almost all elements from crystals of both populations towards a single olivine rim composition. This rim composition, however, is not represented by any of the olivine macrocryst compositions, indicating that the carrier liquid was different to any of the melts parental to the macrocrysts. This carrier liquid thus scavenged macrocrysts from various mush piles comprising the lower Icelandic crust before erupting at the surface. Modelling the concentration profiles of moderately incompatible elements (Ni, Mn, Co) results in timescales of 2-8 months for the process of scavenging and eruption. Highly incompatible element profiles (Ti, V and Y) are significantly shorter, potentially reflecting the continued differentiation of the carrier liquid during ascent. This is corroborated by Cr profiles, which uniquely show sigmoidal shapes, consistent with crystallisation of Cr-spinel during transport.

Our olivine trace element data shows that even the most primitive magmatic olivines on Earth may reflect melt-modifying processes such as melt mixing, rather than equilbrium with primary mantle melts. Such interpretations cannot be made from microprobe data alone. Therefore, trace element measurements in olivine are an essential tool for identifying the most primitive stages of magma differentiation.

2.19

Thermochemical controls on the diversity of magma chemistry sampled by volcanoes

Gregor Weber, Guy Simpson & Luca Caricchi

Department of Earth Sciences, University of Geneva, Rue des Maraîchers 13, CH-1205 Geneva (gregor.weber@unige.ch)

The geochemical diversity of magmas is attained at inaccessible depth within the Earth and at times sampled by volcanic eruptions. Unravelling the geochemical record of volcanic rocks consequently holds important but enigmatic information about processes occurring within magma plumbing systems, which ultimately are of value for volcanic hazard assessment, the genesis of ore deposits and geodynamics. Detailed mapping, geochronology and chemical analysis of volcanic complexes has revealed that some volcanoes produce magmas of monotonous chemistry throughout their lifecyle, while others tend to erupt magmas covering the entire range from basalt to rhyolite. The underlying reasons for such different behavior are not well understood.

We present results from thermal modelling of magma injection in the mid- to lower crust (20-30 km depth) coupled with experimental phase equilibria in order to compute the temporal evolution and compositional diversity of magma geochemistry as a function of recharge rates and crustal thermal state. Our results demonstrate that low magma fluxes (<0.002 km^3 yr^{-1}) at relatively hot or deep crust produce less geochemical diversity compared to large magma injection rates (>0.002 km^3 yr^{-1}) into cooler or shallower crust. This indicates that the thermal structure, resulting from different injection rates and temperature variation within the surrounding crust is a primary control on the compositional variability of magmas present within plumbing systems. We compared the modelling outcomes to various natural datasets, which show striking similarity. Our study shows that heat transfer and phase petrology can be used to constrain otherwise inaccessible variables like rates of magma input and the thermal architecture of magmatic systems from geochemical analysis of volcanic rocks.

P 2.1

Mn-Cr chronological constraints on the thermal evolution of ordinary chondrite parent bodies

Aryavart Anand[1], Jonas Pape[1,2], Martin Wille[1], Beda Hofmann[1,2] & Klaus Mezger[1]

[1]Institute of Geological Sciences, University of Bern, Baltzerstrasse 1+3, CH-3012, Bern (aryavart.anand@geo.unibe.ch)a
[2]Naturhistorisches Museum Bern, Bernastrasse 15, CH-3005, Bern

Ordinary chondrites (OCs) were metamorphosed to varying degrees ranging from un-equilibrated petrologic type 3 to equilibrated type 6. OCs of different petrologic types are considered to sample different depths of an "onion-shell"-structured parent body[1]. Thus, they can yield information on the time of accretion and subsequent thermal evolution of undifferentiated planetesimals in the early Solar System. The short-lived ^{53}Mn-^{53}Cr ($t_{1/2} \approx 3.7$ Ma) chronometer is suitable to investigate the timing and extent of such early Solar System processes.

Chromite ($FeCr_2O_4$) occurs as an accessory mineral (0.2-1 wt%) in all OC groups (i.e. H, L & LL). It has an Mn/Cr ratio near zero (≈0.01) and hence, preserves the Cr isotopic composition (i.e. ^{53}Cr/^{52}Cr) of its host at the time of isotopic closure, which corresponds to the growth of chromite in the samples of low petrologic type. Chromites from the highest grade samples may record cooling below the closure temperature of the Mn-Cr system.

Model ages for the formation of chromite in OCs of different petrologic types can be obtained by comparing their Cr-isotope composition with the Cr-isotope evolution of a chondritic reservoir, using Solar System initial ε^{53}Cr and chondritic ^{55}Mn/^{52}Cr values and under the assumption of a canonical ^{53}Mn/^{55}Mn ratio[2]. In order to be able to systematically resolve the ingrowth of ^{53}Cr over a time span of a few Myrs, Cr isotope abundances need to be measured with high precision using Thermal Ionization Mass Spectrometry (TIMS).

Here we report first results for the model ages of chromite separated from three un-equilibrated type 3 and four equilibrated type 6 OC meteorites. Chromite grains from type 3 OCs show an average model age of ~3.5 Ma after the formation of the Solar System, while chromite grains from type 6 OCs record average age of ~9.3 Ma. The calculated mean ages correlate with the petrologic degrees of metamorphism of the host meteorites, which strongly supports an "onion-shell" structure of their parent body. Additionally, these ages better constrain the time of accretion and onset of metamorphism on the chondrite parent body at ~3.5 Ma.

REFERENCES

[1]Trieloff, M., Jessberger, E. K., Herrwerth, I., Hopp, J., Flénl, C., Ghélis, M., Bourot-Denise, M., Pellas, P. (2003). Structure and thermal history of the H-chondrite parent asteroid revealed by thermochronometry. Nature, 422 (6931), 502–506.
[2]Trinquier, A., Birck, J. L., Allègre, C. J., Göpel, C., & Ulfbeck, D. (2008). ^{53}Mn-^{53}Cr systematics of the early Solar System revisited. Geochimica et Cosmochimica Acta, 72 (20), 5146–5163.

P 2.2

Genesis of Early Archaean Continents: Constraints from Initial Sr- and Hf-Isotopes from Apatite and Zircon in the Western Dharwar Craton

Arathy Ravindran[1], Klaus Mezger[1], S. Balakrishnan[2], Ellen Kooijman[3], Melanie Schmitt[3], Dewashish Upadhyay[4], Jasper Berndt[5]

[1]Institut für Geologie, Universität Bern, Bern, Switzerland
(correspondence: arathy.ravindran@geo.unibe.ch)
[2]Department of Earth Sciences, Pondicherry University, Puducherry, India
[3]Department of Geosciences, Swedish Museum of Natural History, Stockholm, Sweden
[4]Department of Geology and Geophysics, IIT Kharagpur, Kharagpur, India
[5]Institut für Mineralogie, WWU, Münster, Germany

Crustal evolution models are primarily based on radiogenic isotope systematics in Archaean rocks with some preferential bias towards rocks formed after 3.0 Ga. The key problem is the scarcity of exposures of rocks older than 3.0 Ga and their common overprint by metamorphism and extensive deformation that obscure primary features including mineralogy and isotope systematics. This later (partial) reprocessing makes it difficult to obtain precise and accurate initial isotope compositions that can be used to reconstruct their petrogenesis. However, minerals such as apatite can preserve initial $^{87}Sr/^{86}Sr$ (Tsuboi and Suzuki, 2003) and zircon can preserve initial $^{176}Hf/^{177}Hf$ (Mezger and Krogstad, 1997). In addition, the U-Pb system in zircon records the time of mineral growth. The U-Pb ages and isotope information from minerals that preserve initial isotope composition (at least partially) are particularly powerful to reconstruct crust-mantle evolution prior to 3.0 Ga.

Igneous zircon grains from TTG gneisses record U-Pb ages ranging from 3.4 to 3.1 Ga. Rare detrital zircons from metasediments yield a maximum $^{207}Pb/^{206}Pb$ age of 3.6 Ga. Single apatite crystals from granitoids yield initial $^{87}Sr/^{86}Sr$ ~0.7013 that indicate a maximum mantle derivation age of 3.7 Ga for their precursor material. $^{87}Sr/^{86}Sr$ values in apatite from mafic rocks are close to the value expected for the BSE at that time. The Rb-Sr isotope system implies that only small amounts of felsic evolved continental crust existed (Dhuime et al., 2015) prior to the formation of the Dharwar Craton that started at ca. 3.6 Ga. Sm-Nd and Lu-Hf isotope systematics in felsic and mafic rocks are consistent with mantle depletion starting at 3.8 Ga.

REFERENCES

Tsuboi, M. & Suzuki, K., 2003: Heterogeneity of initial $^{87}Sr/^{86}Sr$ ratios within a single pluton: evidence from apatite strontium isotopic study, Chem. Geo., 199, 189-197

Mezger, K. & Krogstad, E. J., 1997: Interpretation of discordant U-Pb ages: An evaluation, J. metamorphic Geol. 15, 127-140.

Dhuime, B., et al., 2015: Emergence of modern continental crust about 3 billion years ago, Nature, 8, 552-555

P 2.3

Microbial mat growth rates inverted from Δ14C profiles

Franziska R. Blattmann[1,2], Timothy I. Eglinton[2], Negar Haghipour[2], Tessa S. van der Voort[3] & Tomaso R.R. Bontognali[4,5]

[1]Institute of Earth Surface Dynamics, University of Lausanne, Géopolis, 1015 Dorigny
[2]Erdwissenschaflticher Departement, ETH Zürich, Sonneggstrasse 5, 8092 Zürich
[3]Campus Fryslân, University of Groningen, Wirmurdijk 34, Leeuwarden, Netherlands
[4]Space Exploration Institute, Fbg de l'Hôpital 68, 2000 Neuchâtel
[5]Department of Environmental Sciences, University of Basel, Klingelbergstrasse 27, 4056 Basel, Switzerland

Microbial mats –a multi layered sheet of microorgansims– are among the earliest forms of life to have inhabited our planet. Some microbial mats produce laminated sedimentary structures called stromatolites that are present in sediments dating as far back as the Early Archean. Despite their importance for the study of the evolution of early life on Earth and their relevance in the search for life on Mars, little is known about microbial mat growth rates. Past studies have attempted to derive growth rates using various methods, but the interpretation of this data has been ambiguous (Ginsburg et al., 1954; Bahniuk Rumbelsperger, 2013). Consequently, it remains unclear how much time is recorded in stromatolitic sequences. Radiocarbon analysis of microbial mats is often hampered by the presence of allochthonous organic particles that are trapped within the authochthonous biomass. This study provides modeled radiocarbon measurements of microbial mats from two Qatari sabkha. The inhospitable environment of the Qatari desert leads to nearly all organic matter being produced in-situ via photosynthesis and therefor mirroring a clearer radiocarbon signature. The collected radiocarbon data at millimeter-scale vertical profiles through the mats show a bomb spike signal allowing for an inverse Monte Carlo modeling approach. An increase in growth rate throughout the age of the mat can be observed in the modeled data. The data shows that the 45-55 mm thick mats cannot be older than 60 to 70 years of age. The inferred microbial mat growth rate are higher than previously estimated, suggesting that Archean stromatolites may have formed in a relatively short period of time. This in turn sheds a new light on the development of one of the earliest life forms on the planet.

REFERENCES

Bahniuk Rumbelsperger A.M., 2013. Coupling organic and inorganic methods to study growth and diagenesis of modern microbial carbonates, Rio de Janeiro State, Brazil: Implications for interpreting ancient microbialite facies development, PhD Thesis ETH Zurich, ETH No. 20984.

Ginsburg, R.N., Isham, L.B., Bein, S.J. & Kuperberg, J. 1954. Laminated algal sediments of South Florida and their recognition in the fossil record. Marine Laboratory, University of Miami, Coral Gables, Florida: 54-208.

P 2.4

Organic matter flux Characterization by pyroloyse Rock Eval in the Majerda river

Raja Chairi[1], Arbia Triki[1], Nourséne Mahmoud[1]

[1]*Georesources laboratory, Center of Water Research and Technologies, Smartek Borje Cedria. BP273 8020 Soliman, Tunisie*

RE pyrolysis was initially designed to estimate the petroleum potential of sedimentary rocks (Espitalié et al., 1985). It has been considered as a low-cost and a technically less demanding method for the characterization and quantification of soil and modern sediment carbon, as it does not require any previous treatment of the sample (Sebag et al., 2016). These indices were used to reconstruct paleo-environments through the evolution of OM quality and quantity in sedimentary archives (Chairi, 2005, Zaccone et al., 2011), In this study we used this technique to characterize the organic matter delivered and deposited in the most important river of Tunisia : Wadi Majerda (Fig.1). Majerda or Bagrada takes its source near Souk Ahras, in the Constantine (Algeria), then flows east before flowing into the Mediterranean Sea (Gulf of Tunis). Flowing over more than 460 km which 350 in Tunisia. Sediment samples were collected at the old and new mouth of Majerda Wadi (OM and NM) along transverse transect of a depth of 0,45m. Sediments cores are taken every 5 cm and packaged in aluminum trays at 4 °C. 50–100 mg of dried sediment was used for RockEval6 (Vinci Technologies) analysis. The amount of nitrogen was determined with khjeldal, and Fe and Mn were determined by atomic absorption. Sediments of both investigated cores are predominantly clastic and composed of clay and silt, as well as fragments and mostly higher plants. The sediments exhibit a cyclic alternation of light clay and Fe-rich dark green to black laminae throughout the profil. It has been suggested that they result from redox conditions. XRD analyse reveals a monotonous and similar composition for both cores, regardless of the presence of laminae or other structures. It is characterized by illite, kaolinite, type clay minerals, calcite, quartz, halite, pyrite and hematite. TOC concentration of the old mouth Majerda wadi samples ranges between 1,22% and 2,63%. The values decrease in the deepest part (1%). The TOC concentrations in the new mouth of Majerda wadi range between 1,13% and 1,59%. The values are distributed in two deposit periodes. This pattern shows a high OM accumulation, greater export of organic sediment and weak dilution of OM content by mineral input. The C/N ratio distinguishes between terrestrial and aquatic sources (Kunz et al., 2011). The C/N values range between 6 and 13 in new mouth and between 9 and 73 in old mouth. These values demonstrate a significant contribution from terrestrial plants to the old mouth sediments and high contribution from phytoplankton and epiphytes in new mouth. Degradation of phytoplankton and epiphyticites materials in the water column will also increase C/N. A reverse correlation between S2 and TpS2 can be noted: a decrease in temperature is systematically accompanied by an increase in S2 in old mouth. This feature suggests the delivery of fresh and/or slightly weathered organic particles to the sediments. The lack of correlation between these parameters in the new mouth suggests an intense intake of detrital organic matter. The HI vs OI diagram also displays two distinct groups. The first one refers to highly variable HI values (140– 200 mg·HC/g·Corg) and OI values (240- 300 mg·O_2/g·C_{org}), whereas the second one has lower HI values (32– 135mg·HC/ g·C_{org}) and OI values varying from 94 to about 190 mg·O_2/g·C_{org}. The HI values progressively decrease along profiles. This process reflects a dehydrogenation of organic compounds during early diagenses.

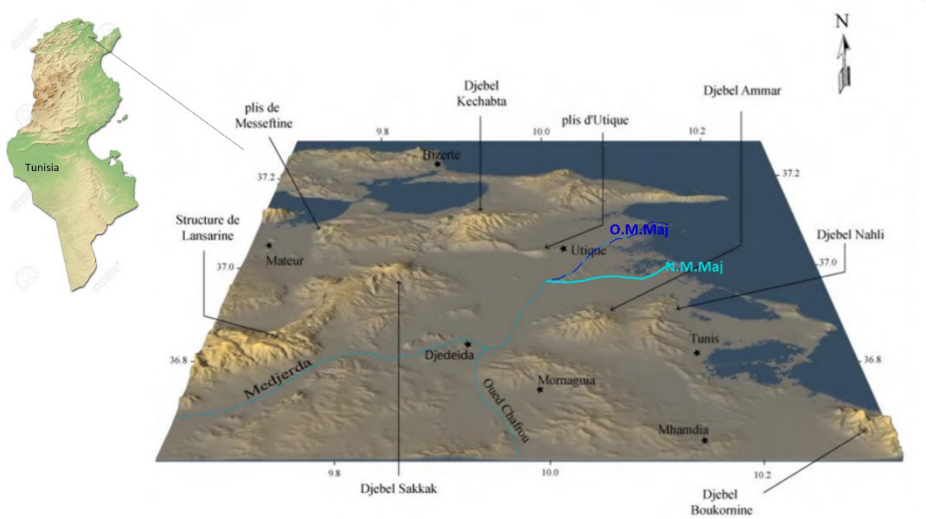


Figure 1 : Study location and sampling

There is a progressive increase of OI, resulting from the loss of C and H. This change is explained by a progressive oxidative transformation (mineralization and dehydrogenation) of organic compounds. In Majerda cores NM and OM similarly have thick oxic layer (6-12 cm and 7-14 cm), high Mn concentration up to 20 mg g-1 and TOC > 1% (tab.). Mn oxides may be employed by bacteria for the purpose of utilizing pools of refractory OM such as humic and fulvic acids, and furthermore may partially oxidize such complex carbohydrates. Higher (466-475°C) TpS2 results for Mouth Majerda (MM) sediments support that more oxygen-containing compounds contribute to OI values. Fe and Mn vertical profile have high concentrations in a surface layer, then decreasing to low and relatively constant concentrations at depth. The generally high T_{peak} values suggest that much OM distributed throughout MM could be composed of humic or fulvic acids because T_{peak} temperatures between 440 C and 470 °C are typically represented by these types of compounds in other systems (Hetényi et al., 2006). The vertical distribution of Mn in MM sediments also demonstrates that surface recycling of Mn oxides is in corrolation with accumulation and preservation of carbonates (r2 0,8).

REFERENCES

Chairi, R., 2005 Sedimentological study of sediment from an hypersaline system of oriental Tunisia in recent Quaternary: Moknine Sebkha. Quaternaire. 16.2. 107-117

Espitalié, J., Deroo, G. &Marquis, F., 1985. La pyrolyse Rock- Eval et ses applications; première partie. Revue de l'Institut Français du Pétrole 40, 563-579

Kunz, M.j., Anselmetti, est, A., Wehrli, B., ring, S.& Senn, D.B., 2011. Sediment accumulation and carbon, nitrogen, and phosphorus deposition in the large tropical reservoir, Lake Kariba (Zambia/Zimbabwe). J. Geophysical Research, 116, G03003, doi:10.1029/2010JG001538

Sebag, D., Verrecchia, E.P., Cécillon, L., Adatte, T., Albrecht, R., Aubert, M., Bureau, F., Calleau, G., Copard, Y., Decaëns, T., Disnar, J.-R., Hetényi, M., Nyilas, T. & Trombino, L., 2016. Dynamics of soil organic matter based on new Rock-Eval indices. Geoderma 284, 185–203.

Zaccone, C., Casiello, G., Longobardi, F., Bragazza, L., Sacco, A., Miano, T.M., 2011. Evaluating the "conservative" behavior of stable isotopic ratios ($\delta^{13}C$, $\delta^{15}N$, and $\delta^{18}O$) in humic acids and their reliability as paleoenvironmental proxies along a peat sequence. Chemical Geology 285, 124–132.

P 2.5

Maghemite (γ-Fe_2O_3) as a black pigment on a late 18th century tiled stove from Fribourg

Marino Maggetti[1], Bernard Grobéty[1] & Christoph Neururer[1]

[1]Department of Geosciences, Earth Sciences, University of Fribourg, Chemin du Musée 6, CH-1700 Fribourg (marino.maggetti@unifr.ch)

The black painting of a tiled stove attributed to the Fribourg manufacture of Johann Baptist Nuoffer, stylistically dated to the years 1780-1785, contains Mn-bearing, well shaped Fe-oxydes embedded in a Fe-rich glassy matrix. These crystals are interpreted as "recycled" hammerscale grains. According to experimental firings under air at 600°C, an iron steel will be coated with a complex oxydation layer (Iordanova et al. 2000). It is in fact a triple layer (Birosca et al. 2003, 2005; Dungworth & Wilkes 2007), consisting, from the inside to the outside, of wüstite (FeO), magnetite (Fe_3O_4) and hematite (α-Fe_2O_3). The hammering of a blacksmith breaks this very brittle layer into thousands of small particles (= hammerscale), a cheap potters black pigment. A combination of analytical techniques were employed in order to determine the exact crystallographic nature of this phase: (1) Optical microscopy observations on the diamond-polished sample; (2) Subsequent extensive scanning electron microscopy analyses coupled with an energy-dispersive spectrometer on the ultra-high polished sample (textural and chemical informations). This so-called "Siton" polishing of the sample surface reveals also the atomic structure on a submicron scale via electron backscattered diffraction; (3) transmission electron microscopy on a lamella produced by the focused ion beam technique, which increases the certainty of the crystals chemical composition and its lattice structure. In opposition to what has been already published, these crystals are maghemite (γ-Fe_2O_3) - not wüstite, magnetite nor hematite.

REFERENCES

Birosca, S., Dingley, D. & Higginson, R. L. 2004: Microstructural and microtextural characterization of oxide on steel using electron backscatter diffraction, Journal of Microscopy, 213, 3, 235-240.

Birosca, S., West, G. D. & Higginson, R. L. 2005: Microstructural investigation of the oxide scale on low carbon steel, Metal 2005, 1-8.

Dungworth, D. & Wilkes, R. 2007: An Investigation of Hammerscale. Technology Report, English Heritage Research Department Report Series no. 26.

Iordanova, I., Surtchev, M., Forcey, K. S. & Krastev, V. 2000: High-temperature surface oxidation of low-carbon simming steel, Surface and Interface Analysis, 30, 158-160.

P 2.6

Geochemistry and diagenesis of fossil tetrapod bones from the Late Triassic of Northern Switzerland

Annette Maurer[1], Christian A. Meyer[1], Leander Franz[1]

[1]*Department of Environmental Sciences, Quaternary Environmental Geology, University of Basel, Switzerland*

The objects of investigation are three fossil tetrapod bones from the Late Triassic. Two samples (FR1 and FR2) are bone fragments of *Plateosaurus engelhardti* from the clay pit Gruhalde in Frick (AG) that have been excavated from the upper part of the Gruhalde Member, Klettgau Formation (Norian). The deposits consist of greyish to light purple marl and some channels filled with dolomitic sandstones (Jordan et al., 2016). The third sample originates from a *temnospondyle amphibian* (?*Mastodonsaurus sp.),* which comes from the a 'bonebed' in the Belchen member of the Klettgau Formation (Rhaetian) in Schönthal (BL). The Rhaetian-'bonebed' is a conglomerate with a sandstone matrix (Omari, 2017). Both 'bonebeds' contain reworked faunal elements from mud flat playas, carbonate lakes or fluvial channels occurring within a wide seasonally dry alluvial plain (Meyer, 2017).

The samples were analysed with reflected and transmitted light microscopy and Raman spectroscopy. The results reflect different states of weathering due to varying depositional conditions and allow to draw conclusions about chemical and physical parameters of the depositional environment. Bioapatite (modelled as hydroxylapatite ($Ca_5[(OH)/(PO_4)_3]$)) is generally unstable in a range of varying geochemical conditions and dissolves easily. The alteration of hydroxylapatite (HAP) into a more stable phase like fluorine-enriched apatite requires particular physiochemical and microbial conditions during early diagenesis (Keenan, 2017).

The samples from Frick and Schönthal differ in their preservation of the bone structures and the composition of minerals as a result of different deposition and alteration. The bone structures (Cortex, spongiosa and saversian canals) of the samples from Frick are well preserved. The cortex completely consists of Fluorapatite ($Ca_5[F/(PO_4)_3$), which implies a complete alteration of bioapatite (modelled as Hydroxylapatite) ($Ca_5[(OH)/(PO_4)_3]$ into fluorapatite (FAP). Furthermore, the samples contain hematite (Fe_2O_3) and Calcite, which crystallized in cracks and voids.

The sample FR1 additionally contains Cu-rich minerals and iron sulphides. In some voids relicts of Chalcopyrite ($CuFeS_2$) were found, which formed due to percolating Cu-rich fluids. At the surface of the sample, Malachite ($Cu_2(CO_3)OH_2$) and Childrenite ($FeAlPO_4(OH)_2$) occur.

In contrast to FR1, the sample FR2 does not contain any iron sulphides but its alteration product Hematite. The voids are filled with different minerals like Quartz, Claudetite (As_2O_3) and Ankerite ($Ca(Fe,Mg,Mn)(CO_3)_2$). The lack of chalcopyrite leads to the conclusion of a longer exposition to oxidation than FR1 or a different composition of the percolating fluids. The bone structures of the sample NdS from Schönthal are strongly blurred by weathering. Further, no Harversian canals are present because of a complete replacement by pyrite (FeS_2) aggregates. The compacta and spongiosa is granular and contain a variation of different minerals like Bukovskyite ($Fe_2(AsO_4)(SO_4)(OH)x7H_2O$) Goethite (FeOOH), Quartz, Albite ($Na[AlSi_3O_8]$), Barite ($BaSO_4$) and carbonates. Noticeable is the absence of Apatite, which is due to the lack of required conditions to enable the alteration of HAP into the more stable FAP.

REFERENCES

P. Jordan, J.S. Pietsch, H. Bläsi, H. Furrer, N. Kündig, N. Looser, A. Wetzel, G. Deplazes 2017: The middle to late Triassic Bänkerjoch and Klettgau formations of northern Switzerland. Swiss Journal of Earth Sciences Vol. 109, Issue 2, pp 257–284

Ch. A. Meyer, A. Wetzel, E. Kustatscher 2017: The Norian Bonebeds of Northern Switzerland - "Deep in the Motherlode - It's Falling Like Water, Always Coming Down From Those Hills". Abstract European Association of Vertebrate Palaentologists. Zitteliana 91, p.63

S.W. Keenan, A. Summers Engel 2016: Early diagenesis and recrystallization of bone. Geochimica at Cosmochimica Acta 196 pp 209-221

K.M. Tanner 1978: Die Keuper-Lias Fundstelle von Niederschönthal, Kanton Baselland. Bulletin der Vereinigung Schweiz. Petroleum-Geologen und Ingenieure p. 13-23

P 2.7

$Ca_3Ti_2^{4+}H_2Si_2O_{12}$ – A new hydrogarnet?

Julien Reynes[1], Jörg Hermann[1] & Pierre Lanari[1]

[1]*Institute of Geological Sciences, University of Bern, Baltzerstrasse 3, 3012 Bern, Switzerland (julien.reynes@geo.unibe.ch)*

Garnet is a common mineral in high-pressure metamorphic rocks. Its structural formula does not contain any structural OH/H_2O groups, though it has been shown that significant amount of H_2O can be incorporated in the mineral lattice, where H^+ substitutes for cations (1-10 000 ppm wt. H_2O) (Aines and Rossman 1984a; Rossman and Aines 1991).

It has been proposed that the silicon vacancy point defect, with 4 H^+ substituting to a Si^{4+}(Cohen-Addad et al. 1967), is the main point defect incorporating water in garnet. However, the uniqueness of this hydrous point defect is questioned. Several observations support the possibility of other hydrous point defects: 1) Infrared spectra show up to 10 bands in the OH stretching region of garnet for a single sample, indicating that different environments are occurring around OH groups 2) the infrared peak positions vary with major element garnet chemistry 3) The affinity of garnet for OH groups varies with composition 4) FTIR OH bands show different behaviour/ speed when H is diffusing out of the lattice (Blanchard and Ingrin 2004; Kurka 2005; Reynes et al. 2018). Other nominally anhydrous minerals such as Olivine have been already intensively studied and it has been shown in the last decade that several point defects – in addition to Si vacancy help to incorporate OH groups in the lattice (Padron-Navarta et al. 2014).

In the quest of identifying new hydrous point defects in garnet, this study proposes an alternative approach to investigate the relation of water incorporation as a function of garnet composition. We developed an algorithm to stack maps of major element composition acquired by electron microprobe and OH maps acquired by high resolution Fourier transform infrared spectroscopy with different resolutions. Once the superimposition is complete, it is possible to compute the structural formula of garnet for the whole map, taking into account the H content.

This method has been applied to three hydrous Ca-rich garnets: one grossular (Ca-Al garnet), one Cr-Andradite (Ca-Cr/Fe^{3+} garnet) and one Ti-Andradite (Ca-Ti/Fe^{3+} garnet). The results suggest a 1/1 relationship between Ti and H content in the garnet structure. Therefore, a new hydrous point defect, consisting of $2H^+$ replacing one Si^{4+} in tetrahedral site with charge compensation achieved by the two Ti^{4+} in octahedral site is proposed. The theoretical endmember is $Ca_3Ti_2^{4+}H_2Si_2O_{12}$.

This new finding has some important geological consequences. For a given amount of water, twice as many Si vacancies are needed to host the H^+ compared to the classical hydro-garnet substitution, with implications for the rheology of garnet bearing rocks. Moreover, the charge balance will be significantly affected for water-rich garnet impacting on the calculated Fe^{2+}/Fe^{3+} ratio, which can be sensitive to oxygen fugacity. Identifying different hydrous point defects in garnet is also essential to constrain retentivity of OH groups in the crystal structure. As garnet is stable over a large P-T field it is able to carry water to the deep mantle.

REFERENCES

Aines RD, Rossman GR (1984a) The hydrous component in garnets: pyralspites American Mineralogist 69:1116-1126.

Blanchard M, Ingrin J (2004) Hydrogen diffusion in Dora Maira pyrope Physics and Chemistry of Minerals 31:593-605.

Cohen-Addad C, Ducros P, Bertaut EF (1967) Etude de la Substitution du groupement SiO_4 par $(OH)_4$ dans les composés $Al_2Ca_3(OH)_{12}$ et $Al_2Ca_3(SiO_4)_{2.16}(OH)_{3.36}$ de type grenat Acta Crystallographica 23:220-230.

Kurka A (2005) Hydrogen in Ca-rich garnets : diffusion and stability of OH-defects. Toulouse III Paul Sabatier

Padron-Navarta JA, Hermann J, Neill HO (2014) Site-specific hydrogen diffusion rates in forsterite Earth and Planetary Science Letters 392:100-112.

Reynes J, Jollands MC, Hermann J, Ireland T (2018) Experimental constraints on hydrogen diffusion in garnet Contributions to mineralogy and Petrology 173:68-70.

Rossman GR, Aines RD (1991) The hydrous components in garnets: Grossular-hydrogrossular American Mineralogist 76:1153-1164.

P 2.8

Highlighting complex textures by major and trace element mapping in high-pressure garnet

Thomas Bovay[1], Alex Bisch[2], Francesca Piccoli[1], Pierre Lanari[1], Daniela Rubatto[1]

[1]Institut für Geologie, University of Bern, Baltzerstrasse 3, CH-3012 Bern (thomas.bovay@unibe.ch)
[2]Département des sciences de la Terre, ENS de Lyon, 46 allée d'Italie, FR-69364 Lyon

Electron microprobe X-ray mapping analysis is a powerful tool to study quantitative major elements zoning in minerals. Trace elements zoning can provide supplementary information on the mechanisms of mineral growth and bulk rock element fractionation dynamic. Trace element mapping offers more complete information than profiles or spot analysis, but remains underexplored.

Here we present major and trace element maps performed on garnet with a complex zoning from a high-pressure garnet schist (Theodul Glacier Unit, Western Alps). Major element mapping is applied to highlight multiple growth stage textures and estimate pressure-temperature condition of mineral crystallisation. Trace element 2D maps with a pixel size of 16*11.42 µm were obtained with an automated LA-ICP-MS system. Because trace elements and in particular REE+Y diffuse very slowly in garnets, this is a powerful tool to understand and characterize successive fluid-rock interaction.

Major element results show that a first garnet generation with a unique chemical composition grew at 550 °C and 20 kbar. This garnet grow stage is successively fractured and replaced at peak metamorphism (560 °C and 25 kbar). The last generation present a sharp chemical transition and overgrowth during the retrograde path at 540 °C and 18 kbar. Major and trace element mapping are coherent, preserving the sharp chemical transition of the last replacement event, where REE + Y decrease sharply. V, Cr and Zn are the only elements to be enriched in the last garnet generation. These results and the trace element budget suggest that the last garnet generation is associated with input of external fluid poor in trace element likely coming from the surrounding ultramafic rocks.

P 2.9

Oxygen isotope characterization of the silicic Jurassic volcanics from Chon Aike Province (Patagonia): Investigating the origin of rhyolites linked to crustal melting

Michelle Foley[1], Zoé Guillhermin[1], Susanne Seitz[2], Benita Putlitz[1], Lukas Baumgartner[1]

[1]University of Lausanne, Geopolis Building, 1020 Lausanne, Switzerland (michelle.foley@unil.ch)
[2]Vanderbilt University, 5726 Stevenson Center, Nashville TN 37240, USA

The role of crustal melting in the generation of large-volume, highly silicic magmas is a much-debated topic. We present oxygen isotope data (in-situ SIMS and laser-fluorination) of the rhyolites comprising the Chon Aike Silicic Province (CASP) to characterize the potential magmatic source material and the crustal contribution in the generation of these widespread, voluminous melts. The Chon Aike is thought to be one of the largest silicic igneous provinces in the world, with an estimated volume of >235,000km^3 including exposures in both Patagonia and West Antarctica (Pankhurst *et al*., 1998). Previous geochronological studies demonstrate that volcanism swept across the region over ~30 My, but the eruptive episodes are inferred to concentrate into three periods of peak magmatism during the Jurassic: V1 (188-178 Ma), V2 (172-16 Ma), and V3 (162-153 Ma) (Pankhurst *et al*., 2000). We focus our study on the latter two periods of volcanism: the V2 Chon Aike Formation in the Deseado Massif (DM) region and the V3 El Quemado Complex with outcrops confined to the eastern Andean margin.

We sampled ignimbrites and rhyolitic lava flows from various localities of the El Quemado Complex and the Chon Aike Fm. across the Santa Cruz province of Argentina (Patagonia). Samples are silicic in composition (>70 wt % bulk SiO_2) and dominated by quartz +/- 2 feldspar.

Both zircon and quartz record high $\delta^{18}O$ values, ranging from 8-10 ‰ and 9-13 ‰, respectively. We show that quartz phenocrysts preserve their original magmatic composition and textures, even where alteration is prevalent. Alteration in the CASP region often results in a high bulk rock signature (10-17 ‰). In one rhyolite flow (DM) we distinguish two quartz generations, one magmatic with 9‰ and second younger one with a low $\delta^{18}O_{qtz}$ value of 2.3 ‰ and corresponding low $\delta^{18}O_{whole\ rock}$ (5.5 ‰). The observed high magmatic $\delta^{18}O$ values signify a significant crustal sediment component - supporting a petrogenic model of extensive partial melting of a crustal (sedimentary-rich) source in the generation of the CASP melts.

The high $\delta^{18}O$ rhyolites in the Chaltén region yield U/Pb ages ranging from 147 to 155 Ma, thus belonging to the youngest episode (V3) of Jurassic volcanism. We note the presence of inherited cores, preserving Proterozoic ages as old as 1300 Ma, which provides good evidence for the recycling of an older basement. Further work to identify potential source rocks and quantify the nature of the crustal input is in progress.

REFERENCES

Pankhurst, R.J., Leat, P.T., Sruoga, P., Rapela, C.W., Márquez, M., Storey, B.C. & Riley, T.R. 1998: The Chon Aike province of Patagonia and related rocks in West Antarctica: A silicic large igneous province. Journal of Volcanology and Geothermal Research 81, 113-136

Pankhurst, R.J., Riley, T.R., Fanning, C.M. & Kelley, S.P. 2000: Episodic Silicic Volcanism in Patagonia and the Antarctic Peninsula: Chronology of Magmatism Associated with the Break-Up of Gondwana. Journal of Petrology 41, 605-625

P 2.10

Epidote as a geochronometer in veins

Veronica Peverelli[1], Tanya Ewing[1], Martin Wille[1], Daniela Rubatto[1], Pierre Lanari[1], Igor M. Villa[1,2], Marco Herwegh[1], Alfons Berger[1]

[1]Institut für Geologie, University of Bern, Baltzerstrasse 1+3, CH-3012 Bern (veronica.peverelli@geo.unibe.ch)
[2]Università di Milano-Bicocca, I-20126 Milano

Much attention has been paid to the role of fluids in the crystalline continental crust as they mediate mass transfer, and influence chemical and physical processes such as crustal metamorphism. Important and clear evidence of fluid flow are veins at different crustal levels. Epidote, whose potential as a mineral chronometer and geochemical tracer is still poorly known, is a common mineral in veins and represents a promising proxy to unravel their long-term fluid history. Epidote is a robust mineral that mainly records brittle deformation, without being reset by dynamic recrystallization processes. Epidote can incorporate radioactive as well as non-radiogenic trace elements, and thus may serve as both geochronometer and geochemical tracer. By exploiting these two qualities of epidote we aim at obtaining information on fluid flow during vein formation. We investigated epidote veins from the Albula region (Albula Granite, Eastern Alps), from Grimsel Pass and from the Gelmersee area (Zentraler Aare Granite, Aar Massif, Central Alps), and from the Heyuan Fault (Yashanian Granite, Guangdong Province, China). To constrain the timing of formation of such veins, we developed an analytical protocol for in situ LA-ICPMS U-Pb dating of epidote. Such measurements are challenging because, relative to well-established U-Pb geochronometers, epidote has low U concentrations and incorporates high concentrations of initial Pb. Our approach uses radioactivity imaging (i.e. a Beta-scanner) in order to target epidote zones with the highest U concentrations for in situ U-Pb dating by LA-ICPMS. We have established the suitability of allanite as a sufficiently matrix-matched standard for epidote in spot analysis mode, given the lack of an epidote standard. We have successfully applied the isochron approach to three epidote veins from the Aar Massif, one from the Albula region and one from the Heyuan Fault, thus obtaining reliable U-Pb ages as well as initial $^{207}Pb/^{206}Pb$ compositions. The ages measured in veins from Grimsel Pass and from the Gelmersee area can be ascribed to the Handegg phase (~20-17 Ma) of Alpine deformation. We were hence able to exclude our initial hypothesis that these epidote veins might have recorded fluid flow during the Jurassic. The initial $^{207}Pb/^{206}Pb$ compositions indicate a uranogenic inherited component, which is isotopically different between Grimsel Pass and the Gelmersee area, indicating isotopic heterogeneity in the fluid(s) circulating in the Zentraler Aare Granite during the same Alpine phase. The vein from the Albula region yielded a Paleocene age and its initial $^{207}Pb/^{206}Pb$ ratio is consistent with a two-stage evolution model Pb composition. The vein from Heyuan Fault gave an age on the boundary between Early and Late Cretaceous and is consistent with stratigraphic and structural relations in the area. Its initial $^{207}Pb/^{206}Pb$ composition indicates a uranogenic inherited component. One epidote vein from Grimsel Pass yielded a data set which does not meet the criteria for the isochron approach (i.e. same age and initial Pb isotopic composition for all analyzed grains). The data suggest that either 1) grains of different formation ages are present or 2) the U-Pb system of some grains was affected by secondary (i.e. chemical and/or physical) processes. Our in situ laser ablation data will be discussed in reference to solution MC-ICPMS bulk measurements of U and Pb isotopes in vein-epidote micro-separates from the same samples. Our results show that the development of U-Pb dating of epidote can provide a valuable new chronometer for dating fluid-related processes recorded in veins from a wide range of geological settings. The current challenge is to increase the precision of the isochron ages, which is in the order of 5-25%. Despite the relatively large uncertainties, such ages are still relevant within the geological history of the areas of interest and provide useful ages where no other datable mineral is present.

P 2.11

Internal structure of a felsic intrusion: the Catedral granite, Torres del Paine, Patagonia

Lorenzo Giacomazzi[1], Lukas P. Baumgartner[1]

[1]*Institut des sciences de la Terre, University of Lausanne, Géopolis, CH-1015, Lausanne (lorenzo.giacomazzi@unil.ch)*

The Torres del Paine igneous complex (TPIC) in southern Chile, is a well preserved and exposed intrusion of Miocene age. It is composed of a mafic complex (PMC) at the bottom and a granitic laccolith (TPL) on the top (Leuthold et al., 2012). Based on field observations and high precision dating, three units were defined inside the TPL (Michael et al. 2008). They intruded by underaccretion over the short period of 90±40 Ky. Individual units intruded in a brittle fashion, hence we call each unit a magmatic batch. In contrast, the PMC formed by overaccreation (Leuthold et al., 2012). Here we present new field and textural data on the youngest granite batch.

The youngest and largest batch is the Catedral granite or unit (III). It occupies a volume of ~54 km^3 (Leuthold et al. 2012). Evidences of magmatic pulses inside this batch (Catedral granite) are recognized on the field due to changes in rock fabrics, such as (1) textures, (2) mineral modal abundances, (3) occurrence of mafic enclaves and (4) grain size. Contacts between pulses are mostly ductile, with local brittle dyking. They are often accentuated by the presence of biotite and hornblende schlieren-like accumulations. Dyke injections and structural crosscut relations were used to determine the relative time of emplacement. This reveal that pulses intruded in a random order, rather than by under- or over-accretion. Pulses are generally sub-horizontal and variable in size. Their thickness is up to a few tens of meters and some of the larger individual pulses can be followed up to at least a kilometre. Hence pulse sizes seem to range from a few 10^3 m^3 to over 10^5 m^3 of individual pulses intruding at rates high enough to maintain partially molten, ductile environments. Microscopic observations indicate a broad variety of textures. Cumulus and miarolitic textures are present in the granites and can strongly vary between individual pulses. The outstanding preservation of magmatic textures also allow to identify the method of melt escape: melt was mobilized and “escaped” individual pulses through neighbouring pulses by coalescence of melt porosity into microgranitic and aplitic small (cm to decimetre) dykes.

Hence detailed mapping and petrology allows to identify the hierarchy which forms a shallow intrusion: rapid and arbitrarily intruding pulses are alternating with periods of relative quiescence, during which time the batches cooled likely below their solidus.

REFERENCES

Leuthold, J., Müntener, O., Baumgartner, L. P., Putlitz, B., Ovtcharova, M., and Schaltegger, U. 2012: Time resolved construction of a bimodal laccolith (Torres del Paine, Patagonia), Earth and Planetary Science Letters, 325-326:85-92.

Michel, J., Baumgartner, L., Putlitz, B., Schaltegger, U., and Ovtcharova, M. 2008: Incremental growth of the Patagonian Torres del Paine laccolith over 90 ky, Geology, 36(6):459-462.

P 2.12

Understanding minor elements in iron bloomery slag from archaeological excavations

Ildiko Katona Serneels[1], Vincent Serneels[1]

[1]*Department of Geosciences, University of Fribourg, Switzerland*

Before the development of the blast furnace in the 14th century AD and the production of cast iron in the liquid state, iron was made by smelting iron ores in a small furnace, the bloomery. The conditions in the furnace (oxygen fugacity, temperature, time) are strong enough to reduce part of the iron oxides into metallic iron but not to melt the metallic phase. The unreduced iron oxides and the other substances present in the ore must form a liquid slag. The main components of this slag are fayalite (Fe_2SiO_4), hercynite ($FeAl_2O_4$), wüstite (FeO) and leucite ($KAlSi_2O_6$).

The minor elements in the smelting slag are inherited from the different components of the system: the iron ore, the charcoal ashes and the partially fused internal lining of the furnace walls.

Several minor elements, like Phosphorus, Titanium, Manganese, Chromium, Vanadium, Cobalt and Nickel are frequently abundant in various types of iron ores. Their presence and concentrations are related to the ore forming processes. During the smelting process, highly reducible minor elements (like Nickel, Cobalt and Copper) will partition massively in the metallic mass. On the other hand, unreducible minor elements (like Titanium and Barium) will be trapped into the silca-rich slag. Mildly reducible minor elements (like Phosphorus, Manganese, Chromium and Vanadium) will partition in a more complex way depending on the conditions in the furnace.

During the cooling of the slag, the minor elements will be trapped preferentially in the first crystallising mineral at high temperature. The partitionning process is strongly influenced by the oxygen fugacity in the furnace and the state of oxidation of the considered cation.

Chemical data obtained from minerals in recently studied smelting slag will be presented.

P 2.13

Reconstruction of the supply of lithic materials in the Roman city of Aventicum (VD, Switzerland)

Morgane Surdez[1], Vincent Serneels[1]

[1]*Department of Geosciences, University of Fribourg, Chemin du Musée 6, CH-1700 Fribourg (morgane.surdez@unifr.ch)*

Aventicum (VD, Switzerland) was the capital of the Helvetians during Roman times. Many rocks were used in this city, mainly for architectural purposes, put also for utilitarian (e.g. millstones, inscriptions) and decorative (e.g. marble veneers, mosaics, sculptures) objects.

We can identify three different areas from which rocks were imported to Aventicum. The first one is the immediate proximity of the city, where we can find molasse, shelly sandstone, calcareous tufa, fluvio-glacial deposits. These materials are easy to exploit and to transport to the city. However it is in the second area, the Jura mountains, that we find limestones, which are abundantly used in Avenches. The rocks from this area are at a greater distance but could be quite easily imported into the Roman city by lacustrine and fluvial transport. The third sector contains the more remote resources, such as alpine or Mediterranean marbles, French basalts, Asian gemstones. Considerable efforts in terms of transport are necessary, showing a real desire from the Helveto-Romans to hold objects produced from these materials.

The first step of this PhD thesis in archaeometry is to characterise the different rocks used in Aventicum during Roman times, in order to determine their provenance. The second part will be to reconstruct the supply routes of these lithic materials, considering the quantity of each rock type. It will contribute to a better understanding of the reasons behind the choices of these different materials.

P 2.14

Geochronology of the Terre Adélie Craton (East Antarctica)

Maria Naumenko-Dèzes[1], Yann Rolland[1,2], Sylvain Gallet[1]

[1]Université Côte d'Azur, CNRS, OCA, IRD, Géoazur, 250 rue Albert Einstein, Sophia Antipolis 06560 Valbonne, France. (marie@geosphere.ch)
[2]EDYTEM, Université de Savoie – CNRS, UMR 5204, Le Bourget du Lac, France.

The Terre Adélie craton (East Antarctica) is an example of complex continental crust, which underwent several high-grade deformation phases during Neoarchean to Mesoproterozoic times (e.g., Fitzsimons, 2000). At least two tectono-thermal events have affected the whole Terre Adélie Craton, which resulted in superimposed ductile strain fields (Ménot et al., 2005; Lamarque et al., 2016). However, it remains controversial which part of the mineral fabric observed at the scale of the Terre Adélie Neoarchean basement can be attributed to the Neoarchean and which to the Paleoproterozoic deformation phases (Ménot et al., 2005; Duclaux et al., 2008; Lamarque et al., 2016). The combination of several geochronometers, or the dating of several minerals, within the same rock, in relation to specific structural sites in the field (shear zones, dykes, undeformed rocks…) allows to pinpoint the different tectonic events which occurred during the long-lived evolution of continents (e.g., Bosse and Villa, 2019).

Twenty-two samples from the Terre Adélie were chosen from the collection of samples gathered during the missions of 1998 and 2004. Bt and Amph pairs were hand picked for Ar/Ar dating in two laboratories. Fifty-three single grain 40Ar/39Ar dating laser step-heating measurements were carried out at Géoazur in Nice University (France) on the ARGUS VI mass-spectrometer, ten samples were additionally measured with oven step-heating routine in University of Milano Bicocca (Italy) on the Nu Instruments Noblesse rare gas mass spectrometer.

The comprehensive dataset obtained and compiled in this study allowed us to give a new interpretation to the earlier results. The ages are lying in the range of 1800-1500 Ma which corresponds to the second Paleoproterozoic deformation phase that affected the whole Terre Adéle Craton, including the Dumont D'Urville basin. It was sufficiently high grade to reset all the biotites and most of the amphiboles which crystallized before in the Neoarchean basement, even in cases where the granulite facies texture is well preserved. Given the variability of ages obtained in narrow outcropping zones, we suggest that the age groups are representative of a petro-chronological evolution related to superimposed deformation / fluid flow events rather than cooling in relation to a long-lived regional-scale thermal event. Based on the probability distribution curves of amphiboles and biotites at the scale of the Terre Adélie Craton, three to five stages of recrystallization can be discretized.

REFERENCES

Bosse, V., Villa, I.M., 2019. Petrochronology, hygrochronology of tectono-metamorphic events. Gondwana Research, doi: 10.1016/j.gr.2018.12.014.

Duclaux, G., Rolland, Y., Ruffet, G., Ménot, R. P., Guillot, S., Peucat, J. J., et al., 2008. Superimposed Neoarchaean and Paleoproterozoic tectonics in the Terre Adélie Craton (East Antarctica): evidence from Th–U–Pb ages on monazite and 40Ar/39Ar ages. Precambrian Research 167(3-4), 316-338.

Fitzsimons, I.C.W., 2000. A review of tectonic events in the East Antarctic shield and their implications for Gondwana and earlier Supercontinents. Journal of African Earth Sciences 31 (1), 3–23.

Lamarque, G., Bascou, J., Maurice, C., Cottin, J. Y., Riel, N., Ménot, R. P., 2016. Microstructures, deformation mechanisms and seismic properties of a Palaeoproterozoic shear zone: The Mertz shear zone, East-Antarctica. Tectonophysics 680, 174-191.

Ménot, R.P., Pêcher, A., Rolland, Y., Peucat, J.J., Pelletier, A., Duclaux, G., Guillot, S., 2005. Structural setting of the Neoarchean terrains in the Commonwealth Bay Area (143–145◦E), Terre Adélie Craton, East Antarctica. Gondwana Research 8, 1–9.

P 2.15

Pumpellyosites as markers of chemically evolved hydrothermal discharge in the oceanic crust, and their relation to massive sulfide (VMS) deposits

Samuel Weber[1], Larryn W. Diamond[1]

[1]Rock–Water Interaction Group, Institute of Geological Sciences, University of Bern, Baltzerstrasse 3, 3012 Bern (samuel.weber@geo.unibe.ch)

Seawater–basalt interactions are crucial for the formation of black-smoker type volcanogenic massive sulfide (VMS) deposits at the seafloor and they influence the chemical composition of the oceans. Reactions of fresh basalts with downwelling seawater add Mg and Na to the rock and leach Ca, leading to «spilite» alteration (chlorite+albite+Fe-oxides+titanite±epidote±quartz±calcite; Alt, 1995). After seawater has chemically evolved via such reactions, it may generate Ca-enriched, Na-Mg-depleted «epidosite» alteration (epidote+quartz+Fe-oxides+titanite; Richardson et al., 1987) along the upwelling path of its circulation cycle. In addition to epidosites, Harper (1995) described pumpellyosites (pumpellyite+quartz+chlorite±epidote) in the Josephine ophiolite (USA), reflecting chemical changes similar to epidosites. Pumpellyosites formed close to epidosites, but stratigraphically higher up, near to the paleo-seafloor and were therefore interpreted to form from the cooling epidosite fluid.

Following the discovery of huge epidosites in the volcanic pile of the Semail ophiolite, Oman (Gilgen et al., 2016) we have now found ~1 km^2 outcrops of intense, pervasive pumpellyosite alteration higher in the lava sequence, up to 30 m below the paleo-seafloor. In contrast to the dark blue-green Fe^{2+}-rich Josephine pumpellyosites, the Oman examples are a striking mustard colour, reflecting high Fe^{3+} contents. Further, their Ca-enriched, Na- and Mg-depleted bulk-rock compositions are very similar to the underlying epidosites. Accordingly, these pumpellyosites also appear to be low-*T* equivalents of epidosite alteration. Thus, they mark sites at which highly evolved hydrothermal fluids in the oceanic crust discharge onto the seafloor. Their metasomatic fingerprint contrasts strongly with the chlorite–quartz alteration found below black-smoker vents. Whether the evolved fluids that form pumpellyosites and epidosites can form VMS deposits is highly questionable, as there is no sign of mineralisation on the seafloor above the newly discovered pumpellyosites.

REFERENCES

Alt, J.C. 1995: Subseafloor Processes in Mid-Ocean Ridge Hydrothermal Systems, Geophysical Monograph, 91, 85-114

Gilgen, S.A., Diamond L.W. & Mercolli, I. 2016: Sub-seafloor epidosite alteration: Timing, depth and stratigraphic distribution in the Semail ophiolite, Oman, Lithos, 260, 191-210

Harper, G. 1995: Pumpellyosite and prehnitite associated with epidosite in the Josephine ophiolite – Ca metasomatism during upwelling of hydrothermal fluids at a spreading axis, Geological Society of America Special Papers, 296, 101-122

Richardson, C.J., Cann, J.R., Richards, H.G. & Cowan, J.G. 1987: Metal-depleted rott zones of the Troodos ore-forming hydrothermal systems, Cyprus, Earth and Planetary Science Letters, 84, 243-253

P 2.16

Rate of eruptible magma assembly preceding Toba's super-eruptions

Ping-Ping Liu[1,2,3]*, Sun-Lin Chung[2,4*], Xian-Hua Li[3], Qiu-Li Li[3], Mei-Fu Zhou[5], Yu-Ming Lai[6], Azman A. Ghani[7], Theodora Sihotang[8], Tom E. Sheldrake[9], Guy Simpson[9], Luca Caricchi[9]

[1]Key Laboratory of Orogenic Belts and Crustal Evolution, School of Earth and Space Sciences, Peking University, Beijing, China
[2]Institute of Earth Sciences, Academia Sinica, Taipei, Taiwan
[3]Institute of Geology and Geophysics, Chinese Academy of Sciences, Beijing, China
[4]Department of Geosciences, National Taiwan University, Taipei, Taiwan
[5]Department of Earth Sciences, the University of Hong Kong, Hong Kong
[6]Department of Earth Sciences, National Taiwan Normal University, Taipei, Taiwan
[7]Department of Geology, University of Malaya, Kuala Lumpur, Malaysia
[8]Samosir Geoarea Management Board, Toba Caldera Geopark, Indonesia
[9]Department of Earth Sciences, University of Geneva, Geneva, Switzerland

Accumulation of enormous amounts of hot and eruptible magma (<50 vol.% crystals) in growing magma reservoirs is essential for super-eruptions. However, the timescales of reservoir construction and relative amounts of potentially eruptible and injected magma remain poorly constrained. Here, we integrate zircon petrochronology and thermal modelling to constrain the rate of eruptible magma accumulation at the Toba volcano in Indonesia, a system that produced two super-eruptions on Earth over the last 1 million years. Our results show that within this system magma has been accumulated since at least 2.2 Ma at a rate of about 4 cubic kilometres per millennium, 20-50% of which is eruptible. Thus, the Toba plumbing system contains today about 150 cubic kilometres of potentially eruptible magma. Our approach can be applied to other active volcanoes to gauge the volume of potentially eruptible magma present today in their subvolcanic systems.

P 2.17

Consequences of magma-CO_2 interaction for explosive volcanism at Colli Albani (Italy)

Corin Jorgenson[1], Luca Caricchi[1], Gregor Weber[1], Guido Giordano[2], Felix Marxer[3], Peter Ulmer [3], & Peter Tollan[4]

[1]Department of Earth Sciences, University of Geneva, Rue de Maraîchaire 13, CH-1205 Genève, (corin.jorgenson@etu.unige.ch)
[2]Department of Science Geology, Università Degli Studi Roma Tre, Via Ostiense, 159, 00154 Roma
[3]Department of Earth Sciences, ETH Zurich, Sonneggstrasse 5, 8092 Zurich, Switzerland
[4]Institute of Geological Sciences, University of Bern, Baltzerstrasse 1+3, CH-3012 Bern

Understanding the processes that trigger explosive eruptions in densely populated areas is important for volcanic hazard assessment. Located 30 km from the city of Rome, Colli Albani is a caldera complex that is currently experiencing seismic and degassing activity, and intermittent uplifts possibly related to magmatic intrusions. This ultrapotassic volcano has produced a series of large eruptions between 600 and 355 ka (up to 63 km^3 DRE per eruption) creating pyroclastic flows extending up to 33 km from the eruptive centre (Giordano & CARG team, 2010). These ignimbrites are mafic in composition, which is rarely observed for such explosive events, as the rheological properties of mafic melts typically favour effusive eruptions. The cause of this unusual explosivity is thought to be related to magma-CO_2 interaction (Freda et al. 2011; Giordano & CARG team, 2010). However, the origin of the CO_2 and its role in driving explosive volcanism are not well constrained. We test this hypothesis by analysing crystal zonation patterns and melt inclusions in products of both explosive and effusive eruptions to determine the evolution of magma chemistry and volatile content before eruption and to determine whether the explosivity of the eruptions is linked to specific magma properties. Melt inclusions hosted in leucite and clinopyroxene have been homogenized using piston cylinder experiments at 7 kbar, temperatures ranging from 1200-1350 °C and run times from 0.5-4 hours. Detailed petrography and mineral chemistry will be combined with determination of volatile contents to gain quantitative insights into magma source conditions, accumulation and/or loss of the excess fluid phase, and the evolution of intensive parameters prior to eruption. These data will be used in conjunction with thermodynamic modelling (rhyolite-MELTS) to evaluate if magma-CO_2 interaction is a physically plausible scenario for driving explosive volcanism at Colli Albani and to assess whether magma-CO_2 interaction at Colli Albani is better explained by carbonate assimilation or by flushing of a magma reservoir with CO_2 from depth.

REFERENCES

Freda, C., Gaeta, M., Giaccio, B., Marra, F., Palladino, D.M., & Scarlato, P. 2011: CO_2-driven large mafic explosive eruptions: The Pozzolane Rosse case study from the Colli Albani Volcanic District (Italy). Bull Volcanol. 73(3), 241–56.

Giordano, G., & CARG Team. 2010: Stratigraphy, volcano tectonics and evolution of the Colli Albani volcanic field. The Colli Albani volcano. Geol Soc London, Spec IAVCEI Publ. 3, 43-98.

P 2.18

Probabilistic graphical models to assess tectonic controls on arc volcanism

Tom Sheldrake[1], Luca Caricchi[1]

[1]Département des sciences de la Terre, Université de Genève, Rue des Maraîchers 13, 1205 Genève, Switzerland (thomas.sheldrake@unige.ch)

The record of eruptions is often sparse because volcanoes can remain dormant and not erupt for many centuries or millennia. Comparing volcanoes over these long timescales is thus difficult, as the spectrum of eruptive behaviour that is observed at an individual volcano is unlikely to have encompassed what is naturally possible or even has possibly occurred. To address this issue a common approach is to group volcanoes, often by geographical region, to understand how the average eruptive behaviour varies as function of different independent parameters. However, the scarcity of the eruption record is further confounded by recording biases associated with the age and size of volcanic eruptions, as well as the location of a volcano itself, leading to analyses that focus on regions or datasets that are well studied and well recorded. We investigate approaches to incorporate valuable observations from regions in which observations are sparse or limited. We use probabilistic graphical models, in combination with ensemble methods to understand the role that regional tectonics has in influencing the geochemistry, style and magnitude of volcanic eruptions.

P 2.19

Experimental model for lava fountaining: the case study of 26 January - 24 June 2000 at south east crater (Mt. Etna, Italy)

Alessandro Musu[1,4], Daniele Morgavi[1], Laura Spina[2], Rosa Anna Corsaro[3], Diego Perugini[1]

[1]Department of Physics and Geology, University of Perugia, Piazza dell'Università, 1, 06123 Perugia, Italy.
[2]Istituto Nazionale di Geofisica e Vulcanologia, Sezione di Roma 1, Roma, Italy.
[3]Istituto Nazionale di Geofisica e Vulcanologia, Osservatorio Etneo, Sezione di Catania, Catania, Italy.
[4]Department of Earth Sciences, University of Geneva, Rue des Maraîchers 13, CH-1205 Geneva, Switzerland.

Basaltic volcanoes represent a large portion of the active volcanoes worldwide providing up to the 70% of sub-aerial volcanic discharge. Is therefore not surprising the ever-increasing number of studies devoted to the investigation of the link between plumbing system dynamics and eruptive style. Basaltic eruptive activity may vary widely from lava effusion up to rare violent Plinian eruptions. However, the most iconic explosive activities of basaltic volcanoes are represented by Strombolian explosions and lava fountains. To justify the onset, periodicity and the transition between the above-mentioned eruptive styles, different hypothesis on the degassing dynamics have been made. Here, we make use of a laboratory volcano, Mt. Etna, to test the validity of these assumptions and to calculate different volcanological parameters (e.g. erupted volume and gas flux in the plumbing system). In particular, we focus on an exceptional series of lava fountains observed in 2000 at South East Crater, with a multi-parametric approach. First, we investigate the pattern of geochemical data to infer the evolution of magmatic source. Thin sections from selected lava fountain episodes are analyzed and the correlations between the 2000 and the 2011-12 eruptions, which represent another incredible cyclic series of fountain activity, are also studied. Then, we assumed the collapse foam model CF (Jaupart and Vergniolle, 1989) as the reference source model for the 2000 eruption, looking for the best parameters that allows to fit the observed pattern and eruptive behavior (e.g. intermittence time, erupted volume of lavas etc.). Moreover, we performed several experiments using the experimental apparatus of Jaupart and Vergniolle (1988, 1989) having different viscosity from 0.001 Pas to 10 Pa s to constrain the effect of viscosity onto the rate of foam collapse. The experimental apparatus was reproduced in two different sizes in order to test the efficiency of the machine at different scales either with water or silicone oil.

REFERENCES

Jaupart C. and Vergniolle S. (1988). Laboratory models of Hawaiian and Strombolian eruptions. Nature, 331 (6151), 58.
Jaupart C. and Vergniolle S. (1989) The generation and collapse of foam layer at the roof of a basaltic magma chamber. J. Fluid Mech. 203, 347 – 380.

P 2.20

Geochemistry Of The Sturtian-Aged Hamama Iron Formations: Implication On The Origin Of Neoproterozoic Banded Iron Formations Of The Arabian-Nubian Shield

Yasser Abd El-Rahman[1], Jens Gutzmer[2], Xian-Hua Li[3], Thomas Seifert[2], Chao-Feng Li[3]

[1]Geology Department, Cairo University, Giza 12613, Egypt (yasser@sci.cu.edu.eg)
[2]Department of Mineralogy, TU Bergakademie Freiberg, 09596 Freiberg, Germany
[3]Institute of Geology and Geophysics, Chinese Academy of Science, Beijing 100029, China

Neoproterozoic time is characterized by the sudden reoccurrence of banded iron formations after a one billion year hiatus in the sedimentary record. The origin of these Neoproterozoic iron formations exposed in the Arabian-Nubian Shield is a matter of debate. Both non-glaciogenic exhalative zipper-rift hypothesis (Basta et al., 2011) and glaciogenic Snowball Earth hypothesis (Stern et al., 2006) were proposed to justify the formation of these iron-rich sedimentary rocks in the Eastern Desert of Egypt.

The Neoproterozoic iron formation deposits are exposed in the central segment of the Eastern Desert of Egypt, which constitutes the northwestern extension of the Arabian-Nubian Shield. One of these iron-formation is the Wadi Hamama area. In this area, mafic and felsic volcanic and volcaniclastic rocks of an intra-oceanic island-arc setting host multiple, thin iron-formation units. Precise age constraints on these deposits are provided by zircon yielded from the volcaniclastic rocks alternating with the iron bands. The obtained age (ca. 695 Ma) is correlated with the well-recognized Sturtian glaciation episode.

The geochemical data of the Hamama iron-formations indicate the minimal detrital contribution. Thus, these data reflect the signature of either the hydrothermal fluids contributed to their deposition and/or the basin conditions in which these iron-formations deposited. Europium anomalies, which are commonly used as a proxy to identify hydrothermal contributions to iron-formations, of the Hamama iron-formations range from 0.8 to 1.73 with an average of 1.16. These results indicate that iron was most likely sourced from low-temperature hydrothermal fluids vented into the basin, which is restricted within this arc system, which is supported from the geochemistry of the host volcanic rocks. The Hamama iron-formations display a low Pr/Yb_{SN} ratio averaging 0.26 and do not show any Ce anomaly, which is similar to many modern iron-rich crusts formed in oxygenated ocean. The Hamama iron-formations display positive εNd(t) values ranging from 2.3 to 5.4, which are different from negative εNd(t) values characterizing other glaciogenic Neoproterozoic Rapitan-type iron-formations. These findings refute the necessary connection between the formation of Neoproterozoic iron-formations of the Arabian-Nubian Shield and glaciation.The results of these analyzed iron-formations ascribed their formation to the exhalative hydrothermal fluids similar to modern exhalites formed in oxygenated basins. The zipper-rift hypothesis attributed the formation of Neoproterozoic iron-formations to extensive hydrothermal activities in rift basins related to the breakup of Rodinia after 750 Ma. However, the Egyptian iron formations and the rest iron-formation deposits of the Arabian-Nubian Shield are associated with arc-related volcanic and volcaniclastic rock assemblages, which are unrelated to rifting of Rodinia, but instead are linked to Neoproterozoic juvenile crustal growth through accretion and assembly of island arc terranes. The abundance of iron-formations in the ANS could be related to extensive submarine hydrothermal systems associated with and preserved within the largest amounts of arc materials involved in the intense growth of the large Neoproterozoic juvenile crust.

REFERENCES

Basta, F.F., Maurice, A.E., Fontboté, L., Favarger, P. 2011: Petrology and geochemistry of the banded iron formation (BIF) of Wadi Karim and Um Anab, Eastern Desert, Egypt: Implications for the origin of Neoproterozoic BIF, Precambrian Research, 187, 277-292.

Stern, R.J., Avigad, D., Miller, N.R., Beyth, M. 2006: Evidence for the Snowball Earth hypothesis in the Arabian-Nubian Shield and the East African Orogen, Journal of African Earth Sciences, 44, 1-20.

3. Stable isotope geochemistry: development and applications

Afifé El Korh, Andres Rüggeberg, Nicolas Greber

TALKS:

3.1 Decraene M.N., Marin-Carbonne J., Thomazo C., Olivier N., Philippot P., Deloule E.: Deciphering microbial signatures in stromatolites through micrometric in situ iron and sulfur isotope analyses.

3.2 El Korh A., Luais B., Boiron M.-C., Cividini D.: Multi-isotope study (Ge, Fe, O) of hydrothermal metamorphism in the Limousin ophiolite

3.3 Hammerli J., Kemp T.: How does anatectic melt receive its isotopic fingerprint? A case study from the Halls Creek Orogen, WA, Australia

3.4 Kaufmann A., Pettke T., O'Sullivan E., Wille M.: Molybdenum isotope fractionation between melt, exsolved fluid and hydrothermal minerals during the magmatic-hydrothermal transition

3.5 Marin-Carbonne J., Thomazo C., Decraene M.N., Saitoh M., Alleon J., Olivier N.: Microscale Fe and S isotope compositions of Archean pyrites can constrain past microbial metabolism and post deposit processes

3.6 O'Sullivan E., Nägler T., Babechuk M.: Tracing anthropogenic δ^{98}Mo in riverine water: Implications for palaeo-redox reconstruction

3.7 Pohlner J.E., El Korh A., Chiaradia M., Klemd R., Grobéty B.: Fe and O isotope study of eclogites and gneisses in the Münchberg Massif, Germany

3.8 Vho A., Lanari P., Rubatto D., Hermann J.: Fluid production and transfer in subduction zones: Insights from an integrated thermodynamic and δ^{18}O fractionation model

POSTERS:

P 3.1 Ahmad Q., Wille M., Rosca C., König S.: Molybdenum isotope systematics at convergent plate margins – the effect of deep sea pelagic sediments

P 3.2 Greber N.D., Aarons S.M., Dauphas N., Pettke T.: First order validation of the titanium isotope thermometer

P 3.3 Hoffmann J., Mezger K.: Stable isotope anomalies in chondrules – Insights into the pantry of the early Solar System

P 3.4 Rüggeberg A., Raddatz J.: Constraining past environmental changes of cold-water coral mounds with geochemical proxies in corals and foraminifera

3.1

Deciphering microbial signatures in stromatolites through micrometric *in situ* iron and sulfur isotope analyses.

Marie-Noëlle Decraene[1,2], Johanna Marin Carbonne[1], Christophe Thomazo[3], Nicolas Olivier[4], Pascal Philippot[5] & Etienne Deloule[2]

[1]Institut des sciences de la Terre, University of Lausanne, CH- 1015 Lausanne (marie-noelle.decraene@unil.ch)
[2]CRPG-CNRS, BP20, 54501 Vandoeuvre les Nancy, France
[3]UMR CRNS 5561 Biogéosciences, University of Burgundy, Dijon, France
[4]Laboratoire Magmas et volcans, University Clermont Auvergne, 63038 Clermont-Ferrand, France
[5]Géosciences Montpellier, University of Montpellier, France

Stromatolites are laminated organosedimentary structures formed under the influence of microbial consortium. The study of actual stromatolites helps to constrain chemical reactions at the biofilm scale and the role of microbial metabolisms on mineralization (Dupraz et al., 2005). The identification of the microbial communities in Archean stromatolites is yet still discussed due to the absence of microfossils. The preservation of primary microbial signatures is also challenged by the post depositional influence recorded in Archean sediments. Microbial metabolisms as Dissimilatory Iron Reduction (DIR) and Microbial Sulfate Reduction (MSR) are thought to be well established on the early Earth (Vargas et al., 1998; Ohmoto et al., 1993) and led to diagnostic fractionation of iron and sulfur isotopes, up to -3‰ and -70‰ respectively, during Fe^{3+}-oxide and sulfate reduction (e.g. Crosby et al., 2007; Sim et al., 2011). Micrometric syngenetic sedimentary pyrites (FeS_2) closely associated with organic matter are widespread in stromatolites through geological times. These sulfides can be precipitated through abiotic reactions or microbial activity using DIR and MSR metabolic pathways. We propose to explore Fe and S isotope signatures of micro-pyrites as a proxy of the early traces of microbial activity using SIMS analyses. Iron isotope analyses were performed using the new Hyperion Radio-Frequency source in CRPG Nancy and SwissSIMS Lausanne. This microscale approach, applied on Archean (2.7 Ga stromatolites of the Tumbiana Formation, Western Australia) and Triassic (250 Ma sediments of the Sonoma Basin, USA) samples, allows to obtain a spatial resolution of 3µm (Fe) (Fig.1) and 10µm (S) and a reproducibility on Balmat pyrite standard better than 0.24‰ (2σ) on δ^{56}Fe and 0.13‰ (2σ) on δ^{34}S. The comparison of these data yields a large view of the evolution of the isotopic signatures through geological time and provides original constraints about pyrite formation at local scale.

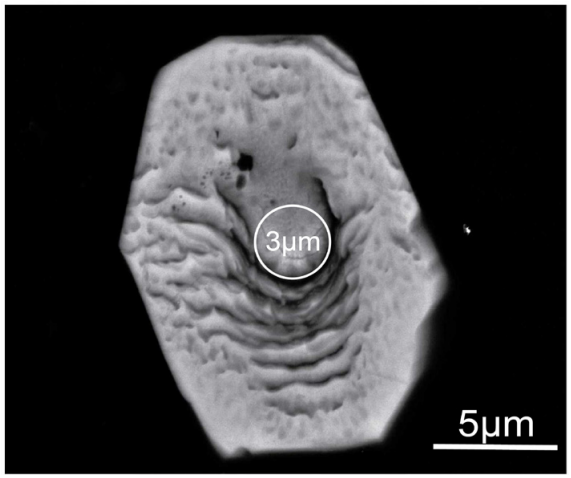


Figure 1. Primary beam spot used for iron isotope analyses in a micro-pyrite from the 2.7Ga Tumbiana Formation.

REFERENCES

Crosby, H. A., Roden, E. E., Johnson, C. M., & Beard, B. L. (2007). The mechanisms of iron isotope fractionation produced during dissimilatory Fe (III) reduction by Shewanella putrefaciens and Geobacter sulfurreducens. Geobiology, 5(2), 169-189.

Dupraz, C., & Visscher, P. T., 2005. Trends in microbiology, 13(9), 429-438.

Vargas, M., Kashefi, K., Blunt-Harris, E. L., & Lovley, D. R., 1998. Nature, 395(6697), 65.

Ohmoto, H., Kakegawa, T., & Lowe, D. R. (1993). 3.4-Billion-year-old biogenic pyrites from Barberton, South Africa: sulfur isotope evidence. Science, 262(5133), 555-557.

Sim, M. S., Bosak, T., & Ono, S. (2011). Large sulfur isotope fractionation does not require disproportionation. Science, 333(6038), 74-77.

Vargas, M., Kashefi, K., Blunt-Harris, E. L., & Lovley, D. R. (1998). Microbiological evidence for Fe (III) reduction on early Earth. Nature, 395(6697), 65.

3.2

Multi-isotope study (Ge, Fe, O) of hydrothermal metamorphism in the Limousin ophiolite

Afifé El Korh[1], Béatrice Luais[2], Marie-Christine Boiron[3] & Damien Cividini[2]

[1]*Unit of Earth Sciences, Department of Geosciences, University of Fribourg, Chemin du Musée 6, CH-1700 Fribourg, Switzerland (afife.elkorh@unifr.ch)*
[2]*Centre de Recherches Pétrographiques et Géochimiques (CRPG), UMR 7358 CNRS-Université de Lorraine, 15 rue Notre Dame des Pauvres, BP 20, F-54501 Vandœuvre-lès-Nancy Cedex, France*
[3]*GeoRessources, Université de Lorraine, CNRS, UMR 7359, Boulevard des Aiguillettes, BP 70239, F-54506 Vandœuvre-lès-Nancy, France*

Non-traditional stable isotope geochemistry in ophiolites is a powerful tool for the understanding of geochemical processes during hydrothermal alteration (or hydrothermal metamorphism) in ancient oceanic lithosphere. Ge and Fe isotope fractionation can be significant during low-temperature (T) hydrothermal processes (< 350°C), but also under high-T hydrothermal or magmatic conditions. Thus, Ge and Fe isotopes can be employed as tracers of hydrothermal vs. magmatic processes in the ancient oceanic lithosphere.

While O isotope fractionation is mainly controlled by T and fluid flows during hydrothermal alteration on (sub-)seafloor, Ge and Fe isotope fractionation during hydrothermal processes strongly depends on the redox conditions and the chemistry of fluids. In the altered oceanic crust (AOC), hydrothermal alteration may result in: 1) Ge depletion in the presence of hydrothermal sulfides during high-T alteration along hydrothermal vents or, 2) Ge enrichment due to Ge adsorption by iron hydroxides (Escoube et al., 2015). Moreover, the heavier Fe isotopes are preferencially incorporated into the Fe^{3+}- phases. Thus, the AOC may display variable Ge and Fe isotopic compositions, depending on the nature of hydrothermal vent fluids and products: Fe^{2+}-rich sulfides (low δ^{74}Ge and δ^{56}Fe) or Fe^{3+}-rich deposits (clays, Fe-hydroxides: high δ^{74}Ge and δ^{56}Fe) (Rouxel et al. 2003; Escoube et al., 2015).

In this study, we have measured non-traditional Ge and Fe isotopes and traditional O isotopes in series of metagabbros and serpentinites from the Limousin ophiolite (French Massif Central) to decipher the different signatures of hydrothermal metamorphism. The Limousin ophiolite belongs to the upper part of the Middle Allochthon domain of the Variscan belt. Serpentinisation of peridotites and troctolites, and amphibolite facies metamorphism of gabbros and mafic dykes occurred during intensive seafloor hydrothermal alteration under low-pressure conditions (~ 0.2 GPa) and temperatures from high-T late-magmatic conditions to low-T greenschist–zeolite metamorphic facies (serpentinisation: ≤ 500°C; amphibolite facies: 570–750°C; Berger et al., 2005).

Ge and Fe isotope ratios ($\delta^{74}Ge_{NIST3120}$ ± 0.02–0.10‰; $\delta^{56}Fe_{IRMM-014}$ ± 0.01–0.04 ‰; 2σ SE) were measured in bulk samples using a NeptunePlus MC-ICPMS (ThermoFisher Scientific) after sample dissolution and element separation through ion exchange chromatography columns at the CRPG-Nancy (Luais, 2012; Liu et al., 2014). O isotopes were measured by on-line CO_2 fluorination using a Thermo-Finnigan MAT 253 gas source mass spectrometer at the ISTE of the University of Lausanne.

Amphibolites display low $Fe^{3+}/\Sigma Fe$ ratios (0.11–0.14) and MORB-like δ^{56}Fe values (+0.03 to +0.17‰). δ^{18}O values are typical of high-T hydrothermally altered MORB (+6.2 to +6.6‰). δ^{74}Ge values show a small range (+0.72 to +0.77‰) and are heavier than most basalts and gabbros (+0.37 to +0.74‰; see Rouxel and Luais, 2017). The δ^{18}O slightly decreases with the increase of the δ^{56}Fe, indicating a slight fractionation of the δ^{56}Fe towards lighter values during hydrothermal alteration. However, no δ^{74}Ge vs. δ^{56}Fe correlation is observed, indicating that Ge isotope fractionation has prevailed over Fe isotope fractionation during hydrothermal alteration of basic rocks. Reducing conditions have enhanced Ge isotope fractionation towards compositions heavier than MORB.

Contrary to amphibolites, serpentinites are strongly oxidised rocks ($Fe^{3+}/\Sigma Fe$: 0.6–0.7) and display δ^{18}O values (+5.0 to +6.1‰) typical of hydrothermally altered ultrabasic rocks. They display similar to heavier δ^{74}Ge values (+0.48 to +0.93‰) than ultrabasic rocks (+0.46 to +0.76‰; for a review see Rouxel and Luais, 2017), as well as heavier Fe isotopic composition (+0.15 to +0.18‰) than partially to totally serpentinised abyssal peridotites (-0.10‰ to +0.11‰; e.g. Craddock et al., 2013). The δ^{74}Ge shows a slight positive correlation with the δ^{56}Fe, indicating concomittant Ge and Fe isotope fractionation towards heavier values during hydrothermal alteration. The δ^{18}O increases with the decrease of the δ^{74}Ge and, to a lesser extent, of the δ^{56}Fe, suggesting both Ge and Fe fractionation during hydrothermal alteration. However, δ^{56}Fe values display a larger deviation from ultrabasic rocks than δ^{74}Ge and δ^{18}O values, suggest that oxidising conditions have favoured the fractionation of Fe isotopes to a larger extent than Ge isotopes.

The present study corroborates former results obtained on subducted high-pressure metabasites (El Korh et al., 2017a, b): Fe isotope composition of the oxidised rocks mainly expresses the signature of the protolith composition and subsequent fractionation during low-T hydrothermal alteration, while only (re)hydration reactions in a reducing environment can trigger Ge isotope fractionation towards heavier compositions than those of basalts.

REFERENCES

Berger, J., Féménias, O., Mercier, J.C.C. & Demaiffe, D. 2005: Journal of Metamorphic Geology, 23, 795-812.
Craddock, P.R., Warren, J.M. & Dauphas, N. 2013: Earth and Planetary Science Letters, 365, 63-76.
El Korh, A., Luais, B., Boiron, M.C., Deloule, E. & Cividini, D. 2017a: Chemical Geology 449, 165-181.
El Korh, A., Luais, B., Deloule, E. & Cividini, D. 2017b: Contributions to Mineralogy and Petrology, 172:41.
Liu, P.P., Zhou, M.F., Luais, B., Cividini, D. & Rollion-Bard, C. 2014: Earth and Planetary Science Letters,399, 21-29.
Luais, B. 2012: Chemical Geology 334, 295-311.
Escoube, R., Rouxel, O., Edwards, K., Glazer, B. & Donard, O.F.X. 2015: Geochimica et Cosmochimica Acta 167, 93-112.
Rouxel, O. & Luais, B. 2017: Reviews in Mineralogy & Geochemistry 82, 601-656.
Rouxel, O., Dobbek, N., Ludden, J. & Fouquet, Y. 2003: Chemical Geology, 202, 155-182.

3.3

How does anatectic melt receive its isotopic fingerprint? A case study from the Halls Creek Orogen, WA, Australia

Johannes Hammerli[1] & Tony Kemp[2]

[1]Institut für Geologie, University of Bern, Baltzerstrasse 1-3, CH-3012 Bern (johannes.hammerli@my.jcu.edu.au)
[2]School of Earth Science, The University of Western Australia, Perth 6009, WA, Australia

Anatexis plays an important role for the production of crustal melts, for feeding large igneous bodies, and for the differentiation of the crust. However, geochemists often have to rely on radiogenic isotope analyses of granitic rocks to deduce the melt source and timing of melt production. In igneous rocks, apparent isotope inconsistencies and isotope decoupling are often perplexing to interpret without fully understanding melting processes, melt origins, and melt extraction at the source – a critical knowledge gap that can lead to mis- interpretation of isotopic data. Well exposed anatectic terranes provide the opportunity to study melt evolution within the source rocks and how extracted melt receives its geochemical fingerprint. In this study we investigate the isotopic evolution of radiogenic (U-Pb, Sm-Nd, Lu-Hf) and stable (O) isotope systems on a whole rock and (sub-) mineral scale in migmatites and their protoliths. The study site exposes a spectacular window into anatexis in the middle/lower crust where source rocks, external melt, and residual cumulates can be studied (Oliver and Barr, 1997). The studied migmatitic terrane belongs to the ~1850 Ma Halls Creek Orogen and with the radiogenic clocks starting in the Paleoproterozoic, the protracted evolutionary path of the isotope systems allows identifying potential isotope disequilibria induced during anatexis. Given the well constrained and exposed anatectic terrane, this setting allows to address the following key questions:

1. Are (isotope) disequilibrium melting processes possible as claimed in previous studies?

2. What is the role of garnet cumulates in terms of the Hf isotope signature of melt and residual material over time (garnet has as a strong Lu-Hf affinity and over time could evolve to highly radiogenic Hf signatures due to it high Lu/Hf ratio)?

3. How representative are the Hf isotope signatures of anatectic zircon rims in terms of the whole rock values and what role do the garnet cumulates play (see above)?

4. What is the magnitude and length-scale of isotope variations induced by infiltration of externally derived melts?

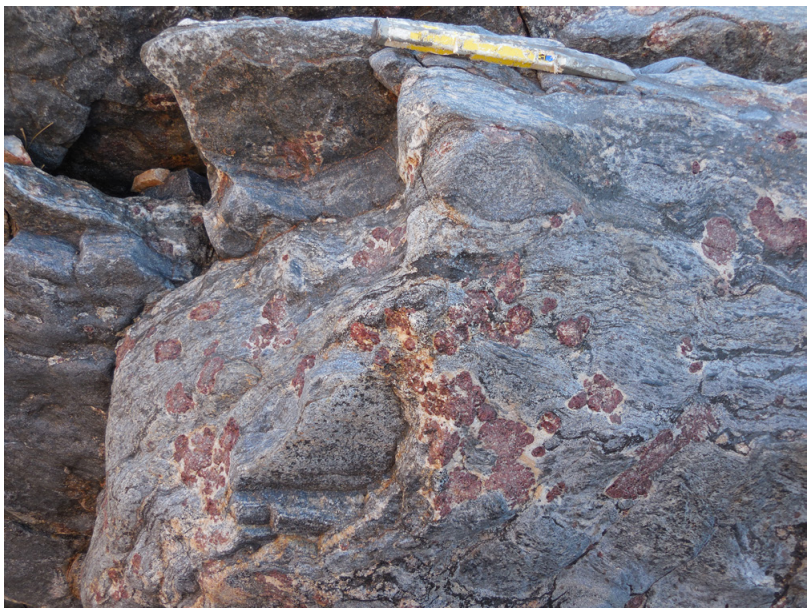


Figure 1. Residual garnet cumulates after melt extraction in a migmatite of the Halls Creek Orogen.

REFERENCES

Oliver, N.H.S., & Barr, T. 1997: The geometry and evolution of magma pathways through migmatites in the Halls Creek Orogen, Western Australia, Mineralogical Magazine 14, 3-14.

3.4

Molybdenum isotope fractionation between melt, exsolved fluid and hydrothermal minerals during the magmatic-hydrothermal transition

Anne Kaufmann[1], Thomas Pettke[1], Edel O'Sullivan[1], Martin Wille[1]

[1]*Institute of Geological Sciences, University of Bern, Baltzerstrasse 1+3, CH-3012 Bern (anne.kaufmann@geo.unibe.ch)*

Molybdenum isotopes of igneous rocks show a much larger variability (up to 0.6‰ $\delta^{98/95}$Mo) than has previously been assumed for the continental crust (0-0.2‰). Two processes have been put forward to account for this, (i) magmatic fractionation (Voegelin et al., 2014) and (ii) source variability delivered from the subducting slab to arc magmas. Moreover, studies focusing on magmatic-hydrothermal mineralisation have discovered a large spread in Mo isotope compositions of molybdenites, which cannot be explained by mass-dependent fractionation alone (Greber et al., 2011, 2014). Data acquired so far document increasingly heavier δ^{98}Mo with progressive hydrothermal evolution (Greber et al., 2014), hinting at significant fractionation between an increasingly heavy aqueous fluid while lighter isotopes are bound in precipitating MoS_2. On the other hand, Shafiei et al. (2015) observed the opposite trend with heavier $\delta^{97/95}$Mo values (0.0 - +0.92‰) of early stage molybdenites followed by a late stage with $\delta^{97/95}$Mo values restricted to -0.31 - +0.27‰. They postulated this to reflect the involvement of multiple fluid types (brine, vapour, aqueous liquid) with different physico-chemical properties that dominated during the two mineralisation stages. All these observations indicate that significant Mo isotope fractionation can occur during high-temperature processes.

We investigate the magmatic-hydrothermal transition using miarolitic cavities of the Torres del Paine igneous complex (Patagonia, Chile). They formed during successive stages of magma emplacement at shallow crustal levels (0.75 – 1 kbar) and document the magmatic-hydrothermal history from approx. 750°C down to <300°C. Bulk rock δ^{98}Mo ratios vary between +0.05 and +0.46 ‰ $\delta^{98}Mo_{NIST}$, a range reported for other calc-alkaline magmas elsewhere (e.g., Wille et al., 2018; Willbold and Elliott, 2017). Cavity mineral (amphibole, biotite, titanite, and molybdenite) and aqueous fluid isotopic measurements are currently underway; preliminary data indicate that biotite has a very light isotopic signature (<-1 ‰ $\delta^{98}Mo_{NIST}$) compared to the bulk rocks, whereas molybdenite exhibits moderately light $\delta^{98}Mo_{NIST}$ values of -0.24 to -0.20‰. Together, this data set allows the quantification of isotopic distribution coefficients between minerals and aqueous fluid, a necessary step in better understanding the relevant processes producing isotopic variability in the continental crust.

REFERENCES

Greber, N. D., Hofmann, B. A., Voegelin, A. R., Villa, I. M. & Nägler, T. F. 2011: Mo isotope composition in Mo-rich high- and low-T hydrothermal systems from the Swiss Alps, Geochimica et Cosmochimica Acta 75, 6600-6609.

Greber, N. D., Pettke, T. & Nägler, T. F. 2014: Magmatic–hydrothermal molybdenum isotope fractionation and its relevance to the igneous crustal signature, Lithos 190-191, 104-110.

Shafiei, B., Shamanian, G., Mathur, R. & Mirnejad, H. 2015: Mo isotope fractionation during hydrothermal evolution of porphyry Cu systems, Mineralium Deposita 50, 281-291.

Voegelin, A. R., Pettke, T., Greber, N. D., von Niederhausern, B. & Nägler, T. F. 2014: Magma differentiation fractionates Mo isotope ratios: Evidence from the Kos Plateau Tuff (Aegean Arc), Lithos 190, 440-448.

Willbold, M. & Elliott, T. 2017: Molybdenum isotope variations in magmatic rocks, Chemical Geology 449, 253-268.

Wille, M., Kramers, J. D., Nagler, T. F., Beukes, N. J., Schroder, S., Meisel, T., Lacassie, J. P. & Voegelin, A. R. 2007: Evidence for a gradual rise of oxygen between 2.6 and 2.5 Ga from Mo isotopes and Re-PGE signatures in shales, Geochimica et Cosmochimica Acta 71, 2417-2435.

Wille, M., Nebel, O., Pettke, T., Vroon, P. Z., Konig, S. & Schoenberg, R. 2018: Molybdenum isotope variations in calc-alkaline lavas from the Banda arc, Indonesia: Assessing the effect of crystal fractionation in creating isotopically heavy continental crust. Chemical Geology 485, 1-13.

3.5

Microscale Fe and S isotope compositions of Archean pyrites can constrain past microbial metabolism and post deposit processes

Johanna Marin Carbonne[1], Christophe Thomazo [2], Marie-Noelle Decraene[1], Masafumi Saitoh[1], Julien Alleon[1] and Nicolas Olivier[3]

[1]Institut des Sciences de la Terre, Université de Lausanne (johanna.marincarbonne@unil.ch)
[2]Biogeosciences Université de Bourgogne Franche Comté, Dijon, France
[3]Laboratoire Magma et Volcans, Université Clermont Auvergne, Clermont Ferrand, France

The identification of microbial signatures preserved in the geological record is crucial for understanding life evolution in the Early Earth. Iron and sulfur isotopes offer the most direct means to track the biogeochemical cycling of these elements through time, but their joint use as biomarker of specific metabolic activity has been relatively limited to date. Archean sediments contain small sulfides, that can be formed either by abiotic processes (reaction between H_2S and Fe(II)) or by metabolic activity like microbial sulfate reduction (MSR) or dissimilatory iron reduction (DIR). We have developed a microscale approach using correlative microscopy and SIMS analyses. In situ Fe and S isotope analyses as well as high-resolution mineralogy of pyrites in Archean sediments from the Buck Reef Chert (3.41 Ga, basal member of the Kromberg Formation, South Africa) and the Mendon (3.33 Ga, South Africa) Formations reveal not only post-depositional metasomatic influence but also a well-preserved primary microbial signature inherited from early diagenetic reactions in the sediment. This microscale approach allows us to distinguish microbial signatures from late overprints. Our results demonstrate the existence of microbial iron respiration as early as 3.26 Gyr ago, providing new time calibration of the tree of life for this type of metabolism.

3.6

Tracing anthropogenic δ^{98}Mo in riverine water: Implications for palaeo-redox reconstruction

Edel O'Sullivan[1], Thomas Nägler[1] and Michael Babechuk[2]

[1]University of Bern (edel.osullivan@geo.unibe.ch)
[2]Memorial University of Newfoundland

The reconstruction of the Earth's changing surface oxygenation has benefited greatly from the use of Mo isotopes in marine sediments as a palaeo-redox proxy. Here the extent of Mo removal by oxic sediments is calculated by mass balance models assuming steady state conditions between the inputs and outputs of Mo to and from the ancient ocean. Unlike the outputs of Mo which are preserved in sedimentary rocks, the continental inputs of Mo to the ocean in the past must be estimated based on the modern global riverine average. First publications have shown that global rivers are isotopically highly variable and consistently heavy up to δ^{98}Mo ~1.9‰ compared to the average upper continental crust of ~0.0‰. It has been argued that this isotopic offset might originate from weathering of isotopically heavy black shales, evaporites and sulfides, and mechanisms of fractionation by adsorption onto Fe-Mn oxyhydroxides in suspended particles and soils.

Here we demonstrate the influence of an isotopically heavy anthropogenic Mo source on the natural composition of the Ottawa River, with implications for mass balance modelling of the ancient ocean. The Ottawa River, Canada, has previously been identified as having an anomalously heavy δ^{98}Mo close to seawater, which cannot be accounted for by previous explanations, and indicates the existence of an additional Mo source or sink. We collected 32 water samples from the Ottawa River, its tributaries and surrounding lakes. Filtered samples were analysed for major and trace elements as well as δ^{98}Mo.

Our results reveal a progressive upstream trend towards heavy δ^{98}Mo up to 3.0‰, different to samples from tributaries and lakes with a constant δ^{98}Mo of 1.1‰. Positive correlation between δ^{98}Mo and [Mo] indicate a binary mixing between δ^{98}Mo released by natural weathering of the catchment, and a single, isotopically heavy point source located upstream. A potential source might be Cu-Au porphyry mining activities in the Abitibi Greenstone Belt, in the headwaters of the river. Direct contamination from dissolution of isotopically light MoS_2 molybdenite is unlikely to explain the heavy Mo signature of the source waters. Alternatively, adsorption of Mo onto Fe-oxides within the waste-rock storage facilities has previously been shown to fractionate Mo in mine drainage water, releasing a highly reduced, heavy δ^{98}Mo source into the surrounding waters. We hypothesise that a similar mechanism of Mo removal occurring in these mining regions has altered the δ^{98}Mo of the Ottawa River.

Anthropogenic alteration of the isotopic composition of natural river water challenges the use of modern large river systems as analogues for ancient input parameters in mass balance models. If the impact of anthropogenic input is found to affect rivers on a global scale, palaeo-redox reconstructions may need to be refined.

3.7

Fe and O isotope study of eclogites and gneisses in the Münchberg Massif, Germany

Johannes E. Pohlner[1], Afifé El Korh[1], Massimo Chiaradia[2], Reiner Klemd[3] & Bernard Grobéty[1]

[1]Unit of Earth Sciences, Department of Geosciences, University of Fribourg, Chemin du Musée 6, 1700 Fribourg (johannes.pohlner@unifr.ch)
[2]Department of Earth Sciences, University of Geneva, Rue des Maraîchers 13, 1205 Genève
[3]GeoZentrum Nordbayern, Universität Erlangen-Nürnberg, Schlossgarten 5a, 91054 Erlangen

Fe isotopes provide a promising tool to trace fluid-rock interactions and mass transfer in subducting lithosphere due to redox-sensitive isotope fractionation (phases rich in Fe^{3+} preferentially incorporate the heavier isotopes). Our study aims at understanding to which extent the Fe isotopes in the subducted crust reflect (1) igneous protolith formation, (2) subsequent low-temperature (LT) alteration, or (3) fluid-rock interactions during the subduction-exhumation cycle.

The Münchberg Massif represents a nappe pile within the Variscan orogen. MORB-type eclogites and gneisses of the uppermost nappe (Hangendserie) show variable degrees of amphibolite facies retrogression. A dark, kyanite-free eclogite (Mg# <65, Al_2O_3 <15.5 wt.%, MORB signature) is distinguished from a light, Ky-bearing eclogite (Mg# >65, Al_2O_3 >15.5 wt.%, more arc-like signature, usually higher Cr and lower HFSE contents, positive Eu/Eu*). δ^{56}Fe values of dark (–0.068 ± 0.018 to –0.007 ± 0.003‰) and light eclogites (–0.053 ± 0.002 to +0.014 ± 0.024‰) overlap. Both types comprise the lowest δ^{56}Fe of subduction-related eclogites ever measured, being lighter than MORB and comparable with some arc basalts. δ^{56}Fe tends to increase with Mg# and Eu/Eu* and to decrease with FeO_{tot}, Sc, Ni, V and Zn. Fluid-mobile elements are decoupled from δ^{56}Fe. $Fe^{3+}/\Sigma Fe$ (0.13–0.30) do not strongly vary with δ^{56}Fe and are highest in the dark eclogites of Fattigau, which also have high δ^{18}O (+10‰). Dark Weissenstein eclogites have more mantle-like δ^{18}O values (+5.0 to 5.6‰), whereas δ^{18}O of light eclogites from Oberkotzau and Weissenstein are slightly higher (+6.3 to 6.9‰). Within every locality, δ^{18}O and $Fe^{3+}/\Sigma Fe$ appear to be independent from each other. Gneisses from Weissenstein do not show large variations in δ^{18}O (+10.0 to 11.0‰) or $Fe^{3+}/\Sigma Fe$ (0.07 to 0.10).

It appears that δ^{56}Fe is still largely controlled by protolith signatures. Presumably the light eclogites originated from plagioclase-rich cumulates, and the dark eclogites represent the complementary differentiates. Enrichment of heavy Fe in high-$Fe^{3+}/\Sigma Fe$ cumulate phases (e.g., plagioclase or magnetite) can explain the unusual decrease of δ^{56}Fe during magmatic differentiation. LT alteration, which appears to be modest for most samples, most likely caused secondary oxidation in some cases, but not necessarily a change of δ^{56}Fe. Fe isotope fractionation during HP metamorphism cannot be excluded. Loss of heavy Fe during slab dehydration or a specifically composed protolith mantle source are possible explanations for the unusually light δ^{56}Fe. Retrogression does not seem to have influenced the eclogite Fe isotope signatures.

3.8

Fluid production and transfer in subduction zones: Insights from an integrated thermodynamic and $\delta^{18}O$ fractionation model

Alice Vho[1], Pierre Lanari[1], Daniela Rubatto[1,2] & Jörg Hermann[1]

[1]*Institute of Geological Sciences, University of Bern, CH-3012 Bern, Switzerland (alice.vho@geo.unibe.ch)*
[2]*Institut de Sciences de la Terre, University of Lausanne, CH-1015 Lausanne, Switzerland*

Oxygen isotope geochemistry is a powerful tool for investigating rocks that interacted with fluids, to assess fluid sources and quantify the physical conditions of fluid-rock interaction.

We present an integrated modelling approach applied to multi-rock open systems. It combines thermodynamic- and oxygen isotope fractionation-modelling based on internally consistent databases. This technique was applied to subduction zone metamorphism to predict the possible range of $\delta^{18}O$ values for mineral phases and aqueous fluids at various pressure-temperature (P-T) conditions in the subducting slab. The evolution of mineral assemblage and $\delta^{18}O$ values of each phase is calculated along a defined P-T path for a system composed by a sequence of oceanic crust (mafic) with sedimentary cover (pelitic or carbonatic) of known initial chemical composition and bulk $\delta^{18}O$. In this system, fluid-rock interactions may occur as consequence of infiltration of an external fluid into the mafic rocks or transfer into the metasediments of the fluid liberated by dehydration reactions occurring in the mafic rocks. The model quantifies (1) the effect of the dehydration reactions on the bulk $\delta^{18}O$ of a rock during prograde metamorphism, (2) the effect of the influx into a subducting rock of an external fluid of distinct isotopic signature and (3) the final amount and isotopic signature of the fluid leaving the multi-rock system, e.g. infiltrating an upper unit or the mantle wedge. The effects of interaction with externally-derived fluids on the mineral and bulk $\delta^{18}O$ of each rock were quantified for two typical compositions of metabasalts and metasediments with external fluid influx from serpentinite dehydration.

We confirm that variations in $\delta^{18}O$ due to mineral fractionation and/or excess fluid loss are typically negligible (i.e. < 1 ‰). The effect of temperature variation over a range of ~150 °C on the mineral $\delta^{18}O$ is phase dependent and may be significant (> 1 ‰). On the other hand, the interaction with an external fluid of different oxygen isotope composition leads to shifts in bulk and mineral $\delta^{18}O$ values that depend on the degree of fluid/rock interaction and on the $\delta^{18}O$ difference between the rock and the fluid. This change can be dramatic (i.e. > 10 ‰). In the considered system, quartz and garnet are the most suited minerals to track such changes in oxygen isotope ratio. A comparison between natural samples and modelling results is possible as the oxygen isotope composition of quartz and garnet can be measured *in situ* by SIMS with good precision (down to ± 0.2–0.3‰ in $\delta^{18}O$, 2σ). The fluid released by the subducting slab has typically a $\delta^{18}O$ higher than the mantle value (5.5 ‰) and has the potential to extensively serpentinize the mantle wedge at the slab-mantle interface and to modify its bulk oxygen isotope composition. Significant modification of the slab-mantle interface are expected to occur already after 0.35 My of ongoing subduction.

The presented modelling strategy provides a new way to investigate different degrees of interaction between external fluids and the associated sink lithology and to evaluate the consequences of closed system *vs* open system behaviour with respect to oxygen isotopes during the evolution of a rock. Measured oxygen isotope compositions in minerals, intra-grain or bulk $\delta^{18}O$ variations at different scales, can be compared with the results of the model for the specific scenarios. If the measured isotopic compositions are not consistent with the behaviour of a closed system, the presented model can be used to determine potential fluid sources, to estimate the degree of fluid-rock interaction and the metamorphic conditions at which this happened.

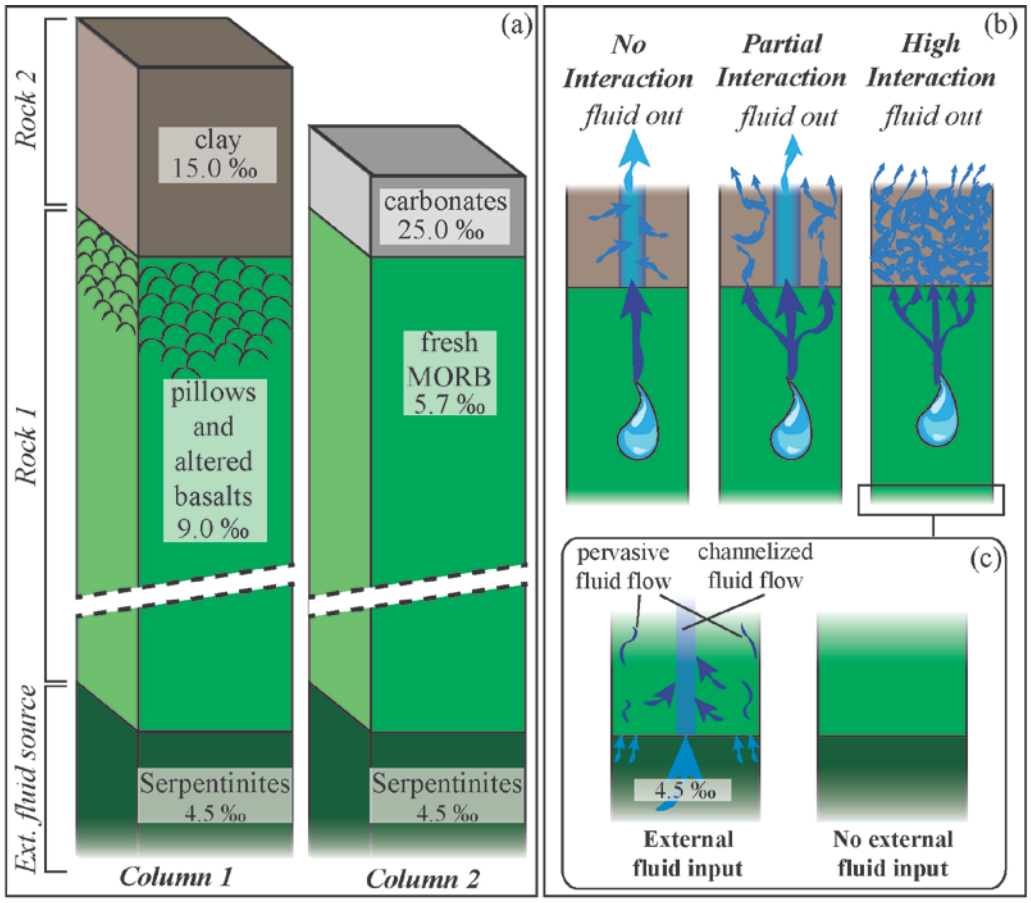


Figure 1. Schematic geometry of the model. (a) The target column is composed by two rock types that can be infiltrated by an external fluid deriving from a third layer located beneath them. (b) Schematic representation of the three interaction cases (no interaction case, partial interaction case, high interaction case) between metabasalts and metasediments. (c) Possible scenario at the base of the column. As a consequence of serpentine breakdown, ultramafic fluid may infiltrate the MORB, exchange with it and affect the fluid infiltrating the sedimentary cover.

P 3.1

Molybdenum isotope systematics at convergent plate margins – the effect of deep sea pelagic sediments

Qasid Ahmad[1], Martin Wille[1], Carolina Rosca[2], Stephan König[2]

[1]*Insitute of Geological Sciences, University of Bern, Baltzerstrasse 1+3, CH-3012 Bern (qasid.ahmad@geo.unibe.ch)*
[2]*Department of Geosciences, University of Tübingen, Hölderlinstrasse 12, DE-72074 Tübingen*

Subduction zone magmatism at convergent plate margins is closely associated with the formation of continental crust through geological history. These settings are also characterized by the highest mass fluxes between crust and mantle, where the slab-derived fluids (and possibly slab melts) facilitate the element transfer into the mantle wedge. Recently, Mo and its isotopes have been applied to investigate the slab-mantle wedge transport and ultimately the incorporation of this element into arc lavas. Significant stable Mo isotope fractionation is induced during Earth's surface processes leading to distinct Mo concentrations and Mo isotopic ratios in different marine sediments. One sedimentary endmember are Mn-rich deep sea pelagic clays with a high authigenic Mo concentration, which dominate the sedimentary subduction input at the Tonga Trench due to its remote location from continental shelf areas.

To better constrain if and how subducted sediment imprint the recycling of Mo at subduction zones, new Mo isotopic analyses on arc volcanic rocks (basalts and basaltic andesites) from the Tongan subduction zone are presented. Additionally, pelagic sediment and altered oceanic crust samples from IODP site 595 were analyzed. Together with major and trace element concentration data, this approach allows us to calculate the isotopic mass balance between Mo input by subducted continental material (SCM) and Mo output at arc magmatism. This is necessary to evaluate the role of sub arc processes on the Mo budget and the isotopic input on Mo to the deeper mantle. In comparison with published Mo isotopic data from other convergent margin settings with different SCM input, our new data will constrain the role of sediments on Mo recycling at arc settings.

P 3.2

First order validation of the titanium isotope thermometer

Greber Nicolas D.[1], Aarons Sarah M.[2], Dauphas Nicolas[3], Pettke Thomas[1]

[1]*Institut für Geologie, Universität Bern, 3012, Bern (nicolas.greber@geo.unibe.ch)*
[2]*Scripps Institution of Oceanography, California 92093, USA*
[3]*Origins Laboratory, Department of the Geophysical Sciences and Enrico Fermi Institute, The University of Chicago, Chicago, IL 60615, USA*

Pioneering studies by Millet and Dauphas (2014) and Millet et al (2016) showed that stable Ti isotopes exhibt significant mass-dependent variations in magmatic rocks, whereby basalts are isotopically lighter than more evolved lithologies. Stable isotope theory predicts that isotope fractination is driven by the contrast in element bonding and that weaker bonds (high coordination) prefer light isotopes. Consequently, the observed fractination of Ti isotopes is likely due to the presence of 4-, 5-, and 6-fold coordinated Ti in silicate melts and minerals. Another virtue of stable isotopes is that the degree of isotopic fractination is negatively correlated with temperature. Therefore, minerals that incorporate 6-fold Ti (e.g. ilmenite, magnetite) should be isotopically lighter than minerals that contain Ti in 4-fold coordination (e.g. olivin, quartz), and the difference in the isotopic composition between these mineral phases is expected to be dependent on the temperature of crystallization (or last isotopic equilibration). Recently, Aarons et al. (subm.) presented ab initio calculations of Ti-O bond strenght of various minerals, which allow to predict the temperature dependent difference of minerals in their Ti isotopic compositions.

Here we test the applicability of these calculations on mineral separates (olivine, biotite, feldspar, quartz, magnetite) of 5 rocks from the Kos magmatic suite (Greece) that range in composition from basaltic to rhyolitic. Thermodynamic modelling and conventional mineral thermometers indicate that advanced fractional crystallisation occurred in a shallow magma chamber under H_2O saturated conditions and low temperature (~750-650 °C) prior to eruption of the system (Bachmann et al. 2012). Within a given rock, magnetite is lightest, biotite is intermediate and felspar, olivine an quartz are heaviest in their Ti isotopic compositions. Applying the predicted Ti isotope fractionation between Fe-Ti-oxides (6-fold, mgt) and neso- and tectosilicates (4-fold, ol, fspt, qz) suggests crystallization temperatures of 1180 °C for the basalt, 770, 760, 650 °C for three andesites/dacites and 600 °C for a rhyolithic pumice. These temperatures agree largely with the previously suggested crystallization conditions (but the rhyolite temperature is low) and indicate that Ti isotopes have the potential to become a valuable magmatic thermometer.

REFERENCES

Aarons, Sarah et al., subm., Controls on titanium isotope fractionation in tholeiitic and calc-alkaline magmas, *Geophys Res L.*

Bachmann, Olivier et al., 2012, Evolution of silicic magmas in the Kos-Nisyros volcanic center, Greece. *Contrib Mineral Petrol* 163.

Millet, Marc-Alban, et al., 2016, Titanium stable isotope investigation of magmatic processes on the Earth and Moon. *EPSL* 449.

Millet, Marc-Alban, and Nicolas Dauphas, 2014, Ultra-precise titanium stable isotope measurements by double-spike high resolution MC-ICP-MS. *JAAS* 29.8.

P 3.3

Stable isotope anomalies in chondrules – Insights into the pantry of the early Solar System

Jan Hoffmann[1], Klaus Mezger[1,2]

[1]*Institut für Geologie, Universität Bern, Baltzerstrasse 1–3, 3012 Bern, Switzerland*
[2]*Center for Space and Habitability, Universität Bern, Gesellschaftsstrasse 6, 3012 Bern, Switzerland*

Chondrules are millimetre-sized, igneous rocks and major components of chondrites, the chemically most primitive meteorites in our solar system. The high abundance of chondrules in the most common meteorite classes and early formation ages of ca. 1.8–3.0 Ma after CAI formation (Pape et al., 2019) suggest that chondrules were a common ingredient in the early Solar System, thus, may have played a major role between the time of condensation of solids from the solar nebula and the time of accretion of planetary bodies. However, their formation process(es) and later incorporation into their host bodies remain enigmatic.

Physical models were developed that show that chondrules might be a by-product of planetesimal collision, whereas cosmochemical constraints favour the melting of dust aggregates in flash-heating events (e.g. Connolly & Jones, 2016). A valid model for chondrule formation needs to satisfy all aspects that can be drawn from textural, mineralogical and chemical observations. Several authors proposed a complementary relationship between chondrules and chondrite matrices on both the elemental and isotopic scale (e.g. Hezel et al., 2018), while the whole rock is always chondritic. If this holds true, it would imply a closely intertwined genetic connection between both components and put constraints on the chondrite-forming region and the dynamics of accretion of material that ends up in chondrules and later in chondrites. In this context a key question relates to the distribution of elements and isotopes throughout the solar nebula in particular.

The study of stable isotope anomalies offers an opportunity to pin-point contributions of nucleosynthetic processes (e.g. super novae explosions) and injection of anomalous material into the solar nebula. Such anomalies have been reported for several elements in chondrites, refractory inclusions and, to a lesser extent, in chondrules (e.g. Burkhardt et al., 2017), suggesting compositionally distinct regions in the solar nebula.

Here, we will present results from the investigation of the petrographic properties of chondrules using micro-computed tomography (µCT). This relatively new and quickly emerging method allows a non-destructive textural and mineralogical analysis of precious material like extraterrestrial samples. These studies are complemented by analyses of the isotopic composition of Ca in individual chondrules and adjacent matrices using thermal ionization mass spectrometry. The results provide constraints on the degree of isotopic heterogeneity in the feeding zone of different chondrite classes and the process of chondrule formation, particularly the physical models that invoke pre-existing planetesimals.

REFERENCES

Burkhardt, C., Dauphas, N., Tang, H., Fischer-Gödde, M., Qin, L., Chen, J.H., Rout, S.S., Pack, A., Heck, P.R., Papanastassiou, D.A. 2017: In search of the Earth-forming reservoir: Mineralogical, chemical, and isotopic characterizations of the ungrouped achondrite NWA 5363/NWA 5400 and selected chondrites. Meteoritic and Planetary Science 52, 807-826.

Connolly, H.C. & Jones, R.H. 2016: Chondrules: The canonical and noncanonical views. Journal of Geophysical Research: Planets 121, 1885-1899.

Hezel, D.C., Bland, P.A., Palme, H., Jacquet, E., Bigolski, J. 2018: Composition of Chondrules and Matrix and Their Complementary Relationship in Chondrites. In: Chondrules (Ed. by Russell, S.S., Connolly, H.C., Krot, A.N.). Cambridge University Press, 91-121.

Pape, J., Mezger, K., Bouvier, A.-S., Baumgartner, L.P. 2019: Time and duration of chondrule formation: Constraints from 26Al-26Mg ages of individual chondrules. Geochimica et Cosmochimica Acta 244, 416-436.

P 3.4

Constraining past environmental changes of cold-water coral mounds with geochemical proxies in corals and foraminifera

Andres Rüggeberg[1] & Jacek Raddatz[2]

[1]Faculty of Science and Medicine, Science Section, Dept. of Geosciences – Geology, Switzerland, University of Fribourg, Chemin du Musée 6, CH-1700 Fribourg, Switzerland.
[2]Institute of Geosciences, Goethe University Frankfurt, Altenhöferallee 1, D-60438, Frankfurt am Main, Germany.

Cold-water coral reefs and mounds are and have been biodiversity hotspots of the deep sea. As their occurrence depends on specific environmental parameters, gaining hindsight on changing ocean conditions under on-going climate change is the key to a better understanding of cold-water coral mound development through time. A convenient technique for reconstructing the palaeoenvironment during periods of cold-water coral mound growth is by extracting geochemical proxies from biologically mediated carbonates.

In this review, we focus on probably the two most abundant calcareous archives, i.e. cold-water Scleractinia and Foraminifera, with an overview of a selection of geochemical proxies ($\delta^{18}O$, $\delta^{13}C$, Δ_{47}, $\delta^{11}B$, Me/Ca ratios) used in these aragonitic and calcitic skeletons from cold-water coral mounds. A particular emphasis is set on constraining proxies for for temperature, salinity, seawater density, seawater carbonate systems parameters (pH, CO_3^{2-}), nutrients, oxygen and water mass tracers.

4. Palaeontology

Torsten Scheyer, Christian Klug, Lionel Cavin

Schweizerische Paläontologische Gesellschaft
Commission for the Swiss Journal of Palaeontology

TALKS:

4.1 Alleon J., Bernard S., Olivier N., Thomazo C., Marin-Carbonne J.: Molecular characteristics of organic microfossils in Paleoarchean cherts

4.2 Antcliffe J.B., Jessop W., Daley A.C.: Prey fractionation in the Archaeocyatha and its implication for the ecology of the first animal reef systems

4.3 Bastiaans D., Kroll J.F., Jagt J.W.M., Schulp A.S.: Cranial pathologies in a Late Cretaceous mosasaur from the Netherlands: behavioral and immunological implications.

4.4 Daley A.C., Antcliffe J.B., Lheritier M.: Understanding the fossil record of arthropod moulting using experimental taphonomic approaches

4.5 Dziomber L., Foth C., Joyce W.G.: A geometric morphometric study of turtle shells

4.6 Evers S.W.: A new hypothesis of turtle relationships provides insights into the evolution of marine adaptation, and turtle diversification

4.7 Fau M., Villier L., Ewin T.: Diversity of early Forcipulatacea (Asteroidea)

4.8 Ferrante C., Cavin L.: Weird coelacanths from the Triassic of Switzerland

4.9 Frey L., Coates M.I., Rücklin M., Klug C.: A new early symmoriid with an unusual jaw articulation from the Late Devonian of Morocco

4.10 Friesenbichler E., Hautmann M., Bucher H.: Palaeoecology of benthic macroinvertebrates from three Middle Triassic carbonate platforms

4.11 Friesenhagen T., Knappertsbusch M.: *Globorotalia menardii* reflects AMOC: Test-Size Evolution of *G. menardii* as a new Proxy for the AMOC Strength

4.12 Galasso F., Schneebeli-Hermann E.: Environmental influence on spore-pollen morphology during the Mesozoic

4.13 Gueriau P., Laibl L., Pérez Peris F., Lustri L., Daley A.C.: Soft part preservation reveals a high diversity of large bivalved arthropods in the Fezouata Biota (Early Ordovician, Morocco)

4.14 Jobbins M., Klug C.: Famennian thylacocephalans from Morocco and their role in Late Devonian foodwebs

4.15 Laibl L., Gueriau P., Peris P.F., Lustri L., Antcliffe J.B., Daley A.C.: Early post-embryonic development of marrellomorph arthropod from the Early Ordovician of Morocco

4.16 Lustri L., Gueriau P., Daley A.C.: A new stem Euchelicerate from the early Ordovician Fezouata Biota

4.17 Lynch S., Balcarcel A., Sánchez-Villagra M.R.: The Evolution Of The Camelidae

4.18 Maridet O., Gueriau P., Lu X.-Y., Costeur L.: Did dormice ever glide? Reinvestigation of *Glirulus aff. lissiensis* from the late Miocene of Saint-Bauzile (Ardéche, France)

4.19 Meyer C.A., Klein H., Wizevich M.C., Stecher R.: Triassic Sauropodomorph tracks with Gondwanan affinities from the Central Austroalpine Nappes of Switzerland

4.20 Pérez-Peris F., Laibl L., Vidal M., Daley A.: Morphology and evolution of basal Cheirurina (Trilobita) from the Fezouata Biota (Lower Ordovician, Morocco)

4.21 Plateau O., Foth C.: Ontogenetic patterns of cranial modularity along the theropod-bird transition

4.22 Pohle A., Jell P.A.: Filling the gap: a forgotten fauna of Cambrian nautiloid cephalopods from Australia and its implications

4.23 Scheyer T.M., Hutchinson J.R., Strauss O., Delfino M., Carrillo-Briceño J.D., Sánchez R., Sánchez-Villagra M.R.: Anatomy of the girdle regions of the giant *Purussaurus mirandai* (Caimaninae, Alligatoridae) from the Miocene of Venezuela

4.24 Spiekman S.N.F., Neenan J.M., Fraser N.C., Rieppel O., Fernandez V., Scheyer T.M.: Synchrotron microtomography and bone histology of *Tanystropheus* reveal its cranial morphology and the identification of a separate, small-sized species

4.25 Torres Ladeira M., Frey L., Coates M., Ginter M., Klug C.: A new cladoselachid chondrichthyan from the Famenian of Marocco

4.26 Żylińska A., Daley A.C.: Moulting or protection – enrolment strategies in *Strenuella polonica* Czarnocki, 1926 (Ellipsocephalida, Trilobita) from Cambrian Series 2 of the Holy Cross Mountains, Poland

POSTERS:

P 4.1 Bastiaans D., Hartman A.-F., Alkindi M., Schulp A.S.: The First Dinosaurian Braincase from the Middle East: An Enigmatic Ornithopod Braincase from the latest Cretaceous Al-Khod Formation of Oman.

P 4.2 Knappertsbusch M., Eisenecker J., Binggeli D.: AMOR2 follows AMOR – an improved robot for orientation and imaging of planktonic foraminifera

P 4.3 Mennecart B., Dubied M., Solé F.: Talking about brain dead and a giant among the dwarfs: new data on the Swiss Hyaenodonta (Mammalia)

4.1

Molecular characteristics of organic microfossils in Paleoarchean cherts

Julien Alleon[1], Sylvain Bernard[2], Nicolas Olivier[3], Christophe Thomazo[4], & Johanna Marin-Carbonne[1]

[1]ISTE, Université de Lausanne, Lausanne, Switzerland.
[2]IMPMC, Sorbonne Université, Paris, France.
[3]LMV, Université Clermont Auvergne, Clermont-Ferrand, France.
[4]Biogéosciences, Université de Bourgogne Franche Comté, Dijon, France.

The Archean geological record contains key information to document the emergence and the evolution of early life. Claims for traces of paleobiological activity in such ancient rocks are, however, very often controversial (Bernard and Papineau, 2014; Alleon and Summons, 2019; Javaux, 2019).

Fossilization processes and the increase of temperature and pressure conditions associated with diagenesis and metamorphism inevitably alter the original biochemical signatures of organic molecules. At a certain stage, biotic and abiotic organic structures may become undistinguishable (Bernard and Papineau, 2014; Alleon and Summons, 2019). Numerous Precambrian cherts (*i.e.* silica-rich rocks) are well known for hosting morphologically preserved fossilized microorganisms (*e.g.*, Knoll *et al.*, 2016; Lepot *et al.*, 2017). Recently, spatially resolved investigations using synchrotron-based XANES microspectroscopy revealed that molecular information about the organic precursor of 3.4 Ga microfossils, was preserved in the Strelley Pool Chert, Pilbara Craton, Western Australia (Figure 1), despite a metamorphic history so far believed to be incompatible with such preservation (lower greenschist facies - peak temperature ≅ 300 °C; Alleon *et al.*, 2018). Laboratory experiments showed that silica-organic interactions are likely to play a key role in the molecular preservation of microorganisms fossilized in cherts (Alleon *et al.*, 2016). Altogether, these results demonstrate that ancient organic microfossils may exhibit a high level of chemical preservation in appropriate settings independent of a long and complex geological history.

Here, we use spatially resolved microspectroscopy techniques, including STXM-based XANES spectroscopy, to investigate the chemical nature and molecular preservation of individual microfossils from the 3.4 Ga Buck Reef Chert (Kaapvaal Craton, South Africa). The latter have heterogeneous elemental and molecular compositions that differ significantly from those of the Strelley Pool Chert. The slightly higher peak temperature conditions (≅ 350 °C) they experienced during their geological history may partially explain these differences, although their molecular characteristics were likely initially distinct.

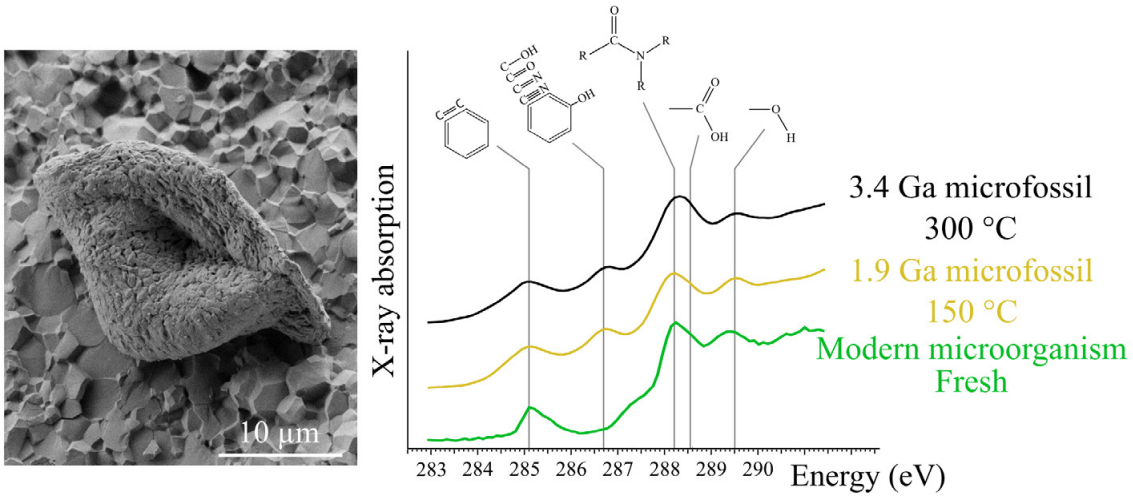


Figure 1. Left: Scanning electron microscope image showing a lenticular organic microfossil from the 3.4 Ga Strelley Pool chert. Right: X-ray absorption spectra collected at the carbon *K* edge for microfossils from the 3.4 Ga Strelley Pool chert (black) and the 1.9 Ga Gunflint chert (yellow), compared to a spectrum of a modern microorganism (green). The absorption features indicate the presence of similar molecular functional groups in both microfossils in ancient microfossils, despite they experienced different peak temperatures during their geological history (peak temperature is indicated in °C). Data are reproduced from Alleon *et al.* (2018).

REFERENCES

Alleon, J., Bernard, S., Le Guillou, C., Daval, D., Skouri-Panet, F., Pont, S., Delbes, L., & Robert, F. 2016: Early entombment within silica minimizes the molecular degradation of microorganisms during advanced diagenesis, Chemical Geology 437, 98-108.

Alleon, J., Bernard, S., Le Guillou, C., Beyssac, O., Sugitani, K., & Robert, F. 2018: Chemical nature of the 3.4 Ga Strelley Pool microfossils, Geochemical Perspectives Letters 7, 37-42.

Alleon, J., & Summons, R.E. 2019: Organic geochemical approaches to understanding early life, Free Radical Biology and Medicine.

Bernard, S., & Papineau, D. 2014: Graphitic carbons and biosignatures, Elements 10, 435-440.

Javaux, E.J. 2019: Challenges in evidencing the earliest traces of life, Nature 572, 451-460.

Knoll, A.H., Bergmann, K.D., & Strauss, J.V. 2016: Life: the first two billion years, Philosophical Transactions of the Royal Society B 371, 20150493.

Lepot, K., Addad, A., Knoll, A.H., Wang, J., Troadec, D., Béché, A., & Javaux, E.J. 2017: Iron minerals within specific microfossil morphospecies of the 1.88 Ga Gunflint Formation, Nature Communications 8, 14890.

4.2

Prey fractionation in the Archaeocyatha and its implication for the ecology of the first animal reef systems

Jonathan B. Antcliffe[1], William Jessop[2], and Allison C. Daley[1]

[1]Institut des Sciences de la Terre, Bâtiment Géopolis, UNIL-Mouline, CH-1015 Lausanne (jonathan.antcliffe@unil.ch)
[2]Oxford University Department of Zoology, South Parks Road, Oxford, UK

Archaeocyaths are the most abundant sponges from the Cambrian period, forming the first animal reef communities over 500 million years ago. The Archaeocyatha are index fossils for correlating rocks of similar ages globally, because of their abundance, extensive geographic distribution, their detailed anatomy and well established taxonomy. Their ecological significance remains incompletely explored yet they are known to strongly competitively interact unlike modern sponges. This study examines the feeding ecology of the fossil remains of Siberian archaeocyath assemblages. As suspension feeders, archaeocyaths filtered plankton from the water column through pores in their outer wall. Here we outline a new method to estimate the limit on the upper size of plankton that could be consumed by an archaeocyath during life. The archaeocyaths examined were predominantly feeding on nanoplankton and microplankton such as phytoplankton and protozooplankton. Size-frequency distributions of pore sizes from six different Siberian archaeocyath assemblages, ranging from Tommotian to Botoman in age, reveal significantly different upper limits to the prey consumed at each locality. Some of the assemblages contain specimens that could have fed on larger organisms extending in to the mesoplankton including micro-invertebrates as a possible food resource. These results show that during the establishment of the first animal reef systems, prey partitioning was established as a way of reducing competition. This method has applicability for understanding the construction and the functioning of the first reef systems, and could be applied to understanding nutrient flow and prey partitioning in modern reef systems and fossil phanerozoic reef systems, as well as more broadly informing reef development though time and space.

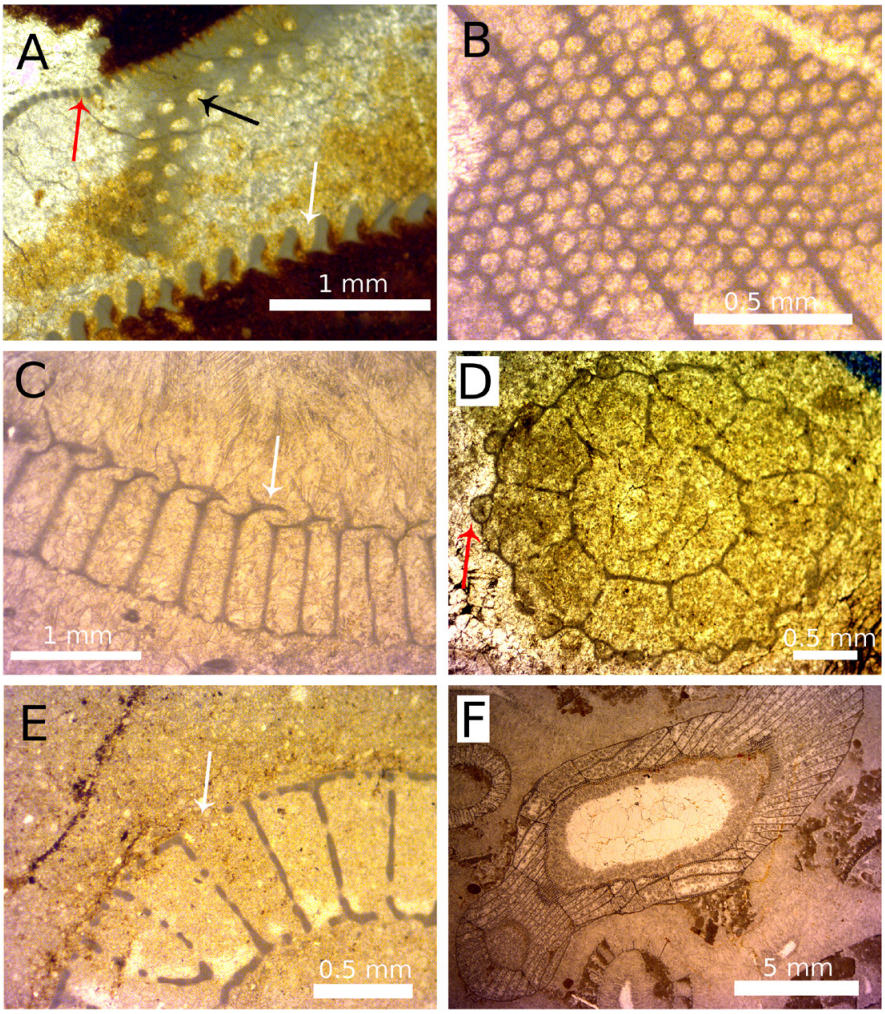


Figure 1. A range of features associated with the pores of archaeocyaths. A: the three major pore types: red arrow = outer wall pore; black arrow = septal pore; white arrow = inner wall canal. B: Varying pore sizes seen in slightly oblique section, with pores becoming more elliptical (to sub-polygonal) to the right side of the image. C: Annuli are plate-like features (white arrow) which restrict the pore width, and may add spiny and ornate coverings to the pore. D: Tumuli are sphere-like coverings (red arrow) over pores that have one or more openings to allow transit of particles. E: An example of a broken outer wall, producing a space in the wall much larger than the original pore. F: The irregular growth of archaeocyaths (e.g. if the specimens turns through 90o during growth) means that a single section can intersect the specimen in such a way that transverse, oblique, and longitudinal sections can be seen in a single specimen in thin section.

4.3

Cranial pathologies in a Late Cretaceous mosasaur from the Netherlands: behavioral and immunological implications.

Dylan Bastiaans[1,2,3], Jeroen J.F. Kroll[4], John W.M. Jagt[2], Anne S. Schulp[2,3]

[1]*Universität Zürich, Paläontologisches Institut und Museum , Karl-Schmid-Strasse 4, 8006 Zürich, Switzerland*
[2]*Natuurhistorisch Museum Maastricht, Maastricht, the Netherlands*
[3]*Naturalis Biodiversity Center, Leiden, the Netherlands*
[4]*MUMC+, Department of Radiology, Maastricht, the Netherlands*

On rare occasions, diseases and injuries sustained during the lifetime of an organism can be preserved in the fossil record, in the form of osseous lesions and exostoses. Palaeopathology, or the study of these ancient records of disease and trauma, may provide insight in disease acquisition, soft tissue anatomy, healing strategies and even behavioural aspects of extinct organisms. Although many paleopathological surveys have been undertaken in dinosaurs and archosaurs in general, most squamates have been largely understudied (e.g. Foth et al., 2015). Research on pathologies in mosasaurs (extinct Late Cretaceous marine squamates), however, took off early, with some of the first examples recognised at the end of the 19th century. These (mostly descriptive) works were succeeded by cases concerning both traumatic (e.g. Lingham-Soliar, 1998; Everhart, 2008) and non-traumatic conditions (e.g. Mulder, 2001; Schulp et al., 2004) prompting the first hypotheses on their underlying behavioural implications.

Multiple pathological specimens of various mosasaur genera have been recovered from the type Maastrichtian (SE Netherlands, NE Belgium), providing a glimpse into the interactions and trophic relationships of these marine squamates in this latest Cretaceous ecosystem (e.g. Lingham-Soliar, 1998; Schulp et al., 2004). Despite these efforts, the immunological implications of these pathologies have been fully neglected. Many pathological studies rely on external morphological comparisons only, despite the availability of histological, isotopic and modern radiological techniques.

Here we report on a palaeopathological case study of a recently discovered specimen of the globidensine mosasaur *Prognathodon* cf. *sectorius* (NHMM 2012 072) from the type Maastrichtian area and display the opportunities provided by modern day integrative approaches (e.g. CT and 3D-visualizations).The specimen was recovered from the upper Maastrichtian Lixhe 3 Member (Gulpen Formation) near Maastricht, the Netherlands. The similarities in extent, location and degree of healing of the anomalous bony structures on the anterior side of the upper jaw strongly suggest a common origin. The individual in all likelihood was bitten in the snout by a large, possibly conspecific mosasaur — and survived this attack. The specimen described here is among the very few with clear and unambiguous evidence of intraspecific agonistic interactions amongst mosasaurs. Despite significant injuries, including partial amputation of the premaxilla, this mosasaur initially recuperated from the encounter, but succumbed to the resulting subsequent infectious processes. Radiological and morphological features suggest chronic osteomyelitis which led to loss of bone within the left maxilla, which most likely hampered its ability to feed, resulting in the demise of this individual. This case study further illustrates the potential of integrative three-dimensional approaches in palaeopathological studies to provide a much more comprehensive and detailed description of alterations and underlying physiological processes. This allows for a detailed description of the immunological response of these animals, which in the case of NHMM 2012 072 seems much more akin the mammalian response than to its extant squamate relatives. Highly detailed scanning and 3D-visualizations allow for large evolutionary analyses on the exact osseous response to pathogens in an immunological context, thus providing information on the evolution of the immune response in fossil taxa.

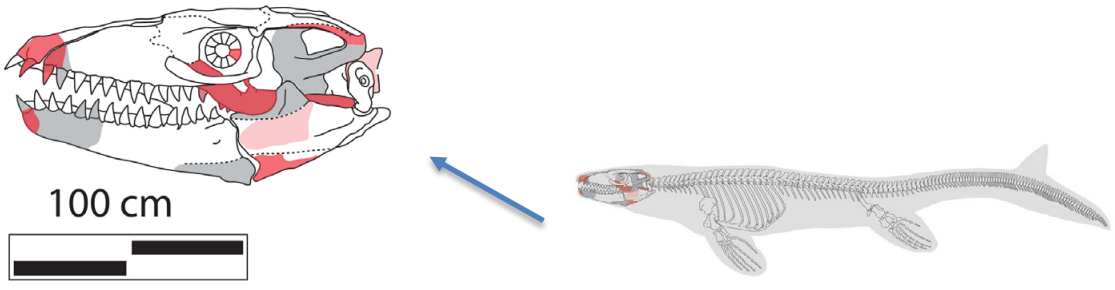


Figure 1. Completeness of the skull of the globidensine mosasaur NHMM 2012 072 (nicknamed “Carlo”), with **red** depicting the right side and **grey** the left side.

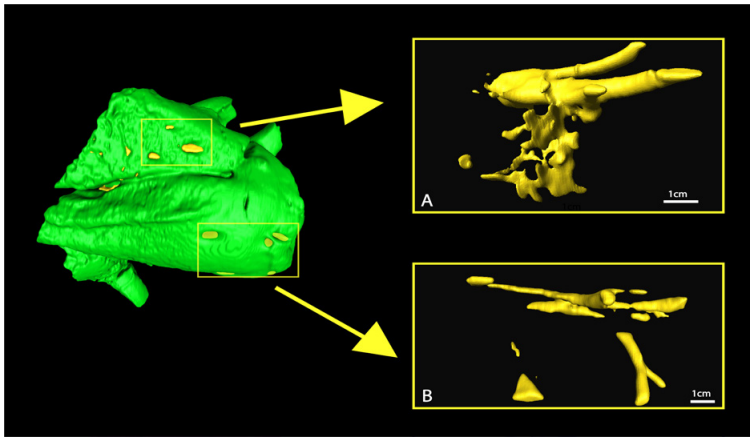


Figure 2. A reconstruction of the (A) pathological alterations associated with chronic infection and (B) normal neuroanatomical structures in the upper jaws and snout (i.e. maxilla and premaxilla, respectively) of NHMM 2012 072.

REFERENCES

Foth, C., Evers, S.W., Pabst, B., Mateus, O., Flisch, A., Patthey, M., Rauhut, O.W. 2015. New insights into the lifestyle of *Allosaurus* (Dinosauria: Theropoda) based on another specimen with multiple pathologies. PeerJ, 3, e940, 1-33.

Lingham-Soliar, T. 1998. Unusual death of a Cretaceous giant. Lethaia 31, 308-310.

Everhart, M.J., 2008. A bitten skull of *Tylosaurus kansasensis* (Squamata: Mosasauridae) and a review of mosasaur-on-mosasaur pathology in the fossil record. Transactions of the Kansas Academy of Science 111, 251-262.

Mulder, E.W.A. 2001. Co-ossified vertebrae of mosasaurs and cetaceans: implications for the mode of locomotion of extinct marine reptiles. Paleobiology, 27, 724-734.

Schulp, A.S., Walenkamp, G.H.I.M., Hofman, P.A.M., Rothschild, B.M., & Jagt, J.W.M. 2004. Rib fracture in *Prognathodon saturator* (Mosasauridae, Late Cretaceous). Netherlands Journal of Geosciences/ Geologie en Mijnbouw 83, 251-254.

4.4

Understanding the fossil record of arthropod moulting using experimental taphonomic approaches

Allison C. Daley[1], Jonathan B. Antcliffe[1] & Mickaël Lheritier[2]

[1]*Institute of Earth Sciences, University of Lausanne, Geopolis, CH-1-15 Lausanne, Switzerland (allison.daley@unil.ch)*
[2]*Université Claude Bernard Lyon 1, Department des Sciences de la Terre, Bâtiment Géode, 2 rue Dubois, 69622 Villeurbanne, France.*

The arthropod fossil record has revealed that this animal phylum has been diverse and abundant for over 500 million years, providing important insight into major events such as the Cambrian Explosion and the Great Ordovician Biodiversification Event (Daley et al. 2018). Detailed descriptive works focused on anatomy and functional morphology provide critical information on the phylogenetic relationships and evolution of the arthropod phylum. To achieve the best possible interpretations of arthropod fossils, aspects of their life history strategies and preservation should also be taken into account. In particular, growth and development of arthropods is characterised by moulting, or ecdysis, where the hardened exoskeleton must be periodically shed. This means that a single arthropod individual produces multiple empty moulted exuviae during their life, but only one carcass upon death. Both moults and carcasses are known in the fossil record (Figure 1), but they can only be easily distinguished in a few select groups (e.g. trilobites), and opinion is divided on the relative preservation potential of moults versus carcasses (Daley & Drage 2015). Such information is important to establish because it can contribute to more accurate quantitative paleoecological studies on fossil arthropod communities, and be combined with ontogenetic information to examine life history strategies of extinct taxa.

Further insight into the arthropod fossil record can be gained by using experimental taphonomy approaches, during which decay of modern arthropod analogues is observed at regular intervals under varying parameters. Such experiments provide, for example, information on how soft and hard tissues react under different conditions, their rate of decomposition, and the order of character loss (Briggs & Kear 1994; Sansom et al. 2011). We observed the decay of the red cherry shrimp (*Neocaridina davidi*) in four contrasted conditions: in fresh water versus in highly saline water, and adult shrimp versus juveniles. Adult and juvenile shrimps were euthanized with deoxygenated water, and the condition of a list of characters were coded while they decayed in either fresh water or hypersaline water. Decay stages can be examined using digital photography, multispectral macroimaging, or cryo-SEM (Antcliffe & Hancy, accepted). We also recorded the oxygen level in 200mL of fresh water containing a single decaying adult shrimp, with readings taken every 24 hours using a UNISENSE Microsensor Multimeter. Results show that juveniles decayed must faster than adults in both fresh and hypersaline conditions, and that hypersaline conditions slowed down decay of both juvenile and adults. Soft tissues forming the visceral mass lost coherency within the first few days, corresponding to the period of time d a drastic decrease in oxygen was observed by the Microsensor readings. Such results provide a baseline from which to develop further studies examining the preservation and proportions of adults and juveniles found in the crustacean fossil record, for example at localites such as Upper Jurassic Solnhofen Lithographic Limestones (Bavaria), where hypersaline stagnant conditions contributed to exceptional preservation of soft tissues. At this locality and others, empty moulted exuviae make up a large proportion of the arthropod fossil record (Daley & Drage 2015), and so future experimentation will compare the decay sequence and preservation potential of moults and carcasses. This study forms part of a wide-ranging research strategy that seeks to understand the evolution of moulting in arthropods over their entire history.

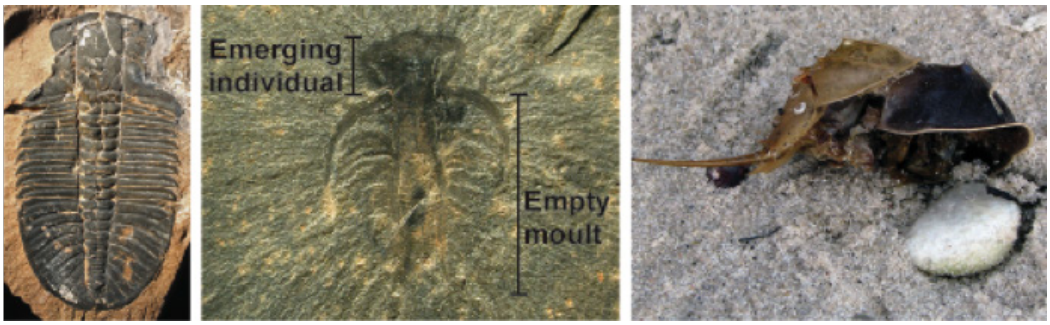


Figure 1. Fossil and extant arthropod moults. From left to right: A trilobite empty moult (Image credit: H. Drage); *Marrella* from the Burgess Shale preserved mid-moult (Image credit: D. Garcia-Bellido; and a modern horseshoe crab in the act of moulting (Image credit: Wikimedia Commons). Modified from Daley & Drage (2015).

REFERENCES

Antcliffe, J.B., & Hancy, A.D. Anoxia can increase the rate of decay for cnidarian tissue: using *Actinia equina* to understand the early fossil record. Geobiology, accepted.

Briggs, D.E.G., & Kear, A.J. 1994. Decay and Mineralization of Shrimps. Palaios, 9, 431-456.

Daley, A.C., & Drage, H.B. 2015. The fossil record of ecdysis, and trends in the moulting behaviour of trilobites. Arthropod Structure & Development, 45, 71-96.

Daley, A.C., Antcliffe, J.B., Drage, H.B., & Pates, S. 2019. Early fossil record of Euarthropoda and the Cambrian Explosion. PNAS, 115, 5323-5331.

Sansom, R.S., Gabbott, S.E., & Purnell, M.A. 2010. Non-random decay of chordate characters causes bias in fossil interpretation. Nature, 463, 797-800.

4.5

A geometric morphometric study of turtle shells

Laura Dziomber[1], Christian Foth[1], Walter G. Joyce[1]

[1]*Department of Geosciences, University of Fribourg, Chemin du Musée 6, CH-1700 Fribourg, Switzerland (laura.dziomber@unifr.ch)*

The turtle shell is unique among tetrapods and its presence defines the clade Testudinata. Turtles have proven themselves to be successful since they first appeared in the Late Triassic as they colonized a large diversity of environments, ranging from dry land to ponds, rivers, and the open ocean, and survived all major extinction events.

Although the turtle shell is universally composed of the dorsal carapace and the ventral plastron, variation is apparent in its exact composition (i.e., the number of bones and scutes) and in its morphology, ranging from domed, to flat, to tectiform, and tear-drop shaped. The turtle shell has been hypothesized to provide several adaptive advantages to its owner, including not only physical defense against predators, but also perhaps thermoregulation, pH regulation, and mate recognition. The shell has also been proposed to possibly have ecological significance, in that herbivorous turtles may have more voluminous shells, terrestrial turtles more highly domed shells, or aquatic turtle more stream-lined shells, but only a few of these purported correlations have been investigated in a global context. This is one reason why the ecology of the most basal known turtles is still under discussion.

To explicitly test for a correlation between shell shape and ecology, we assembled a 3D dataset of 70 extant turtles and 3 fossils, in particular, the Late Triassic *Proganochelys quenstedti* and *Proterochersis robusta* and the Late Jurassic *Plesiochelys bigleri*, all from Central Europe. 3D models were obtained using surface scanning and photogrammetry and morphology was captured through the use of landmarks and semi-landmarks. The known habitat ecology of turtles was classified using the webbing of their forelimbs as a proxy. Principle component analysis (PCA) highlights much overlap between habitat groups, but phylogenetic discriminant analysis (pFDA) suggests significant differences. However, while *Plesiochelys bigleri* tends to cluster with marine turtles, the two Triassic species do not cluster with extant forms at all. It, therefore, may not be possible to characterize their ecology using the methods we chose.

4.6

A new hypothesis of turtle relationships provides insights into the evolution of marine adaptation, and turtle diversification

Serjoscha W. Evers[1]

[1]*Department of Geosciences, University of Fribourg, Chemin du Musée 4, CH-1700 Fribourg (serjoscha.evers@googlemail.com)*

Evolutionary transitions to marine habitats occurred frequently among Mesozoic reptiles, but chelonioid sea turtles are the only clade that survives to the present. Thus, chelonioids provide the chance to investigate macroevolutionary questions, such as the mode and tempo of morphological evolution during this ecological transition informed by total evidence approaches that integrate fossil and recent data. However, uncertainties about turtle phylogeny (e.g. Joyce 2007; Cadena & Parham 2015), particularly the relationships of several secondarily marine groups from the Mesozoic have prohibited a rigorous assessment of divergence times of marine clades, and of patterns of flipper evolution.

I address these issues by reconciling previously available data with novel observations based of a large database of 3D cranial models derived from >150 CT scans of living and extinct turtles (Fig. 1). This resulted in a new phylogenetic dataset, formulated using a consistent coding strategy that accounts for hierachical homologies of observed variation. Parsimony and Bayesian phylogenetic analyses, incorporating explicit statistical hypothesis tests demonstate that two major clades (outside pleurodires) evolved a secondarily marine lifestyle: chelonioids and angolachelonians (Evers & Benson 2019). Angolachelonians comprise all non-pleurodiran marine Mesozoic–Paleogene turtles. The chelonoioid crown-group evolved during the early Late Cretaceous, and their stem group extends into the Early Cretaceous by inclusion of protostegids. The general flipper morphology of chelonioids was established early on their stem-lineage (Fig. 2), and further morphological innovations appeared at the origin of extant subclades Cheloniidae and Dermochelyidae (Evers et al. 2019). Chelonioid inner ears show increased semicircular canal thickness with increased diving ability, which mirrors observations from sauropterygians (Neenan et al. 2017), potentially providing evidence for a pattern of marine adaptation in the inner ear across reptiles more generally.

Americhelidians, i.e. chelonioids plus their extant sister clade, the chelydroids, are inferred to have a North American origin, but geographic expansion of protostegids occurred rapidly during the Early Cretaceous. The inference of an earlier diversification of americhelydians implies that crown-clades of turtles in general diversified earlier and faster than previously thought. My findings indicate that a total of three independent origins of marine life in Jurassic–Cretaceous turtles gave rise to speciose, long-lived clades (chelonioids, angolachelonians, bothremydid pleurodires). All three clades survived the K/Pg boundary, indicating high survivorship compared to other marine reptiles. Angolachelonians and bothremydids become extinct by the early Neogene, coincident with global cooling, and only chelonioids survived to the present.

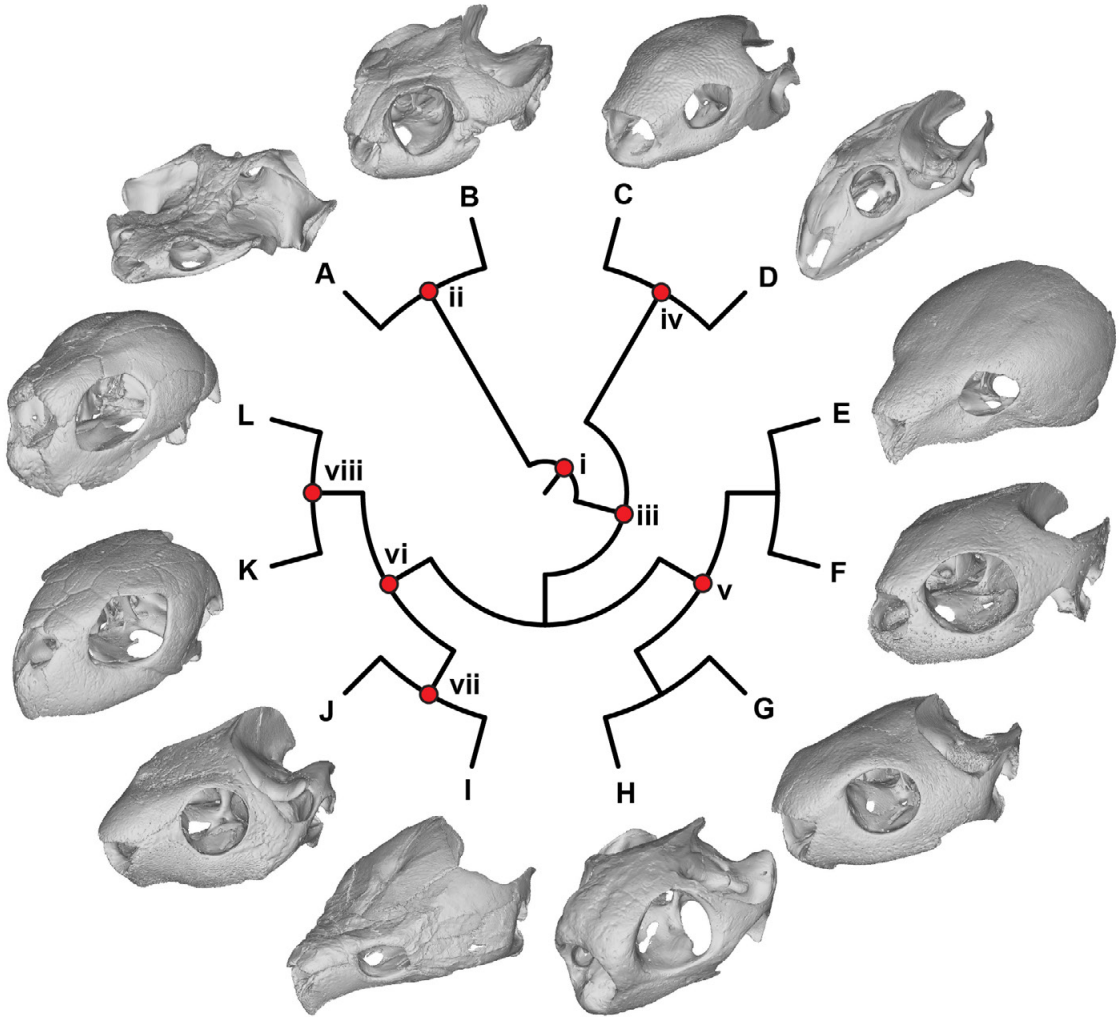


Figure 1. 3D renderings of extant turtle species representing major turtle clades, exemplifying the data used in my study. **A**, *Chelus fimbriatus* (NHMUK 81.9.72.4), representing Cheliidae; **B**, *Pelomedusa subrufa* (SMF 70540), representing Pelomedusoides; **C**, *Carettochelys insculpta* (NHMUK 1903.7.10.1), representing Carettochelyidae; **D**, *Apalone spinifera emoryi* (FMNH 22178), representing Trionychidae; **E**, *Platysternon megacephalum* (SMF 69684), representing Platysternidae; **F**, *Chrysemys picta*, representing Emydidae (NHMUK 76.1.31.19); **G**, *Geoclemys hamiltoni*, representing Geoemydidae (NHMUK 87.9.30.1); **H**, *Gopherus polyphemus* (FMNH 211815), representing Testudinidae; **I**, *Macrochelys temminckii* (FMNH 22111), representing Chelydridae; **J**, *Sternotherus minor* (FMNH 211696), representing Kinosternidae; **K**, *Lepidochelys olivacea* (SMNS 11070), representing Cheloniidae; **L**, *Dermochelys coriacea* (UMZC R3031), representing Dermochelyidae. Note that Plemodusidae and Podocnemididae are summarized as Pelomedusoides and that Dermatemydidae is not listed separately. Labelled internal nodes represent important clades: *i*, Testudines (crown-group turtles); *ii*, Pleurodira; *iii*, Cryptodira; *iv*, Trionychia; *v*, Testudinoidea; *vi*, Americhelydia; *vii*, Chelydroidea; *viii*, Chelonioidea.

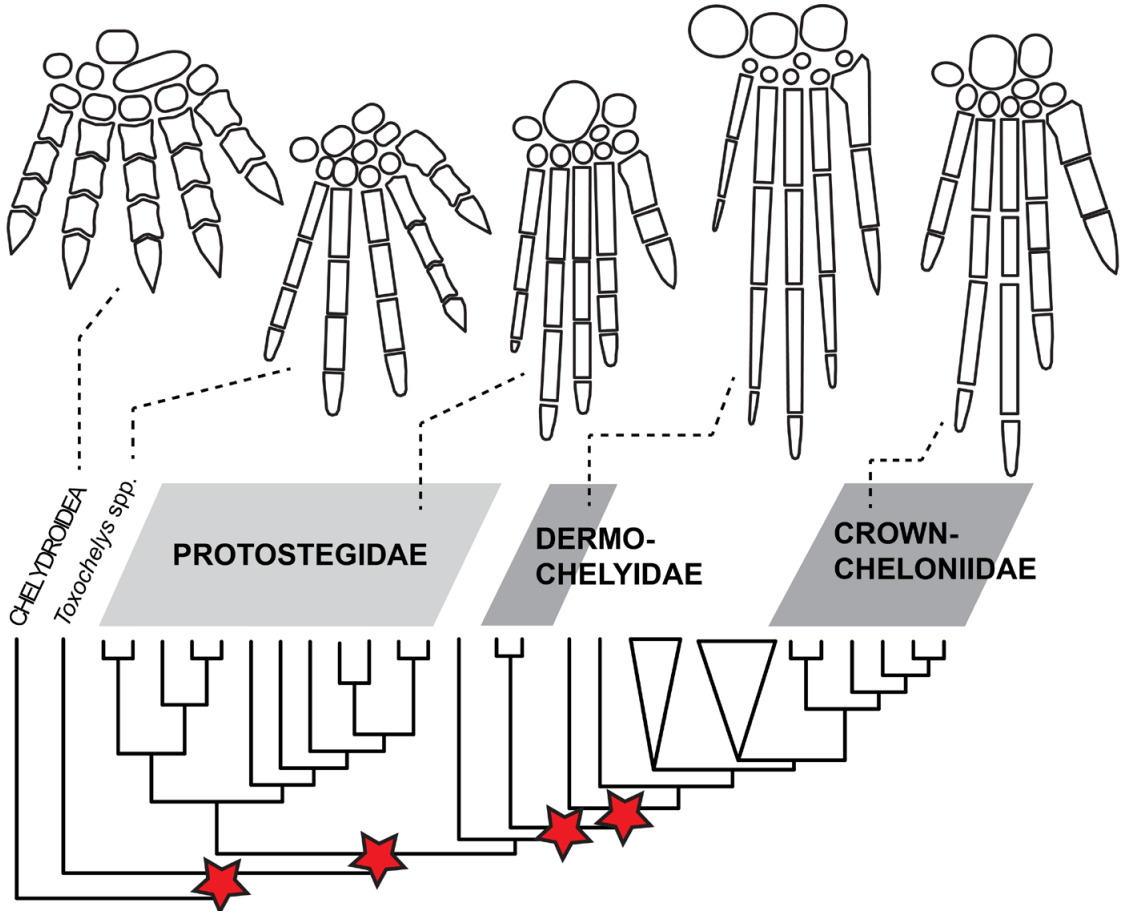


Figure 2. Summary phylogeny and schematic flipper morphology for respresantatives of all chelonioid subclades. Red stars indicate burst of morphological innovations.

REFERENCES

Cadena, E.A., & Parham, J.F. 2015: Oldest known marine turtle? A protostegid from the Lower Cretaceous of Colombia, PaleoBios, 32(1), 1-42.

Evers, S.W., & Benson, R.B.J. 2019: A new phylogenetic hypothesis of turtles with implications for the timing and number of evolutionary transitions to marine turtles, Palaeontology, 62, 93-134.

Evers, S.W., Barrett, P.M., & Benson, R.B.J. 2019: Anatomy of *Rhinochelys pulchriceps* (Protostegidae) and marine adaptation during the early evolution of chelonioids, PeerJ, 7, e6811.

Joyce, W.G. 2007: Phylogenetic relationships of Mesozoic turtles, Bulletin of the Peabody Museum of Natural History, 48(1), 3-103.

Neenan, J.M., Reich, T., Evers, S.W., Druckenmiller, P.S., Voeten, D.F.A.E., Choiniere, J.N., Barrett, P.M., Pierce, S.E., & Benson, R.B.J. 2017: Evolution of the sauropterygian labyrinth with increasingly pelagic lifestyles, Current Biology, 27(24), 3852-3858.

4.7

Diversity of early Forcipulatacea (Asteroidea)

Marine Fau[1], Loïc Villier[2] & Timothy Ewin[3]

[1]Department of Geosciences, University of Fribourg, Chemin du Musée 6, 1700 Fribourg, Switzerland
[2]Centre de Recherche en Paléontologie - Paris, Sorbonne Université, 4 place Jussieu, 75005 Paris, France
[3]Department of Earth Sciences, The Natural History Museum London, Cromwell Road, South Kensington, London, UK, SW7 5BD, United Kingdom

Asteroidea (also called sea stars or starfish) is a class comprised of about 2'000 extant and 600 extinct species. It is generally accepted that all extant orders emerged during the Jurassic period, and then had about 200 million years of independent evolutionary history. The study of Jurassic fossils is therefore essential to understanding the initial diversification of all extant sea stars. The clade Forcipulatacea, comprised of about 400 extant species, is morphologically well-defined. However, its fossil record is relatively sparse with all representatives being assigned to two extant families; the Asteriidae and the Zoroasteridae, or erected as exclusively extinct families. We here reappraise four fossil forms from the Jurassic of England that belongs to Forcipulatacea, but has not always been recognized as such: *Asterias gaveyi* Forbes 1850, *Compsaster spiniger* Wright 1880, *Ophidiaster davidsoni* de Loriol and Pellat 1874 and *Terminaster cancriformis* Quenstedt 1876.

Extensive observation of these four fossils, including key details of the abactinal skeleton, ossicle spination and, where present, pedicellariae, combined with detailed comparative anatomical studies of extant taxa suggest that they need re-assignment. A phylogenetic analysis comprising 29 extant forcipulataceans and the 4 fossil forms was performed. More than a hundred characters were derived from the skeleton with emphasis on the organisation of the abactinal skeleton, as most of the synapomorphies of the extant clades (i.e., for the Asteriidae, the Stichasteridae) address the abactinal skeleton structure.

The results of the phylogenetic analysis place *A. gaveyi* and *T. cancriformis* along the stem of crown Zoroasteridae, supported at this position by their compact abactinal skeleton and the lack of crossed pedicellariae. These two fossils challenge previous hypotheses regarding the homology of the unique row of marginals in zoroasterids, as two rows of marginals can be identified in *T. cancriformis. Ophidiaster davidsoni* is retrieve within the Stichasteridae, and *C. spiniger* within the Asteriidae. Although the latter possesses crossed pedicellariae, there is no trace of a wreath organ, which is the most distinct synapomorphy of Asteriidae. The position of the fossils in the tree suggests an early diversification of Forcipulatacea during the Jurassic. The reanalysis of these taxa demonstrates that the early diversity of the Forcipulatacea was greater than previously thought and challenges existing perceptions of the evolutional history of this major clade.

4.8

Weird coelacanths from the Triassic of Switzerland

Christophe Ferrante[1,2], Lionel Cavin[2]

[1]Department of Earth Sciences, University of Geneva, Rue des Maraîchers 13, 1205 Genève (christophe.ferrante@ville-ge.ch)
[2]Department of Geology and Palaeontology, Natural History Museum of Geneva, CP 6434, 1211 Genève 8

Coelacanths, or actinistians, form a clade of sarcopterygian fishes with two living species and about 50 extinct genera. This group is well known for its relatively conservative morphology, with representatives showing a generalized Bauplan since the Early Devonian (Zhu et al., 2012). Species showing a body morphology that differentiates from the generalized model are known in the Devonian, Carboniferous and Triassic. *Foreyia maxkuhni* from the Middle Triassic Prosanto Formation in Canton Graubünden, Switzerland, is one of these deviant forms recently described. This species shows a mosaic of plesiomorphic and apomorphic characters for coelacanths, although a cladistic analysis placed it as the sister of *Ticinepomis* at the base of the extant latimeriid family (Cavin et al., 2017).

The ongoing description of coelacanth material from the famous Middle Triassic Monte San Giorgio site collected in the 20th century and kept in the Palaeontological Institute and Museum, University of Zurich, provides new information about the distribution of characters and consequently about the phylogeny of coelacanths. It likely represents a new taxon. Some superficial features, such as the dermal ornamentation and proportionally huge head compared to the body are reminiscent of *Foreyia*. Other characters, e.g. the tightly sutured bones on the cheek, the shape of the cleithrum and of the extrascapular series are evocative of primitive coelacanths. Some characters, e.g. the peculiar shape of the dentary appear to share characteristics with derived genera. Eventually, postcranial features are autapomorphic.

The Prosanto and Besano formations in Cantons Graubünden and Ticino, respectively, are yielding an expectedly high diversity of coelacanths (Ferrante et al., 2017), such as *Ticinepomis* (Rieppel, 1980) and *Heptnaema* (Renesto & Stockar, 2018.), which show a conservative morphology. Others, such as *Foreyia* and the new taxon display a very unusual anatomy.

REFERENCES

Cavin, L., Mennecart, B., Obrist, C., Costeur, L. & Furrer, H. 2017: Heterochronic evolution explains novel body shape in a Triassic coelacanth from Switzerland. Scientific Reports, 1-7.

Ferrante, C., Martini, R., Furrer, H. & Cavin, L. 2017: Coelacanths from the Middle Triassic of Switzerland and the pace of actinistian evolution. Research & Knowledge, 3, 59-62.

Renesto, S., & Stockar, R. 2018: First record of a coelacanth fish from the Middle Triassic Meride Limestone of Monte San Giorgio (Canton Ticino, Switzerland). Rivista Italiana di Paleontologia e Stratigrafia (Research In Paleontology and Stratigraphy), Riv. It. Paleontol. Strat., 124, 639-653.

Rieppel, O. 1980: A new coelacanth from the Middle Triassic of Monte San Giorgio, Switzerland. Eclogae Geologicae Helvetiae 73/3, 921-939.

Zhu, M., Yu, X., Lu, J., Qiao, T., Zhao, W. & Jia, L. 2012: Earliest known coelacanth skull extends the range of anatomically modern coelacanths to the Early Devonian: Nature Communications, 3, 772.

4.9

A new early symmoriid with an unusual jaw articulation from the Late Devonian of Morocco

L. Frey[1], M. I. Coates[2], M. Rücklin[3] and C. Klug[1°]

[1]Paläontologisches Institut und Museum, University of Zurich, Karl-Schmid-Strasse 4, CH-8006 Zürich °(chklug@pim.uzh.ch).
[2]Department of Organismal Biology and Anatomy, University of Chicago, 1027 E. 57th St., USA-60637 Chicago.
[3]Naturalis Biodiversity Center, Postbus 9517, 2300 RA, Leiden, The Netherlands.

The Symmoriida comprise some morphologically peculiar chondrichthyan genera like *Akmonistion*, *Damocles*, *Falcatus* or *Stethacanthus*. Most symmoriids were described from the Carboniferous and many are characterized by strangely modified dorsal fin spines or spine brush-complexes and moderately small body sizes. We discovered a new small symmoriid in the Famennian of the Maïder region. The specimen is exceptionally well preserved and allows to assess several previously unknown aspects of its palaeobiology such as the function of the jaw articulation in this group. The functional morphology of mandibular and branchial arches in early chondrichthyans is poorly known because of the lack of articulated and undistorted fossil material. A three-dimensional model based on CT-scans of this new symmoriid shows the undeformed mandibular and branchial arches such as the hyoids and ceratohyals allowing the reconstruction of mandible movement during feeding. The way the Meckel's cartilages rotate around their sagittal axes was previously unknown from chondrichthyans and probably became extinct with the demise of the symmoriid clade. At the same time, the new species corroborates that the cranial morphology (in contrast to the remarkably modified dorsal fins and spines) of Palaeozoic symmoriiforms is quite conservative and allowed to falsify the aphetohyoidean hypothesis for these early chondrichthyans, because in the new taxon, the hyoid is tightly attached to the lower jaw.

4.10

Palaeoecology of benthic macroinvertebrates from three Middle Triassic carbonate platforms

Evelyn Friesenbichler[1], Michael Hautmann[1], Hugo Bucher[1]

[1]Paläontologisches Institut und Museum, University of Zurich, Karl-Schmid-Strasse 4, CH-8006 Zurich (evelyn.friesenbichler@pim.uzh.ch)

The main recovery phase after the end-Permian mass extinction took place during the Middle Triassic and coincided with the re-establishment of large carbonate platforms. Did the resurgence of these large carbonate platforms affect the diversification of benthic macroinvertebrates and which evolutionary changes were involved in the colonization of this new habitat type? To answer these questions, quantitative ecological analyses were performed on benthic communities from three Middle Triassic carbonate platforms: (1) An early Middle Anisian *Tubiphytes*-microbial buildup (North Dobrogea, Romania), (2) the late Anisian carbonate platform of the Latemar (Dolomites, Italy) and (3) the Late Ladinian – Early Carnian Schlernplateau beds (Dolomites, Italy). The *Tubiphytes*-microbial buildup represents one of the oldest Triassic carbonate reefs, which was formed on the upper slope of a distal platform in relatively deep water. The Latemar carbonate platform represents an atoll, with a wellstratified platform interior that contains the investigated fauna. The Schlernplateau beds represent an open lagoon in a platform interior. The investigated faunas were compared with other Middle and Early Triassic faunas in terms of species richness and trophic composition. This comparison shows an increase in species richness during the Middle Triassic, which coincides with the main phase of recovery after the end-Permian mass extinction. During this recovery phase, bivalves that dominated Early Triassic benthic communities continued to diversify, but gastropods diversified quicker and outnumbered bivalves by the end of the Middle Triassic in carbonate platform settings. We hypothesise that the co-evolution between carbonate producers and benthic faunas, as well as the increase in environmental heterogeneity in the context of carbonate platforms resurgence were factors that contributed to this shift in taxonomic composition.

4.11

Globorotalia menardii reflects AMOC: Test-Size Evolution of *G. menardii* as a new Proxy for the AMOC Strength

Thore Friesenhagen[1,2], Michael Knappertsbusch[1]

[1]*Natural History Museum Basel, Augustinergasse 2, CH-4001 Basel, Switzerland*
[2]*Department Umweltwissenschaften, University of Basel, Bernoullistrasse 32, CH-4056 Basel*
(thore.friesenhagen@unibas.ch)

The Atlantic Meridional Overturning Circulation (AMOC) is known to have a huge impact on the climatic system of the northern hemisphere via northern directed heat transport from low to high latitudes. Thus, changes of its strength probably played a major role for climatic events, like the 8.2 ka event on a relatively small timescale [e.g. Alley & Ágústdóttir, 2005] or the Northern Hemisphere Glaciation on a long timescale [e.g. Steph et al., 2010].

Recently, the long-term (10^5 years) strength of the AMOC was reconstructed by others using stable isotopes like $\delta^{18}O$, $\delta^{13}C$, and Nd/Hf ratio [Dausmann et al., 2017]. Here, we propose that the test-size of the planktonic foraminifer *Globorotalia menardii* may serve as another, new proxy for the relative interglacial AMOC strength. New in our research is the observation that our measurements of test-size changes in the tropical Atlantic throughout the last 8Ma remarkably correlate positive with the reconstruction of AMOC strength from the literature. This correlation is probably caused by the ecology of *G. menardii* as a thermocline dweller. The test size seems to change along with the development and/or the depth of the thermocline, which in turn is affected by long-term changes in the AMOC strength [dos Santos et al., 2010]. Thus, the test-size evolution of *G. menardii* may be a valuable tool to reconstruct the local relative thermocline development and/or depth evolution during interglacial times, whereas longer time-series of test-size evolution possibly allow the reconstruction of the AMOC strength.

Currently, work is in progress about the test-size evolution of *G. menardii* from the western Indian Ocean IODP Site 1476A for the past 6.5Ma. Its position within the Mozambique Channel qualifies this core to be a key site for testing the Agulhas Leakage Hypothesis. This hypothesis proposes the dispersal of Indian Ocean biota into the Atlantic Ocean via the Agulhas Current and may explain a “sudden” test-size increase event of *G. menardii* in the tropical Atlantic Ocean during the Gelasian [Knappertsbusch, 2016]. Preliminary results will be interpreted in terms of whether or not the data set agrees with the above idea about a thermocline-controlled size evolution.

REFERENCES

Alley, R. B. and Ágústdóttir, A. M. (2005). The 8k event - cause and consequences of a major Holocene abrupt climate change. *Quaternary Science Reviews*, 24(10–11):1123–1149.

Dausmann, V., Frank, M., Gutjahr, M., and Rickli, J. (2017). Glacial reduction of AMOC strength and long–term transition in weathering inputs into the Southern Ocean since the mid–Miocene: Evidence from radiogenic Nd and Hf isotopes. *Paleoceanography*, 32(3):265–283.

dos Santos, R. A. L., Prange, M., Castañeda, I. S., Schefuß, E., Mulitza, S., Schulz, M., Niedermeyer, E. M., Damsté, J. S. S., and Schouten, S. (2010). Glacial-interglacial variability in Atlantic meridional overturning circulation and thermocline adjustments in the tropical North Atlantic. *Earth and Planetary Science Letters*, 300(3-4):407–414.

Knappertsbusch, M. W. (2016). Evolutionary prospection in the Neogene planktic foraminifer Globorotalia menardii and related forms from ODP Hole 925B (Ceara Rise, western tropical Atlantic): evidence for gradual evolution superimposed by long distance dispersal? *Swiss Journal of Palaeontology*.

Steph, S., Tiedemann, R., Prange, M., Groeneveld, J., Schulz, M., Timmermann, A., Nürnberg, D., Rühlemann, C., Saukel, C., and Haug, G. H. (2010). Early Pliocene increase in thermohaline overturning: A precondition for the development of the modern equatorial Pacific cold tongue. *Paleoceanography*, 25(2).

4.12

Environmental influence on spore-pollen morphology during the Mesozoic

Francesca Galasso[1] and Elke Schneebeli-Hermann[1]

[1]*Paläontologisches Institut und Museum, University of Zurich, Karl-Schmid-Strasse 4, CH-8006, Zürich (francesca.galasso@pim.uzh.ch)*

The Permian/Triassic biotic crisis (PTB) is considered as one of the five most severe mass extinction events in geological time. Environmental perturbations caused a significant decrease in faunal diversity. However, the plant record shows a different pattern. Historically, an almost complete loss of vegetation was suggested; however, recent studies show that almost all major plant linages survived the PTB. Global environmental changes have been postulated as potential causes (e.g. changing pCO_2, climate, sea-level, or SO_2 emission).

Recent work on teratomorph spores and pollen grains ("the science of malformation/abnormalities") shows a higher occurrence of abnormal structures associated with/during the PTB and Triassic-Jurassic mass extinctions and intervals with rapid changes in the carbon isotope curve.
The Smithian-Spathian Boundary (SSB) event was one of the most significant biotic events in the aftermath of the PTB extinction. The SSB interval coincides with a positive carbon isotope excursion, a preceding vegetation turnover from lycopods-to gymnosperm-dominated vegetation, with subsequently climatic turnover from rather humid to more arid conditions.

Here we present occurrence and relative abundance data of teratomorph spores and pollen grains from the Nammal section (Pakistan) straddling the SSB. In 25 samples, at least 300 sporomorphs were counted, recording the quantitative distribution of normal and teratomorphic grains. Furthermore, normal and malformed spore tetrads and modifications of sporomorphs color are described. The encountered variety of abnormalities and the wealth of combinations of these encouraged the establishment of two identification schemes (i.e. one for lycopods and one for gymnosperms). These schemes or guidelines shall help to quantify the morphological patterns and distinguish between morphological changes due to poor preservation and malformation due to environmental effects. This allows testing whether teratology in spores and pollen can work as a means of identifying and quantifying ecological disturbance in the fossil record, specifically around the PTB.

4.13

Soft part preservation reveals a high diversity of large bivalved arthropods in the Fezouata Biota (Early Ordovician, Morocco)

Pierre Gueriau[1], Lukáš Laibl[1], Francesc Pérez Peris[1], Lorenzo Lustri[1] & Allison C. Daley[1]

[1]*Institute of Earth Sciences, University of Lausanne, Géopolis, CH-1015 Lausanne, Switzerland (pierre.gueriau@unil.ch)*

The Early Ordovician Fezouata Biota (late Tremadocian, ca. 478 Ma) from Morocco has yielded a diverse arthropod fauna, including basal stem-lineage arthropods such as Radiodonta and Lobopodia, the oldest examples of horseshoe crabs, and new informative specimens of enigmatic taxa such as marrellomorph arthropods (Van Roy et al. 2010, 2015a, b). The Fezouata Biota also contains abundant remains of bivalved arthropod carapaces, with lengths ranging from a few millimeters to several centimeters. Besides isolated hemispherical valves with cardinal spines typical of Isoxyida, absence of soft parts has so far precluded other carapaces being assigned to any specific arthropod group, as bivalved carapaces evolved in a wide range of groups homoplastically, and are seen in bradoriid, ostracod, diplostracan, phyllocarid and thylococephalan crustaceans, as well as in a series of large Cambrian 'bivalved arthropod taxa' such as *Branchiocaris*, *Canadaspis* and *Odaraia*.

Here, we describe new bivalved arthropod specimens with soft parts from the Fezouata Biota. The new anatomical details highlighted using optical photography and contrast-enhanced UV-near-infrared macro-imaging show anteriorly directed appendages associated with an elongated, narrowing backwards bivalved carapace, reminiscent of thylacocephalan crustaceans. Isolated carapaces further display a well-defined anterior notch similar to the anterior optic notch present in most thylacocephalans. Another specimen, dorsoventrally flattened with suboval valves in 'butterfly position', displays a peculiar radiating pattern on the valves, as well as part of the trunk including seven segments, the last one being longer than the others. A third specimen preserves two segments and a tapering telson with unsegmented articulated furca, which strongly suggests phyllocarid affinities for these last two forms. The precise affinities of these few fossils remain to be determined, but they clearly indicate a high diversity of bivalved arthropod taxa in early Ordovician marine communities along the West Gondwanan margin, and we can expect that new fossil finds and/or the use of new imaging techniques may reveal an even higher diversity of these organisms.

REFERENCES

Van Roy, P., Orr, P.J., Botting, J.P., Muir, L.A., Vinther, J., Lefebvre, B., el Hariri, K., & Briggs, D.E.G. 2010: Ordovician faunas of Burgess Shale type, Nature, 465, 215-218.

Van Roy, P., Briggs, D.E.G., & Gaines, R.R. 2015a: The Fezouata fossils of Morocco; an extraordinary record of marine life in the Early Ordovician, Journal of the Geological Society, 172, 541-549.

Van Roy, P., Daley, A.C., & Briggs, D.E.G. 2015b: Anomalocaridid trunk limb homology revealed by a giant filter-feeder with paired flaps, Nature, 522, 77-80.

4.14

Famennian thylacocephalans from Morocco and their role in Late Devonian foodwebs

Melina Jobbins[1], Christian Klug[1]

[1]*Paläontologisches Institut und Museum, University of Zurich, Karl-Schmid-Strasse 4, CH-8006 Zurich (melina.jobbins@pim.uzh.ch)*

Thylacocephalans are pelagic arthropods with an erratic fossil record stretching from the Silurian, possibly Cambrian, to the Cretaceous. In many of the few localities where they occur, they are quite abundant. This holds true for the Famennian Thylacocephalan Layer in the Maider Basin (eastern Anti-Atlas) (Frey et al. 2018). This small epicontinental basin hosts some strata with taphonomic properties of a Konservat-Lagerstätte yielding exceptionally preserved gnathostomes and invertebrates. In a thin argillaceous interval in the earliest middle Famennian, thylacocephalans occur in such great numbers that they became eponyms of this unit. Therein, we discovered the two new thylacocephalan taxa *Concavicaris submarinus* sp. nov. and *Madenecaris iugumata* sp. nov., which represent the first records of this group from Africa. In the CT-imagery, the holotype of *Concavicaris submarinus* sp. nov. revealed anatomical details including its eyes, pleiopods, some muscles and other structures. Sedimentary facies and faunal composition of the Thylacocephalan Layer suggest that these animals populated the water column above the low-oxygen bottom waters. The Thylacocephalan Layer is also rich in articulated remains of chondrichthyans and placoderms. Accordingly, these putative crustaceans likely represented an important component of their diet (Williams 1990). The abundance of thylacocephalans in other Konservat-Lagerstätten such as the Cleveland Shale (USA; Williams 1990), the Gogo Formation (Australia; Briggs et al. 2011) and the Famennian of the Holy Cross Mountains (Poland; Broda et al. 2015) underline their pivotal role in Late Devonian pelagic foodwebs.

REFERENCES

Briggs, D., Rolfe, W., Butler, P., Liston, J. & Ingham, J. 2011: Phyllocarid crustaceans from the Upper Devonian Gogo Formation, Western Australia. J. of Syst. Palaeontol. 9, 399-424.

Broda, K., Wolny, M. & Zatoń, M. 2015: Palaeobiological significance of damaged and fragmented thylacocephalan carapaces from the Upper Devonian of Poland. Proc. Geol. Asso. 126, 589-598.

Frey, L., Rücklin, M., Korn, D. & Klug, C. 2018: Late Devonian and Early Carboniferous alpha diversity, ecospace occupation, vertebrate assemblages and bio-events of southeastern Morocco. Palaeogrogr., Palaeoclimatol., Palaeoecol. 496, 1-17.

Williams, M. 1990: Feeding behavior in Cleveland Shale fishes. Evolutionary paleobiology of behavior and coevolution 273-287.

4.15

Early post-embryonic development of marrellomorph arthropod from the Early Ordovician of Morocco

Lukáš Laibl[1], Pierre Gueriau[1], Frances Pérez Peris[1], Lorenzo Lustri[1], Jonathan B. Antcliffe[1] & Allison C. Daley[1]

[1]Anom Lab, Institute of Earth Sciences, University of Lausanne, Géopolis, CH-1015 Lausanne (lukas.laibl@unil.ch)

Marrellomorphs are marine arthropods known from several Cambrian to Devonian localities. The majority of recent phylogenies resolved this group as stem-Mandibulata (Legg 2013, Wolfe 2017) or at least as stem-Crustacea (Ortega-Hernández et al. 2013, Stein et al. 2013, Du et al. 2018, Chen et al. 2019), although its phylogenetic position is subject of continuous discussions (see Aria and Caron 2017 for an example of different topology). The post-embryonic development of Marrellomorpha is insufficiently known, as specimens of early stages are rare. Consequently, we know almost nothing about life-history strategies in its members. In this contribution, we describe numerous early post-embryonic stages of a marrellomorph arthropod from the Fezouata Formation (Lower Ordovician) of Morocco. These are small (ranging from two to four mm in sagittal length) and morphologically similar to adults. The only differences observed in the juveniles when compare with adults are: (i) a lower number of trunk segments; (ii) slender and straight spines on the cephalic shield; (iii) proportionally shorter secondary spines on the cephalic shield; and (iv) proportionally shorter podomeres in trunk endopods.

The morphology of both first and second antennae, and of the trunk exopods are identical to those of adults specimens. From such observations, several conclusions can be drawn. Firstly, the cephalic spines, their secondary spines and trunk endopods show allometric growth, but the shape change during development is generally minor. Secondly, the lower number of trunk segments confirm anamorphic type of development (i.e. adding segments during moulting), although it is difficult to determine whether the segment addition was halted at some point (= hemianamorphosis) or not (= euanamorphosis). Finally, the striking similarity between the early developmental stages and the adults implies direct development in this taxon, at least for the developmental sequence starting at about two mm in length onwards. This suggests that no niche differentiation took place during development of this taxon, as is supported also by the co-occurrence of early stages and adults at some localities. Considering the phylogenetic position of Marrellomorpha, it is likely that direct anamorphic development is ancestral either for total group Mandibulata or total group Crustacea, revealing the developmental origins of the most diverse arthropod group in existence today.

REFERENCES

Aria, C. & Caron, J.-B. 2017: Burgess Shale fossils illustrate the origin of the mandibulate body plan, Nature, 545, 89-92.

Chen, X., Ortega-Hernández, J., Wolfe, J.M., Zhai, D., Hou, X., Chen, A., Mai, H. & Liu, Y. 2019: The appendicular morphology of *Sinoburius lunaris* and the evolution of the artiopodan clade Xandarellida (Euarthropoda, early Cambrian) from South China. BMC Evolutionary Biology, 19, 165.

Du, K-s., Ortega-Hernández, J., Yang, J. & Zhang, X-g. 2018: A soft-bodied euarthropod from the early Cambrian Xiaoshiba Lagerstätte of China supports a new clade of basal artiopodans with dorsal ecdysial sutures, Cladistics, 35, 269-281.

Legg, D.A., Sutton, M.D. & Edgecombe, G.D. 2013: Arthropod fossil data increase congruence of morphological and molecular phylogenies, Nature Communications, 4, 2485.

Ortega-Hernández, J., Legg, D.A. & Braddy, S.J. 2013: The phylogeny of aglaspidid arthropods and the internal relationships within Artiopoda, Cladistics, 29, 15-45.

Stein, M., Budd, G.E., Peel, J.S. & Harper, D.A.T. 2013: Arthroaspis n. gen., a common element of the Sirius Passet Lagerstätte (Cambrian, North Greenland), sheds light on trilobite ancestry, BMC Evolutionary Biology, 13, 99.

Wolfe, J.M. 2017: Metamorphosis Is Ancestral for Crown Euarthropods, and Evolved in the Cambrian or Earlier, Integrative and Comparative Biology, 57, 499-509.

4.16

A new stem Euchelicerate from the early Ordovician Fezouata Biota

Lorenzo Lustri[1], Pierre Gueriau & Allison C. Daley[1]

[1]*Institut des sciences de la Terre, Université de Lausanne, Geopolis, CH-1015 Lausanne (lorenzo.lustri@unil.ch)*

The Fezouata Formation in southeastern Morocco is an Early Ordovician Lagerstätte that preserves a wide variety of non-biomineralized taxa and anatomical features (Van Roy et al. 2011, Van Roy et al. 2015, Lefebvre et al 2016). This site is noteworthy because it preserves a mix of Cambrian Explosion fauna and more typical Paleozoic marine taxa, as exemplified by the arthropods from this site, which includes radiodonts and other stem lineage taxa as well as crustaceans and a wide variety of euchelicerates. Two different undescribed euchelicerates are particularly abundant, one of them being the oldest occurrence of horseshoe crabs in the fossil record, and the other having been ascribed to a closely related clade known as the "synziphosurines" because of the lack of a fused opisthosoma.

Synziphosurina is a paraphyletic clade of taxa of various affinities, including stem members of Euchelicerata and of the lineages leading to Eurypterida, Xiphosura and Arachnida (Lamsdell, 2013, 2016; Selden et al 2015). An in-depth study of the Fezouata shale material is required to clarify the evolution and phylogeny of early xiphosurids and synziphosurines, and the relationship between them and other euchelicerates.
Here we described a new synziphosurine taxon from the Fezouata shale, known from more than 300 specimens. Specimens were examined using microscopy then photographed, and a limited number of specimens were selected for 3D surface rendering and synchrotron radiation X-ray tomographic microscopy.

This taxon is characterized by the presence of a semi-circular prosoma with an apical carapace spine, an ophthalmic ridge, and a pair of antero-ventrally oriented genal spines. Appendages are biramous. There are eleven opisthosomal targites, with no sign of fusion, and the first of them is not reduced to a ring like articulation but instead is fully developed. The second to the sixth targites possess a highly developed axis with two nodes connecting the axis to the pleura, which are present from the first to the seventh segments. On the ventral side opercula are present. The last four targites do not bear pleura and are fused with sternites that are fused to form a circular shaped segment. The pre-telson segment bear two pair of spines at each side of the base of the telson, which shows a bifurcation on the distal part.

Only three taxa of Synziphosura have been found with preserved appendages: *Offacolus kingi* (Sutton et al 2002) and *Dibasterium durgae* (Briggs et al 2012) from the Silurian Lagerstätte of Herefordshire and *Weinbergina opitzi* (Stürmer & Bergström 1981) from the Devonian Lagerstätte of Hunsrück Slate. All of them are at least 50 Ma younger than our taxon. The new Fezouata Biota species possesses some characters in common with these taxa, such as biramous prosomal appendages similar in morphology to those of the Herefordshire species, but also characters of the Prosomapoda euchelicerates, such as the ophthalmic ridge (Lamsdell 2013).

We undertook a phylogenetic analysis to clarify the phylogenetic position of the group. Two different datasets (Legg, 2013; Selden et al. 2015) have been used and compared to using both Parsimony and Bayesian methods to increase the reliability of our result. Our taxon resolves as a stem-euchelicerate with Prosomapoda affinities, and fills a gap in the transitional series that represents early euchelicerate evolution. Linking our new findings on euchelicerate diversity during the Great Ordovician Biodiversification Event to the earliest origin of the phylum, as recorded in the Cambrian Burgess Shale-type biotas, provides a more complete picture of euarthropod evolution during these major events.

REFERENCES

Briggs, D. E., Siveter, D. J., Siveter, D. J., Sutton, M. D., Garwood, R. J., & Legg, D. (2012). Silurian horseshoe crab illuminates the evolution of arthropod limbs. Proceedings of the National Academy of Sciences, 109(39), 15702-15705.

Lamsdell, J. C. (2013). Revised systematics of Palaeozoic 'horseshoe crabs' and the myth of monophyletic Xiphosura. Zoological Journal of the Linnean Society, 167(1), 1-27.

Lamsdell, J. C. (2016). Horseshoe crab phylogeny and independent colonizations of fresh water: ecological invasion as a driver for morphological innovation. Palaeontology, 59(2), 181-194.

Lefebvre, B., El Hariri, K., Lerosey-Aubril, R., Servais, T., & Van Roy, P. (2016). The Fezouata Shale (Lower Ordovician, Anti-Atlas, Morocco): a historical review. Palaeogeography, Palaeoclimatology, Palaeoecology, 460, 7-23.

Legg, D. A. (2014). Sanctacaris uncata: the oldest chelicerate (Arthropoda). Naturwissenschaften, 101(12), 1065-1073.

Selden, P. A., Lamsdell, J. C., & Qi, L. (2015). An unusual euchelicerate linking horseshoe crabs and eurypterids, from the Lower Devonian (Lochkovian) of Yunnan, China. Zoologica Scripta, 44(6), 645-652.

Van Roy, P., Briggs, D. E., & Gaines, R. R. (2015). The Fezouata fossils of Morocco; an extraordinary record of marine life in the Early Ordovician. Journal of the Geological Society, 172(5), 541-549.

Van Roy, M., Ververken, C., Beirnaert, E., Hoefman, S., Kolkman, J., Vierboom, M., ... & Jacobs, S. (2015). The preclinical pharmacology of the high affinity anti-IL-6R Nanobody® ALX-0061 supports its clinical development in rheumatoid arthritis. Arthritis research & therapy, 17(1), 135.

Sutton, M. D., Briggs, D. E., Siveter, D. J., Siveter, D. J., & Orr, P. J. (2002). The arthropod Offacolus kingi (Chelicerata) from the Silurian of Herefordshire, England: computer based morphological reconstructions and phylogenetic affinities. *Proceedings of the Royal Society of London. Series B: Biological Sciences*, *269*(1497), 1195-1203.

Stürmer, W., & Bergström, J. (1981). Weinbergina, a xiphosuran arthropod from the Devonian Hunsrück Slate. *Paläontologische Zeitschrift*, *55*(3-4), 237-255.

4.17

The Evolution of the Camelidae

Sinéad Lynch, Ana Balcarcel & Marcelo Sánchez-Villagra

*Paläontologisches Institut und Mu*seum, Karl-Schmid-Strasse 4, 8006 Zürich, Switzerland

The Camelidae appeared during the middle Eocene epoch in North America and became a highly diversified group until its drastic decline in the late Pleistocene. (Honey et al., 1998) Today only members of two tribes, Lamini (*Lama, Vicugna*) and Camelini (*Camelus*), are extant. Both of these tribes originated in the Miocene and migrated to the Old World and South America approximately 3 Mya ago. (Webb, 1974)

Even though the fossil record of camelids is fairly extensive, their phylogeny remains uncertain. For example, while the genus *Camelops* was placed within the Lamini in the latest morphology-based phylogeny, (Scherer, 2013) genomic data indicate a closer relationship with the Camelini. (Heintzman et al., 2015) Similarly, the position of *Aepycamelus* among other Camelidae remains ambiguous.

We described a near-complete Lamini fossil specimen from the early/middle Pleistocene of Argentina is currently housed at the Institute of Paleontology of Zürich. It is aged to approximately 1 Mya and preserves a suite of cranial morphologies rarely captured in a single specimen.

Our aims are to clarify and update the phylogeny of the Camelidae, concentrating on craniomandibular and dental characters, as we investigate the position of this new Argentinian specimen. In order to do so, we added a wider range of species to the analysis, reviewed and added characters to reflect more accurately the morphological disparity within the Camelidae.

We will be presenting the results of this analysis, as well as a preliminary description of this Argentinian specimen's endocast.

REFERENCES

Heintzman, P.D., Zazula, G.D., Cahill, J.A., Reyes, A.V., MacPhee, R.D.E., and Shapiro, B. (2015). Genomic Data from Extinct North American *Camelops* Revise Camel Evolutionary History. Mol Biol Evol *32*, 2433–2440.

Honey, J., Harrison, J., and Stevens, M. (1998). Evolution of Tertiary Mammals of North America (Cambridge University Press, New York).

Scherer, C.S. (2013). The Camelidae (Mammalia, Artiodactyla) from the Quaternary of South America: Cladistic and Biogeographic Hypotheses. Journal of Mammalian Evolution *20*, 45–56.

Webb, S.D. (1974). Pleistocene llamas of Florida, with a brief review of the Lamini. In Pleistocene Mammals of Florida, (Gainesville: University Presses of Florida.), pp. 170–213.

4.18

Did dormice ever glide? Reinvestigation of *Glirulus* aff. *lissiensis* from the late Miocene of Saint-Bauzile (Ardéche, France)

Olivier Maridet[1,2], Pierre Gueriau[3], Xiaoyu Lu[1,2] & Loïc Costeur[4]

[1]Jurassica Museum, Rte de Fontenais 21, CH-2900 Porrentruy (olivier.maridet@jurassica.ch)
[2]Dpt of Geosciences, University of Fribourg, Chemin du Musée 6, CH-1700 Fribourg
[3]Institute of Earth Sciences, University of Lausanne, Géopolis, CH-1015 Lausanne
[4]Naturhistorisches Museum Basel, Augustinergasse 2, CH-4051 Basel

Among extant mammals, except bats that have achieved an evolution toward active flight, the vast majority of species remain terrestrial or aquatic. The only exceptions are a few gliding species of Diprotodontia (Metatheria), Dermoptera (Eutheria) and Rodentia, the so-called “flying squirrels” (Eutheria). Today, only two families of rodents include gliding species: Anomaluridae and Sciuridae. Both families possess convergent adaptations: an elongation of anterior limbs and phalanges, a fold of skin connecting the forelimbs and hind limbs called patagium, and additional cartilaginous bones allowing to stretch the patagium during the glide.

In the fossil record, two other families are known to have evolved similar adaptations: Eomyidae (extinct) and Gliridae (which includes extant dormice) (Jackson & Thorington 2012). The latter is known thanks to a single beautifully preserved specimen of *Glirulus* aff. *Lissiensis* (Figure 1) from Saint-Bauzile (late Miocene, France; Métais & Sen 2018), exhibiting soft tissue remains interpreted as a possible patagium. This discovery is especially surprising because none of the extant species of dormice can glide. The first study of this fossil specimen was published by Mein & Romaggi (1991). At the time, the authors only compared the anatomy of *G.* aff. *Lissiensis* with that of *Glirulus japonicus*, considered to be its closest extant relative, yet no osteologic adaption to gliding was observed on the fossil specimen. We reconstructed *G.* aff. *Lissiensis* in 3D using X-ray tomography (CT-scan), allowing for the visualization of its whole anatomy (one side of the bones being otherwise concealed in the sediment), and more details about the preservation of the specimen. Additionally, further anatomic comparisons are now possible with other extant glirids (including now also a CT-scan of *G. japonicus* for more detailed comparisons) and other gliding mammals. The skeleton of *G.* aff. *Lissiensis* shows morphological features generally observed in terrestrial or aquatic rodents, but never in gliding mammals. A statistic comparison of the skeleton proportions with other mammal species also questiones the gliding adaptation. The gliding interpretation of this specimen is consequently only based on the presence of a possible patagium. If it is indeed a patagium, it would imply that Gliridae adapted to gliding without any convergent evolution with other gliding rodent, and gliding mammals in general. Concerning *G.* aff. *Lissiensis* preservation, first observations indicate a significant deformation of the specimen during fossilization processes. Soft tissues preservation appear more complex than previously described and extends beyond the theoretical position of a patagium, thus questioning this interpretation. Further chemical characterisation of theses soft tissues using infrared spectroscopy and synchrotron-based X-ray fluorescence major-to-trace elemental mapping (e.g. Manning et al. 2019) must be done to ensure the anatomic interpretation of the preserved organic matter.

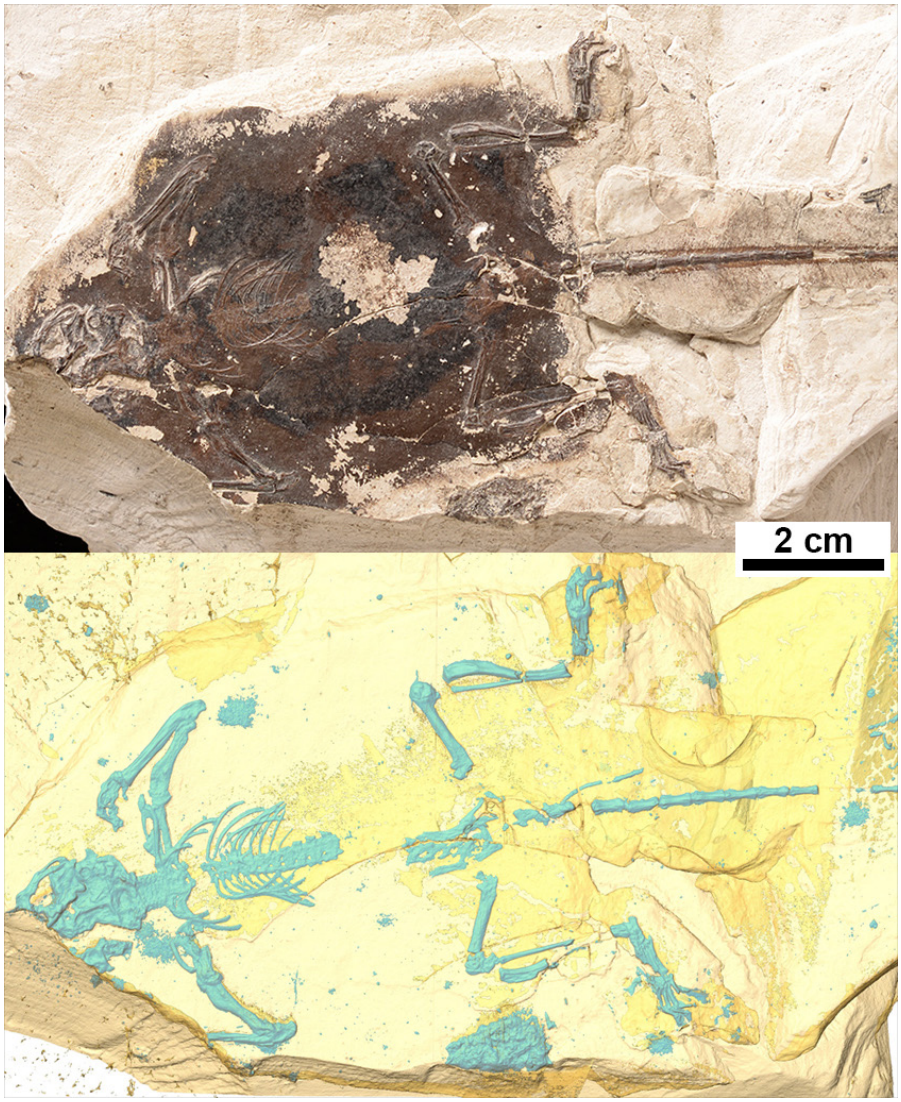


Figure 1. *Glirulus* aff. *lissiensis* from the late Miocene of Saint-Bauzile (Ardéche, France). Top: optical photograph; bottom: 3D rendering based on X-ray tomography.

REFERENCES

Jackson, S.M., & Thorington Jr., R.W. 2012: Gliding Mammals: Taxonomy of Living and Extinct Species, Smithsonian Contributions to Zoology, 638, 1–117.

Manning, P.L. et al. 2019: Pheomelanin pigment remnants mapped in fossils of an extinct mammal, Nature Communications, 10, 2250.

Mein, P., & Romaggi, J.P. 1991 : Un Gliridé (Mammalia, Rodentia) planeur dans le Miocène supérieur de l'Ardèche: une adaptation non retrouvée dans la nature actuelle, Géobios, M.S.13, 45–50.

Métais, G., & Sen, S. 2018: The late Miocene mammals from the Konservat-Lagerstätte of Saint-Bauzile (Ardèche, France), Comptes Rendus Palevol, 17, 479–493.

4.19

Triassic Sauropodomorph tracks with Gondwanan affinities from the Central Austroalpine Nappes of Switzerland

Christian A. Meyer[1], Hendrik Klein[2], Michael C. Wizevich[3] & Rico Stecher[4]

[1]*Departement Umweltwissenschaften, University of Basel, Bernoullistrasse 32, CH-4056 Basel, Switzerland (chris.meyer@unibas.ch)*
[2]*Saurierwelt Paläontologisches Museum, Alte Richt, D-92318 Neumarkt, Germany*
[3]*Departement ofGeological Sciences , Central Connecticut State University, 1615 Stanley Street, New Britain, CT 06050, USA*
[4]*Bündner Naturmuseum, Masanserstrasse 31, CH-7000 Chur, Switzerland*

We report on a new dinosaur tracksite in the Hauptdolomit Formation of the S-charl unit at Piz S-Chalambert Dadaint (Val d'Uina, Scuol). The site was discovered in 2018 by a local hunter on the western ridge at 2840 m a.m.s.l. and could only be accessed by us using ropes and helicopters.

The footprints occur in the uppermost part of the Hauptdolomit Formation which consist of a series of buff to grey dolomites with stromatolites. The surface is slightly inclined (27^0) and covers ~50 m^2. Three trackways are present, the longest can be followed for almost 12 m. The main trackway (TR1) contains 14 consecutive left and right pes impressions. Only the right pedes (FL: 36.5 cm; FW: 32.5 cm) are well preserved. They display four distinct digit impressions, although in some, only three digits are visible. The left pedes of the trackway show elongated, kidney-shaped impressions that result from digit IV and the heel only (Fig. 1). The average pace is 87.5 cm and stride is 154.4 cm respectively. A second trackway (TR 2) displays only these partial impressions, and the third trackway (TR 3) has three steps, only one being reasonably well preserved. The left pes imprint of TR 3 is elongated (FL: 50 cm; FW: 40 cm), oval shaped, with three well-marked, inwardly curved digits (Fig. 2).

TR 1 and TR 2 are similar in size and overall footprint morphology to those reported from the Ela Nappe and the Quattervals Nappe (Meyer et al. 2013; Furrer 1993; Furrer & Lozza 2008; Fig. 1A). They share some similarities with the Gondwanan ichnotaxon *Pseudotetrasauropus* from the Lower Elliot Formation of Lesotho and South Africa (d'Orazi Porchetti & Nicosia 2007) and with footprints described as *Otozoum grandcombensis* from the Norian of Grand Combe in Southern France (Gand et al. 2000), which were attributed to prosauropods. TR 3 (Fig. 2) is a hitherto unreported and different morphotype that shows some resemblance with *Tetrasauropus* from the Lower Elliot Formation of southern Africa, the more plantigrade pes imprint with digits strongly pointing inward, but lacks manus imprints.

The reported sites and ichnofauna from the Central Austroalpine Nappes (see Meyer et al. 2007, 2013) support the evidence of a wide spread, highly diverse ichnofauna including small and larger theropods (?*Grallator* isp., *Eubrontes* isp.), and sauropodomorphs with possible prosauropods (?*Pseudotetrasauropus* isp., ?*Tetrasauropus* isp.), and early sauropods. Remarkable is the lack of chirotheriid footprints that are common in Upper Triassic siliciclastic facies of the Germanic Basin and in North America.

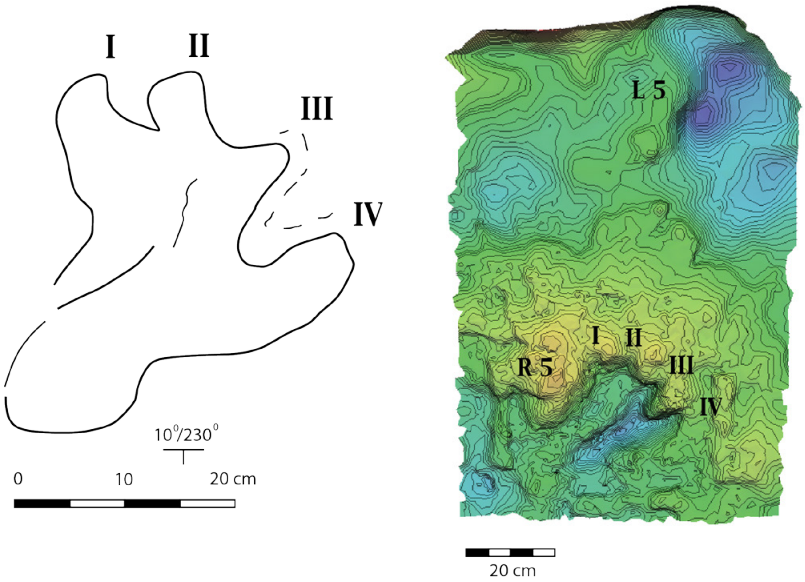


Figure 1. Left: TR 1, R 5 (tracing) Right: TR 1, R 5 and L 5 (photogrammetric model)

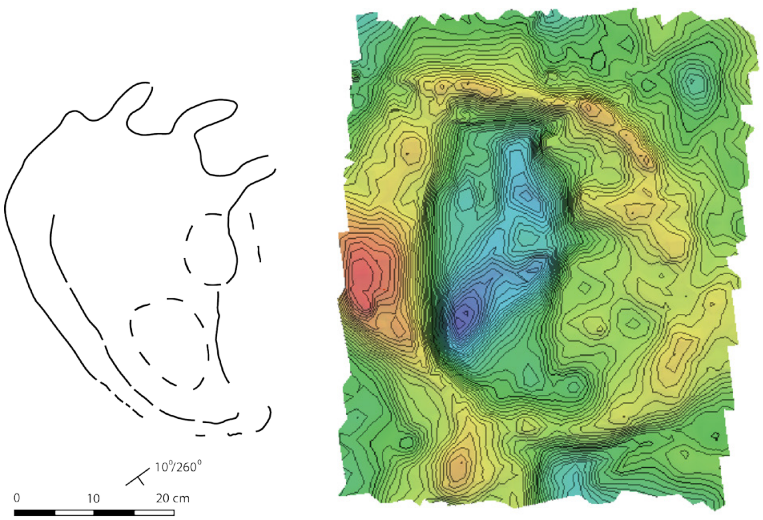


Figure 2. Left: TR 3, L 1 (tracing) Right: TR 3, L 1 (photogrammetric model)

REFERENCES

Furrer, H. 1993: Dinosaurier im Schweizerischen Nationalpark. Cratschla, Ediziuns specialas 1: 4–24.

Furrer, H. & Lozza, H. 2008: Neue Funde von Dinosaurierfährten im Schweizerischen Nationalpark. Cratschla 1: 17–21.

Gand, G., Vianey-Liaud, M., Demathieu, G. & Garric, J. 2000: Deux nouvelles traces de pas de dinosaures du Trias supérieur de la bordure Cévenole (La Grand-Combe, Sud-Est de la France). Geobios 33: 599–624.

Meyer Ch. A., Thüring, B.,Costeur, L. & S. Thüring, S. 2007: The early rise of sauropods – Evidence from the Late Triassic of the Eastern Swiss Alps. Abstracts 7th Meeting European Association of Vertebrate Palaeontologists, Berlin.

Meyer, Ch. A., Marty, D., Thüring, B., Stecher, R. & Thüring, S. 2013: Dinosaurierspuren aus der Trias der Bergüner Stöcke (Parc Ela, Kanton Graubünden, SE-Schweiz). Mitteilungen der Naturforschenden Gesellschaft beider Basel 14: 135 – 144.

d'Orazi Porchetti, S. & Nicosia, U. 2007: Re-Examination of some large Early Mesozoic Tetrapod from the African Collection of Paul Ellenberger. Ichnos 14: 219 – 245.

4.20

Morphology and evolution of basal Cheirurina (Trilobita) from the Fezouata Biota (Lower Ordovician, Morocco)

Francesc Pérez-Peris[1], Lukas Laibl[1,2], Muriel Vidal[3] and Allison Daley[1]

[1]Institute of Earth Sciences, University of Lausanne, Géopolis, CH-1015 Lausanne, Switzerland
[2]The Czech Academy of Sciences, Institute of Geology, Rozvojová 269, 165 00 Prague 6, Czech Republic
[3]Univ. Brest, CNRS, IUEM Institut Universitaire Européen de la Mer, UMR 6538 Laboratoire Géosciences Océan, Place Nicolas Copernic, 29280 Plouzané, France

Pilekiinae is a group of phacopid trilobites of the suborder Cheirurina, a widespread group that was a major component of Ordovician to Devonian marine ecosystems. The fossil record of pilekiids starts in the Upper Cambrian and finishes in the Darriwilian (Middle Ordovician) (Adrian, 2013). Most pilekiid taxa are from Tremadocian, being the most common cheirurines at this period. Pilekiids are generally considered to be the basal-most members of the Cheirurina, and therefore they are crucial for understanding the early evolution and morphological diversification of the group.

In the Fezouata Shale (Lower Ordovician, SE Morocco), numerous species of pilekiids have been described (Corbacho & Vela, 2011). Owing to taphonomical and morphological variability, it is possible that the group has been split into too many species. In this contribution, numerous specimens have been studied in order to clarify the taxonomy and to re-describe the morphology of cheirurids from the Lower Ordovician of Morocco. Morphological and biostratigraphical data suggest that most of the described species are co-specific and belong to genus *Anacheirurus.* Comparison with other basal cheirurids from Bohemia, North America, United Kingdom and Norway suggest that the Moroccan taxa show numerous ancestral characters, such as the morphology of the pleural furrows and the glabella.

In addition, a few specimens preserve the post-antennal appendages. This exceptional preservation allows us to describe the limbs of *Anacheirurus* and compare them with those other trilobites. Similar to other trilobites, *Anacheirurus* had three pairs of cephalic biramous appendages and then one pair associated each thoracic tergite. No pygidial appendages are preserved in our material. The post-antennal biramous appendages are composed of a protopodite (coxa), an exopodite (or gill branch) and an endopodite (walking leg). The protopodite seems to be attached below the axial ring in a lateral position relative to the sagittal axis. There is no evidence for spines on the protopodite or along the inner edge of the gnathobase. Each endopodite has seven podomeres. The appendages on the posterior part of the thorax show prominent spines on the second, third and fourth podomere. The last podomere is reduced into a small tripartite segment with three little claws. The exopodite consists of a flap, divided in two different parts by an articulation structure. The proximal lobe of the exopodite is bigger, and its external rim bears long, robust bristles. The bristles are arranged into a fan-like shape, are directed backwards, and overlap the posterior exopodite flap. The distal lobe is smaller and also bears long bristles, but shorter than those of the proximal one.

The limb morphology of *Anacheirurus* show a combination of characters that is typical for both Cambrian and Ordovician trilobites (Whittington & Almond, 1987; Zeng et al., 2017; Holmes et al., 2019). For example, the elongated rectangular shape of the protopodite is most similar to the Ordovician trilobites *Triarthruss eatoni* or *Ceraurus pleurexanthemus.* The endopodite's proximal spinosity resembles *Thriarthus eatoni.* The distal podomere with three claws is a pattern observed in various trilobites, like *Thriarthrus eatoni, Olenoides serratus, Chotecops fernandi, Cryptolithus tesselatus, Hongshiyanaspis yiliangensis, Eoredlichia intermedia* or *Redlichia rex.* Finally, the exopodites are similar to Cambrian forms such as *Olenoides serratus, Hongshiyanaspis yiliangensis, Eoredlichia intermedia* or *Redlichia rex,* with some variations in the number of lobes and the length of the distal bristles. In trilobites, the morphology of the exopodite seems to be more variable than the morphology of the endopodite, which is rather conserved across different taxa. These differences in exopodite morphology between trilobites have been interpreted as being driven by adaptations to particular environments or varying modes of life, rather than reflecting any phylogenetic signal (Zeng et al., 2017). From this point of view, the appendage morphology of *Anancheirurus* is important because this species comes from stratigraphic levels that are associated with the Great Ordovician Biodiversification Event and reveals the faunal transition from Cambrian to post-Cambrian ecosystems. Indeed, the unusual combination of ancestral and derived characters in the *Anacheirurus* appendages may be attributed to more specific adaptations of trilobites in the post-Cambrian world.

REFERENCES

Adrain, J. M. 2013: A synopsis of Ordovician trilobite distribution and diversity, Geological Society, London, Memoirs, 38, 297-336.

Holmes, J. D., Paterson, J. R., & García-Bellido, D. C. 2019: The trilobite Redlichia from the lower Cambrian Emu Bay Shale Konservat-Lagerstätte of South Australia: systematics, ontogeny and soft-part anatomy. Journal of Systematic Palaeontology, 1-40.

Whittington, H. B., & Almond, J. E. 1987: Appendages and habits of the Upper Ordovician trilobite Triarthrus eatoni. Philosophical Transactions of the Royal Society of London. B, Biological Sciences, 317, 1-46.

Zeng, H., Zhao, F., Yin, Z., & Zhu, M. 2017: Appendages of an early Cambrian metadoxidid trilobite from Yunnan, SW China support mandibulate affinities of trilobites and artiopods. Geological Magazine, 154, 1306-1328.

4.21

Ontogenetic patterns of cranial modularity along the theropod-bird transition

Olivia Plateau[1], Christian Foth[1]

[1]*Department of Geosciences, University of Fribourg, Chemin du Musée 6, CH-1700 Fribourg (olivia.plateau@unifr.ch)*

Extant birds represent a living branch of theropod dinosaurs. Due to their highly derived morphology, the transitional processes from terrestrial non-avian theropods to volant birds are still subject of many scientific debates. The skull of extant adult birds for instance is strongly integrated, showing a high degree of bone fusion in combination with cranial kinesis. Thus, bird skulls are extremely derived when compared to their theropod ancestors. Several studies investigating these differences, using geometric morphometrics (Bhullar et al. 2012, Felice & Goswami 2017) or anatomical networking (Werneburg et al. 2019), imply that the skull evolution of birds was primarily driven by paedomorphic heterochrony.

While geometric morphometrics allows quantifying variation of shape itself, anatomical networking focusses strictly on bone contacts, but is actually more sensitive to processes related to bone fusion. As the latter process is characteristic for the postnatal skull ontogeny of extant birds, the goal of this studies is to investigated changes in the cranial network of 41 extant birds during postnatal ontogeny, and compared them with those of non-avian theropods.

Our results demonstrate that the skulls of early juvenile birds are much more complex in terms of bone numbers, bone contacts and modularity than those of their adult counterparts. However, strong correlations between the increase of skull size and decrease of complexity, indicate that this reduction is a continuous process, showing any signs of rapid ontogenetic shifts. Due to their high complexity, the skull network of early juvenile birds resembles that of non-avian theropods, including *Archaeopteryx* and *Ichthyornis*, indicating that the highly integrated skull morphology of adult birds evolved in last common ancestor of the crown group of extant birds.

While previous shape analyses suggest that paedomorphic heterochrony affected the skull shape of extant birds, our study indicates that the derived ossification and modularity patterns seen in modern bird skulls result from a peramorphic heterochrony. Thus, the simultaneous occurrence of oppositional heterochronic processes (paedomorphosis vs. peramorphosis), indicates that the skull evolution of birds was much more complex than previously thought.

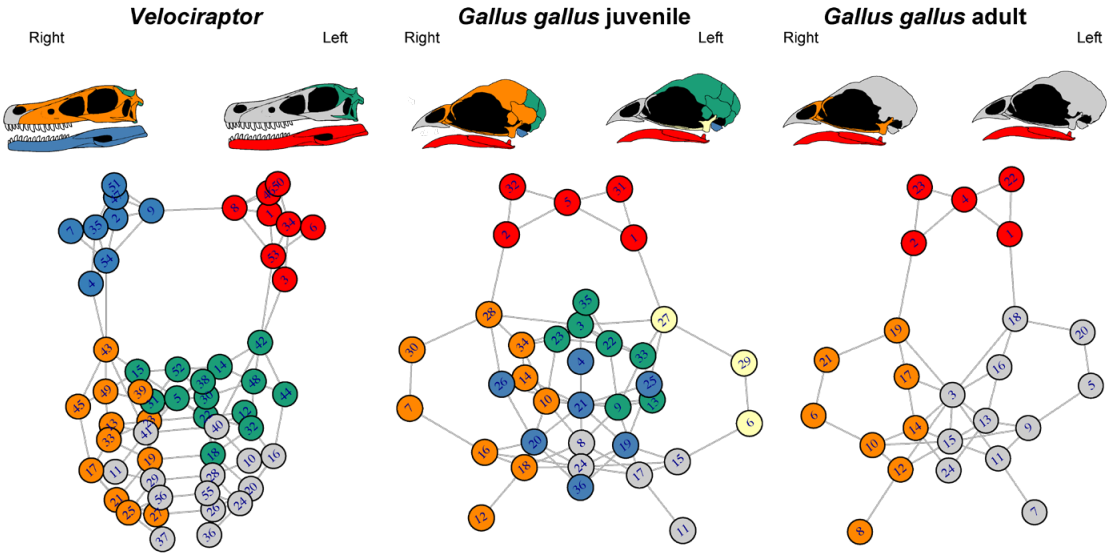


Figure 1. Reconstruction of the skull modularity in lateral view and results of the networking analyses in a non-avian theropod (*Velociraptor*) and a extant bird (*Gallus gallus*) in different ontogenetic stages. Different colours represent the different skull modules. Grey: snoot part, orange lateral or jugular bones, green: root part, red and blue: mandibular bones.

REFERENCES

Bhullar, B. A. S., Marugán-Lobón, J., Racimo, F., Bever, G. S., Rowe, T. B., Norell, M. A., & Abzhanov, A. 2012: Birds have paedomorphic dinosaur skulls, Nature, 487, 223–226.

Felice, R. N, & Goswami, A. 2017: Developmental origins of mosaic evolution in the avian cranium, Proceedings of the National Academy of Sciences, U.S.A. , 115, 555-560.

Werneburg, I., Esteve-Altava, B., Bruno, J., Ladeira, M. T., & Diogo, R. 2019: Unique skull network complexity of *Tyrannosaurus rex* among land vertebrates, Scientific Reports, 9, 1520.

4.22

Filling the gap: a forgotten fauna of Cambrian nautiloid cephalopods from Australia and its implications

Alexander Pohle[1] & Peter A. Jell[2]

[1]*Paläontologisches Institut und Museum, Universität Zürich, Karl-Schmid-Strasse 4, CH-8006 Zürich (alexander.pohle@pim.uzh.ch)*
[2]*School of Earth Sciences, The University of Queensland, AUS-4072 St Lucia QLD*

Cephalopods constitute an important part of modern marine ecosystems. Due to their enormous diversity and good preservation potential, Palaeozoic and Mesozoic externally shelled groups (ammonoids and nautiloids) are of great importance to both stratigraphers and evolutionary biologists. Their origins can be traced back to the late Cambrian (Jiangshanian, Furongian), where diverse faunas have been described mainly from North China (Chen & Teichert 1983). Reports from other parts of the world are rather scarce, but there is evidence of Cambrian cephalopods from North America and possibly also Kazakhstan and Siberia. Thus, late Cambrian cephalopods appear to have been restricted to tropical regions (Fang et al. 2019). Furthermore, after an initial diversification boost in the *Acaroceras-Sinoeremoceras* zone (middle Stage 10), cephalopods seem to have gone almost extinct in the latest Cambrian *Mictosaukia* zone (latest Stage 10) with only few unidentifyable specimens known worldwide. This decline has been described as the "late Trempealeauan Eclipse" (Chen & Teichert 1983; Fang et al. 2019).

Here, we present a fauna of late Cambrian nautiloids from Australia that was collected in the 1980ies by Dr. Mary J. Wade, former curator of the Queensland Museum. She started but never managed to finish several manuscripts on this fauna. Remarkably, despite extensive correspondance between her and several contemporary nautiloid experts such as C. Teichert, R.H. Flower and Chen J.Y. and even a short mention of the material in one of her articles (Wade 1988), the knowledge about the existence of this material has apparently disappeared from today's literature on fossil nautiloids.

The material originates from Black Mountain, western Queensland and probably represents the latest Cambrian. Protactinocerids and ellesmerocerids are abundant in three distinct horizons of the lower Ninmaroo Formation (Druce et al. 1982). The lowest horizon contains *Protactinoceras* and *Acaroceras* or *Ectenolites* and falls within the *Miktosaukia* zone. Thus, it is slightly younger than the Chinese material. The youngest of the nautiloid horizons contains mainly very small specimens and is possibly already earliest Ordovician in age. Conodonts from these horizons are currently being investigated and might refine their stratigraphic position.

The nautiloids from Black Mountain are remarkable in several regards. 1) Taxonomy: The majority of the previously described Cambrian cephalopods from China are only available as longitudinal sections. The specimens from Black Mountain are preserved as silicified internal moulds, thus they provide new insights on the three-dimensional morphology of Cambrian cephalopods. Most importantly, the new material made it clear that members of the order Protactinocerida possess a siphuncle with a strong bilateral symmetry instead of the radial symmetry found in siphuncles of other cephalopods. This is likely also the reason why Chen & Teichert (1983) established a number of separate genera that probably can be synonymized, since the supposed "genera" can be reproduced in the same specimen by cutting the shell obliquely or otherwise off the dorso-ventral symmetry axis. 2) Palaeogeography: Until now, Cambrian cephalopods were mostly known from China. The Australian specimens increases the knowledge on nautiloid cephalopods significantly, as this material is available in at least similar numbers. 3) Cephalopod evolution: The Queensland nautiloids represent the first evidence of identifiable cephalopods from this time interval. Thus, the "late Trempealeauan Eclipse" might not be as severe as previously thought and there is evidence that cephalopods continued to flourish through the Cambrian–Ordovician boundary. The absence of cephalopods from other latest Cambrian deposits could be explained by taphonomy. Alternatively, Australia might has served as a refugium for nautiloid cephalopods.

In summary, the rediscovery of the specimens from Queensland, Australia allows us to fill several gaps in the knowledge of Cambrian nautiloids.

REFERENCES

Chen, J.Y. & Teichert, C. 1983: Camrbian cephalopods from China. Palaeontographica, Abteilung A 181, 1–102.

Druce, E.C., Shergold, J.H. & Radke, B.M. 1982: A reassessment of the Cambrian-Ordovician boundary section at Black Mountain, western Queensland, Australia. In: The Cambrian–Ordovician boundary: sections, fossil distributions and correlations (Ed. by Bassett, M.G. & Dean, W.T.). National Museum of Wales Geological Series 3, 193–209.

Fang, X., Kröger, B., Zhang, Y.D., Zhang, Y.B. & Chen, T.E.: Palaeogeographic distribution and diversity of cephalopods during the Cambrian–Ordovician transition. Palaeoworld 28, 51–57.

Wade, M.J., 1988: Nautiloids and their descendants: Cephalopod classification in 1986. New Mexico Bureau of Mines and Mineral Resources, Memoir 44, 15–25.

4.23

Anatomy of the girdle regions of the giant *Purussaurus mirandai* (Caimaninae, Alligatoridae) from the Miocene of Venezuela

Torsten M. Scheyer[1], John R. Hutchinson[2], Olivier Strauss[1], Massimo Delfino[3,4], Jorge D. Carrillo-Briceño[1], Rodolfo Sánchez[5], & Marcelo R. Sánchez-Villagra[1]

[1]Universität Zürich, Paläontologisches Institut und Museum, Karl Schmid-Strasse 4, CH-8006 Zurich (tscheyer@pim.uzh.ch)
[2]Structure and Motion Lab, Department of Comparative Biomedical Sciences, Royal Veterinary College, Hatfield, United Kingdom
[3]Dipartimento di Scienze della Terra, Università di Torino, Via Valperga Caluso 35, I-10125 Torino, Italy
[4]Institut Català de Paleontologia Miquel Crusafont, Universitat Autònoma de Barcelona. Edifici ICTA-ICP, Carrer de les Columnes s/n, Campus de la UAB, E-08193 Cerdanyola del Vallès, Barcelona, Spain
[5]Museo Paleontológico de Urumaco, Urumaco, Estado Falcón, Venezuela

Crown-group Crocodylia, the alligators and caimans, crocodiles, gharials, and their closest extinct relatives, are amphibious and carnivorous large reptiles found in various aquatic environments in the Tropics and Subtropics. With a low flattened body profile and long powerful tails, they are well suited for swimming, but all also venture on land for frequent basking and for nesting and oviposition, while employing various types of locomotor patterns on land, including bounding and galloping gaits in some taxa. Independent of size, taxonomy, and locomotory capabilities, however, the precaudal vertebral count in all crown-group crocodylians is remarkably conservative, consisting of 9 cervicals, 15 dorsals and 2 sacrals (e.g. Hoffstetter and Casc 1969). It is only among non-Crocodylia crocodylomorphs such as the terrestrial *Notosuchus* from the Late Cretaceous and marine teleosauroids from the Jurassic, that deviation from this pattern is evident. These animals also show higher disparity in their girdle morphology compared to crown crocodylians, presumably due to their different lifestyles. He we report on the first member of crown-Crocodylia, the giant caimanine *Purussaurus mirandai*, that has three (instead of two) sacrals, two true or primordial sacral vertebrae and one dorsosacral, which articulate with the ilium. *Purussaurus* is so far the only giant crocodylian (with body lengths exceeding 10 m) from the Miocene of northern South America for which most of the postcranium is adequately known and described, including robust fore- and hind limbs. Following description of non-pathological dorsosacrals in Triassic Archosauriformes and recent discussion of hox gene expression in relation to axial compartmentalisation in the literature, we propose that an earlier timing of gene expression of *Hox11* and partial suppression of *Hox10* could be coupled with the formation of an additional dorsosacral in *P. mirandai*. The deviant vertebral count in this extinct species is also supported by the ilium morphology, which shows three distinct attachment areas for sacral ribs in several specimens, thus ruling out a pathological condition of a single individual. In addition, the proximal bone surface of the pubis differs from that of other crown crocodylians in that the lateral part of the surface is angled and thus impossible to articulate with the ischium when the medial part is in articulation. In the pectoral region, *P. mirandai* has narrow scapular blades oriented dorsally and posteriorly, ventromedially and slightly posteriorly oriented coracoids, as well as a narrow scapulocoracoid contact (lacking an anterior expansion) between both girdle elements- a condition that again differs strongly from extant crocodylians. A very wide and robust deltoid crest of the scapula indicates a well-developed origination site of the *deltoideus clavicularis* muscle in *P. mirandai*, which likely strengthened the anchoring of the humerus to the shoulder girdle and facilitated lifting of the heavy forelimbs during limb protraction. We speculate that the girdle morphology, the 'three sacral' condition, together with the robustness of the limb bones encountered in *P. mirandai*, are related to the giant size and body mass that these animals attained. In particular, a stiffened sacral region could help reduce transmission of motions from the tail to the anterior body during tail-driven locomotion such as swimming.

REFERENCES

Hoffstetter, R. & Gasc, J.-P. 1969: Vertebrae and ribs of modern reptiles. In: C. Gans, A.d.A. Bellairs, and T.S. Parsons (eds.), Biology of the Reptilia. Vol. 1 Morphology A, 201-310. Academic Press, London.

4.24

Synchrotron microtomography and bone histology of *Tanystropheus* reveal its cranial morphology and the identification of a separate, small-sized species

Stephan N. F. Spiekman[1], James M. Neenan[2], Nicholas C. Fraser[3], Olivier Rieppel[4], Vincent Fernandez[5], Torsten M. Scheyer[1]

[1]Universität Zürich, Paläontologisches Institut und Museum, Karl-Schmid-Strasse 4, 8006 Zürich, Switzerland
[2]Oxford University Museum of Natural History, Parks Road, Oxford OX1 3PW, UK
[3]National Museums Scotland, Chambers St, Edinburgh EH1 1JF, UK
[4]Field Museum of Natural History, 1400 S Lake Shore Dr, Chicago, IL 60605, USA
[5]European Synchrotron Radiation Facility, 71 Avenue des Martyrs, 38000 Grenoble, France

Tanystropheus is one of the most iconic taxa originating from the UNESCO World Heritage site of Monte San Giorgio in Switzerland and Italy and one of the most enigmatic Triassic reptiles due to its unique body plan. It is characterized by a hyper elongate and stiff neck that was longer than the body and tail combined and consisted of only 13 extremely elongated vertebrae and accompanying ribs. The function of this neck and the lifestyle of *Tanystropheus* remain unclear, with both largely terrestrial and fully aquatic lifestyles having been proposed (e.g. Renesto, 2005; and Nosotti, 2007). Two skull morphotypes of *Tanystropheus* are known, a small-sized morphotype with largely tricuspid dentition and a large-sized morphotype bearing fang-like teeth, previously considered to represent juveniles and adults of the same species, respectively. Although the cranial morphology of the small morphotype is well-documented, the skull of the large morphotype has remained enigmatic due to compression or incompleteness of available specimens.

We synchrotron µCT-scanned a virtually complete skull of the large morphotype, which allows for a detailed cranial reconstruction (Fig. 1). Our findings show that the disparity in cranial morphology between the two morphotypes exceeds the amount of variation that could be attributed to ontogeny and that the morphotypes thus represent different species. This conclusion is corroborated by long bone histological sections including a femur of a specimen of the small morphotype. The cross section of this femur clearly exhibits over 10 lines of arrested growth (LAGs), as well as an external fundamental system (EFS), indicating its skeletal maturity (Fig. 2). The small morphotype therefore represents a separate, smaller species that co-occurred with the larger morphotype. The strongly reduced overall size and tricuspid dentition of the former indicate that it preyed on small sized invertebrates such as crustaceans, and as such occupied a different niche than the latter. The highly specialized neck of *Tanystropheus* was thus able to facilitate more lifestyles than was previously appreciated.

A detailed study of the synchrotron µCT-scan, as well as re-analysis of other specimens, further provides many new insights into the cranial morphology of the large morphotype in both functionally and phylogenetically important aspects. The dentition is profoundly specialized towards catching fast swimming prey such as fish and squid, with large fang-like marginal teeth anteriorly, as well as a row of fang-like vomerine teeth. The postorbital region differs strongly from previous interpretations and includes a dorsoventrally tall squamosal. Detailed observation of the squamosal-quadrate articulation indicates the skull of *Tanystropheus* was streptostylic, which has implications for jaw mobility and prey acquisition. Finally, the atlas-axis complex and the braincase, including the endocast and inner ear, are presented, and a complete skull reconstruction is provided. The large morphotype of *Tanystropheus* shows many derived cranial features in comparison to other tanystropheids and “protorosaurs”, particularly in the braincase, postorbital region, and snout, indicating Tanystropheidae were a morphologically diverse group. Furthermore, the dentition and shape of the skull indicates *Tanystropheus* hunted in an aquatic environment, providing further evidence for an at least semi-aquatic lifestyle for the large morphotype of *Tanystropheus*.

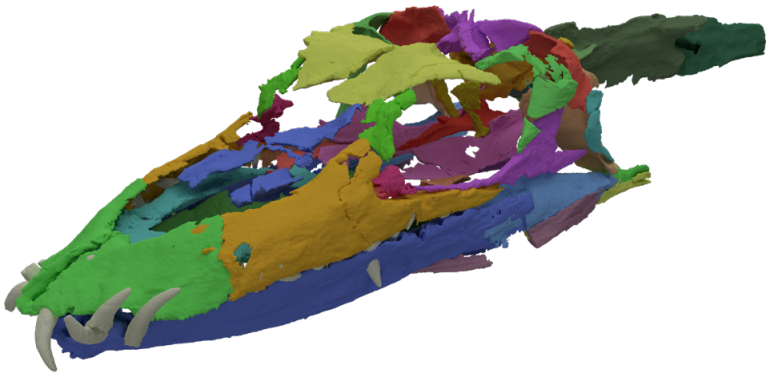


Figure 1. Reconstructed skull of the large morphotype of *Tanystropheus* PIMUZ T 2790 in angled view based on the synchrotron µCT-scan.

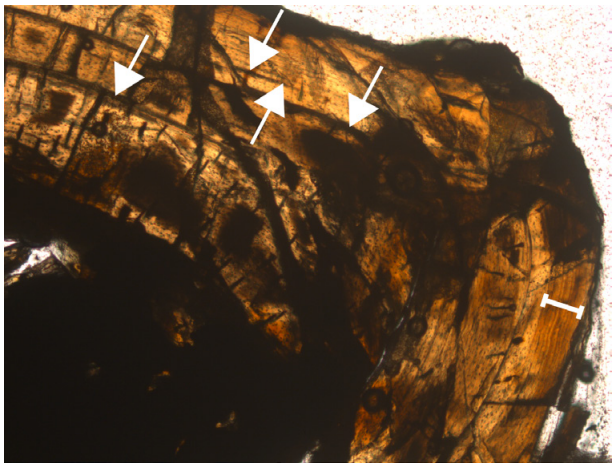


Figure 2. Histological section of the cortex of the femur of the small morphotype specimen PIMUZ T 1277 indicating several LAGs (indicated by white arrows) and the EFS containing at least eight LAGs (indicated by white line).

REFERENCES

Renesto, S. 2005: A New Specimen of *Tanystropheus* (Reptilia Protorosauria) from the Middle Triassic of Switzerland and the Ecology of the Genus, Rivista Italiana di Paleontologia e Stratigrafia, 111 (3), 377-394.

Nosotti, S. 2007: *Tanystropheus longobardicus* (Reptilia, Protorosauria): Re-interpretations of the Anatomy Based on New Specimens from the Middle Triassic of Besano (Lombardy, Northern Italy), Società Italiana di Scienze Naturali e Museo Civico di Storia Naturale, 35 (3).

4.25

A new cladoselachid chondrichthyan from the Famenian of Marocco

Marta Torres Ladeira[1], Linda Frey[1], Michael Coates[2], Michał Ginter[3] & Christian Klug[1]

[1]Paläontologisches Institut und Museum, University of Zurich, Karl-Schmid-Strasse 4, CH-8006 Zürich (marta.torresladeira@pim.uzh.ch; chklug@pim.uzh.ch)
[2]Department of Organismal Biology and Anatomy, University of Chicago, 1027 E. 57th St., USA-60637 Chicago
[3]Faculty of Geology, University of Warsaw, al. Żwirki i Wigury 93, PL-02-089 Warszawa

Cladoselache is the best studied genus of Devonian chondrichthyans, sometimes displaying exceptional preservation both in the Cleveland Shale of Ohio and in the Famennian shales of Morocco. From the desert of the Moroccan Anti-Atlas (southern part of Maïder Basin), we present new materials of a similar chondrichthyan. They are representatives of a new taxon of Devonian symmoriid chondrichthyans, which were found in the early middle Famennian Thylacocephalan Layer. They co-occur with other chondrichthyans such as *Phoebodus* and cladodonts as well as placoderms and rare osteichthyans (Frey et al. 2018). The most abundant macrofossils, however, are carapaces of the eponymic thylacocephalans. The red coloration of the sediment derives from altered pyrite (Frey et al. in press) and is interpreted as reflecting poorly oxygenated conditions of the bottom waters in the Maïder Basin. The chondrichthyans considered here measure between 1 and 2 m in length and are exceptionally preserved including cartilage, muscles, liver remains, skin denticles and stomach contents (Frey et al. in press). The caudal part is more rarely preserved and all specimens are dorsoventrally or laterally compacted. The body proportions resemble those of other symmoriids, such as *Cobelodus* and *Symmorium*; the dentition is cladodont and the overall morphology of the body is close to that of *Cladoselache*. Amongst other particular characters, the presence of a single, posterior dorsal fin, absence of an extension of the anterior dorsal fin, the Y-shaped pelvic plate, and the large size of the scapulocoracoid, makes these specimens worthy off their own taxonomic group.



Figure 1. Skeleton of a chondrichthyan resembling *Cladoselache* from the middle Famennian (Late Devonian) of the southern Maïder Basin (Morocco), which was embedded with the venter upward. The skull is seen in ventral view, with the left and right Meckel's cartilage visible, the branchial arches posterior to the skull, the anterior dorsal fin spine, and the shoulder girdle. Parts of the palatoquadrates extend laterally below the lower jaws. The posterior part of the skeleton is not preserved.

REFERENCES

Janvier, P. 1996: Early vertebrates, No. QE851 J36.

Frey, L., Rücklin, M., Korn, D., & Klug, C. 2018: Late Devonian and Early Carboniferous alpha diversity, ecospace occupation, vertebrate assemblages and bio-events of southeastern Morocco. Palaeogeography, palaeoclimatology, palaeoecology, 496, 1-17.

Frey, L., Pohle, A., Rücklin, M. & Klug, C. (in press): Fossil-Lagerstätten and preservation of vertebrates and invertebrates from the Devonian of Morocco (eastern Anti-Atlas). – Lethaia.

Frey, L., Coates, M., Ginter, M., Hairapetian, V., Rücklin, M., Jerjen, I., & Klug, C. (submitted): Morphology, phylogenetic relationships and ecomorpholohy of the early elasmobranch Phoebodus.

4.26

Moulting or protection – enrolment strategies in *Strenuella polonica* Czarnocki, 1926 (Ellipsocephalida, Trilobita) from Cambrian Series 2 of the Holy Cross Mountains, Poland

Anna Żylińska[1] & Allison C. Daley[2]

[1]*Faculty of Geology, University of Warsaw, Żwirki i Wigury 93, 02-089 Warszawa, Poland (anna.zylinska@uw.edu.pl)*
[2]*Institute of Earth Sciences, University of Lausanne, Geopolis, CH-1015 Lausanne, Switzerland*

Enrolment in trilobites is considered as a protective response of the animal to rapid and unfavourable environmental changes (such as salinity, oxygenation, and sediment influx) and/or biotic factors (such as predation) (Babcock & Speyer 1987). Enrolled trilobite exoskeletons may also reflect moulting strategies (see overview in Drage & Daley 2016). A case study to distinguish between individuals that enrolled for protection and fossils that represent flexed moults was performed on a dataset comprising c. 200 specimens of the ellipsocephalid trilobite *Strenuella polonica* Czarnocki, 1926 from the Cambrian of the Holy Cross Mountains, Poland.

Strenuella polonica is one of the most characteristic fossils of the Cambrian Series 2 *Holmia-Schmidtiellus* assemblage zone, being also the first identified early Cambrian trilobite from the area, already recognised in 1915. Its taxonomic status has since been subject to prolonged debate and only recently clarified (Żylińska 2013). *Strenuella polonica* was a medium-sized (length of about 30 mm and posterior cephalic width of about 20 mm), micropygous and relatively spinose trilobite. The cephalon is characterised by a strongly convex glabella with three distinct lateral glabellar furrows, a posteriorly directed occipital spine, and librigenae with large backward directed spines. The thorax is composed of 13 segments, of which the 4th is the widest, with pleurae terminated by short, backward directed spines. Each axial ring has a small hook-like spine that is located posteriorly and curved backwards. The longest hook-like spines occur on segments 4th to 8th. The small pygidium has short spines located on the pygidial margin.

Strenuella polonica was capable of spiral enrolment, as demonstrated by around 50 enrolled individuals displaying various strategies – completely enrolled, semi-enrolled, or with a thorax, pygidium or cranidium flex (Fig. 1). Two modes of enrolment were observed: 1) bending of the thorax at the level of the 4th, 5th or 6th segment, resulting in semi-enrolled individuals with the cephalon not entirely deflected from the thorax axial plane (Fig. 1A), and 2) simultaneous bending of cephalon and thorax at the level of the 4th, 5th or 6th segment, resulting in completely enrolled individuals (Fig. 1B). In mode 2), the cephalon could have been first deflected from the axial plane, followed by bending of the thorax, as evidenced by specimens with a deflected cephalon but an outstretched thorax, perhaps preserving the first enrolment step.

The modes of enrolment in *Strenuella polonica* may have had different causes. In some cases, this likely provided protection against potential predators, as was suggested by Żylińska & Kin (2010), owing to the spinosity of the exoskeleton and that most spines gained their functionality in an enrolled state. Enrolment could also have been a response to sudden unfavourable changes in the environmental conditions, for example storms, as suggested by Stachacz (2013) based on descriptions of the local depositional setting. Lastly, moulting strategies may have involved partial enrolment, with vigorous movements of the individual and flexing of the exoskeleton occurring during shedding. In this scenario, pleural spines could have provided purchase against the sediment to facilitate exuviation (Drage et al. 2018). Enrolment in the trilobite *Strenuella polonica* may have been a flexible strategy for survival and development.

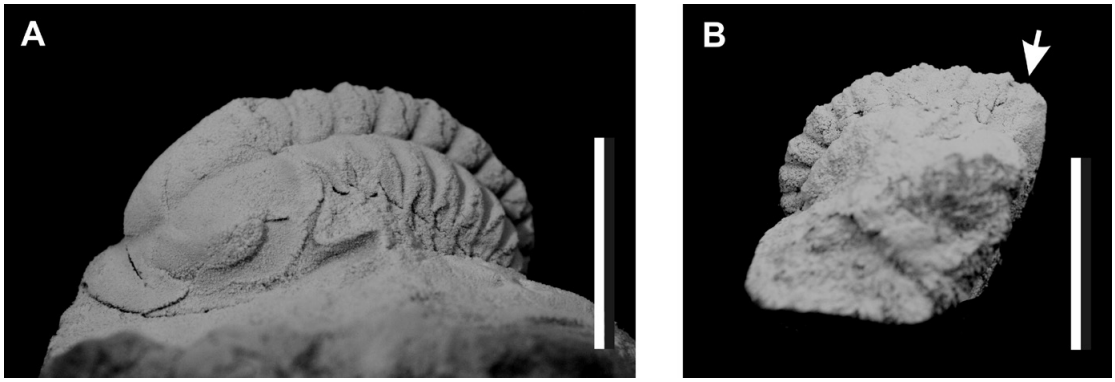


Figure 1. *Strenuella polonica* Czarnocki, 1926 from the *Holmia–Schmidtiellus* Zone, Cambrian Series 2, Holy Cross Mountains, Poland. A. semi-enrolled specimen 100/AB 32-16 from Adrian Kin collection. B. completely enrolled specimen UJ 214P/T16 from Michał Stachacz collection. Arrow indicates flex between cephalon and thorax. Scale bar is 10 mm.

REFERENCES

Babcock, L.E. & Speyer, S.E. 1987: Enrolled trilobites from the Alden Pyrite Bed, Ledyard Shale (Middle Devonian) of Western New York. J. Paleont., 61, 539–548.

Drage, H.B. & Daley, A.C. 2016: Recognising moulting behavior in trilobites by examining morphology, development and preservation: Comment on Błażejowski et al. 2015. Bioessays, 38, 981–990.

Drage, H.B., Holmes, J.D., García-Bellido, D.C. & Daley, A.C. 2018: An exceptional record of Cambrian trilobite moulting behaviour preserved in the Emu Bay Shale, South Australia. Lethaia, 51, 473-492.

Stachacz, M. 2013: Trilobites, their traces and associated sedimentary structures as indicators of the Cambrian palaeoenvironment of the Ociesęki range (Holy Cross Mountains, Poland). Geol. Quart., 57, 745–756.

Żylińska, A. 2013: The oldest Cambrian trilobites from the Holy Cross Mountains, Poland: taxonomic, stratigraphic and biogeographic reappraisal. Acta Geol. Pol., 63, 57–87.

Żylińska, A. & Kin, A. 2010. Defence strategy in *Strenuella polonica* Czarnocki (Ellipsocephalidae, Trilobita) from the Cambrian of the Holy Cross Mountains. In: XXI Konferencja Naukowa Sekcji Paleontologicznej PTG (Ed. by Zatoń, M., Krawczyński, W., Salamon, M. & Bodzioch, A.), Żarki-Letnisko, 13-16 września 2010, 91–93. (In Polish)

P 4.1

The First Dinosaurian Braincase from the Middle East: An Enigmatic Ornithopod Braincase from the latest Cretaceous Al-Khod Formation of Oman.

Dylan Bastiaans[1,2,3], Axel-Frans Hartman[4], Mohammed Alkindi[5], Anne S. Schulp[2,3]

[1]Universität Zürich, Paläontologisches Institut und Museum , Karl-Schmid-Strasse 4, 8006 Zürich, Switzerland
[2]Natuurhistorisch Museum Maastricht, Maastricht, the Netherlands
[3]Naturalis Biodiversity Center, Leiden, the Netherlands
[4]Shell International Exploration and Production B.V., The Hague, the Netherlands
[5]German University of Technology in Oman, Halban, Sultanate of Oman

The Arabian vertebrate fossil potential had been largely unexplored until the last two decades. Although its fossil record has improved considerably in terms of quantity, it still largely consists of poorly preserved undiagnostic material (Buffetaut et al., 2015). The dearth of diagnostic material has hampered paleobiogeographic reconstructions for Afro-Arabia resulting in older models postulating a refugium for relict taxa and endemic faunas, especially during the Late Cretaceous. Recent studies on the improved faunal composition of some southern continents paint a different and more complex picture, one of extensive faunal connectivity between various Gondwanan landmasses and possibly even Eurasia (Agnolin et al., 2010). Here we describe a newly discovered enigmatic ornithopod braincase from the type locality of the Al-Khod Conglomerate Formation of Oman. This formation fills an important spatio-temporal gap, given its position in between Africa and Eurasia, its long palaeogeographic relationship with Africa and being latest Cretaceous I (i.e. post-Cenomanian) in age (Sallam et al., 2018).

Although immensely undersampled and never systematically excavated, it has produced one of the most taxonomically diverse latest Cretaceous faunas for any Gondwanan landmass (incl. turtles, neosuchian crocodyliforms and non-avian dinosaurs) and a significant portion of all dinosaur records from the Arabian Peninsula (e.g. Schulp et al., 2008, Buffetaut et al., 2015). The braincase is assigned to Ornithopoda on the basis of: a U-shaped occipital condyle, the dorsoventral proportions of the posterior aspect of the braincase and the angle of the exoccipital-supraoccipital contact. Unlike typical ornithopods it displays short and laterally restricted basipterygoid processes, prominent basal tuberi and a peculiar dorsal skull margin. Endocranial features including a very narrow and steep median ridge, the morphology of the inner ear and the hypoglossal arrangement are more typical of ornithopods. A unique combination of features: separate canal for the ophthalmic branch of the trigeminal nerve (CN V), the large fossa above the cerebral carotid foramen, and an almost total absence of a floccular recess, justify an identification as a non-hadrosaurid ornithopod.

This braincase adds support to the idea of large non-hadrosaurid ornithopods existing on the Afro-Arabian plate. It is crucial to determine the exact phylogenetic position of the specimen, whether being closely related to Eurasian taxa or whether this population represents endemic archaic refugia taxa without clear phylogenetic relatives in the Late Cretaceous. Trans-Tethys intercontinental connectivity between Afro-Arabian and Eurasian faunas was previously suggested for both sauropod and ornithopod taxa (Sallam et al., 2018). Paradoxically the generally small size of the morphologically peculiar taxa recovered from the Al-Khod Fm. seems to suggest at least periodic isolation. Hadrosauroids may have been more prominent in Afro-Arabia during the Late Cretaceous than currently represented by the vertebrate fossil record, as indicated by tracks from Cameroon and Yemen, and fragmentary and isolated material from Angola, Jordan and Sudan (e.g. Schulp et al., 2008).

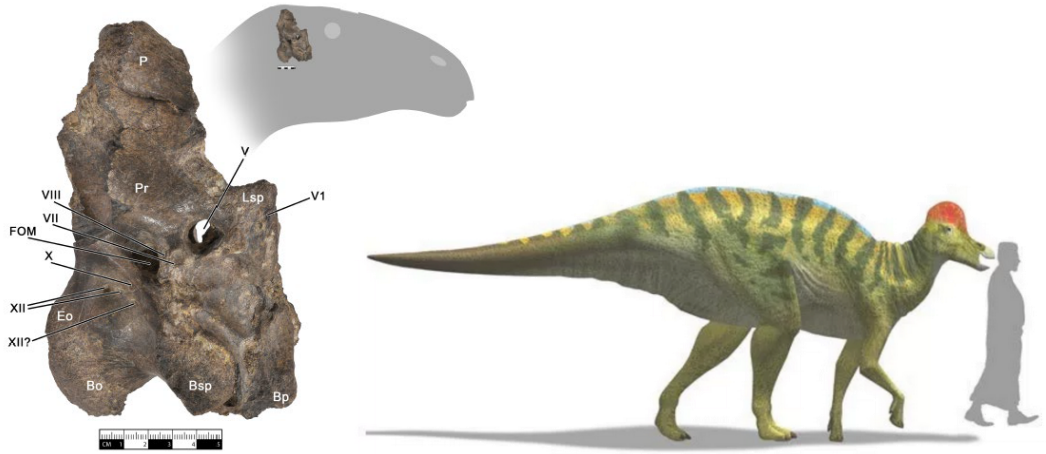


Figure 1. A generalized and conservative reconstruction of the size of the cranium of the Al-Khod non-hadrosauroid ornithopod in right lateral view. Note the robustness of the cranium, the extra foramen for CN XII, and seemingly short basipterygoid processes. Scale bar is 5 cm.

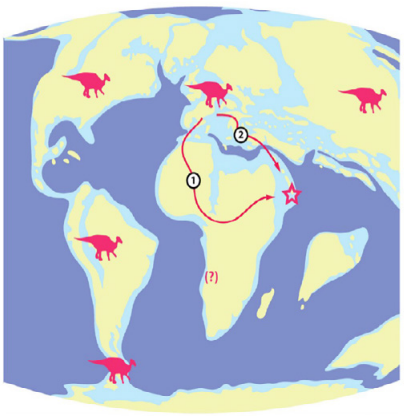


Figure 2. The potential dispersal routes for Eurasian hadrosauroids to the Late Cretaceous Arabian archipelago of Oman (Buffetaut et al., 2015).

REFERENCES

Agnolin, F.L., Ezcurra, M.D., Pais, D.F., and Salisbury, S.W. 2010. A reappraisal of the Cretaceous non-avian dinosaur faunas from Australia and New Zealand: evidence for their Gondwanan affinities. *Journal of Systematic Palaeontology,* 8(2), 257-300.

Sallam, H.M., Gorscak, E., O'Connor, P.M., El-Dawoudi, I.A., El-Sayed, S., Saber, S., Kora, M.A., Sertich, J.J.W., Seiffert, E.R., and Lamanna, M.C. 2018. New Egyptian Sauropod Reveals Late Cretaceous Dinosaur Dispersal Between Europe and Africa.

First Dinosaur Tracks from the Arabian Peninsula – Schulp, A.S., Al-Wosabi, M., Stevens, N.J. 2008. *PLoS ONE* 3(5): 1-4.

Buffetaut, E., Hartman, A.F., Al-Kindi, M., Schulp, A.S. 2015. Hadrosauroid Dinosaurs from the Late Cretaceous of the Sultanate of Oman.

P 4.2

AMOR2 follows AMOR – an improved robot for orientation and imaging of planktonic foraminifera

Michael Knappertsbusch[1], Jean Eisenecker[1] & Daniel Binggeli[2]

[1]Naturhistorisches Museum Basel, Augustinergasse 2, CH-4002 Basel (michael.knappertsbusch@unibas.ch)
[2]Fachhochschule Nordwestschweiz, Hochschule für Technik, Klosterzelgstrasse 2, CH-5210 Windisch

Morphometric shell measurements are a necessity to quantitatively map and record the biogeography and evolution of planktonic foraminifera, an information that is still notoriously underrepresented in the taxonomic literature. For a robust picture about morphological evolution knowledge about a species‘ variation over its global paleobiogeography is required at stratigraphically high resolution, which demands the study of thousands of specimens. Such a requirement is often a limitation to research projects due to the incredibly time-consuming labour of specimen orientation and imaging.

During our efforts of mapping morphological boundaries of extant and extinct menardiform globorotalids (Neogene tropical planktonic foraminifera) through time (Knappertsbusch, 2016) automated devices were developed, that help orientate and image specimens in reflected light at improved efficiency and precision. The first of these robots - AMOR - (Automated Measurement system for shell mORphology) has been built several years ago (Knappertsbusch et al., 2009) and has proven to be of great advantage for gathering the desired morphological data. AMOR consists of a motorized tilting stage allowing pitch and roll movements coupled with an motorized binocular microscope from Leica. The software of AMOR is encoded in LabView and includes standard core-functions for X- and Y tilting and translation, centering, automagnification, and autofocussing of specimens mounted in keel view. Before saving to disk, images are autorotated for vertical alignment on the monitor. These functions can be operated either in manual mode when handling single specimens, or in automatic mode for scanning series of specimens in a multicellular slide. After image collection shell parameters are extracted and analyzed using separate digital image and morphometric software. Early versions of AMOR were limited to *Globorotalia menardii* with a rather strict, quasi-symmetric biconvex geometry in keel view. Newer versions of the algorithm allow orientation of spiro- and umbilico-convex profiles, or menardiforms with a circular periphery in aequatorial view (e.g., *G. miocenica*, *G. multicamerata*).

We learnt, that in natural populations automated orientation of shells cannot be satisfactorily achieved using a single, universal algorithm because of too strong deviation of specimens from the model shape, that forms the basis for that algorithm. Instead, more (sub-)species specific algorithms are needed in order to best orientate specimens into the desired standard view for imaging. This became possible by scripting functions in the more recent AMOR v. 3.28 software applying AutoIt scripting language from Jonathan Bennett and the AutoIt team: This approach allows a case-dependent combination of the above mentioned core-functions, and which proved to be an elegant solution for increasing flexibility. It enables us in future to create a „portfolio“ of adapted scripts for processing particular morphologies without the need of re-programming sophisticated LabView code.

To further expand on this concept and other reasons made re-building of existing AMOR inavoidable. The follow-up device - AMOR2 - was completed (see Figure 1). It integrates improved hardware, updated software (AMOR v. 4.2), extended core-functions, and has a modified Graphical User Interface where core-functions and numeric input controls / numeric output indicators are scriptable. This new robot is now available for our ongoing research about prospecting patterns of morphological evolution in menardiform globorotalids along Agulhas‘ trackway (see Knappertsbusch and Friesenhagen (2018) and the contribution of Friesenhagen during the present Swiss Geoscience Meeting).

An important aspect of our newer development is that portfolio’s with AMOR allow to extend to other morphogroups than menardiform globorotalids. In this context we bear on the dream that different laboratories may in future build similar devices and network for morphology-based phylogenetic reconstruction at unprecedented stratigraphic resolution.

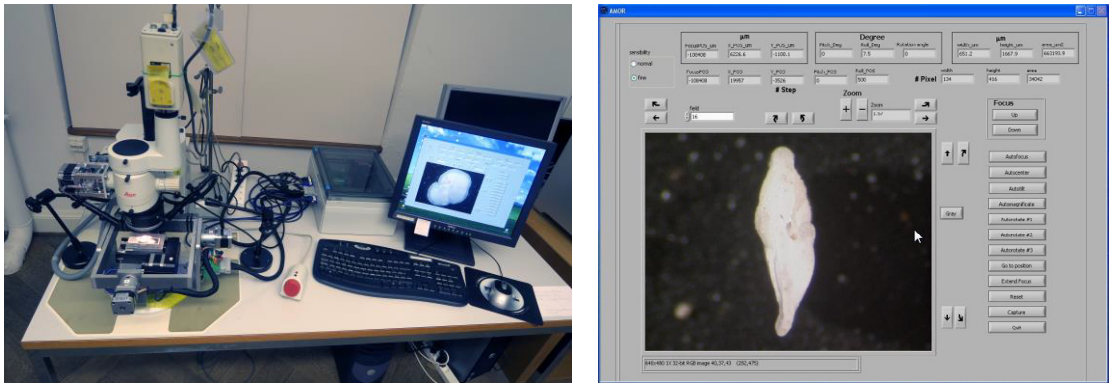


Figure 1. Left, robot AMOR2 with controller box containing drivers for stage and motorized zoom. Right, Graphical User Interface of software that drives AMOR2 (e.g., AMOR v. 4.2) in single specimen mode and with scriptable buttons & input/output fields.

REFERENCES

Knappertsbusch, M., Binggeli, D., Herzig, A., Schmutz, L., Stapfer, S., Schneider, C., Eisenecker, J., & Widmer, L. (2009). AMOR - A new system for automated imaging of microfossils for morphometric analyses. Palaeontologia Electronica, 12(2); 1-20. http://palaeo-electronica.org/2009_2/165/index.html

Knappertsbusch, M. (2016). Evolutionary prospection in the Neogene planktic foraminifer Globorotalia menardii and related forms from ODP Hole 925B (Ceara Rise, western tropical Atlantic): evidence for gradual evolution superimposed by long distance dispersal ? Swiss Journal of Palaeontology, 135, 205-248.

Knappertsbusch M., & Friesenhagen T. (2018). Morphological evolution of menardiform globorotalids are different in the Atlantic and Pacific oceans. Poster presentation. Symposium 10: Celebrating 50 Years of International Ocean Drilling (1968-2018), Abstract Volume 16th Swiss Geoscience Meeting Bern, 30th November – 1st December 2018, pp. 300-301. https://geoscience-meeting.ch/sgm2018/wpcontent/uploads/SGM_2018_Abstract_Book.pdf

More info: https://www.micropal-basel.unibas.ch/

P 4.3

Talking about brain dead and a giant among the dwarfs: new data on the Swiss Hyaenodonta (Mammalia)

Bastien Mennecart[1], Morgane Dubied[2], Floréal Solé[3]

[1]Naturhistorisches Museum Basel, Augustinergasse 2, CH-4001 Basel (mennecartbastien@gmail.com)
[2]UMR6282 Biogéosciences, Université de Bourgogne, 6 Boulevard Gabriel, F-21000 Dijon (morgane.dubied@u-bourgogne.fr)
[3]Royal Belgian Institute of Natural Sciences, Rue Vautier 29, B–1000 Brussels (fsole@naturalsciences.be)

The hyaenodonts were the most numerous and diverse carnivorous mammals during the Eocene of Europe. Their phylogenetical concepts within the clade Hyaenodonta and their relationships with the other mammals remain today unclear. Numerous propositions based on the extinct Northern American faunas lead to the conclusion that the hyaenodonts were less competitive in many ways than the contemporaneous Carnivora. Indeed, we observe a direct competition of these taxa in Northern America during the Eocene (ca. 56-34 Mya), the period of their local decrease in diversity. A less efficient lever arm for the carnassial complex due to backward located large and secant teeth, a less evolvable dental morphology due to the posterior position of the carnassials (= secant teeth dedicated to cut the meat), and a supposed smaller size of their brain are often supposed at the origin for the extinction of this entire clade. However, hyaenodonts are known in Africa and Eurasia until the middle Miocene (ca. 12 Mya).

Egerkingen localities (Canton of Solothurn, Switzerland) are three karstic infillings that have been excavated since 1890. They are designated α, β, and γ and date from the Lutetian, Middle Eocene. The localities α and β constitutes the reference locality for the European reference level MP14 (generally noted Egerkingen $\alpha + \beta$) ca. 43 Mya. Quarry γ is considered as slightly older and possibly close to MP13 reference level ca. 44 Mya. At that time, the Hyaenodonta flourished in Europe. No less than eight different species of Hyaenodonta are currently described in Egerkingen localities. Here we present *Cartierodon egerkingensis* Solé & Mennecart, 2019, a new species of Hyaenodonta from Egerkingen, and the first virtual endocranial reconstruction (Dubied et al. 2019) studied in this clade with *Proviverra typica*.

Cartierodon is represented by numerous dental elements (Figure 1). Calculations based on the teeth size show that this Hyaenodonta of ca. 30 kg was from far the largest carnivorous mammal known in Europe between 50 Mya and 40 Mya, all the others not exceeding 20 kg. Reaching this size allowed *Cartierodon* to open a new ecological niche. He was, as far as we know, the only one able to eat larger species than itself. Moreover, the peculiar dental morphology proves that he was a bone-cracking predator.

On the other size of the hyaenodont spectrum, *Proviverra typica* (ca 0.5 kg) is an emblematic European Hyaenodonta (Figure 1), which was first described based on fossils from Egerkingen. Comparing the morphology of the holotype virtual endocast with natural cast of Hyaenodonta already published shows that there is an increase in complexity in the convolutions. Moreover, we observed an increase in relative size of the encephalon within the Hyaenodonta history. The analysis of the encephalization quotient – the relative volume size of the "brain" materialized by the empty volume inside the braincase – reveals that the endocast of *Proviverra* is very large in comparison to its bodymass. Generally speaking, the endocranium of the Hyaenodonta is not smaller than those of fossil Carnivora or even some extent Carnivora. Therefore, the extinction of Hyaenodonta may not be linked to the relative size of their brain.

Few are currently known on the Hyaenodonta evolution. Further investigation is necessary to better understand the reasons of their European and African success as well as the cause(s) of their total extinction.

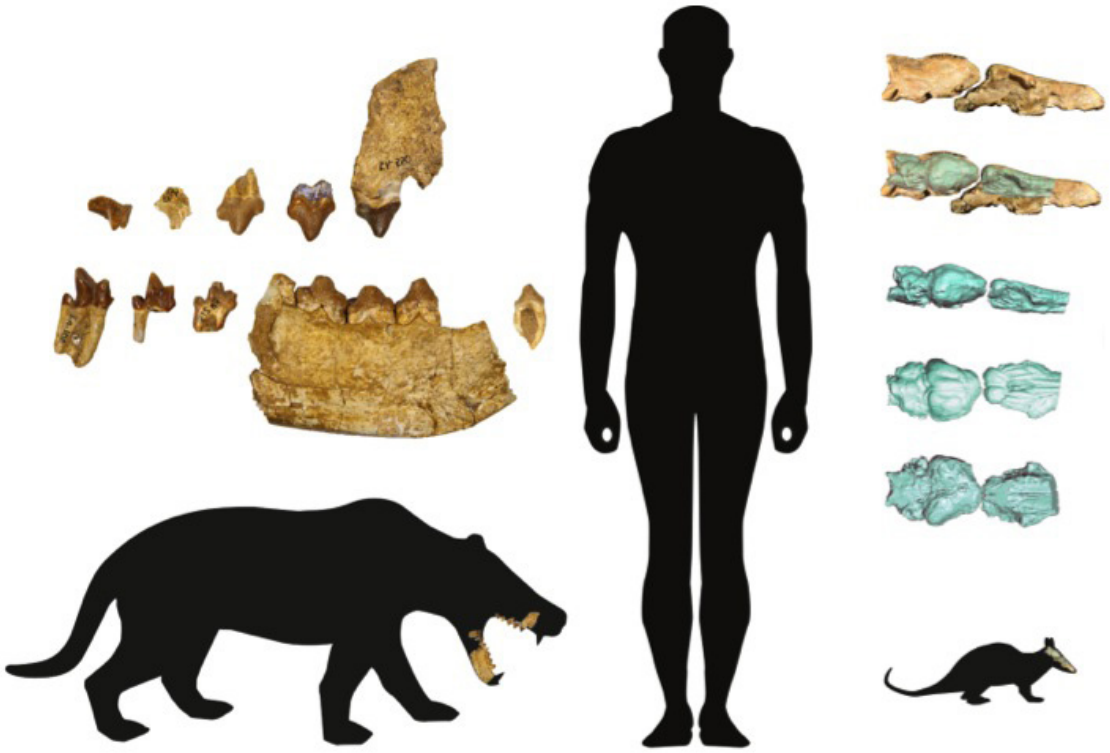


Figure 1. Fossils and outline illustrations with comparison to human size of *Cartierdon egerkingensis* (left) and *Proviverra typical* (right).

REFERENCES

Dubied, M., Solé, F. & Mennecart, B. 2019: The cranium of *Proviverra typica* (Mammalia, Hyaenodonta) and its impact on Hyaenodont phylogeny and endocranial evolution, Palaeontology DOI 10.1111/pala.12437.

Solé, F. & Mennecart, B. 2019: A large Hyaenodont from the Lutetian of Switzerland expands the body mass range of the European mammalian predators during the Eocene, Acta Palaeontol. Pol. 64(2), 275-290.

05. Stratigraphy

Alain Morard, Reto Burkhalter, Oliver Kempf & Ursula Menkveld-Gfeller

Swiss Commitee for Stratigraphy (SKS/CSS),
Swiss Palaeontological Society (SPG/SPS),

TALKS:

5.1 Fantasia A., Adatte T., Spangenberg J.E., Thibault N.R., Mattioli E., Bernárdez E., Bodin S.: Towards a better understanding of the Aalenian (Middle Jurassic) palaeoenvironmental changes

5.2 Ruchat A., Adatte T., Spangenberg J.E.: Expression of the Toarcian Ocean Anoxic Event (TOAE) in Shallow Environments from Central Atlas, Morocco

5.3 Sharma N., Vérité J., Watkins S., Valero L., Whittaker A., Garcès M., Puigdefabregas C., Guillocheau F., Adatte T., Castelltort S.: Upstream versus downstream controls on a natural sediment routing system from source-to-sink

5.4 Tremblin M., Spangenberg J.E., Adatte T., Fillon C., Lasseur E., Serrano O., Roig J Y., Calassou C., Guillocheau F., Castelltort S.: Documentation of the first stable isotopic records of the North Pyrenean foreland basin

5.5 Zuchuat V., Sleveland A.R.N., van Soelen E., Twitchett R.J., Svensen H., Turner H., Augland L.E., Hammer Ø., Hauksson B.T., Midtkandal I., Planke S.: A tale of a core and a river section: ultra-high-resolution, multidisciplinary analysis of the Permian-Triassic boundary from central Spitsbergen, Svalbard

POSTERS:

P 5.1 Garefalakis P., Schlunegger F.: Extracting information on sediment- and water-fluxes from coarse-grained deposits in the Swiss Molasse

P 5.2 Lauper B., Deplazes G., Vogel H., Jaeggi D., Wohlwend S., Ariztegui D., Foubert A.: XRF chemostratigraphy to unravel depositional and diagenetic processes across a diachronous lithostratigraphic transition (Middle Jurassic, northern Switzerland)

P 5.3 Rime V., Negga H., El Korh A., Salzmann A., Addate T., Kidane T., Atnafu B., Foubert A.: Danakil Evaporites: how to build a salt giant?

P 5.4 Shahzad A., Munir-Ul- Hassan Munir, Adatte T.: Characterization of the Paleocene/Eocene boundary in the Indus Basin, NW margin of Indian Plate, Pakistan: Preliminary Results

P 5.5 Valero L., Beamud B., Garcés M., Sharma N., Tremblin N., Watkins S.E., Guillocheau F., Puigdefàbregas C., Castelltort S.: A new completelly dated source-to-sink profile

P 5.6 Watkins S.E., Sharma N., Valero L., Tremblin M., Zaki A.S., Arlaud F., Castelltort S.: Fluvial deposits: is there a fundamental difference in architecture between upstream and downstream driven aggradation?

5.1

Towards a better understanding of the Aalenian (Middle Jurassic) palaeoenvironmental changes

Alicia Fantasia[1], Thierry Adatte[2], Jorge E. Spangenberg[3], Nicolas R. Thibault[4], Emanuela Mattioli[5], Enrique Bernárdez[6] & Stéphane Bodin[1]

[1]Department of Geoscience, Aarhus University, 8000 Aarhus C, Denmark (alicia.fantasia@geo.au.dk)
[2]Institute of Earth Sciences (ISTE), University of Lausanne, 1015 Lausanne, Switzerland
[3]Institute of Earth Surface Dynamics (IDYST), University of Lausanne, 1015 Lausanne, Switzerland
[4]Department of Geosciences and Natural Resource Management, University of Copenhagen, 1350 Copenhagen K, Denmark
[5]Université de Lyon, UCBL, ENSL, CNRS, LGL-TPE, F-69622 Villeurbanne, France
[6]Department of Geology, University of Atacama, Copiapó, Atacama, Chile

The Jurassic Period was punctuated by repeated carbon cycle perturbations, climate changes, and faunal/floral turnovers. Among them, the Toarcian Oceanic Anoxic Event and the Early Bajocian Event are the most studied ones. To date, in stark contrast to the previously mentioned events, the Aalenian stage (Middle Jurassic) remains largely understudied, leaving an important gap in our knowledge and understanding of palaeoenvironmental and palaeoclimatic conditions between the Toarcian and Bajocian events. There are several lines of evidence indicating that the Aalenian was marked by climatic change, carbon cycle disturbances, and faunal turnovers. Nevertheless, the hitherto studied sections are restricted to European basins and there is no comprehensive continuous Aalenian dataset published thus far from successions of regions outside Europe. Hence, there are still large uncertainties concerning the causes and consequences of the Aalenian palaeoenvironmental and palaeoclimatic changes and their regional vs global significance. In this study, we have selected two expanded successions, namely Le Brusquet (Vocontian Basin, SE France) and El Peñon (Andean Basin, N Chile), in order to compare the most complete records of the Aalenian interval from the northern and southern hemispheres. The successions are composed of marl and limestone alternations. High-resolution sedimentological, geochemical, mineralogical, biostratigraphic (calcareous nannofossils) and cyclostratigraphic datasets have been generated on both successions to assess the palaeoenvironmental change, and constrain the duration of the Aalenian and associated environmental change. Our carbon isotope records of bulk organic matter ($\delta^{13}C_{org}$) reveals trends similar to previously published $\delta^{13}C_{org}$ curves from the European area, suggesting the occurrence of repeated carbon cycle perturbations of global significance throughout the Toarcian-Aalenian interval.

5.2

Expression of the Toarcian Ocean Anoxic Event (TOAE) in Shallow Environments from Central Atlas, Morocco

Arnaud Ruchat[1], Thierry Adatte[1] & Jorge E. Spangenberg[2]

[1]Institute of Earth Sciences (ISTE), University of Lausanne, 1015 Lausanne, Switzerland (thierry.adatte@unil.ch)
[2]Institute of Earth Surface Dynamics (IDYST), University of Lausanne, 1015 Lausanne, Switzerland

The Toarcian Ocean Anoxic Event (TOAE) took place in the early Jurassic (~183 My) and is characterised by the widespread deposition of organic matter-rich black shales in deep basins, and by a negative carbon isotope excursion (NCIE) reflecting profound environmental changes. This event is well documented in the sedimentary record of deeper marine settings, in which the TOAE is marked by the presence of organic-rich shales. However, the recording of the TOAE in shallower environments is less common, due to incomplete sediment records, to sea-level fluctuations and the lack of good biostratigraphy markers.

Here we present data gathered from a new extremely shallow section in Morocco (Dadès Gorges, Central Atlas), which was located along the northern Gondwana margin. This section consists of alternating dolomitic limestones and paleosols, associated with the presence of several dinosaur tracks and other sedimentary features such as stromatolites, ripple marks, mud cracks and fossil roots. This section shows a significant increase in mercury (Hg) located just below a negative excursion in $^{13}C_{carbonate}$ isotopes (-3) that we attributed to the TOAE-NCIE, which coincides with several cyclical episodes of emersion. Bulk rock and clay mineralogy indicate an increase in weathering intensity in the upper part of the section marked by higher phyllosilicates quartz and kaolinite contents.

The upper part of the section shows a gradual decrease in the number of carbonate beds coinciding with increased clay-rich intervals. The carbonates interbedded with the clay levels are almost entirely composed of an accumulation of stromatolites reflecting extreme conditions, which coincide with the TOA-NCIE.

These results confirm the presence of the TOAE-NCIE even in the most shallow environments of the Tethys. The observed Hg anomalies have been globally recorded and are probably linked with the volcanic activity from the Karoo Ferrar province. This marker combined with stable isotopes is therefore a very promising correlative tool.

5.3

Upstream versus downstream controls on a natural sediment routing system from source-to-sink

Nikhil Sharma[1], Jean Vérité[2], Stephen Watkins[1], Luis Valero[1], Alex Whittaker[3], Miguel Garcès[4], Cai Puigdefabregas[5], François Guillocheau[2], Thierry Adatte[6], Sebastien Castelltort[1]

[1]Department of Earth Sciences, University of Geneva, Rue des Maraîchers 13, 1205 Genève, Switzerland
[2]Gèosciences Rennes, Campus Beaulieu, Université de Rennes 1, 35042 Rennes cedex, France
[3]Department of Earth Science and Engineering, Imperial College London, South Kensington, London SW7 2AZ, England
[4]Department of Stratigraphy, Paleontology and Marine Geosciences, C/ Martí i Franquès, s/n, University of Barcelona, 08028 Barcelona, Spain
[5]Department of Earth and Ocean Dynamics, University of Barcelona, C/ Martí i Franquès, s/n, 08028 Barcelona, Spain
[6]Institute of Earth Sciences (ISTE), University of Lausanne, Bâtiment Géopolis, 1015 Lausanne, Switzerland

The Middle Eocene Climatic Optimum (MECO) represents an episode of widespread warming about 40 million years ago. It is characterised by gradual warming over a period of 500,000 years and rise in ocean temperatures of about 5° C in the mid and high-latitudes (Sluijs et al., 2013). Contrary to the traditional understanding of downstream factors controlling fluvial successions, we here propose to test our hypothesis that upstream factors rather than downstream factors control fluvial architecture through changes in the sediment supply and water discharge with paleoslope as a measurable proxy to quantify these changes. We test this hypothesis in a natural system, the Escanilla sediment routing system which corresponds to the Middle Eocene Climatic Optimum. The Escanilla formation is an overall prograding succession consisting of 1000 m thick alluvial and fluvial deposits at the southern-margin of the Tremp-Graus Basin in Spain. Multiple sections were sampled close to the source, and at intermediate and distal part of the system for paleohydraulics (grain size and cross-set measurements, flow direction, channel geometry) and for paleoclimatic reconstructions from fine-grained floodplain samples (XRD, XRF, clay mineral separation, stable isotopes). We present here the preliminary results of this multi-proxy approach across the MECO.

REFERENCES

Sluijs, Appy & E. Zeebe, Richard & Bijl, Peter & M. Bohaty, Steven. (2013). A middle Eocene carbon cycle conundrum. Nature Geoscience. 6. 429-434. 10.1038/ngeo1807

5.4

Documentation of the first stable isotopic records of the North Pyrenean foreland basin

Maxime Tremblin[1], Jorge E. Spangenberg[2], Thierry Adatte[2], Charlotte Fillon[3], Eric Lasseur[4], Olivier Serrano[4], Jean-Yves Roig[4], Sylvain Calassou[3], Francois Guillocheau[5], Sébastien Castelltort[1]

[1]Department of Earth Sciences, University of Geneva, Rue des Maraîchais 13, 1205 Genève, Switzerland
[2]Institute of Earth Sciences (ISTE), University of Lausanne, Batiment Geopolis, 1015 Lausanne, Switzerland
[3]TOTAL, CSTJF, Avenue Larribau, F-64018, Pau Cedex, France
[4]BRGM, French Geological Survey, 45060, Orléans Cedex, France
[5]Géosciences-Rennes, UMR 6118 Université de Rennes 1 – CNRS, OSUR, 35042 Rennes cedex, France

The late Paleocene and the Eocene represent the last “greenhouse” period characterized by relatively high atmospheric CO_2 concentrations and warm surface temperatures. This longterm climatic state is punctuated by several transient hyperthermal events. The maximum warming episode record is known as the Paleocene-Eocene thermal maximum (PETM). This event is associated with an increase of temperatures of 4-8°C, by a 2-6 ‰ negative carbon isotope excursion (CIE) and by a large shift in biotic communities. The source of the carbon and whether it was released in one or numerous steps remain controversial.

The PETM is widely recorded from pelagic, hemipelagic and continental settings but is again poorly recorded in shallow water successions. This absence is due to the lack of adequate sections covering this time interval and to apparent problems which bring complexity in the use of carbon isotopes as environmental and stratigraphic proxies in these shallow-water depositional environments. However, these environments are key locations to link continental and open marine settings. Furthermore the high sedimentation rate which charaterizes these environments have the potential to preserve expanded CIE records and can offer an opportunity to better understand the nature and the causes of the PETM.

In this study, we present the first high resolution stable isotopic records ($\delta^{18}O$ and $\delta^{13}C$) of the North Pyrenean foreland basin (Lussagnet, Aquitaine Basin) from the end of the Paleocene to the middle Eocene. Our first results show two important negative excursions in the bulk-rock $\delta^{13}C$ signature. The prominent negative excursion is interpretated as the carbon isotope excursion of the Paleocene-Eocene thermal maximum and the second one as the pre-onset excursion (POE). This event, which suggests two massive releases of carbon at the onset of the PETM, was first recorded in continental pedogenic carbonates but remains poorly constrained in oceanic settings. To study if these events could be associated with a large release of volcanic carbon, a mercury (Hg) analysis was carried out, for which preliminary results are presented. Our work confirms that hyperthermal events of the Paleogene can be well recorded in shallow water successions and can be used as powerful stratigraphic tools for these depositional environments, in addition to providing information on the climatic perturbations associated with the PETM.

5.5

A tale of a core and a river section: ultra-high-resolution, multidisciplinary analysis of the Permian-Triassic boundary from central Spitsbergen, Svalbard

Valentin Zuchuat[1], Arve R.N. Sleveland[1], Els van Soelen[1], Richard J. Twitchett[2], Henrik Svensen[3], Holly Turner[4], Lars Eiving Augland[1], Øyvind Hammer[4], Bjarki T. Hauksson[5], Ivar Midtkandal[1], & Sverre Planke[3,6]

[1]Department of Geosciences, University of Oslo, Sem Sælands Vei 1, 0371 Oslo, Norway (valentin.zuchuat@geo.uio.no)
[2]Natural History Museum, Earth Sciences Department, London, UK
[3]Center for Earth Evolution and Dynamics (CEED), Department of Geosciences, University of Oslo, Norway
[4]Natural History Museum, University of Oslo, Pb. 1172 Blindern, 0318 Oslo, Norway
[5]Geodata AS, Schweigaards gate 28, Oslo, Norway
[6]Volcanic Basin Petroleum Research (VBPR), Oslo Science Park, Oslo, Norway

95% of marine and 75% of terrestrial species vanished in less than 60 ± 48 ky as a consequence of the End-Permian Mass Extinction (Hochuli et al., 2010; Burgess and Bowring, 2015). It is associated with a sharp and important $\delta^{13}C_{org}$ negative excursion worldwide (Horacek et al., 2007; Meyer et al., 2011; Grasby et al., 2013; Grasby et al., 2016; Foster et al., 2017; Wang et al., 2019). Research on the Permian-Triassic boundary (PTB) of the northern margins of Pangea (exposed today in the High-Arctic region) has traditionally relied on field observations, and data resolution was consequently determined by outcrop condition and accessibility. The aim of this work was to provide a high-quality, multidisciplinary analysis of the Permian-Triassic boundary interval at a never-yet-achieved resolution in the Arctic region, by the collection and analysis of two sedimentary cores.

The drilling operation conducted in Deltadalen, Central Spitsbergen, allowed for a near-complete recovery of two 90 m cores drilled across the Vikinghøgda Formation, the Permian-Triassic Boundary, and the Kapp Starostin Formation. The analyses conducted on the core comprise: (i) classic sedimentology analysis of the recovered material; (ii) U-Pb dating of zircon crystals extracted from the collected tephra layer; (iii) an optical and electron microscopy analysis of selected samples;(iv) a complete XRF-scan of the entire core, from which elemental concentration and elemental ratios were calculated, including Si/Al, Zr/Rb, Ti/Al, Fe/K, V/Cr, whereas the U/Th ratio is derived from XRF-analysis of hand-specimen; (v) geochemical analyses which delivered the $\delta^{13}C_{org}$, Total Organic Carbon and Hydrogen Index values of the core; (vi) and the interpretation of palynofacies. Evolutionary spectral analyses were conducted on the five XRF-derived environmental proxies between the dated tephra bed at 84.90 m and the Induan-Olenekian Boundary at 29.68 m, in order to identify cyclical patterns.

The discovery of *H. parvus* in the river section of Deltadalen is the first ever documented specimen in Svalbard. It places the PTB ca. 4 m above the base of the Vikingøgda Formation, within the Reduviasporonites chalastus assemblage zone. The *H. parvus* specimen recovered from concretion level 3 and the 252.13 ± 0.62 Ma tephra bed occurs ca. 2.50 m above the extinction event and is in association with the sharp negative shift towards more negative $\delta^{13}C_{org}$ values. This lag between the extinction event and the FAD has also been reported from the Canadian Arctic and Greenland, confirming a delayed appearence of the Triassic-defining conodont on the northern margin of Panthalassa with respect to GSSP (Yin et al., 2001). This further supports the call for a re-assessment of the definition of the base Induan, which is highly diachronous as officially defined today.

The sedimentation rate dramatically accelerated during the Induan, during which sediments accumulated 6 to 20 time faster than during the Permian. This augmented sedimentation rate in the Triassic is thought to be linked to an increased runoff. However, this study's climatic proxies indicate a transition towards a more arid climate in the earliest Triassic. This northwards migration of an arid climatic belt was linked to increased CO_2 concentration in the atmosphere. However, both an extreme high atmospheric CO_2 concentration and northwards expantion of an arid climatic belt contradicts with models associated with elevated CO_2 concentration. Such as the mid-Cretaceous Supergreenhouse period, during which an arid climatic belt migrated southwards. This contradiction is thought to be related to an extremely rapid expulsion of CO_2 in the atmosphere by the Siberian Traps.

Last but not least, the second major $\delta^{13}C_{org}$ negative excursion documented in DD-1 corresponds to the so-called Dienerian Crisis. This C-isotopic negative shift has now been recognised in both Tethyan and Panthalassic sections, suggesting that the Dienerian Crisis was a global event. Diminished oxygen levels in the water might have been linked to a slowed-down ocean circulation. However, the occurence of two thin tephra layers in Deltadalen during the $\delta^{13}C_{org}$ negative shift suggests that the worsening of the environmental conditions could have also been impacted by volcanic activity.

REFERENCES

Burgess, S.D., Bowring, S., & Shen, S.Z. (2014). High-precision timeline for Earth's most severe extinction. Proceedings of the National Academy of Sciences, 111(9), 3316-3321.

Foster, W.J., Danise, S., Price, G. D. & Twitchett, R. J. (2017). Subsequent biotic crises delayed marine recovery following the late Permian mass extinction event in northern Italy. PLoS ONE, 12, e0172321. DOI: 10.1371/journal.pone.0172321

Grasby, S.E., Beauchamp, B., Embry, A., & Sanei, H. (2013). Recurrent Early Triassic ocean anoxia. Geology, 41(2), 175-178.

Grasby, S.E., Beauchamp, B., Bond, D.P., Wignall, P.B., & Sanei, H. (2016). Mercury anomalies associated with three extinction events (Capitanian crisis, latest Permian extinction and the Smithian/Spathian extinction) in NW Pangea. Geological magazine, 153(2), 285-297.

Hochuli, P.A., Hermann, E., Vigran, J.O., Bucher, H., & Weissert, H. (2010). Rapid demise and recovery of plant ecosystems across the end-Permian extinction event. Global and Planetary Change, 74(3-4), 144-155.

Horacek, M., Richoz, S., Brandner, R., Krystyn, L., & Spötl, C. (2007). Evidence for recurrent changes in Lower Triassic oceanic circulation of the Tethys: The δ13C record from marine sections in Iran. Palaeogeography, Palaeoclimatology, Palaeoecology, 252(1-2), 355-369.

Meyer, K. M., Yu, M., Jost, A. B., Kelley, B. M., & Payne, J. L. (2011). δ13C evidence that high primary productivity delayed recovery from end-Permian mass extinction. Earth and Planetary Science Letters, 302(3-4), 378-384.

Wang, X., Cawood, P. A., Zhao, H., Zhao, L., Grasby, S. E., Chen, Z. Q., & Zhang, L. (2019). Global mercury cycle during the end-Permian mass extinction and subsequent Early Triassic recovery. Earth and Planetary Science Letters, 513, 144-155.

Yin, H., Kexin, Z., Jinnan, T., Zunyi, Y., & Shunbao, W. (2001). The global stratotype section and point (GSSP) of the Permian-Triassic boundary. Episodes, 24(2), 102-114.

P 5.1

Extracting information on sediment- and water-fluxes from coarse-grained deposits in the Swiss Molasse

Philippos Garefalakis[1] & Fritz Schlunegger[1]

[1]*University of Bern, Institute of Geological Sciences, Baltzerstrasse 1 + 3, CH-3012 Bern, Switzerland (philippos.garefalakis@geo.unibe.ch)*

Sedimentation within foreland basins typically results in large-scale coarsening- and thickening-upward successions caused by the subsidence of the foreland plate, progressive progradation of the thrust belt and larger sediment fluxes (DeCelles & Giles 1996). Increase of grain size ("coarsening") and thickness of sedimentary beds ("thickening") either results from a change in the depositional axis, a shift from a marine to a terrestrial setting, or as a consequence of a progradation of fan-systems where coarser-grained deposits migrate onto finer-grained material situated at more distal positions. Because these changes are to large extents controlled by the evolution of the adjacent mountain belt and autocyclic dynamics within the basin, the sedimentary architecture of foreland basins, and particularly grain size patterns, bear fundamental information on the tectonic and erosional history of the orogen and of the basin itself. Besides information on the facies-relationship patterns from the clastic detritus, the deposited material and grain size can also be used to determine data on sediment- and water-fluxes.

The Swiss part of the north Alpine foreland basin has been intensively explored for its sedimentary architecture and facies relationship, and the deposits have been put in a chronological framework (e.g. Matter et al. 1980; Schlunegger et al. 1996; Kempf & Matter 1999). The Swiss Molasse basin and its sedimentary fill is characterized by two coarsening- and thickening-upward mega sequences. These Oligocene to Miocene successions have been classically divided into four lithostratigraphic groups (Matter et al. 1980). The first transgressive-regressive cycle comprises the Lower Marine Molasse (UMM) and the Lower Freshwater Molasse (USM) groups, and the second cycle comprises the Upper Marine Molasse (OMM) and the Upper Freshwater Molasse (OSM) groups. Marine sediments (UMM, OMM) have been deposited within an open marine and coastal environment and consist of sand- and mudstones. The terrestrial freshwater deposits (USM, OSM) comprise transverse-oriented alluvial megafans (usually conglomerates and sandstones) that were established adjacent to the Alps, and axial-directed river-systems (mostly sand- and mudstones alternations) at more distal positions. While the areal extent, facies relationship and chronological framework of such systems have been well explored (e.g. Schlunegger et al. 1996), only few studies focused on the question of how changes of sediment concentration, or shifts in water- and sediment-fluxes, are potentially recorded by these successions.

In this study, we focus on the coarse-grained sediment fraction, i.e. conglomerates, deposited at both proximal and distal positions in relation to the Alpine thrust. The fieldwork is carried out in the eastern Swiss Molasse basin along already dated sections (Kempf & Matter 1999) encompassing USM- and OSM-sediments. Facies-analyses of these sedimentary archives revealed that sediments at proximal sites were deposited on alluvial megafans by a transverse-oriented system of braided rivers. These streams gradually changed into more confined channel belts at distal sites, which converged with an axial-directed river system at farther positions. We aim to explore patterns and changes of sediment-flux and water-discharge. We proceed by collecting data about grain size and stacking patterns of conglomerates in the field, which we combine with the results of hydrological flume experiments. In this context, digital photographs of conglomerates were taken at each site, and diameters of the particles are determined using grain size measuring programs. These data are used to infer changes of sediment- and water-fluxes through time, which builds the basis to reconstruct the erosional dynamics of the sediment routing systems in the Alps and the depositional processes of the streams in the basin. We ultimately use this information to infer the tectonic and geodynamic evolution in the hinterland, because the related processes are mirrored by distinct stratigraphic responses in the sedimentary archives.

REFERENCES

DeCelles, P.G. & Giles, K.A. 1996: Foreland basin systems, Basin Research, 8, 105–123.

Kempf, O. & Matter, A. 1999: Magnetostratigraphy and depositional history of the Upper Freshwater Molasse (OSM) of eastern Switzerland. Eclogae Geol. Helv. 92, 97–103.

Matter. A., Homewood. P., Caron, C., Rigassi. D., Van Stuuvenberg, J., Weidmann. M. & Winkler, W. 1980: Flysch and Molasse of Western and Central Switzerland. In: Geology of Switzerland, a guidebook (Part B) (Ed. by Trümpy, R.), Wepf Basel, 261–293.

Schlunegger, F., Burbank, D.W., Matter, A., Engesser, B. & Mödden, C. 1996: Magnetostratigraphic calibration of the Oligocence to Middle Miocene (30–15 Ma) mammal biozones and depositional sequences of the Swiss Molasse Basin. Eclogae Geol. Helv. 89, 753–788.

P 5.2

XRF chemostratigraphy to unravel depositional and diagenetic processes across a diachronous lithostratigraphic transition (Middle Jurassic, northern Switzerland)

Bruno Lauper[1], Gaudenz Deplazes[2], Hendrik Vogel[3], David Jaeggi[4], Stephan Wohlwend[5], Daniel Ariztegui[6] & Anneleen Foubert[1]

[1]Departement of Geosciences, University of Fribourg, Chemin du Musée 6, CH-1700 Fribourg (bruno.lauper@unifr.ch)
[2]Nagra, Hardstrasse 73, CH-5430 Wettingen
[3]Institute of Geological Sciences and Oeschger Centre for Climate Change, Universiy of Bern, Baltzerstrasse 1+3, CH-3012 Bern
[4]Federal Office of Topography swisstopo, Seftigenstrasse 264, CH-3084 Wabern
[5]Geological Institute, ETH Zürich, Sonneggstrasse 5, CH-8092 Zurich
[6]Department of Earth Sciences, University of Geneva, Rue des Maraîchers 13, CH-1205 Geneva

In northern Switzerland, the Opalinus Clay (OPA), an argillaceous to silty mudstone formation, is overlain by successions of sandy bioclastic marls and limestones capped by oolitic ironstone beds (Passwang Formation and eastern equivalent; upper confining unit, abbreviated UCU). This Aalenian lithostratigraphic transition is diachronous and evidences high vertical and lateral variability.

Considering the differing bio- and lithostratigraphy across this transition, the delineation of the OPA/UCU boundary is not always evident rendering correlation between different sections difficult.

The aim of the present study is to assess the potential use of semi-quantitative X-ray fluorescence (XRF) chemostratigraphy along this complex transition. Sections from four drillcores covering the OPA/UCU transition (Mont Terri, Riniken, Weiach and Benken) were measured with an ITRAX XRF core scanner and compared to petrographical and quantitative geochemical data.

The results evidence that XRF core scanning can be used to understand better the depositional and diagenetic processes shaping the OPA/UCU transition. The position of the OPA/UCU boundary is re-discussed using specific elemental proxies. The elemental records reveal a sedimentary discontinuity at the OPA/UCU boundary induced by sediment bypassing, supporting the basal sequence stratigraphic framework proposed by Burkhalter (1995). However, its relation to an overall regressive phase at the OPA/UCU boundary could not be established and remains hypothetical.

REFERENCES

Burkhalter, R. M. 1995: Ooidal ironstones and ferruginous microbialites: origin and reation to sequence stratigraphy (Aalenian and Bajocian, Swiss Jura mountains), Sedimentology, 42, 57-74.

P 5.3

Danakil Evaporites: how to build a salt giant?

Valentin Rime[1], Haileyesus Negga[1], Afifé El Korh[1], Alexandre Salzmann[1], Thierry Addate[2], Tesfaye Kidane[3], Balemwal Atnafu[4], and Anneleen Foubert[1]

[1]Department of Geosciences, University of Fribourg, Ch. Du Musée 6, Fribourg, Switzerland. (valentin.rime@unifr.ch)
[2]Faculty of Geosciences and Environment, Géopolis, Lausanne
[3]School of Agricultural, Earth and Environmental Sciences, University of KwaZulu-Natal Durban, South Africa.
[4]*School of Earth Sciences, Addis Ababa University, Ethiopia.*

The formation of salt giants remains an actively debated topic. Several mechanism are invoked to explain the thick evaporite successions found in many sedimentary basins around the world. It has been argued that the lack of modern analogues prevents an actualistic approach to the problem. The Danakil depression in northern Afar (Ethiopia) however feature a thick (up to 2000m) evaporite sequence where halite is still depositing nowadays.

This study presents a 600 m Pleistocene to Holocene core record drilled in the center of the Danakil basin. Multi-proxy analysis (facies, geochemistry, mineralogy, organic carbon content and micropaleontology) allowed to identify the alternation of different mechanisms explaining the thick evaporite succession: marine seawater evaporation, evaporation of saline pans (playas), continental reworking of salts, seepage and hydrothermal fluid circulation. Correlation of the core facies with sediments outcropping at the margin of the basin, allowed to constrain the age of the sediments. Most of the evaporite deposition took place after the MIS5e marine transgression in the basin. The deposition continued until now, recording also major environmental changes during the late Pleistocene to Holocene, such as the African Humid Period.

This study has been funded through the Swiss National Science Foundation (SNF project SERENA – SEdimentary REcord of the Northern Afar 200021_163114).

P 5.4

Characterization of the Paleocene/Eocene boundary in the Indus Basin, NW margin of Indian Plate, Pakistan: Preliminary Results

Amir Shahzad[1], Munir-Ul- Hassan Munir[1], Thierry Adatte[2]

[1]Institute of Geology, University of Azad Jammu and Kashmir, Muzaffarabad, Pakistan
[2]Institute of Earth Sciences (ISTE), University of Lausanne, Lausanne 1015, Switzerland

The early Palaeogene climate was marked by long-term global warming, beginning in the late Paleocene (Selandian,~59 Ma) and culminating in the earliest Eocene (Paleocene-Eocene Thermal maximum, PETM~56 Ma). This event is globally related with the extinction of deep benthic foraminifera, the diversification of both planktic foraminifera and mammals. Mercury anomalies coincident with PETM intervals have been observed in several sections (e.g Zumaya, Esplugafreda, Spain, Zomet, Negev, Israel, Wadi Nukhul and Beida, Egypt) and support the role of volcanism (North Atlantic Igneous Province) to initiate the concomitant warming and sea-level rise characterizing the PETM.

The Paleocene/Eocene (PE) boundary appears to be present in marine successions located along the NW margin of Indian plate in the Indus basin, Pakistan; but these sections are still poorly studied. The current project is focused on five sections characterized by different paleoenvironments, varying from relatively deep (outer shelf) shales and marls with planktonic foraminifera to shallow sandstones and carbonates with large benthic foraminifera. The main goal of the project is to characterize the PETM in these poorly studied sections using a multiproxy approach including sedimentology, micropaleontology, mineralogy (bulk and clay mineralogy) and geochemistry (stable isotopes, major and trace elements, organic matter, and mercury).

REFRENCES

Zachos, J.C., Pagani, M., Sloan, L., Thomas, E. & Billups, K. 2001. Trends, rhythms and aberrations in global climate 65 Ma to present. Science, 292, 686-693.

P 5.5

A new completely dated source-to-sink profile

Luis Valero[1], Bet Beamud[2], Miguel Garcés[3], Nikhil Sharma[1], Maxime Tremblin[1], Stephen E. Watkins[1], François Guillocheau[4], Alex C. Whittaker[5], Cai Puigdefàbregas[3] & Sébastien Castelltort[1].

[1]Département des Sciences de la Terre, Université de Genève, Rue des Maraîchers,13, CH-1205, Genève.
[2]Laboratori de Paleomagnetisme de Barcelona (CCiTUB-CSIC), Solé i Sabarís s/n, 08028, Barcelona.
[3]Departament de Dinàmica de la Terra i l'Oceà, Facultat de Ciències de la Terra, Marti i Franqués s/n, 08028, Barcelona.
[4]Département des Geosciences, Université de Rennes 1/CNRS (UMR 6118), Rennes.
[5]Department of Earth Science and Engineering, Imperial College London, SW7 2AZ London

Here we present the results of a new magnetostratigraphy for a middle Eocene record of the South Pyrenean foreland basin in Spain. The new Lascuarre section (*ca.* 650 m thick) provides new ages for fluvial (Capella Fm.), lacustrine (Escanilla Limestone), and fluvial to alluvial (Escanilla Fm.) systems. We show that the Capella Fm is of Lutetian age and the Escanilla Fm. is Bartonian. These results fill a chronostratrigraphic gap in the sedimentary record of the Tremp-Graus-Ainsa basin.

Integration of our Lascuarre chronology with other magnetostratigraphic studies in the region allows for a complete snapshot of the entire source to sink system. This new data permits a comprehensive study of the propagation of upstream and downstream signals. Due to the quality of data, outcrops, and accessibility, our new correlation profile opens the possibility to study the source-to-sink expression of multiple drivers, and constitutes a, *de facto,* giant natural laboratory.

An evaluation of the impact of the orbital cycles in the complete source-to-sink system is also being carried out. If successful, we will have an enhanced understanding of the mechanisms by which the climatic signals can be transferred along the sediment routing systems, and a high-resolution chronology.

P 5.6

Fluvial deposits: is there a fundamental difference in architecture between upstream and downstream driven aggradation?

Stephen E. Watkins[1], Nikhil Sharma[1], Luis Valero[1], Maxime Tremblin[1], Abdallah S. Zaki[1], Frédéric Arlaud[1] & Sébastien Castelltort[1]

[1]Department of Earth Sciences, 13 rue de Maraîchers, University of Geneva, 1205 Geneva, Switzerland (stephen.watkins@unige.ch)

Stratigraphic architecture of fluvial deposits is often interpreted as a record of changes in accommodation created by absolute sea-level change, subsidence, or a combination of both (downstream drivers). An increase or decrease in accommodation causes the fluvial system to respond by either aggrading or degrading to a new equilibrium slope. However, in recent years the role of upstream drivers, such as water discharge and sediment supply (volume and grain-size distribution), in controlling equilibrium slopes has become more apparent, yet we still lack significant understanding of these upstream processes. It is important to be able to differentiate between stratigraphy influenced by upstream and downstream drivers in the field because fluvial deposits represent an important archive of environmental changes. Traditionally, often downstream drivers are invoked to explain past accommodation changes, but in actuality there is often little or no constraint on the cause of these space changes. At present there is still no well-documented examples of upstream versus downstream driven stratigraphic architecture. One way to address this issue is by undertaking analogue modelling (i.e. flume experiments) as this permits the isolation of individual parameters, such as water discharge, and allows us to investigate their role on the fluvial system in a controlled environment.

In the first part of the project that we present here, we investigate how sediment aggradation within a channel develops through time via a series of flume experiments. We have designed and manufactured a narrow (0.05 m), long (2.25 m) flume with an initial gradient of zero. We aim to (i) replicate existing flume studies (e.g., Van Berg Van Saparoea & Potsma, 2008) to compare our results with theirs; (ii) investigate the role of upstream drivers by using a variety of different water discharges, sediment supplies and sediment concentrations; (iii) carry out a series of experiments varying downstream drivers (i.e. sea-level) which theoretically produce the same amount of aggradation as the upstream parameters we have used do, we will then be able to compare any similarities or differences in stratigraphy. In the second part of the study we will use these results to scale up to a fully three-dimensional analogue model (i.e. a wide flume, approximately 1 m) that produces channels and floodplains. We can then investigate how the upstream and downstream changes seen in the narrow flume are translated into the wider flume. This project is carried out in conjunction with a field-based study also presented here at SGM: *Upstream versus downstream controls on a natural sediment routing system from source-to-sink (Sharma et al. 2019)*. Where field data collection is utilised in the calculation of palaeoslopes before, during and after the Mid-Eocene Climatic Optimum (MECO).

REFERENCES

Van Den Berg Van Saparoea, A. -P., Postma, 2008: Control of climate change on the yield of river systems. In: *Recent advances in models of siliciclastic shallow-marine stratigraphy*: *Introduction and Perspectives* (Ed. By G. J. Hampson, R. Steel, P. M. Burgess & R. Dalrymple) SEPM (Society for Sedimentary Geology) Special Publication, 90, p.15-33

6. Seismic Hazard and Risk in Switzerland: From Science to Mitigation

Donat Fäh, Katrin Beyer, Blaise Duvernay

Schweizerischen Gesellschaft für Erdbebeningenieurwesen und Baudynamik (SGEB)

TALKS:

6.1 Bergamo P., Hammer C., Panzera F., Perron V., Fäh D.: Assessing the Sensitivity of Site Condition Parameters towards seismic local Amplification and their potential Use for Site Response Prediction

6.2 Chieppa D., Hobiger M., Fäh D.: Investigations of the Swiss Molasse basin down to large depth using passive seismic methods: a case study in Herdern

6.3 Hallo M., Imperatori W., Panzera F., Fäh D.: Joint probabilistic self-adapting inversion on properties of near-surface layers from dispersion and ellipticity curves

6.4 Häusler M., Michel C., Burjánek J., Fäh D.: Fracture Network Imaging on the Preonzo rock slope instability using resonance mode analysis

6.5 Hobiger M., Imperatori W., Bergamo P., Panzera F., Fäh D.: Borehole seismometer stations of the Swiss Strong Motion network

6.6 Kremer K., Grolimund R., Gassner-Stamm G., Strasser M., Wirth S.B, Fäh D.: A prehistorical geo-event database of Switzerland for paleoseismology

6.7 Lontsi A.M., Shynkarenko A., Hobiger M., Bergamo P., Kremer K., Fäh D.: Offshore Microtremor Horizontal-to-Vertical (H/V) spectral Ratio at Lake Lucerne (Switzerland): Spatio-temporal Variability and Contribution to Slope Stability Assessment

6.8 Martakis P., Reuland Y., Dertimanis V., Chatzi E.: Monitoring-Driven Seismic Assessment of Existing Masonry Buildings

6.9 Meng Z., Ancey C.: The effects of slide cohesion on impulse waves generated by landslides

6.10 Perron V., Panzera F., Bergamo P., Hammer C., Imperatori W., Moeri A., Wehrens P., Volken S., Mayoraz R., Christe P., Fäh D.: Assessing the earthquake's site response in the Swiss Rhône Valley: a multi-scale study

6.11 Savoy R., Zainal H., Khodaverdian A., Lestuzzi P.: Fragility curves for two specific buidling types in Switzerland

POSTERS:

P 6.1 Gascon L., Michel C., Devaux M., Lestuzzi P.: Implementation of seismic scenarios for the city of Yverdon-les-bains

P 6.2 Panzera F., Bergamo P., Fäh D.: Towards an improvement of the macroseismic amplification map for Switzerland

P 6.3 Herren M., Häusler M., Maurer H., Burjánek J., Fäh D.: Hunting a hidden fracture on a rock slope instability using active seismic techniques

P 6.4 Kremer K., Anselmetti F.S., Bacigaluppi P., Boes R.M., Evers F.M., Fäh D., Fuchs H., Hilbe M., Kopf A., Lontsi A., Nigg V.,Shynkarenko A., Stegmann S., Strupler M., Vetsch D.F , Wiemer S.: Assessing the causes, consequences and hazard of lake tsunamis in Switzerland with a multidisciplinary project

P 6.5 Shynkarenko A., Kremer K., Lontsi A.M., Hobiger M., Bergamo P., Kirk H., Hilbe M., Fabbri S., Anselmetti F.S., Fäh D.: “Good practice” of conducting an array OBS survey in a lake: possible challenges and pitfalls

P 6.6 Nigg V., Wohlwend S., Hilbe M., Bellwald B., Anselmetti F.S.: A tsunamogenic delta collapse in an Alpine lake and its coastal impact around 700 AD

6.1

Assessing the Sensitivity of Site Condition Parameters towards seismic local Amplification and their potential Use for Site Response Prediction

Paolo Bergamo[1], Conny Hammer[1], Francesco Panzera[1], Vincent Perron[1] & Donat Fäh[1]

[1]Swiss Seismological Service (SED), ETH Zürich, Sonneggstrasse 5, CH-8092 Zürich (paolo.bergamo@sed.ethz.ch)

One of the main objectives of the "Site Response" module of the "Risk Model Switzerland" project is the replacement of the current macroseismic amplification map of the Swiss territory (Fäh et al., 2011), with the ambition of producing several frequency-dependent seismic response layers. The strategy devised for this purpose involves the extrapolation of the local amplification experimentally reconstructed at instrumented sites (Edwards et al., 2013), using site condition parameters (SCPs) as support layer for the extrapolation. Therefore, an extensive dataset of site condition information, or proxies, has been compiled for the sites hosting seismic stations of the Swiss network (Bergamo et al., 2018); the dataset comprises parameters from estimated V_S profiles (e.g. V_{S30}), from H/V obtained from noise measurements (e.g. f_0), topographical parameters (e.g. slope, terrain class), geological/geophysical parameters and categorizations. The proxy dataset has been paired with an ensemble of empirical Fourier amplification functions (one from each station), sampled at ten frequencies (0.5-20 Hz). For data completion and comparison, the Swiss database of SCPs and amplification functions has been accompanied by an analogous dataset referring to Japanese Kik-net stations (Aoi et al. 2004).

In this work, we have investigated the relation between site condition information and amplification functions using two parallel approaches:

- In the first method, we use statistical tools to evaluate the sensitivity of the various proxies towards the corresponding amplification factors at each frequency. For continuous-variable proxies (e.g. V_{S30}), we used univariate linear regressions (Figure 1a). As for discrete, classification proxies (e.g. the geological categorization), we evaluated their capability to subdivide the total population of stations into subgroups having significantly different behaviors (Welch 1947, Figure1b). The systematic application of these tools enabled us to rank the various proxies in terms of strength of their correlation with amplification, at each frequency. Besides, we assessed whether the same SCPs behave in a similar way at the Swiss and Japanese sites.
- As for the second method, we used a neural network (NN) approach (Bishop 1995) to attempt the prediction of local amplification from proxies. The Japanese and Swiss databases were subdivided into a training and a validation subset, so to first calibrate a NN structure and then evaluate its performance in predicting site response (Figure 1c). With the NN we tested the performance of various typologies and combinations of SCPs.

We highlight the complementarity of the two methods; the first statistical approach provided a list of the most "promising" proxies for amplification prediction with the NN, as well as the proxies exhibiting similar behavior at Swiss and Japanese sites (so that the two datasets could be combined, hence improving the robustness of the neural network structure).

The main outcomes from the two approaches are the following: i) as expected, "direct" proxies (from V_S profiles, H/V measurements) perform generally better than "indirect" proxies (from geology, topography). The first group shows stronger correlation with amplification in the intermediate (1-6.7 Hz) frequency band, the latter at lower frequencies (< 3.3 Hz); ii) more complete, frequency-dependent parameters (e.g. quarter-wavelength velocity, Poggi et al. 2012) are more effective than single-value proxies (e.g. V_{S30}); iii) in general, "direct" proxies are related to amplification in a similar way in Switzerland and Japan (see Figure 1a); "indirect" proxies exhibit different behaviors; iv) the use of NN for the prediction of amplification from "direct" proxies, although achieving discrete results, has highlighted the need to employ a larger training dataset (more than the 350 sites available). This issue is less severe for "indirect" proxies, which cover a larger number of stations.

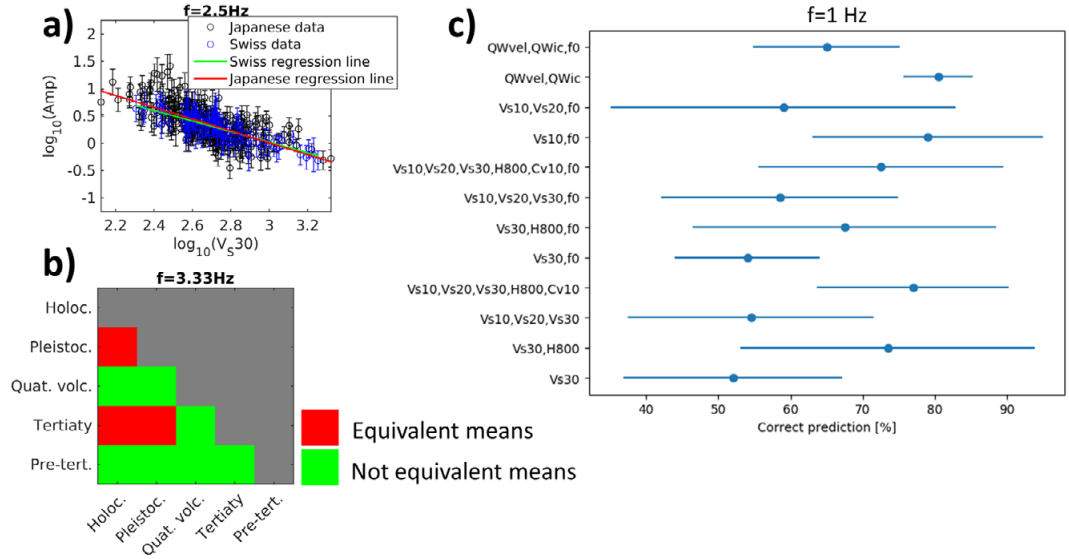


Figure 1 a) Example of linear regression of amplification factors at 2.5 Hz *vs* V_{S30}, Swiss and Japanese data. The scaling of amplification with the proxy is statistically equivalent at Swiss and Japanese sites. b) Japanese data: collation of mean amplification factors (at 3.33 Hz) between pairs of stations' subgroups defined by the geological age categorization. c) Swiss and Japanese data: predictive performance of NN at 1.0 Hz for different groups of direct proxies.

REFERENCES

Aoi S. et al., 2004: Strong Motion Seimsograph Network operated by NIED: K-net and KiK-net. JJAEE, vol. 4, no.3, 65-74.

Bergamo P. et al., 2018: Ongoing development of the site response module in the ERM-CH project. 16th Swiss Geoscience Meeting, abstract 7.6, 216-217.

Bishop. C. M. 1995: Neural Networks for Pattern Recognition. Oxford University Press, Oxford, 482 pp

Edwards B. et al., 2013: Determination of Site Amplification from Regional Sesimsicity. Seismological Research Letters, 84, no. 4, 611-621.

Fäh D. et al., 2011: ECOS-09 Earthquake Catalogues of Switzerland, Release 2-11 Report and Database, SED, Report SED/RISK/R/001/20110417

Poggi V. et al., 2012: The quarter-wavelength average velocity: a review of some past and recent application developments. 15th WCEE

Welch, B.L. 1947: The generalization of Student's problem when sevaral different population variances are involved. Biometrika, 34 (1-2), 28-35.

6.2

Investigations of the Swiss Molasse basin down to large depth using passive seismic methods: a case study in Herdern

Dario Chieppa [1], Manuel Hobiger[1] & Donat Fäh[1]

[1]Swiss Seismological Service (SED), Zurich Switzerland (dario.chieppa@sed.ethz.ch)

A good way to investigate the subsurface is through the recording of ambient seismic vibrations, because their use makes us independent of the occurrence of earthquakes, especially in areas of moderate seismicity like Switzerland. Ambient seismic vibrations mainly consist of Rayleigh and Love waves and allow the investigation of the subsurface at different scales, from few hundreds of meters to several kilometers. Site characterization studies generally explore the subsurface down to few hundred meters (Hobiger et al 2016, Maranò et al 2017, Michel et al 2014, Poggi et al 2017), while the deep structures are often investigated using tomographic techniques. In this work, we show the potential of using surface waves to investigate the deep subsurface and the possibility to reconstruct the velocity profile down to several kilometers using passive seismic arrays of sizes up to 30 km diameter.

The study area is the Swiss Molasse basin, a sedimentary basin stretching from Geneva to Constance, whose sedimentary thickness changes from less than a kilometer in the north to more than five in the south. We will present the final results of our measurements centered at the village of Herdern (TG), in northern Switzerland, where two arrays of seismic sensors with minimum and maximum interstation distances of 12.7 m to 900 m and 790 m to 29.6 km, respectively, were deployed. The small array was aimed at reconstructing the velocities of the shallow layers, as generally used for site characterization analysis, while the big array pointed to identify the deep structures as, for example, the geological transition between the sedimentary cover and the crystalline basement. The recorded data were analyzed using single-station (H/V and ellipticity curves) and array processing (three-component high-resolution FK, SPAC and Wavefield Decomposition) techniques, interpreted and finally inverted. A joint inversion was performed using the fundamental modes of Rayleigh and Love wave dispersion curves together with the ellipticity angle curve. The inverted velocity profile shows investigation depth potential down to 5 km and good fit with all the inverted data (Chieppa et al 2019).

6.3

Joint probabilistic self-adapting inversion on properties of near-surface layers from dispersion and ellipticity curves.

Miroslav Hallo[1], Walter Imperatori[1], Francesco Panzera[1], Donat Fäh[1]

[1]Schweizerischer Erdbebendienst (SED), ETH Zürich, Sonneggstrasse 5, CH-8092 Zürich (miroslav.hallo@sed.ethz.ch)

The physical properties of near-surface soil and rock layers play a fundamental role in seismic site response estimate, the latter being an essential element for reliable seismic hazard analysis. These properties (S- and P-wave velocities, Poisson's ratio and density) can be inferred from measured surface wave dispersion and ellipticity curves by applying non-linear inversion procedures. Nevertheless, the results are known to exhibit significant inherent non-uniqueness, since two or more very different velocity models may provide a similar fit to data. Standard non-linear inversion techniques (e.g. gradient methods, optimization neighbourhood algorithm) explore various velocity models in order to find a global minimum of the data misfit resulting in a single representative velocity model. Other velocity models, which might provide a similar fit, remain hidden in these standard approaches. Our research is focused on the development and application of a probabilistic approach to inference of 1D layered velocity models from measured dispersion and ellipticity curves based on the trans-dimensional parameterization of the model space. This approach efficiently explores various velocity models and produces an ensemble of models explicitly following the posterior trans-dimensional conditional probability on the models' properties. A statistical analysis of this ensemble can highlight which features are reliable (e.g. dominant layers and their boundaries, etc.), and which are arbitrary because of the non-uniqueness of the problem (e.g. poorly constrained layer boundaries, layers with uncertain properties, etc.).

In particular, we parameterize the velocity models by utilizing sets of Voronoi nuclei as in Bodin et al. (2012), and we use the Geopsy software package (http://www.geopsy.org/) for forward computations. Next, we use a Bayesian probabilistic framework (e.g. Tarantola 2005), where the measured data (i.e. dispersion and ellipticity curves) and model parameters (i.e. physical properties, thickness and number of layers) are related through multi-dimensional conditional probability density functions. As the number of layers (i.e. number of Voronoi nuclei) is not constrained, the dimension of the model space (i.e. number of model parameters) may vary. For exploration of such trans-dimensional model space we utilize a reversible-jump Markov chain Monte Carlo algorithm (Green 1995). This algorithm is enhanced by the parallel tempering of Markov chains on multiple deployed computational (MPI) nodes, where each two chains are allowed to perform a temperature swap (Sambridge et al. 2006, Fig.1). The used algorithm (of birth-death type) explores the model space by a random walk with three possible move types: 1. "perturb move" - randomly perturb layer parameters; 2. "birth" - introduction of a new layer; 3. "death" - removal of an arbitrary layer (see Fig.1). The proposed velocity model is then accepted or rejected based on a generalized Metropolis-Hastings acceptance probability (Green 1995). The velocity models sampled during the random walk through the model space create an ensemble of solutions drawn from the conditional posterior probability density on model parameters.

To summarize, our approach provides a rigorous evaluation of the velocity models from dispersion and ellipticity curves considering the inherent non-uniqueness of this inverse problem. The output includes the most probable values supplemented with uncertainties of the inferred parameters. This information can be used to evaluate the reliability of the inferred velocity models and may be relevant for seismic site-response purposes.

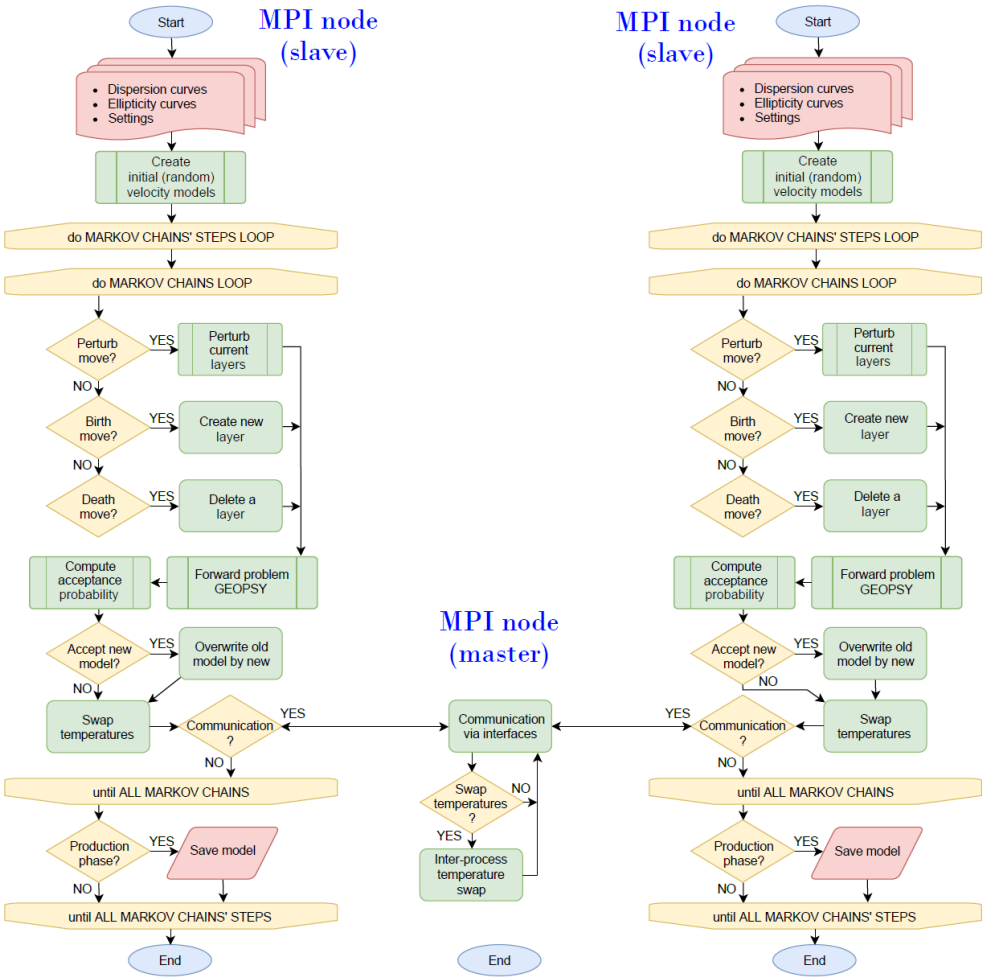


Figure 1. Flowchart diagram of our approach workflow. Arrows shows flow order, red rhomboids indicate inputs and outputs, yellow diamonds are conditional operations, yellow horizontal bars show main loops, and green rectangles represent operations or subroutines.

REFERENCES

Bodin, T., Sambridge, M., Tkalčić, H., Arroucau, P., Gallagher, K., Rawlinson, N. 2012: Transdimensional inversion of receiver functions and surface wave dispersion, Journal of Geophysical Research, 117, B02301.

Green, P.J. 1995: Reversible jump Markov chain Monte Carlo computation and Bayesian model determination, Biometrika, 82(4), 711–732.

Sambridge, M., Gallagher, K., Jackson, A., Rickwood, P. 2006: Transdimensional inverse problems, model comparison and the evidence, Geophysical Journal International, 167, 528–542.

Tarantola, A. 2005: Inverse Problem Theory and Methods for Model Parameter Estimation, Society for Industrial and Applied Mathematics, Philadelphia.

6.4

Fracture Network Imaging on the Preonzo rock slope instability using resonance mode analysis

Mauro Häusler[1], Clotaire Michel[2], Jan Burjánek[3] & Donat Fäh[1]

[1]Swiss Seismological Service, ETH Zurich, Sonneggstrasse 5, CH-8092 Zurich (mauro.haeusler@sed.ethz.ch)
[2]Risk&Safety AG, Bahnhofstrasse 92, CH-5001 Aarau, Switzerland
[3]Institute of Geophysics of the Czech Academy of Sciences, Boční II/1401141 31 Prague 4 – Spořilov, Czech Republic

Coseismic landslides and rockfalls are among the most devastating secondary effects of earthquakes. In Switzerland, a country of moderate seismicity, such effects occured, for example, following the 1946 Mw 5.8 Sierre earthquake at Rawilhorn. Combining geospatial susceptibility proxies, such as topography, with models for peak ground acceleration allows for estimating the likelihood of earthquake-induced mass movements on a regional scale (Cauzzi et al., 2018). However, to evaluate the coseismic landslide hazard on a specific slope, detailed investigations on site are required. Therefore, it is of crucial importance to understand the dynamic response of a slope and its dynamic behavior during strong ground shaking.

Describing the dynamic response of rock slopes can be achieved by measuring ambient seismic vibrations. It is generally observed that the seismic wavefield polarizes perpendicular to open fractures and that unstable slopes exhibit strong wavefield amplifications. Kleinbrod et al. (2019) established a classification scheme for ambient seismic recordings on rock slope instabilities with two end members: depth-controlled and volume-controlled sites. Depth-controlled sites are characterized by the presence of propagating surface waves and a broad ramp of increasing amplification towards higher frequecies. In contrast, volume-controlled sites exhibit normal mode behavior due to standing wave phenomena within compartments clearly separated by well-defined fracture sets.

Normal mode analysis is a well established technique in civil engineering to assess the structural integrity and the dynamic response of the object studied. We performed frequency domain decomposition (FDD) modal analysis on ambient vibration data acquired on an unstable rock site with a volume larger than 150’000 m^3 near Preonzo, Canton of Ticino, Switzerland (Häusler et al, 2019, see Fig. 1). We show that the high ground motion amplification and the clear polarization pattern identified by FDD compare well to previous studies that are based on site-to-reference spectral ratios and time-frequency polarization analysis (Burjánek et al., 2018). In addition, FDD allows for a better detection of higher modes, which can be used to efficently map dominant fracture sets. This is of special interest on rock slope instabilities where little or no surface expressions of fractures are developed and where geodetic monitoring systems are not installed yet.

Enhanced FDD additionaly provides the damping parameters (energy loss) and an improved estimate of the resonance frequency. These parameters are especially relevant for long term monitoring since they are expected to change with increasing damage, either rapidly after strong ground shaking or other external loading or gradually due to progressive degradation of the rock mass over time (e.g. Michel et al., 2011).

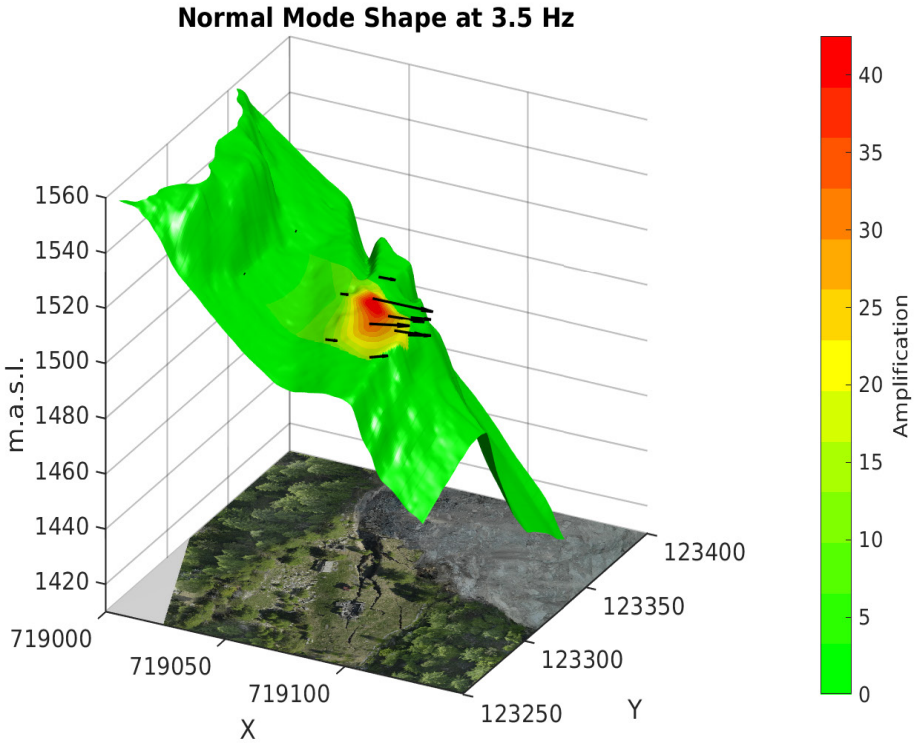


Figure 1. Normal mode shape at 3.5 Hz at the unstable rock slope Preonzo, Switzerland. The modal deflection is perpendicular to the open tension cracks and reaches high amplification factors of more than 30 compared to stable reference bedrock (orthophoto courtesy Canton of Ticino).

REFERENCES

Cauzzi, C., D. Fäh, D. J. Wald, J. Clinton, S. Losey, and S. Wiemer. 2018, ShakeMap-based prediction of earthquake-induced mass movements in Switzerland calibrated on historical observations. Natural Hazards, 92, no. 2

Burjánek, J., Gischig, V., Moore, J. R., & Fäh, D. 2018, Ambient vibration characterization and monitoring of a rock slope close to collapse. Geophysical Journal International, 212(1), 297–310. Doi: 10.1093/gji/ggx424

Häusler, M., Michel, C., Burjánek, J., & Fäh, D. 2019, Fracture network imaging on rock slope instabilities using resonance mode analysis. Geophysical Research Letters, 46, 6497– 6506. Doi: 10.1029/2019GL083201

Kleinbrod, U., Burjánek, J., & Fäh, D. 2019, Ambient vibration classification of unstable rock slopes: A systematic approach. Engineering Geology, 249, 198–217. doi: 10.1016/j.enggeo.2018.12.012

Michel, C. , Zapico, B. , Lestuzzi, P. , Molina, F. J. & Weber, F. 2011, Quantification of fundamental frequency drop for unreinforced masonry buildings from dynamic tests. Earthquake Engng. Struct. Dyn., 40: 1283-1296. doi: 10.1002/eqe.1088

6.5

Borehole seismometer stations of the Swiss Strong Motion network

Manuel Hobiger[1], Walter Imperatori[1], Paolo Bergamo[1], Francesco Panzera[1], Donat Fäh[1]

[1]Schweizerischer Erdbebendienst, ETH Zürich, Sonneggstrasse 5, 8092 Zürich (manuel.hobiger@sed.ethz.ch)

In Switzerland, historical earthquakes did not only produce damage because of strong ground-shaking, but also by triggering secondary events, such as landslides, rock falls, soil liquefaction or tsunamis in lakes. For the earthquake of Visp (25 July 1855, M 6.2), for example, wide-spread liquefaction is reported in the Rhone valley.

In general, liquefaction occurs in soils with a high amount of surficial unconsolidated sand and silt, and shallow water table. Such soils are mostly found in alluvial basins. In historical times, such soils were normally of too bad quality to construct large buildings. Nowadays, it is technically possible to build houses in such areas, for example by using long pillars for the foundation of a building. As the building density increased over the last centuries, many buildings have been constructed in such areas.
In case of a strong earthquake, liquefaction is likely to happen in those areas and the liquefaction potential depends on the level of ground shaking and therefore depend on the magnitude and distance of the earthquake and the local site effects.

Since 2009, the renewal and extension project of the Swiss Strong Motion network (SSMNet) is ongoing (Michel et al., 2014; Hobiger et al., 2017). A total of 100 new free-field seismic accelerometer stations are planned to be installed in Switzerland within this project until the end of 2021. These stations shall be mainly placed in areas of high seismic risk, i.e. in agglomerations, industrial and touristic areas, and at important infrastructures. The focal areas of important historical earthquakes are also targeted, as well as locations with special site effects, such as sites vulnerable to landslides, special geological site conditions, or sites susceptible of liquefaction. Four out of the 100 new stations are planned to be borehole stations at sites with a liquefaction potential.

A first borehole station, called SVISP, was built in 2015 on the Lonza area in Visp within the framework of the COGEAR project. This station consists of three seismic sensors located at depths of 15 m, 58 m and 102 m, respectively, and a surface sensor. In addition, six pore-pressure sensors are installed at depths between 5 and 15 m. The station SVISP might have to be relocated soon because of constructions at the site.

Out of the four new borehole stations of the SSMNet renewal project, a first one, SBUS, was built in Buochs (NW) close to the shore of Lake Lucerne (Fig. 1) and went operational in May 2019. This station consists of two seismic sensors at depths of 26 m and 100 m, respectively, and a surface sensor. Six pore-pressure sensors are installed at depths from 5 to 17 m. Two other stations are planned to be built in Collombey-Muraz (VS) and Sennwald (SG). The fourth station would be the relocated SVISP station.



Figure 1. Photo of the array measurements at the new borehole site in Buochs (NW), close to the shore of Lake Lucerne from October 2017. The new station was built in the foreground, close to the tree on the right.

As each borehole installation represents a considerable investment, the underground at the potential stations has been investigated in detail before taking the decision of building such a station there, using CPT measurements, active and passive seismic methods. We will give an overview of the different pre-installation measurements, show some example recordings of the borehole stations and show results of the data analysis of the running stations.

REFERENCES

Michel, C., Edwards, B., Poggi, V., Burjánek, J., Roten, D., Cauzzi, C., Fäh, D. 2014: Assessment of site effects in alpine regions through systematic site characterization of seismic stations, Bull. Seismol. Soc. Am., 104(6), 2809–2826.

Hobiger, M., Fäh, D., Scherrer, C., Michel, C., Duvernay, B., Clinton, J., Cauzzi, C., Weber, F. 2017: The renewal project of the Swiss Strong Motion Network (SSMNet). Proceedings of the 16th World Conference on Earthquake Engineering (16WCEE), Santiago de Chile, Chile, January 9-13, 2017.

6.6

A prehistorical geo-event database of Switzerland for paleoseismology

Katrina Kremer[1], Remo Grolimund[1], Gabriela Gassner-Stamm[1], Michael Strasser[3], Stephanie B. Wirth[4], Donat Faeh[1]

[1]Swiss Seismological Service, Institute of Geophysics, Sonneggstrasse 5, 8092 Zurich, Switzerland
[2]Insitute of Geological Sciences and Oeschger Centre for Climate Change Research, University of Bern, CH-3012 Bern
[3]Department of Geology, University of Innsbruck, Austria
[4]Centre for Hydrogeology and Geothermics, University of Neuchatel, Neuchatel, Switzerland

Paleoseismological evidences are indispensable for identifying large prehistoric earthquakes and to extend the temporal coverage of historical and instrumental earthquake catalogues. Diverse traces of potential earthquakes can be identified in the geological record and can be constrained within a certain time period. We collected all published information on past geo-events covering mainly the past 20,000 years. The database includes published and unpublished data from sedimentological, archeological, speleological, and geomorphological research. This unique dataset allows identifying periods of enhanced occurrence of geo-events. In analogy to lake systems that have been used in past paleoseismological studies, enhanced occurrence of geo-events of all types can be further discussed as potentially earthquake-triggered. The acquired dataset shows enhanced occurrence at around 450, 1600, 2200, 4500, 6000, 9700 cal yr BP. For the most recent period (450 calibrated year before present; cal yr BP), the increased occurrence of geo-events is an effect of the historical earthquakes in 1356, 1584 and 1601 AD, documented in written sources. The other phases of increased occurrence of geo-events confirm former phases identified based on lake sediments. Even though dating uncertainties are large (e.g. 14C calibration range) and an unequivocal attribution of earthquakes as trigger mechanism is not possible, the database reflects the natural hazard potential of a region and represents valuable information for seismic hazard assessment. Furthermore, despite the uncertainty regarding the definition of the trigger mechanism, we propose that the database can be used to validate and improve earthquake-hazard models.

6.7

Offshore Microtremor Horizontal-to-Vertical (H/V) spectral Ratio at Lake Lucerne (Switzerland): Spatio-temporal Variability and Contribution to Slope Stability Assessment

Agostiny Marrios Lontsi[1], Anastasiia Shynkarenko[1], Manuel Hobiger[1], Paolo Bergamo[1], Katrina Kremer[1,2], Donat Fäh[1]

[1]Swiss Seismological Service, ETH Zürich, Switzerland, Sonneggstrasse 5 8092 Zürich (agostiny.lontsi@sed.ethz.ch)
[2]Institute of Geological Sciences and Oeschner Centre for Climate Change Research, Univ. of Bern, Switzerland, Hochschulstrasse 4, 3012 Bern

The microtremor horizontal-to-vertical (H/V) spectral ratio has emerged as a single-station method within the seismic ambient-noise analysis field by its capability to quickly estimate the frequency of resonance at a site and, through inversion with additional constraints, the average velocity profile (E.g. Bard 1998, Fäh et al. 2003, Lontsi et al. 2015). For seismic hazard assessment, this information is of importance both onshore and offshore civil engineering and exploration seismology. With the advances in amphibious seismic instrumentation, high quality seismic data are emerging from the offshore environment. These data aid to characterize the sediments of the lake/ocean bottom and to assess the volume of sediment cover susceptible to failure in case of an earthquake. Failed slopes could in turn lead to a tsunami (Hilbe and Anselmetti 2014). Within the SNF-Synergia project ”Lake Tsunamis: Causes, Controls, and Hazard”, we deploy amphibious seismometers at selected locations with sediments that are susceptible to failure. We used the existing high-resolution bathymetric map to optimize the site selection. For the test sites at Weggis (Fig.1) and Chrüztrichter we evaluate the spatio-temporal variability of the estimated offshore microtremor H/V spectral ratio. This is necessary (1) to assess the stability of the H/V spectral ratio measured in the lake, (2) to test the diffuse nature of the noise wavefields in the lake, and to use appropriate tools and constraints for the inversion of the estimated H/V spectral ratio curves. Engineering frequencies ranging from 0.2 to 50 Hz are used as they aid in practice to resolve structures ranging from few to hundreds of meters.

REFERENCES

Bard, P.-Y. 1998: Microtremor measurements: a tool for site effect estimation? State-of-the-art paper, Effects of Surface Geology on Seismic Motion, 3, 1251-1279.

Fäh, D., Kind, F., & Giardini, D. 2003: Inversion of local S-wave velocity structures from average H/V ratios, and their use for the estimation of site-effects, Journal of Seismology, 7(4), 449-467.

Hilbe, M. & Anselmetti, F. 2014: Signatures of slope failures and river delta collapses in a perialpine lake (Lake Lucerne, Switzerland), Sedimentology, 61(7), 1883-1907.

Lontsi, A.M., Sánchez-Sesma, F.J., Molina-Villegas, J.C., Ohrnberger, M., & Krüger, F. 2015: Full microtremor H/V(z, f) inversion for shallow subsurface characterization, Geophysical Journal International, 202(1), 298-312.

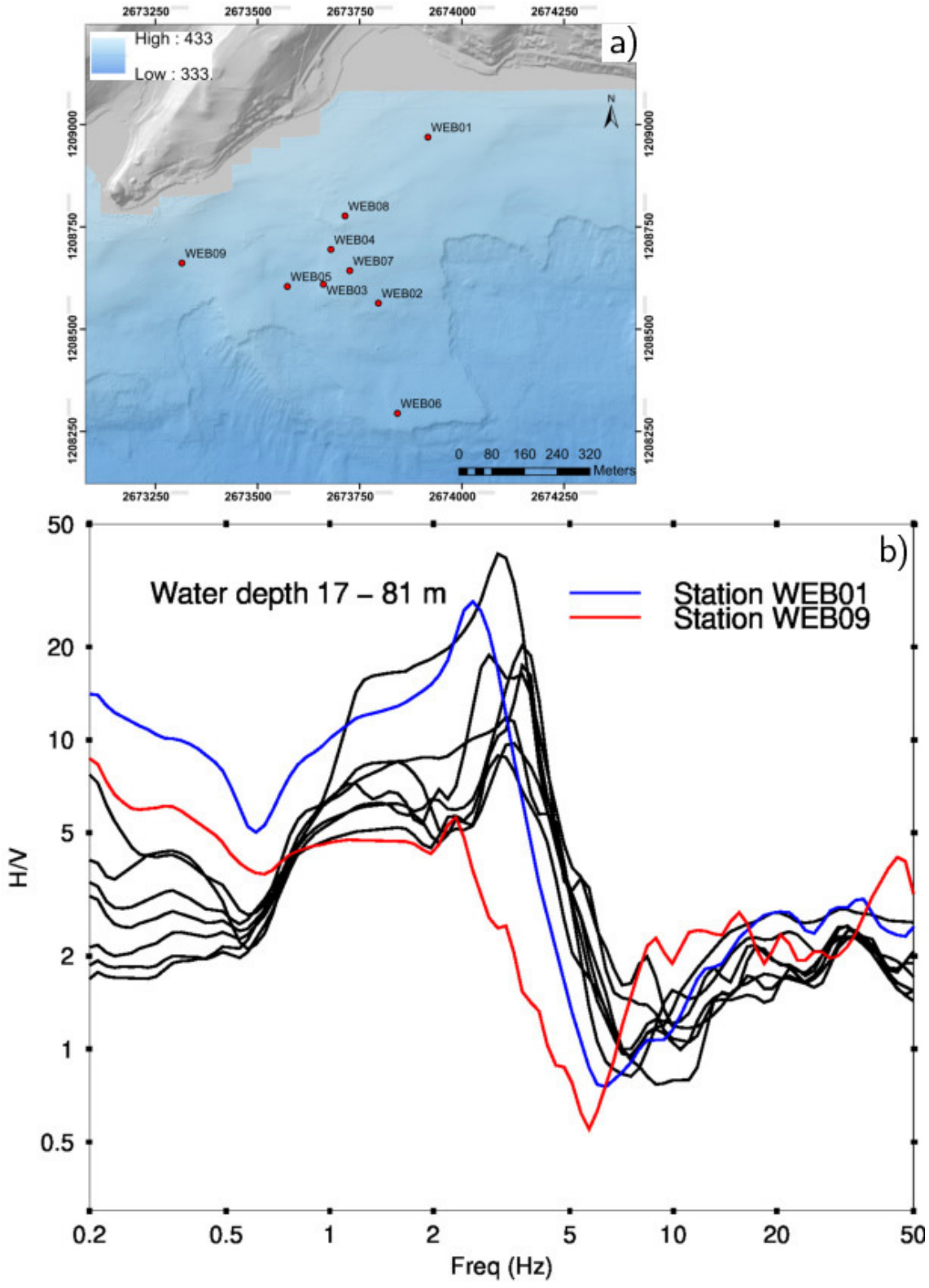


Figure 1 a) Test site at Weggis. The location of the amphibeous seismometers is shown with the red dots. b) Offshore microtremor horizontal-to-vertical spectral ratio from 9 stations. The water depth for the sensors ranges from 17 to 81 m.

6.8

Monitoring-Driven Seismic Assessment of Existing Masonry Buildings

Panagiotis Martakis[1], Yves Reuland[1], Vasileios Dertimanis[1], Eleni Chatzi[1]

[1]*Institute of Structural Engineering and Monitoring, ETH, Zurich, Switzerland., Stefano-Franscini-Platz 5, CH-8093 Zurich (martakis@ibk.baug.ethz.ch)*

Earthquake is the natural hazard with the largest loss potential even for sites of moderate seismicity, such as Switzerland, where the seismic assessment of existing buildings is undermined by the perception that low seismic hazard translates to low seismic risk. However, the interpreteation of a low occurence probability into low risk is misleading due to the catastrophic consequences of rare earthquake events. Central Europe has not experienced strong ground motions in the past century, in contrast to the Mediterranean countries, where earthquakes have triggered massive seismic retrofit campaigns and the adaption of strict regulations for seismic design and assessement. Thus, a large part of the existing building stock in central European countries is not designed to fulfill current, if any, seismic standards. In addition, most of them have already exceeded their design life span and influence of ageing on material properties remains unknown. As a consequence, seismic vulnerability of the existing building stock is nowadays highly uncertain.

A large portion of the aged building stock comprises masonry as a main constituent. Given the inherent uncertainties of masonry as a composite material and the corresponding difficulty to reliably capture the nonlinear response of such structures, data-driven health monitoring provides an efficient way to reduce the epistemic uncertainty, to validate modeling assumptions, and to identify the structural health. This work comprises an effort to analyse the existing building stock in Switzerland from a structural perspective with focus on the seismic performance. As refined seismic assessment of the entire building stock is economically and technically impossible, representative buildings of the dominant categories will be selected to apply vibration-based monitoring methodologies and calibrate appropriate numerical models. The ultimate goal of this research is to refine the vulnerability assessment of the existing building stock based on dynamic measurements and to define damage-sensitive features tailored to the different structural typologies.

This information will serve as a reference for engineering practice and aims to enhance reliability assessment via monitoring-based seismic evaluation of individual buildings and infrastructure systems. Furthermore, the refinement of the vulnerability assessment will help to upgrade the seismic risk map of Switzerland and thus, support decision makers on the management of large building portofolios including strucures that were not desinged to fullfill the current seismic standards or have already exceeded their design life span.

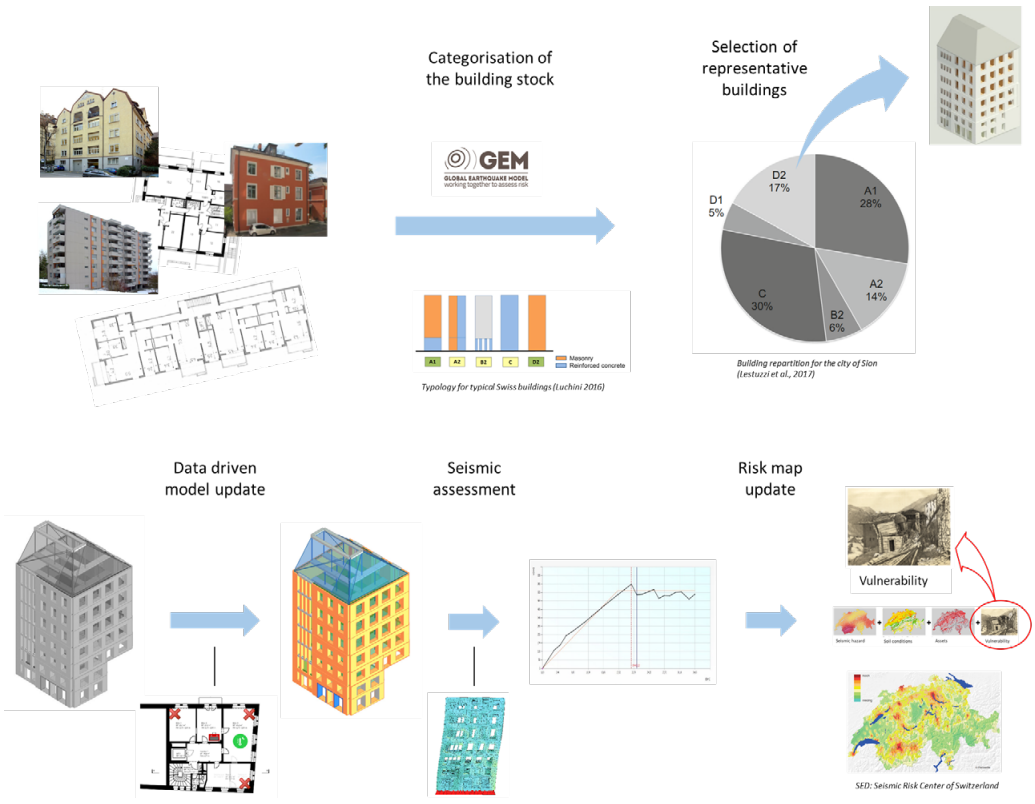


Figure 1. Graphical demonstration of the proposed methodology towards the refinement of the seismic vulnerability assessement of the existing builiding stock based on novel monitoring tools.

REFERENCES

C. Michel, A. Karbassi, and P. Lestuzzi, “Evaluation of the seismic retrofitting of an unreinforced masonry building using numerical modeling and ambient vibration measurements,” Eng. Struct., vol. 158, no. December 2017, pp. 124–135, 2018.

J. Snoj, M. Österreicher, and M. Dolšek, “The importance of ambient and forced vibration measurements for the results of seismic performance assessment of buildings obtained by using a simplified non-linear procedure: Case study of an old masonry building,” Bull. Earthq. Eng., vol. 11, no. 6, pp. 2105–2132, 2013.

S. Hans, C. Boutin, E. Ibraim, and P. Roussillon, “In situ experiments and seismic analysis of existing buildings. Part I: Experimental investigations,” Earthq. Eng. Struct. Dyn., vol. 34, no. 12, pp. 1513–1529, 2005.

Y. Reuland, A. Jaoude, P. Lestuzzi, and I.F.C. Smith. “Usefulness of ambient-vibration measurements for seismic assessment of existing structures” 4th International Conference on Smart Monitoring, Assessment and Rehabilitation of Civil Structures, Zurich, Switzerland, ETH-Zurich, 2017.

C. Luchini “Development of displacement-based methods for seismic risk assessment of the existing building stock.”, Ph.D. thesis, University of Genova, Italy, 2016.

P. Lestuzzi, S. Podesta, C. Luchini, A. Garofano “Validation and improvement of Risk-UE LM2 capacity curves for URM buildings with stiff floors and RC shear walls buildings”, Bulletin of Earthquake Engineering, vol. 15, issue 3, pp. 1111-1134, 2017.

6.9

The effects of slide cohesion on impulse waves generated by landslides

Zhenzhu Meng[1], Christophe Ancey[1]

[1]Environmental Hydraulics Laboratory, École Polytechnique Fédérale de Lausanne, 1015 Lausanne, Switzerland (zhenzhu.meng@epfl.ch)

When gravity-driven mass flows, such as avalanches and landslides, enter bodies of water, they can generate large impulse waves whose effects can be devastating. Experimental studies of impulse wave formation have mostly used rigid blocks or granular materials to mimic landslides at the laboratory scale. These studies have deduced that material deformability plays a key part in wave formation: the more rigid the sliding mass, the higher the impulse wave. It is, however, still unclear whether higher wave amplitudes arise solely from lower deformability. Indeed, blocks are not only rigid, but they are also cohesive, whereas granular media are deformable and cohesionless. To shed light on this issue, we ran experiments using two deformable materials of equal density, one exhibiting no cohesion (soft 15-mm diameter balls) and the other exhibiting cohesion (a viscoplastic polymeric gel called Carbopol Ultrez 10). A finite volume of material was released at the top of a chute, penetrated a body of water and generated impulse waves. We monitored how the mass slid and interacted with the water volume. Using high-speed cameras, we measured maximum wave heights, amplitudes and lengths of the leading wave. We used dimensionless groups to reduce the dimension of the parameter space, making it possible to carry out a regression analysis. Viscoplastic slides generated larger wave amplitudes but shorter wave lengths than granular materials. Surprisingly, the wave features did not depend on the polymer concentration. In other terms, impulse wave features were not found to be dependent on the cohesion of the deformable material landslides causing them, within the range of concentrations tested.

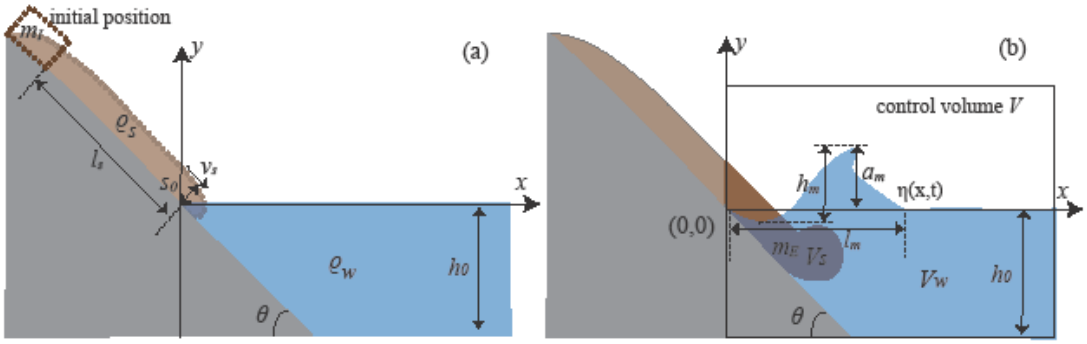


Figure 1. Sketch of the wave generated by releasing slide material into a body of water.

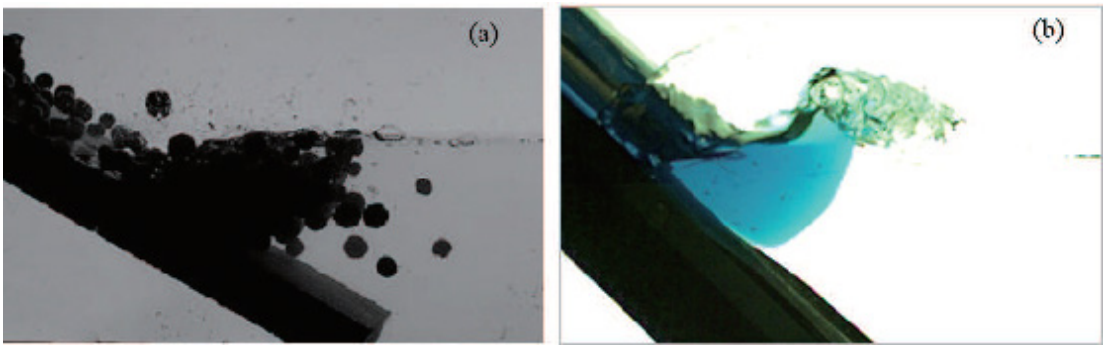


Figure 2. Sketch of the wave generated by releasing slide material into a body of water.

REFERENCES

Zitti, G., Ancey, C., Postacchini, M. and Brocchini, M., 2016. Impulse waves generated by snow avalanches: momentum and energy transfer to a water body. Journal of Geophysical Research: Earth Surface, 121(12), pp.2399-2423.

Meng, Z., 2018. Experimental study on impulse waves generated by a viscoplastic material at laboratory scale. Landslides, 15(6), pp.1173-1182.

Ancey, C. and Cochard, S., 2009. The dam-break problem for Herschel–Bulkley viscoplastic fluids down steep flumes. Journal of Non-Newtonian Fluid Mechanics, 158(1-3), pp.18-35.

6.10

Assessing the earthquake's site response in the Swiss Rhône Valley: a multi-scale study

Vincent Perron[1], Francesco Panzera[1], Paolo Bergamo[1], Conny Hammer[1], Walter Imperatori[1], Andreas Moeri[2], Philip Wehrens[2], Stephan Volken[2], Raphael Mayoraz[3], Pierre Christe[3] & Donat Fäh[1]

[1]Swiss Seismological Service (SED), ETH Zürich, Sonneggstrasse 5, CH-8092 Zürich (vincent.perron@sed.ethz.ch)
[2]Federal Office of Topography (swisstopo), Seftigenstrasse 264, CH-3084 Wabern
[3]Canton du Valais, département de la mobilité, du territoire et de l'environnement /
Service des forêts, des cours d'eau et du paysage, rue de la Dent-blanche 18A, CH – 1950 Sion

The area of the Rhône Valley in canton Valais is one of the most seismically active areas of Switzerland. Moreover, the thick and soft sedimentary deposits of the Rhône valley are prone to increase significantly both the amplitude and the duration of the seismic signal. Thus, it is essential to estimate the so-called "site effects" to better define the seismic hazard. This study aims to evaluate the site response in the Rhône valley at different scales and is carried out in the framework of the "Site Response" module of the "Risk Model Switzerland".

At the regional scale of the entire valley, the amplification can be estimated from a 3D-model of the subsurface, derived from the geological and geophysical data available for the region. This 3D-model of the sedimentary deposit in the Rhône valley is develop in collaboration between Canton Valais, SED and swisstopo. We are at the first step which corresponds to the improvement of a geological and geophysical model between Gampel and Brig, and a model for the area around Sion. Geophysical measurements and existing borehole information are used to better constrain the models. Geophysical data are mainly constituted by the fundamental resonance frequency of the site, estimated from the spectral ratio between the horizontal and the vertical component (HVSR) of ambient vibrations recorded on a single station. Moreover, the entire velocity profile is also available at several places where the seismic ambient vibrations were recorded by a dense array of seismic stations.

At the local scale, site effects can be estimated with high spatial resolution by performing dense measurements in an area of special interest (Michel et al., 2017). Such measurements were performed for the Sion area, from Vétroz to Saint-Leonard. A dense grid of almost 300 ambient-vibration measurements approximately every 250m has been performed during two field campaigns in 2019. A very detailed map of the fundamental frequency of resonance of the soil can be deduced from these measurements which help addressing the spatial distribution of the seismic-wave amplification in the Rhône valley, and might help to improve the resolution of the geological model locally.

At the scale of some specific sites, the site response can be accurately estimated at all frequencies from earthquake recordings. However, to record enough earthquakes, seismic stations have to be deployed over a long period of time (>1 year). For this purpose, 12 seismic stations were deployed in summer 2018 in the canton Valais. These stations help improving the distribution of permanent stations already present in this region. The amplifications with respect to the Swiss rock reference (Poggi et al., 2011) are estimated from the spectral fitting approach of Edwards et al. (2013). This approach accounts for the source and for the propagation term of the ground motion in order to provide amplification values which can be compared between all stations in Switzerland. The spatial variation of the site response is also estimated locally by performing direct spectral ratios between neighboring stations, assuming that the source and the propagation term are similar for close stations.

6.11

Fragility curves for two specific buidling types in Switzerland

Romain Savoy[1], Hajand Zainal[1], Alireza Khodaverdian[1] & Pierino Lestuzzi[1]

[1]*Ecole Polytechnique Fédérale Lausanne (EPFL), Station 18, CH-1015 Lausanne, Switzerland.*
(alireza.khodaverdian@epfl.ch)

Earthquake is one of most hazardous natural events that may cause catastrophic losses in term of lives and finances. Various studies and past evidence showed that some European countries, such as Switzerland, are vulnerable to large-magnitude earthquakes (Asteris *et al.*, 2014) although Switzerland is characterised as a low-to-moderate seismic zone in Europe. Large-scale seismic damage assessments are of importance to evaluate the consequence potential losses due to earthquakes; the knowledge on vulnerability of existing buildings plays a major role in a realistic estimate of damages. Since large-scale damage assessments are carried out for a region where buildings with different characteristics exist, buildings with the almost similar behaviour during the earthquake are first grouped together and vulnerability analyses are carried out for limited building types (D'Ayala *et al.*, 2014; Hancilar *et al.*, 2014). In this context, we focus on two special Swiss building types; The first type represents a row of masonry buildings which is common in Basel and the second one is a representative of single family houses with soft floor in Lausanne. Several numerical models of these building types with different geometric characteristics are developed and dynamic simulations are carried out using the applied element method. Finally, fragility curves, which link the different damage grades to a measure of the ground motion intensity (e.g. spectral acceleration), are presented for the proposed building types.

REFERENCES

Asteris, P. G. *et al.* (2014) 'Seismic vulnerability assessment of historical masonry structural systems', *Engineering Structures*, 62–63, pp. 118–134. doi: 10.1016/j.engstruct.2014.01.031.

D'Ayala, D. *et al.* (2014) *Guidelines for analytical vulnerability assessment of low/mid-rise buildings – methodology. Vulnerability Global Component Project. GEM Technical Report*.

Hancilar, U. *et al.* (2014) 'Earthquake vulnerability of school buildings: Probabilistic structural fragility analyses', *Soil Dynamics and Earthquake Engineering*. Elsevier Ltd, 67, pp. 169–178.

P 6.1

Implementation of seismic scenarios for the city of Yverdon-les-bains

Lauriane Gascon[1,2], Clotaire Michel[3], Mylène Devaux[2], Pierino Lestuzzi[4]

[1]Department of Geoengineering, Ecole des Mines de Nancy, Campus Artem - 92 Rue Sergent Blandan, 54042 Nancy (lauriane.gascon1@etu.univ-lorraine.fr)
[2]HEIA-FR, iTEC, HES-SO/Haute Ecole Spécialisée de Suisse Occidentale, Boulevard de Pérolles 80, CH-1705 Fribourg (mylene.devaux@hefr.ch)
[3]Risk&Safety AG, Bahnhofstrasse 92, CH-5001 Aarau (michel@risksafety.ch)
[4]EPFL, ENAC IIC-IMAC, CH-1015 Lausanne, (pierino.lestuzzi@epfl.ch)

The computation of earthquake scenarios is useful for authorities to prepare crisis management. It is necessary to define contingency plans, determine which areas will be most affected and organise rapid rescue actions.

The hereby-presented study focuses on the city of Yverdon-les-Bains, which is located in a low seismicity area, i.e. zone Z1 according to Swiss standard SIA 261. Since 1500, about forty earthquakes that have been recorded by the Swiss Seismological Service (SED) (Mw between 3 and 6) have occurred within a 10 km radius circle around the city (Fäh et al., 2011). Most of these earthquakes have an magnitude of less than 4 and an intensity observed at Yverdon-les-bains of less than V. Among them, three events are known to have caused some damage to the city: the Mw=5.2 Mathod earthquake in 1846, the Mw=4.7 Sainte-Croix earthquake in 1898 and the Mw=5.0 Bioley-Magnoux earthquake in 1929.

The implementation of seismic scenarios for Yverdon-les-bains is based on a database of the building stock that was developed through a building-by-building survey and a specific taxonomy defined for Swiss buildings (Lestuzzi et al, 2016). Regarding the computation of ground motion, the deaggregation of the Swiss hazard of 2015, a ground motion prediction equation developed for Switzerland (see Wiemer et al., 2016) and the amplification from the microzonation study of Yverdon (Lacave et al., 2009) have been used.

Two approaches to determine seismic scenarios were selected for the study: a probabilistic method (Michel et al., 2017) and a simplified method based on the attenuation of design ground motion with distance. Three earthquake scenarios were defined on the basis of Mathod and Bioley-Magnoux historical events and one event compatible with a 475-year return period. The latest was based on the hazard deaggregation developped for the city of Lausanne by SED and is characterized by a magnitude Mw=4.5, an epicenter located north of Yverdon-les-bains, 7.5 km away from the city centre.

The obtained results show a reasonable match between both approaches and the observations. All scenarios show relatively low damage in the city (a large majority with slight damages or no damage). These results are corroborated with those obtained by applying an empirical method. Site effects are notable in the area of Yverdon-les-bains (deep alluvial basin) and their significance on damage is discussed.

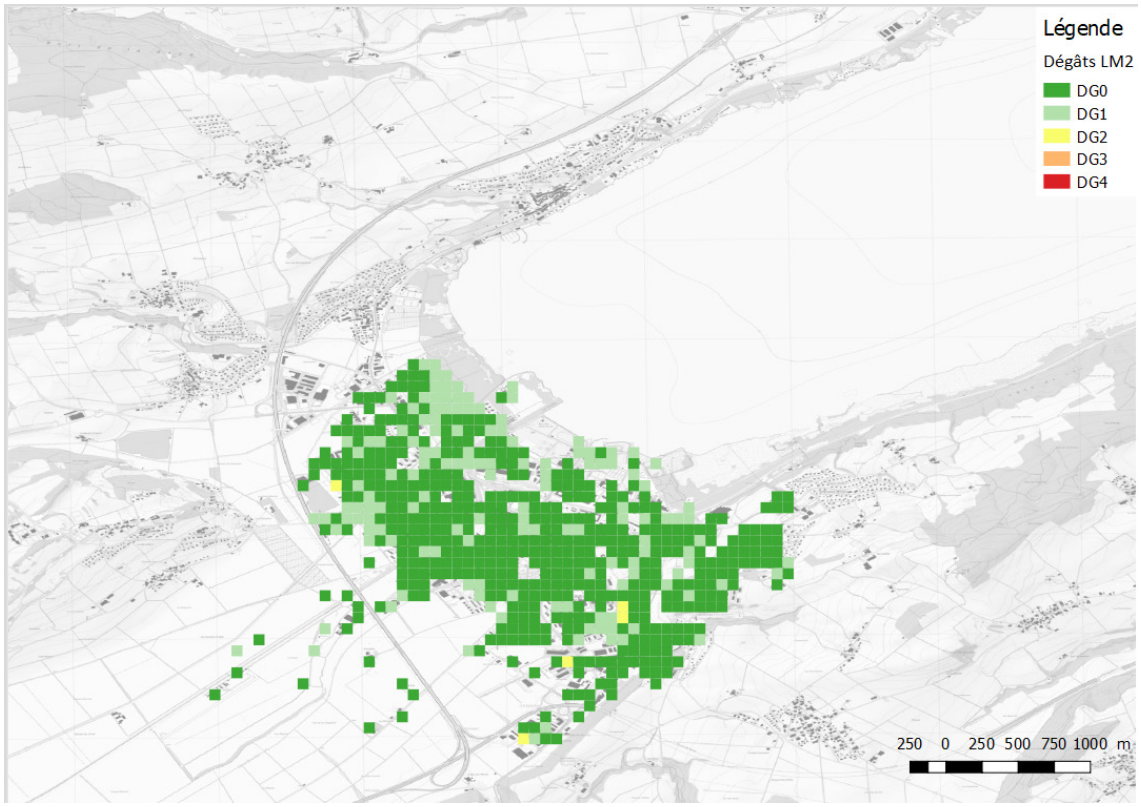


Figure 1 : Damage map with pragmatic method and LM2 typology for Yverdon-les-Bains and the earthquake compatible with a 475-year return period

REFERENCES

Fäh, D., Giardini, D., Kästli, P., Deichmann, N., Gisler, M., Schwarz-Zanetti, G., Alvarez-Rubio, S., Sellami, S., Edwards, B., Allmann, B., Bethmann, F., Wössner, J., Gassner-Stamm, G., Fritsche, S., Eberhard, D., 2011. ECOS-09 Earthquake Catalogue of Switzerland Release 2011 Report and Database. Public catalogue, 17. 4. 2011. Swiss Seismological Service ETH Zurich, Report SED/RISK/R/001/20110417.

Lacave C., Koller M., Bailly T., Microzonage sismique spectral de la région d'Yverdon. Rapport RT 289.03, Résonance Ingénieurs-Conseils SA pour l'ECA-Vaud, 2009

Lestuzzi P., Podestà S., Luchini C., Garofano A.,Kazantzidou-Firtinidou D., Bozzano C., Bischof P., Haffter A., Rouiller J.-D. (2016). "Seismic vulnerability assessment at urban scale for two typical Swisscities using Risk-UE methodology". Natural Hazards, vol. 84/1, pp. 249-269.DOI 10.1007/s11069-016-2420-z

Michel C., Hannewald P., Lestuzzi P., Fäh D., Husen S. "Probabilistic mechanics-based loss scenarios for school buildings in Basel (Switzerland)", Bulletin of Earthquake Engineering, 15(4), 1471-1496, 2017.

Wiemer S, Danciu L, Edwards B, Marti M, Fäh D, Hiemer S, Wössner J, Cauzzi C, Kästli P, Kremer K (2016) Seismic hazard model 2015 for Switzerland. Zürich. doi:10.12686/a2

P 6.2

Towards an improvement of the macroseismic amplification map for Switzerland

Francesco Panzera[1], Paolo Bergamo[1], Donat Fäh[1]

[1]Swiss Seismological Service, ETH Zurich, Sonneggstrasse 5, CH-8092 Zurich
(francesco.panzera@sed.ethz.ch)

A detailed estimate of seismic hazard needs seismic site effects evaluation in order to quantify amplification due to geological settings (Roten et al. 2008; Panzera et al. 2016; Michel et al. 2017). Macroseismic data in urban areas have already been used to identify amplification zones (e.g. Sbarra et al. 2012), whereas few cases exist at national level (e.g. Sousa and Oliveira, 1997; Fäh et al., 2011). Although this amplification map might hold on average on a national scale, the map is not applicable locally. However, it is very useful for seismic risk and shake map applications, to identify damage prone areas (e.g. Wald 2014).

A macroseismic amplification map, estimating ΔIm as difference between observed and expected macroseismic intensity using an intensity prediction equation, was developed for Switzerland using a collection of macroseismic intensity data points of past earthquakes and geological-tectonic classes (Fäh et al. 2011). Through geophysical and seismological data acquired by the Swiss Seismological Service, the map was checked and validated. Geophysical data are shear-wave velocity profiles measured at the seismic stations. The earthquake recordings are used to retrieve empirical amplification functions at the sensor locations using spectral modelling (Edwards et al., 2013).

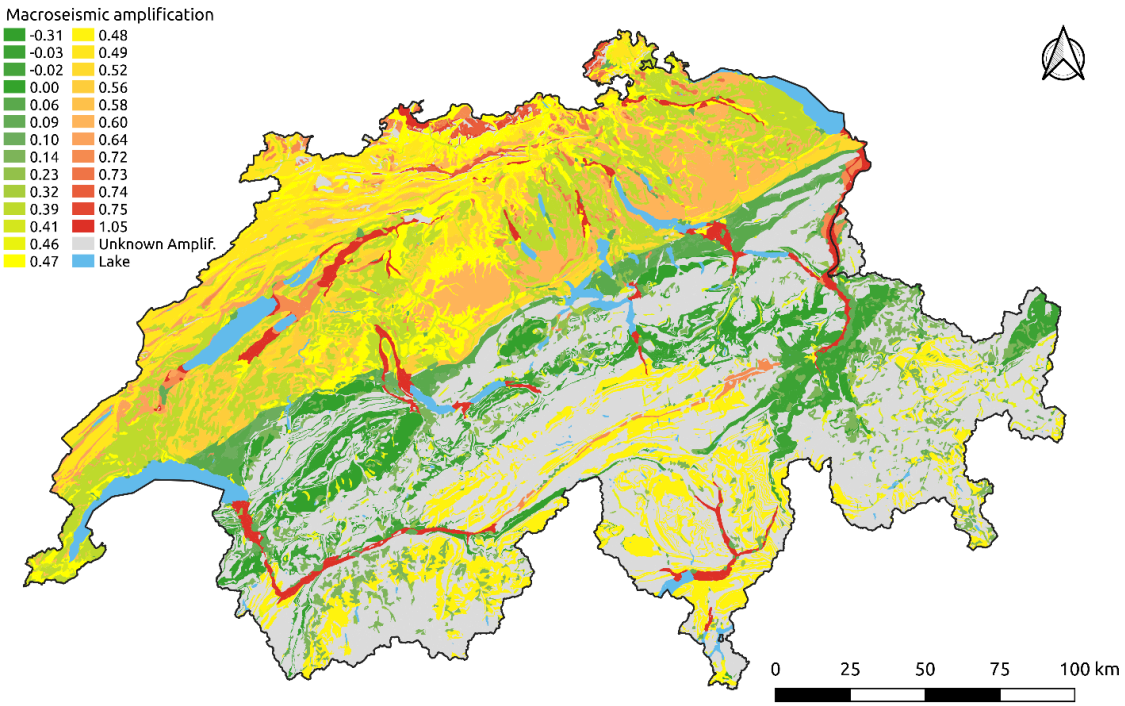


Figure 1. Site amplification map for Switzerland obtained from the analysis of macroseismic data (modified from Fäh et al. 2011).

Macroseismic amplification factors ΔIs for each considered seismic station were computed from empirical amplification factors. Moreover, a macroseismic amplification factor ΔIm was assigned to each seismic station according to macroseismic amplification map.

Correction factors $d\Delta I$ as difference between ΔIs and ΔIm are used to estimate the adjustment to Swiss reference rock conditions (Poggi et al. 2011) used in the computation of the Swiss seismic hazard map. The reference soil condition of the Swiss macroseismic amplification map, in terms of average shear wave velocity, were also verified. The study allowed linking macroseismic-intensity observations with experimental geophysical data, highlighting a good correspondence. However, statistical significance tests point out that the seismic stations are not evenly distributed among the various geological-tectonic classes of the macroseismic amplification map, so that its revision could merge classes with similar behaviour and/or by defining a new classification scheme.

REFERENCES

Fäh, D., et al. 2011: ECOS-09 Earthquake Catalogue of Switzerland, Release 2011 Report and Database, Swiss Seismological Service ETH Zurich, Report SED/RISK/R/001/20110417.

Michel, C., Fäh, D., Edwards, B., Cauzzi, C. 2017: Site amplification at the city scale in Basel (Switzerland) from geophysical site characterization and spectral modelling of recorded earthquakes, Physics and Chemistry of the Earth 98, 27-40.

Panzera, F., Lombardo, G., Imposa, S, Grassi, S., Gresta, S., Catalano, S., Romagnoli, G., Tortorici, G., Patti, F., Di Maio, E. 2018: Correlation between earthquake damage and seismic site effects: The study case of Lentini and Carlentini, Italy, Engineering Geology 240, 5, 149-162.

Poggi, V., Edwards, B., Fäh, D. 2011: Derivation of a Reference Shear-Wave Velocity Model from Empirical Site Amplification. Bulletin of the Seismological Society of America, 101(1), 258–274

Roten, D., Fäh, D., Olsen, K.B., Giardini, D. 2008: A comparison of observed and simulated site response in the Rhone valley, Geophys. J. Int. 173, 958–978.

Sbarra, P., De Rubeis, V., Di Luzio, E., Mancini, M., Moscatelli, M., Stigliano, F., Tosi, P., Vallone, R. 2012: Macroseismic effects highlight site response in Rome and its geological signature, Nat. Hazards, 62, 425–443, DOI 10.1007/s11069-012-0085-9

Sousa, M.L., Oliveira, C.S. 1997: Hazard Mapping Based on Macroseismic Data Considering the Influence of Geological Conditions, Nat. Hazards 14, 207-225. doi:10.1007/BF00128267.

Wald, D.J. 2011: Earthquakes, Shake Map. In: Gupta H.K. (eds) Encyclopedia of Solid Earth Geophysics. Encyclopedia of Earth Sciences Series. Springer, Dordrecht.

P 6.3

Hunting a hidden fracture on a rock slope instability using active seismic techniques

Michèle Herren[1], Mauro Häusler[1], Hansruedi Maurer[2], Jan Burjánek[3] & Donat Fäh[1]

[1]*Swiss Seismological Service, ETH Zurich, Sonneggstrasse 5, CH-8092 Zurich (mauro.haeusler@sed.ethz.ch)*
[2]*Institute of Geophysics, ETH Zurich, Sonneggstrasse 5, CH-8092 Zürich*
[3]*Institute of Geophysics of the Czech Academy of Sciences, Boční II/1401141 31 Prague 4 – Spořilov, Czech Republic*

In mountainous countries, such as Switzerland, large mass movements pose a significant threat to infrastructures and settlements situated inside and along valleys. This is particularly the case during strong earthquakes. Moreover, this hazard increases progressively, considering the current climate change and the increasing density of engineered structures in these regions. Therefore, it is necessary to understand the geometry, failure mechanisms, and volumes of potentially unstable slopes. One of these instabilities is the Walkerschmatt rock slope in the Matter Valley, Switzerland. Numerical modelling of ambient seismic vibrations at this rock slope revealed indications of a large-scale compliant fracture that is not evident by geological mapping, since no clear surface expressions are observable (Burjánek et al, 2019).

In order to resolve this uncertainty, we performed an active seismic survey including multicomponent recordings along four lines, two of them in combination with a vertical source and two with an inclined impact source (Herren, 2019). In addition, a synthetic dataset was generated that simulated recordings perpendicular to the potential fracture in order to verify the utilized methods. We applied seismic refraction tomography and a variety of surface wave techniques, which have proven their efficiency in previous studies. In addition, we introduce a newly developed surface wave method based on the analysis of the two-dimensional particle motion of Rayleigh waves in time domain (hodograms). Other studies showed that ambient vibrations of unstable slopes are polarized perpendicularly to open fractures (Burjánek et al, 2012). Therefore, we assume to observe a similar behavior when analyzing waveforms from active seismic sources (e.g. sledgehammer).

Almost all methods applied to the synthetic data set and to an open and clearly visible fracture resulted in well-detectable anomalies. However, the results of the measured lines crossing the location of the predicted hidden fracture are not as clear (Fig. 1). Observed small-scale features may indicate some fracturing, but they cannot be distinguished from noise with adequate certainty. The anomalies are less distinct than expected for such a large crack if compared to the result of the open fracture and to the synthetic data. Therefore, we cannot confirm the existence of a fracture by active seismic methods as proposed by numerical modelling. However, if the fracture is heavily infilled or very narrow, it might not be observable with the techniques applied.

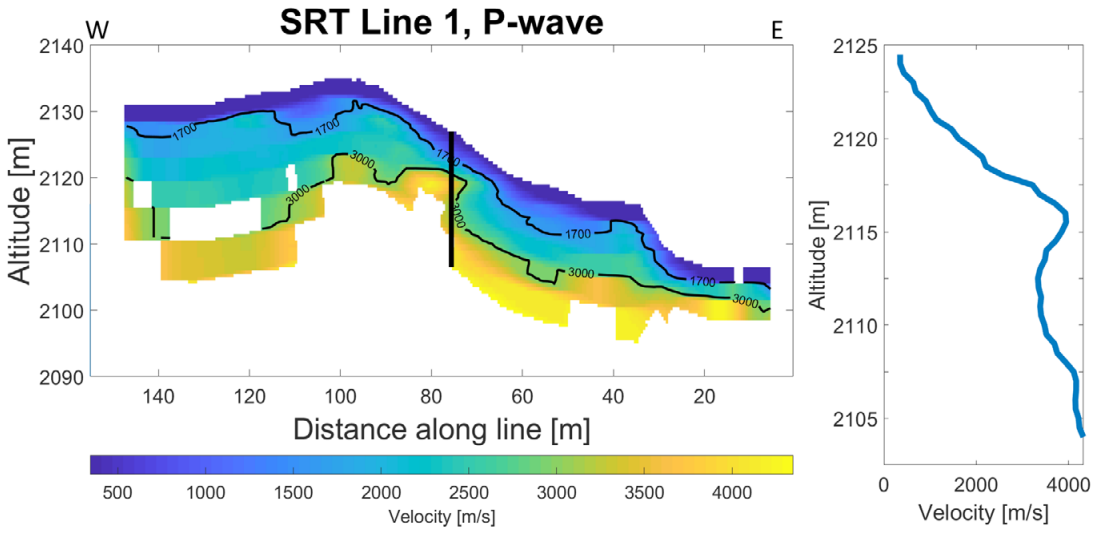


Figure 1. P-wave velocity profile on the rock slope instability Walkerschmatt, Valais, Switzerland. The black line indicates the location of the 1D-profile plottet in the right panel. The location expected for the hidden fracture is situated between profile meter 90 and 140.

REFERENCES

Burjánek, J., U. Kleinbrod, and D. Fäh (2019). Modeling the seismic response of unstable rock slopes with deep compliant fractures, submitted to J. Geophys. Res. Solid Earth.

Burjánek, J., J. R. Moore, Y. F. X. Molina, & D. Fäh. 2012, Instrumental evidence of normal mode rock slope vibration. Geophysical Journal International, 188, no. 2,559-569. doi: 10.1111/j.1365-246X.2011.05272.x.

Herren, M. 2019, Detection of sub-vertical fractures on the rock slope instability Walkerschmatt using seismic methods. MSc Thesis, ETH Zurich.

P 6.4

Assessing the causes, consequences and hazard of lake tsunamis in Switzerland with a multidisciplinary project

Katrina Kremer[1,2], Flavio S. Anselmetti[2], Paola Bacigaluppi[3], Robert M. Boes[3], Frederic M. Evers[3], Donat Faeh[1], Helge Fuchs[3], Michael Hilbe[2], Achim Kopf[4], Agostiny Lontsi[1], Valentin Nigg[2], Anastasiia Shynkarenko[1], Sylvia Stegmann[4], Michael Strupler[1], David F. Vetsch[3] & Stefan Wiemer[1]

[1]Swiss Seismological Service, ETH Zürich, Sonneggstrasse 5, 8092 Zurich
[2]Institute of Geological Sciences and Oeschger Centre for Climate Change Research, Univ. of Bern, Bern
[3]Laboratory of Hydraulics, Hydrology and Glaciology (VAW), ETH Zurich, Hönggerbergring 26, 8093 Zürich
[4]MARUM, University of Bremen, Leobener Strasse 8, 28359 Bremen

Historical reports and recent studies have shown that Swiss lakes have experienced tsunamis in the past. The causes of these tsunamis can be seismic or aseismic. These tsunamis are mainly generated by mass-movement processes displacing large volumes of water. Some examples of such events in Switzerland are the 563 AD Lake Geneva tsunami caused by a rockfall-induced delta failure, the 1601 AD Lake Lucerne tsunami caused by earthquake-triggered sublacustrine mass movements, and the 1687 AD Lake Lucerne tsunami that was caused by a delta failure.

Nowadays, the shorelines of many Swiss lakes are densely populated and host important infrastructures. The occurrence of lake tsunamis in Switzerland is known, however, we still miss a workflow to assess the hazard related to tsunamis. Within this framework of an interdisciplinary project (Lake Tsunamis: Causes, Consequences and Hazard), funded by the Swiss National Science Foundation and the Federal Office for the Environment, aims towards better understanding the key concepts of lake-tsunami processes using Swiss lakes as a laboratories.

The major objectives of this project are to investigate a) the diverse causes of lake tsunamis, b) the geotechnical and sedimentological properties of unstable slope sediment, c) the potentially unstable sediment volumes on charged slopes, d) the wave generation, propagation and shore run-up, e) the onshore and shallow offshore tsunami deposits and d) their related hazard. In this contribution, we will present the main objectives and advances of this interdisciplinary project.

P 6.5

"Good practice" of conducting an array OBS survey in a lake: possible challenges and pitfalls

Anastasiia Shynkarenko[1], Katrina Kremer[1], Agostiny Marrios Lontsi[1], Manuel Hobiger[1], Paolo Bergamo[1], Henning Kirk[2], Michael Hilbe[3], Stefano Fabbri[3], Flavio S. Anselmetti[3], Donat Fäh[1]

[1]Swiss Seismological Service, ETH Zürich, Sonneggstrasse 5, CH-8092 Zürich (a.shynkarenko@sed.ethz.ch)
[2]Alfred Wegener Institute – Helmholtz Centre for Polar and Marine Research, Am Handelshafen 12, D-27570, Bremerhaven
[3]*Geological* Institute and Oeschger Centre for Climate Change Research, University of Bern, Baltzerstrasse 1+3, CH-3012, Bern

Passive array measurements of ambient seismic vibrations and earthquake signals are widely and successfully used onshore in order to resolve the shear wave velocity structure, and to characterize the seismic response and stability of soil deposits. Similar experiments can be carried out in the subaquatic realm (offshore), but with numerous technical and logistical challenges. While onshore, orientation and timing of seismometers are well constrained, this is not the case for the offshore measurements. Therefore, a specific workflow is required to overcome potential pitfalls.

One of the goals of the Synergia Project "Lake Tsunamis: Causes, Controls and Hazard" is to study submerged slopes in terms of their stability (static conditions), and their seismic response and potential during earthquakes. We deployed arrays of Ocean Bottom Seismometers (OBS, Fig. 1) in Lake Lucerne (Central Switzerland) to assess the seismic response of the slopes and resolve their characteristic fundamental frequency of resonance and shear wave velocity structure.
Planning of the campaigns and operation of the OBSs together with the subsequent data processing require specific preparatory steps and supplementary measurements (e.g. multibeam, airgun, differential GPS etc.). This includes site selection and the design of array geometries (Fig. 2), determination and correction of instrument positions, orientation of the seismometers and time-drift corrections of the recording systems.

We present our experience, and propose what we call "good practice" of array OBS investigations in the lake realm. This is based on several OBS campaigns in Lake Lucerne carried out between 2018 and 2019. Our workflow includes stages from campaign preparation to data processing. Targers are the fundamental frequency of resonanse of the sites, based on the horizontal-to-vertical spectral ratios, and dispersion curves of surface waves including Scholte and Love waves. It is visible in the observed fundamental frequencies and dispersion curves, that characteristics of lake sediments are very different from what we find onshore.

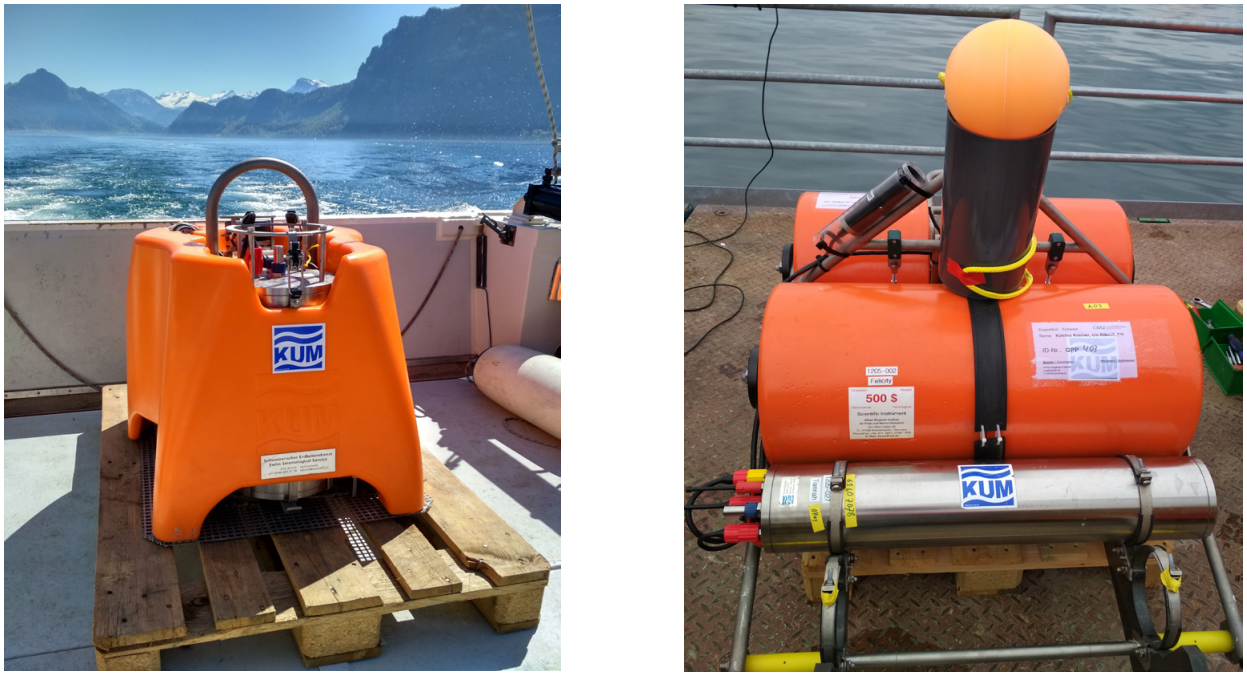


Figure 1. Two configurations of Ocean Bottom Seismometers used in the arrays: Nammu (left) and Lobster (right). Both intsruments are produced by KUM, Kiel.

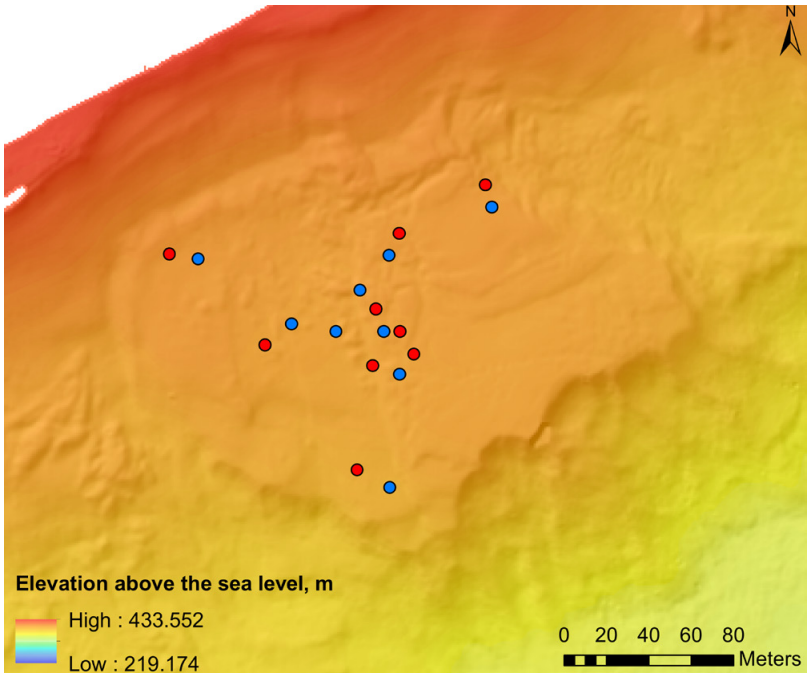


Figure 2. An example of spiral-arm design of OBS array geometry (Site: Ennetbürgen, Lake Lucerne). Blue dots: planned array geometry; red dots: obtained array geometry due to the drift of free-fall OBSs in the water column.

P 6.6

A tsunamogenic delta collapse in an Alpine lake and its coastal impact around 700 AD

Valentin Nigg[1], Stephan Wohlwend[2], Michael Hilbe[3], Benjamin Bellwald[4], & Flavio S. Anselmetti[3]

[1]Institute of Geological Sciences and Oeschger Centre for Climate Change Research, University of Bern, Baltzerstrasse 1+3, CH-3012 Bern (valentin.nigg@geo.unibe.ch)
[2]ETH Zurich, Sonneggstrasse 5, CH-8092 Zurich
[3]Institute of Geological Sciences and Oeschger Centre for Climate Change Research, University of Bern, Baltzerstrasse 1+3, CH-3012 Bern
[4]Volcanic Basin Petroleum Research (VBPR), Oslo Science Park, Gaustadalléen 21, NO-0349 Oslo

Subaqueous mass movements are able to generate tsunamis in the marine and lacustrine realm (e.g. 2018 Sulawesi Earthquake, Palu City tsunami (Takagi et al. 2018); AD 563 Lake Geneve delta collapse tsunami (Kremer et al. 2012)). These tsunami events are caused by the displacement of large water masses, which are initiated by the emplacement of large subaqueous mass movements. Mass-movement volume, Froude number and water depth at the triggered site are the most critical parameters in tsunami generation (Harbitz et al., 2014; Hilbe and Anselmetti, 2015), and determine the tsunami magnitude and runup. Such subaqueous mass movements can be triggered by large earthquakes by amplified ground shaking acceleration, but also aseismically by spontaneous delta collapses resulting from overloading and high sedimentation rates.

Seismic data and sediment cores from Lake Sils in the Upper Engadin (SE Switzerland) revealed in previous studies a large mass-movement deposit of at least 6.5 Mio m^3 originated from a deltaic collapse around 700 AD (Blass et al. 2015). Regional paleoseismic reconstruction indicate that this delta collapse likely occured during a strong prehistoric earthquake (Bellwald et al. 2012). Based on subaqueous mass-movement and tsunami propagation/inundation modelling, we argue that this deltaic collapse was able to trigger a tsunami in Lake Sils. This hypothesis is supported by onshore and shallow-water offshore sediment cores recovered along the shoreline at Sils Baselgia on the northwestern edge of the lake. The sediment cores contain a fining upwards coarse-grained clastic sediment deposit with imbricated pebbles overlying an organic-rich soil horizon as it is typical for tsunami deposits (Monecke et al. 2008). Moreover, the excavation of an underground garage ~200 m inland from today's lake shore in Sils-Baselgia in 1964 showed that this clastic layer contained four Roman votive altars. We argue that this former sanctuary was built during Roman times and then became buried upon tsunami inundation related to the mass movement from 700 AD. This interpretation is supported by sedimentological analysis and radiocarbon dating.

REFERENCES

Bellwald, B., 2012; Paleoseismologic implications of the sediment stratigraphy in Lake Silvaplana (Engadine, Eastern Switzerland), MSc Thesis ETH Zürich, 96 pp.

Blass, A., Anselmetti, F.S., Grosjean, M. and Sturm, M., 2005: The last 1300 years of environmental history recorded in the sediments of Lake Sils (Engadine, Switzerland). Eclogae Geologicae Helvetiae, 98(3), pp.319-332

Harbitz, C.B., Løvholt, F. and Bungum, H., 2014: Submarine landslide tsunamis: how extreme and how likely?. Natural Hazards, 72(3), pp.1341-1374.

Hilbe, M. and Anselmetti, F.S., 2015: Mass movement-induced tsunami hazard on perialpine Lake Lucerne (Switzerland): Scenarios and numerical experiments: Pure and Applied Geophysics 172, 545-568.

Kremer, K., Simpson, G. and Girardclos, S., 2012: Giant Lake Geneva tsunami in ad 563. *Nature Geoscience*, *5*(11), p.756.

Monecke, K., Finger, W., Klarer, D., Kongko, W., McAdoo, B. G., Moore, A. L., & Sudrajat, S. U., 2008: A 1,000-year sediment record of tsunami recurrence in northern Sumatra. Nature, 455(7217), 1232.

Takagi, H., Pratama, M.B., Kurobe, S., Esteban, M., Aránguiz, R. and Ke, B., 2019: Analysis of generation and arrival time of landslide tsunami to Palu City due to the 2018 Sulawesi Earthquake. *Landslides*, *16*(5), pp.983-991.

7. Deep geothermal energy and CO_2 storage

Larryn Diamond, Paul Bossart, Benoît Valley

TALKS:

7.1 Berger, A., Herwegh, M.: Instantaneous high porosities versus long-term dynamic porosity evolution within the Grimsel breccia fault (Aar-Massif): Insights from cockade bearing breccias

7.2 Dutler N., Valley B., Gischig V., Krietsch H., Villiger L., Doetsch J., Jalali M., Amann F.: Hydromechanical observation from the in-situ hydraulic fracturing (HF) experiment

7.3 Eruteya, O.E., Guglielmetti L., Makhloufi,Y., Moscariello A.: 3-D Static Model to Characterize Geothermal Reservoirs for High-Temperature Aquifer Thermal Energy Storage (HT-ATES) in the Geneva Area, Switzerland

7.4 Ferreira De Oliveira G., De Haller A., Guglielmetti L., Makhloufi Y., Moscariello A.: Characterization of Lower Cretaceous-Upper Jurassic geothermal reservoirs using chemostratigraphy and automated quantitative petrography: examples from the Geneva Basin.

7.5 Fryer, B., Ma, X., Siddiqi, G., Laloui, L.: Critically-stressed EGS reservoir stimulation in reverse faulting stress regimes using stress preconditioning

7.6 Gilles Waleffe: Observation of rate and magnitude of induced seismicity under damage-controlled tensile fracturing

7.7 Guglielmetti L., Eichinger F., Moscariello A.: Geochemical Characterization of Deep Geothermal Waters Circulation in Carbonatic Geothermal Reservoirs of the Geneva Basin (GB)

7.8 Kong X.-Z., Kittilä A., Jalali M., Somogyvari M., Evans K.F., Saar, M.O. : Flow path characterization at the Grimsel Underground Rock Laboratory using solute tracer tests

7.9 Krietsch, H., Villiger, L., Brixel, B., Gischig, V., Doetsch, J., Jalali, M.R., Amann, F.: Current seismo-hydro-mechanical interpretations of the in-situ hydraulic stimulations at the Grimsel Test Site

7.10 Nussbaum C., Guglielmi Y., Cappa F., Birkholzer J., Ajo-Franklin J., Robertson M., Cook P., Lanyon G.W., Bossart P.: Imaging the long-term loss of faulted host rock and caprock integrity (FS-B experiment), Mont Terri Rock Laboratory

7.11 Omid Moradian: Fault Reactivation and Associated Induced Seismicity under Cyclic Loading

7.12 Owusu J.P., Moradian O.: Observation of Cracking in Damage Controlled Tensile Fracturing

7.13 Rinaldi A.P., Zappone A., Grab M., Wenning Q., Roques C., Guglielmi Y., Madonna C., Obermann A., Nussbaum C., Wiemer S.: The CS-D experiment at the Mont Terri Laboratory: site-characterization and preliminary results of long-term injection

7.14 Ritz V. A., Rinaldi A. P., Castilla R., Colas E., Meier P. M., Wiemer S., and the COSEISMIQ team: Preliminary Geomechanical Modelling of the Hengill Geothermal Field

7.15 Rossi E., Jamali S., Saar M.O., Rudolf von Rohr Ph.: Advanced hybrid thermo-mechanical drilling technology to facilitate deep geo-resource exploitation

7.16 Valley B., Miller S. A.: Favourability maps for deep geothermal in Switzerland

7.17 Wanner C., Waber H.N., Bucher K.: Geochemical evidence for large-scale and long-term topography-driven groundwater flow in orogenic crystalline basements

7.18 Zabihian F., Moradian O.: The Effects of Normal Stress on the Transition Between Stable Sliding and Stick-slip in Crystalline Rock Faults

POSTERS:

P 7.1 van den Heuvel D.B, Alt-Epping P., Wanner C., Mäder U., Diamond L.W.: Investigating mineral reactions during high-temperature aquifer thermal energy storage (HT-ATES)

P 7.2 Guglielmetti L., Perozzi, L. ., Dupuy D., Martin F., Métraux V., Meyer, M., Mijic G., Moscariello A., Nawratil De Bono C., Radogna P.V.: High-resolution gravity data to characterize density variations and reduce uncertainty in geothermal reservoirs of the Geneva basin (GB)

P 7.3 Niederau J., Ebigbo A., Saar M.O.: Model-based characterization of subsurface heat transport processes in Canton Aargau

P 7.4 Alt-Epping P., Diamond L.W., Wanner C.: Regional scale models of fluid flow in the orogenic hydrothermal system at Grimsel Pass, Switzerland

P 7.5 Perrochet L., Preisig G., Valley B.: Assessing fault criticality using seismic monitoring and fluid pressure analysis

P 7.6 Quiroga G.E., Rubino J.G., Solazzi S.G., Barbosa N.D., Holliger K.: Effects of fracture connectivity on Rayleigh wave dispersion

P 7.7 Sotelo E., Solazzi S. G., Rubino G. J., Barbosa N. D., Holliger K.: Poroelastic effects of the damaged zone on fracture reflectivity

P 7.8 Jaeggi D., Hesser J., Chao Li, Nussbaum C., Bossart P.: Predictive HM-modeling in the heterogeneous Opalinus Clay of the Mont Terri rock laboratory and validation with monitoring data from a mine-by test

P 7.9 Wenning Q., Madonna C., Zappone A.: Anisotropic elastic properties and permeability of Opalinus shale from the 'Main Fault' and host formation within Mont Terri

P 7.10 Zhou Y., Pugnetti M., Foubert A., Neururer C., Biedermann A.R.: Characterization of 3D pore shape and distribution in sedimentary rocks with different porosity by X-ray microcomputed tomography

P 7.11 Pugnetti M., Zhou Y., Biedermann A.R.: Anisotropy of Magnetic Susceptibility to investigate the pore fabric of rocks with various porosity using ferrofluid impregnation: First results and method improvements

P 7.12 Vouillamoz N., Vouillamoz J., Clerc de Senarclens M., Rincón Hanna D., Nuijten G.: Will deep geothermal enable Switzerland to be carbon neutral by 2050?

P 7.13 von Rothkirch J., Ejderyan O., Stauffacher M.: Bridging the gap between Places and Sites: Including place factors in the site selection process of CO_2 storage projects

7.1

Instantaneous high porosities versus long-term dynamic porosity evolution within the Grimsel breccia fault (Aar-Massif): Insights from cockade bearing breccias

Alfons Berger[1] and Marco Herwegh[1]

[1]*Institut für Geologie, University of Bern, Baltzerstrasse 1+3, CH-3012 Bern (alfons.berger@geo.unibe.ch)*

This study presents structural and petrophysical data from the Grimsel breccia fault (GBF), a still active fault-bound hydrothermal system in the crystalline basement of the southern central Aar Massif. The naturally formed rocks divide into breccias, cataclasites, cockade-bearing breccias and a damage zone surrounding the GBF. The latter consisting of fractured gneisses and mylonites. The most porous parts of the GBF often contain cockade structures or their tectonically overprinted remnants.

Cockades are indicators for a high permeability and porosity. They are clasts completely surrounded in 3D by spheroidal-hydrothermal growth rims. The core of the cockades either consists of cataclasites or re-fragmented cockades clearly documenting a brittle origin. The growth rims must precipitate while the cores are in suspension within a fluid jet. This peculiar cockade formation requires (a) instantaneous fracturing, (b) high-speed injection of the fluid and (c) high porosities [Berger and Herwegh, 2019]. All these processes occur during a local seismic event producing such cockade structures. Once the velocity of the injecting fluid jet reduces, the cockades settle down and either are remobilized again into a suspension state with the next fluid pulse (aftershock) or become cemented during a stagnant fluid stage (interseismic period). With cementation, porosity decreases and may even clogg. It requires then a new main rupture to re-fracture the system and start the seismic-interseismic cockade cycle again. These cockade layers have sizes of mm to decimeters and are embedded in cataclasites or breccias. Depending on the timing and number of overprints the cockade layers are the most porous rocks inside the GBF but their porosity changes with time and is therefore highly dynamic. In active hydrothermal systems such as the GBF, these cockade layers and breccias are the dominant present day fluid pathways. The estimated porosities are in the range of 20-25vol%. In contrast cemented cataclasites show porosities of about 5-15%. Both values are fundamentally different to those of adjacent gneisses, which show porosities below 2 %. For geological time intervals, this clearly indicates that only repeated seismic fracturing is an effective way to locally open very high porosities. These porosities are connected with high dynamic permeability. In contrast, slow brittle deformation also enhances porosity, but much less efficient and with lower values.

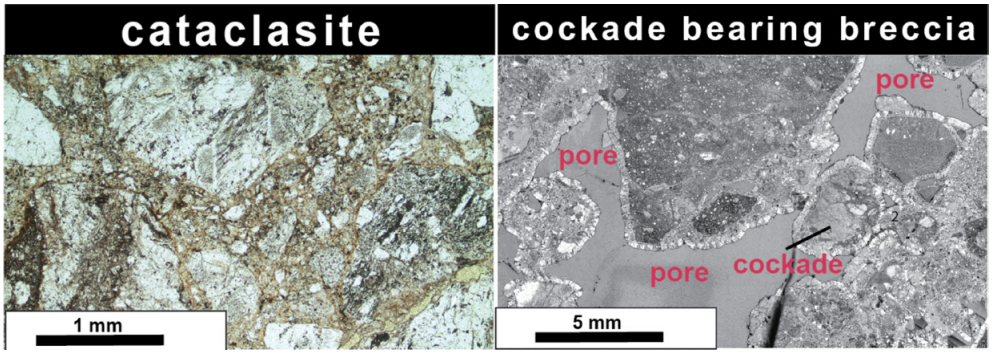


Fig. 1: thin section photographs of an cataclasite and cockade bearing breccia. Note the fundamental different porosity

REFERENCES

Berger, A., Herwegh, M., 2019. Cockade structures as a paleoearthquake proxy in upper crustal hydrothermal systems. Nature Scientific Reports, 9, 9209.

7.2

Hydromechanical observation from the in-situ hydraulic fracturing (HF) experiment

Dutler Nathan[1°], Valley Benoît[1], Gischig Valentin[2], Krietsch Hannes[3], Villiger Linus[3], Doetsch Joseph[3], Jalali Mohammadreza[4], Amann Florian[4]

[1]*Centre for Hydrogeology and Geothermics, University of Neuchâtel*
[2]*CSD Engineers, Bern*
[3]*Dep. of Earth Sciences, ETH Zurich*
[4]*Dep. of Engineering Geology and Environmental Management, RWTH Aachen*
°*nathan.dutler@unine.ch*

A total of six hydraulic fracturing (HF) experiments were conducted at the Grimsel Test Site (GTS), Switzerland, with the aim to improve our understanding of processes associated with high-pressure fluid injection into a moderately fractured crystalline rock mass. The HF test intervals were distributed over two inclined boreholes using an injection interval length of one meter. The injection protocol was kept similar for all tests. The surrounding, exceptionally well-characterized rock mass is accessed with 12 boreholes which allow high-resolution monitoring of fracture fluid pressure, temperature, strain and micro-seismicity.

Injection rates and injection pressures in the open intervals are recorded and rock mass deformation is monitored with uniaxial strain (FBG) sensors (Dutler et al., 2019). The results of different tests and cycles will be presented within this contribution. As an example, Figure 1 presents pressure-controlled step test of one experiment. In Fig. 1a the location of the injection interval and the FBG sensor at 31.8 m depth in FBS1 (radial distance to the injection location is ~6 m) can be observed. Also shown are the time series for the aforementioned FBG sensor and the injection pressure (Fig. 1b). The linked FBG reading with the injection pressure (Fig. 1c) show almost linear opening with increasing injection. At approximately 3.5 MPa, the pressure varies during opening until pressure stabilise at 4.25 MPa and the FBG reading indicate progressive tension until shut-in. The delay time between is due to the different measurement locations. Therefore, pressure decay at the injection interval before the FBG reading indicate closure. The fracture closes with a rate of 5 m/m/MPa.

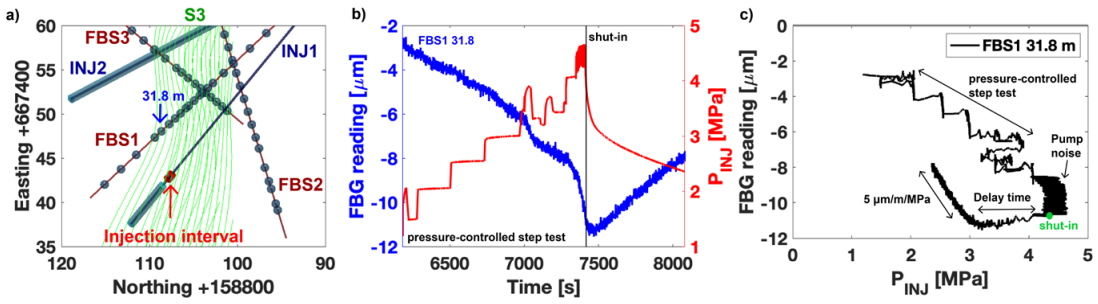


Figure 1: a) Overview of the injection location and the FBG sensor in FBS1. b) The timeseries of the FBG reading at 31.8 m and the injection pressure are presented for the pressure-controlled step test. c) presents the FBG reading vs the injection pressure for the two timeseries from b).

REFERENCES

Dutler, N., Valley, B., Gischig, V., Villiger, L., Krietsch, H., Doetsch, J., … Amann, F. (2019). Hydraulic fracture propagation in a heterogeneous stress field in a crystalline rock mass. *Solid Earth Discussions*, 1–41. https://doi.org/10.5194/se-2019-111

7.3

3-D Static Model to Characterize Geothermal Reservoirs for High-Temperature Aquifer Thermal Energy Storage (HT-ATES) in the Geneva Area, Switzerland

Ovie Emmanuel Eruteya[1], Luca Guglielmetti[1], Yasin Makhloufi[1] & Andrea Moscariello[1]

[1]Department of Earth Sciences, University of Geneva, Rue des Maraîchers 13, CH-1205 Geneva (ovie.eruteya@unige.ch)

In the framework of the GEOTHERMICA ERA-NET co-funded project-HEASTORE, one of the main challenges related to assessing the technical feasibility and sustainability of High Temperature (~25°C to ~90°C) Aquifer Thermal Energy Storage (HT-ATES) is subsurface characterization. In this study, we aim to develop a 3-D geologically robust static model in order to characterize the subsurface at the GEo-01 geothermal exploration borehole and possibly identify candidate intervals suitable for HT-ATES within the Lower Cretaceous Carbonates in the Geneva Area. In order to achieve this, we analyzed a suite of subsurface datasets encompassing two-dimensional seismic reflection data integrated with petrophysical data and well report from the GEo-01 well recently drilled in the framework of the Geothermie2020 program and other proximal boreholes. Seismic interpretation reveals a well-developed flower structure deforming the Mesozoic and parts of the Cenozoic sediments. Petrophysical analysis suggests the Lower Cretaceous Formation is tight, generally characterized by low porosity and permeability values. However, the presence of fracture networks and faults deforming a substantial part of this unit may promote localized fluid circulation. Three candidate intervals have been identified as potential Lower Cretaceous targets (CT) suitable for HT-ATES in fractured intervals characterized by tested water outflows and devoid of hydrocarbon impregnation: (1) Grand Essert Fm / Pierre Jeune de Neuchatel + Marnes d'Hauterives Fm [CT1], (2) Vuache Fm - Chambotte- Chambotte inférieur [CT2] and (3) Goldberg Fm [CT3]. The 3-D static model developed in this study will be used as input for numerical heat flow and predictive THMC models for the Geneva Basin. Importantly, our findings highlight the need for subsurface data augmentation in the Geneva Basin. It also shed light on the implication of the subsurface manifestation of hydrocarbons as geohazard to heat storage and other geo-energy related projects at large.

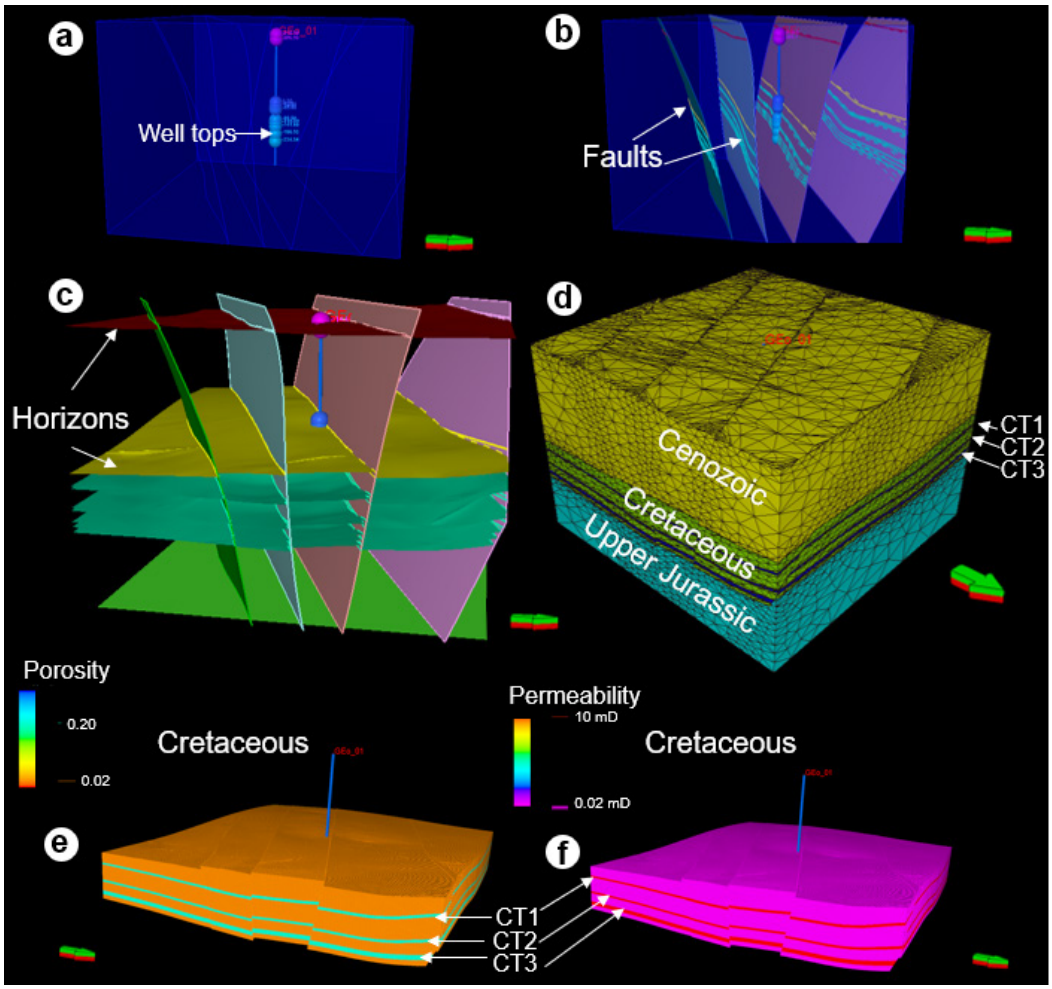


Figure 1. (a) Volume of interest (b) Faults interpreted (c) Fault and Horizons interpreted (d) Layering with the three candidate intervals for HT-ATES CT 1, CT2 and CT3. (e) Porosity model (f) Permeability model.

7.4

Characterization of Lower Cretaceous-Upper Jurassic geothermal reservoirs using chemostratigraphy and automated quantitative petrography: examples from the Geneva Basin.

Gustavo Ferreira De Oliveira[1], Antoine De Haller[1], Luca Guglielmetti[1], Yasin Makhloufi[1], Andrea Moscariello[1]

[1]*Department of Earth Sciences, University of Geneva, Rue de Maraîchairs 13, CH-1205 Geneva (andrea.moscariello@unige.ch)*

The stratigraphic, sedimentological and compositional characteristics of the Mesozoic sedimentary sequence outcropping in the Geneva Basin and neighbouring reliefs have been subject of several studies in the past (Brentini, 2018; Rusillon, 2018). On the other hand, very little knowledge exists regarding these characteristics in the subsurface. This work presents the results of a detailed investigation of the sedimentary record encountered in 3 wells drilled in the Geneva Basin in both the Canton if Geneva and surrounding France.
The deepest of the three wells, is the GEo-01 and was drilled in the context of the GEothermie 2020 Program (Moscariello, 2016) in order to assess the geothermal potential the Geneva Basin subsurface. This well crossed the Oligocene and Lower Cretaceous units, reaching total depth in the Upper Jurassic. The other two wells, Grilly and Crozet have a total length of ca 250 m and were drilled for hydrogeological prospection in neighbouring France, at the foothill of the Jura. The sedimentary sequences encountered in these 3 boreholes is composed mainly by a succession of carbonate strata presenting variable degree of clastic components, intercalated with thinner layer of marls and shales. Integrated chemostratigraphic (ICP-MS) and automated petrography (QEMSCAN) analyses on ditch cuttings samples, joined with quality-check investigation using conventional petrography, were therefore carried out to define key stratigraphic units based on geochemical and mineralogical composition.

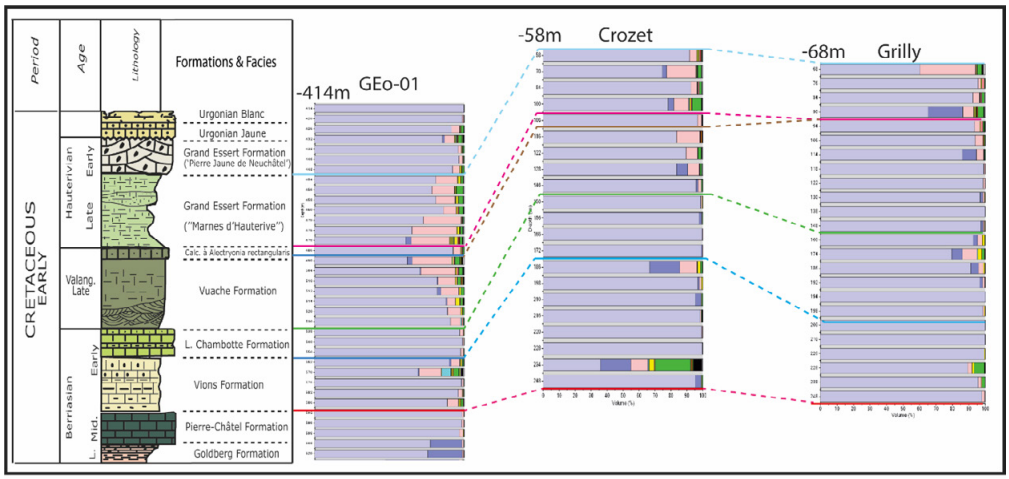


Figure 1. Stratigraphic correlation for the GEo-01, Crozet and Grilly wells. The continuity of the various formations forming the Lower Cretaceous succession has been detected based on QEMSCAN automated mineralogy.

The variations in concentration of specific groups of chemical elements (major and rare earth elements) and minerals, allowed us to identify several units consistent with the established lithostratigraphic and chronostratigraphic subdivision and key markers, corresponding also to important sequence stratigraphic surfaces, which can be used to drive inter-well correlation and reservoir properties description.
This study demonstrate the usefulness of using chemical and petrographic information to establish a first order stratigraphic subdivision which can be used for assisting reservoir characterization studies and 3D reservoir modelling providing a solid stratigraphic and reservoir subdivision framework both at reservoir and basin scale.

REFERENCES

Brentini, M. 2018: Impact d'une donnée géologique hétérogène dans la gestion des géo-ressources: Analyse intégrée et valorisation de la stratigraphie à travers le bassin genevois (Suisse, France). Terre & Environnement 140, 230 pp.

Moscariello, A. 2016: Geothermal exploration in SW Switzerland. *Proceedings* European Geothermal Congress 2016 Strasbourg, France, 19-24 Sept 2016, 10 pp.

Rusillon E. 2018: Characterisation and rock typing of deep geothermal reservoirs in the Greater Geneva Basin (Switzerland & France). Terre & Environnement 141 (2018), 252 pp.

7.5

Critically-stressed EGS reservoir stimulation in reverse faulting stress regimes using stress preconditioning

Barnaby Fryer[1], Xiaodong Ma[2], Gunter Siddiqi[3], & Lyesse Laloui[1]

[1]EPFL, Route Cantonale, 1015 Lausanne (barnaby.fryer@epfl.ch)
[2]Swiss Competence Center for Energy Research – Supply of Electricity (SCCER-SoE) & Chair for Geothermal Energy and Geofluids, ETH Zürich, Zürich
[3]Swiss Federal Office of Energy, Bern

Hydrothermal wells could greatly benefit from stimulation treatments that can be directed. This might allow them to target specific areas of a reservoir (such as known highly-permeable fracture zones), avoid faults, or prevent overlap with other wells – maximizing reservoir usage. In this work it is shown how stimulation treatments could be directed by modifying the reservoir stresses.

The proposed methodology has been investigated numerically, using a 2-D, plane strain, sequentially coupled fully implicit flow and linear elastic mechanical simulator.

The methodology is based around the idea that stresses in the subsurface can be altered through fluid production/injection activities (e.g. Segall 1989). To begin, one well is stimulated as usual - in this case in a reverse faulting stress regime. Then, the second well is drilled into the stimulated region of the first well. At this stage, both the first and second wells are produced. The advantage of this is that it alters the stresses outside of the stimulated region of these two wells. Specifically, the horizontal stress will decrease and the vertical stress will slightly increase in regions at the same depth but outside of the already stimulated area. As this is a reverse faulting stress regime, this makes shear failure less likely. Next, a third well is stimulated in this stress-altered zone. This stimulation treatment will be influenced by the altered stress field such that it is directed away from the first two wells. The stress changes caused by the preconditioning production phase are relatively small (on the order of 0.5 MPa in the region between the wells) and therefore do not affect the shear failure occurring near this third well during stimulation. However, these stress changes become significant at distances farther away from the stimulating well as the pore pressure changes at larger distances from the stimulating well are smaller. This then inhibits shear failure in the regions closest to produced area, resulting in a stimulation treatment which preferentially stimulates areas away from the first two wells. While the results presented here were for reverse faulting stress regimes, the methodology works similarly for strike-slip faulting stress regimes.

One potential disadvantage of the extra production phase is that it induces stress changes above and below the producing wells. Specifically, it induces compressive horizontal stress changes and tensile vertical stress changes. As this is a reverse faulting stress regime, these stress changes can lead to shear failure (similar to the production-induced seismicity reported by Segall 1989). However, it should be noted that the production rates used to produce these wells during the preconditioning phase are significantly less than rates which are considered economical for, for example, EGS wells (Ziagos et al., 2013). This implies that, were this shear failure to be seen during the preconditioning phase, it also would have been seen during the normal field life of the producing well of the doublet pair under normal circumstances.

REFERENCES

Ladner, K., & Häring, M. 2009: Hydraulic characterisation of the Basel 1 Enhanced Geothermal System, Geothermal Resources Council Transactions, 33, 199-204.

Miller, S. 2015: Modeling enhanced geothermal systems and the essential nature of large-scale changes in permeability at the onset of slip, Geofluids, 15, 338-349.

Segall, P. 1989: Earthquakes triggered by fluid extraction, Geology, 17, 942-946.

Ziagos, J., Phillips, B., Boyd, L., Jelacic, A., Stillman, G., & Hass, E. 2013: A technology roadmap for strategic development of enhanced geothermal systems, Proceedings: Thirty-Eighth Workshop on Geothermal Reservoir Engineering, Stanford University, Stanford.

7.6

Observation of rate and magnitude of induced seismicity under damage-controlled tensile fracturing

Gilles Waleffe[1], Dr. Omid Moradian[1]

[1]*Earth Sciences Department, ETH Zurich, Soneggstrasse 5, CH-8006 Zurich (waleffeg@ethz.ch)*

Brazilian Fracturing experiments were performed on Grimsel Granodiorite (n=20) and Central Aar Granite (n=15) to analyse the effect of fatigue and creep loading on the tensile strength and induced seismicity. To see a potential influence of the anisotropy observed in Grimsel Granodiorite, one half of the experiments were performed parallel, the other half perpendicular to foliation. Brazilian Fracturing experiments do not consider any confining and pore pressure. The fracture mechanics do also not include thermo-mechanical and hydro-mechanical effects, however, the purpose is to come up with a promising, damage-controlled loading protocol that can possibly lead to a basis for an injection protocol for further hydraulic fracturing experiments performed in-situ or at laboratory scale.

Fatigue loading protocols were determined to be progressive – where the stress is increasing progressively by each cycle applied – and cyclic, where the stress is held constant for 10 cycles, followed by an increase for the next 10 cycles etc as shown in Figure 1 below. The creep loading protocols were loaded monotonically with a lower loading rate than the standardized and reference monotonic loading (M_{ISRM}). The loading rates for the creep experiments were calculated based on the duration and maximum stress of progressive and cyclic experiments, respectively. Acoustic Emissions (AE) were measured and analysed for all experiments.

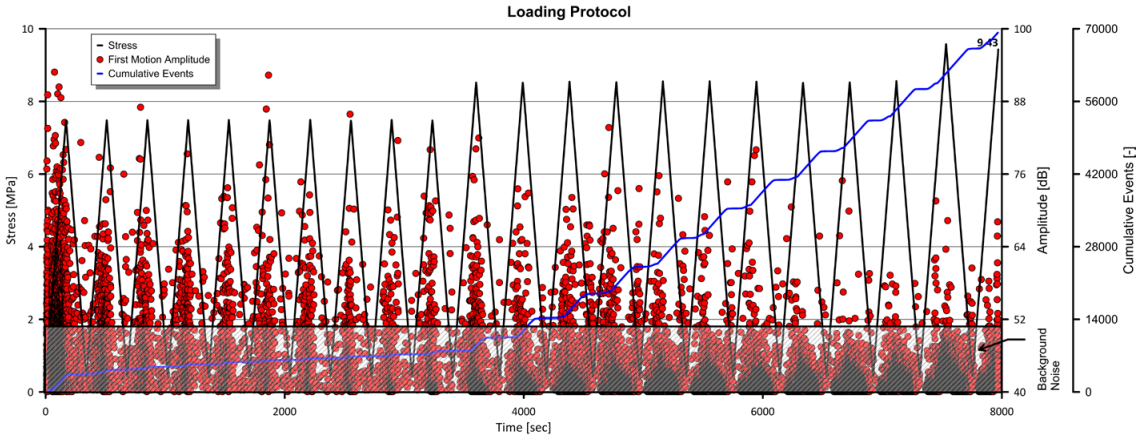


Figure 1. Example of a loading protocol for a cyclic Brazilian experiment performed on Central Aar Granite. Red dots indicate the registered acoustic emissions (i.e. seismic events), the blue line is representing the cumulative AE curve, the black line the applied stress up to failure (=tensile strength).

It was observed that the effect of anisotropy, heterogeneity and grain size seem to be more dominant on the tensile strength than the applied loading mechanisms for Grimsel Granodiorite specimens. However, the maximum amplitude of the measured AE's were reduced and the b-value increased for all loading mechanisms compared to monotonic loading. Furthermore, it was observed that the b-value for the last cycle was most of the time higher than the b-value for the whole experiment (as shown in Figure 2 below). This result seems to be surprisingly, since the failure occurs with the biggest seismic events, resulting in a low b-value for monotonic loading, while for cyclic we see higher b-values indicating lower seismicity.

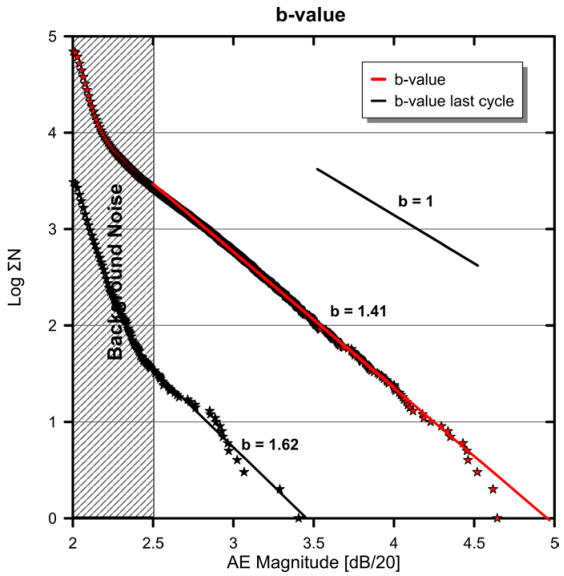


Figure 2. Obtained b-values from the magnitude-frequency curve for experiment shown in Figure 1. Red best fit= whole registered AE from whole experiment, black best fit = registered AE from last cycle only.

The results obtained from this work are promising to reduce the induced seismicity by different mechanical fracturing. In general, the most promising loading mechanisms throughout different foliation angles seem to be cyclic and creep monotonic.

7.7

Geochemical Characterization of Deep Geothermal Waters Circulation in Carbonatic Geothermal Reservoirs of the Geneva Basin (GB)

Guglielmetti Luca[1], Eichinger Florian[2]. Moscariello Andrea[1],

[1]Department of Earth Sciences, University of Geneva. Rue des maraichers 13, 1205 Geneve (Switzerland)
[2]Hydroisotop GmbH. Woelksetr. 9, D-85301 Schweitenkirchen (Germany)

This study focuses on the interpretation of geochemical data collected at springs and at two deep geothermal exploration wells located on the edges and within the Geneva Basin (GB Canton of Geneva, Switzerland). The sampling sites have been selected across one North-South trending sections following the main groundwater flow from the recharge zone to the deep geothermal reservoirs in the Mesozoic carbonatic units. These formations have been drilled by two geothermal exploration wells; the 745 m deep GEO-01 well, where water with a temperature of 34°C and an artesian flow rate of 50l/s is encountered, and at the 2530 m deep Thonex-01 well, which produces app. 0.1 l/s by artesian flow at reservoir temperature of 80°C. Major ions, trace elements, stable isotopes of Oxygen and Hydrogen, Tritium, Sulphur and Carbon isotopes as well as noble gas samples have been collected and analysed. The analyses aim at characterizing the fluid circulation in terms of recharge zone, origin of the water, mean residence times, reservoir temperature, and water-rock interactions. The interpretations show that the geothermal waters have a meteoric origin with the main recharge zone being located in the Jura Mountains towards the North. The infiltration is dominated by secondary porosity controlled by intense fracture conditions. Infiltrating water circulates in the Mesozoic Units and the groundwater flow direction is controlled by the geometry of these formations, which gently dip towards south with a 3° average dip. Fracture zones associated to sub-vertical strike- slip faults represent the main corridors where waters as well as hydrocarbons and dissolved gas rise towards the surface. Moreover, the highly porous and permeable karstified horizons at the Lower Cretaceous level and the reef complex in the Upper Jurassic represent very promising potential geothermal reservoirs across the whole Geneva Canton for heat production with temperatures ranging from about 30°C to more than 110°C.

REFERENCES

Muralt, R. (1999). Processus hydrogéologiques et hydrochimiques dans les circulations profondes des calcaires du Malm de l'arc jurassien. (Verwendet in SGPK-Publikation Nr. 39). https://doi.org/Hydrovaud, PNR61, VD_3D, Synclinal_Delemont

Nawratil de Bono, C. (2018). GEo-01 : The first GEothermie 2020 P&D well in the Canton of Geneva - Preliminary results. SCCER SoE Annual Conference 2018. SCCER - Swiss Competence Center for Energy Research Supply of Electricity.

Sanjuan, B., Gal, F., Millot, R., Dezayes, C., Jirakova, V., Frydrych, V., Hopmann, J. (2016). Final Report on chemical geothermometers and tracers.

7.8

Flow path characterization at the Grimsel Underground Rock Laboratory using solute tracer tests

Xiang-Zhao Kong[1], Anniina Kittilä[1], Mohammadreza Jalali[2], Márk Somogyvári[3], Keith F. Evans[1], Martin O. Saar[1]

[1]Geothermal Energy and Geofluids Group, Institute of Geophysics, ETH Zurich, CH-8092, Zurich, Switzerland (xkong@ethz.ch)
[2]Department of Engineering Geology and Hydrogeology, RWTH Aachen, Aachen, Germany
[3]Department of Hydrogeology, TU Berlin, Berlin, Germany

The sustainable development and utilization of geothermal energy is one of the recommended approaches to meet the increasing demand for global renewable energy. In particular, Switzerland has set an ambitious goal of increasing the supply of electricity from deep geothermal energy from 0 to 4.4 TWh by 2050. It is known that the productivity of a geothermal reservoir is strongly influenced by the characteristics of flow paths between the injection and the production wells. In this study, we report solute tracer tests that were conducted as part of a pre- and post-stimulation hydraulic characterization of the In-Situ Stimulation and Circulation (ISC) experiment at the Grimsel Underground Rock Laboratory in Switzerland. Our tracer tests aim at understanding and characterizing the changes in the hydraulic properties controlling fluid flow in the fractured crystalline rock mass induced by hydraulic stimulation.

During the ISC experiments, a total of nine solute tracer tests were conducted in the manner of the cross-well short-pulse test framework. These nine experiments yielded 5 and 18 tracer breakthrough curves (BTCs) before and after the hydraulic stimulations, respectively. Analysing the tracer BTCs and their intrinsic temporal moments, we delineate hydraulic properties of the connected flow paths in the fractured crystalline rock mass before and after the hydraulic stimulation. Our analyses focus on the tracer residence time distribution curves and the spatial distribution of hydraulic conductivities evaluated by tomographic inversion. The calculated tracer swept volumes increased considerably at all three monitoring locations, suggesting that new and/or additional flow paths were accessed by the tracers after the hydraulic stimulations. Moreover, the tomographic inversion of the hydraulic conductivity distribution indicated an increase in the geometric mean of hydraulic conductivity and a decrease in the heterogeneity of hydraulic conductivity distribution. These observations suggest that the stimulated rock volume became hydraulically more conductive, where the injected fluid travelled through fractures with higher hydraulic conductivities than before hydraulic stimulations. Our study provides a valuable framework for field-scale geothermal reservoir characterizations.

REFERENCES

Kittilä, et al. 2019: Field Comparison of DNA-Labeled Nanoparticle and Solute Tracer Transport in a Fractured Crystalline Rock, Water Resources Research, DOI: 10.1029/2019WR025021.

Kittilä, et al. 2019: Characterization of the effects of hydraulic stimulation with tracer-based temporal moment analysis and tomographic inversion, Submitted to Geothermics.

7.9

Current seismo-hydro-mechanical interpretations of the in-situ hydraulic stimulations at the Grimsel Test Site

Hannes Krietsch[1], Linus Villiger[2], Benard Brixel[1], Valentin Gischig[3], Joseph Doetsch[1], Mohammadreza Jalali[4] & Florian Amann[4]

[1]Department of Earth Sciences, ETH Zurich, Sonneggstr. 5, CH-8092 Zurich (hannes.krietsch @sccer-soe.ethz.ch)
[2]Swiss Seismological Service, ETH Zurich, Sonneggstr. 5, CH-8092 Zurich
[3]CSD Ingenieure, Hessstr. 27d CH-3097 Bern
[4]Department of Engineering Geology & Hydrogeology, RWTH Aachen, Lochnerstr. 4-20, DE-52056 Aachen

In 2017, six decameter-scale hydraulic shearing test were conducted at the Grimsel Test Site (GTS) in the framework of the In-Situ Stimulation and Circulation (ISC) experiment. In each of these experiments one cubic meter of water was injected in a 1 m long injectoin interval. The injections targeted two different types of pre-existing shear zones. One shear zone type is allocated within two meta-basic dykes, which host a highly fractured zone in-between. The other shear zone type is characterized by very few discrete fractures, that are initially poorly connected to the overall fracture network and the highly fractured zone.

To capture the seismological, hydraulic and mechanical response of the test volume, a comprehensive monitoring system was installed along ten dedicated boreholes inside the test volume and along the tunnel walls surrounding it.
The experiments indicated the high complexity of rock mass responses at this scale. These responses included poro-elastic stress transfer coupled with shearing induced stress redistributions. Fracture normal opening and shear dislocation were observed, as well as fracture initiation and competitive fracture opening. Based on the fluid pressure monitoring, it is interpreted that the fluid flows very channelized along the shear zones, but can reorient in terms of flow direction during ongoing stimulation. The pressure monitoring system also allowed to distinguish between hydraulically and mechanically induced pressure perturbations. Thus, an inner zone of diffusion-controlled hydro-mechanical rock mass responses can be distinguished from a mechanically-controlled far-field zone. The extent of these zones was confirmed by active seismic surveys conducted during stimulation.

The seismic responses vary for the two different shear zone types. It was observed that the stimulations targeting the shear zones associaded with the highly fractured zone and initially high permeable strucutres induced an increased seismic response. In contrast, stimulations of shear zones assoziated with only dicrete fractrues and initially low permeable structures further away from the highly fractured zone, were more efficient in terms of permeability enhancement, with a lower seismic response.

7.10

Imaging the long-term loss of faulted host rock and caprock integrity (FS-B experiment), Mont Terri Rock Laboratory

Christophe Nussbaum[1], Yves Guglielmi[2], Fréderic Cappa[3], Jens Birkholzer[2], Jonathan Ajo-Franklin[4], Michelle Robertson[2], Paul Cook[2], Bill Lanyon [5] & Paul Bossart[1]

[1]Swiss Geological Survey, Federal Office of Topography swisstopo, CH-2882 St-Ursanne (christophe.nussbaum@swisstopo.ch)
[2]Lawrence Berkeley National Laboratory, Energy Geoscience Division, Berkeley, CA, 94720
[3]Côte d'Azur Observatory, Géoazur, University of Côte d'Azur, CNRS, 06560 Sophia-Antipolis
[4]Department of Earth, Environmental and Planetary Sciences, Rice University, Houston, TX, 77005
[5]Fracture Systems Ltd, Tregurrian, St Ives, Cornwall

Understanding fault reactivation and post-reactivation with possible self-sealing as a result of subsurface fluid injection is crucial in investigating geological CO_2 sequestration. The potential for fault reactivation and subsequent self-sealing is also important in assessing the performance of radioactive waste repositories in shale formations. Since 2015, two semi-controlled fault reactivation experiments, named FS (2015-2018) and FS-B (2018-ongoing), have been conducted in a fault zone intersecting the Opalinus Clay at 300 m depth in the Mont Terri Rock Laboratory (Canton of Jura, Switzerland). In 2015, repeated injections in five borehole intervals set at different locations within the fault zone showed that injected fluids can only penetrate the fault planes when they are at or above the Coulomb failure pressure, highlighting complex mixed opening and slip-activation modes. Rupture modes are driven by complex fault geometry. One key parameter is the way the initial very low permeability of the fault dynamically increases at failure. We observed poro-elastic stress transfer in a large volume around the rupture patch, producing pore-pressure drops of ca. 4*10-4 MPa in the host rock 20 m away from the ruptured (activated) fault patch. Since 2015, the pressure in the ruptured patch has not recovered, remaining ca. 0.45 MPa below its initial value. This unexpected result shows a long-term modification of the hydraulic response of the fault zone that is clearly related to irreversible changes caused by the reactivation. In 2018, we initiated the FS-B experiment targeting the time-lapse three-dimensional imaging of long-term fluid flow and rupture in a 100 m-scale fault zone volume including the previous FS volume. Five inclined holes were drilled parallel to the Main Fault dip at a distance of ca. 2 to 5 m from the fault core "boundary", with three boreholes drilled in the hangingwall and two boreholes drilled in the footwall (Figure 1). An active seismic source-receiver array will be deployed in autumn 2019 in the five inclined boreholes. It will be coupled to nearby three-dimensional displacement and pore-pressure measurements distributed in the three vertical boreholes drilled across the fault zone. This system will allow us to track the variations of p- and s-wave velocities during fault leakage associated to rupture and any possible post-rupture self-sealing processes. Pre-calibrations show that the system resolution is ca. 3* 10-4 m/s for 3*10-7 Pa stress changes, thus in the range of the expected signals.

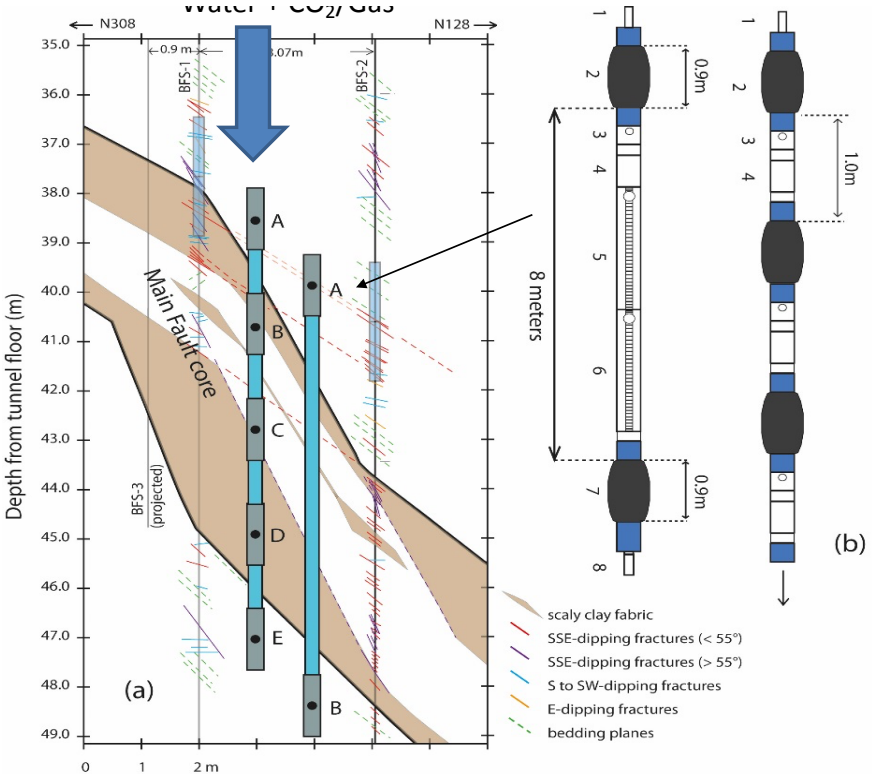


Figure 1. Design of the FS-B experiment. Conceptual vertical section of the fault zone (Main Fault) and the proposed geometry for both the injection vertical holes equipped with distributed fault 3D-displacement extensometers (SIMFIP), and the seismic tomography (five inclined holes parallel to the fault zone, not shown here). The 8 m-long interval will allow injection into the entire fault core, while conducting (i) nearfield pressure-deformation-acoustic and seismic monitoring with sensors set on the SIMFIP, and (ii) crosshole active imaging and a passive seismic monitoring from the inclined holes.

7.11

Fault Reactivation and Associated Induced Seismicity under Cyclic Loading

Omid Moradian[1]

[1]Department of Earth Sciences, ETH Zurich, Switzerland (omid.moradian@erdw.ethz.ch)

Increase of pore pressure and consequently decrease of effective normal stress can cause fault slip and induce earthquakes during fluid injection in engineering applications such as enhanced geothermal systems (EGS), wastewater disposal, and CO_2 sequestration. This happens because a large volume of the high-pressure fluid is injected in the rock mass in a continuous or monotonic manner.

Several studies have been done to investigate the effect of stress states, pore-pressure, fluid properties, injection volume, injection rate, fault geometry, and fault roughness on the sliding mechanisms and induced seismicity of the faults during fluid injection. However, an effective solution to controlling the induced seismicity, which can be applied with confidence, does not exist yet.

Recently, efforts to reduce the effects of fault induced seismicity by fluid injection have focused on developing softer stimulation techniques such as cyclic or fatigue loading. In this research, we conducted an extensive experimental investigation on sliding fault activations and assessed the effect of monotonic and cyclic loading paths on the fault slip and associated induced seismicity (acoustic emissions) in crystalline rocks.

The results showed that compared to monotonic loading, the cyclic loading could cause not only the failure of the fault under a lower strength but also with a smaller stress drop, hence it decreases the maximum seismic magnitude of the induced earthquakes. Nevertheless, cyclic loading on the faults generated a higher number of low-amplitude acoustic emissions (higher b-value) as it releases the seismic energy of the fault gradually.

7.12

Observation of Cracking in Damage Controlled Tensile Fracturing

Jerry Peprah Owusu[1], Omid Moradian[1]

[1]Department of Earth Sciences, ETH Zurich, Sonnegstrasse 5, 8092 Zurich.
(owusuj@student.ethz.ch, omid.moradian@erdw.ethz.ch)

In deep geothermal systems, the creation of large fracture networks by hydraulic fracturing (HF) is an essential task for heat absorption enhancement in low permeability rocks. This is because fluid flow should occur within many fractures that sweep a large surface area of the rock mass in order to absorb an appreciable amount of heat energy.

Over the years, the conventional injection protocol for hydraulic stimulation has been performed by the monotonic mechanism, where the pressure of the injection fluid in the well is continuously increased until the rock fractures in tension. Therefore, the working hypothesis of this research is to help develop an optimized methodology for a successful hydraulic stimulation for geothermal energy projects by investigating the effect of different loading mechanisms/protocols/paths, loading rates, anisotropy and grain size on the complexity of tensile fractures from the Brazilian experiment.

Although the hydraulic tensile fracturing mechanism is affected by confining pressure, pore pressure and thermo-hydro-mechanical loading rather than mechanical loading, the Brazilian tensile fracturing test was selected for this research since it still has close failure mechanism to the hydraulic tensile fracturing.

The laboratory experiments in this thesis were conducted on anisotropic Grimsel Granodiorite and Isotropic Central Aar Granite. Forty-five (45) samples were tested, which include fifteen (15) isotropic materials and thirty (30) anisotropic materials. Fourteen (14) of the tested anisotropic materials were investigated under Monotonic High Rate Loading for the assessment of the influence of grain size on the fracture complexity by eliminating the effect of the loading mechanism. There were five (5) loading actions under which the specimens were tested. These are the Monotonic High Rate Loading, Monotonic Medium Rate Loading, Monotonic Low Rate Loading, Progressive Loading, and Cyclic Loading.

Tested specimens were analyzed by image analysis tools to compute two fracture complexity parameters, which are the Tortuosity and the Total Fracture Length. Correlations were then made between the explored objectives and the fracture complexity parameters. In conclusion, Low rate cyclic loading in a high feldspathic Grimsel Granodiorite with foliation oriented parallel to the loading action, proved to create higher fracture complexity comparing to other loading paths.

7.13

The CS-D experiment at the Mont Terri Laboratory: site-characterization and preliminary results of long-term injection

Antonio P. Rinaldi[1], Alba Zappone[1], Melchior Grab[2], Quinn Wenning[2], Clement Roques[2], Yves Guglielmi[3], Claudio Madonna[2], Anne Obermann[1], Christophe Nussbaum[4], Stefan Wiemer[1]

[1]Swiss Seismological Service, ETHZ, Sonneggstrasse 5, CH-8092 Zürich, Switzerland (antoniopio.rinaldi@sed.ethz.ch)
[2]Swiss Competence Center for Energy Resource, ETHZ, , Sonneggstrasse 5, CH-8092 Zürich, Switzerland
[3]Energy Geosciences Division, LBNL, 1 Cyclotron Rd., 94720 Berkeley, CA, USA
[4]Federal Office of Topography, swisstopo, Route de la Gare 63, CH -2882 St-Ursanne, Switzerland

Understanding potential caprock failure through fault zone leakage is crucial for the safe, long-term containment of a CO_2 storage site. Thus, the presence of faults in caprocks will greatly affect the site characterization process in terms of the safety assessment. The CS-D experiment at the Mont Terri Lab aims to investigate caprock integrity by determining CO_2-rich water mobility in a fault zone. We monitor for geochemical and geomechanical changes induced by fluid injection for prolonged time, with the goal to better understand mechanisms of CO_2 leakage, and develop strategies to detect/monitor/predict it. The experiment offers a unique opportunity to develop improved, and more integrated monitoring technologies (Zappone et al., 2018; 2019). In particular, a multi component monitoring network of stress propagation within the fault will be integrated with the three-dimensional displacement probe (Guglielmi et al., 2013), and will be employed in parallel with other monitoring systems (micro-seismicity and active seismic monitoring, cross-hole electrical resistivity monitoring, axial deformation, geochemical fluid sampling).

Injection activities started in December 2018, with multiple step up tests at pressures up to 6 MPa, in order to define the hydraulic response of the fault. Tests were interrupted in May 2019 due to tunnel excavations for the extension of the Mont Terri Underground Rock Laboratory and the final breakthrough in proximity of the experiment site. The excavation was recorded by our monitoring system, and constitutes an extremely valuable calibration for our instrumentation. A prolonged injection of CO_2 saturated brine at constant head pressure started in June 2019 and will continue for the next months. At the conference, we will present the analysis of the data collected during the site characterization (hydraulic, geophysics, and core analysis) as well as the preliminary results the continuous injection.

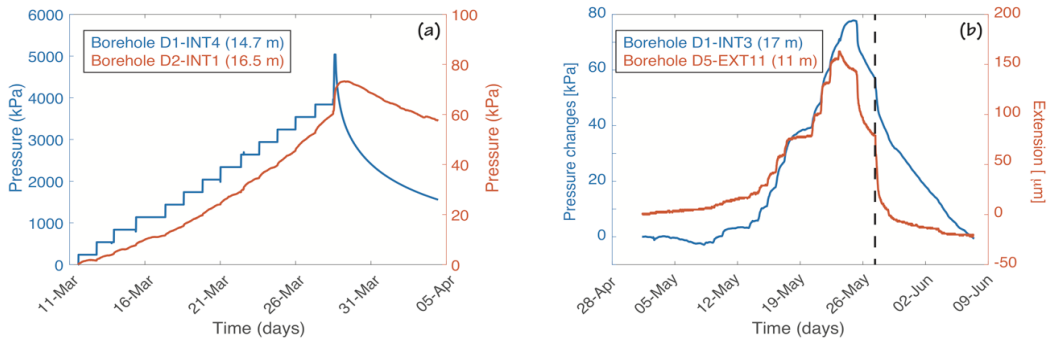


Figure 1. (a) A Prolonged Step Test (constant head with step of 1 day). The blue line is pressure changes at injection point, while the red curve is the response at the monitoring point. (b) Recording of pressure changes (blue) and deformation (red) in two boreholes located next to the excavation front. The dashed line represents the time of breaktrough (May 27th)

REFERENCES

Guglielmi Y., Cappa F., Lançon H., Janowczyk J.B., Rutqvist J., Tsang C.F., Wang J.S.Y. 2013. ISRM Suggested Method for Step-Rate Injection Method for Fracture In-Situ Properties (SIMFIP): Using a 3-Component Borehole Deformation Sensor. Rock Mech. Rock Eng. 47(1). DOI: 10.1007/s00603-013-0517-1

Zappone, A., Rinaldi A.P., Grab M., Obermann A., Madonna C., Nussbaum C., Wiemer S. 2018. CO_2 sequestration: studying caprock and fault sealing integrity, the CS-D experiment in Mont Terri, In: Proceedings of the EAGE Fifth CO_2 Geological Storage Workshop, Utrecht, The Netherlands. doi: 10.3997/2214-4609.201803002

Zappone A., Grab M., Rinaldi A.P., Madonna C., Obermann A., Guglielmi Y., Nussbaum C., Wiemer S. 2019. CSD-Experiment: Caprock and Fault Sealing Integrity by a 1:1 scale in-situ experiment Test plan. Mont Terri Technical Note TN 2019-36

7.14

Preliminary Geomechanical Modelling of the Hengill Geothermal Field

Vanille A. Ritz[1], Antonio P. Rinaldi[1], Raymi Castilla[2], Elisa Colas[2], Peter M. Meier[2], Stefan Wiemer[1] and the COSEISMIQ Team

[1]Swiss Seismological Service at ETH, Sonneggstrasse 5, CH-8092 Zürich, Switzerland (vanille.ritz@sed.ethz.ch)
[2]Geo-Energie Suisse AG, Reitergasse 11, CH-8004 Zürich, Switzerland

Monitoring micro-seismicity during operations of a geothermal field is crucial for the understanding of seismic hazard and the reservoir evolution. Induced earthquakes in the context of a geothermal project are on the one hand an important tool to enhance the permeability and thus productivity of reservoirs and to image structure and processes. On the other hand, felt and/or damaging earthquakes are a major threat to societal acceptance and regulatory license to operate. With the adaptive data driven tool RISC (Real-Time Induced Seismicity Controller), we aim at managing and mitigating the risk posed by induced earthquakes during stimulation and operations, while at the same time insuring and optimising the productivity. RISC is developed as part of the EC Geothermica project COSEISMIQ (www.geothermica.eu/projects/coseismiq/). The demonstration site lies in the Hengill volcanic region located in the South-West of Island, which hosts two power plants (Hellisheiði and Nesjavellir) with a total production capacity of 423 MWe and 433MWth. The production of energy and heat in accompanied by reinjection of the spent geothermal water in dedicated areas. These reinjection area have been showing very different seismic responses to drilling and injection operation. We invetigate these different behaviours by performing preliminary numerical modelling for two of the reinjection regions, using the hybrid simulatorTOUGH2-Seed. Future analysis will aim, on the one hand, at understanding the physical processes happening at the different sites, and on the other hand, at evaluating the performance of such code for future application in RISC..

REFERENCES

Gunnarsson, G., & Aradóttir, E. S. (2015). The deep roots of geothermal systems in volcanic areas: boundary conditions and heat sources in reservoir modeling. Transport in Porous Media.

Rinaldi, Antonio Pio & Nespoli, Massimo. (2017). TOUGH2-Seed: a coupled fluid flow and mechanical-Stochastic approach to model injection-induced seismicity. Computers & Geosciences.

Ritz, V. A., Rinaldi, A. P., Castilla, R., Colas, E., Meier, P. M. & Wiemer, S. (2020). Preliminary Modelling Activities for an Adaptive Traffic Light System for the Hengill Geothermal Field. In Proceedings world geothermal congress.

7.15

Advanced hybrid thermo-mechanical drilling technology to facilitate deep geo-resource exploitation

Edoardo Rossi[1,2], Shahin Jamali[3], Martin O. Saar[1], and Philipp Rudolf von Rohr[1]

[1]Geothermal Energy and Geofluids group, ETH Zürich, Sonneggstr. 5, 8092 Zürich, Switzerland (rossie@ethz.ch)
[2]Institute of Process Engineering, ETH Zürich, Sonneggstr. 3, 8092 Zürich, Switzerland
[3]International Geothermal Center GZB, Lennershofstr. 140, 44801 Bochum, Germany

To meet the increasing worldwide energy demand in the next decades, the access to geothermal heat from deep reservoirs can play a fundamental role in the global energy supply. Deep wells to extract geothermal energy in more challenging and deeper environments, require major costs, mainly related to the involved drilling operations. Indeed, drilling costs are found to increase exponentially with depth and, furthermore, they occur in an early, considerably high-risk phase of the project (Tester 2006). Drilling of deep wells into hard rocks represents a major challenge for conventional rotary drilling systems, featuring high rates of drill bit wear with consequent bit replacement and high non-productive time (NPT), low rates of penetration (ROP) and poor process efficiency (Fay 1993).

Therefore, with the aim of improving the overall economics to access deep resources in hard rocks, advanced drilling technologies, based on alternative rock-breaking mechanisms are investigated worldwide. We propose to use a combined thermo-mechanical drilling (CTMD) technology to intensify the drilling process in deep, hard rocks. This method is based on thermally-assisting conventional drilling using a flame-jet (Rossi 2018), and is expected to facilitate drilling in hard rocks with a consequent reduction of the overall costs. In order to prove the feasibility and demonstrate the drilling performance of this technology, we field-test the method under relevant process conditions. We provide evidence that combining a thermal assistance to conventional drilling can greatly improve drilling performance parameters in hard granite rocks, commonly found formation in deep geothermal drilling projects.

REFERENCES

Tester, J.W., Anderson, B., Batchelor, A., Blackwell, D., DiPippo, R., Drake, E., Garnish, J., Livesay, B., Moore, M.C., & Nichols, K. 2006: The future of geothermal energy, Technical Report: Idaho National Laboratory.

Fay, H. 1993: Practical evaluation of rock-bit wear during drilling, SPE Drilling & Completion SPE-21930-PA 8(2), 99-104.

Rossi, E., Kant, M.A., Madonna, C., Saar, M.O., & Rudolf von Rohr, Ph. 2018: The effects of high heating rate and high temperature on the rock strength: Feasibility study of a thermally assisted drilling method, Rock Mechanics and Rock Engineering 51(9), 2957-2964.

7.16

Favourability maps for deep geothermal in Switzerland

Benoît Valley[1] & Stephen A, Miller[1]

[1]Center for Hydrogeology and Geothermics, University of Neuchâtel, Emile Argand 11, CH-2000 Neuchâtel (benoit.valley@unine.ch)

In support to the Swiss energy strategy, which aims to produce 5% of the Swiss electricity demand with deep geothermal energy by 2050, the Swiss geological survey (swisstopo) is compiling subsurface information to help geothermal prospection and exploration. Access to this database provides opportunities for reviewing the geothermal potential of Switzerland using a quantitative play- fairway approach.

In this contribution, we first review the available data sets and propose a conceptual classification of geological and structural settings favourable for deep geothermal projects. The data and information we used include the following elements:

- Hydrostratigraphy (Chevalier et al. 2010)
- Mechanical stratigraphy (Hergert et al., 2015)
- Geomol horizon model (swisstopo)
- Geomol fault model (swisstopo)
- Geomol temperature model (swisstopo)
- Heat flow map (swisstopo)
- Spring and thermal spring locations (Hydr. Atlas of CH, Sonney and Vuataz; 2008)
- Evaluation of regional flow pattern
- Stress field estimation with a Swiss-scale finite element stress simulation
- Earthquake catalogue of Switzerland (download from SED website)

We defined 11 favourability criteria computed from one or a combination of the datasets listed above. For each criteria, we computed a favourability index ranging from 0 (=unfavourable) to 1 (= favourable). We performed our analyses on a 1km x 1km grid covering the extent of the geomol model. In addition, we focus on two specific temperature levels: 80°C and 120°C, being the typical minimum temperature level for direct use and electricity production, respectively. The favourability criteria include elements related to:

- thermal regime (heat flow and temperature);
- lithological controls (aquifer vs. aquiclude formations);
- rock mass damage (seismic events density, distance to faults, von Mises stress);
- in-situ stress conditions computed using a swiss-scale finite element stress model (slip tendency, dilation tendency) and;
- indications of deep-seated flow (flow pattern, regional springs, thermal springs).

We joined the 11 criteria in a combined favourability index, and Figure 1 shows an example of a favourability map for 120°C target temperature. Sharp contrasts in favourability are highlighted on the Swiss plateau and these contrasts can guide exploration. However, this has to be considered as a preliminary approach and also at a scale that is not appropriate for local scale exploration planning. Future approaches will include more detailed analyses of the elements leading to the combined favourability map. Another important element will be to include data from exploration projects in order to base the weighting scheme on a more robust method. The methodology and results presented here are bound to evolve when more data becomes available.

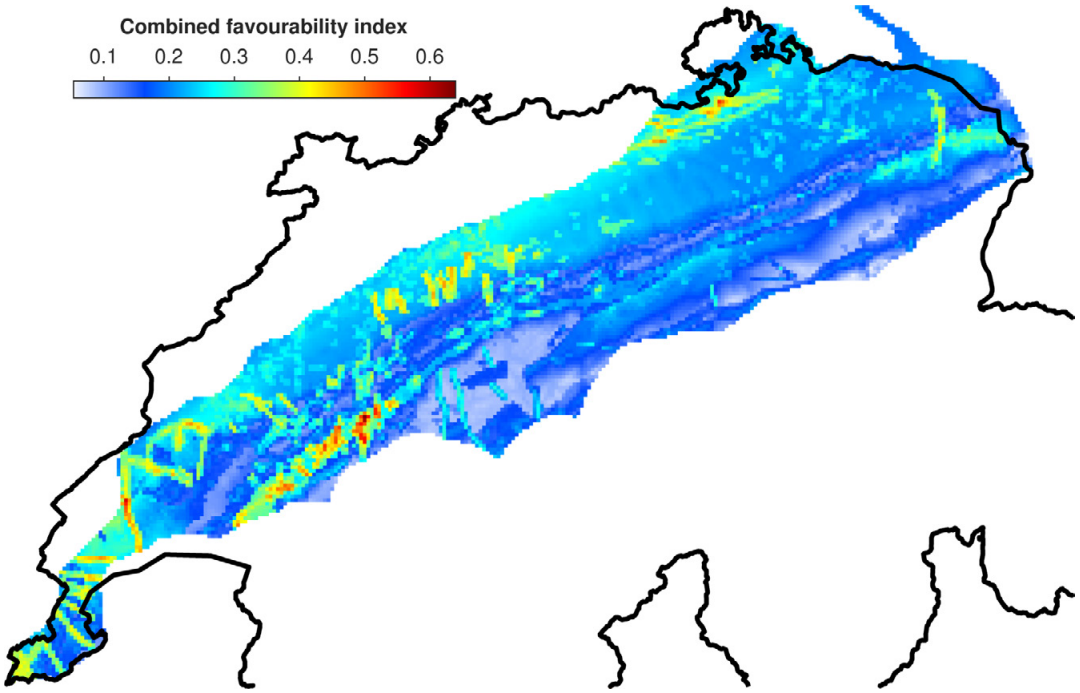


Figure 1. Combined favourability index for deep geothermal project with 120°C target temperature.

REFERENCES

Chevalier G, Diamond LW, Leu W (2010) Potential for deep geological sequestration of CO_2 in Switzerland: a first appraisal. Swiss J Geosci 103:427–455. doi: 10.1007/s00015-010-0030-4

Hergert T, Heidbach O, Reiter K, et al (2015) Stress field sensitivity analysis in a sedimentary sequence of the Alpine foreland, northern Switzerland. Solid Earth 6:533–552. doi: 10.5194/se-6-533-2015

Sonney R, Vuataz F-D (2008) Properties of geothermal fluids in Switzerland: a new interactive database. Geothermics 37:496–509

7.17

Geochemical evidence for large-scale and long-term topography-driven groundwater flow in orogenic crystalline basements

Christoph Wanner[1], H. Niklaus Waber[1], Kurt Bucher[2]

[1]Rock-Water Interaction Group, Institute of Geological Sciences, University of Bern, Baltzerstrasse 3, CH-3012 Bern, Switzerland (wanner@geo.unibe.ch)
[2]Mineralogy and Petrology, University of Freiburg, Albertstr. 23b, D-79104 Freiburg, Germany

Detailed knowledge about the circulation of meteoric water in amagmatic, orogenic belts is fundamental for assessing the potential of such settings for geothermal power production. To get more general insight into these large-scale hydrological processes, we have conducted large-scale (20 x 10 x 9 km) thermal-hydraulic-chemical (THC) simulations of meteoric water circulation in the orogenic, crystalline basement of the Aar Massif in the Central Alps, Switzerland. Model results were compared to numerous geochemical and isotopic analyses of groundwater discharging into the longest and deepest tunnel of the world, the Gotthard railbase tunnel located within the model domain. Explicitly considering the surface topography and stable water isotopologues in our model was sufficient to reproduce all key characteristics of the tunnel inflows (e.g. salinity and temperature distribution, tunnel discharge rates, $\delta^{18}O$ values, up- and downward directed flow zones inferred from geochemical constraints). This quantitatively confirms that surface topography operates as the governing control on fluid flow in orogenic crystalline basements with meteoric water infiltration occurring at high altitude and resulting upward directed flow zones (i.e. exfiltration) along major valleys. Owing to the low flow rates (<2 m/year), computed residence times of the longest flow paths were above 100 k years, confirming that groundwater and/or porewater in orogenic crystalline basements may act as an archive for palaeohydrologic variations. Moreover, simulation results show that down to the lower model boundary at 9 km depth, penetration of meteoric water is not limited by the decrease in permeability with depth that is typically observed in granitic rocks. This suggests that advective fluid transport in orogenic crystalline basement likely reaches the brittle-ductile transition zone. Without the occurrence of major fault zones, however, the permeability and hence the flow rates are too low for the formation of major thermal anomalies despite that meteoric water attains temperature well above 150 °C during such deep circulation. Nevertheless, based on the upward directed flow zones identified along major valleys our simulations suggest that positive temperature anomalies preferentially form when steeply-dipping, major faults zones with elevated permeability intersect with valley floors. Since such conditions are frequently found in the Alps as manifested by the occurrence of thermal springs, we conclude that orogenic geothermal systems are promising plays for geothermal power production.

7.18

The Effects of Normal Stress on the Transition Between Stable Sliding and Stick-slip in Crystalline Rock Faults

Farid Zabihian[1], Omid Moradian[1]

[1]*Engineering Geology Group, Department of Earth Sciences, ETH Zurich, Sonneggstrasse 5, 8092 Zürich, Switzerland (fzabihian@ethz.ch)*

Hydraulic fracturing and hydraulic shearing stimulations in the crystalline basement rocks are used to increase the permeability of the rock mass in the enhanced geothermal systems (EGS). While the fluid is injected, it increases the pore pressure and changes the stress field around the pre-existing faults that might have been already under a critical stress state and very prone to slip. This pore pressure increase leads to a decrease in the effective normal stress which eventually causes fault activation even in farther distances from the injection borehole.

It has been widely accepted that faults fail in a spectrum of slip behavior from aseismic to seismic slip. However, among different frictional mechanisms involved in fault reactivation, stable sliding and stick-slip are the two common mechanisms that have been investigated the most. The stable sliding process is the steady slip of the fault surfaces under constant stress states with no measurable radiating seismic energy. If for any reasons such as fluid injection the effective normal stress on a fault changes, a transition from stable sliding to stick-slip may happen in the fault behavior leading to a large stress drop and a seismic slip. This transition in the frictional mechanism has been considered as the failure mechanism of many injection-triggered earthquakes.

To investigate the effects of normal stress on rock faults and the friction sliding regimes, constant normal load direct shear experiments were conducted on fault surfaces in granite with variations in the effective normal stress. Shear displacement, dilatancy, and acoustic emission (AE) signals were measured to monitor the behavior of the tested faults.

The results showed that once the normal stress was increased, the AE events started increasing gradually with higher seismic magnitudes. The shear stress also increases and the fault behavior changes from stable sliding to stick-slip. In the decreasing normal stress conditions, a noteworthy decrease happens in shear stress and also in rate and magnitude of the AE signals indicating stable sliding behavior. Regarding the friction coefficient, once the normal stress is increased, a significant drop is observed in the friction coefficient. However, in the reduction period of normal stress, the coefficient of friction is increased with smaller amounts.

In general, the results show that changing the normal stress, whether increase or decrease, has a substantial effect on the stable or unstable slip behavior of the faults and the associated induced seismicity.

P 7.1

Investigating mineral reactions during high-temperature aquifer thermal energy storage (HT-ATES)

Daniela B. van den Heuvel, Peter Alt-Epping, Christoph Wanner, Urs Mäder, Larryn W. Diamond

Institute of Geological Sciences, University of Bern, Baltzerstrasse 1+3, CH-3012 Bern (daniela.vandenheuvel@geo.unibe.ch)

As part of the Swiss Energy Strategy 2050, Switzerland aims to increase the use of surplus heat from industry (e.g. municipal waste incinerators) for district heating. While heat generation from these industrial sources is more or less constant, the heating demand is characterised by seasonal fluctuations. In order to overcome this mismatch of demand and supply, excess thermal energy can be stored in sandstone- and carbonate-aquifers during summer and recovered and fed into the district heating network during winter. In order to increase the potential of aquifer thermal energy storage (ATES), new pilot projects planned within the framework of the GEOTHERMICA-Heatstore project aim for higher injection temperatures (60 to 110 °C). As the reservoir fluids are in equilibrium with calcite and/or dolomite, heating them up will result in carbonate mineral precipitation, potentially clogging surface installations and reservoir porosity.

In order to quantitatively investigate the mineral reactions expected during ATES, we are performing laboratory experiments on drill core samples from the target formations under the conditions planned for the HT-ATES system. By measuring changes in the fluid composition as a function of time, we can infer the stoichiometry and kinetics of mineral dissolution and precipitation reactions. In addition, we are investigating different conditions (variations in temperature and fluid composition) in order to generate data transferrable to other reservoir formations. We are also investigating the effectiveness of potential mitigation strategies such as conditioning of fluids by CO_2 addition or the usage of carbonate inhibitors.
All of our experimental data is fed into 3D THC models representing the two pilot sites planned in Switzerland (in Geneva and Bern). The models will be used to guide development of the sites as well as help to predict the long-term behaviour of the reservoir formation. In addition, the models can be used as a planning tool to develop more HT-ATES systems inside and outside of Switzerland in the future.

P 7.2

High-resolution gravity data to characterize density variations and reduce uncertainty in geothermal reservoirs of the Geneva basin (GB)

Guglielmetti L.[1], Perozzi, L.[1]., Dupuy D.[3], Martin F. [2], Métraux V.[3], Meyer, M.[2], Mijic G.[1], Moscariello A.[1], Nawratil De Bono C.[2], Radogna P.V.[2]

[1]Department of Earth Sciences, University of Geneva. Rue des maraichers 13, 1205 Geneve (Switzerland)
[2]Services Industriels de Genève. Chemin du Château-Bloch 2, 1219 Le Lignon (Switzerland)
[3]GEO2X SA. Rue de Chamblon 34, 1400 Yverdon-les-Bains (Switzerland)

This paper focuses on the acquisition and processing of gravity data collected in the Canton of Geneva in the framework of the InnoSuisse funded project GECOS (Geothermal Energy Chance of Success). The goals of GECOS is to reduce the costs and the exploration risk for geothermal exploration by integrating high resolution data acquisitions such as gravity, S-waves reflection seismic and 3D DAS VSP (Distributed Acoustic Sensing Vertical Seismic Profiling). The main geological challenges in geothermal exploration in the Geneva area are the characterization of the lithological heterogeneities and the fault zones affecting potential geothermal targets in the Quaternary sediments, Oligocene Molasse sequence and the Mesozoic Units. The study area covers the central part of the Canton of Geneva and overlaps with the location of two geothermal exploration wells drilled by SIG in the framework of the Geothermie 2020 program. A total of 1714 new stations were collected in 71 days of field work thanks to the collaboration between the University of Geneva and GEO2X SA. The goal of the survey has been to constrain the lateral density variations associated to lithological anisotropies in the Quaternary, Oligocene Molasse and in the Mesozoic carbonate sequence. The results of the survey showed that the new stations produced a dramatic increase in resolution compared to the gravity data available at the regional scale. In particular Quaternary deposits are much better constrained than before, which is a crucial step forward as these sediments are known to be lithologically and geometrically heterogeneous and locally can host hydrocarbon gas pockets, which can represent an element of risk for drilling operations. 3D inversion processing allowed producing a realistic 3D density model down to about 1000m in depth, where the main present-day geothermal targets are located, proving that gravity can be a powerful tool for prospection and possibly for time-lapse monitoring of production.

REFERENCES

Abdelfettah, Y., Schill, E., & Kuhn, P. (2014). Characterization of geothermally relevant structures at the top of crystalline basement in Switzerland by filters and gravity forward modelling. Geophysical Journal International, 199(1), 226–241.

Klingele, E. (2006). Systematic analysis of the Bouguer anomalies of Switzerland. Jahresberichte 2006, Schweizerische Geophysikalische Kommission SGPK, 13.

Mauri, G., Marguet, L., Jansen, G., Marti, U., Baumberger, R., Allenbach, R., Miller, S. A. (2017). Combined use of land gravity data and 3D geological model to imagine deep geological basin: the case of la Broye, Switzerlan. Proceedings of 46th IASTEM International Conference, (February). Seoul.

P 7.3

Model-based characterization of subsurface heat transport processes in Canton Aargau

Jan Niederau[1], Anozie Ebigbo[1], Martin O. Saar[1]

[1]*Geothermal Energy and Geofluids Group, Department of Earth Sciences, ETH Zürich, Switzerland, Sonneggstrasse 5, CH-8092 Zürich*
(jan.niederau@erdw.ethz.ch)

In a referendum in May 2017, Switzerland decided to phase out nuclear power in favor of further developing renewable energy sources. This is part of the Swiss Energy Strategy 2050 which also states that around 4'400 GWh per year of electricity should be provided by deep geothermal installations. To help facilitate potential future deep geothermal projects, this project aims at characterizing, for instance, the heat transport in potential geothermal reservoir systems by numerical modeling and uncertainty evaluation. For this, we present an iterative workflow to connect geological and heat transport modeling which also considers uncertainties in input data and their effect on simulation results.

This workflow is applied to a pilot study in the Canton of Aargau. There, a known surface heat-flow anomaly exists with measured specific heat-flow values of up to 140 mW m^{-2} (Medici and Rybach, 1995), thus an area of interest for deep geothermal energy exploration. We want to characterize the heat-flow distribution in the vicinity of the anomaly in more detail to facilitate future assessment of the geothermal potential of this region. To achieve a complete characterization of the heat-flow values as well as their spatial uncertainty, we develop a workflow comprising: (i) assimilation and homogenization of different types of geologic data, (ii) development of a geological model with focus on important heat transport parameters, and (iii) numerical simulations of the dominant heat transport processes. For step (i), we closely cooperate with colleagues at the Georessources Switzerland Group (ETH Zürich), who re-compile available and new data, relevant for heat-transport characterization. By integrating new data, they aim to update published maps of the shallow heat flow in Switzerland (Medici & Rybach, 1995).

Due to its nature as a pilot study, the developed workflow needs to be integrative and adaptable. This means that data generated during the course of the project can easily be integrated in the modeling and simulation process, and that the generated workflow should easily be adaptable to other regions for potential future studies.

One further goal of this project is that the generated models and simulations provide insights into the nature of the heat-flow anomaly in Northern Switzerland and to test the hypothesis that upward migration of deep geothermal fluids along structural pathways is the origin of this particular heat-flow anomaly. For instance, the localized increase in heat flow, which is also shown in earlier surface heat-flow data (Medici and Rybach, 1995) may be caused by advective heat transport along Paleozoic faults in the crystalline basement. These are most likely normal faults bounding the so-called Permo-Carboniferous trough(s) of which all besides the major, northernmost one (see Fig. 1), are merely presumed to exist (Naef and Madritsch, 2014).

By inferring the main parameters for controling the heat-flow anomaly in Northern Switzerland, e.g. fault permeability, a model can focus on assessing these parameters and their (spatial) uncertainty. This is achieved by combining (geometrical) uncertainty of geological 3D models with (parametric) uncertainty of numerical heat-transport models in a Bayesian framework. Results can be presented as maps, for instance, comprising average heat-flow values, as well as their (spatial) uncertainty.

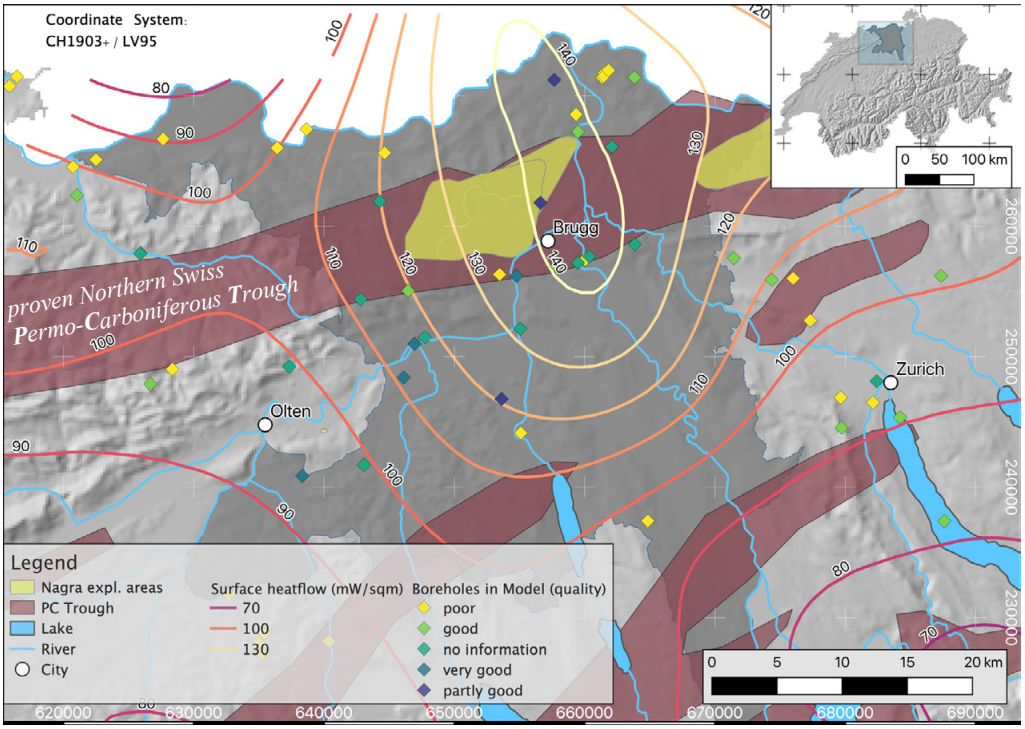


Figure 1. Thematic map of the project area in the Canton Aargau. Relevant boreholes in the area are colored by their data quality, based on the classification of Schärli and Kohl (2002). Permo-Carboniferous troughs are outlined based on Leu (2008). The heat-flow contours are based on Medici and Rybach (1995).

REFERENCES

Leu, W.: Permokarbon-Kartenskizze (Rohstoffe). Kompilation eines GIS-Datensatzes auf der Basis von bestehenden Unterlagen (Bereich Schweizer Mittelland). Nagra Arbeitsber. NAB 08-49, (2008).

Medici, F., and Rybach, L.: Geothermal map of Switzerland 1995:(heat flow density) (No. 30). Commission Suisse de géophysique, (1995).

Naef, H., and Madritsch, H.: Tektonische Karte des Nordschweizer Permokarbontrogs: Aktualisierung basierend auf 2D-Seismik und Schweredaten. Nagra Arbeitsbericht NAB 14-017, (2014).

Schärli, U. and Kohl, T.: Archivierung und Kompilation geothermischer Daten der Schweiz und angrenzender Gebiete. ISSN 0253-1186, Swiss Geophysical Commission (Beiträge zur Geologie der Schweiz: Geophysik, Nr. 36), (2002).

P 7.4

Regional scale models of fluid flow in the orogenic hydrothermal system at Grimsel Pass, Switzerland

Peter Alt-Epping, Larryn W. Diamond & Christoph Wanner

Institute of Geological Sciences, University of Bern, Baltzerstrasse 3, CH-3012 Bern (alt-epping@geo.unibe.ch)

Thermal waters at temperatures ranging between 17 - 28 °C discharge at a rate of ≤ 10 L/min into a tunnel underneath Grimsel Pass (2164 m) in the Central Alps. Fluid discharge occurs at the intersection with a brecciated fault zone (Grimsel Breccia Fault (GBF)), a late Neogene exhumed strike-slip fault (Belgrano et al, 2016). The chemical composition of the water sampled in the tunnel shows that the water is a mixture of old geothermal water and younger cold water. Both components have meteoric isotope signatures, but the thermal water is derived from a higher altitude. Residence times of the old and young waters are ≤30 ky and ~7 years, respectively (Waber et al., 2017).

The breccia in the GBF formed about 3 Ma years ago. It shows hydrothermal alteration by heated meteoric water at about 165 °C (Hofmann et al., 2004). However, results from Na-K geothermometry on present-day fluid samples indicate the maximum temperature at depth could be as high as 250 °C. Given the local geothermal gradient this corresponds to a circulation depth of meteoric water to at least 9 km (Diamond et al., 2018).

The breccia in the GBF has a sub-vertical, pipe-like structure in 3D, and it constitutes a permeable linkage zone between parallel segments of the main shear-zone. Another such linkage zone exists in the Sidelhorn area to the west (Belgrano et al., 2016). Thus, it can be expected that these permeable linkage zones are common structural features along the fault. In this study we use numerical modelling to better understand the regional flow system leading to discharge of thermal water at Grimsel Pass. Questions we aim to answer include the following:

1) What is the role of the GBF in generating upflow under Grimsel Pass?
2) What causes infiltration of meteoric water to a depth of at least 9 km?
3) What is the permeability (k) of the fault and its permeability distribution that reproduces flow rates and temperatures observed at the thermal springs?
4) What conditions induce mixing of the ascending hydrothermal fluid with shallow groundwater at mixing ratios observed at the springs?

To answer these questions a thermal-hydraulic model was constructed, using the high performance reactive transport code PFLOTRAN (www.pflotran.org). The model incorporates the topography of the region as the top boundary and extends to a depth of 12.5 km. The upflow zone at Grimsel Pass is incorporated as a vertical permeable conduit (k = 1e-13 m^2) within a low permeability granitic rock (k = 3e-20 m^2).

Simulations confirm that the GBF, if represented as an unconfined permeable vertical plane extending into the high mountains towards the west and to depths of 12.5 km, can sustain hydrothermal upflow at Grimsel Pass. The driving force of flow is the increase in recharge elevation towards the west. The infiltration of meteoric recharge becomes progressively deeper towards the west and can easily exceed the 9 km circulation depth consistent with geochemical evidence (Fig. 1A). The region around Lake Oberaar constitues a broad discharge zone of groundwater from shallower depths (Fig. 1) which indicates a (relatively minor) contribution of groundwater to the source of the river Aare. Local hill-and-valley topography induces shallow groundwater flow which at Grimsel Pass leads to mixing of the ascending thermal water with cold meteoric water recharging in the Sidelhorn area. This type of mixing is consistent with geochemical evidence from the thermal springs.

Models calibrated to match discharge rates and temperatures at the thermal springs suggest permeabilities of the GBF between 1e-15 m^2 and 1e-14 m^2. At permeabilities exceeding 5e-15 m^2 (fault-zone width of 100 m), the flow system in the fault becomes unstable and convection cells begin to form which induce transient flow and transient temperature conditions at the discharge site.

Although meteoric water can infiltrate the fault to depths > 9 km without permeability forcing (e.g. a homogeneous permeability distribution), results indicate that significant mixing of fluids from different circulation depths occurs in the upflow zone (Fig. 1A). This is inconsistent with obervations which suggest a distinct geochemical signature of the spring water acquired at a depth > 9 km. To preserve this signature, mixing during upflow has to be minimal. We propose a permeable pipe-like breccia zone, analogous the upflow conduit at Grimsel Pass, situated at higher elevation in the west and acting as the preferential path of meteoric recharge into the deep fault zone (Fig. 1B). Such focussed recharge would lead to focussed inflow into the deep section (> 9 km) of the upflow zone.

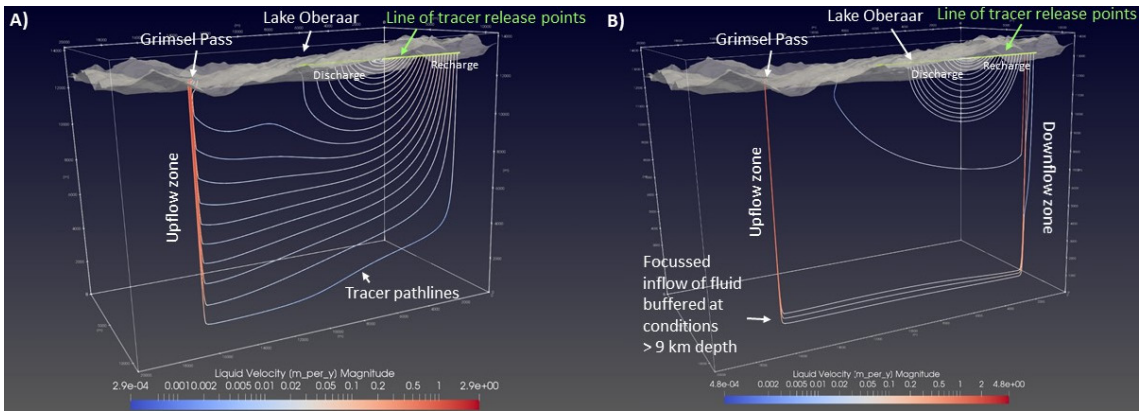


Figure 1. Flow pattern as tracer pathlines in the fault plane assuming a homogeneous permeability of 1e-15 m^2, (A) without and (B) with recharge through a permeable breccia pipe. Only in scenario B can the ascending fluid preserve the chemical signature obained at > 9 km depth.

REFERENCES

Belgrano, T.M., Herwegh, M. & Berger, A., 2016: Inherited structural controls on fault geometry, architecture and hydrothermal activity, an example from Grimsel Pass, Switzerland, Swiss J. Geosci., 109, 345-364

Diamond, L.W., Wanner, C. & Alt-Epping, P. 2018: Penetration depth of meteoric water in orogenic geothermal systems. Geology, 46, 1063-1066.

Hofmann, B.A., Helfer, M., Diamond, L.W., Villa, I., Frei, R., & Eikenberg, J., 2004: Topography-driven hydrothermal breccia mineralozation of Pliocene age a Grimsel Pass, Aar Massif, Central Swiss Alps: Schweizerische Mineralogische und Petrographishe Mitteilungen, v. 84, No 3, p. 271-302

Waber, H.N., Schneeberger, R., Mäder, U.K., Wanner, C., 2017, Constraints on evolution and residence time of geothermal water in granitic rock at Grimsel (Switzerland), 15th Water-Rock Interaction Symposium, WRI-15, Procedia Earth and Planetary Science 17, 774-777

P 7.5

Assessing fault criticality using seismic monitoring and fluid pressure analysis

Léa Perrochet[1], Giona Preisig[1], Benoît Valley[1]

[1]*Centre for Hydrogeology and Geothermics (CHYN), University of Neuchâtel, Rue Emile-Argand 11, CH-2000 Neuchâtel (lea.perrochet@unine.ch)*

Better understanding fault criticality, the proximity of a fault to shear failure, is of primary interest when planning underground projects. Stress perturbations in the surroundings of a critically stressed fault, resulting from human activities, can affect the fault's stability – and eventually lead to a forced interruption of projects due to seismic risk.
Changes in the stress state also occur naturally. It has been observed (Miller 2008) that in karstic regions, an increase in groundwater pressure following significant recharge (precipitations and/or seasonal snowmelt) can result in a fault re-activation, inducing microseismicity.

The aim of this study is to combine the natural microseismicity and groundwater level fluctuations observations to estimate the fault criticality. The research is carried out on two major strike-slip faults on the northern shore of Lake Neuchâtel (Fig.1) – La Lance Fault and La Ferrière Fault – most likely critically stressed according to their position in the global stress-regime. Data acquisition mainly consists in hydrogeologic and seismic monitoring. The objectives are to have continuous discharge rates of the major karstic springs and to produce a seismic catalog for the area of interest. Combining both data sets will allow to determine relations between increasing spring discharge rates and low magnitude earthquakes and eventually to acquire a quantitative knowledge on what pressure change is affecting the fault's stability. This knowledge will be used to develop a straighforward methodology to assess fault criticality. In addition, the study of a possible time lag between aquifer response and fault activation, as well as back-analysis of seismic events can provide, respectively, important information about the deep-seated fluid circulation and the local stress-regime.

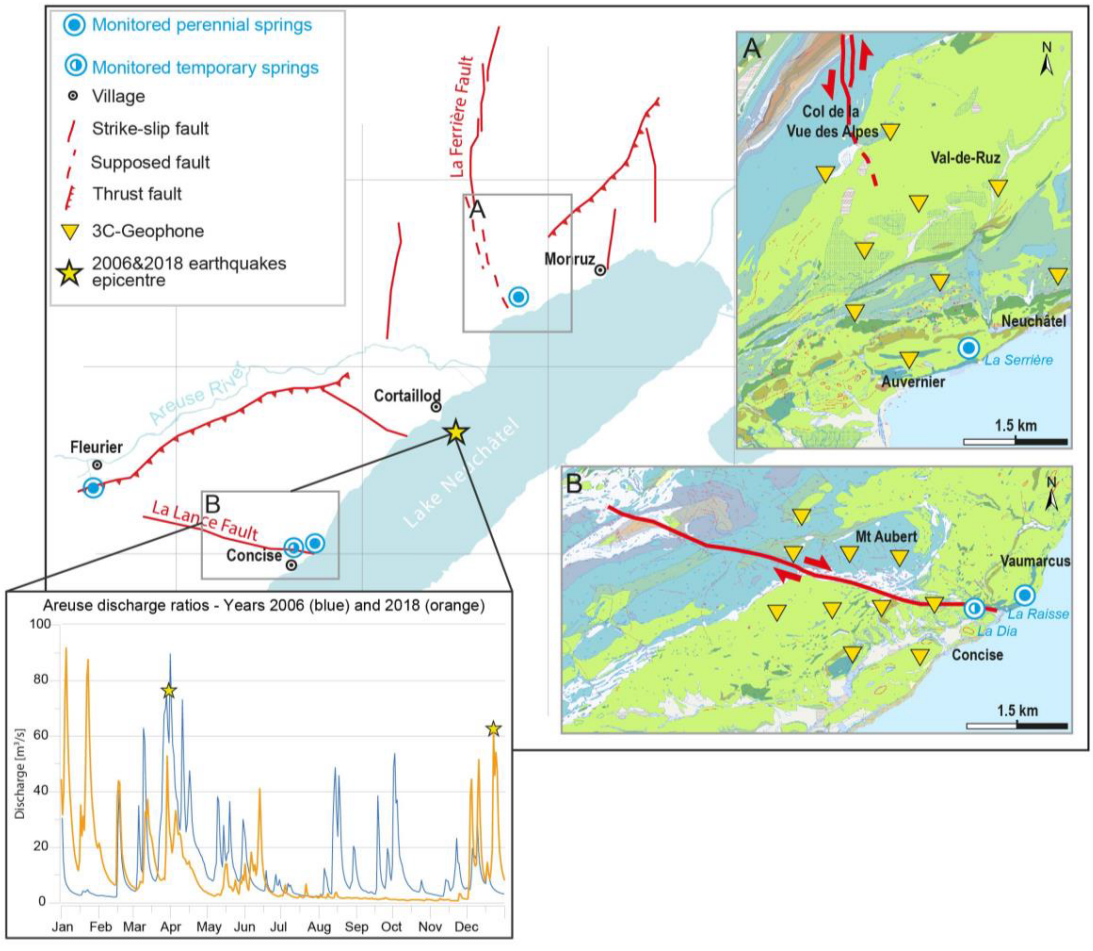


Figure 1. Situation map of the research area. Showing major strike-slip and thrust faults, monitored karstic springs and future position of the 3-Channel geophones for microseismic monitoring. Also shown epicentre of 2006 and 2018 seismic events and associated Areuse river discharge ratios. Data from the geological map (Geocover, https://www.map.geo.admin.ch), the Swiss Seismological Service (https://www.seismo.ethz.ch), and the Federal Office for the Environnment – Hydrological data and forecasts (https://hydrodaten.admin.ch).

REFERENCES

Miller, S. A. 2008: Note on rain-triggered earthquakes and their dependence on karst geology. Geophysical Journal International 173(1), 334-338.

P 7.6

Effects of fracture connectivity on Rayleigh wave dispersion

Gabriel E. Quiroga[1], J. Germán Rubino[2], Santiago G. Solazzi[1], Nicolás D. Barbosa[3], and Klaus Holliger[1].

[1]Applied and Environmental Geophysics Group, Institute of Earth Sciences, Université de Lausanne, Lausanne, Switzerland.
[2]CONICET, Centro Atómico Bariloche-CNEA, San Carlos de Bariloche, Argentina.
[3]Department of Earth Sciences, University of Geneva, Geneva, Switzerland.

The use of passive seismic techniques to monitor geothermal reservoirs allows to assess the risks associated with their exploitation and stimulation. One key factor in geothermal reservoirs is fracture connectivity, as changes in this parameter can affect the permeability and productivity of the system. Notably, seismic attenuation, anisotropy, and velocity are sensitive to changes in the mechanical and hidraulic properties of rocks. In this work, we study the effects of fracture connectivity on Rayleigh wave dispersion accounting for frequency-dependent poroelastic effects. For that, we consider a three-layer medium (Figure 1) which consists of a water saturated and fractured granite layer characterized by unconnected or connected fracture networks. We used an upscaling approach based on Biot's poroelasticity theory to determine the effective properties associated with these two scenarios. This procedure allows to obtain P- and S-wave velocities accounting for fluid pressure diffusion effects. Finally, we compute the corresponding Rayleigh wave dipersion curves. Our results show that Rayleigh wave dispersion curves exhibit a significant sensitivity to fracture connectivity and, thus, that they have the potential to be employed to detect changes in fracture connectivity as well as related properties in geothermal reservoirs.

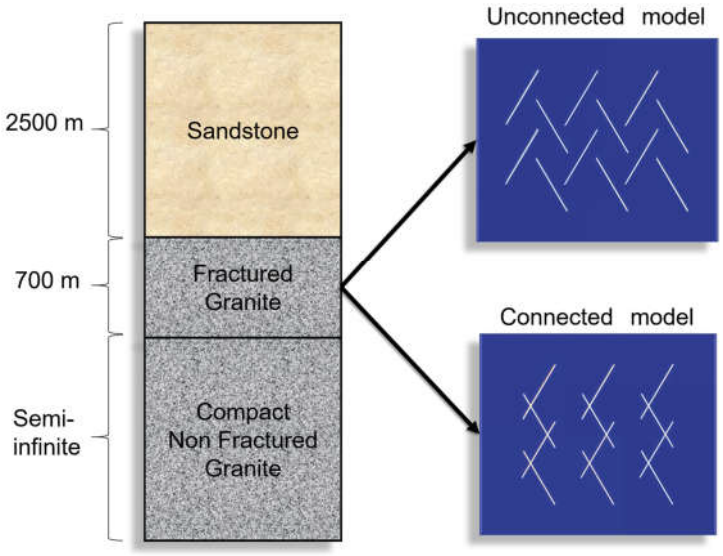


Figure 1. Schematic illustration of the considered three-layer model. The panels on the right show representative samples associated with the fractured reservoir models analyzed in this work.

P 7.7

Poroelastic effects of the damaged zone on fracture reflectivity

Edith Sotelo[1], Santiago G. Solazzi[1], J. Germán Rubino[2], Nicolás D. Barbosa[3], and Klaus Holliger[1]

[1]Institut des Sciences de la Terre, Université de Lausanne, Lausanne, Switzerland (edith.sotelogamboa@unil.ch)
[2]Centro Atómico de Bariloche, Consejo Nacional de Investigaciones Científicas y Técnicas, San Carlos de Bariloche, Rio Negro, Argentina
[3]Université de Genève, Genève, Switzerland

The presence of fractures has a predominant influence on the hydraulic and mechanical behavior of fractured rock systems. In this context, studies show the existence of a microfractured zone, generally referred to as the damaged zone, surrounding fractures and faults (Mitchell and Faulkner, 2012). The permeability changes associated with the damaged zone can enhance fluid pressure diffusion in the vicinity of fractures as seismic waves travel through the system. This process, together with the inherent mechanical weakness of damaged zone, are expected to affect the reflectivity of the fracture system. Following Barbosa et al. (2016), we investigate these effects using Biot's theory of poroelasticity (Biot, 1962). Under this framework, we consider a reference model (Figure 1a) and a model with a damaged zone (Figure 1b), and we compute the reflectivities at the background-fracture interface and background-damaged zone interface, respectively.

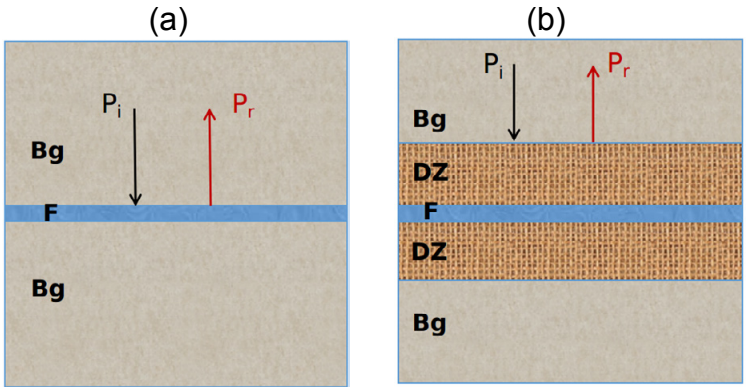


Figure 1. (a) Reference model and (b) model with damaged zone. $\mathbf{P_i}$ is the normally incident fast P-wave, $\mathbf{P_r}$ is the reflected P-wave, **Bg** is the background rock, **DZ** is the damaged zone, and **F** is the fracture.

Our results show that accounting for the permeability enhancement of the damaged zone increases the reflectivity of the system (Figure 2a). This effect is explained by the increase of fracture compliance when fluid pressure diffusion occurs from the fracture into the damaged zone. Mechanical weakening of the damaged zone increases the reflectivity as well (Figure 2b) due to an enhancement of the mechanical contrast with respect to the intact background.

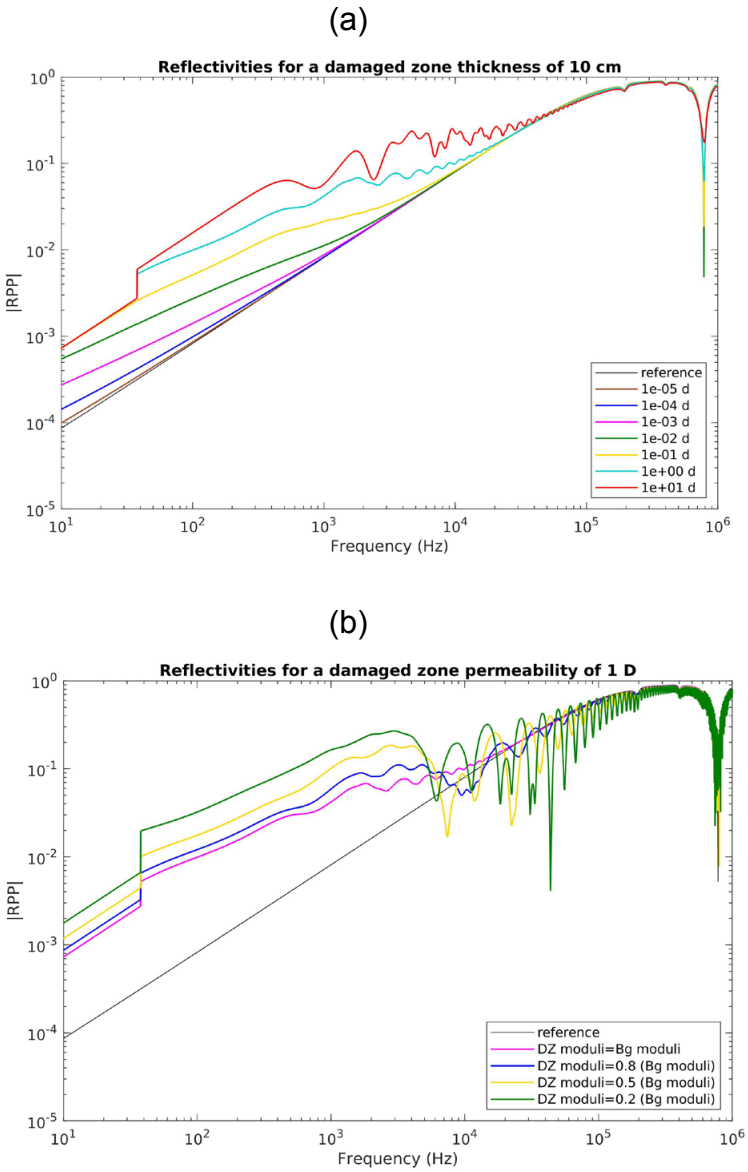


Figure 2. Absolute value of P-wave reflectivity (|RPP|) versus frequency for models with a damaged zone with (a) different values of permeability and (b) with weaker moduli. The frame bulk and shear moduli of the damaged zone decrease by 20%, 50%, and 80% with respect to their reference values (background rock). We assumed a damaged zone thickness of 10 cm, a background permeability of 10^{-6} D, a fracture permeability of 100 D, and, unless stated otherwise, the properties of the damaged zone are the same as those of the background.

REFERENCES

Barbosa, Nicolás D., J. Germán Rubino, Eva Caspari, Marco Milani, and Klaus Holliger (2016) “Fluid pressure diffusion effects on the seismic reflectivity of a single fracture.” The Journal of the Acoustical Society of America 140(4), 2554-2570.

Biot, M. A. (1962). “Mechanics of deformation and acoustic propagation in porous media.” Journal Applied Physics 33, 1482–1498.

Mitchell, T. M., and D. R. Faulkner (2012). “Towards quantifying the matrix permeability of fault damage zones in low porosity rocks.” Earth and Planetary Science Letters 339, 24-31.

P 7.8

Predictive HM-modeling in the heterogeneous Opalinus Clay of the Mont Terri rock laboratory and validation with monitoring data from a mine-by test

David Jaeggi[1], Jürgen Hesser[2], Chao Li[3] , Christophe Nussbaum[1] & Paul Bossart[1]

[1]Swisstopo, Seftigenstrasse 264, 3084 Wabern, Switzerland (david.jaeggi@swisstopo.ch)
[2]BGR, Stilleweg 2, 30655 Hannover, Germany
[3]INTERA, Hardstrasse 73, 5430 Wettingen, Switzerland

The Mont Terri rock laboratory was initiated in 1996 with 8 niches followed by a research tunnel in 1998. Since then the laboratory has been expanded every 10 years, mainly in the shaly facies of the Opalinus Clay. In March 2018, south of the existing laboratory, we extended the Mont Terri rock laboratory, mostly in the sandy facies of the Opalinus Clay (Ga18). In October 2019, this extension will be finished, resulting in more than 500 m of additional galleries and niches for new experiments. In the frame of this extension, we conducted for the first time a mine-by test investigating a sheet of sandy facies and carbonate-rich sandy facies sandwiched between shaly facies. This so-called MB-A experiment (hydro-mechanical characterization of the sandy facies before and during excavation) consists of two lateral niches for instrumentation and monitoring, and a test gallery of 30 m length oriented perpendicular to the lateral niches (Figure 1). Instrumentation based on 26 boreholes with lengths up to 40 m comprises pore-pressure transducers, extensometers, inclinometers and stress monitoring stations. It was finished several months before excavation of the test section was started to assure equilibration close to the initial conditions. We carried out excavation of the test gallery running parallel to bedding strike in May 2019 sequentially in daily advances of 2 m. The horseshoe-shaped gallery was lined with two layers of sprayed shotcrete of 20 cm total thickness. Concreting of the invert was done after finishing the entire gallery.
Here we present data from predictive modeling to estimate the hydro-mechanical behavior of the rock mass during excavation that was carried out for two heterogeneous, anisotropic cases: i) 3D-elastic and ii) 2D-APD (anisotropy, plasticity, damage) (Parisio, 2016). Initial predictive modeling was corrected to effective daily advances and sensor locations (Jaeggi & Madaschi, 2017, Li, 2018). We also present monitoring data and qualify the modeling results for the two different approaches. The elastic calculation predicts a rotation of early time, near-field pore-pressure reduction from perpendicular to parallel to bedding for later times. In contrast, the APD simulation predicts plastic volumetric dilation and a linked pore-pressure reduction along bedding. In general, monitored peak pore water pressures were higher than predicted, with a remarkable phase shift depending on distance and spatial position with respect to the drift. Compared to the elastic calculations, monitored deformations were clearly underestimated and are still low compared to the APD calculation. The overall behavior of the excavation in the sandy facies was, unexpectedly, not so different from earlier excavations in shaly facies (Lisjak et al., 2015). A large volume of the rock mass was influenced by the excavation works of Ga18, which became manifest in large-scale pore-water pressure changes and long-range deformations of existing galleries.

The acquired dataset of the mine-by test will be used in the future to calibrate our hydro-mechanical models. We need sound constitutive laws in the sandy facies for the understanding of rock mechanics and hydraulics. The outcomes of the MB-A experiment build an important input for CO_2 caprock integrity and long-term safety.

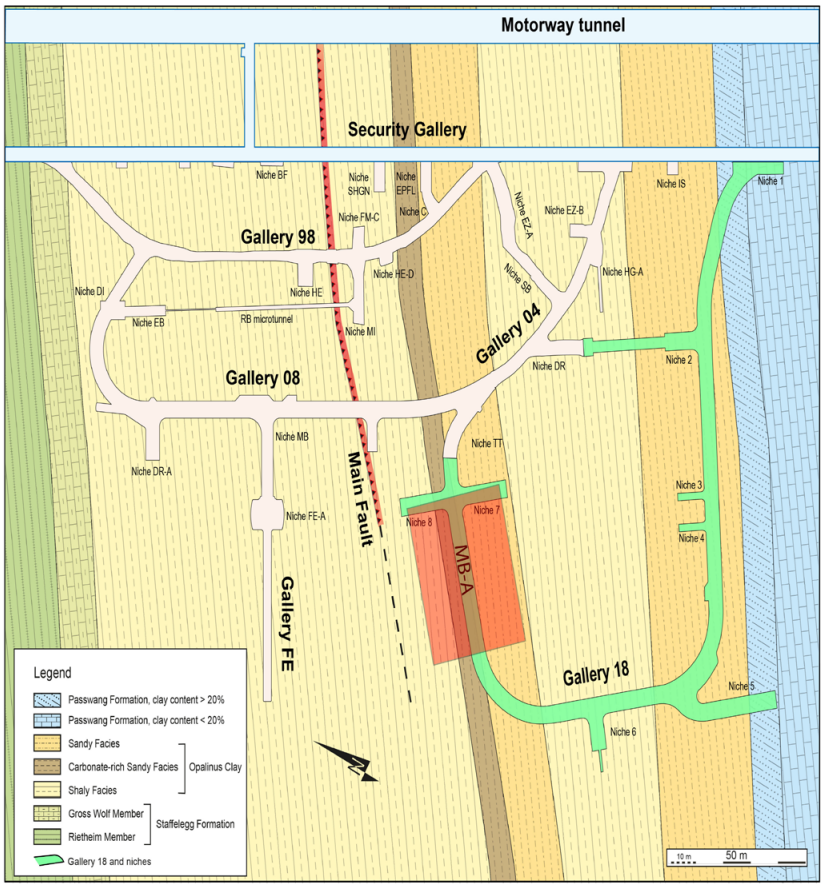


Figure 1. Location of the MB-A mine-by test in the new part (Ga 18) of the Mont Terri rock laboratory.

REFERENCES

Jaeggi, D. & Madaschi, A. (2017): MB-A (Mine-by test in sandy facies) Experiment: Predictive modeling using Code_Aster – model setup and results, Mont Terri Project Technical Note, TN2017-85.

Li, C. (2018): Numerical modelling of tunnel excavation for the MBA experiment, Mont Terri Project Technical Note, TN2018-70.

Lisjak, A., Grasselli, G., Müller, H. & Vietor, T. (2015): The excavation of a circular tunnel in a bedded argillaceous rock (Opalinus Clay): short-term rock mass response and FDEM numerical analysis. Tunn Undergr Sp Tech 45, 227-248.

Parisio, F. (2016): Constitutive and numerical modeling of anisotropic quasi-brittle shales, Thesis EPFL, No 7053.

P 7.9

Anisotropic elastic properties and permeability of Opalinus shale from the 'Main Fault' and host formation within Mont Terri

Quinn Wenning[1], Claudio Madonna[1], & Alba Zappone[2]

[1]Department of Earth Sciences, ETH Zurich, Sonneggstrasse 5, 8092 Zurich (quinn.wenning@erdw.ethz.ch)
[2]Department of Mechanical and Processess Engineering / Swiss Seismological Survey, ETH Zurich

This study focuses on measurements of elastic properties and permeability of both the Opalinus shale host formation and the so-called 'Main Fault' within the Mont Terri Rock Laboratory. Given the formation's potential to serve as both a caprock for carbon capture and storage and as the host for nuclear waste disposal, understanding the hydro-mechanical properties of the Opalinus shale is of significant importance. During the drilling phase of the CS-D experiment within Mont Terri, approximately 200 m of core was recovered and preserved in air-tight aluminium packing. We selected core material from both the host rock 'shaley' facies and from within the Main Fault. The samples from the shaley facies develops anisotropic fabric due to bedding, while the samples from the Main Fault have foliation that developed due to shearing along the fault. As such, we have measured directional variations in seismic velocities, porosity, and permeability, perpendicular and parallel to the foliations in the recovered core. The seismic velocity and permeability measurements were made systematically under hydrostatic confinement. We measured permeability at 3, 5, 7, and 10 MPa confining pressure using the transient pressure step technique with argon. Seismic velocities were made at corresponding pressures and then up to 200 MPa. The high-pressure measurements allow for extrapolation of the permeability and elastic properties to realistic gas reservoir conditions and beyond. As expected, the results show that the foliation controls both seismic velocities and permeability. In both cases the seismic velocity and permeability is significantly higher parallel to both the bedding and structural foliations. Permeability measurements perpendicular to bedding and structural foliation are both on the order of 10^{-20} to 10^{-22} m^2, and in some cases above 5 MPa confining pressure the flow was below the detection limit of the apparatus. Measured permeability parallel to bedding and structural foliation is one to two orders of magnitude larger, however given the fissile nature of the Opalinus, it is difficult to rule out whether or not this increase is due to desiccation cracks in the sample.

P 7.10

Characterization of 3D pore shape and distribution in sedimentary rocks with different porosity by X-ray microcomputed tomography

Yi Zhou[1], Michele Pugnetti[1], Anneleen Foubert[2], Christoph Neururer[2] & Andrea R. Biedermann[1]

[1]*Institut für Geologie, University of Bern, Baltzerstrasse 1+3, CH-3012 Bern (yi.zhou@geo.unibe.ch)*
[2]*Department of Geosciences, University of Fribourg, Chemin du Musée 6, CH-1700 Fribourg*

Pore fabrics describe pore shape and pore network distribution. The shape-preferred orientation and distribution of pores lead to anisotropic physical properties, for example permeability. The preferred orientation of connected pores results in strong permeability anisotropy, which in turn controls the preferred flow direction. The thorough understanding of preferred flow paths is essential for the exploitation of fluid resources, such as groundwater, geothermal energy, or hydrocarbon. One way of relating pore fabrics to physical properties is digital rock physics. In this study, we use X-ray microcomputed tomography (XRCT) as an advanced way to directly assess the 3D pore fabric in sedimentary rocks. Two types of porous sedimentary rock samples have been used in our experiments, respectively, ~5%-porosity sandstone (Swiss Molasse Basin, Switzerland) and ~50%-porosity calcarenite samples (Apulia, Italy). Porosity on discrete samples is measured by pycnometry. XRCT data were analysed to quantify and visualize pore shape and distribution. XRCT has the advantage that the digitized 3D pore fabric of rocks can be directly used for modelling and process simulation in fluid flow studies. These XRCT-derived data will be compared to a new indirect method of pore fabric characterization, the magnetic pore fabric determination, by impregnating ferrofluid and measuring magnetic susceptibility of the samples. That method, once fully understood, has the potential to characterize in an effective and rapid way the average pore shape and orientation. This will allow more samples to be analysed for pore fabric characterization in hydrocarbon and geothermal studies, making it possible to investigate regional-scale variations.

P 7.11

Anisotropy of Magnetic Susceptibility to investigate the pore fabric of rocks with various porosity using ferrofluid impregnation: First results and method improvements

Michele Pugnetti[1], Yi Zhou[1], Andrea R. Biedermann[1,2]

[1]Institute of Geological Sciences, University of Bern, Baltzerstrasse 1+3, CH-3012 Bern, Switzerland (michele.pugnetti@geo.unibe.ch)
[2]Institute of Geophysics, ETH Zurich, Sonneggstrasse 5,CH-8092 Zurich, Switzerland

Pore fabric analysis is important in oil and gas exploration, hydrogleology, hydrothermal characterization and extraction of fluid from underground structures. However, it can be challenging when the lithologies involved show a wide range of porosities with anisotropic properties. Many properties of porous rocks can be anisotropic (permeability, elastic wave propagation, electrical resistivity, magnetic susceptibility). For example, the anisotropy of permeability determines the easiest direction of groundwater flow or the easiest direction to extract oil or gas from the subsurface, while elastic anisotropy defines the direction of fastest wave propagation. The anisotropy of these properties is largely controlled by the pore structure (pore dimensions, shape and orientation). A method to analyse the pore fabric of a range of lithologies showing different porosities is the magnetic pore fabrics method, initially proposed in the 90's. Here, this method is tested with a special focus on impregnation methods (and their efficiency) and frequency-dependence magnetic susceptibility on three types of rocks with low (5-10%), medium (10-30%) and high (30-50%) porosity. The experimental procedure starts with water and oil-based ferrofluid (fluid with suspension of 10nm particles of magnetite) impregnation of drilled cores. The quality of impregnation was checked using magnetic method. After successful impregnation, the anisotropy of magnetic susceptibility was measured at different frequencies in 15 directions to create an ellipsoid of the anisotropy. Since the observed data show that the magnetic susceptibility of the ferrofluid is significantly larger than the susceptibility of the rock, the direction of maximum susceptibility reflects the preferred pore elongation direction. Ferrofluid impregnation is a challenging and important step and its efficiency depends mainly on the porosity and pore throat of the porous medium and the fluid properties. The results of this study show that: (1) Verify the impregnation efficiency is a key point to ensure the uniform distribution of the ferrofluid inside the pores and its improvement is vital for the reliability of the Magnetic Pore Fabric anisotropy results because it's one of the factors that have the strongest influence on the susceptibility measurements. (2) The method used for impregnation strongly affects the impregnation efficiency, however it also depends on the porosity of the material, the type of ferrofluid and its wetting and viscous properties. (3) The type and concentration of ferrofluid are other factors that affect the impregnation efficiency and the magnitude of anisotropy. (4) In all cases the impregnated samples show a strong frequency dependence in magnetic susceptibility measurements. For this purpose, future works should investigate in detail the correlation between frequency dependence magnetic susceptibility and the pore size distribution.
The future development of the project will show which combination of type of ferrofluid, impregnation method and impregnation efficiency determination will provide the optimum response as a function of the physical characteristic of the porous samples (interconnected porosity, pore throat pore shape and orientation).

P 7.12

Will deep geothermal enable Switzerland to be carbon neutral by 2050?

Naomi Vouillamoz[1], Jonathan Vouillamoz[2], Martin Clerc de Senarclens[2], Daniel Rincón Hanna[3] & Guido Nuijten[4]

[1]Seismo Earth AG, Schwadernauweg 33, CH-2504 Biel/Bienne (naomi.vouillamoz@seismo-earth.com)
[2]CSGE Sàrl, Conseils en Stratégies Géo-Environementales, Rue des Voisins 8, CH-1205 Genève
[3]Legacy Foundry, Wiesenstrasse 13, CH-8834 Schindellegi
[4]Pöyry Finland Oy/Rock & Tunnel Engineering, Jaakonkatu 3 (PL 500), 01620 Vantaa, Finland

Switzerland has two existential challenges:

1. It must become carbon neutral by 2050; and
2. It must find ways to reduce foreign energy dependency.

The Energy Strategy 2050 is promising but insufficient. Deep Geothermal Energy (DGE) could be the primary solution to achieving both goals.

Existential challenges:
Global greenhouse gases emissions have reached an all-time high in 2018 (Global Carbon Project 2018). On August 28, 2019, the Swiss Government declared Switzerland's imperative to become carbon neutral by 2050. In 2018, 73% of Switzerland's energy originated from non-renewable sources, such as oil, gas, coal and nuclear.

The Energy Strategy 2050 presents a shift towards more renewable energy sources, such as hydropower, solar photovoltaic, wind and deep geothermal energy, in the form of electricity.

While the strategy is promising, it hardly seems achievable for three reasons:

1. **Time**: at the current rate (40-60 MW of added renewable capacity per year), replacing non-renewable with renewable sources will take at least 46 years for nuclear, plus 61, 155, and 59 additional years to replace oil, fuels and gas respectively (BFE, 1999, 2018, 2019). Assuming an optimistic 2% annual growth of the current renewable installation rate, it will take a century to replace nuclear, oil, fuel and gas!
2. **Resources**: deployment of solar and wind renewable is heavily dependent on technologies requiring raw materials that are mined using cheap and abundant fossil energy.
3. **Energy Return on Energy Invested (ERoEI)**: the functioning of our economics and society is estimated to require ERoEI above 9:1. Recent studies indicate ERoEI for solar PV getting below 3:1 in sunny Spain and below unity for moderate insolated countries like Switzerland or Germany (Weißbach et al., 2013; Ferroni and Hopkirk, 2016; Hall, 2018).

A solution to two problems:
Deep geothermal energy offers the greatest theoretical potential to solve both problems. However, current technologies have not proven yet the capability of installing a 5 MW plant and are often criticized for induced seismicity.

Seismo Earth AG located in Biel/Bienne, Switzerland, is developing a patent-pending technology for deep geothermal heat exchange in industrial power production. Given the strategic importance of the challenges, the viability and sustainability of renewable energy sources must be scrutinized. Our research and technology development focus on increasing the efficiency of DGE plants, applying a systemic optimization of raw material and energy needs inputs, considering the whole plants life cycle. Our goal is to present an alternative answer.

REFERENCES

Bundesamt für Energie BFE - Office fédéral de l›énergie OFEN 1999: Schweizerische Gesamtenergie Statistik 1998/2017/2018 - Statistique Globale Suisse de l›Energie 1998/2017/2018.

Ferroni, F. & Hopkirk, R. J. 2016: Energy Return on Energy Invested (ERoEI) for photovoltaic solar systems in regions of moderate insolation, Energy Policy 94, 336–344.

Global Carbon Project (2018): Carbon budget and trends 2018.

Hall, C. A.S. 2018: Energy Return on Investment. A Unifying Principle for Biology, Economics, and Sustainability, Lecture Notes in Energy 36, Springer International Publishing.

Weißbach, D., Ruprecht, G., Huke, A., Czerski, K., Gottlieb, S. & Hussein, A. 2013: Energy intensities, EROIs (energy returned on invested), and energy payback times of electricity generating power plants, Energy 52, 210–221.

P 7.13

Bridging the gap between Places and Sites Including place factors in the site selection process of CO_2 storage projects

Juanita von Rothkirch, Olivier Ejderyan, Michael Stauffacher

ETH Zürich

Geological CO_2 storage is a key technology for facilitating the removal of carbon dioxide from the atmosphere. However, the progression of CO_2 storage has been hindered by public opposition to some particular cases, once sites for the project implementation were selected. As numerous experiences on contested technologies have shown, public participation processes determine whether communities become a door or barrier for the emplacement of projects in local contexts. Yet there is much literature on the importance of early public engagement for normative, substantive and instrumental reasons, there are no tools for integrating social aspects early on in the site selection process. This thesis constitutes an exploratory study of the upstream inclusion of social characteristics and concerns in the site selection process for CO_2 storage in Switzerland. It starts with an evaluation on the social aspects which matter for the emplacement of CO_2 storage. Then, it analyzes whether it is possible to map selected social aspects using GIS, for including them in the selection process. It extracts the characteristics of potential locations in Switzerland and explores the locations using cluster analyses. Finally, it reflects on the potential uses and limitations of this approach. This thesis presents a concrete framework for including place factors in the site selection process, consisting on a typology of place factors, maps for their visualization and a frame for reflection. This framework can constitute a first step in an iterative process which requires the input of diverse stakeholders.

8. Quaternary environments: landscapes, climate, ecosystems and human activity during the past 2.6 million years

Naki Akçar, Christine Pümpin, Gaudenz Deplazes, Stephanie Wirth, Jean Nicolas Haas, René Löpfe, Loren Eggenschwiler and Marc Luetscher

Swiss Society for Quaternary Research (CH-QUAT)

TALKS:

8.1 Affolter S., Fleitmann D., Häuselmann A., Leuenberger M.: Speleothem-based temperature reconstruction over the past 14000 years from Milandre Cave, Switzerland

8.2 Amini Tehrani N., B.Naimi, Jaboyedoff M.: Toward community predictions: multi-scale modelling of mountain breeding birds' habitat suitability and landscape preferences

8.3 Amsler H.E., Ikehara M., Geibert W., Kuhn G., Jaccard S.L.: Bottom water oxigenation across a transect in the SW Indian Ocean since the last glacial inception

8.4 Bolland A., Rey F.,Tinner W.,Heiri O.: Using chironomids to assess Lateglacial climate evolution in at Burgäschisee, Switzerland

8.5 Bomou B., Rachoud-Schneider A.-M., Spangenberg J., Gärtner M., Haas J.-N., Adatte T.: Paleoenvironmental reconstruction of the Amburnex paleolake (Switzerland) during the Late Glacial and the Holocene.

8.6 Courtney-Mustaphi C.: Land use and land cover changes in western Serengeti over the past few hundred years

8.7 Deák J., Preusser F., Chauvière F.: Cotencher cave: a site with an exceptional preserved sedimentary sequence recording Late Pleistocene climatic and environmental changes in Swiss Jura Mountains

8.8 Dieleman C., Christl M., Vockenhuber C., Akçar N.: Tracking the Pace of Landscape Evolution during the Deckenschotter Times

8.9 Gegg L., Buechi M.W., Ebert A., Deplazes G., Madritsch H., Anselmetti F.S.: Deformation features in glacially overridden karst: evidence for subglacial hydrofracturing?

8.10 Heer A.J.: A glimpse of the sedimentary history of the Rhine Valley, eastern Switzerland – new contribution from quartz OSL dating.

8.11 Jeannin P.-Y, Doumenc F., Guerrier B.: Impact of climate change on the conservation of paleolotihic paintings in caves

8.12 Keller L., Moro D.G., Spillmann T., Deplazes G., Madritsch M.: Mapping Bedrock Topography of the Lower Aare Valley Using Seismic Surface Waves

8.13 Serra E., Valla P.G., Gribenski N., Magrani F., Carcaillet J., Delaloye R., Grobety B., Braillard L.: Late-glacial to Holocene sediment dynamics in high Alpine regions (Sanetsch Pass, Switzerland)

8.14 Vogel H., Wagner B., Francke A., Friedrich T., Donders T., Lacey J.H., Leng M.J., Regattieri E., Sadori L., Wilke T., Zanchetta G. et al.: Mediterranean rainfall variability and its phase relationship with the African monsoon – A 1.36 million year record from Lake Ohrid

8.15 Zaki A.S:, Schuster M., Giegengack R., Gupta S., Haghipour N., King G.E., Herman F., El-wakil M., Khairy H., Ahmed S., Eltayeb S.A., Watkins S.E., Castelltort S.: Late-Quaternary inverted palaeochannels record high precipitation rates and episodic flooding in the Sahara: Implications for Holocene human dispersal

POSTERS:

P 8.1 Buechi M.W., Deplazes G., Gegg L., Landgraf A., Madritsch H., Anselmetti F.S.: Reconstructing the landscape evolution of Northern Switzerland using overdeepened glacial basins

P 8.2 Burkhalter C., Bichet V., Ivy-Ochs S., Akçar N.: Last Glacial Maximum glaciation in the Jura mountains

P 8.3 Cojean A.N.Y., Bartosiewicz M., Lehmann M.F., Kremer K., Wirth S.B.: Different lacustrine pockmark systems in Lake Thun, Switzerland, and their potential influence on the hydrological and biogeochemical budget of the lake

P 8.4 Czerski D., Mosetti L., Vergani C.R., Pellegrini M., Federici-Schenardi M., Gillioz M., Nogara G., Scapozza C.: Evolution of fluvial environments and history of human settlements on the Ticino river alluvial plain

P 8.5 Gegg L., Buechi M.W., Deplazes G., Madritsch H., Mueller D., Preusser F., Anselmetti F.S.: The glaciation history of the overdeepened Lower Aare Valley: insights from scientific drilling and outcrop data

P 8.6 Hajdas I., Eggenschwiler L.,Maurer M.,Röttig M.B.: The fading ^{14}C “Bomb pulse” and consequences for geochronology

P 8.7 Kamleitner S., Ivy-Ochs S., Monegato G., Gianotti F., Martin S., Christl M.: First Beryllium-10 exposure ages from the LGM Ticino-Toce glacier

P 8.8 Kremer K., Schweizer N., Fabbri S., Anselmetti F.S., Gilli A., Wirth S.B.: Traces of a large prehistoric rockfall in Lake Thun (Switzerland)

P 8.9 Luetscher M., Moseley G.E., Boch R., Cheng H., Edwards R.L., Spötl C.: The expression of Heinrich Event 2 in Alpine speleothems

P 8.10 Makri S., Tylmann W., Vogel H., Grosjean M.: Investigating meromixis dynamics in varved lake sediments of Lake Jaczno, Poland using high resolution hyperspectral imaging and XRF data

P 8.11 Märki L., Lupker M., Gajurel A., Haghipour N., Schide K., France-Lanord C., Lavé J., Morin G., Gallen S., Eglinton T.: Organic and inorganic long-term carbon budget of Himalayan erosion after the 2015 Gorkha earthquake

P 8.12 Negga H., Rime V., Hailu A., Jaramillo-Vogel D., Braga C.J., Atnafu B., Kidane T., Foubert A.: Coupling of Pleistocene sea level fluctuations with coralgal reef growth in the Danakil Depression (Afar, Ethiopia)

P 8.13 Reber R., Heuberger S., Nibourel L., Galfetti T.: The challenge of compiling a Swiss gravel and sand occurrence map

P 8.14 Rigoussen D., Diaz N., Mokatse T., Verrecchia E.: Origin of calcium in Ca-carbonate deposits from a sandy siliceous basin (Chobe Enclave, North Botswana): first results

P 8.15 Schläfli P., Gobet E., Tinner W., Leeuwen v.J., Vescovi E., Douillet G., Schwenk M., Bandou D., Schlunegger F.: Towards a chronologically constrained Eemian (MIS 5e) pollen biostratigraphy in Switzerland

P 8.16 Schwenk M.A:, Bandou D., Schläfli P., Douillet G.A., Schlunegger F.: New insights into the Quaternary fill of the overdeepened Aare Valley

P 8.17 Steinemann O., Ivy-Ochs S., Hippe K., Christl M., Haghipour N., Synal H.-A.: Rock basins, riegels and gorges: decipgering glacial overdeepenings

P 8.18 Studer A.S., Mekik F., Ren H., Martínez-García A., Sigman D.M., Haug G.H.: Foraminifera-bound nitrogen isotope evidence for similar rates of water column denitrification in the eastern Pacific during the last ice age and the Holocene

P 8.19 Tomonaga Y., Horstmann E., Deplazes G., Kipfer R.: 4He/U-Th dating of pore waters from Quaternary sediments in Switzerland: potential and challenges

P 8.20 Weidlich R., Rüggeberg A., Makovsky Y., Bialik O., Foubert A.: Morphological and Petrographic Characterisation of Seep Carbonates from the South-Eastern Mediterranean Sea

P 8.21 Wirth S.B., Zander P., Gilli A., Grosjean M.: Hyperspectral imaging spectroscopy applied to Lake Cadagno: resolving the short-term response of meromixis and aquatic productivity to climatic and environmental events

P 8.22 Klein K., Groβ-Schmölders M., Alewell C., Leifeld J..: Using analytical pyrolysis-derived molecular biomarkers to identify changes in chemical composition with depth in natural and drained Finnish mires

P 8.23 Yeşilyurt S., Fredin O., Romundset A., Christl M., Vockenhuber C., Akçar N.: Lateglacial deglaciation and glaciostatic uplift in northern Norway

P 8.24 Ivy-Ochs S., Steinemann O., Luetscher M., Fischer U.H., Vockenhuber C.: The connection between low rates of glacial erosion on limestone bedrock and relief development in the Alps

8.1

Speleothem-based temperature reconstruction over the past 14000 years from Milandre Cave, Switzerland

Stéphane Affolter[1,2], Dominik Fleitmann[3], Anamaria Häuselmann[4] and Markus Leuenberger [1]

[1]Climate and Environmental Physics, Physics Institute, University of Bern, Switzerland (affolter@climate.unibe.ch)
[2]now at: International Foundation High Altitude Research Stations Jungfraujoch and Gornergrat, Bern, Switzerland
[3]Department of Environmental Sciences, Quaternary Geology, University of Basel, Switzerland
[4]Geological Institute, University of Bern, Switzerland

Stalagmites – a powerful continental archive – are able to provide essential knowledge about past climate variability. At the Climate and Environmental Physics Division of the University of Bern, we recently developed a method to extract microliter amounts of water from stalagmites and further analyse their water isotopes (Affolter et al., 2014). We applied this method to two stalagmites M6 and M8 from Milandre Cave, Jura Mountains. Due to physically constrained processes, water isotopes in modern precipitation at the study site are highly correlated to surface air temperatures, which allows us to transpose this relationship into the past and estimate the temperature variability of central Europe over the past 14000 years (Affolter et al., 2019).

The inferred temperature reconstruction shows a very similar pattern in the temperature evolution as the Greenland and the western Mediterranean Sea areas, and provides further evidence fro the existence of a Holocene Thermal maximum between approximately 10000 to 6000 years ago. In addition, our results also confirm a marked gradient in temperature between central and northern Europe during the early Holocene, making a discussion of a global temperature reconstruction difficult. Finally, our temperature reconstruction from Milandre Cave allows us to address the so-called "Holocene temperature conundrum" which describes a discrepancy between paleoclimate data and climate model simulation, which simulate a distinct warming during the Holocene. Our results suggest that seasonality in the proxy records is not the main cause for the conundrum.

REFERENCES

Affolter, S., A. D. Häuselmann, D. Fleitmann, R. Lawrence Edwards, H. Cheng, M. Leuenberger, "Central Europe temperature constrained by speleothem fluid inclusion water isotopes over the past 14,000 years", Science Advances, 5, 2019.

Affolter, S., D. Fleitmann, M. Leuenberger, "New online method for water isotope analysis of speleothem fluid inclusions using laser absorption spectroscopy (WS-CRDS)", Climate of the Past, 10, 1291-1304, 2014.

8.2

Toward community predictions: multi-scale modelling of mountain breeding birds' habitat suitability and landscape preferences

N. Amini Tehrani[1], B. Naimi[1], M. Jaboyedoff[1]

[1]Faculty of Geosciences and Environment, University of Lausanne, CH–1015 Lausanne, Switzerland (Nasrin.AminiTehrani@unil.ch)
[1]Faculty of Science, Institute for Biodiversity and Ecosystem Dynamics, University of Amsterdam, 1090 GE Amsterdam
[1]Faculty of Geosciences and Environment, University of Lausanne, CH–1015 Lausanne, Switzerland

It is important and challenging to model the fine-scale uncertainties in distributions of highly mobile species such as birds. Across a large mountain area of the western Swiss Alps, we used occurrence data (presence-only points) of bird species to find suitable modelling solutions and build reliable distribution maps to deal with biodiversity and conservation necessities of bird species at finer scales. To know better, how bird species and their complex environment interact, we have performed a multi-scale modelling method using focal variables in different scales to evaluate the efficient scale of each environmental predictor where they are influential. We used 12 neighboring window sizes (0.1 to 5 km) to explore the effect of species-specific scales of influence of each variable, and then to identify the best radius for each focal variable (land cover and land use), we fitted univariate models for each species to identify the most efficient scale of influence of each predictor. The final set of variables obtained from the previous stage was then employed to build ensemble of small models (ESMs) at a fine spatial resolution of 100 m and generate species distribution maps as conservation tools for nature practitioners. We could build useful habitat suitability models for the three groups of species (all the 91-bird species, species listed as least concern (LC), near threatened (NT) and as Vulnerable (VU), Endangered (EN)) in the national red list. Our results are consistent with this finding that, in general, the most important variables were in the group of bioclimatic variables including "Bio11"= Mean Temperature of Coldest Quarter, and "Bio 4"= Temperature Seasonality, then in the focal variables including "Forest", "Orchard", and "Agriculture area" that linked to forest structures such as tree and vegetation covers. Distribution maps are useful to identify most threatened species and their area and to optimize conservation efforts for identifying bird hotspots and ESMs present a powerful strategy for a better understanding of ecology and distribution of bird species in a complex and heterogeneous area.

8.3

Bottom water oxigenation across a transect in the SW Indian Ocean since the last glacial inception

H. Eri Amsler[1], Minoru Ikehara[2], Walter Geibert[3], Gerhard Kuhn[3], Samuel L. Jaccard

[1]University of Bern, Institute of Geological Sciences and Oeschger Centre for Climate Change Research, Bern, Switzerland (helen-eri.amsler@geo.unibe.ch)
[2]Center for Advanced Marine Core Research, Kochi University
[3]Alfred-Wegener-Institut Helmholtz-Zentrum für Polar- und Meeresforschung, Bremerhaven, Germany

On glacial-interglacial timescales the Southern Ocean plays a major role in modulating climate oscillations. On the one hand upwelling and outcropping of nutrient-rich deep water releases CO_2 to the atmosphere while on the other hand atmospheric CO_2 is taken up by phytoplankton and sequestered in the deep ocean [1]. Varying the balance between these processes can directly affect the storage of respiratory carbon in the ocean interior. This is reflected in the concentration of dissolved oxygen in deep water. Bulk sedimentary authigenic uranium (auth.U) is a useful tracer for oxygenation in marine sediments and can help document temporal changes in bottom water oxygenation resulting from changes in circulation and/or export production.

Here we present auth. U records from marine sediment cores spanning a meridional transect in the Indian sector of the Southern Ocean, a region that has yet received little attention. Increased sedimentary accumulation of auth. U. during the last ice age in all cores suggests that the deep southern Indian Ocean was more poorly ventilated and thus contributed to sequester remineralized carbon away from the atmophere. These observations support previous findings suggesting that the Southern Ocean played a dominant role in the partitioning of CO_2 between the subsurface ocean and the atmosphere during the last ice age.

REFERENCES

[1] Sigman, D. M. & Boyle, E. A. 2000: Glacial/interglacial variations in atmospheric carbon dioxide. Nature 407, 859-869.

8.4

Using chironomids to assess Lateglacial climate evolution in at Burgäschisee, Switzerland

Alexander Bolland[1,2], Fabian Rey[1,2], Willy Tinner[2], Oliver Heiri [1,2]

[1]Geoecology, Department of Environmental Sciences, University of Basel, Switzerland (alexanderwilliam.bolland@unibas.ch)
[2]Institute of Plant Sciences & Oeschger Centre for Climate Change Research, University of Bern, Switzerland

Chironomid-based temperature reconstructions which extend back into the Early Lateglacial prior to 14,700 cal BP in central Europe are few, and none are reliably dated in northern Switzerland. New pollen evidence displaying Early Lateglacial warming in the Swiss Plateau lowlands as early as 16,000 cal BP (Rey et al 2017) exemplifies this knowledge gap. Currently the only temperature reconstructions available for comparison can be found South of the Alps (Samartin et al 2012). Therefore, the production of a new well temporally constrained chironomid assemblage record for northern Switzerland is essential. The information derived from this new record will contribute to our understanding of Early Lateglacial environment and climate evolution on the Swiss Plateau which can then be used to corroborate the new observations of Early Lateglacial warming derived from pollen and macrofossil data.

Chironomids have been sampled from lake sediments retrieved from Burgäschisee, a small, well studied lake on the Swiss Plateau. Pollen analysis from Burgäschisee has shown vegetational turnover during the Early Lateglacial at 16,000 cal BP (Rey et al 2017) which describes the transition from tundra to shrub tundra prior to the onset of the Bölling interstadial (ca. 14,700 cal BP). Here, in parallel, we present the first well dated chironomid assemblage record for the Swiss Plateau Early Lateglacial on a centennial scale, and explore lake and climate development for the period 14,000 - 18,000 cal BP. The results indicate that the cold stenothermic taxa *Sergentia coracina*-type dominated the chironomid assemblage throughout the period preceding the Bölling warming. Despite the persistence dominance of *Sergentia coracina*-type there are changes observed in the sub dominant chironomid taxa, with cold stenotherms such as *Paratanytarsus austriacus*-type and *Micropsectra radialis*-type becoming less abundant and replaced with types indicative of warmer conditions such as Dicrotendipes nervosus-type. These changes are concurrent with the vegetational shift from tundra to shrub-tundra at 16,000 cal BP in the Burgäschisee record. Furthermore these results are coeval with results from South of the Alps at Lago di Origlio in the Ticino lowlands, which show pollen-inferred afforestation and chironomid-inferred warming (Samartin et al 2012). This implies that there was circum-alpine climatic warming after the end of Heinrich Event 1 which was substantial enough to release major vegetation reorganizations.

REFERENCES

Rey, F., Gobet, E., van Leeuwen, J. F. N., Gilli, A., van Raden, U. J., Hafner, A., Wey, O., Rhiner, J., Schmocker, D., Zünd, J., & Tinner, W. 2017: Vegetational and agricultural dynamics at Burgäschisee (Swiss Plateau) recorded for 18,700 years by multi-proxy evidence from partly varved sediments. Veg Hist Archaeobot 26(6), 571–86.

Samartin, S., Heiri, O., Lotter, A. F., & Tinner, W. 2012: Climate warming and vegetation response after Heinrich event 1 (16,700–16,000 cal yr BP) in Europe south of the Alps. Clim Past 8, 1913–1927.

8.5

Paleoenvironmental reconstruction of the Amburnex paleolake (Switzerland) during the Late Glacial and the Holocene.

Brahimsamba Bomou[1], Anne-Marie Rachoud-Schneider[2], Jorge Spangenberg[1], Marina Gärtner[3], Jean-Nicolas Haas[3], Thierry Adatte[1]

[1]Institute of Earth Sciences, University of Lausanne, Unil-Mouline, Geopolis, 1015 Lausanne, Switzerland (brahimsamba.bomou@unil.ch)
[2]Musée et Jardins botaniques cantonaux, Av. de Cour 14bis, 1007 Lausanne, Switzerland
[3]Department of Botany, University of Innsbruck, Sternwartestrasse 15, 6020 Innsbruck, Austria

Created by the retreat of a Würm ice sheet, numerous glacial paleolakes took place in the Western Swiss Jura. One of them, in the Amburnex Valley, have evolved in well-developed peatland which is a humid zone ecosystem particularly vulnerable to current climate change. During the Late Glacial period, this peatland was a glacial lake characterized by a significant accumulation of lacustrine sediment deposits.

Using a multiproxy approach, this project aims to reconstruct the paleoclimatic and the paleoenvironmental evolution recorded in lacustrine sediments and peatbog deposits since the last 13'000 years, and to investigate if major volcanic episodes have been recorded throughout this period.

High resolution analyses have been performed at cm-scale on a 7 m-thick sedimentary core. Starting with a morainic deposit from the Würm period, this core shows three meters of lacustrine deposits overlain by four meters of peatland deposits.

A multiproxy approach based on palynological analyses, grain-size analyses, mineralogical analyses (XRD) and geochemical analyses (TOC, Nitrogen, Phosphorus and Mercury contents; major and trace elements; organic carbon isotopes) have been used to characterize the hydrological and climatic fluctuations, the trophic level and the origin of organic matter in order to reconstruct the paleoenvironmental and paleoclimatic evolution in this area. Mercury anomalies recorded in the sediment can be a robust tracer of volcanic activity in absence of tephra layers. The latter are indeed not always well preserved in sediments due to mineralogical transformation, Hg anomalies could therefore be a reliable tool to characterize atmospheric volcanism fallouts such as the Laacher See Tephra event (Eifel, Germany), the Icelandic tephra (Iceland), the Italian Volcanic Province tephra (Italy) and the Puy de la Nugère tephra (Massif Central, France).

8.6

Land use and land cover changes in western Serengeti over the past few hundred years

Colin Courtney-Mustaph

Geoecology, University of Basel, Klingelbergstrasse 27, 4056 Basel, Switzerland
(colin.courtney-mustaphi@unibas.ch)

Tropical savannah ecosystems are highly dynamic systems that experience rapid changes in vegetation cover due to interactions between climate, soil, fire and herbivory. Anthropogenic modifications and interventions have rapid and long-lasting legacies on the landscapes. Several major changes have occurred over the past few centuries in northern Tanzania - including defaunation, increasing agricultural area, population increases, re-faunation and protected area designations, deforestation/afforestation, introduced species, topsoil erosion, and emerging pollutants. As part of a multidisciplinary project on trajectories of land use and land cover changes across the western Serengeti, Tanzania, we use Quaternary science approaches that couple palaeoenvironments with archaeology and historical ecology to generate a temporal context to modern changes. A lacustrine sediment core was collected in Speke's Gulf, southern Lake Victoria, that was lead-210 dated using gamma spectroscopy and analysed for physical sedimentology, charcoal and pollen. The sediment core provides a record of land cover changes over the past 200 years and can be compared with local oral histories, colonial government records, historical maps and air photographs, and published datasets. Initial data shows a decreasing pattern of organic content in the sediments and decreasing clay content. Silts increase after the mid-nineteenth century, as populations increased, agricultural expansion continued, and deforestation may have contributed to increased erosion of several river systems flowing into the southeastern quadrant of Lake Victoria (see also Dutton et al., 2019 Sci of Total Env 664: 148-160). The lake sediment record aggregates an environmental change signal from several ecosystem components, such as savannahs, riverine, woodlands and montane forests. European descriptions of the area emerge missionary workers in the mid1800s and from explorers and sporthunters from 1890s-1920s; mining prospectors 1920s-1960s, and park wardens and ecologists 1950s onward. Compiling local histories with palaeoenvironmental datasets improves the resolution and interpretation of the complementing datasets. The data adds to our understanding of regional land cover and land use changes in an area with several UNESCO world heritage sites, and competing yet lucrative land use activities (ecotourism, agriculture, and mining).

8.7

Cotencher cave: a site with an exceptional preserved sedimentary sequence recording Late Pleistocene climatic and environmental changes in Swiss Jura Mountains

Judit Deák[1], Frank Preusser[2], François-Xavier Chauvière[1]

[1]Office du patrimoine et d'archéologie Neuchâtel, section Archéologie, Laténium, espace Paul-Vouga, CH-2068 Hauterive (judit.deak@ne.ch)
[2]Sedimentary Geology and Quaternary Research, Institute of Earth and Environmental Sciences, University of Freiburg

The heterometric and colorful sedimentary sequence of Cotencher cave (Jura Mountains, Neuchâtel) attracted the attention of scientific community since more than 150 years. This site is famous for its Mousterian archaeological finds and for animal remains belonging to more than 60 species: some of them already completely extinct (ex: *Ursus spelaeus, Panthera leo spelea*) ; others living in markedly colder environments compared to the ones prevailing in our region (ex*: Rangifer tarandus, Vulpes lagopus*); and some of them still living in the studied area (ex: Capra rupicapra, Capra ibex). Palaeontological, archaeological and geaorchaeological studies performed in the past highlighted already climatic changes recorded by palaeontological remains and by sediments preserved in this cavity. In addition, these investigations attempted already to link the observed feature with a complex history of glaciers passages in the region.

The geaorchaeological study carried out since 2016 in the frame of interdisciplinary *Cotencher Project* permitted recognition of a set of additional soil-sedimentary characteristics, that allowed a novel understanding of processes responsible for deposition of these sediments and their archaeological and palaeontological components. Our interdisciplinary study permitted also to unravel and date climatic events that where little or not documented in the studied regions. This is due to the fact that during the Last Glacial Maximum most of the formers sediments have been eroded. These results reinforce the reputation of the Cotencher cave as a place of exceptional preservation of natural processes and prehistoric human activities.

REFERENCES

Deák, J., Preusser, F., Cattin, M.-I., Castel, J.-C., and Chauvière, F.-X.: New data from the Middle Palaeolithic Cotencher cave (Swiss Jura): site formation, environment, and chronology, E&G Quaternary Sci. J., 67, 41–72, https://doi.org/10.5194/egqsj-67-41-2019, 2019.

8.8

Tracking the Pace of Landscape Evolution during the Deckenschotter Times

Catharina Dieleman[1], Marcus Christl[2], Christof Vockenhuber[2] & Naki Akçar[1]

[1]Institut für Geologie, University of Bern, Baltzerstrasse 1+3, CH-3012 Bern (catharina.dieleman@geo.unibe.ch)
[2]Laboratory of Ion Beam Physics, ETH Zurich, Otto-Stern-Weg 5, 8093 Zurich

Swiss Deckenschotter document the landscape changes in the northern Alpine Foreland during the Early and Middle Pleistocene. They are characterised by a succession of glacio-fluvial sediments intercalated with glacial and/or overbank deposits (Graf, 1993). This succession has been separated into Höhere Deckenschotter (HDS) and Tiefere Deckenschotter (TDS) by a significant phase of incision (Graf and Müller, 1999). During the Quaternary, glaciers overrode the Swiss northern Alpine Foreland at least 13 times, of which the pace of eight advances can be tracked in the HDS and TDS sequences (Schlüchter, 1988). They have been for a long time correlated with the Günz and Mindel glaciation after Penck and Brückner. HDS were attributed to the Günz glaciation and TDS to the Mindel. The landscape evolution during the Deckenschotter time is still poorly understood as well as their chronology. Recently, HDS and TDS deposits were dated using depth-profile, burial and isochron-burial dating techniques and a new chronology has been established. This chronology suggests that HDS and TDS are around 2 Ma and around 1 Ma old, respectively (Akçar et al., 2014, 2017; Claude et al., 2017, 2019)Swiss Geological Society.The Swiss Deckenschotter ("cover gravels". However, the existing chronology based on mammal fossils found in one site at Irchel, which are attributed to Neogene Mammal Zone 17 (2.5 – 1.8 Ma; Bolliger et al., 1996) is challenged by the new one, since 2 Ma old deposits are located at the same morphostratigraphical position as 1 Ma old ones (Claude et al., 2019). Therefore, how far can the approach "*same elevation means same age*" explain the chronology? Within this context, we focus, in this study, on the Deckenschotter deposits at Irchel, the area around Mandach and Lake Constance, in order to reconstruct the timing of the Early and Middle Pleistocene glaciations with isochron-burial dating and to implement these results into a more complex landscape evolution model than thought so far.

To achieve these goals, eleven new Deckenschotter sites were selected after a reconnaissance study in the field: three HDS sites at Irchel, three HDS and three TDS sites in the area around Mandach, as well as one HDS and one TDS site in the region of Lake Constance. We applied following strategy for sampling in the field: one sediment sample consisting of quartz pebbles and at least nine clasts of different sizes, shape and lithology per site were sampled. After the quartz isolation from these samples, five samples (with the lowest total Al concentration) and the sediment sample were further processed for the cosmogenic ^{10}Be and ^{26}Al analysis at the accelerator mass spectrometry facilities at ETH Zurich. In addition, sedimentology at the sampling sites will be analysed to reveal the sediment source, paleoflow regime, transportation mechanisms and depositional environment. First results will be presented.

REFERENCES

Akçar, N., Ivy-Ochs, S., Alfimov, V., Claude, A., Graf, H.R., Dehnert, A., Kubik, P.W., Rahn, M., Kuhlemann, J., Schlüchter, C. 2014: The first major incision of the Swiss Deckenschotter landscape. Swiss J. Geosci. 107, 337–347. https://doi.org/10.1007/s00015-014-0176-6

Akçar, N., Ivy-Ochs, S., Alfimov, V., Schlunegger, F., Claude, A., Reber, R., Christl, M., Vockenhuber, C., Dehnert, A., Rahn, M., Schlüchter, C. 2017: Isochron-burial dating of glaciofluvial deposits: First results from the Swiss Alps. Earth Surf. Process. Landforms 42, 2414–2425. https://doi.org/10.1002/esp.4201

Bolliger, T., Fejfar, O., Graf, H., Kaelin, D. 1996: Vorläufige Mitteilung über Funde von pliozänen Kleinsäugern aus den höheren Deckenschottern des Irchels (Kt. Zürich). Eclogae geol Helv 89, 1043–1048.

Claude, A., Akçar, N., Ivy-Ochs, S., Schlunegger, F., Kubik, P.W., Christl, M., Vockenhuber, C., Kuhlemann, J., Rahn, M., Schlüchter, C. 2019: Changes in landscape evolution patterns in the northern Alpine Foreland during the. Geol. Soc. Am. Bull. 1–23. https://doi.org/10.1130/B31880.1/4691963/b31880.pdf

Claude, A., Akçar, N., Ivy-Ochs, S.D., Schlunegger, F., Kubik, P.W., Dehnert, A., Kuhlemann, J., Rahn, M., Schlüchter, C. 2017: Timing of early Quaternary gravel accumulation in the Swiss Alpine Foreland. Geomorphology 276, 71–85. https://doi.org/10.1016/j.geomorph.2016.10.016

Graf, H.R. 1993: Die Deckenschotter der zentralen Nordschweiz. ETH Zurich.

Graf, H.R., Müller, B. 1999: Das Quartär: Die Epoche der Eiszeiten., in: Bolliger, T. (Ed.), Geologie Des Kantons Zürich. Thun: Ott Verlag, pp. 71–95.

Schlüchter, C. 1988: The deglaciation of the Swiss-Alps : a paleoclimatic event with chronological problems. Bull. l'Association française pour l'étude du Quat. 25, 141–145. https://doi.org/10.3406/quate.1988.1875

8.9

Deformation features in glacially overridden karst: evidence for subglacial hydrofracturing?

Lukas Gegg[1], Marius W. Buechi[1], Andreas Ebert[2], Gaudenz Deplazes[3], Herfried Madritsch[3], & Flavio S. Anselmetti[1]

[1]Institute of Geological Sciences & Oeschger Centre for Climate and Climate Change Research, University of Bern, Baltzerstrasse 1+3, CH-3012 Bern (lukas.gegg@geo.unibe.ch)
[2]Geo Explorers AG, Wasserturmstrasse 1, *CH*-4410 Liestal
[3]National Cooperative for the Disposal of Radioactive Waste (Nagra), Hardstrasse 73, CH-5430 Wettingen

Water pressures at the ice-bed interface of warm-based and polythermal glaciers are known to undergo extreme fluctuations, e.g. during jökulhlaups. Consequently, evidence for the interaction of pressurized subglacial water with the bed substrate is well-known from modern and ancient subglacial settings (Van der Meer et al., 2009). We present what could be considered the expression of such an interaction below a Mid-Pleistocene glacial overdeepening in the Swiss Alpine foreland.
Our project investigates the overdeepened section of the Lower Aare Valley, at the confluence of the Aare with Reuss and Limmat. Right below the sedimentary infill of the valley, one of our scientific boreholes – QBO Gebenstorf-Brüel – recovered heavily karstified Jurassic limestones in a depth of >100 m (Fig. 1, Gegg et al., in prep.). The karst conduits are infilled by blue clay of presumably Eocene age ("Boluston"). Besides phenomena attributed to karstification, we observe an intense brecciation of the karstified limestone accompanied by the intrusion of the clayey karst filling into fractures of the cavity walls and microstructures indicative for viscous deformation in the clay matrix.
While a tectonic origin of these overprinting phenomena is quite likely considering the local setting (e.g. Miocene brittle faulting related to the formation of the adjacent Jura fold-and-thrust belt), our contribution will also discuss how these fracturing and injection features could relate to high-pressure water pulses at the former ice-bed contact in a major overdeepening.



Fig. 1: Karstified and brecciated limestone from drillhole Gebenstorf-Brüel (116.2-116.5 m depth)

REFERENCES

Gegg, L., Kuster, A.M., Deplazes, G., Madritsch, H. & Buechi, M.W. (in prep.): Quaternary borehole QBO Gebenstorf-Brüel (QGBR) data report, Nagra Arbeitsbericht NAB 19-02.

Van der Meer, J.J.M., Kjær, K.H., Krüger, J., Rabassa, J. & Kilfeather, A.A. 2009: Under pressure: clastic dykes in glacial settings, Quaternary Science Reviews 28, p. 708-720.

8.10

A glimpse of the sedimentary history of the Rhine Valley, eastern Switzerland – new contribution from quartz OSL dating.

A.J. Heer[1],°

[1]Institute of Geography, University of Bern, Hallerstrasse 12, CH-3012 Bern
°Corresponding author; Email: heer@giub.unibe.ch; Telephone: 0041 79 607 5125;

At the 13th of October 2018 a fragment of late Roman belt plaque ("Propellerbeschlag") was found in a construction pit in the small alpine town of Bad Ragaz, Rhine Valley, eastern Switzerland. The related sedimentary profile (from the top to the bottom) contained: loamy colluvium of loess origin, cross bedded sands and gravels of the Rhine River including intercalated smaller soil and colluvium layers; and finally massive, coarse gravels interpreted as sediments of the Late Glacial Rhine River. The presence of the belt plaque and the funds awarded from the Archaeological Survey of the Kanton St. Gallen, opened the unique opportunity to apply OSL dating to the sediments in order to contribute to better understanding of the postglacial landscape history of the Rhine Valley and of the human settlement after the glacial meltdown. Because it has been anticipated that incomplete bleaching may be an issue, loess sediment from neighbouring "Tiergarten" Rock in the Seez Valley was included in the dating.

Based on a total of eleven OSL samples grouped in three profiles, two radiocarbon samples, the archaeological determination of the age of the belt plaque fragment and the known historical and pre-historical events in the Rhine and Seez Valleys, 16000 years of landscape history and up to 2000 years of human settlement had been confirmed in the research site by this study. To the extend known, this was the first application of the quartz OSL dating to the sediments in this part of the Rhine and Seez Valleys. In particular, the investigation of the loess revealed a thermally unstable medium component. The young colluvium samples were challenging due to the quartz's low sensitivity and the often poor sediments' bleaching.

REFERENCES

Ivy-Ochs S. et al. 2008. Chronology of the last glacial cycle in the European Alps. JQS 23(6-67) 559-573
Heer A.J., Adamiec G., Moska P. 2012. How many grains are there on a single aliquot? Ancient TL Vol. 30 No. 1

8.11

Impact of climate change on the conservation of paleolotihic paintings in caves

Pierre-Yves Jeannin[1], Frédéric Doumenc[2], Beatrice Guerrier[2]

[1]Swiss Institute for Speleology and Karst-Studies, SISKA (pierre-yves.jeannin@isska.ch)
[2]Laboratoire FAST, Univ. Paris-Sud, CNRS, Université Paris-Saclay, F-91405, Orsay, France

Weathering processes in caves are weak and slow. Most usual weathering processes are in fact strongly reduced in fossil caves: no rain, no frost, no overheating by solar radiation, no vegetation, no light and UV, no life. Time is “stopped” in caves.
This is why many archaeological artifacts are found in caves all over the world.
However, to what extent is it really true? Why some Paleolithic paintings are damaged or even disappeared? Are all caves really the same?

The answer is clearly “no”! Active caves (traversed by significant water fluxes) are exposed to some dissolution and erosion. Among fossil caves, there is a transition zone between the deep part of the cave (or of the karst massif) and the outside conditions (heterothermic zone). In this zone, condensation of air humidity on cave walls may be quite significant. It leads to the formation of a water film on the wall, which can dissolve the rock surface. This humid surface is also a favorable place for bacteria to develop. These microorganisms may influence the chemistry of the thin water film at the wall, possibly leading to more complex weathering processes. For example, vermiculations are patterns of particles formed on cave walls. Under some circumstances, particles “glued” on cave wall since “ever” (e.g. Paleolithic paintings) may migrate (damaging the paintings). This process threatens some of the paintings of Lascaux cave, and is thus being investigated in detail.

Condensation is controlled by the convection of outside air into the cave, which is defined by heat exchange between the respective temperature of the rock, of cave air and of outside air.

Temperature contrasts always lead to condensation or evaporation conditions at cave walls. Long term simulations of rock and air temperature in Lascaux cave (France) indicates that, after a change in outside temperature, it takes at least 50 years for the rock to be in equilibrium with the regional climate. During this period of time, more condensation than usual will take place, leading to more water, bacteria, dissolution and vermiculations… In other words, climate change seems to accelerate the weathering of some archaeological features in caves.

8.12

Mapping bedrock topography of the Lower Aare valley using seismic surface waves

Lorenz Keller[1], Giancarlo Dal Moro[2], Thomas Spillmann[3], Gaudenz Deplazes[3], & Herfried Madritsch[3]

[1]roXplore gmbh, Oberfeldstrasse 6, CH-8514 Amlikon (lorenz@roxplore.ch)
[2]Eliosoft, IT-Udine
[3]Nagra, Hardstrasse 73, CH-5430 Wettingen

The knowledge of bedrock topography of glacially overdeepend Quaternary valleys provides important constraints to the layout of geological repositories for radioactive waste materials in Switzerland (Nagra, 2008). For this reason Nagra currently investigates these valleys at various locations including the Lower Aare Valley around the village of Gebenstorf where the Aare river dissects the Jura Mountains (cf. poster presentation by Gegg et al. 2019). It is a challenging exploration area with limited possiblities for drillings and difficult geophysical surveying conditions.

In spring 2019, we conducted a seismic 2D test survey in the area using combinations of active and passive surface wave data. Test objectives were (1) to validate seismic surface wave analyses methodologies for mapping bedrock topography below Quaternary deposits of up to 100 m thickness, and (2) optimising field parameters for a possible later extension of the survey.

The exploitation of active and passive data collected by a single 3C sensor as well as by 2D geophone arrays facilitated the survey design in an area where geophysical surveying is challenged by rivers, transport infrastructure and dense population. The finally selected crooked-line layout consisted of three types of measurements:

(I) Ambient microtremor measurements at 38 evenly spaced stations.
Each station provided a fundamental frequency from horizontal to vertical spectral ratio (H/V ratio) analyses.

(II) Active data (sledgehammer source and 3C geophone) on every 3rd station.
Joint inversion of Rayleigh wave group velocity spectra and H/V ratio provided shear wave velocity information in the form of 1D depth profiles.

(III) Ambient microtremor measurements with L-shaped geophone arrays (array dimension 90 x 190 m) over the central part of the Quaternary valley. The outcome of the array analyses are 1D shear wave velocity profiles with higher accuracy in areas with deeper Quaternary sediments.

Figure 1 shows the processed H/V ratio with picks of the fundamental frequency along the profile. The fundamental frequency is well constrained on sections where Quaternary sediments overlay Malm limestone. Ambiguous H/V ratios that appear in the eastern part of the line indicate that Molasse rocks (mainly silt-/sandstone, marl) between Malm limestone and Quaternary units likely influence our depth analyses.

We averaged the shear wave velocities of overlaying sediments in horizontal direction and used such mean shear wave velocities at each station to convert the peak frequency of the H/V curves to bedrock depths according to Roesset (1970). Obtained depth estimations correspond very well with the base Quaternary depth of 65 m that was observed in the recent Gebenstorf-Vogelsang (QGVO; Gegg et al. 2019) borehole (Figure 1). This validation confirms a high accuracy of our bedrock depths in areas with high impedance contrast between bedrock and overlaying sediments. Ambiguities in our analyses may lead to inaccurate depth estimates in the eastern section of the test line (distance larger than 1000 m in Figure 1).

In conclusion, the surface wave measurements provided accurate constraints to the base of the Quaternary valley.

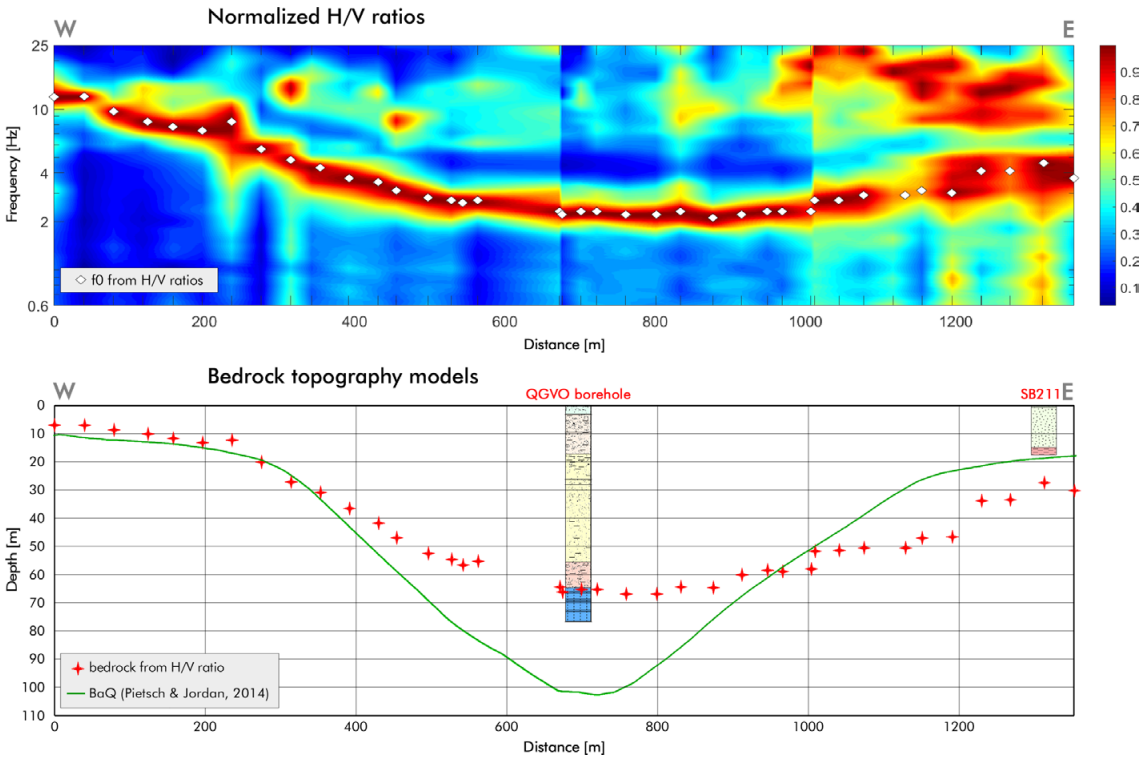


Figure 1. Top: Normalized H/V ratio curves along the test line.
Bottom: Reconstructed bedrock depths (red crosses) and a-priori bedrock model by Pietsch & Jordan (2014; green line).

REFERENCES

Gegg L., Buechi M.W., Deplazes G., Madritsch H., Mueller D., Preusser F. & Anselmetti F.S. 2019: The glaciation history of the overdeepened Lower Aare Valley: insights from scientific drilling and outcrop data. Swiss Geoscience Meeting 2019.

Nagra 2008: Vorschlag geologischer Standortgebiete für ein SMA- und ein HAA-Lager: Geologische Grundlagen. Nagra Technischer Bericht NTB 08-04. Nagra, Wettingen, Schweiz.

Pietsch, J. & Jordan, P. 2014: Digitales Höhenmodell Basis Quartär der Nordschweiz – Version 2014 und ausgewählte Auswertungen. Nagra Arbeitsbericht NAB 14-02. Nagra, Wettingen, Schweiz.

Roesset, J.M. 1970: Fundamentals of soil amplification. In: Hansen R. (ed) – Seismic design of nuclear power plants. Cambridge/Mass, 489pp.

8.13

Late-glacial to Holocene sediment dynamics in high Alpine regions (Sanetsch Pass, Switzerland)

Elena Serra[1,2] Pierre G. Valla[3,1,2] Natacha Gribenski[1,2] Fabio Magrani[1,2] Julien Carcaillet[3] Reynald Delaloye[4] Bernard Grobety[4] Luc Braillard[4]

[1]*Institute of Geological Sciences, University of Bern, Switzerland*
[2]*Oeschger Centre for Climate Change Research, University of Bern, Switzerland*
[3]*Institute of Earth Sciences, Univ. Grenoble Alpes, CNRS, Univ. Savoie Mt Blanc, IRD, IFSTTAR,, France*
[4]*Department of Geosciences, University of Fribourg, Switzerland*
(elena.serra@geo.unibe.ch)

Widespread loess deposits accumulated during the last glaciations in low-elevation regions of Europe, and are often used as paleo-environmental archives (e.g. Muhs, 2013; Martignier et al., 2015). High-elevation aeolian deposits occur also in the European Alps and the Jura Mountains where they have been interpreted as proxies for Late-glacial glacier retreat (Montandon, 1940; Spaltenstein, 1985). However, active geomorphic processes result in complex sediment dynamics within high Alpine regions which may prevent the direct use of such aeolian deposits as paleo-environmental indicators.

This study aims to deepen our understanding of pre- and post-depositional histories of high-altitude aeolian deposits located in formerly glaciated alpine settings. We focus on the Sanetsch Pass (Switzerland), where aeolian-like sediments were identified on a high-elevation platform covered by patterned ground (2680 m a.s.l.) as well as in the stratigraphy of an alluvial fan located in the fluvio-glacial plain at lower altitude (2100 m a.s.l.). Our multi-methodological approach, combining stratigraphy, sedimentology, micromorphology, mineralogy, geochemistry and geochronology (TCN and OSL), allows us to constrain the sediment provenance, the processes and timing of sediment deposition/reworking, and to propose a possible connectivity between the two investigated sites (i.e. sediment cascade).

Our results suggest that the sediments from the high-elevation platform are a primary aeolian deposit with allochthonous origin, deposited before or during the Younger Dryas (YD, 12.9-11.6 ka ago) and then affected by cryoturbation. Following YD glacier retreat, widespread aeolian deposits in the Sanetsch area, bedrock derived and glacial deposits were transported away from the slopes and accumulated in the fluvio-glacial plain, rapidly building up alluvial fans (12.3-9.1 ka ago) that were periodically submerged by an ephemeral ice-dammed lake (10.6-10.1 ka ago). This paleo-environmental reconstruction highlights the complex sediment dynamics and potential post-deposition processes occurring in high-elevation Alpine settings, making therefore aeolian sediments not immediately suitable as paleo-environmental proxies. Overall, this study demonstrates the importance of a multimethodological approach to reconstruct sediment dynamics and connectivity which may link distinct geomorphic landforms in high Alpine regions.

REFERENCES

Martignier, L., Nussbaumer, M., Adatte, T., Gobat, J.M. and Verrecchia, E.P., 2015: Assessment of a locally-sourced loess system in Europe: The Swiss Jura Mountains, Aeolian Research, 18, 11-21.

Montandon, F., 1940: Le loess d'Evionne (Valais), Études Rhodan, 16, 75-103.

Muhs, D.R., 2013: The geologic records of dust in the Quaternary, Aeolian Research, 9, 3-48.

Spaltenstein, H., 1985: Caractérisation de deux sols alpins minces sur calcaire dur dans le lapiaz du Sanetsch, Bulletin de la Société vaudoise des sciences naturelles, 77(367), 245-254.

8.14

Mediterranean rainfall variability and its phase relationship with the African monsoon – A 1.36 million year record from Lake Ohrid (N Macedonia & Albania)

Hendrik Vogel[1], Bernd Wagner[2], Alexander Francke[3], Tobias Friedrich[4], Timme Donders[5], Jack H. Lacey[6],Melanie J. Leng, Eleonora Regattieri, Laura Sadori, Thomas Wilke, Giovanni Zanchetta, Christian Albrecht, Adele Bertini, Nathalie Combourieu-Nebout, Aleksandra Cvetkoska, Biagio Giaccio, Andon Grazhdani, Torsten Hauffe, Jens Holtvoeth, Sebastien Joannin, Elena Jovanovska, Janna Just, Katerina Kouli, Ilias Kousis, Andreas Koutsodendris, Sebastian Krastel, Markus Lagos, Niklas Leicher, Zlatko Levkov, Katja Lindhorst, Alessia Masi, Martin Melles, Anna M. Mercuri, Sebastien Nomade, Norbert Nowaczyk, Konstantinos Panagiotopoulos, Odile Peyron, Jane M. Reed, Leonardo Sagnotti, Gaia Sinopoli, Björn Stelbrink, Roberto Sulpizio, Axel Timmermann, Slavica Tofilovska, Paola Torri, Friederike Wagner-Cremer, Thomas Wonik & Xiaosen Zhang

[1]Institute of Geological Sciences & Oeschger Centre for Climate Change Research, University of Bern, Baltzerstr. 1+3, 3012 Bern, Switzerland (hendrik.vogel@geo.unibe.ch)
[2]Institute of Geology and Mineralogy, University of Cologne, Germany
[3]School of Earth, Atmospheric, and Life Science, University of Wollongong, Wollongong, New South Wales, Australia
[4]International Pacific Research Center, University of Hawaii at Manoa, Honolulu, HI, USA
[5]Palaeoecology, Department of Physical Geography, Utrecht University, Utrecht, The Netherlands
[6]National Environmental Isotope Facility, British Geological Survey, Nottingham, UK

Mediterranean climates are characterized by strong seasonal contrasts between dry summers and wet winters. Changes in winter rainfall are critical for the regional socioeconomic development but are difficult to simulate accurately and reconstruct on Quaternary timescales. This is partly because the underlying mechanisms of change and their persistence remain unexplored.

A multinational science team co-sponsored by the ICDP recovered sedimentary drill core records from Lake Ohrid (N Macedonia, Albania) in 2013 capturing the entire sedimentary sucession. The DEEP record from the lake depocenter covers the past 1.36 Myrs continuously and sensitively records changes in the regions hydrology, thereby enabling the analysis of Mediterranean rainfall variability in response to different underlying orbital geometries, global ice volume and atmospheric greenhouse gas concentrations over multiple glacial–interglacial cycles. The record suggests that, over the past 1.36 Myrs, wet winters in the northcentral Mediterranean tend to occur with high contrasts in local, seasonal insolation and a vigorous North African summer monsoon. Our proxy time series from Lake Ohrid, together with a 784 kyr transient climate model hind cast, further suggests that increased sea-surface temperatures amplify local cyclogenesis while also refueling North Atlantic low-pressure systems that enter the Mediterranean during phases that are characterized by low continental ice volume and high atmospheric carbon dioxide concentrations. Comparison with modern reanalysis data shows that current drivers of the amount of rainfall in the Mediterranean share some similarities to those that drive the reconstructed increases in precipitation.

8.15

Late-Quaternary inverted palaeochannels record high precipitation rates and episodic flooding in the Sahara: Implications for Holocene human dispersal

Abdallah S. Zaki [a1], Mathieu Schuster[b], Robert Giegengack[c], Sanjeev Gupta[d], Negar Haghipour[e], Georgina E. King[f], Frédéric Herman[f], Mostafa El-wakil[g], Hossam Khairy[g], Salah Ahmed[g], Saleh A. Eltayeb[h], Stephen E. Watkins[a], Sébastien Castelltort[a]

[a1] *Department of Earth Sciences, University of Geneva, Geneva, Switzerland. (Abdallah.zaki@etu.unige.ch)*
[b] *Institut de Physique du Globe de Strasbourg, UMR7516, CNRS, Strasbourg Cedex, France*
[c] *Department of Earth & Environmental Science, University of Pennsylvania, Philadelphia PA USA*
[d] *Department of Earth Sciences and Engineering, Imperial College London, UK*
[e] *Geological Institute, ETH Zürich, Zürich, Switzerland*
[f] *Institute of Earth Surface Dynamics, University of Lausanne, Lausanne, Switzerland*
[g] *Geological Survey of Egypt, Cairo, Egypt*
[h] *Department of Geology, University of Aswan, Aswan, Egypt*

Palaeodischarge and sediment load estimates of the Nile River, cave speleothems, dust fluxes, fossil groundwater, and abrupt fluctuations of lake levels suggest climate oscillation during the Late Quaternary over the eastern Sahara (e.g., Foucault and Stanley, 1989; Hoffmann et al., 2016). In the southern part of the Egyptian Sahara, remnants of Late Quaternary rivers are well preserved as inverted river channels (Giegengack, 1968; Zaki and Giegengack, 2016) (Fig. 1). Artifacts and pottery shards collected from sediments deposited in these rivers indicate that they are of Late Quaternary ages. The objectives of this study are: (1) to estimate precipitation rates throughout the Late Quaternary climate oscillation based on palaeohydrologic reconstructions, through measurements of median grain sizes (D50) and channel geometries; and (2) to constrain the absolute ages of these rivers by employing ^{14}C and Optically-Stimulated Luminescence dating (OSL). Our reconstructions of palaeoprecipitation values indicate that precipitation rates were in the range of 60 to 70 ($\pm$17) mm/h (Fig. 1). These rates of precipitation are huge compared to modern analogs, including Brule River near Florence WI (0.152 mm/h) and Catherine Creek at Montour Falls (1.1. mm/h). Although one sample yielded a date of 11,055 ± 107 years, the ^{14}C ages of six samples collected from three of the paleochannels yielded ages of 7,097 ± 87 to 8,839 ± 105 years for five samples. These ages coupled with estimates of precipitation rates provide quantitative support to the model of Kuper and Kröpelin (2006), according to which dispersal of human settlements from the southern part of the Egyptian Sahara to the northwestward 8,500 to 7,000 years ago was a direct response of a climatic perturbation towards hazardous environments. Potentially, our geochronological results define for the first time, the period over which such climatic conditions persisted, and prevented human reoccupation.

ACKNOWLEDGEMENTS
This work is funded by the Swiss Confederation excellence fellowships program (fellowship No: 2017.1006).

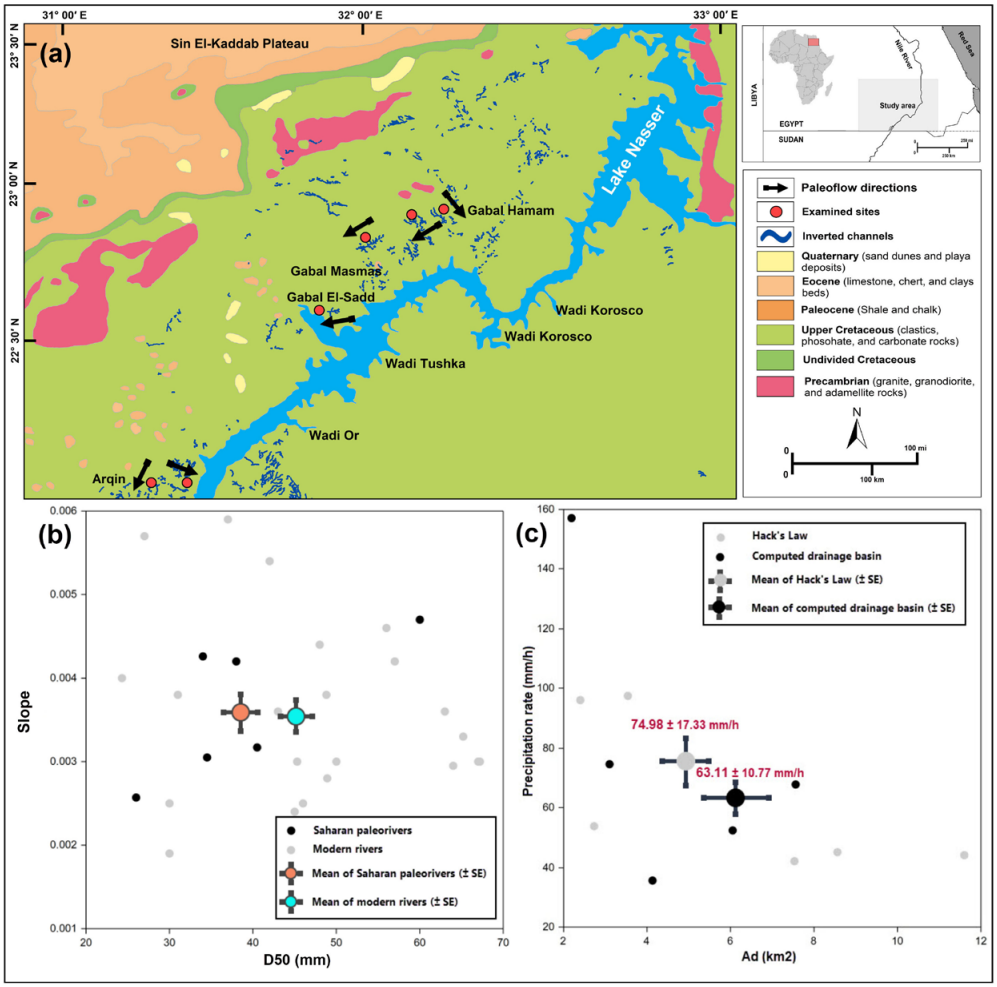


Fig. 1. (**a**) Geological map of southern Egypt showing the distribution of inverted palaeorivers. Red dots indicate the selected inverted river channels. (**b**) Plots of D50 and calculated paleoslopes of the inverted palaeorivers in the context of real measurements from modern rivers. (**c**) Palaeoprecipitation rates based on computed drainage area over the inverted paleorivers, following Hack's law.

REFERENCES

Zaki, A. S., Giegengack, R., 2016. Inverted topography in the southeastern part of the Western Desert of Egypt. Journal of African Earth Sciences 121, 56-61.

Foucault, A., and Stanley, D.J., 1989. Late Quaternary paleoclimatic oscillations in East Africa recorded by heavy minerals in the Nile delta: Nature, 339,44–46.

Hoffmann, D. L., Rogerson, M., Spötl, C., Luetscher, M., Vance, D., Osborne, A., Fello, N., Moseley, G. (2016). Timing and causes of North African wet phases during the last glacial period and implications for modern human migration, Sci. Rep.-UK, 6, 36367, https://doi.org/10.1038/srep36367, 2016.

Giegengack, R.F., 1968. Late Pleistocene History of the Nile Valley in Egyptian Nubia.Unpublished Ph.D. Thesis, Yale University.

Kuper, R., Kröpelin, S., 2006. Climate-controlled Holocene occupation inthe Sahara: Motor of Aftica's evolution. Science 313, 803–807.

P 8.1

Reconstructing the landscape evolution of Northern Switzerland using overdeepened glacial basins

Marius W. Buechi[1], Gaudenz Deplazes[2], Lukas Gegg[1], Angela Landgraf[2], Herfried Madritsch[2] & Flavio S. Anselmetti[1]

[1]Institut für Geologie & Oeschger-Zentrum für Klimaforschung, Baltzerstrasse 1+3, 3012 Bern (marius.buechi@geo.unibe.ch)
[2]Nagra, Hardstrasse 73, 5430 Wettingen

Glacial overdeepenings are excellent archives for the glaciation history and the Quaternary landscape evolution of Northern Switzerland. The spatial coverage of well-studied overdeepened basins, however, is low and the significance of these individual studies at a more regional scale remains to be clarified. We present the status and first results of an ongoing research project in which we investigate some of the most prominent overdeepened glacial basins between the Aare and Rhine Rivers in Northern Switzerland.

The investigations focus on two main research goals: 1) Refining the Middle to Late Pleistocene glaciation history of Northern Switzerland using a combination of the sedimentary archives in glacially overdeepened basins and former fluvial channels. 2) Identifying the mechanisms and controls of overdeepening subglacial erosion. We use a multi-method approach – including geophysical methods and scientific drilling – to characterise the geometry, sedimentary infill and age of these overdeepenings. Furthermore, these data allow us to study the relationship of overdeepened basins with bedrock and other elements of the Quaternary glacial landsystem.

P 8.2

Last Glacial Maximum glaciation in the Jura mountains

Claudia Burkhalter[1], Vincent Bichet[2], Susan Ivy-Ochs[3], Naki Akçar[1]

[1]Geologisches Institut, University of Bern, Baltzerstrasse 1+3, CH-3012 Bern (claudia.burkhalter@students.unibe.ch)
[2]Laboratoire Chrono-environment, Université de Franche-Comté, 16 route de Gray, 25030 Besançon cedex, France
[3]Labor für Ionenstrahlphysik , ETH Zürich, Otto-Stern-Weg 5, CH-8093 Zürich

During the Last Glacial Maximum (LGM; 22.1 ± 4.3 ka; Shakun and Carlson, 2010), a local ice-cap covered the Jura Mountains.
Outlet glaciers advanced all the way down to the lowlands, and reached amongst others the valley d'Ain. Glaciers blocked the Ain River and caused the building of an ice-dammed lake in the valley. As the glacial geomorphic features and deposits have not been subjected to building, construction and/or production activities, they are well-preserved. LGM advance and deglaciation of the glaciers are geomorphologically well documented (J.F. Buoncristiani & M. Campy 2004, C. Kasse 2013). However, their chronology is only reconstructed indirectly, for instance, by analysing the palynology of the lacustrine deposits, counting of annual varves in the lake sediments and correlating the stable isotopes (e.g., $\delta^{18}O$) with the global marine isotope stages (J.F. Buoncristiani & M. Campy 2004)).

The aim of this study is to explore the Late Pleistocene deposits and related geomorphologic features in the valley d'Ain in detail and to reconstruct the chronology of the glacio-lacustrine deposits. To reach this goal, a detailed geomorphological map will be prepared. In addition, detailed sedimentological analysis (grainsize distribution, clast petrography, morphometry and fabric)will be conducted to investigate the catchment area, transport mechanisms and depositional environment. In the end, the chronology of the sediments will be reconstructed by depth-profile dating with terrestrial cosmogenic nuclides.

REFERENCES

Buoncristiani Jean-Francois & Campy Michel 2004: Expansion and retreat of the Jura ice sheet (France) during the last glacial maximum, Sedimentary Geology 165, 253-264

Kasse Cornelis 2013: Fluvial response to rapid high-amplitude lake-level changes during the Late Weichselian and early Holocene, Ain River valley, Jura, France, Boreas, Vol 43, 403-421

Shakun Jeremy D. & Carlson Anders E.: A global perspective on Last Glacial Maximum to Holocene climate change, Quarternary Science Reviews 29, 1801-1816

P 8.3

Different lacustrine pockmark systems in Lake Thun, Switzerland, and their potential influence on the hydrological and biogeochemical budget of the lake

Adeline N.Y. Cojean[1], Maciej Bartosiewicz[2], Moritz F. Lehmann[2], Katrina Kremer[3] and Stefanie B. Wirth[1]

[1]Centre for Hydrogeology and Geothermics, University of Neuchatel, Rue Emile-Argand 11, CH-2000 Neuchâtel (adeline.cojean@unine.ch)
[2]Department of Environmental Sciences, University of Basel, Bernoullistrasse 30, CH-4056 Basel
[3]Swiss Seismological Service (SED), ETH Zürich, Sonneggstrasse 5, CH-8006 Zürich

Pockmarks are crater-like depressions formed by upward transport of fluid and gas through the unconsolidated sediment column. The fluid flow through marine pockmarks is considered to enhance hydrological and biogeochemical exchanges between the water column and the seafloor. While a similar relevance can be expected in lakes, the importance of lacustrine pockmarks in this regard is virtually unexplored.

Lake Thun is an excellent system to study lacustrine pockmarks as it exhibits several sites with different sedimentological and biogeochemical regimes. The Daerligen pockmark site, which is located close to the mouth of the Aar river, is characterized by evident signs of methane (CH_4) ebullition, and high CH_4 concentration from ~2.4 to 8.9 mM within the sediments. At Tannmoos, spikes in electrical conductivity detected during a survey with a remotely operated vehicle (ROV) indicate a hydrological connection with the groundwater system in the Triassic bedrock. The third pockmark site is located adjacent to the rock wall of the Beatenberg karst system and might thus be associated with large groundwater discharge into the lake.

Further biogeochemical and molecular analyses (e.g. 16S rRNA sequencing) of the sediments and the water column will help to better assess the influence of methane emission and groundwater discharge via these pockmarks on the biogeochemistry and microbial community of the lake, as well as to expand our limited knowledge on the mechanism of lacustrine pockmarks in general.

P 8.4

Evolution of fluvial environments and history of human settlements on the Ticino river alluvial plain

Dorota Czerski[1], Luisa Mosetti[2], Rossana Cardani Vergani[2] & Michele Pellegrini[2], Maruska Federici-Schenardi[2], Mattia Gillioz[2], Giorgio Nogara[2], Cristian Scapozza[1]

[1]Istituto scienze della Terra, Scuola universitaria professionale della Svizzera italiana (SUPSI), Campus Trevano, CH-6952 Canobbio (dorota.czerski@supsi.ch, cristian.scapozza@supsi.ch)
[2]Sezione archeologia, Ufficio dei beni culturali del Cantone Ticino, Viale Stefano Franscini 30a, CH-6501 Bellinzona

In recent times many geomorphological and geoarchaeological studies were carried out at many locations on the Piano di Magadino (Scapozza & Opizzi, 2013). The age and stratigraphy of the deposits were determined using the radiocarbon dating method on organic matter debris and charcoals. This, combined with an accurate sedimentological characterization of the deposit, archaeological observations and dating, allowed interpreting the palaeoenvironmental conditions and depositional context for the studied sedimentary and archaeological sequences.

This contribution resumes dating and stratigraphy determined in the archeological sites in Progero (2'715'900/1'114'530, CH1903+ / LV95), Gudo (2'716'720/1'114'800; Figure 1) and Giubiasco–Palasio (2'721'902/1'114'942), for the last site the dating analysis is ongoing.

The observations together with other historical information (Scapozza, 2013) and results from other research projects on the Ticino river alluvial plain (Scapozza et al., 2017) highlighted eight phases of enhanced hydrosedimentary activity since the Bronze Age: 1500–1440 BC (Middle Bronze Age), 1285–760 BC (Late Bronze Age/Early Iron Age), 400–370 BC (Late Iron Age), 200–170 BC (Late Iron Age), 10–340 AD (Roman Period), 540–1000 AD (Early Middle Ages), 1178 AD (High Middle Ages) and 1690–1868 AD (Modern Epoch) (Scapozza & Czerski, 2019).



Figure 1. View from upslope of the archeological worksite and of the L-shaped wall on the site of Gudo, Via alla Chiesa (photo Cristian Scapozza, IST-SUPSI). The massive L-shaped wall is placed chrono-stratigraphically between the two phases of enhanced hydrosedimentary activity of the Iron Age, which suggests both a stable human settlement in the area during this time and the need to build a dam to contain river water from the valley floor and / or slope.

REFERENCES

Scapozza, C. 2013: L'evoluzione degli ambienti fluviali del Piano di Magadino dall'anno 1000 a oggi, Archivio Storico Ticinese, 153, 60-92. http://repository.supsi.ch/3155/

Scapozza, C., & Oppizzi P. 2013: Evolution morpho-sédimentaire et paléo-environnementale de la plainde fluvio-deltaïque du Ticino pendant l'Holocène récent (Canton du Tessin, Suisse), Géomorphologie : relief, processus, environnement, 19(3), 265-286. http://journals.openedition.org/geomorphologie/10289

Scapozza, C., & Czerski D. 2019: Geomorfologia della Svizzera italiana / Die Geomorphologie der Südschweiz, Archeologia svizzera, 42(2), 8-13.

Scapozza, C., Castelletti, C. & Czerski D. 2017: Nuove datazioni per la storia dell'evoluzione olocenica degli ambienti fluviali del Piano di Magadino (Cantone Ticino, Svizzera), Bollettino della Società ticinese di Scienze naturali, 105, 97-102. http://repository.supsi.ch/8625/

P 8.5

The glaciation history of the overdeepened Lower Aare Valley: insights from scientific drilling and outcrop data

Lukas Gegg[1], Marius W. Buechi[1], Gaudenz Deplazes[2], Herfried Madritsch[2], Daniela Mueller[3], Frank Preusser[3], & Flavio S. Anselmetti[1]

[1]Institute of Geological Sciences & Oeschger Centre for Climate and Climate Change Research, University of Bern, Baltzerstrasse 1+3, CH-3012 Bern (lukas.gegg@geo.unibe.ch)
[2]National Cooperative for the Disposal of Radioactive Waste (Nagra), Hardstrasse 73, CH-5430 Wettingen
[3]Institute of Earth and Environmental Sciences, Albert-Ludwigs-University Freiburg, Albertstr. 23b, D-79104 Freiburg

During the Pleistocene, extensive and repeated glaciations covered the foreland of the European Alps and carved up to several hundred meters deep trough structures, termed overdeepened valleys. These sediment traps were later, sometimes over the course of multiple subsequent glaciations, infilled with sub-, pro-, or non-glacial deposits. Therefore, overdeepened valleys can serve as excellent archives of pre-LGM glaciations, whose relics were otherwise largely obliterated by the following ice advances. However, timing and processes of formation of pre-LGM overdeepenings in the Alpine foreland are discussed controversially.

To gain insights into the pre-LGM glacial and fluvial history of Northern Switzerland and to constrain the process of subglacial erosion, we currently investigate the overdeepened section of the Lower Aare Valley as well as a nearby glaciofluvial paleochannel. Our study area is situated just beyond the local LGM, at the confluence of the rivers Aare, Reuss, and Limmat. There, the valley is deeply incised (>100 m below surface) into the substratum composed of Jurassic carbonates. The project comprises four scientific drillings and is complemented by field work.
In 2018, we recovered more than 350 m of drill cores. Here, we present first results of our sedimentological, geochronological, geotechnical as well as geophysical analyses.

REFERENCES

Gegg, L., Kuster, A.M., Schmid, D. & Buechi, M.W. 2018: Quaternary boreholes QBO Riniken 1 & 2 (QRIN1 & QRIN2) data report, Nagra Arbeitsbericht NAB 18-40.

Gegg, L., Kuster, A.M., Schmid, D., Lemke, K., Deplazes, G., Madritsch, H. & Buechi, M.W. 2019: Quaternary borehole QBO Untersiggenthal (QUST) data report, Nagra Arbeitsbericht NAB 19-01.

Gegg, L., Kuster, A.M., Deplazes, G., Madritsch, H. & Buechi, M.W. (in prep.): Quaternary borehole QBO Gebenstorf-Brüel (QGBR) data report, Nagra Arbeitsbericht NAB 19-02.

Gegg, L., Kuster, A.M., Amschwand, D., Huber, M., Deplazes, G., Madritsch, H. & Buechi, M.W. (in prep.): Quaternary borehole QBO Gebenstorf-Vogelsang (QGVO) data report, Nagra Arbeitsbericht NAB 19-03.

P 8.6

The fading ^{14}C "Bomb pulse" and consequences for geochronology

Irka Hajdas[1], Lorent Eggenschwiller[1], Mantana Maurer[1] and Maria Bellen Röttig[1]

[1]*Laboratory of Ion Beam Physics, ETH Zurich (hajdas@phys.ethz.ch)*

Radiocarbon is a naturally occurring isotope, produced by secondary cosmic rays. During the last 200 years the pristine pool of cosmogonic ^{14}C in the atmosphere and connected reservoirs (biosphere, ocean, soils etc.,), has been perturbed by human activities. Two anthropogenic effects left their imprint on the ^{14}C concentration of the atmosphere: combustion of fossil fuels leading to dilution of the atmosphere with 'old' carbon dioxide since the start of the industrial revolution (Suess effect) and nuclear tests of the 1950/60ties creating an excess of artificially produced ^{14}C (Bomb pulse). This time marker of the mid-20th century is a useful tool in numerous applications including the proposed onset of the Anthropocene (Zalasiewicz et al., 2015). Here we present results of radiocarbon analysis performed on leaves collected at various location around the world. The measured ^{14}C concentration at urban sites clearly indicate the fossil fuels component. The clean air leaves reflect the global trend of ^{14}C atmosphere 'ageing' due to the Suess effect. We discuss the implication this development has on radiocarbon based chronologies of the future radiocarbon based chronology.

REFERENCES

Zalasiewicz J, Waters CN, Williams M, Barnosky AD, Cearreta A, Crutzen P, Ellis E, Ellis MA, Fairchild IJ, Grinevald J, Haff PK, Hajdas I, Leinfelder R, McNeill J, Odada EO, Poirier C, Richter D, Steffen W, Summerhayes C, Syvitski JPM, Vidas D, Wagreich M, Wing SL, Wolfe AP, Zhisheng A, and Oreskes N. 2015. When did the Anthropocene begin? A mid-twentieth century boundary level is stratigraphically optimal. Quaternary International 383: 196-203.

P 8.7

First Beryllium-10 exposure ages from the LGM Ticino-Toce glacier

Sarah Kamleitner[1], Susan Ivy-Ochs[1], Giovanni Monegato[2], Franco Gianotti[3], Silvana Martin[4] & Marcus Christl[1]

[1]Laboratory of Ion Beam Physics, ETH Zürich, Otto-Stern-Weg 5, CH-8093 Zurich (kamsarah@phys.ethz.ch)
[2]Institute of Geosciences and Earth Resources, CNR, Via G. Gradenigo 6, I-35131 Padua
[3]Department of Earth Sciences, Università degli Studi di Torino, Via Valperga Caluso 35, I-10125 Torino
[4]Department of Geoscience, Università degli Studi di Padova, Via G. Gradenigo 6, I-35131 Padua

Recent studies underpinned by isotopic dating (Ivy-Ochs et al. 2018, Monegato et al. 2017), have greatly improved our knowledge on the timing of the Last Glacial Maximum in the Italian Alps. While detailled glacial chronologies of several foreland glaciers exist, the Verbano piedmont lobe, which was fed by the Ticino and Toce glaciers remains chronologically unconstrained. Moreover, authors greatly disagree on former ice margins and the formation age of the preserved morainic amphitheatre.
As the Ticino-Toce catchment was linked to both the Vorderrhine and the Rhone ice domes, LGM timing and extent as well as ice retreat into the mountains is of particular interest with respect to the glaciers draining to the northern sides of the Alps (Reuss & Rhine glacier).
The present study provides the first surface exposure ages from glacially deposited erratic boulders of the Verbano piedmont lobe. Numerical dating is further combined with geomorphological mapping, sedimentological data and petrographic analysis to reconstruct ice surface geometry and flow patterns of the Ticino-Toce paleo-glacier.

REFERENCES

Ivy-Ochs, S., Lucchesi, S., Baggio, P., Fioraso, G., Gianotti, F., Monegato, G., Graf, A.A., Akçar, N., Christl, M., Carraro, F., Forno, M.G., Schlüchter, C. 2018: New geomorphological and chronological constraints for glacial deposits in the Rivoli-Avigliana end-moraine system and the lower Susa Valley (Western Alps, NW Italy), Journal of Quaternary Science, 33/5, 550-562.

Monegato, G., Scardia, G., Hajdas, I., Rizzini, F., Piccin, A. 2017: The Alpine LGM in the boreal ice-sheets game, Scientific Reports, 7, 2078.

P 8.8

Traces of a large prehistoric rockfall in Lake Thun (Switzerland)

Katrina Kremer[1,2], Nora Schweizer[1], Stefano Fabbri[2], Flavio S. Anselmetti[2], Adrian Gilli[3], Stefanie B. Wirth[4]

[1]Swiss Seismological Service, ETH Zürich, Sonneggstrasse 5, CH-8092 Zurich
[2]Insitute of Geological Sciences and Oeschger Centre for Climate Change Research, University of Bern, CH-3012 Bern
[3]Geological Institute, ETH Zurich, Sonneggstrasse 5, CH-8092 Zurich
[4]Centre for Hydrogeology and Geothermics (CHYN), University of Neuchatel, Emile-Argand 11, CH-2000 Neuchatel

Rockfalls and landslides constitute major natural hazards in the Alpine realm. When triggered on slopes adjacent to lakes, rockfalls can generate impulse waves that can cause additional damage. As a result, lake sediments are excellent natural archives that can record the traces of such devastating events.

The combination of data from a high-resolution bathymetric map (multibeam), from airgun and pinger reflection seismic data and the sediment record of the first 10 m (long gravity cores) show traces of a large rockfall deposited at the northern shore area of Lake Thun. The deposits are found directly offshore of the village of Merligen where also a property Ralligen is located. The rockfall is identified by large blocks on the bathymetric map, chaotic to transparent facies on the reflection seismic profiles and by mixed sediment features in the sedimentary record. Following a historical report, a rockfall occurred in the village of Ralligen in 598/599 AD. This document also mentions ‘dead fish washed ashore’ and a ‘cooking lake’ (Fredegarius, 1888) suggesting also the occurrence of an impulse wave due to the rockfall. Radiocarbon ages reveal, however, that the rockfall deposits we observe are not related to the historical event but to a prehistoric event. The historical rockfall might be recorded further up in the sediment column by a 20 cm thick deposit of mixed sediments. In the reflection seismic, no indications for a younger mass movement have been found. Thus, the Ralligen rockfall might have been much smaller than the prehistorical rockfall.

REFERENCE

Fredegarius (1888) Chronicarum quae dicuntur Fredegarii Scholastici, Liber IV. In : Momenta Germaniae Historica (MGH) (Ed. B. Krusch), Script, Rev. Mer. 128pp.

P 8.9

The expression of Heinrich Event 2 in Alpine speleothems

Marc Luetscher[1], Gina E. Moseley[2], Ronny Boch[3], Hai Cheng[4], R. Lawrence Edwards[5], Christoph Spötl[2]

[1]Swiss Institute for Speleology and Karst Studies (SISKA), Rue de la Serre 68, CH-2301 La Chaux-de-Fonds
[2]University of Innsbruck, Institute of Geology, Innrain 52, A-6020 Innsbruck
[3]Graz University of Technology, Institute of Applied Geosciences, Rechbauerstraße 12, A-8010 Graz
[4]Institute of Global Environmental Change, Xi'an Jiaotong University, Xi'an 710049, China.
[5]Department of Earth Sciences, University of Minnesota, Minneapolis, 55455 Minnesota, USA

Terrestrial archives of the last glacial maximum (LGM) are remarkably rare across Switzerland which was largely covered with ice (Bini et al., 2009). Characterizing the LGM paleoclimate is nonetheless critical to reconstruct the glacier dynamics and thus understand processes which drove the regional landscape evolution. The Sieben Hengste cave system (7H) has revealed continuous deposition of speleothems across the LGM, suggesting that glacier build-up took advantage of enhanced southerly moisture advection between 26.5 and 23.5 ka (Luetscher et al., 2015). Surprisingly, the 7H record reveals only a buffered oxygen isotope signal at the time of Heinrich event 2. Here, we compare this original record with two new speleothems recovered nearby the initial sampling site. These stalagmites are characterized by a markedly distinct petrography indicating contrasted hydrological regimes. We discuss the paleoclimate interpretation of these groups of speleothems and suggest that the northern Alps may have been subject to enhanced summer aridity during the time period covering Heinrich stadial 2. These results are compared with regional sedimentary records and discussed with respect to the Alpine glacier dynamics during the LGM.

REFERENCES

Bini, A. et al., 2009. Switzerland during the Last Glacial Maximum (LGM). 1:500000, Federal Office of Topography Swisstopo.

Luetscher M., Boch R., Sodemann H., Spötl C., Cheng H., Edwards R.L., Frisia S., Hof F., Müller W., 2015. North Atlantic storm track changes during the Last Glacial Maximum recorded by Alpine speleothems. Nature Communications, 6:6344. doi: 10.1038/ncomms7344.

P 8.10

Investigating meromixis dynamics in varved lake sediments of Lake Jaczno, Poland using high resolution hyperspectral imaging and XRF data.

Stamatina Makri [1], Wojciech Tylmann [2], Hendrik Vogel [3], Martin Grosjean [1]

[1]University of Bern,Institute of Geography & Oeschger Centre for Climate Change Research, Bern, Switzerland (stamatina.makri@giub.unibe.ch
[2]University of Gdansk, Faculty of Oceanography and Geography, Gdansk, Poland
[3]University of Bern, Institute of Geological Sciences & Oeschger Centre for Climate Change

Lake ecosystems are very sensitive to environmental changes, of both climatic and human induced origin. Eutrophication and meromixis can occur naturally as part of the lake evolution or much faster due to external forcing, leading to altered biogeochemical cycles and anoxia. Yet, not much is known about events of paleoproductivity, meromixis and hypoxia in the past due to analytical difficulties and lack of effective proxies. The assessment of the causes and dynamics of such changes require long term, high-resolution data.

The varved lake sediment record of meromictic Lake Jaczno has so far been analyzed for the last 1700 years, revealing its great potential for a long-term assessment of the causes and dynamics of meromixis and hypoxia (Butz et al., 2017). Here we analyze a 12-meter sediment record utilizing recent developments in novel hyperspectral imaging (HSI) techniques combined with XRF scanning. This study completes a series of applications across Europe (Greece, Switzerland, and Poland). The aim is to show how and when meromixis/hypoxia established and vanished over Holocene time scales and which where the forcing factors (erosional input, land use change, climate). For this, we perform HSI scanning at very high spectral (3 nm) and spatial (40 µm pixel size) resolution, able to detect sedimentary pigments at sub-millimeter scale. We use hyperspectral indices to infer quantitatively {Chl a and chlorins} as an indicator for aquatic primary production and Bacteriopheophytin a (Bphe a) as an indicator for meromixis (Butz et al., 2016). Bphe a is a diagenetic product of Bacteriochlorophyll a, produced by anoxygenic phototrophic bacteria in the chemocline. Pigment compositions are inferred from sets of spectral indices, such as the Relative Absorption Band Depths (RABD). Indices are calibrated with absolute pigment concentrations of selected samples of the sediment sequence as measured by HPLC, using linear regression models (e.g average RMSEP of 9% or 200 µg g-1). Chronology is based on radiocarbon dating of terrestrial plant microfossils. In addition, we measured relative changes in sedimentary element composition by high resolution XRF scanning and the organic matter and carbonate content by LOI/CNS analysis.

Preliminary results show a strong link of the lake mixing regime with catchment processes. Meromixis is present during periods of a closed and more stable landscape around the lake (i.e. without human disturbance). Remarkably, meromixis is interrupted mainly by the presence of an open landscape around the lake during periods of intense deforestation and soil erosion in the catchment.

REFERENCES

Butz C, Grosjean M, Goslar T, Tylmann W, (2017): Hyperspectral imaging of sedimentary bacterial pigments: a 1700-year history of meromixis from varved Lake Jaczno, northeast Poland, J Paleolimnol 58:57–72

Butz C, Grosjean M, Poraj-Górska A, Enters D, Tylmann W. (2016): Sedimentary Bacteriopheophytin a as an indicator of meromixis in varved lake sediments of Lake Jaczno, north-east Poland, AD 1891–2010, Glob. Planet. Change 144: 109–118.

P 8.11

Organic and inorganic long-term carbon budget of Himalayan erosion after the 2015 Gorkha earthquake

Lena Märki[1], Maarten Lupker[1], Ananta Gajurel[2], Negar Haghipour[1,3], Katherine Schide[1], Christian France-Lanord[4], Jérôme Lavé[4], Guillaume Morin[5], Sean Gallen[6], Timothy Eglinton[1]

[1]Geologisches Institut, ETH Zürich, Sonneggstrasse 5, CH-8092 Zürich (lena.maerki@erdw.ethz.ch)
[2]Central Department of Geology, Tribhuvan University, Kathmandu, Nepal
[3]Laboratory of Ion Beam Physics, Otto-Stern-Weg 5, CH-8093, Zürich
[4]CRPG, CNRS-Université de Lorraine, Rue Notre Dame des Pauvres 5, F-54500 Vandoeuvres-lès-Nancy
[5]UMPC, Chemin du Lazaret 181, F-06230 Villefranche-sur-mer
[6]Department of Geosciences, Colorado State University, USA-80592 Fort Collins

The erosion of mountain ranges plays an important role in the carbon cycle by controlling the magnitude of the main geological carbon sinks namely silicate weathering and organic carbon export. Here, we investigate the impact of extreme and rare events on the carbon budget of continental erosion by quantifying the response of weathering and organic carbon fluxes to the April 2015 Gorkha earthquake (Mw 7.8) in central Nepal.

We acquired daily river suspended sediment and water samples during 3 post-earthquake monsoon seasons (2015-2017) from the Narayani River, a large trans-Himalayan tributary of the Ganges. Samples collected in 2010 from the same location provide a pre-earthquake comparison point. Organic carbon sources and fluxes are constrained using suspended sediment load estimates, the total organic carbon content and radiocarbon isotopic compositions of the sediments. Silicate weathering fluxes are quantified using river water dissolved elemental compositions. These two complementary datasets allow us to make a geological carbon budget of Himalayan erosion before and after the earthquake.

Our preliminary results confirm that carbon drawdown from the burial of organic carbon of the Central Himalaya is about 3 times more important than the silicate weathering carbon sink (e.g. France-Lanord and Derry, 1999). We show that co-seismic landsliding during the Gorkha earthquake did not significantly influence the carbon budget of erosion. However, the magnitudes of total organic carbon export and of silicate weathering fluxes are strongly correlated to the total river discharge of a monsoon season. We therefore suggest that the long-term carbon budget of this Himalayan catchment is mainly controlled by the monsoon intensity rather than by rare but intense co-seismic events as has been suggested in other systems.

REFERENCES

France-Lanord, C., & Derry, L. A. 1997 : Organic carbon burial forcing of the carbon cycle from Himalayan erosion. Nature 390, 65-67.

P 8.12

Coupling of Pleistocene sea level fluctuations with coralgal reef growth in the Danakil Depression (Afar, Ethiopia)

Haileyesus Negga[1], Valentin Rime[1], Addis Hailu[1], David Jaramillo-Vogel[1], Juan Carlos Braga[3], Balemwal Atnafu[2], Tesfaye Kidane[4], and Anneleen Foubert[1]

[1]Department of Geosciences, University of Fribourg, Switzerland (haileyesusalemu.negga@unifr.ch)
[2]School of Earth Sciences, Addis Ababa University, Ethiopia
[3]Department of Stratigraphy and Paleontology, University of Granada, Spain
[4]Department of Geology, School of Agricultural, Earth and Environmental Sciences, College of Agriculture, Engineering and Sciences, University of Kwazulu-Natal, Westville Campus, Durban, South Africa

The Danakil Depression is an active rift system located in the northern part of the Afar. The rifting is associated to the break-up of the Afro-Arabian plateau since Oligocene times. The presence of several Pleistocene coral reef terraces at the western and eastern margins of the basin evidence several cycles of Red Sea incursions and subsequent desiccation. Core and seismic data in the central part of the basin record thick evaporite sequences alternating with marine marls, and support the hypothesis of repeated marine incursion and desiccation.

Marine deposits consist of diverse fringing coralgal reef units and calcarenites. The coralgal reef terraces correspond to transgression of the Red Sea in the basin during the Pleistocene marine isotope stage 5e (MIS 5e) and marine isotope stage 7 (MIS 7). This study focus on facies variations within the MIS 7 framestones. Field mapping in the central part of the western margin has been combined with sedimentary petrography (thin section analyses), XRD and stable isotope analyses on the bulk matrix. The MIS 7 coralgal reef consist of a grainstone with few massive corals at the basal unit. On top of this unit lies a pillarstone unit with more coral diversity. Branching Porites dominate the middle unit of the reef. The upper unit of the reef is a domestone characterized by high diversity of massive corals and red algae. Decimeter-scaled algal crusts and hardgrounds are present in the middle and upper reef units

The MIS 7 reef growth pattern is mainly aggradational. Stable isotope values in combination with the facies patterns evidence the presence of 2 major shallowing upward sequences. short term sea level fluctuations and active neotectonic changes may have been responsible for small-scaled changes within the reef unit.

P 8.13

The challenge of compiling a Swiss gravel and sand occurrence map

Regina Reber[1], Stefan Heuberger[1], Lukas Nibourel[1], Thomas Galfetti[2]

[1]Fachgruppe Georessourcen Schweiz, Departement Erdwissenschaften, ETH Zürich, Sonneggstrasse 5, 8092 Zürich (regina.reber@erdw.ethz.ch)
[2]Landesgeologie, Bundesamt für Landestopografie swisstopo, Seftigenstrasse 264, 3084 Wabern

With an extraction rate of more than 30 million tons per year, sand and gravel represent the most used raw material resource in Switzerland. These important materials are mainly extracted from Quaternary deposits in the Swiss Alpine Foreland. However, the diversity of depositional settings of these sediments is high and their composition varies strongly.

Our project aims at establishing a Switzerland-wide sand and gravel occurrence map on the basis of published geological data. Yet, the majority of Quaternary deposits are documented in approx. 40 map sheets of the Geological Atlas of Switzerland (GA 1:25'000), which were produced over the past 85 years by numerous authors working with different mapping styles and interpretation techniques.

The challenge is to harmonise these Quaternary data sets (geometries and attributes) and to validate the necessary generalisation with local data points (i.e. with data from present-day/historical extraction sites, borehole data, where available). We present an approach to address this challenge in a pilot region.
The ultimate goal, however, is to provide a novel, standardised workflow to be applied at the national scale.

P 8.14

Origin of calcium in Ca-carbonate deposits from a sandy siliceous basin (Chobe Enclave, North Botswana): first results

Dimitri Rigoussen[1], Nathalie Diaz[1], Thuto Mokatse[1] & Eric P. Verrecchia[1]

[1]*Institute of Earth Surface Dynamics, Geopolis, University of Lausanne, Lausanne Switzerland (dimitri.rigoussen@unil.ch)*

How can the formation of calcium carbonate deposits be explained in large siliceous sandy basins? This type of apparent paradox has been documented in the Sahara (Dietrich et al., 2017), the Simpson Desert (Australia), as well as in the Kalahari Basin, where the Chobe Enclave is found. The Chobe Enclave, situated in northern Botswana, is limited by two main faults, the Chobe and the Linyanti faults. This high and flat plateau belongs to a graben system possibly associated to the Okavango Rift Zone. Large deposits of terrestrial limestones have been observed in this area, deposited during the last 100 ka (Diaz et al., 2019) and probably due to alternations of paleo-fluvial/lacustrine/palustrine environments. The presence of such deposits is unexpected because the whole area lies on 80 to 200 m of Kalahari quartz sands and possible sources of inherited carbonates are extremely remote. Although the source of the carbonate ion can easily be attributed to the atmosphere through biogenic or abiotic pathways, the source of calcium remains unclear. Therefore, the aim of this study is to recognize the potential sources of calcium in this quartz dominated environment.

Two sources of Ca^{2+} have been hypothesized in the Chobe Enclave: (i) the first one is the episodic water flow of the Zambezi and Kwando rivers, originating from Angola and Zambia watersheds, and which could have contributed to the regional water input throughout the Late Pleistocene and the Holocene; these rivers displace ions resulting from the weathering of the Karoo basalts and shield metamorphic rocks; (ii) the second source is the groundwater, which could have been enriched in ions during hydrothermal weathering of the deep basement rocks. Therefore, geochemical analyses have been performed in order to get major and trace elements, REEY, and Sr isotopes contained in the calcium carbonate phases to trace the potential sources of ions provided to the system during calcite precipitation; in addition, clumped isotopes have been used to emcompass the possible temperatures at which calcite formed.

In terms of mineralogy, the carbonate beds are composed of calcite, quartz (likely from aeolian origin), barite ($BaSO_4$), sepiolite (a fibrous clay) and some other phyllosilicates. Barite is a mineral often attributed to hydrothermal sources (Goldberg et al., 1969), whereas sepiolite suggests a strongly evaporitive environment (Galan and Pozo, 2011), making the origin of these beds potentially complex.

Regarding the elemental compositions of the carbonate phases, they vary laterally and according to depth. Ba and Sr concentrations are three times higher than the average concentration of NASC, the global terrestrial reference. The REEY concentrations (normalized to PAAS) display two anomalies, (i) a slight negative anomaly of cerium in some samples likely due to river transportation (Tostevin et al., 2016), (ii) a positive anomaly of europium, which is probably related to a hydrothermal influence (Tostevin et al., 2016). Moreover, Sr isotope ratios point to more radiogenic values in the carbonate phase than in the surrounding basalts, which are the closest potential source of Ca in the area. Therefore, the Karoo basalts cannot be the only source of calcium of terrestrial carbonate in the Chobe Enclave. Finally, clumped isotopes point out an average precipitation temperature of 25°C.

To conclude, this preliminary study seems to support that sources for calcium have two end-members. Indeed, the calcium contained in the Chobe Enclave carbonate can solely originate from neither rivers nor hydrothermal groundwater. The calcium pathways in the region are then fairly complex and influenced by changes due to rainfall, hydrothermal pulses, and river inputs. Moreover, some of these factors have certainly be affected by neotectonics, making the formation framework of these terrestrial carbonates even more complex.

REFERENCES

Diaz, N., Armitage, S.J., Verrecchia, E.P., Herman, F., 2019: OSL Dating of a carbonate island in the Chobe Enclave, NW Botswana. Quaternary Geochronology 49, 172-76.

Dietrich, F., Diaz, N., Deschanmps, P., Ngounou Ngatcha, B., Sebag, D., Verrecchia, E., 2017. Origin of calcium in pedogenic carbonate nodules from silicate watersheds in the Far North Region of Cameroon: Respective contribution of in situ weathering source and dust input, Chemical Geology 460, 54-69.

Galán, E., Pozo, M., 2011: Palygorskite and sepiolite deposits in continental environments. Description, Genetic Patterns and Sedimentary Settings. In Developments in Clay Science 3, 125-73.

Goldberg, E.D., Somayajulu, B.L.K., Galloway, J., Kaplan, I.R., Faure, G., 1969: Differences between barites of marine and continental origins, Geochimica and Cosmochimica Acta 33, 287-289.

Margane, A., Bäumle, R., Schildknecht, F., Wierenga, A., 2005: Groundwater Investigations in the Eastern Caprivi Region - Main Hydrogeological Report. Investigation of Groundwater Resources and Airborne-Geophysical Investigation of Selected Mineral Targets in Namibia, Volume IV.GW.2.1.

Tostevin, R., Shields, G.A., Tarbuck, G.M., He, T., Clarkson, ö.O., Wood R.A., 2016: Effective use of cerium anomalies as a redox proxy in carbonate-dominated marine settings, Chemical Geology 438, 146-162.

P 8.15

Towards a chronologically constrained Eemian (MIS 5e) pollen biostratigraphy in Switzerland

Patrick Schläfli[1,2], Erika Gobet[2], Willy Tinner[2], Jacqueline van Leeuwen[2], Elisa Vescovi[2], Guilhem Douillet[1], Michael Schwenk[1], Dimitri Bandou[1] & Fritz Schlunegger[1]

[1]*Institute of Geological Sciences, University of Bern, Baltzerstrasse 1+3, CH-3012 Bern (patrick.schlaefli@geo.unibe.ch)*
[2]*Institute of Plant Sciences and Oeschger Centre for Climate Change Research, University of Bern, Altenbergrain 21, CH-3013 Bern*

The last interglacial (Eemian, c. 127 – 110 ka BP) has been a major focus of recent research efforts because its warmer-than-today conditions offer unique possibilities to assess vegetational responses to a warmer climate in the future.
So far the biostratigraphy and the pollen-inferred plant succession of the Eemian have not been fully characterized and deciphered. In fact, palynological records from the Swiss North Alpine forelands (Wegmüller 1992; Welten 1982, 1988) are lacking well constrained independent internal chronologies. It is the major scope of this project to improve the characterization and the temporal calibration of Eemian biostratigraphic records.

To address this scope, we performed a pollen analysis on palaeolake deposits of supposed Eemian age, retrieved in a technical drilling at the SW-margin of perialpine lake Thun. Local pollen assemblage zones (LPAZ) were calculated with the optimal partitioning approach and correlated with the reference record from Gondiswil, the only physically dated (U/Th; 115.7 ± 4.8 ka BP) and most complete Eemian record in the study area (Wegmüller 1992). The correlation is based on optical and numerical methods (DCA).

We show that our novel record represents a fragmentary Eemian archive. The bottom part of the section was sedimented during late-glacial conditions prior to Termination II. Hydrological changes in the region lead to increased gravel input and caused a hiatus within the sequence during the onset of the last interglacial. Full interglacial conditions established right after the hiatus with abundant thermophilous taxa *Taxus baccata* and *Hedera helix*. We interpret this part as the local thermal maximum of the last interglacial.

For the chronological framework we will use the pollen-inferred vegetation and climate signals of both, the novel and the reference record, for correlation with two vegetation-independent ($\delta^{18}O$, $\delta^{13}C$) climate records from speleothems from the Swiss Alps, both having well constrained internal chronologies (U/Th) (Luetscher et al. 2019; Wilcox et al. 2019).
The planned analyses would represent a major scientific advance in Quaternary biostratigraphy, as they would for the first time generate an independently dated Eemian biostratigraphic record in the perialpine region. In addition, refining and chronologically constraining the Eemian biostratigraphies with state-of-the-art approaches would allow better foundations for biostratigraphic comparisons of European sediment archives.

REFERENCES

Luetscher, M., Moseley, G.E., Festi, D., Hof, F., Spötl, C., Edwards, R.L. 2019: The last interglacial (MIS-5e) in Alpine speleothems: the Sieben Hengste record (Switzerland) [Abstract]. International Association for Quaternary Research. Congress (20th: 2019: Dublin, Ireland). (2019). XVI INQUA Congress programs with abstracts: July 25-31, 2019, Dublin Convention Center, Dublin, Ireland.

Wegmüller, S. 1992: Vegetationsgeschichtliche und stratigraphische Untersuchungen an Schieferkohlen des nördlichen Alpenvorlandes. Denkschriften der Schweizer Akademie der Naturwissenschaften 102, Birkhäuser Verlag, Basel.

Welten, M. 1982: Pollenanalytische Untersuchungen im jüngeren Quartär des nördlichen Alpenvorlandes der Schweiz. Beiträge zur Geologischen Karte der Schweiz, N.F. 156. Schweizerische Geologische Kommission, Zürich.

Welten, M. 1988: Neue pollenanalytische Untersuchungen über das Jüngere Quartär des nördlichen Alpenvorlandes der Schweiz, Mittel- und Jungpleistozän. Beiträge zur Geologischen Karte der Schweiz, N.F. 162. Schweizerische Geologische Kommission, Zürich.

Wilcox, P., Spötl, C., Honiat, C., Edwards, L. 2019: Speleothem record from the Swiss Alps highlights Last Interglacial climate variability [Abstract]. International Association for Quaternary Research. Congress (20th: 2019: Dublin, Ireland). (2019). XVI INQUA Congress programs with abstracts: July 25-31, 2019, Dublin Convention Center, Dublin, Ireland.

P 8.16

New insights into the Quaternary fill of the overdeepened Aare Valley

Michael A. Schwenk[1], Dimitri Bandou[1], Patrick Schläfli[1], Guilhem A. Douillet[1], Fritz Schlunegger[1]

[1]*Institut für Geologie, Universität Bern, Balzerstrasse 1+3, CH-3012 Bern*
(michael.schwenk@geo.unibe.ch)

Glacially overdeepened troughs have attracted the scientific community since their discovery. Discussions on their geometries, spatial extents, and hypotheses on their formation ages and mechanisms have been highly controversial. A century of research and drilling activity combined with geophysical surveys left no doubt that they exist. Overdeepenings are bedrock depressions that are located in modern landscapes where glaciers still exist, and they were discovered on plateaus adjacent to mountain belts where thick piedmont glaciers covered a large portion of the landscape. They lie below the current base level and are filled with sediment or currently host lakes. Locally, the sedimentary fill is several hundred meters thick, and thus these troughs apparently contain invaluable archives of the past climate and ice-dynamics. Overdeepenings are a common feature in the Alps and in their forelands. Within Switzerland, one example of an overdeepening is located in the Aare Valley. Here, a single continuous trough stretches from within the Alps into the Molasse foreland. The research history of this overdeepening reaches back more than forty years. Research on overdeepenings, including the one along the Aare Valley, saw different peaks throughout these years. Nevertheless, the complex multi-glaciation history of the Alps and their Swiss part in particular has remained unknown to a deficient extent. Since 1989, no drilling had been conducted in the middle Aare Valley for scientific purposes. Here, we present the results of a new drilling campaign that was conducted earlier in the year 2019. This drilling, situated in Bern-Bümpliz, penetrated a total of 210 m-long suite of non-consolidated Quaternary deposits before ending in Molasse bedrock and discloses a succession made up of lake deposits, glacial till and large-scale cross-beds. The material has been retrieved in a liner, thus offering perfect conditions for analyzing the sedimentary structures at high resolution. The age of this succession is not known, yet preliminary OSL analyses suggest that the topmost sediments are older than 200 ka. This campaign adds to older drillings from the 1980's (Preusser et al., 2005; Schlüchter, 1989; Welten, 1982)pollen analyses and luminescence dating. The sedimentary sequence comprises about 70 m of lacustrine deposits, overlain by about 39 m of coarse glacial outwash interpreted to represent at least two independent ice advances. Pollen analyses of the apparently complete limnic sequence reveal a basal late glacial period followed by three warm phases that are interrupted by two stadial periods (Meikirch complex and reveals more information on sedimentation history in the middle Aare Valley around Bern. With this campaign, we want to increase our understanding of the glaciation history in the Aare Valley and compare it to other areas around the Swiss Alps. Therefore, we display and discuss our findings in comparison with the results of former scientific drillings in the middle Aare Valley.

REFERENCES

Preusser, F., Drescher-Schneider, R., Fiebig, M., Schlüchter, C., 2005. Re-interpretation of the Meikirch pollen record, Swiss Alpine Foreland, and implications for Middle Pleistocene chronostratigraphy. J. Quat. Sci. 20, 607–620.

Schlüchter, C., 1989. Thalgut: Ein umfassendes eiszeitstratigraphisches Referenzprofil im nördlichen Alpenvorland. Eclogae Geol. Helv. 277–284.

Welten, M., 1982. Pollenanalytische Untersuchungen im Jüngeren Quartär des nördlichen Alpenvorlandes der Schweiz. Beiträge zur Geol. Karte der Schweiz-Neue Folge 156, 179 pp.

P 8.17

Rock basins, riegels and gorges: deciphering glacial overdeepenings

Olivia Steinemann[1], Susan Ivy-Ochs[1], Kristina Hippe[2], Marcus Christl[1], Negar Haghipour[2] & Hans-Arno Synal[1]

[1]Laboratory of Ion Beam Physics, ETH Zürich, Otto-Stern-Weg 5, CH-8093 Zürich (okronig@phys.ethz.ch)
[2]Institute of Gological Sciences, Freie Universität Berlin, Malteserstrasse 74-100, 12249 Berlin
[3]Geological Institute, ETH Zürich, Sonneggstrasse 5,CH-8092 Zürich

In the last decades, with the ongoing retreat of the Trift glacier (central Swiss Alps), the remarkably high (150 m) cross-valley riegel, the approximately 100 m deep gorge cutting through the riegel and the associated overdeepened rock basin upvalley became revealed. Because, the bedrock riegel only became exposed some years ago, this offers the possibility to determine the glacial erosion depth and erosion rates within the footprint of the Little Ice Age (LIA) extent. Detailed knowledge about how much the Late Holocene glacier(s) abraded the cross-valley riegel gives new insights in how and how fast glaciers were able to shape this distinct glacial landscape. A combined approach of field survey, cosmogenic nuclide analysis (^{10}Be and in-situ ^{14}C) and numerical modelling was used to determine the spatial glacial erosion pattern on the bedrock riegel. Two transects were sampled; one perpendicular to the ice-flow direction from outside the LIA extent down to the riegel, the other parallel to the ice-flow direction, across the riegel. The total of ten samples were all analysed for ^{10}Be and in-situ ^{14}C. A combination of two nuclides helps to gain additional information about the duration of the last glacier coverage. The results show that the area outside of the LIA extent was constantly exposed since the retreat of the Egesen stadial glacier (11.7 ka). The perpendicular transect shows a trend of increasing erosion rates from LIA marginal position down to the riegel. The parallel transect revealed substantially high erosion all across the riegel. This led us to the conclusion that the riegel was not persisting due to limited glacial erosion.

P 8.18

Foraminifera-bound nitrogen isotope evidence for similar rates of water column denitrification in the eastern Pacific during the last ice age and the Holocene

Anja S. Studer[1,2], Figen Mekik[3], Haojia Ren[4], Alfredo Martínez-García[5], Daniel M. Sigman[2], Gerald H. Haug[5,6]

[1]Department of Environmental Sciences, University of Basel, Basel, Switzerland (anja.studer@unibas.ch)
[2]Department of Geosciences, Princeton University, Princeton, NJ, USA
[3]Grand Valley State University, Department of Geology, Allendale, USA
[4]Department of Geosciences, National Taiwan University, Taipei 106, Taiwan
[5]Max Planck Institute for Chemistry, Climate Geochemistry Department, Mainz, Germany
[6]Department of Earth Sciences, ETH Zurich, Zurich, Switzerland

The $\delta^{15}N$ of N export in the far-eastern equatorial Pacific is sensitive to the $\delta^{15}N$ of nitrate supply from the subsurface to the euphotic zone, which is elevated by water column denitrification in the eastern Pacific oxygen-deficient zones. Bulk sediment $\delta^{15}N$ records from the eastern equatorial Pacific extending back to the last ice age resemble records from along the eastern margin of the Pacific Ocean, with lower $\delta^{15}N$ during the last ice age than in the Holocene. This low glacial $\delta^{15}N$ has been interpreted to reflect a reduction in water column denitrification. In two sediment cores from the Eastern Equatorial Pacific (EEP) that exhibit this glacial-age lowering in bulk sediment $\delta^{15}N$, we measured foraminifera-bound nitrogen isotopes (FB-$\delta^{15}N$) in two subsurface dwelling species *Neogloboquadrina dutertrei* and *Neogloboquadrina pachyderma (dextral)* over the last 35ka. While several major millennial scale features are shared between the bulk sediment $\delta^{15}N$ and FB-$\delta^{15}N$ records, FB-$\delta^{15}N$ contrasts with the bulk sediment $\delta^{15}N$ record by showing a similar FB-$\delta^{15}N$ during the last ice age and Holocene. We propose that the lower glacial $\delta^{15}N$ in bulk sediment is an artifact, possibly related to an increase in exogenous N inputs during the last ice age and/or a glacial weakening of sedimentary diagenesis due to lower deep water oxygen. If so, the previous inference of large-scale ice age reductions in water column denitrification in the eastern Pacific may be incorrect. In both cores, there is an early deglacial maximum in FB-$\delta^{15}N$. While this may indicate a deglacial maximum in eastern Pacific denitrification, an analogous FB-$\delta^{15}N$ peak in records from further west in the equatorial Pacific raises the alternative possibility of a change in the $\delta^{15}N$ of the nitrate supply to the equatorial Pacific via the Equatorial Undercurrent.

P 8.19

^{4}He/U-Th dating of pore waters from Quaternary sediments in Switzerland: potential and challenges

Yama Tomonaga[1], Edith Horstmann[1], Gaudenz Deplazes[2], Rolf Kipfer[1]

[1]Eawag, Swiss Federal Institute of Aquatic Science and Technology, Überlandstrasse 133, CH-8600 Dübendorf (yama.tomonaga@eawag.ch)
[2]NAGRA, National Cooperative for the Disposal of Radioactive Waste, Hardstrasse 73, CH-5430 Wettingen

Dating based on the ^{4}He/U-Th method can be used to estimate the residence time of pore waters in very low-permeable rocks and consolidated sediments. The residence time is inferred from the time necessary to accumulate radiogenic ^{4}He measured in the pore water being produced by the decay of U and Th in the sediment matrix (Torgersen & Clarke, 1985). In the Jurassic Opalinus Clay, the pore water still contains the signature of the original marine formation water that was entrapped during sediment deposition. The pore water composition was altered only by diffusive processes (Gimmi et al., 2007; Mazurek et al., 2011). The fact that even ~100-Ma-old water signatures can be preserved in their original pore space suggests that such preservation might also be possible in much younger dense glacial deposits. The ^{4}He concentrations measured in the pore waters of glacial tills were translated into mean residence times of 15-25 kyrs (Hendry et al., 2005) that agree rather well with the expected depositional ages of 25-31 kyrs (Wassenaar & Hendry, 2000). These observations, as well as evidence from lacustrine sediments (Tomonaga et al., 2014, 2015), suggest that, if the solute transport in the pore space is sufficiently attenuated, even unconsolidated sediments can “store” and host “old” pore waters.

In the present work we investigate if the ^{4}He/U-Th dating of pore waters can be used as a novel tool to complement the luminescence dating of unconsolidated Quaternary sediments. We applied the ^{4}He/U-Th method to date pore waters in the time range of 10 to 100 thousands of years which covers the age range of the sedimentary depositions targeted by the Quaternary drillings (QBOs) managed by the National Cooperative for the Disposal of Radioactive Waste (Nagra) in Switzerland. In particular, we focus on fine-grained lacustrine sediment layers that might provide low-permeability conditions suitable for the preservation of radiogenic ^{4}He concentrations in the pore space.

We report the preliminary results of the ^{4}He/U-Th dating based on the measurements conducted in sediment samples from the first QBOs, highlighting potential and challenges of the method with respect to the studied glaciofluvial sediments of the Swiss Midland.

REFERENCES

Gimmi T., Waber H.N., Gautschi A., & Rübel A. 2007: Stable water isotopes in pore water of Jurassic argillaceous rocks as tracers for solute transport over large spatial and temporal scales. Water Resour. Res. 43(4).

Hendry, M. J., Kotzer, T.G., & Solomon, D.K. 2005: Sources of radiogenic helium in a clay till aquitard and its use to evaluate the timing of geologic events. Geochim. Cosmochim. Acta 69(2), 475–483.

Mazurek, M., Alt-Epping, P., Bath, A., Gimmi, T., Waber, H.N., Buschaert, S., De Cannière, P., De Craen, M., Gautschi, A., Savoye, S., Vinsot, A., Wemaere, I., & Wouters, L. 2011: Natural tracer profiles across argillaceous formations. Appl. Geochem. 26(7), 1035–1064.

Tomonaga, Y., Brennwald, M. S., & Kipfer, R. 2015: Attenuation of noble-gas transport in laminated sediments of the Stockholm Archipelago. Limnol. Oceanogr. 60(2), 497–511.

Tomonaga, Y., Brennwald, M.S., Meydan, A.F., & Kipfer, R. 2014: Noble gases in the sediments of Lake Van - Solute transport and palaeoenvironmental reconstruction. Quat. Sci. Rev. 104, 117–126.

Torgersen, T., & Clarke, W.B. 1985: Helium accumulation in groundwater, I: an evaluation of sources and the continental flux of crustal ^{4}He in the Great Artesian Basin, Australia. Geochim. Cosmochim. Acta 49, 1211–1218.

Wassenaar L.I., & Hendry M.J. 2000: Mechanisms controlling the distribution and transport of ^{14}C in a clay-rich till aquitard. Groundwater 38(3), 343–349.

P 8.20

Morphological and Petrographic Characterisation of Seep Carbonates from the South-Eastern Mediterranean Sea

Reinhard Weidlich[1], Andres Rüggeberg[1], Yizhaq Makovsky[2,3], Or Bialik[3] and Anneleen Foubert[1]

[1]Department of Geosciences, University of Fribourg, Chemin du Musée 6, CH-1700 Fribourg (reinhard.weidlich@unifr.ch)
[2]The Hatter Department of Marine Technologies, Leon H. Charney School of Marine Sciences, University of Haifa, ISR-3498838 Haifa
[3]The Dr. Moses Strauss Department of Marine Geosciences, Leon H. Charney School of Marine Sciences, University of Haifa, ISR-3498838 Haifa

Seep-carbonates are valuable archives to reconstruct past seepage activity in sedimentary basins. They appear in different varieties, depending on the conditions of formation. While carbonate chimneys often form in regions of focused seepage, chemoherms and carbonate crusts occur mainly in regions of diffuse seepage. In this study, we present preliminary seep-carbonate data collected during the EUROFLEETS 2 SEMSEEP expedition onboard the R/V AEGAEO in 2016. Thirty-six hours of ROV dive videos, and seep-carbonates recovered from box core samples and collected during ROV dives have been investigated. ROV video footage suggests the occurrence of three different types of seep-carbonates (chimneys, carbonate slabs and chemoherms) around the Palmachim Disturbance (PD) and the Levant channel. While in water depths around 600 to 700 meters chemoherms and carbonate slabs up to 15 meters in size are located, the abundance of chimneys in water depths around 1200m increase significantly. Authigenic carbonates have been visualized through 3D high-resolution X-ray micro-computer tomography to understand the internal variation of the authigenic cements and carbonate phases. Micro-tomography in combination with classical petrographical microscopy (thin sections) and XRD analyses allowed to identify the different cement generations. Results of the carbonate crusts and nodules recovered from the box cores evidence the occurrence of three generations of micritic cements, one of them being enriched in fossils. Crusts from the carbonate chimneys reveal two different cement generations, one micritic cement and one distinct microcrystalline phase. The individual cement phases possibly indicate different phases of seep activity. Further research will focus on the thorough geochemical characterisation of the different cement generations to identify the origin of the methane and type of seepage activity.

P 8.21

Hyperspectral imaging spectroscopy applied to Lake Cadagno: resolving the short-term response of meromixis and aquatic productivity to climatic and environmental events

Stefanie B. Wirth[1], Paul Zander[2], Adrian Gilli[3] & Martin Grosjean[2]

[1]Centre for Hydrogeology and Geothermics, University of Neuchâtel, Rue Emile-Argand 11, CH-2000 Neuchâtel (stefanie.wirth@unine.ch)
[2]Institute of Geography and Oeschger Centre for Climate Change Research, University of Bern, Erlachstrasse 9a, CH-3012 Bern
[3]Geological Institute, ETH Zurich, Sonneggstrasse 5, CH-8092 Zurich

Applying hyperspectral imaging spectroscopy (HSI) to lake sediment records allows tracking hypoxia and aquatic primary productivity at extraordinary resolution (70 μm pixel size) (Butz et al. 2017; Schneider et al. 2018). A new HSI data set for Lake Cadagno allows us to revisit its Holocene sediment record (Wirth et al. 2013) and to track the response of meromixis and aquatic productivity to climatic changes and to short-term events such as floods and subaquatic slides at unprecedented resolution.

We concentrate on two pigment groups: the Bacteriopheophytins (Bphe) (at a Relative Absorption Band Depth RABD 845 nm) as a proxy for the abundance of anoxic phototrophic bacteria that are indicative of meromixis, and the chloropigments (Chlorophylls-a,b and their derivatives) used as a proxy for aquatic productivity (RABD of 655-680 nm). Additionally, we calibrated the RABD indices to absolute pigment concentrations using spectrophotometer analysis (n=22; r^2=0.92 and RMSEP ~ 10% for Bphe; r^2=0.71 and RMSEP ~ 16% for chloropigments).

With the new data set we are able to resolve that: (i) meromixis was not directly established after ceasing of the post-glacial clastic input ~9800 years ago but that it was preceded by the emergence of aquatic productivity; (ii) periods with increased flood occurrence in the second half of the Holocene led to intermittent interruptions of the water-column stratification indicated by low Bphe concentrations; and that (iii) massive subaquatic slides also led to a weakening of meromixis that reestablished to its full stability only after recovery of the aquatic productivity.

This new HSI data is in line with the current knowledge about meromixis and hypoxia in Lake Cadagno for the entire Holocene but reveals now the full dynamics of the lake behavior at exceptionally high temporal resolution.

REFERENCES

Butz, C., Grosjean, M., Goslar, T. and Tylmann, W. 2017: Hyperspectral imaging of sedimentary bacterial pigments: a 1700-year history of meromixis from varved Lake Jaczno, northeast Poland. J Paleolimnol 58, 57-72.

Schneider, T., Rimer, D., Butz, C. and Grosjean, M. 2018: A high-resolution pigment and productivity record from the varved Ponte Tresa basin (Lake Lugano, Switzerland) since 1919: insight from an approach that combines hyperspectral imaging and high-performance liquid chromatography. J Paleolimnol 60, 381-398.

Wirth, S.B., Gilli, A., Niemann, H., Dahl, T.W., Ravasi, D., Sax, N., Hamann, Y., Peduzzi, R., Peduzzi, S., Tonolla, M., Lehmann, M.F. and Anselmetti, F.S. 2013: Combining sedimentological, trace metal (Mn, Mo) and molecular evidence for reconstructing past water-column redox conditions: The example of meromictic Lake Cadagno (Swiss Alps). Geochimica et Cosmochimica Acta 120, 220-238.

P 8.22

Using analytical pyrolysis-derived molecular biomarkers to identify changes in chemical composition with depth in natural and drained Finnish mires

Kristy Klein[1], Miriam Groß-Schmölders[2], Christine Alewell[2], Jens Leifeld[1]

[1]Agroscope, Climate and Agriculture Group, Reckenholzstraße 191, CH-8046 Zürich
[2]Environmental Geosciences, University of Basel, Bernoullistrasse 32, CH-4056 Basel

While in their pristine state, peatlands are a vitally important terrestrial sink for carbon (C), impacts from climate change, agriculture/forestry, and extraction are resulting in increased aerobic decomposition in drained and degraded ecosystems – shifting their C balance from sink to source. To better understand the effect this degradation has on global C stores, analysis methods are needed to more effectively delineate between indicators of net peat growth (C sequestration) and indicators of increased (aerobic) decomposition (C loss) in peatland profiles, especially when these changes cannot be easily observed using botanical macrofossils. Molecular biomarkers can help to distinguish between periods of aerobic and anaerobic conditions, allowing researchers to track changes in organic matter (OM) chemical composition following shifts in palaeoclimatic conditions.

To characterize and compare changes in chemical composition between degraded and natural peatlands, abundance of various OM biomarkers from cores collected from drained and natural sites in an ombrotrophic peatland in Lakkasuo, Finland were analyzed using pyrolysis-gas chromatography mass spectrometry (Py-GC/MS). Changes in relative percent abundance of molecular biomarkers in different chemical classes were compared (lignin, Sphagnum phenols, aromatics, lipids, n-containing compounds etc.), and used to identify shifts in vegetation with depth, as well as indicators for increased microbial activity. To assess whether the data reflected larger C and N stoichiometric changes in the cores, molecular composition “fingerprint” data were also compared to data obtained using bulk elemental analysis. Differences were observed in relative percent abundance between lignin, phenolic, and n-containing chemical classes between the drained and natural sites, suggesting that molecular composition within a peatland profile can provide detailed information about previous ecosystem conditions and decomposition states in a peatland. These chemical shifts are related to changes in isotopic signal abundance (^{13}C and ^{15}N) as part of a larger project.

P 8.23

Lateglacial deglaciation and glaciostatic uplift in northern Norway

Serdar Yeşilyurt[1], Ola Fredin[2,3], Anders Romundset[2], Marcus Christl[4], Christof Vockenhuber[4], Naki Akçar[1]

[1]*Institute of Geological Sciences, University of Bern, Baltzerstrasse 1-3, 3012 Bern, Switzerland*
[2]*Geological Survey of Norway (NGU), Leiv Eirikssons vei 39, 7491 Trondheim, Norway*
[3]*Norwegian University of Science and Technology (NTNU), 7491 Trondheim, Norway*
[4]*Laboratory of Ion Beam Physics (LIP), ETH Zurich, Otto-Stern-Weg 5, 8093 Zurich*

During the cold periods of the Quaternary, global volume of ice increased and, as a result, ice sheets were built at high latitudes, such as the Scandinavian Ice Sheet (SIS) during and after the Last Glacial Maximum (LGM). Due to the loading of up to few kilometers thick ice mass, the lithosphere sank into the mantle. At the end of the LGM, it began to rise as response to the unloading due to the rapid melting, which is called as glacio-isostatic uplift. Today, well-preserved geomorphological evidences of deglaciation of the SIS and glacio-isostatic uplift are exemplified in Finnmark, northern Norway, where the timing of these events is not fully understood yet. In this study, we focus on the coupling of post-LGM deglaciation of the SIS and glacio-isostatic uplift. Therefore, we reconstruct the chronology of deglaciation by dating the moraines and that of glacio-isostatic uplift by the raised shorelines in Finnmark, northern Norway. To do that, surface exposure and depth-profile dating techniques were used. 25 rock surface samples from the glacially transported boulders on the moraines, 16 sediments samples along the depth profiles into the delta and terrace deposits, and 46 flat cobbles from the storm deposits on the raised shorelines were collected for ^{36}Cl and ^{10}Be analysis. Our first results showed that the Scandinavian Ice Sheet started to retreat from northernmost Finnmark at ca. 14-15 ka, while it was separated from Barents Sea Ice Sheet and continental shelf was deglaciated. Thus, marine limit was either carved into the bedrock or indicated by shoreline deposits following Lateglacial deglaciation. For instance, we dated the marine limit in the south of Nordkinn Peninsula located at + 55 m today to ca. 13 ka. The elevation of this raised shoreline level soars from north of Finnmark toward the south because of shoreline gradients and pattern of greater uplift in inner regions.

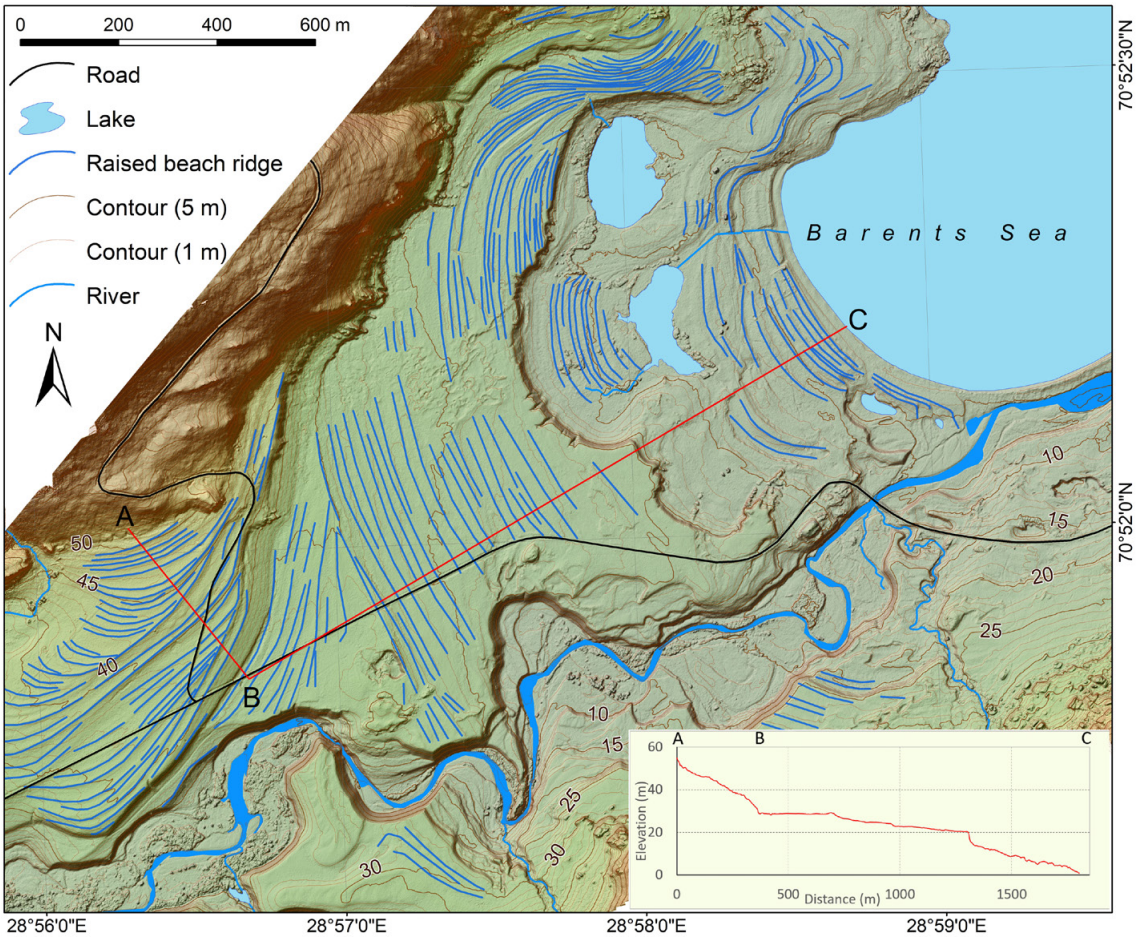


Figure 1. Geomorphological map of Spoatnajohka delta in Finnmark, including a cross section

P 8.24

The connection between low rates of glacial erosion on limestone bedrock and relief development in the Alps

Susan Ivy-Ochs[1], Olivia Steinemann[1], Marc Luetscher[2], Urs H. Fischer[3], Christof Vockenhuber[1]

[1]Laboratory of Ion Beam Physics, ETH Zürich, Otto-Stern-Weg 5, 8093 Zürich (ivy@phys.eth.ch)
[2]Swiss Institute for Speleology and Karst Studies (SISKA), Rue de la Serre 68, 2301 La Chaux-de-Fonds
[3]NAGRA, Hardstrasse 73, 5430 Wettingen

We look at the striking contrast between subglacial erosion rates measured on limestone (Steinemann et al., 2019) vs. those measured on gneiss bedrock (Wirsig et al., 2017). We use cosmogenic nuclides to determine how deeply a glacier has eroded. The sites are glacier forefields exposed just in the last few years in the Alps. In theory, limestone is more erodible than gneiss (Kühni and Pfiffner, 2011), thus it should be much easier to abrade beneath a sliding glacier. Nevertheless, our quantifications of glacial erosion show that the limestone rates are magnitudes lower than the gneiss rates.

At the Tsanfleuron glacier site in Switzerland, evidence of glacial erosion is abundant. But the true magnitude (depth of rock removed by the glacier) is difficult to gauge based on observations alone. The obvious appearance of highly polished rock surfaces within the Little Ice Age-glacier footprint belies our determination based on 36Cl concentrations that very little rock was removed during late Holocene glacier advances. The underlying limestone is part of a well-studied karst system (Gremaud et al., 2009). Within just a few meters of the ice margin meltwater is seen to pour into karst shafts. Meltwater beneath the glacier is and was likely immediately and efficiently channeled down into the karst system. Glacier sliding, and thus erosion, is directly linked to the presence of water at the base of a glacier on a hard bed. Loss of water inhibits sliding, erosion slows (Braakhekke, Ivy-Ochs and Fischer 2017, and references therein).

Until now, observations at glaciated karst regions have been contrastingly interpreted as indicating either profound or insignificant glacial erosion. Our results suggest that in areas with well-developed karst systems it is the inability of glaciers to effectively erode limestone itself that leads to those areas gaining topographic dominance with time. After numerous Quaternary glaciations over hundreds of thousands of years, high limestone plateaus of the Alps developed and were preserved. As the glaciers cleared away easier to erode overlying (silicate) rocks and eroded down to the massive limestones, the plateau character emerged. Because the plateau surfaces are low in relief, a negative feedback develops; glacier velocity and sliding and consequently erosion are reduced even further. On the other hand, clearly some limestone terrains in the Alps are strongly glacially incised. What factors lead to certain areas of limestone being eroded less than their neighbors such that high standing plateaus form? As shown at the Tsanfleuron site, near horizontal, very thick-bedded, weakly fractured, massive limestone bedrock favors this process.

REFERENCES

Braakhekke, J., Fischer, U.H., & Ivy-Ochs, S. 2017: Effects of limestone beds on glacial hydrology, erosion, sediment transport and associated landforms: a literature review, NAB 17-26.

Gremaud, V., Goldscheider, N., Savoy, L., Favre, G., & Masson, H. 2009: Geological structure, recharge processes and underground drainage of a glacierised karst aquifer system, Tsanfleuron-Sanetsch, Swiss Alps, Hydrogeology Journal, 17, 1833-1848.

Kühni, A., & Pfiffner, O.A. 2001: The relief of the Swiss Alps and adjacent areas and its relation to lithology and structure: topographic analysis from a 250-m DEM, Geomorphology, 41, 285-307.

Steinemann, O., Ivy-Ochs, S., Grazioli, S., Luetscher, M., Fischer, U.H., Vockenhuber, C., & Synal, H.A. 2019: Quantifying glacial erosion on a limestone bed and its relevance for landscape development, Earth Surface Processes and Landforms (in revision).

Wirsig, C., Ivy-Ochs, S, Reitner, J.M., Christl, M., Vockenhuber, C., Bichler, M., & Reindl, M. 2017: Subglacial abrasion rates at Goldbergkees, Hohe Tauern, Austria, determined from cosmogenic 10Be and 36Cl concentrations, Earth Surface Processes and Landforms, 42, 1119-1131.

9. Geomorphology

Nikolaus Kuhn, Christoph Graf, Isabell Kull, Geraldine Regolini, Isabelle Gärtner-Roer, Margreth Keiler, Christophe Lambiel, Christian Scapozza, Reynald Delaloye, Negar Haghipour

Swiss Geomorphological Society

TALKS:

9.1 de Palézieux L., Leith K., Loew S.: River channel perturbations resulting from active landsliding in the High Himalaya of Bhutan

9.2 Delaloye R., Barboux C., Gärtner-Roer I., Lambiel C., Pellet C., Phillips M., Scapozza C.: Toward the first national rock glacier inventory in the Swiss Alps (SwissRG2020)

9.3 Litty C., Charreau J., Blard P.H., Pik R., Nomade S.: Potential climatic control on Quaternary denudation rates of tropical volcanic islands

9.4 Magrani F., Valla P., Gribenski N., Serra E.: Swiss glacial overdeepenings: spatial patterns and morphometric analysis of hidden geomorphic features

9.5 Shynkarenko A., Lontsi A.M., Kremer K., Stegmann S., Hobiger M., Bergamo P., Kopf A., Fäh D.: First steps to create a comprehensive geophysical and geotechnical model of submerged slopes in Lake Lucerne

9.6 Truttmann S., Hardmeier S., Herwegh M., Schreurs G., Ebert A.: Assessing the effect of pre-existing structures on the Moosfluh landslide (Great Aletsch Glacier) by using remote sensing techniques and field observations

9.7 Vivero S., Lambiel C.: Unmanned aerial vehicles and feature tracking for monitoring rock glacier kinematics

9.8 Wang Y., Willett S.D.: The importance of non-vertical flux in the interpretation of detrital cosmogenic nuclide concentrations for basin-wide erosion rates

POSTERS:

P 9.1 Braillard L., Magnin J., Charrière M., Monney N., Jeanrenaud P., Gremaud J.: Augmented reality for geosciences: the example of the didactic trail Novi Lé (Lake of Gruyère, FR)

P 9.2 De Pedrini A., Cristian S., Christian A.: The 1513 Monte Crenone rock avalanche. Numerical model and geomorphological analysis

P 9.3 Haghipour N., Burg J.-P., Lupker M., Christl M.: Surface behavior of the Makran accretionary wedge in Iran from ^{10}Be analyses of river sands and terraces

P 9.4 Hirschberg J., McArdell B.W., Molnar P.: Calibration and sensitivity analysis of a sediment cascade model

P 9.5 Josset J., Bontognali T., Hofmann B., Meister Y., Kuhn N.J.: Close-up imaging simulation in the Marslabo of the University of Basel

P 9.6 Lupker M., Hippe K., Wacker L., Haghipour N., Blard P.H., Lavé J.: Tracing sediment processes with paired cosmogenic nuclides (in-situ ^{14}C & ^{10}Be)

P 9.7 Rüegg A., Preisig G.: JuraHydroSlide: identifying the principal hydrogeologic ingredients for predicting landslide activity in Jura Mountains

P 9.8 Milani S.A., Mousazadeh F., Rafiei R.: Morphodynamic Evaluation of Barchan Movement in Robat-e-Posht Badam, Iran

P 9.9 Scapozza C., Ambrosi C., Siro D.C., Lambiel C.: Schmidt hammer exposure-age dating of (peri-) glacial landforms thanks to R-values calibration by historical data in the Southern Swiss Alps

P 9.10 Van Leeuwen C.C.E., Cammeraat L.H., Kuhn N.J., Fister W., Vos H.C.: A Cross-Comparison between a Traditional Portable Straight-Line Wind Tunnel and PI-SWERL over an Altitude Gradient

P 9.11 Zhang Z., Walter F., He S.: Extracting landslide dynamics from seismic signals based on empirical Green's function

9.1

River channel perturbations resulting from active landsliding in the High Himalaya of Bhutan

Larissa de Palézieux[1], Kerry Leith[1], Simon Loew[1]

[1]Geological Institute, ETH Zurich, Sonneggstrasse 5, CH-8092 Zurich
(larissa.depalezieux@erdw.ethz.ch)

Both direct, and indirect hazards associated with large landslides contribute to significant risks to societies living in close contact with high-relief terrain. Understanding the location and the process of formation of slope instabilities in mountainous regions is an important first step to reducing such risks. These are, however, difficult to constrain due to the long time-scales of formation and the plethora of pre-conditioning factors involved. Of the pre-conditioning factors, several have been studied in the past (e.g. Blöthe et al., 2015; Tsou et al., 2014; Grämiger et al, 2017) suggesting a strong correlation between landslide occurrence and active erosional processes.

The fluvial valleys of NW Bhutan preserve a long record of fluvial erosion, which was not interrupted by glacial erosion in the recent past. Throughout the region this record is expressed in sequences of terraces and knickpoints, characteristic river profiles, and broad alluvial plains. In addition, the topography and the erosional processes shaping it are strongly influenced by the high relief of the Himalayan mountain chain and the particular climatic conditions.

In this study we analyse variations in planform and longitudinal channel morphology with respect to landslides intersecting these rivers in order to identify active landslides interacting with the river channel development. When considered in association with streampower and / or indicators of incision rate, these properties can provide a quantitative measure of relative landslide activity. We see a spatial correlation between excess topography and channel steepness with both landslide size and mode of interaction with the stream network: areas of high relief and with high channel steepness tend to coincide with weathering-limited systems and also larger landslides, compared to areas of low relief and low channel steepness, where the system is transport-limited and with on average smaller, but more numerous landslide surfaces.

REFERENCES

Blöthe, J. H., Korup, O., & Schwanghart, W. (2015). Large landslides lie low: Excess topography in the Himalaya- Karakoram ranges, 43(6), 523–526. https://doi.org/10.1130/G36527.1

Grämiger, L. M., Moore, J. R., Gischig, V. S., Ivy-Ochs, S., & Loew, S. (2017). Beyond debuttressing: Mechanics of paraglacial rock slope damage during repeat glacial cycles. Journal of Geophysical Research: Earth Surface, 122(4), 1004–1036. https://doi.org/10.1002/2016JF003967

Tsou, C. Y., Chigira, M., Matsushi, Y., & Chen, S. C. (2014). Fluvial incision history that controlled the distribution of landslides in the Central Range of Taiwan. Geomorphology, 226, 175–192. https://doi.org/10.1016/j.geomorph.2014.08.015

9.2

Toward the first national rock glacier inventory in the Swiss Alps (SwissRG2020)

Reynald Delaloye[1], Chloé Barboux[1], Isabelle Gärtner-Roer[2], Christophe Lambiel [3], Cécile Pellet[1], Marcia Phillips[4], Cristian Scapozza[5]

[1]Department of Geosciences – Geography, University of Fribourg, Switzerland
[2]Department of Geography, University of Zurich, Switzerland
[3]Institute of Earth Surface Dynamics, University of Lausanne, Switzerland
[4]WSL Institute for Snow and Avalanches Research SLF, Davos, Switzerland
[5]Institute of Earth Sciences, SUPSI, Canobbio, Switzerland

Rock glaciers are the most common landforms associated to the mountain periglacial (permafrost) landscape. They are essential periglacial items of the Earth geomorphological heritage but are mostly not identifiable for people lacking background in mountain geomorphology. Inventorying rock glaciers is basically making them to exist (and to become visible). So far, scientific motivations for producing an exhaustive rock glacier inventory and/or for exploiting it have been various : enhancing geomorphological landscape; modelling (past and/or present) permafrost occurrence; studying climate and paleo-climate; investigating hydrological significance or assessing geohazards. Whatever the motivation for producing or exploiting an inventory, it has to follow standardized guidelines to avoid or at least minimize potential discrepancies between producers and users.

In Switzerland, rock glaciers have already been inventoried in various regions over the last decades (e.g. Phillips and Reynard, 1996, Delaloye and Morand 1998, Frauenfelder et al, 2003, Barboux et al. 2014, Ambrosi et al. 2018). These inventories have been based on different methodologies: using a (geo)morphological approach based on the visual identification of rock glacier features of the (imaged) landscape and DEM-derived products or/and using a kinematical approach based on the detection of surface motion (e.g. InSAR-derived inventories). However, they rely in particular on the unequal availability of initial datasets (e.g. satellite imagery) and have been performed at different times in various projects and therefore make an assemblage and completion not feasible.

The objective is now to update the existing inventories and to include missing areas in order to produce a unique standardized rock glacier inventory over the entire Swiss Alps reflecting the situation around 2020.

This initiative (2019-2023) will apply the international standard guidelines currently in elaboration by the *Rock glacier inventory and kinematics* IPA (International Permafrost Association) Action Group (2018-2020). The latter intends to sustain the first steps toward the organization and the management of a network dedicated to rock glacier mapping and inventorying at a global scale. It also promotes the integration of permafrost creep rate (rock glacier kinematics) as a potentially new associated parameter to Essential Climate Variable (ECV) Permafrost within the Global Climate Observing System (GCOS) initiative characterizing the ongoing evolution of mountain permafrost in as many as possible mountain ranges over the Earth.

REFERENCES

Ambrosi, C., Castelletti, C., Scapozza, C., Czerski, D. & Schenker, F., 2018: The new landslide and rock glacier inventory map of Canton Ticino. *Geophysical Research Abstracts* 20, EGU2018-2358, General Assembly 2018.

Barboux, C., Delaloye R. & Lambiel, C., 2014 : Inventorying slope movements in an Alpine environment using DInSAR. *Earth Surface Processes and Landforms*, 39/15, 2087-2099. DOI: 10.1002/esp.3603

Delaloye R. & Morand, S., 1998: Les glaciers rocheux de la région d'Entremont (Alpes valaisannes): inventaire et analyse spatiale à l'aide d'un SIG. *Mitt. VAW / ETH Zürich* 158, 75-86

Frauenfelder, R., Haeberli, W. & Hoelzle, M., 2003: Rockglacier occurrence and related terrain parameters in a study area of the Eastern Swiss Alps. *Permafrost*, Proc. 8ICOP Zurich, Phillips, Springman & Arenson (eds), Swets & Zeitlinger, Lisse, ISBN 90 5809 582 7

Phillips, M. & Reynard, E., 1996 : Influence régionale du climat et de la morphologie sur la distribution du permafrost: l'exemple des Hautes Alpes Calcaires. *Rapports de recherche UKPIK* 8, Institut de Géographie, Universsité de Fribourg, 197-206.

9.3

Potential climatic control on Quaternary denudation rates of tropical volcanic islands

Camille Litty[1], Julien Charreau[1], Pierre Henri Blard[1], Raphael Pik[1], Sébastien Nomade[2]

[1]Centre de Recherches Pétrologiques et Géochimiques, CRPG Nancy, France
[2]Laboratoire des Sciences du Climat et de l'Environnement, Gif-sur-Yvette, France

Denudation of emerged surfaces strongly influences the CO_2 cycle and the climate evolution through chemical weathering of silicates, which consumes atmospheric CO_2, and fluxes of sediments, which deeply modifies the chemical composition of the oceans and buries organic carbon. In order to better understand the long term carbon cycle and the associated climate evolution, it is important to better quantify the total continental denudation rates and better understand the associated controlling factors. Denudation rates at the basin scale can be quantified by measuring cosmogenic isotopes in river sediments. This technique may moreover provide denudation rates averaged over long time period (10^2-10^3a). However, cosmogenic denudation rates have been mainly based on quartz rich lithologies through ^{10}Be analyses. On volcanic islands, where basaltic and andesitic petrologies are predominant, ^{10}Be cannot be used in an easy and direct way and the denudation rates at the geological scale remain poorly constrained. Yet, according to decenal geochemical measurment of disolved load in river, the weathering of volcanic islands, especially in tropical area, is particularly intense and may represent a significant CO_2 sink. It is therefore critical to better constrain also in tropical volcanic islands the denudation rates at the geological time scale. This could be achieve by measuring cosmogenic ^{3}He in olivine and pyroxene in river sediments.

Here we focused our analysis on the San Antao island (Cabo Verde archipelago) where we measured the cosmogenic ^{3}He in olivine and pyroxene of 29 river sand bars. San Antao has the advantage of having a relatively homogeneous, basaltic lithological composition and stable tectonics, but a strong rainfall gradient between the NE and SW, which allows us to quantitatively investigate the impact of precipitation on erosion rates. The obtained denudation rates will then be used to estimate the rate of weathering and the amount of CO_2 consumed by this process.
This study therefore provides for the first time and from an innovative technique, the spatial distribution of denudation rates on a volcanic island located in a tropical zone.

9.4

Swiss glacial overdeepenings: spatial patterns and morphometric analysis of hidden geomorphic features

Fabio Magrani[1], Pierre Valla[1,2], Natacha Gribenski[1], Elena Serra[1]

[1]*Institute of Geological Sciences and Oeschger Centre for Climate Change Research, University of Bern, Baltzerstrasse 1, CH-3012 Bern (fabio.magrani@geo.unibe.ch)*
[2]*Institute of Earth Sciences (ISTerre), Université Grenoble Alps, Université Savoie Mont Blanc, CNRS, IRD, IFSTAR, 38000 Grenoble, France*

Alpine glacial overdeepenings consist of hidden geomorphic features shaped by glacial erosion and water, with up to hundreds of meters carving over the Quaternary. These features are presently filled by overlying (post-)glacial sediment or water from lakes. Accessing their bedrock contact through geophysical investigations allows to determine their spatial occurrence and geometry (Dürst-Stucki & Schlunegger, 2013). For the Swiss foreland, both their spatial distribution, morphometric characteristics and Quaternary evolution during glaciations remain poorly constrained (Preusser et al., 2010).

This study consists in the morphometric analysis of glacial overdeepenings (ODs), mostly in the Swiss Alpine foreland and adjacent valleys, to get quantitative constrains on both their 3D geometry and spatial relationships. Our objective is to understand how much the bedrock resistance, local and regional settings and drainage network control the location and geometry of such ODs. To that aim, a combined bedrock model derived from Dürst-Stucki & Schlunegger (2013) and Mey et al. (2016) was compiled to better constrain the Quaternary sediment thickness both in the low-relief (Swiss Alpine foreland) and in the high-relief (Swiss Alps) regions. Modelled ODs for regions under modern glaciers (Haeberli et al., 2016) were also used for quantitative comparisons with ODs in ice-free areas (our dataset).

An automated GIS-routine was designed to identify and extract ODs features using four different filtering criterions: area, maximum depth, slope and basin connectivity. Differences in overdeepenings' spatial trends (area, length, width, sediment thickness, elongation and orientation) and the potential influence of lithology and hydrological network were investigated for the whole Switzerland (163 ODs in total). A more detailed analysis was conducted for big overdeepened features (length > 5 km, 31 ODs), in which cross-section profiles, shape-factors (V to U-shaped), drainage confluences and transversal valley asymmetry were computed.

Our results suggest a continuous trend for ODs' geometry between ODs under current ice and in ice-free areas. Overdeepenings' elongation ratios, mean and maximum depths show good correlation with their areas. From a hydrological perspective, the number of rivers confluences seem to be a good proxy for ODs' volumes. While drainage flow can help explain ODs' elongations, bedrock resistance explains well the maximum depths and widths of the analyzed features. On the other hand, no clear relationship was found between area and elongation. Cross-section calculations showed a correlation between depths and shape factors, demonstrating that V-shaped cross-profiles occur mostly for deeper ODs. This might be related to a more efficient subglacial water system.

The investigation of spatial patterns suggest stronger relationships with local controls (such as drainage area and lithology) than with broader regional settings (e.g. mountain vs foreland areas). This analysis will, ultimately, contribute to identifying possible controls related to overdeepenings formation and development, allowing a better understanding of erosive processes by glaciers during Quaternary times.

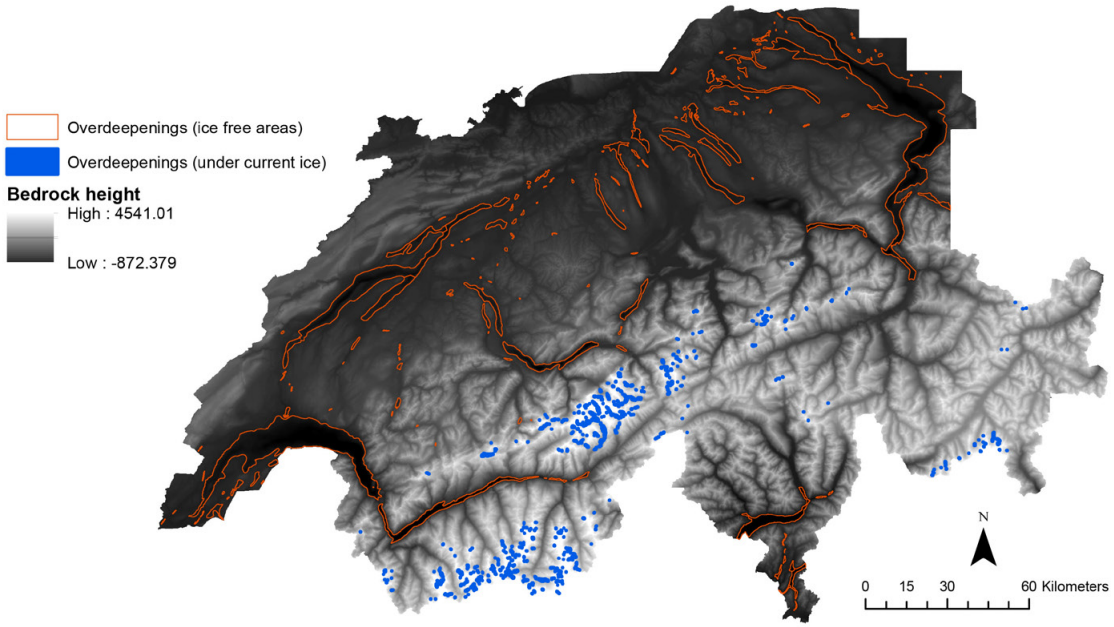


Figure 1. Overdeepenings location and bedrock elevation model. ODs under current ice from Haeberli et al. (2016) dataset.

REFERENCES

Dürst-Stucki, M., & Schlunegger, F. 2013: Identification of erosional mechanisms during past glaciations based on a bedrock surface model of the Central European Alps. Earth Planet. Sci. Lett, 384, 57.

Haeberli, W., Linsbauer, A., Cochachin, A., Salazar, C., & Fischer, U. H. 2016: On the morphological characteristics of overdeepenings in high-mountain glacier beds. Earth Surface Processes and Landforms, 41(13), 1980–1990.

Mey, J., Scherler, D., Wickert, A.D., Egholm, D.L., Tesauro, M., Schildgen, T.F., Stecker, M.R. 2016: Glacial isostatic uplift of the European Alps. Nature Communications, 7, 10.

Preusser, F., Reitner, J.M., Schlüchter, C. 2010: Distribution, geometry, age and origin of overdeepened valleys and basins in the Alps and their foreland. Swiss J. Geoscience, 103, 407.

9.5

First steps to create a comprehensive geophysical and geotechnical model of submerged slopes in Lake Lucerne

Anastasiia Shynkarenko[1], Agostiny Marrios Lontsi[1], Katrina Kremer[1], Sylvia Stegmann[2], Manuel Hobiger[1], Paolo Bergamo[1], Achim Kopf[2], Donat Fäh[1]

[1]Swiss Seismological Service, ETH Zürich, Sonneggstrasse 5, CH-8092 Zürich (a.shynkarenko@sed.ethz.ch)
[2]MARUM – Center for Marine Environmental Sciences, University of Bremen, Leobener Strasse 8, D-28359, Bremen

Both seismically and aseismically triggered slope failures in lakes can cause a substantial damage to the infrastructure and population as they can be tsunamigenic. Despite the smaller spatial scale in comparison to tsunamis in oceans, they can nevertheless pose a considerable hazard for the densely populated lake shores.

Lake Lucerne in central Switzerland has experienced damaging tsunamis in the past few centuries: in 1601, caused by earthquake-triggered mass movements, and in 1687, caused by the spontaneous collapse of Muota river delta. Nowadays there are still substantial sediment packages on some of Lake Lucerne's slopes which have a potential to fail providing the presence of critical conditions.

Potential slope failure scenarios in lakes can be investigated based on slope stability analysis taking into account the influence of different triggering factors, among which earthquakes appear to be the most important. The volume of the potentially unstable mass can define whether a tsunami generation is possible or not.

In this study, the stability of submerged slopes of Lake Lucerne is investigated. To model the behavior of lake slopes under different conditions, we are creating a geophysical and geotechnical model of sediment coverage on the slopes. For this purpose numerous seismological and geotechnical investigations are being conducted since 2018: more than 150 cone penetration tests (CPTu) and core retrievals and more than 100 ocean bottom seismometer (OBS) deployments have being carried out so far (Fig.1). All the data is being processed and analyzed in order to retrieve the main sediment properties, such as fundamental frequency of resonance, shear wave velocity, undrained shear strength, density, grain size distribution etc. Based on the new data obtained during this extensive field work, and on the available bathymetry map and reflection seismic dataset, a 3D model of slopes structure and sediment properties distribution in Lake Lucerne will be created.

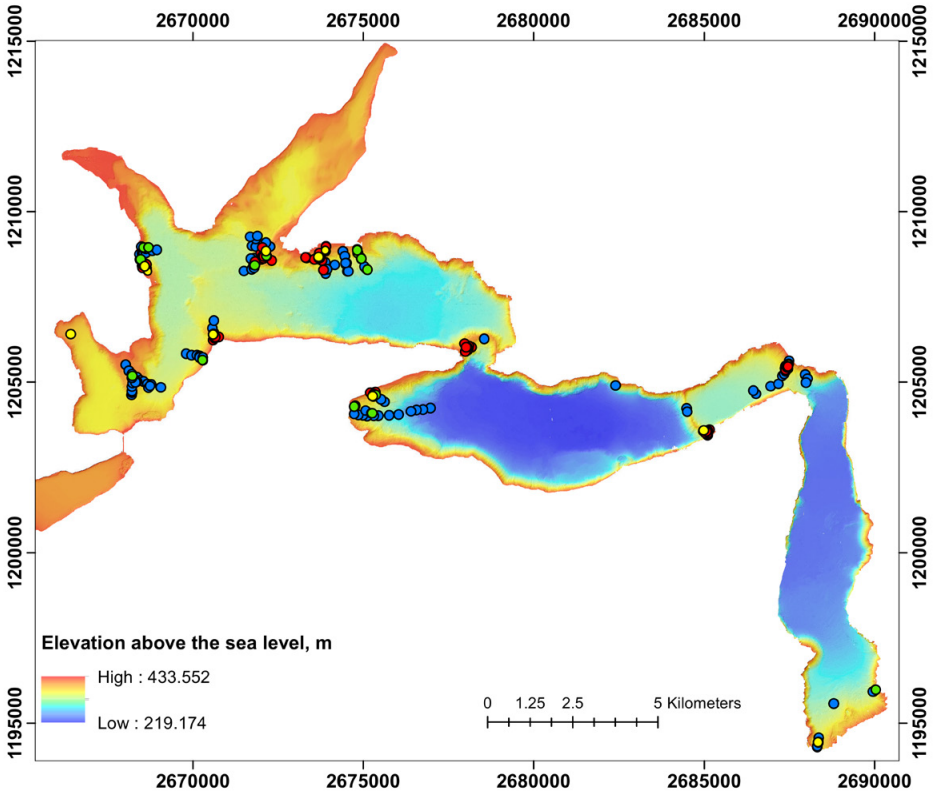


Figure 1. Map of the locations where seismological or geotechnical investigations were carried out. Red and yellow dots: Ocean Bottom Seismometer deployments; green dots: coring sites; blue dots: cone penetration testing sites.

9.6

Assessing the effect of pre-existing structures on the Moosfluh landslide (Great Aletsch Glacier) by using remote sensing techniques and field observations

Sandro Truttmann[1], Sibylla Hardmeier[1], Marco Herwegh[1], Guido Schreurs[1] & Andreas Ebert[2]

[1]Institute of Geological Sciences, University of Bern, Baltzerstrasse 1+3, CH-3012 Bern (sandro.truttmann@gmail.com)
[2]Geo Explorers AG, Wasserturmplatz 1, 4410 Liestal

The Moosfluh landslide at the tongue of the current extent of the Great Aletsch Glacier is one of the largest active landslides in the European Alps. Several historical slope failures attributed to the retreat of the Great Aletsch Glacier have been recorded in the Aletsch valley. In the gneisses and granodiorites of the Aar Massif hosting the landslide, pre-existing deformation structures play a key role in slope destabilization.

In this study, a combination of fieldwork and remote sensing techniques is used to assess the effect of pre-existing deformation structures on the Moosfluh landslide. Fieldwork data and lineament mapping on orthophotos allow to identify and characterize pre-existing deformation structures and landslide-induced fracture patterns. Digital Image Correlation (DIC) is used to reconstruct horizontal surface velocities from orthophoto image pairs, which combined with a novel approach for landslide deformation analysis give spatially high-resolution information on landslide kinematics and the related surface deformation. By linking the knowledge of pre-existing deformation structures and landslide-induced deformation, we obtain detailed information on the landslide processes and their evolution in space and time.

The landslide evolution from 2008 to 2018 can be reconstructed with high spatial resolution. Surface deformation analysis reveals the concentration of active deformation along former narrow ductile and brittle shear zones, allowing to directly link pre-existing deformation structures with landslide deformation processes. Brittle reactivation of these shear planes and fracture propagation between exfoliation joints results in a pervasive 3D fracture pattern, which is responsible for the current disintegration of the rock mass. Toppling is the main gravity-driven mass movement process in the upper part of the slope. A complex interplay between toppling processes and pre-existing, valley-parallel exfoliation joints allows the transition from toppling to sliding mechanism by an upward connection of fractures and the formation of a continuous basal rupture surface. The results from this study show that the lateral detachment processes differ on either side of the Moosfluh landslide, which can also be explained by lateral differences in the geometry of pre-existing deformation structures. 3D disintegration further leads to enhanced rockfall activity in oversteepened slopes. A temporal stabilization of the landslide is recorded after 2017, which might be caused by the self-stabilizing properties of flexural toppling. Particularly with further glacier retreat, renewed acceleration of the landslide can however not be excluded.

9.7

Unmanned aerial vehicles and feature tracking for monitoring rock glacier kinematics

Sebastián Vivero[1] & Christophe Lambiel[1]

[1]*Institute of Earth Surface Dynamics (IDYST), University of Lausanne, Bâtiment Géopolis UNIL Mouline, CH-1015 Lausanne (sebastian.viveroandrade@unil.ch)*

Rock glacier kinematics are commonly derived from repeated measurements carried out by terrestrial geodetic surveys. In the Swiss Alps, and under the coordination of PERMOS office, continuous long-term kinematics records are obtained since 2000 for several rock glaciers (PERMOS, 2019). These records provide a robust and updated picture of the state of rock glacier kinematics, which allows a better understanding of the dynamics of mountain permafrost.

This study introduces a new method to quantify rock glacier kinematics and their associated uncertainties derived from six consecutive UAV surveys of Tsarmine rock glacier, Valais Alps, Switzerland. Since 2016, we have been executed UAV surveys with a SenseFly eBee RTK device concomitant with the acquisition of in-situ kinematic measurements using differential GNSS equipment. Sequences of high-density 3D point clouds for Tsarmine and its environs using SfM-photogrammetry were generated. Co-registration and feature tracking methods were performed on the multitemporal orthomosaics and DEMs.

Using customised UAV surveys and their resulting 3D data, rock glacier geometric changes can be studied in high detail. Results indicate a good fitness between in-situ GNSS measurements and UAV-derived displacements, where the flow structure of Tsarmine shows a regular profile of increasing velocities towards the terminus (up to 7 m/y). Moreover, the general assessment of the 3D-models allows computing not only horizontal displacements but also elevation changes. UAV monitoring approaches can be advantageous for accessing difficult terrain, as they can be easily customised to deliver high resolution and frequency of observations in comparison with other remote sensing or ground survey methods.

REFERENCES

PERMOS (2019). Permafrost in Switzerland 2014/2015 to 2017/2018. Edited by J. Noetzli, C. Pellet, and B. Staub, Cryospheric Commission of the Swiss Academy of Sciences.

9.8

The importance of non-vertical flux in the interpretation of detrital cosmogenic nuclide concentrations for basin-wide erosion rates

Yanyan Wang[1], Sean D. Willett[1]

[1]*Geological Insititute, Department of Earth Sciences, ETH Zurich, Sonneggstrasse 5, CH-8092 Zurich (yanyan.wang@erdw.ethz.ch)*

Detrital cosmogenic nuclides (DCN) concentrations are generally interpreted in terms of the mean rate of catchment surface lowering. This is based on the relationship that DCN concentration depends on the production of cosmogenic nuclides integrated over the catchment area divided by the volume of rock moving through that surface per unit time, giving the unit of a flux. Conventional catchment-averaged erosion rate is thus a vertical mass flux. In general, the mass flux results from motion of the rock through the Earth's surface in any direction, not just in the vertical. In many geomorphic or tectonic settings, the change of the surface is better described by horizontal motion of the rock with respect to the surface, thus defining a horizontal flux. For example, in tectonically-quiescent escarpments on rift margins, the mass flux of an escarpment-draining basin can be approximated to be purely horizontal and the mass flux is determined by the rate of escarpment retreat. Similarly, tectonic motion on low-angle faults results in horizontal rock motion with respect to the surface, if erosion maintains a constant surface.

Assuming equilibrium of cosmogenic nuclides production and transport means that rock trajectory has no impact on the total production of cosmogenic nuclides. The effect of non-vertical rock motion is to change only the solid rock flux and thus the dilution of the cosmogenic nuclides. For a given direction (dip and azimuth) for the instantaneous rock motion, we can determine the velocity producing a given DCN concentration, and we present those expressions here.

We demonstrate and test this method using published DCN data from rift-margins where landscape evolution is dominated by retreat of an escarpment (Braun, 2008). We estimated retreat directions and converted DCN concentrations into fluxes and thus retreat velocities. We focused on data from the Western Ghats where we analyzed 24 basins and found escarpment retreat rates of 160 to 2480 m/Ma (Figure 1). These rates are consistent with near-constant retreat rates since rifting at 65 Ma. We also analyzed data from Brazil, South Africa, the southern Appalachians, and east Australia, finding rates on the order of 100s to 1000s of m/Ma. The high concentrations of DCNs from passive margins thus do not imply static landscapes with only low rates of change. The retreat rates from our method is consistent with ndependent scaling relationship between retreat rate and channel steepness as proposed by Willett et al. (2018).

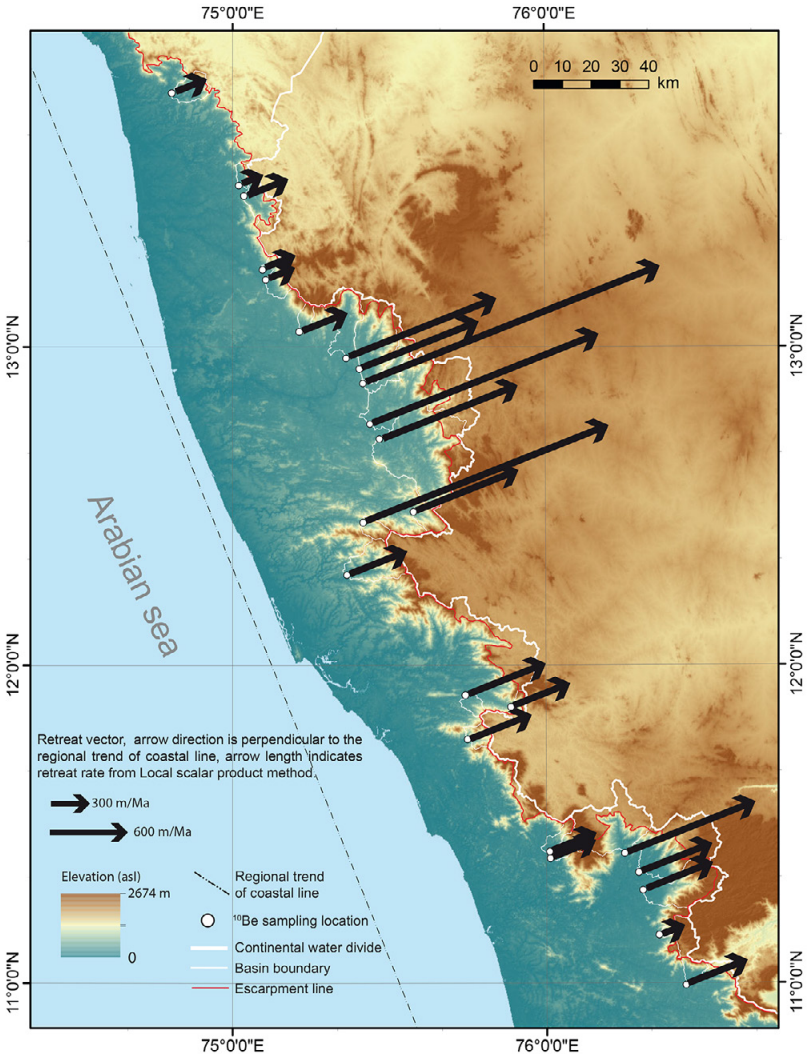


Figure 1. Escarpment retreat rates in the normal direction of the reference coastal line on the topography base map of southern Western Ghats, India. Arrows represent the escarpment retreat vector: the azimuth denotes the retreat direction while the length denotes the retreat rate in that direction. Cosmogenic nuclide concentrations are from Mandal et al., (2015).

REFERENCES

Braun, J. (2018), A review of numerical modeling studies of passive margin escarpments leading to a new analytical expression for the rate of escarpment migration velocity, *Gondwana Research*, *53*, 209-224, doi:10.1016/j.gr.2017.04.012.

Mandal, S. K., M. Lupker, J.-P. Burg, P. G. Valla, N. Haghipour, and M. Christl (2015b), Spatial variability of 10Be-derived erosion rates across the southern Peninsular Indian escarpment: A key to landscape evolution across passive margins, *Earth and Planetary Science Letters*, *425*, 154-167, doi:10.1016/j.epsl.2015.05.050.

Willett, S. D., S. W. McCoy, and H. W. Beeson (2018), Transience of the North American High Plains landscape and its impact on surface water, *Nature*, *561*(7724), 528-532, doi:10.1038/s41586-018-0532-1.

P 9.1

Augmented reality for geosciences: the example of the didactic trail Novi Lé (Lake of Gruyère, FR)

Luc Braillard[1], Julien Magnin[2], Martin Charrière[3], Nathanaël Monney[3], Philippe Jeanrenaud[4] & Jérôme Gremaud[5]

[1]*Department of Geosciences, University of Fribourg (luc.braillard@unifr.ch)*
[2]*Agence DEP/ART, Rue Netton-Bosson 9, CH-1632 Riaz*
[3]*DNA Studios, Rue de Vevey 75, CH-1630 Bulle*
[4]*Vidinoti SA, Passage du Cardinal 1, CH-1700 Fribourg*
[5]*Atelier 11a, Rue du Vieux-Pont 57, CH-1630 Bulle*

Novi Lé (New Lake in local dialect) is a didactic trail created in 2019 around the Lake of Gruyère. It comprises 30 panels distributed into seven walks, which provides information about the lake, its natural environment and its (pre-)history. Four panels are specifically dedicated to geosciences. They tell stories about the glaciers, the palaeo-lake of Gruyère, the influence of bedrock on topography, and the landscape evolution since deglaciation. When scanned with a smartphone or a tablet, each panel starts an interactive animation, designed to be attractive and didactic. The panels will be available at the poster session to test the app and exchange ideas and experiences about the use of augmented reality to explain and promote geosciences in the general public.



Figure 1. Trailer of Novi Lé: launch it by scanning the image once the app has been downloaded.

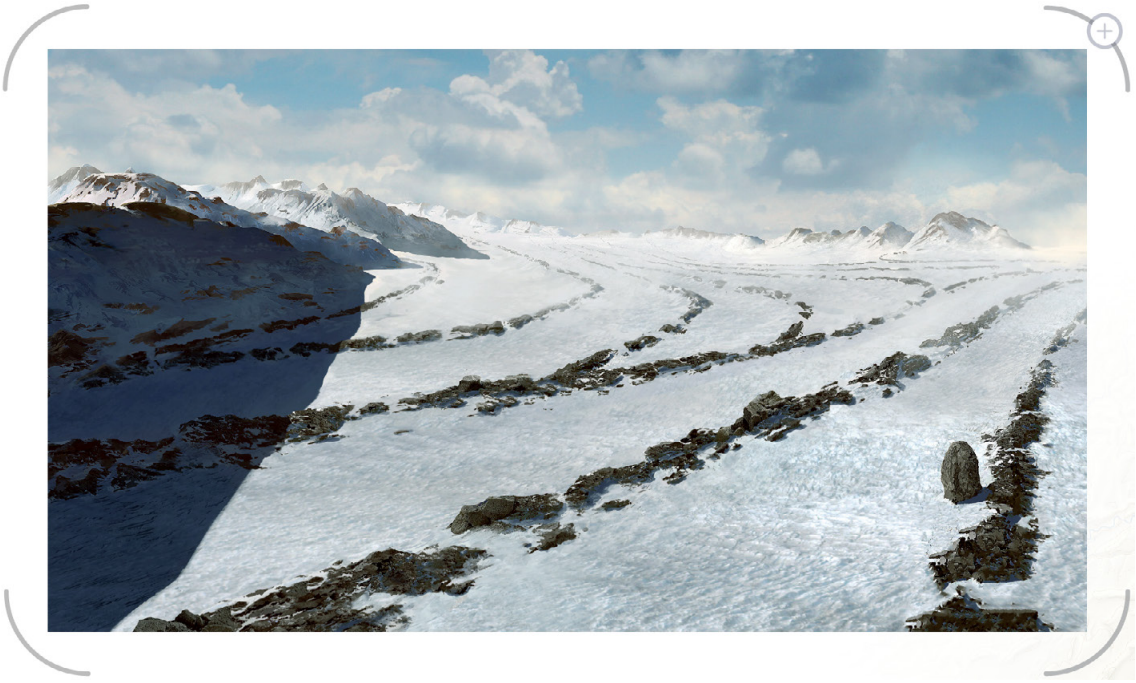


Figure 2. The Gruyère region during the last glacial maximum (ca. 20 ka ago). Confluence between the Valais (right) and Sarine (left) palaeo-glaciers.
Scan the image to start the animation.
© dna studios / L. Braillard, 2019.



Figure 3. Landscape evolution since the deglaciation.
Scan the image to start the animation.
© dna studios / J. Gremaud, 2019.

P 9.2

The 1513 Monte Crenone rock avalanche. Numerical model and geomorphological analysis

De Pedrini Alessandro [1], Scapozza Cristian [1] & Ambrosi Christian [1]

[1]Istituto scienze della Terra (IST), Scuola universitaria professionale della Svizzera italiana (SUPSI), Campus Trevano, 6952 Canobbio, Switzerland (alessandro.depedrini@supsi.ch)

The Monte Crenone rock avalanche of 30th September 1513 is one of the most catastrophic natural events in Switzerland and throughout the Alps. The enormous mass of rock that broke away from the western slope of Pizzo Magn or Mount Crenone, estimated at 50-90 million cubic meters, caused the complete damming of the course of the Brenno river, leading to the formation of a basin that extended from Biasca to the Castello di Serravalle in Semione (De Antoni et al. 2016). On 20th May 1515 the basin formed behind the dam overflowed, giving rise to a wave of more than 10 meters high that led to devastation in the territories downstream to reach Lake Maggiore (Scapozza et al. 2015).

In this project, we analyze the dynamics of the 1513 rock avalanche, trying to reconstruct the event through a numerical model, calculated with the software RAMMS::Debrisflow (RApid Mass Movement Simulation) provided by the Federal Institute for the Study of Snow and Avalanches (SLF/WSL).

The realization of the numerical model was preceded by the reconstruction of the topography before the landslide. This first phase of work, included a geological survey of the landslide body, the analysis of digital data (orthophotos, digital topographic maps, shaded model derived from swissALTI3D) and the collection of previous historical data.

The observation of the stratigraphic data obtained from the 701.27 and 701.30 boreholes (part of the geotechnical studies for the Chiasso-San Gottardo highway) of the GESPOS database (GEstione Sondaggi, POzzi e Sorgenti) of the Institute of Earth Sciences SUPSI was essential to understand the landslide body thickness and volume in the deposition zone.
From the first phase of data collection and interpretation, we then moved on to the actual reconstruction of the digital model of the terrain before the landslide. This operation was carried out using ESRI's ArcGIS software, which made it possible recreating multiple models of the pre-event topography and thus finding the most realistic solution applicable to the subsequent RAMMS model (Figure 1).

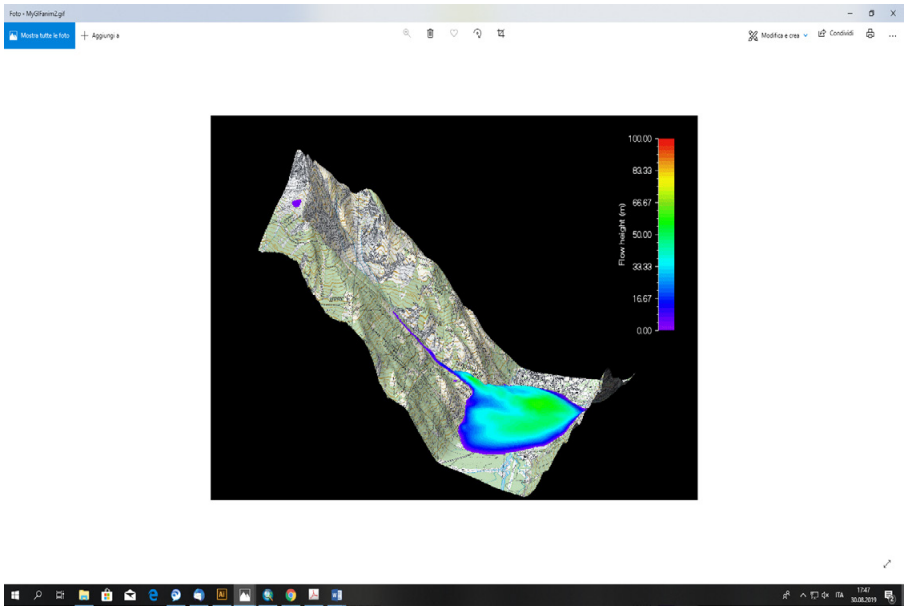


Figure 1. Final numerical model obtained by the Ramms Debris Flow software, (developed by WSL Institute for Snow and Avalanche Research SLF and the Swiss Federal Institute for Forest, Snow and Landscape Research WSL)

REFERENCES

De Antoni S., Scapozza C., Tognacca C., Zucca M., Bernasocchi M., Bruni-Coduri Y. & Chiaravalloti E. 2016. La Buzza di Biasca attraverso le immagini e i documenti. 1515–2015. Biasca, Comune di Biasca, 128 p.

Scapozza C., Tognacca C., Ambrosi C. & Seno S. 2015. 20 maggio 1515: la "Buzza" che impressionò l'Europa. Bollettino della Società ticinese di scienze naturali 103: 79–88.

P 9.3

Surface behavior of the Makran accretionary wedge in Iran from ^{10}Be analyses of river sands and terraces.

Negar Haghipour [1,2] Jean-Pierre Burg[1], Maarten Lupker[1] & Marcus Christl[2]

[1]Department of Earth Sciences, ETH Zurich, Sonneggstrasse 5, 8092 Zürich, Switzerland
[2]Laboratory of Ion Beam Physics, Department of Physics, ETH Zurich, Otto-Stern-Weg 5, 8093 Zurich, Switzerland

The Makran subduction zone hosts in SE Iran and SW Pakistan one of the largest exposed accretionary wedges in the world. However, the western and eastern Makran accretionary wedge differ remarkably in topography and seismicity. While the eastern Makran experienced large earthquakes (e.g. Mw 8.1 in 1945), the western part is seismically quieter. Besides, the surface topography shows more maturity in the western than in the eastern part.

How topography evolves with wedge accretion and whether the topography reached steady states are open questions. We measured catchment wide ^{10}Be in five major catchments draining intramountain basins of the on-shore Iranian Makran. Combined with data from previous studies on incision rates from fluvial terraces found in the same catchments, we provide new arguments for the steady state topography of the wedge on a regional scale.

Another aim of this study was to examine the possible temporal variability of CRN-derived signals driven by climate changes during the Pleistocene and Holocene by comparing modern river derived denudation rates with paleo estimates obtained on the fluvial terraces. Results complement existing information on temporal changes in sediment fluxes, which might point to climatic events in this part of Southwest Asia.

P 9.4

Clibration and sensitivity analysis of a sediment cascade model

Jacob Hirschberg[1,2], Brian McArdell[1] & Peter Molnar[2]

[1]Swiss Federal Institute WSL, Zürcherstrasse 111, CH-8903 Birmensdorf (jacob.hirschberg@wsl.ch)
[2]Institute of Environmental Engineering, ETH Zürich, Stefano-Franscini-Platz 5, CH-8093 Zürich

Investigating geomorphological processes in a modelling framework is crucial for (a) gaining understanding of the interactions between climate, weathering and sediment history, for (b) conducting studies on climate change impacts and for (c) hazard scenario assessment. In the Alps and on a small catchment scale (~0.1 – 10 km^2), the high-resolution input data needed for determinstc and physically-based models are often missing or highly uncertain. Consequently, the outputs of such models often lack significance. Thus, geomorphological processes are often investigated in stochastic frameworks in combination with parameterising well-established concepts. These parameters only have limited physical meaning and need to be calibrated. Consequently, the conceptual models should be examined on their sensitivity to those parameters to avoid overinterpretation of the results and highlight knowledge gaps.

SedCas (Bennett et al., 2014) is a sediment cascade model developed for reproducing debris-flow first-order characteristics such as magnitude, frequency and seasonality. The model consists of a hydrological and a hillslope module and is forced by climatic variables (precipitation and temperature) as well as a magnitude-frequency distribution of hillslope failures providing sediments to the channel. The land-use types (forest, bedrock/scree) are lumped into hydrological response units represented as linear reservoirs. SedCas operates at hourly time steps, which is a representative time scale for debris-flow triggering.

SedCas was developed for the Illgraben, a highly debris-flow prone catchment in the canton of Valais, Switzerland, with an average of 3-4 debris flows yearly. While debris-flow dynamics at the outlet of the catchment are observed since 2003 with a force plate (McArdell et al., 2007), data to calibrate the hydrological module is missing (e.g. discharge measurements, soil properties). Therefore, we calibrate eight parameters of SedCas (Table 1) in a Monte Carlo approach using posterior analysis and quantify the model's sensitivity to uncertainty in the parameters using Sobol' indices (Sobol, 2001). Sobol' indices express the proportion of variance in the model output, which can be attributed to the uncertainty of the specific parameter.

Preliminary results reveal that with the approach of posterior analysis, debris-flow paramters can be well constrained whereas for the hydrological parameters (storage capacities and residence times), a wide range of parameter values can lead to similar results (Figure 1). The findings of this study has implications for future applications of SedCas. We will use the model to assess climate change impacts on sediment yield and debris-flow activity. Therefore, this study provides objectively obtained measures for the significance of model outputs.

Parameter	Name	Unit	Range
Storage capacity forest, upper layer	Vwcap11	mm	1 - 50
Storage capacity forest, lower layer	Vwcap12	mm	1 - 50
Storage capacity scree	Vwcap2	mm	1 - 50
Mean residence time forest, upper layer	k11	h	2 - 400
Mean residence time forest, lower layer	k12	h	2 - 400
Mean residence time scree	k2	h	2 - 48
Max sediment concentration	smax	-	0.45 - 0.9
Specific debris-flow triggering discharge	qdf	mm/h	0.1 - 10

Table 1: List of parameters from the SedCas model which are subject to calibration and sensitivity analysis.

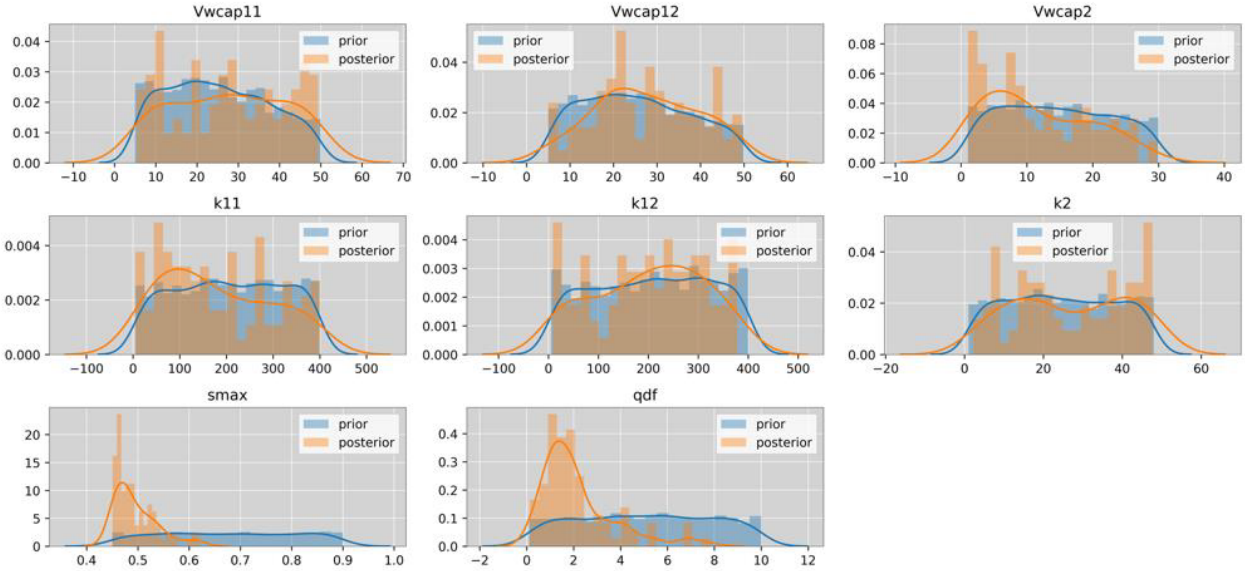


Figure 1. Histograms of the parameters listed in Table 1. Prior parameter distributions are uniform and blue (n=2000). The posterior distributions (orange, n=100) consist only of parameter sets with behavioural model results (i.e. within accepted limits).

REFERENCES

Bennett, G. L., Molnar, P., McArdell, B. W., & Burlando, P. 2014: A probabilistic sediment cascade model of sediment transfer in the Illgraben. Water Resources Research, 50(2), 1225-1244.

McArdell, B. W., Bartelt, P., & Kowalski, J. 2007: Field observations of basal forces and fluid pore pressure in a debris flow. Geophysical Research Letters, 34(7).

Sobol, I. M. 2001: Global sensitivity indices for nonlinear mathematical models and their Monte Carlo estimates. Mathematics and computers in simulation, 55(1-3), 271-280.

P 9.5

Close-up imaging simulation in the Marslabor of the University of Basel

Jean-Luc Josset[2], Tomaso Bontognali[2,1], Beda Hofmann[3], Yardena Meister[1], Nikolaus J. Kuhn[1°]

°1 University of Basel, Physical Geography, Environmental Sciences, Basel, Switzerland (nikolaus.kuhn@unibas.ch)
[2]Space Exploration Institute, Neuchâtel, Switzerland,
[3]Natural History Museum, Bern, Switzerland

Close-up imagers such as MAHLI or CLUPI are often described as the equivalent of a geoscientist's hand lense mounted on a rover. Compared to the use of a hand lense by a geoscientist in the field, the use of such imagers for extracting information, e.g. on rock properties, rock formation or their potential to contain biosignatures, is biased. The difference between the tools is caused by the resolution and spectral recording capacity of the imager, as well as the environmental conditions when an image is taken. During rover missions, ideal conditions to take close-up images are rare or require extra time, energy and data transmission volume. Preparing the use of close-up imagers during a mission is therefore essential for maximizing the scientific output of rover operations. The Marslabor of the University of Basel aims at providing the opportunity to test the operations of close-up imagers in situations that resemble those during a rover mission to another planetary body. The main elements of the Marslabor are a Marsyard with variable surface conditions, in particular surface color and roughness, lighting simulating different positions of the sun at various degrees of intensity and atmospheric diffusion, and a small rover carrying a commercial camera with macro-lense offering a field of view similar to the ExoMars Close-up Imager (CLUPI). The aims of the tests conducted in the University of Basel's Marslabor are (i) the identification of the best lighting for the recognition of biosignatures, (ii) rock identification from the furthest possible distance during rover drives, and (iii) integration of close-up imagers in rover exploration cascades.

REFERENCES

Josset J-L., Westall F., Hofmann B.A., Spray J., Cockell C., Kempe S., Griffiths A.D., De Sanctis M.C., Colangeli L., Koschny D., Föllmi K., Verrecchia E., Diamond L., Josset M., Javaux E.J., Esposito F., Gunn M., Souchon-Leitner A.L., Bontognali T.R.R., Korablev O., Erkman S., Paar G., Ulamec S., Foucher F., Martin P., Verhaeghe A., Tanevski M., Vago J.L. (2017) The Close-Up Imager Onboard the ESA ExoMars Rover: Objectives, Description, Operations, and Science Validation Activities. ASTROBIOLOGY. Volume 17, Numbers 6 and 7 (2017) 595-610.

P 9.6

Tracing sediment processes with paired cosmogenic nuclides (in-situ ^{14}C & ^{10}Be)

Maarten Lupker[1], Kristina Hippe[2], Lukas Wacker[3], Negar Haghipour[1,3], Pierre-Henri Blard[4] & Jérôme Lavé[4]

[1]Geologisch Institut, ETH Zürich, Sonneggstrassse 5, CH-8092 Zürich (maarten.lupker@erdw.ethz.ch)
[2]Institute of Geological Sciences, Freie Universität Berlin, Malteserstrasse 74-100, 12249 Berlin
[3]Ion Beam Physics, ETH Zürich, Otto-Stern-Weg 5, CH-8093 Zürich
[4]CRPG Nancy, 15 rue Notre Dame des Pauvres, 54500 Vandoeuvre

Cosmogenic nuclides, such as ^{10}Be, measured in detrital river sediments are widely used to derive denudation rates and sediment fluxes at the scale of entire catchments. Pairing ^{10}Be with another short-lived nuclide such as in-situ ^{14}C (5700 years half-life) allows tracing erosion and sediment processes occurring on Holocene time-scales to be traced at the Earth's surface.

In this contribution we use paired ^{10}Be - in-situ ^{14}C measurements in detrital sediments produced by the rapidly eroding Himalayan range to better quantify how sediments are produced and transferred from source to sink. ^{10}Be and in-situ ^{14}C data from trans-Himalayan rivers show that the concentration of in-situ ^{14}C relative to ^{10}Be is lower than what would be expected if sediments were produced by steady-state superficial erosion of the landscape. Such apparent offset between ^{10}Be and ^{14}C concentrations may be explained by the erosion and mobilisation of sediments from large, deep-seated landslides. In that case, we show that it is possible to use paired ^{10}Be and in-situ ^{14}C measurements in detrital sediments to evaluate the average landslide depth and recurrence time averaged over the scale of entire catchments.

Once the sediments are exported to the lowlands, the paired ^{10}Be - in-situ ^{14}C concentrations measured in sediments are mainly sensitive to sediment transfer processes in the floodplain. Sediment storage in alluvial settings leads to the partial shielding of sediments from cosmic rays and results in the rapid decay of ^{14}C in comparison to ^{10}Be. Our preliminary data obtained from the sediments sampled at the mouth of the Ganges in Bangladesh has ^{10}Be-^{14}C signatures close to those measured in the trans-Himalayan rivers mentioned above, suggesting a rapid sediment transfer of sediments through the floodplain separating the Himalayan range from the Bay of Bengal.

P 9.7

JuraHydroSlide: identifying the principal hydrogeologic ingredients for predicting landslide activity in Jura Mountains

Arnaud Rüegg[1], Giona Preisig[1]

[1]*Centre for Hydrogeology and Geothermics, University of Neuchâtel, Rue Emile-Argand 11, CH-2000 Neuchâtel (arnaud.ruegg@unine.ch)*

Landslides phenomena are a type of natural hazard that can compromise people's safety and infrastructures, especially in mountainous areas. Each year in Switzerland, several accidents and damage to infrastructure are recorded in the Alps, on the Plateau or in the Jura massif due to landslide activities. Thus, in 2018, landslides have been introduced in the governmental program for protecting and alerting the Swiss population against natural hazards. However, large-scale predictions of landslide activity can be tedious and complex due to their high dependence on local rock and soil properties, as well as environmental conditions. In addition, monitoring systems of slope deformation for anticipating incipient failure or enhanced slope activity are simply too expensive for covering large spatial and temporal scales. Thus, the objective of the *JuraHydroslide* project is to find alternative hydrogeologic indicators and develop innovative tools for making short- and long-term predictions of landslide activity in the Jura Mountains, as well as assess the interaction between karst systems and slope stability. The study sites are distributed along the Jura massif to cover several types of landslides, such as permanent deep-seated landslides, superficial spontaneous landslides, peat landslides or rock avalanches. Particular attention will be paid to the role of groundwater in these different landslide phenomena, especially in the triggering and propagation aspects of these natural processes. The pre-historic Chasseral landslide (Nods, BE), described as a rock avalanche, takes part in the first development step of the *JuraHydroslide* project, by exploring its geometrical properties, via the acquisition and processing of Electrical Resistivity Tomographies (ERT).This permits the assessment of pre-failure and post-failure geologic and hydrogeologic conditions. Hence, this landslide was studied in order to precisely assess the thickness of the deposit area along multiple ERT cross sections, the source and deposit volumes, the travel angle, the travel distance and the mean flow velocity (Fig. 1). These field data will be used to constrain numerical models of slope stability and landslide propagation for evaluating and better understanding the triggering and propagation mechanisms.

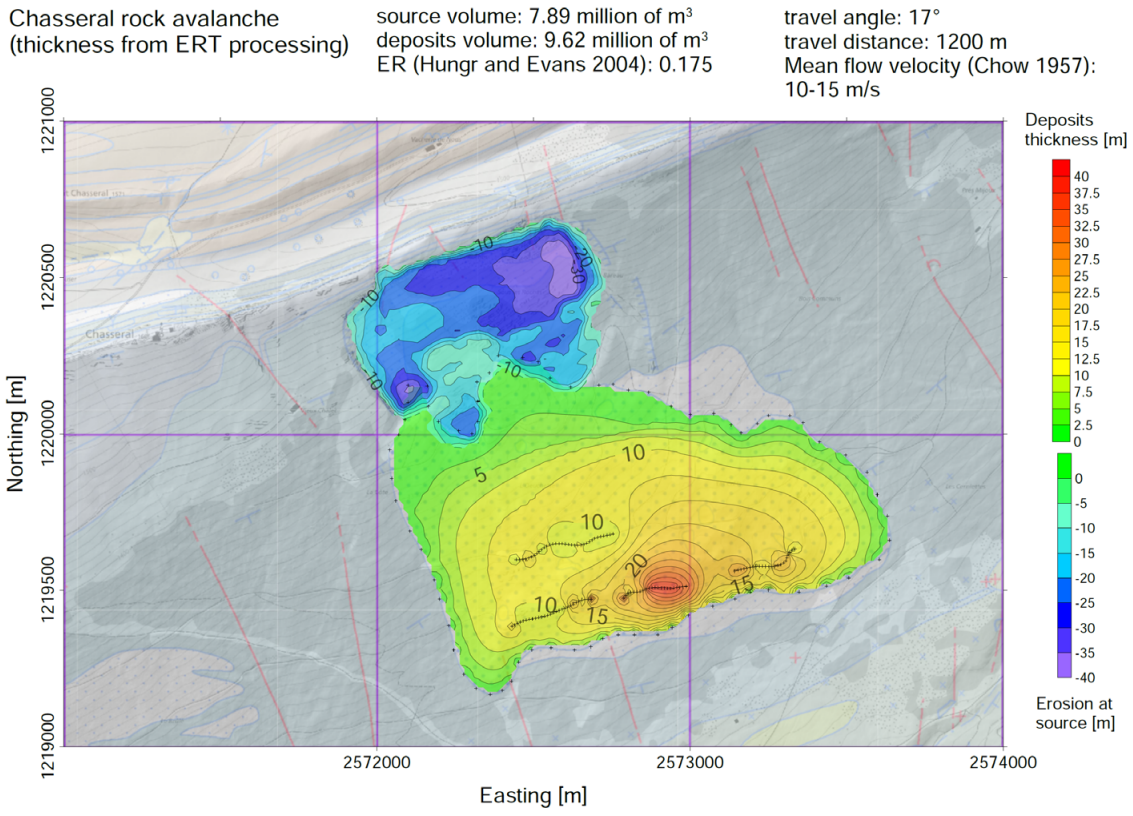


Fig. 1: Geomorphologic and kinematical properties of the Chasseral rock avalanche derived from high resolution ERT profiles, analyses of the digital elevation model swissALTI3D from swisstopo and geostatistical modelling.

P 9.8

Morphodynamic Evaluation of Barchan Movement in Robat-e-Posht Badam, Iran

Alireza Salehipour Milani[1], Fatemeh Mousazadeh[2], Rasoul Rafiei[3]

[1]Departmet of Physical Geography, University of Shahid Beheshti, Evin, Tehran, Iran, (ar.salehipour@gmail.com)
[2]Departmet of Physical Geography, University of Shahid Beheshti, Evin, Tehran, Iran 3Departmet of Physical Geography, University of Shahid Beheshti, Evin, Tehran, Iran

Introduction

More than 50% of Iran area located in arid and semi-arid regions including deserts and playas geomorphological units. Sand dune and barchans area are the most important landform in desert environments of Iran. There are more than 20 relatively large Erg in Iran, as well as numerous small sand dune field with an area of about 36,000 square kilometers (Mahmoudi, 1991). Dynamics of this landforms affect human settlements, as well as the economic and commercial buildings, road and rails roads and cause a serious threat to human societies. The studied area is located in central parts of Iran, between Yazd and Tabas and near the Robat-e-poshtbadam regins. The movements of sand dune especially barchans in this region are causing damage and blocking Yazd Tabas. Hence morphodynamics investigations of sand dunes and barchans are essential in this region. In this study, 35 individuals' barchans were studied and movement rate and direction of movement was calculated to obtain dynamics of barchans and control sand dunes movements in study area.

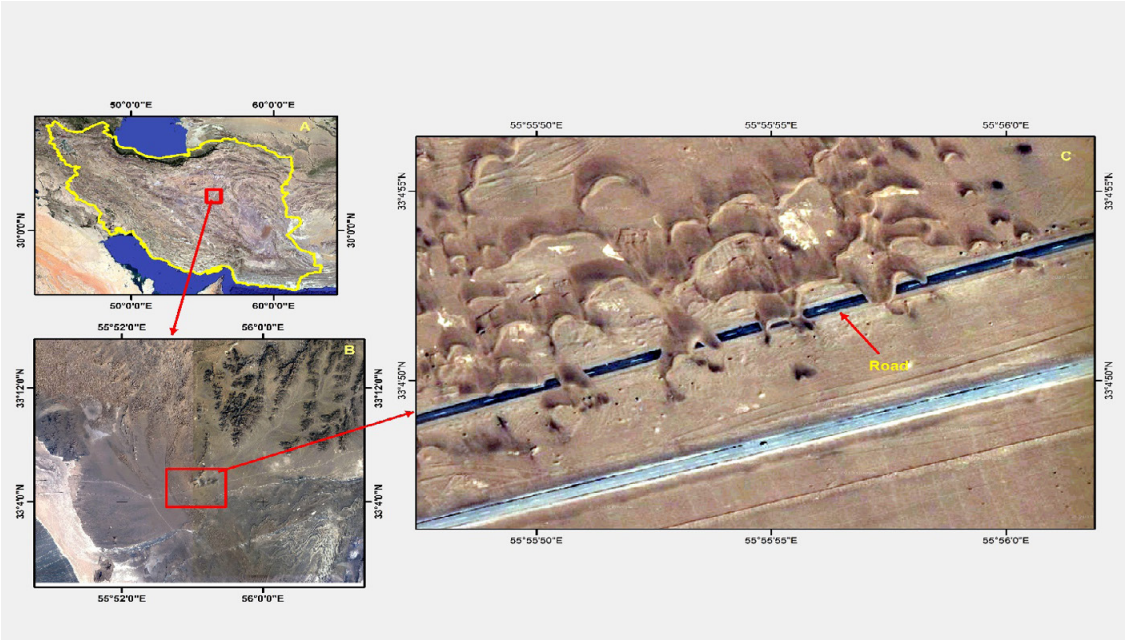


Fig1. A: Locations of Study area in Iran (red quadrangle), B: Study Area, C: Effects of barchan movement on blocking Major Road in study area

Material and Method

Quick bird satellite data are used to calculate rate and direction of barchan dune movement between from 2005 to 2012. This process was automatically extracted from these images using Geographic Information System (GIS) and spatial analysis techniques provided by image processing software. the migration distance of each barchan dune (D) in meter is equal to the average length of lines that connecting every two corresponding points; the obtained migration distance which refers to the whole period (2005 and 20112)was averaged to express the yearly movement rate for each barchan dune (m/year)Equation 1; also, the barchan movement direction (A) in degree clockwise from north is automatically extracted, the barchan migration rate and direction are expressed by the equations2 (Boulghobra and Hadda Dridi ,2016). in order to investigation wind characteristic role migration rate and direction Wind rose diagram generated using annual.

$$D = \sqrt{(y_2 - y_1)^2 + (x_2 - x_1)^2} \qquad (1)$$

$$A = 180/pi * \alpha tan\left((y_2 - y_1)\right)/(x_2 - x_1)) \qquad (2)$$

Discussion and Results

point-to-point geo correlation on fine resolution imagery between 35 individual barchans in study area allowed accurately

measuring the barchan movement rate and direction; results showed that the movement rate in posht badam region ranged from 6.6 to 20 m/year) during the period 2005-2012. The obtained direction of barchan movement is ranging from South east South. Composite meteorological records derived from Iran Meteorological Organization including wind speed and directions suggests causes of this direction and tare of barchan fluctuations is a variability in regional wind regime. The results indicate that Quick Bird images, is useful tools for mapping, analyse and monitor the spatial and temporal behaviour of barchan including: mobility, speed and directions in arid regions.

REFERENCES

Boulghobra, N., & Hadda Dridi. 2016: Fine resolution imagery and GIS for investigation the morphological characteristics, and migration rate of barchan dunes in the erg sidi moussa dunefield near in- salah (Algeria), Geographia Technica, 11(2),14 – 21.

Mahmoudi, faraj Allah. 1991: Dynamic Geomorphology,Payamnour publication

P 9.9

Schmidt hammer exposure-age dating of (peri-) glacial landforms thanks to R-values calibration by historical data in the Southern Swiss Alps

Cristian Scapozza[1], Christian Ambrosi[1], Chantal Del Siro[2] & Christophe Lambiel[2]

[1]*Istituto scienze della Terra, Scuola universitaria professionale della Svizzera italiana (SUPSI), Campus Trevano, CH-6952 Canobbio (cristian.scapozza@supsi.ch)*
[2]*Institut des dynamiques de la surface terrestre, Université de Lausanne, Quartier UNIL-Mouline, CH-1015 Lausanne*

Within the framework of scientific researches related to geomorphological and climatic evolution of the Alps during Lateglacial and Holocene, only few studies were carried out on periglacial sedimentary terrains. In order to reconstitute the palaeoenvironmental history of the alpine periglacial domain, this research has focused on the morphostratigraphy of periglacial and glacial landforms of the Splügenpass region (transnational pass between Switzerland and Italy) and of the upper part of Val Scaradra (north-eastern part of the Ticino Canton).

The surface dating was performed with the analysis of Schmidt hammer rebound values (R-values). The joint utilisation of palaeogeographical method, allowing the reconstruction of past glacier and rock glacier extensions, and the definition of age-calibration curves of R-values on historical constructions and thanks to historical cartography, allowed Schmidt hammer exposure-age dating (SHD) and the definition of relative chronologies with high temporal resolution.

In the Splügenpass region, Schmidt hammer R-values measured on metagranite porphyr of the Suretta-Nappe ("Rofna-Porphyr") were calibrated thanks to two historical retaining walls for a mule track, attributed respectively to the Roman Epoch (1.65 ka cal BP) and to the Late Middle Ages (0.7 ka cal BP) (Figure 1). Thanks to SHD, it was possible to establish a chronology of the Lateglacial glacier retreat and to date rock glaciers and talus slopes development. The results show that Splügenpass was ice free since 15.8 ± 2.6 ka cal BP, whereas the Splügenpass rock glacier started its formation during the Lateglacial Interstadial (the minimal age of the front is of 12.6 ± 2.6 ka cal BP).

In the upper Val Scaradra, R-values were measured on large boulders of the proglacial area of the Vadrecc di Scaradra (Scaradra glacier) composed by micaschists and paragneisses of the Adula-Nappe (Del Siro, 2019). From a Younger Dryas lateral moraine to the glacier portal, several Holocene terminal moraines were studied by SHD in order to determine the glacier fluctuation during the last centuries (Scapozza, 2014). Schmidt hammer R-values were calibrated thanks to historical topographic maps of the area: (1) the original relief for the Dufour Map (Topographical Map of Switzerland, sheet OA 443, Feuille XIX. Sect. 2, 1:50'000) cartographed by Hermann Siegfried in 1854; (2) the editions of the Sheet 504/ Olivone of the Siegfried Map (Topographical Atlas of Switzerland, 1:50'000; the first edition is from 1872) and; (3) the editions of the Sheet 1253/Olivone of the National Map of Switzerland 1:25'000 (the first edition is from 1966).

The SHD age-calibration based on historical surfaces of known age highlights a non-linear behaviour of surface weathering from the Lateglacial to the Late Holocene. These investigations will also improve the knowledge of the potential use of SHD for numerical-age dating in alpine geomorphological studies, a field of research that is currently rapidly developing and that can be an alternative to Cosmogenic Nuclides dating in the understanding of complex glacial-periglacial-paraglacial landsystems.

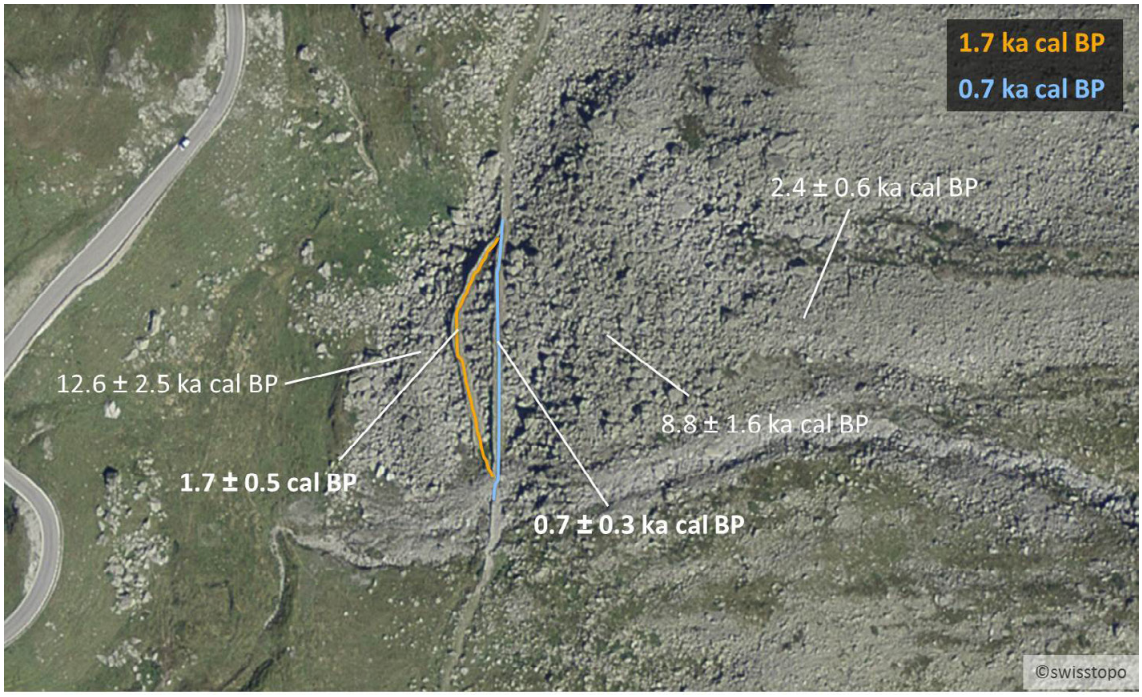


Figure 1. SHD show a probable evidence of final “relictification” between the Roman Period and the Late Middle Ages. Orthophoto: Swiss Federal office of topography swisstopo.

REFERENCES

Del Siro, C. 2019: Les fluctuations des glaciers après le Petit Âge Glaciaire. Datation de cordons morainiques dans le Val Scaradra avec la méthode du marteau de Schmidt et l’analyse de cartes historiques. Travail de Bachelor, Université de Lausanne.

Scapozza, C. 2014: Appunti climatici e glaciologici sulle descrizioni della Valle di Blenio tra Settecento e Ottocento, Archivio Storico Ticinese, 155, 38-63. http://repository.supsi.ch/5751/

P 9.10

A Cross-Comparison between a Traditional Portable Straight-Line Wind Tunnel and PI-SWERL over an Altitude Gradient

Cynthia C.E. van Leeuwen[1], L.H. Cammeraat[1], Nikolaus J. Kuhn[2], Wolfgang Fister [2] & Heleen C. Vos [2]

[1]*Institute for Biodiversity and Ecosystem Dynamics, Ecosystem and Landscape Dynamics Group, University of Amsterdam, PO Box 94240, Amsterdam 1090 GE, The Netherlands (cce.vanleeuwen@gmail.com)*
[2]*Physical Geography and Environmental Change, University of Basel, 4056 Basel, Switzerland*

Dust emissions by soils, primarily originating from hot and cold (semi-) deserts, can have a large effect on the Earth's system. Long distance transport of suspended dust potentially affects air circulation systems, biogeochemical cycles of oceanic and terrestrial ecosystems, soil characteristics and geomorphology. To generate dust emission, a particular wind velocity must be exceeded: the threshold friction velocity. Most research focused on the relation between wind velocities and dust emission has been carried out at sea level, where a high air pressure, and thus high air density, is present. Studies on the effect of low air density conditions are primarily focused on extra-terrestrial environments. However, more recent research demonstrated that the intensity of wind erosion on Earth decreased with decreasing air density. These findings form the basis for this research, which aims to *establish the relationship between threshold friction velocities and PM_{10} dust emission, taking changing air density into account, while comparing two types of instruments: a traditional portable straight-line wind tunnel, and a new type of instrument, the PI-SWERL.* The research is divided into two components: 1) a cross-comparison between a traditional portable straight-line wind tunnel and the PI-SWERL, and 2) a study on the influence of decreasing air density on the threshold friction velocity for PM_{10} emission by employing the PI-SWERL in the field. It was found that compared to the wind tunnel, the PI-SWERL measured significantly different threshold friction velocities for one of the materials, which can possibly be attributed to the experimental set-up. To obtain data about the effect of changing air density on the threshold friction velocity and dust emission potential of soils, four field locations at different altitudes in Switzerland were chosen to create an altitude gradient. When testing the PI-SWERL in the field, a highly significant positive linear relationship between the threshold friction velocity for PM_{10} emission and air density was found. Furthermore, a significant negative linear relationship between the PM_{10} emission potential and air density was found, as the PM_{10} emission decreased with decreasing air density. Despite the different measured thresholds for PM_{10} emission, it is believed that the PI-SWERL can be used to study certain aspects of wind erosion. For future research, several adjustments need to be done to the experimental design to reduce variance between replicates and improve reproducibility.

REFERENCES

Bagnold, R. (1941). The physics of wind blown sand and desert dunes. London: Methuen.

Etyemezian, V., Nikolich, G., Ahonen, S., Pitchford, M., Sweeney, M., Purcell, R., Kuhns, H. (2007). The portable in situ wind erosion laboratory (PI-SWERL): a new method to measure PM10 windblown dust properties and potential for emissions. Atmospheric Environment, 41(18), 3789–3796.

Han, Q., Qu, J., Dong, Z., Zu, R., Zhang, K., Wang, H., & Xie, S. (2014). The effect of air density on sand transport structures and the adobe abrasion profile: a field wind-tunnel experiment over a wide range of altitude. Boundary-layer meteorology, 150(2), 299–317.

Iversen, J. D. & White, B. R. (1982). Saltation threshold on earth, mars and venus. Sedimentology, 29(1), 111–119.

Middleton, N. (2017). Desert dust hazards: a global review. Aeolian research, 24, 53–63.

White, B. & Mounla, H. (1991). An experimental study of froude number effect on wind- tunnel saltation. Aeolian grain transport 1 (pp. 145–157). Springer.

P 9.11

Extracting landslide dynamics from seismic signals based on empirical Green's function

Zhen Zhang[1], Fabian Walter [2], Siming He[1]

[1]Key Laboratory of Mountain Hazards and Surface Process, Institute of Mountain Hazards and Environment, Chinese Academy of Sciences, Chengdu, 610041, China (zhangzhen@imde.ac.cn)
[2]Laboratory of Hydraulics, Hydrology and Glaciology, ETH Zurich, Zurich, 8093, Switzerland

Over the last two decades, many studies have attempted to estimate the source characteristics of landslide using seismic signals. Based on the single-force source model, the landslide force history can be obtained by inverting long-period seismic signals (Ekström and Stark, 2013). When the inverted force-time function of the landslide is combined with field observations, the landslide's dynamics can be reconstructed. However, the higher-frequency seismic signals cannot be used to invert the force-time function of the event because calculatingthe Earth's higher-frequency elastic response ('Green's functions') requires a crustal velocity model at a precision, which is usually not available (Allstadt, 2013).

Moreover, our understanding of physical sources models for the high-frequency seismic signals is still incomplete. In this paper, we use seismic signals generated by a smaller landslide that have occurred at the same place as larger ones as the empirical Green's function (EGF) to obtain the main landslide dynamics from high-frequency signals. This avoids the requirement to calculate Green's function. When the source of the smaller landslide is simple, the dynamics of the main event can be described as the combination of simple mass motions. Using the EGF, we obtain the apparent force-time function of the landslide based on the EGF by inverting the higher-frequency seismic signals. Based on this apparent force-time function, we can obtain more detailed landslide dynamics. This paper thus shows that the EGF can be used to quantitatively estimate the dynamics of a landslide.

REFERENCES

Allstadt, K. 2013: Extracting source characteristics and dynamics of the August 2010 Mount Meager landslide from broadband seismograms, Journal of Geophysical Research: Earth Surface, 118(3):1472-1490.

Ekström, G. & Stark, C.P. 2013: Simple scaling of catastrophic landslide dynamics, Science, 339(6126):1416-1419.

10. Soil: Formation, Processes, and Conservation

Klaus Jarosch, Tobias Sprafke, Tatenda Lemann, Volker Prasuhn

TALKS:

10.1 Boivin P., Dupla X., Lemaître T., Deluz C., Gondret K., Sauzet O.: Carbon sequestration in Swiss arable land: insights from the case of Geneva Canton

10.2 Deluz C., Nussbaum M., Sauzet O., Gondret K., Boivin P.: Monitoring the soil organic carbon with farmers. The case of Geneva canton climate plan

10.3 Deluz C., Sebag D., Verrecchia E., Boivin P.: Organic matter quality in arable land as influence by clay content and cropping system

10.4 Fischer A., Wendling M., Sebag D., Charles R., Bayon L.R.C.: Evaluation of earthworms as soil quality indicator for the farmers

10.5 Foetisch A., Filella M., Fischer D., Muntwyler A., Watts B., Witte K., Bigalke M.: A method of extraction and analysis of nanoplastics in soils

10.6 Grand S., Turberg V., Fayolle A., Unc A.: The podzolization process in a context of land disturbance

10.7 Gudrun Schwilch: KEYNOTE: Soil protection in Switzerland between policy and practice

10.8 Keel S.G., Anken T., Büchi L., Chervet A., Fliessbach A., Flisch R., Huguenin-Elie O., Mäder P., Mayer J., Sinaj S., Sturny W., Wüst-Galley C., Zihlmann U., Leifeld J.: Loss of soil organic carbon in Swiss long-term agricultural experiments over a wide range of management practices

10.9 Millière L., Gussone N., Bindschedler S., Verrecchia E.P.: Growth conditions and Ca sources of pedogenic needle fibre calcite (NFC)

10.10 Rodrigues L., Sprafke T., McKey D.: The ephemeral legacy of nutrient management in tropical seasonal wetland Anthrosols

10.11 Rowley M.C., Grand S., Adatte T., Verrecchia E.P.: The cascading influence of $CaCO_3$ on the pedogenic trajectories and biogeochemistry of the subalpine soils at the Nant valley, Switzerland.

POSTERS:

P 10.1 Grand S., Viret F., Turberg V., Marmier V., Verrecchia E.P. SWISSOIL: a pedagogical multimedia resource in soil science

P 10.2 Keller R., Sprafke T., Waroszewski J., Ndjigui P.-D., Tchawa P., Veit H.: Soil color and geochemistry along a W-E transect on the S-Cameroon Plateau

P 10.3 Lauer F., Peticzka R., Sprafke T.: Cover beds of local and aeolian deposits influence soil evolution along a hillslope in N-Bavaria

P 10.4 Musso A., Ketterer M.E., Egli M.: Soil erosion rates over time derived from two high Alpine soil chronosequences

P 10.5 Sprafke T., Veit H.: Pedogenesis – a matter of perspective? Case studies from the temperate and the tropical zone

P 10.6 Van Thuyne J., Verrecchia E.: Are Fungus-Growing Termites Major Contributors To Sediment Grain-Size Distributions In Subtropical Environments?

P 10.7 Dietrich F., Diaz N., Deschamps P., Sebag D., Verrecchia E.P.: Quaternary calcium transfer in semi-arid African landscapes: pedogenic nodules and the geochemical cascade

P 10.8 Jarosch K.A., Chen H., Lima A.B., Westphal Muniz A., McLaren T., Müller C., Frossard E., Oberson A.: Factors governing soil phosphorus availabilty in Amazonian Dark Earth

10.1

Carbon sequestration in Swiss arable land: insights from the case of Geneva Canton

Pascal Boivin[1], Xavier Dupla[1], Téo Lemaître[1], Cécric Deluz[1], Karine Gondret[1] & Ophélie Sauzet[1]

[1]HEPIA Sols et Substrats, HES-SO Genève, 150 route de Presinge, 1254 Jussy (pascal.boivin@hesge.ch)

The canton of Geneva has adopted a climate plan compatible with the objectives adopted at the COP21 conference. Among measures, the measure 6.4 projected to sequestre 15'000 t of CO_2 per year in the topsoil of arable land. Investigations were performed to define how this objective should be achieved. Each field was analysed for Soil Organic Carbon (SOC) content at least every ten years with international standards whose results are available in the canton database. Therefore, the annual change in SOC was quantified for more than 600 fields for which the field limits were unchanged between 2 analyses. The annual rates of SOC ranged between -30‰ and +45‰ (Figure 1). In average, the SOC content was decreasing before 2000 and increased later-on, in connection with the introduction od conservation agriculture and reduced tillage methods (Figure 2). The cropping practices corresponding to the range of observed rate of SOC change were analysed in 60 farms, thus leading to a general model of SOC change according to cropping practices. This meta-analysis underlined the potential and limits of conservation agriculture practices, and allowed to define the priority actions to conduct for increased carbon sequestration in arable land.

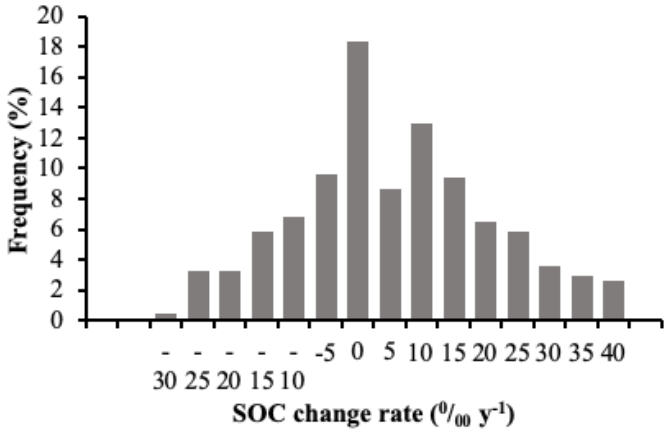


Figure 1. Histogram of the annual SOC change rate for 600 fields of the canton of Geneva.

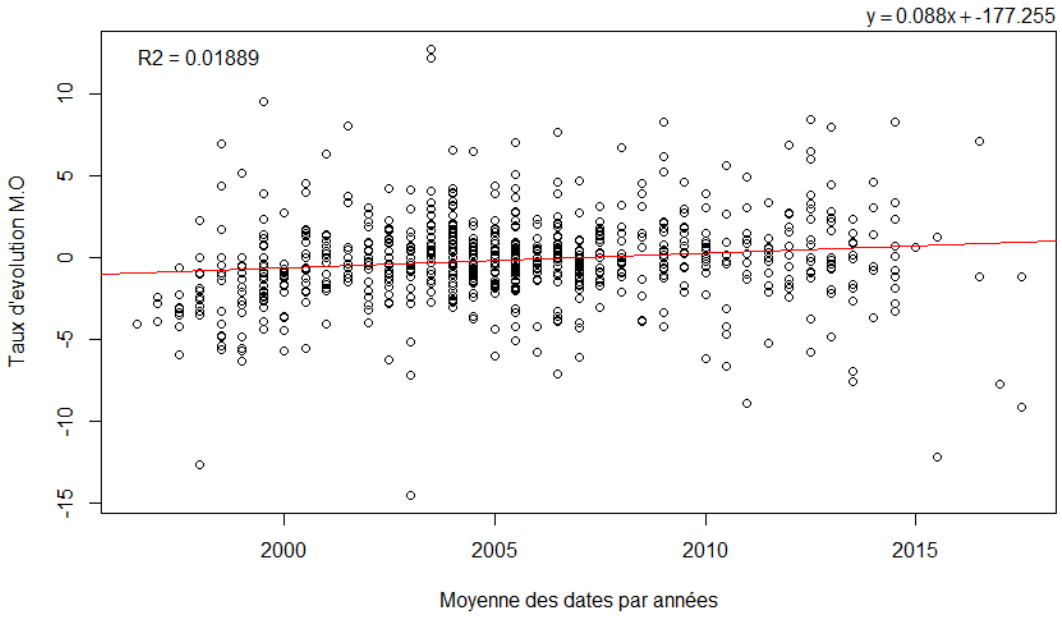


Figure 2 – Time evolution of the annual rate of SOC change in Geneva Arable land.

10.2

Monitoring the soil organic carbon with farmers. The case of Geneva canton climate plan

Cédric Deluz[1], Madlene Nussbaum[2], Ophélie Sauzet[1], Karine Gondret[1] and Pascal Boivin[1]

[1]University of Applied Sciences and Arts Western Switzerland, HEPIA Soils and Substrates, Route de Presinge 150, 1254 Jussy Geneva, Switzerland (pascal.boivin@hesge.ch)
[2]Bern University of Applied Sciences, School of Agricultural, Forest and Food Sciences (BFH-HAFL), Länggasse 85, 3052 Zollikofen, Switzerland

Increasing soil organic carbon (SOC) content is crucial for soil quality restauration and climate change mitigation. SOC monitoring is indispensable to the corresponding policies and should provide results at farm scale to allow for incentives. In Switzerland farmers perform mandatory analyses of the SOC content of the 0-20 cm topsoil of every field, based on a composite sample, at least every ten years. The corresponding results were stored in a database in canton of Geneva. The minimum detectable change (MDC) calculated based on the observed SOC changes was 0.013 % g g-1 at canton scale (2700 fields). Three representative fields were extensively sampled to simulate different sampling strategies and determine best sampling guidelines for farmers. Collecting 20 aliquots with a gouge on the field diagonals was considered the best sampling compromise with MDCs of about 0.1 % g g-1 and a sampling duration of 20 mn. Compared to this procedure, former farmers' sampling was not biased in average but showed a variance of 0.22% g g-1 due to smaller number of aliquots and varying sampling depths. Based on the best sampling results and assumptions on farm-scale SOC variance or SOC differences, the MDCs at farm scale ranged from 0.21 to 0.12 % g g-1 (5 fields) and 0.09 to 0.05 % g g-1 (30 fields), respectively (Figure 1). These MDCs are small compared to published monitoring networks MDCs, and allow determining SOC change rates at farm scale, thus representative an inexpensive and potentially efficient monitoring in the frame of soil quality or climate mitigation incentives.

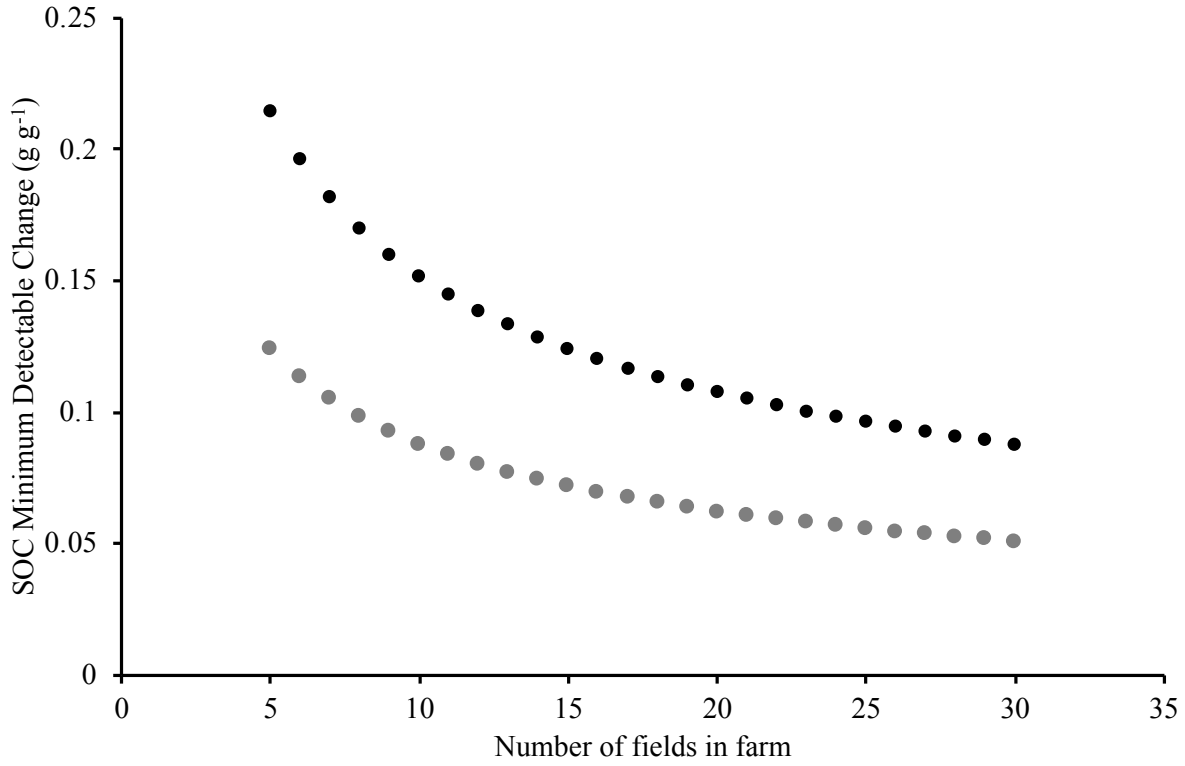


Figure 1. Minimum Detectable Change of SOC at farm scale, as a function of the number of fields. Black dots: calculated using Eq. (2) and the estimated variance of the difference between two consecutive analyses at farm scale; grey dots: calculated using Eq. (3) and the estimated variance of SOC content at farm scale.

10.3

Organic matter quality in arable land as influence by clay content and cropping system

Cédric Deluz[1], David Sebag[2], Eric Verrecchia[3] & Pascal Boivin[1]

[1]HEPIA Sols et Substrats, HES-SO Genève, 150 route de Presinge, 1254 Jussy (cedric.deluz@hesge.ch)
[2]Normandie Univ, UNIROUEN, UNICAEN, CNRS, M2C, 76000 Rouen, France
[3]Institute of Earth Surface Dynamics, Faculty of Geosciences and the Environment, Bât. Geopolis Université de Lausanne, 1015 Lausanne – Switzerland

Fifty fields from the Swiss plateau, cropped with Conservation Agriculture (CA) or conventional tillage (CT) since at least 10 years, were sampled for structure quality and soil analyses down to 40 cm depth. The organic matter (OM) quality was analysed with Rock-Eval pyrolisys. The relationships between cropping practices, depth, clay content, Soil Organic Carbon (SOC) content and OM quality were then discussed. AC and CT differed mostly by the location of SOC, with higher content on the topsoil in CA, and lower below 20 cm depth, compared to CT. OM quality was influenced by SOC content, showing increasing labile forms proportion with increasing SOC content. SOC to clay ratio, however, seemed to be the major determinant of OM quality, with the 0.1 ratio corresponding to a threshold above which changes in SOC content are mostly accounted for by labile forms, and conversely. This 0.1 SOC:clay ratio was already highlighted as a threshold for structural and physical behavour of the soil, thus leading to the hypothesis that the degradation of mid-recalcitrant forms under this ratio are responsible for structure degradation. Moreover, these results call for caution when interpreting field experiments with respect to OM quality, which appears to be driven by SOC:Clay ratio rather than cropping practices in this study.

10.4

Evaluation of earthworms as soil quality indicator for the farmers

Alyssa Fischer[1], Marina Wendling[2], David Sebag[3], Raphaël Charles[2], Renée-Claire Le Bayon[1]

[1]Functional Ecology Laboratory, Institute of Biology, Faculty of Science, Université de Neuchâtel, Rue Emile-Argand 11, CH-2000 Neuchâtel
[2]Research Institut of Organic Agriculture (FiBL), Antenne romande, Avenue des Jordils 3, CH-1001 Lausanne
[3]Normandie Univ, UNIROUEN, UNICAEN, CNRS, M2C, 76000 Rouen, France

The role of earthworms on soil functioning has been widely demonstrated and their potential as a bioindicator has been explored several times. As part of the “Progrès Sol“ project, this work aims to evaluate the perspective of earthworms as a soil quality self-diagnosis tool for farmers. To do this, the earthworm communities were studied using simple methods on twenty agricultural plots in the canton of Vaud. The crop management techniques were characterized to determine the influence of cultural practices. Laboratory analyses were conducted to characterize soil properties between sites as well as earthworm faeces. Earthworms are proving to be a good indicator of soil disturbance. Regardless of the cropping system, reduced tillage and the presence of grassland limit the impact of cropping practices. The presence of legumes in the rotation and the addition of organic matter are also favourable to earthworms. This work did not establish a link between the earthworm communities and the differences in the physico-chemical properties of the plots. On the other hand, the results showed that the nutritional behaviour of earthworms influences the properties of the organic matter present in the faeces. Measuring the abundance of earthworms appears to be the best compromise among the measures tested between the simplicity of the indicator and the produced information. This study also recommends using full extraction to collect earthworms, waiting for a minimum of 50 mm of cumulative rainfall over the 30 days preceding the sampling and setting a critical abundance threshold at 120 individuals/m^2 above which agricultural practices can be considered favourable for earthworm populations.

10.5

A method of extraction and analysis of nanoplastics in soils

Alexandra Foetisch[1], Montserrat Filella[2], Daniela Fischer[1], Anna Muntwyler[1], Benjamin Watts[3], Katharina Witte[3], Moritz Bigalke[1]

[1]Institute of Geography, University of Bern, Hallerstrasse 12, 3000 Bern (alexandra.foetisch@giub.unibe.ch)
[2]Department F.-A. Forel, Universityof Geneva, Boulevard Carl-Vogt 66, CH-1205 Geneva
[3]Paul Scherrer Institute, CH-5232 Villigen PSI

The world plastic production is steadily increasing and some of the produced plastics end up in soils and might affect soil properties and soil health. The effect of the plastics strongly depend on its size and shape. Nanoplastics (NP) are in the <1µm size range and might either be emitted directly (e.g. from, cosmetics or road dust) or form from bigger plastics by decomposition, UV induced breakdown or physically forced breakdown. In agricultural ecosystems, NP can induce negative effects on a variety of soil organisms and their occurrence might affect soil ecology and fertility. The research about NP in soils is still at its very beginning due to the complex matrix soil represents and technical limitations in the analysis of NP. Samples preparation and analysis are more challenging compared to microplastics. Indeed, infrared or Raman spectroscopy, which are normally used in microplastic research, are limited to the >1µm range and does not allow for the analysis of smaller particles.

This study focuses on soils under two different landuse. First, agricultural soils, which are exposed to plastic input because of agricultural practices, as sewage sludge application or the use of plastic mulch. Second, road sided soils exposed to plastic pollution coming from tyre abrasion on the road. With the aim of characterizing NP pollution in the first 20 cm of agricultural and road sided soils, we tested the extraction of NP from soils samples by the following sequence: size fractionation, density separation, oxidation of natural organic and ultrafiltration to extract and concentrate and clean the NP. Samples are deposited on a 1 mm silicon-nitride (Si_3N_4) membrane. Particles are located on the membrane with a Scanning Electron Microscope (SEM) (Figure 1 A) and their elemental composition is analysed by energy dispersive X-ray spectroscopy (EDX) analysis. The identification of the NP is done by scanning transmission X-ray microscopy (STXM) at the Swiss Light Source synchrotron. The STXM method can image NP with a resolution of about 30 nm (Figure 1 B) and identify the plastics via near edge X-ray absorption fine spectra (NEXAFS) at the carbon K-edge (Figure 1 C).

The method was suitable to extract polystyrene nanobeads of 1000, 500, 250 and 100 nm from spiked soil and particles between 150 and > 1000 nm in natural samples. However, analysis show that natural organic matter particles remain in the sample. Those particles make the identification of plastic more laborious. Indeed, it is not possible to differentiate plastic and natural organic matter (NOM) particles visually or with an EDX analysis. Furthermore, dissolved organic matter can precipitate while drying the sample creating a background interfering with the particles spectra.

Current work is focusing on two main aspects. The first one is to improve removal of organic matter with different incubation time of H_2O_2 and by alkalinisation of sample in order to remove humic acids from solutions. The second one is to increase particles concentration on Si3N4 membranes by concentrating the sample by evaporation or the use a perforated membrane as a filter.

Nonetheless, preliminary results already showed that the protocol is suitable to extract plastic nanoparticles from natural soil samples. Coupled with STXM analysis, the method allows for imaging and identifications of the NP and thus offers the possibility for a characterisation of NP in the environment.

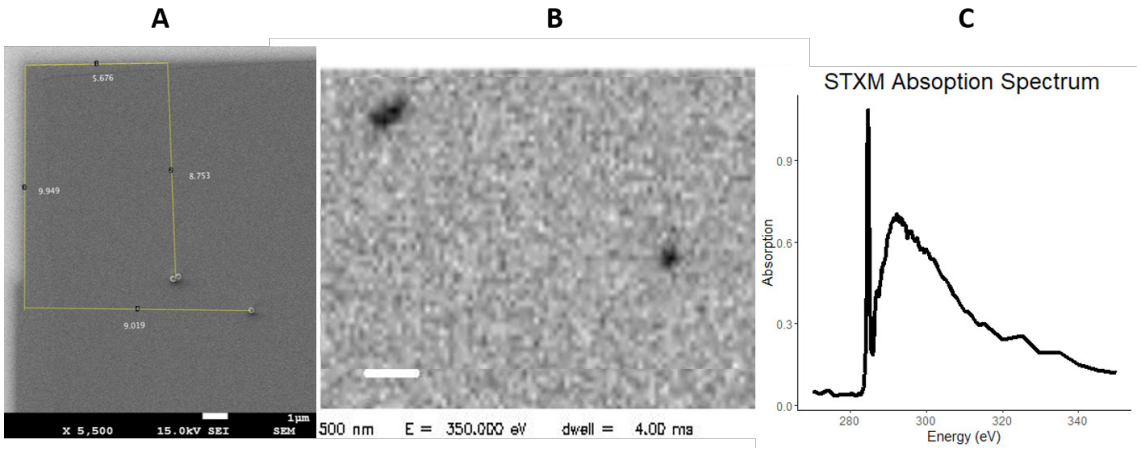


Figure 1. (A) SEM picture of a membrane's corner carrying 250 nm Polystyrene (PS) beads. Position of the beads is measured according to the edge of the membrane. (B) STXM picture of the same particles than in (A). (C) Absorption spectrum of a PS beads with the STXM.

10.6

The podzolization process in a context of land disturbance

Stephanie Grand[1], Valentine Turberg[1], Anaïs Fayolle[1] & Adrian Unc[2]

[1]Faculty of Geosciences and Environment, University of Lausanne, CH-1015 Lausanne (stephanie.grand@unil.ch)
[2]Boreal Ecosystems and Agricultural Sciences, Memorial University of Newfoundland, Canada

The podzolization process involves the intensive leaching of the upper soil layer and the subsurface accumulation of illuviated organic matter, iron and aluminium. The resulting sola, called podzols in many classification systems, are widespread on coarse-textured acid parent materials under cool climates where precipitation exceeds evapotranspiration. Most often, podzols naturally support forest or heath vegetation. Due to the growing demand for food and forest product as well as the push for locally-sourced commodities, the area of podzolic land coming under human influence is increasing in many parts of the world.

This talk explores the effects of land-use change such as forest harvest or conversion to agriculture on the podzolization process. Using examples from Canada and the Swiss Alps, we show that land disturbance often causes a change in the quantity and the quality of organic matter in podzols. Land disturbance can also affect the forms and distribution of iron and aluminium in the profile. Our data suggest that the amount of poorly crystalline Fe and Al varies according to climate and land use, in turn affecting the ability of podzols to accumulate and stabilize organic matter. Future research needs surrounding this largely unexplored feedback loop are discussed.

10.7

Soil protection in Switzerland between policy and practice

Gudrun Schwilch

Federal Office for the Environment FOEN, Soil and Biotechnology Division, 3003 Bern (gudrun.schwilch@bafu.admin.ch)

In Switzerland, the problem of soil degradation persists despite numerous studies and significant improvements. Analysis shows that the non-renewable resource of soil is suffering both qualitative and quantitative damage. This suggests that it may be difficult to retain soil functions in the long-term. Although various measures have helped to prevent an increase in certain types of soil pollution and there has even been a decrease in some types of pollution, Switzerland does not have a sustainable approach to dealing with soil, a basic natural resource. Soil has been protected by legislation in Switzerland only since 1983, when the Environment Protection Act (EPA) was passed. The EPA and the Soil Pollution Ordinance (SoilPO) are the legal basis for soil protection in Switzerland. The federal government strives to improve soil protection on various levels. However, there has been limited success to date because at the cantonal and communal levels financial and human resources are still very scarce. Newly emerging challenges include climate mitigation and adaptation, plant protection products or (micro-)plastic.

In most cases, the effect of soil degradation involves economic and ecological costs for society, such as with on- and off-site effects of soil erosion. The Swiss agricultural policy system is based on a system of direct payments (subsidies) to compensate farmers for the different types of services they deliver to society. This system supports prevention of soil erosion indirectly, e.g. by defining a minimal crop rotation or an optimal soil coverage. Furthermore, financial support is given to farmers, for example for applying conservation tillage. In Switzerland, agro-environmental policies are the result of negotiation and compromise rather than optimal expert determination. Despite their comprehensiveness, inconsistencies remain, leading to an ineffective implementation.

10.8

Loss of soil organic carbon in Swiss long-term agricultural experiments over a wide range of management practices

Sonja G. Keel[1], Thomas Anken[2], Lucie Büchi[3,°], Andreas Chervet[4], Andreas Fliessbach[5], René Flisch[6], Olivier Huguenin-Elie[7], Paul Mäder[5], Jochen Mayer[6], Sokrat Sinaj[3], Wolfgang Sturny[4], Chloé Wüst-Galley[1], Urs Zihlmann[7], Jens Leifeld[1]

[1]Climate and Agriculture, Agroecology and Environment, Agroscope, 8046 Zürich (sonja.keel@agroscope.admin.ch)
[2]Digital Production, Competitiveness and System Evaluation, Agroscope, 8356 Ettenhausen
[3]Field crop systems and Plant nutrition, Plant Production Systems, Agroscope, 1260 Nyon
[4]Bern Office of Agriculture & Nature, Soil Conservation Service, 3052 Zollikofen
[5]Research Institute of Organic Agriculture, 5070 Frick
[6]Water Protection and Substance Flows, Agroecology and Environment, Agroscope, 8046 Zürich
[7]Forage Production and Grassland Systems, Animal Production Systems and Animal Health, Agroscope, 8046 Zürich
[8]Soil Fertility and Soil Protection, Agroecology and Environment, Agroscope, 8046 Zürich
°present address: Natural Resources Institute, University of Greenwich, Chatham, England

Soil carbon sequestration (SCS) is one of the cheapest and technically least demanding carbon dioxide (CO_2) removal technologies. It is defined as a change in land management that leads to an increase in the soil C content and therefore a net uptake of CO_2 from the atmosphere. For a realistic assessment of SCS on agricultural soils, it is critical to evaluate how much carbon (C) can be stored under actual agricultural practices. This includes e.g. typical crop rotations or fertilization strategies and depends on resources that are available (e.g. farmyard manure) and affordable for farmers.
We evaluated changes in soil organic carbon (SOC) stocks using data from eleven long-term field experiments on cropland and permanent grassland in Switzerland that included common local practices. Surprisingly topsoils (~0-0.2 m) lost C at an average rate of 0.29 t C ha^{-1} $year^{-1}$, although many of the investigated treatments were expected to lead to SOC increases. Based on a linear mixed effects model we showed that SOC change rates were driven by amounts of C inputs to the soil (from harvest residues and organic fertilizer), the duration of soil cover and the size of the initial SOC stock. The type of land use (grassland vs. cropland) or soil tillage (conventional ploughing vs. no tillage) had no significant effect. Our analysis suggests that current efforts to manage soils sustainably need to be intensified and complemented with further techniques if Switzerland wants to achieve the goal of the 4p1000 initiative, a multistakeholder platform aiming at increasing SOC storage. Using a model-based SOC inventory, we will assess the potential to increase SCS at the national scale.

10.9

Growth conditions and Ca sources of pedogenic needle fibre calcite (NFC)

Millière L.[1,2], Gussone N.[1], Bindschedler S.[3] and Verrecchia E.P.[2]

[1]*Institut für Mineralogie, Universität Münster, Corrensst. 24, D-48149 Münster*
[2]*Institute of Earth Surface Dynamics, Faculty of the Geosciences and the Environment, University of Lausanne, Geopolis Campus, CH-1015 Lausanne*
[3]*Institute of Biology, Faculty of Sciences, University of Neuchâtel, Rue Emile Argand 11, CH-2000 Neuchâtel*

Needle fibre calcite (NFC) and nanofibres are microscopic features of secondary calcium carbonate accumulation commonly observed in soils and caves. Both NFC and nanofibre morphologies correspond to a needle-shaped monocrystal. NFC has an average diameter of 1-2 µm and a length reaching 10^2 times its width, while nanofibres have an average width of 50-150 nm and lengths from 10 to 100 times their width. Three main groups previously identified by Millière et al. (2011) and corresponding to specific microscopic arrangements, have been identified in the Swiss Jura Mountains: simple needles (SN) corresponding to the original form of NFC, which can evolve into simple needles with calcitic overgrowths (SNO), and simple needles with nanofibres (SNN). It is suggested that both NFC and nanofibres are related to the presence of fungi, but despite intense work, its origin and the processes involved in its formation are still under debate. To better constrain their formation processes, different NFC morphotypes (SN, SNO, SNN) and a late calcitic cement (LCC) from the same soil depth, have been sampled in the Swiss Jura Mountains.

Strontium and calcium isotopic compositions and Sr/Ca ratios in the different reservoirs of NFC, soil water, throughfall, inorganic cements, as well as host rock, have been analysed to determine the Ca sources and to investigate the formation mechanisms.

$^{87}Sr/^{86}Sr$ ratios of the various NFC types and LCC suggest that the contribution of Ca from the main Ca sources differs between NFC and LCC, implying different precipitation processes. In addition, the three microscopic morphological groups of NFC (SN, SNO, SNN) displayed Sr isotopic compositions different from each other, emphasizing a direct relationship between the NFC morphotypes and the origin of the Ca. Sr/Ca ratios and $\delta^{44/40}Ca$ values of NFC and LCC crystal are used to determine possible differences in their growth rate and/or micro-environment during their formation. Crystals described as simple needles (SN) are enriched in ^{44}Ca and depleted in Sr compared to LCC, suggesting that the elongated shape of the SN crystal cannot be related to a rapid precipitation rate, but rather to a slow precipitation under semi-enclosed conditions. In contrast, LCC has a stronger enrichment in light Ca isotopes and is less depleted in Sr relative to the soil solution, suggesting more rapid precipitation. SNN and SNO overlap with the SN but are on average lighter in Ca isotopes and have higher Sr contents. Overall, NFC and LCC are explainable by calcite precipitation according to the Sr and Ca systematics of inorganic calcite of Tang et al. (2008), with different precipitation rates and degrees of Ca and Sr consumption. Specifically, SN correspond to values of a calcite formed in a restricted environment, supporting the fungal hypothesis for the origin of NFC.

REFERENCES

Millière L., Gussone O., Bindschedler S., Moritz T. & Verrecchia EP. 2019: Origin of strontium and calcium in pedogenic needle fibre calcite (NFC), Cemical Geology 524: 329-344.

Millière L., Hasinger O., Bindschedler S., Cailleau G., Spangenberg JE. & Verrecchia EP. 2011: Stable carbon and oxygen isotope signature of pedogenic needle fibre calcite: further insight into its origin and relationship with soil conditions, Geoderma 161: 74-87.

Tang J., Dietzel M., Böhm F., Köhler SJ. & Eisenhauer A. 2008: Sr^{2+}/Ca^{2+} and $^{44}Ca/^{40}Ca$ fractionation during inorganic calcite formation: II. Ca isotopes, Geochimica et Cosmochimica Acta 72: 3733-3745.

10.10

The ephemeral legacy of nutrient management in tropical seasonal wetland Anthrosols

Leonor Rodrigues[1/2], Tobias Sprafke[1], Doyle McKey[2]

[1]Institut of Geographie, University of Bern, Hallerstrasse 12, CH-3012 Bern (Leonor.rodrigues@giub.unibe.ch)
[2]Centre d'Écologie Fonctionnelle et Évolutive, CNRS UMR 5175, 1919 Route de Mende, 34293 Montpellier 5, France.

Anthrosols, man-made soils, vary widely in their characteristics and the degree to which evidence of past human activities is preserved. Over at least 500 years, Terras Pretas do Índio, or Amazonian Dark Earths (ADEs), have remained far more fertile than the surrounding natural soils and research on their history and functioning has found wide applications for agronomy, bioenergy and carbon storage. Another widespread type of pre-Columbian Anthrosols in Amazonia has attracted comparably little attention: raised fields (RFs), large earthworks constructed in order to farm in seasonally inundated wetlands. To date, pre-Columbian RFs have been mostly regarded simply as a technique to minimize flood risk, as there is no convincing evidence of nutrient management. A promising analogue of the long-abandoned RFs in the Amazon Basin is present-day RF agriculture in similar environments of the Congo Basin. We studied three RFs in detail, spanning different periods of cultivation, material addition and fallow on seasonal to multi-decadal timescales. To evaluate their properties and functioning we used a multi-methodological approach including sedimentology, geochemistry and micromorphology. Our results reveal that the way RFs are managed does result in a considerable improvement of soil fertility when they are active. On the other hand, we show that evidence of human management disappears within years to decades. This relatively fast process leads to a clear loss of information on how they were constructed and how they functioned when they were active, hampering the interpretation of ancient agricultural systems. These findings clearly show that comparison with present-day active systems can yield important insights for interpreting ancient agricultural systems.



Figure 1. Present-day raised field (400 cm x 400 cm x 170 cm) in the Congo Basin, during the dry season. The field can be flooded up to 150 cm during the high-water season.

10.11

The cascading influence of $CaCO_3$ on the pedogenic trajectories and biogeochemistry of the subalpine soils at the Nant valley, Switzerland.

Rowley, M. C., Grand, S., Adatte, T., Verrecchia, E. P.

Université de Lausanne, IDYST, Geopolis, 1015 Lausanne, Switzerland
(mike.rowley@unil.ch)

Soil research in temperate to cool and humid regions has typically focused on acidic soils; there has been relatively little investigation into the effects of calcium carbonate ($CaCO_3$) on unamended soil properties or function in humid environments like the subalpine soils of Switzerland. The object of this study was to characterise the effects of small concentrations of $CaCO_3$ on the pedogenic trajectories and soil biogeochemistry of a humid subalpine valley in Switzerland (Nant valley, Vaud).

To isolate the influence of $CaCO_3$ from other pedogenic variables, six profiles were selected that had developed under almost identical conditions for soil formation (climate, topography, vegetation structure, time since deglaciation, silicate mineralogy and texture). The main difference between the profiles was that three contained small concentrations of $CaCO_3$ (< 6.2 %; thereafter, '$CaCO_3$-bearing') and the remaining three contained no detectable $CaCO_3$ (thereafter, '$CaCO_3$-free').

The presence of $CaCO_3$ was associated with cascading changes in soil biogeochemistry of these soils that had formed under otherwise similar conditions. These changes included higher pH, an order of magnitude higher extractable Ca, twice as much soil organic carbon, and a higher proportion of poorly crystalline Fe forms. The higher pH at the $CaCO_3$-bearing site was attributable to the weak buffering provided by dissolution of the small concentrations of $CaCO_3$, which also maintained the relatively higher extractable Ca concentrations. Exchangeable Ca (Ca_{Exch}) and other reactive Ca forms could be stabilising SOC, contributing to its accumulation through sorption to mineral surfaces and/or occlusion within aggregates. The increased pH, Ca_{Exch} and SOC concentrations at the $CaCO_3$-bearing site could in turn also be inhibiting the crystallisation of disordered Fe forms, contributing to the further retention of SOC; but additional investigation is required to confirm this effect and isolate the exact mechanisms.

Overall, this study shows that the presence of small amounts of $CaCO_3$ in the humid subalpine soils of the Nant valley has a far-reaching influence on soil formation and biogeochemistry. This study further supports the idea that indicators of Ca prevalence may have the potential to improve regional SOC estimates.

P 10.1

SWISSOIL: a pedagogical multimedia resource in soil science

Stephanie Grand, Fanny Viret, Valentine Turberg, Vincent Marmier, Eric Verrecchia

Faculty of Geoscience and Environment, University of Lausanne, CH-1015 Lausanne (stephanie.grand@unil.ch)

SWISSOIL is a teaching resource for pedology hosted at the University of Lausanne. The aim of the project was to improve access to field educational activities on soils for university students as well as school children and the general public. SWISSOIL has two main components:

1. A physical basis, consisting in five permanent soil pits maintained in the Dorigny forest on the University of Lausanne campus; and
2. A multimedia website (wp.unil.ch/swissoil) providing interpretive information on soil profiles.

The permanent soil pits are marked by a wood enclosure and freely accessible along the trails of the Dorigny forest. A QR code is present at each site directing visitors to the web resource. The website features both introductory and advanced pedological information. Introductory material, designed for novice students and the general public, includes a basic explanation of soil formation processes, visuals (soil pictures) and short presentation videos. Advanced content includes technical soil descriptions, micromorphological characterization and results of mineralogical, chemical and physical analyses.

The SWISSOIL resource allows students to make field observations on soil profiles at their own pace. The detailed information provided on the website forms the basis for a practical exercise in which students are asked to integrate their own observations with existing data to answer an integrative question on soil quality and conservation. Many activities and excursions targeting a wide range of audiences (young children, nature enthusiasts, alumni, winegrowers, *etc*.) have also made use of SWISSOIL, showing that there is an unmet demand for soil interpretive resources. SWISSOIL has received the 2019 prize from the Swiss Society of Pedology (SSP – BGS) for innovation in soil conservation and public awareness.

P 10.2

Soil color and geochemistry along a W-E transect on the S-Cameroon Plateau

Rea Keller[1], Tobias Sprafke[1], Jarosław Waroszewski[2], Paul-Desiree Ndjigui[3], Paul Tchawa[4] & Heinz Veit[1]

[1]Institute of Geography, University of Bern, Hallerstrasse 12, CH-3012 Bern (rea.keller@students.unibe.ch)
[2]Institute of Soil Science and Environmental Protection, Wroclaw University of Environmental and Life Sciences, ul. Grunwaldzka 53, PL-50-357 Wrocław
[3]University of Yaounde I, Dep. of Earth Sciences, P.O. Box 812, Yaounde, CAM
[4]University of Yaounde I, Dep. of Geography, P.O. Box 755, Yaounde, CAM

Soil has important functions for nature and society. Large regions of Central Africa, especially those covered by rainforest, lack consistent spatial information on soil distribution and properties. According to the Soil Map of the World 1:5M (FAO/UNESCO 1973), the S Cameroon plateau is mainly covered by Ferralsols; an earlier pedological map of Cameroon (1:1M) differentates yellow and red ferralitic soils for this region (Ségalen & Martin 1966). More detailed and more recent spatial information using the international soil classification (WRB 2015) is practically not available. Applying the WRB requires training and - even more challenging – laboratory data for final classification of several soil types. In order to fill the current gap, we carried out an initial survey along roadcuts of a 200 km W-E transect through the S-Cameroon plateau. The region is largely covered by secondary rainforest and made up of gneiss from the Panafrican orogeny. Weathering profiles had a thickness of > 40 m, whereas soil classifications usually consider the first 2 m. We focused on describing sections above stone lines / petro-/pisoplinthic horizons / saprolite, which varied in thickness between 0.3 to 7.4 m. 63 locations were sampled in their upper and lower parts for laboratory measurements of color (spectrophotometer), geochemistry (portable XRF), and organic matter. Seven reference profiles were sampled in detail for analyzes of Fed/Feo, base saturation, cation exchange capacity, carbon / organic matter content, grain size distribution according to WRB (2014) requirements. Our study reveals an unexpected variability in soil cover thickness, colors and morphologies along the studied transect. Based on our dataset we expect to provide unprecedented detail in soil differentiation for the South of Cameroon.

REFERENCES

FAO & UNESCO (1973): Soil Map of the World 1:5 000 000. UNESCO, Paris. Sheet VI-3.

IUSS Working Group WRB (2015): World reference base for soil resources 2014, update 2015. World Soil Resources Reports 106. FAO Rome, 181pp.

Segalen, P. & Martin, D. (1966): Carte Pédologieque du Cameroun Oriental a l'echelle de 1:1 000 000. France, ORSTOM (2 sheets).

P 10.3

Cover beds of local and aeolian deposits influence soil evolution along a hillslope in N-Bavaria

Felix Lauer[1], Robert Peticzka[2], Tobias Sprafke[3]

[1]Institute of Geography, Friedrich-Schiller-University of Jena, Loebdergraben 32, DE-07743 Jena (felix.lauer@uni-jena.de)
[2]Institute of Geography and Regional Research, University of Vienna. Althanstrasse 14 (UZA II), A-1090 Wien
[3]Institute of Geography, University of Bern, Hallerstrasse 12, CH-3012 Bern

The pedosphere is the interface of all natural spheres and provides an important research field to investigate environmental processes and changes through time. Quantifying rates of soil production is a major challenge in Earth Sciences, leading to the development of new methods (e.g. based on cosmogenic nuclides) and models of increasing complexity. For the temperate zone the role of allochtonous additions from upslope and from deposition by wind to soil parent materials is widely accepted, which makes it difficult to calculate soil production rates. Such cover beds are assumed to have formed during the cold stages of the Pleistocene and they determine the pathway of soil formation and their properties (Kleber & Terhorst 2013).

This study aims to identify slope deposits with variable dust admixture on a catena with variable lithology in Northern Bavaria. Six profiles were examined in detail in a catena from the hilltop to the footslope covering diverse Triassic bedrocks of the Lower Muschelkalk (limestone) and Upper Buntsandstein (silty claystone and sandstone). A small area on a midslope plateau is covered by up to 2 m of loess. In addition to field descriptions, a spectrophotometer measured color changes throughout the soil profile, complemented by basic soil parameters (pH, carbonate content). As granulometry is an important aspect of soil classification, we used and compared three different methods, i.e. sieve/pipette, sieve/Sedigraph and laser particle sizer (Mastersizer 2000). The latter clearly underestimates clay contents, but determines the modes of grain size distribution, which informs about the contribution of aeolian silt.

A variable influence of slope processes and aeolian additions to soil parent materials is visible in all soil profiles alonge the slope, which has considerable influence on soil properties and classification: Even though the local lithology is highly variable, all soils classify as Cambisols (WRB 2015) or Braunerde after the German soil mapping key (Ad-hoc-AG Boden 2005) with differing properties; the exception are Luvisols (Parabraunerden) found on loess.

REFERENCES

Ad-hoc-Arbeitsgruppe Boden 2005: Bodenkundliche Kartieranleitung. Schweizerbart›sche Verlagsbuchhandlung, 5. Ed., Hannover, 438 pp.

Kleber, A. & Terhorst, B. 2013: Chapter 1 - Introduction. In: Mid-Latitude Slope Deposits (Cover Beds) (Ed. by A. Kleber & B. Terhorst). Developments in Sedimentology 66, 1-8.

IUSS Working Group WRB 2015: World Reference Base for Soil Resources 2014, update 2015. In: World Soil Resources Reports 106. FAO, Rome.

P 10.4

Soil erosion rates over time derived from two high Alpine soil chronosequences

Alessandra Musso[1], Michael E. Ketterer[2], Markus Egli[1]

[1]Department of Geography, University of Zurich, Winterthurerstrasse 190, 8057 Zurich, Switzerland (amusso@geo.uzh.ch)
[2]Department of Chemistry and Biochemistry, Northern Arizona University, 700 South Osborne, Flagstaff, AZ 86011-5698, USA

Erosion and sedimentation are important drivers in the degradation of soil quality worldwide. Mountainous landscapes are strongly shaped by soil relocation processes due to their variable and steep relief. The high-Alpine soils we see today started to develop since the Late Pleistocene/Early Holocene and mostly have formed on the glacial till left by the retreating glaciers. Soil chronosequences are a powerful tool widely used on moraine sequences to examine soil development over time. Soil formation is the net difference between soil production and denudation or erosion. How erosion rates change over time has so far only rarely been investigated.

The aim of this study was therefore to assess how soil age affects soil erosion rates. We investigated two chronosequences in the Swiss Alps: one was established in the (siliceous) proglacial area of the Stein glacier at Sustenpass, and the other one in the (calcareous) proglacial area of Griess glacier near Klausenpass. The quantification of soil relocation processes is often done using Fallout Radionuclides (FRN). During the last few years 239+240Pu have been increasingly used due to advantages over other isotopes (e.g. long half-life). FRNs originate from nuclear weapons tests which were conducted most intensely during the early 1960s. Erosion (or sedimentation) rates can be modelled using a reference site that is compared to the site of interest. The investigated soils at Sustenpass have ages varying from 30 a to 10 ka; the soils at Klausenpass from 110 a to c. 14 ka. We collected data on both the physical and chemical soil properties, and quantified the Pu inventories and soil redistribution rates.

Soil erosion decreased from 4 – 4.2 t ha^{-1} yr^{-1} to 1.7 t ha^{-1} yr^{-1} after several millennia of soil development. The highest soil erosion occurred at the youngest sites and almost no erosion was detectable at the oldest sits. This confirms that young soils are the most vulnerable to surface erosion and that soil erosion exhibits distinct temporal dynamics.

The physical and chemical soil properties change substantially during the first decades and centuries of soil development and affect the composition and density of the plant cover. More water is retained and more nutrients are available for plant up-take thanks to the weathering of minerals and physical breakdown of larger particles. With time, deeper rooting plants are able to establish a dense cover which stabilises and protects the soil surface from erosion. After about 10 ka, erosion rates on vegetated moraine slopes is almost zero.

P 10.5

Pedogenesis – a matter of perspective? Case studies from the temperate and the tropical zone

Tobias Sprafke[1], Heinz Veit[1]

[1]*Institute of Geography, University of Bern, Hallerstrasse 12, 3012 Bern. (tobias.sprafke@giub.unibe.ch)*

Soils are the complex interface of the major geospheres at the earth's surface and provide essential services for nature and society. Knowledge on the processes and rates of soil formation through time helps understanding variations of soil properties in space and raises awareness that soil is a limited ressource.

During the last decades, researchers from different scientific background have worked on pedogenesis; yet there exits little conceptual work for a unified concept on soil formation. To overcome this limitation, we compile case studies from the tropical and the temperate zone that address and quantify significant aspects of soil formation.

The determination of soil production rates under assumed steady state conditions, especially based on terrestrial cosmogenic nuclides (TCN), provides a quantitative basis for our understanding of soil and landscape evolution. However, research from Central Europe has revealed that paleoclimatic shifts resulted in alternating phases of morphodynamic activity with enhanced slope processes and morphodynamic stability characterized by soil formation. Grain size distribution, mineralogy and geochemical provenance tracers can reveal aeolian additions to soils and their parent materials. The presence of allochtonous material leads to significant overestimations of soil production rates. Luminescence dating increasingly determines time periods of slope processes and strong aeolian deposition. Recent studies use this technique to understand and quantify bioturbation processes.

Based on our literature review and own research in the temperate and tropical zone, we conclude that future work needs to mutually integrate the "biomantle" (e.g. Johnson et al. 2005) and the "cover bed" concepts (Kleber & Terhorst 2013). This leads to an appropriate selection of complementary research tools to evaluate soil formation through time in different regions worldwide.

REFERENCES

Kleber, A. & Terhorst, B. 2013: Chapter 1 - Introduction. – A. Kleber & B. Terhorst (Eds.): Mid-Latitude Slope Deposits (Cover Beds). – Developments in Sedimentology 66. Elsevier, pp. 1-8.

Johnson, D.L., Domier & J.E.J., Johnson, D.N. 2005: Reflections on the nature of soil and its biomantle. Annals of the Association of American Geographers 95, pp. 11–31

P 10.6

Are Fungus-Growing Termites Major Contributors To Sediment Grain-Size Distributions In Subtropical Environments?

John Van Thuyne[1,2], Eric P. Verrecchia[1]

[1]Institute of Earth Surface Dynamics, University of Lausanne, CH-1015 Lausanne (john.vanthuyne@unil.ch)
[2]VanThuyne-Ridge Research Centre, Chobe Enclave, Kasane, Botswana

Fungus-growing termites (FGT) have long been considered as ecosystem engineers (Jones, 1990) for the modifications they bring to the soil, their ability to concentrate nutrients, and their capacity to create patches of fertile land. Although FGT have obvious specific capabilities to change their environment, there are only a few studies that have highlighted their ability to modify the grain-size distributions of the sediments and soils that are forming the environment where they develop (Jouquet, 2002). Therefore, the aim of this study is to document the potential impact of FGT in an environment in which sands are dominating grain-size distributions, but also, where some concentrations of fine material, in this case diatomites, are found, offering the opportunity to compare the impact of FGT on two different and contrasting grain-size settings. In other words, this work proposes to compare two distinct substrata one fine, one coarse, on which FGT built mounds. The sedimentary modifications carried out by termites between these two parent materials and associated constructed mounds are assessed using techniques mostly based on grain-size distributions and soil micromorphology. Only very few studies have combined both methods to highlight the role FGT play in the selection of grain-sizes to build their epigeal mounds (Abe, 2009). In order to conduct this investigation, two FGT mounds where selected in the Chobe Enclave, northen Botswana, in the surroundings of the VTR Research Center. Two types of sediments were chosen, one coarse (dominated by sands) and one fine (dominated by fine silt). The key questions of this study lie on the capacity of fungus-growing termites (i) to adapt to any kind of parent material to build their mounds, (ii) and to enrich or deplete this parent soil to meet their texture requirements in terms of mound stability and appropriate settings to insure the success of the colony. Therefore, it is demonstrated that ,whatever a given parent material, the result in their construction will converge to a required optimum; in other words, by selecting, transporting, and mixing at will the various grain-sizes at disposition from the surrounding environment, fungus-growing termites reach the mandatory texture adapted to the functions and properties for their mounds.

REFERENCES

Abe, S.S. 2009: Soil-particle selection by the mound-building termite Macrotermes bellicosus on a sandy loam soil catena in a Nigerian tropical savanna. Journal of Tropical Ecology 25:449-452.A

Jones, J.A. 1990: Termites, soil fertility and carbon cycling in dry tropical Africa: a hypothesis. Journal of Tropical Ecology,6: 291-305.

Jouquet, P. Lepage, M. 2002: Termite soil preferences and particle selections: strategies related to ecological requirements. Insectes Sociaux, 49:1-7.

P 10.7

Quaternary calcium transfer in semi-arid African landscapes: pedogenic nodules and the geochemical cascade

Fabienne Dietrich[1], Nathalie Diaz[1], Pierre Deschamps[2], David Sebag[1,3,4] and Eric P. Verrecchia[1]

[1]Earth Surface Dynamics Institute, Lausanne University, Switzerland
[2]Aix-Marseille Univ, CNRS, IRD, INRA, Coll France, CEREGE, Aix-en-Provence, France
[3]Normandie Université, UNIROUEN, UNICAEN, CNRS, M2C, 76000 Rouen, France
[4]HSM, LMI Picass'Eau, IRD, Université de Montpellier, Montpellier, France

Calcium (Ca) is a key element of the Earth's system and closely related to the carbon cycle. Weathering of silicate releases Ca, which is exported and sequestered into the oceans. However, pedogenic Ca-carbonate constitutes a Ca-trapping pathway on continents that has not received the attention it deserves. Significant accumulations of pedogenic carbonate nodules associated with paleo-Vertisols, inherited from the Late Quaternary, are widespread in the Far North Region of Cameroon, although formed in a carbonate-free watershed. A previous study using Sr isotopes showed that Ca sources of carbonate nodules are local granite and Saharan dust (Dietrich et al., 2017). This suggests that Ca is kept in the soil system after weathering. However, the Ca sedimentary and biogeochemical pathways by which Ca is transferred from sources, i.e. the granite and the Saharan dust, to the trapping compartment, i.e. the carbonate nodules, remained unclear. This present study used major, trace, and rare earth element distributions of carbonate nodules, as well as of the various other Ca compartments of the landscape, in order to document these pathways. Three main processes transferred Ca from its source, in granite and dust, to a trapping compartment, i.e. pedogenic carbonate nodules. The first process involved the weathering of a granitic bedrock, which produced a saprolite. The residual products were then mixed with Saharan dust to form the host sediment of the nodules. The second process is related to clay minerals, products of weathering, which accumulated Ca and other alkaline cations during Vertisol development. Weathering products, i.e. clays and oxides, as well as vegetation and soil organic matter, have to be considered as transient compartments of Ca. At the end of the African Humid Period, drier climate conditions prevailed, enhancing the precipitation and preservation of pedogenic carbonate nodules. Ca was then incorporated and sequestered into the nodules, until the present-day. Consequently, during the last twenty thousand years, an important part of the Ca was transferred from upstream granite to downstream nodules of pedogenic carbonate developed in Vertisols (Diaz et al., 2018). Mass balance calculations in soil profiles demonstrated that the Ca accumulation in carbonate nodules exceeded the Ca released by the chemical weathering of the parent material, highlighting the role of Vertisols as Ca-trappers. Therefore, an important part of Ca is still sequestrated in the soil system and has not been yet transferred into rivers. Consequently, at the landscape scale, the paleo-Vertisols have acted as Ca-trapping systems (pedogenic carbonate nodules), emphasizing the significant role of Vertisols in terrestrial Ca balances, as they cover large areas on continents. Moreover, such a spatial relationship between sources and transient trapping compartments leads to a new concept of "geochemical cascade" similar, in terms of geochemistry, to the concept of "sediment cascade" developed by continental sedimentologists.

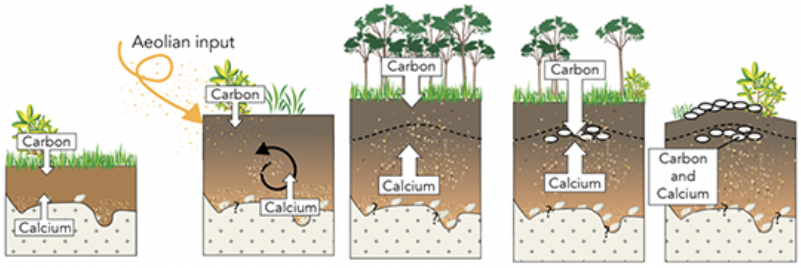


Figure 1. Ca location through time: Ca is transferred from granite and dust sources to carbonate nodules, highlighting the role of Vertisols as Ca- and C-trappers.

REFERENCES

Diaz N., Dietrich F., Sebag D., King. G.E., Valla P.G., Durand A., Garcin Y., de Saulieu G., Deschamps P., Herman F., Verrecchia E.P. 2018: Pedo-sedimentary constituents as paleoenvironmental proxies in the Sudano-Sahelian belt during the Late Quaternary (southwestern Chad Basin). Quatern. Sci. Rev., 191, 348-362.

Dietrich F., Diaz N., Deschamps P., Ngounou Ngatcha B., Sebag D. and Verrecchia E.P. 2017: Origin of Calcium in pedogenic carbonate nodules from silicate watersheds in the Far North Region of Cameroon: respective contribution of in situ weathering source and dust input. Chem. Geol., 460, 54–69.

P 10.8

Factors governing soil phosphorus availabilty in Amazonian Dark Earth

Klaus A. Jarosch[1], Hao Chen[2], Amanda Barbosa Lima[3], Aleksander Westphal Muniz[4], Timothy McLaren[5], Christoph Müller[3], Emmanuel Frossard[5], and Astrid Oberson[5]

[1]Institute of Geography, Soil Science, University of Bern, Bern, Switzerland (klaus.jarosch@giub.unibe.ch)
[2]College of Resources and Environmental Sciences, China Agricultural University, Beijing 100193, PR China,
[3]Department of Plant Ecology (IFZ), Justus-Liebig University Giessen, Giessen, Germany,
[4]Embrapa Amazônia Ocidental, Manaus, Brazil,
[5]Institute of Agricultural Sciences, ETH Zurich, Zurich, Switzerland

Strongly weathered soils in tropical regions are often poor in nutrients and suffer from low soil fertilty. Amazonian Dark Earth (ADE) is an exception to this rule, as it often shows increased soil fertility compared to surrounding soils, likely linked to its increased concentration of soil organic matter and macronutrients such as phosphorus (P). For P, there is little knowledge whether the higher P availability is a result of increased biological processes (such as organic P mineralization) or physico-chemical processes (such as sorption/desorption), or both. Using the ^{33}P isotopic pool dilution approach we aimed to quantify the exchangeability of inorganic P as well as organic P mineralization rates of ADE under secondary forest and a cassava plantation. For that, ^{33}P labelled ADE as well as surrounding soil (highly weathered, no “dark earth” features) under both land use systems (forest and cassava) were incubated for a period of 14 days. P-concentrations and specific activity of the added ^{33}P tracer were determined on four time points in the water-extractable P pool as well as in the microbial P pool (resin-fumigation method). ADE showed generally increased concentrations of total P and loosely bound P (water extractable P; resin extractable P) compared to surrounding soils. Isotopically exchangeable P was similar in both analyzed ADEs (approx. 150 mg kg^{-1} soil after 7 days), yet significantly higher compared to surrounding soils (30 to 90 mg kg^{-1} soil after 7 days). A numerical model used to estimate P transformation rates suggests the dominance of physicochemical processes over biological processes in ADE under both land use systems. However, biological processes were at least doubled in ADE, compared to surrounding soils. We conclude that the higher P availability in ADE is largely caused by increases in the exchangeable inorganic P pool. While biological processes (mineralization/microbial immobilization) were increased in ADE compared to surrounding soils, their net effect on P availability remains small.

11. Cryospheric Sciences

Matthias Huss, Martin Heggli, Theo Jenk, Nadine Salzmann, Daniel Tobler, Andreas Vieli

Swiss Snow, Ice and Permafrost Society

TALKS:

11.1 Balasubramanian S., Hoelzle M., Oerlemans J., Wangchuk S., Keller F., Lehning M.: A first attempt to model an Artificial Ice Reservoir (Ice Stupa) using a simple energy balance approach

11.2 Compagno L., Zekollari H., Huss M., Farinotti D.: Physically-based modelling of the future evolution of Scandinavian and Icelandic glaciers

11.3 Foehn A., Hernández G.J., Schaefli B., Cesare D.G., Rinaldo A.: Correcting solid precipitation gauge undercatch in quantitative precipitation estimates for snow modelling in Alpine catchments

11.4 Koenig C.E.M., Hilbich C., Hauck C., Arenson L.U.: Ground Temperature within Mountain Permafrost Zones of the Central Andes

11.5 Landmann J., Ogier C., Huss M., Farinotti D.: Real-time glacier mass balance monitoring with low-cost sensors: first experiences

11.6 Leinss S., Wicki R., Holsteiner S., Bafelli S., Bühler Y.: Snow Avalanche Detection in Sentinel-1 and TerraSAR-X Radar Satellite Images

11.7 Manconi A., Loew S., Glueer F.: Rock mass disintegration at the Moosfluh slope, Switzerland

11.8 Mazzotti G., Malle J., Essery R., Webster C., Jonas T.: Canopy structure influences on energy fluxes to the forest snowpack: observations and modelling

11.9 Mölg N., Ferguson J., Bolch T., Vieli A.: On the influence of debris cover on glacier surface morphology

11.10 Ogier C., Werder M.A., Huss M., Walter F., Farinotti D.: Comprehensive field measurements of the supra- and sub-glacial drainage of Lac des Faverges, Glacier de la Plaine Morte, in summer 2019.

11.11 Portenier C., Wunderle S.: SnowNet – a deep learning approach for automatic snow and cloud classification in public webcam images

11.12 Silva L., Nehrbass-Ahles C., Schmidely L., Schmitt J., Fischer H., Stocker T.: Flat CO_2: a reconstruction from the last interglacial

11.13 Steiner L., Biland N. , Grimm D.: Quantification of Snow Water Equivalent Using GNSS Refractometry and Standard GNSS Software

11.14 Storni E., Loew S., Hugentobler M., Manconi A: Monitoring and Analysis of Landslide-Glacier Interactions (Great Aletsch Glacier, Switzerland)

11.15 Walter A., Lüthi M.P., Funk M., Vieli A.: Changes in calving activity and front geometry of a marine terminating outlet glacier over six years

POSTERS:

P 11.1 Barandun M., Rivera A., Grobety B., Fang L., Schwikowski M.: Light absorbing impurities in the Olivares Catchment, Central Chile

P 11.2 Carlen P., Church G., Grab M., Maurer H., Farinotti D.: Detecting and characterising englacial features on Oberaletsch Glacier using ground-penetrating radar

P 11.3 Chmiel M., Walter F., Preiswerk L.: Monitoring an unstable hanging glacier in the Swiss Alps using icequake repeaters and seismic coda wave interferometry

P 11.4 Church G.,Grab M.,Schmelzbach C.,Bauder A.,Maurer H.: Englacial drainage network temporal evolution using impendance inversion from ground-penetrating radar

P 11.5 Geibel L., Landmann J., Farinotti D.: "SnowIceSen": An Automated Tool to Map Snow and Ice on Glaciers with Sentinel-2

P 11.6 Grab M., Langhammer L., Hellmann S., Church G., Bauder A., Rabenstein L., Schmid L., Maurer H.: The total glacier ice volume in the Swiss Alps

P 11.7 Groos A.R., Mayer C., Lambrecht A., Erlwein S., Schiwkowski M.: High-elevation snow accumulation studies at the Biafo-Hispar glacier system in the Central Karakoram

P 11.8 Kronenberg M., Machguth H., Eichler A., Schwikowski M., Ruethi M., Heule M., Hoelzle M.: No firn changes in Central Asia?

P 11.9 Lindner F., Roux P., Walter F., Gimbert F.: Do ice dynamics and glacier hydraulics cause englacial variations detectable with seismology?

P 11.10 Lüthi M.: Observing glacier motion in extremely high resolution

P 11.11 Morgenthaler J., Jouvet G., Bauder A.: Modelling the age of ice of Rhonegletscher

P 11.12 Sergeant A., Chmiel M., Walter F., Lindner F., Chaput J., Mordret A., Roux P., Gimbert F.: Passive seismic imaging of glaciers with ambient seismic noise and glacier seismicity

P 11.13 Fang L., Cao F., M.Schwikowski, Jenk T.: Enhancement of carbonaceous aerosol during the 20th century by anthropogenic activities

P 11.14 Hauck C., Hilbich C., Mollaret C., Pellet C.: Permafrost monitoring by reprocessing and repeating historical geophysical measurements

P 11.15 Hilbich C., Hauck C., Pellet C., Isaksen K., Etzelmüller B.: Permafrost degradation in Norway documented through repeated geophysical surveys after 10 and 20 years

P 11.16 Wicky J., Hauck C.: Thermal effects of natural air convection in the active layer of rock glaciers

P 11.17 Pruessner L., Phillips M., Huss M., Farinotti D.: Modelling rock glacier thermal regime using GERM: first results and comparison to Snowpack

P 11.18 Wee J., Delaloye R.: Glacier forefields in mountain permafrost environments (Swiss Alps)

P 11.19 Guidicelli M., Gugerli R., Salzmann N.: Improving temporal and spatial estimates of solid precipitation and accumulation in high mountain regions

P 11.20 Gugerli R., Salzmann N., Huss M., Desilets D.: Continous and autonomous snow water equivalent measurements by a cosmic ray sensor on a Swiss Glacier

11.1

A first attempt to model an Artificial Ice Reservoir (Ice Stupa) using a simple energy balance approach

Suryanarayanan Balasubramanian[1], Martin Hoelzle[1], J.Oerlemans[2], Sonam Wangchuk[3], Felix Keller[4], Michael Lehning[5]

[1]University of Fribourg, Fribourg, Switzerland (suryanarayanan.balasubramanian@unifr.ch)
[2]Institute for Marine and Atmospheric Research, Utrecht University, Utrecht, The Netherlands
[3]Himalayan Institute of Alternatives, Leh, India
[4]Academia Engiadina, Samedan, Switzerland
[5]WSL Institute for Snow and Avalanche Research, Davos, Switzerland

Artificial Ice Reservoirs (AIRs, also called icestupas) have been successful in storing water during winter and releasing the water during spring and summer (M. Nusser 2018). This has made them a vital fresh water resource for irrigation in dry environments. Many different forms of AIRs do exist and not many studies have tried to model them.

We will present simulations of the most important physical processes that causes the formation and melt of AIRs using one dimensional equations governing the heat transfer, vapour diffusion and water transport of a phase changing water mass. For this purpose, an AIR was constructed in Schwarzsee region in the Canton of Fribourg, Switzerland. Meteorological data in conjunction with fountain discharge data was measured. According to the model, the Schwarzsee AIR was able to store and discharge 850 litres or 3.7 percent of all the water sprayed over a duration of 40 days.

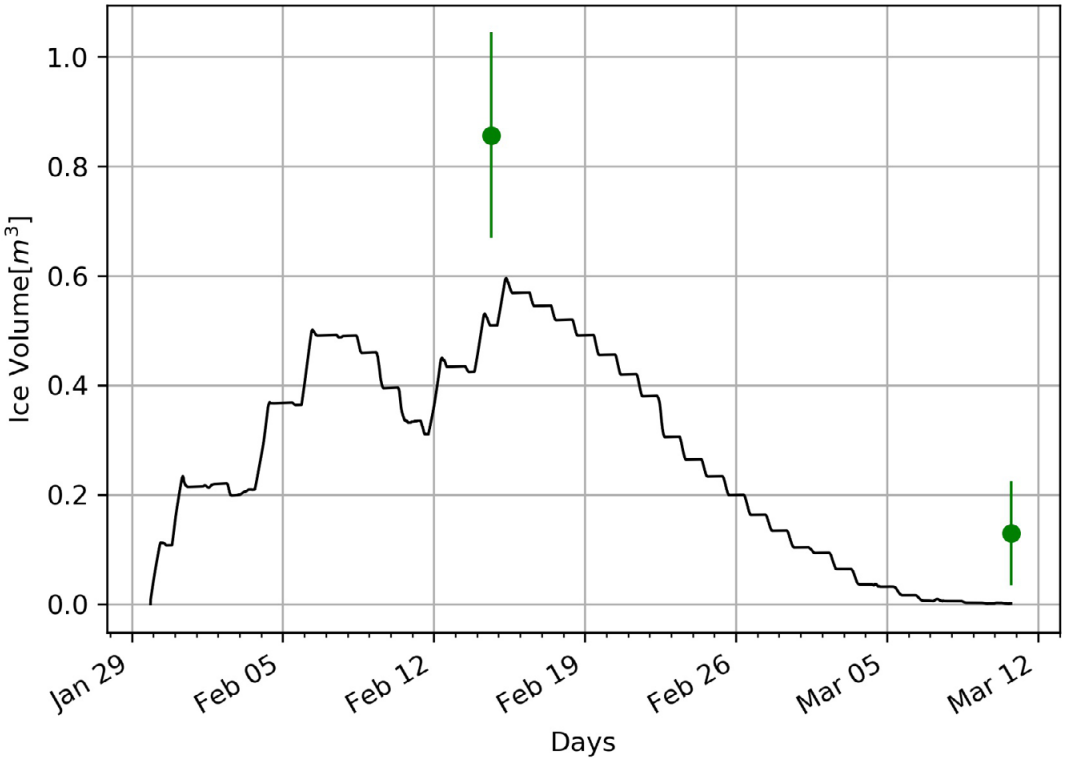


Figure 1. Daily Ice Volume of Schwarzsee AIR. Validation measurements are indicated through green line segments.

REFERENCES

M. Nusser 2018, “Socio-hydrology of artificial glaciers in ladakh, India: assessing adaptive strategies in a changing cryosphere,” Regional Environmental Change, https://doi.org/10.1007/s10113-018-1372-0.

11.2

Physically-based modelling of the future evolution of Scandinavian and Icelandic glaciers

Loris Compagno[1,2], Harry Zekollari[1,2,3], Matthias Huss[1,2,4], Daniel Farinotti[1,2]

[1]Laboratory of Hydraulics, Hydrology and Glaciology (VAW), ETH Zürich, Switzerland,
[2]Swiss Federal Institute for Forest, Snow and Landscape Research (WSL),
[3]Delft University of Technology, TUDelft, Holland, and
[4]Department of Geosciences, University of Fribourg, Switzerland

Due to global climate change, the majority of glaciers worldwide are losing volume. This trend is expected to continue in the future, with serious consequences for sea level, water availability, and hydropower production. In this study, we used a further developed version of the GloGEMflow model (Zekollari et al., 2019) to predict the evolution of Scandinavian and Icelandic glaciers until 2100. GloGEMflow explicitly accounts for both surface mass balance and ice flow. The model is initialized with three distinct observational climate dataset and reanalysis products (E-OBS, ERA-I, ERA-5), while future climate is prescribed by both global circulation models (GCMs) and with high-resolution regional climate models (RCMs). Different climatological models are used to create an ensemble and to analyze glacier model sensitivity. The mass-balance model is calibrated with glacier-specific geodetic ice volume change data (Zemp et al., 2019).

Under various representative concentrations pathways, we find that by 2100, Scandinavian glaciers might have lost between 63 % and 96 % of their 2018 ice volume. In the same time period, Icelandic glaciers are expected to lose only between 22 % and 59 % of their ice volume (Figure 1). The results indicate a large spread in glacier response to future climate, depending on future CO_2 concentration.

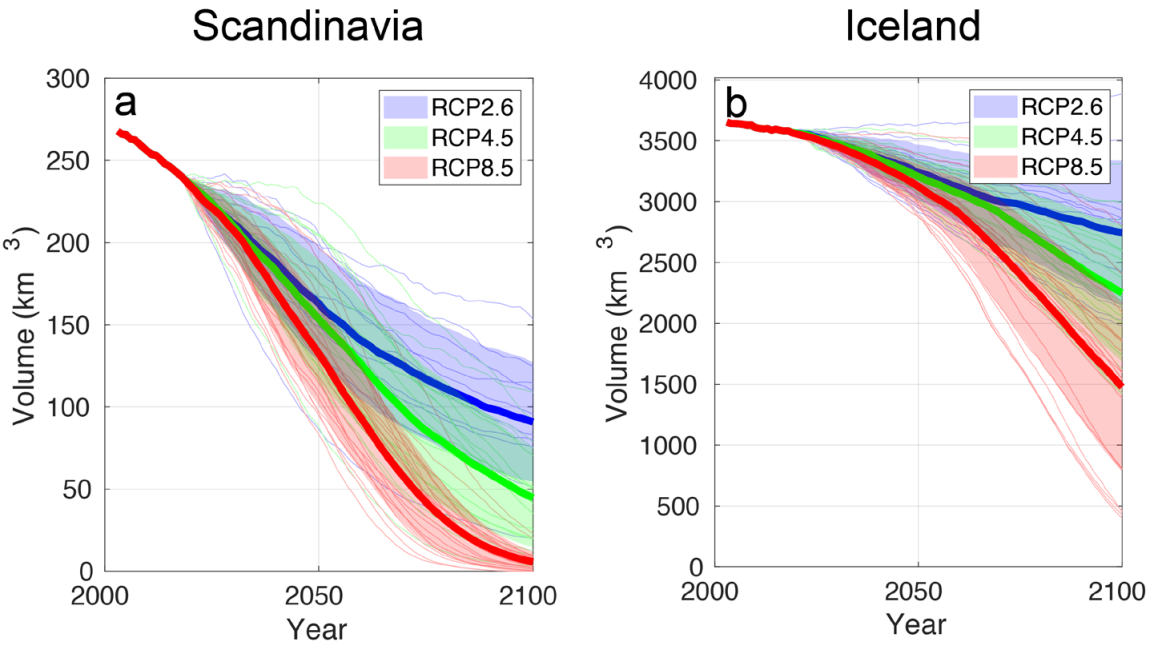


Figure 1: Volume evolution of (a) Scandinavian and (b) Icelandic glaciers using ERA-5 to initialize the model and various RCMs to simulate the future. Thin lines correspond to the individual RCM chains and the thick lines show the RCP mean. The transparent bands are one standard deviation.

REFERENCES:

Zekollari, H., Huss, M. & Farinotti, D. Modelling the future evolution of glaciers in the European Alps under the EURO-CORDEX RCM ensemble. The Cryosphere 13, 1125–1146 (2019).

Zemp, M. et al. Global glacier mass changes and their contributions to sea-level rise from 1961 to 2016. Nature 568, 382–386 (2019).

11.3

Correcting solid precipitation gauge undercatch in quantitative precipitation estimates for snow modelling in Alpine catchments

Alain Foehn[1], Javier García Hernández[2], Bettina Schaefli[3], Giovanni De Cesare[1] & Andrea Rinaldo[4]

[1]Platform of Hydraulic Constructions (LCH), Ecole Polytechnique Fédérale de Lausanne (EPFL), Station 18, CH-1015 Lausanne (alain.foehn@alumni.epfl.ch)
[2]Centre de recherche sur l'environnement alpin (CREALP), Rue de l'Industrie 45, CH-1950 Sion
[3]*Institute of Earth Surface Dynamics (IDYST), University of Lausanne (UNIL), Quartier UNIL-Mouline, Bâtiment Géopolis, CH-1015 Lausanne. Now at Institute of Geography, University of Bern, Switzerland*
[4]Laboratory of Ecohydrology (ECHO), Ecole Polytechnique Fédérale de Lausanne (EPFL), Station 18, CH-1015 Lausanne

Reliable quantification of solid precipitation remains a challenge due to gauge undercatch by precipitation gauges in snowy, windy conditions. Accordingly, quantitative precipitation estimates (QPE) based on uncorrected gauge data generally lead to underestimation in the interpolated precipitation fields, which ineluctably results in a negative volume bias in snow or hydrological models [Pollock et al. 2018].

In this study, a methodology to define a global correction factor to be applied to hourly solid precipitation values before computing QPEs is proposed. Four different QPEs are used as input for a snow temperature-index model. These include the CombiPrecip [Sideris et al. 2014] product of MeteoSwiss (QPE1) and the spatial product of precipitation combining radar data with gauge data from the networks of MeteoSwiss and MeteoGroup developed by Foehn et al. [2018] (QPE2) as well as two variants of QPE2 including correction factors for solid precipitation of 1.2 and 1.3 (QPE2-120 and QPE2-130, respectively). A temperature-index snow model is calibrated on absence and presence of snow as obtained from MODIS snow-covered area products [Hall et al. 2016]. The simulated snow amounts are compared to snow water equivalent (SWE) observations at 10 monitoring stations located in the Valais alpine region from the Swiss Institute for Snow and Avalanche Research (SLF).

Results suggest that applying a correction factor of 1.2 considerably reduces the bias between simulated and observed SWE values (Figure 1). The results encourage further developing the approach to integrate other parameters such as the wind speed for the solid precipitation correction instead of using constant factors.

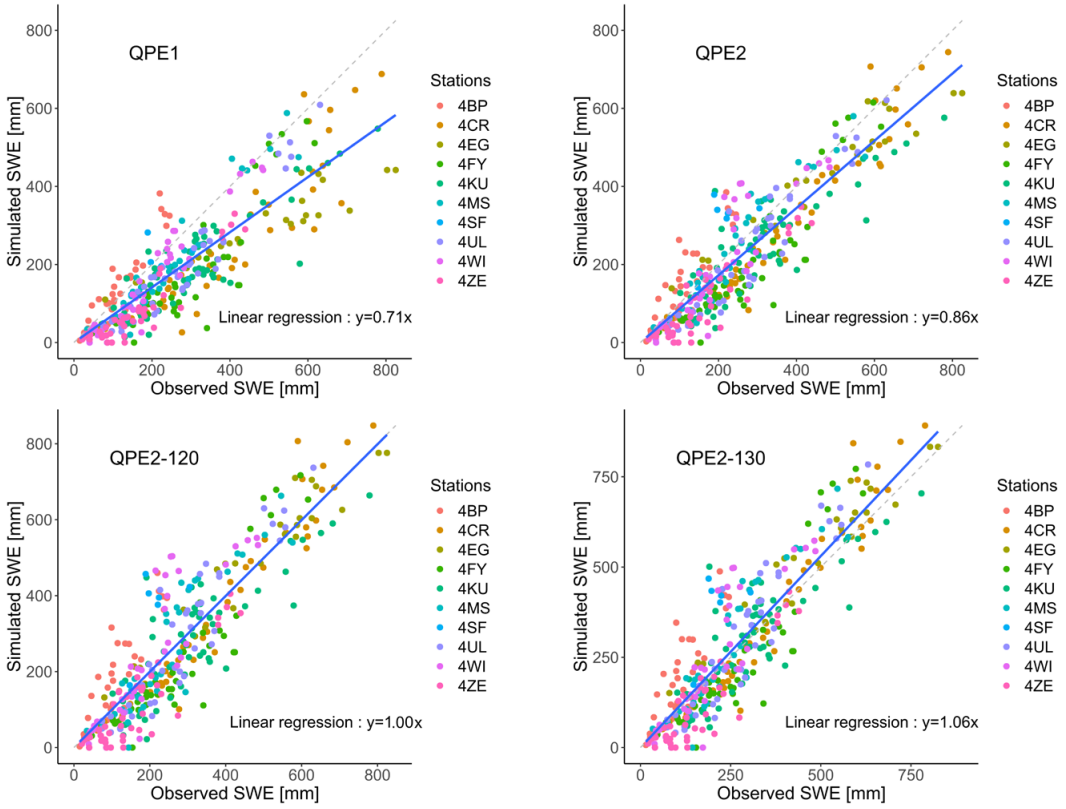


Figure 1. Simulated vs. observed SWE for the four QPE products. The gray dashed line indicates a slope of 1. Number of observations: 367.

REFERENCES

Foehn, A., García Hernández, J., Schaefli, B. & De Cesare G. 2018: Spatial interpolation of precipitation from multiple rain gauge networks and weather radar data for operational applications in Alpine catchments. Journal of Hydrology, 563, 1092–1110.

Hall, D., Salomonson, V., Riggs, G. 2016a: MODIS/Aqua and MODIS/Terra Snow Cover Daily L3 Global 500m Grid, Version 6.

Pollock, M. D., & coauthors, 2018: Quantifying and mitigating wind-induced under catch in rainfall measurements. Water Resources Research, 54 (6), 3863–3875.

Sideris, I. V., Gabella, M., Erdin, R. & Germann U. 2014: Real-time radar-rain-gauge merging using spatio-temporal co-kriging with external drift in the alpine terrain of Switzerland. Quarterly Journal of the Royal Meteorological Society, 140 (680), 1097–1111.

11.4

Ground Temperature within Mountain Permafrost Zones of the Central Andes

Cassandra E.M. Koenig[1], Christin Hilbich[1], Christian Hauck[1] & Lukas U. Arenson[2]

[1]Department of Geosciences, University of Fribourg, Chemin du Musée 4, CH-1700 Fribourg
[2]BGC Engineering Inc., Vancouver BC, Canada

The hydrological role of ground ice in the Central Andes is poorly understood because quantitative research within the region is scarce. Consequently, there are conflicting opinions about the importance of permafrost and related landforms as a strategic water resource in Chile and Argentina. This could have negative economic and environmental consequences for local communities if the application of incorrect conclusions needlessly hinders development or causes scarce water resources to be mis-managed.

Project developers in Chile and Argentina are required by legislation to consider the evolution of cryoforms in environmental impacts assessments of their projects. Industry site characterization and monitoring campaigns are therefore compiling valuable data for quantifying the thermal state of the periglacial environment in the central Andes. Such data are critical for developing thermal-hydrologic models to assess the potential contribution from ground ice melt to the hydrological cycle. We present the first coordinated effort to compile existing ground temperature datasets in mountain permafrost regions of the Central Andes and examine relationships with key climate and borehole attributes. Ground temperature data for periods up to 9 years were available from thermistor strings installed at sites located between 34°S and 27°S at a transect along the Chile-Argentine border. The dataset includes measurements within cold and warm permafrost where average ground surface temperatures are above 0°C, as well as locations outside permafrost zones with ground temperatures remaining above 0°C along the profiles.

While these observations suggest that permafrost, where present, is in a state of degradation, there is currently no discernible warming trend in ground temperature with time. Similarly, there is no observable increase in active layer thickness for the period of data examined. It is noted, however, that the existing dataset is not yet sufficient to evaluate long-term changes to the subsurface thermal regime. Ongoing monitoring will provide valuable data for assessing potential trends under climate warming, which may be used to estimate melt water volumes within local catchments.

11.5

Real-time glacier mass balance monitoring with low-cost sensors: first experiences

Johannes Landmann[1,2], Christophe Ogier[1,2], Matthias Huss[1,2,3] & Daniel Farinotti[1,2]

[1]Versuchsanstalt für Wasserbau, Hydrologie und Glaziologie (VAW), Swiss Federal Institute of Technology (ETH), Hönggerbergring 26, CH-8093 Zürich (landmann@vaw.baug.ethz.ch)
[2]Eidgenössische Forschungsanstalt für Wald, Schnee und Landschaft (WSL), Zürcherstrasse 111, CH-8903 Birmensdorf
[3]Département des Géosciences, Université de Fribourg, Chemin du Musée 4, CH-1700 Fribourg

In the context of climate change, hydropower production and numerous public requests, real-time information on glacier mass balance is of high interest. Blending different types of direct and indirect observations makes it possible to infer glacier mass changes from monthly to even daily time scales.

Here, we make a first step, and put seven low-cost cameras on three glaciers in Switzerland during summer 2019 (Glacier de la Plaine Morte, Rhonegletscher and Findelgletscher) at heights between 2240 and 3015 masl. The cameras are mounted on a self-made stake construction floating on the glacier surface (see Figure 1) and take images of a 2cm-marked ablation stake every 20 minutes. By using the Swiss mobile network, we transfer the so-recorded surface elevation changes to our servers in real-time. The surface height changes are then converted into a mass balance estimate. Correlations between different stations on the same glacier and between glaciers are calculated. Further, we assimilate the observed daily mass balance values into a temperature index melt model ensemble (cf. Hock, 2003) and compare the assimilated mass balances to model runs not knowing about observations (Figure 2). The high temporal frequency of the information allows modelled mass balance to be constrained at daily intervals. Uncertainty arises during night time, when images are not taken and when melt up to approx. 3cm w.e. can occur.

To reduce uncertainties, future work aims at automating the readings of the monitored mass balance stakes by means of image correlation, and at merging the in situ measurements with optical satellite observations.

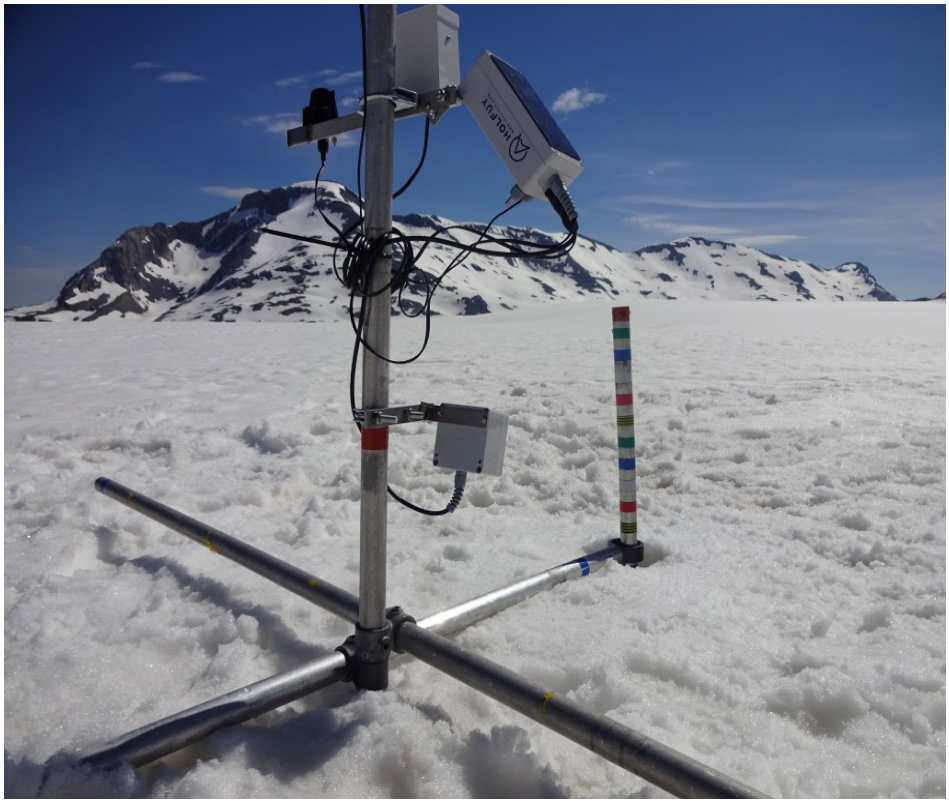


Figure 1. Camera setup on Glacier de la Plaine Morte. A 2cm ring-marked mass balance stake is drilled into the ice, while the attached camera floats on the surface. Pictures are taken at regular intervals to document the stake melt-out, and are sent to a server in real-time using the Swiss mobile network.

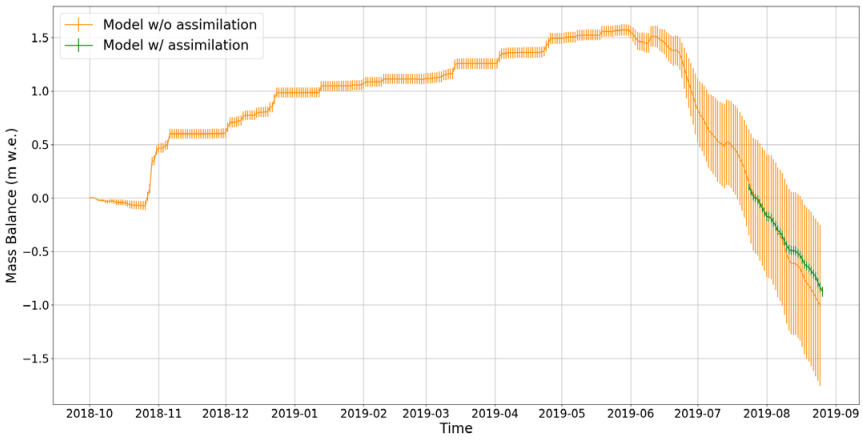


Figure 2. Modeled and assimilated daily evolution of the glacier-wide mass balance at Findelgletscher between October 2018 and end of August 2019. The green (orange) line shows the estimated evolution when the camera observations are (are not) assimilated. Error bars indicate the standard deviation of the model ensembles.

REFERENCES

Hock, R. 2003: Temperature-Index Melt Modelling in Mountain Areas. Journal of Hydrology, 282, 104-115.

11.6

Snow Avalanche Detection in Sentinel-1 and TerraSAR-X Radar Satellite Images

Silvan Leinss[1], Raphael Wicki[1], Sämi Holsteiner[1], Simone Bafelli[1], Yves Bühler[2]

[1]Institute of Environmental Engineering, ETH Zürich, CH 8093 Zürich, (leinss@ifu.baug.ethz.ch)
[2]WSL-Institute of Snow and Avalanche Research SLF, CH- 7260 Davos

In January 2018 two extreme snow fall events happened in Switzerland, rising the avalanche warning twice to level 5, on 9th of January in the district Visp and on 22nd of January for most of the Swiss alps. Due to the cut-off of valleys and ski resorts, information about avalanches was scarce. In such cases, high resolution optical satellite imagery is currently used to provide an analysis of the avalanche events, at least if cloud-free images can be acquired. To asses the potential of weather-independent radar satellites, we analyzed 2-meter resolution TerraSAR-X images and 10-meter resolution Sentinel-1 images and compared them to optical 1.5m resolution SPOT-6 data.

Avalanches were mapped manually by visual inspection of single radar backscatter images and also by visual inspection of change detection RGB composites created from 2 consecutive backscatter images. The comparison of radar results to the current standard of optical SPOT-6 satellite images showed that radar images are a valuable, comparable and possibly cheap alternative.

We found that both, radar and optical data have geometric limitations: in optical images, avalanches are difficult to detect in the sun shadow. In radar images, no information exists in the radar shadow and avalanches in layover areas are difficult to detect and cannot be correctly orthorectifiifed. Nevertheless, in areas visible for both optical and radar satellites, detection results are comparable to each. Still, the lower resolution Sentinel-1 data often miss smaller avalanches.
Remarkably, we found that the combination of multiple operationally and freely available Sentinel-1 images can provide comparable results to pairs of expensive and only on-demand available, high resolution TerraSAR-X images. The combination of different polarizations and orbits by an incoherent average of radar speckle enhances not only the effective resolution, but allows for an almost complete coverage of entire Switzerland especially in the difficult terrain of the Swiss Alps which is in single images affected by shadow and layover. As a demonstration, we present a Sentinel-1 change detection image covering entire Switzerland for the first period around the first avalanche event on 9th January.

11.7

Rock mass disintegration at the Moosfluh slope, Switzerland

Andrea Manconi[1], Simon Loew[1] & Franziska Glueer[2]

[1]Department of Earth Sciences, Engineering Geology, ETH Zurich, Zurich, Switzerland (andrea.manconi@erdw.ethz.ch)
[2]now at Swiss Seismological Service (SED), ETH Zurich, Zurich, Switzerland

The Moosfluh rock slope, located in the vicinity of the current tongue of the Great Aletsch glacier, Switzerland, hosts one of the largest active instabilities of the European Alps. Despite at this location accelerated slope displacement has been detected over the past decade, the rapid evolution observed between September and November 2016, locally reaching tens of meters, was largely unexpected. During this “crisis phase”, the rock mass experienced substantial internal deformation mainly composed of toppling, formation of tensile scarps, and basal sliding. The large internal deformation caused also several local failure events in the form of single block falls and/or rock mass collapses of moderate size. Here we focus on the post-crisis, i.e. the period going between spring 2017 until today. The deformation occurring at the Moosfluh slope is still large and rock failure events regularly occur, however, not in a dramatic fashion as observed in fall 2016. In particular, we focus on the joint analysis of the information obtained from the optical imagery acquired with high temporal frequencies and the seismic waveforms associated to rock failure events.

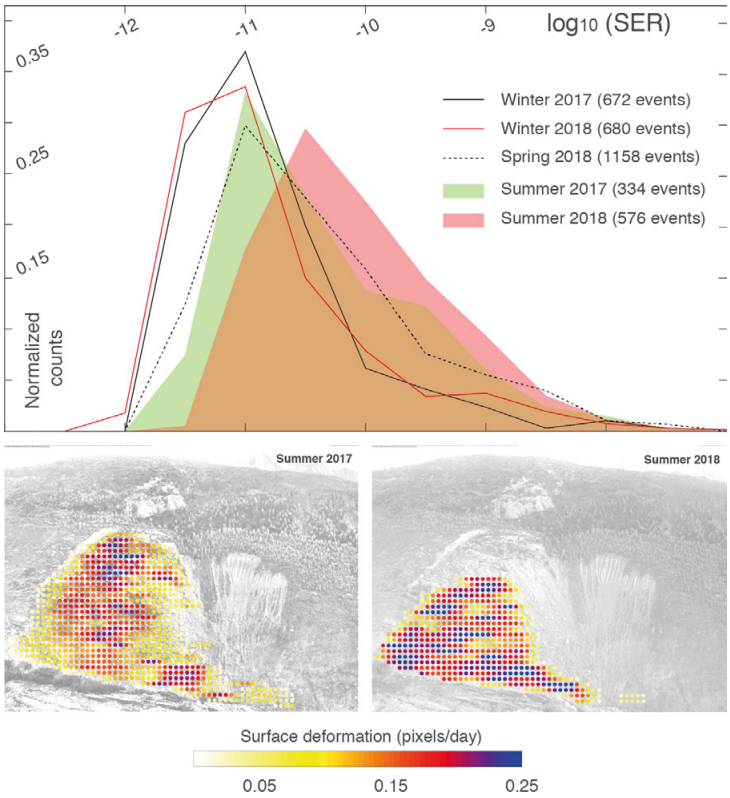


Figure 1. (top) Analysis of the catalogue showing differences in seismic energy release (SER). This change was associated to a change of the surface deformation style (Digital Image Correlation results shown at the bottom).

11.8

Canopy structure influences on energy fluxes to the forest snowpack: observations and modelling

Giulia Mazzotti[1,2], Johanna Malle[1,3], Richard Essery[4], Clare Webster[1,4], Tobias Jonas[1]

[1]WSL Swiss Federal Institute for Snow and Avalanche Research SLF, Davos, Switzerland
[2]Laboratory of Hydraulics, Hydrology and Glaciology VAW, ETH Zurich, Zurich, Switzerland
[3]Department of Geography and Environmental Sciences, Northumbria University, Newcastle upon Tyne, UK
[4]School of Geosciences, University of Edinburgh, Edinburgh, UK

Forest canopies strongly affect snowpack energetics during wintertime. In discontinuous forest stands, spatiotemporal variations in radiative and turbulent fluxes create complex snow distribution and melt patterns. As increasingly detailed canopy structure datasets are becoming available, canopy-induced energy exchange processes can be explicitly represented in high-resolution snow models. Yet, assessing canopy representation strategies for a variety of weather and canopy patterns necessitates in-situ measurements of the sub-canopy micrometeorological conditions.

In this study, we designed and deployed observational systems to capture spatial and temporal variations of incoming short- and longwave radiation, air and snow surface temperatures in subalpine and boreal forest stands. For all measured quantities, combining fixed sensor arrays and sensor assemblies mounted on a motorized cable car system and on a handheld stabilized gimbal yielded 1) time series at point locations, 2) spatiotemporal patterns along linear transect of varying canopy density, and 3) snapshots in time of 2-dimensional spatial distributions across forest discontinuities.

We then applied the multi-physics modelling framework FSM2 to obtain concurrent, spatially distributed simulations of the forest snowpack at high resolution (2m). By comparing modelled sub-canopy radiative and turbulent fluxes to observational data, model performance could be evaluated at the level of individual energy balance components, under various meteorological conditions and across canopy density gradients. We show which canopy representation strategies within FSM2 best succeed in reproducing snowpack energy transfer dynamics in discontinuous forested environments.

11.9

On the influence of debris cover on glacier surface morphology

Mölg, N., Ferguson, J., Bolch, T., Vieli, A.

Universität Zürich, Winterthurerstrasse 190, 8057 Zürich
(nico.moelg@geo.uzh.ch)

Various feedback mechanisms shape the intensity and the connections of processes that affect the evolution of debris-covered glaciers. While topics like mass balance, sub-debris melt and influence of ice cliffs and supraglacial ponds have received large attention during the past years, only few studies combined different processes to investigate the characteristic evolution of the surface morphology to sharpen the knowledge of glacier evolution on a wider spatial and temporal scale, although the morphology of many debris-covered glaciers is remarkably different from that of debris-free glaciers. In particular their tongues often show surfaces of high relief with abundant ice cliffs and experience surprisingly high mass loss despite the insulating debris.

We analysed the evolution of the surface features of Zmuttgletscher, a debris-covered glacier in Switzerland, over a period of 140 years using time series of historic maps, high resolution digital elevation models, and glacier velocities, as well as data on debris cover extent and thickness. Over time, the debris cover has expanded up-glacier, and moraine ridges have formed in the prolongation of the uppermost debris bands. Ridge prominence increased during periods of negative mass balance, and throughs developed in debris-free areas between ridges and persisted also after a continuous debris cover had developed. The changing surface morphology inhibits across-glacier meltwater flow, both supra- and subglacially. Accordingly, we found that large cryo-valleys with ice cliffs have formed down-glacier of the throughs where meltwater runoff accumulates. The meanders of these valleys have enlarged over time, especially by ice cliff backwasting at steep slopes, and most of the glacier width today is affected by such high-relief erosion features. We found that about 75% of all ice cliffs are located in this high-relief zone. The volume of the erosion features has increased by a factor of five since the 1980s, but is still small in comparison to the high glacier-wide thinning rates.

11.10

Comprehensive field measurements of the supra- and sub-glacial drainage of Lac des Faverges, Glacier de la Plaine Morte, in summer 2019.

Christophe Ogier[1] , Mauro A. Werder[1], Matthias Huss[1,2,3], Fabian Walter[1] & Daniel Farinotti[1,2]

[1]Versuchsanstalt für Wasserbau, Hydrologie und Glaziologie (VAW), Swiss Federal Institute of Technology (ETH), Hönggerbergring 26, CH-8093 Zürich (ogier@vaw.baug.ethz.ch)
[2]Eidgenössische Forschungsanstalt für Wald, Schnee und Landschaft (WSL), Zürcherstrasse 111, CH-8903 Birmensdorf
[3]Département des Géosciences, Université de Fribourg, Chemin du Musée 4, CH-1700 Fribourg

Glacier de la Plaine Morte, located in the Bernese Alps, is the largest plateau glacier in the European Alps. Since 2011, the ice-marginal Lac des Faverges drains annually through englacial and subglacial hydraulic channels with lake volumes up to $2x10^6$ m^3 and typically within only a few days. This causes floods and damage downstream along the Simme river. Since the lake volume is expected to continue to increase in the future (Huss et al., 2013), a 1.3km-long canal was dug at the glacier surface in April-June 2019. The intention was to progressively evacuate the lake water toward a nearby active moulin. On 10th July, the lake level reached the canal spillway elevation, corresponding to a volume of $1.35x10^6$ m^3, and started to drain through the canal (Figure 1). In early August, the canal was no longer able to drain the lake and its level remained constant (at a low volume of about $0.5x10^6$ m^3). On the 24th August, the remaining water suddenly drained subglacially, within 48h. The discharge at Simme river, however, did not show a pronounced peak.

Here, we present a comprehensive set of field measurements that were carried out during the 48 days of drainage and present insights into the temporal evolution of the event. The measurements aimed at quantifying both the drainage-canal erosion and lake discharge through time. The data set includes the incision rate of the canal into the ice, water temperature, seismic recording of hydraulic tremor, lake level and discharge measurements.



Figure 1: Lake runoff into the 2 meters-wide canal. Imprints of daily canal incision are well visible on the side walls.

REFERENCES

Huss, M., Voinesco, A., & Hoelzle, M. 2013: Implications of climate change on Glacier de la Plaine Morte, Switzerland, Geogr. Helv., 68, 227–237.

11.11

SnowNet - a deep learning approach for automatic snow and cloud classification in public webcam images

Céline Portenier[1], Stefan Wunderle[1]

[1]*Institute of Geography and Oeschger Centre for Climate Change Research, University of Bern, Hallerstrasse 12, CH-3012 Bern (celine.portenier@giub.unibe.ch)*

Terrestrial photography offers a huge potential to study the variability of snow cover on a high spato-temporal scale. A vast amount of readily available public webcam images can be used to complement and validate satellite-derived snow cover products. However, an accurate and automatic snow classification is of major importance. Additionally, the detection of adverse cloud cover and fog and its distinction from the snow cover is an enormous challenge.

Most existing classification approaches are threshold- or pixel-based. Therefore, the accuracy of these methods is insufficient under difficult conditions. Varying illumination due to daytime, weather, or shadowing hinder the application of threshold-based approaches. Moreover, the lack of global context for pixel-based techniques makes snow-cloud distinction ill-posed.

We propose to train a deep convolutional neural network on appropriate training data to predict snow and cloud coverage with per-pixel accuracy. For this purpose, we leverage manually labeled webcam images to train and evaluate the proposed network. To improve the accuracy of our network, we incorporate global context in the prediction for each pixel. This is achieved by considering an entire image patch instead of only a small local neighborhood to predict a single pixel. We evaluate our approach by comparing the performance of our trained network to state-of-the-art hand-crafted snow classification techniques.

11.12

Flat CO_2: a reconstruction from the last interglacial

Lucas Silva[1], Christoph Nehrbass-Ahles, Loïc Schmidely, Jochen Schmitt, Hubertus Fischer, Thomas Stocker

Climate and Environmental Physics, Physics Institute, University of Bern, Sidlerstrasse 5, CH-3012 Bern
[1](silva@climate.unibe.ch)

Antarctic ice cores provide high-resolution greenhouse gas records and open a clear window to the climate of the Earth of the past 800 kyr. The record for atmospheric CO_2 nevertheless hides fine structure on the sub-millenial scale in many intervals of lesser data resolution. Restricted ice availability and difficulties with traditional CO_2 dry extraction techniques inhibit high-resolution datasets. Here we present a novel CO_2 dataset from EPICA Dome C covering the Marine Isotope Stages 5 and 6. Discrete sampling with a centrifugal ice microtome achieved state-of-the-art ±1ppm in precision and improved seven-fold the resolution of the previous dataset. The reconstruction uncovers a long and stable interglacial period from 127 to 115 kyr at 277 ppm. There are hints of rapid CO_2 incursions during Termination II, a feature only seen so far during Termination I. We also find that rates of CO_2 change and timing of events match with another highly-resolved CO_2 record from MIS9-11. Together these features point to further CO_2 behavioral patterns between past interglacial periods and underline the importance of the study of past interglacials to our overarching understanding of the Holocene.

REFERENCES

Lüthi, D. et al 2008: High-resolution carbon dioxide concentration record 650,000–800,000 years before present. Nature, 453, 379-382

Bereiter, B., Stocker, T. F., and Fischer, H. 2013: A centrifugal ice microtome for measurements of atmospheric CO_2 on air trapped in polar ice cores. Atmos. Meas. Tech., 6, 251-262

Marcott, S. 2014: Centennial-scale changes in the global carbon cycle during the last deglaciation. Nature, 514, 616-619

11.13

Quantification of Snow Water Equivalent Using GNSS Refractometry and Standard GNSS Software

Ladina Steiner[1], Nadine Biland[2], and David Grimm[2]

[1]Institute of Geodesy and Photogrammetry, ETH Zurich, Switzerland (ladinasteiner@ethz.ch)
[2]Institute of Geomatics, University of Sciences and Arts of Northwestern Switzerland (FHNW), Switzerland

Extensive amount of water stored in snow covers has a high impact on flood development during snow melting periods. Early assessment of the snow water equivalent in mountain environments enhance early-warning and thus prevention of major impacts. Sub-snow GNSS techniques are lately suggested to determine liquid water content, snow water equivalent or considered for avalanche rescue. This technique is affordable, flexible, and provides accurate and continuous observations independent on weather conditions.

The potential to quantify snow water equivalent above a GPS antenna placed underneath a snowpack is evaluated using phase based differential GPS processing. In contrary to previous studies, standard off-the-shelf GNSS processing softwares are used and evaluated regarding the possibility to accurately determine snow water equivalent. One commercial software, Leica Infinity, and one open-source software, RTKLib, are thereby investigated.

Data is provided from a measurement network, which is set-up at the WSL SLF test site “Weissfluhjoch” consisting of a GPS reference station above the snow pack and a geodetic and low-cost GPS antenna mounted on the ground underneath the snowpack. The provided data are analysed for the winter seasons 2016/17. The results are compared to three reference sensors snow pillow, snow scale, and manual SWE observations provided by the WSL SLF, and results obtained from a high-end GNSS processing using the scientific Bernese GNSS software. Results of this point-wise estimation of snow water equivalent agree very well with all reference sensors within 10 percent over one complet dry and wet snow seasons.

11.14

Monitoring and Analysis of Landslide-Glacier Interactions (Great Aletsch Glacier, Switzerland)

Enea Storni[1], Simon Loew[1], Marc Hugentobler[1], Andrea Manconi[1]

[1]*Engineering Geology, Department of Earth Sciences, ETH Zürich, Sonneggstrasse 5, 8092 Zürich*

Valley glaciers might influence stability and movement rates of adjacent paraglacial landslides. However, detailed studies concerning the interactions between glacier ice and the mechanical behaviour of rock slopes are very rare. This Master Thesis deals with a detailed in-situ investigation of the displacement field of the Great Aletsch Glacier and the adjacent Moosfluh Landslide Landslide. The overall goal of the thesis is to better understand the dynamics which are acting at an active landslide-glacier interface. Main research questions are if landslide displacements cause modifications of the ice flow or vice versa if the viscous ice of the glacier has an effect on the creeping movement velocities and stability of an adjacent deep rock slope instability.

The Moosfluh landslide is a Deep-Seated Gravitational Slope Deformation (DSGSD) located near the currently retreating tongue of the Great Altesch Glacier. We have performed repeat UAV-based photogrammetric surveys (august 2018) and applied Digital Image Correlation (DIC) techniques, to record high-resolution surfaces movement's patterns for 74 h of both the landslide and glacier. A geomorphological analysis of the mapping area was done involving also previous airbourne pictures in order to properly detect the ice-contact boundary. In the end, observed displacements and modelled velocities have been compared from a statistical points of view in order to validate the performed work. Results show that the rapid movement of the landslide (up to 0.7 m displacement in 74 hours) has clear influence on the glacier vector field. This influence tends to be higher near the ice-contact boundary and decrease within a distance of about 100 m from the rock slope instability. Using the multiphysics simulation software COMSOL, the glacier-landslide system was modeled. Input parameters obtained during the UAV survey were used to calculate the glacial flow under the presence of an active landslide. The obtained vector field was finally compared with the field data supporting the idea that the observed glacial vector field is significantly influenced by the presence of the adjacent active landslide.

11.15

Changes in calving activity and front geometry of a marine terminating outlet glacier over six years

Andrea Walter[1,2], Martin P. Lüthi[1], Martin Funk[2], Andreas Vieli[1]

[1]Department of Geography, University of Zurich, Winterthurerstr. 190, 8057 Zürich (andrea.walter@geo.uzh.ch)
[2]ETH Zürich, VAW, Hönggerbergring 26, 8093 Zürich

By using a terrestrial radar interferometer, pressure sensors and a time-lapse camera we observed an outlet glacier in West-Greenland over six years. With the terrestrial radar interferometer we investigated additionally an outlet glacier with different characteristics in geometry and ice flow in Northwest-Greenland during two field campaigns. The resulting very detailed dataset provides us new insights on the calving process and the changes in front geometry. A comparison of the three different datasets offers us also a validation of the used methods. With the time-lapse camera alone, all calving events of different sizes and styles can be detected, but not quantified. The pressure sensors and the terrestrial radar interferometer are limited to calving events of a minimal size, but the terrestrial radar interferometer allows us to quantify the volumes of aerial calving events and calving waves measured with the pressure sensors enable us to distinguish between aerial and subaquatic events. We find that the calving style and size as well as the front geometry is mainly controlled by the bed topography and the presence of a subglacial discharge plume. The location of the plume can change from year to year, which leads also to changes in the calving pattern. Calving style and pattern as well as glacier velocity patterns and geometry changes are additionally compared with environmental conditions such as the temperature and the presence of ice-mélange in the proglacial fjord. The results will enable us to better understand the ongoing changes of the marine terminating outlet glaciers in Greenland.

P 11.1

Light absorbing impurities in the Olivares Catchment, Central Chile

Martina Barandun[1,2], Andres Rivera[3], Bernard Grobety[4], Ling Fang[1], Margit Schwikowski[1]

[1]Analytical Chemistry, Paul Scherrer Institute, Villigen, Switzerland,
[2]University of Fribourg, Unit of Geography, Geoscience, Fribourg, Switzerland
[3]Laboratorio de Glaciología, Centro de Estudios Científicos, Valdivia, Chile
[4]University of Fribourg, Unit of Geology, Geoscience, Fribourg, Switzerland

Light absorbing impurities (LAIs) such as mineral dust, organic material or black carbon can reduce the albedo on a glacier surface considerably. The lowered albedo values provoke a set of positive feedback mechanisms that enhance snow and ice melt. The glaciers located in the Olivares catchment in Central Chile are reported to have lost a substantial amount of mass in recent years (Rivera, 2019). Rowe et al. (2019) and Alfonso et al. (2019) showed important anthropogenic LAI content in snow for Central Chile. They also highlighted not only the effect of black carbon but also of mineral dust in snow.

Despite its importance, the complex effects of LAIs on ice albedo and the associated impact on ablation increase on the Olivares glaciers are so far not well understood. More investigation is required (1) to identify the origin of LAI pollution in snow and ice, (2) to quantify the related change in albedo and (3) to estimate the effect of such albedo changes on the ablation processes. To identify potential LAI sources, we combine the results from laboratory, remote sensing and field measurements. We use field spectrometry (Analysis Spectral Device (ASD) FieldSpec Pro, Boulder, USA) and Hyperspectral Imaging Microscope Spectrometry (HIMS by CytoViva, Inc.) to collect spectral reflectance properties of 65 surface ice and snow samples as well as of the containing LAI particles on Olivares Alfa, Beta, Paloma Norte and Juncal Sur.

The spectral information together with the LAI composition and concentration provided by mineralogical and chemical analysis enables in a second step to quantify the individual contribution of each LAI component. Organic carbon (OC) and elemental carbon (EC) are determined with a recently developed thermal-optical method (Swiss_4S), quantified with a non-dispersive infrared (NDIR) detector using an OC/EC analyzer (Sunset Laboratory Inc., USA). We use X-Ray Diffractometry (XRD) to assess the mineralogical composition and analyse trace element concentrations in the surface ice samples with inductively coupled plasma optical emission spectrometry (ICP-OES). For each tracer element, we calculate enrichment factors above the natural background to identify possible anthropogenic pollution through external LAI sources.

Using remote sensing, we aim to extrapolate the collected LAI concentration/composition and spectral properties to the entire glacier surface through establishing a relationship with surface reflectance maps from spatially distributed shortwave broadband albedo maps from Landsat images. The albedo maps are compare to the signatures of the representative surface material measured with the ASD FieldSpec, which serve as endmembers for surface classification on the Landsat Images.

First results show high concentration of mineral dust and rather low concentrations of EC which is in line with Rowe et al. (2019). HIMS analysis on Olivares Alfa, Beta and Paloma Norte confirm mineral dust as the predominant material of the LAIs. Preliminary XRD analysis show that the samples contain large amounts of quartz, chloride, andesite and muscovite. A first analysis of the ASD FieldSpec data indicates slightly lower reflectance values (field of measurement of 4 by 4 meters) at Olivares Alfa in comparison with the other sampling location (Fig. 1). This is in line with previous assessments of albedo on Landsat satellite images and of a permanently installed albedometer (CODELCO report, 2018).

Comparison of the LAI concentrations with values from Central Asia and Switzerland indicates elevated quantities of mineral dust in comparison to OC and EC. The origin of the mineral dust can on the one hand be natural erosion and, on the other hand, might origin from anthropogenic dispersible mineral dust such as from the deposition sites of the close by copper mine activities. However, the origin of the mineral dust is so far unclear and needs more profound assessments. Furthermore, the effect of LAIs on the glacier surface albedo remains unclear. Possible reasons for the difference in the reflectance can originate from elevated mineral dust concentration but might be connected to a more complex set of feedback mechanism such as increased melt water retention at the glacier surface. The spatio-temporal effect of LAIs on glacier albedo and the associated melt will be investigated in further analysis for the sample sites but also on glacier-wide and catchment scale using the full archive of Landsat surface reflectance data from 2000 to present. Comparison to unaffected glaciers and times are of crucial importance to identify possible anthropogenic effects (e.g. mining activities, air pollution of the capital city Santiago).

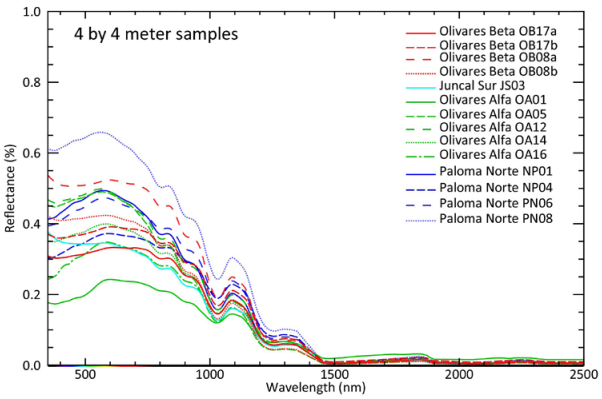


Figure 1: Reflectance spectra measured for a field of 4 by 4 meters at different ablation stake locations at glacier Olivares Alfa, Beta, Paloma Norte and Juncal Sur.

REFERENCES

Alfonso, J. A., Cordero, R. R., Rowe, P. M., Neshyba, S., Casassa, G., Carrasco, J., ... & Feron, S. (2019). Elemental and Mineralogical Composition of the Western Andean Snow (18° S–41° S). Scientific reports, 9(1), 8130.

Rivera, A. (2019). Los glaciares de Chile central a seis décadas de los trabajos de Louis Lliboutry. In: Turrel, M. El hombre que descifró los glaciares Louis Lliboutry. Aguas Andinas, pp. 250-255, Santiago de Chile, Chile.

Rowe, P. M., Cordero, R. R., Warren, S. G., Stewart, E., Doherty, S. J., Pankow, A., ... & MacDonell, S. (2019). Black carbon and other light-absorbing impurities in snow in the Chilean Andes. Scientific reports, 9(1), 4008.

P 11.2

Detecting and characterising englacial features on Oberaletsch Glacier using ground-penetrating radar

Pascale Carlen[1], Gregory Church[1,2], Melchior Grab[1,2], Hansruedi Maurer[2], Daniel Farinotti[1]

[1]*Department of Earth Sciences, Institute of Geophysics ETH Zürich, Zürich, Switzerland (pcarlen@student.ethz.ch, church@vaw.baug.ethz.ch)*
[2]*Laboratory of Hydraulics, Hydrology and Glaciology (VAW), ETH Zürich, Zürich, Switzerland*

A ground-based radar survey using a PulsEkko 50 MHz system was conducted on the Oberaletsch Glacier, Valais in February 2019 in order to detect and characterize the glacier's bedrock. We were able to detect a large overdeepening at the glacier's tongue, which could result in a proglacial lake with continued retreat of Oberaletsch Glacier. Additionally, a number of englacial features were detected. Different hypothesis for such englacial features were determined and compared to previous study oberservations on other temperatre glaciers.

As shown in the figure, two englacial features were identified; 1) a transparent layer overlying a high amplitude zone of scattering and, 2) a strong continuous englacial reflection. Both englacial features have been mapped across the survey area providing an insight into their spatial distribution.

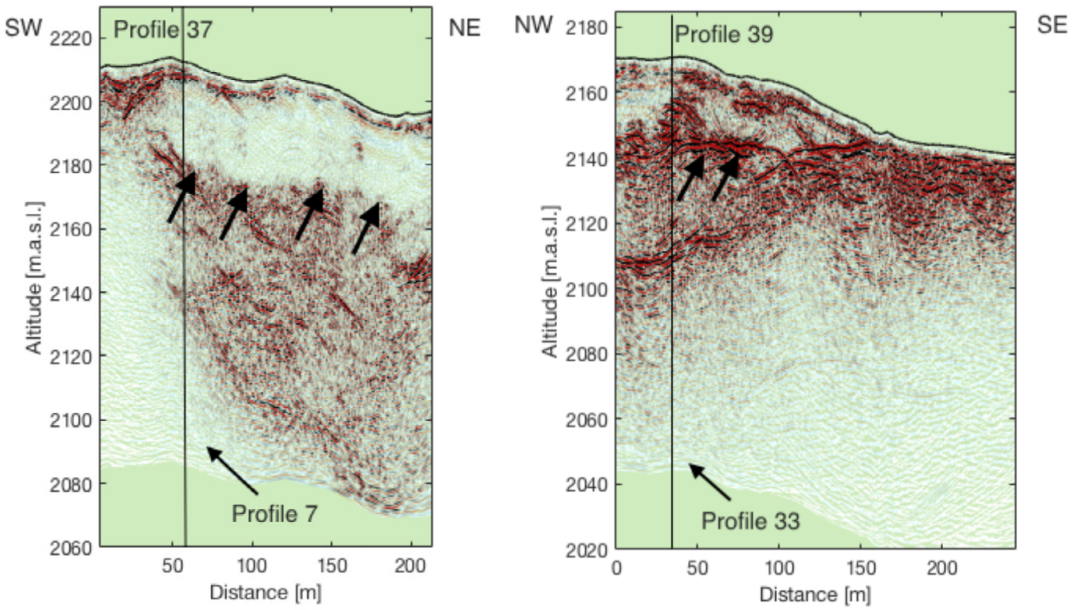


Figure: Profile 37 (left – Feature 1), GPR profile with the transparent layer and the englacial scattering horizon; profile 39 (right – Feature 2), GPR profile with a strong continuous reflector (black arrows).

The radar transparent zone, feature 1, was observed across the entire survey area. This transparent layer resembles cold ice in polythermal glaciers. However, it is argued that this transparent layer can be attributed to ice lacking in water. This has also been observed on Bench Glacier, Alaska (Brown, Harper and Bradford, 2009).

The strong continuous reflections, feature 2, was observed in the lower regions of the glacier. This englacial feature can potentially be attributed to an englacial water channel. However, by relying solely on GPR data, the interpretation and analysis of the observed englacial features is difficult and ambiguous. More research is thus required for a better understanding and an unambiguous interpretation of the nature of the englacial features.

These englacial features are ubiquitous within temperate glaciers and a thorough understanding will provide improvements in glacio-hydrology modelling.

REFERENCES

Brown, J., Harper, J. and Bradford, J. (2009) 'A radar transparent layer in a temperate valley glacier: Bench Glacier, Alaska', *Earth Surface Processes and Landforms*, 34(11), pp. 1497–1506. doi: 10.1002/esp.1835.

P 11.3

Monitoring an unstable hanging glacier in the Swiss Alps using icequake repeaters and seismic coda wave interferometry

Małgorzata Chmiel[1], Fabian Walter[1] and Lukas Preiswerk[1,2]

[1]Laboratory of Hydraulics, Hydrology and Glaciology, ETH Zurich, Zurich, Switzerland (chmiel@vaw.baug.ethz.ch)
[2]Forensic Technology & Discovery Services, Ernst & Young AG, Maagplatz 1, Zurich, Switzerland

High-altitude glaciers frozen to steep mountain faces are inherently unstable and produce catastrophic break-off events (Faillettaz et al., 2015). The hanging glacier on Switzerland's Mount Eiger periodically produces ice avalanches, which threaten tourist activity and a train line located in the avalanche runout path (Margreth et al., 2017). Reliable forecasting remains a challenge as physical processes leading to rupture events are not fully understood yet and/or difficult to observe.

The hanging glacier on Mount Eiger was intensely monitored in 2016 as crevasses and ice flow speed suggested that a large break-off event was impending. Among different instruments, such as an interferometric radar measuring ice motion, an automatic camera, an infrasound array, and four 3-component seismometers (natural frequency: 1 Hz) were installed on the glacier between April and August 2016 (stations EIG1:EIG4, Figure 1a). Avalanche activity, snow fall and other factors associated with high altitude conditions posed severe challenges for instrument maintenance. However, one station was recording continuously for 4.5 months, and up to three seismic stations operated simultaneously.

On 25 August 2016 an ice mass of 15,000 m^3 broke off the hanging glacier. We investigate the local microseismic activity and icequake occurrence recorded by the seismic array before, during and after the rupture event. We find no straightforward correlation between the icequake detections and the break-off event. However, we find thousands of repeating seismic events with practically identical waveforms. We group the repeating events into clusters based on the similarity of the waveforms. Figure 1b shows one of the clusters with 290 repeating events recorded at the vertical component of station EIG 2. Figure 1c shows a normalized average of repeating event waveforms (continuous black line) and the amplitude variation from the average (dashed black line). The direct P-waves and Rayleigh waves are marked with a red dashed box, and coda waves (waves reflected at the boundaries of the glacier and scattered at the pervasive fracturing within the hanging glacier) are marked with a blue dashed box.

Based on the clusters of repeating events, we perform a statistical analysis of microseismic activity and test seismic coda wave-interferometry [CWI: Snieder et al., (2002), Campillo and Paul, (2003)] as a means to monitor englacial elastic properties. First results indicate changes in englacial fracture state, which may be related to variations in ice motion. This suggests that though technically challenging, on-ice seismic measurements provide new insights into fracture processes within the ice influencing the stability of avalanching glaciers.

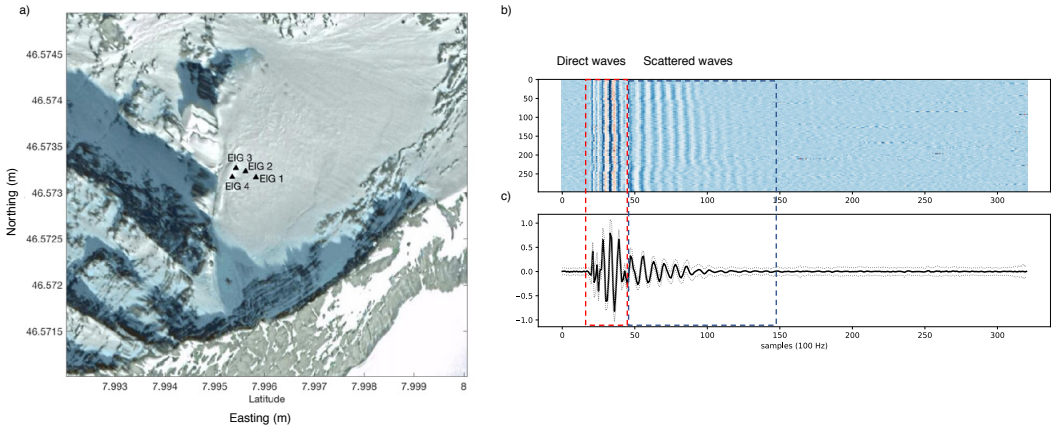


Figure 1. a) Four stations installed on Mount Eiger glacier (EIG1:EIG4). b) One of the clusters with 290 repeating events recorded at the vertical component of station EIG 2. Direct waves are marked with a red box, and scattered waves are marked with a blue box. c) Normalized average of repeating event waveforms (continuous black line) and the amplitude variation from the average (dashed black line).

REFERENCES

Faillettaz, J., Funk, M., and Vincent, C. 2015: Avalanching glacier instabilities: Review on processes and early warning perspectives, Rev. Geophys., 53, 203– 224.

Margreth, S., Funk, M., Tobler, D., Dalban, P., Meier, L., Lauper, J. 2017: Analysis of the hazard caused by ice avalanches from the hanging glacier on the Eiger west face, Cold Regions Science and Technology, 144, 63-72.

Snieder, R., Grêt, A., Douma, H., Scales, J. 2002: Coda Wave Interferometry for Estimating Nonlinear Behavior in Seismic Velocity, Science, 295, 2253-2255.

Campillo, M., Paul, A. 2003: Long-Range Correlations in the Diffuse Seismic Coda, Science, 299, 547-549.

P 11.4

Englacial drainage network temporal evolution using impendance inversion from ground-penetrating radar

Gregory Church[1,2], Melchior Grab[1,2],Cédric Schmelzbach[2], Andreas Bauder[1], Hansruedi Maurer[2]

[1]Laboratory of Hydraulics, Hydrology and Glaciology (VAW), ETH Zürich, Zürich, Switzerland (church@vaw.baug.ethz.ch)
[2]Department of Earth Sciences, Institute of Geophysics ETH Zürich, Zürich, Switzerland

Glacier hydraulic drainage systems are continuously evolving throughout the melt season on alpine glaciers. Englacial drainage systems impact glacial dynamics by routing surface meltwater to the glacier's base and facilitating basal lubrication which often results in basal slip (Cuffey and Paterson, 2010). Therefore, advanced knowledge of such drainage systems is essential.

This study was conducted within the ablation zone of the Rhone Glacier, Switzerland. Repeated ground-penetrating radar (GPR) surveys were acquired between 2017 and 2019 in order to investigate the glacier's drainage system evolution. Additionally, we drilled six boreholes in and around the drainage network in summer 2018 to provide ground truth measurements. Direct observations were also made into the englacial conduit network using a GeoVISIONTM Dual-Scan borehole camera.

GPR is highly sensitive to the presence of water and is therefore a suitable tool to monitor englacial drainage evolution. We studied the seasonal evolution of the englacial drainage network by inverting GPR data for impedance contrasts using an amplitude inversion workflow (Schmelzbach, Tronicke and Dietrich, 2012)which controls GPR wave velocity and reflectivity. Conventional tools like common midpoint (CMP based upon the seismic reflection impedance inversions. The reflectivity analysis provided an indication of the englacial network's geometry and the water content. Our inversion results indicated the englacial network was inactive during the winter season (November-May) with low reflectivity values between 0 and -0.1 (Figure 1 top). Whereas, the drainage system became activated between May and July and flowed through a meandering channel network, imaged with GPR, with high reflectivity around -0.3, indicating the likely presence of water (Figure 1 bottom).

The englacial drainage network shut down and became inactive between two GPR surveys in October and December. Alongside the inversion results, we are able to draw conclusions on the geometry using a GPR thin layer modelling analysis. The englacial drainage network seems to remain active across three melt seasons, thereby indicating that conditions in temperate glaciers can provide long term fluid flow paths, even though englacial drainage networks can be inactive throughout the winter.

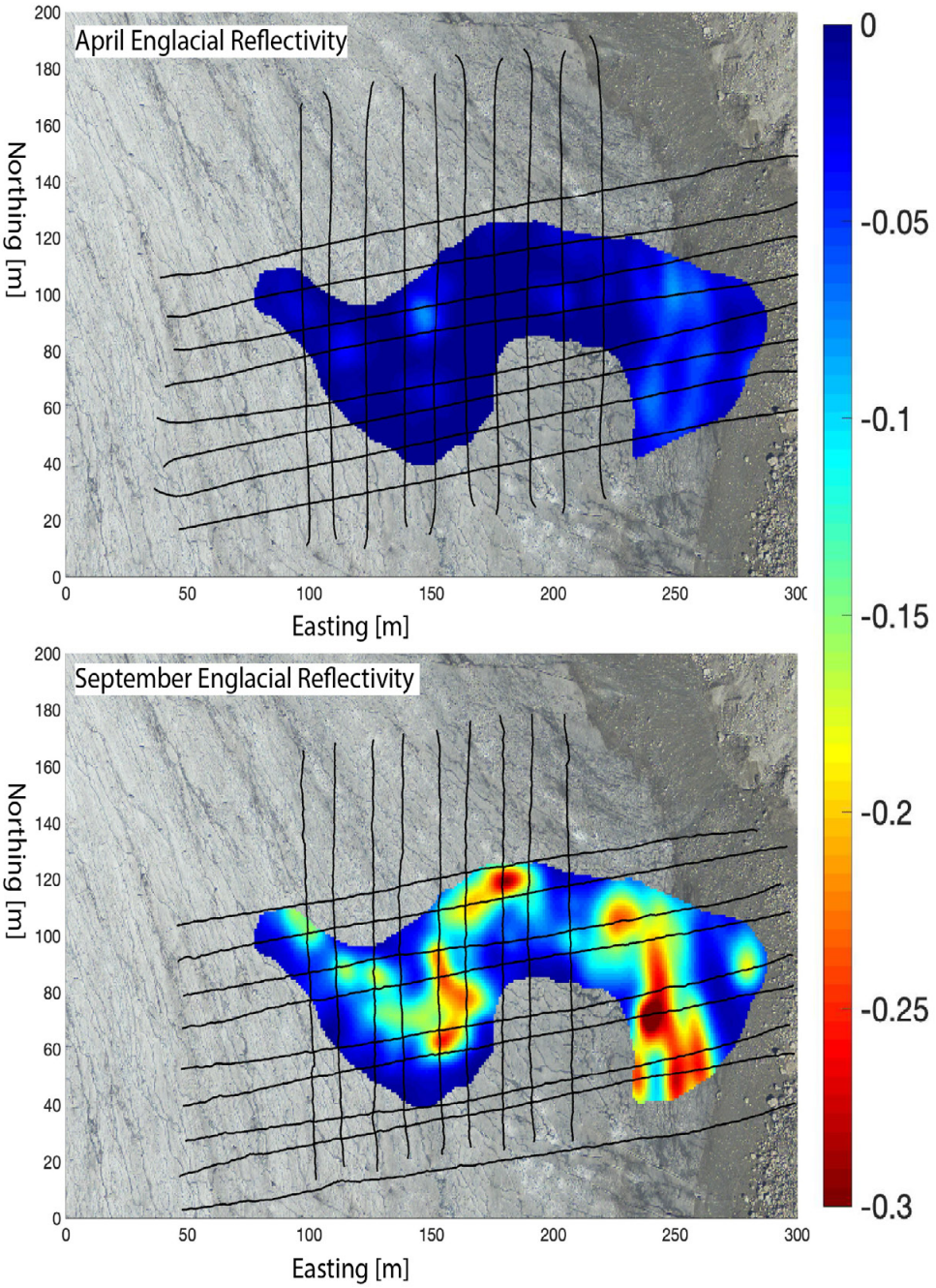


Figure 1: Top: Englacial reflectivity inverted from GPR data acquired in April (winter). Bottom: Englacial reflectivity inverted from GPR data acquired in September (summer). In both plots the black lines represent the GPR profiles from their respective montly acquisitions.

REFERNCES

Cuffey, K. M. and Paterson, W. S. B. (2010) *The Physics of Glaciers, Fourth Edition*. Fourth Edi. Academic Press.

Schmelzbach, C., Tronicke, J. and Dietrich, P. (2012) 'High-resolution water content estimation from surface-based ground-penetrating radar reflection data by impedance inversion', *Water Resources Research*, 48(8), pp. 1–16. doi: 10.1029/2012WR011955.

P 11.5

“SnowIceSen”: An Automated Tool to Map Snow and Ice on Glaciers with Sentinel-2

Lea Geibel[1,2], Johannes Landmann[1,2] & Daniel Farinotti[1,2]

[1]*Versuchsanstalt für Wasserbau, Hydrologie und Glaziologie (VAW), Swiss Federal Institute of Technology (ETH), Hönggerbergring 26, CH-8093 Zürich (geibell@student.ethz.ch)*
[2]*Eidgenössische Forschungsanstalt für Wald, Schnee und Landschaft (WSL), Zürcherstrasse 111, CH-8903 Birmensdorf*

An automated classification of snow cover on glaciers using optical remote sensing data is challenging, but has the potential to frequently constrain glacier mass balance estimates and improve glacier modeling. In the past, there have not been many approaches to fully automate the workflow of mapping snow, firn and ice facies on glaciers. Recent earth observation initiatives, such as the European Space Agency’s Copernicus programme, offer great opportunities to complement in situ measurements with observations from space. The Sentinel-2a and Sentinel-2b optical satellites, for example, offer revisiting times of 2-4 days at mid-latitudes, and a spatial resolution of 10 m. In this study, we test the use of such data over Switzerland.

We developed the open source Python tool “SnowIceSen” (https://github.com/lgeibel/snowicesen) which uses Sentinel-2 data to distinguish snow and firn cover from ice surfaces. This tool automates image availability checks for a given time and glacier, downloads the data, performs terrain correction, and excludes debris and cloud-covered areas. After image pre-processing, snow and ice are distinguished by using three classification algorithms: the ASMAG algorithm (Automated Snow Mapping on Glaciers) by Rastner et al. (2019), a method presented in Naegeli et al. (2018), and an alternate version of the latter introducing more flexible parameters for the multi- step classification. All three algorithms make use of snow and ice spectral reflectance properties and partly introduce additional geometric rules to confine the model results.

We validate algorithm performance against a manually created dataset of 430 snow distributions. The validation scenes are weighted with the glacier area to account for the glaciers contribution to the overall mass balance, and are uniformly distributed over the time for which data is processed. The evaluation shows that the performance varies greatly with the conditions under which the images are acquired: for a snow cover of 30-80% and low cloud coverage, the snow maps created by the ASMAG algorithm and the alternate version of the method by Naegeli et al. show good agreement with the manual snow maps (average Cohen’s Kappa of 0.58 and 0.56 respectively). Contrarily, for high snow cover (over 80%) and cloud coverage higher than 30%, the agreement is often very low (Cohen’s Kappa under 0.1). This shows that image conditions can severely hamper the application of a fully automated workflow as implemented in SnowIceSen. Often encountered problems are small contrasts between snow and ice reflectance, erroneous cloud cover detection, as well as terrain and cloud induced shadows. Improvements in the algorithm performance might be possible through additional rule-based classifiers in the future.

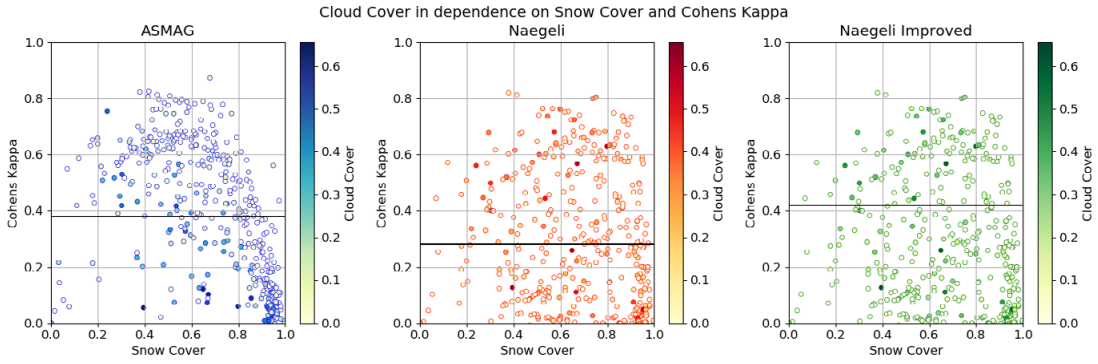


Figure 1. Performance (Cohen’s Kappa) of Snowicesen’s snow cover maps as a function of the snow cover (x-axis) and the cloud cover (color of the dots). The three panels correspond to the three implemented algorithms, the horizontal line shows the average Cohen’s Kappa for all scenes (ASMAG: 0.38, Naegeli, 0.28, Naegeli alternate: 0.42). Validation is performed against manually delineated snow cover extents extracted from 430 scenes. Cohen’s Kappa for each scene (Kappa=1 means perfect agreement, Kappa=0 means no agreement) is low for high snow cover and high cloud cover and better for medium snow cover for the ASMAG and alternate Naegeli algorithm. The original method by Naegeli et al. shows no clear dependence, and a generally lower Kappa.

REFERENCES

Copernicus Sentinel data 2015-2018. Retrieved from Copernicus Open Access Hub between June 2nd and August 5th 2019, processed by ESA.

Rastner, P., Prinz, R., Notarnicola, C., Nicholson, L., Sailer, R., Schwaizer, G.& Paul, F. 2019: On the Automated Mapping of Snow Cover on Glaciers and Calculation of Snow Line Altitudes from Multi-Temporal Landsat Data, Remote Sensing, 11, 1410.

Naegeli, K., Huss, M., Hoelzle, M. 2019: Change detection of bare-ice albedo in the Swiss Alps, The Cryosphere, 13. 397-412.

P 11.6

The total glacier ice volume in the Swiss Alps

Melchior Grab[1,2], Lisbeth Langhammer[1], Sebastian Hellmann[1], Gregory Church[1,2], Andreas Bauder[2], Lasse Rabenstein[3], Lino Schmid[4] & Hansruedi Maurer[1]

[1]Institute for Geophysics, ETH Zurich, Sonneggstrasse 5, 8092 Zürich (melchior.grab@erdw.ethz.ch)
[2]Laboratory of Hydraulics, Hydrology and Glaciology, ETH Zurich, Hönggerbergring 26, 8092 Zürich
[3]Drift & Noise Polar Services GmbH, Hohenlohestr 8, 28209 Bremen

In earlier studies the total ice volume in the Swiss Alps for the year 1999 as been estimated to be 74 ± 9 km^3 (Farinotti et al., 2009) and 65 ± 20 km^3 (Linsbauer et al., 2012). These estimates were based on glaciological modeling. Ground penetrating radar (GPR) data of some glaciers have been used to validate the models. Until 2015, around 1500 km of GPR profiles have been recorded on Swiss glaciers by various researchers, with some of them being used for the Swiss-wide ice tickness estimates mentioned above.

For our new study, we additionally acquired around 1100 km of GPR profiles since 2016, with the helicpoter-borne GPR system AIR-ETH (Langhammer et al., 2019a) and the corresponding processing software GPRglaz (Grab et al., 2018), both developed for this purpose. To obtain continuous maps of the ice thickness and the bedrock topography, we recently established the Glacier Thickness Estimation (GlaTE) algorithm (Langhammer et al., 2019b). It enables to invert for the three-dimensional ice thickness of Alpine glaciers based on glaciological modeling (after Clarke et al., 2013) and observable data constraints (glacier outlines, digital elevation model, by Swisstopo), while adequately accounting for the ice thickness obtained from GPR-measurements.

The GlaTE algorithm has now been used to calculate the total ice volume in the Swiss Alps, taking into account the large amount of accessable data recorded during earlier years and the new data recorded with AIR-ETH. The resulting distribution of the ice thickness is shown in Figure 1. In contrast to the earlier studies, this ice thickness map is based on much more field data, such that Swiss-wide around 80% (large pie-diagram in Figure 1) of the obtained ice volume is constrained by GPR data. For individual subregions, the ratio of GPR-constrained volume estimates versus ice volumes estimated by glaciological modeling only, are shown with the small pie-diagrams. From the ice thickness map, the total ice volume in the Swiss Alps will be calculated and presented during the Swiss Geoscience Meeting 2019.

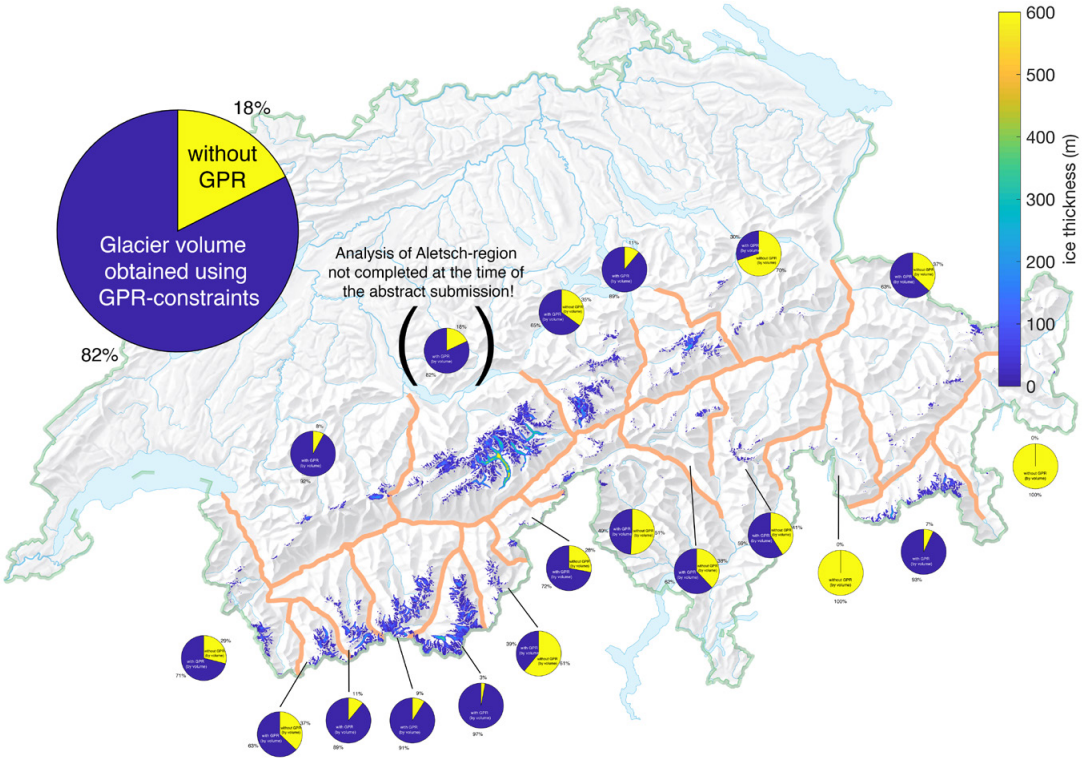


Figure 1. Glacier thickness map obtained during our study. Note that the color-range is clipped to 600 m. Maximum ice thickness at Konkordiaplatz is approximately 850 meters. Around 80% of the total ice volume is estimated using our GPR-constrained GlaTE algorithm, whereas 20% are obtained from glaciological modeling without GPR constraints. Small pie-diagrams show this ratio for different subregions.

REFERENCES

Clarke, G. K., Anslow, F. S., Jarosch, A. H., Radić, V., Menounos, B., Bolch, T., & Berthier, E, Ice volume and subglacial topography for western Canadian glaciers from mass balance fields, thinning rates, and a bed stress model. Journal of Climate, 26(12), 4282-4303, 2013.

Farinotti, D., M. Huss, A. Bauder, & M. Funk, An estimate of the glacier ice volume in the Swiss Alps. *Global and Planetary Change*, *68*(3), 225-231, 2009

Grab, M., A. Bauder, F. Ammann, L. Langhammer, S. Hellmann, G. J. Church, L. Schmid, L. Rabenstein, and H. R. Maurer. "Ice volume estimates of Swiss glaciers using helicopter-borne GPR—an example from the Glacier de la Plaine Morte." In 2018 17th International Conference on Ground Penetrating Radar (GPR), pp. 1-4. IEEE, 2018.

Langhammer, L. Rabenstein, L. Schmid, L., A. Bauder, M. Grab, P. Schaer, & H. Maurer, Glacier bed surveying with helicopter-borne dual-polarization ground-penetrating radar. *Journal of Glaciology*, *65*(249), 123-135, 2019a.

Langhammer, L., M. Grab, A. Bauder, & H. Maurer, Glacier thickness estimations of alpine glaciers using data and modeling constraints. *The Cryosphere*, *13*(8), 2189-2202, 2019b.

Linsbauer, A., F. Paul, & W. Haeberli, W, Modeling glacier thickness distribution and bed topography over entire mountain ranges with GlabTop: Application of a fast and robust approach. *Journal of Geophysical Research: Earth Surface*, *117*(F3), 2012.

P 11.7

High-elevation snow accumulation studies at the Biafo-Hispar glacier system in the Central Karakoram

Alexander Raphael Groos[1], Christoph Mayer[2], Astrid Lambrecht[2], Sabrina Erlwein[3], Margit Schiwkowski[4]

[1]Institute of Geography, University of Bern, Hallerstrasse 12, CH-3012 Bern (alexander.groos@giub.unibe.ch)
[2]Geodesy and Glaciology Group, Bavarian Academy of Sciences and Humanities, Alfons-Goppel-Str. 11, D-80539 Munich
[3]Chair for Strategic Landscape Planning and Management, Technical University of Munich, Emil-Ramann-Str. 6, D-85354 Freising
[4]Laboratory of Environmental Chemistry, Paul Scherrer Institute, Forschungsstrasse 111, CH-5232 Villigen PSI

The Karakoram in the northwestern part of High Mountain Asia is one of the most extensively glacierised areas outside the polar regions and an important fresh water source for millions of people living in the Indus Basin. The mountain range has increasingly attracted attention in recent years due to an anomalous glacier stability, which contrasts the progressing ice mass loss elsewhere in the Himalaya. Decreasing summer temperatures and increasing winter precipitation are discussed as potential causes for the anomaly. However, the lack of weather stations and glaciological investigations above 3,000 m a.s.l. hampers the corroboration of this hypothesis. To study the spatio-temporal variations of snow accumulation across the Central Karakoram, we repeated a Canadian research expedition from 1986 (Hewitt et al. 1989; Wake 1989) and investigated eight snow pits between 4,388 and 5,202 m a.s.l. in the accumulation zone of the Biafo-Hispar glacier system. Snow density measurements were performed in the field to quantify the elevation-dependent annual snow water equivalent and compared to the 30-year-old results from Hewitt et al. (1989) and Wake (1989). In addition, snow water samples were retrieved in 10 cm intervals for analysis of the stable isotope O^{18} and the chemical fingerprint of several detected dust events.



Figure 1. Snow accumulation studies at Biafo Glacier in the Central Karakoram in 1986 (left side) and 2019 (right side).

REFERENCES

Hewitt, K., Wake, C.P., Young, G.J. & David, C. 1989: Hydrological Investigations at Biafo Glacier, Karakoram Range, Himalaya; An Important Source of Water for the Indus River. Annals of Glaciology 13, 103-108.

Wake, C.P. 1989: Glaciochemical Investigations as a Tool for Determining the Spatial and Seasonal Variation of Snow Accumulation in the Central Karakoram, Northern Pakistan. Annals of Glaciology 13, 279-284.

P 11.8

No firn changes in Central Asia?

Marlene Kronenberg[1], Horst Machguth[1], Anja Eichler[2,3], Margit Schwikowski [2,3,4], Max Ruethi[4], Martin Heule[5] & Martin Hoelzle[1]

[1]Departement of Geosciences, University of Fribourg, Chemin de Musée 4, CH-1700 Fribourg (marlene.kronenberg@unifr.ch)
[2]Laboratory of Environmental Chemistry, Paul Scherrer Institute, CH-5232 Villigen
[3]Oeschger Centre for Climate Change Research, University of Bern, CH-3012 Bern
[4]Department of Chemistry and Biochemistry, University of Bern, CH-3012 Bern
[5]Abteilung Strahlenschutz und Sicherheit, Paul Scherrer Institute, CH-5232 Villigen

For polar glaciers, it has been shown that firn properties are strongly affected by climate change (e.g. Bezeau et al., 2013; Machguth et al., 2016). Changes within the firn area, where snow densifies into glacier ice, affect the glacier dynamics and glacier mass balance. Only a few studies investigate firn on mountain glaciers. Despite the importance of firn temperature monitoring for mountain ranges with cold and polythermal glaciers such studies are regionally biased and focus on sites in the European Alps (Hoelzle, 2011). However, repeated firn investigations in data sparse regions such as Central Asia are necessary to detect firn changes. Furthermore, such data allow to increase our process understanding and to address uncertainties in mass balance estimates for data sparse regions.

Here, we use legacy firn core data (1970s – 1990s) from two glaciers that represent different climatic settings in Central Asia. (i) Gregoriev ice cap is situated in the Inner Tien Shan, where the precipitation maximum occurs during summer months and the annual precipitation is about 360 mm water equivalent (w.eq.). (ii) Abramov glacier is located in the Pamir Alay and receives maximum precipitation during winter. Kislov (1980) described a strong precipitation gradient across the glacier surface with up to 1800 mm w.eq. yr^{-1} in the accumulation area. At both sites, ~17 m long firn cores were drilled in 2018. Firn cores were shipped to Switzerland and analysed for water stable isotopes, black carbon and major ions at the Paul Scherrer Institute, Villigen. Chemical measurements allow determining the annual accumulation rates of the Abramov firn core for 2011-2017. In the Gregoriev core, chemical records are partly disturbed by melting and accumulation rates are low.Thus, for dating, annual layer counting was complemented with identifying the year 1986 (Tschernobyl accident) based on total beta activity measurements. Accordingly, the mean annual accumulation rate in the Gregoriev core is ~320 mm w.eq. in the period ~1975-2018. The comparison of recent firn characteristics with legacy data shows that accumulation at both sites has undergone no substantial changes over the past 5 decades. This is surprising as both glaciers have experienced a substantial mass loss over the respective periods despite their different climatic setting. These results point out, that more in situ data from remote areas is necessary to increase our process understanding.

REFERENCES

Bezeau, P., Sharp, M., Burgess, D. & Gascon, G. 2013: Firn profile changes in response to extreme 21st-century melting at Devon Ice Cap, Nunavut, Canada J. Glaciol., 59, 981-991.

Hoelzle, M., Darms, G., Lüthi, M. P. & Suter. S. 2011: Evidence of Accelerated Englacial Warming in the Monte Rosa Area, Switzerland/Italy. The Cryosphere 5(1), 231–43.

Kislov, B. V. 1982. Formirovanie i Režim Firnovo-Ledjanoj Tolŝi Gornogo Lednika [Formation and Regime of the Firn-Ice Stratum of a Mountain Glacier]. (In Russian). SARNIGMI, Tashkent.

Machguth, H., MacFerrin, M., van As, D. Box, J.E., Charalampidis, C., Colgan,W., Fausto, R.S., Meijer, H.A.J., Mosley-Thompson, E. & van de Wal, R.S.W., 2016. Greenland Meltwater Storage in Firn Limited by Near-Surface Ice Formation. Nature Climate Change 6, 390–93.

P 11.9

Do ice dynamics and glacier hydraulics cause englacial variations detectable with seismology?

Fabian Lindner[1], Philippe Roux[2], Fabian Walter[1] & Florent Gimbert[3]

[1]*Laboratory of Hydraulics, Hydrology and Glaciology, ETH Zürich, Hönggerbergring 26, CH-8093 Zürich (lindner@vaw.baug.ethz.ch)*
[2]*Institut des Sciences de la Terre, Université Grenoble Alpes, France*
[3]*Institut des Géosciences de l'Environment, Université Grenoble Alpes, France*

Ice flow causes spatio-temporal variations in englacial stresses which may result in crevassing (Colgan et al, 2016). Through crevasses, meltwater produced at the surface may reach the glacier bed via existing conduits or hydrofracturing, where it modulates the hydraulic head of subglacial discharge (Fountain & Walder, 1998).

Changes in the englacial stress and fracture state as well as the englacial water content affect the bulk properties of the ice and thus its seismic wave velocities. By measuring the medium's response between seismic sensors repeatedly, seismic interferometry allows to detect such variations in subsurface velocity (e.g. Sens-Schönfelder & Wegler, 2006). Here, we apply an interferometric approach called virtual-reflector seismology (Weemstra et al., 2017) to a 98-geophone dataset from Glacier d'Argentière. The geophones were deployed for six weeks in a regular grid of 50 m on the tongue of the glacier. The dense grid of sensors allows the retrieval of virtual reflections within the array, which increases the monitoring capabilities of englacial changes (Lindner et al., 2018).

Based on icequakes which illuminate the glacier, we propose to retrieve interferometric responses allowing englacial monitoring with subdaily resolution. Comparison of potential temporal changes in englacial velocities with time series of subglacial water pressure and basal motion (measured in subglacial tunnel facilities), as well as surface ice motion allows us to address the following questions: How do ice flow modulations affect the englacial fracture state? Can we detect variations in water content of englacial void spaces resulting from subglacial water pressure variations?

REFERENCES

Colgan, W., Rajaram, H., Abdalati, W., McCutchan, C., Mottram, R., Moussavi, M. S., & Grigsby, S. 2016: Glacier crevasses: Observations, models, and mass balance implications. *Reviews of Geophysics*, *54*(1), 119-161.

Fountain, A. G., & Walder, J. S. 1998: Water flow through temperate glaciers. *Reviews of Geophysics*, *36*(3), 299-328.

Lindner, F., Weemstra, C., Walter, F., & Hadziioannou, C. 2018: Towards monitoring the englacial fracture state using virtual-reflector seismology. *Geophysical Journal International*, *214*(2), 825-844.

Sens-Schönfelder, C., & Wegler, U. 2006: Passive image interferometry and seasonal variations of seismic velocities at Merapi Volcano, Indonesia. *Geophysical research letters*, *33*(21).

Weemstra, C., Wapenaar, K., & Van Dalen, K. N. 2017: Reflecting boundary conditions for interferometry by multidimensional deconvolution. *The Journal of the Acoustical Society of America*, *142*(4), 2242-2257.

P 11.10

Observing glacier motion in extremely high resolution

Martin P. Lüthi

[1]Geographical Institute, University of Zurich, Winterthurerstr. 190, 8057 Zürich (martin.luethi@geo.uzh.ch)

Interferometric radar systems, such as the Gamma GPRI, have been used to observe glacier motion at high spatial and temporal resolution. In many cases the signal is severly distorted by atmospheric noise. Instead of the theoretical minute interval, displacement data has to be averaged for many minutes, and even then the accuracy is poor.

Here, we present a novel method to cope with the phase noise caused by the atmosphere, and show how a much better time and space resolution can be achieved. The method is illustrated at the examples of a steep glacier in the Alps and for tidewater glaciers in Greenland.

P 11.11

Modelling the age of ice of Rhonegletscher

Joël Morgenthaler[1], Guillaume Jouvet[1,2], Andreas Bauder[1]

[1]Laboratory of Hydraulics, Hydrology and Glaciology (VAW), Swiss Federal Institute of Technology (ETH), Hönggerbergring 26, CH-8093 Zurich (mjoel@student.ethz.ch)
[2]Geographical Institute, University of Zurich, Winterthurerstrasse 190, CH-8057 Zurich

The dynamics of temperate alpine glaciers are the result of two main processes: internal plastic deformation (vertical ice shearing) and sliding over the bedrock. However, the ratio between shearing and sliding is often difficult to estimate due to lack of direct observations. Most of the time, we have only to rely on information from the glacier surface to give insights on basal processes (Cuffey & Paterson, 2010).

Here we use a modelling approach to investigate the surface age distribution of Rhonegletscher under different shearing/sliding conditions. First, we modelled diagnostically the ice flow field using the Stokes model Elmer/Ice and computed particle streamlines of stationary 2D and 3D glacier geometries. In turn, this allows us to characterize the surface age distribution of ice and to evidence how basal motion influences the surface age distribution of Rhonegletscher.

Second, we run our model prognostically by coupling to a mass balance model to simulate the dynamic evolution of Rhonegletscher from 1874 to present time similarly to Jouvet et al. (2009). From the resulting ice flow field, we compute backward-in-time trajectories of ice particles (Jouvet & Funk, 2014) passing by an ice core extracted in 2017 at the terminus of Rhonegletscher in order to infer the modelled age of ice and to compare to independent results of analytic dating methods.

REFERENCES

Cuffey, K., & Paterson, W. 2010. The Physics of Glaciers, Elseiver, Burlington

Jouvet, G., & Funk, M. 2014: Modelling the trajectory of the corpses of mountaineers who disappeared in 1926 on Aletschgletscher, Switzerland, Journal of Glaciology, 60(220), 255-261.

Jouvet, G., Huss, M., Blatter, H., Picasso, M., & Rappaz, J. 2009: Numerical simulation of Rhonegletscher from 1874 to 2100, Journal of Computational Physics, 17(228), 0021-9991.

P 11.12

Passive seismic imaging of glaciers with ambient seismic noise and glacier seismicity

Amandine Sergeant[1], Malgorzata Chmiel[1], Walter Fabian[1], Lindner Fabian[1], Chaput Julien[2], Mordret Aurélien[3], Roux Philippe[3], Gimbert Florent[4]

[1]Laboratory of Hydraulics, Hydrology and Glaciology, ETH Zurich, Zurich, Switzerland (sergeant@vaw.baug.ethz.ch)
[2]Department of Geological Sciences, University of Texas El Paso, El Paso, USA
[3]ISTerre, Université de Grenoble Alpes, Grenoble, France
[4]Institut des Geosciences et de l'Environement (IGE), IRD, Université de Grenoble Alpes, Grenoble, France

Ambient noise interferometry has revolutionized seismic characterization of the Earth's crust at local to global scales. The underlying techniques use continuous records of seismic background noise primarily generated by ocean and climate activity to estimate the elastic properties of the propagation medium beneath one seismic array (e.g. Shapiro et al, 2005). Seismic interferometry is rooted in the fact that the elastic impulse response between two seismic sensors (the Green›s function) can be reconstructed via the cross-correlation of ambient noise seismograms recorded at the two sites (Wapenaar, 2004). Consequently, passive noise techniques can image and monitor the subsurface without the need for artificial active seismic sources. In this study, we apply such methods to obtain the seismic velocity structure of a glacier's subsurface using different types of passive seismic measurements in different glacier settings (Alps and Greenland). Ice melting and brittle ice failure are responsible for a wide spectrum of seismicity which is recorded on seismometers deployed directly on the ice (Figure 1a), and which includes numerous near-surface crevasse icequakes (10^2-10^3 daily events) and high-frequency (>1Hz) continuous seismic noise generated by meltwater flow (Figure 1b).

An equipartitioned wavefield illuminating the propagation medium in all directions is a pre-requesite for obtaining accurate Green's functions. Such condition can be reached in (i) the presence of equally-distributed sources around the recording network and/or (ii) in strong-scattering media as seismic scatterers act like secondary sources to create a diffuse homogeneized wavefield in all propagation directions. These two scenarios are hardly met in glaciers as (i) microseismicity is often confined to narrow regions such as crevasse zones or other water-filled englacial conduits, and (ii) due to homogeneity of ice, which tends to suppress seismic scattering. This imposes strong limitations on the Green's function convergence from cross-correlations of glacier seismograms (Walter et al, 2015; Preiswerk and Walter, 2018). We address this difficulty by investigating different patterns of glacier seismic wavefields: a favorable distribution of icequakes and noise sources recorded on a dense array on Glacier d'Argentière (France), a dominant noise source constituted by a moulin within a smaller seismic array on the Greenland ice-sheet, and crevasse-generated scattering at Gornergletscher (Switzerland).

Surface meltwater flow through englacial channels produces sustained ambient seismic sources in glacier d'Argentière and thus favorable conditions for Green's function estimates on a regular grid of 98 sensors. From the velocity measurements of reconstructed Rayleigh waves, we invert bed properties and depth profiles, and map seismic anisotropy introduced by crevassing and englacial conduits. In Greenland, advanced signal processing allows to "denoise" the cross-correlation functions and remove the moulin source signature. At Gornergletscher, cross-correlation of icequake coda waves shows evidence for a small yet significant homogeneous wavefield likely due to crevasse scattering. Cross-correlations of optimized coda time-windows enable compution of accurate Green's functions and estimate seismic velocities beneath the array.

This study introduces new processing schemes inspired from crustal seismology to investigate the glaciers' structure from naturally occurring glacier seismicity. It opens ways for monitoring any glacier changes from passive seismic measurements.

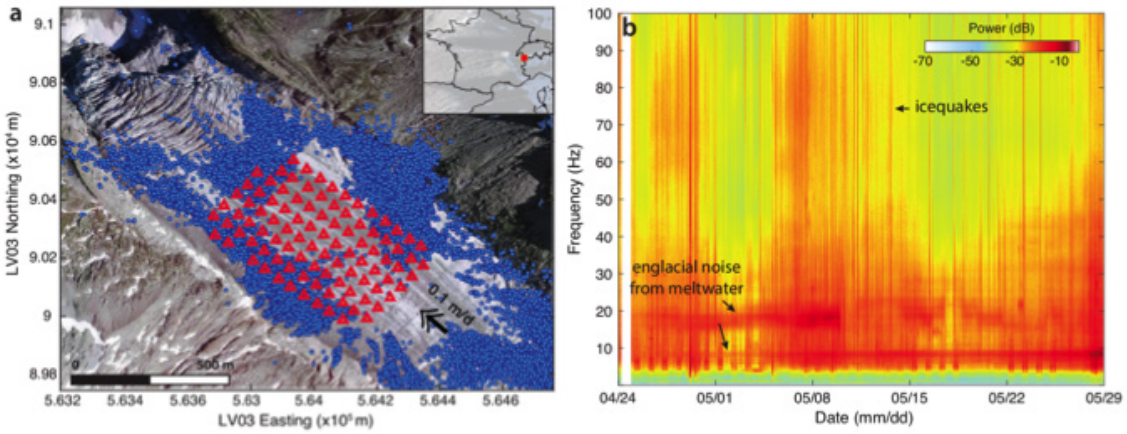


Figure 1. (a) Crevasse icequake locations (blue dots) and seismic stations (red triangles) deployed in Glacier d'Argentière (France). (b) One-month spectrogram of continuous seismic recording in Argentière. About 3000 icequakes related to brittle ice failure are recorded every day. High-frequency (1-20 Hz) ambient noise is recorded continuously over the melting season and attributed to glacier hydrology. Recorded seismicity is used to compute the elastic response of the illuminated medium beneath the array and estimate the glacier subsurface's elastic properties and structure.

REFERENCES

Preiswerk, L. E. and Walter, F. 2018: High-Frequency (>2 Hz) Ambient Seismic Noise on High-Melt Glaciers: Green's Function Estimation and Source Characterization, Journal of Geophysical Research: Earth Surface.

Shapiro, N. M., Campillo, M., Stehly, L., and Ritzwoller, M. H. 2005: High-resolution surface-wave tomography from ambient seismic noise, Science, 307, 1615–1618.

Walter, F., Roux, P., Röösli, C., Lecointre, A., Kilb, D., and Roux, P. 2015: Using glacier seismicity for phase velocity measurements and Green's function retrieval, Geophysical Journal International, 201, 1722–1737.

Wapenaar, K. 2004: Retrieving the elastodynamic Green's function of an arbitrary inhomogeneous medium by cross correlation, Physical review letters, 93, 254 301.

P 11.13

Enhancement of carbonaceous aerosol during the 20th century by anthropogenic activities

Ling Fang[1], Fang Cao[2], M. Schwikowski[1,3] & Theo Jenk[1]

[1]*Laboratory for Environmental Chemistry, Paul Scherrer Institute, CH-5232 Villigen PSI, Switzerland (ling.fang@psi.ch)*
[2]*Yale-NUIST Center on Atmospheric Environmental, Nanjing University of information Science and Technology, 210044 Nanjing, China*
[3]*Oeschger Centre for Climate Change Research, University of Bern, CH-3012 Bern, Switzerland*

Carbonaceous particles which comprise organic carbon (OC) and black carbon (BC; depending on the analytical technique applied also referred to as elemental carbon, EC) are of increasing interest globally because of their influences on the radiative balance of the Earth via direct and indirect effects(Pöschl et al., 2005). However, the magnitude of the anthropogenic activities effect on earth climate is still uncertain, one of reason is due to the lack of knowledge about interaction between biogenic volatile organic compounds (VOC) and the anthropogenic emissions. EC exclusively originates from fossil-fuel combustion and biomass burning, while OC sources are complex. OC can be emitted directly as primary organic aerosol (POA) from biogenic sources, biomass burning and fossil-fuel combustion or can be formed in the atmosphere as secondary organic aerosol (SOA). Recent studies suggest that SOA formation rates are not adequately constrained in current models limiting accurate modeling of their climate effect (Hodzic et al., 2016; Shilling et al., 2013). Furthermore, changes in temperature, land cover and CO_2 have effect on biogenic VOC emissions (Acosta Navarro et al.,2014). Laboratory and field measurement indicate the production of SOA could increase by 20-200% on average due to nitrogen-oxides emission at pristine location (Shrivastava et al., 2019). All these anthropogenic and natural perturbations have effect on carbonaceous aerosol loading which in return could modified the climate.

Biogenic SOA production enhanced by anthropogenic emission have been study in laboratory and chamber experiment for decades. Here we present a 340-year concentration record of carbonaceous particles from Fiescherhorn ice core (Swiss Alps) to prove the enhancement of SOA formation by anthropogenic activities. Carbonaceous aerosol increased by a factor of three at the end of 20th century compare to pre-industrial background. Radiocarbon based source apportionment shows that fossil fuel combustion contributed to 35%. European BVOCs emission increase associate with enhanced SOA production are the main reasons of increase in non-fossil origin carbonaceous aerosol. However, this increase in non-fossil SOA due to anthropogenic activities is not reflected in the emission estimates of OC and NMVOC in the source regions with a mismatch up to one magnitude in the second half of the 20th century. Thus, bottom-up emission inventories seem to heavily underestimate the atmospheric OC loading by not accounting adequately for changes in SOA formation due to climate change and anthropogenic activities, limiting the capacity of current models in estimating aerosol forcing.

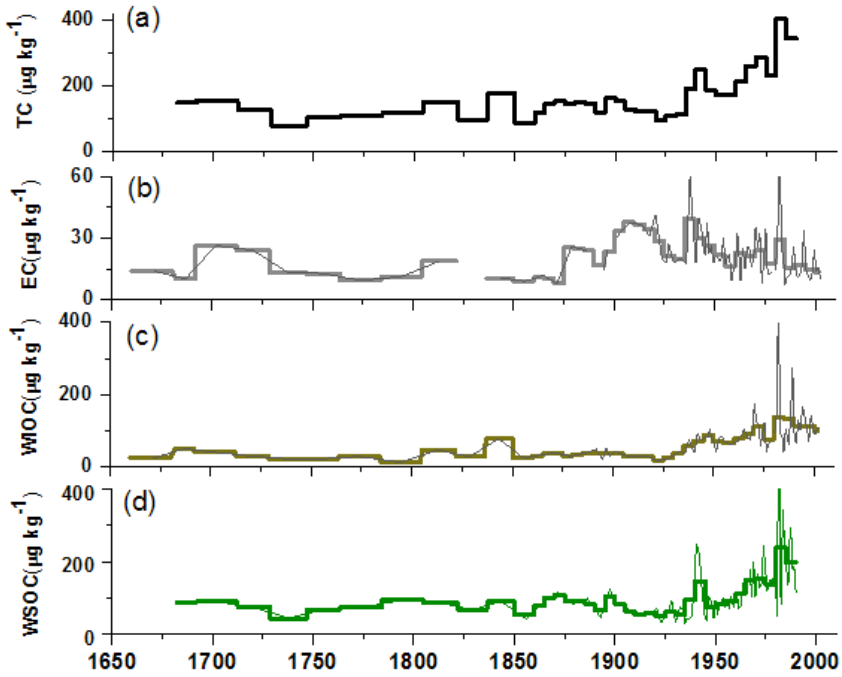


Figure 1. FH concentration record of a) total carbon (TC), b) elemental carbon (EC), c) water-insoluble organic carbon (WIOC) and d) water-soluble organic carbon (WSOC) covering the period 1660–2002. TC is the sum of EC, WIOC and WSOC.

REFERENCES

Acosta Navarro, J.C., S. Smolander, H. Struthers, E. Zorita, A.M. Ekman, J. Kaplan, A. Guenther, A. Arneth, and I. Riipinen, Global emissions of terpenoid VOCs from terrestrial vegetation in the last millennium. Journal of Geophysical Research: Atmospheres, 2014. 119(11): p. 6867-6885.

Hodzic, A., P.S. Kasibhatla, D.S. Jo, C.D. Cappa, J.L. Jimenez, S. Madronich, and R.J. Park, Rethinking the global secondary organic aerosol (SOA) budget: stronger production, faster removal, shorter lifetime. Atmos. Chem. Phys., 2016. 16(12): p. 7917-7941.

Pöschl, U.J.A.C.I.E., Atmospheric aerosols: composition, transformation, climate and health effects. 2005. 44(46): p. 7520-7540.

Shilling, J.E., R.A. Zaveri, J.D. Fast, L. Kleinman, M.L. Alexander, M.R. Canagaratna, E. Fortner, J.M. Hubbe, J.T. Jayne, A. Sedlacek, A. Setyan, S. Springston, D.R. Worsnop, and Q. Zhang, Enhanced SOA formation from mixed anthropogenic and biogenic emissions during the CARES campaign. Atmos. Chem. Phys., 2013. 13(4): p. 2091-2113.

Shrivastava, M., M.O. Andreae, P. Artaxo, H.M. Barbosa, L.K. Berg, J. Brito, J. Ching, R.C. Easter, J. Fan, and J.D.J.N.c. Fast, Urban pollution greatly enhances formation of natural aerosols over the Amazon rainforest. 2019. 10(1): p. 1046.

P 11.14

Permafrost monitoring by reprocessing and repeating historical geophysical measurements

Christian Hauck[1], Christin Hilbich[1], Coline Mollaret[1], Cécile Pellet[1]

[1]*University of Fribourg, Departement of Geosciences, Chemin du Musée 4, CH-1700 Fribourg*

Geophysical methods and especially electrical techniques have been used for permafrost detection and monitoring since more than 50 years. However, only after the development of 2-dimensional tomographic measurement and processing techniques i.e. Electrical Resistivity Tomography (ERT) in the late 1990's, these methods became generally available and were applied on many mountain permafrost sites in the European Alps. Due to the large contrast in electrical resistivity between unfrozen and frozen material, ERT is well suited to detect, but also to monitor frozen ground, and more specifically the ground ice content.

Within the Swiss permafrost network PERMOS, operational ERT measurements are conducted since 2005 for the monitoring of the changes in subsurface ground ice content at five permafrost stations in the Swiss Alps on a yearly basis (Hilbich et al. 2008, PERMOS 2019). A thorough analysis of this data set has shown its high quality and robustness against potential error sources related with the harsh high mountain field conditions and has indicated common climatic trends at all sites, i.e. a decreasing trend of mean specific resistivity (associated with permafrost thawing) since the first measurements in 1999 (Mollaret et al. 2019).

Because of the comparatively large efforts needed for continuous and long-term ERT monitoring, only a very small number of operational ERT monitoring sites exist worldwide in permafrost terrain. However, a much larger number (estimated to be > 500) of permafrost sites with singular ERT measurements exist, many of them published in the scientific literature. These data sets are neither included in a joint database nor have they been analysed in an integrated way. Within a newly GCOS Switzerland-funded project (REP-ERT) we address this important historical data source. Whereas singular ERT data from different permafrost occurrences are not easily comparable due to the local influence of the geologic material on the obtained electrical resistivities, their use as baseline for repeated measurements and subsequent processing and interpretation in a climatic context is highly promising and can be effectuated with low efforts.

In this presentation we will give an overview over existing historical ERT profiles on permafrost terrain and show first results of resistivity changes from repeated ERT data over time spans of more than 10 years from different regions, landforms and subsurface compositions.

REFERENCES

Hilbich, C., Hauck, C., Delaloye, R. & Hoelzle, M. (2008): A geoelectric monitoring network and resistivity-temperature relationships of different mountain permafrost sites in the Swiss Alps. Proceedings Ninth International Conference on Permafrost, Fairbanks, Vol. 1, Kane D.L. and Hinkel K.M. (eds), Institute of Northern Engineering, University of Alaska Fairbanks, 699-704.

Mollaret C, Hilbich C, Pellet C, Flores-Orozco A, Delaloye R, and Hauck C. (2019). Mountain permafrost degradation documented through a network of permanent electrical resistivity tomography sites, The Cryosphere, accepted.

PERMOS 2019. Permafrost in Switzerland 2014/2015 to 2017/2018. Noetzli, J., Pellet, C., and Staub, B. (eds.), Glaciological Report (Permafrost) No. 16-19 of the Cryospheric Commission of the Swiss Academy of Sciences, 104 pp, doi:10.13093/permos-rep-2019-16-19.

P 11.15

Permafrost degradation in Norway documented through repeated geophysical surveys after 10 and 20 years

Christin Hilbich[1], Christian Hauck[1], Cécile Pellet[1], Ketil Isaksen[2], Bernd Etzelmüller[3]

[1]Department of Geosciences, University of Fribourg, Chemin du Musée 4, CH-1700 Fribourg (christin.hilbich@unifr.ch)
[2]Norwegian Meteorological Institute, Oslo, Norway
[3]Department of Geosciences, University of Oslo, Oslo, Norway

The evolution of mountain permafrost in Norway has been studied since more than 20 years. During the European PACE project (Permafrost and Climate in Europe, 1998 – 2001, Harris et al. 2009) a 129 m deep borehole was drilled on Juvvasshoe in Jotunheimen (southern Norway), and as part of the Norwegian CRYOLINK and TSP Norway projects a series of shallower boreholes was drilled at several mountain sites in northern and southern Norway (cf. Christiansen et al. 2010, Farbrot et al. 2013). In addition, at all borehole sites geophysical surveys using refraction seismic tomography (RST) and electrical resistivity tomography (ERT) were conducted to characterise the ground composition (e.g. Hauck et al. 2004, Etzelmüller et al. 2009).

Previous studies already evidenced ongoing permafrost degradation, partly including considerable thickening of the active layer and the formation of taliks (e.g. Farbrot et al. 2013). At the Juvvass site the observed warming trend could also be confirmed with ERT monitoring over a 10 year-period (Isaksen et al. 2011).

In summer 2019, ERT and RST surveys have been repeated at 4 different sites (including 10 individual boreholes and geophysical profiles) in northern Norway (after 11 years) and in southern Norway (after 10 and 20 years). We here present the observed long-term changes in electrical resistivity and seismic p-wave velocity at a) Iskoras/Finnmark and b) Guolasjavri/Troms (Northern Norway) as well as at c) Juvvasshoe/Jotunheimen and d) in the Tron massif (southern Norway) and relate them to the observed borehole temperature evolution. In addition, the change in ground ice content is modelled with the 4-phase model for exemplary profiles (Hauck et al. 2011).

REFERENCES

Christiansen HH, Etzelmüller B, Isaksen K, Juliussen H, Farbrot H, Humlum O, Johansson M, Ingeman-Nielsen T, Kristensen L, Hjort J, Holmlund P, Sannel AB, Sigsgaard C, Åkerman HJ, Foged N, Blikra LH, Pernosky MA, Ødegård RS, 2010. The thermal state of permafrost in the nordic area during the international polar year 2007–2009. Permafrost and Periglacial Processes 21: 156-181. doi:10.1002/ppp.687

Etzelmueller B, Hauck C, Hilbich C, Isaksen K, Farbrot H and Lewkowicz AG, 2009. Geophysical sounding and thermal monitoring in northern Norway –TSP-Norway. Geophysical Research Abstracts, Vol. 11, EGU2009-3585.

Farbrot H, Isaksen K, Etzelmüller B, Gisnås K 2013. Ground Thermal Regime and Permafrost Distribution under a Changing Climate in Northern Norway. Permafrost and Periglacial Processes 24(1):20-38. https://doi.org/10.1002/ppp.1763

Isaksen K, Ødegård RS, Etzelmüller B, Hilbich C, Hauck C, Farbrot H, Eiken T, Hygen HO, Hipp T 2011. Degrading mountain permafrost in southern Norway - spatial and temporal variability of mean ground temperatures 1999-2009. Permafrost and Periglacial Processes 22(4):361-377, doi 10.1002/ppp.728.

Harris C, Arenson L, Christiansen H, Etzelmüller B, Frauenfelder R, Gruber S, Haeberli W, Hauck C, Hoelzle M, Humlum O, Isaksen K, Kääb A, Kern-Lütschg M, Lehning M, Matsuoka N, Murton J, Nötzli J, Phillips M, Ross N, Seppälä M, Springman S, Vonder Mühll D 2009. Permafrost and climate in Europe: monitoring and modelling thermal, geomorphological and geotechnical responses. Earth Science Reviews 92(3-4): 117-171.

Hauck C, Isaksen K, Vonder Mühll D, Sollid JL 2004. Geophysical surveys designed to delineate the altitudinal limit of mountain permafrost: an example from Jotunheimen, Norway. Permafrost and Periglacial Processes 15(3):191-205. https://doi.org/10.1002/ppp.493

Hauck C, Böttcher M & Maurer H. 2011. A new model for estimating subsurface ice content based on combined electrical and seismic data sets. The Cryosphere 5(2): 453-468.← use the «Abstract_References» pre_defined style

P 11.16

Thermal effects of natural air convection in the active layer of rock glaciers

Jonas Wicky[1], Christian Hauck[1]

[1]Alpine Cryosphere and Geomorphology Group, Department of Geosciences, University of Fribourg, Chemin du Musée 4, 1700 Fribourg (jonas.wicky@unifr.ch)

The thermal regime of alpine permafrost is complex and not fully understood yet, among other things, because of the heterogeneity of the material composition. The main governing processes are heat conduction, radiation and heat convection. Heat convection can be either natural convection or forced convection, which is often also referred as advection. In our study, we focus on natural convection of air within the active layer of rock glaciers. In permafrost modelling air convection is often neglected or parametrized (eg. Pruessner et al., 2018; Scherler et al., 2014), but it has been observed and described in field based studies (Hanson and Hoelzle, 2004; Panz, 2006). We solve a heat conduction equation coupled with Darcy's law in COMSOL Multiphysics over a 2D grid to explicitly model air convection and thus be able to assess its effects on the ground thermal regime. Our model is forced and validated with measured temperature data from PERMOS (2019) at various field sites in the Swiss Alps.

Our long-term simulations show that the ground permeability is the most sensitive parameter governing air convection. On field sites with a high ground permeability (order of magnitude 10^6 m^2), convection plays a crucial role and is required to model measured borehole temperatures. Sites with a lower ground permeability show less sensitivity to air convection. The simulations show an onset of natural convection at the critical Rayleigh number as theoretically expected. Our results also confirm that under a warming climate the coarse blocky layer has the potential to delay permafrost degradation on certain landforms. The internal convective air circulation and not only the low conductivity of air in the coarse blocky surface layer leads to cooler ground temperatures.

REFERENCES

Hanson, S., and Hoelzle, M. (2004). The thermal regime of the active layer at the Murtèl rock glacier based on data from 2002. Permafr. Periglac. Process. 15, 273–282.

Panz, M. (2006). Analyse von Austauschprozessen in der Auftauschicht des Blockgletschers Murtèl-Corvatsch, Oberengadin. Master thesis (unpubl.). Ruhr Universität.

PERMOS (2019). PERMOS Database. Fribourg and Davos, Switzerland: Swiss Permafrost Monitoring Network doi:DOI:10.13093/permos-2019-01.

Pruessner, L., Phillips, M., Farinotti, D., Hoelzle, M., and Lehning, M. (2018). Near-surface ventilation as a key for modeling the thermal regime of coarse blocky rock glaciers. Permafr. Periglac. Process. 29, 152–163.

Scherler, M., Schneider, S., Hoelzle, M., and Hauck, C. (2014). A two-sided approach to estimate heat transfer processes within the active layer of the Murtèl-Corvatsch rock glacier. Earth Surf. Dyn. 2, 141–154.

P 11.17

Modelling rock glacier thermal regime using GERM: first results and comparison to Snowpack

Luisa Pruessner[1,2], Marcia Phillips[3], Matthias Huss[1] & Daniel Farinotti[1,2]

[1]*Laboratory of Hydraulics, Hydrology and Glaciology (VAW), ETH Zurich, Zurich, Switzerland (pruessner@vaw.baug.ethz.ch)*
[2]*Swiss Federal Institute for Forest, Snow and Landscape Research WSL, Birmensdorf, Switzerland*
[3]*WSL, Swiss Federal Institute for Snow and Avalanche Research, SLF, Flüelastrasse 11, CH-7260 Davos Dorf, Switzerland*

Rock glaciers have recently come more into focus as potential water sources due to the diminishing of clean-ice glaciers in Alpine regions (Brighenti et al. 2019). In order to quantify the runoff contribution from rock glaciers it is necessary to model their thermal regime and ice content evolution at the catchment scale.

The distributed Glacier Evolution and Runoff Model (GERM; Huss et al., 2008; Farinotti et al., 2012) has been extended to allow for the inclusion of spatio-temporal changes in permafrost and, hence, corresponding changes in the ice content of rock glaciers. GERM is an empirical model used for modelling runoff from glaciated basins at the catchment scale and above. High mountain catchments often contain rock glaciers, which need to be treated differently due to their unique characteristics. The coarse blocky surface layer characteristic of rock glaciers allows for air flow and thus different modes of heat transport than purely conductive. Previous modelling work done with the physics-based Snowpack model (Pruessner et al., 2018) has shown that ventilation is necessary to reproduce the measured low winter temperatures, thus this effect is included in a parameterised form in GERM. The model solves the conduction-diffusion equation using a Crank-Nicholson scheme; phase changes and water transport are accounted for. The aim here is to have a simple model that can readily be applied to the larger scale while still retaining the important processes.

Both GERM and Snowpack are run at three sites in the Swiss Alps: Murtèl-Corvatsch, Schafberg and Ritigraben. These sites were chosen because good borehole temperature measurements were available for a period of more than ten years. The results of the two models were then intercompared and validated using direct ground temperature measurements at the point scale. While GERM is less complex than Snowpack it is still able to reproduce the main features of the temperature timeseries (Fig. 1).

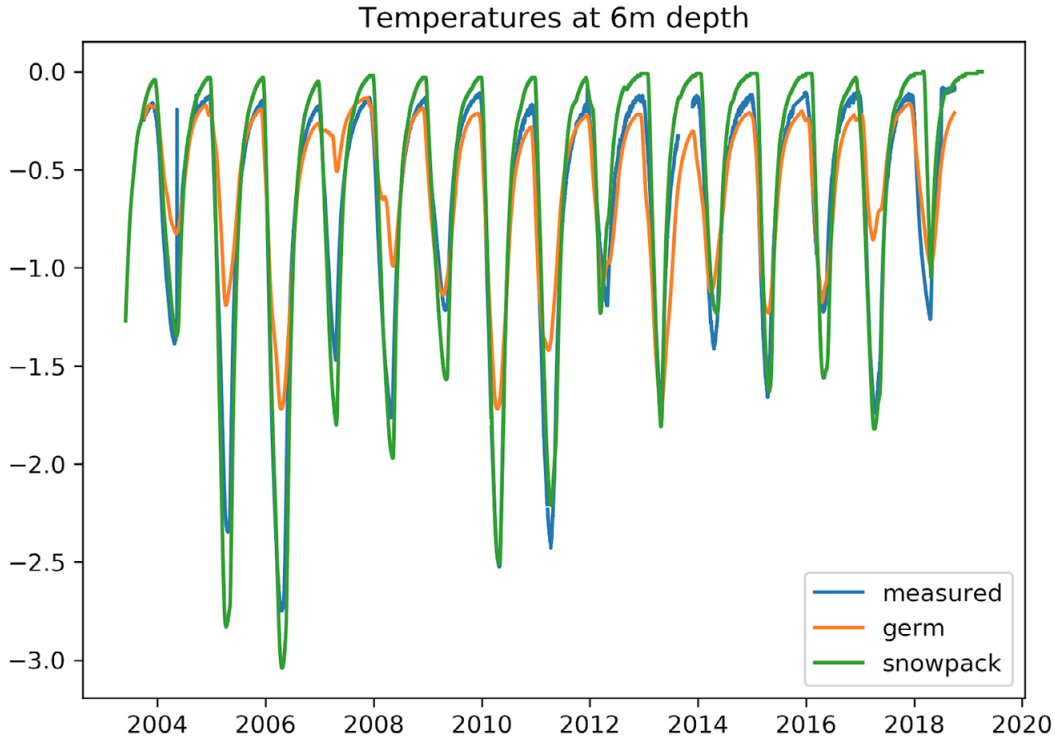


Figure 1. Modeled and measured ground temperatures at the Ritigraben site at approx. 6m depth. Modeled temperatures have a normalised root mean square error of 0.144 K (GERM) and 0.135 K (Snowpack).

REFERENCES

Brighenti, S., Tolotti, M., Bruno, MC., et al. 2019: After the peak water: the increasing influence of rock glaciers on alpine river systems. Hydrological Processes, 1– 20.

Huss, M., Farinotti, D., Bauder, A., & Funk, M. 2008: Modelling runoff from highly glacierized alpine drainage basins in a changing climate. Hydrological Processes, 22:3888–3902.

Farinotti, D., Usselmann, S., Huss, M., Bauder, A., & Funk, M. 2012: Runoff evolution in the Swiss Alps: projections for selected high-alpine catchments based on ENSEMBLES scenarios. Hydrological Processes, 26:1909–1924.

Pruessner, L., Phillips, M., Farinotti, D., Hoelzle, M. & Lehning, M. 2018: Near-surface ventilation as a key for modeling the thermal regime of coarse blocky rock glaciers. Permafrost and Periglacial Processes, 29: 152– 163

P 11.18

Glacier forefields in mountain permafrost environments (Swiss Alps)

Julie Wee[1] & Reynald Delaloye[1]

[1]*Department of Geosciences, University of Fribourg, Ch. du Musée 4, CH-1700 Fribourg (julie.wee@unifr.ch)*

Repeated sequences of glacial and interglacial have strongly orchestrated multi-phased geomorphic processes in glacier forefields in permafrost environments, and contributed to their present-day morphology and dynamical behaviour (Maisch et *al*., 2003). In the Alps, glaciers and frozen landforms have coexisted and episodiacally interacted throughout the entire Holocene. In the context of this study, the focus is attributed to the Little Ice Age (LIA), the last important glacial period, as it has a direct influence on today's morphodynamic processes in glacier forefields. Indeed, LIA glacier forefields located within the belt of discontinuous permaftrost are complex systems sitting astride the glacial, paraglacial and periglacial research frontier. These recently deglaciated environments have been characterized as transient systems pursuing a state of equilibrium by adjusting to non-glacial conditions, and are therefore subject to intense geomorphological activity, especially under the current conditions of a warming climate (Lane et *al*., 2016; Bosson et *al*., 2015). Present-day landforms existing in these systems are legacies of the interrelations between glacial and permafrost-driven morphodynamics and are therefore precious proxies for the understanding of the spatio-temporal evolution of permafrost in glacier forefield systems since the LIA.

Specifically, this project aims at

- inventorying the occurrence of mass-wasting processes of glacitectonized (potentially) frozen sediments in LIA glacier forefields within the belt of mountain permafrost from the western to the eastern Swiss Alps;
- assessing the spatio-temporal dynamical evolution (decadal time frame) of selected glacier forefields in mountain permafrost environments, and specifically of the associated mass-wasting glacitectonized frozen sediments;
- providing in-situ data on the current state of permafrost/ground ice through geophysical prospection and to assess the evolution of permafrost/ground ice by repeating historical geophysical measurements (20-year interval);
- compiling, analysing and integrating existing datasets of more than 20-year of permafrost monitoring in glacier forefields (ground surface temperature, kinematics and geophysical data).

The combination of a complete inventory of permafrost-driven mass-wasting processes in glacier forefields in mountain permafrost environments, a thorough analysis of current and historical aerial images (and remotely sensed data, e.g. InSAR), and the repetition of existing geophysical surveys will allow a detailed assessment of the processes behind the spatio-temporal evolution of glacier forefields in mountain permafrost environments.

REFERENCES

Bosson, J.-B., Lambiel, C., Deline, P., Bodin, X., Schoeneich, P., Baron, L. and Gardent, M. (2015). The influence of ground ice distribution on geomorphic dynamics since the Little Ice Age in proglacial areas of two cirque glacier systems. Earth Surface Processes and Landforms, 40, 666-680.

Lane, S.N., Bakker, M., Gabbud, C., Micheletti, N., Saugy, J.N., 2016. Sediment export, transient landscape response and catchment-scale connectivity following rapid climate warming and Alpine glacier recession. Geomorphology 277, 210–227.

Maisch, M., Haeberli, W., Frauenfelder, R. and Kääb, A. (2003). Lateglacial and Holocene evolution of glaciers and permafrost in the Val Muragl, Upper Engadin, Swiss Alps. Swets & Zeitlinger, 717-722.

P 11.19

Improving temporal and spatial estimates of solid precipitation and accumulation in high mountain regions

Matteo Guidicelli[1], Rebecca Gugerli[1] & Nadine Salzmann[1]

[1]Departement of Geosciences, University of Fribourg, Chemin du Musée 4, CH-1700 Fribourg (matteo.guidicelli@unifr.ch)

The scarcity and the considerable uncertainties of precipitation observation and estimation in high mountain regions are a major drawback for enhancing our understanding of climatic-cryospheric processes and limits the reduction of uncertainties in related climate impact studies.

We aim at tackling this research need by combining methods from atmospheric and cryospheric sciences. Here, we present a concept and first results for a study in the Swiss Alps. Based on weather radar (Rad4Alp network of MeteoSwiss) and ground measurements from two swiss glaciers (glacier de la Plaine Morte and Findelengletscher), a spatially and temporally highly resolved estimate of solid precipitation is produced. The distinction between solid and liquid precipitation is performed establishing a linear relationship between 0°C and a temperature threshold, as well as applying an hydrometeor classification based on dual-polarization characteristics (Besic et al., 2016). Available standard mass balance observations and temporally highly resolved measurements obtained through a cosmic ray sensor (Gugerli et al., 2019) are used to validate the model.

Moreover, solid precipitation estimations of the NWP model COSMO-1 are analyzed too. The finer topography of COSMO-1 does not exclude erroneous elevation, causing model uncertainties. Therefore, COSMO-1 estimations are post-processed, combining them with very high resolution topographical parameters and other auxiliary meteorological variables showing correlations with the error of COSMO-1 (e.g. relative humidity, wind direction and wind speed). Advanced supervised techniques of machine learning are exploited in order to model non-linearities. The highly resolved product built in the first step is used as ground truth data.

Finally, a similar approach involving regional and global climate models is also applied to distribute the data in space and time and to asses the related future evolution and impacts for the environment and societies.

REFERENCES

Besic, N., Figueras I Ventura, J., Grazioli, J., Gabella, M., Germann, U. et al.: Hydrometeor classification through statistical clustering of polarimetric radar measurements: a semi-supervised approach, Atmospheric Measurement Techniques. Vol. 9, num. 9, p. 4425-4445. DOI: 10.5194/amt-9-4425-2016.

Gugerli, R., Salzmann, N., Huss, M., and Desilets, D.: Evaluating continuous and autonomous snow water equivalent measurements by a cosmic ray sensor on a Swiss glacier, The Cryosphere Discuss., https://doi.org/10.5194/tc-2019-106, in review, 2019.

P 11.20

Continuous and autonomous snow water equivalent measurements by a cosmic ray sensor on a Swiss glacier

Rebecca Gugerli[1], Nadine Salzmann[1], Matthias Huss[1/ 2] and Darin Desilets[3]

[1]*Department of Geosciences, University of Fribourg, Chemin de Musée 4, 1700 Fribourg, Switzerland (rebecca.gugerli@unifr.ch)*
[2]*Laboratory of Hydraulics, Hydrology and Glaciology (VAW), Swiss Federal Institute of Zurich, Hönggerbergring 26, 8093 Zürich, Switzerland*
[3]*Hydroinnova LLC, Albuquerque, NM, USA*

The annual amount of snow accumulation in high mountain regions is a key parameter in many research fields related to climate change impacts and adaptation, or hydrology and glaciology. Therefore, it is important to have reliable and continuous snow water equivalent (SWE) measurements. However, such measurements are challenging in high mountain regions because of the harsh environment with cold and windy conditions, the remoteness and the complex topography.

The cosmic ray sensor (CRS) is a device that estimates SWE continuously through cosmic ray neutron fluxes. We placed this sensor directly on the glacier surface (below the snow pack) of the Glacier de la Plaine Morte (Switzerland) where it has been measuring since October 2016. To validate the CRS estimates of SWE, we use 15 manual field measurements (snow pits, snow probings) obtained during three winter seasons (2016-2019). On average, the CRS overestimates the manual measurements by +2%±11% (Fig.1 a,d). A sonic ranging sensor (SR) that was installed next to the CRS provides continuous snow depth (SD) measurements. These are on average -1%±5% lower than manual measurements (Fig. 1b,d). From the daily SD and SWE observations, we calculate the bulk snow density which overestimates manual observations by +1%±8% on average (Fig.1c,d).

With this measurement setup, we were able to analyse the evolution of snow density over three winter seasons (Fig.2). In Fig.2, we see that the snow density has a similar evolution for all three distinct winter seasons. The accumulation period is characterised by the lowest densities and snowfall events results first in a decrease of snow depth followed by an increase. When the seasonal maximum in SD is reached, the snow pack enters a period of densification before ablation begins. During the ablation phase, SWE and SD decrease continuously while the snow density remains almost constant.

We conclude that the CRS is a suitable measurement device for continuous observation of snow accumulation in high mountain regions. The CRS requires no flat surface, no signal reception from satellites or a fixed location as many other similar and promising devices do. Validated by our field measurements, it also shows a good agreement. However, several uncertainties in the data processing of the CRS data remain which need further investigations.

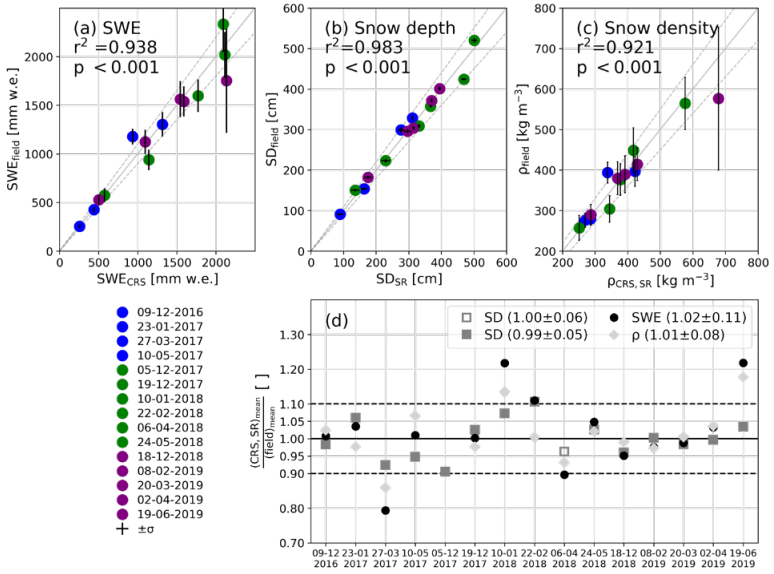


Figure 1. Manual and autonomous measurements for SWE (a), SD (b) and snow density (ρ, c). (d) shows the over- and underestimations of the individual field campaigns for SD (squares), SWE (dots) and snow density (diamonds).

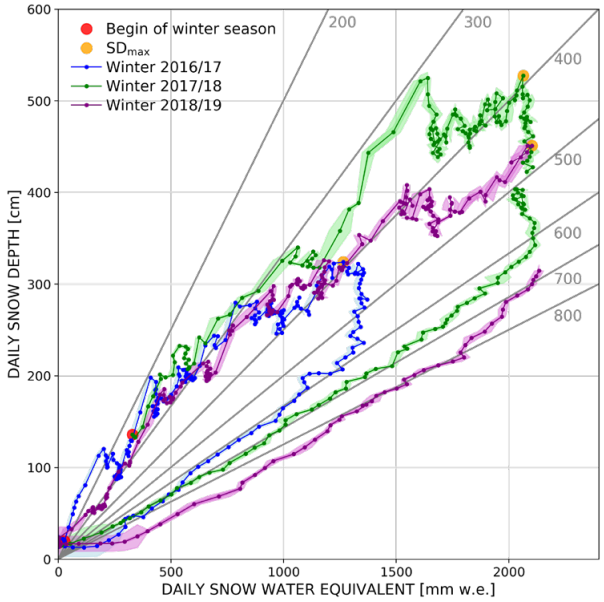


Figure 2. Daily SD and SWE for the winter seasons of 2016-17 (blue), 2017-18 (green) and 2018-19 (purple). Orange dots represent the seasonal maxima of SD.

REFERENCES

Gugerli, R., Salzmann, N., Huss, M., and Desilets, D. (2019) Evaluating continuous and autonomous snow water equivalent measurements by a cosmic ray sensor on a Swiss glacier. The Cryosphere Discuss., in review.

Howat, I.M., De La Peña, S., Desilets, D., and Womack, G. (2018) Autonomous ice sheet surface mass balance measurements from cosmic rays, The Cryosphere, 12, 2099-2108.

Schattan, P., Baroni, G., Oswald, S.E., Schöber, J., Fey, C., Kormann, C., Huttenlau, M., and Achleitner, S.: (2017). Continuous monitoring of snowpack dynamics in alpine terrain by aboveground neutron sensing. Water Resources Research, 53, 3615-3634

12. Hydrology, Limnology and Hydrogeology

Peter Molnar, Michael Doering, Tobias Jonas, Sandra Pool, Michael Sinreich, Sanja Hosi

Swiss Society for Hydrology and Limnology SGHL
Swiss Hydrological Commission CHy
Swiss Hydrogeological Society SGH

TALKS:

12.1 Arnoux M., Cochand F., Hunkeler D., Brunner B., Schaefli B., Jonas T.: Groundwater and discharge regime evolution with climate change in Alpine catchments

12.2 Beria H., Larsen J.R., Ceperley N.C., Michelon A., Schaefli B.: Increased snowpack ephemerality augments groundwater recharge in the mid-elevation belt of the Swiss Alps

12.3 Botter M., Burlando P., Fatichi S.: Solute generation and C-Q relations: is solute input frequency or depth of solute generation the key-player?

12.4 Cochand F., Hunkeler D., Sinreich M., Brunner P.: Modelling recharge by precipitation at the Swiss scale

12.5 Doda T., Ramón C., Ulloa H., Wüest A., Bouffard D.: Density currents induced by differential cooling in a small temperate lake: seasonality in their occurrence and magnitude

12.6 Kiewiet L., Wicki A., van Meerveld H.J., Seibert J.: Explaining shallow groundwater concentrations with surface and bedrock topography, and soil and bedrock composition

12.7 Mastrotheodoros T., Pappas C., Molnar P., Burlando P., Manoli G., Fatichi S.: Dissecting the water tower of Europe: a high-resolution ecohydrological modelling of the European Alps

12.8 Mettra F., Blanckaert K., Lemmin U., Barry D.A.: Sediment connectivity in the Rhône Basin: from an isolated thunderstorm at Illgraben to a turbidity current in deep Lake Geneva

12.9 Michel A., Brauchli T., Wever N., Epting J., Lehning M., Huwald H.: Stream Temperature Evolution in Switzerland simulated with downscaled CH2018 Climate Change Scenarios

12.10 Perego R., Pera S., Bulgheroni M., Boaga J., Galgaro A.: Hydro/thermogeological state of the Maggia river delta: potential shallow geothermal energy implications

12.11 Weatherl R., Salgado M.H., Schirmer M.: Identifying sources and processes impacting groundwater recharge in the human environment

12.12 Wirth S.B., Bouffard D., Cojean A., Zopfi J.: Giant pockmarks in Lake Neuchatel, Switzerland: new multi-proxy evidence for lacustrine groundwater discharge

POSTERS:

P 12.1 Brauchli T., Michel A., Lehning M., Schaefli B., Huwald H.: Stream temperature and discharge evolution over the last 50 years in Switzerland

P 12.2 Cotte G., Vennemann T.: Does the Rhône River fertilise Lake Geneva ? (in the context of its re-oligotrophisation)

P 12.3 Epting J., Huggenberger P.: Thermal potential of urban tunnel infrastructures in unconsolidated rock groundwater resources

P 12.4 Scheidler S., Dresmann H., Huggenberger P., Epting J.: Geothermal use of an Alpine aquifer – Davos pilot study

P 12.5 Etter S., Stobl B., Seibert J., Meerveld v.H.J. (Ilja): Accuracy of citizen science water level class observations

P 12.6 Jeannin P.: KMC : a comparison of various models for assessing karst hydrology

P 12.7 Li Z., Sun H., Zhang Y., Sibatov R.T.: Continuous time random walk model for non-uniform bed-load transport

P 12.8 Peel M., Musy S., Popp A., Alvarez P.A., Purtschert R., Hunkeler D., Brunner P.: Getting the most out of environmental tracers in complex alluvial systems

P 12.9 Peleg N., Molnar P.: Temperature effects on extreme rainfall modify catchment response

P 12.10 Pool S., Frances F., Garcia-Prats A., Puertes C., Pulido-Velazquez M., Sanchis-Ibor C., Schirmer M., Yang H., Jimenez-Martinez J.: Modelling the effect of irrigation modernization on groundwater recharge

P 12.11 Popp A.L., Pardo-Alvarez A., Schilling O.S., Musy S., Scheidegger A., Peel M., Purtschert R., Hunkeler D., Brunner P., Kipfer R.: Elucidating stream-groundwater interactions using real-time, in situ noble gas analysis and numerical modeling

P 12.12 Saurwein D.: Towards decadal hydro-glaciological forecasts for the hydropower sector

P 12.13 Tu L., Zander P., Szidat S., Vogel H., Grosjean M.: The influence of trophic history and lake mixing regime on long-term phosphorus fractions retention in sediments of deep, eutrophic lakes: a case study from Lake Burgäschi, Switzerland

P 12.14 Wicki A., Stähli M., Hauck C., Lehmann P.: Soil hydrological monitoring for regional landslide early warning

12.1

Groundwater and discharge regime evolution with climate change in Alpine catchments

Marie Arnoux[1], Fabien Cochand[1], Daniel Hunkeler[1], Philip Brunner[1], Bettina Schaefli[2] & Tobias Jonas[3]

[1]The Centre for Hydrogeology and Geothermics of University of Neuchâtel, University of Neuchâtel, Rue Emile-Argand 11, CH-2000 Neuchâtel (marie.arnoux@unine.ch)
[2]Institute of Earth Surface Dynamics, University of Lausanne, CH-1015 Lausanne
[3]Institute for Snow and Avalanche Research, Flüelastrasse 11, CH-7260 Davos Dorf

The hydrology of alpine areas is highly sensitive to climate change, especially on a seasonal time scale. Recent studies suggest a general decrease in snow accumulation and a shift of snow-influenced discharge event towards earlier periods of the year. Depending on future scenarios, these snow-cover changes can be combined with warm and dry summers. The associated seasonal magnitude of discharge regime change is most likely influenced by groundwater storage. However, hydrogeological data are very limited in these areas, mainly because of the difficulty to develop monitoring networks in Alpine Terrain. The dynamics of alpine groundwater processes and their influence on catchment response to climate change remains therefore poorly understood. In fact, the role of groundwater is rarely considered explicitly in hydrological studies.

In order to highlight the influence of groundwater storage on discharge regime evolution with climate change, we run recent climate change scenarios for Switzerland (CH2018) with hydrological and hydrogeological models for several alpine catchments across Switzerland. The results provide insights on how groundwater and discharge dynamics are affected by climate change in alpine areas. Winter low flows will move toward summer low flows in the future. However, the intensity of summer low flows will be buffered by the dynamic groundwater storage in the catchments and therefore the combination of their unconsolidated aquifer units. These dynamics have implications for water management at larger scale which should be considered in the future, as only some alpine rivers will continue to sustain low flow periods in downstream valleys.

12.2

Increased snowpack ephemerality augments groundwater recharge in the mid-elevation belt of the Swiss Alps

Harsh Beria[1], Joshua R. Larsen[2,3], Natalie C. Ceperley[1], Anthony Michelon[1] & Bettina Schaefli[1,4]

[1]Institute of Earth Surface Dynamics (IDYST), University of Lausanne (UNIL), Switzerland (harsh.beria@unil.ch)
[2]School of Geography, Earth and Environmental Sciences, University of Birmingham, United Kingdom
[3]The Birmingham Institute of Forest Research (BIFoR), University of Birmingham, United Kingdom
[4]Now at, Institute of Geography, University of Bern

A warming climate brings with it changes in the spatiotemporal distribution of precipitation with significant implications for water resources availability. Higher air temperatures, a direct consequence of global warming, will result in greater proportion of precipitation falling as liquid rain than as snow. Snowmelt has been previously shown to be more efficient at recharging groundwater aquifers than an equivalent amount of rainfall. Lower amount of future snowfall along with increased snow cover intermittency increases uncertainty in groundwater recharge patterns in mountainous parts of the world.

Using a combination of stable water isotopes and baseflow recession analysis based on streamflow measurements spread across 39 headwater catchments in Switzerland, we show that ephemeral snowpacks that accumulate and melt during winters contribute disproportionately more to groundwater recharge than seasonal snowpacks that accumulate during winters and melt over the ensuing spring and summer period. We also identify an elevational divide currently existing at 1500 m a.s.l. in Switzerland, separating catchments dominated by ephemeral and seasonal snowpacks. This divide will move higher up to around 2000 m a.s.l. with a 2.5°C increase in air temperature, resulting in higher groundwater recharge in catchments between 1500 – 2000 m a.s.l. The increased winter recharge will come at a cost of lower summer flows, making summer baseflow more dependent on summer rainfall, increasing the likelihood of mid-summer droughts. Our study has important implications for changes in water resources availability in the Swiss Alps that are likely transferable to other mountainous regions in the world.

12.3

Solute generation and C-Q relations: is solute input frequency or depth of solute generation the key-player?

Martina Botter[1], Paolo Burlando[1], Simone Fatichi[1]

[1]*Institute of Environmental Engineering, ETH Zurich, Zurich, Switzerland (botter@ifu.baug.ethz.ch)*

Understanding how different solutes are exported and how their concentrations change in rivers is an open question for catchment hydrology, which is particularly challenging due to the general lack of solutes input data.

In order to gain information on the role of the solute generation in the export dynamics, this study collects and compares publicly available or published solutes concentrations data at the outlet of 585 catchments across 9 countries around the world. The magnitude of the concentrations of different solutes (Ca^{2+}, Mg^{2+}, K^{+}, Na^{+}, Cl^{-}, NO_3, DOC and DRP) is compared and its spatial variability across catchment and temporal variability within catchments is quantified by means of the metrics CV-time and CV-space. The solute behavior, defined by the b-exponent of the C-Q relation $C = aQ^b$, which can determine chemostatioc ($b \approx 0$), diluting ($b<0$) or enriching ($b>0$) dynamics, is also investigated. Evidence in the data analysis suggests that both the timing and the vertical distribution of the solute supply play a role in determining the dynamics of the solute concentrations at the catchment outlet.

The concentrations of exogenous solutes (i.e. solutes often linked to anthropogenic sources such as Na^{+}, Cl^{-}, NO_3 and DRP) exhibit not only higher variability in time than concentrations of geogenic solutes (i.e., Ca^{2+}, Mg^{2+}, K^{+}) and DOC, but also more variable behavior ranging between highly diluting to enriching for NO_3 and DRP and severely diluting for Na^{+}, Cl^{-}. When combining the CV-time with the b-exponent, two clear clusters emerge. One group of solutes with low temporal variability and pronounced dilution behavior, including the geogenic solutes (Ca^{2+}, Mg^{2+}, K^{+}) and the salt species (Na^{+}, Cl^{-}), and another group including nutrients (NO_3, DRP and DOC) with larger and highly variable CV-time and nearly zero or slightly positive b-exponent. We associate the higher variability in time to a more sporadic rather than continuous input typical of the exogenous solute applications and ascribe the different b-exponent behaviors mainly to the vertical distribution of the solute supply. Based on this evidence, we design numerical experiments and run simulations with a tracer-aided distributed hydrological model to test the relative contribution of these two factors as determinats of the solute behavior.

The results of the numerical simulations represent well the various CV-time/b-exponent relations observed in nature and therefore allow to corroborate our hypotheses. Numerical experiments prove that decreasing the depth of solute generation reduces the values of b, from chemostatic to strongly diluting. Instead, enriching behavior is obtained either assigning a threshold on soil moisture above which the solute export is activated or introducing residence-time dependant solute degradation in the groundwater when the solute enters the catchment through deposition. These results support the hypothesis that the vertical distribution of the solute supply drives the C-Q relations.

In summary, while the input frequency has an impact on CV-time and adds some uncertainty to C-Q relations, the vertical distribution of solute generation plays the key-role in the determination of the solute behavior for highly diluting (Na^{+}, Cl^{-}), weakly diluting (Ca^{2+}, Mg^{2+}, K^{+}) and enriching solutes (e.g., DOC).

12.4

Modelling recharge by precipitation at the Swiss scale

Fabien Cochand[1], Daniel Hunkeler[1], Michael Sinreich[2] & Philip Brunner[1]

[1]The Centre for Hydrogeology and Geothermics of University of Neuchâtel (CHYN), rue Emile-Argand 11, CH-2000 Neuchâtel (fabien.cochand@unine.ch)
[2]Federal Office for the Environment FOEN, Hydrology Division, Hydrogeology Section, Papiermühlestr. 172, CH-3063 Ittigen

Groundwater recharge by precipitation is one of the key components of the groundwater water balance. It is therefore crucial to establish reliable estimations of recharge whenever a hydrogeological study is carried out. However, recharge is often roughly estimated or used as a calibration parameter to close the water balance. This study presents a novel methodology for estimating recharge for Switzerland at a fine resolution (125mx125m).

From a physical point of view, recharge occurs via infiltration of a fraction of precipitation through variably-saturated vertical flow. Infiltration is reduced by evapotranspiration (ET) processes through the soil before contributing to the saturated zone (the aquifer). These processes have been studied for a long time with lysimeters, and can be simulated using numerical simulators which couple the Richards and surface flow equations. We developed “Numerical lysimeters” to estimate recharge using HydroGeoSphere (HGS, Aquanty (2017)). The HGS model allows for the fully-coupled simulation of surface flow, subsurface variably-saturated flow and ET.

Figure 1a shows the conceptual model and the required data for simulating recharge. The soil is represented by a collum on top of which a positive flux representing precipitation and a negative flux representing potential evapotranspiration (PET) are applied. The surface allows for the consideration of different surface properties and slopes that reflect land-use and topography. Different soil properties (such as hydraulic conductivity or van Genuchten parameters) and various ET are also considered to reproduce different unsaturated flow conditions, rainfall interception and ET processes. At the bottom of the collum, a seepage boundary condition (BC) is set and the vertical flow reaching this BC is considered to represent groundwater recharge.

To employ the approach at a Swiss scale, major assumptions have to be made due to limited availability of data. Alpine regions are excluded because of the lack of data. To keep the computations trackable, Switzerland is divided in 267 areas, each being attributed to a set of climatic parameters (precipitation and temperature). The identification of these regions is based on statistics of the meteoswiss grid-data products (MeteoSwiss, 2013). For each identified area, daily rainfall and temperature (converted in PET) are extracted, again using grid-data products from the period 1999 - 2018. Subsequnetly, each climatic area is spatially discretized in 125x125m cells and a HGS lysimeter model is created for each cell. This resolution corresponds to the coarsest resolution of the available data, i.e. the soil properties data (FOAG, 2015). A total of 20’025 models were run and the results were post-processed to obtain daily, monthly or annual mean recharge rates (figure 1b) at the Swiss scale. Finally, model results are validated using lysimeter observations and other recharge estimation studies.

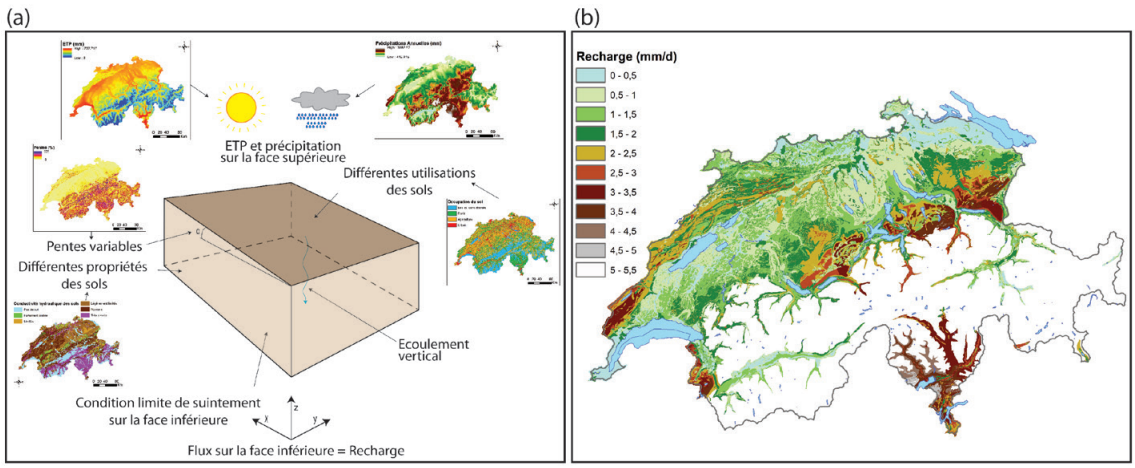


Figure 1: a) Numerical lysimeter using HGS and b) simulated annual mean recharge

REFERENCES

Aquanty: HydroGeoSphere, a three-dimensional numerical model describing fully- integrated subsurface and surface flow and solute transport. Waterloo, ON, Canada., 2017.
FOAG: Digital soil suitability map of Switzerland - Permeability, Federal Office for Agriculture (FOAG), 2015.
MeteoSwiss: MeteoSwiss Grid-Data Products, Federal Office of Meteorology and Climatology MeteoSwiss, 2013.

12.5

Density currents induced by differential cooling in a small temperate lake: seasonality in their occurrence and magnitude

Tomy Doda[1,2], Cintia Ramón[1], Hugo N. Ulloa[2], Alfred Wüest[1,2] & Damien Bouffard[1]

[1]Eawag, Swiss Federal Institute of Aquatic Science and Technology, Surface Waters - Research and Management, Seestrasse 79, CH-6047 Kastanienbaum (tomy.doda@eawag.ch)
[2]Physics of Aquatic Systems Laboratory, École Polytechnique Fédérale de Lausanne, Station 2, CH-1015 Lausanne

Differential cooling occurs in the littoral region of lakes, during calm and cold nights in summer and continuously in fall/winter. For uniform heat loss over the lake surface, shallower regions cool faster than deeper regions leading to horizontal density gradients. Nearshore waters become negatively buoyant and start to plunge creating a cold downslope density current that can reach the pelagic zone (Monismith et al. 1990).

This cross-shore flow, also referred to as “thermal siphon”, has the potential to transport biogeochemical constituents offshore and deeper into the water column (James & Barko 1991; MacIntyre & Melack 1995; Brothers et al. 2017). However, its significance for the lake ecosystem remains unknown. Thermal siphon has been observed in the field during specific cooling events (e.g., Monismith et al. 1990; James & Barko 1991; Fer et al. 2002), but never monitored over long time series where potential variability might be identified. The driving conditions of the flow are expected to change over time but their effects on the occurrence and magnitude of the density current are unclear.

To fill these gaps, we collected temperature and velocity data over several months in Rotsee, a small (0.5 km^2) eutrophic lake located near Lucerne (Switzerland). The lake has an elongated shape and is well protected from wind, making it a potential site to observe thermal siphons.
Two vertical moorings, both composed of a chain of thermistors and an upward-looking Acoustic Doppler Current Profiler (ADCP), were deployed in the littoral region (mooring MT, 4 m depth) and the pelagic region (mooring MB, 16 m depth). They measured temperature and velocity over the entire water column from March to November 2019, providing information on the background stratification (MB) and the occurrence of thermal siphon (MT).
In addition, several short-term campaigns were performed during the fall period in 2018 and 2019 to increase the spatial and temporal resolution of the measurements. They consisted of three additional moorings M1-M3 and cross-shore transects of CTD (Conductivity-Temperature-Depth) profiles.
Finally, meteorological forcing was obtained from a weather station close to the lake shore.

Our observations reveal that thermal siphon is characterized by both short-term (~hours) and long-term (~days) temporal variability.
In fall, differential cooling leads to horizontal temperature gradients on the order of 10^{-3} °C/m (Figure 1) and produces a thermal siphon during both day and night. The cold density current is roughly 1-2 m thick, can reach a speed of 3 cm/s (Figure 2), and creates a microstratification close to the sediment of around 0.2 °C over approximately 2 m (Figure 1). As expected, periods of higher flow match periods of stronger microstratification (Figure 2).
In spring/summer, thermal siphon can occur during periods of low wind and strong night-time cooling. Inertial effects make it persist well after the end of the cooling period, often until the middle of the day. Its occurrence is clearly dependent on several factors, including surface cooling, low wind intensity and strong background stratification.

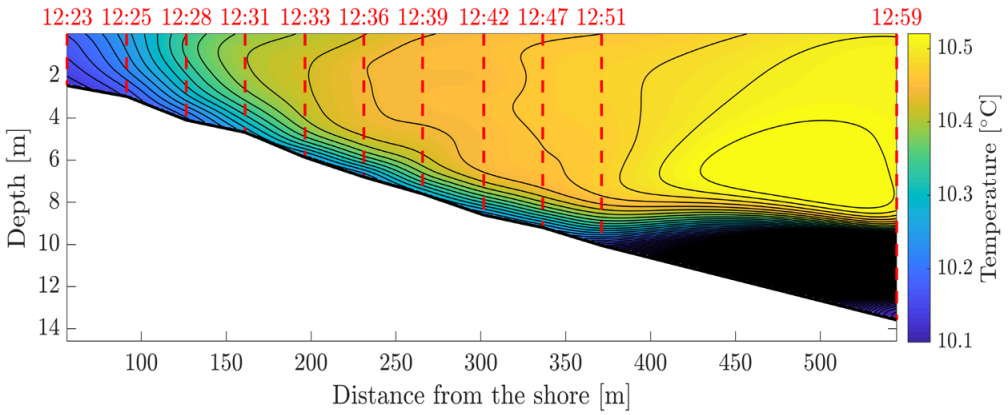


Figure 1. Interpolated cross-shore transect of temperature measured in Rotsee on November 20, 2018. The red dashed lines show the location of the 11 CTD profiles from which temperature was interpolated. Time is indicated in red for each profile and 0.02°C isotherms are represented by black lines.

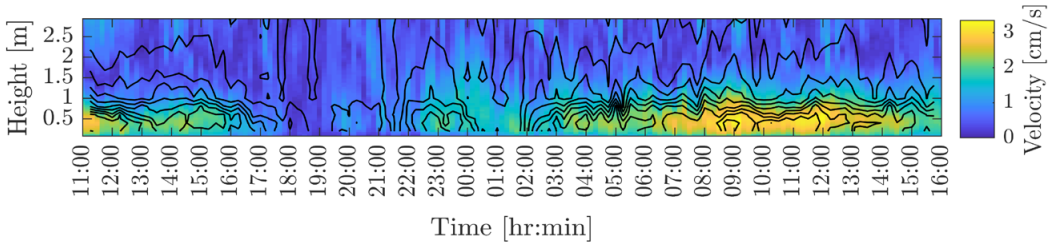


Figure 2. Velocity magnitude (norm) measured at M2 (6 m depth) over the first three meters above the bottom on November 20-21, 2018. The black lines represent the 0.03°C isotherms from temperature differences relative to the surface.

REFERENCES

Brothers, S., Kazanjian, G., Köhler, J., Scharfenberger, U., & Hilt, S. 2017: Convective mixing and high littoral production established systematic errors in the diel oxygen curves of a shallow, eutrophic lake. *Limnology and Oceanography: Methods, 15* (5), 429–435.

Fer, I., Lemmin, U., & Thorpe, S. 2002: Winter cascading of cold water in Lake Geneva. *Journal of Geophysical Research: Oceans, 107*(C6), 3060.

James, W. F., & Barko, J. W. 1991: Estimation of phosphorus exchange between littoral and pelagic zones during nighttime convective circulation. *Limnology and Oceanography, 36* (1), 179–187.

MacIntyre, S., & Melack, J. M. 1995: Vertical and horizontal transport in lakes: linking littoral, benthic, and pelagic habitats. *Journal of the North American Benthological Society, 14* (4), 599–615.

12.6

Explaining shallow groundwater concentrations with surface and bedrock topography, and soil and bedrock composition

Leonie Kiewiet[1], Adrian Wicki[2], Ilja van Meerveld[1], Jan Seibert[1,3]

[1]Department of Geography, University of Zurich, Winterthurerstr. 190, 8057 Zurich (leonie.kiewiet@geo.uzh.ch)
[2]Swiss Federal Research Institute WSL, Mountain Hydrology and Mass Movements, Zürcherstrasse 111, CH-8903 Birmensdorf
[3]Swedish University of Agricultural Sciences, Department of Aquatic Sciences and Assessment, Uppsala, Sweden

Concentrations of major- and trace elements in shallow groundwater depend on the composition and reactivity of the material and contact time. Topography influences the hydraulic gradient and, thus the flow velocity and chemistry. We investigated the importance of surface and bedrock topography, as well as soil and bedrock chemistry to describe shallow groundwater chemistry in a small pre-alpine headwater in the Swiss pre-Alps. The catchment is underlain by Flysch bedrock, which is a reworked carbonate rock that is deposited in deep-water.

We sampled groundwater at more than 40 wells during nine baseflow snapshot campaigns. All wells were drilled until the bedrock (determined by manual augering) and screened over the entire length. There was a large spatial variability in shallow groundwater compositions, with concentrations varying over five orders of magnitude for elements such as calcium, manganese and zinc (Kiewiet *et al.,* 2019)(Kiewiet, von Freyberg, & van Meerveld, 2019). The spatial variability in concentrations was larger than the temporal variability in the average concentrations for the different measurement campaigns, indicating that local factors affect shallow groundwater chemistry. There were consistent patterns of high and low concentrations for the nine snapshot campaigns. Random forest and principal component analysis suggested that surface topography does not explain the concentrations of major and trace elements. Clustering of the wells using the mean relative difference (MRD) from the catchment average for each well and element resulted in four groundwater clusters, which had significantly different median values for surface topographic characteristics and water level dynamics, but the differences were not big enough to predict chemistry across the catchment from surface topography alone.

We therefore investigated the depth to bedrock, the distribution of soil moisture, and the bedrock and soil composition to better understand what caused the differences in concentrations. We took electrical resistivity tomography (ERT) measurements at key locations in the catchment using Wenner-Schlumberger arrays at 0.8 m spacing. Inversion results (Figure 1) indicate that the depth of the wells reflected the depth to the bedrock closely at shallower soil sites, but slightly understimated the depth to bedrock at sites where the soil and regolith layers were thicker. We found that in some locations, the bedrock topography was rugged, and that the surface topography was not always a smoother version of the bedrock topography. Soil moisture at the ERT measurement locations varied, which probably contributed to the spatial variability we observed in the groundwater concentrations.

We performed leaching experiments on three soil samples and two bedrock samples to investigate which elements are released by interaction with water (methods cf. Hissler *et al.*, 2015). We took samples from riparian soil, hillslope soil, and hillslope topsoil as a reference for atmospheric inputs. We furthermore took samples from rather thickly banked sandy carbonate bedrock and thinly banked, silty carbonate bedrock. We found that higher concentrations of transition metals and trace metals were released from the soil samples than the bedrock samples at low acidity (0.05 N HAc). In the second leaching stage (1 N HCl) the release of magnesium, and calcium was particularly high for the silty bedrock, which corresponds to anomalously high concentrations of magnesium in shallow groundwater sampled close to this outcrop.

Our results show that although surface topography affects water movement, it is not sufficient to describe spatial variations in shallow groundwater chemistry. The combined effect of surface and bedrock topography need to be considered together with the chemical composition of soil and bedrock to understand the spatial variability of shallow groundwater composition.

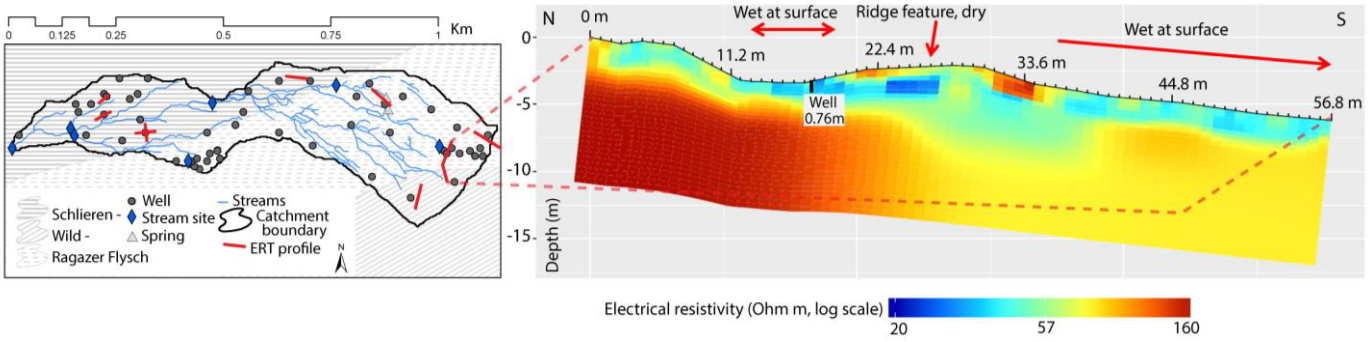


Figure 1: (left) map of the Studibach catchment with locations of the ERT profiles indicated in red and (right) detailed resistivity profile at one location

REFERENCES

Kiewiet, L., von Freyberg, J., & van Meerveld, H. J. (Ilja). 2019. Spatiotemporal variability in hydrochemistry of shallow groundwater in a small pre-alpine catchment: The importance of landscape elements. Hydrological Processes, 1–21.

Hissler, C., Stille, P., Juilleret, J., François, J., Perrone, T., & Morvan, G. 2015. Elucidating the formation of terra fuscas using Sr – Nd – Pb isotopes and rare earth elements. Applied Geochemistry, 54, 85–99

12.7

Dissecting the water tower of Europe: a high-resolution ecohydrological modelling of the European Alps

Theodoros Mastrotheodoros[1], Christoforos Pappas[2], Peter Molnar[1], Paolo Burlando[1], Gabriele Manoli[1], and Simone Fatichi[1]

[1]Institute of Environmental Engineering, ETH Zurich, Zürich, Switzerland (simone.fatichi@ifu.baug.ethz.ch)
[2]Département de géographie and Centre d'études nordiques, Université de Montréal, Montréal, QC, Canada

Mountain ecosystems are intrinsically heterogeneous because the complex terrain creates steep gradients in climate, soil, and vegetation cover. This heterogeneity complicates our understanding and representation of mountain hydrological processes. Here, we used the fully distributed, process-based ecohydrological model Tethys-Chloris (T&C) to perform a high spatiotemporal resolution simulation of the entire European Alps (257,000 km^2). By analysing hourly simulation results over three years (2000-2003) with a spatial resolution of 250x250 m^2 across the study domain, we quantify: (1) the components of the hydrological budget in different seasons and how streamflow may respond to increasing temperature; (2) the role of vegetation water stress or lack of thereof on the Alpine water balance during summer. Uncalibrated ecohydrological simulations were tested in reproducing spatiotemporal patterns of observed snow cover (in more than 550 stations) and discharge (in more than 350 stream gauges). Results are on average unbiased in terms of streamflow magnitude and snow cover duration. Correlations between observed and simulated discharge at the daily scale are typically greater than 0.7. Due to the challenge of projecting climate change forcing in mountainous areas at such a high resolution, we used a space-for-time substitution based on the current climate simulations to infer how an increase in air temperature affects the ecohydrological response. Our results suggest that total annual runoff over the entire Alpine area is strongly controlled by precipitation and therefore it is very resilient to changes in temperature, despite evapotranspiration being energy-limited and temperature-dependent. For instance, a +3°C scenario affects annual runoff similarly to a decrease of only 3% in precipitation. However, patterns of runoff production are spatially complex and several dry areas may become considerably drier in a warmer climate. Results are quite different when the focus is on the growing season only, where evapotranspiration is a significant component of the water budget and an increase in temperature modifies the hydrological response. For instance, evapotranspiration considerably contributed to reduce water yield during the 2003 growing season because vegetation benefited from the unusually warm and sunny conditions in a large part of the Alpine region at higher elevations. In summary, model results with high spatiotemporal resolution are providing novel insights into the underlying ecohydrological processes and help us to better understand the response of Alpine water resources to climatic changes.

12.8

Sediment connectivity in the Rhône Basin: from an isolated thunderstorm at Illgraben to a turbidity current in deep Lake Geneva

François Mettra[1,2], Koen Blanckaert[3], Ulrich Lemmin[4] & David Andrew Barry[4]

[1]*Institute of Earth Surface Dynamics, University of Lausanne, Géopolis, CH-1015 Lausanne (francois.mettra@unil.ch)*
[2]*Invited researcher at Institute of Hydraulic Engineering and Water Resources Management, TU Wien, Karlsplatz 13/222, A-1040 Vienna*
[3]*Institute of Hydraulic Engineering and Water Resources Management, TU Wien, Karlsplatz 13/222, A-1040 Vienna*
[4]*Ecological Engineering Laboratory, Lausanne Federal Institute of Technology, Station 2, CH-1015 Lausanne*

In the Rhône canyon of Lake Geneva (Figure 1), turbidity currents are occasionaly present in summer. Based on velocity measurements in the canyon and discharge measurements at Porte du Scex in the Rhône 6 km upstream of Lake Geneva (Figure 1), Lambert and Giovanoli (1988) hypothesized that Rhône River floods and slides of sublacustrine deltaic deposits are the main causes of these turbidity currents. Here, we present another type of initiation: a strong sediment event along the sediment cascade of the Rhône basin, ending in a deep lake turbidity current without a significant increase in water discharge of the Rhône River. Using data available at the Illgraben catchment in Wallis (McArdell, 2016), at Porte du Scex, and our own velocity measurements in the Rhône canyon (Figure 1), we are able to follow the release of a strong sediment pulse from source to sink. At Illgraben, a debris flow, reaching the Rhône River, is triggered by a short and intense convective storm that does not significantly increases the Rhône water discharge (Bennett, 2014). Eleven to thirteen hours later, the fine sediment cloud is observed at Porte du Scex, which is situated 84 km further downstream, and subsequently a turbidity current is measured in the canyon. The observations demonstrate the high and fast sediment connectivity between specific high-alpine areas and the deep part of Lake Geneva.

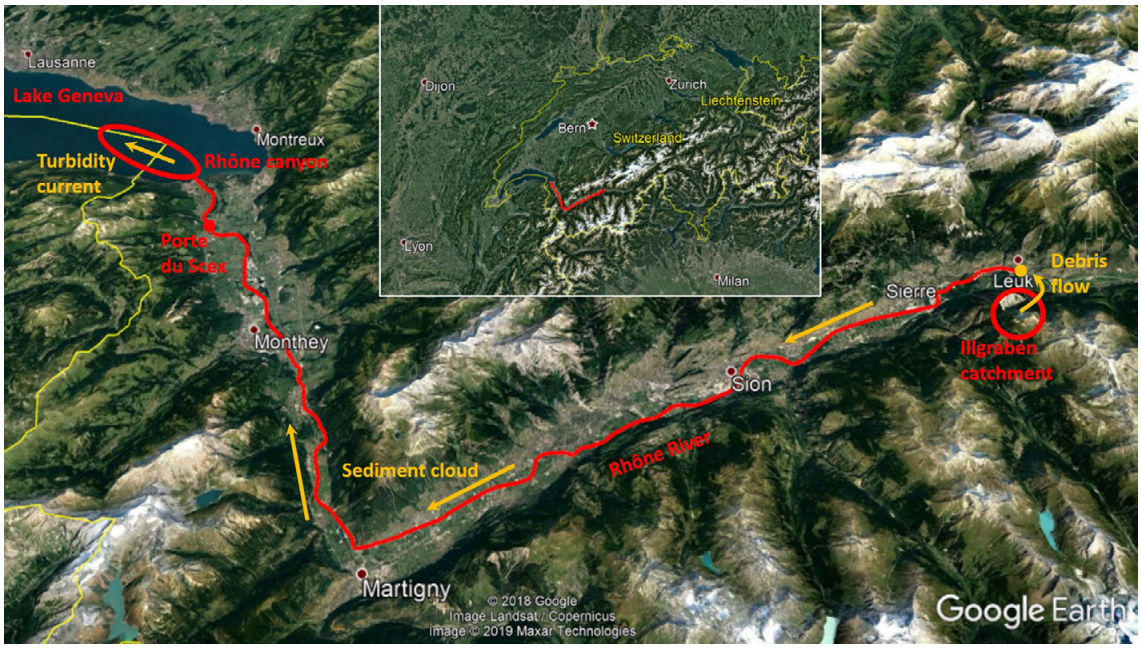


Figure 1. Situation of the observation sites in the upper Rhône catchment and processes involved in the sediment cascade from high alpin slopes to Lake Geneva during a strong sediment event.

REFERENCES

Bennett, G. L., Molnar, P., McArdell, B. W., & Burlando, P. 2014: A probabilistic sediment cascade model of sediment transfer in the Illgraben. Water Resources Research, 50(2), 1225-1244.

Lambert, A., & Giovanoli, F. 1988: Records of riverborne turbidity currents and indications of slope failures in the Rhone delta of Lake Geneva, Limnology and Oceanography, 33(3), 458-468.

McArdell, B. W. 2016: Field measurements of forces in debris flows at the Illgraben: Implications for channel-bed erosion. International Journal of Erosion Control Engineering, 9(4), 194-198.

12.9

Stream Temperature Evolution in Switzerland simulated with downscaled CH2018 Climate Change Scenarios

Adrien Michel[1,2,3], Tristan Brauchli[1,4,5], Nander Wever[6], Jannis Epting[3] Michael Lehning[1,2], & Hendrik Huwald[1,2]

[1]Ecole Polytechnique Fédérale de Lausanne (EPFL), (adrien.michel@epfl.ch)
[2]WSL Institute for Snow and Avalanche Research SLF, Davos, Switzerland
[3]University of Basel (UniBas)
[4]University of Lausanne (UNIL)
[5]Centre de Recherche sur l'Environnement Alpin (CREALP)
[6]University of Colorado, Boulder

Climate change already has affected many components of our natural environment. Numerous studies have attempted and succeeded in quantifying the observed impact on air temperature, glacier volume, snow cover duration, shifts in vegetation, phenology and many more. While it is very likely that climate change has and will also have an important effect on the temperature of streams with consequences for water quality, the aquatic fauna and fluvial ecosystem services, very little information and quantitative predictions are available on this topic. This study investigates numerically the response of selected streams in Switzerland to the future forcing as provided by the CH2018 climate change scenarios for Switzerland. The approach uses a sequence of physical models composed of Snowpack, Alpine3D and StreamFlow. The simulations are forced by using CH2018 scenarios which have been down-scaled to an hourly time step using a novel approach based on a delta method which preserves the seasonal aspect of the climate change scenario. Preliminary results suggest that the observed warming of water temperature will continue with any of the scenarios used (RCP2.6, RCP 4.5, RCP8.5) due to the rise of air temperature and the decrease in discharge in summer. As a consequence, river ecosystems will be impacted and current legal limits for the usage of water for cooling in the energy production sector and in the industry will be reached more often in the future. These results are analysed and interpreted by comparing to a present-day reference situation and in view of a recent, comprehensive analysis of historical stream temperature data in Switzerland (Michel et al., 2019).

REFERENCES

Michel, A., Brauchli, T., Lehning, M., Schaefli, B., & Huwald, H.: Stream temperature evolution in Switzerland over the last 50 years, Hydrol. Earth Syst. Sci. Discuss., https://doi.org/10.5194/hess-2019-366, in review, 2019.

12.10

Hydro/thermogeological state of the Maggia river delta: potential shallow geothermal energy implications

Rodolfo Perego[1], Sebastian Pera[1], Monica Bulgheroni[1], Jacopo Boaga[2] & Antonio Galgaro[2]

[1]Institute of Earth Science, SUPSI, Campus Trevano, CH-6952 Canobbio, Switzerland (rodolfo.perego@supsi.ch)
[2]Department of Geosciences, Università degli Studi di Padova, Italy

In Cantone Ticino, located in southern Switzerland, there is a constant growth of subsurface heat exploitation through the use of shallow geothermal systems (SGS) both closed and open-loop. Such a density (10 probes/km^2 if we consider only major valleys, where population density is greater) will raise issues regarding short probe distances and adjoining probe fields that will influence ground temperatures and system performances in the long term.

The scope of the present work is to study the processes governing interferences between closed and open loop systems to obtain results that in turn would be used to efficiently allocate ground heat, in a long-term sustainable manner.
We identified an interesting case study where mutual interactions between closed and open systems could be analyzed: the delta of Maggia river, a torrential regime stream that flows into Lake Maggiore and hosts the cities of Locarno and Ascona. In this area there is a large presence of both closed and open SGS at relatively small distances. In particular, an area in the north-western part of the Maggia delta (which already hosts many SGS) within the city of Locarno will be interested by the installation of large closed-loop systems. To properly study the local interactions between SGS, firstly the regional actual conditions from both groundwater level and temperature had to be assessed.

The workplan therefore started with the hydrogeological and thermal characterization of the case study subsurface in order to acquire information aimed at the creation of a regional scale numerical model. The steady-state simulation of initial piezometric level and groundwater temperature will be subsequently implemented in the local scale numerical model which will be used to assess the mutual interferences between closed-loop and open-loop SGS.

To build the physical model of the Maggia delta available literature was initially analyzed [1] and field work was performed. Different campaigns of passive microseismic measurements were planned and executed, in order to detect the shape of the lithological discontinuity between thick Quaternary alluvial sediments and the underlying bedrock formation [2]. The collected signals and spectral ratio, along with literature data, were investigated and used to produce a 3D continuous reconstruction of the bedrock top throughout the study area. Moreover, a groundwater monitoring network was conceived and applied from scratch. Piezometric level and groundwater temperature measurements [3] were performed in order to hydrogeologically and thermally characterize the subsurface. A regional numerical model was consequently developed with the commercial software FEFLOW [4] to represent average hydrogeological conditions (both for hydraulic head and temperature), considering the period between 2015 and 2018. The regional flow and heat transport model [Figure 1] is currently under calibration against both hydraulic head and temperature observations. It will provide insights on the regional behavior of the groundwater. Moreover the regional model will describe the initial conditions for the local scale assessment, where the mutual impact of closed and open geothermal systems will be investigated in detail.

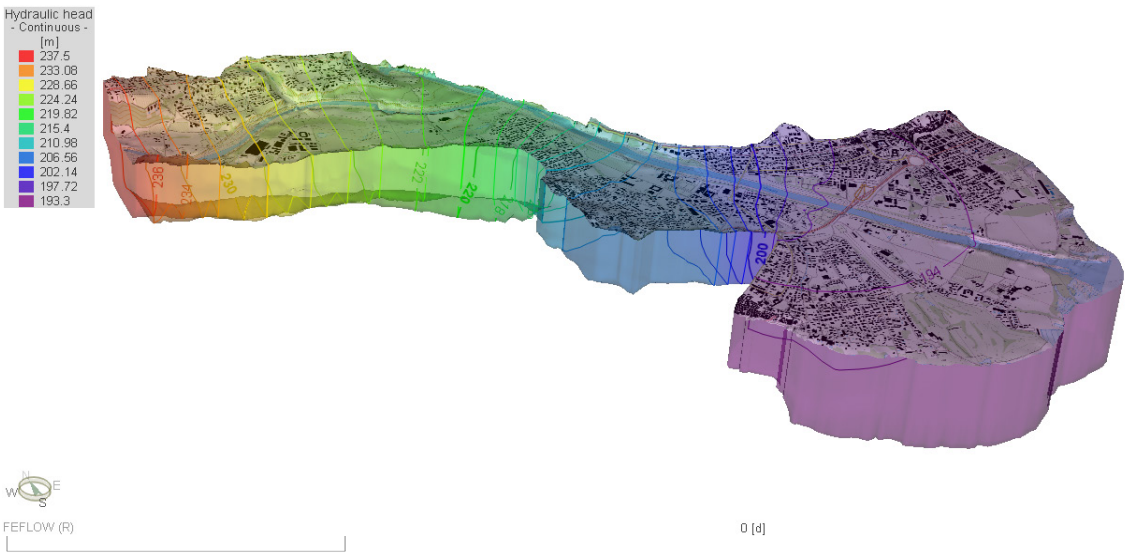


Figure 1 - Hydrogeological model of the Maggia river delta with preliminary results of the calculated hydraulic head

REFERENCES

Fondazione Lerici 1970: Studio geofisico dei fondovalle del Canton Ticino, eseguito per conto della Sezione Cantonale delle Bonifiche e del Catasto, Bellinzona. Milano, Fondazione Ing. C.M. Lerici, Ricerca No. 535

Trevisani, S., Boaga, J., Agostini, L., & Galgaro, A. 2017: Insights into bedrock surface morphology using low-cost passive seismic surveys and integrated geostatistical analysis. Science of The Total Environment, 578, 186-202.

Farr, G. J., Patton, A. M., Boon, D. P., James, D. R., Williams, B., & Schofield, D. I. 2017: Mapping shallow urban groundwater temperatures, a case study from Cardiff, UK. Quarterly Journal of Engineering Geology and Hydrogeology, 50(2), 187-198.

Diersch, H. J. G. 2005: FEFLOW finite element subsurface flow and transport simulation system. Inst. for Water Resources Planning and System Res., Berlin

12.11

Identifying sources and processes impacting groundwater recharge in the human environment

Robin Weatherl[1,2], Maria Henao Salgado[3,1], Mario Schirmer[1,2]

[1]*Swiss Federal Institute of Aquatic Science and Technology (Eawag)*
[2]*University of Neuchâtel Center for Hydrogeology and Geothermie (CHYN)*
[3]*ETH Zürich Institute of Environmental Engineering (IfU)*

Understanding groundwater dynamics around areas of human influence is of critical importance for ensuring sustainable resource management in the 21st century and beyond. Groundwater supplies in agricultural or urban areas are at a particular risk of quality degradation due to their proximity to human activity. These supplies are also at risk of depletion due to heightened consumption in such areas. These risks and the dynamics that feed into them can no longer be determined considering natural controls only. Exploitation of the land can have significant impacts on a local water cycle, by changing the magnitude of existing parameters, changing the nature of surface water-groundwater interactions, changing infiltration pathways, or creating new, artificial sources and sinks of groundwater. All of these changes are consequential for the resulting quality of a groundwater body.

We intend to present here the results of a site investigation being carried out in a small catchment aquifer located in the Canton of Zürich, Switzerland. We have tested a number of methods in an attempt to characterize the above-mentioned anthropogenic groundwater dynamics. A first approach involves the estimation of groundwater recharge via water balance. Our water balance has attempted to account for changes in runoff and evapotranspiration terms due to changes in land cover, and has considered the impact of artificial source and sink terms from infrastructure and from practices such as groundwater pumping and irrigation. We have then made use of synthetic organic compounds (here referred to as *micropollutants*) as indicators of specific recharge sources and potential pathways from the surface into the water. Micropollutants are fully absent in the natural environment and thus offer unequivocal evidence of input from the human environment when measured in groundwater. They may be used to trace input from treated or untreated wastewater, irrigation runoff, and surface waters. Micropollutant datasets at our site have proven to be highly censored, requiring appropriate statistical methods (including a robust regression on order statistics) for proper interpretation that avoids bias. Emphasis is given to these statistical methods as they are fundamental to the analysis of micropollutant datasets, yet are often ignored in the environmental sciences. Finally, stable water isotopes and inorganic chemistry are used as independent validation (or dissention) of the conclusions drawn from micropollutant data. From these analyses, a conceptual model of the modified water cycle in this catchment is offered.

Contact Information: Robin Weatherl, Department of Water Resources and Drinking Water, Eawag, Email: robin.weatherl@eawag.ch

12.12

Giant pockmarks in Lake Neuchatel, Switzerland: new multi-proxy evidence for lacustrine groundwater discharge

Stefanie B. Wirth[1], Damien Bouffard[2], Adeline Cojean[1] & Jakob Zopfi[3]

[1]Centre for Hydrogeology and Geothermics, University of Neuchatel, Rue Emile-Argand 11, CH-2000 Neuchâtel (stefanie.wirth@unine.ch)
[2]Eawag, Seestrasse 79, CH-6047 Kastanienbaum
[3]Department of Environmental Sciences, University of Basel, Bernoullistrasse 30, CH-4056 Basel

Four giant pockmarks (80 to 150 m in diameter) are located in Lake Neuchatel, Switzerland, along its northern shore and adjacent to the karst system of the Jura Mountains (Reusch et al. 2015, 2016). Two pockmarks have a ~60 m-deep chimney filled with mud; two are funnel-shaped 12 m and 29 m deep holes. We present evidence for the presence of groundwater in the chimneys and active lacustrine groundwater discharge (LGD) at both pockmark types. Temperature, electrical conductivity and Ca^{2+} concentrations of the pore water in the chimneys show values typical for karst water. TOC and TIC indicate that the chimney mud consists of liquefied sediments from the entire deglacial to Holocene lacustrine sediment succession. Mini mud volcanoes apparent on the suspension surface imaged with a remotely operated vehicle (ROV) localize the groundwater exit points and confirm LGD. LGD is further corroborated by electrical conductivity anomalies detected above the lutoclines and within a funnel-shaped pockmark during the ROV survey. We conclude that the giant pockmarks in Lake Neuchatel represent a type of subaquatic spring that connects the water body of the lake with the karst system. Quantifying LGD via the pockmarks will be an essential next research step in order to assess their lake-wide relevance. Overall, this study underlines the existing need for research on the connectivity of lakes and oceans with groundwater systems for completing our understanding of the hydrological cycle.

REFERENCES

Reusch, A., Loher, M., Bouffard, D., Moernaut, J., Hellmich, F., Anselmetti, F.S., Bernasconi, S.M., Hilbe, M., Kopf, A., Lilley, M.D., Meinecke, G. & Strasser, M. 2015: Giant lacustrine pockmarks with subaqueous groundwater discharge and subsurface sediment mobilization, Geophysical Research Letters, 42, 3465-3473.

Reusch, A., Moernaut, J., Anselmetti, F.S. and Strasser, M. 2016: Sediment mobilization deposits from episodic subsurface fluid flow—A new tool to reveal long-term earthquake records? Geology, 44, 243-246.

P 12.1

Stream temperature and discharge evolution over the last 50 years in Switzerland

Tristan Brauchli[1,2,4], Adrien Michel[1,3], Michael Lehning[1,3], Bettina Schaefli[4,5] & Hendrik Huwald[1,3]

[1]*Ecole Polytechnique Fédérale de Lausanne (EPFL), tristan.brauchli@crealp.vs.ch*
[2]*Centre de Recherche sur l'Environnement Alpin (CREALP), Sion*
[3]*WSL Institute for Snow and Avalanche Research SLF, Davos, Switzerland*
[4]*University of Lausanne (UNIL)*
[5]*Institute of Geography, University of Bern, Bern*

Stream temperature and discharge are key variables for water resources management but also for ecosystems: they strongly influences the fauna and flora along with biogeochemical cycles. In a changing climate, river water temperature is generally assumed to increase (due to a change of the energy budget) while streamflow should decrease during summer months (low base flow, droughts). The amplitudes of these changes are however hard to quantify given the complexity of the system and the natural climate variability. In addition, many anthropogenic activities (hydropower plants, river correction and lake regulation) significantly impact river systems and associated water temperatures.

In Switzerland, hydrological observations are available since the beginnning of the 20th century. However, few studies have quantified stream discharge and temperature trends. In the present study (Michel et al., 2019), we propose a robust countrywide historical analysis: the data set is composed of 52 gauging stations measuring water temperature and discharge back to 1960. The stations are clustered into coherent entities based on their hydrological regime (snow or ice vs rain-dominated, natural vs disturbed discharge). Thanks to a seasonal-trend decomposition (STL), we show how climate change differently impacts the various types of rivers. Stream temperature has significantly increased over the past 5 decades, with positive trends for all four seasons. The mean trends for the last 20 years are +0.37 °C per decade for water temperature, resulting from joint effects of trends in air temperature (+0.39 °C per decade) in discharge (−10.1 % per decade) and in precipitation (−9.3 % per decade). For a longer time period (1979–2018), the trends are +0.33 °C per decade for water temperature, +0.46 °C per decade for air temperature, −3.0 % per decade for discharge and −1.3 % per decade for precipitation. We furthermore show that in alpine streams, snow and glacier melt compensates air temperature warming trends in a transient way. Lakes, on the contrary have a strengthening effect on downstream water temperature trends at all elevations. The identified stream temperature trends are furthermore shown to have critical impacts on ecological temperature thresholds, especially in lowland rivers, suggesting that these are becoming more vulnerable to the increasing air temperature forcing. Resilient alpine rivers are expected to become more vulnerable to warming in the near future due to the expected reductions in snow- and glacier melt inputs.

REFERENCES

Michel, A., Brauchli, T., Lehning, M., Schaefli, B., & Huwald, H.: Stream temperature evolution in Switzerland over the last 50 years, Hydrol. Earth Syst. Sci. Discuss., https://doi.org/10.5194/hess-2019-366, in review, 2019.

P 12.2

Does the Rhône River fertilise Lake Geneva ? (in the context of its re-oligotrophisation)

Cotte Gabriel[1], Vennemann Torsten[1]

[1]*IDYST, University of Lausanne, Géopolis 1015 Lausanne (Gabriel.Cotte@unil.ch)*

After a period of eutrophication during the 60's and 70's with annual average of total phosphorus reaching 90 μgP/L, Lake Geneva has been on the way of re-oligotrophisation. Since the 80's, after Swiss and French measures were taken to limit the phosphorus input into the lake, the concentration decreased to 10 μgP/L (CIPEL, 2018). Despite this important reduction, the amount of biomass measured every years does not decline. Nowadays, because the phosphorus becomes a limiting factor earlier and earlier during the season, it is important to evaluate (i) which nutrients are coming from the river inputs, (ii) where it is transported and (iii) how it is metabolized.

The Rhône River is the principal tributary to Lake Geneva, both in terms of discharge of water and sediment load (CIPEL, 2018). Therefore, it influences the physical and chemical properties of the lake and so the lake ecological functioning as primary production (Bouffard and Perga, 2016).

The objective of this study is to determine the potential chemical gradient related to the Rhône water intrusion in the river-lake transition zone and how it can influence locally the phytoplancton growth.

During 2019, a consortium of researchers from the ISE (UNIGE), the ECOL (EPFL) and the IDYST (UNIL) organised field campaigns at different seasons in order to establish the link between hydrodynamics, chemistry and biology in the Rhône rivermouth area. Three transects were definied by ADCP profiling: one longitudinal and two transversals, in and out of the near field, defined as the area where the Rhône is still visible in terms of current velocities (Fig.1). Systematic depth sampling (2.5, 5, 7.5, 10, 15, 20, 30, 100 m, bottom) and CTD profiles were done using a Rosette autosampler at the different sampling locations. As it been shown that the stable H- and O-isotope composition of water for this Alpine lake is a powerful tool to trace the Rhône River intrusion (Halder et al., 2013), this method was used to determine the river mixing rates. Major ions and cations as well as the phytoplancton communities and concentrations have been analysed.
In this contribution, we'll focuse on the nutrient dispersion linked to the Rhône intrusion and show how it can change depending on the Rhône discharge, the lake stratification and the wind conditions.

REFERENCES

Bouffard, D. and Perga, M.-E., 2016 Are flood-driven turbidity currents hot spots for priming effect in lakes?, Biogeosciences, 13, 3573-3584.

Conseil scientifique de la commission internationale pour la protection des eaux du Léman contre la pollution. 2018. Rapports sur les études et recherches entreprises dans le bassin lémanique. Campagne 2017. CIPEL.

Halder, J., L. Decrouy, and T. W. Vennemann, 2013. Mixing of Rhône River water in Lake Geneva (Switzerland- France) inferred from stable hydrogen and oxygen isotope profiles. J. Hydrol. 477: 152–164.

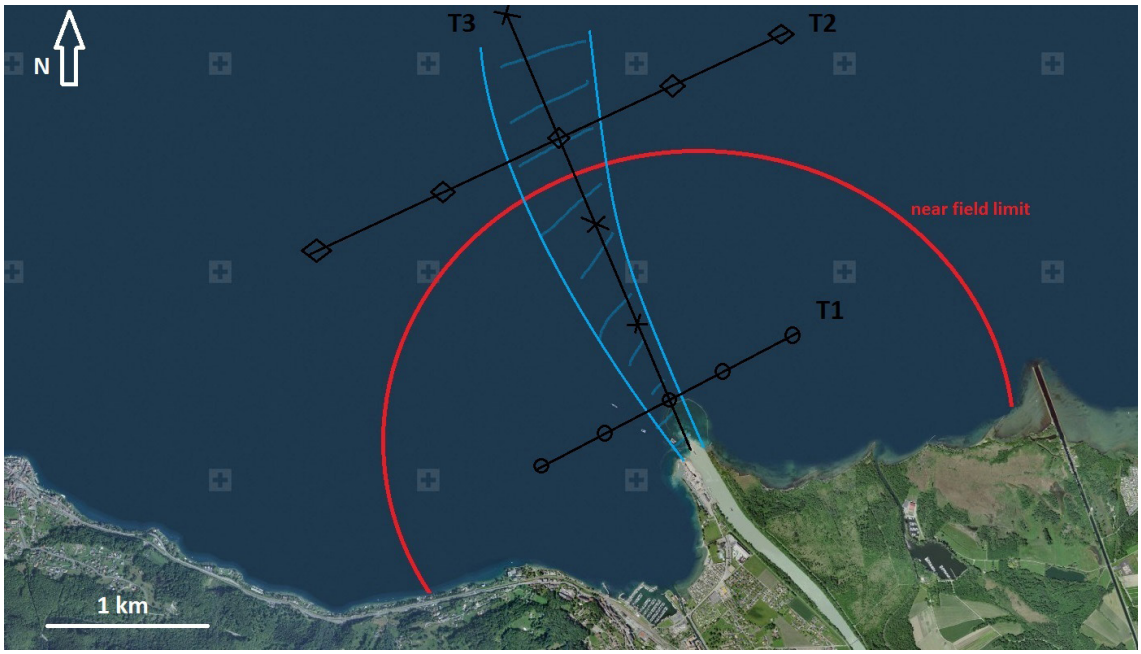


Figure 1. Sampling locations in the Rhône rivermouth area in Lake Geneva.

P 12.3

Thermal potential of urban tunnel infrastructures in unconsolidated rock groundwater resources

Jannis Epting[1], Peter Huggenberger[1]

[1]*Applied and Environmental Geology, Department of Environmental Sciences, University of Basel, Bernoullistrasse 32, CH-4056 Basel (jannis.epting@unibas.ch)*

The current development of energy geostructures often lacks the scientific foundations and knowledge of how the various systems interact in the shallow subsurface and influence the hydraulic and thermal regimes in the subsurface.
This contribution in collaboration with the SFOE (SI/501646-01) presents preliminary evaluation elements for geothermal potential assessment and thermal influences of planned tunnel infrastructures for the urban agglomeration of Basel (Switzerland).

In dependence of the tunnel type (motorway or railway) as well as its location related to the geological and hydrogeological settings different solutions for shallow geothermal energy systems (SGE) are investigated. 'Passive' and 'active' SGE have been evaluated, including heat-exchanging segments installed in tunnel lining structures and thermal exploitation of water circulating in culvert systems.

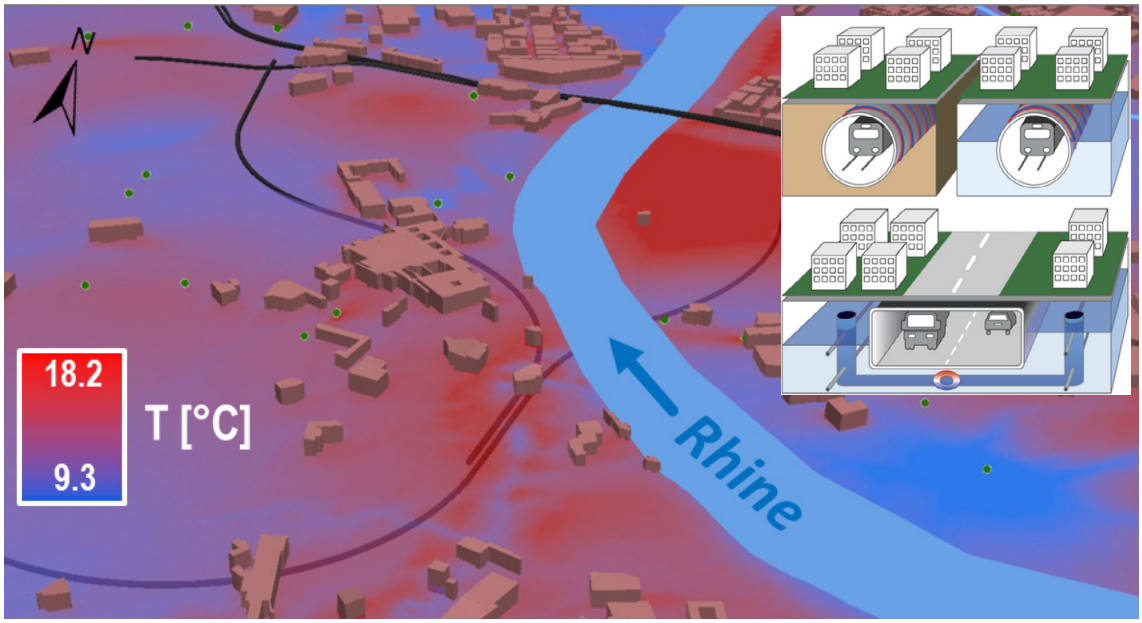


Figure 1. Groundwater temperatures and urban subsurface constructions, including progression of planned and existent tunnels, at the bend of the river Rhine in the city of Basel, Switzerland.

REFERENCES

Epting J., Baralis M., Künze R., Mueller M.H., Insana A., Barla M. & Hug-genberger P. 2019: Geothermal Potential of Tunnel Infrastructures – Development of Tools at the City-Scale of Basel, Switzerland. Geothermics

P 12.4

Geothermal use of an Alpine aquifer – Davos pilot study

Stefan Scheidler[1], Horst Dresmann[1], Peter Huggenberger[1], Jannis Epting[1]

[1]Applied and Environmental Geology, Department of Environmental Sciences, University of Basel, Bernoullistrasse 32, CH-4056 Basel (jannis.epting@unibas.ch)

Topographically induced Alpine regional groundwater flow systems below the unconsolidated valley fillings constitute a substantial unused geothermal resource.

Within the framework of the INTERREG VB project GRETA (shallow geothermal energy in the Alpine region), we developed a method to quantify the groundwater flux of complex alpine aquifers. The basis of the study is a regional-scale hydraulic groundwater model, which is based on a 3D tectonic model of the Davos region in Switzerland.
Favourable conditions for an energetic exploitation are related to large-scale topography differences between groundwater recharge and potential exfiltration areas in the valleys, thanks to the 3D geometry of the large-area tectonic nappe units with their root zone located within river valleys.

In general, the proposed concept could be applied to a variety of similar geological and hydrogeological conditions in the tourist regions of the Alpine belt.

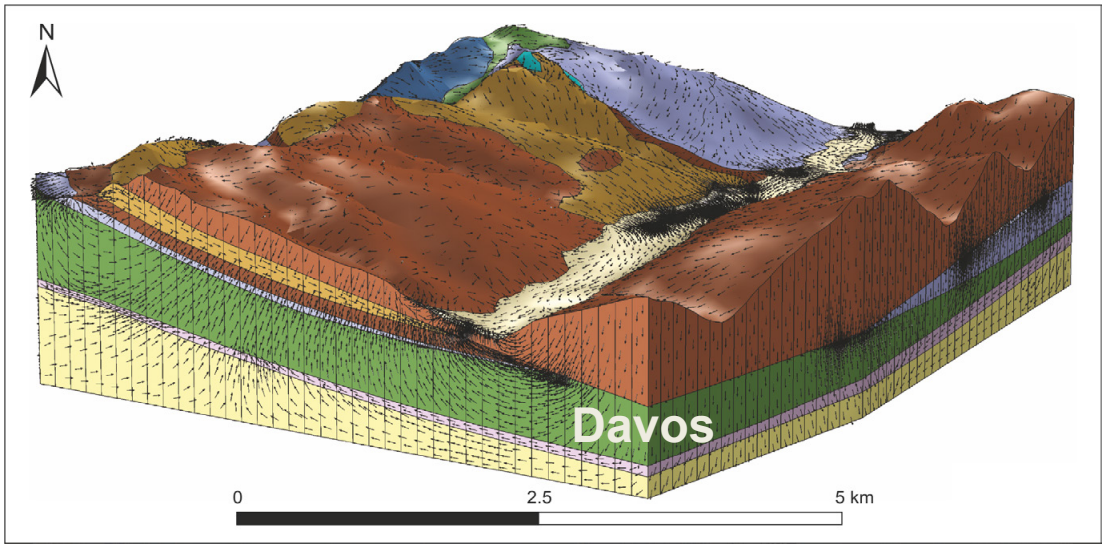


Figure 1. Result of regional scale groundwater modelling: the arrows represent the flow direction.

REFERENCES

Scheidler S., Anders B., Regli C., Bolay S., Huggenberger P. 2019: Geothermal use of an Alpine aquifer – Davos pilot study. Grundwasser

Scheidler, S., Huggenberger, P., Butscher, C. and Dresmann, H. 2019: Tools to simulate changes in hydraulic flow systems in complex geologic settings affected by tunnel excavation. Bulletin of Engineering Geology and the Environment 78(2), 969-980

P 12.5

Accuracy of citizen science water level class observations

Simon Etter[1], Barbara Strobl[1], Jan Seibert[1,2] & H.J. (Ilja) van Meerveld[1]

[1]Department of Geography, University of Zurich, Winterthurerstrasse 190, 8057 Zurich, Switzerland (simon.etter@geo.uzh.ch)
[2]Department of Aquatic Sciences and Assessment, Swedish University of Agricultural Sciences, P.O. Box 7050, 75007 Uppsala, Sweden.

We will present the first results of real citizen generated WL-class time series from the CrowdWater project. The CrowdWater citizen science project (www.crowdwater.ch, Seibert et al., 2019) aims to collect hydrological data in remote regions where hydrological data are scarce. Previously, we assessed the accuracy of streamflow and water level class (WL-class) estimates from passers-by in street surveys (Strobl et al., 2019). For the WL-class estimates, citizens compared the actual water level in a stream with a picture of the stream taken at a different time in which a sticker of a staff gauge was placed as a reference. To asses the potential value of crowd-sourced water level class and streamflow data for hydrological model calibration we used these errors to create synthetic datasets that represented the characteristics of citizen generated time series of streamflow or water level class data. These data were then used to calibrate a hydrological model which we evaluated by comparing the simulations to the measured streamflow (Etter et al. (2018), Etter et al. (submitted)).

Because the surveys with the passers-by may be influenced by the presence of experts at the site, in this study we evaluated the accuracy of citizen science based stream level class observations using data collected with the CrowdWater app and survey sheets. Since the launch of the “CrowdWater | SPOTTERON” smartphone application in spring 2017 (Seibert et al. (2019) and Figure 1 - left), citizen scientists can start their own timeseries at any stream. For this study we selected eight such locations across Switzerland and Austria where measured water level data was available by national or local authorities. Furthermore, we collected WL-class data with survey sheets where passers-by estimated WL-classes independently (Figure 1 - right) at 13 locations across Switzerland where streamlevel data were available from the Federal Office of the Environment, the École Polytechnique Fédéderale de Lausanne or measured by ourselves. We compared the crowdsourced and measured timeseries to assess the accuracy of the crowdsourced data and their ability to represent the streamflow dynamics over time. We show that the accuracy of the crowd-sourced water level class data varied for the different streams and the quality of the reference image.

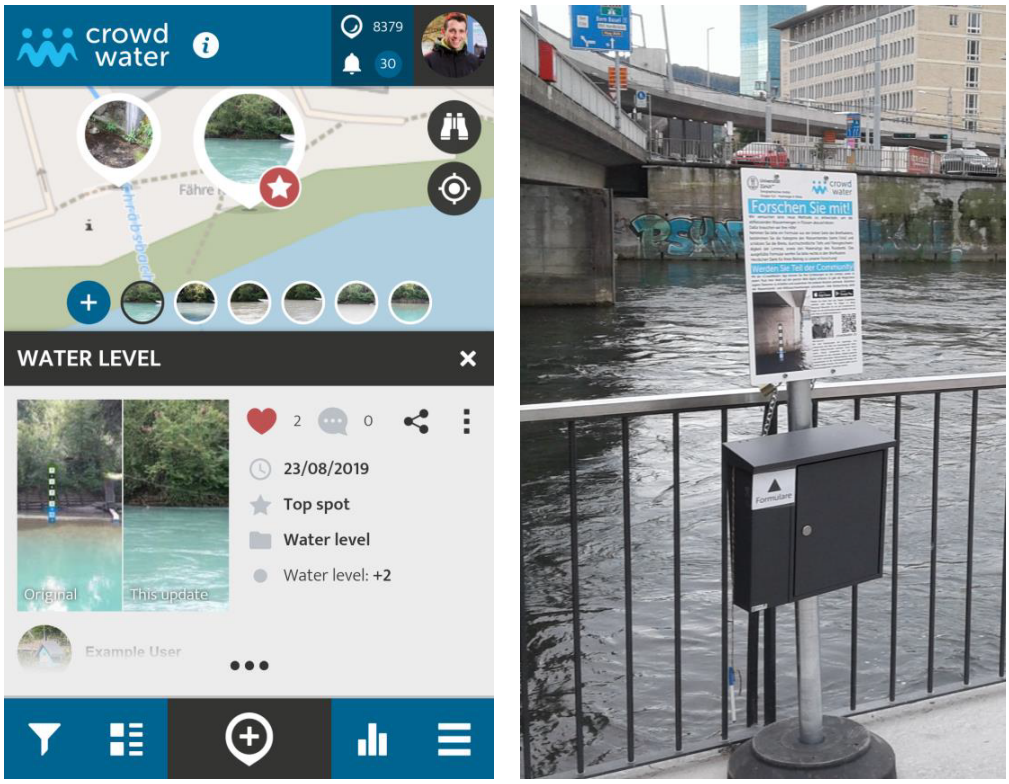


Figure 1. Left: Screenshot of the CrowdWater | SPOTTERON smartphone application. On the lower left, the reference picture with a virtual staff gauge and a picture of the stream at a the time of the contribution. The citizen scientist chose the level +2 for the new observation based on the comparison with the reference image. Right: CrowdWater station at the Limmat in Zurich, Switzerland. Passers-by could independently submit their observations using forms and the letterbox. The reference picture was provided on a sign board with information about CrowdWater and the explanation of how to contribute.

REFERENCES

Etter, S., Strobl, B., Seibert, J. and van Meerveld, I.: Value of uncertain streamflow observations for hydrological modelling, Hydrol. Earth Syst. Sci., 22, 5243–5257, doi:https://doi.org/10.5194/hess-22-5243-2018, 2018.

Etter, S., Strobl, B., van Meerveld, H. J. (Ilja) and Seibert, J.: Value of crowd-based water level class observations for hydrological model calibration, submitted to Water Resources Research (Aug 2019).

van Meerveld, H. J., Vis, M. J. P. and Seibert, J.: Information content of stream level class data for hydrological model calibration, Hydrol. Earth Syst. Sci., 21(9), 4895–4905, doi:10.5194/hess-21-4895-2017, 2017.

Seibert, J., Strobl, B., Etter, S., Hummer, P. and van Meerveld, H. J.: Virtual Staff Gauges for Crowd-Based Stream Level Observations, Front. Earth Sci., 7, doi:10.3389/feart.2019.00070, 2019.

Strobl, B., Etter, S., van Meerveld, I. and Seibert, J.: Accuracy of crowdsourced streamflow and stream level class estimates, Hydrol. Sci. J., (Special issue on hydrological data: opportunities and barriers), 1–19, doi:10.1080/02626667.2019.1578966, 2019.

P 12.6

KMC : a comparison of various models for assessing karst hydrology

Pierre-Yves Jeannin[1]

[1]*Swiss Institute for Speleology and Karst-Studies, SISKA (pierre-yves.jeannin@isska.ch)*

The idea of the Karst Modelling Challenge (KMC) was to invite various research groups to apply their models to the same data set in order to compare approaches and results, and finally to discuss advantages and disadvantages of the respective approaches.

Data from the Milandre underground laboratory (Switzerland) are used for the comparison. The first step in the challenge is to simulate spring hydrograph from measured meteorological data. Ten research groups are participating.
The definition of common evaluation criteria, as well as of time steps for the simulations lead to some interesting discussions. The Kling-Gupta Evaluation criteria (KGE) was considered as the best criteria, and an hourly time-step was chosen for the given catchment area. Volume conservation as well as Nash-Sutcliffe criteria are being considered in the evaluation too.

Most models provided reasonable results, some of them being very close to measured discharge rates. The required effort for conducting the simulation exercise ranged between a few hours to several weeks depending on the models. The best results were mainly obtained by the simplest models (least number of parameters, i.e. black-box type of models), which appear to be the most efficient for the given exercise. However, the next (future) step of the challenge will be to simulate the spatial distribution of heads and flow-rates within the karst massif, which will be difficult with the simplest models...

P 12.7

Continuous time random walk model for non-uniform bed-load transport

ZhiPeng Li[1], HongGuang Sun[1], Yong Zhang[2], Renat T. Sibatov [3]

[1]College of Mechanics and Materials, Hohai University, Nanjing, Jiangsu 210098, China (zhipenghhu@gmail.com)
[2]Department of Geological Sciences, University of Alabama, Tuscaloosa, AL 35487, United States
[3]Ulyanovsk State University, 42 Leo Tolstoy str., Ulyanovsk 432017, Russia

Bed-load transport along widely graded river-beds typically exhibits anomalous dynamics, whose efficient characterization may require parsimonious stochastic models with pre-defined statistics involving the waiting time and hop distance distributions for sediment particles. This study employs a continuous time random walk (CTRW) model to characterize bed-load particle motions on a widely graded gravel-bed with cluster microforms built in our lab. Flume experiments guide the selection of the Mittag-Leffler (M-L) function as the waiting time distribution function, and the Lévy a -stable density for the hop distance distribution function in the CTRW model. Monte Carlo simulations show that the resulting CTRW model can well capture the observed flume experimental data (with either a continuous or an instantaneous source) with coexisting super- and sub-dispersion behaviors in the bed-load transport process. Analyses further discover the dual impact of clusters on the dynamics of fine sediment particles, namely, some particles are more likely to be blocked or trapped by clusters, while others have a high probability to be accelerated by the ``flow accelerating belts" between the clusters. Therefore, with proper statistical distributions and relevant parameters for sediment waiting times and hop distances, the CTRW model may efficiently capture the complex dynamics in sediment transport.

P 12.8

Getting the most out of environmental tracers in complex alluvial systems

Morgan Peel[1], Stéphanie Musy[2], Andrea Popp[3], Alvaro Pardo Alvarez[1], Roland Purtschert[2], Daniel Hunkeler[1], Philip Brunner[1]

[1]Centre d'hydrogéologie et de géothermie, Université de Neuchâtel, Emile Argand 11, CH-2000 Neuchâtel (morgan.peel@unine.ch)
[2]Climate and Environmental Physics, University of Bern, Silderstrasse 5, CH-3012 Bern
[3]Department Water Resources & Drinking Water, Eawag, Überlandstrasse 133, CH-8600 Dübendorf

Alluvial aquifers and adjacent streams play a critical role for drinking water supply and irrigation. However, a sound characterization of the spatial and temporal dynamics of water in alluvial systems remains elusive, due to highly anisotropic subsurface properties as well as complex interactions between surface water (SW) and groundwater (GW).

The combination of multiple environmental tracers with different chemical properties and measurement time-scales can provide valuable information on GW/SW mixing ratios and exchange dynamics. However, the interpretation of tracer concentrations in terms of GW residence time often relies on simplified approaches (e.g. assuming homogenous aquifer properties, simplified geometries, uniform tracer inputs, …), which are unable to capture the complexity of dynamic natural systems. One promising yet seldom-used method is the explicit simulation of environmental tracers in physically-based numerical models of alluvial aquifer systems, which can realistically account for most processes affecting measured tracer concentrations.

This study aims to explore in which circumstances and to what extent the explicit simulation of tracers can improve the reliability of numerical models, and better help constrain the properties of alluvial aquifers.

As a first step in this endeavour, a comprehensive dataset was collected during a unique 6-week transient pumping test at an important alluvial aquifer in Switzerland (Emme site). Over this period, the GW abstraction rate was gradually increased from zero to 35'000 l/min, providing the optimal conditions for analysing how tracer measurements reflect system transience. Multiple environmental tracers (^{222}Rn, ^{37}Ar, stable noble gases) were acquired at high spatial and temporal resolutions before, during, and after the experiment. Moreover, core samples recovered from the test site were used to quantify the variability of subsurface ^{222}Rn production rates in the study area.

The acquired dataset forms the basis of a future numerical model, in which measured tracer concentrations and spatially variable ^{222}Rn production rates will be explicitly simulated and integrated into the calibration process. This will allow systematic exploration of the data worth of tracers in terms of informing model parameters and reducing predictive uncertainties of model outputs.

P 12.9

Temperature effects on extreme rainfall modify catchment response

Nadav Peleg[1] & Peter Molnar[1]

[1]*Institute of Environmental Engineering, ETH Zurich, Zurich, Switzerland (nadav.peleg@sccer-soe.ethz.ch)*

Heavy rainfall is expected to intensify with increasing temperatures. The rainfall spatial characteristics also change with increasing temperature, but the type of change (e.g. increase or decrease in the area of the storm) depends on many factors, such as the local vertical uplift conditions (convection) and available humidity. These changes can affect streamflow and sediment transport volumes and peaks. Using a combination of a numerical rainfall generator model and a landscape evolution model, we explored the sensitivity of the hydro-morphological response to heavy rainfall at the small-scale of minutes and hundreds of meters. We examined two types of rainfall, stratiform and convective, using a design storm that represents a typical extreme rainfall event in Alpine region. The design storm was modified to follow different spatial rainfall scenarios, associated with increasing temperatures. We found that the response of the stream discharge and sediment yields are sensitive to changes in the rainfall structure at the small-scale, in particular to changes in the areal rainfall intensity and in the area of heavy rainfall, which controls the total rainfall volume. Surprisingly, the hydro-morphologic response was less sensitive to changes in the peak rainfall intensity. The response was also found to be more sensitive to convective rainfall than stratiform rainfall because of localized runoff and erosion production.

P 12.10

Modelling the effect of irrigation modernization on groundwater recharge

Sandra Pool[1,2], Felix Frances[3], Alberto Garcia-Prats[3], Cristina Puertes[3], Manuel Pulido-Velazquez[3], Carles Sanchis-Ibor[4], Mario Schirmer[1,5], Hong Yang[2,6] & Joaquin Jimenez-Martinez[1,7]

[1]Department of Water Resources and Drinking Water, Eawag, Überlandstrasse 133, CH-8600 Dübendorf (sandra.pool@eawag.ch)
[2]Department Systems Analysis, Integrated Assessment and Modelling, Eawag, Überlandstrasse 133, CH-8600 Dübendorf
[3]Research Institute of Water and Environmental Engineering (IIAMA), Polytechnic University of Valencia, Camino de Vera s/n, E-46022 Valencia
[4]Valencian Center for Irrigation Studies, Polytechnic University of Valencia, Camino de Vera s/n, E-46022 Valencia
[5]Centre of Hydrogeology and Geothermics (CHYN), University of Neuchâtel, Rue Emile-Argand 11, CH-2000 Neuchâtel
[6]Department of Environmental Science, University of Basel, Bernoullistrasse 32, CH- 4056 Basel
[7]Department of Civil, Environmental and Geomatic Engineering, ETH Zurich, Stefano-Franscini-Platz 5, CH-8093 Zürich

The region of Valencia (Spain) is one of the major citrus producers in Europe. The high citrus productivity in the prevailing semi-arid conditions can only be sustained by irrigation with a considerable volume of freshwater. With the aim of moving towards a more sustainable use of freshwater resources, during the last decades national and regional governments have promoted the installation of pressurized drip irrigation systems to replace traditional flood irrigation schemes. However, the (positive) effect of such a modernization on the regional water balance is highly debated. The aim of this study is therefore to improve the understanding of the hydrological functioning of a landscape under irrigation modernization. The core of this study is a distributed hydrological model that was specifically adapted to model the difference in evapotranspiration as a function of irrigation method and crop type. Information about irrigation transition and irrigation volumes at farm level was used to run the model at the aquifer scale of about 500 km^2. Model simulations were checked for plausibility at different spatiotemporal scales for three variables. First, the annual water balance was evaluated with respect to the evaporative index of flood- and drip-irrigated fields. Second, seasonal dynamics of groundwater fluctuations were evaluated at 22 observation wells. And third, daily dynamics of soil moisture in drip-irrigated fields were assessed for their reliability based on process understanding gained at an experimental plot. We found that a spatially distributed multi-variable evaluation was an essential step in evaluating the success of the implementation of drip and flood irrigation into the hydrological model. The results will ultimately help to improve the prediction of groundwater recharge under changing conditions, such as irrigation modernization or climate change.

P 12.11

Elucidating stream-groundwater interactions using real-time, in situ noble gas analysis and numerical modeling

Andrea L. Popp[1], Alvaro Pardo-Alvarez[2], Oliver S. Schilling[3], Stephanie Musy[4], Andreas Scheidegger[1], Morgan Peel[2], Roland Purtschert[4], Daniel Hunkeler[2], Philip Brunner[2], Rolf Kipfer[1]

[1]Department of Water Resources and Drinking Water, Eawag, Swiss Federal Institute of Aquatic Science and Technology, Überlandstrasse 133, CH-8600 Dübendorf (andrea.popp@eawag.ch)
[2]Centre d'Hydrogeologie et de Geothermie, University of Neuchatel, CH-2000 Neuchatel
[3]National Centre for Groundwater Research and Training, Flinders University, AUS-5042 Adelaide
[4]Climate and Environmental Physics, University of Bern, CH-3012 Bern

The quality and quantity of shallow, alluvial groundwater in mountainous areas are particularly vulnerable to the effects of climate change as well as increasing pollution from agriculture and urbanization. Understanding groundwater mixing and travel times in such systems is thus crucial to sustain a safe and sufficient water supply. We used a novel combination of real-time, in situ noble gas analysis to quantify groundwater mixing ratios and travel times during a two-month groundwater pumping test carried out at a drinking water wellfield in the Emmental. Transient groundwater mixing ratios were calculated using He/Ar time series combined with a Bayesian end-member mixing model. Having identified the fraction of recently infiltrated river water allowed us to estimate the mean groundwater travel times using Radon-222. Additionally, we calculated groundwater mixing ratios using a previously calibrated groundwater model built with the physically-based flow simulator *HydroGeoSphere*. The two independently obtained groundwater mixing ratios (i.e., tracer-based and model-based) are in excellent agreement for the majority of our observation time. Our findings show that (i) mean travel times of recently infiltrated river water are in the order of two weeks, (ii) for the majority of the experiment, the fraction of recently infiltrated river water in the sampled groundwater pumping well is high (~70%), and (iii) increased groundwater pumping only has a marginal effect on groundwater mixing ratios and travel times. These insights emphasize that groundwater in pre-alpine alluvial valleys is highly vulnerable to potential pollution originating from surface water due to the high fraction of recently infiltrated river water and short groundwater travel times.

P 12.12

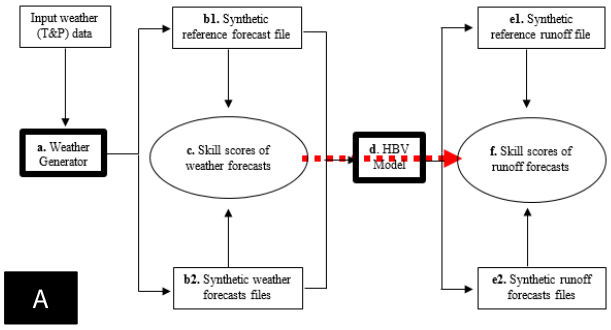
Towards decadal hydro-glaciological forecasts for the hydropower sector

Davide Saurwein[1]

[1]*Institute of Earth Sciences, University of Applied Sciences and Arts of Southern Switzerland, Campus Trevano, Via Trevano, CH-6952 Canobbio (davide.saurwein@supsi.ch)*

Hydropower and water resources management are an important issue in most countries of the world, included Switzerland. The scientific community is currently engaged to produce numerical models and simulations which aim at understanding the most important concurring factors of climate with the support of different tools and methods, at both regional and global scales. In this case, the purpose is to simplify reality while reducing errors and uncertainties related to streamflow prediction. The latter uncertainties can be due to different sources, such as the initial hydrologic conditions of a catchment, the hydrological model's input data and structure, or a too high amount of subjectivity which is applied while implementing such modelling procedures (Beven, 2012).

The aim of this work is to investigate the propagation of uncertainties from the input meteorological forecasts to the resulting streamflow predictions. A weather generator has been used to create synthetic weather decadal forecasts (Ailliot *et al.*, 2015). These forecasts have then been fed into the hydrological model *Hydrologiska Byråns Vattenbalansavdelning* (HBV), and simulations have been run in order to obtain corresponding runoff forecasts. The accuracy of the meteorological and runoff forecasts has been calculated with similar statistical metrics with the aim to assess uncertainty propagation. Three statistical metrics, defined as "skill scores", have been applied for this purpose (Hamill and Juras, 2006). The experiment was performed for two glacierized catchments located in the Swiss Alps, Findelen and Gries. The simulations were performed by assuming different scenarios of glacier extent in order to observe the influence of the amount of ice present in the catchment on the results. The effect of a varying input glacier extent on simulated runoff has then been studied, together with an assessment of the modifications on the hydrological regime. Simulations have been run by applying the recently-implemented glacier routine in the hydrological model with different settings in order to analyze how skill transfer can be affected. In addition, a sensitivity analysis has been performed on parameters and routines of the hydrological model in order to study their contribution to model efficiency.



Skill Score name	Mathematical formula	Variability range
Root Mean Square Error (RMSE)	$\sqrt{\frac{1}{N}\sum_i (f_i - o_i)^2}$	0 (best score) < RMSE < ∞ (worst score)
Reduction of Variance (RV)	$1 - \frac{\frac{1}{N}\sum (f_i - o_i)^2}{var_f^2}$	-∞ (worst score) < RV < 1 (best score)
Correlation Coefficient (CC)	$\frac{\frac{1}{N}\sum_i^N (f_i - \bar{f}) * (o_i - \bar{o})}{sd_f * sd_o}$	-1 (worst score) < CC < 1 (best score)

B

Figure 1. Methodology of the project. (A) General description of the methodology; (B) Skill scores used for the quantification of decadal forecasts.

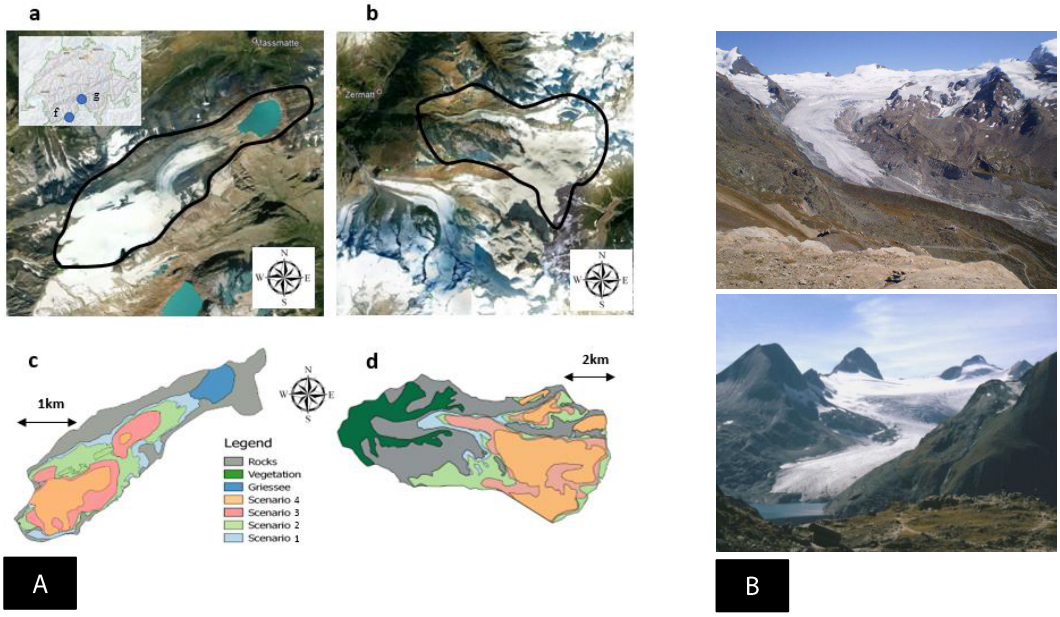


Figure 2. (A) Geographic situation of Gries and Findelen glacierized catchments. In the localization map of the two catchments, "f" indicates the Findelen catchment, while "g" represents the Gries catchment. (B) Visual representations of Findelen glacier (upper picture) and Gries glacier (lower picture).

It has been observed that the influence of precipitation on runoff forecasts is lower than the one of temperature for highly-glacierized catchments. This influence increases with diminishing glacierization. In a hypothetical ice-free catchment, the effect of precipitation on skill transfer tends to become more relevant, for both Findelen and Gries catchments. Other important factors of skill transfer are the lead time from which a forecast is produced and the application of different settings of the glacier routine of the hydrological model.

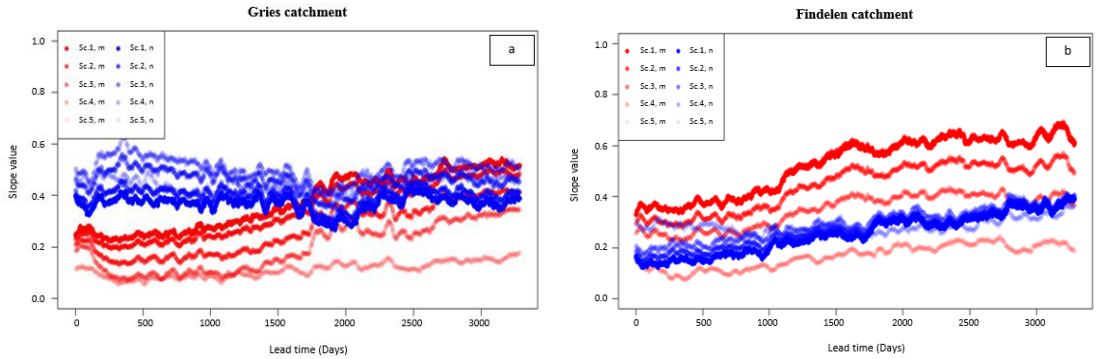


Figure 3. Evolution of slope parameters 'm' and 'n', the colour saturation is related to the degree of glacierization related to each Scenario ("*Sc.*" in the figure).

REFERENCES

Ailliot, P., Allard, D., Monbet, V. & Naveau P. 2015: Stochastic weather generators: an overview of weather type models, Journal de la Société Française de Statistique 156, 101-113.

Beven, K. 2012: Rainfall-Runoff Modelling (2nd Edition), Wiley-Blackwell Editors, Lancaster University, UK.

Hamill, T.M. & Juras J. 2006: Measuring forecast skill: is it real skill or is it the varying climatology? Quarterly Journal of the Royal Meteorological Society 132, 2905-2923.

P 12.13

The influence of trophic history and lake mixing regime on long-term phosphorus fractions retention in sediments of deep, eutrophic lakes: a case study from Lake Burgäschi, Switzerland

Luyao Tu[1], Sönke Szidat[2], Hendrik Vogel[2], Paul Zander[1], Martin Grosjean[1]

[1]Oeschger Centre for Climate Change Research and Institute of Geography, University of Bern, Switzerland
[2]Oeschger Centre for Climate Change Research and Institute of Chemistry and Biochemistry, University of Bern, Switzerland

Lake eutrophication and anoxic conditions in the hypolimnion can influence the sediment phosphorus (P) release on short time scales, which is the main cause of the delay of lake recovery in many freshwater deep lakes (Burley et al., 2001). It is yet not clear how long-term sediment P-fraction retention responded to hypolimnion-water redox conditions and eutrophication history in the further past. In this study, we investigated the P species and changes of P-fraction retention in sediment profiles since the early 1900s in Lake Burgäschi, a deep eutrophic lake in Swiss Plateau. The changes of sediment P-fraction retention were assessed with respect to lake trophic evolution (sedimentary green-pigments proxy; Schneider et al., 2018), hypolimnion oxygenation regime (Fe/Mn ratio proxy; Zarczynski et al., 2019) and sediment geochemical characteristics. The results show that dominant factors controlling the long-term retention of labile P-fractions (NaCl-TP, NaBD-TP, and NaOH-TP) were autochthonous Fe-and Mn preserved in anoxic sediments, which were determined by past redox conditions in hypolimnion water. The considerable declines in total P and these labile P fractions retention during 1977 to 2017 CE were suggested to be related to eutrophication-incurred anoxic conditions and hypolimnetic withdrawal restoration in the lake during the period. By comparison, refractory HCl-P (Ca-P) fraction retention, to a large extent, resulted from authigenic $CaCO_3$-P precipitation and increased with higher eutrophic levels. Large amounts of Ca-P fraction predominated in the surface sediments after 1977 CE, indicating a potential negative feedback to eutrophication. The study implies that in seasonally-stratified deep lakes like Lake Burgäschi, hypolimnetic withdrawal might be an effective restoration method to reduce the retention and availability of sediment P.

REFERENCES

Burley, K. L., E. E. Prepas, and P. A. Chambers, 2001, Phosphorus release from sediments in hardwater eutrophic lakes: the effects of redox-sensitive and-insensitive chemical treatments: Freshwater Biology, v. 46, p. 1061-1074.

Schneider, T., D. Rimer, C. Butz, and M. Grosjean, 2018, A high-resolution pigment and productivity record from the varved Ponte Tresa basin (Lake Lugano, Switzerland) since 1919: insight from an approach that combines hyperspectral imaging and high-performance liquid chromatography: Journal of Paleolimnology, p. 1-18

Zarczynski, M., A. Wacnik, and W. Tylmann, 2019, Tracing lake mixing and oxygenation regime using the Fe/Mn ratio in varved sediments: 2000year-long record of human-induced changes from Lake Zabinskie (NE Poland): Sci Total Environ, v. 657, p. 585-596.

P 12.14

Soil hydrological monitoring for regional landslide early warning

Adrian Wicki[1], Manfred Stähli[1], Christian Hauck[2], Peter Lehmann[3]

[1]Swiss Federal Research Institute WSL, Mountain Hydrology and Mass Movements, Zürcherstrasse 111, CH-8903 Birmensdorf (adrian.wicki@wsl.ch)
[2]University of Fribourg, Departement of Geosciences, Chemin du Musée 4, CH-1700 Fribourg
[3]Eidgenössische Technische Hochschule Zürich, Institute of Biogeochemistry and Pollutant Dynamics, Universitätstrasse 16, CH-8092 Zürich

In mountainous terrain, rainfall-induced shallow landslides pose a serious risk to people and infrastructure due to a widespread occurrence and the short time interval between activation and failure. Regional landslide early warning systems (LEWS), which are mostly based on empirically derived rainfall exceedance thresholds, have demonstrated to be a valuable tool to inform decision makers about the imminent landslide danger or to issue warnings to the public.

Recent studies have shown that the forecast quality of LEWS can be improved significantly after the inclusion of soil hydrological measurements. In Switzerland, it could be demonstrated that soil moisture data alone from existing monitoring networks inhibits specific information about the regional landslide activity, particularly the antecedent wetness state and the increase of soil moisture during an infiltration event (Wicki et al., in preparation). Questions remain whether the predominantly flat measurement sites are representative for critical saturated conditions at landslide prone hillslopes and which instrumentation is most suitable to monitor these conditions.

To answer this, a hillslope and a flat location in a landslide prone area in the Napf region (Swiss Prealps) were equipped with soil moisture probes, tensiometers, electrical resistivity tomography (ERT) profile lines and shallow groundwater wells. Differences in the hydrological dynamics between the two sites are analysed to assess the representativeness of flat sites for critical hydrological conditions at hillslope locations. Further, different sensor types are compared with regards to their ability to detect such conditions and their suitability for the use in a real-time monitoring system.

First results from summer 2019 indicate that the local topography imposes distinct differences on the soil moisture dynamics. Near the surface, soil moisture variability is larger at the flat site which can be attributed to higher evaporation rates (aspect, shading), less surface runoff and different soil properties. At the hillslope site, soil wetness variability is higher at depth due to subsurface flow near the shallow bedrock interface. Further, it could be shown that soil moisture probe readings can be affected considerably by the installation surroundings, and near-surface tensiometers can be rapidly out of measurements range during very dry conditions. While both effects are problematic with respect to the use in a monitoring system, the combination of the two sensor types can help to partially cope with these problems.

13. Public Engagement with Climate Change: Interdisciplinary Challenges

Moritz Gubler, Marc Eyer, Adrian Brügger, Kathrin Nägeli, Maurice Skelton

Swiss Association for Geographic Education (VGDch)

TALKS:

13.1 Cologna V., Siegrist, M.: The role of trust for climate change mitigation and adaptation behaviour: a meta-analysis

13.2 Gadient-Brügger A., Gubler M.: To strike or not to strike? Motivations of young people in Switzerland to (not) participate in climate strikes

13.3 Gubler M.: Climate change concern among adolescents – a matter of perceived distance?

13.4 Linsbauer A., Christen J., Imhof A., Meeus B., Millhäusler A., Lochmatter A.: «Expedition 2 Grad» – A climate change experience in Virtual Reality at Great Aletsch glacier: Implementation, exhibition success and first results from the evaluation

13.5 Reinfried S.: Patterns of Interpretation of Climate Change in Teachers' Statements and Consequences for Climate Communication in Teaching

13.6 Schrot O., Peduzzi D., Keller L.: Can we build cognitive adaptive capacity through climate change education? If yes, how can it be assessed by scientific means?

13.1

The role of trust for climate change mitigation and adaptation behaviour: a meta-analysis

Viktoria Cologna[1], Michael Siegrist[1]

[1]*Institute for Environmental Decisions, ETH Zürich, Universitätstrasse 22, 8092 Zürich, Switzerland*

Choosing between different mitigation and adaptation behaviours can be a complex cognitive task, especially when knowledge of climate change is low. Trusting experts can help to alleviate the cognitive complexity of evaluating behavioural decisions due to serving as a heuristic in decision making. Gaining a deeper understanding of how trust in certain actors influences individuals' mitigation and adaptation behaviours is, therefore, key. We present results of a meta-analysis that examines the role of trust in institutions, scientists, industry, environmental groups and people in general, in relation to different mitigation and adaptation behaviours. By drawing on data from 53 studies conducted in over 21 different countries, we find that trust in scientists and environmental groups is strongly associated with mitigation and adaptation behaviours. Conversely, this association is weak for individuals' trust in institutions and industry, while it is negligible for general trust measures. We discuss the implications that these findings have for climate scientists and how experts could potentially increase trust levels to foster engagement in mitigation and adaptation behaviours.

In a second study, we explored (among other factors) how trust in the Swiss government and in climate scientists influences participation in the Fridays for Future climate strikes in Switzerland with a sample (N = 638) of university students. We find that trust in the Swiss government to act on climate change decreases the likelihood of participation, while trust in climate scientists to provide correct information on climate change increases the likelihood of participation. We explore and discuss determinants of large-scale collective action on climate change.

13.2
To strike or not to strike? Motivations of young people in Switzerland to (not) participate in climate strikes

Adrian Gadient-Brügger[1] & Moritz Gubler[2,3,4]

[1]*Institut für Marketing und Unternehmensführung, Universität Bern, Engehaldestrasse 4, CH-3012 Bern (adrian.gadient@imu.unibe.ch)*
[2]*Institut für Forschung, Entwicklung und Evaluation, Pädagogische Hochschule Bern, Fabrikstrasse 8, CH-3012 Bern (hmoritz.gubler@phbern.ch)*
[3]*Oeschger-Zentrum für Klimaforschung, Universität Bern, Hochschulstrasse 4, CH-3012 Bern*
[4]*Geographisches Institut, Universität Bern, Hallerstrasse 12, CH-3012 Bern*

Since the first climate strikes in December 2018, ten thousands of students across multiple Swiss cities regularly stepped out of schools, demanding the declaration of climate emergency and climate justice. Accompanied by remarkable amounts of media attention and controversial discussions among the public, the climate strike movement received encouragement from political and scientific communities. However, relatively little is known about potential drivers and dynamics of this new form of collective engagement for climate change, as well as how it is perceived by adolescents and young adults.

To explore individual motivations for participating – or not – in climate strikes and to examine speculations of the media and public discourse about them, two online-surveys with closed- and open-ended questions were conducted in February and May-August 2019. Answers from a total of 6'605 (study 1: *N*=888; study 2: *N*=5'717) students (14 - 25 years) of which ca. 44% and 33% respectively participated in the strikes were analysed using a mixed-methods approach.

Preliminary results show that the majority of strikers was motivated for participation by concerncs about the environment and humanity, by the urgency and severity of climate change, and by the aim to foster action among the public and politicians. The most prominent reasons for not participating in the strikes were the fear of negative consequences due to absence in school or at work and the belief that participating would be hypocritical without acting in a climate-friendly way in everyday-life.

13.3

Climate change concern among adolescents - a matter of perceived distance?

Moritz Gubler[1,2,3], Adrian Brügger[4], & Marc Eyer[5]

[1]Institut für Forschung, Entwicklung und Evaluation, Pädagogische Hochschule Bern, Fabrikstrasse 8, CH-3012 Bern (moritz.gubler@phbern.ch)
[2]Oeschger-Zentrum für Klimaforschung, Universität Bern, Hochschulstrasse 4, CH-3012 Bern
[3]Geographisches Institut, Universität Bern, Hallerstrasse 12, CH-3012 Bern
[4]Institut für Marketing und Unternehmensführung, Universität Bern, Engehaldestrasse 4, CH-3012 Bern
[5]Institut Sekundarstufe II, Pädagogische Hochschule Bern, Fabrikstrasse 8, CH-3012 Bern

Effective climate change education and communication strategies need to take into account people's perceptions and beliefs. A root difficulty is that the general public tends to perceive climate change as a psychologically distant phenomenon - something that, if at all, happens not here, not now, and not to oneself. This may make it difficult to imagine its impact and seriousness and consequently, the perceived personal relevance and concern about the issue may be low. Lack of concern is problematic because concern is a key factor for triggering climate action. However, previous studies examining distance perceptions and concern about climate change have almost exclusively focussed on samples of the general public made up of adults. Thus, little is known about how psychologically distant or close climate change is perceived by a highly relevant and so far overlooked population segment: adolescents.

In this study, we explored Swiss adolescents' (N = 587, 14 – 17 years) perceptions of psychological distance to climate change risks and how it relates to their concerns about it. Based on a closed-ended questionnaire conducted in October and November 2018, we used multiple linear regression models to reveal linkages between risk perceptions and climate change concern. Furthermore, latent profile analysis allowed for a classification of the students with regard to patterns of similar distance perceptions.

Our findings show that adolescents perceived climate change to be a certain and present risk. However, they perceived climate change to rather affect other places and other people more than themselves. Regression analysis revealed a significant inverse relationship between distance and concern: respondents who felt psychologically closer to the phenomenon expressed greater concern. In addition, we identified four distinct perception types which also differed with regard to their level of concern about climate change. The findings contribute to the understanding of how young people perceive climate change, which should assist in designing education and communication strategies to make it more salient for individual engagement.

13.4

«Expedition 2 Grad» – A climate change experience in Virtual Reality at Great Aletsch glacier: Implementation, exhibition success and first results from the evaluation

Andreas Linsbauer[1 2], Jonas Christen[3], Andreas Imhof[4], Bruno Meeus[1] Andrea Millhäusler[5], Alessandra Lochmatter[6]

[1]Département de Géosciences, Université de Fribourg, Chemin du Musée 4, 1700 Fribourg (andreas.linsbauer@unifr.ch)
[2]Geographisches Institut, Universität Zürich, Winterthurerstrasse 190, 8057 Zürich
[3]Knowledge Visualization, Zürcher Hochschule der Künste, Pfingstweidstr. 96, 8031 Zürich
[4]Abteilung Forschung und Entwicklung, Pädagogische Hochschule Graubünden, Scalärstrasse 17a, 7000 Chur
[5]Schweizerischer Nationalpark, Schloss Planta-Wildenberg, 7530 Zernez
[6]World Nature Forum, UNESCO-Welterbe Swiss Alps Jungfrau-Aletsch, Bahnhofstrasse 9a, 3904 Naters

Climate change has become a major topic in various media channels and is important for the general public and in Swiss politics. Young people started activism all over Switzerland with “climate strikes”, the recently launched “Gletscherinitiative” is about to be submitted and the Federal Council now aims for a climate-neutral Switzerland by 2050. The general interest in the topic of climate change is high and further increasing.

Our SNF Agora project “The 2°C target in the Alps – An Experience in Virtual Reality” also known as «Expedition 2 Grad» (http://www.expedition2grad.ch/) is placed within this field of interest. The main objective of «Expedition 2 Grad» is to make the production and the consequences of climate change tangible in virtual reality (VR) and to offer tools to rethink and re-imagine society’s relation to nature. At a tablet-station and with a VR-headset vistitors undertake an expedition around the Great Aletsch glacier and interactively experiences the effects of increasing temperatures on the alpine environment since the 19th century. John Tyndall, a 19th century English physicist, mountaineer and a pioneer in climate science, accompanies the users on their expedition. He acts as a storyteller and explains the very basic concept of how humanity got to a point where it could influence the global climate. Tyndall takes the users on a journey through time watching the retreat of the glacier until 2100 when most of its mass will have disappeared. Throughout this journey through space and time, emotions are triggered and the users experience the region of Aletsch through the eyes of their grandparents and of future generations.


Figure 1. The scientist and mountaineer John Tyndall (1820-1893), guides the viristors at the «Expedition 2 Grad».through space and time

This VR-experience with tablet station and VR-headset is open to all museum visitors. However, the main target audience of the project are school classes of Secondary and Gymnasium level (12-17 years). Our approach is to combine emotional involvement with a space for debate about the causes and possible actions to take. School classes get involved in such reflective debates thanks to the accompanying pedagogical program offered by the partner museums. A key point is a final discussion guided by experts. It aims to show the participants different ways of action and to motivate them to take responsibility for an own contribution in solving the climate problem. The audience should not leave with a guilty conscience, but should become aware that an individual can inspire others by own actions, that one can find alternative solutions with like-minded people and that collectively organized, one can influence politicians and decision-makers.


Figure 1. The Aletsch glacier in virtual reality, a view from the Eggishorn nowadays (left) and in future (middle). An the rigth site, youths experiencing the «Expedition 2 Grad» at Nationalparkzentrum, Zernez.

An important additional component is the pedagogical evaluation by a web-based questionnaire in which the users of the VR-experience answer several questions, to test aspect of the VR-experience (e.g. realistic experience, wellbeing, helpfulness of several elements) and possible effects of program-participation on the severity of problem-perception concerning climate change and retreat of glaciers. The 33 classes participating the program at the visitor center of the Swiss national park in Zernez were surveyed three times: bevor/ after the program and with a delay of a month.

First results indicate that participants perceive the VR-experience as realistic, feel comfortable and rarely bored. This impression depends not on age or prior experience with VR-technology (except of wellbeing). Even bevor program-participation participants indicate high values of concern on climate change and glacier retreat (an indicator for motivation building). After the program, this values increase significantly (but with small effect size). As general indicator for satisfaction with the whole program, 84% of participants recommend (or mostly/rather recommend) their family and friends to participate at the “Expedition 2 Grad”. For the second implementation of the program at the Word Nature Forum in Naters, the results could be used for program adaptions and for refining the evaluation procedure.

P 13.5
Patterns of Interpretation of Climate Change in Teachers' Statements and Consequences for Climate Communication in Teaching

Sibylle Reinfried

GeoEduc, Didaktische Beratung, Flühgasse 33, CH-8008 Zürich (reinfried@geoeduc.ch)

Teacher language is an essential factor in the construction of meaning by learners. An explorative pilot study investigated how teachers communicate climate change. The aim was to discover frames of interpretation in teacher statements in order to generate supra-individual patterns of interpretation by using a combination of qualitative and quantitative methods. Interviews with eight secondary school teachers served as data source. Three patterns of interpretation could be identified, two of which can influence the interpretation of climate change among recipients in such a way that they can promote willingness to act, while the third pattern can inhibit motivation to act.

REFERENCES

Reinfried, S., & Künzle, R. 2019: Deutungsmuster des Klimawandels in Aussagen von Lehrpersonen und Konsequenzen für die Klima-Kommunikation im Unterricht. Zeitschrift für Geographiedidaktik, 47(2), 1-22.

P 13.6

Can we build cognitive adaptive capacity through climate change education? If yes, how can it be assessed by scientific means?

Oliver Schrot[1], Dunja Peduzzi[1] & Lars Keller[1]

[1]*Institut für Geographie, University of Innsbruck, Innrain 52f, AUT-6020 Innsbruck (Oliver.Schrot@uibk.ac.at)*

Earth's climate is changing and climate-related impacts become increasingly apparent. For example, the heatwave over continental Western Europe in July 2019 was found to be closely linked to human interference, making record-breaking heatwaves much more likely (Vautard et al. 2019). Today's young people, like teenagers, already are affected by extreme temperatures, and they will be challenged by other climate-related phenomena throughout their life-times. Consequently, they are increasingly asked to develop knowledge, respectively skills for solving challenges related to climate change (CC), and for safeguarding a more sustainable future (Gharabaghi & Anderson-Nathe, 2018).

Against this background, CC education comes as a strategy to foster young peoples' engagement with CC effects. CC education may build young learners' cognitive adaptive capacity, which is understood as an individual's intellectual ability to process thoughts and actions related to CC adaptation. In detail, cognitive adaptive capacity, as described by Grothmann and Patt (2005), is determined by (1) subjective risk perception and (2) subjective coping appraisal. Subjective risk perception depends on one's (1a) perception of being exposed to CC (i.e., perceived probability), and one's (1b) assessment on the degree of harmful CC effects occuring to him/her (or not) (i.e., perceived severity). In contrast, subjective coping appraisal is determined by one's (2a) general belief in protective actions (i.e., perceived adaptation efficiacy), and one's (2b) self-assessment of being capable to perform adaptive actions (i.e., perceived self-efficacy) (see Figure 1).

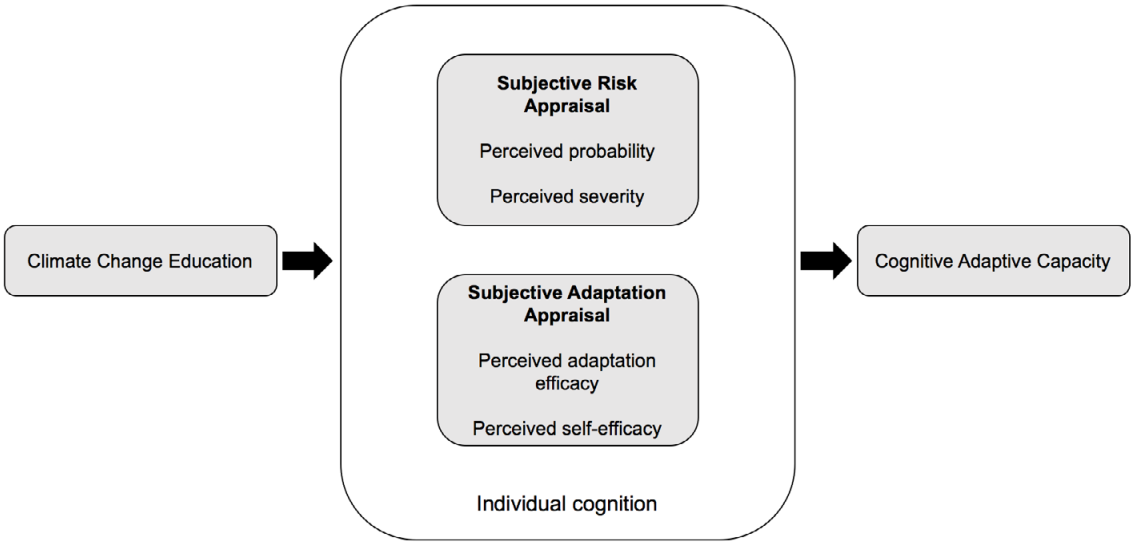


Figure 1: Climate change education targeting young peoples' cognitive adaptive capacity, adapted from Grothmann and Patt (2005)

Now, this research hypothesizes that CC education may build teenagers' cognitive adaptive capacity, as inquiry-based learning confronts teenagers' with adaptation strategies to local/regional CC risks (Keller et al. 2019). In this context, the research-education cooperation *Generation F³ - Fit for Future* is presented, in which 175 high-school students collaborated with 57 scientific and non-scientific experts on CC adaptation in North Tyrol (Austria) and South Tyrol (Italy) in school years 2017/18 and 2018/19. *Generation F³ - Fit for Future* encouraged students to carry out their own research project dealing with current challenges related to CC adaptation in their home-regions.

In methodological terms, a web-based questionnaire yielded treatment and control group students' (N=235) dimensions of cognitive adaptive capacity. Then, a Wilcoxon-signed rank test was applied to evaluate potential changes in high-school students' dimensions of cognitive adaptive capacity prior and after CC education, respectively inquiry-based learning. Quantitative data will be triangulated with findings from problem-centered interviews (N=45). In a final step, documentary method will be used to contrast performances from intervention and control group students.

Findings suggest that CC education, respectively inquiry-based learning positively affects two dimensions of high-school students' cognitive adaptive capacity, mainly (2a) perceived adaptation efficacy and (1b) perceived severity of CC effects. Little evidence comes with (2b) perceived self-effiacy. First qualitative findings confirm that CC education was capable to strengthen high-school students' cognitive skills necessary to solve local/regional problems in CC adaptation and deepened their understanding of adaptation measures. Effects are unequal across school classes. As fuzziness is inherent to the concept of cognitive adaptive capacity itself, mixed-methodologies and qualitative competence-oriented testing are recommended for further research addressing young peoples' cognitive adaptive capacity.

REFERENCES

Gharabaghi, K., & Anderson-Nathe, B. 2018: Children and youth in the era of climate change, Child & Youth Services, 39(4), 207-210 doi:10.1080/0145935X.2018.1557882

Grothmann, T., & Patt, A. 2005: Adaptive capacity and human cognition: The process of individual adaptation to climate change, Global Envrionmental Change, 15(3), 199-213 doi: 10.1016/j.gloenvcha.2005.01.002

Keller, L., Stötter, J., Oberrauch, A., Kuthe, A., Körfgen, A., & Hüfner, K. 2019: Changing Climate Change Education: Exploring moderate constructivist and transdisciplinary approaches through the research-education co-operation *k.i.d.Z.21*, GAIA-Ecologocal Perspectives for Science and Society,28(1),35-43 doi:10.14512/gaia.28.1.10

Vautard, R., Boucher, O., van Oldenborgh, G.J., Otto, F., Haustein, K., Vogel, M.M. … & van Alst, M. 2019: Human contribution to the record-breaking July 2019 heatwave in Western Europe. Retrieved from https://www.worldweatherattribution.org/wp-content/uploads/July2019heatwave.pdf 11/08/2019

14. Environmental Biogeochemistry of Trace Elements

Montserrat Filella, Moritz Bigalke, Adrien Mestrot, Andreas Voegelin, Lenny Winkel

TALKS:

14.1 Filella M.: Fact-checking when working outside the biogeochemist 'comfort zone': lessons learned when trying to understand tantalum and tellurium behaviour in the environment

14.2 Grolimund D., Frasca B., Leupin O.X., Savoye S., Winkel L.H.E., Curti E., Michelot J., Wittebroodt C.: Reactive transport of redox-sensitive Selenium in geological media: New insights from an inside view

14.3 Guan H., Crespi M.C., Caggìa V., Liu X.W., Mestrot A., Bigalke M.: Plant and microbiome-dependent effects on arsenic speciation in soil water

14.4 Jiskra M., Sonke J.E.: Source attribution of mercury in freshwater fish using stable mercury isotope fingerprints

14.5 Kaegi R., Gogos A., Wielinski J., Voegelin A.: Distinguishing between anthrogogenic and natural CeO_2 inputs into watewater systems

14.6 Marafatto F.F., Ferreira-Sanchez D., Dähn R., Grolimund D., Voegelin A.: Thallium redox speciation in soil Mn concretions imaged by synchrotron X-ray spectroscopy

14.7 Mestrot A., Caplette J., Gfeller L., Lei D., Liao J., Xia J., Zhang H., Feng X.: Release and biovolatilisation of antimony from contaminated soils

14.8 Schmidt F., Schäffer A., Lenz M.: Environmental fate of perovskite photovoltaics

14.9 Slaveykova V.I., Regier N., Beauvais-Flueck R., Cosio C., Majumdar S., Keller A.: Insigth from omics to uncover the effect of mercury compounds to phytoplankton

14.10 Stanisic L., Caplette J.N., Pfister S., Lepke T., Mestrot A.: Improvement of antimony analyses in soil matrices

14.11 Wick S., Baeyens B., Peña J., Pfenninger N., Voegelin A.: Thallium adsorption onto clay minerals and Mn oxides in soils

14.12 Wiggenhauser M., Aucour A.-M., Telouk P., Campillo S., Bureau S., Landrot G., Ma F.J., Sarret G.: Cadmium transfer in contaminated soil-rice systems: insights from solid-state speciation and isotope fractionation

14.13 Wilson S.C., Doherty S., Tighe M., Milan L.: INVITED TALK: Arsenic and antimony speciation, sequestration, mobilisation and dispersion in a highly contaminated river catchment: Differences revealed for improved risk assessment.

POSTERS:

P 14.1 Tercier-Waeber M., Abdou M., Bakker E., Schäfer J., Novellino A., Alloisio S., Bonofiglio L., Petersen W., Blandfort D.: Innovative autonomous field monitoring of bioavailable metal species, macronutrients, phytoplankton to deeper understand their behaviour, interaction and fate (MEPHY)

P 14.2 Catrouillet C., Hirosue S., Manetti N., Peña J.: Arsenic removal from manganese-containing groundwaters using Fe(0) electrocoagulation – modelling

P 14.3 Cossart T., Garcia-Calleja J., Pedredo Z., Ouerdane L., Tessier E., Kavanagh K., Worms I., Amouroux D., Slaveykova V.: Bioaccumulation and biotransformation of mercury compounds: Focus on green algae and cyanobacteria

P 14.4 Gehin G.: Towards an approach to assess the reactivity of biogenic manganese oxides

P 14.5 Ingold P., Wanner C.: Stability and As adsorption of nanocrystalline Al-hydroxysulfates forming during acid rock drainage

P 14.6 Li M., Slaveykova V.I.: Cocktail effect of nanoTiO_2 mixtures with mercury to green alga Chlamydomonas reinhardtii

P 14.7 Mahat S., Gfeller L., Jenni L., Mestrot A.: Bioaccumulation of mercury in the terrestrial food chain: method development and first results

P 14.8 ThomasArrigo L., Gubler R., Kretzschmar R.: Arsenic adsorption and oxidation by Fe(II)-activated magnetite and maghemite

P 14.9 Linqiong W., Slaveykova V.I.: Response of ammonia oxidizing archaeal and bacteria microbial to co-contamination of decabromodiphenyl ether and copper in river sediments

P 14.10 Wille M., Kurzweil F., Dellwig O.: Mn authigenesis at the Landsort Deep, Baltic Sea and its impact on Mo isotopes

P 14.11 Zelano I.O., González Holguera J., Peña J.: Oxidation of bioavailable carbon substrates by Mn oxides and the competition effect with bacteria

14.1

Fact-checking when working outside the biogeochemist 'comfort zone': lessons learned when trying to understand tantalum and tellurium behaviour in the environment

Montserrat Filella[1]

[1]Department F.-A. Forel, University of Geneva, Boulevard Carl-Vogt 66, CH-1205 Geneva (montserrat.filella@unige.ch)

Tantalum (Ta) and tellurium (Te), that were formerly considered scientific curiosities, have now become essential for new applications and significant dispersion in the environment is to be expected in the near future. However, trying to understand and predict their environmental behaviour rapidly becomes a frustrating exercise: scarce and unreliable data, even on total concentrations in the various environmental compartments; lack of 'reasonable' analytical methods; poor knowledge of the behaviour of the elements even in simple, aqueous systems (solution chemistry being considered as a relic of the past, most thermodynamic data is more than 50 years old, when existing). These difficulties that might look irrelevant since, finally, Ta and Te do not look as being serious environmental problems, are just the tip of the iceberg: the same situation exists for many other elements of the periodic table as soon as you are not interested in Hg, As, Pb, Cd, etc. On the other hand, gathering the needed information is a tedious, time-consuming exercise that usually does not go further than the elaboration of narrative reviews; a rather old-fashioned approach in these times of AI. All these questions will be explored through the discussion of Ta and Te case-studies.

14.2

Reactive transport of redox-sensitive Selenium in geological media: New insights from an inside view

Daniel Grolimund[1,1], Benjamin Frasca[2,3], Olivier X. Leupin[4], Sebastien Savoye[2], Lenny H.E. Winkel[5], Enzo Curti[1], Jean-Luc Michelot[3], Charles Wittebroodt[6]

[1]Paul Scherrer Institute, CH-5232 Villigen PSI, Switzerland
(1correspondence: daniel.grolimund@psi.ch)
[2]CEA, F-91191 Gif-sur-Yvette, France
[3]CNRS–Université de Paris-Sud, F-91405 Orsay, France
[4]NAGRA, CH-5430 Wettingen, Switzerland
[5]ETHZ & EAWAG, CH-8600 Dübendorf, Switzerland
[6]IRSN, F-92265 Fontenay Aux Roses, France

The environmentally safe disposal of radioactive waste is a major and pressing challenge for modern societies. Safety assessment calculations identified ^{79}Se in high level radioactive waste as a key radionuclide that could contribute to the release of radioactivity in the biosphere. Se(IV) was identified as the predominant form in vitrified high level waste. The oxyanionic character of ^{79}Se in combination with its long half-life of $3.27 \cdot 10^5$ years causes an enhanced risk potential for radiotoxic impairment of the biosphere.

The prevailing redox conditions in the spreading medium and corresponding speciation strongly influence the fate of Se. Reduced Se species [Se(0), Se(-II)] exhibit a low solubility in aqueous systems resulting in a limited mobility and bioavailability. Under oxidizing conditions, the Se speciation is dominated by the oxyanions $Se^{IV}O_3^{2-}$ and $Se^{VI}O_4^{2-}$, which have higher solubities. In addition to these higher solubities, clay based engineered and geological barrier systems are inefficient in retaining dissolved Se and other anionicspecies via sorption, due to the predominantely negatively charged mineral surfaces. Thus anionic nuclides might eventually diffuse from the repository through the hostrock reaching the biosphere.

The present study visualizes in-situ micro-scale reactive transport of Se(IV) within undisturbed natural samples of two potential deep argillaceous hostrock formations (Opalinus and Upper Toarcian claystone). To characterize the transport and Se-mineral interactions in the micro-heterogenous clay rock matrix, we used a combination of synchrotron-based micro-imaging techniques – μXRF, μXRD, and μXAS – to record comprehensive sets of two-dimensional, multimodal chemical images. An illustrative sub-set is depicted in Figure 1. These chemical maps reveal the reactive (solute) transport pattern of Se within the clay rock, the corresponding spatial distribution of the Se oxidation state as well as their correlation with geochemical heterogeneity represented by elemental and mineral phase distributions.

Such spatially resolved chemical information from within the undisturbed porous medium turned out to be a necessity concerning the identification of the most relevant reactive transport processes (see also, e.g., Grolimund et al., 2016; Kaplan et al., 2017; Crean et al., 2014).

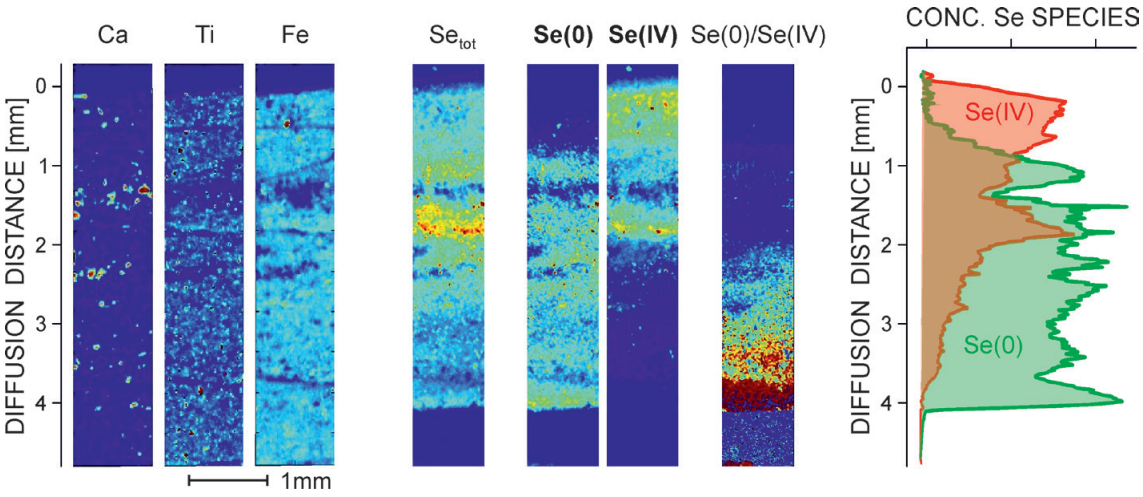


Figure 1. Reactive transport of Se(IV) within undisturbed Opalinus claystone. Geochemical heterogeneity illustrated by elemental distribution maps of major elements (left panel). Redox state specific reactive transport pattern of Se (middle panel). Integrated diffusion profiles (right panel).

REFERENCES

Grolimund, D., Wang, H.A.O, Van Loon, L.R., Marone, F., Diaz, N., Kaestner, A., & Jakob, A., Microscopic Chemical Imaging: A Key to Understand Ion Mobility in Tight Formations, CMS Workshop Lecture Series, Chapter 9, 105-128, in: Filling the Gaps – from Microscopic Pore Structures to Transport Properties in Shales (T. Schäfer, R. Dohrmann, and H.C. Greenwell, editors). CMS Workshop Lectures, 21. The Clay Minerals Society, Chantilly, Virginia, USA. ISBN - 978-1-881208-46-4, (2016).

U. Kaplan, U., Amayri, S., Fröhlich, D.R. , Drebert, J., Grolimund, D., Borca, C.N., & Reich, T., Geochemical Interactions of Plutonium(VI) with Opalinus Clay Studied by Spatially Resolved Synchrotron Radiation Techniques, Environ. Sci. Technol., 51, 7892-7902, (2017).

Crean, D.E., Livens, F.R., Stennett, M.C., Grolimund, D., Borca, C.N., & Hyatt, N.C., Microanalytical x-ray imaging of depleted uranium speciation in environmentally aged munitions residues, Env. Sci. Technol., 48/3, 1467-1474, (2014).

14.3

Plant and Microbiome-dependent Effects on Arsenic Speciation in Soil Water

Hang Guan [1], Miquel Coll Crespi[1], Veronica Caggìa[2], Xiaowen Liu[1], Adrien Mestrot[1], Moritz Bigalke[1]

[1]Institute of Geography, University of Bern, Hallerstrasse 12, CH-3012 Bern (hang.guan@giub.unibe.ch)
[2]Institute of Plant Sciences, University of Bern, Altenbergrain 21, CH-3013 Bern

Arsenic (As) is a trace metalloid known as “the king of poisons”. Due to natural processes and anthropogenic activities, As is ubiquitous in various environmental compartments. As is also a class one carcinogen and its high toxicity correlates with a host of human diseases e.g. skin cancer. The speciation of As largely regulates its mobility, bioavailability and toxicity in the environment. As speciation is not only driven by inorganic parameters (pH, redox) but also controlled by the interactions with plants and microbiota. We performed an experiment to investigate the cascading health effects of As through the food chain from soil to humans. As the first part of the experiment we will report on the effects of plants and soil microbiota on As speciation in soils. Soil microbiota can enzymatically transform As from inorganic to less-toxic organic forms.

In the experiment, we set up nine experimental groups: three soil treatments (normal soil (NS), sterilized soil (SS) and first-sterilized soil reconditioned with microbiome (SM)) intersecting with three As concentration groups (0, 100 and 200 ppm). In each treatment group, 10 pots with maize plants and three pots without maize were cultivated. For the As treatments we spiked soil with different levels of As. After soil incubation for two months to allow for equilibration of the As with the soil, we grew 99 maize plants and regularly determined As speciation in the soil pore water with HPLC-ICP-MS.

The recent findings related to As speciation in the soil pore water: the presence of plants reduced the concentration of all As species in the pore water. Comparing between plant and no-plant groups, almost all plant groups had lower As concentrations as well as smaller proportions of organic As species. After four months, As concentrations have dramatically decreased in both 100 and 200 plant-groups (from 320.46 to 105.85 $\mu g\ L^{-1}$ and from 986.74 to 418.61 $\mu g\ L^{-1}$, respectively). This is partly because of As uptake and translocation in plants. Moreover, compared to 100 groups, the less-toxic organic As species in the 200 groups were one order magnitude smaller, which confirmed the observed stronger phytotoxic symptoms in 200-plants. Besides, microbiome do play a key role in As speciation. Almost all As species showed this variation pattern: NS < SS < SM, which reveals the importance of microbes in controlling the speciation of As. More analyses are being performed to explain the reasons behind this sequence such as the profiling of soil microbial community and characterization of bacterial and fungal soil communities.

14.4

Effects of the vegetation mercury pump on seasonal variations in atmospheric mercury concentrations

Martin Jiskra[1]

[1]*Umweltgeowissenschaften, University of Basel, Bernoullistrasse 30, CH-4056 Basel (martin.jiskra@unibas.ch)*

Mercury is a top priority global pollutant threatening human and ecosystem health. Anthropogenic mercury emissions are emitted and transported through the atmosphere as gaseous elemental mercury (Hg0) before being deposited on land and ocean. Strong seasonal variations in atmospheric Hg0 concentrations are observed in the Northern Hemisphere, with maxima in winter and minima in summer. The seasonality of atmospheric Hg0 has mainly been attributed to seasonal variations in anthropogenic Hg0 emissions peaking in winter due to high energy production for heating or seasonal variation in photochemically driven Hg0 oxidation with maximum rates in summer. Here, I present evidence that the seasonal variation of anthropogenic mercury emission can not fully explain atmospheric Hg0 seasonality and that the oxidation of atmospheric Hg0 is overestimated. I will discuss Hg0 drawdown by vegetation – the vegetation mercury pump – as alternative to explain variations in atmospheric Hg0 concentrations. Atmospheric Hg0 concentrations correlate with CO_2, known to exhibit a strong seasonal variation driven by vegetation assimilating CO_2 in summer. Both trace gases, Hg0 and CO_2, show a strong correlation with satelite-derived vegetation activity data. This suggests that the uptake of Hg0 by vegetation plays a dominant role in atmospheric Hg0 cycling. In this presentation I will also touch on how the vegetation mercury pump may have changed in the recent decades due to increases in net primary production and how Hg0 uptake by vegetation may be affected by climate change.

REFERENCES

Jiskra, M., Sonke, J. E., Obrist, D., Bieser, J., Ebinghaus, R., Myhre, C. L., Pfaffhuber, K. A., Wangberg, I., Kyllonen, K., Worthy, D., Martin, L. G., Labuschagne, C., Mkololo, T., Ramonet, M., Magand, O., Dommergue, A. 2018: A vegetation control on seasonal variations in global atmospheric mercury concentrations. Nat. Geosci. 11, (4), 244-250.

14.5

Distinguishing between anthrogogenic and natural CeO_2 inputs into watewater systems

Ralf Kaegi[1], Alexander Gogos[2], Jonas Wielinski[1] & Andreas Voegelin[1]

[1]Eawag, Ueberlandstrasse 133, CH-8600 Dübendorf (ralf.kaegi@eawag.ch)
[2]Empa, Lerchenfeldstrasse 5, CH-9014 St. Gallen

A rigorous assessment of the impact of engineered nanomaterials (ENM) on the (aquatic) environment requires a clear separation between inputs related to anthropogenic activities and natural sources. Based on the case of ceriumdioxide (CeO_2)-(nano)particles (NP) detected in sewage sludge, we present a novel approach to quantitatively differentiate between anthropogenic and natural Ce inputs into wastewater systems.

CeO_2-NP are used in different industrial applications, eventually resulting in their release into the environment. Recent mass flow models suggest that a major fraction of the anthropogenic CeO_2-NP are discharged to wastewater systems. With retention rates of > 95 % in wastewater treatment plants (WWTP), the majority of the CeO_2-NP will be accumulated in sewage sludge. The digested sludge system, therefore, can be regarded as an efficient sampling system, averaging the Ce inputs from natural and anthropogenic sources over roughly 30 days, corresponding to the typical sludge age of the anaerobic digestion.

Based on the results of a previous screening study, in which we assessed the elemental concentration in digested sewage sludge in 64 WWTPs across Switzerland, 5 sludge samples were selected for more detailed characterization. In addition to the sludge samples, 6 soil samples from different localities were also investigated. These soil samples served as references for geogenic Ce inputs into WWTPs, assuming that the Ce present in these soil samples was exclusively of natural origin. The contents of the rare earth elements (REE) La, Ce, Eu, Er, and Dy in all slude and soil samples were quantified by acid digestion and inductively plasma mass spectrometry (ICP-MS). The oxidation state of Ce in all samples was assessed by X-ray absorption spectroscopy (XAS) at the Ce L_{III}-edge.

Cerium in soils and sediments is dominantly present as Ce(III) in minerals such as allanite, bastnaesite or monazite. Engineered CeO_2-(NP), are expected to exclusively contain Ce(IV). Therefore, the oxidation state of Ce in sewage sludge may be used to estimate the fractions of Ce related to anthropogenic activities. XAS analyses showed that Ce in soil samples was up to ~70% Ce(III) and ~30% Ce(IV). For the estimation of the anthropogenic inputs from measured Ce oxidation state in sludge samples, we thus assumed that natural Ce consisted of 70 % Ce(III) and 30 % Ce(IV) and that anthropogenic Ce inputs were exclusively Ce(IV). Complementarily, fractions of anthropogenic Ce inputs were derived from the contents of the REE La, Ce, Eu, Er, and Dy. Engineered of $Ce(O_2)$ was assumed to be free of other REEs, whereas natural Ce inputs were described by the average Ce/REE ratios (normalized by the respective post archean Australian shale (PAAS) ratios) derived from the 5 soil samples.

The five estimates based on the Ce oxidation state and on the four Ce/REE ratios (Ce/La, Ce/Eu, Ce/ Er, Ce/Dy) indicated that Ce in four of the five investigated sludge samples was mainly (60-100%) CeO_2 of anthropogenic origin, whereas Ce in one sludge was dominated by natural inputs. Estimates based on Ce/Eu, Ce/Dy and Ce/Er ratios were in excellent agreement with each other, but substantially deviated from estimates based on Ce oxidation state and Ce/La ratios. The considerable mismatch between Ce/La-based estimates and estimates based on the other Ce/REE ratios can be attributed to additional and variable anthropogenic inputs of La that are unrelated to anthropogenic Ce inputs. The considerable deviation between the quantifications derived from the oxidation state and the results obtained from the Ce/REE ration (excluding La) is most probably related to variable fractions of Ce(III) in anthropogenic Ce inputs, in contrast to our assumption that Ce from anthropogenic activities is exclusively Ce(IV). The fact that the results from the Ce/Eu, Ce/Er and Ce/Dy ratios are very comparable suggests that Eu, Dy and Er have negligible contents in engineered / anthropogenic materials that reach the wastewater stream.

Thus, based on (normalized) Ce/Eu, Ce/Dy and Ce/Er ratios, we were able to reliably estimate the fraction of anthropogenic inputs of Ce into wastewater systems. An extension of this analyses to additional REE will further substantiate our findings. Assuming that the dominant fraction of the anthropogenic Ce particles is classified as ENM, our results will eventually allow calibrating current mass flow models of ENMs with experimental data.

14.6

Thallium redox speciation in soil Mn concretions imaged by synchrotron X-ray spectroscopy

Francesco Femi Marafatto[1,2], Dario Ferreira-Sanchez[2], Rainer Dähn[2], Daniel Grolimund[2], Andreas Voegelin[1]

[1]Eawag, Ueberlandstrasse 133, CH-8600 Dübendorf
[2]Paul Scherrer Institut, Forschungstrasse 111, CH-5232 Villigen PSI

Thallium, a highly toxic trace metal, occurs in the environment as relatively soluble Tl(I) and, to a lesser extent, insoluble Tl(III). Tl(I) is both chalcophile and lithophile, substituting K in minerals such as illite and ocurring in metal sulfides. Thallium can also sorb to Mn oxides via both non-oxidative and oxidative uptake mechanisms. The oxidative uptake was only found to occur on hexagonal vacancy-bearing birnessite [1, 2].

The aim of this study was to evaluate the extent of Tl sequestration in soil Mn concretions, both oxidative and non-oxidative, using synchrotron and laboratory based X-ray imaging. To this end, we analyzed soil samples from the Erzmatt (Buus), in the Swiss Jura Mountains, which are geogenically rich in Tl [3]. The association of Tl with clay minerals and Mn concretions was assessed by analyzing soil thin-sections prepared on thermally conductive Si wafers with micro-focused (µ-) X-ray techniques, including laboratory X-ray fluorescence spectrometry (XRF) as well as synchrotron-based XRF and X-ray absorption spectroscopy (XAS) with a spatial resolution of ~5 µm. Measurements were conducted in a liquid helium-cooled cryostat, to reduce potential beam damage.

Our results show that with an increasing Tl/Mn molar ratio results in a decreasing average Tl oxidation state, consistent with an increase in non-oxidative Tl uptake. Furthermore, the trends in Tl average oxidation state with Tl/Mn loading are consistent with laboratory studies on Tl adsorption and oxidation on synthetic Mn oxides [5]. Semiquantitative µ-XRF results on the distribution of Tl between the clay matrix and Mn concretions are in line with results from sequential chemical extractions. In particular, the results indicate that the majority of Tl in these soils has been sequestered by incorporation into micaceous clay minerals. Minor fractions of Tl associated with Mn oxides however may be relevant with respect to short term Tl dynamics driven by cyclic soil redox variations. In conclusion, these spectroscopic results from natural soil samples combined with laboratory studies on the sorption of Tl by synthetic Mn oxides and clay minerals [1,2,4], allow to better constrain the relevance of different sorbent phases for Tl sequestration in soils.

REFERENCES

[1] Peacock, C. L. and E. M. Moon (2012). Geochim. Cosmochim. Acta 84: 297-313. [2] Cruz-Hernandez, Y., et al., (2019). Geochim. Cosmochim. Acta 248: 356-369. [3] Voegelin, A., et al., (2015). Environ. Sci. Technol. 49: 5390-5398. [4] Wick et al. (2018). Environ. Sci. Technol. 52: 571-580.
[5] Wick et al. (2019). *In review.*

14.7

Release and biovolatilisation of antimony from contaminated soils

Adrien Mestrot[1], Jaime Caplette[1], Lorenz Gfeller[1], Da Lei[2], Jie Liao[2], Jicheng Xia[2], Hua Zhang[2] & Xinbin Feng[2]

[1]Institute of Geography, Univeristy of Bern, 3012, Bern, Switzerland (1correspondence: adrien.mestrot@giub.unibe.ch)
[2]State Key Laboratory of Environmental Geochemistry, Institute of Geochemistry, Chinese Academy of Sciences, 550081 Guiyang, P.R. China

Antimony (Sb) is a naturally occurring, potentially carcinogenic, metalloid that can be remobilised from soils due to flooding. This is an issue because Sb released in the soil solution can potentially travel to the groundwater and be taken up by biota. Microorganisms can take up Sb and transform it to different chemical species For example, to the volatile forms of Sb (stibines) which are genotoxic and understudied. Here we investigated the effect of flooding and organic matter amendments on the release of Sb to the soil solution and the formation of volatile Sb by performing soil incubations under controlled conditions and by direct field sampling. We focused our work on contaminated Swiss shooting range soils and mine impacted rice paddies.

Our first incubation experiments on Swiss shooting range soils consisted of four treatments held at constant temperature (30°C) and humidity (70%) for 42 days. Our results indicate that volatile Sb is produced from Swiss shooting range soils under flooded conditions and enhanced by organic matter addition.

We also observed the in-situ production of volatile Sb from rice paddy fields near the Xikuangshan mine in China during a sampling campaign in 2018. Our results, the first field measurements of volatile Sb emanating from soils, indicate up to 390.65 mg ha^{-1} y^{-1} of volatile Sb is produced from the investigated paddy fields. We will also present and discuss Sb concentrations in soils, soil solution and irrigation water in the area.

The release and biovolatilisation of Sb in rice paddy soils sampled during the same field campaign was then investigated in the laboratory during a second incubation experiment. The first results from this trial will be presented and discussed.

14.8

Environmental fate of perovskite photovoltaics

Felix Schmidt[1,2], Andreas Schäffer[2], Markus Lenza[3]

[1]Institute for Ecopreneurship, School of Life Sciences, University of Applied Sciences and Arts Northwestern Switzerland, Switzerland (felix.schmidt@fhnw.ch)
[2]Institute for Environmental Research, RWTH Aachen University, Worringerweg 1, 52074 Aachen, Germany
[3]Sub-Department of Environmental Technology, Wageningen University, 6700 AA, Wageningen, the Netherlands

Achieving climate neutrality is one of the major challenges our society is facing. Renewable energies are likely to play an increasing and essential role in attaining net-zero emissions. The photovoltaic (PV) market is still dominated by Si-based technology (90% of the total PV energy production in 2017[1]). Recently, thin-film PV based on new absorber materials have emerged, such as perovskite solar cells[2]. These have given rise to potential application outside the range of rigid glass wafer-based technology via roll-to-roll (R2R) and sheet-to-sheet (S2S) processing on flexible (PET) substrates[3,4].

Perovskite photovoltaics promise a low-cost and efficient alternative to conventional Si-based solar cells. However, perovskite solar cells crucially rely on Pb- and/or Sn-based absorber materials, which are of environmental and toxicological concern. Until now, laboratory experiments quantifying leaching of metals and associated toxicological aspects have been addressed on a very rudimentary stage only[5,6].

Here, we present more detailed experiments to realistically assess metal transformations determining the environmental fate of perovskite photovoltaic constituents. More specifically, we use a set of complex and biologically active environmental compartments (e.g. soil/sediment-water microcosms) for laboratory and outdoor experiments. A focus is given to changes in aqueous speciation as well as sequestration mechanisms on solid-phases.The data serves to calculate predicted environmental concentrations (PEC) of toxic PV ingredients in the frame of environmental risk assessment.

REFERENCES

1. ISE. *Photovoltaics Report*. (2019).
2. Green, M. A., Ho-Baillie, A. & Snaith, H. J. The emergence of perovskite solar cells. *Nat. Photonics* **8**, 506 (2014).
3. You, J. *et al.* Low-temperature solution-processed perovskite solar cells with high efficiency and flexibility. *ACS Nano* **8**, 1674–1680 (2014).
4. Roldán-Carmona, C. *et al.* Flexible high efficiency perovskite solar cells. *Energy Environ. Sci.* **7**, 994–997 (2014).
5. Hailegnaw, B., Kirmayer, S., Edri, E., Hodes, G. & Cahen, D. Rain on methylammonium lead iodide based perovskites: Possible environmental effects of perovskite solar cells. *J. Phys. Chem. Lett.* **6**, 1543–1547 (2015).
6. Babayigit, A., Ethirajan, A., Muller, M. & Conings, B. Toxicity of organometal halide perovskite solar cells. *Nat. Mater.* (2016).

14.9

Insigth from omics to uncover the effect of mercury compounds to phytoplankton

Vera I. Slaveykova[1], Nicole Regier[1], Rebecca Beauvais-Flueck[1], Claudia Cosio[1], Sanghamitra Majumdar[2], Arturo Keller[2]

[1]Environmental Biogeochemistry and Ecotoxicology, Department F.-A. Forel for environmental and aquatic sciences, Earth and Environmental Sciences, Faculty of Sciences, University of Geneva, 66, boulevard Carl-Vogt, CH-1211 Geneva 4, Switzerland (vera.slaveykova@unige.ch)
[2]Bren School of Environmental Science and Management, 2045 Bren Hall, University of California Santa Barbara, CA 93106, USA

Using a combination of transcriptomics and metabolomics, the present study focusses on the effect of Hg compounds on green alga *Chlamydomons reinhardtii*, as a representative of the freshwater phytoplankton. To this end the response of *C. reinhardtii* to short-term exposure to a large concentration range of inorganic mercury (IHg) and methylmercury (MeHg) was studied, together with determination of intracellular Hg contents. RNAseq, next generation sequencing technology, was used to examine mercury-induced perturbations of cellular metabolic pathway and to detect the earliest stages of the toxicological response. Metabolic variations were further quantified by targeted liquid chromatography – mass spectrometry metabolomics. Obtained results demonstrated an increase of the intracellular Hg and MeHg contents with the concentration in the exposure medium. The number of up- or down- regulated transcripts increased with the intracellular Hg contents of both IHg and MeHg. For comparable intracellular content, the number of the dysregulated transcripts was higher for MeHg than for IHg supporting stronger impact of MeHg on algae as compared to IHg. The expression of several metal transporters' genes was affected by both species, showing that they might be involved in a transport of Hg within the cells. Exposure to MeHg dysregulated the expression of genes involved in motility, energy metabolism, lipid metabolism, and transport and antioxidant enzymes, while IHg induced similar alterations but only at highest exposure concentration (Beauvais-Flueck et al., 2017). MeHg induced increase of the percentage of the cells experiencing oxidative stress, while no oxidative stress was detected for IHg exposure. Targeted metabolomics confirmed an alteration of multiple patways in green alga when exposed to IHg or MeHg, including carbohydrate metabolism, energy and lipid metabolism, amino acid metabolism. The results of this study contribute to significant improvement of the understanding concerning Hg compounds adverse outcome pathways in green algae, as well as to the development of sensitive biomarkers in support to biomonitoring efforts of mercury monitoring programs in aquatic systems.

REFERENCES

Beauvais-Flueck, R., Slaveykova, V.I. & Cosio, C. 2017: Cellular toxicity pathways of inorganic and methyl mercury in the green microalga Chlamydomonas reinhardtii, Scientific Reports, 2017, 7, 8034.

14.10

Improvement of Antimony Analyses in Soil Matrices

Lucija Stanisic[1], Jaime N. Caplette[1], Stephanie Pfister[1], Thomas Lepke[2] & Adrien Mestrot[1]

[1]*Institute of Geograpfy, University of Bern, Hallerstrasse 12, CH-3012 Bern*
[2]*Federal Office for the Environment FOEN, Contaminated sites Section, Worblentalstrasse 68, CH-3063 Ittigen*

In the environment Antimony (Sb) is a toxic trace element of growing environmental interest and is regarded as a priority pollutant by the USEPA and the EU. In Switzerland, shooting ranges are heavily polluted by Sb and other trace elements due to weathering of the bullets. However, assessing the risks posed by Sb is difficult due to inherent analytical issues. These are for example memory effects in the sample introduction system, incomplete sample digestion, and bullet fragments causing measurement heterogeneity.

Sb exhibits strong retention in the ICP-MS sample introduction system. Typically, a longer rinsing time is required to reduce the risk of memory effects between samples. This results in a longer sample analysis cycle raising the costs of individual measurements (e.g., time, instrument upkeep, argon gas, etc.). Inefficient rinsing procedures can affect the quality of the analysis. We compared common cleaning procedures (e.g., NH_4OH-H_2O_2-MQ, EDTA-H_2O_2-MQ, 1% HNO_3) to prevent Sb carry-over and the effect of sample matrix on ICP-MS analysis (e.g., HCl vs HNO_3).

Acid digestion methods are strongly dependent on the matrix composition. To be effective, sample digestion must efficiently destroy the matrix and release Sb in a form compatible with the chosen analytical method (e.g., inductively coupled plasma mass spectrometry (ICP-MS)). However, Sb can be adsorbed and/or complexed after digestion or even be lost through volatilization during the digestion. Therefore, different digestion procedures for total analysis of Sb were tested with CRMs and spiked soils to optimize Sb recoveries in soil matrices (e.g., open and closed vessel digestion, aqua regia, HNO_3, HBF_4-HNO_3). Optimized digestion procedures will be presented.

Fine bullet fragments of Sb (< 200 µm) may have an impact on the measured Sb concentration in (a homogenized) sample. Since the fine residues contain high Sb concentrations this can cause a discrepancy in the total Sb concentration in the soil. Therefore, we separated fine fragments of bullets from the soil by magnet and by sedimentation and measured the fragment size. To quantify the discrepancy, we analyzed the samples in which the fine fragments were removed and compared the Sb concentration to the samples that contained the fine residues. Furthermore, we will compare the obtained Sb concentrations by the ICP-MS with the measurements of X-ray fluorescence spectrometry.

Different digestion and cleaning procedures were tested to improve time of sample analysis while increasing the accuracy and reproducibility of the analysis.

14.11

Thallium adsorption onto clay minerals and Mn oxides in soils

Silvan Wick[1], Bart Baeyens[2], Jasquelin Pena[3], Numa Pfenninger[1], and Andreas Voegelin[1]

[1]Eawag, Überlandstrasse 133, CH-8600 Dübendorf (silvan.wick@eawag.ch)
[2]Paul Scherrer Institute, CH-5232 Villigen PSI
[3]Institute of Earth Surface Dynamics, Faculty of Geosciences and Environment, University of Lausanne, CH-1015 Lausanne

Thallium (Tl) is a toxic trace element. It occurs in the environment as monovalent Tl^{I} and, to a lesser extent, as trivalent Tl^{III}. The clay mineral illite and the Mn-oxide birnessite have long been postulated to be key sorbents for Tl in soils and sediments. Direct spectroscopic evidence for the sequestration of Tl by illite and birnessite in soil was found in a study on the speciation of Tl in geogenically Tl-rich soils from the Erzmatt (Swiss Jura mountains) (1). In a laboratory study, we confirmed that Tl^{I} exhibits a high affinity for adsorption onto illite and modelled Tl adsorption using a 3-site cation exchange model previously developed to quantify the adsorption of Cs^{+}, Rb^{+}, NH_4^{+} and K^{+} onto illite (2). Recent results on Tl sorption onto Mn-oxides confirm that high-affinity oxidative Tl^{I} uptake dominates on vacancy-containing hexagonal birnessite, whereas Tl^{I} adsorbs less strongly and without oxidation onto triclinic birnessite and tectomanganates (3). The aim of the present study is to gain complementary insights into the roles of Tl sorption onto clay minerals and Mn-oxides in soil by determining the adsorption, solubility, and exchangeability of geogenic and freshly spiked Tl in soils from the Erzmatt.

The extraction of 36 Erzmatt topsoil samples with geogenic Tl contents from 3 to 1000 mg/kg with 10 mM $CaCl_2$ (soluble Tl) and with 1 M NH_4-acetate (exchangeable Tl) showed that on average 3.6±1.6% of the geogenic Tl was NH_4-acetate exchangeable and revealed a nearly linear relationship between soluble and exchangeable Tl. Tl L_{III}-edge X-ray absorption spectra of 12 soils suggested that most soil Tl was Tl^{I} associated with illite. The solubility of the exchangeable geogenic Tl could be described with the model for Tl adsorption onto illite. In combination, these findings indicate that the major fraction of geogenic Tl in these soils was fixed in the interlayers of illite, and that short-term Tl solubility was controlled by a minor fraction of Tl adsorbed onto illitic clay minerals. Additional insights into the relevance of clay minerals and Mn-oxides for Tl sorption was obtained from Tl sorption isotherms on Tl spiked Erzmatt soils and from a sequential extraction, which indicated that Mn-oxides may adsorb similar fractions of total soil Tl as clay minerals, although their relevance in the Erzmatt soils is limited because of the high fractions of structurally incorporated Tl in clays.

REFERENCES

(1) Voegelin, A. et al. (2015): *Thallium speciation and extractability in a thallium- and arsenic-rich soil developed from mineralized carbonate rock*, Environmental Science and Technology, v.49, 5390-5398.
(2) Wick, S. et al. (2018): *Thallium adsorption onto illite*, Environmental Science and Technology, v.52, 571-580.
(3) Wick, S. et al.: Thallium sorption onto Mn-oxides (in review).

14.12

Cadmium transfer in contaminated soil-rice systems: insights from solid-state speciation and isotope fractionation

Matthias Wiggenhauser[1], Anne-Marie Aucour[2], Philipp Telouk[2], Sylvain Campillo[1], S. Bureau[1], G. Landrot[3], Jian Feng Ma[4], Géraldine Sarret[1]

[1]Institut des Sciences de la Terre (ISTerre), Université Grenoble Alpes, CNRS, France. (matthias.wiggenhauser@univ-grenoble-alpes.fr)
[2]ENS de Lyon, Université de Lyon, CNRS, France
[3]Synchrotron SOLEIL, Samba Beamline, France
[4]Institute of Plant Science and Resources, Okayama University, Japan

Staple crops such as rice are our major sources of cadmium (Cd). Therefore, a fundamental understanding of processes that control Cd accumulation in crops is crucial. To this end, we combined synchrotron solid state speciation analysis with Cd isotope process tracing in contaminated soil-rice systems. The main principle of this approach is that (i) synchrotron solid state speciation techniques (XANES) identify snapshots of Cd speciation in soil and rice compartments at the time of sampling (ii) while mass balances and isotope ratios provide information on how Cd speciation controls the mobility of Cd during plant growth. With this combined approach, we aimed to provide a holistic view on major processes that determine the Cd distribution in soil-rice systems.

We grew rice (*Oryza sativa* L.) in pots that contained wet and flooded soils that were spiked with 15 mg Cd [kg soil]$^{-1.}$ We cultivated two rice accessions which have functional and non-functional vacuolar Cd transporter to retain Cd in roots. The rice was harvested at flowering stage. For analysis of stable Cd isotope ratios, samples were purified and measured using MC-ICPMS. For bulk XANES analysis, samples were frozen with liquid nitrogen immediately after harvest.

Cd transfer from soil to rice was about two times higher in the wet (1940-2552 µg [kg soil]$^{-1}$) compared to the flooded soil (917-1000). Cd-sulfide was the dominating species in the flooded soil at flowering (76 %) while rice plants that grew on flooded soils were enriched in heavy isotopes ($\delta^{114/110}$Cd = -0.36 to -0.38 ‰) compared to the rice that grew on the wet soil (-0.44 to -0.56 ‰). The rice accessions with functional Cd root vacuolar transporter accumulated 5.1 to 7.4 times more Cd in roots than in shoots and retained light Cd isotopes in the roots ($\Delta^{114/110}Cd_{shoot\text{-}root}$ = 0.16 to 0.19 ‰). In contrast, the rice without functional vacuolar Cd transporter accumulated 1.4 to 2.9 times more Cd in shoots than in roots while less or no isotope fractionation occurred between shoot and root (-0.02 to 0.08 ‰). Regardless the treatment, all Cd was bound to S ligands in roots.

Our combined approach identified Cd-sulfide precipitation as major process that reduced the transfer of Cd from soil to rice. At the conference, the role of pH change and increased sorption of Cd to dissolved organic matter during flooding will be discussed by complementing the data set with Cd speciation modelling and isotope ratios in soil solution. Within the plant, Cd vacuolar sequestration controlled Cd retention in roots and Cd isotope fractionation between root and shoot. We will present a conceptual model that illustrates that a combination of ligand exchange, membrane transport, and Cd chelation retains Cd in roots of Cd contaminated soil-rice systems.

14.13

Arsenic and antimony speciation, sequestration, mobilisation and dispersion in a highly contaminated river catchment: Differences revealed for improved risk assessment (Invited Talk).

Susan C. Wilson[1], Steven Doherty[1], Matthew Tighe[1] & Luke Milan[1]

[1]School of Environmental and Rural Science, University of New England, Armidale, NSW 2351, Australia (swilso24@une.edu.au)

The Macleay River Catchment in northern New South Wales, Australia, exhibits the largest dispersed co-contamination of antimony (Sb) and arsenic (As) in the southern hemisphere. Several thousand tonnes of Sb and As have entered the river system and been dispersed from the historic operations at the Hillgrove Mine to the coastal floodplain 300km distant at the Pacific Ocean. The contamination in this near neutral to basic catchment has been the focus of concentrated reseach effort to understand and explain the mobility of the two metalloids, considering the processes underlying metalloid dispersion from primary sources, sequestration in secondary minerals, the predominant metalloid species in different parts of the catchment and differences between Sb and As. The metalloids are primarily hosted by stibnite and arsenopyrite (Ashley et al. 2007) but oxidation processes for stibnite are much less understood than those of arsenopyrite. Our work is filling important knowledge gaps needed in risk assesment and environmental management (Wilson et al. 2010).

Sediment, suspended sediment and water samples collected over 10 years from 13 important geomorphological and ecological confluences through the length of the river system provide insights about the metalloid mobilisation processes. Antimony in stream water can exceed 1000 µg L^{-1} in the upper catchment but concentrations decrease rapidly compared to As with distance from the mine. In surface waters Sb is present only as the oxidised Sb(V) oxyanion; in contrast As(III) can account for up to 60 % of total dissolved As at some sites, although As(V) predominates through the waterway as a whole. Arsenic concentrations can exceed those of Sb in hyporheic and sub-oxic waters likely due to reductive dissolution of Fe host-phases. In the lower catchment the dissolved and suspended As load in the water column become relatively more important compared with Sb.

Scanning electron microscopy and thin section analysis of mineralised fragments from the upper catchment stream bed show oxidised rims of mixed-valence Sb oxides surrounding primary stibnite. Grains of high purity Sb_2O_3 are identified in upper catchment sediment samples using electron microprobe analyses. Synchrotron X-ray absorption spectroscopy confirms Sb predominantly as secondary mineralised oxidation products of stibnite through the upper catchment sediment. Arsenic is identified only in association with iron oxide grains at up to 2.5 % of total grain weight, and not as primary mineral phases such as arsenopyrite.

River sediment fractionation shows a gradual increase in the smaller size fraction down river, with iron significantly positively correlated with total As and Sb in the lower Macleay River, but only with As in the upper catchment. Sequential extraction of sediment fractions reveals a large proportion of total Sb (59 – 88 %) and As (59 – 82 %) in the residual fraction of upper catchment samples, whilst residual As (51 – 71 %) is significantly greater than Sb (27 – 53 %) in the sediments of the lower river. Antimony in sediment is more water soluble than As throughout the catchment (0.6 – 2.2 % total Sb; 0.4 – 1.4 % total As). Metalloid association with amorphous phases is significant (up to 29 – 49 % of total As and 22 – 64 % of Sb in the lower catchment) and increases with distance from the upper catchment source.

Overall our results clearly illustrate the different behaviour of Sb and As in this co-contaminated river system. Rapid oxidation of the stibnite ore results in primarily mineral Sb oxide forms in the upper Macleay River sediment that release Sb(V) to the river water. The Sb becomes progressively and strongly sequestered with amorphous phases in the lower part of the catchment. In contrast, the mobilisation of As is driven by association with Fe hydroxyoxides and redox changes throughout the dispersal pathway.

REFERENCES

Ashley, P.M., Graham, B., Tighe, M. & Wolfenden, B.J. 2007. Antimony and arsenic dispersion in the Macleay River catchment, New South Wales, Australia: a study of the environmental geochemical consequences. Australian Journal of Earth Sciences, 54, 83-103.

Wilson, S.C., Lockwood, P.V., Ashley, P.M. & Tighe, M. 2010. The chemistry and behaviour of antimony in the soil environment, with comparisons to arsenic. Environmental Pollution, 158, 1169-1181.

P 14.1

Innovative autonomous field monitoring of bioavailable metal species, macronutrients, phytoplankton to deeper understand their behaviour, interaction and fate (MEPHY)

Mary-Lou Tercier-Waeber[1], Melina Abdou[1], Eric Bakker[1], Jörg Schäfer[2], Antonio Novellino[3], Susana Alloisio[3], Luca Bonofiglio[3], Wilhelm Petersen[4], Daniel Blandfort[4]

[1]University of Geneva, Sciences II, 30 Quai E.-Ansermet, 1221 Geneva 4, Switzerland (melina.abdou@unige.ch)
[2]University of Bordeaux, Allée Geoffroy Saint-Hilaire, 33615 Pessac, France
[3]ETT S.p.A., via Sestri 37, 16154 Genoa, Italy
[4]Helmholtz Zentrum Geesthacht, Max Planck Str. 1, D-21502 Geesthacht, Germany

Trace metals are distributed under various physical-chemical forms including dynamic (bioavailable) species. Reciprocal interactions exist between bioavailable metal species and phytoplankton activity. Considering the short temporal scale involving primary production processes, understanding of these interactions requires high resolution monitoring.

The MEPHY field campaign was performed at the COSYNA Stationary FerryBox platform (COSYNA_SFB) from May 6 to 16, 2019. Located at the mouth of the Elbe River (German Southern North Sea), this sampling site is characterized by Spring and Summer phytoplankton blooms. The Elbe River is also impacted by anthropogenic sources of trace metals and macronutrients originating from an urbanised and industrialised watershed.

The objective of our field study was two-fold: 1) the study of the dynamic behaviour of the bioavailable fraction of a range of trace metals, algal-bacterial species, and macronutrients; 2) the assessment of the sources and behavior of the metals, phytoplankton and macronutrients targeted and of their interactions.

To this purpose, two innovative sensing tools were installed in parallel to the COSYNA FerryBox: an integrated multi-channel Trace Metal Sensing Module (TMSM); and a miniature, low-cost multiwavelength fluorometer, based on Advanced Luminescence-Based Phytoplankton Analysis and Classification Appliance (ALPACA). The TMSM and ALPACA enable real-time detection of respectively the bioavailable fraction of a range of essential or toxic trace metals, and discrimination of relevant phytoplankton groups combined with an approximation of the cell density respectively. Preliminary outcomes observed with these new sensing tools coupled to those of master bio-physicochemical parameters and macronutrients recorded by the COSYNA FerryBox are presented. Potentiality provided by synergising these tools with FerryBox sensors to (i) extend capability of coastal area sentinel systems; ii) assess bio-chemical processes which regulate the transport and behavior of trace metals and nutrients; ii) study relationships between micro- nutrients/pollutants, macro-nutrients and phytoplankton (community, diversity, bloom), are discussed.

P 14.2

Arsenic removal from manganese-containing groundwaters using Fe(0) electrocoagulation - modelling

Charlotte Catrouillet[1], Sachiko Hirosue[1], Nathalie Manetti[1] & Jasquelin Peña[1]

[1]Unversity of Lausanne IDYST, Geopolis, CH-1015 Lausanne, Switzerland (charlotte.catrouillet@unil.ch)

Arsenic (As) occurs naturally in some groundwaters that serve as the main source of drinking water for people worldwide, especially in South-East of Asia (Bengladesh, India, etc.). This large-scale contamination of groundwater and the high toxicity and carconegicity of As is responsible for millions of deaths around the world. Therefore, strategies to remove As from water using efficient and low-cost treatement systems are critically needed. Iron(0) electrocoagulation (EC) has gained attention as a low-cost method for As removal from groundwater because it has short supply chain and low energy requirements (small solar panels or car battery provide sufficient power) and, is easy to operate. In EC, a current is passed through an Fe(0) electrode, such that Fe(0) is oxidized to Fe(II). The production of Fe(II) generates reactive oxidants that readily oxidize As(III) to As(V) – a less toxic form of As, and Fe(II) to Fe(III), which forms nanoscale iron precipitates that remove As from solution (Li et al., 2012 ; Nidheesh and Singh, 2017). However, the mechanism and efficiency of As removal depend strongly on the chemical composition of the groundwater.

The co-occurrence of high concentrations of As and Mn has been documented in several places, including the Peruvian Amazon (de Meyer et al., 2017). Recent work shows that like As,[3] Mn(II) can be removed from water using an EC system through the oxidation of Mn(II) to Mn(III) by reactive oxidants (i.e., $OH^{\bullet}$ or Fe(IV)) and its incorporation into Fe oxides (Hug and Leupin, 2003). These studies suggest that As and Mn compete for the same pool of oxidants in an EC system and, therefore that the efficiency of As removal may be lowered by the presence of Mn. The main goal of this work is thus to understand the extent to which As and Mn are removed during EC when aqueous As(III) and Mn(II) are initially present in the groundwater. In addition, knowledge of the speciation of As and Mn in the solid phase is needed in order to understand the mechanism of contaminant removal (oxidation and sorption) at the different conditions (concentrations of Mn, pH, oxidants). Finally, based on our results, the mechanisms of oxidation of As, Fe and Mn by Fe(IV) and $OH^{\bullet}$ will be modeled in order to simulate diverse Mn- and As-containing waters.

In this study, experiments were conducted using a simple $NaCl/HCO_3^-$ electrolyte with either 10 and 100 µM As(III) and 0 and 100 Mn(II) at pH values 4.5, 6.5 and 8.5. In addition, 250 µM H_2O_2 was added to the experiments to favor the production of $OH^{\bullet}$ and Fe(IV) oxidants instead of $O_2^{\bullet-}$, which does not oxidize As(III) at appreciable rates relative to $OH^{\bullet}$ and Fe(IV). All the experiments were conducted in triplicate and speciation of the aqueous and solid phase (as determined by X-ray absorption spectroscopy, Stanford Synchrotron Radiation Lightsource, BL 4-1) followed over time for 32 minutes.

Results showed that in the absence of Mn, the 10 µg L^{-1} (WHO recommendation) is achieved at pH 4.5 and 6.5 but would require longer time of EC at pH 8.5. Arsenic oxidation was quasi complete after 32 min of EC for all pH. In the presence of Mn, the kinetics and mechanism of As removal varied but still reached As levels below the WHO limit for pH 4.5.Specifically, As in the aqueous and solid phase showed greater As oxidation at pH 4.5 (by $OH^{\bullet}$) than at pH 8.5 (by Fe(IV)), whereas, greater Mn oxidation was observed at pH 8.5 than at pH 4.5. While Mn(II) oxidation to Mn(III,IV) by Fe(IV) competes with As(III) oxidation to As(V), favorable As(III) sorption allowed for As removal from solution. This work shows that the kinetics of As and Mn oxidation and mechanisms of removal from the aqueous phase to the solid phase vary strongly according to the type of oxidant present in the system (e.g., $OH^{\bullet}$ and Fe(IV), respectively). Furthermore, these data can be used to constrain the constants of oxidation of Mn by $OH^{\bullet}$ and Fe(IV), which are needed before a kinetic model to predict As removal.

REFERENCES

Li, L., van Genuchten, C., Addy S.E.A., Yao, J., Gao, N. & Gadgil, A.,J. 2012: Modeling As(III) Oxidation and Removal with Iron Electrocoagulation, Environmental Science & Technology, 46, 12038-12045.

Nidheesh, P.V., & Singh, T.S.A. 2017: Arsenic removal by electrocoagulation process: Recent trends and removal mechanism, Chemosphere, 181, 418-432.

Hug, S.J., & Leupin, O. 2003: Iron CatalyzedOxidation of Arsenic(III) by Oxygen and by Hydrogen Peroxide: pH-dependent Formation of Oxidants in the Fenton Reaction, Environmental Science & Technology, 37, 2734-2742.

de Meyer, C., Carpio, P.A., Stengel, C., & Berg, M. 2017: Arsenic, manganese and aluminium contamination in groundwater resources of Western Amazonia (Peru), Science of the Total Environment, 607-608, 1437-1450.

van Genuchten, C. & Peña, J. 2017: Mn(II) Oxidation in Fenton and Fenton Type Systems: Identification of Reaction Efficiency and Reaction Products, Environmental Science & Technology, 51, 2982-2991.

P 14.3

Bioaccumulation and biotransformation of mercury compounds: Focus on green algae and cyanobacteria

Cossart Thibaut[1], Garcia-Calleja Javier[2], Pedredo Zoyne[2], Ouerdane Laurent[2], Tessier Emmanuel[2], Kavanagh Killian[1], Worms Isabelle[1], Amouroux David[2], Slaveykova Vera[1].

[1]Environmental Biogeochemistry and Ecotoxicology, Department F.-A. Forel for environmental and aquatic sciences, Earth and Environmental Sciences, Faculty of Sciences, University of Geneva, Uni Carl Vogt, Bvd Carl-Vogt, CH-1211 Geneva 4, Switzerland.
[2]CNRS – Université de Pau et Pays de l'Adour, Institut des Sciences Analytiques et de Physico-Chimie pour l'Environnement et les Matériaux, UMR 5254, 64000 Pau, France.

Phytoplankton could influence biogeochemistry of mercury directly by accumulating and bio transforming mercury species, and indirectly by excreting bioligands which could influencing different abiotic and biotic transformations. Nevertheless, the role of phytoplankton, such as green algae and cyanobacteria, in Hg transformation is still not well understood. The overall goal of the present work is to get insights on the role of phytoplankton in biotic Hg transformations in the freshwaters. Since the biotic transformations are intracellular, the uptake of inorganic (IHg) and monomethylmercury (MeHg, CH_3Hg^+), their cellular distribution and transformation in green alga *Chlamydomonas reinhardtii*, and cyanobacterium *Synechocystis* sp. were studied. To this end, the alga and cyanobacteria, grown to the exponential and stationary growth phases and exposed to ^{199}IHg or ^{201}MeHg. The cellular accumulation of IHg or MeHg and distribution between membrane and cytosol fractions were quantified by isotopic dilution analysis gas chromatography coupled to inductively coupled plasma mass spectrometry. The ratios between the difference of control isotope concentration after and before incubation and the measured isotope concentration before incubation in the whole cells and the cellular fractions were used to determine the Hg transformations.

The results demonstrated a rapid accumulation of IHg and MeHg green alga and cyanobacterium. However the cellular concentrations were species- and growth phase- dependent. Under comparable exposure conditions, *Synechocystis* sp. accumulated about twice more IHg than *C. reinhardtii*. No measurable Hg transformations have been found in cyanobacteria cells under the studied conditions, green alga cells are able to demethylate MeHg in the cytosolic fraction and more specifically in stationary phase of growth. The results have important implications for the improved understanding of the role of phytoplankton in the aquatic environment as well as for the accumulation of Hg species in the aquatic food webs.

P 14.4

Towards an approach to assess the reactivity of biogenic manganese oxides

Gaïtan Géhin

University of Lausanne, Environmental Geochemistry Lab (gaitan.gehin@unil.ch)

Biogenic manganese oxides (BioMnOx) play key roles in many ecosystems by its capacity to oxidize and interact with numerous metals and organic compounds. Its nanoparticle size, coupled with high valence Mn(IV) and vacancy sites, promote the high reactivity and redox potential(E_H), making manganese oxides (MnOx) the strongest solid oxidant and a valuable material for technological and environmental applications. The mechanisms responsible for the redox potential of BioMnOx are still unclear due to the difficulty to measure the electron transfer on a solid phase. Based on the hypothesis under which the Mn(III) content in the structure influences the oxidation rate and $_{EH}$, we proposed a novel synthetization method capable of precipitating BioMnOx by changing the pH, inducing variations in Mn(III) content. We aimed to overcome the challenging measure of solid phase electron transfer by using the organic molecule ABTS as the electron donor and as the redox probe. The objective was to isolate the mechanisms governing the electron transfer by measuring the redox reactions on different time scales: fast kinetics (0 to 20 sec), midterm (3 to 90 min) and long term reaction extent (4 to 19 days). We precipitated and characterized three BioMnOx containing 0%, 36% and 67% Mn(III,II) using XRD patterns, potentiometric titration and UV-vis spectrophotometry. By comparing them to the abiotic d-MnO_2, we were able highlight the biogenic properties enhancing the first oxidation kinetics (up to 24.9 *µMmin−1*) and inhibiting the midterm electron transfer rates. Our results indicate slower oxidation rate for BioMnOx with increasing Mn(III,II) content. The redox reaction did not reach the equilibrium after 90 min but still highlight the slower kinetics of BioMnOx in comparison to d-MnO_2. Long term reaction extent showed the capacity of all BioMnOx to oxidize the already oxidized $ABTS^{\bullet+}$ testifying of a redox potential above 0.71 V. Our method allowed to quantify the initial oxidation rates for the first time. However, more development is needed to reach the redox reaction equilibrium and to better quantify the ABTS speciation after longer period of time.

P 14.5

Stability and As adsorption of nanocrystalline Al-hydroxysulfates forming during acid rock drainage

Philipp Ingold[1], Christoph Wanner[1]

[1]*Rock-Water Interaction Group, Institute of Geological Sciences, University of Bern, Baltzerstrasse 3, CH-3012 Bern, Switzerland (philipp.ingold@students.unibe.ch)*

In the streambed of a small acidic (*pH ~ 4.0*) mountainous stream located in the Engadin area, Switzerland, white precipitates can be observed, which have formed on boulders (Fig. 1). These precipitates form due to the neutralization of the stream by mixing with several circumneutral tributaries. A Precent study identified basaluminite, a nanocrystalline hydroxysulfate with an idealized stochiometry of $Al_4OH_{10}(SO_4)$•3-5H_2O, as the dominating phase of the white streambed coating (Wanner et al., 2018). Chemical analyses revealed an elevated As concentration of up to 600 µg/g, which is inherited from adsorption of As on basaluminite as well as an anion exchange reaction where SO_4^{2-} in the basaluminite structure is replaced by arsenate anions ($H_2AsO_4^-$). Similar Al-hydroxysulfates are observed downstream of the Fe-Cu mine Servette-Chuc, located in the Aosta Valley in Northern Italy (Tumiati et al., 2008). Their rather low SO_4 content, however, does not seem plausible with the precipitation of pure basaluminite. A potential explanation for the low sulfate content is the transformation of previously formed basaluminite to Al-hydroxides (e.g. $Al(OH)_3$) due to the alkaline pH of ca. 8.0 to which the Aosta Valley precipitates are exposed to during most of the year.

To study the potential transformation of basaluminite and to assess the fate of As during such reactions, we have experimentally investigated (i) the initial formation of Al-hydroxysulfates by titrating the acid mine drainage solution collected at the Servette-Chuc mine in the Aosta Valley (*pH ~ 3.0*) and (ii) the fate of basaluminite sampled in the Engadin area when exposed to a solution with a pH of 8.0 (i.e. stability experiments). Infrared spectroscopy and acid digestion followed by ICP-OES analyses of the precipitates obtained from the titration experiment demonstrate that the precipitates found downstream of the Servette-Chuc mine initially refer to basaluminite.Applying the same analytical techniques to the precipitates used in the stability experiments suggests that the transformation of basaluminite to $Al(OH)_3$ is indeed occuring at pH 8.0 within a few weeks. Chemical analyses of the corresponding solutions, however, showed that such transformation is only associated with a minor mobilization of previously sorbed As. This confirms that basaluminite of similar Al-hydroxysulfates may serve as powerful filter material for the treatment of As contaminated groundwater (Mertens et al., 2012).



Figure 1. Photograph of basaluminite precipitates forming along “Ova Lavirun”, a montainous stream in the Engadin area.

REFERENCES

Tumiati S., Godard G., Masciocchi N., Martin S. and Monticelli D. 2008. Environmental factors controlling the precipitation of Cu-bearing hydrotalcite-like compounds from mine waters. The case of the “Eve verda” spring (Aosta Valley, Italy). European Journal of Mineralogy, 20, 73-94.

Wanner C., Pothig R., Carrero S., Fernandez-Martinez A., Jäger C. & Furrer G. 2018. Natural occurrence of large amounts of nanocrystalline Al-hydroxysulfates: Insights on formation, Al solubility and heavy metal retention. Geochimica Et Cosmochimica Acta 2018, 218, p. 259-269.

Mertens J., Rose J., Kägi R., Chaurand P., Plötze M., Wehrli B. & Furrer G. 2012. Adsorption of arsenic on polyaluminium granulate. Environmental Science & Technology. 46, 7310-7317.

P 14.6

Cocktail effect of nanoTiO$_2$ mixtures with mercury to green alga *Chlamydomonas reinhardtii*

Mengting Li, Vera I. Slaveykova

Environmental Biogeochemistry and Ecotoxicology, Department F.-A. Forel for Environmental and Aquatic Sciences, University of Geneva, Uni Carl Vogt, 66, boulevard Carl-Vogt, CH-1211 Genève 4, Switzerland (Mengting.li@etu.unige.ch)

In aquatic environment nanoparticles are present as complex mixtures with other contaminants which can result in synergism, aditivity or antagonism of their combined action. Despite the fact that the toxicity and environmental risks of engineered nanomaterials have received extensive attention in recent years, their interactions with other contaminants and the subsequent effects to aquatic microorganisms are to explore. In such a context, the present study aims to examine the interactions and effects of cocktails containing nanoTiO$_2$ and mercury compounds, as a representative of priority hazardous substance, to *Chlamydomonas reinhardtii*, as a model phytoplankton specie. It was hypothesized that due to the its high reactivity nanoTiO$_2$ will adsorb Hg compounds and thus decrease its bioavailability and effects to alga, and that the effect will be more pronounced for cocktails containing nanoparticles of smaller primary size. The influence of nanoTiO$_2$ of different primary sizes, 5 nm (anatase, A5), 15 nm (anatase, A15) and 20 nm (anatase/rutile AR20) on inorganic Hg (IHg) and monomethyl Hg (CH_3Hg) effects to algae was studied. The effect of Hg, nanoTiO$_2$ and their mixture on the algal growth, generation of oxidative damage and membrane damage were determined by flow cytometry. In parallel, the stability of nanoTiO$_2$ in terms of hydrodynamic size and surface charge as well as Hg adsorptive capacity of nanoTiO$_2$ were determined. Results showed that the increasing concentrations of nanoTiO$_2$ with different primary size lead to a decrease of Hg-induced effects, due to the adsorption of Hg to nanoTiO$_2$. NanoTiO$_2$ had much higher adsorption capability to IHg than CH_3Hg.The results highlighted the need for improved understanding of the interactions of complex environmental settings containing mixtures of nanomaterials and other contaminants, central for sustainable development of nanotechnology.

P 14.7

Bioaccumulation of mercury in the terrestrial food chain: method development and first results

Sabnam Mahat[1], Lorenz Gfeller[1], Lukas Jenni[2], Adrien Mestrot[1]

[1]*Institute of Geography, University of Bern, Hallerstrasse 12, CH-3012 Bern (sabnam.mahat@giub.unibe.ch)*
[2]*Swiss Ornithological Institute, Luzernerstrasse 6, CH-6204 Sempach*

Mercury's chemistry and biochemistry in aquatic environments has been largely studied but the fate of mercury in the terrestrial environment has been overlooked, even though the majority of total mercury is estimated to be deposited in terrestrial environments. As a result, data on the transfer and bioaccumulation of mercury in terrestrial food webs is scarce. The present study focuses on the fate of mercury and methylmercury in the terrestrial food chain in Switzerland and aims to develop a non-invasive long-term biomonitoring. Firstly, an extensive literature reviews of European studies was conducted in order to determine the concentration of mercury and methylmercury in a range of species and to assist for the selection of species, organs and food chain for our study in Switzerland. Using the collected data, we could show that kidneys of Roe deer was found to be a potentially good indicator of mercury pollution. Secondly, a high-throughput methylmercury extraction and analysis method using acid leaching, organic solvent and back extraction to L-cysteine followed by HPLC-ICP-MS was tested for various organs and tissues. Our tests with Certified Reference Materials showed a recovery of 89.2 ± 7.9 %, 93.4 ± 5.4 % and 100.7 ± 9.1 % for methylmercury in "SRM 2972 Mussel tissue", "NIES CRM 13 Human Hair" and "DOLT-5 Dogfish liver" respectively. Finally, a specific food chain consisting of soil – voles – Barn owl is currently being tested using barn owl feathers and pellets containing hair and bone of voles.

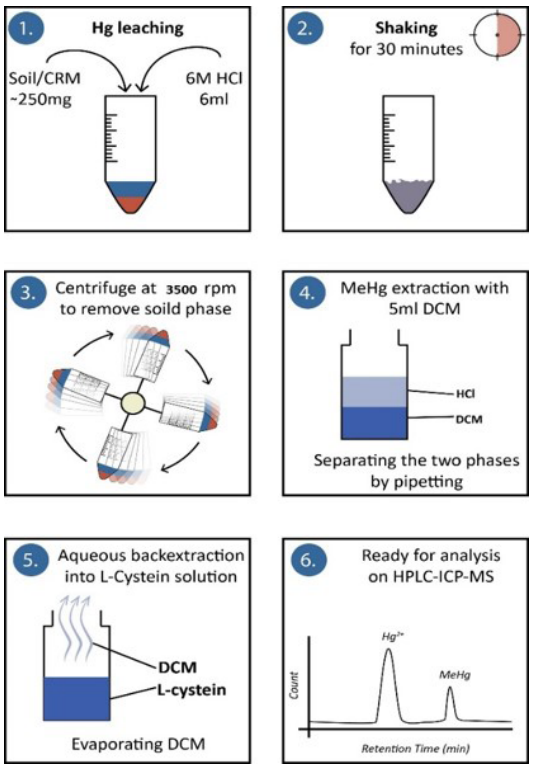


Figure 1. Methylmercury extraction using acid leaching, organic solvent and aqueous back extraction into L-Cysteine and measurement using HPLC-ICP-MS (Gfeller. L, 2017)

REFERENCES

Ritscher A., 2018 : Use, disposal and environmental releases of mercury: An overview of the situation in Switzerland. Federal office of the environment, Bern. State of the environment n°1832 : 56 p

P 14.8

Arsenic Adsorption and Oxidation by Fe(II)-activated Magnetite and Maghemite

Laurel ThomasArrigo[1], Reto Gubler[1], & Ruben Kretzschmar[1]

[1]Soil Chemistry Group, Institute of Biogeochemistry and Pollutant Dynamics, ETH Zurich, 8092 Zurich, Switzerland (laurel.thomas@usys.ethz.ch)

Elevated concentrations of arsenic (As) affect the daily lives of millions of people worldwide, many of whom rely on As-contaminated ground- and surface-waters for drinking, cooking, and irrigation of crops. Because the adsorption behavior of As changes with As redox speciation, the mobility and toxicity of As are greatly dependent on As biogeochemistry. In natural soils and sediments, As redox chemistry is intimately linked to Fe cycling. Under oxic conditions, As is typically present as arsenate (As(V)), a less mobile As species with a high affinity for sorption to Fe(III)-oxides. However, under reducing conditions, the microbially-mediated reduction of Fe(III)-oxides releases solid-phase associated As to solution, where it may act as a terminal electron acceptor in microbial respiration. Thus, arsenite (As(III)), the more mobile and toxic species dominates under reducing conditions.

In the absence of oxygen, secondary Fe mineral phases support the re-adsorption of dissolved As species. At low (micromolar) As concentrations, thermodynamic calculations predict that common Fe(II)/(III)-oxides (e.g. goethite (α-FeOOH) or magnetite ($Fe(II)Fe(III)_2O_4$)) will not oxidize adsorbing As(III) in the absence of oxygen [1]. However, microbially-mediated reduction of Fe(III)-oxides also leads to dissolved ferrous Fe (Fe(II)) in solution. Recently, 'Fe(II)-activated' goethite was reported to oxidize As(III) under anoxic conditions via the Fe(II)-catalyzed formation of a highly reactive Fe(III) surface species [1]. Overall, the presence of Fe(II) reduced As adsorption to goethite [1]. To date, however, it is not known whether an Fe(II)/magnetite system behaves similarly. Magnetite, a thermodynamically stable Fe-oxide, is the end product of Fe(II)-catalyzed transformations of ferrihydrite and lepidocrocite at pH>7, and surpasses goethite in terms of As(III) adsorption at circa-neutral pH [2]. While the presence of Fe(II) may similarly catalyze As(III) oxidation on the surface of magnetite, studies have shown that surface-adsorbed As(V) may be irreversibly incorporated into the magnetite structure, thus resulting in long-term As sequestration [3]. At the same time, this structural incorporation of As(V) may be aided by the presence of Fe(II), which, comparable to goethite [4], triggers recrystallization of magnetite [5]. Therefore, 'Fe(II)-activated' magnetite may represent a significant pathway for long-term As sequestration under reducing conditions.

In this study, Fe(II)-reacted magnetite or maghemite was reacted with As(III) or As(V) for 1 week at neutral pH. Arsenic and Fe adsorption and speciation changes were measured in the aqueous phase, and the stoichometry of the magnetite or maghemite solid phase was determine with acid dissolution and X-ray diffraction. After 1 week, analysis of the unit-cell length (*a*) of (un)reacted magnetite and maghemite X-ray diffraction patterns indicated slight changes in the Fe(II):Fe(III) stoichiometry in accordance with the addition and adsorption of Fe(II). Obtained data from As speciation in solution suggested that up to 15% of As(III) was oxidized in both magnetite and maghemite systems, with higher oxidation and adsorption rates at increasing Fe(II) concentrations. However, As in solution accounted for <15% of As(tot). Higher As adsorption (up to 95%) was recorded in the presence of Fe(II) for both the magnetite and maghemite systems. Conversely, the presence of As appeared to negligibly impact Fe(II) adsorption kinetics, which may be more dependent on initial magnetite stoichiometry.

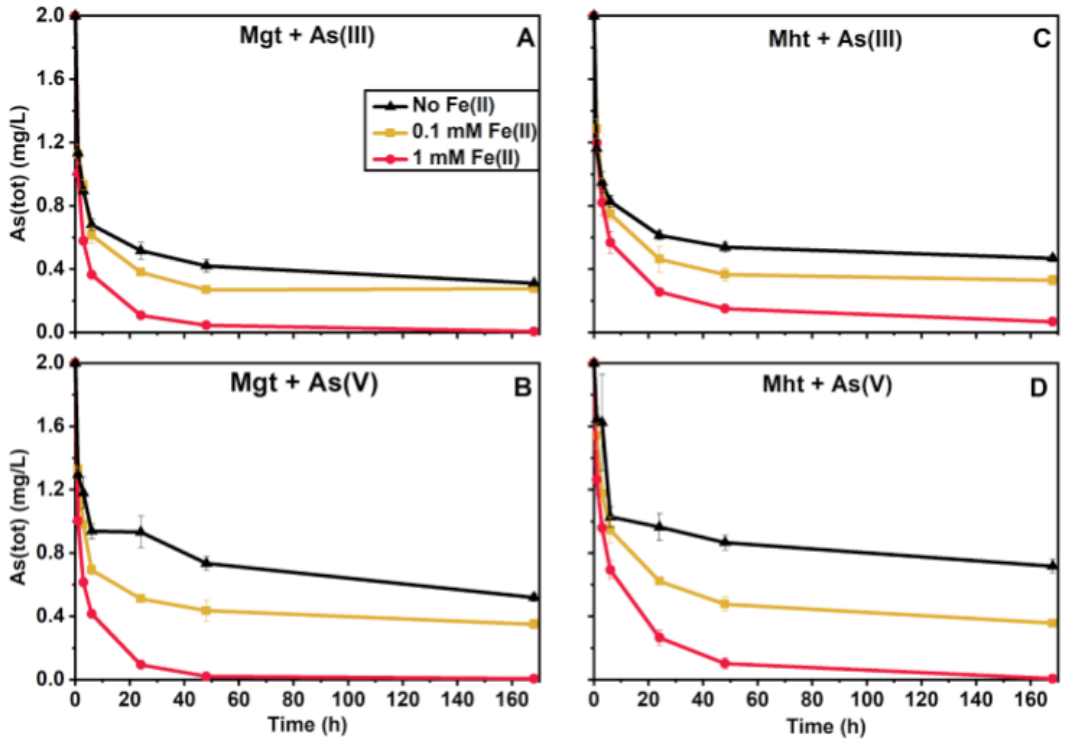


Figure 1. Aqueous As concentrations after adsorption on magnetite (Mgt) and maghemite (Mht) at different $Fe(II)_{aq}$ concentrations. Panels A and C were spiked with arsenite and B and D were spiked with arsenate. Error bars represent the standard deviation from triplicate experiments.

REFERENCES

[1] Amstaetter, K.; Borch, T.; Larese-Casanova, P.; Kappler, A. 2010: Redox transformation of Arsenic by Fe(II)-activated goethite (α-FeOOH). Environ. Sci. Technol., 44, 102-108.

[2] Dixit, S.; Hering, J. G. 2003: Comparison of arsenic(V) and arsenic(III) sorption onto iron oxide minerals: Implications for arsenic mobility. Environ. Sci. Technol., 37, 4182-4189.

[3] Huhmann, B. L.; Neumann, A.; Boyanov, M. I.; Kemner, K. M.; Scherer, M. M. 2017: Emerging investigator series: 5/6 As(v) in magnetite: incorporation and redistribution. Environmental Science-Processes & Impacts, 19, (10), 1208-1219.

[4] Handler, R. M.; Frierdich, A. J.; Johnson, C. M.; Rosso, K. M.; Beard, B. L.; Wang, C.; Latta, D. E.; Neumann, A.; Pasakarnis, T.; Premaratne, W. A. P. J.; Scherer, M. M. 2014: Fe(II)-catalyzed recrystallization of goethite revisited. Environ. Sci. Technol., 48, 11302-11311.

[5] Gorski, C. A.; Handler, R. M.; Beard, B. L.; Pasakarnis, T.; Johnson, C. M.; Scherer, M. M. 2012: Fe atom exchange between aqueous Fe2+ and magnetite. Environ. Sci. Technol., 46, 12399-12407.

P 14.9

Response of ammonia oxidizing archaeal and bacteria microbial to co-contamination of decabromodiphenyl ether and copper in river sediments

Linqiong Wang, Vera Slaveykova[1]

Département F.-A. Forel des sciences de l'environnement et de l'eau & Institut des sciences de l'environnement, Université de Genève, Uni Carl Vogt 66, boulevard Carl-Vogt, CH-1211 Genève 4, Suisse
E-mail: Linqiong.Wang@etu.unige.ch (First author), Vera.Slaveykova@unige.ch (1Corresponding authors)

Ammonia oxidation plays fundamental role in river nitrogen cycle ecosystems, which is normally governed by both ammonia oxidizing archaea (AOA) and bacteria (AOB). The relative distribution of AOA and AOB may mostly depend on the environmental conditions, such as contaminant affection. There is now increasing concern regarding the effect of polybrominated diphenyl ethers (PBDEs) and heavy metals on the environment as e-waste discharge. However, the co-contamination of typical emerging pollutant PBDEs and heavy metal on AOA and AOB communities in river sediments remains unknown. In this study, multiple analytical tools including quantitative PCR (qPCR) and 454-high-throughput pyrosequencing were used to reveal the ammonia monooxygenase (AMO) activity, subunit alpha (*amo*A) genes abundance, and the communities structure of AOA and AOB in river sediment. It was found that the inhibitory of AMO activities were increased with the increase of BDE209 and Cu concentrations. AMO activities was also inhibited and then enhanced as the increasing of incubation time in BDE209 contaminated sediments, while AMO activity and incubation time showed a decrease linear relationship in Cu contamination. Moreover, synergic effects of BDE209 and Cu resulted in higher AMO activity reduction than BDE209 individual pollutant did. AOA and AOB *amo*A genes abundance of co-contaminated sediments were lower than these of individual contamination cases. In addition, compared with AOA genes abundance, AOB *amo*A genes abundance was more easily inhibited than that in the co-contamination cases. AOA *amo*A copies number was declined 75.9% and 83.2% and AOB *amo*A genes abundance was declined 82.8% and 90.0%, at the 20 or 100 mg/kg BDE209 with 100 mg/kg Cu co- contaminated, respectively. The pyrosequencing results showed that a total of one main AOB phylum Proteobacteria and one main AOA phylum Thaumarchaeota across all samples were identified at the phylum level. Meanwhile AOB community structure was obviously altered and AOA community structure was not affected in the same incubation time. These results revealed that AOB community was sensitive to the contaminated environment and played an important role in the ammonia oxidation. This study provided a better understanding of ecotoxicological effects of BDE209 and Cu joint exposure on AOA and AOB in river sediments.

P 14.10

Mn authigenesis at the Landsort Deep, Baltic Sea and its impact on Mo isotopes

Martin Wille[1], Florian Kurzweil[2], Olaf Dellwig[3]

[1]*Instiute of Geological Sciences, University of Bern, Switzerland (martin.wille@geo.unibe.ch)*
[2]*Institute of Geology and Mineralogy, University of Cologne, Germany*
[3]*Leibniz-Institute for Baltic Sea Research, Rostock, Germany*

The formation of Mn oxides in the ocean is thought to require the presence of high-potential oxidants such as free O_2. However, anoxygenic photosynthesis prior to the evolution of oxygenic photosynthesis could also led to Mn^{2+} oxidation. The redox sensitive element Mo is scavenged by Mn oxides. Thereby, isotopically light Mo is preferentially adsorbed. Observed co-variation between authigenic Mn enrichments and Mo isotopic composition ($\delta^{98/95}$Mo) in Archean and Paleoproterozoic marine sediments have therefore been interpreted as evidence for free O_2 in the water column. However, Mn oxides are commonly not preserved due to their reductive dissolution within the sediment, which also affects the cycling of Mo and possibly the sedimentary Mo isotope composition. Therefore, the preservation of primary Mo isotope signatures during early diagenesis needs to be investigated in modern marine analogs.

The Landsort Deep, Baltic Sea, represents an appropriate locality to study the impact of Mn oxides on trace metal cycling and their isotope signatures. Bottom-water redox conditions change on annual to decadal scales due to inflows of O_2-containing waters from the North Sea. While euxinic stagnation periods allow accumulation of dissolved Mn^{2+} in bottom waters, inflows are able to oxidize the entire water body fostering enhanced deposition of Mn-oxides. Anoxic conditions within the sediment provoke the reduction of Mn-oxides and the formation of secondary Mn-carbonate phases.

Here we present Mo isotope data from a dated short core that covers the last ~60 years. The formation of Mn-rich carbonates in these sediments clearly indicates hypoxic but non-euxinic bottom water conditions during deposition. Despite the early diagenetic reduction of Mn and redistribution of Mo, the negative co-variation beween Mn content and $\delta^{98/95}$Mo values indicates the retention of isotopically light Mo during Mn-carbonate formation. This is supported by Mo isotope data from sediment traps and suspended particulate matter. Our results confirm that Mo isotopes in Mn-rich marine sediments are indeed useful to reconstruct temporal changes in depositional redox conditions.

P 14.11

Oxidation of bioavailable carbon substrates by Mn oxides and the competition effect with bacteria

Isabella O. Zelano[1], Julia González Holguera[1], Jasquelin Peña[1]

[1]*Université de Lausanne, CH-1015 Lausanne, Switzerland (jasquelin.pena@unil.ch)*

The residence time of organic biomolecules, including organic acids and carbohydrates, in natural surface soil systems stronlgy depeds on their interaction with mineral phases and microorganisms. Minerals can both stabilize organic substrates through sorption reactions or promote their oxidation, whereasmicroorganisms can use them as a direct source of carbon and electrons, converting them into biomass or mineraling them to CO_2. Manganese oxides (MnOx) are among the strongest abiotic oxidants in soils with reduction potentials that are high enough to drive the oxidation of a broad range of organic molecules. From the Mn side, these reactions can induce the accumulation of Mn(III) in the oxide or dissolution to Mn(II). From the carbon side, we hypothesize that the decarboxylation of organic molecules will induce a cascade of multi-electron oxidative transformation (Wang and Stone 2006), leading to CO_2 production. These reactions may compete with microbial activity by altering the availability of carbon substrates. In this study we investigate the kinetics and mechanism of reaction between glucose, a readily available carbon substrate, and δ-MnO_2 under soil-relevant pH conditions (pH= 5 to 7). Batch experiments were conducted by mixing 5 mM glucose and a 1 mM δ-MnO_2 suspension, in order to have an excess of the electron donor, in presence and absence of the heterotrophic organism *Pseudomonas putida.* Samples were collected over 7 days and reaction products were monitored to compile mass and an electron balances. The extent of reductive dissolution, as measured by $Mn(II)_{aq}$, increased over time and with decreasing pH. However, independently of pH and in both biotic and abiotic conditions, reductive dissolution is precedeed by a rapid increase in the Mn(III) content in the solid phase within 20 minutes of reaction (i.e. up to 40%Mn(III)). In abiotic systems, formic acid is the main oxidation product formed in solution. In biogenic systems, a decrease in total organic carbon (TOC) is observed, suggesting the mineralisation of glucose to CO_2. However, the decrease in TOC is limited in presence of δ-MnO_2, suggesting that oxides can induce a competition for organic substrates with bacteria and alter the pool of available carbon sources for the microbial community.

REFERENCES

Wang, Y., & Stone, A. 2006: Reaction of Mn III,IV (hydr)oxides with oxalic acid, glyoxylic acid, phosphonoformic acid, and structurally-related organic compounds, Geochimica, 70, 4477–4490.

15. Atmospheric Processes and Interactions with the Biosphere +

16. Phenology and seasonality +

17. Aerosols and clouds in a changing world

Christof Ammann, Stefan Brönnimann, Susanne Burri, Martin Steinbacher
Yann Vitasse, Sibylle Stöckli, This Rutishauser
Christopher Hoyle, Ulrich Krieger

ACP – Commission on Atmospheric Chemistry and Physics
Swiss Commission for Phenology and Seasonality (CPS)

TALKS:

15.1 Alpert P.A., Finizio S., Boucly A., Corral Arroyo P., Dou J., Krieger U.K., Padeste C., Ammann M., Watts B.: Chemically Mapping Ice Forming Particles

15.2 Brunner C., Kanji Z.A.: A new Instrument for Continuous Monitoring of Ice Nucleating Particles

15.3 Bühler M., Häni C., Kupper T., Schrade S., Zähner M., Wyss S.A., Mohn J., Ammann C., Brönnimann S.: Assessment of methane emissions from a dairy housing using an inverse dispersion technique

15.4 Dou J., Luo B., Peter T., Alpert P.A., Corral Arroyo P., Ammann M., Krieger U.K.: Photochemical aging processes in iron containing aerosols

15.5 Graf M., Scheidegger P., Looser H., Peter T., Emmenegger L., Tuzson B.: Mid-IR Laser Spectrometer for Balloon-borne Lower Stratospheric Water Vapor Measurements

15.6 Kholiavchuk D., Răchită I.-G., Holobâcă I.-H., Pop O.: Meteorological triggers for snow avalanches in the Borzhava and Chornohora massifs of the Ukrainian Carpathians

15.7 Kilchhofer K., Mahrt F., Kanji Z.A.: Impact of cloud processing on the ice nucleating ability of organic aerosol particles

15.8 Li Y., Riedl A., Aemisegger F., Buchmann N., Eugster W.: Effect of Dew and Fog Water on Swiss Grasslands Using Stable Water Isotopes

15.9 Liu Y., Bachofen C., Klaus V., Duarte G.S., Sun Q., Gilgen A.K., Oliveira Hagen E., Wittwer R., van der Heijden M.G.A., Buchmann N.: Tracking growth phenology and physiology of a cropland in response to experimental drought and different cropping systems

15.10 Schneider L.: Do warmer winters induce more forest and crop pests in Switzerland?

15.11 Schneuwly J., Ammann C.: Large regional differences of soil water limitation effect on ozone induced yield loss for wheat and potato in Switzerland

15.12 Singh R., Singh S., Kumar A., Kumar Y.: Phenological development in mustard (Brassica juncea) crop under varying thermal times

15.13 Singh S., Singh R.: Implication of air pollutants in resilient and sustainable crops production

15.14 Vattioni S.: Exploring Accumulation-Mode H_2SO_4 Versus SO_2 Stratospheric Sulfate Geoengineering In A Sectional Aerosol–Chemistry–Climate Model

15.15 Voglmeier K., Jocher M., Ammann C.: Using the eddy covariance technique to determine the nitrous oxide emissions of an intensively used pasture in Switzerland

15.16 Volk M., Wahl A., Giger R., Bassin S.: Warming, cooling, irrigation and N-deposition effects on the ecosystem C-cycle of subalpine grassland

15.17 Wang Y., Paul S., Jocher M., Alewell C., Leifeld J.: The impact of cover fill on N_2O emissions in drained peatland

POSTERS:

P 15.1 Ammann C., Jocher M., Voglmeier K.: Determining the greenhouse gas budget of two neighboring pastures using the eddy covariance technique

P 15.2 Grimaldi C., Plunkett G., Óladóttir B.A., McConnell J.R., Sigl M.: Icelandic volcanism and climate from Greenland ice cores over the past 3 ka

P 15.3 Osterwalder S., Eugster W., Feigenwinter I., Jiskra M.: First eddy covariance flux measurements of gaseous elemental mercury over a grassland

P 15.4 Chacko M., Mayor S., Crowther T., Niklaus P.A.: Effects of biodiversity on ecosystem functioning across local and landscape scales

15.1

Chemically Mapping Ice Forming Particles

Peter A. Alpert[1], Simone Finizio[1], Anthony Boucly[1], Pablo Corral Arroyo[2], Jing Dou[2], Ulrich K. Kreiger[2], Celestino Padeste[1], Markus Ammann[1], Benjamin Watts[1]

[1]Paul Scherrer Institut, Forschungsstrasse 111, CH-5232 Villigen PSI (peter.alpert@psi.ch)
[2]Eidgenössische Technische Hochschule Zürich, Rämistrasse 101, CH-8092 Zürich, Switzerland

Precipitation is mostly formed via the ice phase in mixed phase clouds, and ice clouds are very relevant for Earths' climate. Freezing or prevention of freezing is common to everyday life, e.g. for food and drug storage, icing and de-icing, etc. However, the ice nucleation process is not well understood, since it occurs on the size scale of clusters of molecules and time scales of molecular fluctuations In this study, we have taken a step toward nanoscale observation of particles that nucleate ice by devolping new instrumentation coupled to a scanning transmission X-ray microscope (STXM) at the Swiss Light Source. We employ near-edge X-ray absorption fine-structure spectroscopy (NEXAFS) to map chemical properties of ice nucleating particles with 35 nm spatial resolution. This is the first time ice nucleation has been measured in-situ in an X-ray microscope. The main technical challenge was temperature control, and thus relative humidity control, while maintaining X-ray transparency. A sketch of our setup is shown in the figure below. X-rays are focused onto our sample through an aperture, which was modified to host a jet of nitrogen with a temperature down to 170 K. The cold jet impinges on the back surface of our sample exposed to water vapour. We verified that ice nucleation can occur on iron containing nano-particles, ferrihydrite, in the figure below. This iron mineral is contained in mineral dust, which itself is assumed to be ice active. When coating ferrihydrite with citric acid, mimicing organic coatings aerosol particles obtain throughout their atmospheric lifetime, we observed a reduction in the efficiency to nucleate ice. However, we suspect this is only due to the fact that citric acid will take up water and solubilze leading to a freezing point depression. Using a newly developed ice nucleation model based off of solution water activity, we can predict the relative humidty and temperature that ice forms.

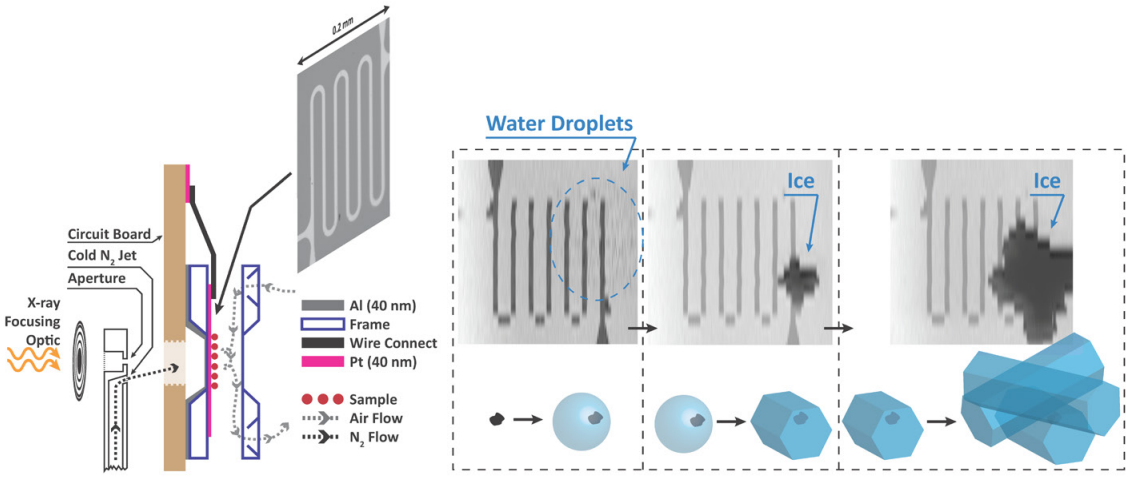


Figure 1. Left: A sketch of the IceCell. Right: Raw STXM images of water condensation and ice nucleation on ferrihydrite particles.

15.2

A new Instrument for Continuous Monitoring of Ice Nucleating Particles

Cyril Brunner[1] and Zamin A. Kanji[1]

[1]*Institute for Atmospheric and Climate Science, ETH Zurich, Zurich, 8092, Switzerland (cyril.brunner@env.ethz.ch)*

The limited knowledge of aerosol-cloud interactions introduces large uncertainties when simulating the cloud radiative forcing in climate models (Boucher et al., 2013). The physical and optical properties, as well as the evolution of precipitation of a cloud is a strong function of the hydrometeor phase. One pathway to form ice crystals in the troposphere is via ice nucleating particles (INPs) which make up only a tiny fraction of all tropospheric aerosols. For accurate climate forecasts and projections, the parametrization of cloud processes and information such as the concentrations of INPs are needed (Demott et al., 2010; Phillips et al., 2013). Presently, no continuous online INP counter is available and the data acquisition still requires a human operator.

To address this restriction, we are developing a fully automated online ice nucleation particle counter, through an adaptation of an existing custom-built instrument, the Horizontal Ice Nucleation Chamber (HINC, Lacher et al., 2017), called HINC-Auto. HINC has successfully been used to detect INP concentrations during numerous field campaigns since 2014. HINC-Auto will be collecting data at the High Altitude Research Station Jungfraujoch (JFJ, 3580 m a.s.l., 46°33’ N, 7°59’ E) by mid-2020 with the goal of publishing the data in near real-time on an open access website. We present results from the first campaign in August 2019 where HINC-Auto was run at the JFJ. Furthermore, we will discuss potential of the new device as wells as the difficulties faced.

REFERENCES:

Boucher, O., Randall, D., Artaxo, P., Bretherton, C., Feingold, G., Forster, P., Kerminen, V.-M., Kondo, Y., Liao, H., Lohmann, U., Rasch, P., Satheesh, S. K., Sherwood, S., Stevens, B. and Zhang, X. Y.: Clouds and Aerosols, in Climate Change 2013: The Physical Science Basis. Contribution of Working Group I to the Fifth Assessment Report of the Intergovernmental Panel on Climate Change, edited by T. F. Stocker, D. Qin, G.-K. Plattner, M. Tignor, S. K. Allen, J. Boschung, A. Nauels, Y. Xia, V. Bex, and P. M. Midgley, pp. 571–658, Cambridge University Press, Cambridge, United Kingdom and New York, NY, USA., 2013.

Demott, P. J., Prenni, A. J., Liu, X., Kreidenweis, S. M., Petters, M. D., Twohy, C. H., Richardson, M. S., Eidhammer, T. and Rogers, D. C.: Predicting global atmospheric ice nuclei distributions and their impacts on climate, Proc. Natl. Acad. Sci., 107(25), 11217–11222, doi:10.1073/pnas.0910818107, 2010.

Lacher, L., Lohmann, U., Boose, Y., Zipori, A., Herrmann, E., Bukowiecki, N., Steinbacher, M. and Kanji, Z. A.: The Horizontal Ice Nucleation Chamber (HINC): INP measurements at conditions relevant for mixed-phase clouds at the High Altitude Research Station Jungfraujoch, Atmos. Chem. Phys., 17(24), 15199–15224, doi:10.5194/acp-17-15199-2017, 2017.

Phillips, V. T. J., Demott, P. J., Andronache, C., Pratt, K. A., Prather, K. A., Subramanian, R. and Twohy, C.: Improvements to an empirical parameterization of heterogeneous ice nucleation and its comparison with observations, J. Atmos. Sci., 70(2), 378–409, doi:10.1175/JAS-D-12-080.1, 2013.

15.3

Assessment of methane emissions from a dairy housing using an inverse dispersion technique

Marcel Bühler[1,2,3] Christoph Häni[3], Thomas Kupper[3], Sabine Schrade[4], Michael Zähner[4], Simon A. Wyss[5], Joachim Mohn[5], Christof Ammann[6], Stefan Brönnimann[1,2]

[1]Oeschger Centre for Climate Change Research, University of Bern, Hochschulstrasse 4, CH-3012 Bern
[2]Institute of Geography, University of Bern, Hallerstrasse 12, CH-3012 Bern (marcel.buehler@giub.unibe.ch)
[3]School of Agricultural, Forest and Food Sciences HAFL, Bern University of Applied Sciences, Länggasse 85, CH-3052 Zollikofen
[4]Ruminants Group, Agroscope, Tänikon 1, CH-8356 Ettenhausen
[5]Laboratory for Air Pollution/Environmental Technology, EMPA, Überlandstrasse 129, CH-8600 Dübendorf
[6]Climate and Agriculture Group, Agroscope, Reckenholzstrasse 191, CH-8046 Zürich

Quantification of gaseous emissions from diffuses sources, e.g. animal farms, is challenging due to their heterogeneity in space and time. The inverse dispersion technique is a promising option, which is increasingly used to determine gaseous emissions from diffuse sources, as it offers high flexibility at reasonable costs. So far, the inverse dispersion technique was only applied under Monin-Obukhov similarity theory conditions, which are often not fulfilled in central Europe. Here we use a simple backward Lagrangian stocastic (bLS) model in combination with open-path tunable diode laser spectrometers up- and downwind of the source in non-homogeneous horizontal and flat terrain and difficult micrometeorological conditions to model methane emissions from a dairy housing and compare it to simultaneously conducted in-house tracer measurements. We could show that the bLS model works also under non-ideal model conditions and that the method can be used to model emissions of sources in areas for which an emission estimate was not possible so far.

15.4

Photochemical aging processes in iron containing aerosols

Jing Dou[1], Beiping Luo[1], Peter A. Alpert[2], Pablo Corral Arroyo[2], Markus Ammann[2], Thomas Peter[1], and Ulrich K. Krieger[1]

[1]Institute for Atmospheric and Climate Science, ETH Zürich, 8092, Zürich (jing.dou@env.ethz.ch)
[2]Laboratory of Environmental Chemistry, Paul Scherrer Institute, 5232, Villigen PSI

Fe^{III}-citrate plays an important role in aerosol aging processes, especially in the lower troposphere, with low intensities of ultraviolet light. The photochemistry of Fe^{III}-citrate has been widely recognized in both solution and solid states. It can absorb light up to around 500 nm, inducing the reduction of Fe^{III} and the oxidation of carboxylate ligands. In the presence of O_2, ensuing radical chemistry will likely lead to more decarboxylation and production of peroxides (e.g., OH•, HO_2• and H_2O_2) and oxygenated volatile organic compounds (OVOC). The peroxides in turn allow the re-oxidation of Fe^{II} to Fe^{III}, closing this photocatalytic cycle, in which Fe acts as a catalyst.

Little is known about how the viscosity of an aerosol might slow these catalytic cycles. To investigate this question, we use an electrodynamic balance. A single mixed FeIII-citrate/citric acid aerosol droplet (radius ~10 µm) is levitated in this balance with well controlled temperature and relative humidity. During photochemical processing under irradiation in the visible (473 nm), mass and size changes of the particle are tracked. We measure a substantial mass loss (80% over 24 hours) of the droplet during photochemical processing due to the evaporation of volatile (e.g., CO_2) and semi-volatile (e.g., ketones) products. We focus the experiments on high viscosity cases (i.e., reduced molecular mobility and low water content), which slows the transport of products and thus affects chemical reaction rates. For a coherent description we developed a numerical model, which includes main equilibria, chemical reactions, and diffusivities of major species. It allows to simulate the concentration gradients of each species inside of the particle, and to derive the size and mass changes. Comparing model output with experimental data enables us to determine or at least constrain some of the crucial parameters, such as equilibrium constants, chemical reaction rates, and liquid phase diffusion coefficients. With such well-defined and physically constrained parameters, we will predict the evolution of products as well as organic acid degradation in the condensed phase under atmospheric conditions.

15.5

Mid-IR Laser Spectrometer for Balloon-borne Lower Stratospheric Water Vapor Measurements

Manuel Graf[1], Philipp Scheidegger[1], Herbert Looser[1], Thomas Peter[2], Lukas Emmenegger[1], Béla Tuzson[1]

[1]Laboratory for Air Pollution & Environmental Technology, Empa Dübendorf, Switzerland (manuel.graf@empa.ch)
[2]Institute for Atmospheric and Climate Science, ETH Zürich, Switzerland

Water vapour is *the* dominant greenhouse gas and its abundance in the upper tropospheric/lower stratospheric region (UTLS, 8-25 km altitude) is of great importance to the Earth›s radiative balance. Reliable predictions of the climate evolution as well as the understanding of certain cloud-microphysical processes require the accurate and frequent measurement of water vapour concentrations at these altitudes. We present a compact and lightweight instrument based on laser absorption spectroscopy (LAS) that addresses the stringent constraints posed by the harsh environmental conditions found in the UTLS. To accomplish this, fundamental reconsiderations were required with respect to traditional, lab-based spectrometers. The key element for high-precision measurements of low abundance gas concentrations by means of LAS is the multipass cell (MPC). It defines both the performance and the size of a spectrometer. Established designs have serious limitations with respect to compactness, weight and/or optical performance. As part of this project, a highly versatile MPC has been proposed and developed, which supports compact and well-controlled beam folding (Graf 2018). The inherent mechanical symmetry of this segmented circular multipass cell (SC-MPC) makes it predestined for mobile applications and rough environmental conditions. As light source, we use a single mode, continuous-wave quantum cascade laser emitting at 6 µm. The collimated laser beam is reflected 64 times within the SC-MPC resulting in an effective optical path length of 6 m. Water vapour amount fractions of <10 ppm can be measured with a precision better than 1% at 1 Hz. Fast response and reduced interference by spurious water desorbing from surfaces is ensured by operating the cell in open-path configuration. Thus, in a balloon-borne setting, the ambient air flows freely through the cell because of the ascending motion. The overall instrument weighs less than 4 kg (including battery) and has an average power consumption of 15 W. Specifically developed hard- and software guarantee stable and autonomous operation during the flight period. Extensive stability assessments in a climate chamber as well as validation experiments using dynamically generated, SI-traceable water vapour mixtures were performed in collaboration with the Swiss Federal Institute for Metrology (METAS). The instrument is currently prepared for deployment aboard meteorological balloons for in-situ measurement of water vapour in the UTLS. This concept represents a paradigm change in portable laser spectroscopy instrumentation and can target many other compounds and research fields, e.g. detection of methane on UAV based platforms.

REFERENCES

[1] Graf, M., Emmenegger, L., & Tuzson, B. 2018: Compact, circular, and optically stable multipass cell for mobile laser absorption spectroscopy, Opt. Lett. 43, 2434-2437

15.6

Meteorological triggers for snow avalanches in the Borzhava and Chornohora massifs of the Ukrainian Carpathians

Dariia Kholiavchuk[1], Ionela Georgiana Răchită[2], Iulian Horea Holobâcă[2], Olimpiu Pop[2]

[1]Department of Physical Geography, Geomorphology and Paleogeography, Yuriy Fedkovych Chernivtsi National University, Kotsyubynsky 2, 58012 Chernivtsi, Ukraine (d.kholyavchuk@chnu.edu.ua)
[2]Faculty of Geography, Babeş-Bolyai University, 5-7 Clinicilor Street, RO-400006, Cluj-Napoca, Romania

Snow avalanches are common natural hazards threatening the tourism mountain areas in the Ukrainian Carpathians. More than 500 avalanche centres are detected here. The sections at altitudes higher than 1,000 m (9.6% of the mountain area) that refer to the Chornohora and Borzhava massifs are the most prone to the avalanche activity and associated ecosystem damages and accidents. Here,15-20 avalanche events a year are observed. An increasing number of avalanche events and avalanche victims are reported in the past decade. Snow and weather regimes are considered to control avalanche activity (Castebrunet et al. 2012). These areas are covered by only two meteorological and snow-avalanche stations with a continuous data series at Play (1343 m a.s.l) and Pogegevskaya(1429 m a.s.l.) that include the observation of 41 avalanche centres. Accordingly, this study involves the time series analysis of meteorological variables and synoptic patterns for the identification of dominant snow avalanche triggers and interpolation for other similar areas in the Ukrainian Carpathians.

The majority of detected avalanches take place on the north-eastern and south-eastern steep slopes with high instability of the snow layer. In the region, 70% of precipitation in the avalanche period from December to April constitute snow. For this period in the last decade, three major meteorological triggers were distinguished –intensive snowfalls, snowstorms, and warming episodes that correspond to the results in Southern Carpathians, Romania (Pop et al. 2018). Intensive snowfalls with a 20-cm increase and snowstorms triggering snow avalanches are maily detected in December and January (Bilanyuk & Tikhanovich 2015.) Warming events with the maximum speed of the surface air temperature increase 1°C per hour are found the dominant trigger in March-April. Besides, differences in the dominance of certain meteorological conditions between the two massifs were found. Snowstorms are the most frequent triggers of snow avalanches in the north-western part of the Ukrainian Carpathians – Borzhava in all the months. Meanwhile, all types of meteorological triggers of snow avalanches are observed in the central part of the Ukrainian Carpathians – Chornohora. Our preliminary results show the increase in the occurrence of wet-snow avalanches associated with intensive precipitation and warming episodes that are correlated with the south-western cyclonic types of regional atmospheric circulation. This work is a contribution to the project ACTIVNEIGE «Activité des avalanches des neige dans les Carpates Orientales Roumaines et Ukrainiennes» (Snow avalanche activity in Romanian and Ukrainian Eastern Carpathians), funded by AUF-IFA RO.

REFERENCES

Bilanyuk, V. & Tikhanovich, I. 2015: Avalanche process in Ukrainian Carpathians. Journal of Education, Health and Sport 5(7), 96-104.

Castebrunet, H., Eckert, N., Giraud, G. 2012: Snow and weather climatic control on snow avalanche occurrence fluctuations over 50 yr in the French Alps. Climate of the Past, 8, 855-875.

Pop O., Holobâcă, I.-H., Mesesan, F., Gavrila, I.-G., Tudose ,T., Burada, C. 2018: Régime des variables climatiques pour les hivers avalancheux dans les monts Parâng (Carpates Méridionales, Roumanie). Les échelles spatiales

Et temporelles fines. Actes du colloque de Nice. XXXI Colloque de L'association Internationale de Climatologie. 4 -7 juillet 2018, Nice.

15.7

Impact of cloud processing on the ice nucleating ability of organic aerosol particles

Kevin Kilchhofer[1], Fabian Mahrt[1] & Zamin A. Kanji[1]

[1]*Institute for Atmospheric and Climate Science, ETH Zurich, Zurich, 8092, Switzerland*

Aerosol particles can interact with clouds by acting as ice nucleating particles (INPs) contributing to significant uncertainties regarding future climate projections (Boucher et al., 2013). Ice formation also influences precipitation formation (Mülmenstädt et al., 2015), highlighting the importance of better constraining ice formation processes in clouds. Organic aerosols (OAs) have been shown to be INPs in the troposphere, even below the homogeneous nucleation temperature of 235K (Knopf et al., 2018). They are either formed from organic precursor gases as secondary organic aerosol or can directly be emitted as primary OA from sources such as ocean and lake surfaces, from biomass burning, and coal combustion. The atmospheric burden of OA is estimated to be approximately 1.7 Tg (Textor et al., 2006) and have been observed in both natural remote and anthropogenically impacted regions (Jimenez et al., 2009).

While OA particles can freeze or form a droplet in a (first) cloud formation cycle, its long atmospheric lifetime of about a week renders it likely that such particles are involved in multiple cloud-cycles. The impact of such a cloud processing on OA physicochemical properties, and potentially altered ice nucleating ability is almost unknown. Previous studies report altered, more porous morphology and particle size (Adler et al., 2013), however the impacts of these alterations on ice nucleation are unknown.

In this work, we investigate if cloud processing impacts the heterogeneous ice nucleation potential of OA particles in either cirrus or mixed-phase cloud environments. A previously used laboratory setup that includes two coupled horizontal ice nucleation chambers described by Mahrt et al. (2019) and atmospherically relevant OA proxies (i.e. levoglucosan and oxalic acid) are used for the measurements. The aim is to determine if there is a detectable change in the ice nucleation ability of OAs in comparison to unprocessed particles. Furthermore, we investigate which properties of the aerosol lead to the any observed change. Experiments are conducted to measure the ice nucleation potential of OA following different relative humidity and temperature trajectories for both the cloud processed particles and unprocessed particles. Our results will aid in furthering our understanding the fate of OA as INPs in relation to their atmospheric lifetime and physicochemical properties.

REFERENCES

Adler, G., T. Koop, C. Haspel, I. Taraniuk, T. Moise, I. Koren, R. H. Heiblum, and Y. Rudich 2013. Formation of highly porous aerosol particles by atmospheric freeze-drying in ice clouds. Proceedings of the National Academy of Sciences, 110(51):20414-20419.

Boucher, O., D. Randall, P. Artaxo, C. Bretherton, G. Feingold, P. Forster, et al. 2013. Clouds and aerosols, Pp. 571{657. Cambridge University Press.

Jimenez, J. L., M. R. Canagaratna, N. M. Donahue, A. S. H. Prevot, Q. Zhang, J. H. Kroll, et al. 2009. Evolution of organic aerosols in the atmosphere. Science, 326(5959):1525-1529.

Knopf, D. A., P. A. Alpert, and B. Wang 2018. The role of organic aerosol in atmospheric ice nucleation: A review. ACS Earth and Space Chemistry, 2(3):168-202.

Mahrt, F., K. Kilchhofer, C. Marcolli, P. Grönquist, R. O. David, M. Rösch, U. Lohmann, Z. Kanji 2019. The impact of cloud processing on the ice nucleation abilities of soot particles at cirrus temperatures. Journal of Geophysical Research: Atmospheres.

Mülmenstädt, J., O. Sourdeval, J. Delanoë, and J. Quaas 2015. Frequency of occurrence of rain from liquid-, mixed-, and ice-phase clouds derived from a-train satellite retrievals. Geophysical Research Letters, 42(15):6502-6509.

Textor, C., S. Michael, G. S, K. S, Y. Balkanski, B. S, T. Berntsen, T. Berglen, O. Boucher, M. Chin, F. Dentener, T. Diehl, R. Easter, F. H, F. D, S. Ghan, P. Ginoux, S. Gong, G. A et al.2006. Analysis and quanti_cation of the diversities of aerosol life cycles within aerocom. Atmospheric Chemistry and Physics, 6.

15.8

Effect of Dew and Fog Water on Swiss Grasslands Using Stable Water Isotopes

Yafei Li[1°], Andreas Riedl[1], Franziska Aemisegger[2], Nina Buchmann[1], Werner Eugster[1]

[1]*Institute of Agricultural Sciences, ETH Zurich, Universitätstrasse 2, CH-8092 Zurich, Switzerland*
[2]*Institute for Atmospheric and Climate Science, ETH Zurich, Universitätstrasse 16, CH-8092 Zurich, Switzerland*

°*Corresponding author: yafei.li@usys.ethz.ch*

Dew and fog have been proven to be essential water sources for plants. Research so far has mainly focused on the effect of dew and fog on arid and desert ecosystems, but rarely on temperate ecosystems; only very limited information is available for temperate grasslands.

Compared to forests, more open canopies of grasslands are expected to be affected by stronger radiative cooling at night, which promotes the formation of dew on leaf surfaces, and the formation of ground radiation fog at the plant boundary layer. Moreover, the rougher surfaces of grasslands are believed to potentially collect more dew and fog water than forests. Under more frequent no-rain days in future summers, the effect of dew and fog on short-statured grassland species is expected to become more beneficial as an additional water source. In 2018, Switzerland experienced the driest April to August period of the last five decades. Our research using stable water isotopes investigates how dew and ground radiation fog affected Swiss grasslands in the extreme summer-2018.

Focusing on an intensively managed grassland located at a valley bottom close to Chamau (ZG), we measured the isotope ratios (δ^2H and $\delta^{18}O$) of near-surface atmospheric water vapor with a cavity ring-down spectrometer (Picarro L2130-i), and the isotope ratios of the liquid-phase water from dew/fog droplets, leaf, root crown and soil with an isotope-ratio mass spectrometer. The isotope signals were then combined with eddy flux and meteorological data to analyze the water vapor dynamics during dew/fog formation, and the interaction of dew/fog with plants and soil. Sampling was carried out during two distinct periods: pre-dew/fog and dew/fog periods. The pre-dew/fog period was defined as the period after sunset before the leaves got wet, while the dew/fog period was defined as the period after leaf wetting before sunrise.

Our results based on the isotope signals of atmospheric water vapor, leaf, root crown and soil water showed that dew/fog water was taken up by leaves, and was also present in top-soil. These results were supported by higher (less negative) leaf water potentials during dew/fog periods than during pre-dew/fog periods. The water vapor isotope signals at the near-surface layer showed deposition and condensation signatures during nights with dew/fog formation, i.e., δ^2H and $\delta^{18}O$ of water vapor in the atmospheric air gradually decreased. While the deuterium excess (d-excess) values of water vapor (d-excess= $\delta^2H - 8*\delta^{18}O$) were positive during the day, they became negative during dew nights, pointing towards non-equilibrium fractionation in supersaturated conditions accompanying a H_2O deposition flux. During dew nights accompanied with ground radiation fog, the d-excess values were relatively stable compared to the dew nights without fog when d-excess gradually decreased. Furthermore, the isotope signals of dew/fog and leaf water were different from each other during pre-dew/fog periods, but became similar during dew/fog periods.

Our research highlights the importance of dew and ground radiation fog as the water sources in temperate grasslands during rainless summer periods that are expected to become more frequent with global warming.

15.9

Tracking growth phenology and physiology of a cropland in response to experimental drought and different cropping systems

Yujie Liu[1], Christoph Bachofen[1], Valentin Klaus[1], Gicele S. Duarte[1], Qing Sun[1], Anna Katarina Gilgen[1], Emily Oliveira Hagen[2], Raphaël Wittwer[2], Marcel G.A. van der Heijden[2], Nina Buchmann[1]

[1]Institute of Agricultural Sciences, Department of Envionmental Systems Science, ETH Zürich, Universitätstrasse 2, CH-8006 Zürich (yujie.liu@usys.ethz.ch)
[2]Ecological Farming Group, Agroscope Reckenholz Tänikon, Reckenholzstrasse 191, CH-8046 Zürich

Plant phenology is highly sensitive to climate change and variability, phenological changes in response to climate change are well documented across all biomes. Drought events, which are projected to increase in both frequency and severity in the future, could strongly affect phenology. Shifts in phenology, such as the length of growing season, might directly link to ecosystem productivity and carbon cycling.

Organic farming and conservation tillage have been proposed as means to better cope with recent agricultural challenges such as environmental impacts from agricultural intensification and the demand for sustainable food production. However, whether drought effects can be mitigated by particular cropping system needs further investigation. Additionallly, it is not well understood how growth phenology relates to crop yields and if growth phenology extracted from phenocam images reflects plant physiological changes, especially in arable systems. We therefore aimed at understanding how drought affects growth phenology in different cropping systems.

We compared organic and conventional farming with intensive and conservation tillage and subjected the four cropping systems to a drought treatment. To observe the changes in growth phenology, we installed time-lapse cameras at plots managed under four different cropping systems. The cameras were mounted to wooden poles at 1.5 m of height with an oblique viewing angle (60° from horizontal) towards north, recording hourly images of the central region (1 m * 1.5 m) of the experimental plots (3 m * 5 m). Images were recorded for a pea and barley mixture in 2018 and winter wheat in 2019. We estimated the length of growing season by extracting the greenness index derived from phenocam image. We hypothesized that (1) a longer growing season leads to higher crop yields, (2) drought causes shifts in phenological phases, especially earlier senescence, and therefore shortens the growing season, (3) cropping systems with conservation tillage mitigate drought effects on growing season length and yield due to improved soil water condition.

First results from the pea-barley mixture show that longer growing season resulted in higher yields. Drought significantly shifted growth phenology, so that the peak of greenness and senescence date occurred earlier. This resulted in a shorter growing season and lower yields in plants under drought compared to control plots. Cropping systems showed no effects on the length of growing season. However, conservation tillage significantly reduced yields, while organic farming had no significant effects. We conclude that phenocam images can well record large yield changes resulting from drought, but not the less severe yield change caused by cropping systems. Future analyses will include plant traits, such as LAI and chlorophyll content in both pea and barley mixture and winter wheat to directly link phenology as observed by the phenocams and plant performance under drought.

Keywords: phenology, drought, cropping systems, yield, physiology

REFERENCES

D'Odorico P, et al. 2015: The match and mismatch between photosynthesis and land surface phenology of deciduous forests. Agric For Meteorol 214–215:25–38.

Keenan C, et al. 2014: Tracking Forest Phenology and Seasonal Physiology Using Digital Repeat Photography: a Critical Assessment. Ecol Appl 24(6):1478–1489.

Richardson AD. 2019: Tracking seasonal rhythms of plants in diverse ecosystems with digital camera imagery. New Phytol 222(4):1742–1750.

Richardson AD, et al. 2013: Climate change, phenology, and phenological control of vegetation feedbacks to the climate system. Agric For Meteorol 169:156–173.

Wittwer RA, Dorn B, Jossi W, van der Heijden MGA. 2017: Cover crops support ecological intensification of arable cropping systems. Sci Rep 7(1):41911.

15.10

Do warmer winters induce more forest and crop pests in Switzerland?

Léonard Schneider[1,2]

[1]Institute of Geography, University of Neuchatel, Espace Tilo-Frey 1, 2000 Neuchatel (leonard.schneider@unine.ch)
[2]Swiss Federal Research Institute WSL, Zürcherstrasse 111, 8903 Birmensdorf

While many studies focuse on the effect of global warming on diverse ecological systems during the spring-summer period, very few are investigating the winter period and its potential changes induced by climate change. With current global warming, warmer winters in Switzerland are already occuring and their frequency might increase. Some insect species which are sensible to extreme cold events in winter could benefit from this by increasing their winter survival rate. Forest pests, such as the pine processionary moth (Thaumetopoea pityocampa), the green spruce aphid (Elatobium abietinum), and some crop pests, such as the southern green stink bug (Nezara viridula) might react to warmer winters. These species are known to be negatively affected by temperatures going from -8°C, for the green stink bug (Chanthy, Martin et al. 2012), to -12°C, for the green spruce aphid (Halldórsson, Docherty et al. 2001) and for the processionary moth (Huchon and Démolin, 1970).

In this study, we examine the trends for winter temperatures in Switzerland, with a special focus on extreme cold events (days with minimal air temperature below -8°C and -12°C). We first analyse daily air temperature between 1975 and 2018 using homogenized data from 18 MeteoSwiss stations. Then, we use available data from CH2018 climatic scenarios to estimate possible trends along the coming century.

Preliminary results showed that a -8°C threshold is still regularly reached at all elevations in Switzerland for the winter period 1975-2018, with a frequency of 100% of the winters above 800m and 86% at lower elevations), except in the South Alps. Climatic scenarios indicate that this frequency might decrease during the next decades under 800m, with less and less winter reaching temperature below -8°C. By the end of the century, this threshold could be reached less than one year every two years at low elevations. The -12°C threshold is already quite unusual under 800 m (frequency of 39%), but occurs almost every winters at higher elevations (frequency of 97%). This frequency might also decrease in the next decades for elevations up to 1700m, and the threshold between 800 and 1700m could be reached only in 50 % of the winters by the end of the century. These results might suggest that (1) crop pests such as the southern green stink bug could overwinter more easily at low elevations in Switzlerand, and (2) that forest pests such as green spruce aphid and pine processionary moth could reach higher elevations by the end of the century.

REFERENCES

Chanthy, P., et al. (2012). “The effects of thermal acclimation on lethal temperatures and critical thermal limits in the green vegetable bug, Nezara viridula (L.)(Hemiptera: Pentatomidae).” Frontiers in physiology 3: 465.

Halldórsson, G., et al. (2001). “The performance of different populations of the green spruce aphid (Elatobium abietinum Walker) at different temperatures.”

Huchon, H. and G. Démolin (1970). «La bioécologie de la Processionnaire du pin: dispersion potentielle, dispersion actuelle.» Revue Forestière Française, 1970, S, fascicule thématique» La lutte biologique en forêt».

15.11

Large regional differences of soil water limitation effect on ozone induced yield loss for wheat and potato in Switzerland

Jérôme Schneuwly[1], Christof Ammann[1]

[1]Agroscope, Reckenholzstr. 191 CH-8046 Zurich, jerome.schneuwly@agroscope.admin.ch

Elevated Ozone (O_3) concentrations are generally prevalent during the crop growing season and can cause significant yield reductions in important food crops. To assess the potential risk, plant stomatal O_3 uptake rates are favorably calculated with deposition models. The species-specific hourly stomatal conductance is calculated based on the Jarvis-type multiplicative algorithm, including meteorological effects and crop phenology. The resulting phytotoxic ozone dose values over a flux threshold (POD_6) allow the estimation of crop specific O_3 induced yield losses.

Given that wheat and potato are among the economically most important food crops and the most O_3 sensitive, the study focused on these two crops. We used data of thirteen O_3 and meteorological measurement sites, distributed among the most important crop growing areas of Switzerland. The DO_3SE model was used for flux calculations and parameterized according to experimental data recorded across Europe, including some adjustments for Switzerland. As shown in earlier studies, soil water limitation is largely influencing the stomatal O_3 uptake by altering the stomatal aperture. To partly validate the soil water model, the modelled wheat evapotranspiration rates were compared with eddy covariance measurements of water fluxes. Different years were modelled to disentangle the influence of contrasting seasonal environmental conditions. Based on the site specific O_3 uptake rates and the respective crop growing area per district an average area weighted potential yield loss for Switzerland was calculated.

Regional and inter-annual differences in meteorological conditions led to considerable variations in soil water conditions and hence also in POD_6 values for wheat. Potato stomatal uptake was much less influenced by soil water and showed a more even distribution of POD_6 values across sites and years. It was found that soil water deficit, observed frequently in the western part of Switzerland, had a large attenuation effect on stomatal O_3 uptake by wheat and on corresponding yield losses. The comparison of modelled evapotranspiration with the water flux measurements over a wheat field showed a reasonable agreement concerning the temporal pattern and the magnitude. However, it was also shown that the model might overestimate stomatal closure in very dry conditions. The estimated nationally and temporally average yield loss was 3.2 ± 1.2% for wheat and 2.4 ± 0.8% for potato.

15.12

Phenological development in mustard (Brassica juncea) crop under varying thermal times

Raj Singh, Surender Singh, Anil Kumar and Yogesh Kumar

Dept of Agril Meteorology CCS Haryana Agricultural University, Hisar-125004, Haryana, India
E-mail: agmetraj@gmail.com

Phenology is the phenomenon of recurring plant and animal life cycle stages, especially their timing and relationships with the environment. Various environmental factors can drive phenological events mainly temperature, relative humidity, daylength, rainfall. Thus, weather and climate play a dominant role in determining both the average timing and specific date in which phenological event will occur at specific locations and years. The connections between phenology and climate go back as far the beginnings of agriculture, when farmers looked to seasonal biological signs to guide their farming activities, the impacts of climatic condiions has been recognized as a crucial element for environmental science that can contribute much to ecological, agricultural and its related studies. Phenology is seasonal timing of life cycle events which is used to help the study of recurring events and its relationship to climate, understanding of plant system and its resources.

Phenology involves the response of living organisms to seasonal and climatic changes of the environment in which they live. Phenological patterns are basic for understanding biological processes and functioning of tropical trees and ecosystems (Tesfaye *et al*., 2011). Plant reproduction and growth are affected by proximate factors such as precipitation, temperature and photoperiod, ecological factors such as plant-animal interaction, for instance pollination and seed dispersal. Therefore, phenological changes may have enormous consequences for plants depending upon the periodical availability of plant resources. The most important environmental cues determining flowering time are considered to be temperature and day length (Reeves and Coupland, 2000). Flowering time distribution in plant populations can be shaped by numerous biotic and abiotic factors, such as pollinator activity (Freeman *et al*., 2003), selection for synchrony with members of same species and other species (Rathcke and Lacey, 1985), temperature and drought. One of the important purposes of phenological observations is to improve understanding of the relationships between meteorological variables and associated biological responses.

Subsequent changes in the timing of phases of the plant life cycle known as phenophases (visible stages of growth and development of crop). They are directly affected by temperature, rainfall and day length. While these factors change through the year in places where there are distinct seasons.The first two factors which is temperature and rainfall are also changing in many regions because of climate change. For example, if climate change causes warmer temperatures, warm weather may occur earlier in the spring season and it may stay warm later into the fall than in years past. It will still get cold in the winter and warm in the summer, but the plant growing season will be longer and that can have big impacts on living things. Plant phenology is strongly controlled by climate and has consequently become one of the most reliable bioindicators of ongoing climate change. This strong dependence on climate have the highest portion of species shifting their phenology in the predicted direction under current climate change (Parmesan and Yohe, 2003). Changes in phenological events like flowering and forced maturity are among the most sensitive biological responses to climate change. A phenological study records the dates on which seasonal phenomena occur which provides important information on how climate change affects ecosystems over time. Phenology has been used as an indicator of climatic difference between two regions and global change over the earth surfaceswith the help of European Environmental Agency and Intergovernmental Panel on Climate Change (IPCC, 2007).Since few studies have assessed the effect of other environmental factors such as precipitation, photoperiod, availability of soil nutrients or soil physical properties and consequently evidence for their impact on phenology remains scarce (Badeck *et al*., 2004).

Phenology is important because it affects whether plants and animals survive in their environments. It is important because our food supply depends on the timing of phenological events. The changes in the timing of phenological events can be used an as indicator of changing climates. Phenology records can help scientists fill in gaps and verify trends in other sources of data to get a more complete picture of the local effects of global climate change. They also help scientists predict changes that may come in the years and decades ahead.İthelpsto understand, respond and prepare for changing climate conditions.This infomation might be helpful for the practices of farmers, resource managers and others stakeholders.

The observations on the phenological events of the mustard crop reflected the influence of weather elements. The dates of sowing make difference significantly in all phenophases. Early sown crop took less number of days for emergence than the normal and late sown crop due to low temperature in late sowing dates. Duration of the reproductive stage became shorter as the date of sowing delayed in the season. This was due to higher temperature experienced in middle and later phenophases under delayed sowing which caused reduction in duration of reproductive phase. High temperature reduced

the days to flowering and days to maturity thus shortening the seed formation period. A highes temperature leads to higher respiration rates, reduces biomass production resulted in smaller and lighter grain therefore lower crop yield. The accumulated growing degree days was less at emergence in late sowing due to comparatively low temperature. The accumulated growing degree days was higher under early sown crop at all the phenophases due to more growing period available to early sown mustard.

REFERENCES

Badeck, F.W., Bondeau, A and Bottcher, K. (2004). Responses of spring phenology to climate change. *New Phytol*. **162**:295–309.

IPCC, (2007). Climate Change 2007: The Physical Science Basis: Summary for Policymakers. IPCC, Geneva, Switzerland. 1-18 pp.

Freeman, R.S., Brody, A.K and Neefus, C.D. (2003). Flowering phenology and compensation for herbivory in Ipomopsis aggregate. *Oecologia*,**136**:394-401.

Reeves, P.H and Coupland, G. (2000). Response of plant development to environment: control of flowering by day length and temperature. *Curr. Opinions in Plant Bio.*,**3**:37-42.

Rathcke, B and Lacey, E. P. (1985). Phenological patterns of terrestrial plants. *Annu.Rev. Ecol. Syst.*,**16**:179–214.

Parmesan, C and Yohe, G. (2003). A globally coherent fingerprint of climate change impacts across natural systems. *Nature*,**421** (69):37–42.

Tesfaye, G., Teketay, D., Fetene, M and Beck, E. (2011). Phenology of seven indigenous tree species in a dry Afromontane forest, southern Ethiopia. *Trop. Eco.*,**52**:229-241.

15.13

Implication of air pollutants in resilient and sustainable crops production

Surender Singh[1] and Raj Singh

Dept of Agril Meteorology CCS Haryana Agricultural University, Hisar-125 004, India
[1]Email: surendersd@yahoo.com

Greenhouse gases (GHGs) warm the surface and the atmosphere with significant implications for rainfall, retreat of glaciers and sea ice, sea level, among other factors. It is well established and recognized that the increase in tropospheric ozone from air pollution (NO*x*, CO and others) is an important greenhouse forcing term. In addition, the recognition of chlorofluorocarbons (CFCs) on stratospheric ozone and its climate effects linked chemistry and climate strongly (Ramanathan and Feng, 2016). Climate change is a serious and long-term challenge that has the potential to affect every part of globe. Increased human activity in the last century altered the concentration of atmospheric greenhouse gases and aerosols, amplifying the process of global warming and climate change. Ever since the Green Revolution first staved off famines in the 1960s, Indian rice and wheat systems have grown over the past half century to play critical roles in the world food economy: India's 1.2 billion people depend primarily on food produced within the country, and other Asian and African nations rely heavily on imports of Indian rice. Rising temperatures because of increased emissions of greenhouse gases (GHGs) have had and will continue to have significant negative impacts on crop yields. The problem of air pollution to has attracted special attention in India due to tremendous increase in size of population, industrialization and urbanization since last few decades. Air pollutants emitted in varying forms adversely affect growth and yield of crops (Singh *et al*., 2018).

Agricultural crops can be injured when exposed to high concentrations of various air pollutants due to intensive developmental activities. Injury ranges from visible markings on the foliage, to reduced growth and yield, to premature death of the plant. The development and severity of the injury depends various factors including the concentration of the particular pollutant. To analyze the air quality at Hisar, air samples were collected using Air Sampler PM1.0. The total mass concentration of PM1.0 samples recorded was above 115 µg/m^3 during the winter season of 2016-17 (115.4 µg/m^3 on 6th Jan, 145.0 µg/m^3 on 7th Feb and 138.0 µg/m^3 on 8th Feb) well above the acceptable limit of 40-60 µg/m^3. Among the total PM concentration, Sulphate contribution was maximum (3.236 to 4.140 µg/m^3) during the season. The pollutants and particulate matter reduces the radiation quality and alter the stomata activities in crops plants consequently more detrimental for plant biological activities. Due to air pollution and anthropogenic climate change impact on crops in India, the yields have levelled off or decreased in recent decades despite continued improvements in agricultural technology (Burney and Ramanathan, 2014) .There is an acute need to not only increase the monitoring programs across all domains, but also to publicly disseminate the information among various stake holders. Air pollution risk assessment of agricultural crops will bring together experts and specialists on air pollution, to discuss the likely impacts of air pollution on agricultural crop production. It will help the decision makers to formulate necessary policy options to reduce the vulnerability of crops to air pollution. While the monitoring stations can be established, legislations amended, and standards improved, these efforts will be a waste, if the regular dissemination of the information is not practiced to raise the awareness for pollution control.

Field experiments on farm scale for GHG emissions estimation under various farming system with agrometeorological interventions will also help immensely for further planning, execution and testing so as to achieve sustenance and resilience crop production.

REFERENCES

Burney, J. and Ramanathan, V. 2014. Recent climate and air pollution impacts on Indian agriculture, PNAS, 111 (46): 16319-16324.

Ramanathan, V. and Feng Y. 2009. Air pollution, greenhouse gases and climate change: Global and regional perspectives, Atmospheric Environment, 43 (1), 37-50.

Singh, S., Tiwari, S., Singh, R. and Chate, M. 2018. Air pollutants concern in field crops under changing environment scenarios, Journal of Agrometeorology, 20 (Spl Issue): 302-306.

15.14

Exploring accumulation-mode H_2SO_4 versus SO_2 stratospheric sulfate geoengineering in a sectional aerosol–chemistry–climate model

Sandro Vattioni[1], Debra Weisenstein[2], David Keith[2], Thomas Peter[1], Gabriel Chiodo[1], Aryeh Feinberg[1] & Andrea Stenke[1]

[1]Institute of Atmospheric and Climate Science, ETH Zürich, Zurich 8092, Switzerland (sandro.vattioni@outlook.com)
[2]Harvard John A. Paulson School of Engineering and Applied Sciences, Cambridge, MA 02138, USA

The continuously increasing dismal prospects for climate change mitigation have boosted research on SSG during the last decade. Stratospheric solar geoengineering (SSG) is a technique that proposes to inject aerosols into the stratosphere to increase the Earth's albedo. SSG could contribute to avoiding some of the adverse impacts of climate change. So far, research has primarily focused on SSG by SO_2 injection due to the natural analogue of volcanos.

In this study, we used the SOCOL-AER global aerosol– chemistry–climate model (Sheng et al. 2015) to compare 21 different SSG scenarios, of which each injected 1.83 Mt S/yr either in the form of accumulation-mode H_2SO_4 droplets (AM H_2SO_4) gas-phase SO_2 or as combinations of both. For most scenarios, the sulfur was continuously emitted at an altitude of 50 hPa (about 20 km) in the tropics and subtropics. We assumed emissions to be zonally and latitudinally symmetric around the Equator. Emissions were injected with a spread between 3.75° S – 3.75° N to 30° S – 30° N.

In the SO_2 emission scenarios, continuous production of tiny nucleation-mode particles results in increased coagulation, which together with gaseous H_2SO_4 condensation, produces coarse-mode particles (see Figure 1). These large particles are less effective for backscattering solar radiation and have a shorter stratospheric residence time than AM H_2SO_2 particles. The green aerosol size range in Figure 1 depicts the sulphate aerosol radius range at which backscattering of solar radiation is at least 70% of the peak efficiency at 0.3 μm. AM-H_2SO_4 size distributions show larger particles concentrations and larger aerosol mass fractions than the equivalent SO_2 emission scenarios. On average, the stratospheric aerosol burden and corresponding all-sky shortwave radiative forcing for the AM H_2SO_4 scenarios are about 37% larger than for the SO_2 scenarios. Sensitivity of the latitudinal spread of the emissions was found to be small. Emitting between 30° N/S instead of 10° N/S only decreases stratospheric burdens by about 10%. This is because an increase in cross-tropopause transport via tropopause folds in scenarios with broad emission spread is nearly compensated by increased gravitational settling rates due to larger coagulation in scenarios that only emit at the Equator. In the case of gaseous SO_2 emissions, limiting the sulfur injections spatially and temporally in the form of point and pulsed emissions reduces the total global annual nucleation, leading to less coagulation and thus smaller particles with increased stratospheric residence times. Pulse or point emissions of AM H_2SO_4 have the opposite effect: they decrease the stratospheric aerosol burden by increasing coagulation and only slightly decrease clear sky radiative forcing.

This study shows that direct emission of AM H_2SO_4 results in higher radiative forcing for the same sulfur equivalent mass injection strength than SO_2 emissions, and that the sensitivity to different injection strategies varies for different forms of injected sulfur. Prospective studies will focus on investigating various materials for SSG such as solid alumina or calcite particles. Due to their chemical, optical and microphysical properties they show the potential of resulting in more effective SSG while simultaneously reducing their adverse effects on stratospheric chemistry.

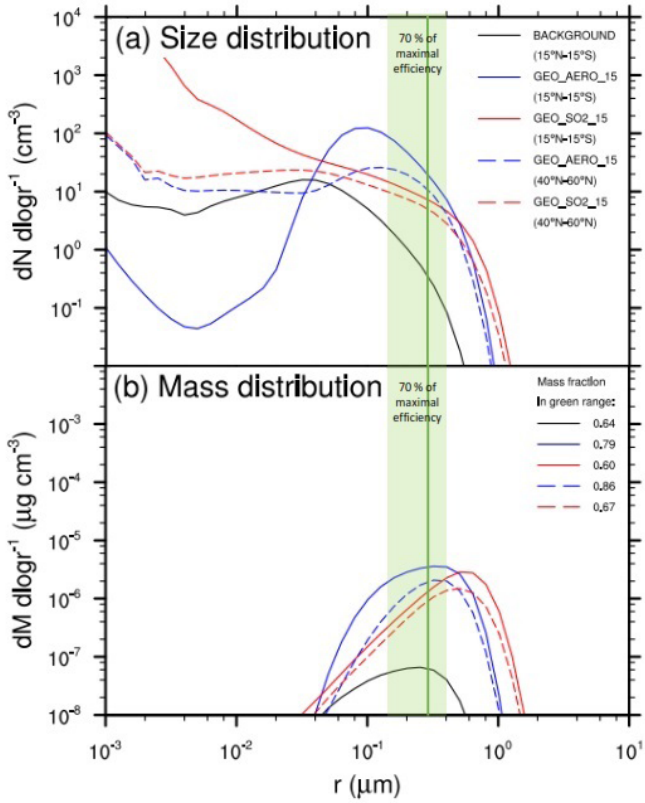


Figure 1. Wet aerosol size (a) and mass (b) distributions of stratospheric aerosol under various scenarios from Vattioni et al. (2019). The AM-H_2SO_4 emission scenarios emitting between 15° N and 15° S (GEO_AERO_15 in blue), the equivalent SO_2 emission scenarios (GEO_SO2_15 in red) and the reference run (BACKGROUND in black) are zonally averaged over 10 years between 15° N and S (continuous lines) and between 40° N and 60° N (dashed lines). Values shown are at 50 hPa in the tropics and at 100 hPa in the northern midlatitudes, i.e., at the levels of peak aerosol mass concentration in the vertical profile. The green size range is defined as the radius at which backscattering efficiency on sulfate aerosols is at least 70 % (i.e., 0.12–0.40 µm) of its maximal value (solid green line at 0.30 µm) following Dykema et al. (2016).

REFERENCES

Dykema, J. A., Keith, D. W., & Keutsch, F. N., 2016, Improved aerosol radiative properties as a foundation for solar geoengineering risk assessment. Geophysical Research Letters, 43(14), 7758–7766. https://doi.org/10.1002/2016GL069258

Sheng, J., D. Weisenstein, B. Luo, E. Rozanov, A. Stenke, J. Anet, H. Bingemer, and T. Peter, 2015, Global atmospheric sulfur budget under volcanically quiescent conditions: Aerosol-chemistry-climate model predictions and validation (2015), J. Geophys. Res., DOI:10.1002/2014JD021985.

Vattioni, S., Weisenstein, D., Keith, D., Feinberg, A., Peter, T., & Stenke, A., 2019, Exploring accumulation-mode H_2SO_4 versus SO_2 stratospheric sulfate geoengineering in a sectional aerosol–chemistry–climate model. Atmospheric Chemistry and Physics, 19(7), 4877–4897. https://doi.org/10.5194/acp-19-4877-2019

15.15

Using the eddy covariance technique to determine the nitrous oxide emissions of an intensively used pasture in Switzerland

Karl Voglmeier[1], Markus Jocher[1], Christof Ammann[1]

[1]*Climate and Agriculture Group, Agroscope, Reckenholzstrasse 191, CH-8046 Zürich (karl.voglmeier@agroscope.admin.ch)*

Nitrous oxide (N_2O) is a very potent greenhouse gas, and the majority of the emissions are associated with intensive livestock production. The magnitude of the emissions typically depends on the nitrogen (N) input to the soil, and on grazed pastures the largest share of the emissions is typically originating from the N applied via fertilization and excreta of the grazing animals. The uneven spatial distribution of the excretion leads to emission hot spots on grazing systems and makes the quantification of the gaseous emissions challenging. Thus, micrometeorological methods that integrate emissions over a larger area like the eddy covariance (EC) method are well suited to quantify the field-scale N_2O emissions of grazed pastures.

We present results of a field experiment carried out in western Switzerland in the years 2013 to 2017. The investigated pasture was grazed by dairy cows in an intensive rotational management. The field was additionally fertilized with organic and mineral fertilizer each year, according to the N requirement of the grassland. The field-scale N_2O fluxes were quantified with the EC technique using a fast response Quantum cascade laser spectrometer for N_2O concentration measurements.

The experimental setup and the environmental conditions resulted in high temporal and spatial dynamics of the N_2O fluxes with highest values typically occurring after mineral fertilization events in the summer month. Using N_2O background parametrizations retrieved from chamber measurements by Voglmeier et al. (2019) for the same site in 2016 and subtracting the background emission from the measured N_2O fluxes allowed us to calculate excreta-related emission factors (EFs) according to the IPCC guidelines. EFs for fertilizer N input were calculated using a pre-defined time window after the fertilizer was applied. The subtracted background emissions during the fertilization events were calculated from the EC measurements outside this time window. We will attribute the observed emissions to the different N inputs and we will discuss potential reasons for the supposedly higher emissions after mineral fertilizer applications in comparison to organic fertilizer emissions.

REFERENCES

Voglmeier, K., Six, J., Jocher, M. & Ammann, C. 2019: Grazing-related nitrous oxide emissions: from patch scale to field scale, Biogeosciences, 16(8), 1685–1703.

15.16

Warming, cooling, irrigation and N-deposition effects on the ecosystem C-cycle of subalpine grassland

Matthias Volk[1], Anne-Lena Wahl[1], Robin Giger[1] and Seraina Bassin[1]

[1]Agroscope, Zurich, Switzerland (matthias.volk@agroscope.admin.ch)

We ran a five-year warming × moisture × atmospheric N-deposition experiment with turf monoliths (ML) from 6 different Alps of equal altitude (2150m) and exposure (S). On the S slope of Piz Cotschen (Unterengadin) 216 ML were replanted at 6 sites along an altitudinal gradient, representing an April - Oct. -1.4° to +3.0°C temperature change (equivalent annual mean -1.7° to +2.4°C). Plant growth was indifferent to -1.4°C cooling, but was rising to c. 40% above control with +1.8°C warming. Surprisingly, neither irrigation, nor +15kg ha^{-1} a^{-1} atmospheric N-deposition treatments yielded a significant growth response.

We quantified the ecosystem CO_2 flux responses using dynamic CO_2 concentration cuvettes and parameterized NEP for the whole period, using light intensity, soil moisture and temperature. We compared the parameterization to soil organic C stock measurements at the beginning and at the end of the experiment.

Soil C stock was found to be slightly reduced with cooling, but was increasing with moderate warming. When April - Oct. warming was greater 1.5°C, after 5 yrs. 0.6 kg C were lost out of a 6.3 kg C m^{-2} stock (0-10cm). NEP parameterizations suggested that $R_{ecosystem}$ was less susceptible to drought than GPP. As a result, we observed a decreased assimilation, but continued respiration under very warm and dry conditions, resulting in substantial ecosystem C loss.

Results will be discussed in the light of our earlier work, that suggests increased C sequestration at low N deposition, but decreased C sequestration at high N deposition (Volk et al., 2016; Volk et al., 2018). At the same time, the effect of rising temperature, accompanied by reduced soil moisture, is expected to make the ecosystem a CO_2 source to the atmosphere (Volk et al., 2011), or at least to reduce potential ecosystem C gains.

REFERENCES

Volk, M., Obrist, D., Novak, K., Giger, R., Bassin, S. & Fuhrer, J. 2011: Subalpine grassland carbon dioxide fluxes indicate substantial carbon losses under increased nitrogen deposition, but not at elevated ozone concentration: Grassland CO_2 flux under O_3 and N deposition. Global Change Biology 17, 366–376.

Volk, M., Enderle, J. & Bassin, S. 2016: Subalpine grassland carbon balance during 7 years of increased atmospheric N deposition. Biogeosciences 13(12): 3807-3817.

Volk, M., Bassin, S., Lehmann, M.F., Johnson, M.G. & Andersen, C.P. 2018: ^{13}C isotopic signature and C concentration of soil density fractions illustrate reduced C allocation to subalpine grassland soil under high atmospheric N deposition. Soil Biology and Biochemistry 125, 178-184.

15.17

The impact of cover fill on N_2O emissions in drained peatland

Yuqiao Wang[1,2], Sonja Paul[1,2], Markus Jocher[1], Christine Alewell [2], Jens Leifeld[1]

[1]Climate and Agriculture Group, Agroscope, 8046 Zürich
(yuqiao.wang@agroscope.admin.ch)
[2]University of Basel, Environmental Geoscience, 4056 Basel

Drainage for agriculture has converted peatlands from a carbon sink to one of the world's main greenhouse gas (GHG) sources. In order to improve the sustainability of managed peatlands in agriculture, and to counteract soil subsidence, mineral soil coverage is becoming a common practice in Switzerland. Cover fills may change the GHG balance from the corresponding organic soil. To explore the effect of cover fill on soil N_2O emission, a field experiment is carried out at the border of Switzerland and Austrain, Rüthi SG to measure the soil – borne N_2O balance from two adjacent sites: drained organic soil without mineral soil cover (DN), and drained organic soil with mineral soil cover (DC). Mineral soil material was applied 12 years ago and varies in thickness between 20 – 80 cm. Both sites have the same farming practice. In our experiment, an automatic chamber system is used for collecting the soil - borne N_2O at an interval of 3 h. Soil moisture, expressd as volumetric water content (VWC),is recorded every 10 min. After six-month's (171 days) of continous measurement, it appears that: (1) The average N_2O emission from DN is 11.72 ± 3.31 mg N_2O-N m^{-2} day^{-1}, and for the DC site it is 1.38 ± 0.68 mg N_2O-N m^{-2} day^{-1}. Hence, mineral soil cover of organic soil seems to induce a strong reduction in N_2O emissions. (2) Exogenous N inputs (mineral nitrogen fertilize and cow slurry) are the main drivers of N_2O emissions. The post exogenous N input N_2O emission peak (post N-input N_2O emission) was found in summer. N_2O peaks occured shortly after the N application and lasted for 2 to 3 weeks before returning to background N_2O emission. At the DC site post N- input N_2O emissions accounted for 79% of the total N_2O emission over the whole measurement period. An equivalent of around 2% of the exogenous N- input was emitted as N_2O. At the DN site, emission peaks after fertilization accounted for 81% of the total N_2O emission, equivalent to around 18% of the exogenous N- input. Background emissions between peak events were 2.60± 2.16 mg N_2O-N m^{-2} day^{-1} at DN and 0.33±0.30 mg N_2O-N m^{-2} day^{-1} at DC. The comparison of peak and background fluxes tentatively indicates that higher average emission rates from the DN site are not only related to fertilization directly, but also to a different response of soil-N. Finally, soil moisture content differed between sites. During the experimental period, the mean daily soil moisture ranged from 15.8%VWC - 49.6%VWC and from 22.6VWC% - 57.2%VWC for DC and DN, respectively. Background N_2O emission increased with soil moisture. In summary, our data from this first experimental period suggest that mineral cover fill could strongly reduce the N_2O emission from drained organic soil, and may therefore be an interesting mitigation option in agriculture.

P 15.1

Determining the greenhouse gas budget of two neighboring pastures using the eddy covariance technique

Christof Ammann[1], Markus Jocher[1], Karl Voglmeier[1]

[1]Climate and Agriculture Group, Agroscope, Reckenholzstrasse 191, CH-8046 Zürich (christof.ammann@agroscope.admin.ch)

Intensive livestock production is a large source of the greenhouse gases (GHG) methane (CH_4) and nitrous oxide (N_2O). However, optimizing grassland management is seen as a potential cost-effective mitigation strategy to counteract these emissions by increasing the soil carbon stock.

We present results of GHG flux measurements in a paired field experiment of two neighboring grazing systems in 2016. Each system was grazed by 12 dairy cows in a rotational grazing management. The systems differed in the energy to protein balance of the diet for the cows (grass with additional maize silage: system M; full grazing system without additional forage: system G) which resulted in different N excretion rates. The field scale emissions of CO_2, CH_4 and N_2O were quantified using two eddy covariance towers, which were installed in the middle of the two systems. The paired field design allowed for a precise comparison of the two systems, as only random uncertainties had to be taken into account. In order to calculate the net ecosystem carbon budget (NECB) of the pasture systems, additional non-gaseous carbon fluxes were either measured (harvest, slurry application) or estimated based on an animal feed demand model (carbon removal/return by grazing/excreta). For the investigated year, the NECB resulted in a significant C sink for system M whereas system G was carbon neutral. We conclude, that this difference was mainly triggered by the external carbon import to the system M through the additionally provided maize silage. Taking the emissions of CH_4 and N_2O into account resulted in a neutral net GHG budget for both pastures.

We will show the individual contributions to the NECB, explain the importance of the individual GHGs to the net GHG budget and illustrate the advantages of a paired field design. Furthermore, we will discuss the outcomes of the study in the context of a similar study on the same pasture in 2013.

P 15.2

Icelandic volcanism and climate from Greenland ice cores over the past 3 ka

Carla Grimaldi[1,2], Gill Plunkett[3], Bergrún A. Óladóttir, Joseph R. McConnell[5], Michael Sigl[1,2]

[1]Climate and Environmental Physics, University of Bern, Bern, Switzerland
[2] Oeschger Centre for Climate Change Research, University of Bern, Bern, Switzerland
[3]Queen's University Belfast, Belfast, UK
[4]University of Iceland, Reykjavík, Iceland
[5]Desert Research Institute, Reno, USA
(carla.grimaldi@climate.unibe.ch)

Volcanic eruptions are considered one of the main causes that can lead to short-term variations in global temperatures. The effects of volcanism on climate can be studied from proxy archives such as polar ice cores, where sulphates and ash layers (tephra) are deposited. Moreover, volcanic layers can provide important absolute chronostratigraphic markers for the ice-record, because they are erupted and deposited instantaneously with respect to geological time-scales.

During the Holocene, Greenland has experienced the deposition of numerous ash layers from Iceland. These tephra layers, can provide independent and precise tie-points for the Greenland record that can be used as time-synchronous marker horizons for different palaeo-archives, allowing a better understanding of past climate changes over the Northern hemisphere. The recognition of Icelandic tephra markers is possible thanks to the availability of published reference geochemical datasets for proximal Icelandic volcanic products, such as the ones from lake cores and soils (e.g., Gudmundsdòttir et al., 2018), that allow for the reconstruction of a complete and detailed tephrostratigraphic framework for Greenland ice cores.

Here, we use sulphur and insoluble particle records from three Greenland ice-cores (TUNU2013; NGRIP; NEEM) to recognize the presence of volcanic fallout (i.e., tephra, volatiles) deposited on the ice-sheet during the last 3 ka. Potential tephra layers in the ice-core records are recognized and targeted for geochemical analyses of single glass shards and compared with Iceland proximal tephrochronological frameworks (e.g., Haflidason et al., 2000) to distinguish tephra of potential Icelandic provenance. The volcanic record is further compared with temperature and sea-ice proxies from ice cores (e.g., $d^{18}O$, MSA) and other archives. We plan to perform geochemical analyses on glass shards from polar ice-cores to define chronostratigraphic markers in the Greenland records and perform detailed multi-proxy analyses linking different records to highlight the effects of Icelandic volcanism on North Atlantic and Northern European climate.

REFERENCES

Gudmundsdottir, E. R., Schomacker, A., Brynjolfsson, S., Ingolfsson, O., and Larsen, N. K. 2018: Holocene tephrostratigraphy in Vestfiroir, NW Iceland. Journal of Quaternary Science 33, 827-839.

Haflidason, H., Eiriksson, J., and Van Kreveld, S. 2000: The tephrochronology of Iceland and the North Atlantic region during the Middle and Late Quaternary: a review. Journal of Quaternary Science 15, 3-22.

P 15.3

First eddy covariance flux measurements of gaseous elemental mercury over a grassland

Stefan Osterwalder[1,2], Werner Eugster[3], Iris Feigenwinter[3] & Martin Jiskra[1]

[1]Environmental Geosciences, University of Basel, 4056 Basel, Switzerland (stefan.osterwalder@unibas.ch)
[2]CNRS, IRD, IGE, Université Grenoble Alpes, 38058 Grenoble, France
[3]Institute of Agricultural Sciences, ETH Zurich, 8092 Zurich, Switzerland

Direct measurements of the net ecosystem exchange (NEE) of gaseous elemental mercury (Hg^0) are crucial to improve our understanding of global Hg cycling and ultimately Hg exposure in humans and wildlife. The lack of long-term, ecosystem-scale measurements causes large uncertainties in Hg^0 flux estimates. Today it remains unclear whether terrestrial ecosystems are net sinks or sources of atmospheric Hg^0. Here, we present the first successful eddy covariance (EC) NEE measurements of Hg^0 over natural, low-Hg background soils (41 - 75 ng Hg g^{-1} topsoil [0-10 cm]) at a managed grassland site in Chamau, Switzerland. We present a detailed validation of the EC technique for Hg^0 based on a Lumex mercury monitor RA-915AM. The flux detection limit derived from a zero-flux experiment in the laboratory was 0.22 ng m^{-2} h^{-1} (maximum) with a 50 % cut-off at 0.074 ng m^{-2} h^{-1}. The statistical estimate of the Hg^0 flux detection limit under real-world outdoor conditions at the site was 5.9 ng m^{-2} h^{-1} (50 % cut-off). Based on our analysis we give suggestions to further improve the precision of the EC system and pinpoint challenges and interferences that occurred during the 34-day pilot campaign in summer 2018. The data were obtained during extremely hot and dry meteorological conditions. We estimated a net summertime grassland-atmosphere Hg^0 flux from -0.6 to 7.4 ng m^{-2} h^{-1} (range between 25th and 75th percentiles). The measurements revealed a distinct diel pattern with significantly lower nighttime fluxes (1.0 ng m^{-2} h^{-1}) compared to daytime fluxes (8.4 ng m^{-2} h^{-1}). Drought stress during the campaign induced partial stomata closure of vegetation which led to a midday depression in CO_2 uptake which did not recover during the afternoon. We suggest that partial stomata closure dampened Hg^0 uptake by vegetation as well, resulting in a NEE of Hg^0 dominated by soil emission. The new Eddy Mercury system seems suitable to complement existing research infrastructures such as ICOS RI in Europe or NOAA Observing Systems in the US built to calculate greenhouse gas balances with direct Hg^0 deposition and emission measurements. We anticipate our Eddy Mercury system to improve knowledge about Hg cycling between ecosystems and the atmosphere and to challenge model simulations on a regional and global scale.

REFERENCES

Osterwalder, S., Eugster, W., Feigenwinter, I., Jiskra, M., 2019. First eddy covariance flux measurements of gaseous elemental mercury (Hg^0) over a grassland. Atmospheric Measurement Techniques Discussions 1–27. https://doi.org/10.5194/amt-2019-278

P 15.4

Effects of biodiversity on ecosystem functioning across local and landscape scales

Merin Chacko[1], Sarah Mayor[1], Thomas Crowther[2], Pascal A. Niklaus[1]

[1]*Department of Evolutionary Biology and Environmental Sciences, University of Zurich, Winterthurerstrasse 190, 8057 Zurich. Correspondence: merinreji.chacko@uzh.ch*
[2]*Department of Environmental Systems Sciences, Institute for Integrative Biology, ETH Zurich, Universitaetsstrasse 16, 8006 Zurich*

Ecosystem functions facilitate the myriad ecosystem goods and services that benefit humans, such as natural pollination of crops, oxygen production and carbon sequestration. Human activities have resulted in the sixth major mass extinction in the history of life on earth. The biodiversity-ecosystem functioning (B-EF) relationship has been widely studied, albeit with experimental model communities consisting of a few dozen species in small plots (~ <100m^2) and conducted generally on grasslands or in microcosms (Brose and Hildebrand, 2016). These experiments have shown a positive decelerating B-EF relationship (Tilman et al, 2014; Paquette & Messier, 2011). It is less broadly understood whether these well-studied local and short-term relationships still hold across larger spatio-temporal scales, where large-scale mechanisms may influence landscape diversity (LD) and landscape functioning (LF) and produce emergent mechanisms that alter the B-EF relationship.

We conducted an observational study of the Koeppen-Geigen hot(dfa) and warm(dfb) summer humid continental climate zones of North America, using a quasi-experimental set up. We applied a grid based on the MODIS 250m Vegetation Index pixels on the region, giving a total of ~74 million plots of 250m^2 extent. Land surface phenology was derived from the 2000-2018 16-day composited MODIS EVI data product (Didan, 2015). Land cover composition was extracted from two 30-m spatial resolution maps of North America, from the North American Land Monitoring System (NALMS), and from GlobeLand30 (Canada Centre for Remote Sensing et al, 2017; Chen et al 2014). A subset of pixels (~140k plots) — for which local BD and LF data was available through the Global Forest Biodiversity Initiative — was chosen to study cross-scale relationships. Plots were optimally picked such that land cover type richness was decorrelated from environmental variables (altitude, slope and aspect), and each composition was equally represented. Preliminary results have shown a positive LD-LF relationship as well as a positive B-LD relationship (Oehri et al, 2017). Further investigation should shed light on any direct LD-LF correlation, or altervatively, indirect facilitation from local biodiversity.

This study furthers the understanding of the effects of biodiversity on ecosystem functioning across the local and landscape scale, as well as understanding the repercussions of biodiversity loss in real-world scenarios, which is of utmost importance to prevent and mitigate its devasting effects on human well-being.

REFERENCES

Brose, U. & Hillebrand, H. 2016: Biodiversity and ecosystem functioning in dynamic landscapes. Philosophical Transactions of the Royal Society B-Biological Sciences, 371, 9.

Canada Centre for Remote Sensing, Canada Centre for Mapping and Earth Observation, Natural Resources Canada, Comisión Nacional para el Conocimiento y Uso de la Biodiversidad, Comisión Nacional Forestal, United States Geologicl Survey. 2017: 2010 Land Cover of North America at 30 meters. Digital raster map, 1st edition, 30m resolution, Commission for Environmental Cooperation, Montreal, Quebec, Canada.

Chen J., Ban Y., Li S. 2014: China: Open access to Earth land-cover map[J]. *Nature*, 514(7523): 434-434. DOI:10.1038/514434c.

Didan, K. 2015: MOD13Q1 MODIS/Terra Vegetation Indices 16-Day L3 Global 250m SIN GridV006. NASA EOSDIS Land Processes DAAC. Available at https://doi.org/10.5067/modis/mod13q1.006. Accessed August 18, 2019.

Oehri, J., Schmid, B., Schaepman-Strub, G., & Niklaus, P. A. 2017: Biodiversity promotes primary productivity and growing season lengthening at the landscape scale. Proceedings of the National Academy of Sciences, 114(38), 10160-10165.

Paquette, A. & Messier, C. 2011: The effect of biodiversity on tree productivity: from temperate to boreal forests. Global Ecology and Biogeography, 20, 170-180.

Tilman, D., Isbell, F. & Cowles, J.M. 2014: Biodiversity and Ecosystem Functioning. Annual Review of Ecology, Evolution, and Systematics, 45, 471-493

18. Remote Sensing of the Spheres

Stefan Wunderle, Mathias Kneubühler, Dominik Brunner, Alain Geiger

Swiss Commission for Remote Sensing
Swiss Geodetic Commission

TALKS:

18.1 Frey O., Werner C.L., Coscione R.: InSAR-based mobile mapping of surface displacements from UAV/car-borne platforms

18.2 Iturrate-Garcia M., Pascal C., Fox N., Woolliams E., Fiscaro P.: EMN Climate and Ocean Observation: A coordinated metrology network supporting ECVs and EOVs measurements

18.3 Kim M., Kuhlmann G., Brunner D.: Downscaling NO_2 satellite observations to high-resolution air pollution maps

18.4 Koutantou K., Mazzotti G., Jonas T., Brunner P.: Ultra-high resolution snow depth mapping using a UAV-based LiDAR scanner

18.5 Los M., Shehaj E., Wegner J.D., D'Aronco S., Geiger A., Brockmann E.: Machine learning assessment for tropospheric pathdelays prediction using meteorological parameters in Switzerland

18.6 Naegeli K., Wiesmann A., Wu X., Neuhaus C., Stengel M., Wunderle S.: Towards a global time series (1982 – 2018) of snow cover extent based on AVHRR GAC data – preliminary results of the ESA CCI+ Snow project

18.7 Schwaerzel M., Emde C., Kuhlmann G., Brunner D., Buchmann B., Berne A.: Effects of spatial variability of NO_2 concentrations on NO_2 remote sensing at city scale studied with a 3D radiative transfer model

18.8 Wingate V.R., Helfenstein I., Röösli C., Schaepman M.E.: GlobDiversity: Remote Sensing-enabled Essential Biodiversity Variables to monitor key biodiversity characteristics at a global scale

POSTERS:

P 18.1 Bernet L., Brockmann E., Mätzler C., Kämpfer N., Hocke K.: Water vapour trends in Switzerland based on data from ground-based microwave radiometry and GNSS ground stations

P 18.2 Manconi A.: Rock slope deformation in the Grimsel Pass region, Switzerland

P 18.3 Patra S., Naegeli K., Wunderle S.: Accuracy study of snow cover maps based on AVHRR data with different spatial resolution

P 18.4 Schuman M.C., Czyz E., Li C., Shimizu K.K., Baldwin I.T., Schaepman M.: Remote Sensing of Ecological Genetics

P 18.5 Strozzi T., Caduff R., Manconi A., Ambrosi C.: Perspectives for the monitoring of very slow landslides in Switzerland with InSAR

P 18.6 Turkoglu M.O., Schindler K., Wegner J.D.: Large-scale crop classification from satellite images

18.1

InSAR-based mobile mapping of surface displacements from UAV/car-borne platforms

Othmar Frey[1,2], Charles L. Werner[1], Roberto Coscione[2]

[1]Gamma Remote Sensing, Worbstrasse 225, CH-3073 Gümligen (frey@gamma-rs.ch)
[2]ETH Zurich, Earth Observation & Remote Sensing, Institute of Environmental Engineering, Leopold-Ruzicka-Weg 4, CH-8093 Zurich.

While current stationary terrestrial radar systems used for the measurement of surface displacements are bound to relatively high frequencies (many of them operating at Ku- or X-band) to ensure a good cross-range resolution, an L-band SAR system, when operated in car-borne mode (or UAV-borne mode), can still achieve a high cross-range resolution on the order of less than 0.5 m up to few meters. The cross-range resolution mostly depends on whether the full range-varying length of the synthetic aperture is obtained for the entire image, which again depends on geometric constraints imposed by the road (car-borne mode), possible flight tracks (airborne/UAV) and the topography. An important advantage and somewhat complementary property to the high-frequency stationary systems is the reduced temporal decorrelation at L-band. While the sensitivity to line-of-sight displacements is lower, the longer wavelength at L-band permits to acquire longer interferometric time series also in natural terrain, where the decorrelation time at Ku-band can be in the order of minutes or less. VTOL UAVs are agile airborne platforms that allow flexible planning and realization of sensor trajectories that are tailored to a specific application. E.g., linear repeat-pass sensor trajectories within a valley can be flown to assess the line-of-sight displacement of a valley slope, irrespective of the direct accessibility of the terrain on the ground. A repeat-pass interferometric campaign has been conducted with the GAMMA L-band SAR mounted on the VTOL UAV Scout B1-100 by Aeroscout GmbH (see Fig. 1). We also present a repeat-pass interferometric phase measurements of the line-of-sight phase component induced by the flow velocity of an alpine glacier obtained in fall 2018 with the GAMMA L-band SAR. In this demonstration case, the GAMMA L-band SAR system is operated in a car-borne mode [6,7]: several repeat-pass SAR acquisitions of an alpine glacier are taken from a car driven along a slightly curved section of a mountain road in central Switzerland. The car-borne SAR data is focused directly to map coordinates involving a digital elevation model by using a time-domain back-projection (TDBP) approach [1-3] & [4,5]. These geocoded complex SAR images then allow to directly form differential interferograms in map coordinates. The feasibility of repeat-pass interferometry using the novel GAMMA L-band SAR on an agile mobile mapping platform is successfully demonstrated with several data examples (see Fig.2 & and 3 and their captions).



Figure 1: GAMMA L-band SAR on Aeroscout's VTOL UAV Scout B1-100, equipped with a Honeywell HGuide n580 INS/GNSS navigation system, at the test site Wolfenschiessen, Switzerland.

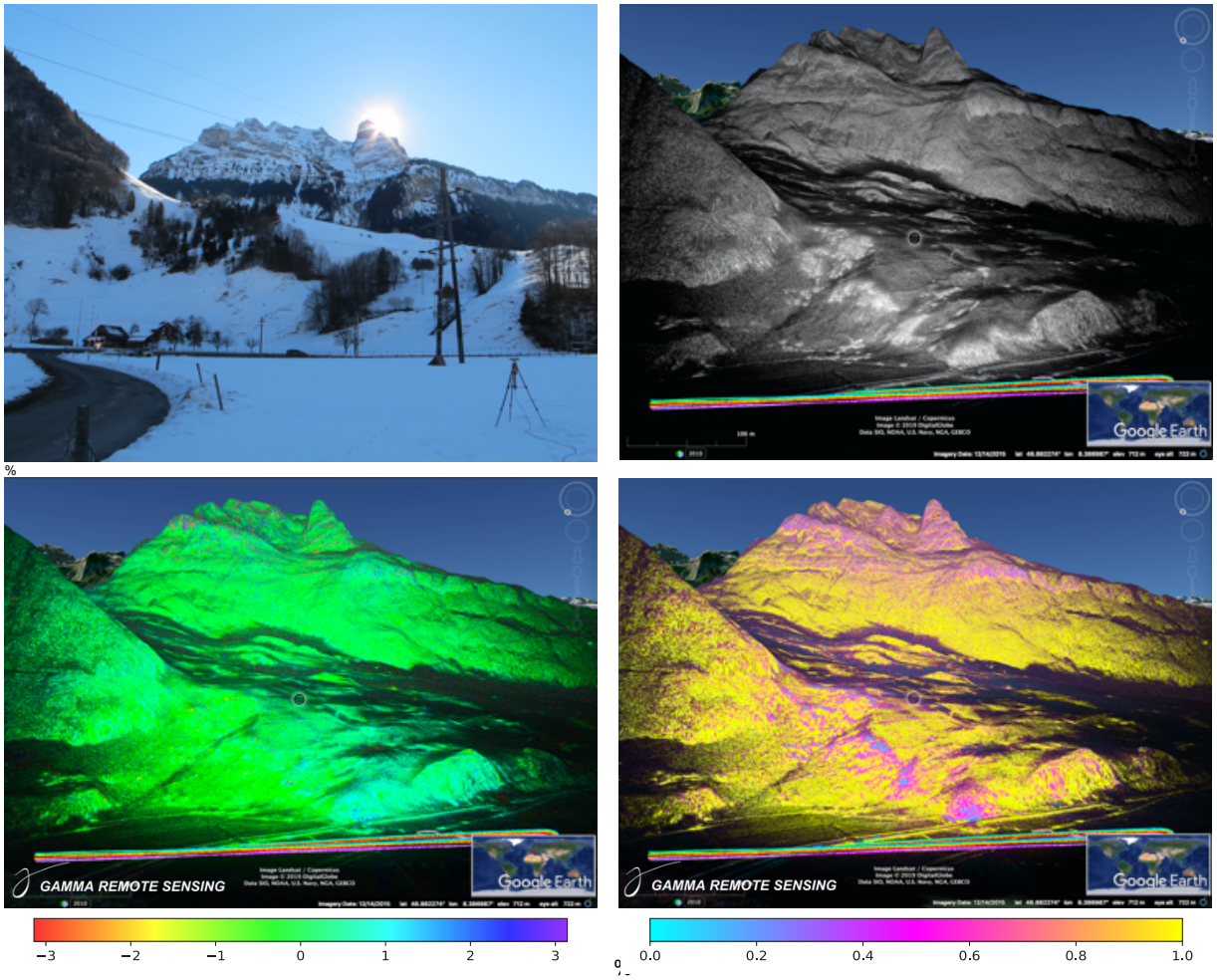


Figure 2: Top left: Area of interest on the campaign day. On the lower right of the photograph, the local GNSS reference station is situated to obtain a highly precise post-processed kinematic GNSS solution of the UAV position. Top right: Google Earth (GE) view of UAV-borne L-band SAR backscatter intensity image with UAV flight trajectories in the foreground. Lower left: View of UAV-borne L-band differential interferometric phase ($-\pi$, π) and, on the lower right, coherence (0,1) for nominally zero spatial baseline and a temporal baseline of 3 minutes. The flight tube of these two repeat-tracks are within 1m radius. With the exception of forested areas in the near range and areas with severe foreshortening a very high coherence is obtained and the interferometric phase is also stable. Since no deformation took place within the 3 minutes time interval the stable phase arround zero is a good indicator for the performance of the interferometric system showing no significant residual phase errors and thus confirming the good performance of the system (see also [8]).

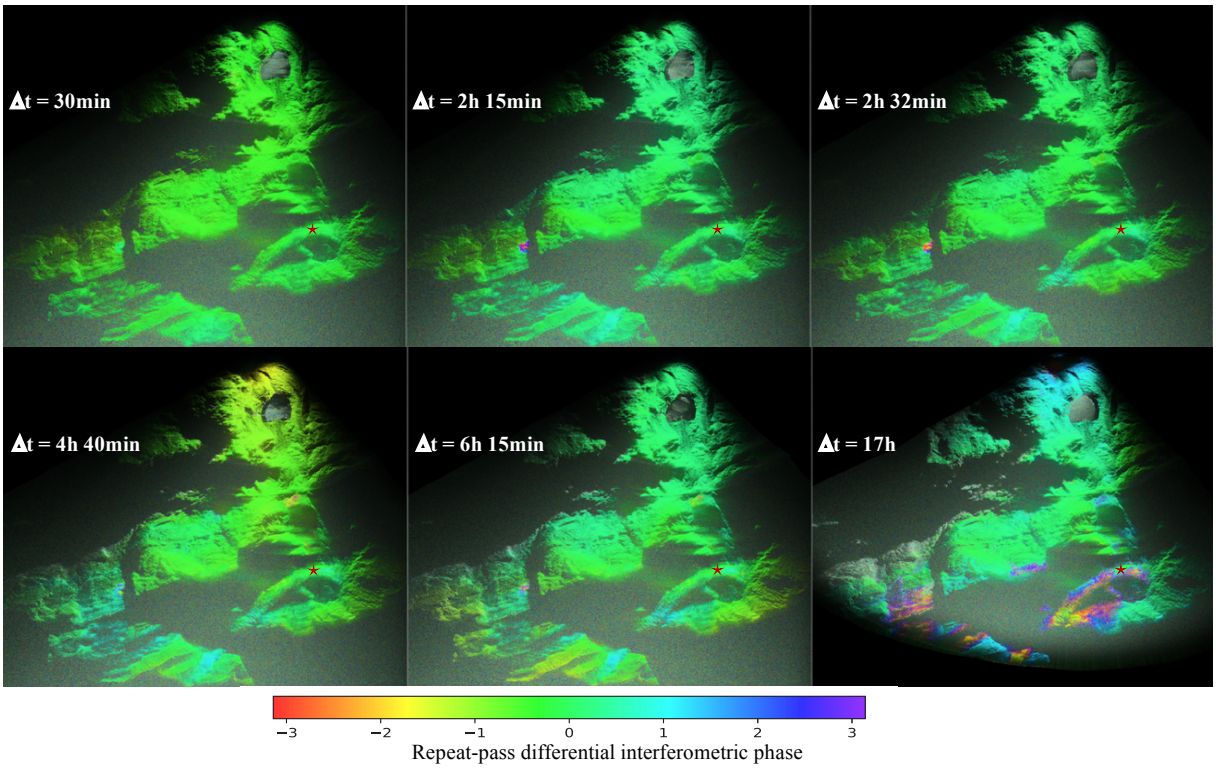


Figure 3. Differential interferograms of the Stein Glacier and the surrounding area in map coordinates (north = up) with temporal baselines of 30 min (upper left), 135 min (upper center), and 152 min (upper right), 280 min (lower left), 375 min (lower center), and 1020 min (=17h) (lower right). The 17h interferogram is obtained between two acquisitions with 1ms chirp duration; hence the limited range distance of ca. 4.68 km. All other interferograms shown are based on acquisitions a 2ms chirp duration. With a carrier frequency of 1.325 GHz (wavelength of 22.6 cm) an interferometric phase value of 2π translates to a line-of-sight displacement of the glacier of 11.3 cm (see also [8]).

REFERENCES

EFERENCES

[1] Frey, O., Werner, C. L., and Wegmuller, U.: “GPU-based parallelized time-domain back-projection processing for agile SAR platforms,” in Proc. IEEE Int. Geosci. Remote Sens. Symp., July 2014, pp. 1132–1135. [Online]. Available: https://ieeexplore.ieee.org/document/6946629

[2] Frey, O., Magnard, C., Rüegg, M., and Meier, E.: “Focusing of airborne synthetic aperture radar data from highly nonlinear flight tracks,” IEEE Trans. Geosci. Remote Sens., vol. 47, no. 6, pp. 1844–1858, June 2009. [Online]. Available: https://ieeexplore.ieee.org/document/4812049

[3] Frey, O., Meier, E., and Nüesch, D.: “Processing SAR data of rugged terrain by time-domain back-projection,” in SPIE Vol. 5980: SAR Image Analysis, Modeling, and Techniques X, 2005.
DOI: https://doi.org/10.1117/12.627647

[4] Ribalta, A.: “Time-domain reconstruction algorithms for FMCW- SAR,” IEEE Geoscience and Remote Sensing Letters, vol. 8, no. 3, pp. 396–400, May 2011.

[5] Stringham, C. and Long, D. G.: “GPU processing for UAS-based LFM-CW stripmap SAR,” Photogrammetric Engineering & Remote Sensing, vol. 80, no. 12, pp. 1107–1115, 2014.

[6] Frey, O., Werner, C. L., Wegmuller, U., Wiesmann, A., Henke, D., and Magnard, C.: “A car-borne SAR and InSAR experiment,” in Proc. IEEE Int. Geosci. Remote Sens. Symp., 2013, pp. 93–96 [Online]. Available: https://ieeexplore.ieee.org/document/6721100

[7] Frey, O., Werner, C. L., Hajnsek, I., and Coscione, R.: “A car-borne SAR system for interferometric measurements: development status and system enhancements,” in Proc. IEEE Int. Geosci. Remote Sens. Symp., 2018, pp. 6508–6511. [Online]. Available: https://ieeexplore.ieee.org/document/8518840

[8] Frey, O., Werner, C. L., Coscione, R.: “Car-borne and UAV-borne mobile mapping of surface displacements with a compact repeat-pass interferometric SAR system at L-band,” Proc. IEEE Int. Geosci. Remote Sens. Symp., July/Aug 2019, pp. 274-277.

18.2

"EMN Climate and Ocean Observation": A coordinated metrology network supporting ECVs and EOVs measurements

Maitane Iturrate-Garcia[1], Céline Pascal[1], Nigel Fox[2], Emma Woolliams[2] & Paola Fiscaro[3]

[1]Gas Analysis Laboratory, Federal Institute of Metrology METAS, Lindenweg 50, CH-3003 Bern (maitane.iturrate@metas.ch)
[2]Earth Observation, Climate and Optical Group, National Physical Laboratory (NPL), Hampton Road, TW110LW, Teddington
[3]Inorganic Chemistry Department, Laboratoire National de Métrologie et d'Essais (LNE), 1 rue Gaston Boissier, 75015 Paris

Six so-called "European Metrology Networks" (EMNs) were set up in 2018 within the European Association of National Metrology Institutes (EURAMET) to promote the coordination between Metrology Institutes as well as with stakeholders for high priority societal and environmental themes. The aim of these EMNs is to analyse the European and global metrology needs and address these needs in a coordinated manner. We present here the "EMN for Climate and Ocean Observation" and its long-term goals.

Essential Climate Variables (ECVs) are physical, chemical, and biological variables that contribute to characterise Earth's climate. The Global Climate Observing System (GCOS) has defined a set of 54 ECVs up to present. In a similar way, the Global Ocean Observing System (GOOS) has defined 31 Essential Ocean Variables (EOVs) that, together with the GCOS oceanic ECVs, aim to provide a better understanding on ocean changes, human impacts and vulnerabilities, and to support the economic and social applications of the ocean system. The measurement of these ECVs entails challenging measurement accuracy to enable the global, multi-decadal observation of small climate trends. Metrological traceability and accuracy applied to measuring techniques of major importance for many ECVs and EOVs, such as remote sensing, will foster meeting those targets.

Remote sensing, particularly from satellites is the only means to achieve a truly global understanding of the planet, with more than 50% of the ECVs only observable from space. One challenge is understanding the transformation of the remote sensed digital count with the bio-geophysical variable of interest, requiring not only robust sensor calibration, but also analysis of retrieval algorithms, validation, with field deployable transfer standards. Although for some environmental monitoring activities, relative instantaneous maps can be adequate, for climate, reliably detecting a trend from a background of natural variability requires multiple decades and consequently satellites to achieve. This places severe challenges on the calibration accuracy of the sensors, their interoperability and the validation of bio-physical products and fundamentally the need for invariant community consensus references, ideally tied to the international system of units (SI), as maintained and disseminated by National Metrology Institutes.

The "EMN for Climate and Ocean Observation" will expand the metrology community's efforts - increasing support to the science, commercial and user community and seeking to build partnerships with remote sensing and in-situ practitioners to merge expertise towards a high quality climate observing system. In particular, METAS, the Swiss national metrology institute is active to support several ECVs, such as greenhouse gases, aerosols precursors and aerosols properties.

18.3

Downscaling NO_2 satellite observations to high-resolution air pollution maps

Minsu Kim[1], Gerrit Kuhlmann[1] & Dominik Brunner[1]

[1]Laboratory for Air Pollution / Environmental Technology, Empa – Swiss Federal Laboratories for Materials Sciences and Technology, Überlandstrasse 129, CH-8600 Dübendorf (minsu.kim@empa.ch)

Nitrogen oxides (NO_x = NO + NO_2) are precursors of ozone (O_3) and particulate matter (PM) that are crucial components of photochemical smog and wintertime air pollution. Concentrations of these air pollutants frequently exceed the legal limits in Switzerland, other European countries, and worldwide. To study the effect of NO_2 on public health, it is important to estimate an unbiased NO_2 exposure of the population, which requires maps of near-surface NO_2 concentrations with a resolution of 1 km or better (Bino et al. 2017).

In October 2017, the TROPospheric Monitoring Instrument (TROPOMI) was launched on-board the Sentinel-5 Precursor satellite. The instrument provides daily global NO_2 maps at a resolution of about 5 km. However, measurements represent a vertical column of NO_2 in the troposphere (Fig. 1 a, c) with a resolution lower than the required 1 km. In this project, we aim at attaining high-resolution maps of near-surface NO_2 concentrations from TROPOMI NO_2 observations by using different data-driven algorithms such as tree-based and neural network models. Besides NO_2 satellite observations, we used land use data (population density, road network, traffic volume, etc.), meteorological data (wind speed, temperature, precipitation, etc.) and geographic data (digital elevation map) for training the models with *in situ* NO_2 observations.

The models were applied to two distinct regions, northern Italy/Switzerland («Alpine region») and Belgium/Netherlands («Benelux region»), to include NO_2 pollution hotspots in Europe and to demonstrate the model performance under a wide range of topographic and meteorological conditions. Figure 1 shows observed and downscaled remotely sensed NO_2 for June and December 2018. Predictions compared well with the observations from ground-based air quality monitoring shown as time-series for two test sites (Fig. 1 e,f). Preliminary results seem consistent with seasonal changes and motivate future efforts of integrating publically available data, including satellite observations, for evaluating human exposure to atmospheric pollutants.

REFERENCES

Bino, M. et al., 2017: Improved Methodologies for NO2 Exposure Assessment in the EU, Study accomplished under the authority of the European Commission, DG-Environment under service contract 070201/2015/SER/717473/C.3, Final report.

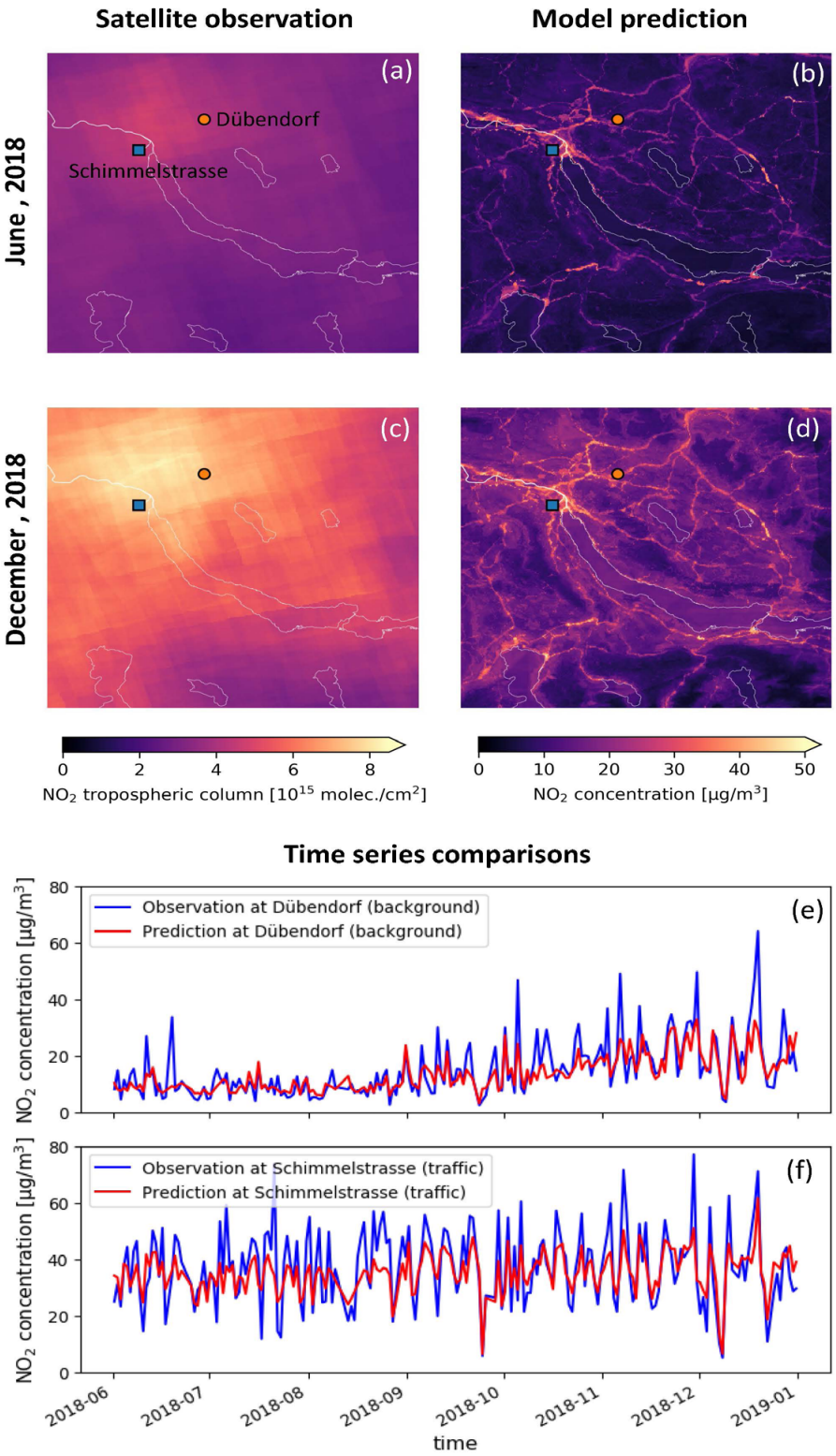


Figure 1: Vertical column density of NO_2 from TROPOMI around the city of Zürich as monthly averages for (a) June, and (c) December, 2018. By using a data-driven algorithm, the satellite observations were downscaled to a resolution of 100 m for both months (b and d, respectively). Predictions of NO_2 concentration time series were compared with observations at (e) Dübendorf (suburban, background, orange circle in a-d) and (f) Schimmelstrasse (urban, near traffic, blue squares in a-d).

18.4

Ultra-high resolution snow depth mapping using a UAV-based LiDAR scanner

Kalliopi Koutantou[1], Giulia Mazzotti[2], Tobias Jonas[2] and Philip Brunner[1]

[1]*Centre for Hydrogeology and Geothermics (CHYN), University of Neuchatel, Rue Emile Argand 11, CH -2000 Neuchâtel, Switzerland (kalliopi.koutantou@unine.ch)*
[2]*WSL Swiss Federal Institute for Snow and Avalanche Research SLF, Fl*üelastrasse 11, CH- 7260 *Davos Dorf, Switzerland*

In forested watersheds with seasonal snowcover, knowledge of the spatial snow accumulation and melt patterns under the forest canopy is of key interest for hydrological applications. While optical sensors fail to obtain data below the trees, UAV-borne laser scanning is a very promising technology for snow depth mapping. In fact, laser altimetry opens new horizons for mapping terrestrial processes. However, Lidar scanning comes along with many challenges: for example, flight plans that allow for the extraction of the highest possible point density need to be developed. Moreover, the processing of the data is demanding and complex.

We use a state-of-the art Altigator Hydra 12 multicopter UAV and a Yellowscan Mapper II Lidar system for mapping the snow depth in a sub-alpine forest in south-eastern Graubünden, Switzerland. Snow-on and snow-off field campaigns took place in March and June 2019. The flights covered a 200*200 m area ranging from isolated larch trees to a closed mixed conifer stand. A flight plan with overlapping patterns yielded high point densities and horizontal and vertical accuracies close to 15 and 5 cm, respectively. For validation purposes, manual in-situ snow depth measurements were taken with a snow probe along pre-defined transects.

Combining two different approaches for extracting snow depth from the 3D point clouds, we propose a workflow to derive snow depth maps for forested areas. Subtraction of digital elevation models (DEMs) and the point to point comparison method are proposed, compared to the reference in situ HS data.
The derived UAV-based snow depth data will allow the investigation of spatial and temporal snow dynamics in terms of canopy structure at the spatial resolution of individual trees.

REFERENCES

Christian Ginzler and Martina L. Hobi(2015) Countrywide Stereo-Image Matching for Updating Digital Surface Models in the Framework of the Swiss National Forest Inventory, Remote Sensing, 7, 4343-4370, doi:10.3390/rs70404343

Giulia Mazzotti, William Ryan Currier, Jeffrey S. Deems, Justin M. Pflug, Jessica D. Lundquist and Tobias Jonas (2019) Revisiting Snow Cover Variability and Canopy Structure within Forest Stands: Insights from Airborne Lidar Data, Water Resources Research, doi:10.1029/2019WR024898

18.5

Machine learning assessment for tropospheric pathdelays prediction using meteorological parameters in Switzerland

Marcelina Los[1], Endrit Shehaj[1], Jan D. Wegner[1], Stefano D'Aronco[1], Alain Geiger[1], Elmar Brockmann[2]

[1]Institute of Geodesy and Photogrammetry, ETH Zurich, Robert-Gnehm-Weg 15, 8093 Zürich, Switzerland (eshehaj@ethz.ch)
[2]Swisstopo, Bern, Switzerland

Atmospheric water vapor experiences high spatio-temporal variability which is reflected in the total tropospheric pathdelays of microwave satellite signals integrated along the zenith direction. This zenith total delays (ZTD) need to be estimated in space geodetic techniques such as GNSS. In this work we provide an alternative method to predict the ZTDs based on meteorological parameters. Indeed, the successful applicability of machine learning to several applications has raised our attention into investigating its potential use to compute the delays caused by the atmosphere into different space geodetic techniques. On the one hand, very accurate meteorological data are available from multiple online sources, advantageously providing many input data for training the network. On the other hand, we can directly use GNSS ZTDs (for example from the swisstopo network over Switzerland) as outputs for the training period. Therefore, GNSS pathdelays are generated without processing any GNSS data, but only using meteorological parameters.

In this work, we provide a preliminary assessment of this technique in which GNSS zenith pathdelays from the AGNES stations in Switzerland and meteorological parameters from the Swiss Meteorological Network (SwissMetNet) have been used for training and validation purposes for a period of 10 years. These stations are distributed all over Switzerland allowing the network to train and validate stations with different altitudes and meteorological conditions. Preliminary results show an accuracy of several mm up to 2 cm depending on the stations location.

18.6

Towards a global time series (1982 - 2018) of snow cover extent based on AVHRR GAC data – preliminary results of the ESA CCI+ Snow project

Kathrin Naegeli[1], Andreas Wiesmann[2], Xiaodan Wu[1,3], Christoph Neuhaus[1], Martin Stengel[4], Rainer Hollmann[4], Stefan Wunderle[1]

[1]Institute of Geography and Oeschger Centre for Climate Change Research, University of Bern, Hallerstrasse 12, CH-3012 Bern (kathrin.naegeli@giub.unibe.ch)
[2]Gamma Remote Sensing Research, Worbstr. 225, CH-3073 Gümligen
[3]College of Earth and Environmental Sciences, Lanzhou University, CN-730000 Lanzhou
[4]German Meteorological Serivce, Frankfurter Straße 135, DE-63067 Offenbach am Main

Knowledge about the snow cover distribution is of high for climate studies, weather forecast, hydrological investigations, irrigation or tourism, respectively. The key aspects are the pronounced albedo change between snow cover and ground, but also water storage influencing run-off in the following spring and summer season. Distribution of snow on the globe is highly variable in space and time. Especially the annual variability of snow extent of the northern hemisphere ranges from 3 to 50 million km^2 from summer to winter. Furthermore, as snow cover is very sensitive to atmospheric temperatures, it is likely to show a significant response to a changing climate. Considering the high dynamic and the vast spatial distribution only satellite data can provide the needed information. For climate studies, a time series of more than 30 years is needed for statistically sound analyses as defined by WMO. Regarding these general conditions the only usable sensor is the Advanced Very High Resolution Radiometer (AVHRR) on the polar orbiting satellites NOAA-6 to -19 and Metop-A to -C providing data from 1982 until today (and most likely until 2025) with daily resolution.

Based on the products of the ESA Cloud cci project we have used the calibrated and geocoded AVHRR GAC (Global Area Coverage) data with a spatial resolution of 4 km including a consistent cloud map. The retrieval of snow extent considers the high reflectance of snow in the visible spectra and the low reflectance values in the near infrared expressed in the Normalized Difference Snow Index (NDSI). Additional thresholds related to topography and land cover are included to derive the fractional snow cover of every pixel.

In this presentation, we show preliminary results of the daily, global snow cover evolution spanning the complete time series of 37 years based on AVHRR GAC data and processed within the ESA CCI+ Snow project. Snow parameters, such as snow cover area percentage (SCA), snow cover duration (SCD), snow cover onset day (SCOD) and snow cover melting day (SCMD), are presented and interpreted. Furthermore, the benefits of this time series of almost 40 years fulfilling the requirements of WMO are highlighted by means of regional comparative assessments with higher resolved satellite data and in view of the climate modelling community.

18.7

Effects of spatial variability of NO_2 concentrations on NO_2 remote sensing at city scale studied with a 3D radiative transfer model

Marc Schwaerzel[1,2], Claudia Emde[3], Gerrit Kuhlmann[1], Dominik Brunner[1], Brigitte Buchmann[1] & Alexis Berne[2]

[1]Laboratory for Air Pollution / Environmental Technology, Empa - Swiss Federal Laboratories for Materials Science and Technology, Überlandstrasse 129, CH-8600 Dübendorf, Switzerland (marc.schwaerzel@empa.ch)
[2]Environmental Remote Sensing Laboratory, EPFL - École Polytechnique Fédérale de Lausanne, Station 2, CH-1015 Lausanne, Switzerland
[3]Meteorologisches Institut München, Ludwig-Maximilians-Universität München, Theresienstr. 37, D-80333 München, Germany

Nitrogen dioxide (NO_2) is a relevant air pollutant with high spatial and temporal variability in cities, because of its strong localized sources combined with a short lifetime of a few hours. The spatial variability can be sampled with ground-based instruments and mapped with airborne or space-based imaging spectrometers. Different from ground-based in situ instruments measuring NO_2 at a single point in space, imaging spectrometers provide information on the total vertical column. For each measured spectrum, an NO_2 vertical column density (VCD) can be derived in two steps: First, a slant column density (SCD) representing the number of NO_2 molecules along the mean path of the photons from the sun to the instrument is fitted to the observed spectrum, and second, the SCD is converted to a VCD using an air mass factors (AMF). AMFs depend on Sun position, instrument viewing direction, surface reflectance and scattering of photons by gases and aerosols in the atmosphere and can be calculated from vertically resolved AMFs (layer-AMFs) with a radiative transfer model (RTM).
AMFs are traditionally computed under the assumption of a horizontally homogeneous atmosphere and land surface, which is not a proper assumption in cities where NO_2 concentrations and surface reflectance have a high spatial variability. To study the effects of horizontal inhomogeneity, we implemented three-dimensional (3D) box-AMFs in the MYSTIC solver of the libRadtran RTM (Emde et al. 2016, www.libradtran.org).

To demonstrate the importance of 3D box-AMFs in the trace gas retrieval, we simulated a NO_x plume emitted from a single stack with the GRAL dispersion model. The total NO_2 columns from the simulation are referred to as true VCDs in the following. We then converted the 3D NO_2 field to NO_2 SCDs using 3D box-AMFs for an imaging spectrometer on an aircraft flying parallel to the plume. From these synthetic SCDs, we calculated back the VCDs using 1D layer-AMFs for the same scenario. Finally, we compared these calculated VCDs to the true VCDs to highlight the errors introduced by using simplified 1D AMFs.

Figure 1a and 1b show the true VCDs obtained from a GRAL simulation and true SCDs calculated with the 3D box-AMFs. Figure 1c and 1d show the VCDs calculated with 1D box-AMFs and the differences between the calculated VCDs and true VCDs. The absolute differences are up to 26 µmol/m² (relative error of 32%) in the plume region. Effects are expected to be even higher for a plume further away from the ground (here the stack emits NO_x in the atmospheric layer between 100 and 200 m).

In conclusion, the new 3D box-AMFs implementation in MYSTIC allows us to study the effect of horizontal inhomogeneities of atmospheric and ground properties on the spatial distribution of box-AMFs and its influence on trace gas retrievals. In cities, where the NO_2 field is complex, not considering 3D box-AMFs can result in significant biases in the NO_2 retrievals.

REFERENCES

C. Emde, R. Buras-Schnell, A. Kylling, B. Mayer, J. Gasteiger, U.
Hamann, J. Kylling, B. Richter, C. Pause, T. Dowling, and L. Bugliaro (2016). The libRadtran software package for radiative transfer calculations (version 2.0.1). Geoscientific Model Development, (5), 1647-1672.

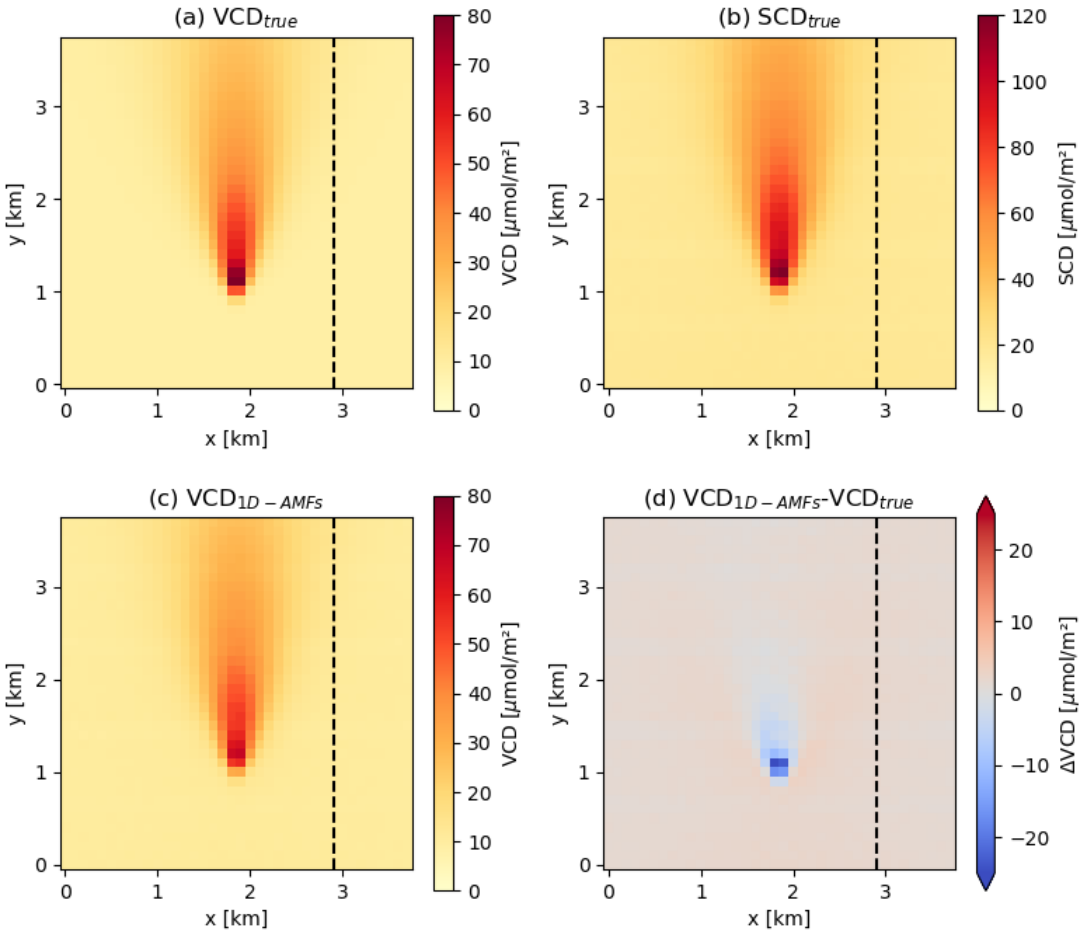


Figure 1. (a) Simulated (true) NO_2 VCDs (b) Synthetic SCDs computed from simulated VCDs combined with 3D box-AMFs for an airborne instrument flying parallel to the y-axis at x=2.9 km (dashed line) and at 6 km above surface. The sun is at a zenith angle of 40° and an azimuthal angle of 90° (west), (c) VCDs calculated from synthetic SCDs and 1D box-AMFs and (d) difference between calculated and true VCDs.

18.8

GlobDiversity: Remote Sensing-enabled Essential Biodiversity Variables to monitor key biodiversity characteristics at a global scale

Vladimir R. Wingate, Isabelle Helfenstein, Claudia Röösli, Michael E. Schaepman

[1]*Dept. of Geography, University of Zurich, Zurich, Switzerland (vladimir.wingate@geo.uzh.ch)*

GlobDiversity is a European Space Agency (ESA) funded project involving a consortium of international research institutes. It is aimed at defining and developing Remote Sensing-enabled Essential Biodiversity Variables (RS-EBV); they comprise a collection of biophysical metrics, derived from satellite remote sensing (RS) datasets, which were shown to be relevant for global biodiversity monitoring. Three RS-EBVs were prioritized for development based on their suitability for biodiversity monitoring and include algorithms for retrieving Land Surface Phenology (LSP), Ecosystem Fragmentation and Canopy Chlorophyll Concentration. They were engineered using current best practices, high resolution Sentinel-2 and Landsat-8 time-series, and are currently being tested on ten pilot sites located across six terrestrial biomes. As a part of GlobDiversity, the University of Zurich (UZH) implemented LSP as a RS-EBV. LSP characterises recurrent biological events in the annual temporal profile of vegetated land surfaces at ecosystem scales, as observed by RS. Importantly, LSP has been widely used to measure the response of terrestrial ecosystems to changes in climate and environmental conditions, as well as a proxy for characterising species composition and ecosystem biodiversity. Currently, the algorithm testing and upscaling phases are taking place, with the objective of implementing the algorithms in an operational cloud computing system and processing them globally. Concurrently, their effectiveness at monitoring biodiversity and their usefulness for conservation applications is being demonstrated in four case studies undertaken by the consortium members. Here, UZH are investigating the biodiversity monitoring and conservation applications of RS-EBVs, particularly LSP, in Kytalyk National Park, Siberia. The focus is on demonstrating how RS-EBVs, together with ancillary datasets, can be used to evaluate the nesting habitat availability and breeding success of the Siberian White crane (*Grus leucogeranus*) and the lesser sand hill crane (*Grus canadensis*).

P 18.1

Water vapour trends in Switzerland based on data from ground-based microwave radiometry and GNSS ground stations

Leonie Bernet[1], Elmar Brockmann[2], Christian Mätzler[2], Niklaus Kämpfer[2], Klemens Hocke[2]

[1]Institute of Applied Physics and Oeschger Centre for Climate Change Research, University of Bern, Bern, Switzerland
[2]Federal Office of Topography, swisstopo, Wabern, Switzerland

Atmospheric water vapour plays a crucial role in the climate system. It is not only a strong greenhouse gas, but also affects many atmospheric processes such as the formation of clouds and precipitation. Water vapour is directly related to changes in temperature, as described by the Clausius Clapeyron relation. Analysing how water vapour changes in time is therefore important in a warming climate.

We asses changes of integrated water vapour (IWV) over Bern, Switzerland, by analysing data from a tropospheric water radiometer (TROWARA). We compared TROWARA data to reanalysis data from the Modern-Era Retrospective analysis for Research and Applications (MERRA2). Further, the data are compared to surrounding ground stations of the Global Navigation Satellite System (GNSS), which are part of the Automated GNSS Network for Switzerland (AGNES). We observe that the different datasets generally agree well, with differences within 10%.
We determined IWV trends of almost 25 years of data and found trends between 1 and 6% per decade. Trend differences depending on seasonal cycle are also presented, with slightly higher trends in spring and autumn. Further we found an altitude dependence of the trends, with larger trends for GNSS stations that lie at higher altitudes.

Our IWV trends are generally consistent with observed temperature changes. This confirms the positive temperature–water vapour feedback in a warming climate. However, we observe that not all data sets show trends that are significantly different from zero at 95% confidence interval. This insignificance of trends for some datasets emphasizes the need to continue to measure water vapour, with the aim to obtain stable long-term time series and to better understand water vapour feedbacks in a changing climate.

GNSS data is of high interest for this endeavour due to its measurement continuity and its good spatial coverage.

P 18.2

Rock slope deformation in the Grimsel Pass region, Switzerland

Andrea Manconi[1], Annette Temperli[2] & Martin Ziegler[1]

[1]Department of Earth Sciences, Engineering Geology, ETH Zurich, Zurich, Switzerland (andrea.manconi@erdw.ethz.ch)
[2]Department of Environmental Sciences, ETH Zurich, Zurich, Switzerland

The investigation of environmental parameters is crucial for the analysis and interpretation of several geo-hazards. In recent years, remote sensing approaches have been extensively applied on radar imagery to study slope instability. Differential Synthetic Aperture Radar Interferometry (DInSAR) is a powerful remote sensing technique capable to retrieve ground displacement in different scenarios. Space-borne DInSAR relies on the availability of images acquired from SAR sensor on board satellites orbiting 800 km above the Earth's surface. By analyzing the phase differences between two subsequent acquisitions over the same area it is possible to identify surface deformation relevant to slope instability with sub-centimetric accuracies.

In this work, we applied DInSAR on the recent ESA Sentinel-1 acquisitions to study slope processes in the Grimsel Pass region. The results show that slopes adjacent to Lake Grimsel and Lake Oberaar are affected by reversible surface displacements during summer periods. High resolution photogrammetric data and UAV-based high-resolution 3D slope models were also used to investigate slope morphology and rock mass fractures, to derive hypotheses on the potential causes of these processes, and to validate the remote sensing results.

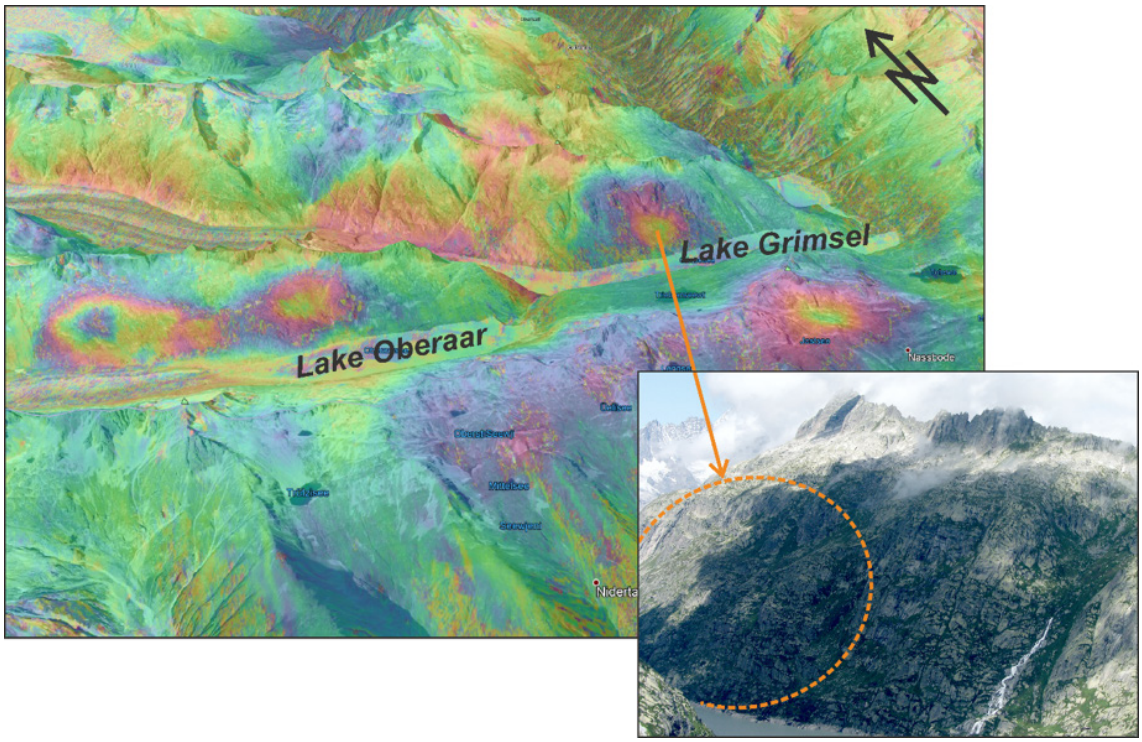


Figure 1. Surface deformation derived from DInSAR in the Grimsel Pass region (summer 2018) and photograph looking at the northern slope of Lake Grimsel.

P 18.3

Accuracy study of snow cover maps based on AVHRR data with different spatial resolution

Soumita Patra[1,2], Kathrin Naegeli[1], Stefan Wunderle[1]

[1]Institute of Geography and Oeschger Centre for Climate Change Research, University of Bern, Hallerstrasse 12, CH-3012, Bern (soumita.patra@guib.unibe.ch)
[2]Birla Institute of Technology, Mesra, Jharkhand, 835215, India

Snow is an essential natural resource and geophysical parameter that represents the largest part of the cryosphere. The significance of snow cover for the climate at a regional and global scale is already recognized. Thus, the proper monitoring of spatial and temporal variability of seasonal snow cover is crucial to understand changes in the climate system including hydrological processes, water management or snow-melt runoff.

The Advanced Very High Resolution Radiometer (AVHRR) provides the unique opportunity to retrieve long time series of more than 35 years to study earth surface process at a global scale on a daily basis. It is important to note that, Local Area Coverage (LAC) and Global Area Coverage (GAC) data from the AVHRR sensor was broadly used for snow cover mapping in the Alps individually. However, the main challenge is the availability of finer resolution LAC data (1.1 km) at a global scale. Therefore, we use reduced resolution GAC data (4.4 km) due to its global availability. To the best of our knowledge, the differences in snow maps occurring due to different resolution from both LAC and GAC data has not yet been investigated. In this study, we thus carry out an in-depth assessment of differences and similarities of winter snow cover products over different topography and land cover types based on AVHRR LAC and GAC data, aiming at estimating the accuracy of GAC snow cover maps for the European Alpine environment.

Here, we present preliminary results of the comparative assessment of LAC and GAC snow cover products. In particular, the influence of the topography and varying land cover types are investigated in order to be able to describe possible reasons for variations between the products. Pixel-wise fractional snow cover extent is obtained by applying the Normalized Difference Snow Index (NDSI) in combination with other band-related thresholds. A series of two winters is used to address the research aim in the regional context of the European Alps. This comparison of snow products based on LAC and GAC data shows their individual assets, points out discrepancies and highlight crucial information to be considered for the derivation of consistent fundamental climate data record.

P 18.4

Remote Sensing of Ecological Genetics

Schuman M.C., Czyz E., Li C., Shimizu K.K., Baldwin I.T., Schaepman M.

Recent, cutting-edge studies have demonstrated the ability of spectroscopic imaging and laser scanning techniques to identify plant species and quantify several biochemical and structural traits, and a few studies have differentiated plant genotypes. While catalogues of species and traits are now being established using multiple approaches, data on genetic diversity is more sporadic, and laborious to collect. Yet genetic diversity is a key determinant of adaptive potential for species in a changing climate. We aim to develop remote sensing approaches to describe plant genetic diversity and its distribution.

P 18.5

Perspectives for the monitoring of very slow landslides in Switzerland with InSAR

Tazio Strozzi[1], Rafael Caduff[1], Andrea Manconi[1] & Christian Ambrosi[2]

[1]Gamma Remote Sensing, Gümligen (BE), Switzerland (strozzi@gamma-rs.ch)
[2]SUPSI, Trevano (TI), Switzerland

Over Switzerland, hazards due to slope instabilities affect about 6% of the territory. It is therefore of outstanding importance to continuously monitor the rate of motion of landslides for the assessment of their hazard and the survey of their activity with time. Satellite Synthetic Aperture Radar (SAR) interferometry (inSAR) is one option for surface deformation monitoring over large areas, now entering an operational phase with the regular availability of Sentinel-1 data since 2014, see various nation-wide maps of land deformation recently released in Norway, Germany and the United Kingdom. Also in Switzerland there is a high interest on deformation maps and time series of surface motion from InSAR.

In our contribution we will discuss, based on results for the Loderio landslide in Canton Ticino, potential and limitations of current satellite SAR data with different carrier frequencies (L-, C- and X-band), ground resolutions (around 10, 20 and 2 meters), time intervals (46, 6, 34 and 11 days) and acquisition strategies (global versus on-demand, free versus commercial data) for the monitoring of very slow landslides (i.e. rates of motion of a few cm/year). Multi-temporal interferometric approaches using large data stacks are applied over this mountainous area, where sparse urbanization, large vegetated areas, snow-cover, layover/shadow, and atmospheric stratification and summer turbulences are introducing special processing challenges.



Figure 1. Photographs of the Loderio landslide.

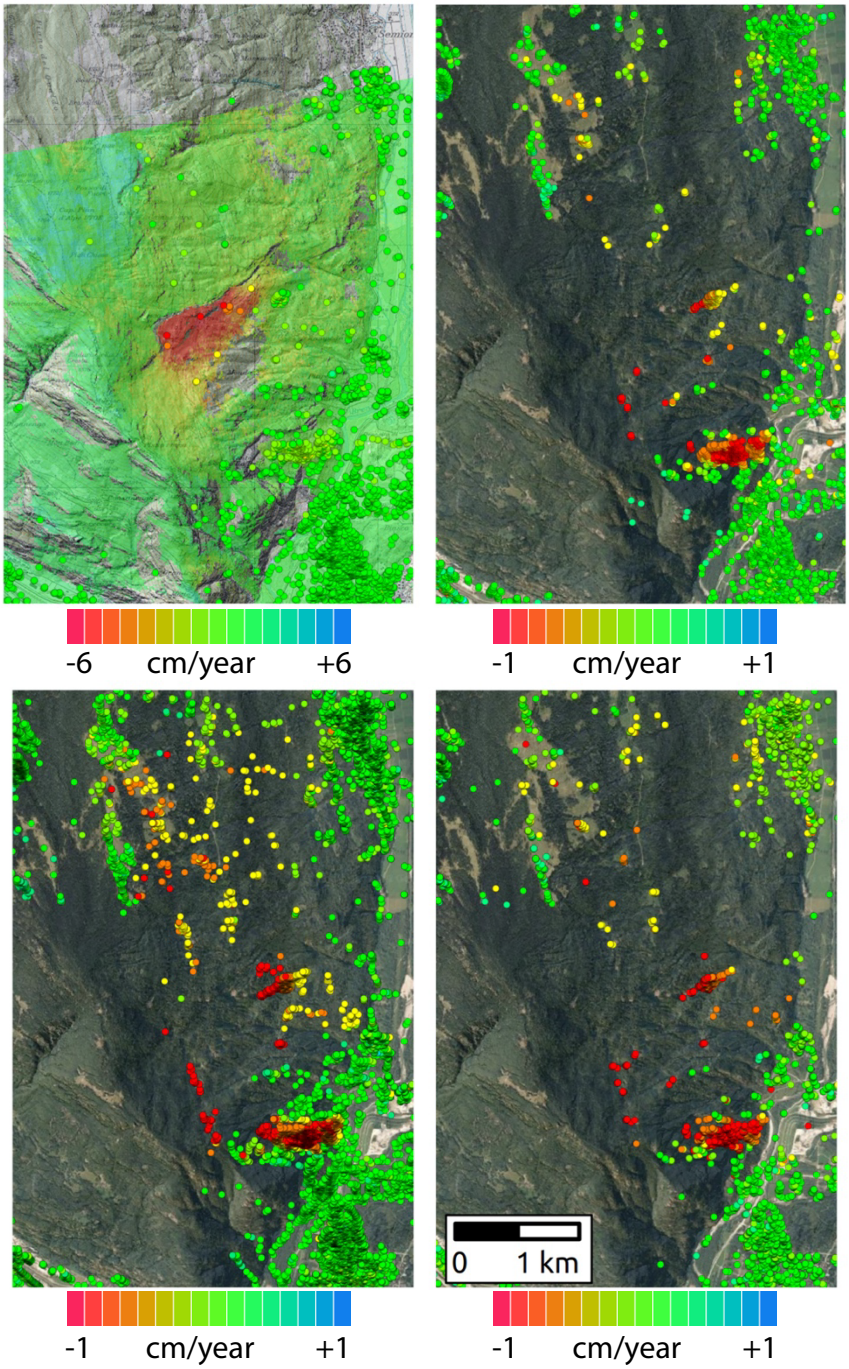


Figure 2. Multi-temporal SAR interferometry on the Loderio landslide using (from left to right, top to bottom) ALOS-2 PALSAR-2 from 2014 to 2018, Sentinel-1 from 2014 to 2018, TerraSAR-X from 2014 to 2017 and Radarsat-2 from 2011 to 2017.

P 18.6

Large-scale crop classification from satellite images

Mehmet Ozgur Turkoglu, Konrad Schindler, Jan Dirk Wegner

EcoVision Lab, Photogrammetry and Remote Sensing, ETH Zurich, 8093, Zurich (ozgur.turkoglu@geod.baug.ethz.ch)

Annual inspections of farmland in Switzerland is a time-consuming process and requires lots of human labor. Each year many farmlands are visited to validate the cultivated crop types reported by farmers and to inspect over-fertilization. These tasks are not only labor-intensive and time-consuming but also do not scale to the entire country in practice. Therefore, the Swiss Federal Office for Agriculture (BLW) has initiated a four-year project in 2018 to develop an automatic system for farmland inspection from satellite images. Within the scope of this project, we are currently working on crop type classification method from publicly available Sentinel-2 images.

Most previous work uses physics-inspired models. They compute one or multiple vegetation-related indexes, form time series, and feed them to a classifier, e.g, a random forest. Such models capture only a limited part of the complex reflectance distribution of the vegetation and its evolution. We posit that this is one of the factors that limit their performance, and undermines their robustness against noise in the data, even when advanced pre-processing techniques are used. Our approach is based on deep learning, which has recently shown great success in prediction tasks, from both image data and time series (e.g. in speech processing). We use a recurrent multi-layer neural network to learn the complex spectral, spatial and temporal patterns that differentiate different crop types from raw data. Our model is fed with a temporal sequence of images and encodes both spectral and temporal information, from which it then predicts the likelihoods of different crop types. We do not do any pre-processing, rather we let the model learn to disregard uninformative and noisy data, such as clouds and cloud shadows.

Here, we present the project aims, the processing methods, preliminary results, and initial validations.

19. Geoscience and Geoinformation – From data acquisition to modelling and visualisation

Nils Oesterling, Massimiliano Cannata, Michael Sinreich

Georesources Switzerland Group
Swiss Geodetic Commission
Swiss Geophysical Commission
Swiss Hydrogeological Society

TALKS:

19.1 Antononic M., Brodhag S., Cannata M., Hoffmann M., Oesterling N.: Presentation und hands-on: Borehole data web-application

19.2 Heck A., Weisgerber J., Westerhaus M., Sumaya H., Even M., Kutterer H., Heck B.: Fusion of SAR-Interferometry, GNSS and Precise Levelling: Latest Deformation Fields in Northern Switzerland derived from PS-InSAR and GNSS

19.3 Iosifescu Enescu.I., Plattner G.-K., Haas-Artho D., Pernas E.L., Steffen K.: Enhancing the Environmental Data Repository EnviDat with a Traditional Spatial Data Architecture

19.4 Kurmann-Matzenauer E., Signer-Michael S.: From a geological map to a 3D-model – and vice versa

19.5 Malard A., Randles S., Hausmann P., Jeannin P., Vogel M., Lopez S., Courrioux G.: Visual KARSYS, a web-tool for modelling karst aquifers in 3D

19.6 Rauch A., Sartori M., Moeri A., Castelltort S.: Tracking mapping style in the Swiss Geological Atlas data set and what we can learn from it

19.7 Su H., Rothacher M.: Water Vapor Comparison between GNSS and MODIS Sensor Retrieval

19.8 Walter F., Wenner M., Marchetti E., Fengler M., Farinotti D.: A data platform for monitoring hazardous mass movements in Alpine terrain

POSTERS:

P 19.1 Bandou D., Schläfli P., Schwenk M., Douillet G.A., Kissling E., Schlunegger F.: Assessing the bedrock surface of overdeepened valleys by 3D gravity modelling

P 19.2 Cannata M., Strigaro D., Antonovic M., Hoffmann M., Shahid I., Ratnayake R., Sudantha BH.: 4onse: open monitoring system

P 19.3 Cannata M., Strigaro D., Lepori F., Capelli C., Brovelli M.A., Rogora M., Veronesi M., Magni D., Buzzi F.: SIMILE, integrated water quality monitoring system

P 19.4 de Lutio R., D'Aronco S., Wegner J.D., Schindler K.: Guided Super-Resolution of Environmental Maps

P 19.5 Hu Y., Gu C., Shao C., Meng Z.: Multi-point Dam Displacement Prediction Based on a Clustering Method

P 19.6 Malard A., Randles S., Hausmann P., Jeannin P., Vogel M., Lopez S., Courrioux G.: Visual KARSYS, a web-tool for modelling karst aquifers in 3D

19.1

Presentation und hands-on: Borehole data web-application

Milan Antononic[1], Sabine Brodhag[2], Massimiliano Cannata[1], Marcus Hoffmann[1], Nils Oesterling[2]

[1]Institute of Earth Sciences, University of Applied Sciences and Arts of Southern Switzerland, Cannobio, Switzerland
[2]Federal Office of Topography SWISSTOPO, Bern, Switzerland

During the last years, a Borehole Data Management System (BDMS) has been developed by the Federal Office of Topography of Switzerland (swisstopo). To facilitate the data exchange procedure, a standalone application built with closed source software is used, but this approach starts to feels too hard working by the users and recently an increasing number of partners start asking for a web-based solution. To fulfill this demand, we developed a new Web Application Prototype, sponsored by swisstopo, using the latest Free and Open Source Technologies. The new application integrates some of the today's best OSGeo projects and will be available in 2020 as a modular open source solution on GitHub and ready to use in a docker container available on Docker Hub. Through two types of authorization, Explorer users are able to search the BDMS for specific boreholes, navigate a configurable user-friendly map, apply filters, explore the stratigraphy layers of each borehole and export all the data in shapefiles, CSV or PDF. Editors are able to manage in detail the information and publish the results after passing a validation process. The application is compliant with the data model for boreholes provided by swisstopo.

REFERENCES

Sabine Brodhag, Nils Oesterling 2014: Datenmodell Bohrdaten https://www.geologieportal.ch/en/knowledge/lookup/data-models/borehole-data-model.html

Nils Oesterling, Sabine Brodhag 2016: Datenmodell Bohrdaten – Module, Bundesamt für Landestopografie swisstopo, Bern

19.2

Fusion of SAR-Interferometry, GNSS and Precise Levelling: Latest Deformation Fields in Northern Switzerland derived from PS-InSAR and GNSS

Alexandra Heck[1], Jakob Weisgerber[1], Malte Westerhaus[1], Hael Sumaya[1], Markus Even[1], Hansjörg Kutterer[1], Bernhard Heck[1]

[1]Geodetic Institute, Karlsruhe Institute of Technology (KIT), Englerstraße 7, D-76131 Karlsruhe (alexandra.heck@kit.edu)

The PS-InSAR (Persistent Scatterer SAR Interferometry) method, GNSS networks and precise levelling provide a unique database to detect recent displacements of the Earth's surface. However, each technique shows its own characteristics in terms of sampling rates, spatial resolution, reference frames and processing models. We focus on developing a fusion technique that takes advantage of the geodetic measurement methods mentioned. This fusion technique has already been applied investigating the intra-plate deformation of the Upper Rhine Graben (URG) located in Central Europe, determine a 3D velocity field which is able to solve the expected tectonic movements below the single-digit millimetre per year range (Fuhrmann et al, 2015).

The previous database consists of

- precise levelling data gathered by the surveying authorities of Germany, France and Switzerland dating back to the end of the 19th century,
- GPS time series between 2002 and 2011 of 85 permanent stations being part of GURN (GNSS Upper Rhine Graben Network) and
- PS-InSAR velocity fields derived from ERS-1/2 and Envisat data acquired between 1992 and 2010.

Some of the analysed GPS time series are less than 4 years, resulting in undesirably high standard deviations of the 3D velocity field. Furthermore, the 3D velocity field shows partially unexpected results at the edge of the investigated area. A current step is therefore to expand the model area and to integrate longer GPS time series into our approach. Besides using data of additional GNSS stations and longer GNSS time series, we also integrate Sentinel-1 data for performing PS-InSAR analysis using the open source software packages SNAP (SentiNel Application Platform) and StaMPS (Stanford Method of Persistent Scatterer).

The presentation will focus on the concept of the fusion approach and will show the latest results of the PS-InSAR evaluation of Sentinal-1 data as well as the GPS PPP (Precise Point Positioning) time series solutions in northern Switzerland.

REFERENCES

Fuhrmann, T., Caro Cuenca, M., Knöpfler, A., van Leijen, F.J., Mayer, M., Westerhaus, M., Hanssen, R.F., Heck, B., 2015: Estimation of small surface displacements in the Upper Rhine Graben area from a combined analysis of PS-InSAR, levelling and GNSS data. Geophysical Journal International, 203 (1): 614-631, doi: 10.1093/gji/ggv328.

19.3

Enhancing the Environmental Data Repository EnviDat with a Traditional Spatial Data Architecture

Ionuț Iosifescu Enescu[1], Gian-Kasper Plattner[1], Dominik Haas-Artho[1], Lucia Espona Pernas & Konrad Steffen[1,2,3]

[1]Swiss Federal Research Institute WSL, Zürcherstrasse 111, CH-8093 Birmensdorf (ionut.iosifescu@wsl.ch)
[2]ETH Zurich
[3]EPF Lausanne

EnviDat (www.envidat.ch) is the environmental data portal and institutional repository of the Swiss Federal Research Institute WSL. With its capability to host and publish data sets, EnviDat focuses on integrating curated data sets from the environmental domain and facilitates efficient and unified access to WSL's environmental monitoring and research data (Iosifescu et al., 2018).



Figure 1. The EnviDat environmental data portal

The integration of existing datasets in EnviDat, currently mainly originating from WSL, is accompanied by their documentation with appropriate metadata. Formal publication of research data with proper citation information and Digital Object Identifiers (DOIs) is supported and encouraged. Extending the EnviDat service to other institutions within the ETH Domain is a mid- to long-term goal of WSL.

Further advances of the EnviDat system are currently being explored, such as geoportal capabilities and spatial data infrastructure (SDI). These will allow EnviDat to include specific support for the discovery, presentation and retrieval of spatial data. Such future portal interface and functionality improvements are interrelated with the EnviDat system architecture and technology stack. EnviDat adopted best practices and standards in data sharing by integrating prominent technologies for data repositories that are available from the wider research data management community.

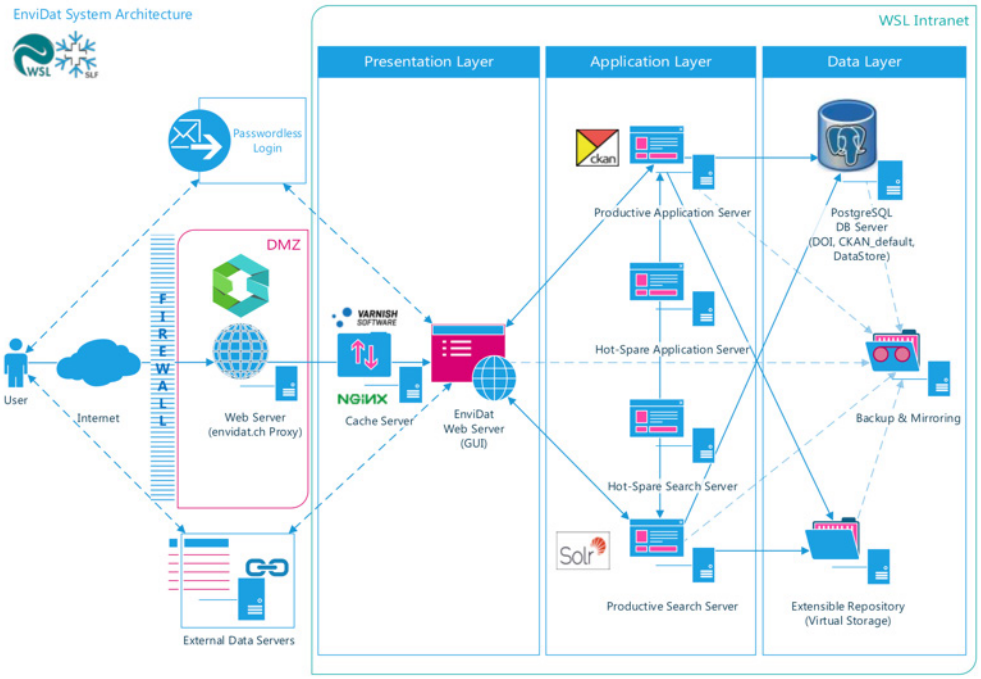


Figure 2. EnviDat three-tier system architecture (Iosifescu et al., 2018)

The EnviDat portal for data providers is leveraging community software such as CKAN, Apache Solr and PostgreSQL, while a three-tier system architecture containing clearly defined data management, application and presentation layers (Iosifescu et al., 2018). In this context, geospatial databases and technologies such as PostgreSQL and PostGIS are already central for EnviDat's additive data discovery mechanism, supporting data users with a more effective search and retrieval of published data based on their geospatial characteristics (Iosifescu et al., 2018). Consequently, the existing EnviDat architecture can be enhanced with additional traditional geoportal components, such as view/mapping and geoprocessing servers (please refer to Iosifescu et al., 2017, for details).

By incorporating full support for spatial data and capabilities, EnviDat is pursuing an innovative convergence of data publishing repositories with geoportals, thus actively bridging the gap between the research data management and the geospatial communities.

REFERENCES

Iosifescu-Enescu, I., Matthys, C., Gkonos, C., Iosifescu-Enescu, C.M., & Hurni L. 2017: Cloud-Based Architectures for Auto-Scalable Web Geoportals towards the Cloudification of the GeoVITe Swiss Academic Geoportal, ISPRS International Journal of Geo-Information, 6(7), 192, DOI:https://doi.org/10.3390/ijgi6070192

Iosifescu Enescu, I., Plattner, G.-K., Espona Pernas, L., Haas-Artho, D., Bischof, S., Lehning, M., & Steffen K. 2018: The EnviDat Concept for an Institutional Environmental Data Portal, Data Science Journal, 17, p.28, DOI:http://doi.org/10.5334/dsj-2018-028

19.4

From a geological map to a 3D-model - and vice versa

Eva Kurmann-Matzenauer1 & Salomè Signer-Michael1

[1]Federal Office of Topography swisstopo, Swiss Geological Survey, Seftigenstrasse 264, CH-3084 Wabern (eva.kurmann@swisstopo.ch)

Ideally, a high density of well logs and seismic interpretations provide a clear picture of the geology of the deeper underground. In reality, outside of areas with intense subsurface exploration and/or production this case is rare: usually the boreholes are far apart, do not reach the desired depth and seismic data is not available. Furthermore, the geological complexity between the sparse input data may excede what can be reproduced by simple interpolation. At shallow depth, geological 2D data (maps, vector data) and associated geological profiles describe the geological context of a large-scale area. The widespread distribution of geological 2D data and their availability, but above all the coherent and consistent geological interpretation on the map sheet, are essential input data for 3D modeling near the surface.

In order to test a nationwide coverage of geological 3D models, the Swiss Geological Survey has created a pilot program focused on the construction of 3D geological models based solely on 2D data, profiles and available drill hole data. Using the Move software (Petroleum Experts, Version 2018.2), several geological 3D models based on the GeoCover vector datasets (© swisstopo) at a scale of 1: 25’000 were created at sites with different geological setting. South of the Jura mountains near Aarau and in the area of Elm, two models were created as part of this feasibility study. In the model of Elm and in two further models in the areas of Hitzkirch and Langnau the modeling was carried out simultaneously to the editing process of the corresponding map sheets of the geological atlas (GA25).
The aim of this study is to (1) develop a methodology for 3D modeling in geologically complex areas, (2) to find out what level of detail can be achieved within a given timeframe and with the available data, and (3) in the case of processing of the GA25 map sheet to give geometric and qualitative feedback on geology or mapping.

We present the workflow and the completed 3D models and highlight the experiences but also the limitations of the chosen 3D modeling approach. Geologists should keep in mind the iterative character of 3D modeling that always returns to 2D data, revealing possible spatial inconsistencies. This in turn means that geological maps may need to be verified in the field and adjusted if needed. This shows that 3D modeling does not always have to lead to a final 3D model, but is also an essential tool for generating bedrock maps or to map a poorly developed geological unit in a spatially consistent way.

19.5

Visual KARSYS, a web-tool for modelling karst aquifers in 3D

Arnauld Malard[1], Stephen Randles[3], Philipp Hausmann[3], Pierre-Yves Jeannin1, Manfred Vogel[3], Simon Lopez[2], Gabriel Courrioux[2]

[1] *SISKA, Swiss Institute for Speleology and Karst Studies, rue de la Serre 68 – CH2300 La Chaux-de-Fonds*
[2] *BRGM, 3 avenue Claude-Guillemin, 45000 Orléans*
[3] *i4ds Institute of 4D Technologies, Fachhochschule Nordwestschweiz, Bahnhofstrasse 6, CH5210 Windisch*

Visual KARSYS is a web-tool available at www.visualkarsys.com. It has been developed to address modelers and end-users working for the documentation and/or the management of geology and groundwater resources in karst areas. It makes possible for modelers to setup projects, to entry geol. and hydrogeol. data and to design geological 3D model in order to subsequently apply the KARSYS approach On one side, Visual KARSYS offers an intuitive interface in which modelers are guided through the steps of the approach. On the other side, Visual KARSYS offers a dedicated output page for end-users which displays formatted data and resulting models built by modelers. Editing and reading permissions can be allotted by the project administrator to different users (both modelers and end-users). End users can arrange data and results as they want (form, layout, views, etc.) and different analysis tools are at their disposal (slicer, drawing tool, etc.). They can export different data or print maps.

Visual KARSYS is actually free-of-use and we encourage users to use it.

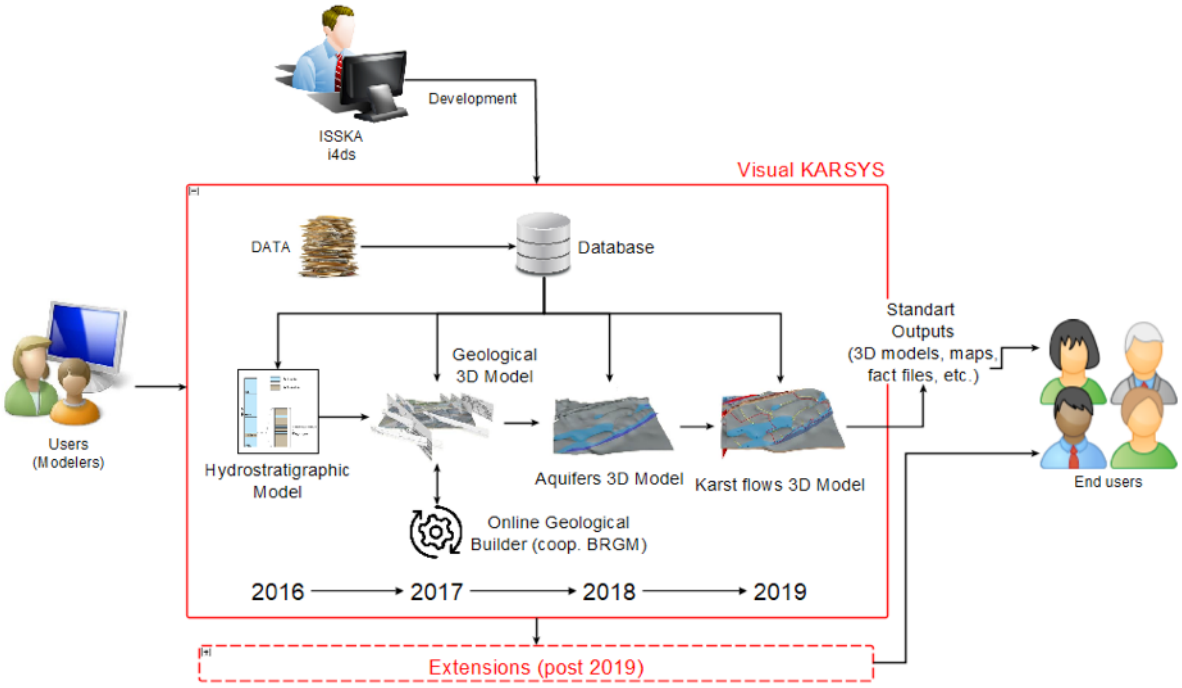


Fig. 1 the four basic steps of Visual KARSYS allow modelers to build 3D aquifer models online which can be seen and exploited by end-users. By the end of 2019, Visual KARSYS is ready for use. Nevertheless, additional extensions may be envisaged for the coming years.

The Visual KARSYS project is supported by the Swiss Federal Office for Environment via the grant for the promotion of environmental technology (2016-2019, UTF 537.13.16).

REFERENCES

Jeannin PY, Eichenberger U, Sinreich M, Vouillamoz J, Malard A et al. (2013) KARSYS: a pragmatic approach to karst hydrogeological system conceptualisation. Assessment of groundwater reserves and resources in Switzerland. Environmental Earth Sciences, 69(3): 999-1013 p.

19.6

Tracking mapping style in the Swiss Geological Atlas data set and what we can learn from it

Anna Rauch[1], Mario Sartori[1], Andreas Moeri[2] & Sébastien Castelltort

[1]*Département des sciences de la Terre, Université de Genève, Rue des Maraîchers 13, CH-1205 Genève (anna.rauch@unige.ch)*
[2]*Office fédéral de topographie swisstopo, Service géologique, Seftigenstrasse 264, CH-3084 Wabern*

Even if unavoidable, geological maps are sometimes pointed at for being a matter of style. In fact, it can hardly be denied that there is a part of personal, contextual, conceptual and temporal influence in each map, which we refer here alltogether to 'style'. This study represents an attempt to better understand style and even learn from it. It aims to observe and describe the map metrics that are strongly related to geological context and that have undergone a significant change during the last decades due to advances in technology, conceptual views and main goals.

Based on the 165 published sheets of the Swiss Geological Atlas (1:25'000), which appeared over a period of 90 years, we analyse the evolution with time of several map parameters, such as the total surface mapped as outcrop, the total fault length or the number of bedrock types. In a second step, we analyse the influence of the geological context and topographic relief on these parameters.

The results show that the complexity of the geological context influences the mappers daringness to interpret. That is one of several factors that typically gives the sheets in the Alps a quite different style than the Jura ones. It is also visible that in more recent years, mappers tend to give unconsolidated deposits more space, display more measurements and add more faults. This leads to more observation- and less interpretation-based maps. At the same time, it gives them a somewhat disjoint and patchy aspect, where deciphering the bedrock structure is much more difficult. This shows the importance of interpreting a bedrock geology map, as defined in swisstopo's data model (swisstopo 2017). The data model separates the interpreted bedrock geology from the observed outcrop boundaries so that neither the general structure comprehension nor the observation fidelity are compromised. We believe that this assessment about style constitute a solid base for a needed discussion about the role of observation and interpretation in geological mapping.

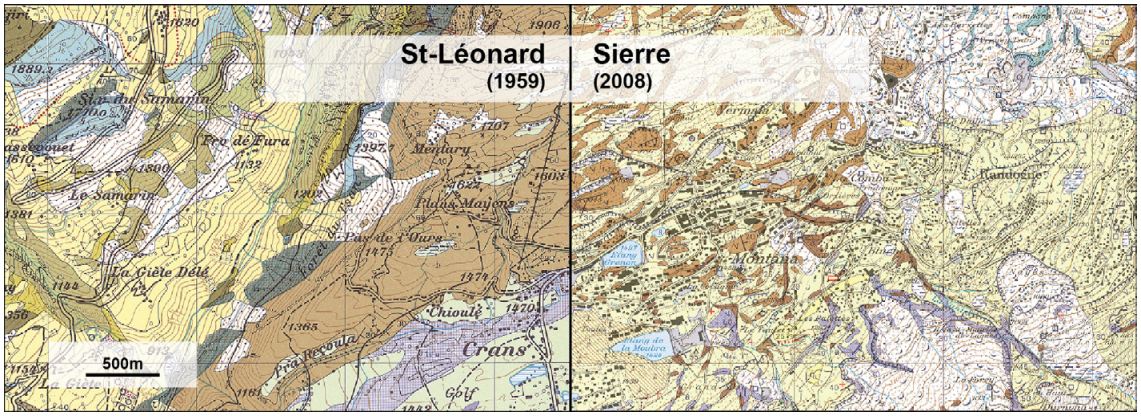


Figure 1. Example of an excerpt of two juxtaposing geological atlas sheets with different styles – on the left the sheet of St-Léonard (Badoux et al., 1959), on the right the sheet of Sierre (Gabus et al., 2008). In this study, the style differences are measured based on the outcrop surface, the fault length as well as the the mean trace length.

REFERENCES

Badoux, H., Bonnard, E.G., Burri, M., & Vischer, A. 1959: Feuille 1286 St-Léonard. – Atlas géol. Suisse 1 :25'000, carte 35. swisstopo.

Gabus, J.H., Weidmann, M., Bugnon, P.-C., Burri, M., Sartori, M. & Marthaler, M. 2008: : Feuille 1287 Sierre. – Atlas géol. Suisse 1 :25'000, carte 111. swisstopo.

Swisstopo 2017: Datenmodell Geologie – Beschreibung im UML-Format und Objektkatalog, Version 3.0. – Bundesamt für Landestopographie swisstopo, 115 p.

19.7

Water Vapor Comparison between GNSS and MODIS Sensor Retrieval

Hang Su[1,2,3] Markus Rothacher[3]

[1]*University of Chinese Academy of Sciences, Beijing, China (suha@ethz.ch)*
[2]*National Time Service Center, CAS, Xi'an, China*
[3]*Institute of Geodesy and Photogrammetry, ETH Zurich, Zurich, Switzerland*

Water vapor is one of the most important greenhouse gases in the world, leading a dominant role in climate change. There are lots of techniques which can measure water vapor directly or remotely. In this work, we compared the water vapor retrieved from GNSS and the MODIS (Moderate Resolution Imaging Spectroradiometer) sensor onboards NASA's Earth Observing System (EOS). For the EOS project, NASA launched two satellites payloads with the MODIS sensor named Terra satellite (1999) and Aqua satellite (2002). The orbital period of the EOS satellites is 12 hours with a day and night resolution of 1 km and 5 km, respectively. We reprocessed 11 years data (from 2002 to 2012) of GNSS data in order to get homogenous results. We computed GPS-only as well as GLONASS-only and combined solutions. Since the GNSS network is sparse and the MODIS sensor provides a grid dataset, we extracted the MODIS data at the GNSS permanent station locations.

During these 11 years, the amplitudes of water vapor vary between 0 and 70 mm. The water vapor difference between GPS and GLONASS is between -1 and +1 mm (Fig. 1) and it is diminishing with time due to the GLONASS constellation replenishment. The difference between MODIS Aqua and MODIS Terra is between -2 and 10 mm (Fig. 2) and it is increasing; this may happen due to the sensor aging. The biggest difference is measured over the equator. This is expected as the amount of water vapor over the equator is larger than in other regions. Finally, we compared GPS with MODIS Aqua. The difference is between -30 and 10 mm (Fig. 3). In the northen hemisphere the difference increases with latitude. However the southern hemisphere shows no significant pattern; the reason may be the sparse GNSS station network in this region.

It is important to noitice that the systematic bias between the techniques still needs to be studied and understood in more details.

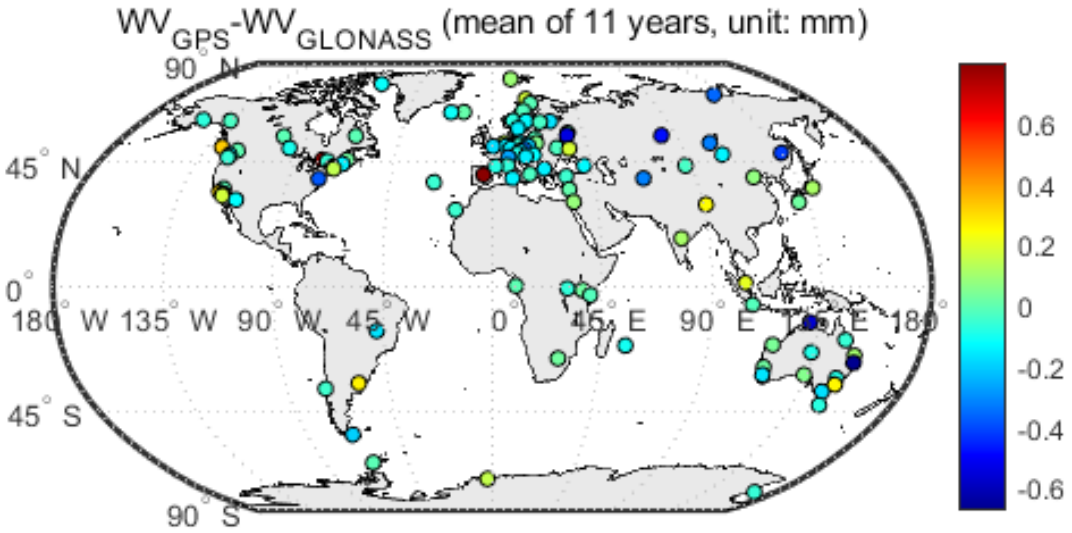


Figure 1. Water vapor differences between GPS and GLONASS

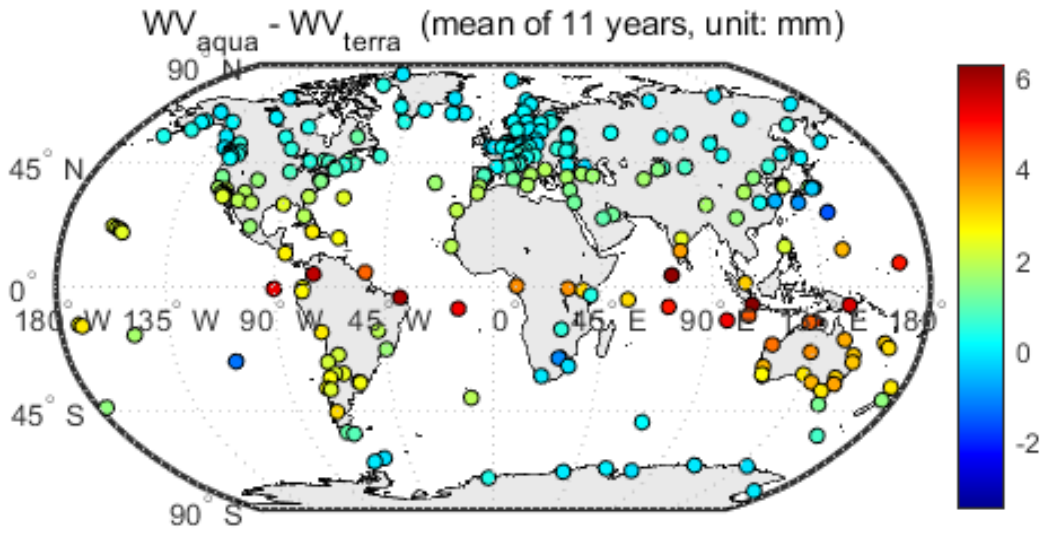


Figure 2. Water vapor differences between MODIS Aqua and MODIS Terra

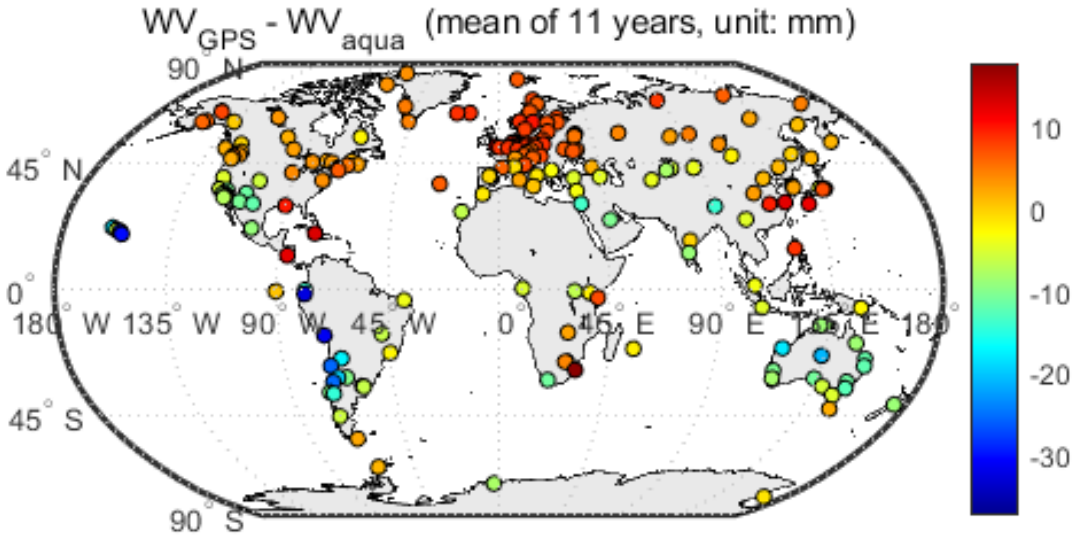


Figure 3. Water vapor differences between GPS and MODIS Aqua

REFERENCES

Parkinson, C. L. 2003. Aqua: An Earth-observing satellite mission to examine water and other climate variables. IEEE Transactions on Geoscience and Remote Sensing, 41(2), 173-183.

Bevis, M., Businger, S., Herring, T. A., Rocken, C., Anthes, R. A., & Ware, R. H. 1992. GPS meteorology: Remote sensing of atmospheric water vapor using the Global Positioning System. Journal of Geophysical Research: Atmospheres, 97(D14), 15787-15801.

Li, Z., Muller, J. P., & Cross, P. 2003. Comparison of precipitable water vapor derived from radiosonde, GPS, and Moderate Resolution Imaging Spectroradiometer measurements. Journal of Geophysical Research: Atmospheres, 108(D20).

19.8

A data platform for monitoring hazardous mass movements in Alpine terrain

Fabian Walter[1], Michaela Wenner[1,2], Emanuele Marchetti[3],
Martin Fengler[4], Elias Hodel[1,2] & Daniel Farinotti[1,2]

[1]*Laboratory of Hydraulics, Hydrology and Glaciology (VAW), ETH Zürich, Hönggerbergring 26, CH-8093 Zürich (walter@vaw.baug.ethz.ch)*
[2]*Swiss Federal Institute for Forest, Snow and Landscape Research WSL, Zürcherstrasse 111, CH-8903 Birmensdorf*
[3]*Dipartimento di Scienze della Terra, UniFI, Via La Pira, 4, I-50121 Firenze*
[4]**Meteomatics AG,** *Lerchenfeldstrasse 3, CH-9014 St. Gallen*

Rapid mass movements, such as rock falls, snow/ice/rock avalanches, debris flows or debris-laden floods constitute severe natural hazards in Alpine terrain. Construction measures can protect roads, settlements and hiking trails from small events, but successful hazard management is increasingly contingent upon rapid detection of ongoing or imminent mass movements. Whereas advanced technologies like Doppler or interferometric radars are capable of detecting precursory acceleration to collapsing rock instabilities, they target small view angles, only. Since gravitational instabilities of mountain faces may threaten entire valleys below, it is necessary to monitor extended areas of Alpine terrain.

Based on elastic wave detection in the air and the ground, it is possible to recognize increased activity before a failure event, and to produce catalogues of mass movements showing their relation to environmental conditions. Nowadays, rapidly advancing drone technology allows acquisition of digital elevation models (DEM's) on demand which can be used to identify fresh and potentially unstable sediment deposits. In addition, weather data can provide important information on heavy precipitation that may trigger avalanches or mobilize sediments. With modern seismological and infrasound monitoring, high-rate DEM time series and increasingly accurate precipitation forecasts, it is therefore possible to fill pivotal observation gaps. This allows us to better understand processes leading to destructive mass movements and help identify or detect specific events.

Unfortunately, none of the mentioned observations in itself is sufficient for monitoring territories prone to mass movements such as debris flow catchments. Seismometers and infrasound sensors may detect even small rock falls over kilometre distances and at sub-second time resolution, yet location and volume estimates are typically inaccurate or even impossible. On the other hand, drone-derived DEM's provide accurate estimates of terrain changes, but they still require the presence of personnel in the field and thus only coarse time series.

Here we present a data platform developed with partners at Swisscom Broadcast (Figure 1), which processes various observation streams pertaining to hazardous mass movements. The platform serves as a visualization tool for incoming seismic, infrasound, weather and drone data. Through state-of-the-art processing of the seismic and infrasound data, dominant noise sources are continuously located. This result then feeds into a detection algorithm. A weather API (Application-Programming-Interface) furthermore yields precipitation estimates on sub-kilometre scale. As the data processing updates results every few tens of seconds, monitoring is practically possible in real-time. Drone-derived DEM's are integrated into the platform and provide volume estimates of mass movements detected with the seismological and infrasound observation.

We have tested the platform at the Illgraben canyon (VS), Switzerland's most active debris flow catchment, producing several events per year (Badoux et al., 2009). Whereas the Swiss Federal Institute for Forest, Snow and Landscape Research (WSL) monitors debris flows at the lower Illgraben reaches with in-torrent sensors, our approach targets the poorly accessible upper catchment (Walter et al., 2017). This region is critical, because mass movements like debris flows initiate here and rapid detection implies extended early warning times. We present the operation of the data platform and discuss to what extent it could serve as a component for early warning operation or hazard management.

REFERENCES

Badoux, A., Graf, C., Rhyner, J., Kuntner, R., & McArdell, B. W. (2009). A debris-flow alarm system for the Alpine Illgraben catchment: design and performance. *Natural hazards*, *49*(3), 517-539.

Walter, F., Burtin, A., McArdell, B. W., Hovius, N., Weder, B., & Turowski, J. M. (2017). Testing seismic amplitude source location for fast debris-flow detection at Illgraben, Switzerland. *Natural Hazards and Earth System Sciences*, *17*(6), 939-955.

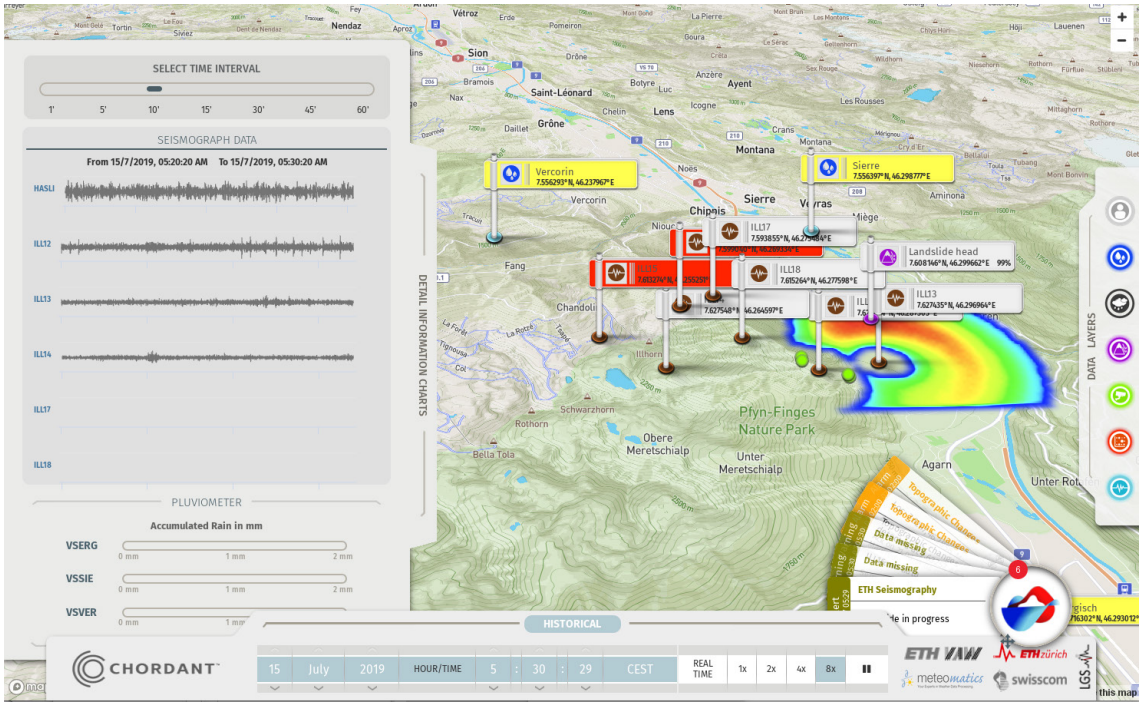


Figure 1. Web application of the data platform monitoring debris flows at Illgraben (VS) developed in collaboration with Swisscom Broadcast. https://www.swisscom.ch/de/business/broadcast.html

P 19.1

Assessing the bedrock surface of overdeepened valleys by 3D gravity modelling

Dimitri Bandou[1], Patrick Schläfli[1], Michael Schwenk[1], Guilhem A. Douillet[1], Edi Kissling[2] & Fritz Schlunegger[1]

[1]Institut für Geologie, Universität Bern, Balzerstrasse 1+3, CH-3012 Bern (dimitri.bandou@geo.unibe.ch)
[2]Institut für Geophysik, ETH Zürich, Sonneggstrasse 5, CH-8092 Zürich

High-resolution information on the topography of landscapes is of prime importance if the scope lies in the specification of the erosional processes.

This also concerns the search for the mechanisms leading to the carving of overdeepened valleys surrounding the European Alps that are now filled with unconsolidated fluvio-lacustrine and glacial sediments.
For some of these valleys within the Alps, the bedrock lies well below sea level today, and in the Alpine foreland, the bedrock lies distinctively below the currently lowest erosional base level such as the river Rhine, for instance. Because of the post-erosional burial of these features, the processes leading to their formation have been contested (Cook and Swift, 2012).

Here, we reconstruct the shape of the buried bedrock surface in the Bern area, the region of confluence of the former Rhone and Aar glaciers.

In this region, the occurrence of overdeepenings, or alternatively tunnel valleys, has already been disclosed locally through drilling (Reber and Schlunegger, 2016).

To achieve our goals, we conduct a high-resolution gravity survey exploiting the density contrast between the bedrock and tunnel valley fill and with densely spaced gravity measurements, adapted to capture the complex regional and residual gravity fields related to the contributions of the Molasse bedrock topography and the Quaternary sediments to this field, respectively. By 3D gravity forward modelling (BGpoly, following Talwani and Ewing, 1960) in combination with the available drill hole information we aim to establish the morphology of the interface between the higher density Molasse bedrock and the lower density Quaternary sediments.

Our first data set consists of several densely spaced gravity profiles across three overdeepened valleys around the city of Bern. This data set will allow us to explore, from a general point of view, the effect of the overdeepening fill on the Bouguer anomaly in the region. We additionally collected gravity data across hills and in quarries that are either underlain by marine or terrestrial Molasse bedrock. This strategy allows us to estimate the in-situ density of the bedrock into which these overdeepenings were carved. The combined data set will be used to constrain a preliminary 3D prismatic model following Nagy (1966) of the bedrock topography underneath the Quaternary cover. The results of this study will guide the strategy for further data collection with the aim to more precisely constrain the bedrock topography model in 3D using BGpoly.

REFERENCES

Cook, S.J., Swift, D.A., 2012: Subglacial basins: Their origin and importance in glacial systems and landscapes.Earth-Science Reviews 115, 332–372.

Nagy, D., 1966: The gravitational attraction of a right rectangular prism. Geophysics, Vol 31, No. 2, 362-371

Reber, R. & Schlunegger, F. 2016: Unravelling the moisture sources of the Alpine glaciers using tunnel valleys as constraints, Terra Nova,Vol 28, No. 3, 202-211

Talwani, M., Ewing, M., 1960: Rapid computation of gravitational attraction of three-dimensional bodies of arbitrary shape. Geophysics 25, 203–225.

P 19.2

4onse: open monitoring system

Massimiliano Cannata[1], Daniele Strigaro[1], Marcus Hoffmann[1], Imran Shahid[2], Rangajeewa Ratnayake[3] & B.H. Sudantha[4]

[1]Institue of earth Sciences, SUPSI, Campus Trevano, CH-6952 Canobbio (massimiliano.cannata@supsi.ch)
[2]Department of Space Science, Institute of Space Technology, Islamabad Highway 1, 44000 Islamabad, Pakistan
[3]Department of Town & Country Planning, University of Moratuwa, Katubedda, Moratuwa, Sri Lanka
[4]Department of Information Technology, University of Moratuwa, Katubedda, Moratuwa, Sri Lanka

The 4onse monitoring system has been designed and developed on the wave of openness, which increasingly pervades not only scientific activity, but also the commercial sectors at different levels. Based on this philosophy, the selected hardware and software technologies have been evaluated in terms of quality, durability and sustainability and are showing very promising results. Unlike conventional systems, where the adoption of closed solutions strongly limits interoperability and data sharing, the designed solution is characterized by a high reproducibility and interoperability, guaranteed by the adoption of open software and standards for the collection and distribution of data. Such a technology can be applied and further developed for monitoring natural and non-natural environments that require low-cost sensor components with a level of quality comparable to conventional systems commonly used. This cost-effective solution is a possible alternative for the implementation of sensor networks in particular in low-income or developing countries in order to manage natural risks or water resources.

The solution consists of three different layers: hardware, server and communication layer. The hardware layer consists of a weather station based on Arduino and sensors measuring environmental variables. This kind of prototype has been validated thanks to the comparison of the time series with the data of an official weather station of the hydro-meteorological network of the Canton Ticino. The second layer is characterized by the server infrastructure that stores the measured data using the istSOS database management system (DBMS), which makes them accessible thanks to the implementation of open standards such as the Sensor Observation Service (SOS) of the Open Geospatial Consortium (OGC). Finally, the communication layer concerns the use of GPRS for the transmission of data from the node to the server that has been optimized in terms of energy and bandwidth consumption in order to guarantee stable and fast communication.
The data are useful for several services like:

- monthly climatic reports available through a dedicated portal (www.zenodo.org) as open data
- a drought monitoring system
- an hydraulic model for the management of water resources and the mitigation of floods due to heavy rain events.

P 19.3

SIMILE, integrated water quality monitoring system

M. Cannata[1], D. Strigaro[1], F. Lepori[1], C. Capelli[1], M. Rogora[2], M.A. Brovelli[3], M. Veronesi[4], D. Magni[5]

[1]University of Applied Sciences and Arts of Southern Switzerland (SUPSI), DACD-IST (massimiliano.cannata@supsi.ch)
[2]IRSA Istituto di Ricerca Sulle Acque, sede di Verbania - VialeTonolli 50 -28922 - Verbania Pallanza (VB)
[3]Politecnico di Milano, Department of Civil and Environmental Engineering, Piazza Leonardo da Vinci, 20133 Milano, Italy
[4]Ufficio della protezione delle acque e dell'approvvigionamento idrico. Via Franco Zorzi 13 6501 Bellinzona.
[5]Direzione Generale Ambiente Energia e Sviluppo Sostenibile (DG AESS) UO Risorse Idriche. Regione Lombardia, Piazza Città di Lombardia 1 - 20124 Milano

Lakes are an invaluable natural and economic resource for the insubric area, identified as the geographical area between the Po River (Lombardy, Italy) and the Monte Ceneri (Ticino, Switzerland). Due to a recognized increased anthropic activity and climate change impacts these precious resource need to be adequately protected. To this end, universities and administrations of the two regions that share the transboundary lakes, started a project name SIMILE whose goal is to provide updated and continuous information to support the management of the lakes. This project is based on long term collaboration actions that the two countries, Switzerland and Italy, have with the CIPAIS commission (http://www.cipais.org/) and aims at introducing innovative information system based on the combination of advanced automatic and continuous observation sensing, high resolution remote sensing data processing, citizen science and ecological and physical models. The project will capitalize the knowledge and experience of the resource managers with the creation of a Bussiness Intelligence platform based on several interoperable geospatial Web services. The use of Open software and data will facilitate its adoption and will contribute to adequately keep the costs limited. The project, started few months ago is here presented and discussed.

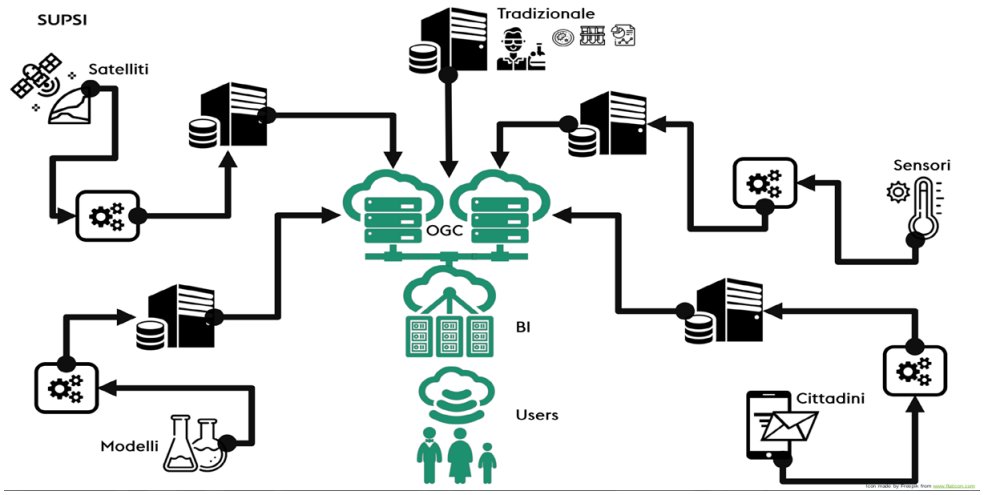


Figure 1. Gebneral architecture of the SIMILE Information System.

P 19.4

Guided Super-Resolution of Environmental Maps

Riccardo de Lutio, Stefano D'Aronco, Jan Dirk Wegner, Konrad Schindler

EcoVision Lab, Photogrammetry and Remote Sensing, ETH Zürich

Environmental mapping often requires extensive and expensive field work, the resolution that can be achieved for these maps is significantly lower than the ground sampling distance of modern earth observation satellites.

Guided super-resolution is a unifying framework for several computer vision tasks where the inputs are a low-resolution **source image** of some target quantity - e.g., a vegetation height map - and a high-resolution **guide image** from a different domain - e.g., a multispectral Sentinel-2 image; and the target output is a high-resolution version of the source, in our example a high-res vegetation height map (note that the sensing principle of several airborne and spaceborne imaging sensors can also be seen as guided super-resolution, where a high-resolution panchromatic channel is fused with colour channels recorded at lower resolution).

The standard way of looking at this problem is to formulate it as a super-resolution task, i.e., the source image is upsampled to the target resolution, while transferring the missing high-frequency details from the guide. Here, we propose to turn that interpretation on its head and instead see it as a pixel-to-pixel mapping of the guide image to the domain of the source image. The pixel-wise mapping is parametrised as a multi-layer perceptron, whose weights are learned by minimising the discrepancies between the source image and the downsampled target image. Importantly, our formulation makes it possible to regularise only the mapping function, while avoiding regularisation of the outputs; thus producing crisp, natural-looking images. The proposed method is unsupervised, using only the specific source and guide images to fit the mapping.

We evaluate our method by super-resolving tree height maps for Switzerland (Ginzler & Hobi 2015). We clearly outperform recent baselines in quantitative comparisons, while delivering visually much sharper outputs. We also show promising preliminary results for the task of creating dense nation-wide maps of biodiversity measures for Switzerland (BDM).

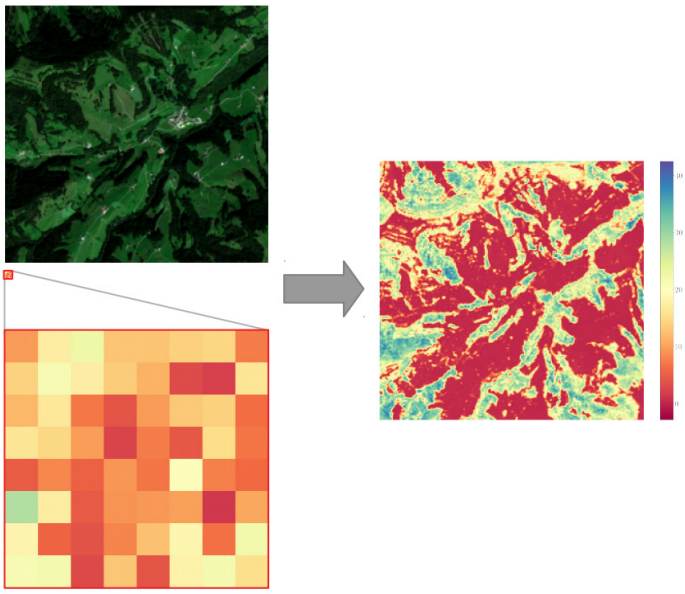


Figure 1. Guided super-resolution: given a low-resolution VHM and a high-resolution guide image, our method predicts a high-resolution VHM. The figure shows an example output of the proposed method, for an upsampling factor of 32X.

REFERENCES

de Lutio, R., D'Aronco, S., Wegner, J. D. & Schindler, K. : Guided super-resolution as pixel-to-pixel transformation, International Conference on Computer Vision (ICCV), 2019.

Ginzler, C. & Hobi, M. L. : Country-wide stereo-image matching for updating digital surface models in the framework of the Swiss National Forest Inventory, Remote Sensing, 2015.

Biodiversity Monitoring Switzerland (BDM) : data and findings up to 2018, http://www.biodiversitymonitoring.ch/en/home.html.

P 19.5

Multi-point Dam Displacement Prediction Based on a Clustering Method

Yating Hu[1,2,3], Chongshi Gu[1,2], Chenfei Shao[1,2], Zhenzhu Meng[3]

[1]College of Water Conservancy and Hydropower Engineering, Hohai University, 210098 Nanjing, China
[2]National Engineering Research Center of Water Resources Efficient Utilization and Engineering Safety, 210098 Nanjing, China
[3]Laboratory of Environmental Hydraulics, École Polytechnique Fédérale de Lausanne, 1015 Lausanne, Switzerland (yating.hu@epfl.ch)

Displacement data modelling is of great importance for the safety control of concrete dams. The commonly used artificial intelligence method modelled the displacement data at each monitoring point individually, i.e., the data correlations between the monitoring points are overlooked, which leads to the over-fitting problem and the limitations in the generalization of model. A novel model combines Gaussian mixture model and Iterative self-organizing data analysing (ISODATA-GMM) clustering and the random coefficient method is proposed in this article, which takes the temporal-spatial correlation among the monitoring points into account. By taking the temporal-spatial correlation among the monitoring points into account and building models for all the points simultaneously, the random coefficient model improves the generalization ability of the model through reducing the number of free model variables. Since the random coefficient model supposed the data follows normal distributions, we use an ISODATA-GMM clustering algorithm to classify the measuring points into several groups according to its temporal and spatial characteristics, so that each group follows one distribution. Our model has the advantage of having a stronger generalization ability.

REFERENCES

Hu, Y., Shao, C., Gu, C. and Meng, Z., 2019. Concrete Dam Displacement Prediction Based on an ISODATA-GMM Clustering and Random Coefficient Model. Water, 11(4), p.714.

Shao, C.; Gu, C.; Yang, M.; Xu, Y.; Su, H. A novel model of dam displacement based on panel data. Struct. Control Health Monit. 2018, 25, e2037.

Mata, J.; Tavares de Castro, A.; Sá da Costa, J. Constructing statistical models for arch dam deformation. Struct. Control Health Monit. 2014, 21, 423–437.

P 19.6

Visual KARSYS, a web-tool for modelling karst aquifers in 3D

Arnauld Malard[1], Stephen Randles[3], Philipp Hausmann[3], Pierre-Yves Jeannin1, Manfred Vogel[3], Simon Lopez[2], Gabriel Courrioux[2]

[1] SISKA, Swiss Institute for Speleology and Karst Studies, rue de la Serre 68 – CH2300 La Chaux-de-Fonds
[2] BRGM, 3 avenue Claude-Guillemin, 45000 Orléans
[3] i4ds Institute of 4D Technologies, Fachhochschule Nordwestschweiz, Bahnhofstrasse 6, CH5210 Windisch

Visual KARSYS is a web-tool available at www.visualkarsys.com. It has been developed to address modelers and end-users working for the documentation and/or the management of geology and groundwater resources in karst areas. It makes possible for modelers to setup projects, to entry geol. and hydrogeol. data and to design geological 3D model in order to subsequently apply the KARSYS approach On one side, Visual KARSYS offers an intuitive interface in which modelers are guided through the steps of the approach. On the other side, Visual KARSYS offers a dedicated output page for end-users which displays formatted data and resulting models built by modelers. Editing and reading permissions can be allotted by the project administrator to different users (both modelers and end-users). End users can arrange data and results as they want (form, layout, views, etc.) and different analysis tools are at their disposal (slicer, drawing tool, etc.). They can export different data or print maps.

Visual KARSYS is actually free-of-use and we encourage users to use it.

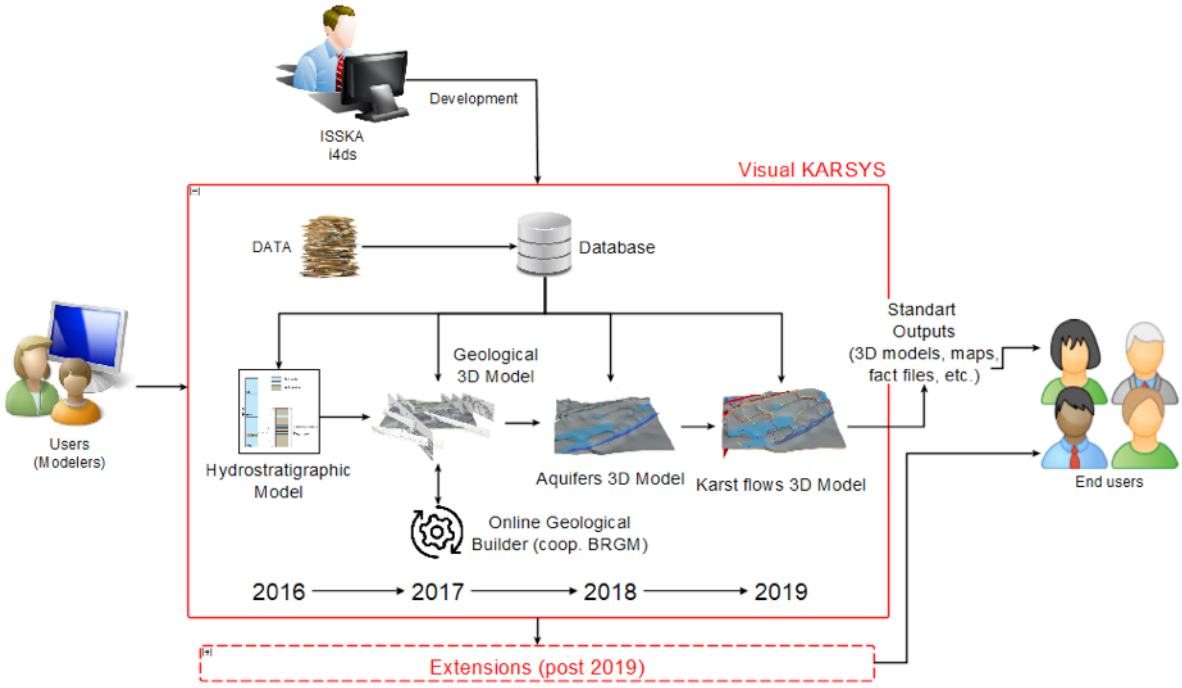


Fig. 1 the four basic steps of Visual KARSYS allow modelers to build 3D aquifer models online which can be seen and exploited by end-users. By the end of 2019, Visual KARSYS is ready for use. Nevertheless, additional extensions may be envisaged for the coming years.

The Visual KARSYS project is supported by the Swiss Federal Office for Environment via the grant for the promotion of environmental technology (2016-2019, UTF 537.13.16).

REFERENCES

Jeannin PY, Eichenberger U, Sinreich M, Vouillamoz J, Malard A et al. (2013) KARSYS: a pragmatic approach to karst hydrogeological system conceptualisation. Assessment of groundwater reserves and resources in Switzerland. Environmental Earth Sciences, 69(3): 999-1013 p.

20. Taking stock of transformative research and education on mountains. What future avenues?

Emmanuel Reynard, Iago Otero, Carolina Adler, Jörg Balsiger

Interdisciplinary Centre for Mountain Research
Forum Landscape, Alps, Parks (FOLAP)
Mountain Research Initiative

TALKS:

20.1 Chapman M., Deplazes Zemp A., Backhaus N.: Donkeys, Deer, and Death around the Swiss National Park: Developing a relational values approach to align environmental values in sustainable development

20.2 Deisenrieder V., Müller S., Knoflach B., Keller L., Geitner C., Stötter H.: Complexity in minds – young peoples pre-concepts about interactions of climate change in High Alpine Mountains spheres

20.3 Jurt C., Bermudez M., L., Adler C., Muñoz V., L., Ticona P., W., Häberli I., Borquez R.: Knowledge flows and co-production of knowledge: rural climate change adaptation of populations near glaciers in Peru and Switzerland

20.4 Otero I.: Wildfire and transformation. Shedding light on the challenges of transformative research in mountains through wildfires

POSTERS:

P 20.1 Bhattacharya S.: Socio-ecological and environmental survey of a cinchona plantation village situated in the Eastern Himalayas, India: Ecotourism and sustainable development perspectives

P 20.2 Galán E., Garmendia E., Andonegi A., Aldezabal A., Barron L.J., del Prado A., Gamboa G., Garcia O., Pardo G.: Integration of ecological, socio-economic and food quality indicators of extensive sheep grazing systems in mountain marginal lands the case of Cantabrian Mountain Range (Northern Spain)

P 20.3 Kronenberg M., Barandun M., Imanalieva P., Naegeli K., Weber H., Tovmasyan K.: Empowering you women from Central Asia on glaciers: A new scientific communications program

P 20.4 Otero I., Reynard E., Darbellay F.: Transformative interdisciplinary research on mountains. The role of serendipity

P 20.5 Peduzzi D., Schrot O., Keller L., Stötter J.: Towards transformation: on the path between climate change challenges, resilience and sustainable development.

20.1

Donkeys, Deer, and Death around the Swiss National Park: Developing a relational values approach to align environmental values in sustainable development

Mollie Chapman[1,2], Anna Deplazes Zemp[1,3], Norman Backhaus[1,2]

[1]University Research Priority Program on Global Change and Biodiversity, University of Zurich, Winterthurerstr. 190, CH-8057 Zurich (mollie.chapman@geo.uzh.ch)
[2]Department of Geography, University of Zurich, Winterthurerstr. 190, CH-8057 Zurich 3Ethics Research Institute, University of Zurich, Zollikerstrasse 117, CH-8008 Zurich

Environmental values are important for many sustainable development and transformation contexts in mountain regions—particularly in participatory decision making (Fish, 2011; see Gregory, Failing, Harstone, Long, & McDaniels, 2012) or ecosystem services assessments (Millennium Ecosystem Assessment, 2003) and implicitly in policies and programs for sustainable development (O›Neill, Holland, & Light, 2008; West, 2006). When values are included in sustainable development efforts, usually one of two approaches is used: instrumental values focus on the benefits from nature for people whereas intrinsic values reflect the idea of nature's value for its own sake.

Yet neither of these approaches effectively captures a wide range of values that motivate many people to care for land, ecosystems and species. For many people, relationships with nature and with other people via nature better characterize how they value and view their biophysical environment. This research project seeks to elaborate a relational values approach to sustainable development with a focus on Swiss alpine agro-ecosystems. Relational values include values such as stewardship and care, kinship and connection towards nature, concepts such as 'eudaemonia' which refers to living a good life in harmony with nature, as well as values around responsibility towards nature (Chan et al., 2016).

Interviews with farmers in the vicinity of the Swiss National Park along with philosophical analysis serve to elaborate an approach to relational values and develop the conceptual foundations of this emerging research area. We present preliminary results from 32 interviews conducted in March 2019 with farmers in Val Müstair and the Lower Engadine. We also discuss the broader implications of a relational values approach for transformative research and education, in particular in agricultural mountain landscapes.

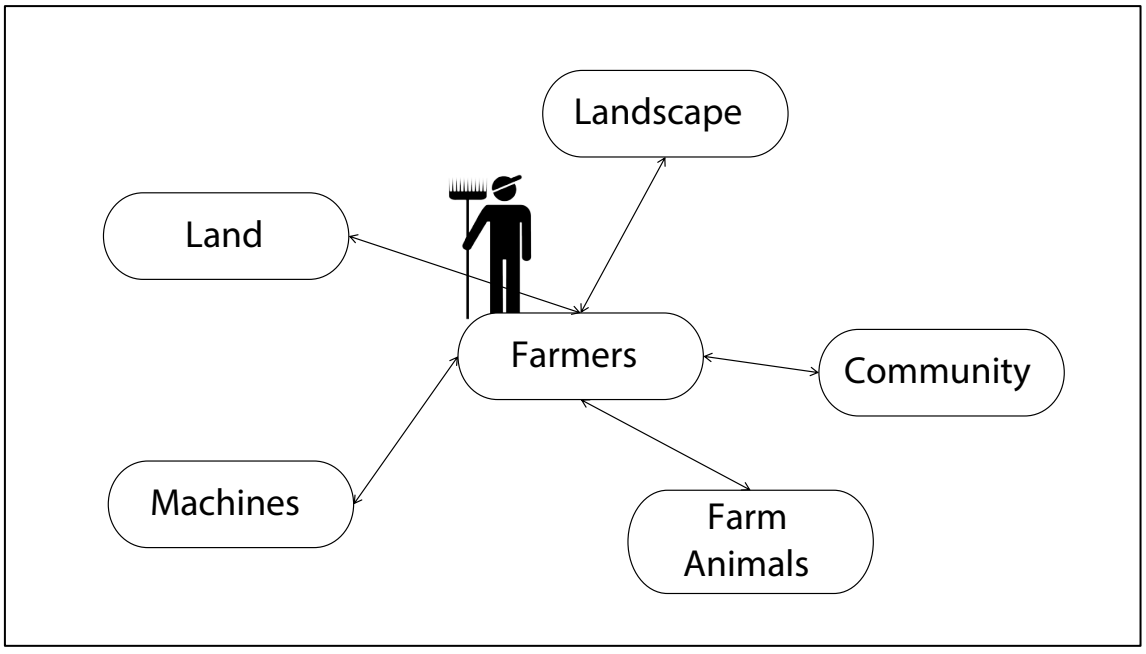


Figure 1. Relationships and Relational Values of Farmers (examples)
Farmers relate to different types of entities in their environment, such as those shown in the figure above. Qualitative interviews with farmers involved a dialogue and conversation guided by the researcher that provides participants with the opportunity to express and reflect upon their valued relationships and examine the limits and motivations for these values.

REFERENCES

Chan, K. M. A., Balvanera, P., Benessaiah, K., Chapman, M., Díaz, S., Gómez-Baggethun, E., et al. (2016). Opinion: Why protect nature? Rethinking values and the environment. *Proc Natl Acad Sci*, *113*(6), 1462–1465. http://doi.org/10.1073/pnas.1525002113

Fish, R. (2011). Environmental decision making and an ecosystems approach: Some challenges from the perspective of social science. *Progress in Physical Geography*, *35*(5), 671–680. http://doi.org/10.1177/0309133311420941

Gregory, R. S., Failing, L., Harstone, M., Long, G., & McDaniels, T. (2012). Structured decision making: a practical guide to environmental management choices. John Wiley & Sons.

Millennium Ecosystem Assessment. (2003). Ecosystems and Human Well-being: A Framework for Assessment. Washington, DC: Island Press.

O'Neill, J., Holland, A., & Light, A. (2008). Environmental Values. Routledge.

West, P. (2006). Conservation is Our Government Now: The Politics of Ecology in Papua New Guinea. *New Ecologies for the Twenty-First Century*. Durham, NC: Duke University Press.

20.2

Complexity in minds – young peoples' pre-concepts about interactions of climate change in High Alpine Mountains spheres

Veronika Deisenrieder[1], Svenja Müller[1], Bettina Knoflach[1], Lars Keller[1], Clemens Geitner[1], Hans Stötter[1]

[1]Department of Geography, University of Innsbruck, Innrain 52f, A-6020 Innsbruck (Veronika.Deisenrieder@uibk.ac.at)

The complex interactions of climate change on different spheres in the High Alpine Mountains with their temporal and spatial delays as well as secondary and feedback effects present great challenges for learners (McNeal et al., 2014). As transformative knowledge about tackling climate change and its consequences ought not to be generated by natural science studies alone, transdisciplinary science-society interactions are required. With today's generation of children and youths who will be confronted by the effects of climate change during their entire lifetime, access to comprehensive interdisciplinar system knowledge is facilitated by a planned research-education cooperation. By applying the scientific learning format of the long-lasting Austrian climate education initiative of *k.l.d.Z.21 – competent into the future* (Keller et al., 2019), an increase of climate change awareness of 14-year old high-school students from Austria and Germany has already been scientifically proven (Kuthe et al., 2019). As an innovative High Alpine research area, Kauner Valley located in the eastern central Alps will be opened up in which students will do their inquiry-based research with the help of visible climate change indicators on soil, permafrost, vegetation and geomorphology at the end of a school year. For providing an effective learning intervention, this paper examines pre-concepts of 350 high school students regarding the effects of climate change on the High Alpine Mountain cryosphere and pedosphere at the beginning of the school year of 2019/2020. Aiming at fostering conceptual change by a transdisciplinary, moderate constructivist learning intervention, in particular replacement, differentiation, coalescence and assimilation (Carey, 1985 &, Krüger, 2007) of pre- and misconceptions regarding the effects of climate change on cryosphere, pedosphere and adjacent fields, like vegetation and geomorphology, will be analysed during an overall time period of three years (Heckmann & Morche, 2019; Moscatelli et al., 2017; Puissant et al., 2017; Zollinger et al., 2015).

By a mixed-method approach, containing an online survey with qualitative and quantitative questions which is further complemented by conceptual maps (Sellmann, Liefländer, & Bogner, 2015), the learning intervention will be analyzed before and after a school year by MaxQData and by IBM SPSS Statistics. Based on these results, the learning settings will be further adapted and developed for enabling transformative climate change education programmes in High Alpine Mountains.

REFERENCES

Carey, S. (1985): Conceptual Change in Childhood (MIT Press series ikn learning, development and conceptual change). Cambridge

Heckmann, T., & Morche, D. (2019). Geomorphology of Proglacial Systems. Cham: Springer International Publishing. https://doi.org/10.1007/978-3-319-94184-4

Keller, L., Stötter, J., Oberrauch, A., Kuthe, A., Körfgen, A., & Hüfner, K. (2019). Changing Climate Change Education: Exploring moderate constructivist and transdisciplinary approaches through the research-education co-operation k.i.d.Z.21. GAIA - Ecological Perspectives for Science and Society, 28(1), 35–43. https://doi.org/10.14512/gaia.28.1.10

Krüger, D. (2007): Die Conceptual-Change Theorie. In D. Krüger, H. Vogt (Eds.): Theorien in der biologiedidaktischen Forschung. Berlin, New York, pp. 81-92.

Kuthe, Alina; Körfgen, Annemarie; Stötter, Johann; Keller, Lars (2019): Strengthening their climate change literacy: A case study addressing the weaknesses in young people's climate change awareness. In: Applied Environmental Education & Communication 47 (2), S. 1–14. DOI: 10.1080/1533015X.2019.1597661

McNeal, K. S., Libarkin, J. C., Ledley, T. S., Bardar, E., Haddad, N., Ellins, K., & Dutta, S. (2014). The Role of Research in Online Curriculum Development: The Case of EarthLabs Climate Change and Earth System Modules. Journal of Geoscience Education, 62(4), 560–577. https://doi.org/10.5408/13-060.1

Moscatelli, M. C., Bonifacio, E., Chiti, T., Cudlín, P., Dinca, L.,

Puissant, J., Mills, R. T. E., Robroek, B. J. M., Gavazov, K., Perrette, Y., Danieli, S. de, . . . Cécillon, L. (2017). Climate change effects on the stability and chemistry of soil organic carbon pools in a subalpine grassland. Biogeochemistry, 132(1-2), 123–139. https://doi.org/10.1007/s10533-016-0291-8

Sellmann, D., Liefländer, A. K., & Bogner, F. X. (2015). Concept Maps in the Classroom: A New Approach to Reveal Students' Conceptual Change. The Journal of Educational Research, 108(3), 250–257. https://doi.org/10.1080/00220671.2014.896315

Zollinger, B., Alewell, C., Kneisel, C., Meusburger, K., Brandová, D., Kubik, P., . . . Egli, M. (2015). The effect of permafrost on time-split soil erosion using radionuclides (137Cs, 239 + 240Pu, meteoric 10Be) and stable isotopes (δ 13C) in the eastern Swiss Alps. Journal of Soils and Sediments, 15(6), 1400–1419. https://doi.org/10.1007/s11368-014-0881-9

20.3

Knowledge flows and co-production of knowledge: rural climate change adaptation of populations near glaciers in Peru and Switzerland

Christine Jurt[1,2], Luis Mujica Bermudez[3], Carolina Adler[4], Luis Vicuña Muñoz[2], William Pino Ticona[5], Isabel Häberli[1], Roxana Borquez[6]

[1]Bern University of Applied Sciences – HAFL, Länggasse 85, 3052 Zollikofen, Schweiz (christine.jurt@bfh.ch)
[2]University of Zurich, Department of Geography, Winterthurerstrasse 190, 8057 Zurich, SChweiz
[3]Pontificia Universidad Católica del Perú, 1801 Universitaria Avenue, San Miguel, Lima 32, Peru
[4]Mountain Research Initiative, Mittelstrasse 43, 3012 Bern, Switzerland
[5]Universidad Nacional de San Antonio Abdad del Cusco, Avenida de La Cultura 773, Cusco 08000, Peru
[6]Kings College, Strand, London WC2R 2LS, United Kingdom

Measures to address climate change adaptation respond to multiple and diverse knowledge demands. However, the types of knowledge that are considered relevant, and how these transform as they flow from source to users, are less understood in context. A project was designed and implemented to identify and clarify the diverse types of knowledge, including information, that are considered as relevant by different actors in a given rural mountain context, as basis for responding to climate change and that transformations that ensue in social-ecological context such as communities in mountains. Through this project, a process to first analyse the flow of knowledge and information from its source, to how it is accessed, understood, valued, and ultimately used, was designed and elaborated. This is important to understand and address as a key condition for improving the co-production of knowledge that is relevant and amenable to the context, given the imperatives to ensure successful and effective adaptation through implementation. These analyses as crucial input for the elaboration of proposed future projects. For the design process, a focus on rural mountain communities living near glaciers, given the current trends surrounding risks from glacial retreat. Following the principles of transdisciplinary research in a transboundary context, it was deemed important to intensify an existing productive collaboration between partners from Peru and Switzerland in this project, and establish a working foundation from which to extend a collaboration also with partners from other mountain regions in the Andean countries such as e.g. Bolivia, Chile or Ecuador as part of a proposed future project. In this presentation, I focus on presenting the results achieved with the whole research team and partners consortium, and engage with the symposium participants to invite feedback.

20.4

Wildfire and transformation. Shedding light on the challenges of transformative research in mountains through wildfires

Iago Otero[1]

[1]*Interdisciplinary Centre for Mountain Research, University of Lausanne, Case postale 4176, CH-1950 Sion 4 (iago.otero@unil.ch)*

As stated in the symposium description, key interdependencies and complexities of environmental problems have not been sufficiently accounted for to fully explore the solutions space in transformative research. In this paper we use wildfires to shed light on this question. Wildfires are treated as empirical phenomena which analysis facilitates a synthetic diagnosis of the key social-ecological links underlying the unsustainability of mountain regions, as well as an attractive entry point for both researchers and practitioners to better grasp the solution space.

My contribution is based on two interrelated research types conducted in the Spanish region of Catalonia during the last years: 1) Analysis of social-ecological relationships and processes underlying wildfire risk through qualitative research (Otero & Nielsen, 2017), and 2) Analysis of my (and my colleagues) attempts to change those relationships and processes through action-research interventions (Otero et al., 2018).

In Catalonia, changing land-uses and settlement patterns (rural outmigration, land abandonment and urbanisation) and a warmer climate have resulted in a very fragile social-ecological system concerning wildfires. After the large wildfires of the 1980s and 1990s, a reconfiguration of the wildfire management system was enacted by the regional government based on a reduction of fires starting and a rapid response with water from fire engines and aerial means. In the late 1990s a group of wildfire fighting specialists was created in the Fire Department that incorporated the use of fire as a prevention and suppression technique and that emphasized the need to understand wildfires as an inherent part of Mediterranean mountains. According to our analysis, the consolidation of this group highlights how learning to coexist with wildfire in Catalonia has triggered a set of transformative processes in institutional arrangements and power relationships of both the wildfire management system and forested mountain ranges. Our data also illustrate why and how coexisting with wildfire under a changing climate entails a dramatic and still incomplete social-ecological transformation in terms of land-uses, settlement patterns, energy supply systems and social values about nature. Efforts so far are unable to reverse the general historical trajectories underlying risk (urbanization and forest transition). Data suggests that in the absence of such systemic changes, management improvements might reinforce risk.

Through several action-research projects co-designed with wildfire managers and other stakeholders, we have tried to intervene in this context in order to transform its main social-ecological relationships and processes underlying risk. In particular, we have focused on the development of participatory planning networks composed of scientists, decision-makers and citizens across governance scales to build resilient landscapes and communities. Our method combined expert knowledge on wildfire regime, participatory co-valuation of landscape, and deliberation about alternative policy options. Integrating the data on landscape values into the wildfire models of the Fire Department allowed us to identify strategic areas where preventive interventions would minimize the loss of social values. In turn, sessions facilitated a debate about transformative measures and policies to reduce wildfire risk down to acceptable levels. Our action-research shows that these networks have the potential to build resilient landscapes by reducing the fuel continuity of mountain ranges, re-defining agency over landscape and fostering re-learning on fire among community members. We identified several challenges that would need to be tackled if the transformative potential of these endeavours is to be maximized: the difficulty of implementing the preventive interventions once the project finishes, institutional and funding obstacles to long-term engagement in trans-disciplinary research projects, and a trade-off between high wildfire risk and democratic management resulting from the current social-ecological setup. Our experience reveals the that legitimacy and conflict management within wildfire planning networks may have a key role to enhance their transformative potential in mountain regions and beyond.

In conclusion, wildfire (social-ecological) studies are well suited to inform research on and for the transformation of mountain regions. First, they facilitate a shift in analytical focus: from managerial improvements (technical knowledge) to the conditions for and implications of their effective implementation (transformative knowledge), including potential side-effects of “solutions”. Second, they show how interventions to accelerate transformations can benefit from such an analysis, as well as some of the challenges ahead. Finally, they suggest that one priority avenue for transformative research in mountains should be the identification of research objects that facilitate synthetic approaches. In the face of pressing environmental problems, such objects could help us to rapidly integrate apparently contrary disciplines and guide us in the acquisition of transformative knowledge.

REFERENCES

Otero, I., Castellnou, M., González, I., Arilla, E., Castell, L., Castellví, J., Sánchez, F., Nielsen, J.Ø. 2018: Democratizing wildfire strategies. Do you realize what it means? Insights from a participatory process in the Montseny region (Catalonia, Spain). PLOS ONE 13, e0204806.

Otero, I. & Nielsen, J.Ø. 2017: Coexisting with wildfire? Achievements and challenges for a radical social-ecological transformation in Catalonia (Spain). Geoforum 85, 234–246.

P 20.1

Socio-ecological and environmental survey of a cinchona plantation village situated in the Eastern Himalayas, India: Ecotourism and sustainable development perspectives

Sayan Bhattacharya[1]

[1]*School of Ecology and Environment Studies, Nalanda University, Bihar, India*
(sbhattacharya@nalandauniv.edu.in, sayan.evs@gmail.com)

The Eastern Himalayas in India demonstrate diverse ecological characters in its varied range of flora and fauna. The local communities also form an integral part of the ecological landscape; deriving various services from the forest and mountain ecosystems. Many scattered hamlets are found in this zone and some of them are proximate to the forests enriched with endemic biodiversity. *Wholesale* (27°1'59" N, 88°51'45"E) is a small village situated in *Kalimpong* district, India and is proximate to *Neora Valley National Park* and *Gorumara National Park* in the Eastern Himalayas. The village has 98 houses with a total population of 451 individuals. *Wholesale* village has extensive coverage of *Cinchona* plantation and is a part of *Dalagaon* division of *Rongo* cinchona plantation in West Bengal, established in 1938. A detail survey of the village was done in April, 2019 to explore the socio-environmental and socio-ecological dynamics of the landscape. Structured questionnaires and semi-structured interviews supplemented by field notes were arranged to collect data from the village. There was particular focus on agriculture, livestock management, traditional water management, waste management, disaster management, biodiversity and ecosystem services. The development of ecotourism was analysed through the number of homestays, modes of communication and promotion, tourist inflow data and ecotourism activities (trekking, bird watching, camping, rafting, cultural visits etc.). Biodiversity of the region was documented by visiting the forest areas in *Neora Valley National Park* and *Gorumara National Park*; possible threats to biodiversity were documented. Management strategies were suggested for conservation of forest biodiversity and sustainable development of the village areas. Coexistence of ecotourism and conservation measures can have significant impact on the sustainable development in the transboundary Himalayan landscapes. Detailed study is needed in the Eastern Himalayan villages to explore the socio-ecological dynamics in the context of climate change.

REFERENCES

Bhattacharya, S., De, S., Shome, A., & Dutta, A. 2019: Socio-environmental survey of a forest hamlet proximate to *Neora Valley* National Park in the Eastern Himalayas, India, Indonesian Journal of Environmental Management and Sustainability, 3, 1-13.

P 20.2

Integration of ecological, socio-economic and food quality indicators of extensive sheep grazing systems in mountain marginal lands the case of Cantabrian Mountain Range (Northern Spain)

Galán, E[2°]., Garmendia, E[1,2°]., Andonegi, A[2, 3]., Aldezabal, A[3]., Barron, L.J[4]., del Prado, A[2]., Gamboa, G. Garcia, O[1]., Pardo, G[2].

[1]Department of Applied Economics-I, University of the Basque Country, UPV/EHU, Gasteiz, Basque Country, Spain.
[2]Basque Centre for Climate Change (BC3), 48940 Leioa, Basque Country, Spain.
[3]Department of Plant Biology and Ecology, Faculty of Science and Technology, University of the Basque Country, UPV/EHU, 48940 Leioa, Basque Country, Spain.
[4]Lactiker Research Group, Faculty of Pharmacy, University of the Basque Country UPV/EHU, Paseo de la Universidad 7, 01006 Vitoria-Gasteiz, Spain
°eneko.garmendia@ehu.eus; elena.galan@bc3research.org

Rural landscapes are facing numerous transformations under the influence of competing global markets, new policies (e.g. the Common Agriculture Policy in Europe), industrialization of the food industry and changing lifestyles, among others. The consequences of these changes are remarkable in mountain areas where extensive sheep grazing systems, developed since ancient times, are at risk. In this context, it becomes critical to assess the ecological, economic and nutritional benefits of these systems in order to ensure their sustainability. Based in a research experience developed over the last 15 years in a mountain area in the Cantabrian Mountain Range (Northern Spain), this article assesses the contribution of mountain sheep grazing in socio-economic, ecological and nutritional terms. With this purpose, we develop an integrated evaluation that combines ecological, socio-economic and food quality indicators. The study shows that in addition to the benefits associated with the production of healthy and high quality food; these systems contribute to biodiversity conservation and rural development, through the generation of employment and income, in mountain marginal lands with low productivity and few economic alternatives. Urgent measures are needed to maintain these benefits and associated socio-cultural values. In addition to the effort of integrating disciplines that work at different scales and narratives, we would like to open the debate on how to include the transformative research approach to our agenda.

P 20.3

Empowering you women from Central Asia on glaciers: A new scientific communications program

Marlene Kronenberg[1,2], Martina Barandun[1,2], Perizat Imanalieva[3], Kathrin Naegeli[4,2], Helga Weber[4], Kristine Tovmasyan[5]

[1]Departement of Geosciences, University of Fribourg, Chemin de Musée 4, CH-1700 Fribourg (marlene.kronenberg@unifr.ch, centralasia@girlsonice.org)
[2]Laboratory of Environmental Chemistry, Paul Scherrer Institute, CH-5232 Villigen
[3]Central Asian Institute for Applied Geosciences, KG-720027 Bishkek
[4]Oeschger Centre for Climate Change Research and Institute of Geography, University of Bern, CH-3012 Bern
[5]UNESCO Almaty office, KZ- 050040 Almaty

“Adventure of science: Women and glaciers in Central Asia” is a program which takes young Central Asian women from diverse backgrounds to an expedition in an alpine environment. The instructor team consists of female scientists and a female mountain guide. During the program, the participants (i) get an introduction into glaciology, cryospheric sciences and environmental change; (ii) they acquire mountaineering and wilderness camping skills; (iii) their observational and critical thinking competences are fostered; and (iv) tailored specific activities provide an introduction into scientific methods. The expedition is surrounded by pre- and post-course events, where the experiences gained by the participants are discussed with a wider public. A further aim of the project is to build up a regional network of female scientists and professionals working in domains affected by climate change.

The idea of the program is based on the “Girls on Ice” (i.e. “Girls on Ice Switzerland”) programs coordinated by “Inspiring Girls Expeditions” (IGE 2019). The basic teaching concepts such as inquiry-based teaching and experimential learning are adopted therefrom. The programs combine science, art and mountaineering subjects. A central course element are scientific projects, which are planned and realised as a team work by participants and supervised by the instructors. The new program is addressed to young adults whereas “Girls on Ice” participants are teenage girls. Therefore, “Adventure of Science: Women and glaciers in Central Asia” includes capacity building components. Whereas “Girls on Ice” mainly aims on the personal development of the participants, “Adventure of science: Women and glaciers in Central Asia” not only aims on making young women more self-confident to proceed a career in male dominated domains, but also envisages to grow a network of young women across national borders.

Participants from different countries in a region prone to conflicts (Tashtemkhanova, 2015) grow together as an expedition team and events organised within the project gather women from different countries to provide platforms of exchange. The program focus on glaciology and the hands-on research project rises the participants’ awareness of the relevance of in-situ data. The project also aims on an institutional impact by highlighting the ongoing changes in mountain environments and the necessity of cryospheric data. Furthermore, local institutions are encouraged to include young female scientists and students into academic activities and research. For the first two years “Adventure of science: Women and glaciers in Central Asia” is organised within the project CICADA financed by the Department of Geosciences of the University of Fribourg and the Swiss Agency for Development and Cooperation in close collaboration with the UNESCO Office in Almaty and local institutions. From the beginning, local women from the different target countries have been part of the organisational and instructor team. A stepwise handover of the program to only local instructors is aimed on.

REFERENCES

IGE 2019, www.inspiringgirls.org.

Tashtemkhanova, R., Medeubayeva, Z. , Serikbayeva, A. & Igimbayeva, M., 2015. Territorial and Border Issues in Central Asia: Analysis of the Reasons, Current State and Perspectives. Anthropologist 22(3), 518–25.

P 20.4

Transformative interdisciplinary research on mountains. The role of serendipity

Iago Otero[1], Emmanuel Reynard[1,2] & Frédéric Darbellay[3]

[1]Interdisciplinary Centre for Mountain Research, University of Lausanne, Case postale 4176, CH-1950 Sion 4 (iago.otero@unil.ch)
[2]Institute of Geography and Sustainability, University of Lausanne, Géopolis, CH – 1015 Lausanne
[3]Inter- and Transdisciplinarity Unit, Center for Children's Rights Studies, University of Geneva (Valais Campus), CH - 1950 Sion

The complexity and urgency of the environmental crisis have triggered calls for research that transcends disciplinary boundaries and that effectively responds to societal challenges since decades. Such a call is prominent in mountain studies, where this kind of research is supposed to play a key role in the transformation of mountain regions towards sustainability. Deeper knowledge of inter- and transdisciplinary research processes on mountains is thus crucial to better understand the prospects and priority avenues for transformative research.

In this paper we explore this topic by drawing on the first year of activities of the Interdisciplinary Center for Mountain Research (ICMR) of the University of Lausanne. The ICMR was created in September 2018 with the goal of promoting interdisciplinary research to contribute to the sustainable development of mountain regions. Our goal is to shed light on the interdisciplinary research processes underway at ICMR and the role that mountains as research objects play in such processes. We are likewise interested in exploring the potential contribution of such processes to the transformation of both mountain regions and researchers. Our methods are based on 1) a series of internal workshops with ICMR members where the goal was to advance interdisciplinary work, and 2) qualitative content analysis of interviews with ICMR researchers and notes from participant observation in workshops. We focus on key aspects that according to the literature on inter- and transdisciplinarity are relevant to diagnose research prospects and thus transformation avenues: researchers' motivations, types of interactions between disciplines, modes of interaction with stakeholders, challenges, learning processes, and leverages for successful work. In addition, we pay attention to serendipity (accidental discovery of things), a crucial element of scientific discovery which has nevertheless received little attention in the literature on interdisciplinarity and transformative research.

Our results show that motivations to engage in interdisciplinary projects ranged from a need to respond to fundamental (disciplinary) research questions to solving concrete societal problems in collaboration with stakeholders. ICMR researchers reported to use diverse ways to make the interaction between disciplines possible, including: quantitative analysis of qualitative data, methodological juxtaposition to answer common research questions across disciplines, and connecting sub-system models to understand landscape dynamics in a holistic way. Challenges faced by interdisciplinary researchers included difficulty of integrating qualitative and quantitative approaches, disparity of disciplinary languages and methods, and lower evaluative performance in terms of publications. ICMR's interdisciplinary research projects had diverse ways to engage non-academic actors. The role of the latter ranged from being only beneficiaries of the project's results (through dissemination) to active co-producers of research questions and methods. A crucial challenge mentioned by our researchers regarding non-academic actors was to actually know what they want from scientific research. The role of intermediaries was highlighted as necessary to ensure a fruitful link with them.

Several factors – somehow contrasting – were listed as leverages of success in ICMR's interdisciplinary projects. On the one hand, a careful planning of interdisciplinary exchange (e.g. including it in the agenda of meetings as a point in itself) was considered crucial. On the other hand, researchers mentioned the importance of having a common site where unexpected interactions between projects from the natural and social sciences can occur (serendipity). Actually, serendipity – being open to unexpected discoveries – emerged in our data as a potentially constitutive element of transformative interdisciplinary research. Not only this was mentioned as a source of significant disciplinary and interdisciplinary discoveries (in topics as distant as glacier flow and ancient history), but it also emerged as the possibility of discovering something unknown in general. Indeed, when talking about their interdisciplinary research projects on mountains, ICMR researchers referred to an unknown world which remains to be discovered. Our data suggest that mountains are particularly suitable objects for transformative interdisciplinary research. This is so not only because they show clearly observable social-ecological interlinkages, but also because via different characteristics – such as beauty or peace – they are able to attract the attention of scientists in such a way that their research can move forward in unexpected, creative and transformative ways.

By shedding light on several aspects of the research processes on mountains underway at ICMR, our paper advances the literature on interdisciplinarity and transformative research in the mountain community and beyond. In particular, it confirms

or nuances some of the debates held in this literature regarding motivations, challenges and leverage factors. In addition, our paper adds the insight that serendipity seems to be a constitutive element of interdisciplinary research, and that being open to the unexpected at the personal and institutional levels can unveil creative solutions to transform mountains, mountain communities and the researchers working on them.

P 20.5

Towards transformation: on the path between climate change challenges, resilience and sustainable development.

Dunja Peduzzi[1], Oliver Schrot[1], Lars Keller[1] & Johann Stötter[1]

[1]Institute of Geographie, University of Innsbruck, Innrain 52f, A-6020 Innsbruck (dunja.peduzzi@uibk.ac.at)

Even if current attempts to terminate anthropogenic emissions of greenhouse gases are successful, future generations will have to cope with many impacts of climate change. For that reason, the development and implementation of appro-priate strategies to adapt to a changing climate is vital, both on a local and on a global scale. In the Alps the capacity to adapt to climate change is higher than in many other mountain areas. Even though, the Alps belong to the regions most affected by the impacts of climate change, their financial power, political stability and existing institutions for interregional and international cooperation provide favourable conditions for effective adaptation (EEA 2009).

Furthermore, there is growing evidence that especially education is a key deter-minant for which adaptation path we choose (Noble et al. 2014). Culture, by evoking collective outlooks and behaviours, is crucial to how societies react to climate-related risks (Adger et al. 2013). Changes in cultural norms and values affect adaptation limits positively or negatively (Klein et al. 2014). Therefore, adequate adaptation to the impacts of a changing climate involves a social learning process (Noble et al. 2014), which can be fostered by educational activities. A central question that needs to be addressed apriori in this context is, though, how we define successful adaptation.

Initially, adaptability has been understood as the capacity to preserve the status quo of natural and human systems by incremental adjustments to observed changes in climate. Recently, potential limits of incremental adaptation to pro-gressing climate change have attracted considerable attention. Facing the uncertainty of the characteristics and cumulative impacts of future climate, transformational adaptation may be essential, altering the system itself (Klein et al. 2014, Noble et al. 2014, O'Brien 2012). Nonetheless, it has to be taken into account that transformational pathways naturally threaten the interests of those who benefit most from the present state (Pelling 2011, cited in O'Brien 2012). This seems to constrain transformational adaptation on different scales and in different ways and also might represent a key challenge for educational ap-proaches concerning the climate change adaptation in the Alps.

We evaluated the potential of an educational project focusing on adaptation to climate change to foster local climate-resilient sustainable development path-ways in North and South Tyrol. The content analysis of posters, presented by secondary school students after a one-year educational intervention incorpora-ting both scientific and lai knowledge, revelead the challenges of such actions.

REFERENCES

Adger, N.W., Barnett, J., Brown, K., Marshall, N. & O'Brien, K. 2013: Cultural dimensions of climate change impacts and adaptation. In: Nature Clim Change 3 (2), 112-117.

EEA 2009: Regional climate change and adaptation: The Alps facing the challenge of changing water resources. European Environment Agency, Copenhagen.

Noble, I.R., Huq, S., Anokhin, Y.A., Carmin, J., Goudou, D., Lansigan, F.P., Osman-Elasha, B. & Villamizar, A. 2014: Adaptation Needs and Options. In: Climate change 2014. Impacts, adaptation, and vulnerability. Part A: Global and Sectoral Aspects. Working Group II contribution to the fifth assessment report of the Intergovernmental Panel on Climate Change (Ed. by Field, C.B., Barros, V.R., Dokken, D., Mach, K.J., Mastrandrea, M.D., Bilir, T.E., Chatterjee, M., Ebi, K.L., Estrada, Y.O., Genova, R.C., Girma, B., Kissel, E.S., Levy, A.N., MacCracken, S., Mastrandrea, P.R. & White L.L.). Cambridge University Press, Cambridge & New York, 833-868.

Klein, R.J.T., Midgley, G.F., Preston, B.L., Alam, M., Berkhout, F.G.H., Dow, K., Shaw, R.M. 2014: Adaptation opportunities, constraints, and limits. In: Climate change 2014. Impacts, adaptation, and vulnerability. Part A: Global and Sectoral Aspects. Working Group II contribution to the fifth assessment report of the Intergovernmental Panel on Climate Change (Ed. by Field, C.B., Barros, V.R., Dokken, D., Mach, K.J., Mastrandrea, M.D., Bilir, T.E., Chatterjee, M., Ebi, K.L., Estrada, Y.O., Genova, R.C., Girma, B., Kissel, E.S., Levy, A.N., MacCracken, S., Mastrandrea, P.R. & White L.L.). Cambridge University Press, Cambridge & New York, 899–943.

O'Brien, K. 2012: Global environmental change II: From adaptation to deliberate transformation. In: Prog. Hum. Geogr. 36 (5), 667-676.

O'Brien, K. & Sygna, L. 2013: Responding to climate change: The three spheres of transformation. In: Proceedings of Transformation in a Changing Climate. University of Oslo, Oslo, 16-23.

21. Human Geographies: Bodies, Cultures, Societies

Karine Duplan, Elisabeth Militz

Swiss Association for Geography (ASG)

TALKS:

21.1 Atakay A.: Queer Bodies, Queering E-Space of Grindr

21.2 Bittel S.: Afghan music in exile: Music in a transnational space

21.3 Brüning L.: Exploring the approach of migration for adaptation in a context of coastal erosion in Senegal: Typology of the consequences of migration on coping strategies

21.4 Chenet M.: Filming the relationship between people and natural environment: Contribution to an embodied environmental geography

21.5 Dijkema C.: Embodied experiences of inequality in a marginalized social-housing neighbourhood in France: How place, gender and class intersect with the effects racialized bodies produce in public space

21.6 Duplan K.: Expatriate as the hero of globalisation? Insights on the production of privileged transnational subjectivities amongst female expatriates in Luxembourg

21.7 Fall J., Sohier E.: Thinking geography visually: Research after the 'Visual Turn'

21.8 Fannin M., Connor K., Kent J.: Blood culture: Reimag(in)ing Life at a Cellular Scale

21.9 Huetz A.: The Moral Geographies of Urban Pleasures: Mapping out Spectacles in Geneva between 1880 and 1920

21.10 Klosterkamp S.: Security, mobility and the body: Negotiating Muslim femininities and power-geometries through/by/in legal institutions

21.11 Lécuyer M.: Producing the container port as a white male area: Inequalities and intersectional domination on the port of Felixstowe, UK

21.12 Leresche N.: Les corps utopiques de la réalité virtuelle

21.13 Mollett S.: Tourism Troubles: Feminist political ecologies of land and body in the making of residential tourism space in Panama

21.14 Pope J.: Intersectionality, an infra-analytical tool for in-between cities?

21.15 Sandoz L., Mittmasser C., Riaño Y., Piguet E.: Everyday transnational practices of migrant entrepreneurs in multiple localities

21.16 Shipp L.: Leaky bodies, leaky data: Apps, data and menstruation

21.17 Thieme S., Fry P.: Teaching visual methodology: Social Learning Video Method as a collaborative practice of learning

21.18 Villacura K.: Housing as an uncertain place: Disempowerment and displacement in the housing system in Sweden

21.19 Willemin R.: Visuality and futurity of unseen water(-scapes) quality

21.1

Queer Bodies, Queering E-space of Grindr

Ali Atakay[1]

[1]*Université de Paris VIII Vincennes-Saint-Denis, 2, Rue de la Liberté, 93526 Saint-Denis*

This paper explores one of the digital cartographies that smartphones offer in our everyday life, cyberspace which has been reformulated by corporeal identities. Frequent utilization of smartphones has expanded the limits of the body image on the one hand, on the other hand, with the different functions and features, the smartphones enable users to extend their identities into cyberspace. By focusing on the geolocation-based dating application for Gay, Trans, Bi and Queer, Grindr, this paper will elaborate on the way the queer bodies are extended in the e-space and how these bodies are construed by the space in which they inhabit. When a user render himself/herself online on Grindr, he or she is also resituated offline via geolocation feature that the application offers. The paper suggests that Grindr enables bodies to queer both the cyber (online) space and physical (offline) space through the representations of different bodily identities that are constructed textually and on imaginary level. To what point Grindr allows bodies to queer the space in which they habit and to what extent queer bodies are allowed to lay claim to the online space offered by Grindr? Grindr not only provides a freedom of browsing online but also render sexual minorities more visible on this semi-public space which cannot be thought outside of physical/offline space. By analyzing the reciprocal and intimate relation between body and e-space as well as online and offline cartographies, this paper elaborates on a phenomenological question to lay claim to the demarcation of e-space and extended bodily contours.

21.2

Afghan Music in Exile: Music in a transnational space

Sarah Bittel

The Graduate Institute Geneva (IHEID) / sarah.bittel@graduateinstitute.ch

Building upon my master's thesis and the resulting research film "Afghan Son(g)s", my paper endeavors to complement an approach developed predominantly by US cultural geographers wherein music defines a place. Through it, I question how definitions of place and music change throughout migration trajectories. My research on Afghan music-making in Geneva further reflects upon research participants' use of social media within their transnational network and how social practices on social media platforms play into practices of music making. I here argue that transnational social interconnections become further accentuated through musical performances, stimulating physical as well as digital movements and exchange and broadening an already extensive transnational network.

Beyond a debate on transnational musical practices and its relation to place, I aim to illustrate how empirical data collection can be blended with research communication and discuss filmmaking's potential as a research method in human geography. Here, film becomes an effective way to capture ambiance, sound and interactions of research participants, allowing the viewer to accompany the researcher in her own explorations by reflecting directly on the acoustic and visual aspects of the research. As such, I situate this research in scholarship that uses visual methods to explore social phenomena, going beyond a common focus on placemaking known from films in geography. The film includes sequences that have been filmed by research participants themselves on their mobile phones, further allowing a reflection on films' participatory possibilities.

21.3

Exploring the approach of migration for adaptation in a context of coastal erosion in Senegal. *Typology of the consequences of migration on coping strategies*

Brüning Loïc

University of Neuchâtel, Institute of geography, Switzerland (loic.bruening@unine.ch)

The commune of Gandiol located in the North of Senegal is affected by a phenomenon of coastal erosion engendered by the anthropic action but also accentuated by climate change. Marine submersions cause salinization of the Senegal River, soils and groundwater in a region that lives mainly from fishing, agriculture and livestock. The sea's rise coupled with the increase in salinity is causing habitat loss and livelihoods for local populations. In the face of these environmental degradations, the use of migration is part of the system of adaptation strategies. Nevertheless, the latter seems particularly preferred to other strategies causing significant male emigration mainly internal to Senegal and new migratory patterns. After presenting the environmental and migratory contexts of Gandiol this paper presents a typology of the consequences of migration on adaptation strategies by mobilizing the emerging approach of *migration for adaptation*. More precisely, the typology is related to the use of monetary remittances by migrants and the effects on the structures of households of male emigration. Through the typology, it shows how remittances are a strong and powerful way for the migrant to maintain links with his home community, but the maintenance of this link can lead to transformations in households receiving remittances. Therefore, this paper examines how the use of migration as adaptative strategy in a context of coastal erosion create new translocal practices within Senegal and re-structure households in Gandiol.

Keywords : Coastal erosion, salinisation, climate change, environmental degradation, migration, adaptation, Senegal, Gandiol

21.4

Filming the relationship between people and natural environment : contribution to an embodied environmental geography

Marie Chenet

University Paris 1 Panthéon-Sorbonne (Marie.Chenet@univ-paris1.fr)

As a researcher in geography, I have produced documentary films of various formats. As a research outcome, a documentary film highlights new relationships between recorded elements and sheds a new light on geographic knowledge. Four of my films address environmental themes, particularly how environmental changes can be lived as a threat and/or as an opportunity, and how people deal with. The films reveal how ambivalent and complex the relationships to nature can be and the necessity of a personal adaptation to live and work in such environments. My films contribute to environmental geography but also to the emerging fields of geography of the body and geography of the emotion. They show bodies in action and highlight the « spatial experience of the bodies » (Barthe-Deloizy, 2011) in natural environment. Filming people documents their physical involvement in a particular environmental context, as well as it shows how the exploitation of natural environment induces specific corporeality. Film is also a good tool to document emotional and affective relationships of people to landscape. These connections are often not taken in account in written texts because of the difficulty to put into words those feelings (Davidson et al., 2005). My films show how these connections are essential to accept hard living and working conditions and how specific feelings can lead to irrational behaviors.
During my presentation, I will highlight these themes by analyzing extracts of my films. Beyond these, I will discuss how filming requires a reflexivity on his or her researcher position.

Barthe-Deloizy F. (2011), « Le corps peut-il être "un objet" du savoir géographique ? »,
Géographie et cultures, n° 80, p. 229-247.
Davidson J., Bondi L., Smith M. (2005), *Emotional geographies*, London and New York, Routledge, 272 p.

21.5

Embodied experiences of inequality in a marginalized social-housing neighborhood in France –how place, gender and class intersect with the effects racialized bodies produce in public space.

Claske Dijkema

PACTE, University of Grenoble-Alpes

One of the results of a five-year long PhD research project on the stigmatization of marginalized social-housing neighborhoods in France, which seeks to develop a decolonial approach to these areas of habitation, is that racialized inhabitants experience inequality in society notably through the negative reactions their bodies produce in public space. It provides information about how they are made to feel “out of place”. These experiences are gendered: men mention frequent identity controls and Muslim women wearing a *hijab* account of the negative reactions their veil provokes in public space, ranging from hostility to disgust. The factor time plays a role here, with a significant shift after the 2015 terrorist attack; the factor place does as well, their bodies produce different effects in different places in the city; and so does the factor class.

The data I will mobilize in this paper presentation have been produced as part of an ongoing experiment with forms of collective knowledge production. This methodological exploration is motivated by a critique of individualized ways of knowledge production that has the disadvantage of extracting knowledge from marginalized neighborhoods in order to nourish the academic debate. It has taken the form of the creation of a *Université Populaire* - community university- in a marginalized social-housing neighborhood in Villeneuve (Grenoble). One cycle of debates has addressed the issue of racism, discrimination and islamophobia in the aftermath of a series of terrorist attacks in France and a second cycle of debates has addressed the question “What is left of the colonial past?”. The results presented here draw on the experiences participants shared throughout these group discussions.

21.6

Expatriate as the hero of globalisation? Insights on the production of privileged transnational subjectivities amongst female expatriates in Luxembourg

Karine Duplan

University of Geneva & University of Neuchâtel (karine.duplan@unige.ch)

This submission draws on the results of my PhD dissertation in political and cultural geography that aims at unveiling the subjective experiences of globalisation of highly skilled female migrants, from an ethnographical case study located in Luxembourg. Positioned at the crossroads of transnational studies, critical mobility studies and migration, this research seeks to question how geographical imaginaries and everyday practices of selected highly skilled migrants take part in the (re)production of the category “expatriate” as a privileged category of migration (Croucher 2012; Fechter and Walsh 2010; Glick-Schiller 2015) that contributes to promote an idealised image of the expatriate as the hero of our globalized era.
In this proposed paper, I intend more specifically to explore the discursive and socio-spatial practices through which selected expatriates in Luxembourg identify themselves as such by putting forward specific sets of values and norms involved with transnational mobility (Massey 2005). I will first disentangle the underlying injunctions that infuse the transnational mobility project as a privilege of cosmopolitan neoliberal elite (Yeoh 2014). I will then scrutinise expatriates’ translocal geographies (Brickel and Datta 2011) through their everyday practices as self-making of an imagined distinctive community. Drawing on an intersectional analysis, I will argue that if the category expatriate contributes to reproduce power relations and hierarchical forms of mobility, it remains useful as a relational category of identity practice of globalisation that expresses a distinctive global sense of place (Massey 1993).

21.7

Thinking geography visually: research after the 'Visual Turn'

Juliet Fall, Estelle Sohier

Department of geography, University of Geneva (Juliet.fall@unige.ch, Estelle.sohier@unige.ch)

Geographers have long been interested in the visual, with map-making, field sketching and landscape analysis being quasi-fetishised practices that marked geography out from other social sciences. It is therefore not new for geographers to think critically about how social worlds are visually constructed, and how such visuality is itself constructed. Nevertheless, this session takes as a starting point that Visual Geographies have undergone a remarkable renewal as part of cultural studies more broadly and, more recently, as part of visual and digital turns in the broader social sciences. In this paper, we aim to map out a space to discuss how geographical practices are changing in a world of images. This serves as the framing presentation for the collective session that brings together geographers interested in thinking critically about visual geographies, and 'mapping out' who and how this is taking place.

Three broad questions frame this paper:
How does the so-called visual turn change how geographers practice research, from how we collect, analyse, and understand increasingly diverse visual material (including film, comics, visual and digital archives, photography, etc.)?
How do we produce images as part of our research, such as through filmmaking, photo-reportage, participatory workshops, drawing, and so on?
How does taking visual geographies seriously change our situated practices as geographers, in how we collect, carry out, share and communicate our research?

21.8

Blood Culture: Reimag(in)ing Life at a Cellular Scale

Maria Fannin[1], Katy Connor[2], & Julie Kent[3]

[1]School of Geographical Sciences, University of Bristol, University Road, Bristol, BS8 1SS, United Kingdom (m.fannin@bristol.ac.uk)
[2]Spike Island, 133 Cumberland Road, Bristol BS1 6UX, United Kingdom
[3]BrisSynBio, University of Bristol, Life Sciences Building, Tyndall Avenue, Bristol BS8 1TQ, United Kingdom

This paper reports on an interdisciplinary project between an artist, a biochemist, a sociologist and a geographer that explores how artistic research as methodology can bring new insights to the technologies of culturing red blood cells. Cell culture is the practice of growing living cells outside the body and in the laboratory. Our aims are threefold – first to discuss the development of new techniques to culture red blood cells on an industrial scale for therapeutic use, second to present the artistic work (making) that resulted from an artistic residency in the research laboratory where the objects of scientific study are red blood cells (erythroctyes) and thirdly, to reflect on and theorise the interdisciplinary dialogue and co-construction of meaning that has shaped our collaboration, a mode of working together that Jane Calvert and Pablo Schyfter call "emergent critique." Central to this analysis is the imag(in)ing of scale – from the macro to the molecular scale. Blood flows within and across bodily boundaries through practices of donation and transfusion; blood travels across healthcare systems and national boundaries. We analyse the corporeal topographies that shape these flows. Located within the research laboratory at the molecular scale, imaging techniques are used to observe the processes of extracting haematopoietic (blood-forming) stem cells from blood and how cells are manipulated, cultured, and cell populations expanded. Shared interest in microscopic imaging/sensing technologies and the visualisation of bodily interiors were a starting point, and artworks were developed to facilitate critical and creative understanding of divisions and commonalities between, as artist Katy Connor writes, "biology and technology, materiality and ethics, as well as the production of new cultural meanings through metaphor."

21.9

The Moral Geographies of Urban Pleasures: Mapping out Spectacles in Geneva between 1880 and 1920

Allison Huetz

Department of geography, University of Geneva (Allison-Laure.Huetz@unige.ch)

The interest of geography in the visual has become a commonplace that authors like Gillian Rose have sought to re-examine by asking the following question: “how exactly is geography visual? » (Rose 2003). This question inevitably leads to the following corollary: “how exactly is the visualization geographical?” (MacDonald, 2009). Based on visual materials and police records, this presentation looks at the creation of moral geographies in Geneva at the turn of the twentieth century. The localization of urban pleasures was a key question in the development of the city. Public shows and spectacles have raised many issues for social reformers and city authorities in terms of public order and moralization of behaviours. The study of their spatial inscription reveals the creation of new « urban visibilities » (Brighenti 2007) that are built at different scales: the street, the neighbourhood and the city.

In my presentation, I will tackle the following methodological questions:
- How to map out spectacles and publics shows in Geneva at the turn of the twentieth century?
- How to use archives and police records to draw up a moral geography of urban pleasures?
- And finally, how can geography help visual studies to examine the role of images in the construction of « urban visibilities »?

21.10

"Security, mobility and the body: Negotiating Muslim femininities and power-geometries through/by/in Legal Institutions"

Sarah Klosterkamp

Department of Human Geography, University of Muenster, Germany (s.klosterkamp@uni-muenster.de)

Syrian Rebel Groups such as *Harakat Ahrar al-Sham*, the so-called *Islamic State* or *Junud al-Sham,* depend on globally linked networks and logistics to exchange personnel, goods and financial resources. European Border security authorities and many researchers in this field have so far mainly focused on male bodies who support logistics networks and supply chains, while the specific role of "juvenile", "female" or "aged" bodies is mostly overlooked. This becomes evident in state protection proceedings involving (German) Foreign Fighters in the Syrian Civil War.

By taking into account empirical data as well as by focusing on the work on (feminist) legal geography (Brickell & Coumo 2019; Jeffrey 2017), feminist geopolitics (Hyndman 2012; Fluri 2017; Smith 2012; Pain & Staeheli 2014; Staeheli & Kofman 2004; Pain 2009, 2014) and socio-legal scholars (Crenshaw 1989; Singelnstein 2016; Krasmann 2006), this talk offers a post-structuralist, intersectional and multi-scalar analysis of how a layered system of patriarchal, racist and Islamophobic patterns exists within legal prosecution and therefore enable other violent networks to operate.

By deploying a feminist perspective on the "global-intimate" (Pratt & Rosner 2012; Mountz & Hyndman 2006) of international terrorism and their logistic infrastructures, this talk aims to exemplify, how bodies can be understood as a side "in which social, cultural, and political meanings are inscribed, understood, and challenged" (Fluri 2017: 144) while at the same time particular "representations of citizenship, privilege, and the lack thereof" (ibid) are carried upon. An intersectional feminist geopolitics analysis like this, emphasizes grounded, empirical accounts that underscore how localized, embodied discourses link to transnational discourses and vice versa consequently redraws the boundaries of the geopolitical. It allows us for a more nuanced understanding of how power operates at multiple scales, across different bodily perceptions and through/by/in legal institutions by discussing hurdles and obstacles of such an intersectional approach at the same time.

REFERENCES

Brickell, K., & Cuomo, D. (2019). Feminist geolegality. *Progress in Human Geography*, *43*(1), 104–122. http://doi.org/10.1177/0309132517735706

Crenshaw, K. (1989). Demarginalizing the Intersection of Race and Sex: A Black Feminist Critique of Antidiscrimination Doctrine, Feminist Theory and Antiracist Politics. *University of Chicago Legal Forum*, *1989*(1), 139–167.

Hyndman, J. (2012). The Geopolitics of Migration and Mobility, *Geopolitics*, 17(2), 243-255, doi: 10.1080/14650045.2011.569321.

Fluri, J. L. (2017). Feminist Political Geography and Geopolitics. In: Oberhauser, Ann M., J. L. Fluri, R. Whitson, and S. Mollett (eds): "Feminist Spaces", London/New York: Routledge, 131–154.

Jeffrey, A. (2017). Legal geography 1: Court materiality. *Progress in Human Geography*, 1–9. http://doi.org/https://doi.org/10.1177/0309132517747746

Krasmann, S. (2006). Der Feind an den Grenzen des Rechtsstaats. In *Foucault: Diskursanalyse der Politik* (pp. 233–250). Wiesbaden: VS Verlag für Sozialwissenschaften. http://doi.org/10.1007/978-3-531-90475-7_11

Pain, R. (2009). Globalized fear? Towards an emotional geopolitics. *Progress in Human Geography*, *33*(4), 466–486. http://doi.org/10.1177/0309132508104994

Pain, R. (2014). Everyday terrorism. *Progress in Human Geography*, *38*(4), 531–550. http://doi.org/10.1177/0309132513512231

Pain, R., & Staeheli, L. (2014). Introduction: intimacy-geopolitics and violence. Area, 46(4), 344–347. http://doi.org/10.1111/area.12138

Singelnstein, T. (2016). Confirmation Bias – Die Bestätigungsneigung als kognitive Verzerrung bei polizeilichen Ermittlungen im Strafverfahren. *Strafverteidiger*, *36*(12), 830–836.

Smith, S. (2012). Intimate Geopolitics: Religion, Marriage, and Reproductive Bodies in Leh, Ladakh. *Annals of the Association of American Geographers*, *102*(6), 1511–1528. http://doi.org/10.1080/00045608.2012.660391

Staeheli, L. A., & Kofman, E. (2004). Mapping Gender, Making Politics: Toward Feminist Political Geographies. In L. A. Staeheli, E. Kofman, & L. Peake (Eds.), *Mapping Women, Making Politics* (pp. 1–14). New York, London: Routledge.

21.11

Producing the container port as a white male area. Inequalities and intersectional domination on the port of Felixstowe, United Kingdom.

Marie Lécuyer[1]

[1]Laboratoire ART-Dev, University of Montpellier 3 Paul Valéry, Rue du Professeur Henri Serre, 34090 Montpellier, France (marie.lecuyer@ens-lyon.fr)

Container ports have become central places in the globalised configuration of economies and circulation of wealth. While transnational maritime flows and port connections have been widely documented (Lau *et alii*, 2017), port areas themselves are hardly considered as relevant spatial units for geographical study. Yet, ports are places of power resting on dynamics of domination and unequal access to employment (Turnbull, 2011).

This paper is based on an ongoing doctoral research about women as marginalised workers on the port of Felixstowe, United Kingdom. Felixstowe is a small single-industry town depending on the jobs provided by the Hong Kongese private port operator and the local transport-related companies. Dock labour has historically been constructed as the exclusive domain of white working-class men under the supervision of white executives as well, producing distinct masculinities (Connell, 1995). Despite attractive salary prospects, the port industry still fails at making its workforce more “diverse”. Combining quantitative secondary data description (UK Census, corporate reports) and qualitative fieldwork (public relations analysis, observation and interviews), this paper addresses the way class and age shape gender and race hierarchies within the port area. I argue that women and/or racialized workers on the port are confined to a few low-ranking positions, because entangled class and age relationships prevent those workers from organizing collectively and gain full access to dock labour. This paper aims at discussing a relevant geographical approach to understand the production of intersectional domination in a broad industrial and private territory, through specific planning policies and neoliberal productive systems.

REFERENCES

Connell, R. 1995: Masculinities. Berkeley: University of California Press.

Lau, Y., Ducruet, C., Ng, K. Y. & Fu, X. 2017: Across the waves: a bibliometric analysis of container shipping research since the 1960s, Maritime Policy & Management, 44/6, 667-684.

Turnbull, P. 2011:‘Port Labor’, in Talley, W. K.:The Blackwell Companion to Maritime Economics. Malden: John Wiley & Sons.

21.12

The utopian bodies of the virtual reality

Nicolas Leresche

Département de Géographie et Environnement, Université de Genève, 1205 Genève (nicolas.leresche@unige.ch)

Virtual reality and its use in tourist and heritage contexts is part of the long tradition of simulation systems as they appeared in the 19th century. Unlike the latter, which build their effects around a partially immobile spectator, virtual reality, in its most advanced form, allows the spectator and his avatar to interact and move around in the simulated worlds. This distinction makes it possible to address two questions specific to the geographical discipline: (i) how does the spectator's position and corporality contribute to the production and understanding of space or the world (virtual or not)? and (ii) what is the importance of mediality in general and visual media in particular in the production and understanding of space (virtual or not) following the digital turn?

For the first question, which refers to phenomenology and critical geography, the position of the spectators concerns as much the perception of the distance (geometric and symbolic) existing between them and the elements composing their environment as it concerns the ability of the latter to position themselves, i.e. to be able to choose or not the distance which seems appropriate to them or which is imposed on them according to "the main axes of social differentiation which are the categories of sex/gender, class, race, ethnicity, age, disability and sexual orientation". The second question refers to the very broad field of Media studies and in particular the German branch of the *Medienwissenshaft*, a field little used by geographers, if not perhaps through the theory of the actor-network theory (ANT) or indirectly through visual studies and their interest for the instrumented gaze.

In order to understand how certain virtual reality devices inform us about these two issues and how they invite us to integrate new theoretical frameworks and new objects into the geographical discipline, I propose to take as case studies a virtual reality exhibition produced in 2019 by the Musée d'Art et d'Histoire de Genève. Conceived in partnership with the Artanim Foundation, this exhibition consisted of a virtual visit to the old city of Geneva as it existed at the time of the Fazist revolution in 1850. Based on data from the digitization of the Magnin relief, a 30 square meter model of the city completed in 1896, this unique experience allowed groups of 4 visitors to walk around the city for 15 minutes.

This experience, at the crossroads of a tourist visit and an illusionary spectacle, represents at least two new features. From a museographic and tourist point of view it is a new tool in terms of didactics of history and geography but it is also a new type of attraction that by means of haptic technology makes the carnal and sensitive body of the spectator the place of vision.

21.13

Tourism Troubles: Feminist political ecologies of land and body in the making of residential tourism space in Panama

Sharlene Mollett

University of Toronto, Department of Human Geography, Centre for Critical Development Studies and the Department of Geography and Planning
(sharlene.mollett@utoronto.ca)

In this address, I examine the ways in which settler colonial logics shape residential tourism development on the Atlantic Coast of Panama. With a focus on the Bocas del Toro archipelago, I entangle feminist political ecological assertions that struggles over nature are embodied struggles with anticolonial feminist understandings of land and body, drawn from a fusion of postcolonial, decolonial and black feminist thought, embedded in the concept of postcolonial intersectionality. Through this lens, I seek to illustrate three key findings. First, settler colonial place making in Bocas is partially articulated in the legal geographies of the Panamanian state's tourism-as-development strategy, a process that invites foreign land ownership. Second, critical development studies in Latin America tends to center indigenous women's livelihoods and rights as emblems of gender mainstreaming and social inclusion. By contrast, I focus on Afro-Panamanian women and illustrate, through ethnographic testimonies, the ways in which settler logics of elimination manifest in the naturalization of Afro-Panamanian women as "maids". Such imaginative and material geographies reflect conventional racial-sexual-gendered histories that take for granted black female servitude and landlessness on the Atlantic coast. Lastly, I will show, notwithstanding the coast's violent past (and present) that a deeper engagement with place-based histories makes *postcolonial intersectional* feminist theorizing a requirement for sustainable development policy with the concomitant recognition that any sustainable tourism policy that erodes local peoples control over land and bodies is not, in fact, *sustainable*. Thus, I argue that Afro-Panamanian women's participation in Bocas' tourism enclave--a project that seeks to erase indigenous and black relations to coastal lands and foster their subjection to foreign nationals--is simultaneously an articulation of their rights to remain on the coast.

21.14

Intersectionality, an infra-analytical tool for in-between cities?

Jill Pope

University of Lausanne

In Belgrade and Belfast, two transitional cities situated at the edge of Europe, discussions of race are often obscured by dominant narratives of ethno-nationalist or sectarian conflict; ambiguous colonial relationships and perceived whiteness. This paper will explore the relevance of intersectionality as an infra-analytical framework for my early doctoral research, exploring whether it is a useful tool to make visible the sometimes-hidden racialized dimensions of urban political practices of violence and resistance in these two cities. This paper discusses whether an intersectional analysis that, following calls from Bilge (2013) and others, puts race back in the frame along with other categories of inequalities, could become an important decolonial tool in these in-between cities, scratching the surface of these dominant narratives. Additionally, it questions whether an intersectional framework is useful to probe my own in-between positionality with respect to my research (McKinnon, 2013).

In doing so, this paper responds not only to calls from scholars who have urged a confrontation of urban politics with critical race theory (Picker, Murji, & Boatcă, 2019) but also to those who have highlighted the need to apply decolonial frameworks to sites such as the former Yugoslav region and Ireland, where race, coloniality and indigeneity are often left out of the picture (Baker, 2018; Karkov & Valiavicharska, 2018; Manolova, Kušić, & Lottholz, 2019; Scanlon & Kumar, 2019). It also acknowledges the need to overlay intersectionality with other conceptual frameworks that recognize the shifting connections between forms of inequality rather than viewing identification as a fixed grid (Puar, 2012).

REFERENCES

Baker, C. (2018). Race and the Yugoslav region: Postsocialist, post-conflict, postcolonial? Manchester: Manchester University Press.

Bilge, S. (2013). INTERSECTIONALITY UNDONE: Saving Intersectionality from Feminist Intersectionality Studies. Du Bois Review: Social Science Research on Race, 10(2), 405–424.

Karkov, N. R., & Valiavicharska, Z. (2018). Rethinking East-European Socialism: Notes Toward an Anti-Capitalist Decolonial Methodology. Interventions, 20(6), 785–813.

Manolova, P., Kušić, K., & Lottholz, P. (Eds.). (2019). Decolonial Theory & Practice in Southeast Europe.

McKinnon, K. (2013). A different kind of difference. Dialogues in Human Geography, 3(2), 213–216.

Picker, G., Murji, K., & Boatcă, M. (2019). Racial urbanities: Towards a global cartography. Social Identities,

Puar, J. K. (2012). 'I would rather be a cyborg than a goddess': Becoming-Intersectional in Assemblage Theory. PhiloSOPHIA, 2(1), 49–66.

Scanlon, L. A., & Kumar, M. S. (2019). Ireland and Irishness: The Contextuality of Postcolonial Identity. Annals of the American Association of Geographers, 109(1), 202–222.

21.15

Everyday transnational practices of migrant entrepreneurs in multiple localities

Laure Sandoz[1], Christina Mittmasser[2], Yvonne Riaño[3], Etienne Piguet[4]

[1]Geography Institute, University of Neuchâtel, Espace Tilo Frey 1, 2000 Neuchâtel (laure.sandoz@unine.ch)
[2]Geography Institute, University of Neuchâtel, Espace Tilo Frey 1, 2000 Neuchâtel (christina.mittmasser@unine.ch
[3]Geography Institute, University of Neuchâtel, Espace Tilo Frey 1, 2000 Neuchâtel (yvonne.riaño@unine.ch)
[4]Geography Institute, University of Neuchâtel, Espace Tilo Frey 1, 2000 Neuchâtel (etienne.piguet@unine.ch)

The activities of self-employed migrants increasingly extend beyond national borders, a phenomenon called transnational migrant entrepreneurship. This involves migrants physically moving across national borders for business opportunities, as well as migrants conducting transnational businesses from their places of residence by moving goods and services. The main objective of this paper is to discuss how the theoretical concept of spatial mobility capital (the ability to be mobile and to strategically use space) can help us to understand the diverse mobilities of migrant entrepreneurs. We map the diverse cross-border mobilities of migrant entrepreneurs and question whether spatial mobility constitutes an asset for migrant entrepreneurship, which can be converted into other forms of capital. The project uses mixed research methods and includes case studies from Switzerland, Spain and South America. We apply an inequality perspective and view spatial mobility as an unequally distributed resource. We propose that certain societal mechanisms, such as migration regimes, gender norms and local characteristics, shape opportunities and constraints for spatial mobility and have an impact on the way transnational migrant entrepreneurs can use transnational resources for their business. Since existing approaches about the concept of spatial mobility capital focus mainly on a local (and urban), rather than a global scale, we want to complement them with a transnational angle. This will enable us to study the different capacities for spatial mobility among transnational migrant entrepreneurs and to elaborate an understanding of spatial mobility capital that encompasses inequalities in transnational space.

21.16

Leaky bodies, leaky data: Apps, data and menstruation.

Laura Shipp[1]

[1]*Royal Holloway, University of London, Egham Hill, Egham, Surrey, TW20 0EX, United Kingdom. (Laura.Shipp.@live.rhul.ac.uk)*

Menstruapps are smartphone applications that allow their users to digitally track their reproductive cycle, sex lives and general health. Millions of menstruators use them globally, be it as an algorithmic fertility awareness method or to learn more about their body's cycle and processes. Yet, this intimate technology remains unexplored in geographical research and beyond. Feminist literature has drawn attention to the geographies of bodies, tissues and interiors (Colls and Fannin, 2013), and begun reconceptualising uterine geographies (Lewis, 2018). Yet, menstrual blood, and fluids imbued with taboo or discomfort still lack engagement (Longhurst and Johnston, 2014).

Through the lens of blood, this paper discusses fluids, flows and leaks, extending the analysis to its digital form. In doing so, it examines how the phone and the menstruapp can be understood as leaky. From this it demonstrates that the data leak more widely can be reconsidered - from large scale leaks such as the WikiLeaks scandal (Springer *et al.,* 2012), towards intimate sites – whilst highlighting the entanglements between the two.

This interdisciplinary work considers intimate leaks and argues that data leaks are intimate. From the ways in which menstruapps may share the data of their leaky subjects as their enter when their period started, from the networks and infrastructures used to transmit that message, to the capital generated through its movement. Overall, the paper considers the leaky geographies of this intimate technology.

REFERENCES

Colls, R., Fannin, M. 2013: Placental surfaces and the geographies of bodily interiors. Environment and Planning A, 45(5), 1087-1104.

Lewis, S. 2018: Cyborg uterine geography: Complicating 'care' and social reproduction. Dialogues in Human Geography, 8(3), 300-316.

Longhurst, R., Johnston, L. 2014: Bodies, gender, place and culture: 21 years on, Gender, Place and Culture, 21(3), 267-278.

Springer, S., Chi, H., Crampton, J., McConnell, F., Cupples, J., Glynn, K., Warf, B., Attewell, W. 2012: Leaky geopolitics: The ruptures and transgressions of WikiLeaks. Geopolitics, 17(3), 681-711.

21.17

Teaching visual methodology: Social Learning Video Method as a collaborative practice of learning

Susan Thieme[1], Patricia Fry[2]

[1]*Institute of Geography, University of Bern (susan.thieme@giub.unibe.ch)*
[2]*Wissenensmanagement GmbH and ETH Zurich (contact@patriciafry.ch)*

Our newly established mLab (medialab) at the Institute of Geography (Bern) is a platform where we explore jointly with students the potential of audio-visual research methodologies. The aim of our presentation is a critical reflection on our last semester first time run course on the *social learning video method*. Our presentation is based on a critical analysis of material generated in the seminar: a content-based video-analysis of the entire course (video records of each meeting), written reflections of the students on the method with specific questions regarding the “visual”, and an in-depth evaluation of the course in exchange with all involved partners.

The central idea of the social learning video method (Fry, 2017, 2018; Fry and Thieme 2019) is to address socially relevant problems and work out solutions together (co-production) with civil society, administration and the private sector. The purpose of the SLV method is to map the different actors and to identify, visualize and make accessible their perspectives and their transformation knowledge. In the seminar the students went through a transdisciplinary work process and produced a social learning video on the topic “Access to and practices of mobility using the example of the Thun railway station”.

The production of the SLV initiated a very strong exchange between the students, the practice partners and the lecturers. The ongoing discussion of the aim of the video, the process of filming (what, whom, when), the discussion of raw material at different stages of the seminar, and the production of the final video (what becomes part of the video and what to leave out) initiated a constant reflection of the process and adaptation whenever needed.

One of the main challenges in the seminar was to keep a balance between the introduction to technical skills, a critical reflection on visual methodology and deepening other topical aspects (e.g. mobility, sustainability, transdisciplinarity). For the students the biggest achievement was that the practice partners not only closely collaborated throughout the whole seminar but now also use the 12 min video for further processes in their institutions.

21.18

Housing as an uncertain place. Disempowerment and displacement in a financialized housing system

Karina Villacura

Urban Studies, Malmö Universitet (karina.villacura@mau.se)

The Swedish welfare system developed from the 1930s and onwards, based on universal principles of access to rights. One of the essential pillars where this universalism expressed was housing, which characterized by the key role of Municipalities both in building and distribution of accommodations. Neo-liberalization of policy experienced from the 1990s have led to a model shift (Grundström and Molina, 2016) changing former housing regime into a monstrous hybrid (Christophers, 2013) that allows a close private/public partnership resulting in the financialization of the Swedish housing system (Grander, 2018). However, those changes do not affect in the same way the whole population. Whereas the presence in the current housing system of high-income earners and social assistance beneficiaries is, in some way, ensured; an important part of the population has severe problems in accessing to housing or meeting the requirements of housing companies –both public and private. This paper focuses on the spatial outcomes of the business-like shift in housing, paying attention to processes of segregation and displacement experienced by disempowered groups and their narratives. Using intersectionality as an analytical tool the discussion aims at unravelling the impacts of policy especially in vulnerable groups that may end up in less secure forms of housing solutions such as informal rental contracts or the overpriced second-hand housing market. One-parent families, precarious workers, young people and non-European immigrants experience the inherent difficulties of a system modified to promote financial gains over social security.

REFERENCES:

Christophers, B. (2013). A Monstrous Hybrid: The Political Economy of Housing in Early Twenty-first Century Sweden. NEW POLITICAL ECONOMY, 18(6), 885–911. https://doi.org/10.1080/13563467.2012.753521

Grundström, K., & Molina, I. (2016). From Folkhem to lifestyle housing in Sweden: segregation and urban form, 1930s–2010s. International Journal of Housing Policy, 16(3), 316–336. https://doi.org/10.1080/14616718.2015.1122695

Grander, M. (2018). For the benefit of everyone?: Explaining the significance of Swedish public housing for urban housing inequality. Malmö universitet, Fakulteten för kultur och samhälle.

21.19

Visuality and Futurity of unseen water(-scapes) quality

Rémi Willemin

[1]Department of Geography, University of Zurich, Winterthurerstrasse 190, CH-8057 Zürich (remi.willemin@geo.uzh.ch)

While debates in Switzerland are increasingly problematizing water pollution as mainly a consequence of agricultural practices, our participatory visual project questions what is perceived as good quality water(-scape) care practices. We look at and co-develop perceptions of practices impacted by or impacting water quality. Participants, selected among farmers in the Jura region, explore how social practices, water, and chemicals (as well as other polluting products) interact and co-create waterscapes revealing various inter-/intra-relations to aquatic ecosystems and water. Based on their pictures, they elicit their perceptions of present waterscapes in Photo-response (Alam et al.2018) like interviews. Moreover, they imagine these waterscapes in probable and aspired futures. This proposed conceptual framework unite hydrosocial territories (Boelens et al. 2016) and chemosocial solidarities (Shapiro and Kirksey 2017) into what could be considered hydro-chemo-social waterscapes. This contribution explores two aspects of future waterscapes: in terms of visuality which “encompasses visual practices of appropriating (spatial) reality and established ways of looking at the world – by society, cultural and social groups, or disciplines” (Schlottmann 2017) as well as in terms of “futurity as care” (Adam & Groves 2007).

REFERENCES

Adam, B. & Groves, C.. 2007: Future Matters: Action, Knowledge, Ethics. BRILL. Leiden, Boston.

Alam, A., McGregor, A., Houston, D. 2018: Photo-Response: Approaching Participatory Photography as a More-than-Human Research Method, Area, 50, 256–65.

Boelens, R., Hoogesteger J., Swyngedouw, E., Vos, J. and Wester, P. 2016: Hydrosocial Territories: A Political Ecology Perspective, Water International, 41, 1–14.

Schlottmann, A. 2017: Visuality. The International Encyclopedia of Geography, 1–3.

Shapiro, N. & Kirksey, E.. 2017: Chemo-Ethnography: An Introduction, Cultural Anthropology, 32, 481–93.

22. Human Geographies: Cities, Regions, Economies

Christian Berndt, Laurent Matthey, Martin Müller

Swiss Association for Geography (ASG)

TALKS:

22.1 Alpermann, H.: Urban redevelopment and its resistance: Learning from La Duchère, Lyon

22.2 Andriamahefazafy M.: The production of uneven benefits from a mobile commodity: the case of tuna from Madagascar

22.3 Baumann H.: Making space for urban Indigenous people in Montreal

22.4 Bernhold C.: Upgrading in and through class differentiation – A case study from agribusiness in Argentina

22.5 Crottaz B.: Corporate social responsibility (CSR) and commodity trading in Switzerland: a potential of redefinition of neoliberalism?

22.6 de Roulet P.: International organisations and the production of dual cities in Africa

22.7 Ginisty K.: Maputo, a smart and a fair city ?

22.8 Herrigel J.: Articulations of diverse forms of labour in (global) commodity chains from a feminist perspective

22.9 Kullman K.: Chemical collectives: alternative designs for environmental health

22.10 Languillon-Aussel R.: Public places in vertical Asian cities – insights from Tokyo and Singapore

22.11 Lehec C.: Graffiti in Palestinian Refugee Camps: from palimpsest walls to public space

22.12 Lupatini M.: Space and citizenship

22.13 Mollett S.: Tourism Troubles: Feminist political ecologies of land and body in the making of residential tourism space in Panama

22.14 Müller M.: How we theorised cities from the North and South but forgot to think with the Easts

22.15 Neville L.: Everyday waste-based practices: exploring politics of space and place from an informal neighbourhood in Cartagena, Colombia

22.16 Pauschinger D.: “We Do Pioneering Work”: Learning and Exemplification of New Technologies in a Digitalised Agriculture

22.17 Wolfe S.D.: Virtual Resistance, Material Consequences: Countering State Projects in (Semi-) Authoritarian Russia

22.1

Urban redevelopment and its resistance: Learning from La Duchère, Lyon

Hendrikje Alpermann

Université de Lausanne, Institute of Geography and Sustainability (IGD)

"…*But what we academics so often forget is (…) the inevitable feelings of loss provoked by the demolitions*…" (Harvey 2012: x-xi).

It was demolitions and the resettlement of thousands of households that provoked public action among two groups of inhabitants in one of France's *grands ensembles*, La Duchère (Lyon). The district has in 2001 been included in national restructuring programs consisting primarily of structural transformation (Mission La Duchère Lyon 2016).

This contribution is based upon empirical research on two similar but very different movements in La Duchère – the *Groupe Inter Quartiers* (*GTI*, later *Conseil Citoyen*) and the *Collectif 230,* fighting for their share in the redevelopment of their district in reaction to top-down urban restructuring plans.

It argues that socio-technical arrangements within urban re-structuring create uneven opportunities for different groups to get heard or involved (Le Galès 2005; Bourdieu 1976; Nonhoff 2007) and create different forms of resistance.The *GTI* was opposing large-scale demolition and later changed its stance with its institutionalization as *Conseil Citoyen*.
The *Collectif 230* didn't feel legitimate to question the restructuring program as a whole as they had no language to get heard (Rancière 2002:35).

The paper investigates how the re-development project and its radical strategy of demolition changes not only the built environment, but also the socio-technical and power relations, interaction and identities within the district – also a firm objective of such policies (Roberts 2000: 17), in the case of La Duchère to change the image and the 'social mix' through demolition and reconstruction (Verhage 2009: 206).

REFERENCES

Bourdieu, Pierre (1976): Entwurf einer Theorie der Praxis auf der ethnologischen Grundlage der kabylischen Gesellschaft. Frankfurt a. M.: Suhrkamp.

Harvey, David (2012): Rebel Cities: From the Right to the City to the Urban Revolution. London/NY: verso.

Le Galès, Patrick (2005): Elusive Urban Policies in Europe. In: Yuri Kazepov (Hg.): Changing Contexts, Local Arrangements, and the Challenge to Social Cohesion. Oxford, Malden: Blackwell, p. 235-254.

Mission La Duchère Lyon (2016): Projet de Territoire Lyon La Duchère 2016-2020.

Nonhoff, Martin (2007): Diskurs, radikale Demokratie, Hegemonie - Einleitung. In: Martin Nonhoff (Hg.): Diskurs - radikale Demokratie - Hegemonie. Zum politischen Denken von Ernesto Laclau und Chantal Mouffe. Bielefeld: Transcript, p. 7-24.

Rancière, Jacques (2002): Das Unvernehmen. Frankfurt a.M.: Suhrkamp.

Rannila, Päivi; Loivaranta, Tikli (2015): Planning as dramaturgy: agonistic approaches to spatial enactment. In: International Journal of Urban and Regional Research 39 (4), p. 788-806.

Verhage, Roelof (2009): Le Renouvellement urbain à La Duchère. In: Paul Boino (Hg.): Lyon: La Production de la ville. Marseille: Paranthèses, p. 194-216.

22.2

The production of uneven benefits from a mobile commodity: the case of tuna from Madagascar

Mialy Andriamahefazafy

Institute of Geography and Sustainability, University of Lausanne, Géopolis CH -1015 Lausanne (mialyzanah.andriamahefazafy@unil.ch)

In Madagascar, tuna fisheries bring important revenues for the country while contributing to local livelihoods of coastal communities. Allowing distant water fishing nations (DWFNs) to access tuna resources in its territorial waters through fishing agreements, Madagascar hosts a tuna cannery that gets its supply from these foreign industrial fleets. The cannery mainly produces tuna cans that are exported in Europe including France, Spain, Germany or Italy. The local tuna fishing mainly provides for the local markets and exports to the neighbouring islands. This paper explores the dual trajectory of tuna from Madagascar, as a local and global commodity. Using political ecology as an approach and more specifically the theory of access by Ribot and Peluso (2003), I explore the means of access to the resources as well as who benefits from the resources. I will show how the industrial fishery, framed by the State and DWFNs as bringing national benefits through revenue and labour opportunities, has also contributed to the limited development of the country's tuna fishery. This is exacerbated by the substantial profits that powerful capitalist firms based in Europe get from the fishery. The paper will also present the importance of tuna fishery at the local level despite a lack of investment from the State. Finally, it will highlight how the fishery is shaped by the mobility of the resources and the fluidity of the Western Indian Ocean.

REFERENCES

Breuil, C. and D. Grima. 2014. Baseline report Madagascar. Ebene, Mauritius: SmartFish Programme of the Indian Ocean SmartFish Programme of the Indian Ocean Commission, Fisheries Management FAO component.

Campling, L. 2012. The tuna 'commodity frontier'- business strategies and environment in the industrial tuna fisheries of the Western Indian Ocean. Journal of Agrarian Change 12(2): 252-278.

Macfadyen, G., B. Rohmer, B. Caillart. et al. 2015. Ex post evaluation of Union financial measures for the implementation of the Common Fisheries Policy and in the area of the Law of the Sea 2007-2013. Final report and annexes. Brussels: European Commission.

Ribot, J.C. and N.L. Peluso. 2003. A theory of access. Rural Sociology 68(2): 153-181.

Sneddon, C. 2007. Nature's materiality and the circuitous paths of accumulation: dispossession of freshwater fisheries in Cambodia. Antipode 39(1): 167-193.

22.3

Making space for urban Indigenous people in Montreal

Heidi Baumann

Department of Geography, University of Zurich, Winterthurerstr 190, CH-8057 Zurich (heidi.baumann@uzh.ch)

For a long time, Indigenous migration to urban areas has been associated with their assimilation into the dominant society (Lévesque 2003:32). As a response to Indigenous people migrating to Canadian cities starting in the 1950s, Friendship Centers emerged, which represent "places of Indigenous resistance and urban community" (Langford 2016:2). Nowadays, more than half of the Indigenous people live in urban areas (Norris, Clatworthy and Peters 2013:33). Indigenous people are subject to a lot of structural socio-economic inequalities, including lower incomes and lower life expectancies (Peters 2005: 51).

The focus of my thesis lies on individual stories of Indigenous people in the city of Montreal, as well as the making of an urban Indigenous space, which is shown through the case of the Native Friendship Center of Montreal (NFCM).

As the literature on Indigenous people often focuses on rural rather than urban areas (cf. Peters and Andersen 2013:2), this research contributes to filling this gap. Using a qualitative methodology, the data was collected through semi-structured interviews and participant observation.

Through the analysis of individual stories, my thesis contributes to a better understanding of the lives of a small part of urban Indigenous people in Montreal. The analysis revealed major frictions between a neoliberal culture, with an individualized and self-responsible subject, and an indigenous culture, which is based on values of family and community.

The NFCM represents an urban node, where conflicting representations get expressed through tensions on the individual level. Navigating through these different representations can be understood as a form of protest and resistance by the individuals.

REFERENCES

Langford, Will (2016), Friendship Centres in Canada, 1959-1977 in The American Indian Quarterly, Vol. 40(1), pp. 1-37.

Lévesque, Carole (2003), "The Presence of Aboriginal Peoples in Quebec's Cities. Multiple Movements, Diverse Issues" in Newhouse, David, and Evelyn Peters (eds.), *Not Strangers in These Parts. Urban Aboriginal Peoples*, Ottawa, Policy Research Initiative, pp. 23-34.

Norris, Mary Jane, Stewart Clatworthy, and Evelyn Peters (2013), "The urbanization of Aboriginal populations in Canada. A Half Century in Review" in Peters, Evelyn, and Chris Andersen (eds.), *Indigenous in the city. Contemporary identities and cultural innovation*, Vancouver, UBC Press, pp. 29-45.

Peters, Evelyn (2005), "Geographies of Urban Aboriginal People in Canada. Implications for Urban Self Governance" in Murphy, Michael (ed.), *Canada: The State of the Federation 2003. Reconfiguring Aboriginal State Relation*, Kingston (ON), Institute of Intergovernmental Relations, pp. 39-76.

Peters, Evelyn and Chris Andersen (2013), "Introduction" in Peters, Evelyn, and Chris Andersen (eds.), *Indigenous in the city. Contemporary identities and cultural innovation*, Vancouver, UBC Press, pp. 1-27.

22.4

Upgrading in and through class differentiation – A case study from agribusiness in Argentina

Christin Bernhold[1]

[1]Department of Geography, University of Hamburg, Bundesstraße 55, D-20146 Hamburg (christin.bernhold@uni-hamburg.de)

Commodity chain studies originated with a critical analysis of the global political economy. In the past decades, however, much of the Global Value Chain (GVC) research has sidelined issues of exploitation and uneven development and instead focused on upgrading as a development strategy. Upgrading, here, is understood as a shift from low-skilled, labour-intensive towards a higher value – technology and knowledge-intensive – production within any industry, including agriculture. This is often accompanied by the implicit assumption that upgrading translates into social enhancement and more and better jobs. Scholars from different currents have criticized a labour-blindness within the related focus on firm-level development. In response, GVC scholars have themselves taken issue with a possible disjuncture between economic upgrading and social gains, and highlighted the need for an additional social upgrading agenda.

From a class-analytical perspective, this paper presents empirical research into the political economy of upgrading in Argentinian agribusiness. Within the framework of a case study, I argue that adverse labour relations are not merely blind spots or by-products of upgrading strategies. Instead, I analyse them as both results and conditions of upgrading, which benefits some actors while for others it instead entails shifting patterns of exploitation. I call this a process of 'upgrading in and through class differentiation.' My paper looks at the particular relations of a successfully upgrading firm to intermediate classes and at the conditions of rural labour, which is outsourced to labour contractors (so called contratistas). In one of the most dynamic branches of the Argentinian economy, salaries and working conditions of those who do the seeding, fumigation, and harvesting in the fields are relatively poor. In this context, I contend that the way in which the capital-labour relation is intermediated by contratistas inheres adverse conditions for struggles for benefits that workers could gain from upgrading. A class analytical perspective helps me understand how these conditions and the exploitative relations, which constantly shift in form but do not disappear under capitalist conditions, are part of the very basis upon which agribusiness upgrading strategies are built.

22.5

Corporate social responsibility (CSR) and commodity trading in Switzerland: a potential of redefinition of neoliberalism?

Baptiste Crottaz

Département de Géographie, Université de Fribourg, Rue du Marché 4, CH- 1700 Fribourg (baptiste.crottaz@unifr.ch)

Since the turn of the 2000s, Switzerland has become a major center for world commodity trading. However, this development has been accompanied by a proliferation of scandals related to the practices of multinationals in producer countries and relayed in the Swiss space, particularly by NGOs. Faced with this pressure, companies in the sector have poposed a response in terms of corporate social responsibility (CSR) incorporating a social and ecological duty. Therefore, this work aims to question the potential of redefinition of neoliberalism, defined as hegemony, contained in this approach. Specifically based on its application to the mining sector, it demonstrates a tool that essentially repels all wills of constrainig regulations, from both private and political actors, while seeking to legitimize the maintenance of neoliberal logic. However, the lack of production alternatives linked to the specificities of the sector highlights the study of the strategy of two NGOs engaged in its reform or its contestation, and to the partially divergent positions on CSR from a more complementary angle than antithetical. Therefore, it can be concluded that while CSR may offer a potential but not sufficient space for engagement, the development of research on other forms of production would be of great interest, especially to open the field of possibiliites of contestation.

22.6

International organisations and the production of dual cities in Africa

Pablo de Roulet[1]

[1]*Département de Géographie et Environnment/Gouvernance de l'Environnement et Développement Territorial, University of Geneva, Uni Carl-Vogt, Boulevard Carl-Vogt 66 (pablo.deroulet@unige.ch)*

Large presence of international organisations supported by numerous humanitarian and development professionals have become a common feature in a number of African cities. The social and material production of new spaces to support aid organisations and their employees translates in new modes of segregation where security procedures constitute unthought-of models of urban planning. Such territorial processes result in forms of dual cities that exchange and communicate in a specific configuration of class and power relations, transforming the urban landscapes of many capital cities in the Global South.

22.7
Maputo, a smart and a fair city ?

Karine Ginisty

Institut de géographie, Université de Lausanne (karine.ginisty@unil.ch)

Cette proposition de communication se propose de revenir sur les transformations de la gouvernance urbaine à Maputo, capitale du Mozambique, en s'appuyant sur l'étude de cas du service de collecte des déchets ménagers. Depuis 2001, la municipalité de Maputo fait l'objet d'une attention particulière de la part des institutions de coopération internationales pour le développement. Dans le cadre des pratiques de transferts de compétences pour la bonne gouvernance (contexte réformes de décentralisation), la coopération allemande (GIZ), puis la coopération japonaise (JICA) sont intervenues pour former à l'élaboration d'un Plan Directeur pour le service public de collecte des déchets. La conduite de ces deux projets de coopération, construits autour du référentiel de la durabilité, a soutenu l'inscription de la trajectoire de Maputo sur celles des *smart cities*. En novembre 2017 est inauguré le système MOPA, financé par la Banque Mondiale, premier *sofware* en *open access* prévue pour une gestion intelligente des déchets dans une ville du Sud. Dans cette perspective, cette communication interroge la trajectoire de Maputo en tant que *smart city* à partir d'une analyse de la construction de son action publique et l'évolution de ses inégalités urbaines.

Cette communication se focalise aussi bien sur les transformations de l'exercice du pouvoir que sur les impacts spatiaux de la gouvernance urbaine à Maputo, conduite depuis 2001 sous l'emprise de la coopération internationale pour le développement. A Maputo, le projet AGRESU (2001-2010), mené par la GIZ, puis le projet de la JICA (2013-2017), se sont traduits par une circulation de référentiels pour penser la durabilité le service public de collecte des déchets ménagers. La rationalité de gouvernement véhiculée par ces deux projets de coopération est celle de techniques de *management* néolibérales, articulées à la publicisation d'enjeux environnementaux. Dans une première partie, je souhaite revenir sur la conduite de ces projets et replacer la focale sur l'adhésion des agents publics à la transformation de leurs pratiques quotidiennes de l'action publique. De 2001 à 2018, l'analyse des différents moments de réappropriation du sens de ces projets de coopération, par les équipes municipales successives, expose le rôle des rapports de pouvoir au sein de la municipalité dans la capacité des agents à s'emparer du référentiel de la durabilité dans l'élaboration du Plan Directeur. Ainsi, si le projet AGRESU a cristallisé une relation conflictuelle entre l'équipe du projet et les élites politiques, dans la perspective d'une ville plus juste, le projet JICA témoigne plutôt de tensions autour d'une confiscation du pouvoir local à des fins néopatrimoniales. Dans une structure de pouvoir décentralisée, la réappropriation de nouvelles techniques de gouvernement s'inscrit dans des registres de pratiques en construction, traversés par des positions divergentes quant au sens de l'action publique. Une seconde partie concerne, ensuite, les transformations spatiales induites par le service de collecte des déchets à Maputo. Une attention particulière est placée sur la réduction des inégalités urbaines entre le centre-ville, hérité de la colonisation, et les quartiers dits périphériques. Loin de s'opposer à la réduction des inégalités urbaines, la rationalité néolibérale véhiculée par ces deux projets de développement été instrumentalisée pour renverser, en partie, des pratiques de pouvoir de l'action publique, clientélistes et néopatrimoniales. L'espace urbain et ses inégalités se transforment donc à Maputo selon la capacité des acteurs internationaux à appréhender les rapports de force de l'action publique, puis de contribuer à la reconfiguration de ces derniers autour des enjeux labélisés du développement. L'échec de la coopération JICA à implanter le tri sélectif illustre le rôle des pratiques de management des coopérants internationaux dans la circulation de modèles urbains et leur ancrage local. Pour conclure, cette communication dresse le cadre de circulation et de réappropriation de la *smart city*, à Maputo, des années 2000 à la seconde moitié des années 2010. La confrontation des différents moments ou contextes de circulation des référentiels de la gouvernance urbaine nourrit une distanciation critique à l'égard d'une littérature construite sur l'existence de modèles urbains, génériques et reproductibles, à l'échelle internationale.

Cette communication s'appuie sur deux matériaux de recherches distincts. Le premier terrain de recherches mobilisé est celui de la thèse de doctorat, de géographie, conduite de 2007 à 2014, sur la question des liens entre les inégalités spatiales d'accès aux services urbains et la justice sociale à Maputo. Lors de cette recherche doctorale, le projet AGRESU, de la coopération allemande, a fait l'objet d'un terrain sur la circulation de leurs techniques de gouvernement et leur réappropriation locale. Cette recherche a permis de mettre en lumière les rapports de pouvoir soulevés par l'adoption d'une conception de l'action publique tournée vers ses publics, ainsi que le rapport des acteurs à la production discursive de la durabilité. Le second terrain concerne, quant à lui, une recherche post-doctorale, qui vient d'être achevée, sur la tenue du projet JICA à Maputo et du projet MOPA pour une plus grande responsabilisation et une participation des habitants dans la gestion des déchets, permises par la technologie. L'adhésion des agents publics et des élites de la municipalité à ces deux projets se révèle pourtant de façade, au regard des coûts du dispositif technique et, surtout, des conflits politiques projetées. La recherche s'est donc intéressée à la stratégie des agents publics mise en œuvre pour produire un discours de la réussite des projets JICA et MOPA dans la vitrine internationale du développement au Mozambique.

22.8

Articulations of diverse forms of labour in (global) commodity chains from a feminist perspective

Johanna Herrigel[1]

[1]*Economic Geography, University of Zurich, Winterthurerstrasse 190, 8057 Zurich*

Recently, scholars have been increasingly concerned with the pervasiveness and ongoing proliferation of unfree, bonded and forced labour in global production. The majority of scholars studying unfree labour in global production assume that ultimately, this issue must and can be addressed within the global capitalist economy. More rarely, scholars conceive of the global capitalist economy as inherently connected to and co-constituted by non-capitalist relations of production and processes of de-proletarianization, including unfree labour. The latter kind of scholarship is insightful with regards to how global commodity chains are constituted through dis/articulations of capitalist and non-capitalist relations of production. However, the general issue with this debate is its exclusive focus on *relations of production* in global commodity chains, thereby eschewing the question of labour falling outside and thus overflowing this specific conceptual framing.
Failing to consider and conceptualize questions of labour beyond 'productive work' is not limited to the aforementioned debate, and indeed is a problem in much of global commodity chains studies. In this paper, I suggest that this lacuna can be solved by revisiting world-system theory conceptualizations of global commodity chains from a feminist perspective. Beyond the combination of capitalist and noncapitalist relations of production, scholars of world-system theory consider how commodities are transferred through diverse modes of exchange – market and nonmarket – along the chain. Importantly, by tracing back labour in global production to the households performing its (re-)production, this scholarship in line with a feminist perspective draws attention to how unpaid housework and unpaid care work provide a 'dark value' appropriated and transferred along global commodity chains. From this, we learn how global commodity chains are constituted by diverse forms of labour crisscrossing binary conceptual distinctions, such as 'productive' and 'reproductive' labour. Empirically attending to and analytically grasping these articulations of diverse forms of labour in global commodity chains is challenging. In line with feminist scholarship, I propose that one way forward is to focus on households and the mundane practices of household members performing and combining diverse forms of labour.

22.9

Chemical collectives: alternative designs for environmental health

Kim Kullman[1]

[1]*Geography, The Open University, Milton Keynes, UK (kim.kullman@open.ac.uk)*

This paper discusses the lifeworld of persons with multiple chemical sensitivities (MCS), a contested environmental illness whose symptoms are often undetectable using standard diagnostic equipment. Revolving around a pragmatist analysis of autobiographical writings, self-help guides, websites and other resources produced by MCS individuals to share knowledge about their condition, it provides new insight into the distinctive coping strategies cultivated by MCS groups to reduce exposure to a chemically saturated planet. Concentrating on the distinctive material culture and informal practices of making among MCS people, from handcrafted air filters to adapted clothing and buildings, the paper develops a geographical account of the diverse forms of indigenous expertise that environmentally ill individuals sustain to manage their situation and to deal with lacking support from the society. It argues that MCS collectives engage in speculative interventions into polluted ways of life, which can open alternative pathways for responses to environmental harms.

22.10

Public places in vertical Asian cities – insights from Tokyo and Singapore

Raphaël Languillon-Aussel[1]

[1]*Department of geography, University of Geneva, Uni-Vogt, Boulevard C. Vogt 66, 1211 Geneva (raphael.languillon@unige.ch)*

In the 2000s and the 2010s, verticality has been a new fronteer for urban growth, especially in Pacific Asia cities. “Vertical sprawl” that has resulted from it has extended cities in two directions: above ground level, and underground. The reasons of cities verticalization are well documented by the scientific literature: land scarcity, land price increasing strategy, disaster prevention (for underground), climate change adaptation… However, cities are not just about juxtaposition of buildings and urban forms: it result from interconnextion between spaces and social interactions between people living and working in it. In that context, connexion between the different layers and levels of vertical cities has becoming a key issue not just in a functionnal dimension, but also from a social, political and symbolic perspective.

In such vertical contexts, public spaces appear to be particularly problematic. If they are close to open spaces in a two-dimension city (especially in European cities), it is not the case anymore in vertical cities, where public spaces could be either underground or located in upper floors (including in urban canoppies and roof top).

The presentation aims to discuss the transformation of the nature of public places in vertical cities. The hypothesis consists in assuming that vertical public places are more relevant in Pacific Asia cities rather than European one because the notion is not initially correlated to open spaces in Asia (as it is in European cities). Assuming that, the author infers that verticalization of cities does not change the nature, the use, the sense or the perception of public space in Asia, contrary to what happens in European cities. The difference relies on the fact that thinking public space in Asia with a European perspective is missunderstanding the deep nature of Asian cities, where a public space is structurally, politically and phylosophically not based on the same criterias nor the same forms or uses.

Taking as case studies Tokyo and Singapore, respectively representating Chinese and Japanese cultural approaches of cities, urban verticality, and public spaces, the presentation will make comparison with European appraoches of public spaces in a vertical build up environment. The final goal is to determine if there would not be any lesson to learn from Asia concerning how to plan public spaces in vertical cities, reversing the transfer of urban models from East to West.

REFERENCES

Caballero, J. A., & Tsukamoto, Y. 2006: Tokyo Public Space Networks at the Intersection of the Commercial and the Domestic Realms, Journal of Asian Architecture and Building Engineering, 5-2, 223-231.

Cybriwsky, R., 1999: Changing patterns of urban public space: Observations and assessments from the Tokyo and New York metropolitan areas, Cities, 16-4, 223-231.

Hee, L., & Ooi G.L. 2003: The politics of public space planning in Singapore, Planning Perspectives, 18-1, 79-103.

Jonas, M. C. 2012: Private use of public open space in Tokyo A study of the hybrid landscape of Tokyo›s informal gardens, Journal of Landscape Architecture, 2, 18-29.

Languillon-Aussel, R. 2017: Verticalisation des quartiers d’affaires et maturité urbaine à Tokyo, Géocarrefour, 91-2, URL: https://journals.openedition.org/geocarrefour/10122.

Ooi G.L., & Hee, L., 2002: Public space and the developmental state in Singapore, International Development Planning Review, 24-4, 433–447.

Yuen, B., Yeh, A., Appold S.J & Ting, J. 2006: High-rise Living in Singapore Public Housing, Urban Studies, 43-3, 583-600.

Yuen, B., & Yien, W.N., 2005: Resident perceptions and expectations of rooftop gardens in Singapore, Landscape and Urban Planning, 73-4, 263-276.

22.11

Graffiti in Palestinian Refugee Camps: from palimpsest walls to public space

Clémence Lehec

Université de Genève & Université Grenoble-Alpes

This paper is the result of a doctoral thesis defended in June 2019 at Geneva University and Grenoble-Alpes University. Updating an article published in the *Articulo Journal of Urban Research* at the end of 2017, the focus will be on the Palestinian graffiti movement that developed in refugee camps as an act of resistance in the late 1960s and continues to this day. This movement was built as part of the struggle against Israeli occupation. To question an ephemeral aesthetic practice in a space where the urban is considered temporary, allows us to reflect on the way in which the inhabitants build a way of living without giving up their request for the right of return. The analysis of graffiti on the streets of the Dheisheh camp in Bethlehem reveals palimpsest walls that allow the refugee community to build common spaces in the political sense of the word. The walls then become a space for debate and the construction of history. Through an examination of visual elements on the walls of refugee camps today, I propose an understanding of the relationship to public space as one where politics is at play, outside of any institutional structures.

22.12

Space and citizenship

Marco Lupatini

Dipartimento Formazione e Apprendimento, Scuola Universitaria Professionale della Svizzera Italiana (DFA/SUPSI) Piazza San Francesco 19, CH-6600 Locarno
Department of Geosciences, University of Fribourg, Chemin du Musée 4, CH-1700 Fribourg

As sustained by Arendt (1960) human action has a deep spatial dimension, which determines and characterize it, and, as she affirms, which confer to it its sense. As revealed by the same author (Arendt, 2003) space is also the result of interaction between people, and it is in this space that all human affairs happen. Lussault (2007), on his side, stresses that human action does not occur on space but with it, and he considers space as an operator influencing human action, and modeling it.

The strong link between human acting and space plays an important role in the education of a dynamic citizen. This concept is here defined in reference to Audigier (2002) and Staeheli (2011) as a person affirming a chosen not an inherited belonging. The link mentioned before, also enters in the formation of a spatial actor. Concept interpreted here in the sense given by Lussault (2007) as individual moved by the need and the will to act, and therefore provided with strategic competencies, margins of maneuvers, capacities of arbitrage and with the capacity to act formed by and for socialization. This link finally also puts the education of a dynamic citizen and the formation of a spatial actor in the frame of the political. Concept described by Bedorf and Röttgers (2010) as a space where different visions regarding the functioning of common life interact.

The presentation aspires to contribute to the reflection on the role of geography teaching in building in future citizens the conscience of the spatiality of human acting. This aim is reached on the base of materials collected both in the frames of a doctoral thesis in progress at the University of Fribourg, and of the professional experience of the author as teachers' trainer at the DFA in Locarno. The selected data contains oral and written productions realized by pupils between 11 and 17 years old, during geography teaching sequences based on the introduction of spatial controversies.

The methodology used for the thesis is the one defined as action research in education (Guay & Prud'homme, 2011). As they stress this methodology could be assimilated to a teachers' training practice. For this reason in spite of the different contexts the collected materials do not substantially differ.

REFERENCES

Arendt, H. (1960). Vita Activa oder vom tätigen Leben. Stuttgart: Kohlhammer.
Arendt, H. (2003). Was ist Politik ? : Fragmente aus dem Nachlass (Piper ed.). München Zürich: Piper.
Audigier, F (2002). L'éducation civique dans l'école française. in Civic and Economic Education in Europe, 2), 8–28
Bedorf, T., et Röttgers, K. (2010). Vorwort. In T. Bedorf, et K. Röttgers (Eds.), Die politische Differenz: zum Denken des Politischen bei Nancy, Lefort, Badiou, Laclau und Agamben (1. Auflage ed., pp. 7–10). Frankfurt am Main: Suhrkamp.
Guay, M.-H. & Prud'homme, L. (2011). La recherche-action. In T. Karsenti, et L. Savoie-Zajc (Eds.), La recherche en éducation : étapes et approches (3e éd., pp. 183-211). Sherbrooke: Éd. du Renouveau Pédagogique Inc. Lussault, M. (2007). L'homme spatial. La construction sociale de l'espace humain. Paris: Éd. du Seuil
Staeheli, L. A. (2011). Political geography: Where's citizenship? Progress in Human Geography, 35 (3), 393–400

22.13

Tourism Troubles: Feminist political ecologies of land and body in the making of residential tourism space in Panama

Sharlene Mollett

University of Toronto, Department of Human Geography, Centre for Critical Development Studies and the Department of Geography and Planning
(sharlene.mollett@utoronto.ca)

In this address, I examine the ways in which settler colonial logics shape residential tourism development on the Atlantic Coast of Panama. With a focus on the Bocas del Toro archipelago, I entangle feminist political ecological assertions that struggles over nature are embodied struggles with anticolonial feminist understandings of land and body, drawn from a fusion of postcolonial, decolonial and black feminist thought, embedded in the concept of postcolonial intersectionality. Through this lens, I seek to illustrate three key findings. First, settler colonial place making in Bocas is partially articulated in the legal geographies of the Panamanian state's tourism-as-development strategy, a process that invites foreign land ownership. Second, critical development studies in Latin America tends to center indigenous women's livelihoods and rights as emblems of gender mainstreaming and social inclusion. By contrast, I focus on Afro-Panamanian women and illustrate, through ethnographic testimonies, the ways in which settler logics of elimination manifest in the naturalization of Afro-Panamanian women as "maids". Such imaginative and material geographies reflect conventional racial-sexual-gendered histories that take for granted black female servitude and landlessness on the Atlantic coast. Lastly, I will show, notwithstanding the coast's violent past (and present) that a deeper engagement with place-based histories makes *postcolonial intersectional* feminist theorizing a requirement for sustainable development policy with the concomitant recognition that any sustainable tourism policy that erodes local peoples control over land and bodies is not, in fact, *sustainable*. Thus, I argue that Afro-Panamanian women's participation in Bocas' tourism enclave--a project that seeks to erase indigenous and black relations to coastal lands and foster their subjection to foreign nationals--is simultaneously an articulation of their rights to remain on the coast.

22.14

How we theorised cities from the North and South but forgot to think with the Easts

Martin Müller[1]

[1]*Institut de Géographie et Durabilité, Université de Lausanne, CH-1015 Lausanne (martin.muller@unil.ch)*

Over the past decade, global urbanism has seen a distinct move towards embracing cities outside the Global North for theory-building and comparative research. In this presentation I welcome this turn towards more inclusive theorizing, but show that the binary geographical imagination of a Global North and a Global South has created its own silences and erasures around what could be termed the Global East – cities and countries, such as those in the former Second World, that fall between North and South. The presentation traces the genealogy of that erasure and outlines the political urgency of 'thinking with a global East' in global urbanism. In so doing, I argue not for an Eastern urbanism, but for a renewed global urbanism that is more than northern.

REFERENCES

Müller, Martin. 2018. "In Search of the Global East: Thinking between North and South." Geopolitics 0 (0): 1–22. doi:10.1080/14650045.2018.1477757.

Müller, Martin. 2019. "Goodbye, Postsocialism!" Europe-Asia Studies 71 (4): 533–550. doi:10.1080/09668136.2019.1578337.

22.15

Everyday waste-based practices: exploring politics of space and place from an informal neighbourhood in Cartagena, Colombia

Laura Neville[1]

[1]*Institute of Geography and Sustainability, University of Lausanne, Mouline – Géopolis, CH-1015 Lausanne (laura.neville@unil.ch)*

Cartagena is a city marked by profound socio-spatial segregation and socio-racial inequality. Its urban development is characterised by displacements of population, both within the city and to the city, significantly affecting the afro-descendent population, who settled largely in the city's so-called periphery. This paper draws upon ethnographic work in an informal neighbourhood located on the edge of the city's main waterbody by focusing on residents' everyday waste-based practices. In this neighbourhood characterised by low state presence and lacking access to urban services, waste appears as more than a discard. For instance, the neighbourhood is expanding due to the construction of informal settlements by filling the waterbody with waste materials. In parallel to this process, waste-based initiatives to improve the neighbourhood's built environment have emerged with the support of corporate social responsibility funded entities.

Against this background, the paper seeks to approach the social production of urban space through the lens of waste from a decolonial urban theory perspective. It engages with Massey's (2005) understanding of space as relational to read residents' everyday waste-based practices in the urban space. The paper's first objective is to shed light on the complexities and paradoxes of the everyday waste-based practices mobilised by residents of an informal neighbourhood. The second objective is to consider what this case suggests about the understanding of politics of space and place from the city margins in an urban neoliberal context.

REFERENCES

Massey, D., 2005: For space, London [etc.]: Sage Publications.

22.16

“We Do Pioneering Work”: Learning and Exemplification of New Technologies in a Digitalised Agriculture

Dennis Pauschinger

[1]*Institut de Géographie, Université de Neuchâtel, Espace Tilo-Frey 1, 2000 Neuchâtel (dennis.pauschinger@unine.ch)*

The digitalisation of agriculture is on the rise. From planting robots and crop management apps to disease detecting software and automated tractors, globally operating companies are presenting “smart farming” solutions as the new future of food production. Much academic and public attention, however, has been paid to how everyday urban life has become more digital, automated and structured by algorithms, often to exercise surveillance by both private and public actors. In geography, there has been much debate addressing how such new technologies and the accompanying policies have travelled globally and are implemented locally in the urban through different scales and specific spaces of learning and exemplification (e.g. McFarlane 2011; McCann & Ward 2011; Söderström 2014). There is way less literature and scientific inquiry of how these processes play out in the rural. Bringing the discussion to the sphere of a digital agriculture there is an opportunity to challenge the common understandings of how new technologies proliferate. This paper therefore draws upon empiricial data from a qualitative case study with a Swiss based but internationally operating start-up that has recently obtained the first authorisation in a joint effort between a coalition of private companies and public instituions to spray pesticides on vineyards and fruit plantations with their home made drone. The paper demonstrates in three main analytical sections 1) the actor-network, 2) the spatial dimensions, and 3) the entrepreneurial improvisation that co-produced in an assembling effort both the regulation and enablement of the sprayer drone. The example opens up the possibility of new understandings of how the exemplification, learning and implementation of new technologies are made possible.

REFERENCES

McCann, E.; Ward, K. (Eds.). 2011. Mobile Urbanism: Cities and the Policymaking in the Global Age. Minneapolis, MN: University of Minnesota Press.

McFarlane, C. 2011: Learning the City. Chichester: Wiley-Blackwell.

Söderström, O. 2014: Cities in Relation: Transnational Connections and Urban Development. Chichester: Wiley-Blackwell.

22.17

Virtual Resistance, Material Consequences: Countering State Projects in (Semi-) Authoritarian Russia

Sven Daniel Wolfe

Department of Geography and Sustainability, University of Lausanne, Quartier Mouline, CH-1015 Lausanne (svendaniel.wolfe@unil.ch)

Over the past decade, Russia's increasing authoritarianism (Gel'man 2015) has resulted in a number of dramatic confrontations between state agents and the general population. While street protests and (sometimes violent) police arrests are the most visible outcomes of these confrontations, the street and the square are not the only places where Russian dissent takes place. Beyond the physicality of marching in public places, the past years have seen a surge in oppositional voices on the Russian internet, taking shape in independent blogs and oriented around local issues. These are then propagated beyond their immediate territories – and indeed beyond Russian borders – through social media, including but not limited to YouTube, Instagram, Twitter, and Facebook.

Building on research that identifies digital spaces as a new sphere for the political (Arora 2015; Vlavo 2012), this paper investigates the material impacts of virtual opposition. Unlike research that connects online activism with mass protest (Radchenko, Pisarevskaya, and Ksenofontova 2012), this paper focuses on the micro level, examining individuals who have engaged in virtual protest – often using the poor quality of urban infrastructure as a starting point – and exploring the consequences of their digital engagements. The paper contrasts the cases of Alexander Valov and Maria Motuznaya, an activist in Sochi and a resident of Barnaul, respectively, with those of Ilya Varlamov and Dmitry Ivanov, two of the Russian internet's most popular urban and political bloggers. On the basis of these four cases, the paper develops a typology of strategies engaged by Russian virtual activists in order to avoid punishment in the context of increasing political closure. It also details the responses of state agencies to these four individuals and explores why Varlamov and Ivanov are allowed to continue work while Valov is in prison and Motuznaya in exile.

REFERENCES

Arora, Payal. 2015. "Usurping Public Leisure Space for Protest: Social Activism in the Digital and Material Commons." *Space and Culture* 18 (1): 55–68. https://doi.org/10.1177/1206331213517609.

Gel'man, Vladimir. 2015. *Authoritarian Russia: Analyzing Post-Soviet Regime Changes*. Pittsburgh: University of Pittsburgh Press.

Radchenko, Darya, Dina Pisarevskaya, and Irina Ksenofontova. 2012. "The Logic of Virtual Protest: The Week After the 2011 Elections." *Forum for Anthropology and Culture*, no. 7: 1–17.

Vlavo, Fidele. 2012. "'Click Here to Protest' Electronic Civil Disobedience and the Imaginaire of Virtual Activism." *Cybercultures*, January, 125–48. https://doi.org/10.1163/9789401208536_009.

23. Human Geographies: Materials, Natures, Politics

Rony Emmenegger, Jevgeniy Bluwstein

Swiss Association for Geography (ASG)

TALKS:

23.1 Andriamahefazafy M.: Tuna materiality and the politics of access to tuna fisheries in the Western Indian Ocean

23.2 Bichsel, C.: Infrastructure on/off Earth

23.3 Bluwstein J.: Global history of conservation landscapism – colonizing landscapes, landscaping colonies

23.4 Brugger A.: Defenders of the flush toilet: the international political economy of feces.

23.5 Emmenegger R.: ROUNDTABLE: Social Science goes Underground: Inter- and Transdisciplinary Reflections

23.6 Florin I.: The utilization of the concept of landscape in the expansionist rhetoric of conservationists: discussions around the Half-earth and Nature needs half visions

23.7 Graefe O., Schlottmann A.: The commercialization of wildlife-conservation in Namibia: Selling nature to save it?

23.8 Hoti S.: Who is The Big Bad Wolf? A political ecology of wolf conservation in Switzerland

23.9 Imhof N.: Making and being rat: A case study of rats in Zurich

23.10 Junquera V., Grêt-Regamey A.: Crop boom dynamics: spatial and temporal dimensions

23.11 Kaufmann, C.: Assembling a Threat to Govern Uncertain Times: Mastering Mercury and Controling Bodies in Artisanal and Small-Scale Gold Extraction in Colombia

23.12 Keller R., Michel A., Backhaus N. : Landscape services: An additional approach to a plurality of worths in protected areas

23.13 Mollett S.: Tourism Troubles: Feminist political ecologies of land and body in the making of residential tourism space in Panama

23.14 Pörtner, E.: Governance of Mobile Phone Radiation

23.15 Rybarikova K.: Decision-making in conservation: Human-wildlife or human-human conflict mitigation? Insights from Namibia.

23.16 Sanchez, J.: Mapping the Urban Political Ecologies of water: concepts, objects and geographies

23.1

Tuna materiality and the politics of access to tuna fisheries in the Western Indian Ocean

Mialy Andriamahefazafy

Institute of Geography and Sustainability, University of Lausanne, Géopolis CH -1015 Lausanne (mialyzanah.andriamahefazafy@unil.ch)

Tuna fisheries in the Western Indian Ocean (WIO) greatly depend on the material behavior of undisciplined tuna resources, with different species being accessible through different types of technology, at different places, and at different depths of the ocean. Tuna becomes an 'actant' in the arena of negotiation of its access. One of the most interesting biophysical features of tuna is its continuous movement in the ocean in research of food. This movement has created social practices. At the country level, the movement of tuna in and out of national waters have created a seasonal fishing that fishers foresee every year. At the regional level, countries of the WIO region and distant water fishing nations are periodically discussing the management of tuna within various platforms. The movement of tuna calls for dialogue and negotiations. Power of different actors is in the end mediated by the materiality of the tuna, requiring fishing countries to negotiate access and providing host countries some leverage for economic development through tuna revenues. The paper expands on the role of materiality into the politics of access to tuna resources in the WIO.

REFERENCES

Bakker, Karen J., and Gavin Bridge. 2006. Material worlds? Resource geographies and the 'matter of nature'. Progress in Human Geography 30 (1):5-27.

Bear, C. 2013. Assembling the sea: materiality, movement and regulatory practices in the Cardigan Bay scallop fishery. Cultural Geographies 20(1): 21-41.

Bennett, J. 2010. Vibrant matter: a political ecology of things. Durham, NC: Duke University Press.

Campling, L. and E. Havice. 2014. The problem of property in industrial fisheries. Journal of Peasant Studies 41(5): 707-727.

Kaplan, David M., Emmanuel Chassot, Justin M. Amandé, Sibylle Dueri, Hervé Demarcq, Laurent Dagorn, and Alain Fonteneau. 2014. Spatial management of Indian Ocean tropical tuna fisheries: potential and perspectives. ICES Journal of Marine Science 71 (7):1728-1749.

23.2

Infrastructure on/off Earth

Christine Bichsel[1]

[1]Departement für Geowissenschaften, Universität Freiburg, Chemin du Musée 4, 1700 Freiburg, christine.bichsel@unifr.ch

This paper focuses on infrastructure for spacefaring. Spacefaring denotes political, economic and cultural practices that shape and are shaped by material or imaginary travels of humans and objects beyond the Earth's atmosphere. Existing social science research of outer space has so far given little attention to exploring the theme of infrastructure. In this paper, I explore the infrastructure of spacefaring both conceptually and on an empirical case study. I argue that a focus on infrastructure provides an entry point to examine the social and material relations, which go beyond, but always refer back to Earth.

23.3

Global history of conservation landscapism - colonizing landscapes, landscaping colonies

Jevgeniy Bluwstein

Department of Geosciences, University of Fribourg, Chemin du Musée 4, CH-1700 Fribourg (jevgeniy.bluwstein@unifr.ch)

Drawing on Kenneth Olwig's work, I suggest that we need to uncover a global history of landscapism to understand how landscape conservation is practiced today across different parts of the world. Whereas European political communities (called landscapes or *Landschaften* before the rise of the nation state) have been appropriated through internal colonization in the wake of European state formation on the continent, (settler-)colonies all over the world have been landscaped by European expansion and appropriation. This variegated global history and geography continues to underpin contemporary practices associated with landscape conservation. Given this global history of landscapism, contemporary landscape perceptions evince narratives of inclusive, peopled spaces in some regions (such as European cultural landscapes), while other regions are appropriated as landscapes that are perceived as inherently threatened by humans (such as African wild landscapes).

23.4

Defenders of the flush toilet: the international political economy of feces.

Andri Brugger

Université de Neuchatel and Eawag

Urban sanitation infrastructure (USI) solutions use the same design principles all over the world, even though the ecological, material and cultural preconditions vary greatly between places. How does USI mediate the relationship between humans, their feces and water and which politics are hindering wastewater to be reused in the 21st century? Through a historical analysis, I explore how the sector guiding paradigms in in USI have shifted over time from public health to environmental health to sustainability. Elaborating on the concept of global socio-technical regimes, I am interested in the co-evolution of social structures and technological artefacts such as centralized wastewater treatment into rigid configurations in which change towards locally adapted and potentially more sustainable infrastructure solutions seem impossible. Wastewater is truly unruly, used as fertilizers until the early 19th century, doomed in the last 150 years as hazardous and nasty it is on the verge of regaining spotlight as the sustainable resource to solve many grand challenges of the 21st century.

23.5

ROUNDTABLE: Social Science goes Underground: Inter- and Transdisciplinary Reflections

Rony Emmenegger

University of Basel, Petersgraben 52, 4056 Basel
(rony.emmenegger@unibas.ch)

Humans are entangled with the Earth not only horizontally, but also vertically. In recent years, this insight has turned the geological underground into a space of social science inquiry and exploration. It has led social scientists to ask, for instance, how the geological underground is opened up for "economic, social and political calculation" (Braun 2000) or how the according geological knowledge claims "affect human life" (Bobette & Donovan 2019). This roundtable explores what a growing body of social science literature on the geos and geo-social formations has to offer for our understanding of the ever-growing significance of the geological underground for modern society. It asks: How are geological knowledge practices shaped by social values, norms and institutional power relations? How does the epistemological uncertainty of geological knowledge shape political decision-making and contestations? And, how does the material constitution of the geos itself affect the way human-Earth relations can be organized? By exploring the relevance of these questions in a variety of specific cases, this roundtable aims at laying a basis for inter- and transdisciplinary reflection, exchange and collaboration.

23.6

The utilization of the concept of landscape in the expansionist rhetoric of conservationists: discussions around the Half-earth and Nature needs half visions

Ian Florin[1]

[1]*Institut des Sciences de l'Environnement – Pôle de Gouvernance de l'Environnement et Développement Territorial, Université de Genève, Boulevard Carl Vogt 66, CH-1205 Genève*

Over the past two decades, growing concerns have emerged about the limited capacity to achieve substantial conservation outcomes on a global scale with existing protected areas. In this context, radical visions to turn half of the earth into a system of interconnected protected areas have recently gained prominence among scientists and practitioners (Dinerstein et al., 2017 ; Wilson, 2016).

Drawing on the current discussions under the *Half-earth* and *Nature needs half* slogans, this paper explores how different definitions of landscape are mobilized in favor or against expansionist dynamics in conservation. On the one hand, I show how they are used to reconcile environmental, social, and economic objectives as well as to emphasize the need to consider natural processes beyond existing protected areas. On the other hand, I describe at how this view is challenged, notably by political ecologists who illuminate challenges in the planning of such visions and their social impacts.

REFERENCES

Dinerstein, E.,Olson, D., Joshi, A., Vynne, C., Burgess, N., Wikramanayake, E., Hahn, N., Palminteri, S., Prashant, H., Noss, R., Hansen, M., Locke, H., Ellis, E., Jones, B., Barber, C., Hayes, R., Kormos, C., Martin, V., Crist, E., Sechrest, W., Price, L., Baillie, J., Weeden, D., Suckling, K., Davis, C., Sizer, N., Moore, R., Thau, D., Birch, T., Potapov, P., Turubanova, S., Tyukavina, A., De Souza, N., Pintea, J., Brito, J., Llewellyn, A., Miller, A., Patzelt, A., Ghazanfar S., Timberlake, J., Klöser, H., Shennan-Fapcon, Y., Kindt, R., Barnekow Lillesø, J-P., Van Breugel, P., Graudal, L., Voge, M., Al-Shammari., K., Saleem, M. 2017 : An ecoregion-based approach to protecting half the terrestrial realm, BioScience, 67 (6), 534-545.

Wilson, E. 2016 : Half-earth, our planet's fight for life. Liveright (New York).

23.7

«Selling nature to save it? Nature conservation as a market in Namibia»

Olivier Graefe[1], Antje Schlottmann[2]

[1]*Université de Fribourg, Dep. de Géoscience, Chemin du Musée 4, CH-1700 Fribourg*
[2]*Institut für Humangeographie, Goethe-Universität Frankfurt a. M., Theodor-W.-Adorno-Platz 6, D-60629 Frankfurt am Main*

African wildlife has long been seen as a resource in form of ivory, skins, trophies, meat and has been integrated in capitalist market development since its beginning. This integration lead to the depletion of wildlife in certain regions or of entire species. Only parks and reserves first created as wildlife sanctuaries succeeded to protect habitats and species under threat. While these sanctuaries have been created and maintained at high financial (not to mention social) costs for the colonial and post-colonial public authorities, wildlife conservation has been turned in a source of profit. Parks and reserves have transformed into tourist attractions and wildlife has been increasingly privatized to different extend. Services like wildlife experiencing, viewing and hunting is dominated by private entrepreneurs and companies but also by nature conservation NGOs. The trade for African wildlife emerged in form of auctions and sells by the catalogues for hunting concessions, trophies and life animals for the purpose of breeding and wildlife viewing in private game reserves. It is estimated that 80 % of the wildlife in Namibia is now in possession of private game farmers and reserves.
This paper will explore the different types of commercialization of wildlife in Namibia and focuses on the changing human – animal relationships induced by the market value given to species.

23.8

Who is The Big Bad Wolf? Exploring social dimensions of human-wildlife relationships : A political ecology of wolf conservation in Switzerland

Shqipe Hoti[1]

[1]Department of Geosciences, University of Fribourg, Chemin du musée 4, CH-1700 Fribourg (shqipe.hoti@unifr.ch)

Wolf recovery in many European countries requires conservation and management in order to ensure its coexistence with humans. Conservationists' agendas, practices, ideology and values may however compete with groups, which do not share the same values and agendas and/or may even be negatively impacted by them. The aim is here to explore the ensuing human-wildlife relationships and conflicts. As the present research is inscribed in a political ecology perspective, the focus is mainly put on groups and communities that are most exposed and impacted by wolf recovery (Hill, 2017) in Switzerland, thus farmers who practice summer mountain pasture.

Conservation programs' and regulations' success or failure depends on communities and stakeholders disposition to collaborate or not. If conservation agendas impact negatively or compete with interests of other interest groups, conflicts may arise and be expressed as conflicts with wildlife even if they are conflicts between humans about wildlife. Tangible material and economic costs due to depredation on livestock is one facet of the problem. This is however only the emerged tip of the iceberg, which conservationists concentrate on to bringing mitigation solutions. Nevertheless, unintended factors do play a much important role in problem perception as do the wildlife value orientations and power relations between human stakeholders. It is increasingly recognized in conservation research that these particular social dimensions and conflicts impact consequently conservation issues.

It is argued here that even if very weakly exposed to depredation, farmers are unhappy with the wolf situation. For them, more important concerns are the management practices and the herd protection measures perceived as imposed and not adapted. Furthermore, the underlying concerns are a lack of decision-making and freedom in the practice of their profession. This concern is, therefore, reinforced and becomes an identity-rooted problem as farmers become always more dependent on state subsidies due to economic changes in the agricultural field. Furthermore, changes in roles that these subsidies assign to them – thus from free producers towards more nature and biodiversity conservationists – are perceived as a threat to their identity and *illusio*. Consequently, these concerns are rather expressed as conflicts with wildlife, which represent a projection surface of underlying concerns, interests, values and needs.

REFERENCES

Hill, C.M., Webber, A.D., Priston, N.E.C. (eds) (2017). *Understanding Conflicts about Wildlife. A Biosocial Approach*, New York, Berghahn Books.

Hill, C. (2017) Introduction. Complex Problems: Using a Biosocial Approach to Understanding Human-wildlife Interactions, *in* Hill, C.M., Webber, A.D., Priston, N.E.C. (eds) *Understanding Conflicts about Wildlife. A Biosocial Approach*, New York, Berghahn Books: 1-14.

23.9

Making rat: Rethinking the city's relationship with nature

Imhof Nadja[1]

[1]*Université de Lausanne, Institut de géographie et durabilité, Mouline-Géopolis, CH - 1015 Lausanne (nadja.imhof@unil.ch)*

This presentation explores the management practices of urban rats in Zurich regarding their framing and placement within the socio-ecological environment. The long shared history between rats and humans has created an abundance of reactions, narratives, symbolic meanings and practices regarding rats. In a time where "nature" is called back into the city, rats are actively taken out with new and bigger pest control campaigns (Poon, 2018; Willsher, 2018). Despite the fact, that the non-dualist idea saying that humans and nature are inherently intertwined (Castree, 2001; Ginn & Demeritt, 2003; Zimmerer, 2000) has been widely accepted in the social sciences, urban politics of nature continue to focus on a certain type of nature in urban environments: green spaces, plants, bees and flowers. Clearly, the rat represents a part of a nature, that no one wants to have anywhere. Yet, they continue to exceed human efforts of managing and controlling them and thrive nevertheless.

Despite connecting the urban with nature and including some non-human actors, most of the urban research is neither post-dualistic nor post-human. Then again, the question of what belongs in post-dualist ecosystems and how to manage them is still a matter of debates in conservation of protected areas and urban natures alike (Braverman, 2015; Castree, 2014; Lorimer, 2015; Mansfield & Doyle, 2017). Following rats to the places they appropriate, continuously transgressing the material boundaries and social framings humans have established for them helps to understand how the politics of nature in urban settings work and how post-dualistic urban ecosystems could look like.

REFERENCES

Lanphere, M., & Pamic J. 1992: K-Ar and Rb-Sr ages of Alpine granite-metamorphic complexes in northern Croatia, Acta Geologica, 22, 97-111.

Sparica, M., Buzaljko, R. & Jovanovic, C. 1984: map sheet Nova Gradiska L 33-107, Osnovna geoloska karta SFRJ 1:100.000. Savezni geoloski zavod, Beograd.

Braverman, I. (2015). Wild Life: The Institution of Nature. Stanford, California: Stanford University Press.

Castree, N. (2001). Socializing Nature: Theory, Practice, and Politics. In N. Castree & B. Braun (Eds.), Social Nature: Theory, Practice, and Politics (pp. 1–21). Malden, MA: Blackwell Publishers.

Castree, N. (2014). Making Sense of Nature: Representation, Politics and Democracy. New York: Routledge.

Ginn, F., & Demeritt, D. (2003). Nature: A Contested Concept. In N. Clifford, S. Holloway, S. P. Rice, & G. Valentine (Eds.), Key Concepts in Geography (2nd ed., pp. 300–311). Retrieved from https://www.researchgate.net/publication/265007577_Nature_A_Contested_Concept

Lorimer, J. (2015). Wildlife in the Anthropocene: Conservation after nature. Retrieved from https://www.upress.umn.edu/book-division/books/wildlife-in-the-anthropocene

Mansfield, B., & Doyle, M. (2017). Nature: A Conversation in Three Parts. Annals of the American Association of Geographers, 107(1), 22–27. https://doi.org/10.1080/24694452.2016.1230418

Poon, L. (2018, August 9). Cities Aren't Smart Enough to Stop Rat Infestations. But That's About to Change. Retrieved August 13, 2018, from CityLab website: https://www.citylab.com/solutions/2017/08/smart-cities-fight-rat-infestations-big-data/535407/

Willsher, K. (2018, June 11). Parisian mayor launches "rat map" to tackle rodent menace. The Guardian. Retrieved from https://www.theguardian.com/world/2018/jun/11/paris-mayor-launches-rat-map-to-tackle-rodent-menace

Zimmerer, K. S. (2000). The Reworking of Conservation Geographies: Nonequilibrium Landscapes and Nature-Society Hybrids. Annals of the Association of American Geographers, 90(2), 356–369.

23.10

Crop boom dynamics: spatial and temporal dimensions

Victoria Junquera, Adrienne Grêt-Regamey[1]

[1]*Institute for Spatial Planning (IRL), Planning of Landscape and Urban Systems (PLUS), ETH Zürich, Switzerland (vjunquer@ethz.ch)*

Expansion of agricultural commodities is the leading cause of deforestation and an important driver of global change (DeFries et al., 2010; Foley et al., 2005; Gibbs et al., 2010). Many instances of large-scale agricultural expansion in recent decades – e.g., soybeans and sugarcane in South and Central America, or oil palm, rubber, and coffee in Southeast Asia – have taken place at very rapid rates, earning them the qualifier of commodity or crop "booms", (e.g., Fox and Castella, 2013; Gatto et al., 2015; Griffin, 2019; Hecht, 2005; Hetherington, 2013; Junquera and Grêt-Regamey, 2019; Mahanty and Milne, 2016; Meyfroidt et al., 2013). Understanding crop boom dynamics is thus essential for designing strategies to address global deforestation and ultimately global change. Crop booms exhibit characteristic dynamics, including non-linearity and unpredictability (Müller et al., 2014). Rapid initial expansion rates are followed by a slowdown and sometimes by a decline or "bust". Because crop booms cause far-reaching and frequently irreversible environmental and socioeconomic changes, they can be considered to cause land "regime shifts". Furthermore, crop booms are bounded in space and time. Spatially, they occur in landscapes defined by a number of factors, including geophysical, historical, cultural, and socioeconomic. Temporally, crop booms start with the adoption of the new crop and end when expansion significantly slows down or when the crop is replaced by a different land use. In this work, we explore questions around the spatiality and temporality of crop booms: What are the markers that define the spatial extent of a crop boom? What are the factors that influence this extent? What are the temporal features that define a boom, and what influences such dynamics? We draw from (i) the regime shifts literature, which has explained crop booms in terms of preconditions, triggers, and reinforcing mechanisms (Ramankutty and Coomes, 2016); (ii) empirical data on the northern Laos rubber boom, and (iii) case study literature on crop booms across geographic regions and commodity types. We propose preliminary conclusions on how a regime shifts lens can help define and explain the spatiality and temporality of crop booms.

REFERENCES

DeFries, R.S., Rudel, T., Uriarte, M., Hansen, M., 2010. Deforestation driven by urban population growth and agricultural trade in the twenty-first century. Nat. Geosci. 3, 178–181. https://doi.org/10.1038/ngeo756

Foley, J.A., Defries, R., Asner, G.P., Barford, C., Bonan, G., Carpenter, S.R., Chapin, F.S., Coe, M.T., Daily, G.C., Gibbs, H.K., Helkowski, J.H., Holloway, T., Howard, E.A., Kucharik, C.J., Monfreda, C., Patz, J.A., Prentice, I.C., Ramankutty, N., Snyder, P.K., 2005. Global Consequences of Land Use. Science (80-.). 309, 570–574. https://doi.org/10.1126/science.1111772

Fox, J., Castella, J.-C., 2013. Expansion of rubber (Hevea brasiliensis) in Mainland Southeast Asia: What are the prospects for smallholders? J. Peasant Stud. 40, 155–170. https://doi.org/10.1080/03066150.2012.750605

Gatto, M., Wollni, M., Qaim, M., 2015. Oil palm boom and land-use dynamics in Indonesia: The role of policies and socioeconomic factors. Land use policy 46, 292–303. https://doi.org/10.1016/j.landusepol.2015.03.001

Gibbs, H.K., Ruesch, A.S., Achard, F., Clayton, M.K., Holmgren, P., Ramankutty, N., Foley, J.A., 2010. Tropical forests were the primary sources of new agricultural land in the 1980s and 1990s. Proc. Natl. Acad. Sci. 107, 16732–16737. https://doi.org/10.1073/pnas.0910275107

Hecht, S.B., 2005. Soybeans, development and conservation on the Amazon frontier. Dev. Change 36, 375–404. https://doi.org/10.1111/j.0012-155X.2005.00415.x

Hetherington, K., 2013. Beans Before The Law: Knowledge Practices, Responsibility, and the Paraguayan Soy Boom. Cult. Anthropol. 28, 65–85. https://doi.org/10.1111/j.1548-1360.2012.01173.x

Junquera, V., Grêt-Regamey, A., 2019. Crop booms at the forest frontier: Triggers, reinforcing dynamics, and the diffusion of knowledge and norms. Glob. Environ. Chang. 57. https://doi.org/10.1016/j.gloenvcha.2019.101929

Mahanty, S., Milne, S., 2016. Anatomy of a boom: Cassava as a 'gateway' crop in Cambodia's north eastern borderland. Asia Pac. Viewp. 57, 180–193. https://doi.org/10.1111/apv.12122

Meyfroidt, P., Vu, T.P., Hoang, V.A., 2013. Trajectories of deforestation, coffee expansion and displacement of shifting cultivation in the Central Highlands of Vietnam. Glob. Environ. Chang. 23, 1187–1198. https://doi.org/10.1016/j.gloenvcha.2013.04.005

Müller, D., Sun, Z., Vongvisouk, T., Pflugmacher, D., Xu, J., Mertz, O., 2014. Regime shifts limit the predictability of land-system change. Glob. Environ. Chang. 28, 75–83. https://doi.org/10.1016/j.gloenvcha.2014.06.003

Ramankutty, N., Coomes, O.T., 2016. Land-use regime shifts: An analytical framework and agenda for future landuse research. Ecol. Soc. 21. https://doi.org/10.5751/ES-08370-210201

23.11

Frames of recognition, ASM formalization and renegotiation of state presence in Colombia

Christoph Kaufmann[1] & Muriel Côte[1]

[1]*Political Geography, University of Zurich, Winterthurerstr. 190, 8057 Zurich, christoph.kaufmann@geo.uzh.ch*

Colombia's economy increasingly relies on a neoliberal extractivist logic for development and the department of Antioquia is its main gold producer. The mines in Segovia and Remedios are particularly productive, contributing approximately 30 percent to the yearly gold extraction in Antioquia (Veiga and Marshall 2017:225). Gold extraction and commodification are also entangled with the armed conflict, as they provide criminal actors with financial income, possibilities for money laundering, and the establishment of public authority (Massé and Le Billon 2017; Rettberg and Ortíz-Riomalo 2016). Formalization and subcontracting of mining activities are key strategies of government institutions to clarify and stabilize access patterns to mineralized land, severe the ties between gold and the armed conflict, and territorialize environmental and safety regulations. Yet, despite the strategic importance of the mining activities in Segovia and Remedios, the power over extraction in this mining region remains highly contested.

The majority of the subsoil in Segovia and Remedios has been privatized, but informal mining persists. Mining titles where different forms of gold extraction overlap are key sites where the frames of recognition (Butler 2009) for artisanal and small-scale gold mining are being negotiated (Côte and Korf 2018). So as to establish control over extraction in this context of regulatory plurality, governmental institutions and title holders advocate for operation contracts (*contratos de operación*) where the title holder allows previously informal miners to extract ore from a part of the mining title. In these schemes, the subcontracted miners manage the everyday mining operations, while the title holder takes care of licenses, processing, and commercialization.

Examining dynamics of artisanal and small-scale mining (ASM) formalization and subcontracting helps to get a sense of the role that ASM plays in the process of a reaffirmation of state control over gold extraction and a renegotiation of political order in a context of macro-political transitions. In this paper, we analyze the construction of frames of recognition for ASM in legal frameworks and the effects of these on mining practices in Segovia and Remedios. We argue that these frames of recognition create more rather than less contestation and violence, that the room for ASM recognition is shrinking, and that this contributes significantly to the invisibilization and criminalization of mining practices that do not 'fit' the state-sanctioned view on extractivism anymore.

REFERENCES

Butler, Judith. 2009. *Frames of War: When Is Life Grievable?* London; New York: Verso.

Côte, Muriel and Benedikt Korf. 2018. "Making Concessions: Extractive Enclaves, Entangled Capitalism and Regulative Pluralism at the Gold Mining Frontier in Burkina Faso." *World Development* 101:466–76.

Massé, Frédéric and Philippe Le Billon. 2017. "Gold Mining in Colombia, Post-War Crime and the Peace Agreement with the FARC." *Third World Thematics: A TWQ Journal* 1–19.

Rettberg, Angelika and Juan Felipe Ortíz-Riomalo. 2016. "Golden Opportunity, or a New Twist on the Resource-Conflict Relationship: Links Between the Drug Trade and Illegal Gold Mining in Colombia." *World Development* 84:82–96.

Veiga, Marcello M. and Bruce G. Marshall. 2017. "Teaching Artisanal Miners about Mercury Pollution Using Songs." *The Extractive Industries and Society* 4(4):842–45.

23.12

Landscape services: An additional approach to a plurality of worths in protected areas

Roger Keller, Annina Helena Michel, Norman Backhaus

Universität Zürich, Geographisches Institut, Winterthurerstrasse 190, 8057 Zürich

Nature and landscape conservation have been contested in various ways. For example, recent attempts to establish new national parks in Switzerland failed. Local residents turned down the projects at the ballots, even though the new approaches followed a "nature for/with people" understanding compared to a "nature for itself" conservation approach (Mace 2014; Michel & Backhaus 2019). The former emphasises the benefits people can draw from nature, which internationally became known as ecosystem services (Millennium Ecosystem Assessment 2005; IPBES 2018). While seen as a useful tool to assess qualities of environmental infrastructure and to sensitise a wider audience to conservation issues, it is also criticised for its monetary bases (Holmes & Cavanagh, 2016). Nowadays, international nature and landscape conservation policies (i.e. CBD or IPBES) often draw on to the ecosystem services approach. The term "landscape services" is related to "ecosystem services" but has a different background, is broader, and has a greater potential for transdisciplinary collaboration (Keller & Backhaus, 2019). Landscape services as a means for nature conservation can be regarded as a mechanistic approach that bears the risk of pitting one service and, consequently, landscape against each other. However, we define "service" more broadly as something that resonates with people when they engage with landscapes (Keller et al. 2019). It fosters discussions that go beyond "protect or not protect", which are shaped by and include a plurality of principles of worth (Michel & Backhaus 2019). Therefore, the landscape services approach can make "conservation" more flexible and inclusive of different perceptions. We will illustrate this with examples from Switzerland.

REFERENCES

Holmes, G., & Cavanagh, C. J. (2016). A review of the social impacts of neoliberal conservation: Formations, inequalities, contestations. *Geoforum*, *75*, 199-209.

IPBES (2018): The IPBES regional assessment report on biodiversity and ecosystem services for Europe and Central Asia. M. Fischer, M. Rounsevell, A. Torre-Marin Rando and A. Mader (eds.). Bonn, IPBES secretariat: 892.

Keller, R., & Backhaus, N. (2019). Integrating landscape services into policy and practice – a case study from Switzerland. *Landscape Research*, *online*.

Keller, R., Clivaz, M., Backhaus, N., & Reynard, E. (2019). *Landschaftsleistungen in Landschaften von nationaler Bedeutung: Forschungsbericht mit Handlungsempfehlungen für Bund, Kantone, Gemeinden, NGOs und Bewirtschaftende*. Zürich: Geographisches Institut der Universität Zürich, Institut de géographie et durabilité de l'université de Lausanne.

Mace, G. M. (2014). Whose conservation? Changes in the perception and goals of nature conservation require a solid scientific basis. *Science*, *345*, 1558-1560.

Michel, A. H., & Backhaus, N. (2019). Unraveling reasons for failed protected areas: Justification regimes and principles of worth in a Swiss national park project. *Environmental Values*, *28*, 171-190.

Millennium Ecosystem Assessment (2005): Ecosystems and human well-being: Synthesis. Washington DC, Island Press.

22.13

Tourism Troubles: Feminist political ecologies of land and body in the making of residential tourism space in Panama

Sharlene Mollett

University of Toronto, Department of Human Geography, Centre for Critical Development Studies and the Department of Geography and Planning
(sharlene.mollett@utoronto.ca)

In this address, I examine the ways in which settler colonial logics shape residential tourism development on the Atlantic Coast of Panama. With a focus on the Bocas del Toro archipelago, I entangle feminist political ecological assertions that struggles over nature are embodied struggles with anticolonial feminist understandings of land and body, drawn from a fusion of postcolonial, decolonial and black feminist thought, embedded in the concept of postcolonial intersectionality. Through this lens, I seek to illustrate three key findings. First, settler colonial place making in Bocas is partially articulated in the legal geographies of the Panamanian state's tourism-as-development strategy, a process that invites foreign land ownership. Second, critical development studies in Latin America tends to center indigenous women's livelihoods and rights as emblems of gender mainstreaming and social inclusion. By contrast, I focus on Afro-Panamanian women and illustrate, through ethnographic testimonies, the ways in which settler logics of elimination manifest in the naturalization of Afro-Panamanian women as "maids". Such imaginative and material geographies reflect conventional racial-sexual-gendered histories that take for granted black female servitude and landlessness on the Atlantic coast. Lastly, I will show, notwithstanding the coast's violent past (and present) that a deeper engagement with place-based histories makes *postcolonial intersectional* feminist theorizing a requirement for sustainable development policy with the concomitant recognition that any sustainable tourism policy that erodes local peoples control over land and bodies is not, in fact, *sustainable*. Thus, I argue that Afro-Panamanian women's participation in Bocas' tourism enclave--a project that seeks to erase indigenous and black relations to coastal lands and foster their subjection to foreign nationals--is simultaneously an articulation of their rights to remain on the coast.

22.14

Goverance of Mobile Phone Radiation: The Socio-Natures of Electromagnetics

Ephraim Pörtner[1]

[1]*Institut für Sozialanthropologie, Lerchenweg 36, CH-3012 Bern*

Mobile phones are pervasive in our lives and the infrastructure for the latest upgrade to 5G (after GSM I & II, UMTS 3G and LTE 4G) is currently being established in Switzerland and beyond. While the usage of phones itself appears for most of little concern, the establishment or upgrade of mobile phone masts is often met with fierce resistance. The stake in such resistance is usually the socio-nature of electromagnetics: the effects of constant exposure to radiation from mobile phone masts and its contested effects on human health and well-being. In the light of conflicting interests and expertise, governing mobile phone radiation becomes a complicated and ambiguous issue. In this contribution, I explore the material-discursive configurations of governing such radiation and the socio-natures of the electromagnetics at stake. And I suggest that the politics of invisible electromagnetic saturation in human environments can be considered an exemplar for risk goverance in the Anthropocene.

22.15

"Decision-making in conservation: human-wildlife or human-human conflict mitigation?" Insights from Namibia.

Katarina Rybarikova

Université de Fribourg, Dep. de Géoscience, Chemin du Musée 4, CH-1700 Fribourg

In a time threatened by climate change and undergoing biodiversity losses, the urge for conservation is at its strongest. Globally implemented policies addressing this issue are generally based on a biological framework compromised by important conceptual weaknesses and the neglect of a social perspective. Human-wildlife conflict (HWC) mitigation overlooks all too often conflicts occurring between the different human stakeholders around conservation, hindering decisions. In Namibia, a community-based natural resource management (CBNRM) is advertised as a silver bullet to tackle needs in conservation and simultaneously empower communities. An analysis of practices in such a system through a political ecology perspective questions the new approach of nature conservation. Establishing the complex constellation of identities affected by a HWC policy allows to first pinpoint the power relations involved and second situate what is at stake. As much as the commodification of nature generates an undeniable economic interest, the present work tries to emphasize that other types of logic must also be considered when conservation policies are to be discussed.

22.16

Mapping the Urban Political Ecologies of water: concepts, objects and geographies

Jérémie Sanchez[1]

[1]*Institut de Géographie et Durabilité, University of Lausanne, Bât. Géopolis, 1015 Lausanne (jeremie.sanchez@hotmail.com)*

This paper synthesizes the theoretical implications of my doctoral research on urban sanitation governance in Myanmar, which I am attempting to frame as an urban political ecological endeavor concerned with 'remaking urban environments' in more equitable and sustainable ways (Véron, 2006; Loftus, 2009). The paper starts by mapping the conceptual, thematic and geographical streams having been followed by scholars publishing in the growing epistemic community known as the "Urban Political Ecology of water" (UPEW) since the 1990s. Second, the paper explores the thematic and geographical gaps that sprinkle the map of UPEW, to show that research on peculiar political-economic contexts – such as Myanmar – and particular political-material nexuses – such as wastewaterscapes – remains rare in UPEW. Third, the paper engages with the empirical shortcomings of UPE as a political project, to suggest that a more practice-oriented and transdisciplinary approach to our fields and writings might have increased potential to fulfill UPE's 'great promises' (Swyngedouw & Kaïka, 2014).

REFERENCES

Loftus, A. (2009). Rethinking Political Ecologies of Water. Third World Quarterly, 30(5), 953–968.

Swyngedouw, E., & Kaika, M. (2014). Urban Political Ecology. Great Promises, Deadlock… and New Beginnings? Documents d'Anàlisi Geogràfica, 60(3).

Véron, R. (2006). Remaking urban environments: the political ecology of air pollution in Delhi. Environment and Planning A, 38(11), 2093–2109.

24. The limits to Earth: thinking social-ecological transitions in a post-extractive economy +

Patrick Bottazzi, Sebastien Boillat

TALKS:

24.1 Augstburger H., Jacobi J., Schwilch G., Rist S.: Agroecosystem Service Capacity Index – A methodological approach

24.2 Boillat S., Sabaly I.K., Bottazzi P.: The agroecological transition in Senegal: a multi-level perspective based on social networks

24.3 Bottazzi P., Boillat S.: Working mitigation and adaptation: rethinking human labour in the age of global environmental change

24.4 Ceddia M.G.: Financialization of agriculture as a spatio-temporal fix to over-accumulation: wealth concentration spurs cropland expansion in the Global South

24.5 Daniel D.: Re-structured Sugar Lands as Governable Spaces

24.6 Dong R. : Discussion on Key Issues of Ecological Planning in New Urban District

24.7 Ellision D.: The Carbon-Water-Energy-Climate Nexus and Forest-Water-People-Climate Systems

24.8 Hanbury H., Moser S., Bader C., Neubert S.: The potential contribution of work time reduction to a post-extractive economy

24.9 Natia J.A., Adams T.: Governing underground resources: Decentralisation, Resource Regimes and Regulatory Complexities in Ghana

24.10 Saadé-Sbeih M., Boistel R.: Geography of Life Cycle Assessment

25. Towards the sustainable management and governance of land resources and land systems

Chinwe Ifejika Speranza, Desiree Daniel, Chidiebere Ofoegbu, Ademola Adenle

TALKS:

25.1 Ademola A.A., Ifejika-Speranza C.: Land Degradation Dynamics in the Nigerian Guinea Savannah Social-Ecological System between 2003-2018.

25.2 Bussard J. : Poster Teaser Introduction: Is tourism compatible with an adequate protection of the geomorphological heritage?

25.3 Ellison D.: Promoting Resilience in the Sahel: The Great Green Wall

25.4 Geiser A.: Farmers' response to agri-environmental governance in Southland, New Zealand

25.5 Inguaggiato C., Tschopp M., Ceddia G., Dimitris C.: Governance structures and competing models on land use: a policy network study of forest law in Salta

25.6 Morenikeji G., Livinus O., Adesina E.A.: Spatial and Temporal Changes in Land Use Land Cover (LULC) and Implications for Food Security in Mararaba Area of Nassarawa State Nigeria

25.7 Oberlack C., Myint W., Messerli P., Gerber J.D.: Governance in telecoupled land systems: the case of Thilawa Special Economic Zone, Myanmar

25.8 Ofoegbu C., Ifejika-Speranza C.: Making Forest Management Work for the Actualization of SDGs and Climate Protection

25.9 Tschopp M., Bardsley N., Inguaggiato C., Graziano C.: Silvopastoral practises adoption by smallholders and private company: is land sharing a solution to stop deforestation in the Chaco Salteño?

25.10 Zepharovich E., Ceddia G.M., Rist S.: Social multi-criteria evaluation of land-use scenarios: Comparing sustainability and environmental justice criteria

POSTERS:

P 25.1 Bussard J.: Is tourism compatible with an adequate protection of the geomorphological heritage?

24.1

Agroecosystem service capacity index – A methodological approach

Horacio Augstburger[1], Johanna Jacobi[2], Gudrun Schwilch[3], Stephan Rist[1,4]

[1]*University of Bern, Centre for Development and Environment (CDE), Hallerstrasse 10; 3012 Bern*
horacio.augstburger@cde.unibe.ch
[2]*University of Bern, Centre for Development and Environment (CDE), Hallerstrasse 10; 3012 Bern*
johanna.jacobi@cde.unibe.ch
[3]*University of Bern, Centre for Development and Environment (CDE), Hallerstrasse 10; 3012 Bern*
gudrun.schwilch@cde.unibe.ch
[4]*University of Bern, Institute of Geography & Centre for Development and Environment (CDE), Hallerstrasse 10; 3012 Bern*
stephan.rist@cde.unibe.ch

Sustainable food systems (FS) require providing food and other goods and services to humans satisfying food security, right to food, income, social justice and resilience, without degrading human health and hiving high environmental performance. The environmental performance of FS can be evaluated using Life Cycle Assessment. However, research on the impact that FS activities, e.g. crop production have on the capacity of farm-based agroecosystems to provide goods and services to humans is still incipient. Our underlying aim was to understand how FS impact on the provision of agroecosystem services and how this relates to the environmental performance of FS, as a basis for supporting decision-making on how to make FS more sustainable. We propose the Agroecosystem Service Capacity (ASC) as a method for assessing farm-based agroecosystem services, it builds on the Ecosystem Service Matrix by Burkhard et al. (2009) and assesses land cover classes against 20 agroecosystem services. The method was applied to eighteen farm-based agroecosystems in Bolivia and Kenya. Here we present two examples for exploring its potentials and limitations. The ASC operates on the basis of land cover class units and permits the calculation of an aggregate ASC-index for farm-based agroecosystems forming part of a specific FS.

KEY WORDS: Agroecosystems, agroecosystem services, land cover classes, food system

24.2

The agroecological transition in Senegal: a multi-level perspective based on social networks

Sébastien Boillat[1], Ibrahima Khalil Sabaly[2], Patrick Bottazzi[1]

[1]*Institute of Geography, University of Bern, Hallerstrasse 12, CH-3012 Bern, Switzerland (sebastien.boillat@giub.unibe.ch)*
[2]*Initiative Prospective Agricole et Rurale, Kër Jacques Faye, Immeuble Bilguiss, 67, Rond-Point VDN - Ouest Foire, Dakar, Sénégal*

Agroecology has the ambition of ensuring food sovereignty while reducing conventional inputs, enhancing ecological processes and increasing social justice in food systems (Gliessman 2016). Its implementation represents a key social-ecological transition towards a post-extractive economy.

In West Africa, NGOs and farmer organizations are promoting agroecology as a means to increase social-ecological resilience and fight poverty. Nevertheless, the up-scaling of agorecological practices and networks has remained relatively limited in the region. The case of Senegal is particularly emblematic with a large agroecological support network that contrasts with the rather limited adoption of practices on the ground.

We characterize the agricultural regime in Senegal using the multi-level perspective (MLP) on socio-technical transitions (Geels and Schot 2007) and use social network analysis to identify lock-ins that hinder the up-scaling of agroecology in the country. Our findings show that first, these lock-ins are enhanced by the national agricultural regime, which consists of firmly established structures such as agricultural policies, education and extension networks, and supply chains all promoting high-input, conventional agriculture. Furthermore, this regime is inserted within a wider landscape of supporting international organizations, international financial institutions and bilateral cooperation agencies around the “feed Africa” discourse. However, we also found that lock-ins are contained within the structure of technological innovation niches themselves, in this case the networks promoting agroecology in Senegal. Niches necessarily need protected conditions to develop. In Senegal, these protected spaces are highly dependent of international non-governmental support networks in both economic and ideological terms. While international networking is rather positively framed, we show that it also bears risks that may hinder the mainstreaming of agroecology, including 1) high fragmentation of agroecological initiatives in both spatial and temporal terms, 2) the reproduction of disagreements and divides around the development of agroecology that exist elsewhere, and 3) the deficient conceptualization of the labor issue in agriculture.

Based on these findings, we identify some leverage points and make recommendations on how to mainstream agroecology in the context of West Africa in general and Senegal in particular.

REFERENCES

Geels, F. and Schot, J. 2007: Typology of sociotechnical transition pathways. Research Policy, 36, 399-417.

Gliesmann, S. 2016. Transforming food systems with agroecology. Agroecology and sustainable food systems, 40, 3, 187-189.

24.3

Working mitigation and adaptation: rethinking human labour in the age of global environmental change

Patrick Bottazzi[1], Sebastien Boillat[1]

[1]*Institute of Geography, University of Bern, Hallerstrasse 12, CH-3012 Bern (patrick.bottazzi@giub.unibe.ch)*

Meeting the challenges of integrated mitigation and adaptation to global environmental change will have tremendous consequences on human labour, although this dimension is usually overlooked. According to a recent ILO estimate, millions of jobs will be lost and even more created by 2030 in several sectors such as circular economy or energy transition (ILO 2018). Such optimistic job creation scenario will nevertheless require profound socio-economic, political and physical transformations. First, restricting the use of fossil fuel energy will have strong consequences on the quality and the quantity of labour inputs required to fulfil fundamental human needs. Second, the increasing instability and unreliability of agro-ecosystems due to extreme climate variability, loss of biodiversity and land degradation will hardly continue to provide food for 7 to 9 billion of people without adequate adaptive measures. Third, there are strong contradictions between corporate financial interests, oligarchic governance and the stake of human adaptation.

For example, a transition from agro-industrial farming to low input farming might require a large share of the human population to integrate the production of food in their everyday work activity. Such a radical change in the agrarian and social structures could be supported by small-scale self-govern communities producing their own adaptation strategies but could also be led by authoritative power structures with consequences on human rights.

To anticipate these multiple transformations, we postulate that labour demand, type of work and social organizations must be re-articulated to fulfill fundamental needs in a post-extractive world increasingly affected by environmental hazards: What are the main human labour transformations we can expect in integrated mitigation and adaptation measures? How can workers emancipate from corporate financial interests, leading to increasing pressures on workers' life quality and their capacity to act according to the emergency of environmental challenges? Adapting labour in view to meet contemporaneous social-ecological challenges requires not only technical innovations but also societal transformations that can enable greater workers' autonomy, help generate new capabilities and establish new modes of recognition and valuation of workers' social and ecological contribution. The emerging fields of environmental labour studies and the political ecology of work help us defining some pathways of understanding.

REFERENCES

ILO (2018). World employment and social outlook 2018. Greening with jobs., ILO.

24.4

Financialization of agriculture as a spatio-temporal fix to over-accumulation: wealth concentration spurs cropland expansion in the Global South

Michele Graziano Ceddia[1]

[1]*Centre for Development and Environment, University of Bern, Mittelstrasse 43, CH-3012 Bern (graziano.ceddia@cde.unibe.ch)*

Agricultural expansion remains the most important proximate cause of deforestation in the Global South, particularly in tropical areas (Aide et al., 2013), with important consequences on carbon emissions, loss of biodiversity and other ecosystem's functions (Baccini et al., 2017; Giam, 2017). The increasing importance of flex-crops commodities (i.e., crops which are suited for both food and non-food uses, like soya, sugar cane and oil palm), is particularly significant in this respect, as it plays a crucial role in the expansion of the agricultural frontier. Over the last ten years there has also been increasing attention to the role of finance in general and foreign capital more in particular, in large scale land acquisitions in the Global South, which in turn put pressure on the remaining forests while exacerbating food security issues (Borras et al., 2012; Cotula, 2012; von Braum and Meinzen-Dick, 2009). These dynamics reflect the convergence of multiple crisis, namely financial, energetic, food and environmental. After the 2008 global financial crisis and the consequent decline in financial returns, investments in land (including both agricultural and urban uses) have become increasingly attractive. In this context, high net worth individuals (HNWI) may have played a role by diverting their wealth from the financial sector towards land and other real assets in search for better yields (Goda and Lysandrou, 2014; Lysandrou, 2011). This in turn suggests a potential effect of rising inequality and wealth concentration among the super-rich in stimulating investments in land. Agricultural expansion appears then as a response to over-accumulation problems through spatio-temporal fixes, in order to perpetuate the process of accumulation 'somewhere else' (Harvey, 2009, 2017). As Marx already noted *"the driving motive and determining purpose of capitalist production is the self-valorisation of capital to the greatest possible extent"* (Marx, 1990, p. 449).
In this paper, I address these issues by looking at 21 countries in Latin America and South East Asia, two regions heavily affected by large-scale land acquisitions, flex-crops area expansion and deforestation. I deploy a number of multivariate statistical models to assess a) whether wealth concentration in the hands of HNWI and the 'search for yield' promote foreign direct investment in agriculture (FDIA) towards the Global South; and b) the impact of FDIA, alongside other capital sources, on the expansion of flex-crops area. The preliminary results suggest that the concentration of wealth was the most important driver of FDIA. Additionally, FDIA are negatively correlated with short-term interest rates. Finally, FDIA have a strong positive impact on the expansion of flex-crop areas in the Global South. By combining the two effects, the results show that a 1% increase in wealth concentration among HNWI leads to a 2.4-10% expansion in the share of agricultural area planted with flex-crops. The results point to the urgenty of addressing wealth inequality in order to protect the remaining forests.

REFERENCES

Aide, T.M., Clark, M.L., Grau, H.R., López-Carr, D., Levy, M.A., Redo, D., Bonilla-Moheno, M., Riner, G., Andrade-Núñez, M.J., Muñiz, M., 2013. Deforestation and Reforestation of Latin America and the Caribbean (2001–2010). Biotropica 45, 262–271. https://doi.org/10.1111/j.1744-7429.2012.00908.x

Baccini, A., Walker, W., Carvalho, L., Farina, M., Sulla-Menashe, D., Houghton, R.A., 2017. Tropical forests are a net carbon source based on aboveground measurements of gain and loss. Science 358, 230–234. https://doi.org/10.1126/science.aam5962

Borras, S.M., Kay, C., Gómez, S., Wilkinson, J., 2012. Land grabbing and global capitalist accumulation: key features in Latin America. Can. J. Dev. Stud. Rev. Can. Détudes Dév. 33, 402–416. https://doi.org/10.1080/02255189.2012.745394

Cotula, L., 2012. The international political economy of the global land rush: A critical appraisal of trends, scale, geography and drivers. J. Peasant Stud. 39, 649–680. https://doi.org/10.1080/03066150.2012.674940

Giam, X., 2017. Global biodiversity loss from tropical deforestation. Proc. Natl. Acad. Sci. 114, 5775–5777. https://doi.org/10.1073/pnas.1706264114

Goda, T., Lysandrou, P., 2014. The contribution of wealth concentration to the subprime crisis: a quantitative estimation. Camb. J. Econ. 38, 301–327. https://doi.org/10.1093/cje/bet061

Harvey, D., 2017. Marx, Capital and the Madness of Economic Reason. Oxford University Press.

Harvey, D., 2009. The "New" Imperialism: Accumulation by Dispossession. Social. Regist. 40.

Lysandrou, P., 2011. Global Inequality, Wealth Concentration and the Subprime Crisis: A Marxian Commodity Theory Analysis. Dev. Change 42, 183–208. https://doi.org/10.1111/j.1467-7660.2010.01680.x

Marx, K., 1990. Capital: a critique of political economy. Penguin Classic.

von Braum, J., Meinzen-Dick, R., 2009. "Land Grabbing" by Foreign Investors in Developing Countries: Risks and Opportunities (IFPRI Policy Brief).

24.5

Re-Structured Sugar Lands as Governable Spaces

Desiree Christina Daniel[1]

[1]*Institute of Geography, University of Bern, Hallerstr. 12, CH-3012 (desiree.daniel@giub.unibe.ch)*

I am presenting how the dissolution of Caroni 1975, the former state-owned sugar company in Trinidad and Tobago, led to the emergence of small-scale agriculture in Caroni as new governable spaces from the political economy of sugar and its neo-liberalisation. The government's 2003 decision to close the state-owned sugar industry due to a lack of profitability and removal of preferential markets for sugar by the EU has shaped current farming activities. From the originally 75000 acres of Caroni lands available, approximately 7000 two-acre plots were distributed via lease agreements to former workers for agricultural usage, with the process of re-distribution still ongoing. With the lease, leaseholders are stipulated to keep the land under agricultural use. However, it is this stipulation that shapes agricultural usage, since the former workers have not all transition into small-holder farming. Thus, lands located within Caroni region are largely occupied by farmers who obtained access through the vernacular market. Those who are renting lands, from former workers usually receive oral permission. I argue that these new governable spaces while intended to advance agricultural productivity have transformed agricultural livelihoods, with farmers dependent on the vernacular land market for informal land access for their livelihoods.

Keywords: agriculture livelihoods, governable spaces, vernacular land market, informal land access

24.6

Discussion on Key Issues of Ecological Planning in New Urban District

Rencai Dong[1]

[1]*State Key Laboratory of Urban and Regional Ecology, Research Center for Eco-Environmental Sciences, Chinese Academy of Sciences, Beijing, 100085, China (dongrencai@rcees.ac.cn)*

As a major form of urbanization in China, the construction of new urban district is the process of transforming the original natural or semi-natural ecosystem into the urban artificial ecosystem from an ecological point of view. It is also the process of transformation, replacement and occupation of ecosystem type. When planning a new district, we should take priority to the forward-looking of its ecological planning, and prevent new ecological environment problems while promoting the overall ecosystem service capacity of the city. Based on the theoretical analysis of characteristics of ecosystem in the construction processes of new urban district, this paper summarized and concluded several key issues of ecological planning in the new district through several typical cases, and put forward the corresponding planning strategies and techniques, so as to provide theoretical support for ecological environmental protection of large-scale development in China.

24.7

The Carbon-Water-Energy-Climate Nexus and Forest-Water-People-Climate Systems

David Ellison[1,2,3]

[1]Adjunct Researcher, Sustainable Land Management Unit, Institute of Geography, University of Bern, Switzerland,
[2]Department of Forest Resource Management, Swedish University of Agricultural Sciences, Umeå, Sweden,
[3]Ellison Consulting, Baar, Switzerland

Rapid population growth, increasing agricultural production, mushrooming urban (and suburban) settlements and the continuous decline of forest cover bode ill for the delicate balance between carbon, water, energy and climate. People-forest-water-climate systems create ever more complex and potentially interactive feedbacks across the carbon-water-energy-climate nexus. Climate change can further exacerbate fundamental imbalances created by the anthropogenic modification of terrestrial landscapes. Globally warming temperatures and declining rainfall (in particular in the tropical and temperate regions), both compound and further aggravate an increasingly grim misuse of planetary resources. Where the forest-water debate is concerned, however, the scientific world remains divided into easily politicized camps, seemingly unable to observe and adequately understand what the other camp is up to. Despite this, as this presentation will demonstrate, many or most of the basic tools necessary for restoring at least a part of the delicate balance between the major ecosystem components of the carbon-water-energy-climate nexus are increasingly well understood and documented. Thus, an optimized ecosystem strategy could effectively use these tools to at least partially address the rapid advance of climate change and its increasingly threatening impacts on the availability of at-risk water resources, and on the million to billions of people and livelihoods who depend on them.

24.8

The potential contribution of work time reduction to a post-extractive economy

Hugo Hanbury[1], Stephanie Moser[1], Christoph Bader[1], Sebastian Neubert[1]

[1]*Centre of Development and Environment, University of Bern, Mittelstreasse 43, CH-3012 Bern (hugo.hanbury@cde.unibe.ch)*

Adaptation strategies in a post-extractive economy will inevitably aim at reducing per capita resource consumption. One such stategy that has received increased attention of late, is the reduction of work time. Both macro- and microlevel research seems to confirm such an effect (Buhl & Acosta 2016; Fitzgerald et al. 2018; Hayden & Shandra 2009; Knight et al.2013; Nässén & Larsson 2015; Nässén et al. 2009; Rosnick 2013; Schor 2005), though more research is still required. The following contribution intends to shed more light on whether the assumption that a reduction of work time leads to a reduction of per capita resource consumption and therefore ultimately contributes to a post-extractive economy holds true. The findings which will be presented at the 17th Swiss Geoscience Meeting 2019 for this purpose are based on explorative qualitative interviews (1), a longitudinal survey (2), as well as a transdisciplinary expert dialogue (3), all of which were, or rather will be conducted within the research project 'Time is Wealth'.

The explorative qualitative interviews (1) were held with 17 Swiss residents employed in the German-speaking part of Switzerland who had reduced their workload in the two years preceding the interviews. A qualitative content analysis of these interviews points in the direction of any sizeable changes in per capita resource consumption due to a reduction of working hours only deriving from specific combinations of changes of individual income and discretionary time over the course of a reduction in working hours, which in turn appeared to depend on the motives behind the study participants' decisions to reduce their workload. In more specific terms, it became evident that only study participants that witnessed both a decrease in income, as well as discretionary time exhibited a decrease in consumption (Hanbury et al. 2018).

While the data collection of the longitudinal survey (2) is still ongoing, a selection of the preliminary results of the completed first wave of the survey (N=735) will be presented at the 17th Swiss Geoscience Meeting 2019. This will gauge how substantiated the assumed effect of work time reduction on per capita resource consumption (measured in CO_2 emissions) is.

The transdisciplinary expert dialogue (3) will take the current societal discourse into consideration by analysing a delphi method-inspired opinion survey with roughly 60 experts from a wide range of fields of both civil society and politics in order to find out how a reduction of working hours could be practically implemented on a societal scale, provided such a reduction is desirable. At this point in time it is not possible to comment on the results of this study, as it finds itself in the data collection phase and will only provide the results of the first data collection phase at the 17th Swiss Geoscience Meeting 2019.

REFERENCES

Buhl, J., & Acosta, J. 2016: Work less, do less?, Sustainability Science, 11(2), 261–276. https://doi.org/10.1007/s11625-015-0322-8

Fitzgerald, J. B., Schor, J. B., & Jorgenson, A. K. 2018: Working Hours and Carbon Dioxide Emissions in the United States, 2007–2013, Social Forces, 96(4), 1851–1874. https://doi.org/10.1093/sf/soy014

Hanbury, H., Moser, S., & Bader, C. 2018: Reducing Working Hours as a Means to Foster Low(er)-Carbon Lifestyles? An Exploratory Study on Swiss Employees, Sustainability, 11(7), 2024. https://doi.org/10.3390/su11072024

Hayden, A., & Shandra, J. M. 2009: Hours of work and the ecological footprint of nations: An exploratory analysis, Local Environment, 14(6), 575–600. https://doi.org/10.1080/13549830902904185

Knight, K. W., Rosa, E. A., & Schor, J. B. 2013: Could working less reduce pressures on the environment? A cross-national panel analysis of OECD countries, 1970–2007, Global Environmental Change, 23(4), 691–700. https://doi.org/10.1016/j.gloenvcha.2013.02.017

Nässén, J., & Larsson, J. 2015: Would shorter working time reduce greenhouse gas emissions? An analysis of time use and consumption in Swedish households, Environment and Planning C: Government and Policy, 33(4), 726–745. https://doi.org/10.1068/c12239

Nässén, J., Larsson, J., & Holmberg, J. 2009: The effect of work hours on energy use. A micro-analysis of time and income effects, ECEEE, ECEEE SUMMER STUDY - ACT! INNOVATE! DELIVER! REDUCING ENERGY DEMAND SUSTAINABLY.

Rosnick, D. 2013: Reduced work hours as a means of slowing climate change, Real-World Economics Review, 63(25), 124–133.

Schor, J. B. 2005: Sustainable consumption and worktime reduction, Journal of Industrial Ecology, 9(1–2), 37–50.

24.9

Governing underground resources: Decentralisation, resource regimes and regulatory complexities in Ghana

James Adam Natia[1], Timothy Adams[1]

[1]*Institute of Geography, University of Bern, Hallerstrasse 12, CH-3012, Bern (james.natia@giub.unibe.ch)*

Decentralisation is a strategy for rolling back the state from rural communities, and as a governance reform for the formalization of private property right. However, the state, as enshrined in the Constitution of Ghana is the ultimate owner of all underground mineral wealth, which reaffirms the State's presence in rural communities. This paradox creates regulatory complexities and uncertainties in right regimes for above-and-underground resources. Therefore, the question that remains is what governance strategies (e.g., centralized or decentralized) can effectively coordinate above-and-underground resource extraction, if resource right regimes become incoherent and inconsistent. This paper presents results from case study research conducted in Bole and Tallensi districts of Ghana. Our aim is to examine the complexity of local social-political relations that artisanal gold miners have to deal with. We relied on the new institutional political ecology to analyse how institutional change happens based on institutional pluralism and the process of institutions shopping. The findings indicate that underground resource governance challenges expose a variety of institutional ambiguities and political conundrum. Artisanal and small-scale miners' claims to land and subterranean resource are legitimized through various mechanisms including autochthonous claim and institutions shopping from legal framework of the national government.

24.10

Geography of Life Cycle Assessment

Myriam Saadé-Sbeih[1,2] Romain Boistel[3]

[1]Institut de Hautes Etudes Internationales et du Développement, Chemin Eugène-Rigot 2, CH-1202 Genève (myriam.saade@graduateinstitute.ch)
[2]Ecole des Ingénieurs de la Ville de Paris, 80 Rue Rebeval, FR-75019 Paris
[3]Ecole des Ponts ParisTech, 6-8 Avenue Blaise Pascal, FR-77420 Champs-sur-Marne

Life Cycle Assessment (LCA) is a multicriteria and comparative methodology quantifying the environmental impacts of a product or a service, covering its entire life cycle (Jolliet et al 2016). It aims at prioritizing actions to improve the environmental performance of production systems throughout their entire life cycle, and avoiding the transfer of impacts between life cycle stages, impact categories, and more recently, geographical areas. Despite the LCA community's ambition to develop a holistic approach assessing the environmental burdens of global economic activities, the method was first dedicated to the quantification of impact scores at a planetary level, based on data constructed mostly for and in Western Europe, Japan and US contexts. Since the late 2000s, extended efforts have been made to promote the LCA method to "non-OCDE countries" (Potting et al 2010). This contribution seeks to understand the circulation and transformation of the LCA methodology through the exploration of the spatial redistribution of its scientific production, at country and city levels. To what extent the dissemination of LCA scientific activities participates to the elaboration of particular understanding of the methodology translated in both methodological developments (databases, models, guidelines) and applications? Drawing from critical political ecology (Forsyth 2003) and geography of science (Grossetti et al 2013) approaches, this research questions more broadly the effects of using normative environmental tools – initially constructed in the "Global North" – in the "Global South".

REFERENCES

Grossetti, M., Eckert, D., Gingras, Y., Jégou, L., Larivière, V. et al. (2013), Cities and the geographical deconcentration of scientific activity : A multilevel analysis of publications (1987-2007). *Urban Studies*, SAGE Publications, 2013, 51(10), 2219-2234.

Forsyth, T. (2003), Critical Political Ecology: The Politics of Environmental Science, Routledge, London.

Jolliet, O., Saadé-Sbeih, M., Shaked, S., Jolliet, A., and Crettaz, P. (2016), Environmental Life Cycle Assessment, CRC Press: New York.

Potting, J., Curran, M.A. & von Blottnitz, H. (2010) From life cycle talking to taking action, The 4th International Conference on Life Cycle Management: The Global Challenge of Managing Life Cycles, International Journal of LCA, 15(4), 326-329.

25.1

Land Degradation Dynamics in the Nigerian Guinea Savannah Social-Ecological System between 2003-2018.

Ademola A. ADENLE[1], Chinwe IFEJIKA SPERANZA[1]

[1]*Institute of Geography, University of Bern, Hallerstrasse 12, CH-3012 Bern, Switzerland.*
(ademola.adenle@giub.unibe.ch)

This study provided a recent view of vegetation dynamics and land degradation situation in the threatened and fragile Nigerian Guinean Savannah (NGS) Agroecological belt, which human and climate (rainfall variability) events have been implicated to drive. Moderate-resolution Imaging Spectroradiometer (MODIS) Normalized Vegetation Index (NDVI, 250m) time series Terra product which compensates for the coarse limitation of previous related large-scale studies and a gridded rainfall observation, from Tropical Applications of Meteorology using SATellite and ground-based observations (TAMSAT, 4km high resolution) were employed and processed differently and together between 2003-2018. The study objectives are to:(i) provide empirical insights on the pattern of savannah vegetation dynamics (ii) exclude rainfall effects from the degradation of savannah (iii) characterize the extent, severity and the geography of human induced degradation across the NGS. The inter-annual variations of vegetation exhibit an alarming anomaly at certain years with a consistent negative, decreasing trend while the profile of monthly anomaly maintains historically seasonal uniformity. Correlation and linear relationships between MODIS and TAMSAT (pixel to pixel) predicted a strong spatio-temporal relationship between vegetation and rainfall over most of the NGS. The exclusion of rainfall effect through the Residual Trend Analysis method (RESTREND), approach produced an NDVI residue with a lowered NDVI value (i.e.0.34 to 0.30) which contrast with the NDVI without accounting for rainfall (i.e. 0.765 to 730). A decreasing trend in NDVI residue in the time series, and continuously negative decreases, but never increase monotonic trend (i.e.-0.96), validate that the prevailing and extensive case of biomass loss was invoked by an accelerated episode of unsustainable human activities. The output from the spatial pattern, extent and severity through Theil-Sen median slope and significant analysis showed that 0.37% (2,480.81 SqKm) and 37.59% (248,920.70 SqKm) of the NGS has noticeably been degraded at P<0.01 and P<0.05 levels of significance respectively, while 13.77% (91,169.44 SqKm) and 0.01%(88.63 SqKm) of the NGS showed improvement in NDVI residue. These results will be used to drive further investigations into the local causative archetype human accelerated degradation across the NGS which are connected to poor land use management and livelihood activities.

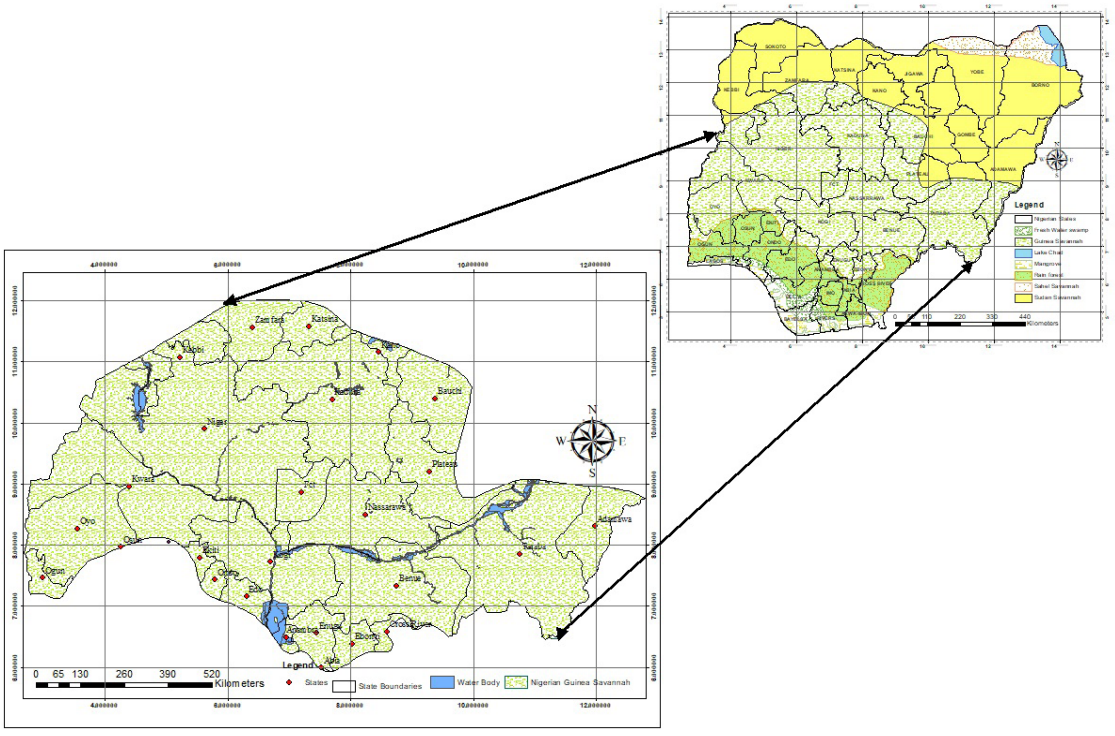


Figure 1. Nigeria Agro-ecological zones showing the Nigerian Guinea Savannah and its state boundary. (Source Adapted from Iloeje, 2001)

25.2

Is tourism compatible with an adequate protection of the geomorphological heritage?

Jonathan Bussard[1]

[1]*Institute of Geography and Sustainability, University of Lausanne - site de Sion, CP 4176, CH-1950 Sion 4 (jonathan.bussard@unil.ch)*

Geoheritage, as part of the natural heritage, is considered by scientists as a testimony of Earth history that has to be protected. However, when exposed to human activities such as tourism, geoheritage can also be considered as a natural resource (Reynard 2005). This is the case, for example, when geosites are part of the tourism offer for their scientific, educational or recreational interest or as part of an attractive landscape, particularly in mountain areas. This raises the question of the compatibility of the exploitation of the resource for tourism purposes with protection needs. In a PhD thesis started in 2019, we try to use several approaches to answer this research question: is tourism compatible with an adequate protection of the geomorphological heritage?

The analysis of the relationship between tourism and its natural environment requires the consideration of many different factors evolving in a complex system. Various approaches, such as geography, natural sciences, economics, political science, sociology, tourism studies, offer complementary perspectives and sources of interpretation on the issue.

Three main approaches will be used to assess the situation of the different case studies:

1. **Natural sciences**: documentation and assessment of the heritage value of a landform, including its “scientific value” and “additional values” (ecological, aesthetic, cultural), by an evaluation method such as the one proposed by Reynard et al. 2016. This first step is very important to define the geosite and why it is necessary to protect it.
2. **Political science**: analysis of the “institutional resource regime”, defined as the combination of the property regime and public policies that regulate the management of natural resources (Knoepfel et al. 2001). This second point allows us to understand how a geosite is presently regulated (as a natural resource).
3. **Geographical approach of tourism**: understanding tourism activity through three main concepts: stakeholders, places and practices (Knafou & Stock 2003). This third analysis is important to determine how a geosite is perceived by tourists and by stakeholders of the tourism sector, including tourism offices, local authorities, tourism services providers, etc. and to better understand the impacts of tourism, seen here as a set of activities and practices that interact with the environment.

REFERENCES

Knafou, R., & Stock, M. 2003. Tourisme, In Dictionnaire de la géographie et de l’espace des sociétés, 931-934. Belin, Paris.

Knoepfel, P., Kissling-Näf, I., & Varone, F. 2001. Institutionelle Regime für natürliche Ressourcen: Boden, Wasser und Wald im Vergleich. Helbing und Lichtenhahn, Basel, Genf, München.

Reynard, E. 2005: Geomorphological sites, public policies and property rights. Conceptualization and examples from Switzerland, Il Quaternario, 18(1), 323-332.

Reynard, E., Perret, A., Bussard, J., Grangier, L., & Martin, S. 2016: Integrated Approach for the Inventory and Management of Geomorphological Heritage at the Regional Scale, Geoheritage, 8(1), 43-60.

25.3

Promoting Resilience in the Sahel: The Great Green Wall

David Ellison[1,2,3]

[1]Adjunct Researcher, Sustainable Land Management Unit, Institute of Geography, University of Bern, Switzerland,
[2]Department of Forest Resource Management, Swedish University of Agricultural Sciences, Umeå, Sweden,
[3]Ellison Consulting, Baar, Switzerland

Many suggest increased tree and forest cover could be beneficial to both resisting the southward expansion of the Sahara and increasing landscape resilience in the W. African Sahel. The severe and extensive drought of the 1970's-1990's led many to undertake projections of future climate, or to promote strategies for improving general climate resilience in the region. The idea for the Great Green Wall (GGW), a band or wall of trees intended to manage desert encroachment, grew out of this period of tremendous upheaval and human tragedy. Millions succumbed to drought, famine, or chose out-migration. In parts of the Sahel, the rural population was decimated. Though the basic conditions in the Sahel have improved since the 1990s, some 30 years on, and despite considerable recovery in the local rainfall regime, we still know far too little about whether an idea such as the GGW can even work. And if it can, under what particular conditions? On the other hand, knowledge about forest-water interactions has improved dramatically over the last several decades. Applying the lens of current knowledge on forest-water interactions to the general concept of landscape restoration as a tool for achieving improved resilience and human welfare in the Sahel provides meaningful input for a potential re-thinking of the GGW strategy. We propose significant revision and upgrading of current knowledge about the principal factors likely to provide and promote landscape resilience in the region. Strategies more broadly focused on updated concepts of the role of forests and water in promoting landscape resilience appear more likely to steer current efforts in useful directions.

Keywords: Great Green Wall, Sahel, Sub-Sharan Africa, forest landscape restoration, forest-water interactions, Ecosystem-based Adaptation

25.4

Farmers' response to agri-environmental governance in Southland, New Zealand

Anna Geiser[1]

[1]*Unit of Geography, University of Fribourg, Chemin de Musée 4, CH-7001 Fribourg (anna.geiser@unifr.ch)*

The case of farming in New Zealand›s district of Southland presents a puzzle where farmers are 'caught' between contradicting governmental policies: On the one hand there is the on-going intensification of agriculture caused by the cut of all governmental subsidies in a neoliberal market in the 1980s, on the other hand there are increasing environmental mitigation demands from both the public and the government (Brown et al. 2019).

The loss of governmental subsidies resulted in conversions of sheep and other types of farms into more lucrative dairying operations. These conversions were attractive for both family farms that were trying to survive, as well as for new investors who were previously not farming in Southland. Conversion to dairy farming is very costly, meaning that the banking sector became heavily involved in farming in Southland, which many farmers were completely unprepared for. In order to finance loans and meet the governmental demands of doubling agricultural exports between 2012 and 2025, farms became more and more intensive (Forney&Stock 2013). This development has severely altered the farming industry of Southland and created a specific institutional environment in which large-scale intensive farming is seen as necessary. This in turn led to increasing environmental problems caused by the agricultural sector in the last 40 years. The nutrient loss measured on dairy farms is high and as a result, water quality has diminished in Southland (Moran et al. 2017). In reaction to this, the regional authorities have been trying to implement more strict agricultural policies, however, pollution has only increased. This has had a severe effect on both quality of life in the area, as well as the tourism sector (Moran et al. 2017). The regional council has now proposed a new agri-environmental governance policy (Water and Land 2020&Beyond Plan), which is supposed to make a more sustainable farming industry possible. In sum, Southland farmers are obliged to increase their farm's output value, while at the same time having to comply with increasingly strict environmental policies. These aims have proven to be incompatible in practice so far.

This examination uses empirical data from interviews and observations gained in the field from November 2018 to February 2019. By employing Pierre Bourdieu's theoretical approach of different forms of capital in his theory of practice, I examine farmers› experiences of this tension and their view on the new policy plan – after all, policies must ultimately be implemented on-farm in order to make a difference. Farmer's responses are assumed to be largely influenced by both habitus and field. According to Bourdieu, farmers are supposed to strive to be 'good farmers' in order to gain social capital, meaning they have an inherent interest in the mitigation of environmental as well as governance problems (Haggerty et al. 2009). In this examination I show why farmers take fault with the new plan, and how they propose to improve it instead. I focus on the issue of water quality management and aim to contribute to a better understanding of farmers' behaviour during governance changes in the neoliberal context of New Zealand, thus influencing the way agri-environmental governance is done (Blackstock et al. 2010).

REFERENCES

Blackstock, K. L., Ingram, J., Burton, R., Brown, K. M. & Slee, B. 2010: Understanding and Influencing Behaviour Change by Farmers to Improve Water Quality. Science of The Total Environment 408(23): 5631–5638.

Brown, P., Daigneault, A. & Dawson, J. 2019: Age, values, farming objectives, past management decisions, and future intentions in New Zealand agriculture, Journal of Environmental Management, 231: 110-120.

Forney, J. & Stock, P. V. 2013: Conversion of Family Farms and Resilience in Southland, New Zealand, International Journal of Sociology of Agriculture and Food, 21(1): pp. 7-29.

Haggerty, J., Campbell, H., & Morris, C. 2009: Keeping the stress off the sheep? Agricultural intensification, neoliberalism, and 'good' farming in New Zealand, Geoforum, 40(5): 767-777.

Moran, E., Pearson, L., Couldreay, M. & Eyre, K. 2017: The Southland Economic Project: Agriculture and Forestry. Technical Report. Publication no. 2017-02. Environment Southland, Invercargill, New Zealand.

25.5

Governance structures and competing models on land use: a policy network study of forest law in Salta

Carla Inguaggiato[1], Maurice Tschopp[1], Graziano Ceddia[1], Christopoulos Dimitris [2]

[1]Centre for Development and Environment, University of Bern, Switzerland;
[2]MODUL University Vienna; Heriot-Watt University

The Gran Chaco Americano is the second biggest forest in Latin America and the third agricultural frontier after the Amazon and the Brazilian Cerrado.

Salta province in the Northwest of Argentina has largest forest coverage in the country. Salta political economy has a strong dependency on the forest, as the province has high forest coverage, a high deforestation rate and many areas of high risk in terms of climate change and social vulnerability.

Salta approved the provincial forest law after long negotiation processes involving actors such as: provincial and national state agencies, NGOs, large scale producers', indigenous people and small-scale farmers' organizations.

This paper aims to understanding how the network position in the policy networks of governance stakeholders' forest use vision relate to the definition and implementation of forest law.

We adopt a mixed methods research design integrating social network analysis with discourse analysis combining quantitative and qualitative analytic techniques. The analysis draws on a unique dataset based on policy network survey addressing stakeholders participating to key committees for the implementation and discussion of forest management policy and on extensive fieldwork. We analyse the co-participation in different policy fields by mapping direct ties among such stakeholders that record their exchange of scientific/technical information, long term mutual support, and meetings. The data collection instrument captures perception of stakeholders on influence of others on forest management governance. It incorporates visions on socio-ecological risks and policy, tenure regularization and forest management policy, to identify policy actors' visions of native forest use.

Policy actors can be classified into three main visions on the land use of native forests: 1) maximizing economic return, 2) protecting livelihood systems and rights of the peoples living on the forest and 3) preserving forest ecosystem services. The classification is the result of content analysis results of stakeholders' qualitative interviews.

In the paper we discuss how the position of these three interest groups in the policy networks structure and their level of reputational influence relates to policy decisions.

25.6

Spatial and Temporal Changes in Land Use Land Cover (LULC) and Implications for Food Security in Mararaba Area of Nassarawa State Nigeria

[1]Morenikeji, G, [1] Livinus, O and [2]Adesina, E.A

[1]Department of Estate Management and Valuation, Federal University of Technology, Minna
[2]Department of Surveying & Geoinformatics, Federal University of Technology, Minna
Contact: gbenga.morenikeji@futminna.edu.ng, joefodsolutions@gmail.com Mobile: +2347036411810

The study will explore land use /cover changes, food production trends and main drivers behind deteriorating agricultural land, relationship between population, land use changes and implications on food production and security. Mararaba area experiences a high rate of land use / cover changes which affecting food production. However, agricultural land fragmentations, population increase and urbanization led to decrease of agricultural land and food production leaving the rural livelihoods food insecure. Land use / cover changes classification and analysis would be done in the area using Landsat TM image in Erdas Imagine while the Soil fertility, Digital Elevation Model (DEM), population density and poverty process would be analyzed and correlated to food production using ArcGIS 10.3 and Statistical Package for Social Sciences (SPSS). Thus, land use land cover data will include farming methods used by farmers in order to map and analyze the land use/ cover changes and implications for food production if the living conditions and standards of rural livelihoods are to be improved and maintained at current levels. The food production data will include livestock products and animal population data in order to map adequately the relationship between land use land cover changes, population growth and food security. The objectives of the study will be to analyze land use land cover changes and implications for food production in Mararaba Area of Nasarawa State, Nigeria using GIS and Remote Sensing techniques. At the end of the study, it will show if food is secure in the area with agricultural land already degraded and densely populated with high poverty levels.

Keywords: Land use/cover, population density, land degradation, food security

25.7

Governance in telecoupled land systems: the case of Thilawa Special Economic Zone, Myanmar

Christoph Oberlack[1,2,°], Win Myint[3], Jean-David Gerber[1,4], Peter Messerli[1,2]

[1]*Institute of Geography, University of Bern, Switzerland*
[2]*Centre for Development and Environment (CDE), University of Bern, Switzerland*
[3]*Environmental Conservation and Community Security Institute (ECCSI), Yangon, Myanmar*
[4]*Centre for Regional Economic Development, University of Bern, Switzerland*
°Corresponding Author: christoph.oberlack@giub.unibe.ch

The emerging lens of telecoupled social-ecological systems offers new opportunities for geographers to refine the analysis of interdependencies among actors in networks that cross established boundaries of social-ecological systems (e.g. interregional commodity trade and investment flows). Changing interdependencies among local and distant actors give rise to changing governance needs and entice novel governance responses in an increasingly networked world. However, debates about networked or polycentric governance and telecoupled land systems remain largely disconnected despite a need to understand performance and change of governance in telecoupled systems. As a consequence, it remains unclear what kind of governance responses are suited to address what kind of sustainability problems in telecoupled systems. This paper presents a case study that analyzes the polycentric governance in a telecoupled system in Myanmar. It assesses how governance interactions triggered telecoupled sustainability problems manifested as negative impacts on access to land in concrete places. Further, it locates the action situations, in which actors transformed some of those sustainability problems. We chose the Thilawa Special Economic Zone in Myanmar as a representative case for this purpose. Primary data were collected through semi-structured interviews, document analysis, and complemented by secondary literature. We analyse the data by process tracing and qualitative content analysis. Analytically, we chose the Networks of Action Situations approach to identify networked spaces of decision-making in telecoupled systems and their critical roles in shaping sustainability outcomes. Tentative results show that problems of livelihood and environmental destruction in the early phase of the Special Economic Zone can be attributed to a lack of linkages between distant action situations and local social-ecological contexts. Subsequently, community resistance in local and distant action situations lead to the creation of new governance spaces, which contributed to transform some of those sustainability problems. We conclude with discussing the emergence of new forms of governance in telecoupled systems; the theorization of problems of sustainability governance problems in telecoupled systems, and particular challenges of telecoupling to environmental and sustainability governance research.

Keywords: Myanmar, Development, Governance, Investment, Trade.

25.8

Making Forest Management Work for the Actualization of SDGs and Climate Protection

Chidiebere Ofoegbu[1] and Chinwe Ifejika Speranza[1]

[1]*Institute of Geography, University of Bern, Bern, Switzerland*

The MOSAIC project is designed to address key challenges faced by rural people and policy-makers in developing countries with respect to forest ecosystem management and protection against climate change impact. The main aim is to assess how to structure forest management practices in order to contribute effectively and efficiently to sustainable wellbeing at local community level while supporting national climate change mitigation and adaptation targets. The MOSAIC project is based on a practice-oriented transdisciplinary approach applying state-of-the-art innovated wellbeing framework to people-centered field research, including qualitative participatory approach and quantitative research methods. Research and synthesis will rely on three REDD+ (Reducing Emissions from Deforestation and forest Degradation plus sustainable forest management) case studies in Nigeria with a strong emphasis on outreach and capacity-building activities, while strengthening local actors' research and monitoring capabilities.

25.9

Silvopastoral practises adoption by smallholders and private company: is land sharing as a solution to stop deforestation in the Chaco Salteño?

Maurice Tschopp[1], Nick Bardsley[1], Carla Inguaggiato[1], Graziano Ceddia[1]

[1]Centre for Development and Environment, Universität Bern, Mittelstrasse 43, 3012 Bern (maurice.tschopp@cde.unibe.ch)

Tropical deforestation and land-use change account for 10% of global greenhouse gas emissions (GE) and represents a significant share of the emissions of south American countries (Harris et al. 2012). The Argentinian semi-arid Chaco has been facing very high deforestation rates in the last three decades. Currently, large-scale soy plantations, as well as cattle companies are the primary drivers of this process (Volante et al. 2016).

Several policies exist to reduce deforestation, but their efficiency is contested (Ceddia & Zepharovich 2017; Nolte 2018). In 2007, Argentina adopted a national law, aiming to reduce deforestation, which incorporates a land-use planning system (Territorial Regulations of Native Forests: OTBN). The OTBN is negotiated and implemented at the province level and it limits productive activities and land-use change in most of the remaining forests. However, the law allows for some specific productive use, including traditionnal sylvopastoral systems, which are presented by the Argentinian state as an alternative to deforestation.

This paper examines the determinants for the adoption of different silvopastoral practises both by smallholders and by large-scale landowners. The paper uses a mixed-methods approach. It builds on a survey with 550 smallholders and on semi-directive interviews with private companies from the Salta province. Our results suggest that smallholders are more disposed to adopt silvopastoral practises than large companies. We discuss the role of different factors in the adoption process, including education level and social capital. We conclude by stressing the key role of farmers' cooperatives and trade unions in shaping such land-use decisions.

REFERENCES

Ceddia, M. G., & Zepharovich, E. (2017). Jevons paradox and the loss of natural habitat in the Argentinean Chaco: The impact of the indigenous communities' land titling and the Forest Law in the province of Salta. Land use policy, 69, 608-617.

Harris, N. L., Brown, S., Hagen, S. C., Saatchi, S. S., Petrova, S., Salas, W., & Lotsch, A. (2012). Baseline map of carbon emissions from deforestation in tropical regions. *Science*, *336*(6088), 1573-1576

Nolte, C., Gobbi, B., de Waroux, Y. L. P., Piquer-Rodríguez, M., Butsic, V., & Lambin, E. F. (2018). Challenges in attributing avoided deforestation to policies and actors: Lessons from provincial forest zoning in the Argentine Dry Chaco. Ecological Economics, 150, 346-352.

Volante, J., Mosciaro, M. J., Gavier-Pizarro, G. I., & Paruelo, J. M. (2016). Agricultural expansion in the Semiarid Chaco: Poorly selective contagious advance. *Land Use Policy*, *55*, 154-165.

25.10

Social multi-criteria evaluation of land-use scenarios: Comparing sustainability and environmental justice criteria

Elena Zepharovich, Michele Graziano Ceddia, Stephan Rist

University of Bern, Centre for Development and Environment (CDE), Hallerstrasse 10; 3012 Bern (elena.zepharovich@cde.unibe.ch)

The increase in deforestation in Latin America is generating a great number of land use conflicts. Diverse stakeholders, such as large-scale producers, indigenous peoples and small-scale famers, compete for land and contest its use. This renders land-use planning essential and at the same time a great challenge because stakeholders hold strongly contrasting perceptions concerning the environmental, social, cultural and economic impacts of deforestation.

The paper contributes to understanding the multi-dimensional implications of deforestation, using a comparative case study in the Argentinean Chaco. We apply the method of social multi-criteria evaluation (SMCE) as it addresses one of the main problems confronted in land-use planning; the conflicting perceptions on what this plan should achieve and how. SMCE simplifies and structures complex decision-making problems, by allowing the use of various evaluation criteria.

Most SMCE studies apply sustainability criteria, including the economic, social and environmental dimension. Even though such indicators are frequently selected in a participatory way, they often do not account for environmental justice, more specific distributional justice (i.e. how are the benefits and harms allocated among actors), procedural challenges (i.e. how decision are made and by whom) and issues of recognition (i.e. respect for difference).

Hence, we apply two sets of criteria: One tackling the general issues of sustainability, and another one, containing criteria of environmental justice, emphasizing distribution, recognition, and procedure. By including the later set of criteria, implications of deforestation become stronger visible.

We use these two sets of criteria to assess four land use scenarios, describing different forms of land use. The scenarios are based on a Q-Method study as well as qualitative interviews with local stakeholders.

On a conceptual side, this paper shows that the selection of the criteria has a strong influence on the results and sheds light on the hegemonic tendencies of mainstream sustainability criteria. In a world, which is increasingly unequal, it is more important than ever to account for justice. From an empirical side, the paper displays the high environmental, social, cultural and economic costs of deforestation in the Argentinean Chaco, as well as the benefits of low deforestation in this area. Finally, our results assist in the creation of dialogues about alternative, more sustainable and environmentally just, futures.